Outer Continental Shelf Environmental Assessment Program

Final Reports of Principal Investigators

Volume 52 **December 1986**

U.S. DEPARTMENT OF COMMERCE
National Oceanic and Atmospheric Administration
National Ocean Service
Office of Oceanography and Marine Assessment
Ocean Assessments Division
Alaska Office

U.S. DEPARTMENT OF THE INTERIOR
Minerals Management Service
OCS Study, MMS 86-0114

"Outer Continental Shelf Environmental Assessment Program Final Reports of Principal Investigators" ("OCSEAP Final Reports") continues the series entitled "Environmental Assessment of the Alaskan Continental Shelf Final Reports of Principal Investigators."

It is suggested that sections of this publication be cited as follows:

Ertec Western, Inc. 1983. Seafloor geologic hazards on the northern Aleutian Shelf. U.S. Dep. Commer., NOAA, OCSEAP Final Rep. 52(1986):1-342

Phillips, L., P. Barnes, E. Reimnitz, and R. Hunter. 1985. Geologic processes and hazards of the Beaufort and Chukchi sea shelf and coastal regions. U.S. Dep. Commer., NOAA, OCSEAP Final Rep. 52(1986):343-820

OCSEAP Final Reports are published by the U.S. Department of Commerce, National Oceanic and Atmospheric Administration, National Ocean Service, Office of Oceanography and Marine Assessment, Ocean Assessments Division, Alaska Office, Anchorage, and primarily funded by the Minerals Management Service, U.S. Department of the Interior, through interagency agreement.

Requests for receipt of OCSEAP Final Reports on a continuing basis should be addressed to:

NOAA-OMA-OAD
Alaska Office
701 C Street
P.O. Box 56
Anchorage, AK 99513

OUTER CONTINENTAL SHELF

ENVIRONMENTAL ASSESSMENT PROGRAM

FINAL REPORTS OF PRINCIPAL INVESTIGATORS

Volume 52

December 1986

U.S. DEPARTMENT OF COMMERCE
National Oceanic and Atmospheric Administration
National Ocean Service
Office of Oceanography and Marine Assessment
Alaska Office

U.S. DEPARTMENT OF THE INTERIOR
Minerals Management Service
Alaska OCS Region
OCS Study, MMS 86-0114

Anchorage, Alaska

The facts, conclusions, and issues appearing in these reports are based on research results of the Outer Continental Shelf Environmental Assessment Program (OCSEAP), which is managed by the National Oceanic and Atmospheric Administration, U.S. Department of Commerce, and funded (wholly or in part) by the Minerals Management Service, U.S. Department of the Interior, through an Interagency Agreement.

Mention of a commercial company or product does not constitute endorsement by the National Oceanic and Atmospheric Administration. Use for publicity or advertising purposes of information from this publication concerning proprietary products or the tests of such products is not authorized.

Content of these reports has not been altered from that submitted by the Principal Investigators. In some instances, minor grammatical, spelling, and punctuation errors have been corrected to improve readability; some figures, charts, and tables have been enhanced to improve clarity in reproduction.

Outer Continental Shelf Environmental Assessment Program

Final Reports of Principal Investigators

VOLUME 52 DECEMBER 1986

C O N T E N T S

SEAFLOOR GEOLOGIC HAZARDS ON THE NORTHERN ALEUTIAN SHELF

by

Ertec Western, Inc.

Final Report
Outer Continental Shelf Environmental Assessment Program
Research Unit 604

June 1983

TABLE OF CONTENTS

LIST OF FIGURES

LIST OF FIGURES (CONT'D)

LIST OF TABLES

LIST OF PLATES

SUMMARY

BACKGROUND

The National Oceanic and Atmospheric Administration (NOAA) contracted the Earth Technology Corporation (Ertec)[1] to perform a geologic hazards evaluation for the Northern Aleutian Shelf. The objective of this hazards evaluation was to identify geologic conditions which could affect the safe development of lease areas on the shelf. These geologic hazards potentially involved faulting, weak seafloor sediments, slope instabilities and scour.

The area of primary interest in the evaluation was bounded by the Alaskan Peninsula and Unimak Island on the south, latitude 57° 00' on the north, longitude 159° 30' W on the east and longitude 165° W on the west. The eastern and western boundaries roughly intersect Port Moller and Unimak Pass, respectively.

A four-part study involving literature review, field geophysical profiling and sediment sampling, laboratory testing, and data interpretation was initiated to identify these potential hazards. The program was managed by Ertec; significant contributions in the field, laboratory and interpretative phases of the study were made by Mesa[2], as a subcontractor to Ertec.

REGIONAL SETTING

The Northern Aleutian Shelf comprises a very flat continental shelf with water depths ranging from 0 to 110 m. Oceanographic and meteorologic conditions are a dominant force in the area. Significant wave heights for

---

[1] Ertec was formerly called Fugro, Inc.

[2] Mesa (Marine Environmental Science Associates), Inc., Whittier, CA.

100-year return periods range from 17 to 23 m, winds can exceed 55 kts, tides vary from 2 to 7 m, and currents can exceed 100 cm/sec. These conditions affect seafloor soils either by direct loading (scour and wave-induced pressure fluctuations) or by loading to structures supported on the soil.

A review of the geologic history for the area indicates that the region has undergone several distinct episodes during its formation. The major change occurred during the Late Mesozoic - early Cenozoic, and was presumably associated with abandonment of a regime involving subduction and transform faulting along the continental margin of the Bering Sea and inception of the present day subduction zone along the Aleutian Arc. This transition is represented by a major unconformity between highly deformed basement rocks and relatively undeformed Cenozoic strata, sedimentary rocks and volcanic rocks. These Cenozoic strata are disrupted only by normal faults which indicate a tensional tectonics regime throughout much of the Cenozoic era.

The present geologic and tectonic environment is dominated by seismicity and volcanism. These processes are primarily related to subduction of the Pacific Plate under the Bering - North American Plate along the Aleutian Trench. Most earthquakes occur along the trench or in a northerly dipping Benioff zone which dips beneath the Aleutian Arc and the study area. However the presence of scattered earthquakes in the upper crust within the study region and the presence of long, potentially active faults indicates that earthquake hazards are significant within the study region. The Aleutian volcanic arc bounds the study region on the southeast, and at least three of the volcanoes in the portion of the arc adjacent to the study area are potentially active.

FIELD PROGRAM

A field program was conducted from the NOAA ship Discoverer in August, September and October of 1980. The objective of the field program was to supplement the existing geologic data base. This objective was accomplished by conducting a geophysial survey and a bottom sampling program. Geophysical equipment included 3.5 kHz, uniboom, air gun, sparker and side-scan systems. Sediment samples were collected with a Van Veen grab sampler, a gravity corer and a vibracorer. A drop penetrometer was used to obtain in situ soil data.

Over 4000 km of geophysical data were collected. Tracklines were oriented approximately north-south and east-west with spacings of 15 to 25 km. Vessel speed ranged from 4 to 5 knots during the survey. The prevalence of crab pots in the area precluded use of side-scan equipment at night, and hence, only partial side-scan coverage was achieved.

Sediment samples and in situ soil resistance data were collected at 60 locations. Only limited sediment penetration (1 to 2 m maximum) could be achieved with the gravity corer, the vibracorer and the drop penetrometer. This is attributed to the very dense, cohesionless nature of the sediments.

LABORATORY TESTING

Sediment samples recovered during the field program were transported to onshore soil testing facilities at Ertec and California State University, Northridge for detailed analyses. The scope of the testing program included geological descriptions and engineering parameter determinations.

Results of the laboratory studies indicate that surficial sediments are very dense silty sands and sands, consisting primarily of quartz, feldspar, hornblende and unidentified opaque minerals. Carbon content is less than 1.0 percent. These sediments have wet unit weights ranging from 18 to 21 kN/m^3; water contents vary from 20 to 40 percent. The compressibility of the material is low; permeability is relatively high; and effective friction angles range from 37 to 41 degrees. Cyclic strength and stiffness are high.

DATA INTERPRETATION AND RESULTS

Literature, field and laboratory data were interpreted and analyzed collectively to enhance existing information about geologic conditions within the study area. The results of this analysis confirm that the shelf is very flat with slopes generally less than 0.5 percent. The area is underlain by three deep basins (depth to 5000 m) filled with Tertiary sediments. Sediment ages within 1 to 2 m of the seafloor range from 11,000 to 12,000 years B.P. Complex faulting occurs at the margins of two basins.

The southeastern portion of the study area is also characterized by earthquakes primarily associated with the subduction of the Pacific Plate beneath the Bering-North American Plate. Based on historic data, a maximum earthquake magnitude of 8 3/4 is postulated for subduction-related events. The historic record for earthquakes in the crust of the study area is considered to be too short to provide a basis for estimating maximum earthquakes; therefore, worldwide empirical data in similar tectonic environments were analyzed. This analysis indicates that a possibility of infrequent earthquakes as large as magnitude 7 3/4 exists. Peak ground accelerations from these earthquakes could vary from 0.1g for the general region to 0.7g near the North Amak Fault Zone.

Sediment stability during static, storm-wave and earthquake loading varies from excellent to poor. The denseness of sediments and the gentleness of slopes should lead to good static stability under normal foundation loading. Storm-wave loading may introduce limited instability due to wave-induced liquefaction in shallow water areas (less than 25 m water depths) or sediment scour. However, the coarseness of surficial sediments within this depth regime suggests that the occurrence of these problems will be limited. Large earthquake-induced ground accelerations will likely cause high excess pore-water pressures near earthquake sources. These sources are located near the Amak and Bristol Bay Fault Zones. The effects of high pore pressures are expected to be small because of the denseness of most sediments.

GEOLOGIC HAZARDS

This evaluation documents several potential geologic hazards which must be considered in the design of offshore facilities. These geologic hazards include earthquake-induced ground accelerations, surface faulting, volcanic ejecta, soil instabilities, shallow gas and gas seeps, and sediment transport. Earthquake-related hazards (accelerations, faulting and sediment instability) and gas seeps are regarded as the most serious hazards. The severity of these hazards is not regarded as being so great that safe development of the area is precluded. Most of the identified hazards can be accomodated by proper site selection and sound engineering design.

CONCLUSIONS AND RECOMMENDATIONS

This geologic hazards evaluation indicates that geologic hazards exist on the Northern Aleutian Shelf but appear to be manageable within the engineering profession's existing state-of-technology. However, it is also clear from this study that site-specific evaluations will be required before pipelines, platforms or other facilities are installed. Future evaluations must include oceanographic and meteorologic studies to enhance understanding of wave, wind and current conditions. Furthermore, more detailed geophysical and sediment testing programs are essential. Sediment sampling programs for large fixed-base structures should include borings to 100 m or more. Future laboratory testing and engineering analyses should quantify soil and foundation behavior under the postulated loading environment.

1.0 INTRODUCTION

1.1 BACKGROUND

This report summarizes the results of a geological hazards evaluation for the southeastern portion of the Northern Aleutian Shelf. The evaluation was conducted by the Earth Technology Corporation (Ertec)* for the National Oceanic and Atmospheric Administration (NOAA) under Contract No. NA 80-RAC 00167. The period of contract performance extended from August 1980 until January 1983.

The geological hazards study was performed in general accordance with a scope of work outlined in NOAA's Request for Proposal (RFP) dated April 21, 1980 (Ref NOAA RFP No. 52-80). The general objective of the study, as outlined in the RFP, was to assess the geologic hazards on the Northern Aleutian Shelf by collecting reconnaissance geophysical, geological and geotechnical data. These data were to be integrated with all available nonproprietary and existing literature information into a regional geologic and geotechnical framework of the study area. Results of the study were to be summarized in a form useable for the petroleum industry in lease-sale evaluations. Additional details about the scope of work are presented in Subsection 1.2.

To accomplish this study, Ertec utilized a team of engineers, geologists and consultants. Dr. Donald Anderson of Ertec served as Project Manager. Messrs. Charles F. Chamberlain and Bruce A. Schell were responsible for field and office geological studies, respectively. Drs. Bill (T.D.) Lu and C. B. Crouse of Ertec were responsible for geotechnical and earthquake engineering studies. Significant phases of the geological studies were conducted by

*At the time of contract award, Ertec was called Fugro Inc. The name of the company changed in 1981.

Drs. Peter J. Fischer and Bruce Molnia of Mesa* as consultants to Ertec. Dr. Dwight Sangrey of Carnegie - Mellon University served as a Chief Scientist on one phase of the field program. NOAA's technical guidance was provided by Messrs. Rod A. Combellick and Laurie E. Jarvella from the Office of Marine Pollution Assessment in Juneau, Alaska; Ms. Jane Carlson served as NOAA's contract administrator.

1.2 SCOPE OF STUDY

The hazards evaluation was carried out in two separate phases. The first phase involved a field program. This was followed by office and laboratory studies during which field data and other published information were reduced, interpreted, summarized and presented.

Field operations were carried out in August, and September and October of 1980. These operations involved

1) collection of side-scan sonar, 3.5 kHz, uniboom, and intermediate resolution ("deeper penetration") seismic reflection data; and

2) collection and description of gravity cores, and measurement of in situ density and shear strengths with a drop penetrometer device.

Upon completion of the field program, a detailed review of existing and new geological and geotechnical data relevant to geological hazards on the Northern Aleutian Shelf was initiated. This phase of the study included

1) collection and synthesis of existing literature concerning environmental and regional geology for the Northern Aleutian Shelf including the shallow structural, sedimentological, and geotechnical framework of the area;

2) analysis and integration of geophysical data with existing information to produce maps and cross-sections of the surficial and shallow geologic relationships in the study area;

*Mesa (Marine Environmental Science Associates), Inc., Whittier, CA.

3) performance of shore-based laboratory tests on selected samples of surficial soils to define geologic characteristics (size, mineralogy, organic and carbonate content, age) and engineering properties (plasticity, static and dynamic strength, compressibility, sonic velocities);

4) interpretation of laboratory and field data to define geologic conditions, earthquake ground motions and geotechnical engineering behavior; and

5) preparation of a final report presenting a detailed geologic-hazard evaluation of the lease sale area.

1.3 ORGANIZATION OF REPORT

The results of this study are summarized in the following text and appendices. Chapters 2, 3, and 4 present the results of data collection from literature reviews, field studies and laboratory testing, respectively. Interpretations about bathymetry, geologic structure, stratigraphy, earthquake conditions, sediment characteristics and geotechnical engineering design considerations are made in Chapter 5. Potential geologic hazards are identified in Chapter 6; conclusions and recommendations are presented in Chapter 7. Appendices to this report contain descriptions of sediment locations and grain-size distributions, results of laboratory testing, descriptions of vibracore samples, and results of liquefaction analyses.

Graphics are presented in two forms: (1) Figures, which are integrated into the text, and (2) Plates, which are all together in a separate section beginning on page 201. These plates also exist in a larger format in the original Volume 2 of this report ("Seafloor Geologic Hazards on the Northern Aleutian Shelf; Volume 2 - Oversized Maps") available from Ertec Western, Inc., 3777 Long Beach Boulevard, Long Beach, CA 90807.

Original data from the field studies have been microfilmed and are located in NOAA's office in Juneau, Alaska. These data include geophysical records, trackline plots, and sediment grain-size distributions.

2.0 REGIONAL SETTING

2.1 LOCATION AND SETTING OF STUDY AREA

The study area encompases approximately 25,000 km in the southeastern section of the Northern Aleutian Shelf in Bristol Bay. It is bounded by the Bering Sea to the north and west and by the glaciated, volcanic terrains of the Alaskan Peninsula and Unimak Island to the south, where elevations range from sea level to over 2850 m (Figures 2-1 and 2-2). The area of study extends eastwards along the northern Alaska Peninsula from Unimak Pass (165° W) to the vicinity of Port Moller (159° 30' W) and north to 57° 00' N latitude.

Generally the seafloor within the study area consists of a very flat and shallow continental shelf which deepens to the southwest. The north shelf is regionally flat having a gradient of approximately 0.02 percent (Sharma, 1974). Water depths in the study area reach 70 m in the northeast and 110 m in the southwest; the average water depth is about 50 m.

A broad gentle trough paralleling the Alaska Peninsula is the most prominent feature of the bottom topography (Plates 3(A) and 3(B)). The area is also characterized by a series of transverse linear ridges which parallels the trend of the Alaska Peninsula. These ridges occur in a 30 to 50 km wide band, and are oriented in various directions, ranging from east-west to west-southwest to east-northeast and exist in maximum water depths which range from 70 to 110 m. The minimum length of the ridges is about 10 km. The area also has three nearly east-west trending structural basins (St. George, Amak and Bristol Bay) (Figure 2-2) which contain sedimentary stratigraphic sections in

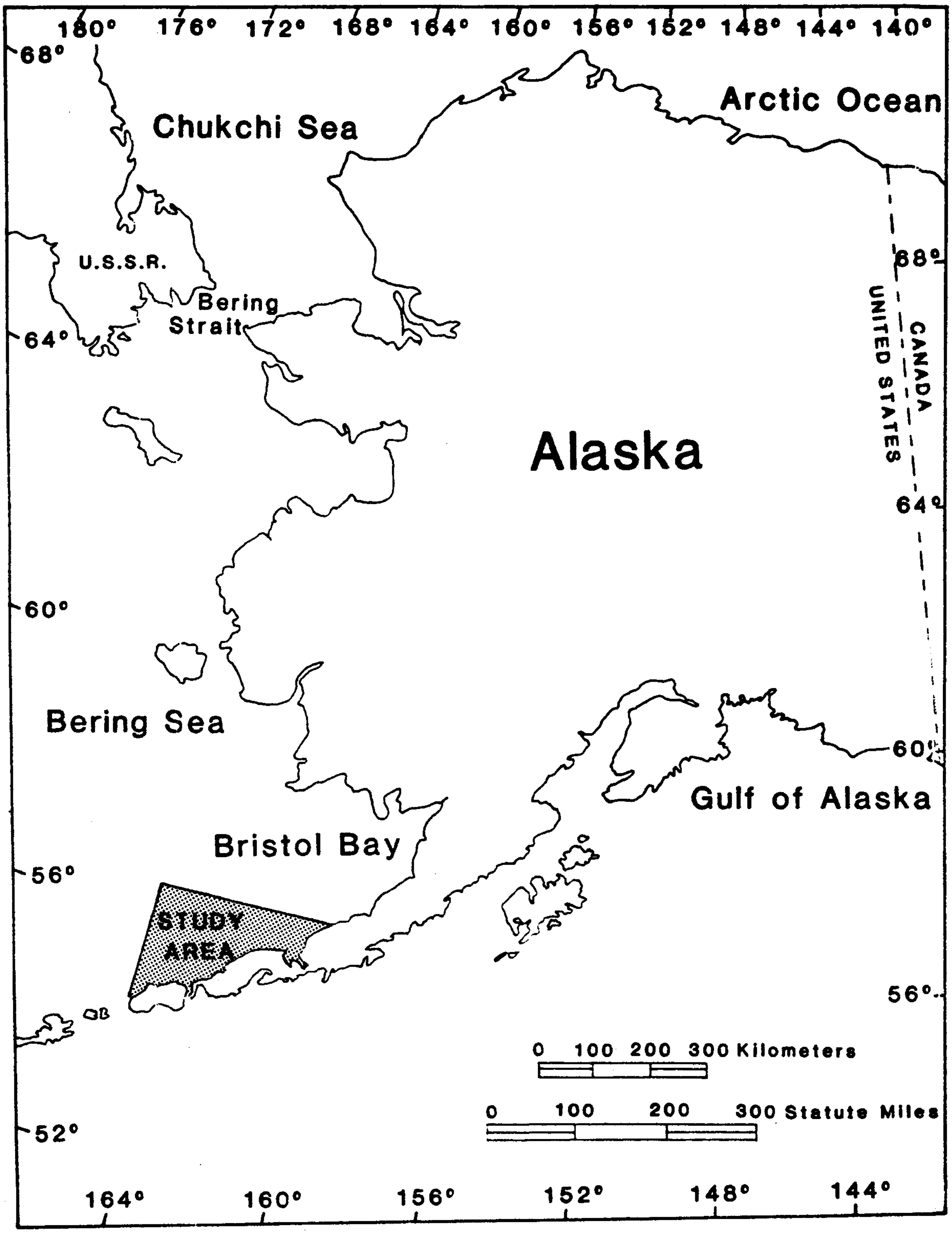

FIGURE 2-1 LOCATION MAP OF THE NORTHERN ALEUTIAN SHELF STUDY AREA

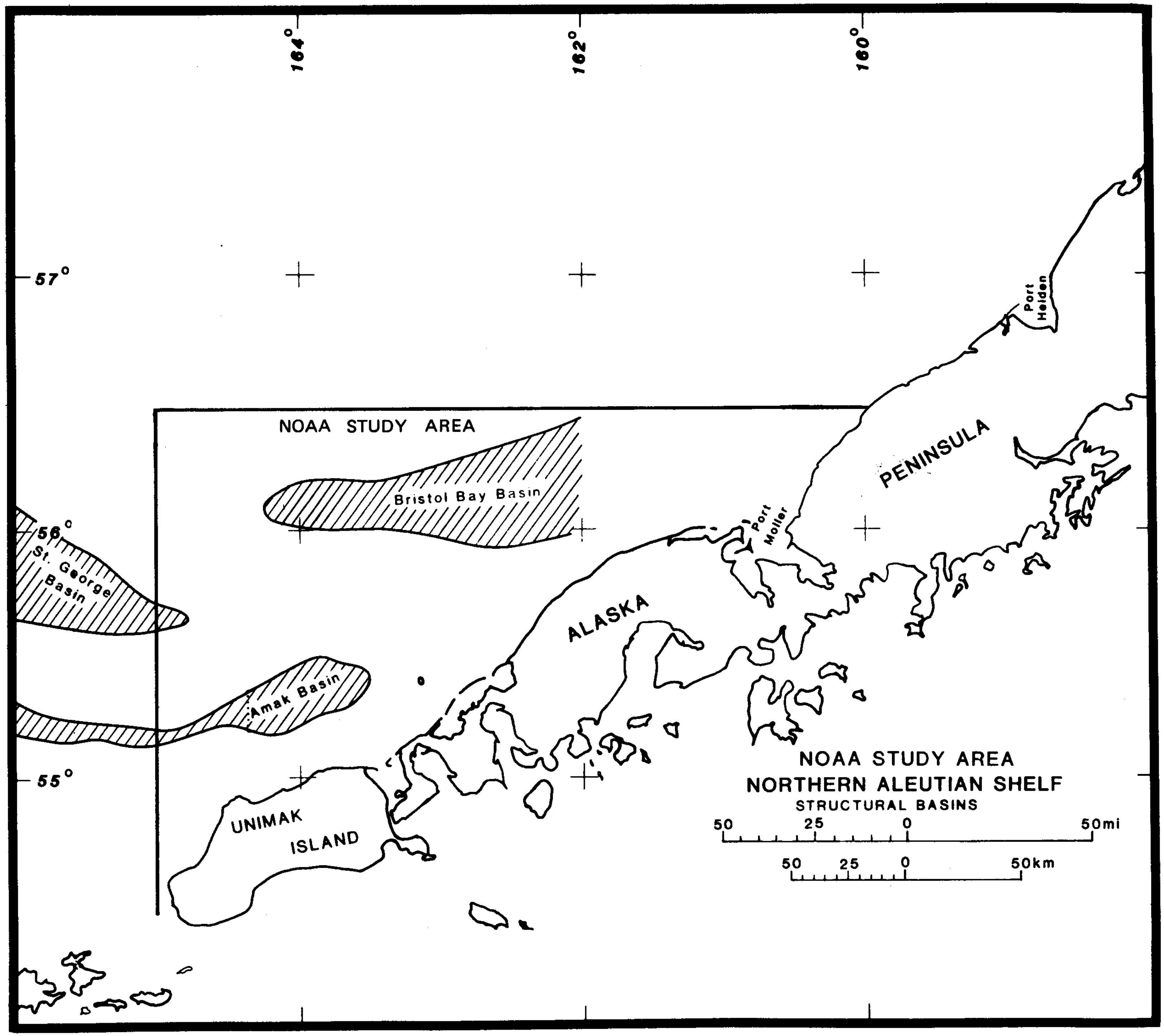

FIGURE 2-2 MAP OF STUDY AREA SHOWING LOCATION OF THE THREE MAJOR SEDIMENTARY BASINS

excess of 4 km thick (Plate VI). These basins are the primary areas of interest with respect to future oil and gas production.

2.2 OCEANOGRAPHY

The study area is within a very dynamic and complex oceanographic area. The large shallow portion of the area is recognized as a high latitude estuary characterized by its variability. Water circulation within the area generally comprises a counter-clockwise gyre with normal current velocities of about 5 cm/sec. Semi-diurnal tides average 2 m on the open shelf and 3.3 m at Port Moller at the eastern edge of the study area (Brower and others, 1977). Climatic conditions, intrusions by oceanic water masses, and fresh water inflow contribute to this variability (Lisitzin, 1966; U.S. Army Corps of Engineers, 1974; Sharma, 1979). Hydrography, general circulation, tides, bottom currents, and long-shore drift parameters of the area are summarized in Figure 2-3. These are discussed separately below.

2.2.1 Hydrography

Many investigators have studied the hydrography within Bristol Bay and the broader Bering Shelf area (Dodimead and others, 1963; Arsen'ev, 1967; Ohtani, 1973; Takenouti and Ohtani, 1974; Kinder, 1977; Schumacher and others, 1979; and Kinder and Schumacher, 1980). Early efforts focused on identifying summer water masses in terms of salinity and temperatures.

The results of these studies generally indicate that four distinct water masses occur on the North Aleutian Shelf: 1) oceanic water, 2) outer shelf water, 3) mid-shelf water, and 4) coastal water. The oceanic water originates from the Pacific Ocean and Bering Sea. This water has a temperature 3 to 5 degrees (°) Centrigrade (C) and a salinity of 33 to 35 parts per thousand (°/oo), respectively. Outer-shelf water is characterized by temperatures of 0.5 to 9.0° C and salinities of 32.7 to 33.0 °/oo. Salinities of 31.0 to 32.6 °/oo and temperatures of 1.8 to 9.0° C are typical of mid-shelf waters. Coastal water has salinities less than 31.0 °/oo and temperatures between 1.3 and 18.2° C.

Kinder and Schumacher (1980) describe a three-domain shelf, for the area. The three domains include coastal, middle and outer shelf regions (Table 2-1, Figure 2-3). The coastal domain is shoreward of the 50 m isobath and is characterized by generally warm, low salinity, vertically well-mixed water lacking stratification. A strong inner front, defined by an enhanced mean salinity gradient, separates the coastal domain from a middle shelf domain. The middle shelf domain is recognized by a strongly stratified two-layered structure extending to approximately the 100 m isobath. A middle front, at about the 100 m isobath, delineates the third or outer shelf domain. The outer shelf domain structure is characterized by a stratified layer with pronounced fine structure, separating surface- and bottom-mixed layers. Beyond the front of the shelf break, ocean water persists. Kinder and Schumacher (1980) suggest that this hydrographic structure is controlled by boundary processes which include tidal and wind stirring, surface cooling, river runoff, and lateral exchange with oceanic water.

2.2.2 General Circulation

The generalized surface circulation pattern for the Northern Aleutian Shelf area is a weak counter clockwise gyre with surface current velocities of

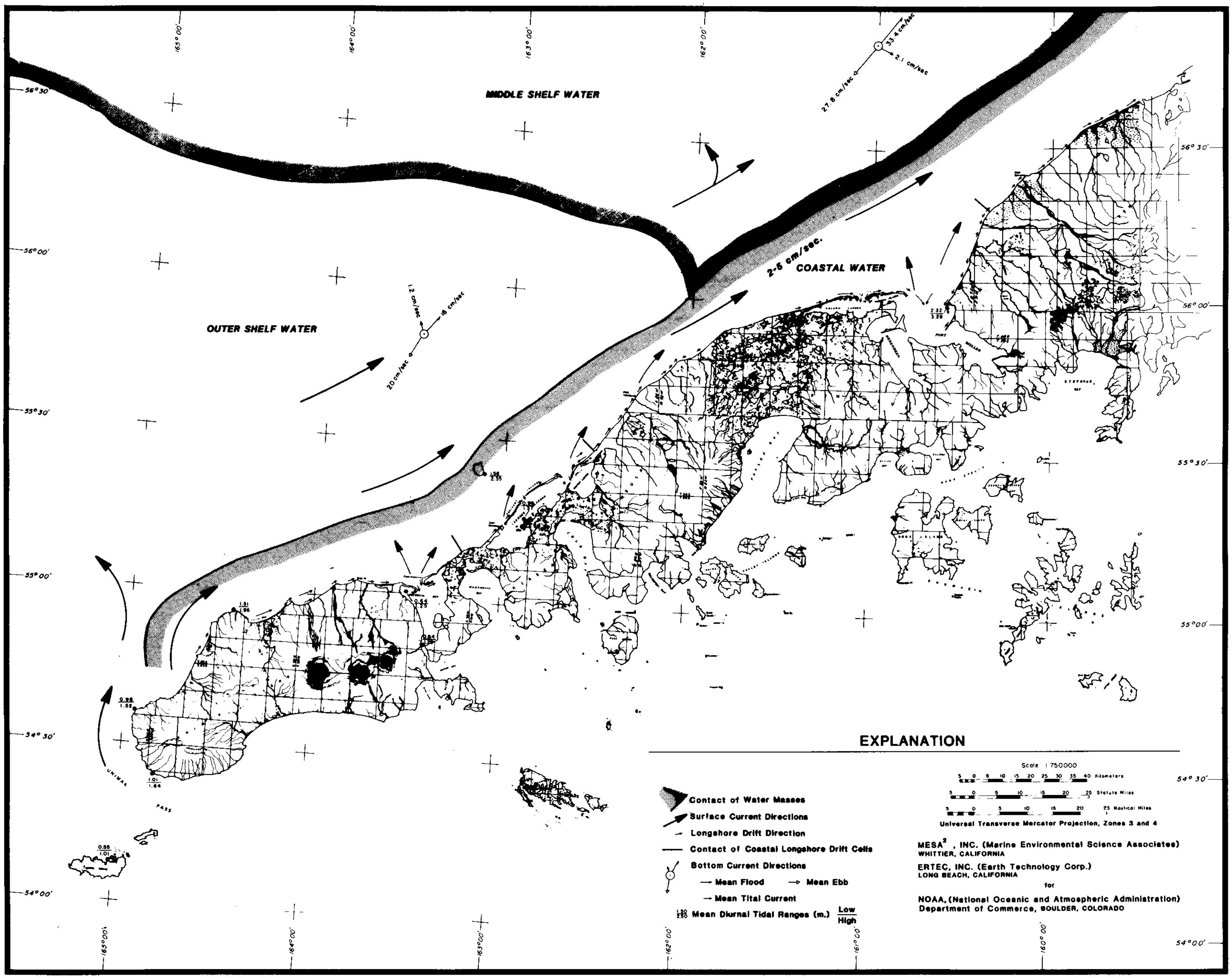

FIGURE 2-3 HYDROLOGY, GENERAL CIRCULATION, TIDES, BOTTOM CURRENTS, AND LONG SHORE DRIFT ON NORTHERN ALEUTIAN SHELF

Table 2-1 Hydrographic Domains - Summer Conditions*

Characteristic	Coastal Shelf	Middle Shelf	Outer Shelf
vertical structure	homogeneous	two layer	surface mixed layer, stratified interior fine-structure, with bottom mixed layer
stratification	very low	very high	moderate
water depth	<50 m	$\leq$50 m - 100 m	$\geq$100 m
temperature	very warm in late summer (8 to 12° C)	very cold bottom temperature throughout summer (-1 to 30° C)	moderate (3 to 6° C)
salinity	generally low (<31.5 ^{o}/oo)	moderate low (31.5 ^{o}/oo)	high (>32^{o}/oo)
influences	river runoff freezing	melting	adjacent water overlying deep basin; Bering Slope Current

*modified from Kinder and Schumacher, 1980

5 cm/sec or less. Figure 2-3 shows a schematic drawing of the surface circulation pattern for Bristol Bay as modified from Kinder and Schumacher (1980). The counterclockwise gyre does not appear to be a geostropic current because neither the extreme meteorological conditions nor the shallow water depths, both characteristic of the area, are conducive to the formation of geostropic circulation. Various investigators have suggested that in the southeastern Bering Sea thermohaline effects, tides, and winds are the forces that drive water mass movement during the portion of the year that the sea is ice free. Generally, the study area is ice free all year.

The mechanics of Bristol Bay circulation are thought to be controlled by southerly and southwesterly winds which tend to drive water eastward toward the head of the bay. The incoming tide from the North Pacific further reinforces this eastward flow which parallels the Alaska Peninsula. At the head of Bristol Bay the eastward flow is mixed with brackish coastal waters that result from high seasonal runoff, and is then deflected northward and westward. Offshore of Cape Newenham the major portion of the water moves northward while a minor quantity flows southerly completing the gyre.

2.2.3 Waves

The Northern Aleutian Shelf area is characterized by severe wave conditions. These waves are generated by local storms. As noted in the preceding subsection, they have a significant impact on water mass stability and general circulation within Bristol Bay.

According to Brower and others (1977), the most critical parameters controlling wave climate for the area include fetch, storm duration, and shallow-depth conditions. During the summer months, winds are predominantly from the south, placing the nearshore portion of Bristol Bay in the lee of the Alaska Peninsula. As a result, most waves are generated locally. During the winter season, winds originate from the northwest in the Bering Sea. Winter storms are significantly more severe than the summer winds from the south. Table 2-2 presents maximum sustained wind velocities and maximum significant and extreme wave heights for the Bristol Bay area.

2.2.4 Tides and Currents

Tides in the study area are dominated by a tidal bulge which enters the Bering Sea through the central and western Aleutian Straits. This bulge progresses as a free wave onto the Bering Shelf. It is dominantly a mixed semi-diurnal tide over the southeastern portion of the shelf. On the open shelf the tidal amplitudes average 2 m. Toward the head of Bristol Bay the largest amplitudes exceed 6 m. The tidal range at Port Moller averages 3.3 m, whereas a 6.9 m range occurs at the Naknek River entrance (Brower and others, 1977).

The natural period of oscillation for the inner bay equals that of the major lunar tide (U.S. Army Corps of Engineers, 1974). This results in a reinforcement of the tidal amplitude toward the head of Bristol Bay. Pearson and others (1981) note that the semi-diurnal tide propagates as a Kelvin Wave along the Alaska Peninsula and appears to be converted to a Sverdrup Wave upon refection in inner Bristol Bay. Tidal oscillations within the bay trend northeast-southwest (Favorite and others, 1961).

Tidal currents in Bristol Bay are nearly reversing along the Alaskan Peninsula and become more cyclonic rotary offshore. Hebard (1961) found tidal currents in the study area having maximum flood velocities exceeding 85 cm/sec

Table 2-2 Maximum Wind and Wave Data

Return period years	Maximum sustained wind (knots) (Thom)*	(Q & F)**	Maximum significant wave (meters) (Thom)	(Q & F)	Extreme wave-(meters) (Thom)	(Q & F)
5	75	75	13.0	10.2	24.0	18.0
10	81	81	15.0	11.2	27.0	20.1
25	90	91	17.5	13.1	31.5	23.8
50	98	98	20.0	14.9	35.5	26.5
100	106	107	22.5	16.8	40.0	29.9

* Thom (1973)

** Quayle and Fulbright (1975)

at Station D (55° 40' N, 163° 30' W) and 41 cm/sec at Station C (56° 40' N, 161° 15' W). Outside the study area maximum flood tidal current velocities were recorded as 51 and 77 cm/sec at two other stations in central Bristol Bay. Hebard (1959) further noted little difference in direction or speed with depth. Mean tidal values in central Bristol Bay were reported at 22 cm/sec (Stations C and D) for the surface and 34 cm/sec (Station C) and 18 cm/sec (Station D) near the bottom. Favorite and others (1961) reported that tidal current velocities exceed 75 to 100 cm/sec inshore and 40 to 50 cm/sec on the open shelf. These measured tidal currents compare well with calculated maximums for open-water conditions (U.S. Army Corps of Engineers, 1974). This tidal current information represents summer values. No studies have measured average current velocity or maximum tidal current velocity during winter or storm conditions. Erosional evidence suggests that significantly higher velocities must exist.

Another source of currents is general water circulation, as discussed in Section 2.2.2. Hebard (1961) reports average surface current velocities from generalized arcolation at Stations C and D as approximately 6 and 3 cm/sec, respectively. Average bottom current velocities are even lower, 2.0 cm/sec at Station C and 1.5 cm/sec at Station D. Hebard's measurements, which were made in June of 1957, involved measuring current velocities at four depths every hour for 38 hours at each of four stations.

2.2.5 Longshore Drift

Longshore drift on the northern coast of the Alaska Peninsula has been divided into a series of longshore drift cells along the coastline (Hunter and others, 1979). Three of these cells occur within the study area. These cells converge at the locations of large bays and diverge a short distance to the northeast of each bay. The long-term effect of wave action in this system of cells is erosion of headlands and deposition in bays, thereby ultimately producing a straightened coastline. In general, the net drift direction along this coast is to the northeast with local reversals near the bays (Figure 2-3).

Waves and wave-driven currents are the primary drift agents, but tidal and other currents may be locally important. The rate of longshore drift increases with increasing wave size. Where wave size is constant, the drift rate is maximum when the waves approach the coastline at an angle of about 45 degrees (Komar, 1976).

2.3 METEOROLOGY

The Northern Aleutian Shelf is in the subarctic climatic zone where the annual weather patterns develop as a result of strong seasonal pressure changes. The U.S. Coast Pilot (U.S. Dept. of Commerce, 1979, p. 297) describes weather in the Bering Sea as follows:

> "The weather over the Bering Sea is generally bad and very changeable. Good weather is the exception, and it does not last long when it does occur. Wind shifts are both frequent and rapid. The summer season has much fog and considerable rain. In early winter, the gales increase, the fogs lessen, and snow is likely any time after mid-September. Winter is the time of almost continuous storminess".

2.3.1 Winds

Southwesterly and southerly winds dominate during the summer; northeasterly winds are common during the winter season. At King Salmon, about 450 km east of the study area, northern winds blow more than 20 percent of the time during the winter. The prevailing wind direction at Port Moller is southerly with average speeds of 9 kts (17 km/hr) but speeds in excess of

55 kts (102 km/hr) have been recorded. At Cold Bay, the mean wind speed is 15 kts (27 km/hr).

Surface currents, vertical water mixing, and water-mass exchange are all influenced by these seasonal wind patterns. The presence of a major storm track in late summer through early winter introduces an additional mechanism influencing general circulation in Bristol Bay.

2.3.2 Precipitation

Precipitation falls primarily as rain during the summer and autumn months (July through October). Measureable precipitation at Port Moller has been recorded 59 percent of the days and trace amounts during an additional 18 percent (Brower and others, 1977). At Port Moller precipitation occurs as much as 77 percent of the month of August. At Cold Bay annual cloud cover is 85 percent, relative humidity is 86 percent, and mean annual precipitation is approximately 84 cm falling on 320 days. On a yearly average, Bristol Bay receives precipitation 44 percent of the time; the average annual accumulation is 50 to 60 cm.

Average snowfall totals 100 to 130 cm/yr from November through April, although it has occurred in all months. Mean annual snowfall at Cold Bay is approximately 140 cm, accumulating on 124 days.

Poor visibility can be a problem all year. Visibility is restricted by land fog and snow in winter and by sea fog and rain in summer. For example, there are an average of 192 foggy days per year at Cold Bay. This weather often interferes with and causes cancellation of aircraft and ship operations.

2.3.3 Temperatures

Mean annual maximum and minimum temperatures at Port Moller are 5.5° C and -2.9° C, respectively, with extremes ranging from approximately +23° C to -23° C (Brower and others, 1977). At Cold Bay, extreme high and low temperatures have been +25° C and -25° C.

2.4 REGIONAL GEOLOGY

The regional geologic setting for the study area is described in the following five subsections (stratigraphy, tectonics, seismicity, volcanism, and magnetics and metallic resources). These summaries, when combined with data collected during the field phase of this evaluation, provide the framework for establishing geologic hazards.

2.4.1 Stratigraphy

Existing stratigraphic studies generally have involved evaluations of shallow rather than deep stratigraphy. No deep core holes exist on the Northern Aleutian Shelf; consequently, all deep stratigraphic interpretations are based on projections of data from wells on the adjacent Alaska Peninsula. Three of these deep interpretations have been presented by the Alaska Geological Society (1975) in their Bristol Bay Region "Stratigraphic Correlation Section" and by McLean (1979). These interpretations were based on borehole data from nine wells drilled on the Alaska Peninsula; four of the wells are located within 15 to 40 km of the study area. Shallow stratigraphy has been investigated in more detail. Generally these investigations involved shallow gravity cores from which sediment composition has been defined. A generalized composite stratigraphic section for the Northern Aleutian Shelf area is shown in Figure 2-4.

2.4.1.1 Deep Stratigraphy

The stratigraphic section for the crust of the Bering and North Aleutian Shelf comprises two major sequences: 1) highly deformed, Mesozoic rocks and 2) slightly deformed Tertiary rocks (Figure 2-4). The lower sequence (Mesozoic rocks) is referred to herein as the basement. These basement rocks were deposited and deformed in conjunction with an ancient phase of plate subduction unrelated to later Tertiary and present tectonic regimes (Cooper and others, 1976; Marlow and others, 1976b), and hence are not discussed in great detail within this report. The following discussion is given to provide only a general framework for the tectonic and geotechnical discussions in subsequent sections of the report.

Basement deposits are overlain unconformably by the Tolstoi Formation (Figure 2-4). The Tolstoi Formation is a Paleocene/Eocene unit with a thickness of 1500+ m. Marine fossils are rare within the formation; however, plant fossils are abundant at the base of the unit. The formation also contains volcanic sandstone units which have poor porosity, presumably due to zeolitic cement (McLean, 1977).

The Tolstoi Formation is overlain by the Meshik and Stepovak Formations which form an Oligocene unit as much as 4550 m in thickness composed of interfingering layers of volcanoclastic and volcanic flow rocks. The Stepovak Formation contains lignite seams in the upper part of the section, and carbonaceous layers occur throughout the section (Marlow and others, 1980). The Meshik Formation contains volcanic breccias and andesitic basalt flows. Both units have marine and non-marine layers.

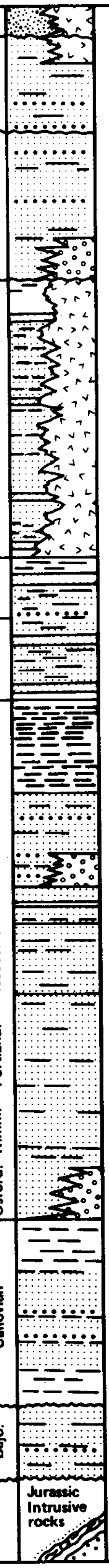

Age			Formation	Description
Cenozoic			Quaternary-Recent Volcanics 300 m ±	Unconsolidated sediments and volcanic rocks
Cenozoic	Tertiary	Pliocene	Milky River Fm (Tpm) 920 m +	Conglomeratic rocks, sandstone and mudstone; clastic fractures. Volcanic derived, fossiliferous, marine and non-marine
Cenozoic	Tertiary	Miocene	Bear Lake Fm (Tmb) 1500 m +	Sandstone and conglomerate with interbedded siltstone, mudstone, and coal, locally fossiliferous, marine and non-marine
Cenozoic	Tertiary	Miocene	Unga Conglomerate Member (Tmbu) Local unconformity	Sandstone, conglomerate, thin mudstone, locally volcanically-derived; locally fossiliferous
Cenozoic	Tertiary	Oligocene	Stapovak Fm (Tos) 4550 m +	Volcanic sandstones and conglomerate and thick beds of black siltstone; all rock types locally carbonaceous with lignite seams in upper part of sequence; locally highly fossiliferous; volcanic flows near base and rare sills throughout; predominantly marine
Cenozoic	Tertiary	Oligocene	Meshik Fm (Tcm)	Volcanic conglomerate sandstone, volcanic breccia, andesite-basaltic extrusive volcanic rocks and local siltstone or shale. Present at surface and in subsurface from Chignik Bay northeast to Ugashik Lakes area; probably interfingers with Stapovak Fm. and upper part of Tolstoi Fm.
Cenozoic	Tertiary	Eocene / Paleocene	Tolstoi Fm (Tct) 1500 m +	Siltstone with interbedded volcanic sandstone and conglomerate; flows, sills, volcanic breccia, non-marine to brackish water environment, rare marine fossils, common plant remains and very abundant in lower part of sequence.
Mesozoic	Late Cretaceous	Senonian	Hoodoo Fm (Kh) 610 m +	Siltstone, silty shale, claystone with fine-grained sandstone. Black to dark gray color. Outer neritic to deep marine environment
Mesozoic	Late Cretaceous	Senonian	Chignik Fm (Kc) 460 m +	Sandstone, siltstone, minor mudstone and conglomerate; shallow marine
Mesozoic	Late Cretaceous	Senonian	Coal Valley Member of Chignik Fm	Conglomerate, sandstone, coal; non-marine
Mesozoic	Early Cretaceous	Neocom.	Herendeen Ls (Khl) 150 m	Calcarenite with abundant Inocar amus prisms
Mesozoic	Early Cretaceous	Neocom.	Staniukovich Fm (Jks) 610 m	Feldspathic sandstone and arkose, thin siltstone, locally abundant Buchia, shallow marine environment
Mesozoic	Late Jurassic	Portland. / Kimm.	Naknek Fm (Jn) 1500 to 3050 m	Claystone and siltstone, predominantly in upper part of unit; lower part consists largely of fledspathic sandstone with some interbedded claystone, siltstone, and conglomerate; locally abundant Buchia and belamnites, shallow marine to naritic environment
Mesozoic	Late Jurassic	Oxford.	Chisik Conglomerate Member (Jnc) 120 m	Pebble to boulder conglomerate consisting of largely granitic debris at base of Naknek Fm; crops out north of Wide Bay
Mesozoic	Middle Jurassic	Callovian		Siltstone and shale with lenses of limestone; marine fossils abundant
Mesozoic	Middle Jurassic	Callovian	Shelikof Fm (Js) 2150 m	Sandstone, siltstone, conglomerate, marine environment
Mesozoic	Middle Jurassic	Callovian		Siltstone, sandy siltstone, sandstone, ash beds and abundant calcitic concretions; marine fossils
Mesozoic	Middle Jurassic	Bajo.	Kialagvik Fm (Jk) 530 m	Sandstone, sandy shale and conglomerate, becomes more sandy near top of unit; marine fossils
Mesozoic			Rare, small outcrops of Early Jurassic, Triassic, and Permian sedimentary rocks	Limestone, chart, volcanic-rich rocks; crop out at Puale Bay northward

FIGURE 2-4 COMPOSITE STRATIGRAPHIC COLUMN FOR THE PROPOSED LEASE SALE AREAS 75 AND 92

The Unga Conglomerate of the Bear Lake Formation overlies the Meshik and Stepovak Formations. This basal conglomerate marks the Oligocene-Miocene boundary. The Bear Lake Formation is approximately 1500 m thick and has its upper and lower contacts bounded by unconformities. Sands, conglomerates and interbedded mudstones with low grade coal (McLean, 1977) characterize the Bear Lake Formation. This formation is considered to be a good hydrocarbon reservoir (Marlow and others, 1976a).

The Milky River Formation overlies the Bear Lake Formation. The base of this formation defines the Miocene-Pliocene boundary. The Milky River Formation is a fossiliferous marine and nonmarine unit of conglomeratic sandstones and mudstones of volcanic origin (Marlow and others, 1980).

2.4.1.2 Shallow Stratigraphy

Approximately 300 m of undifferentiated and partly indurated Quaternary and Holocene sediments and volcanic rocks overlie the Milky River Formation. Quaternary rocks within the study area include the volcanics of Amak Island and the Aleutian Peninsula. Holocene deposits include fluvial sediments of glacial and volcanic origin, much of which are still undergoing active transport, erosion, and deposition.

2.4.1.3 Surficial Sediments

The composition and distribution of surficial sediment from the southeastern Bering Sea have been described by Lisitzin (1966 and 1972), Gershanovich (1968), Askren (1972), Sharma (1974 and 1975) and Sharma and others (1972), with the work by Askren and Sharma being the most relevant to the study area.

Askren suggests that the entire area is covered by at least 3 m of Holocene sediment. According to Askren, all of the study area falls within a "sand province" characterized by a high sand content (greater than 50 percent). He states that the well-sorted character of the "sand province" reflects proximity to mainland and island sediment sources and the influence of strong coastal currents. The presence of sand at depths greater than 50 m in Bristol Bay is believed to be due to the contrast of seasonal wind-wave effects and permanent circulation patterns in Bristol Bay and the shelf to the north.

Sharma (1975) and Sharma and others (1972) describe a much more complicated shelf situation. They suggest that nearshore sediments consist of very poorly sorted gravelly sands which grade to well-sorted, fine-grained sands in the central bay. The far-offshore sediments are very poorly sorted muddy sands. The mean size of the sediments generally decreases with increasing depth and distance from the coast. Two broad depositional environments, an "Inner Continental Shelf" and an "Outer Continental Shelf", are recognized on the basis of silt and clay distribution, the plot of skewness versus kurtosis, and the plot of mean grain size versus sorting coefficient. Sharma sees drainages to the north and east, the Alaska Peninsula to the south, and biogenic processes as being the sources of Bristol Bay sediment.

The Bristol Bay Shelf is described by Sharma (1974, 1975, and 1979) and Sharma and others (1972) as a model contemporary graded shelf. In the sense that mean grain size generally decreases with depth, it is a contemporary graded shelf. However, there is no uniformity in sorting, skewness, or kurtosis across the shelf. If an equilibrium shelf (graded shelf) is considered to be a shelf where sediments are in equilibrium with the prevailing wind, wave, tide, and bottom current conditions; Bristol Bay does not fit this definition in that the only factor that approaches a condition of equilibrium is mean grain size. All other sediment parameters have failed to reach a state of equilibirum.

Concentration of coarse material in scours adjacent to areas of fine sediment, at numerous locations in the study area, also shows a lack of equilibrium conditions (Molnia and others, 1982). It is also uncertain whether the generally graded nature of the shelf may be relict, a carryover from the outwash and fluvial plain conditions that existed prior to the Holocene sea level transgression. Reworking of the relict sediment during post-eustatic sea level rise may account for the tremendous variability in sorting and kurtosis.

Mineralogically, Sharma describes the principal components of the sand fraction as quartz and feldspar in the light fraction; and hypersthene, amphibole, magnetite, and ilmenite, in the heavy fraction. Other heavy minerals present include diopside, garnet, sillimanite, epidote, staurolite, tremolite, sphene, and uralite. Small percentages of illite and chlorite are also present. Sharma uses the composition of the clay fraction to characterize the source area as a region without much chemical weathering. Sharma also observes a decrease in the percentage of heavy minerals with an increase in water depth. Organic carbon content in sediments also increases seaward, coinciding closely with the increase in the clay-size fraction. The maximum organic carbon detected by Sharma was about 0.45 percent. Locations of all historic samples are shown on Figure 2-5 and are tabulated in Appendix I.

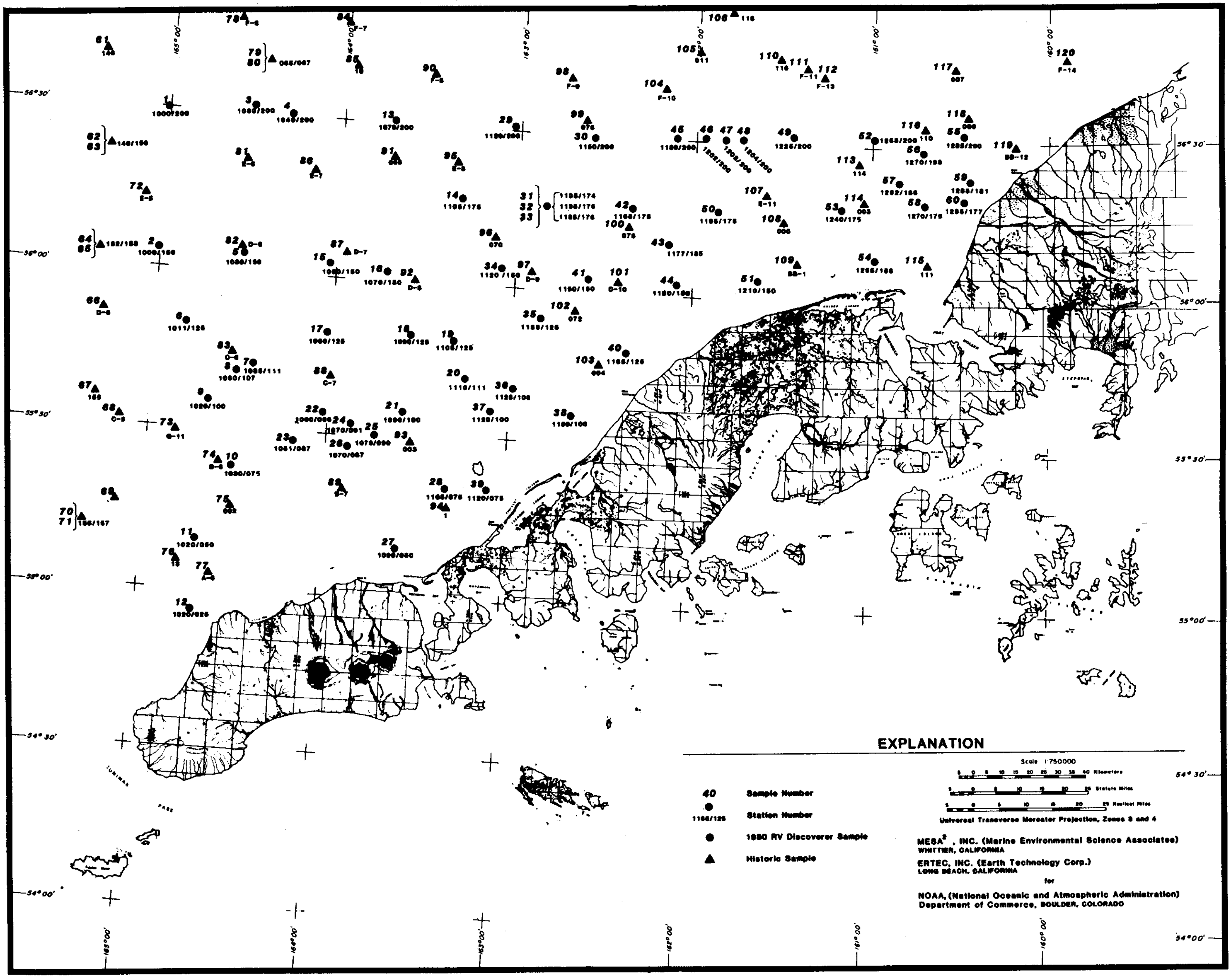

FIGURE 2-5 LOCATION OF SURFACE SEDIMENT SAMPLING STATIONS

2.4.2 Tectonics

The structure and stratigraphy for the Northern Aleutian Shelf indicates that the area has had a complex history of crustal subduction, folding, faulting, uplift, subsidence, and sedimentation. The similarity of Mesozoic rocks on the Alaska Peninsula, the Bering Sea Shelf, and eastern Siberia (Figure 2-6) implies that a continental margin once extended between the Aleutian area and eastern Siberia along the edge of the Bering Shelf (Burk, 1965; Moore, 1972; Cooper and others, 1979; Marlow and Cooper, 1980a).

The basement rocks underlying the area, consisting predominantly of Jurassic and Cretaceous flysch type rocks (Nelson and others, 1974), were deposited during convergence and subduction between the Kula and North American Plates (Grow and Atwater, 1970). The Alaska region, like much of the Pacific margin of North America, may consist of terranes which were tectonically transported (allochthonous) many hundreds of kilometers during Mesozoic and early Tertiary plate tectonic events. These allochtonous terranes may continue beneath the continental shelf to make up much of the Bering Sea basement (McGeary and Ben-Avraham, 1981). By the end of the Mesozoic or early Tertiary, this episode of convergence and consolidation ended and appears to have been followed by regional subsidence and extensional collapse which created a series of submarine ridges and basins. The Bristol Bay, Amak, and St. George basins may have been initiated at that time.

At the end of the Mesozoic or in the early Tertiary, the plate boundary shifted to near the present Aleutian Trench, and the Aleutian arc was formed. Part of the Kula Plate was trapped behind the arc and now forms the abyssal floor of the Bering Sea (Cooper and others, 1976). By mid-Tertiary, the

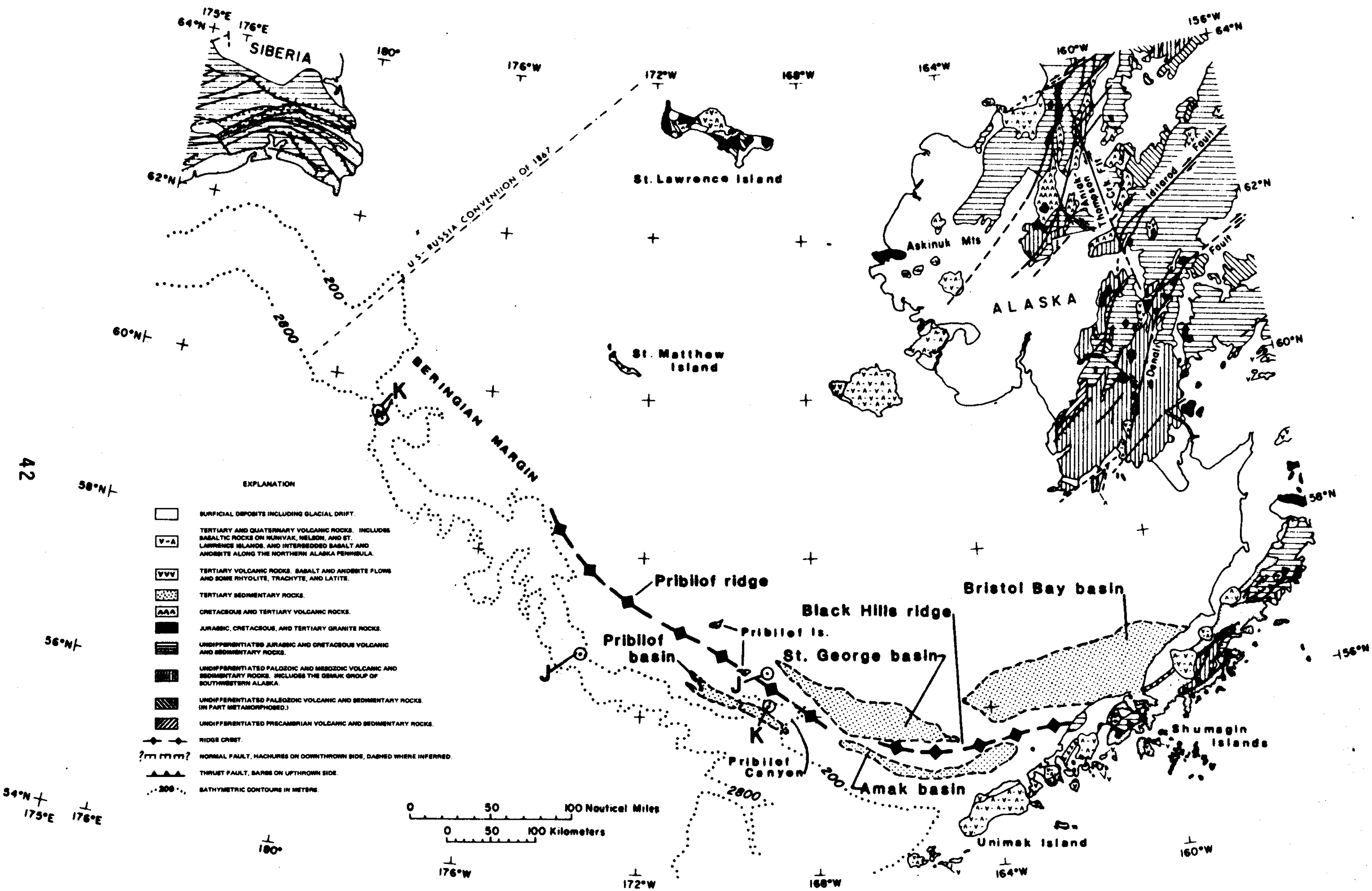

FIGURE 2-6 GENERALIZED GEOLOGY MAP OF WESTERN ALASKA, BERING SEA, AND EASTERN SIBERIA (FROM MARLOW AND COOPER, 1980a)

EXPLANATION

SURFICIAL DEPOSITS INCLUDING GLACIAL DRIFT.

TERTIARY AND QUATERNARY VOLCANIC ROCKS. INCLUDES BASALTIC ROCKS ON NUNIVAK, NELSON, AND ST. LAWRENCE ISLANDS, AND INTERBEDDED BASALT AND ANDESITE ALONG THE NORTHERN ALASKA PENINSULA.

TERTIARY VOLCANIC ROCKS. BASALT AND ANDESITE FLOWS AND SOME RHYOLITE, TRACHYTE, AND LATITE.

TERTIARY SEDIMENTARY ROCKS.

CRETACEOUS AND TERTIARY VOLCANIC ROCKS.

JURASSIC, CRETACEOUS, AND TERTIARY GRANITE ROCKS.

UNDIFFERENTIATED JURASSIC AND CRETACEOUS VOLCANIC AND SEDIMENTARY ROCKS.

UNDIFFERENTIATED PALOZOIC AND MESOZOIC VOLCANIC AND SEDIMENTARY ROCKS. INCLUDES THE GEMUK GROUP OF SOUTHWESTERN ALASKA.

UNDIFFERENTIATED PALEOZOIC VOLCANIC AND SEDIMENTARY ROCKS. (IN PART METAMORPHOSED.)

UNDIFFERENTIATED PRECAMBRIAN VOLCANIC AND SEDIMENTARY ROCKS.

RIDGE CREST.

NORMAL FAULT, HACHURES ON DOWNTHROWN SIDE, DASHED WHERE INFERRED.

THRUST FAULT, BARBS ON UPTHROWN SIDE.

200 BATHYMETRIC CONTOURS IN METERS.

NOTE: DOTTED CIRCLES INDICATE SITES WHERE JURASSIC (J) AND CRETACEOUS (K) SEDIMENTARY ROCKS WERE DREDGED FROM CONTINENTAL SLOPE.

FIGURE 2-6 CONTINUED

continental shelf was submerged for the first time and the basins continued to subside due to sediment loading and crustal tension. The Aleutian arc continued to be plutonically and volcanically active.

During the Pliocene, the arc underwent severe structural deformation which led to development of most of the structures seen today (Burk, 1965). This orogeny seems to correlate with the subduction of a spreading center between the Kula and Farallon lithospheric plates (Grow and Atwater, 1970).

In addition to the tectonic activity, the Pleistocene was time of intermittent glaciation throughout most of the Alaska Peninsula with at least four major glaciations. Sea level rose and fell depending on the amount of water contained as ice in glaciers. The maximum lowering of sea level amounted to about 130 m (Curray, 1965), and this resulted in exposure of most of the Bering Shelf including all of Bristol Bay Basin area.

The present day tectonics of the Bristol Bay area are strongly influenced by subduction of the Pacific Plate under the North American/Bering Plate along the Aleutian Trench. The Alaska-Aleutian Trench has a gently arcuate configuration that extends from the Kamchatka Peninsula on the west to the Gulf of Alaska on the east (Figure 2-7). The subduction zone is bounded by the Kuril-Kamchatka subduction zone on the west and the Queen Charlotte Islands-Fairweather transform fault system on the east. The present rate of subduction of the Pacific Plate along the Aleutian subduction zone varies from about 5.5 cm/yr to 7.6 cm/yr (Figure 2-7).

Under the present tectonic regime, the Aleutian subduction zone changes from 1) a poorly developed sediment-filled trench adjacent to the mainland, to 2) a well-developed trench adjacent to the Alaska Peninsula involving

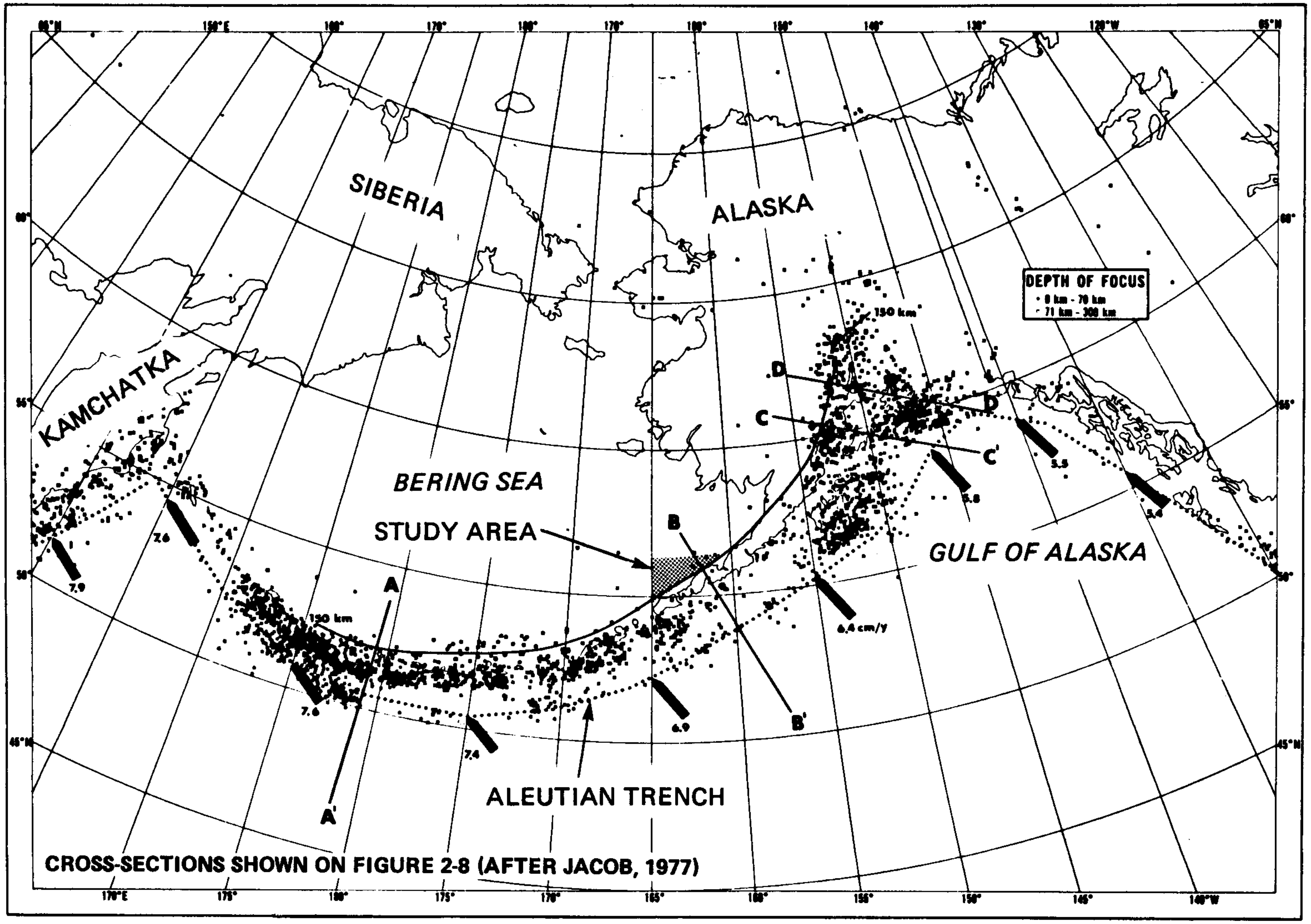

CROSS-SECTIONS SHOWN ON FIGURE 2-8 (AFTER JACOB, 1977)

FIGURE 2-7 REGIONAL SEISMICITY AND RELATIVE MOTION VECTORS ALONG THE ALASKA-ALEUTIAN ARC

subduction of oceanic crust under continental crust, to 3) the well-developed trench west of Unimak Island which involves thrusting of oceanic crust under oceanic crust. These changes indicate that the Aleutian subduction zone comprises several segments each with its own unique combination of tectonic characteristics.

Von Huene and Shor (1969) noted distinct differences in morphology and geology along the Aleutian subduction zone and divided the zone into four distinct segments: 1) the Mainland, 2) East Aleutian, 3) Central Aleutian, and 4) West Aleutian. The Bristol Bay region lies adjacent to the East Segment which occupies the region between the St. Elias and Shumagin Transitions. Along the Aleutian arc other segments can be distinguished based on seismicity characteristics (Spence, 1977) which appear to change across transition zones and tend to support the idea of discrete trench segments.

2.4.3 Seismicity

Earthquake epicenters in the Aleutian area form a prominent curvilinear belt primarily between the Aleutian Trench and the volcanic arc (Figure 2-7). These earthquakes are shallow near the trench and gradually increase in depth northward forming a Benioff Zone that defines the upper portion of the underthrust Pacific lithospheric plate. The angle and the maximum depth of the Benioff Zone changes laterally along the trend of the Arc (Figure 2-8). Near Amchitka, the Benioff Zone is steep and extends to about 250 km deep. In the study area the maximum depth of the Benioff Zone is about 150 to 200 km with about a 40 degree dip. Eastward the earthquakes are generally no deeper than 100 km and the angle of dip ranges from nearly horizontal near the trench to about 20 degrees under the mainland.

LOCATION OF CROSS-SECTIONS SHOWN ON FIGURE 2-7 (FROM JACOB, 1977)

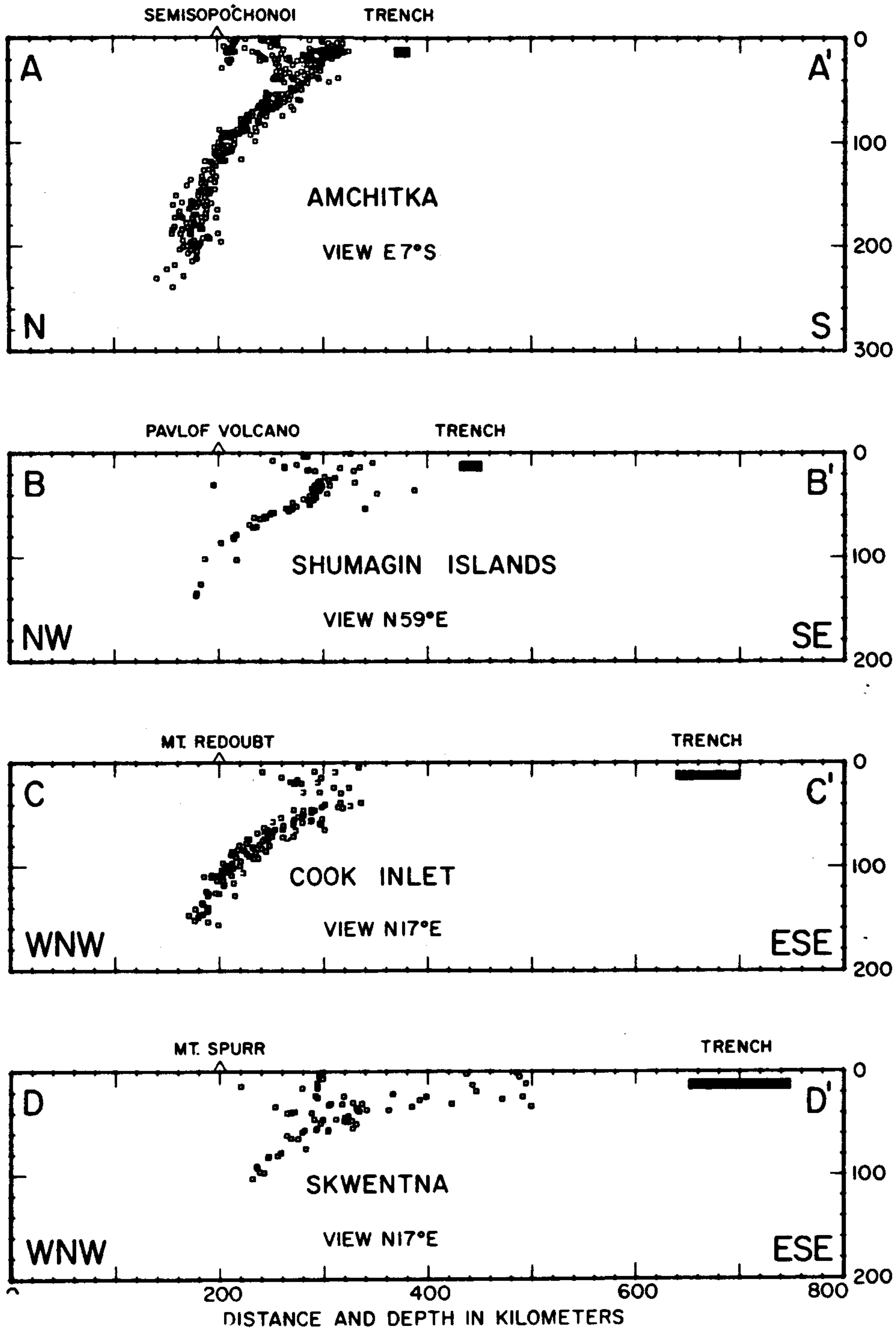

FIGURE 2-8 CROSS-SECTIONS SHOWING BENIOFF ZONE OF THE ALASKA-ALEUTIAN SUBDUCTION ZONE

Not all the earthquakes are directly associated with the subduction zone. Earthquakes also occur in the shallow crust behind and on the arc. These earthquakes are particularly common on the Alaska mainland near the eastern end of the Aleutian subduction zone. Seismicity is poorly documented in the region of the Bering Sea north of the Aleutian Arc but large earthquakes (M_s > 7.0) have occurred in the vicinity of the St. George Basin and the Pribiloff Islands (Davies, 1981) (see Section 5.4 for more-detailed discussion).

2.4.4 Volcanism

Much of the Alaska Peninsula is covered by active volcanoes and volcanic rocks. At least 60 of these volcanic centers have erupted during the past 10,000 years. Commonly, the andesitic volcanoes are characterized by violent and explosive eruptions with widespread volcanic ash fall and with moderately large earthquakes.

At least ten potentially active volcanoes line the southern edge of Bristol Bay basin (Figure 2-9; Table 2-3). The major volcanoes adjacent to the study region are Shishaldin, Pavlof, and Veniaminoff (Plates V(A) and V(B)). None of these have actually erupted in a major destructive eruption in recent times, although Pavlof frequently has given off steam. Table 2-3 gives the dates of the last eruption.

An example of the potential destruction from a volcanic eruption may be that of Mount Katmai, a volcano located on the Alaska Peninsula east of the study region. Mount Katmai erupted in 1912 spreading about 16 cubic km of volcanic debris into the atmosphere. The ash was carried to all parts of the northern hemisphere; near the volcano the ash deposit reached a thickness of more than 15 m and at Kodiak, 160 km to the southeast, it reached a thickness

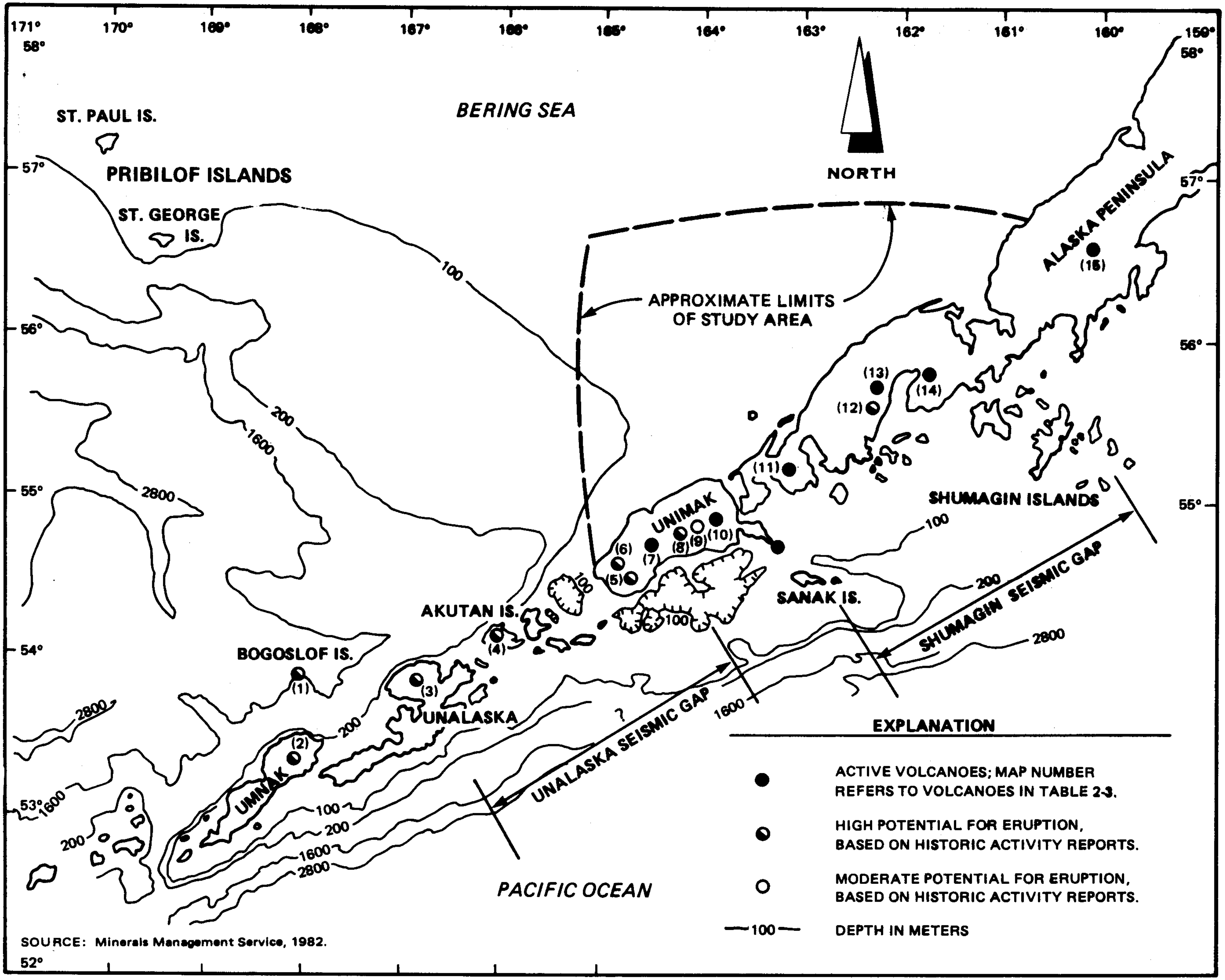

FIGURE 2-9 ACTIVE VOLCANOES IN THE NORTHERN ALEUTIAN SHELF REGION

of about 3 m (Wilcox, 1959). Pumice clogged the nearby Cook Inlet and the skies were darkened several thousand kilometers downwind from the eruption. Hundreds of square kilometers of forestland were converted into an ashy desert and this is still evident today.

Volcanism has also been a dominant process in the past. Volcanic and volcaniclastic rocks dominate the Tertiary record, though all units in this area are limited in areal extent and generally cannot be correlated. Detailed investigations of two Tertiary strato-volcanoes on the Alaskan Peninsula were conducted by Kennedy and Waldron (1955). The volcanoes, Pavlof which is 45 km northeast of Cold Bay and Frosty Peak which is 15 km southwest of Cold Bay, have a long history of eruptions. This history is characterized by long periods of activity separated by brief periods of relative quiescence. The quiet periods are characterized by erosion, sedimentation and glacier buildup. The earliest events, discernible from the geologic record, occurred during the mid-Tertiary when a long period of intense volcanism took place. During this time, Belofski Tuff accumulated to a thickness of more than 1000 m (Waldron, 1961). McLean and others (1978), using fossil evidence, have identified this event as Oligocene in age. Following the accumulation of the Belofski Tuff, numerous other volcanic eruptions continued into the Quaternary (Table 2-3). Late Pleistocene volcanism built the composite summit cone of Frosty Peak. Following the late Pleistocene events, volcanic activity ceased and Frosty Peak and its flows were actively eroded and modified by wind, waves, ice and precipitation.

The chemical composition of these extrusives has not been reported in detail. Waldron (1961) noted that the extrusive volcanic rocks contain less olivine as they become younger. Wilson (1981) summarized the radiometric

Table 2-3 Active Volcanoes in the Vicinity of the Northern Aleutian Shelf

Map No.(#)		Name	Latitude (N)	Longitude (W)	Type of Eruption	Date of Last Eruption
1	*	Bogoslof	53° 56'	168° 02'	Normal Explosion	1931
2	*	Okmok	53° 25'	168° 03'	Normal Explosion, Lava	1945
3	*	Makushin	53° 52'	168° 56'	Normal Explosion	1938
4	*	Akutan	54° 08'	165° 59'	Normal Explosion, Lava	1973
5	*	Westdahl	54° 31'	164° 39'	Normal Explosion, Lava	1967
6	*	Pogromni	54° 34'	164° 41'	Normal Explosion, Lava	1830
7		Fisher	54° 35'	164° 26'	Ash	1826
8	*	Shishaldin	54° 45'	163° 58'	Lava	1965-76
9	†	Isanotski Peaks	54° 47'	163° 13'	Normal Explosion, Ash	1845
10		Roundtop Mt.	54° 48'	163° 35'	---	----
11		Frosty Peak	55° 04'	162° 49'	---	----
12	*	Pavlof	55° 25'	161° 53'	Normal Explosion, Lava	1975-76
13		Pavlof Sister	55° 27'	161° 51'	Ash	1786
14		Dana	55° 38'	161° 13'	---	----
15		Veniaminof	55° 12'	159° 24'	Normal Explosion, Ash	1944

Sources: Minerals Management Service, 1982

* high potential for eruption (based on historic activity reports)
† moderate potential for eruption (based on historic activity reports)
\# Figure 2-9

dating of rocks in the Aleutian Islands and Alaska Peninsula; however, there has been no age dating within the study area outside of a 6.2 million year (m.y.) date of a porphyry copper deposit south of the Herendeen Bay area, 20 km west of Port Moller (Armstrong and others, 1976).

2.4.5 Magnetics and Metallic Mineral Resources

Baily and others (1976) compiled a residual magnetic data map of the Bering Sea which included data collected on 18 separate surveys between 1964 and 1973. Part of this 1976 summary overlaps the Northern Aleutian Shelf study area. Numerous east-west trending magnetic anomalies occur on the map; however, none of the anomalies clearly correlate with basinal configuration or other structure as mapped from the data evaluated in this survey.

Known metallic mineral resources of the Cold Bay Quadrangle, determined by Cobb (1972) from a survey of historic data, are limited to a single placer occurrence of iron oxide. This site, originally mapped by Berryhill (1963), is 7.5 km northeast of Moffet Point. Similar deposits of common metallic opaques can be expected to occur throughout the study area due to the proximity of the source rock (The Aleutian Volcanic Arc) and a depositional environment conducive to concentrations of coarse and heavy particles.

3.0 FIELD PROGRAM

3.1 OPERATIONS

A field program was conducted from aboard the NOAA ship _Discoverer_. The purpose of the program was to supplement existing geophysical (seismic reflection profiles) and geotechnical data on the Northern Aleutian Shelf. The program was accomplished in two phases. These phases were referred to as RP-4-DI-80A, Legs VI and VII. Only 70 percent of sea time during Leg VI and 53 percent of Leg VII were available for field work. The remaining time was spent in transit, transferring equipment, and performing miscellaneous tasks.

During the 24 field days in the study area, 4180 km of seismic profiles were collected on a N-S by E-W grid. Bottom samples and in situ geotechnical data were gathered at 60 stations.

3.1.1. Vessel and Scientific Crew

The NOAA ship _Discoverer_ was used during both legs of the cruise. The _Discoverer_ is a 92-m long oceanographic research vessel, with a 16-m beam and a fully loaded draft of 5.5 m. The _Discoverer_ is equipped with an oceanographic laboratory, deck winches and A-frames, and high-resolution navigational systems to facilitate geophysical and geotechnical research programs. A photograph of the _Discoverer_ is shown in Figure 3-1.

Field operations were carried out in August, September and October of 1980. All field equipment and scientific personnel were mobilized to Kodiak, Alaska before August 25, 1980. Travel to the study area from Kodiak required approximately 72 hours. Of the 20 days assigned to Leg VI, 14 days of field work were accomplished. The remaining six days involved transit time, a

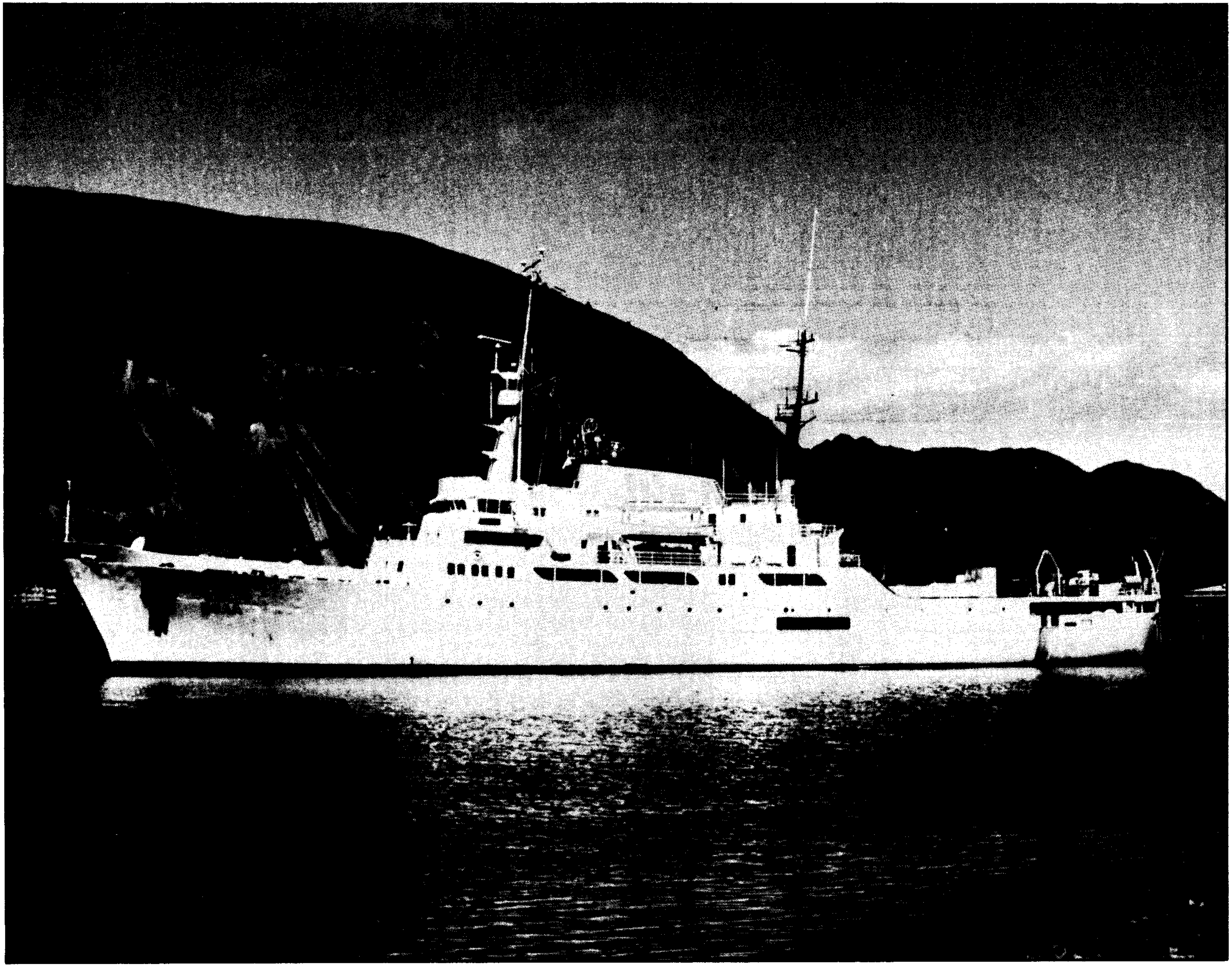

FIGURE 3-1 PHOTOGRAPH OF NOAA SHIP DISCOVERER

medical evacuation to Port Moller, and downtime while untangling the ship from crab-pot lines. Leg VII was assigned 18 days of which 9 1/2 days of field work were accomplished. The remaining time was used in transit, support for another scientific study, and assorted tasks. Demobilization was carried out from Kodiak beginning on October 18, 1982.

The scientific party for Leg VI of the cruise comprised seven personnel. Dr. Peter J. Fischer, Professor of Geological Sciences at California State University at Northridge and Consultant to Ertec, served as Chief Scientist. Mr. Charles F. Chamberlain, Project Geologist at Ertec, was Co-Chief Scientist. During Leg VII, the scientific party was increased to eight with Dr. Dwight Sangrey, Professor of Civil Engineering at Carnegie Mellon University serving as Co-Chief Scientist. Captain Charles H. Nixon was the commanding officer of the Discoverer.

3.1.2 Navigation

Shipboard navigation was provided by LORAN-C and SATNAV with positions recorded every 5 minutes. These data were key-punched and programmed for a "best-fit" navigation solution. The LORAN-C fixes on N-S lines consistently plotted several tenths of a nautical mile to the west of the SATNAV (SM-1 and SM-7) fixes. No suitable explanation for this difference was provided by the Operations Officer on the Discoverer. For simplicity and consistency, the final positions for all tracklines used in this study were based on adjusting the LORAN-C fixes to SM-1 and SM-7 SATNAV positions.

3.2 GEOPHYSICAL SURVEY

The study was designed so that all seismic-reflection trackline data were collected along a preselected grid pattern (Figure 3-2). During the two legs

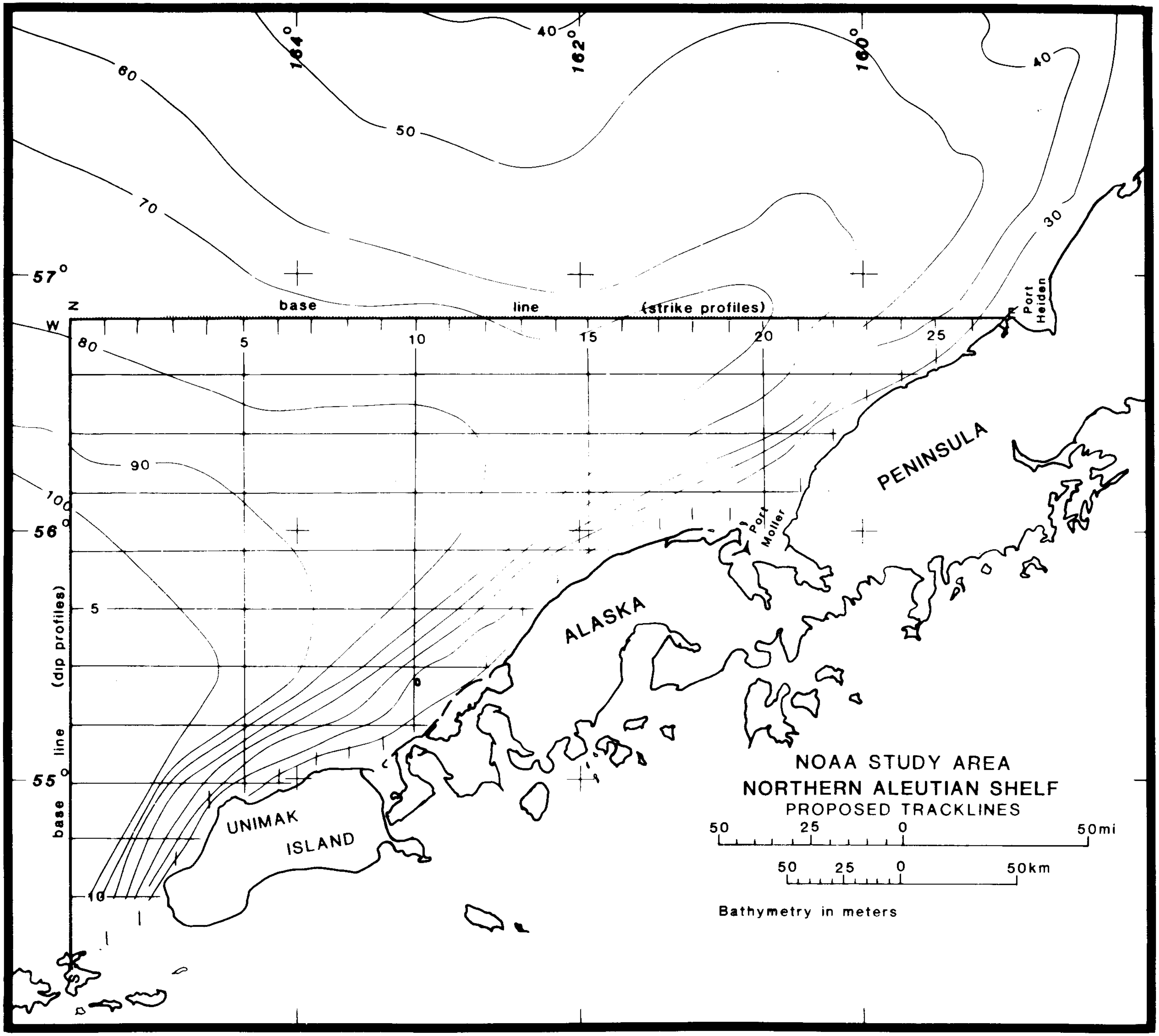

FIGURE 3-2 GEOPHYSICAL TRACKLINE–BASELINE REFERENCE SYSTEM

of the _Discoverer_ cruise, 4180 km of seismic profiles were collected on a N-S by E-W grid (Plates I(A), I(B), II(A) and II(B)).

3.2.1 Trackline Data

All dip lines (N-S orientation) shown in Figure 3-2 and two major strike (E-W orientation) lines were collected. In addition numerous strike-line segments were also collected (Plates I(A) and I(B)). The strike line grid was not completed due to lack of available work time during the cruise.

The dip lines were orientated slightly west of north-south to reflect the trend of the major offshore structural features (Gardner and others, 1979; Marlow and others, 1979; Marlow and Cooper, 1980a and 1980b). The spacing between dip lines was approximately 15 km. The strike lines were oriented at right angles to the dip lines with about a 25 km spacing.

All tracklines were collected and numbered in relation to the "base line" reference system shown in Figure 3-2. This system facilitated easy identification of the line number and located every line by its approximate distance from a "base line." All short lines collected near the core stations during Legs VI and VII were assigned grid numbers and "standard" shot point numbers. This greatly simplified data access and permitted a simplified computer coding of the tracklines.

3.2.2 Geophysical Equipment

All lines shown in Figure 3-2 were profiled using dual airguns (495 cm^3 and 660 cm^3 or 165 and 330 cm^3) and 3.5 kHz sub-bottom profiling systems. Side-scan sonar data were collected only during daylight hours to avoid entantlement of the towed instrument with crab pots in the survey area.

A mini-sparker was used on two dip-line segments. Table 3-1 provides a description of these equipment. Vessel speed during geophysical profiling was 4 to 5 knots.

Two of the primary geophysical systems experienced significant operational problems during the cruise. The intermediate resolution mini-sparker profiling system became inoperative after the explosion of one of its transformers, early in Leg VI, and remained in-operable during the rest of the cruise. The side-scan tow fish collided with a crab pot early in Leg VI. In view of the downtime required to untangle the fish and crab pots and given the prevalance of crab pots in the survey area, a decision was made to operate the side-scan system only during daylight hours.

3.3 SEDIMENT SAMPLING

Sediment information was collected at 60 stations using grab samplers, gravity corers, vibracorers, and a drop penetrometer. Table 3-2 summarizes the numbers of samples by each method; Figure 2-5 identifies the locations of the 60 stations; and Appendix I tabulates the position of each station.

3.3.1 Grab and Gravity Core Samples

Grab samples were collected using a Van Veen sampler. If the lithology was at least slightly cohesive, a gravity core with a 365 kg weight stand and a 1- to 2-m long barrel was deployed. Van Veen samples were recovered at 55 of the 60 stations. Seven gravity cores were recovered from a total of 22 attempts during both legs of the cruise. The average length of gravity cores was 38 cm. Large volume (25 kg) surficial samples were collected at 10 stations during Leg VII of the cruise by taking multiple Van Veen samples.

Table 3-1 Seismic Profiling Systems

Description

EDO-WESTERN (Model 515) - high resolution profiling system (3.5 kHz) low to moderate (with proper booster) penetration (50 m), very high resolution system employing a mounted hull transducer, data are printed on 19 inch graphic recorder. Supplied by Mesa^2.

BOOMER - EPC 200 Joule Boomer - a moderate penetration (up to 75 m), high resolution (30 cm) system employing a towed electromechanical sound source and a towed hydrophone array. Subbottom data are printed on a 19 inch graphic recorder. Supplied by Mesa^2.

BOLT AIR GUN - a high energy, low frequency system utilized for deep penetration seismic profiling. The 40 cubic inch unit is capable of a resolution of ± 3 m; penetration can be varied by changing capacity (1 to 40 cubic inches). Data output presented on 19 inch graphic recorder. Supplied by USGS and Mesa^2.

EDO-WESTERN Side Scan Sonar System - employed a dual channel graphic recorder and transducer towfish to obtain quasi-three-dimensional imagery of sea floor features. The system is complete with 150 m tow cables and power supply. Supplied by Mesa^2.

GEOTECHNICAL SPARKER - 28kJ maximum power, variable frequency system for intermediate-penetration profiling and resolution ($\pm$ 3 m). Data output can be presented in analog form on a graphic recorder and/or on a magnetic tape. Supplied by Mesa^2.

RECORDERS - 2 supplied by NOAA, 1 by Mesa^2.

HYDROPHONES - 2 supplied by USGS, 2 by Mesa^2.

SEDIMENT SAMPLING EQUIPMENT

Gravity Core - Supplied by NOAA.
Vibracore - Supplied by Mesa^2.
Shipek Grab - Supplied by NOAA.
Van Veen Grab - Supplied by NOAA.
Phleger Core - Supplied by NOAA.
Drop Penetrometer - Supplied by Ertec.

Table 3-2 Numbers of Samples Obtained During Sediment Sampling Program

	Number of Samples		
	Leg VI	Leg VII	Total
Stations	40	20	60
Grab Sampling			
Van Veen	39	16	55
Gravity Core	1	7	8
Vibracoring	(not on board)	8	8
Drop Penetrometer Testing	46	43	89

3.3.2 Vibracores

A small vibracore was employed on Leg VII in an attempt to penetrate dense surficial sands encountered during the Leg VI gravity coring operations. The vibracore (built by Mr. Gordon Womack of Sub-Ocean Systems, Inc., Tustin, California) was used when wind and sea state permitted. The Womack corer is hydraulically driven and has a barrel 6 m in length and 7 cm in diameter. The core barrel is supported in a frame for stability. The total weight of the assembly is approximately 2000 kg.

The vibracore was utilized at nine different stations within the study area. These stations were located in areas with potential geologic hazards. Only eight cores were recovered during 17 attempts. The average recovery length was 93 cm with lengths ranging from 15 cm to 216 cm. A summary of vibracoring attempts is presented in Table 3-3; locations of the vibracores are shown in Figure 3-3.

The maximum depth of penetration of the vibracore was considerably less than anticipated. Typically a very dense fine sand was found at the tips of the successful vibracores. Further penetration apparently ceased when this material or layer was reached. Whether the denseness was introduced by the action of the vibracore or actually represents the in situ condition is not known with certainty. However, the areal distribution of the "more successful" vibracore attempts (recovery better than 1 m) coincided with the location of the "more successful" gravity cores, thus suggesting that the hard sediment is an in situ condition.

Table 3-3 Vibracore Summary

Station	Attempts	Recovery	Length Meter
1777/185	1	0	0
1204/200	1	0	0
1202/200	2	1	0.40
1285/181	3	0	0
1070/91	3	1	0.15
			0
			0
1070/87	2	2	0.65
			0.70
1051/87	1	0	0
1020/100	2	2	0.20
			1.05
1000/200	2	2	1.40
			1.95
Totals:			
9 Stations	17	8	6.50 m Total Length Recovered

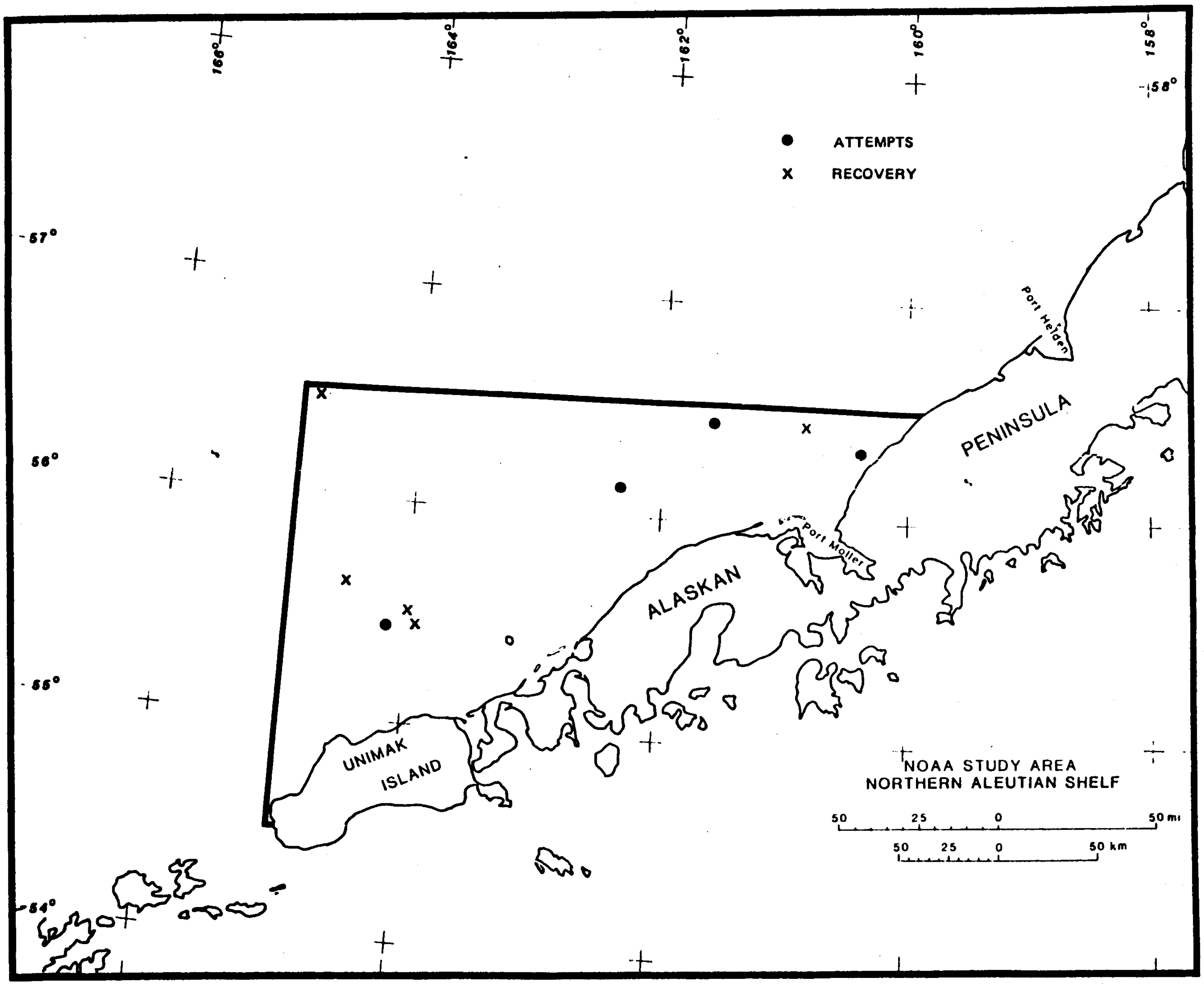

FIGURE 3-3 VIBRACORE LOCATION MAP

3.3.3 Drop Penetrometer

Density and strength information was also obtained by the use of a drop penetrometer developed by Professor R. F. Scott of the California Institute of Technology (Scott, 1967). Figure 3-4 shows a photograph of the drop penetrometer. The penetrometer consists of a 3-m long, 2.5-cm diameter rod with a 10 cm diameter conical tip (60° level) on the end. A 100 kg weightstand containing a mechanical accelerometer is attached to the other end of the rod.

The penetrometer is operated by lowering the system on a winch line to within 10 to 15 m of the seabottom. At this height the penetrometer is allowed to "free-fall" to the seafloor. This sequence is illustrated in Figure 3-5. As the penetrometer falls toward the seafloor and penetrates the bottom, the mechanical accelerometer within the weightstand records the change in acceleration. The acceleration data are subsequently processed to obtain a force-deformation relationship for the soil during the penetration process. This information is then interpreted using conventional geotechnical engineering procedures to estimate density and frictional angles of the sediment.

The drop penetrometer was used 46 times during Leg VI and 43 times during Leg VII. Figure 3-6 shows the drop penetrometer test locations. The results of subsequent interpretations suggested that the maximum cone penetration was less than 1 m, which confirmed observations made during sampling operations regarding the denseness of the sediments.

FIGURE 3-4 PHOTOGRAPH OF DROP PENETROMETER

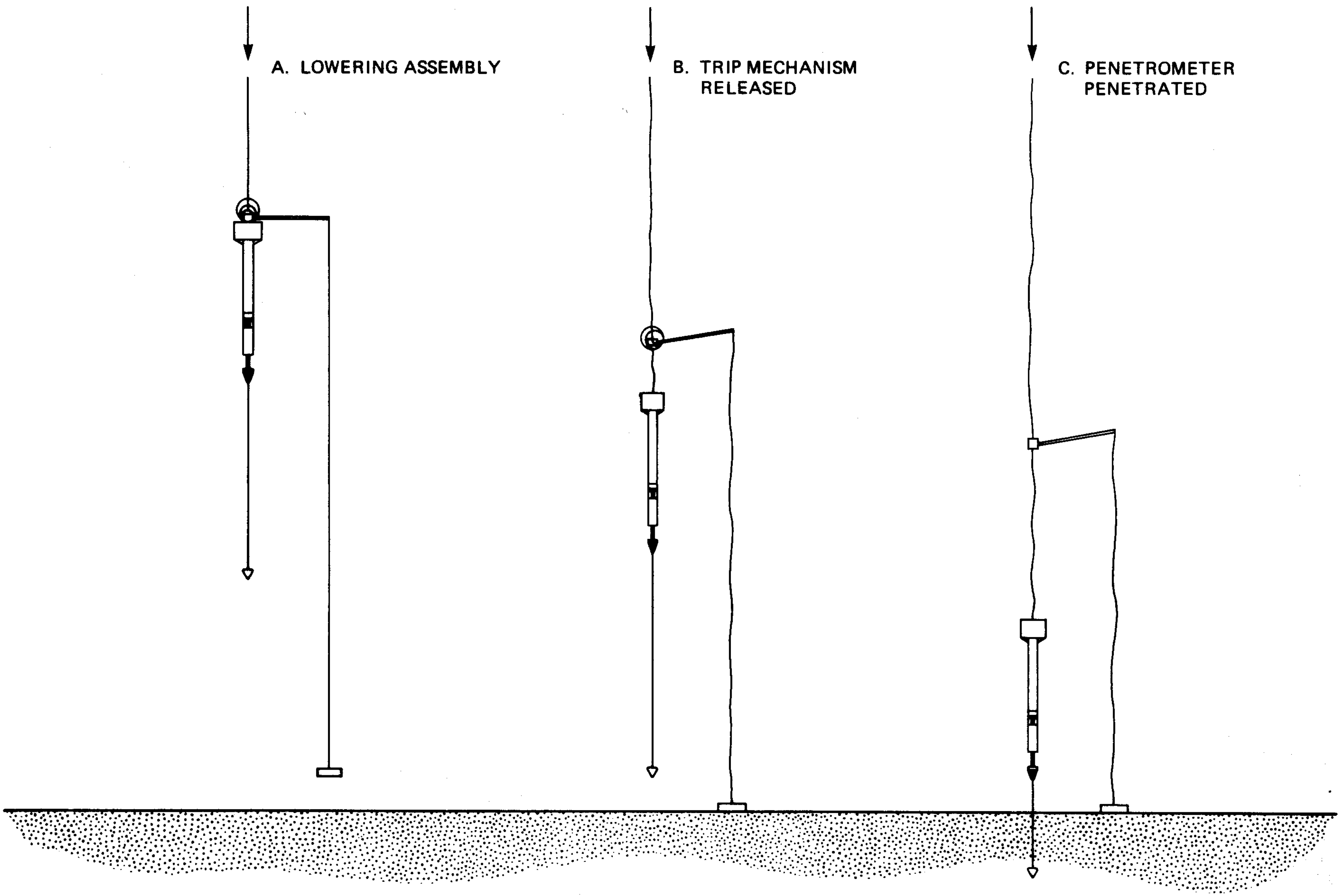

FIGURE 3-5 SCHEMATIC DIAGRAM OF DROP PENETROMETER OPERATION

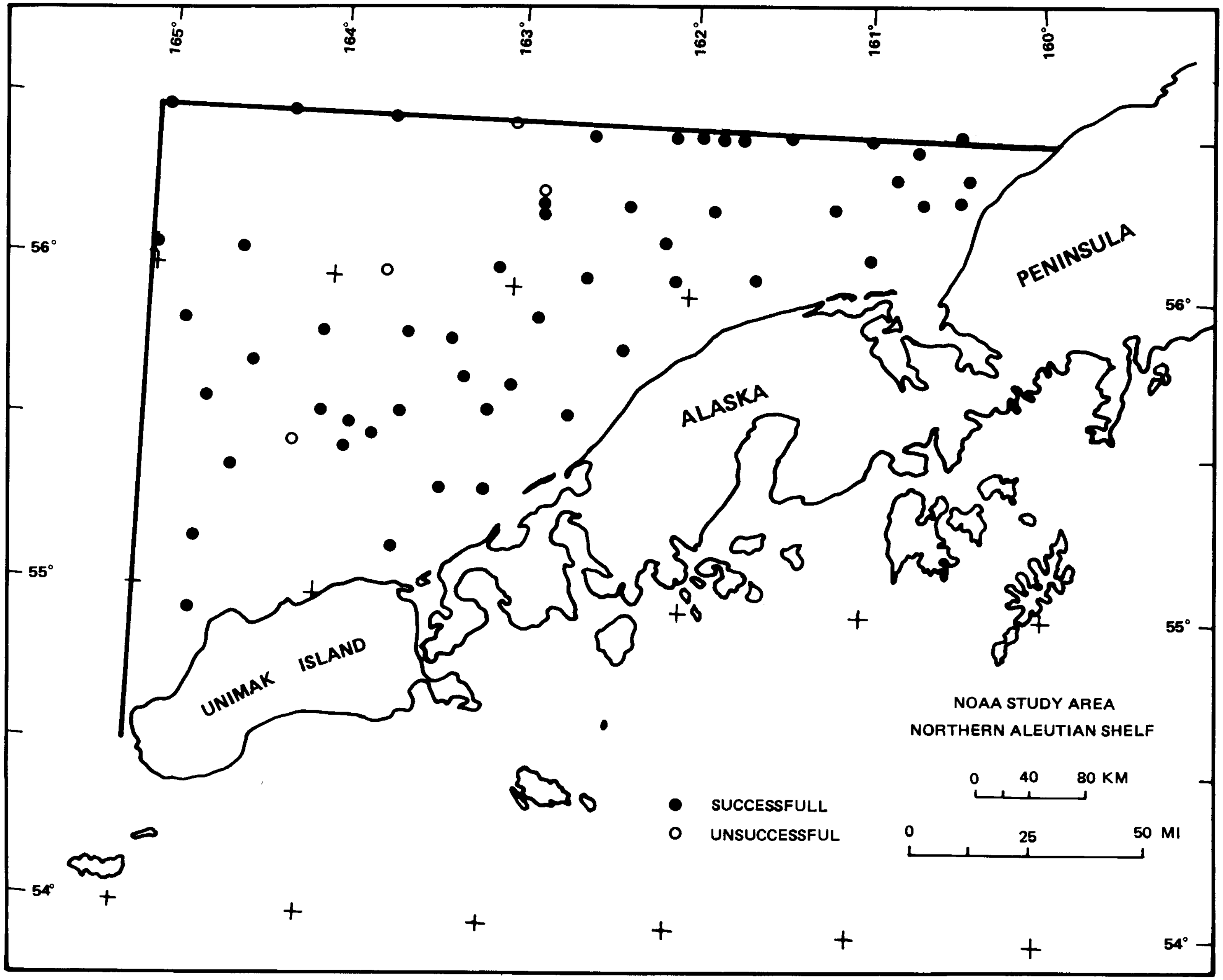

FIGURE 3-6 DROP PENETROMETER TEST LOCATION

4.0 LABORATORY TESTING

4.1 SAMPLE DISTRIBUTION

Sediment samples recovered during the field program were visually classified onboard the survey vessel. From this visual examination, it was determined that all sediments were cohesionless (silts and sands), and hence, it was decided that all laboratory testing would be performed in onshore laboratories. Each sample was then sealed and stored for subsequent laboratory testing. If cohesive (clay) samples had been recovered, the scientific crew was prepared to conduct limited offshore testing including water content and miniature vane shear strength determinations.

The onshore testing program was conducted at Ertec's soil mechanics laboratory located in Long Beach, California and at California State University, Northridge, California. The onshore testing program involved geological description and engineering classification of the sediment samples. The geological description included determination of grain-size distribution, total organic content, carbonate content, bulk mineralogy, X-radiography and radiocarbon dating. Engineering classification included determination of water content, total unit weight, specific gravity, maximum/minimum density, compressibility, permeability, static strength, liquefaction resistance, shear modulus, and material damping properties. Test procedures and results from the tests are described below. Section 5.5 of this report presents a detailed discussion of significant results. Appendix II contains a detailed summary of test results.

4.2 GEOLOGICAL DESCRIPTION

The majority of the geological tests were conducted by the Geological Sciences Department at California State University, Northridge. The purpose of these tests was to establish baseline characteristics of existing sediments.

4.2.1 Grain-size Analyses

Grain-size analyses were performed on 60 samples using an Automatic Particle-Size Analyzer (Gibbs, 1974). The Automatic Particle-Size Analyzer (APSA) utilizes settling procedures to compute grain-size distributions (Hand, 1964, and 1967; McIntyre, 1969). Grain sizes were determined in 0.5 phi intervals. The settling method was used because it exhibits several advantages over the conventional sieving technique. For example, it is precise and accurate so that analyses are completely reproducible; it provides a continuous record of sediment grain-size properties, permitting precise increments of measurement; it provides a measure of hydraulic properties rather than possibly extraneous shape distributions; and it is relatively rapid.

Discussion and comparison of sieving and settling techniques using a variety of settling devices are plentiful in the literature (Emery, 1938; Schlee, 1966; Sengupta and Veenstra, 1968; Felix, 1969; Gibbs and others, 1971; Sanford and Swift, 1971 Reed and others, 1976). In general these comparisons indicate that sieves segregate particles on the basis of minimum properties, while the settling tube directly measures the velocity with which a sediment particle settles through a column of water. Settling velocity is a sensitive function of grain shape, size, density, and surface texture, as well as certain properties of the fluid. Thus, small dense particles may settle with the same velocity as larger, less dense grains.

Twenty-two of the samples were also sieved using methods recommended by the American Society for Testing and Materials (ASTM) to provide comparative data. Samples that contained more than 5 percent silt and clay were further analyzed by standard pipette techniques. Surficial sediments at 13 of the 60 stations had more than 5 percent fines.

Average or graphic mean grain size, inclusive graphic standard deviation (sorting), inclusive graphic skewness, and graphic kurtosis were calculated according to Folk and Ward (1957) and Folk (1974) (see definition of terms in Appendix I). Grain-size parameters, as discussed in Section 5.5, are based upon these measures. Individual grain-size data are tabulated in Appendix I.

4.2.2 Bulk Mineralogy

Sixty samples were examined to determine the bulk mineralogy of the sediments. A minimum of 300 grains were counted using a petrographic microscope. Grains were identified under both plain and polarized light and assigned to one of six mineralogical categories. The categories included quartz, feldspar, hornblende, hypersthene, opaques, and others. Results of the mineralogy studies are summarized in Table 4-1.

4.2.3 Total Organic Carbon and Percent $CaCO_3$

Total organic carbon and percent calcium carbonate ($CaCO_3$) were determined using a modified Bien gasometric digestion assembly and a LECO total carbon analyzer. These methods are based upon the evolution of carbon dioxide (CO_2) from the sample. The volume of CO_2 evolved is directly related to the amount of carbon contained in the sample. Carbon dioxide evolved from both digestion and combustion of carbon compounds in sediments follows a flow pattern modified after Kolpack and Bell (1968). Eleven samples which contained

Table 4-1 Mineralogic Composition Determined from Bulk* Mineralogic Analyses

Sample Number	Quartz (%)	Feldspar (%)	Hypersthene (%)	Hornblende (%)	Opaque (%)	Other (%)
1	31.0	21.7	8.0	8.7	27.7	3.0
2	36.3	24.7	1.0	4.3	25.0	8.7
3	38.3	22.3	9.3	10.7	18.0	1.3
4	28.7	37.3	1.3	6.8	25.3	1.7
5	38.0	27.7	0.7	3.0	27.3	3.3
6	35.3	33.7	0.7	1.0	27.3	2.0
7	27.7	30.0	2.0	2.7	36.0	1.7
8	34.7	33.0	2.7	1.7	27.7	0.3
9	35.8	25.8	0.3	1.3	36.1	0.8
10	25.3	32.7	3.3	2.0	33.0	3.7
11	23.3	17.7	2.0	8.0	46.3	2.7
12	15.3	20.0	13.0	4.3	45.3	2.0
13	31.0	35.0	1.0	1.0	31.3	0.7
14	23.3	24.7	9.0	8.7	27.7	6.7
15	35.0	25.7	3.0	6.7	26.7	3.0
16	23.0	43.7	4.3	1.7	24.0	3.3
17	21.7	37.0	1.7	2.7	35.7	1.3
18	27.7	31.7	2.7	4.0	32.7	1.3
19	28.3	32.0	1.3	2.3	35.3	0.7
20	32.0	21.3	6.3	4.7	32.3	3.3
21	23.0	41.1	3.7	3.4	27.9	0.9
22	34.0	16.0	2.7	10.0	33.0	4.3
23	21.7	20.3	2.7	8.7	32.3	4.7
24	27.7	22.7	5.0	8.7	43.0	3.7
25	35.0	22.7	4.7	8.3	28.7	0.7
26	30.3	30.7	1.3	6.7	28.0	3.0
27	14.3	13.0	15.7	10.7	43.3	3.0
28	12.3	27.0	3.3	5.7	50.3	1.3
29	29.3	27.0	0.3	11.7	28.7	3.0
30	29.7	40.0	0.7	3.0	26.7	0.0
31	20.3	30.7	2.0	8.7	36.0	2.3
32	29.3	21.3	2.7	7.3	36.3	3.0
33	38.3	19.0	7.3	11.7	22.0	1.7
34	40.3	9.3	3.0	11.0	35.0	1.3
35	24.7	21.3	7.7	18.0	28.3	0.0
36	12.3	27.0	13.3	4.0	42.3	1.0
37	26.3	16.7	9.7	9.3	38.0	1.0
38	15.0	13.3	16.3	18.3	41.0	2.3
39	15.0	15.0	6.3	13.7	46.3	3.7
40	12.0	25.7	15.7	21.0	18.7	7.0

*300 Counts

Table 4-1 Mineralogic Composition Determined from Bulk* Mineralogic Analysis (Continued)

Sample Number	Quartz (%)	Feldspar (%)	Hypersthene (%)	Hornblende (%)	Opaque (%)	Other (%)
41	36.3	17.0	9.3	14.3	21.0	2.0
42	26.3	23.0	4.7	9.7	35.0	1.3
43	24.0	27.3	6.7	6.7	32.7	2.7
44	27.7	12.0	16.0	14.3	28.3	1.7
45	32.7	31.3	2.7	5.0	28.0	0.3
46	31.3	26.0	1.7	3.3	37.0	0.7
47	47.0	18.0	3.3	6.3	25.3	0.0
48	26.7	24.7	1.0	7.3	39.7	0.7
49	23.0	27.3	2.7	3.6	41.7	0.7
50	19.7	32.7	6.3	7.7	32.7	1.0
51	17.7	5.3	21.7	22.7	31.3	1.3
52	17.0	22.7	8.7	11.7	34.7	5.3
53	21.3	25.7	6.7	8.0	35.0	3.3
54	17.3	20.7	15.0	12.0	32.3	2.7
55	23.0	21.3	7.3	5.0	39.7	3.7
56	25.7	27.3	3.6	6.7	33.0	3.7
57	19.3	21.3	8.3	14.3	35.0	1.7
58	20.7	24.3	6.0	6.7	41.0	1.3
59	22.7	14.7	15.0	7.3	35.7	4.7
60	24.3	6.3	15.0	8.0	44.3	2.0

* 300 Counts

greater than 5 percent silt and clay were tested. As most resultant numbers were very low, replicates were conducted on each sample to ensure statistical repeatability. Results are summarized in Table 4-2.

4.2.4 Age-Dating

Radioacarbon dating was performed on marine shells from two samples by Dr. R. E. Taylor, Director of the Radiocarbon Laboratory at the University of California, Riverside. No other samples had sufficient carbon to yield useable dates. To determine the dates on the two samples, the outer one-third of the surface of the shell was removed in acid to reduce the chance of contamination. Carbon Dioxide (CO_2) was evolved by 2 normal hydrochloric acid (HCL) in a closed system and collected in liquid nitrogen traps. After being purified, this CO_2 was introduced into a 1.5 liter gas proportional detector. The counting activity of the sample was compared to that of 0.95 NBS (National Bureau of Standards) oxalic acid standard. The age was then expressed in radiocarbon years before present (B.P.) with 5568 used as the ^{14}C half-life and A.D. 1950 = B.P.

The results of the two analyses indicate that sediments at a depth of 7 to 10 cm below the surface have an age of about 12,000 years, i.e.

- Station 1070/91 from 7 cm in 84 m of water — 12,390 $\pm$ 250 years
- Station 1070/87 from 10 cm in 89 m of water — 11,720 $\pm$ 245 years

4.3 ENGINEERING CHARACTERISTICS

The engineering phase of the laboratory program was conducted to characterize the engineering properties of the sediments. Information from this phase formed the basis for conducting various geologic hazards analyses.

Table 4-2 Percentage of Carbon (Organic/Inorganic) and Calcium Carbonate Content for Selected Samples Tests

Sample Number	Total Carbon (%)	Total Organic Carbon (%)	Total Inorganic Carbon (%)	Calcium Carbonate (%)
1	0.48	0.44	0.03	0.28
3	0.49	0.46	0.02	0.22
7	0.40	0.37	0.03	0.26
8	0.36	0.35	0.02	0.16
9	0.44	0.43	0.02	0.15
11	0.44	0.42	0.02	0.13
15	0.34	0.33	0.02	0.14
17	0.36	0.35	0.02	0.16
18	0.30	0.28	0.02	0.13
22	0.33	0.31	0.02	0.15
28	0.30	0.29	0.02	0.13

The laboratory testing program involved determination of 1) index properties and 2) engineering parameters. In general, the engineering laboratory tests were performed in accordance either with American Society for Testing and Materials (ASTM) procedures, or with practices adopted by the geotechnical engineering profession. Laboratory tests were performed on selected soil samples as well as reconstituted samples. Reconstituted samples were prepared using a wet-tamping method with the procedures described by Ladd (1978). Reconstituted samples were prepared to best-estimate, in-situ density values (Section 5.5.5.4). The following paragraphs provide a general description of the testing methods and a summary of test results. Detailed results of these tests are presented in Appendix II.

4.3.1 Total Unit Weight and Water Content

The total (or bulk) unit weight and water content were determined for 46 samples using conventional geotechnical procedures. The total unit weight was computed by measuring the weight of a known volume of material. Subcores of larger samples were made to obtain the unit weight data. Water contents were determined by drying a known weight of sediment and then obtaining the ratio of weight loss to dry weight, in accordance with ASTM D2216. No corrections were made for salt content. Results of these tests are summarized in Table 4-3.

4.3.2 Specific Gravity

Specific gravity tests were conducted on three samples using procedures set forth in ASTM D854. The procedure generally involved determination of the unit weight of the sediment and comparison of this weight to the unit weight of water at 4° C. A dry preparation method was employed. This specific gravity was determined on sediments as they occur naturally (and hence can be referred to as apparent specific gravity). Examination of the sediment particles

Table 4-3 Moisture Content and Unit Weight Values for Selected Samples

Sample Number	Sample Type 1)	Average Depth (cm) 2)	Soil Type 3)	Dry Unit Weight (kN/m^3) 4)	Moisture Content (%)	Total Unit Weight (kN/m^3) 4)
1	V.V.	S	SM (4)	14	34	18
1A	V	0-8	SM (4)	16	26	20
1A	V	78-86	SM (4)	16	23	20
1B	V	0-8	SM (4)	14	35	18
1B	V	63-71	SM (4)	17	21	20
2	V.V.	S	SM (4)	13	43	18
2	G.C.	8	SM (4)	14	36	19
2	G.C.	22	SM (4)	15	30	19
2	G.C.	32	SM (4)	14	34	19
2	G.C.	38	SM (4)	14	37	19
2	G.C.	50	SM (4)	14	33	19
2	G.C.	66	SM (4)	15	31	19
7	V.V.	S	SM (4)	14	32	19
9	V.V.	S	SM (4)	12	40	17
9	V	0-8	SM (4)	15	29	19
9	V	72-80	SM (4)	17	21	21
11	V.V.	S	SM (4)	13	42	18
11	G.C.	3	SM (4)	14	31	18
11	G.C.	8	SM (4)	16	28	20
11	G.C.	22	SM (4)	15	30	20
15	V.V.	S	SM (4)	-	-	-
22	V.V.	S	SM (4)	14	34	19
23	V.V.	S	SP/SM (3)	13	39	18
23	G.C.	5	SP/SM (3)	14	31	18
23	G.C.	17	SP/SM (3)	15	26	19
23	G.C.	21	SP/SM (3)	15	28	20
23	G.C.	33	SP/SM (3)	14	35	19
23	G.C.	41	SP/SM (3)	15	29	19
23	G.C.	64	SP/SM (3)	15	28	19

Notes:
1) V.V. = Van Veen; G.C. = Gravity Corer; V = Vibracorer
2) S = Surface sample
3) Number in parenthesis denotes soil type number described in Section 5.5; letter refers to soil type based on Unified Classification System
4) 1 KN/m^3 = 0.102 g/cm^3

Table 4-3 Moisture Content and Unit Weight Values for Selected Samples

(Cont'd)

Sample Number	Sample Type1)	Average Depth (cm)2)	Soil Type3)	Dry Unit Weight (kN/m3)4)	Moisture Content (%)	Total Unit Weight (kN/m3)4)
26	V.V.	S	SP/SM (3)	16	29	21
26A	V	0-8	SP/SM (3)	16	26	20
26A	V	57-65	SP/SM (3)	16	24	20
26B	V	0-8	SP/SM (3)	15	29	19
27	V.V.	S	SP (2)	15	23	19
28	V.V.	S	SP/SM (3)	-	-	-
35	V.V.	S	SP (2)	16	24	20
37	V.V.	S	SP (2)	16	25	20
39	V.V.	S	SP (1)	15	8	16
41	V.V.	S	SP (2)	17	25	22
43	V.V.	S	SP (2)	17	23	21
49	V.V.	S	SP (2)	16	28	20
50	V.V.	S	SP (2)	17	24	21
54	V.V.	S	SP (1)	18	13	20
55	V.V.	S	SP (1)	15	25	19
279	V	0-8	-	17	20	21
279	V	83-91	-	16	24	20

Notes: 1) V.V. = Van Veen; G.C. = Gravity Corer; V = Vibracorer
2) S = Surface Sample
3) Number in parenthesis denotes the soil type number described in Section 5.5; letter refers to soil type on Unified Classification System
4) 1 $KN/m^3 = 0.102\ g/cm^3$

suggested that no voids exist within the individual particles; therefore, the apparent specific gravity was probably similar to the true specific gravity value of the soil grain. Results of specific gravity tests are summarized in Table 4-4.

4.3.3 Grain-Size Analyses

Grain-size analyses were performed on 34 samples 1) to supplement grain-size data obtained during geological classification and 2) to provide direct information on samples subjected to other engineering tests. These latter data provided a basis for drawing correlations between certain engineering properties and sediment size. Procedures given in ASTM D422 were followed in these tests. In view of the coarseness of the sediments, sieving methods were used on most samples. Test specimens were prepared using a dry preparation method. Results are tabulated in Appendix I.

4.3.4 Maximum and Minimum Dry Unit Weights

Eight maximum and minimum dry unit weight tests were conducted in general accordance with ASTM procedure D2049. These tests were conducted to obtain 1) a basis for judging the relative denseness of sediment in situ and 2) possible ranges of densities if local materials are used for construction. Minimum dry unit weights were obtained by use of the funnelling method; the maximum height of free fall of the soil was maintained constant at 2.5 cm. Maximum dry unit weights were obtained by vibrating a mold containing a sample of soil with a standard vibrator for a specified duration. Results of these tests are summarized in Table 4-5.

4.3.5 Compressibility

The one-dimensional compressibilities of seven samples were measured by conducting oedometer (or consolidation) tests in accordance with procedures

Table 4-4 Specific Gravity Values for Selected Samples

Sample Number	Sample Type[1)]	Soil Type[2)]	Specific Gravity
9	V.V	SM(4)	2.69
36	V.V	SP(2)	2.80
48	V.V	SP(1)	2.74

Notes:

1) V.V. = Van Veen

2) Refer to Table 4-3

Table 4-5 Maximum and Minimum Dry Unit Weight Values for Selected Samples

Sample Number	Soil Type[1]	Maximum Dry Unit Weights (kN/m^3)	Minimum Dry Unit Weights (kN/m^3)
1	SM (4)	14	12
7	SM (4)	14	12
9	SM (4)	15	11
12	SM (4)	14	12
24	SP/SM (3)	16	13
36	SP (2)	20	17
43	SP (2)	17	14
56	SP (2)	17	14
59	SP (1)	19	18

Note:

1) Refer to Table 4-3

described in ASTM D2435. A standard, dead-load consolidometer was used. Three of the test specimens were obtained from gravity cores. These specimens were relatively undisturbed ie., the natural grain structure of the sediment was retained. The other four samples were totally reconstituted to specific density and moisture content values shown in Table 4-6. Information from the oedometer tests provides an indication of the amount of compression the sediment might experience for different stress levels. Results are summarized in Table 4-6 and Appendix II.

4.3.6 Permeability

Six permeability tests were conducted using constant head, triaxial testing methods. Two of the tests were performed on gravity core specimens; the others were performed on reconstituted material. These tests were required to quantify the rate at which excess pore-water pressures would dissipate after storm-wave or earthquake-induced pore pressure increases. Samples were consolidated isotropically to the estimated in situ effective vertical stress and then back-pressure saturated prior to testing. During the test a constant head was applied to the top of the sample, and the resultant outflow from the bottom was measured for a period of time. Permeability characteristics were obtained by plotting and analyzing the cumulative outflow versus time during the tests. Results are summarized in Table 4-7.

4.3.7 Static Triaxial Strength

Fourteen isotropically consolidated, drained triaxial compression tests were conducted on 12 reconstituted and 2 gravity core specimens. The purpose of these tests was to obtain the effective angle of internal friction for the materials. Reconsituted samples were prepared using a moist tamping procedure.

Table 4-6 Compressibility Properties

Sample Number	Sample Type[1)]	Soil Type[2)]	Total Unit Weight (kN/m^3)	Moisture Content (%)	Compression Index, C_c	Recompression Index, C_r	Voids Ratio, e_o
2	GC	SM (4)	19	36	0.18	0.012	1.00
2	GC	SM (4)	19	34	0.19	0.009	0.96
9	R	SM (4)	19	28	0.04	0.005	0.74
23	GC	SP/SM (3)	19	32	0.15	0.008	0.87
24	R	SP/SM (3)	20	25	0.03	0.005	0.68
43	R	SP (1)	20	24	0.04	0.005	0.65
57	R	SP (2)	20	24	0.03	0.003	0.64

Note:

1) GC = Gravity Corer; R = Reconstituted

2) Refer to Table 4-3

Table 4-7 Permeability Characteristics of Selected Samples

Sample Number	Sample Type[1)]	Soil Type[2)]	D_{10} (mm)	D_{50} (mm)	Coefficient of Permeability k (cm/sec)
2	G.C.	SM (4)	0.005	0.055	1×10^{-6}
9	R	SM (4)	-	0.13	2×10^{-5}
23	G.C.	SP/SM (3)	-	0.12	5×10^{-6}
24	R	SP/SM (3)	0.08	0.20	5×10^{-5}
43	R	SP (1)	0.20	0.42	1×10^{-3}
57	R	SP (2)	0.21	0.28	5×10^{-3}

Note:

1) G.C. = Gravity Corer, R = Reconstituted

2) Refer to Table 4-3

Procedures recommended by the Corps of Engineers (EN1110-2-1906) were used to conduct the tests. In general these procedures involved placement of a cylindrical sample of soil in a membrane, consolidation of the sample in a pressure chamber at a specified confining pressure, and shearing by application of an axial load. The rate of loading (0.08 percent per minute) was sufficiently slow to ensure that no excess pore-water pressures developed. Load, deformation and volume change were recorded during the tests.

Standard test procedures were modified slightly during tests on the two gravity core samples. For these tests a multistage testing method was employed. This method involved shearing each sample under three confining pressures. The maximum shearing strain was limited to 2 percent under the first two pressures; the last test was carried out to 20 percent strain. Results of these tests are summarized in Table 4-8. Appendix II contains individual test data.

4.3.8 Liquefaction Resistance

Cyclic simple shear tests were conducted on five gravity core specimens and 12 reconstituted samples. The purpose of these tests was to estimate the resistance of surficial sediments to liquefaction.

Cyclic simple shear tests were performed using a modified version of the Geotechnical Equipment Corporation Model SS-104 cyclic simple shear device (Figure 4-1). Test specimens were confined in wire-bound membranes and consolidated under estimated in situ effective vertical stresses. Pore fluids were back pressured to ensure full saturation. Once saturated, the cylindrical specimens were subjected to a cyclic horizontal shearing load at a frequency of 0.5 Hz. Applied shearing stresses were selected so as to generate

Table 4-8 Shearing Strength Results from Istropically Consolidated, Drained Triaxial Compression Tests (CID)

Sample Number	Sample[1)] Type	Soil[2)] Type	Consolidation Stress (kN/m^2)	Dry Unit Weight (kN/m^3)	Initial Moisture Content (%)	Final Moisture Content (%)	Axial Strain (%)	$q^{3)}$ (kN/m^2)	$p^{3)}$ (kN/m^2)
2	G.C.	SM (4)	69	14	37	26	2	55	125
2	G.C.	SM (4)	138	14	37	26	2	105	243
2	G.C.	SM (4)	276	14	37	26	18	407	683
23	G.C.	SP/SM (3)	69	15	29	-	2	72	141
23	G.C.	SP/SM (3)	138	15	29	-	2	155	293
23	G.C.	SP/SM (3)	276	15	29	-	18	459	735
9	R	SM (4)	69	15	28	26	4	121	188
9	R	SM (4)	138	15	28	28	7	206	344
9	R	SM (4)	276	15	28	27	9	417	693
24	R	SP/SM (3)	69	16	26	28	2	171	240
24	R	SP/SM (3)	138	16	28	28	3	315	453
24	R	SP/SM (3)	276	16	26	27	4	478	754
43	R	SP (1)	69	16	24	25	2	130	199
43	R	SP (1)	138	16	23	26	3	252	390
43	R	SP (1)	276	16	24	25	5	469	744
57	R	SP (2)	69	16	24	27	2	117	186
57	R	SP (2)	138	16	24	27	4	281	419
57	R	SP (2)	276	16	24	26	6	520	796

Notes:

1) R = Reconstituted; G.C. = Gravity Corer

2) Refer to Table 4-3

3) $q = (\sigma_1 - \sigma_3)/2$; $p = (\sigma_1 + \sigma_3)/2$
where σ_1 = major principal stress and σ_3 = minor principal stress

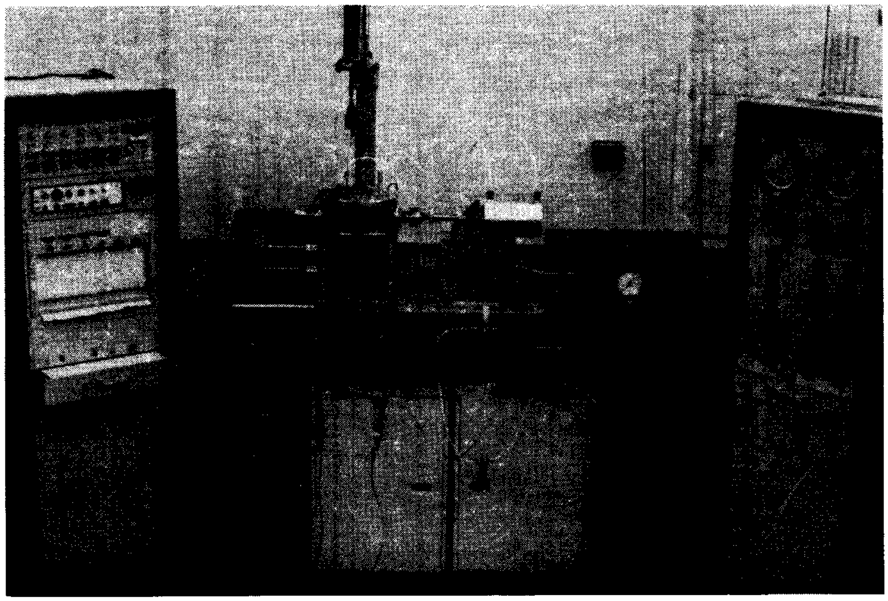

LOADING AND RECORDING SYSTEM

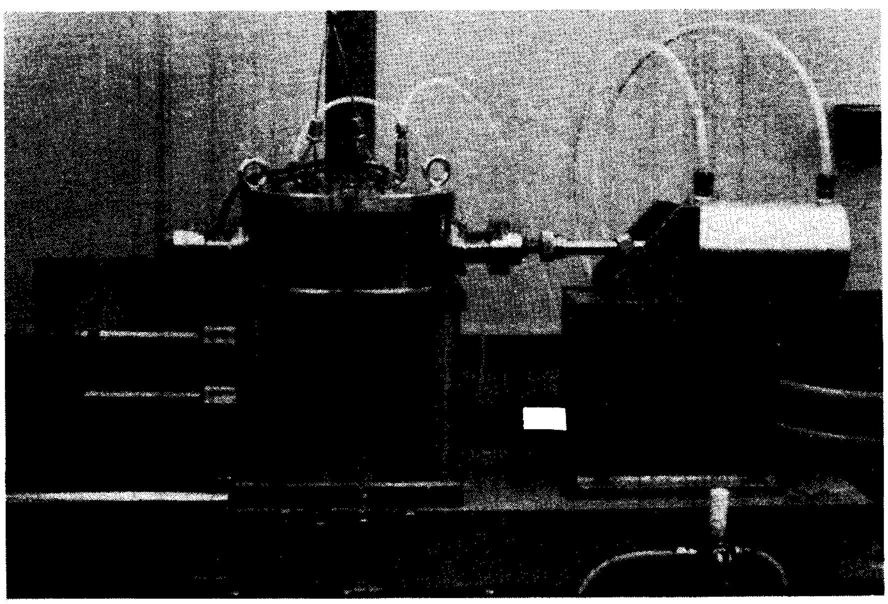

TEST CHAMBER

FIGURE 4-1 PHOTOGRAPHS OF CYCLIC SIMPLE SHEAR EQUIPMENT failure between 5 and 50 cycles. Load, deformation, and pore-water pressure were monitored on a strip chart recorder. Test results were plotted as pore-water pressure ratio and double-amplitude shearing strain versus number of loading cycles. Liquefaction strength was determined at a cyclic shearing strain of 10 percent or at excess pore-water pressures equal to the axial stress at the beginning of the test, whichever occurred first. Information from these tests was used to predict soil response during earthquake or storm-wave loading. Results of these tests are summarized in Table 4-9; individual test data are presented in Appendix II.

4.3.9 Shear Modulus and Damping

Four sets of resonant column and cyclic triaxial tests were conducted on reconstituted samples to define the shear modulus and material damping characteristics of surficial sediments. Test procedures involved first testing a sample in the resonant column device to obtain modulus and damping values over the 10^{-4} to 10^{-2} percent shearing strain range, and then carefully transferring the sample to the cyclic triaxial device to define modulus and damping values over the 10^{-2} to 1 percent strain range.

The resonant column tests were perfomed using a Hardin-type resonant column device (Figures 4-2 and 4-3). During these tests, the samples were first isotropically consolidated under the estimated in situ vertical effective stresses. After consolidation was complete, torsional vibrations were applied to the top of the sample; the bottom was rigidly fixed. Resonant frequency, torque and acceleration were recorded. Using a wave equation analysis, dynamic shear modulus and damping of soils for each strain level were determined.

Table 4-9 Cyclic Simple Shear Test Results

Sample Number	Sample Type	Average Depth (cm)	Soil Type	Dry Unit Weight (kN/m^3)	Moisture Content (%)	Vertical Stress (kN/m^2)	Shear[2] Stress Ratio	Cycles at 5% Strain	Cycles to Initial Lique-faction
9	V.V.	S	SM (4)	15.1	29.5	69	0.24	11	14
9	V.V.	S	SM (4)	15.1	29.5	69	0.29	3	6
9	V.V.	S	SM (4)	15.1	29.5	69	0.19	24	24
9	V.V.	S	SM (4)	15.1	29.5	69	0.16	620	630
24	V.V.	S	SP/SM (3)	15.7	26.6	69	0.17	72	75
24	V.V.	S	SP/SM (3)	15.7	26.6	69	0.21	39	30
24	V.V.	S	SP/SM (3)	15.7	26.6	69	0.30	8	15
43	V.V.	S	SP (1)	16.4	24.3	69	0.22	9	10
43	V.V.	S	SP (1)	16.4	24.3	69	0.29	5	7
43	V.V.	S	SP (1)	16.4	24.3	69	0.17	80	80
57	V.V.	S	SP (2)	16.2	23.3	69	0.21	7	6
57	V.V.	S	SP (2)	16.2	23.3	69	0.17	20	26
57	V.V.	S	SP (2)	16.2	23.3	69	0.13	305	330
57	V.V.	S	SP (2)	16.2	23.3	69	0.14	29	30
1	G.C.	49	SM (4)	14.4	32.1	69	0.22	72	-
1	G.C.	66	SM (4)	14.4	32.1	69	0.27	5	-
1	G.C.	22	SM (4)	14.4	32.1	69	0.22	4	-
11	G.C.	8	SM (4)	15.5	28.4	69	0.26	14	45
23	G.C.	33	SM (4)	14.8	29.5	69	0.20	45	60
23	G.C.	64	SM (4)	14.8	29.5	69	0.23	9	-
23	G.C.	2	SM (4)	14.8	29.5	69	0.30	9	-

Notes:

1) Refer to Table 4-3
2) Shear stress ratio defined as the ratio of cyclic shearing stress to the vertical stress

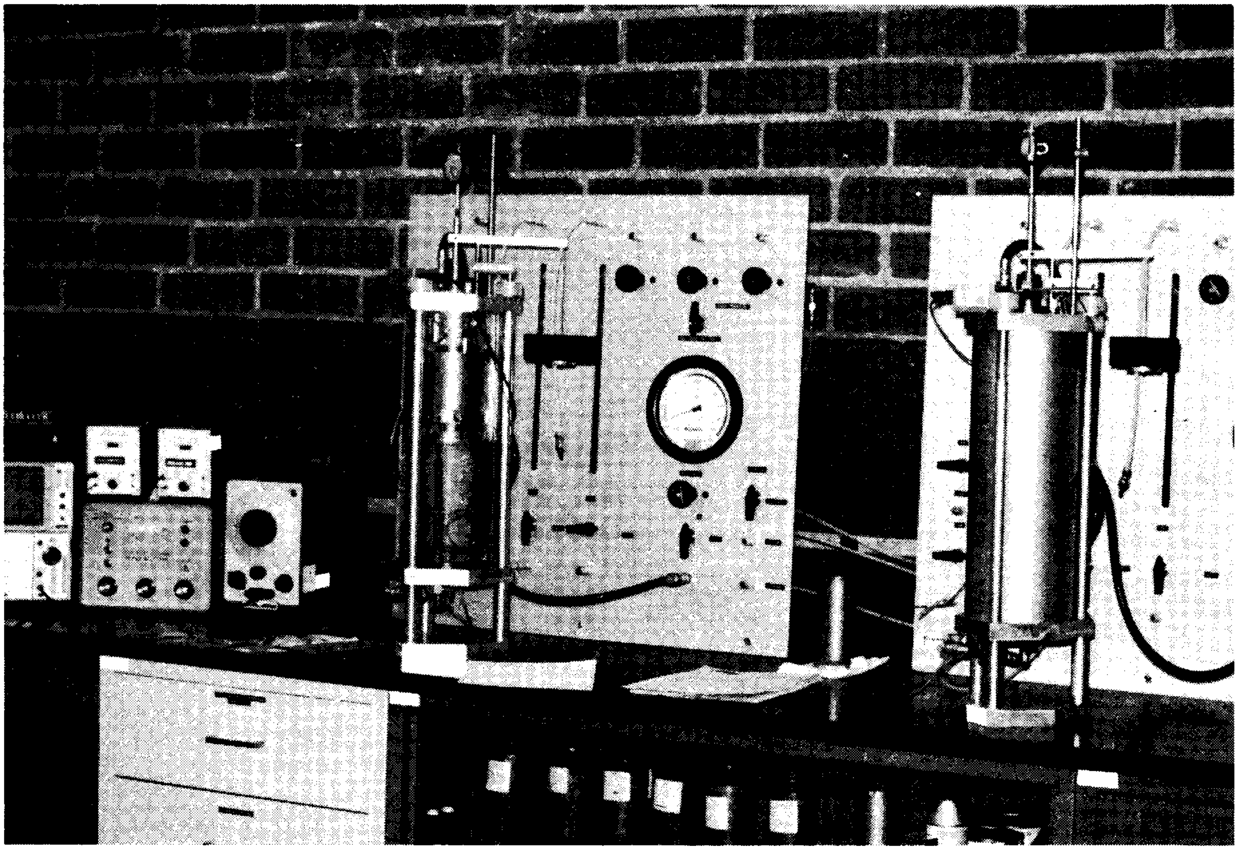

RESONANT COLUMN TEST SETUP

ELECTRONICS FOR RESONANT TEST

FIGURE 4-2 PHOTOGRAPHS OF RESONANT COLUMN EQUIPMENT

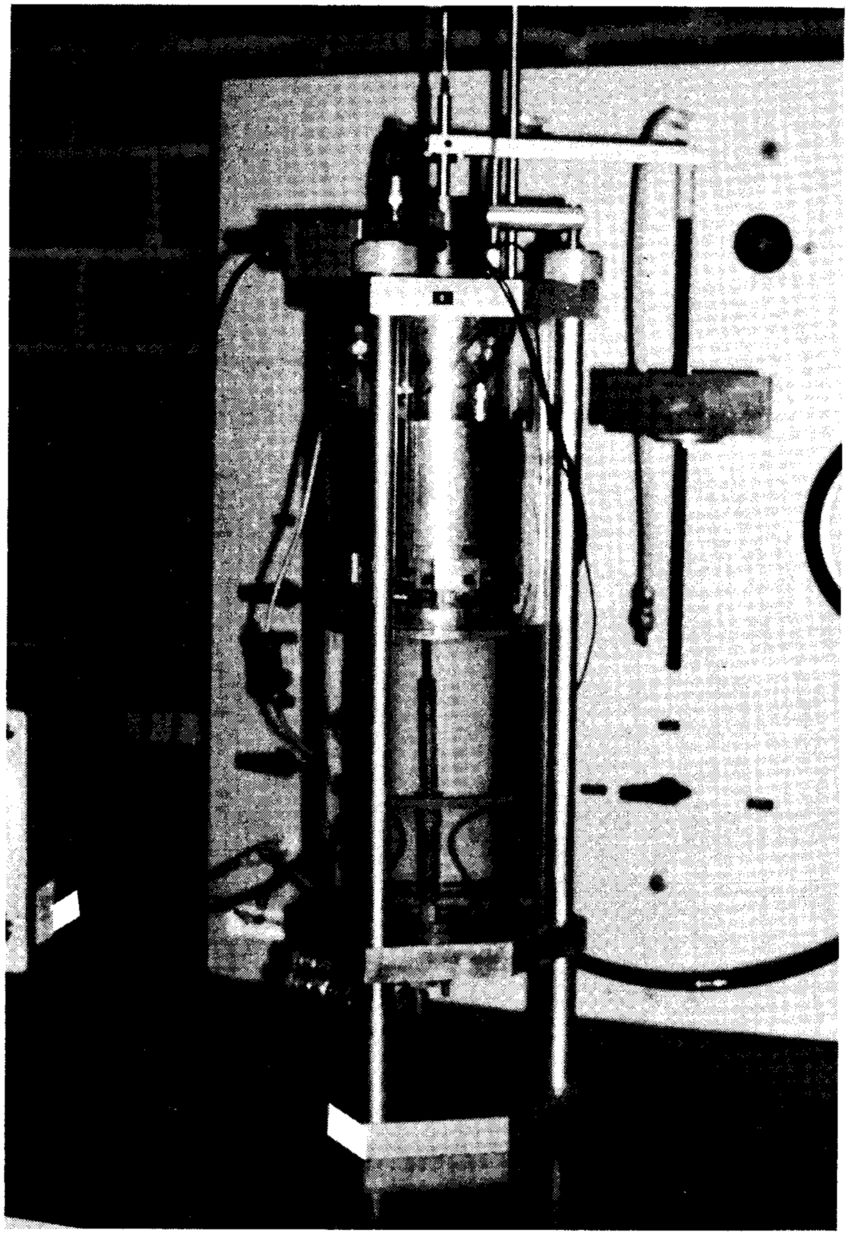

RESONANT COLUMN DEVICE

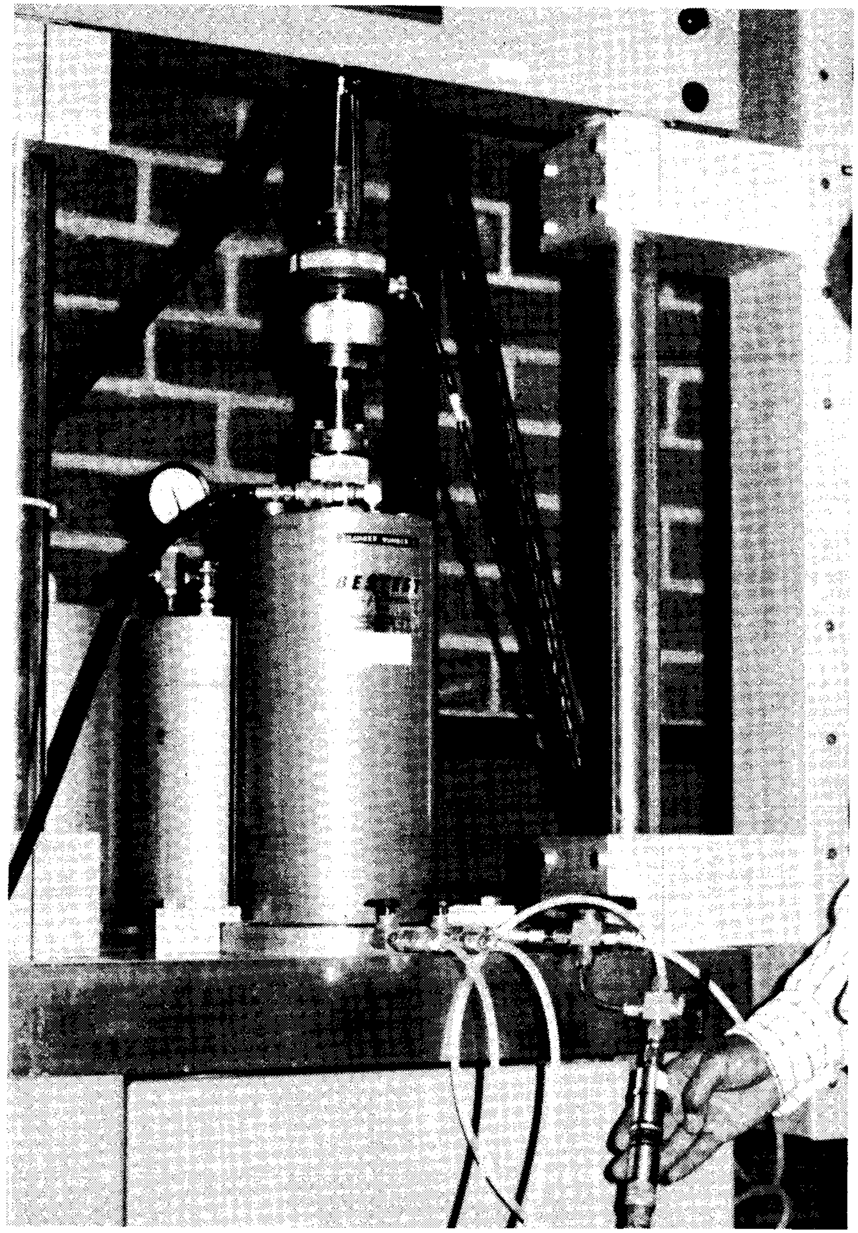

CYCLIC TRIAXIAL CHAMBER

FIGURE 4-3 PHOTOGRAPHS OF RESONANT COLUMN AND CYCLIC TRIAXIAL TEST CHAMBERS

An MTS Model 810 electro-hydraulic loading system, operated in the strain-controlled mode at a loading frequency of 1.0 Hz, was used to perform the cyclic triaxial tests (Figures 4-3 on 4-4). During these tests, the sample was transferred from the resonant column device, and the same consolidation pressure used in the resonant column test was applied. A back pressure was used to induce full saturation, then 15 cycles of loading were applied. Drainage was not permitted during cyclic loading. After the 15th cycle, drainage was allowed. Upon complete dissipation of generated excess pore-water pressures, the next higher strain level loading was applied. Hystersis loops of load versus deformation were recorded to facilitate calculation of secant modulus and damping values. These hysteresis loops were digitized; a computer program was used to convert the measured axial characteristics to shear characteristics. The conversion equations used are:

$$G = E/2(1 + \nu) \qquad (4\text{-}1)$$
$$\gamma = E(1 + \nu)$$

where G is shear modulus, E is Young's modulus, γ is shearing strain and ν is Poisson's Ratio (assumed equal to 0.45). The value of shear modulus obtained at any shearing strain in the cyclic triaxial test was normalized by the maximum modulus for that sample as measured in the resonant column device.

Results of these tests are summarized in Tables 4-10 and 4-11; individual test data are presented in Appendix II.

4.3.10 Sonic Velocities

Sonic velocity measurements were performed on eight samples by Dr. Edward L. Hamilton of the Naval Ocean Systems Center, San Diego, California. All measurements were made with a sound velocimeter. Results of these tests are summarized in Table 4-12.

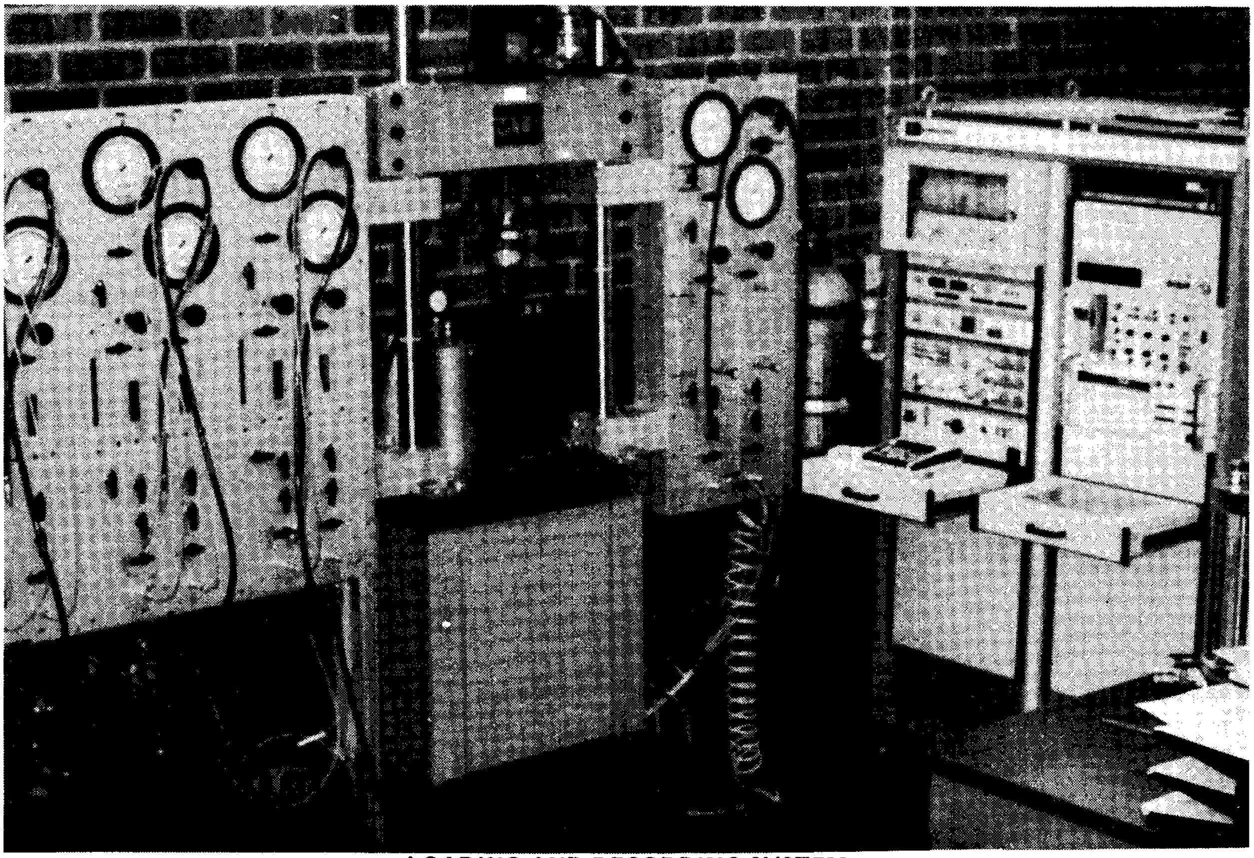

LOADING AND RECORDING SYSTEM

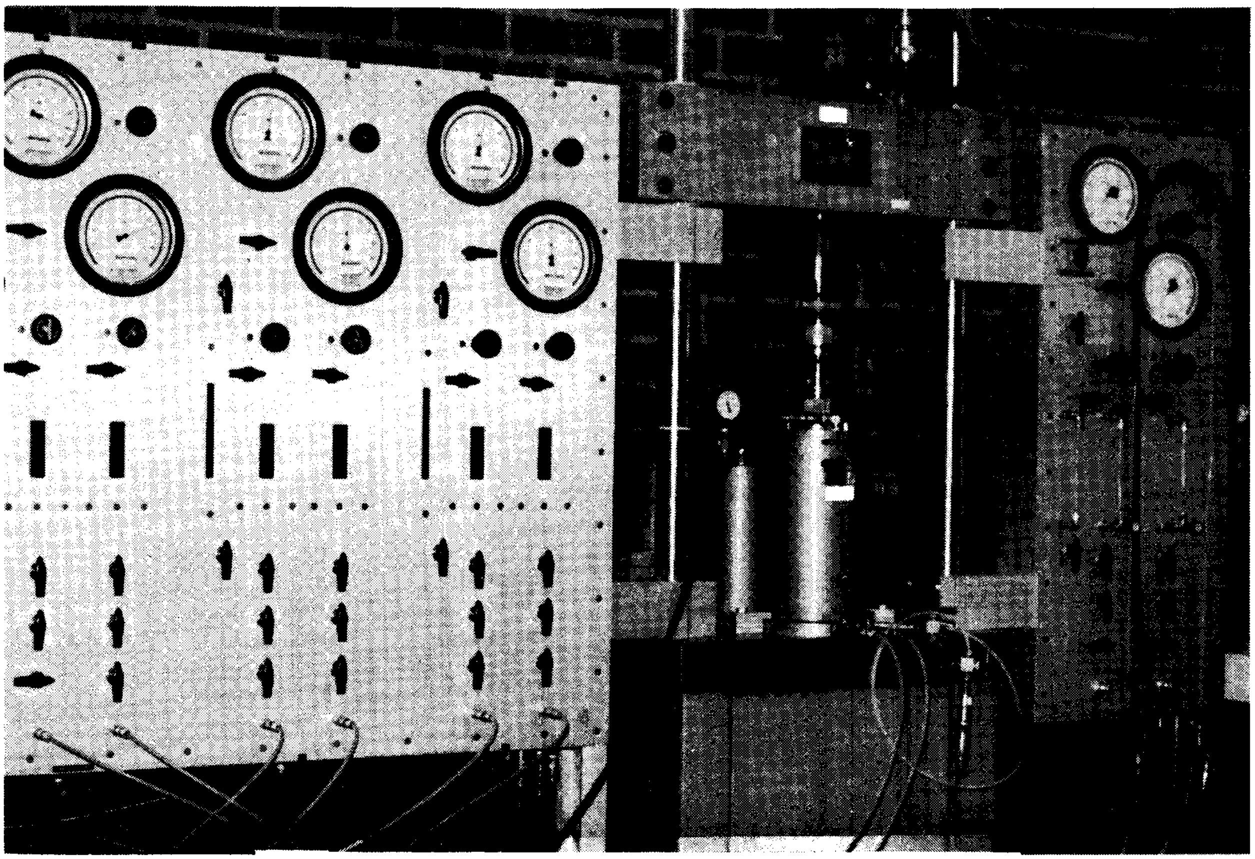

LOADING SYSTEM

FIGURE 4-4 PHOTOGRAPHS OF CYCLIC TRIAXIAL EQUIPMENT

Table 4-10 Low Amplitude Shear Modulus From Resonant Column Tests

Sample Number	Sample[1)] Type	Soil[2)] Type	Dry Unit Weight (kN/m^3)	Water Content (%)	Maximum Shear Modulus (kN/m^2)
9	R	SM (4)	15	14	7.6×10^4
24	R	SP/SM (3)	16	15	1.1×10^5
43	R	SP (1)	16	11	1.2×10^5
57	R	SP (2)	16	10	1.2×10^5

Notes:

1) R = Reconstituted

2) Refer to Table 4-3

Table 4-11 Cyclic Triaxial Test Results

Sample Number	Sample Type	Average Depth (cm)	Soil[1] Type	Dry Unit Weight (kN/m^3)	Moisture Content (%)	Confining Pressure (kN/m^2)	Shearing Strain (%)	Shear Modulus ($10^4 k\ N/m^2$)	Damping Ratio (%)
9	V.V.	5	SM (4)	15	27	138	0.02	7.0	18
9	V.V.	5	SM (4)	15	27	138	0.05	4.8	16
9	V.V.	5	SM (4)	15	27	138	0.10	3.9	15
9	V.V.	5	SM (4)	15	27	138	0.20	2.5	18
9	V.V.	5	SM (4)	15	27	138	0.67	0.5	24
24	V.V.	5	SP/SM (3)	18	27	138	0.02	7.0	5
24	V.V.	5	SP/SM (3)	18	27	138	0.05	4.6	24
24	V.V.	5	SP/SM (3)	18	27	138	0.11	4.5	15
24	V.V.	5	SP/SM (3)	18	27	138	0.20	3.6	16
24	V.V.	5	SP/SM (3)	18	27	138	0.68	1.0	18
43	V.V.	5	SP (1)	16	24	138	0.03	6.8	5
43	V.V.	5	SP (1)	16	24	138	0.05	4.3	21
43	V.V.	5	SP (2)	16	24	138	0.12	3.6	18
43	V.V.	5	SP (2)	16	24	138	0.21	2.4	21
43	V.V.	5	SP (2)	16	24	138	0.72	0.5	22
57	V.V.	5	SP (2)	18	25	138	0.02	9.3	3
57	G.C.	5	SM (4)	18	25	138	0.05	7.7	15
57	G.C.	5	SM (4)	18	25	138	0.10	5.6	16
57	G.C.	5	SM (4)	18	25	138	0.19	3.5	18
57	G.C.	5	SM (4)	18	25	138	0.65	0.8	22

Notes:

1) Refer to Table 4-3

Table 4-12 Sonic Velocity and Other Characteristics of Vibracore Samples

Vibracore Sample Number	Interv. (cm)	Sediment Name (1)	Grain Diameter: Mean mm	Grain Diameter: Mean φ	Grain Diameter: Median mm	Grain Diameter: Median φ	Sand %	Silt %	Clay %	Specific Gravity of Grains (2)	Saturated Unit Weight (g/cm^3)	Porosity %	Velocity (23°C) m/sec	Velocity (23°C) Ratio (3)	Color (4)	Color (5)	Lab. No.
VC 70/87A	0-8	Fine Sand	0.1696	2.56	0.1560	2.68	94.2	03.3	02.5	2.666	1.991	4.01	1805	1.183	5Y 2.5/1	Black	1
VC 70/87A	57-65	Very Fine Sand	0.1241	3.01	0.1111	3.17	*8 .5	12.9	05.6	2.705	2.039	39.6	1845	1.209	5Y 2.5/1	Black	11
VC 70/87B	0-8	Fine Sand	0.1638	2.61	0.1397	2.84	*88.8	07.2	04.0	2.666	1.954	44.0	1804	1.182	5Y 2.5/1	Black	2
VC 20/100	0-8	Very Fine Sand	0.0934	3.42	0.1022	3.29	76.1	19.7	04.2	2.669	1.947	43.8	1729	1.133	5Y 2.5/1	Black	3
VC 20/100	72-80	Fine Sand	0.1550	2.69	0.1560	2.68	*88.8	06.0	05.2	2.706	2.103	35.8	1875	1.229	5Y 2.5/1	Black	4
VC 279	0-8	Very Fine Sand	0.0825	3.60	0.1001	3.32	76.0	16.8	07.2	2.697	2.117	34.6	1896	1.242	5Y 2.5/1	Black	5
VC 279	83-91	Silty Sand	0.0652	3.94	0.0665	3.91	55.4	37.6	07.0	2.677	2.034	38.8	1804	1.182	5Y 2.5/1	Black	6
VC 0/200A	0-8	Silty Sand	0.0728	3.78	0.0764	3.71	57.1	37.8	05.1	2.661	1.995	40.6	1736	1.138	5Y 2.5/1	Black	7
VC 0/200A	78-86	Silty Sand	0.0738	3.76	0.9067	3.37	67.2	25.2	07.6	2.688	2.048	38.4	1789	1.172	5Y 2.5/1	Black	8
VC 0/200B	0-8	Sandy Silt	0.0367	4.77	0.0451	4.47	39.3	49.1	11.6	2.644	1.862	48.2	1698	1.113	5Y 2.5/1	Black	9
VC 0/200B	63-71	Very Fine Sand	0.0921	3.44	0.1081	3.21	*78.2	05.4	05.4	2.685	2.089	35.8	1830	1.199	5Y 2.5/1	Black	10

Notes:
(1) Shepard, 1954
(2) Measured by pycnometer
(3) Ratio: Velocity in sediment/Velocity in sea water at 23° C, 1 atm, and salinity of bottom water; in this case velocity is 1526 m/sec and salinity is 31.8 0/00
(4) Munsell Soil Color Chart
(5) Black color is due to decomposed organic matter
* Includes gravel fraction

5.0 DATA INTERPRETATION AND RESULTS

5.1 BATHYMETRIC MAP

Bathymetric data compiled during this survey were incorporated with existing bathymetric data (i.e. NOAA Bathymetry Map NOS 1711N-18B) to construct new bathymetric maps (Plates III(A) and III(B)) at a scale of 1:250,000 and with a 5-m contour interval. The new data were based on a sonic velocity of 1580 m/sec. No corrections were made for tides, sea-state, transducer depth, temperature, or salinity.

The new contour map (Plates III(A) and III(B)) confirms the existence of a very flat, shallow continental shelf. Water depths vary from 0 to 110 m; slopes along the coastline are generally less than 0.5 percent. Beyond the 90 m isobath, slopes are generally less than 0.02 percent. Although contour lines in the western portion of the study area (Plate III(A)) indicate a more irregular seafloor near the shoreline, the seafloor still must be considered very flat and regular.

5.2 GEOLOGIC STRUCTURE

A geologic structure map (Plates IV(A) and IV(B)) and two structural cross-sections (Plates VI and VII) were interpreted from the analysis of shallow and deep-penetration data gathered during the Discoverer program and during similar programs conducted by Marine Technical Services Company (MTS) and the United States Geological Survey (USGS). Cross Sections A-A' and B-B' (Plates VI and VII respectively) were constructed using 1976 USGS seismic-reflection records (Marlow and Cooper, 1980b) at a scale of 1:250,000 and the NOAA Discoverer (1980) air gun data.

Depths (D) were calculated using Marlow and Cooper's (1980b) equation

$$D = 1.266t + 1.033t^2 - 0.117t^3 \quad \ldots\ldots\ldots \quad (5\text{-}1)$$

where t is the one-way travel time in seconds and D is in kilometers. The following interpretation were made on the basis of these data.

5.2.1 <u>Basement Complex</u>

The surface of the basement complex (Plates VI and VII) was identified and mapped as the interface between the upper well layered sequence (Tertiary (?)), representative of relatively continuous deposition, and the lower sequence (Cretaceous and Jurassic (?)) with a typically noisy signature and few coherent reflectors. A high-amplitude continuous reflector marks this unconformity over most of the study area. Tertiary basin fill within the study area has been previously correlated (Marlow and others, 1980b) to comparably aged clastic and volcanic rock units on the Alaska Peninsula.

The edges of basins were defined at the sharp breaks in slope between the highs and lows in the basement surface. The east-west trending St. George Basin, which lies at the west-central edge of the study area, is the deepest structural basin in the area. The basin floor (basement surface) is approximately 5.1 km deep in the west and rises steeply on its eastern end to approximately 1.2 km. Both Amak Basin, located in the southwest, and Bristol Bay Basin, located in the northeast, are shallower structural basins with maximum depths of approximately 4.8 and 3.8 km, respectively. A basement high, the Black Hills Uplift, separates the Amak Basin from the Bristol Bay and St. George Basins. Shallow-penetration seismic profiles indicate that the Black Hills Uplift extends eastward and rises rapidly from an average depth of 1.0 km to 0.1 km near the Alaska Peninsula. A second basement high

(Plate VI) bounds the northern edge of St. George Basin. This high continues northward as a broad basement platform approximately 1.2 km below the seafloor surface.

5.2.2 Faulting

A number of faults can be identified within the study area. Correlations of fault traces are sometimes approximate because of the widely-spaced reconnaissance grids of the 1976 USGS (90-120 km) and 1980 NOAA *Discoverer* (10-15 km) cruises, and the lack of detailed coverage in the fault areas of the MTS data (Molnia and others, 1982). Nevertheless, based on the relative magnitude of offset and subsurface extent, the correlation of major fault segments appears good.

Separation on major faults is generally normal and increases with depth indicating that the faults formed early in the history of the area and have grown as time progressed. Many of these faults extend upward to near the seafloor and some are associated with surficial sags indicating activity during the Quaternary Period.

The greatest concentration of faults occurs along the southern edge of St. George Basin and the northeastern edge of Amak Basin in the North Amak Fault Zone (Plate IV(A)). These faults are sometimes less than a kilometer apart and form a zone of faults approximately 15 km wide in the area north of Amak Island to about 25 km wide along the western margin of the study area. Along the trace of the North Amak Fault Zone, the sense of displacement changes from downthrown block on the north in the St. George Basin area, to downthrown block on the south in the Amak Basin area. Differential basement formational irregularities may account for this rotational sense along the fault zone. This changing sense of displacement may also be the result of echelon fault segments which may have geometries unique to each of the two basins and may not be correlative along their length.

Major faults also are present along the southern edge of the Amak Basin and just north of the North Amak Fault Zone. These faults are normal faults that strike west-northwest similar to the North Amak fault. Minor faults of limited areal extent, which have much lesser offset than the major faults, are distributed over the entire area. The greatest concentrations of these faults occur at depth along the contact between the basement complex and sedimentary basin-fill (Plate VI). Minor faults are relatively rare in shallow portions of the basin-fill sequence. Surface faults were observed on both shallow- and intermediate-penetration data sets (Plates VIII(A) and VIII(B)). Rarely were any of these faults expressed by steep-sided surficial scarps, but almost all of them had surficial sag zones (Plate V). The locations of these relatively rare, surficial faults coincide with the greatest concentration of major faults as plotted on Plate IV(A) and IV(B).

Compressional folding was not observed in the study area. However, drape folds were observed in association with many fault elements.

5.2.3 Structural Cross-Section A-A'

Cross-Section A-A' (Plate VI) was prepared from the deep, intermediate and shallow penetration seismic data sets. This cross-section traverses southwest to northeast to south-central Bristol Bay Basin (Figure 5-1) along 1976 USGS CDP Lines 1 and 2 (Marlow and Cooper, 1980b), oblique to the major structural trends in the area. Major geologic features along the cross-section include Amak Basin, North Amak Fault Zone, Black Hills Uplift and Bristol Bay Basin.

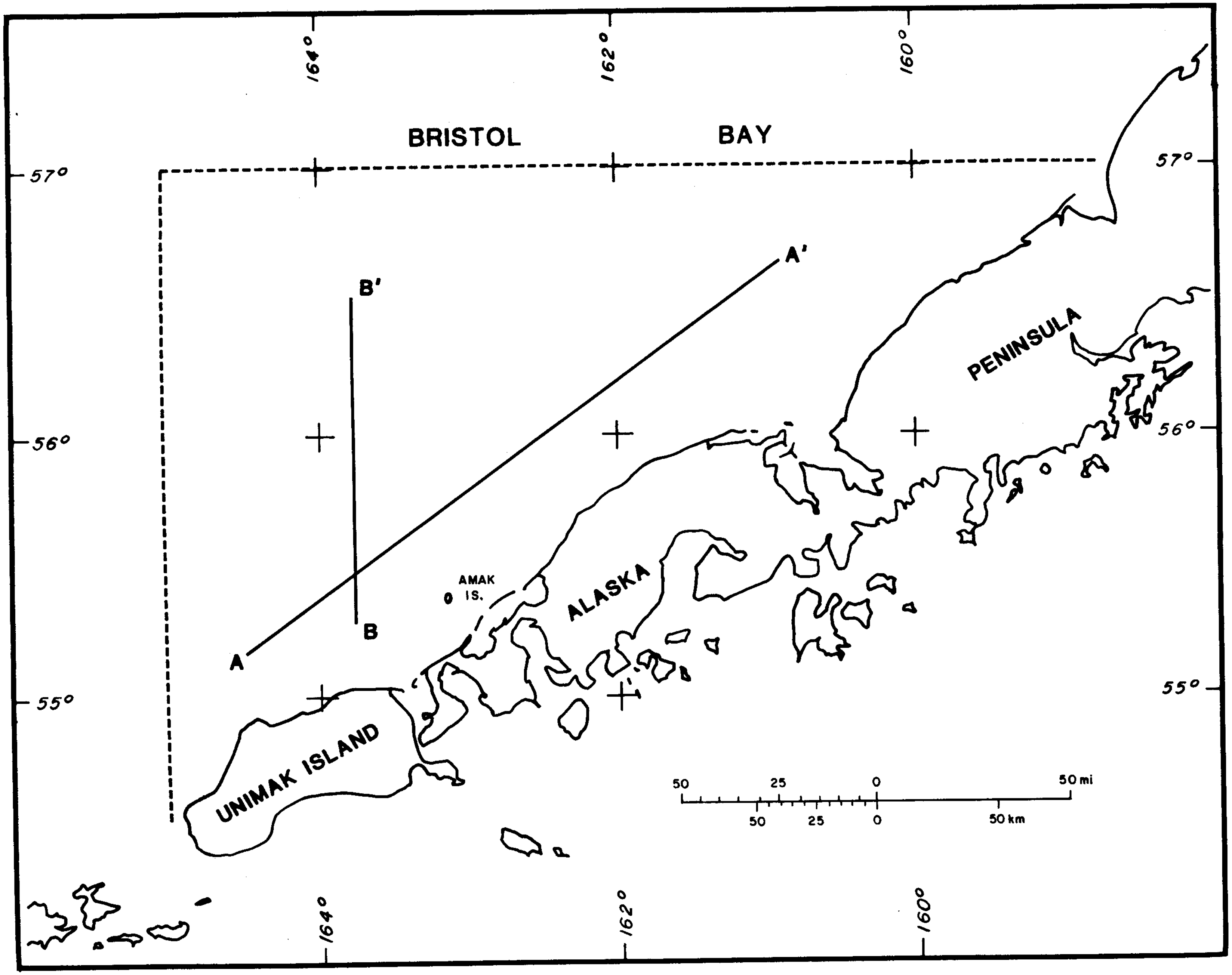

FIGURE 5-1 LOCATION MAP FOR CROSS-SECTIONS A-A' AND B-B'

From this cross-section the Amak Basin was interpreted as a Cenozoic (?) graben bounded on the north by the North Amak Fault Zone and Black Hills Uplift. Tertiary sedimentary fill within the Amak Basin exceeds 4.7 km (Shot Point 700). The Black Hills Uplift is a structural high of the Mesozoic (?) basement. This high rises to within an average depth of 750 m below the seafloor. An intensely faulted 3-km-wide area of the uplift rises to within 550 m of the surface.

The Bristol Bay Basin is a structural depression, 60 km wide, with a maximum Tertiary basin fill of 3.8 km (Shot Point 3600). The regularity and horizontality of the bedding combined with the paucity of large faults and folds, except at the edges of basin, indicate relatively continuous deposition in a fairly stable tectonic environment since early Tertiary time.

The apparent abundance of faults throughout the length of Cross-Section A-A' (Plate VI) is more a result of the orientation of the cross-section oblique to the structural fabric than to the actual abundance of faults. The only major faulting in the study region is the normal fault regime of the North Amak Fault Zone which forms the boundary between Amak Basin and the Black Hills Uplift (Plate VII).

5.2.4 Structural Cross-Section B-B'

Cross-Section B-B' (Plate VII) trends north-south (Figure 5-1) along the 1976 USGS Line 4 (Marlow and Cooper, 1980b) and 1980 Discoverer Line 1079 normal to the major east-west structural trends of the Bristol Bay region.

This cross-section shows the Amak Basin as a graben structure with over 4.7 km of Tertiary basin-fill (Shot Point 2400). The graben is approximately 30 km wide and bounded on the north by a set of major normal faults comprising the North Amak Fault Zone. Within the upper kilometer of basin-fill in the middle of the basin there are numerous minor normal "growth" faults which do not appear to extend to the basement.

Bristol Bay Basin, 20 km north of Amak Basin, is a crustal depression which may be the result of the tensional regime behind the Aleutian Volcanic Arc. However, Bristol Bay Basin is not a simple graben; its geometry appears to be controlled by numerous minor faults along the basement surface. Faulting within the basin appears to have occurred contemporaneously with desposition. Like Amak Basin, Bristol Bay Basin appears to have experienced nearly continuous deposition since early Tertiary time with Tertiary deposits reaching a maximum thickness of over 2 km (Shot Point 1000).

The cross-section shows that the Black Hills Uplift is covered by an average of about 800 m of Tertiary strata. Major faulting within the Black Hills Uplift is limited to its southern extreme, the North Amak Fault Zone. Other faulting within the area is generally limited to minor tensional faulting extending through basement and mid-Tertiary (?) units only. As noted previously, the Black Hills Uplift represents a Mesozoic basement structural high separating Amak and Bristol Bay Basins.

5.2.5 Late Quaternary Stratigraphy

The Late Quaternary geology of the Bering Sea Shelf, north of Unimak Island, and the southern end of the Alaska Peninsula, is shown on Plates VIII(A) and VIII(B). The upper Quaternary stratigraphy is generalized from seismic records and sediment samples. Generally, three stratigraphic units are found above a basal channel-fill unit. These units comprise the Wisconsinan (?) and Holocene (?) (late Quaternary) stratigraphic sequence.

Their combined thickness ranges from 0 to 20 m, as indicated by the isopachs on Plates VIII(A) and VIII(B). Generally, the thickest portion (20 m) is located northeast of Amak Island. General thinning occurs radially away from this location. The thickest occurrence and surrounding isopach configuration displays a somewhat east-west elongation.

The oldest Quaternary unit is interpreted on the basis of seismic signatures as a channel fill sequence. These sediments occur most prominently northwest of Port Moller. The thickness of this unit averages 25 m, with a maximum of 33 m. Because the upper surface of this unit is masked by the seismic bubble-pulse on intermediate-penetration seismic data, its thickness is uncertain. The approximate average depth below the surface in the Port Moller area is 8 m. An average strike of N 40 E and a dip of 0.6° NW was orthographically derived from the orientations of intersecting bedding planes at eight locations within the unit to give a general areal bedding orientation.

A thin, flat-lying, seismically transparent layer believed to be marine sand was recognized only in localized areas unconformably overlying the channel-fill unit described above. Above these two lower units is a thin, locally preserved unit of variable thickness. Core analyses show this layer to consist of moderately dense, very-dark-grey, medium-grained sand with thin interbeds of shell hash. An upper surficial sediment layer, ranging in thickness from 0 to 3 m, is composed of a seismically "transparent", nonindurated grey to very-dark-grey sand, representing modern detritus which is actively mixed by waves and currents.

Shell layers at depths of 7 and 10 cm below sea bottom (Sample Nos. 24 and 26; Station Nos. 1070/91 and 1070/87) were dated by ^{14}C analysis.

Resultant dates were 12,390$\pm$250 years B.P. and 11,729$\pm$245 years B.P. The calculated sedimentation rate for these cores, assuming uninterrupted deposition, is less than 1 cm/1000 years. This rate is considerably less than that suggested by Askren (1972), who estimated a sedimentation rate of 9 cm/1000 years, but is more consistent with the lower bound proposed by Gershanovich (1968), who estimated a rate of 2 to 30 cm/1000 year. The apparent low rate of sedimentation could be a result of the dated shell material being washed in from another area, or of removal of a portion of the overlying sediments during times of lowered sea level. Such an interpretation is suggested by the disarticulated broken nature of the shell material.

5.4 SEISMIC ENVIRONMENT

The general nature and distribution of regional seismicity was presented in Section 2. This section presents more detail on seismic aspects in the study region to provide a background for estimation of maximum credible earthquakes. The intent of this analysis is to provide a basis for preliminary evaluation of the possible adverse effects of earthquakes on geotechnical parameters in the study region. This analysis is based on data readily available at the time of the study so a more-detailed analysis of seismicity and engineering design parameters will be necessary for specific facilities as the area is developed.

Potential sources of earthquakes that might affect future facilities within the Northern Aleutian Shelf region are primarily the Benioff zone, the island arc, the back-arc graben-bounding fault zones (Amak, St. George), and other intrabasin faults. These earthquake sources are shown diagrammatically on Figure 5-2. Potential sources of large earthquakes such as the normal faults

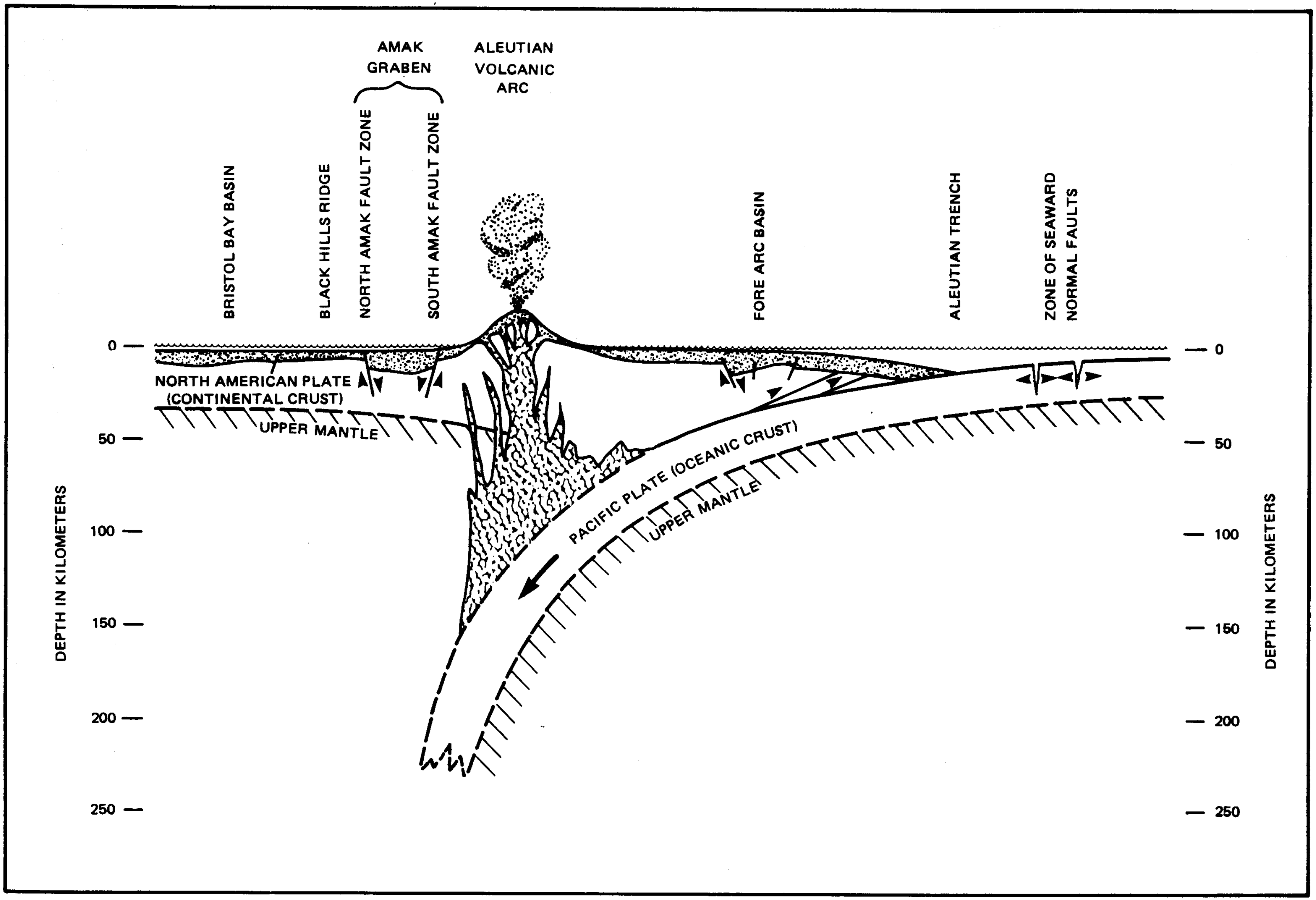

FIGURE 5-2 SCHEMATIC GEOLOGIC CROSS-SECTION OF NORTHERN ALEUTIAN SHELF REGION

seaward of the Aleutian Trench are not considered here because they are clearly not as significant as the nearby features which can generate nearer and larger earthquakes. Based on seismicity and geologic characteristics maximum earthquake magnitudes are estimated for each of these sources. The magnitudes of these earthquakes are surface-wave magnitudes (M_s) which tend to saturate above a magnitude of about 7.75. A moment magnitude scale would probably be a better indicator of the relative size of earthquakes above 7.75, but it is not used in this report because, as the M_s scale tends to saturate at the larger earthquakes, so does the strong ground motion in the near field. Because attenuation relations for strong ground motion developed by earthquake engineers generally use M_s magnitudes without corrections for magnitude saturation, saturation effects are included implicitly in the attenuation relations.

5.4.1 Earthquake Sources

The regional tectonic setting and seismicity of the study region are discussed in Section 2.4.2 and 2.4.3. In these discussions, it is pointed out that the primary cause of earthquakes and tectonic deformation in the Aleutian Island region is subduction of the Pacific lithospheric plate beneath the Bering-North America Plate. Figure 5-2 is a conceptual model of the subduction zone in cross-section and illustrates the geometric relationships of the Amak Basin, Black Hills Uplift, and Bristol Bay Basin to the subduction zone.

As discussed in Section 2.4.3, the vast majority of earthquakes are directly related to subduction of the Pacific Plate and occur along the subducted plate or in the crust directly adjacent to the trench. However, there are several shallow earthquakes on the Aleutian arc and behind the arc (Figure

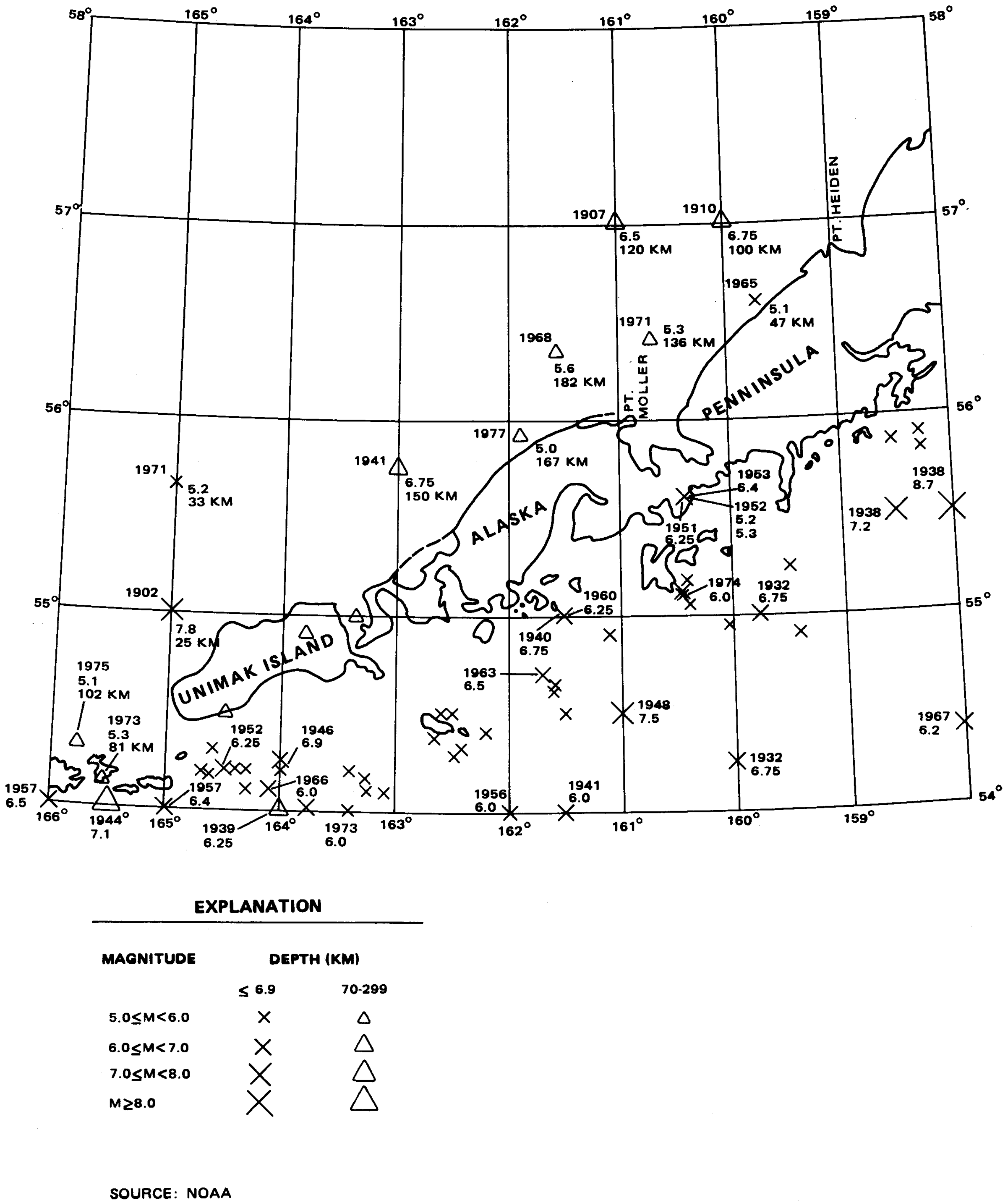

FIGURE 5-3 MAP OF MODERATE TO LARGE MAGNITUDE EARTHQUAKES IN THE NORTHERN ALEUTIAN SHELF REGION

5-3) which may be only indirectly related to the subduction process or which have no obvious relationship to subduction.

According to the NOAA earthquake catalog, in the back-arc area there have been ten shallow earthquakes recorded during the limited time span of the seismicity record (1953 to 1977). The largest of these back-arc earthquakes occurred in 1971 and had a magnitude of 5.2 (Figure 5-3). The largest events on the Aleutian arc were in the 4 to 5 magnitude range. The largest event in the entire region was the M_s 8.7 (Mw = 8.2) magnitude earthquake which occurred east of the Shumagin Islands in 1938 and which is believed to have been associated with the subduction zone. In 1902, a 7.8 magnitude earthquake occurred in the study region but its location in the back-arc region has been considered by most seismologists to have been only a rough approximation. The location of the event, as shown on Figure 5-3, has great uncertainty which could be attributable to minimal seismograph coverage in the early part of the century or possibly to seismic-velocity anomalies. It is generally believed that the earthquake was probably associated with the subduction zone. The large, young, normal faults bounding the Amak and St. George Basins documented during this study, however, may provide a potential source for large-magnitude earthquakes; consequently, it no longer may be possible to simply dismiss the 1902 event as a mislocated event.

According to Davies (1981), there are several earthquakes in the western part of the study area and the St. George Basin region which are not included in the NOAA catalog. These earthquakes are shown on Figure 5-4. The largest of these earthquakes occur in the vicinity of faults associated with the St. George Basin. The strong geologic similarties of the St. George Basin and the Amak Basin suggest that the earthquake potential is probably similar in

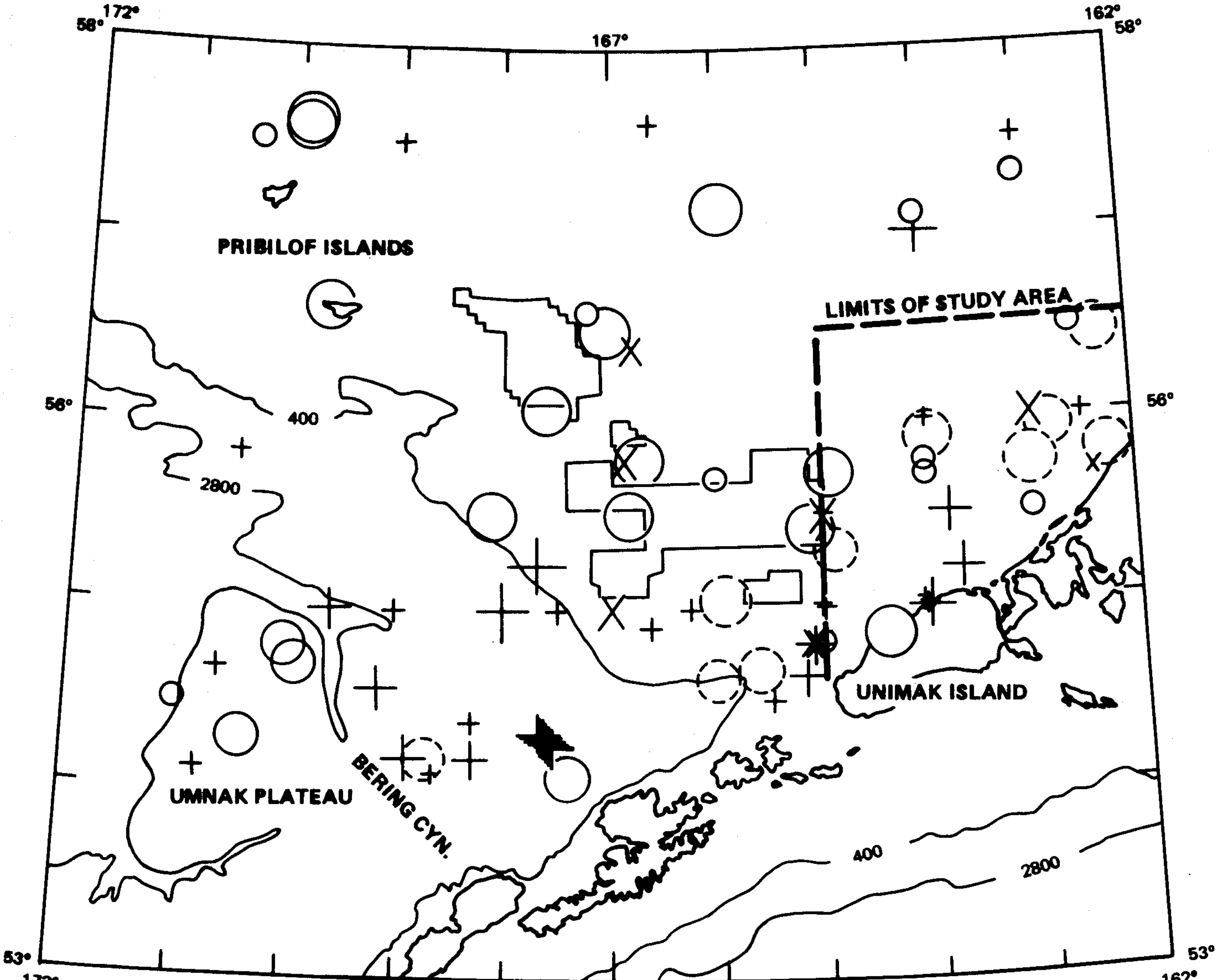

SOURCE: DAVIES, 1981
MINERALS MANAGEMENT SERVICE, 1982.

EXPLANATION

Eqicenter symbols are scaled by magnitude according to height (seconds of latitude) = 6.5 + 1.66 Mag.; crosses represent events with unknown depth; x's those with depths inferred to be shallow; solid circles, those known to be shallow ($Z \leq 75$ km); dashed circles, those known to be deep ($Z \geq 113$ km).

FIGURE 5-4 MAP OF EARTHQUAKES IN THE ST. GEORGE BASIN REGION, 1925 THROUGH 1978

both basins. The largest historic events in the vicinity of the St. George Basin appear to have been the magnitude 7.2 event which occurred in 1925 and intensity I_{MM} = X event which occurred in 1836 (Davies, 1981). Davies (1981) calculated probabilities based on a 22 years teleseismic record and found that the probability is about 11 percent that a randomly selected site within the St. George Basin region will experience strong ground motion in excess of 0.2 g within 40 years and is about 3 percent for 0.5 g.

5.4.2 Maximum Earthquakes

The maximum earthquakes which could be associated with the sources identified in the previous section are listed in Table 5-1. These estimates are based on records which are only about a hundred years long, and this may be too short to characterize, adequately, the earthquake potential. Uncertainties in magnitude estimates arise because the time period between recurrence of the maximum earthquakes for some tectonic features may be longer than the seismic record. To help resolve these uncertainties, empirical fault-length/earthquake-magnitude relationships based on worldwide data and geologic/tectonic relationships in similar tectonic regimes in other areas were examined. In this review it is noted that the maximum earthquake associated with the Benioff Zone is well established compared to the other sources and is fairly well restricted in location relative to any sites in the study area. However, maximum earthquakes associated with the other features, such as volcanoes, shallow faults on the arc, and behind-the-arc grabens are much more speculative.

5.4.2.1 Aleutian Subduction Zone

The maximum earthquakes for the subduction zone are estimated at M_s 8 3/4 and 7 3/4 for shallow and deep source zones, respectively. The 8 3/4 event is

Table 5-1 Estimates of Maximum Earthquakes in the Northern Aleutian Shelf Region

Earthquake Sources	Maximum Earthquake (M_s)
ALEUTIAN SUBDUCTION ZONE	
Thrust Event-Shallow (above 40 to 50 km)	8 3/4
Thrust or Normal Event-Deep (below 40 to 50 km)	7 3/4
MAJOR GRABEN-BOUNDING FAULTS	
North Amak Fault Zone	7 3/4
OTHER LARGE BACK ARC FAULTS	6 1/2
ALEUTIAN ARC	
Volcanic Event and Associated Faults	6
RANDOM EARTHQUAKE	5 1/2

based on the occurrence of a similar-size event in 1938 (M_s=8.7). Such magnitudes are consistent with earthquakes in other subduction zones throughout the world although they appear to be more frequent in the Alaska-Aleutian zone.

The sudduction zone was divided into shallow and deep source zones based on the premise that earthquakes may be characteristically smaller at great depth where there is no direct interface between rigid, brittle crusts of the two colliding plates. The boundary between the two zones is gradational and should be on the order of 40 to 50 km deep (Figure 5-2) based on typical crustal thicknesses in the area and throughout the world in similar environments. The maximum earthquake in the deeper zone is estimated at M_s 7 3/4 because, historically, earthquakes at depth are generally no larger than this magnitude.

5.4.2.2 Major Graben-Bounding Faults

The most significant uncertainty, with respect to earthquake potential in the study region, appears to lie with the normal faults bounding the major structural basins such as the Amak, St. George, and Pribilof grabens. These features may have originated during the late Mesozoic or early Tertiary in response to rifting along a transform boundary (Marlow and Cooper, 1980a), but faults along their margins have moved repeatedly throughout the Cenozoic Era and probably as late as the Holocene Epoch suggesting that they are active at the present time.

These normal-fault-bounded grabens appear to indicate a tensional stress field behind the volcanic arc although a component of lateral movement cannot be ruled out. A tensional stress regime is supported by young alkali basaltic volcanoes in the distant back-arc region which appear to be associated with normal faults and other tectonic features which suggest regional tension oriented roughly north-south (Nakamura and others, 1977). The inferrence of tensional stresses behind the volcanic arc suggests that the grabens are back-arc basins similar to those found behind other volcanic arcs around the globe. If so, earthquake magnitudes should be similar to or compatible with earthquakes in these other back-arc basins.

To determine the characteristics of the back-arc basins, a review of back-arc basins was performed. A complete summary of this review is beyond the scope of this report; however, discussions by Uyeda (1977), Uyeda and Kanamori (1979), Zonenshain and Savostin (1981), and Hsui and Toksoz (1981) suggest that back-arc basins throughout the world can be grouped into the following five major categories:

1) those with continental crust (Peru-Chile, Middle America, Basin and Range province of the western U.S., Alaska-eastern Aleutians, Java-Sumatra);

2) those composed of trapped oceanic crust (western Bering Sea, Caribbean);

3) those with active back-arc spreading (Lau Basin, Marianas, Scotia Sea);

4) those with inactive back-arc spreading (Grenada-Antilles Trough, Sea of Japan, southern Okhotsk); and

5) those with oblique spreading or "leaky" transform faults (Andaman Sea).

Not all investigators agree on which back-arc basins fit into which category, and it seems that several back-arc basins have characteristics of more than one.

In the search for modern analogs of the east Aleutian-Alaska Peninsula region, the following parameters were considered necessary similarities: 1) an active volcanic arc, 2) oceanic crust being subducted under continental crust, and 3) tensional faulting (grabens) behind the volcanic arc. Review of the subduction regimes throughout the world revealed that there are no exact analogs to the Aleutian regime. Most subduction zones fulfill the first criterion; only a few fulfill the second (Java-Sumatra, Japan, western North America, Middle America, and South America); and none fulfill the third criterion very well. The western United States has elements of back-arc grabens in the Great Basin but no longer has the arc; the extensional back-arc region of Japan may have involved more fundamental crustal spreading rather than graben formation, and now appears to be relatively inactive; the tectonic evolution of Java is remarkably similar to the Northern Aleutian Shelf, but Quaternary tectonics in the Java back-arc region are poorly understood and available information is inadequate to construct a soundly based tectonic model.

In addition to the above criteria, seismicity characteristics of back-arc regions were also examined. Typically island arcs have shallow seismicity behind the island arc which forms trends that may be subparallel to the forearc belt of seismicity along the trench. These back-arc seismic events are few in number compared to the forearc region, but commonly include events exceeding magnitude 5 (for example, Japan, south Okhotsk, Java). Apparently the back-arc seismic belts represents a variety of tectonic regimes. In Japan shallow back-arc earthquakes have exceeded magnitude M_s 7 1/2 but focal mechanisms and geologic data indicate reverse faulting; in the south Okhotsk Basin (Kuril back-arc) the focal mechanisms show reverse and normal displacements with strike-slip components (Baranov and Lobkovskii, 1980); behind Java, earthquakes have reached magnitude 6.8 but the tectonic situation is poorly known and no focal mechanism solutions have been determined. According to

Katili and Soetadi (1971), Pliocene and Pleistocene strata in the Java back-arc region are folded and faulted, and a number of the back-arc faults and flexures have large vertical displacements of possible Quaternary age. The available data, however, are not sufficient to confirm whether these basins are similar to those in the study area. Although seismicity is not abundant in the Java back-arc region, there have been several events larger than magnitude 6. The depths of these earthquakes are poorly known but they are crustal events, like those in the Aleutian study area, and most likely are not associated with the Benioff Zone, which is 400 to 700 km deep below the crust where these basins occur.

Another possible analog is the Great Basin, located in the western United States. Although there is no modern subduction zone directly associated with the Great Basin, faults there are caused by tensional forces that appear to be generated by mechanisms similar to those behind some island arcs (mantle convection and upwelling). Because the magnitude of an earthquake is largely a function of rupture area and stress drop, it seems plausible that similar faults, even though they occur in somewhat different tectonic regimes, may generate earthquakes of similar magnitude as long as fault-plane rupture areas are similar in size. Because the graben-bounding faults in the Great Basin are of the same type and size as those in the study region and have generated large events in historic time (1915 - 7.6, 1954 - 7.1, 1932 - 7.3), they may provide an indication of the size of earthquakes possible on major faults bounding the grabens in the Northern Aleutian back-arc region.

As discussed above, the major grabens on the Northern Aleutian shelf do not conform precisely to any existing back-arc basin, so it is difficult to assign earthquake magnitudes based on a comparison to these regions. However, comparison of the size of normal faults that have been associated with large historic earthquakes in other parts of the world indicate that large earthquakes are possible on the major graben bounding faults north of the Aleutians. This is supported by the occurrence of the M=7.2 earthquake which occurred in the vicinity of the St. George graben. Based on these parameters, a maximum earthquake of about M_s 7 3/4 is postulated for major graben-bounding faults in the study area. This is believed to be a very conservative but necessary estimate to ensure that the subsequent engineering analyses account for all plausible conditions. It should also be noted that the recurrence intervals on these types of earthquakes can be very long, on the order of a few thousand years (Wallace, 1977; Schell and others, 1981; Schell, 1982), and therefore, the occurrence of such an event is quite remote during the life of facilities contemplated for the present phase of oil exploration.

5.4.2.3 Other Large Back-Arc Faults

Seismic-reflection data reveal a myriad of faults in the back-arc region, but understanding the nature of these faults is difficult based on the present, widely spread data. Shallow and intermediate-penetration data reveal faults near the surface (Plates V(A) and V(B)). Some of these appear to be growth-type faults related to the subsidence and gravity effects within the basin-fill sediments. As such, they have no connection to basement-involved deformation and probably do not represent a potential source of large earthquakes. Earthquakes in the Gulf of Mexico region where these types of faults are common are generally less than magnitude 6.

The relation to basement is not clear for some other faults in the back-arc region, and some of them appear to have significant lengths. Fault-length/

earthquake-magnitude relationships (Slemmons, 1977) suggest that earthquakes in the 6 to 6 1/2 magnitude range may be possible.

5.4.2.4 Aleutian Arc: Volcano and Associated Faults

Earthquakes associated with the Aleutian Arc may be caused by both volcanoes and fault movements. There are three primary sources of these earthquakes: 1) from the actual volcanic explosion, 2) from fault movements caused by expansion and contraction of the rocks surrounding the magma chambers, and 3) from sympathetic movements on nearby faults. Based on worldwide historic data, the first type does not seem capable of generating large earthquakes, but the second and third types may.

The largest earthquakes known to be associated with volcanism occurred in 1) Hawaii in 1975 where a magnitude 7.2 earthquake accompanied an eruption of Mauna Loa, and 2) Japan in 1914 with a magnitude estimated at 7. Hawaii is a rather unique tectonic environment, and it is not clear whether it should be considered as an analog of the Alaska-Aleutian subduction regime. The 1914 Japanese earthquake is poorly documented, and hence, is also of questionable use. Generally earthquakes associated with volcanic activity are no larger than magnitude 5 to 6. The largest historic event in the site region possibly associated with volcanism had a magnitude of less than 5. Based on these parameters, the maximum earthquake associated with volcanism in the site region is estimated at 6. This is believed to be a reasonably conservative estimate but is probably not as conservative as the estimate of the maximum event associated with the major graben-founding faults.

Fault movement caused by sympathetic movements of nearby faults is subject to considerable uncertainty in the Alaska Peninsula - Unimak Island region due to lack of detailed geologic studies. Beikman (1975) shows several northeast-southwest trending faults along the southern coast of the Peninsula between Pavlof Bay and the Shelikof Strait. The shortest fault is about 40 km long; the longest one is about 70 km long. These faults do not cut Quaternary strata. On Unalaska Island, east-west and northwest-southeast trending faults cut Quaternary volcanics but these features are all relatively short (about 15 km).

Assuming that there are no major late Quaternary faults on the Aleutian Arc adjacent to the study area larger than those already mapped, the magnitude 6 earthquake postulated for the volcanogenic event should be sufficiently conservative to account for fault-related earthquakes.

5.4.2.5 Unknown Earthquake Sources - Random Earthquake

The earthquake hazard analysis must also consider a maximum random earthquake because earthquakes in the back-arc region do not appear to be restricted to the major grabens. However, the maximum random event need not be large because the major tectonic features in the area, the ones capable of generating large earthquakes, are known (Plates V(A), V(B), VI, VII and Figure 5-4). The source of random events could be faults, such as the small growth faults seen on geophysical profiles (Plates IV(A), IV(B) and VII) or faults that are too small or too deep to have been detected by the geophysical survey.

A reasonable random earthquake magnitude is estimated to be about a magnitude 5 1/2 event. This is consistent with earthquakes which have occurred in the region historically but cannot be associated with any known geologic structure.

5.4.3 Earthquake Ground Motions

Peak ground accelerations and scaled time histories were determined for the study area based on the probable and maximum earthquakes postulated for the region. These postulated events were obtained from an evaluation of the tectonics and the seismicity discussed in Sections 2.4.2, 2.4.3, 5.4.1, and 5.4.2. The strong motion accelerograms recorded in Japan and the United States were used to estimate the peak ground accelerations. Representative time histories were selected from this collection of recorded accelerograms and published artificial accelerograms. These time histories were scaled to the peak ground accelerations and subsequently used in the liquefaction analyses presented in Section 5.6.

The recommended ground motions reflect current understanding of the earthquake potential in the Northern Aleutian Shelf region and are considered adequate for liquefaction assessments on a regional scale. The motions are not intended for design purposes. More-detailed studies would be required to determine design criteria for specific sites.

5.4.3.1 Probable and Maximum Earthquakes

Based on the interpretations of the tectonic and seismological data, probable and maximum earthquakes were postulated for the study area. As summarized in Table 5-1, the largest earthquakes were postulated for the Aleutian subduction zone and the North Amak Fault Zone. The Aleutian subduction zone was assigned a magnitude M_s 8 3/4 shallow event and a magnitude M_s 7 3/4 deep event; the North Amak Fault Zone was assigned a magnitude M_s 7 3/4.

The maximum magnitude assignments for the Aleutian subduction zone were also considered probable events because of the frequent occurrence of large magnitude earthquakes within this zone. Although the North Amak Fault Zone and other large back-arc faults were judged capable of producing large-magnitude earthquakes (see Section 5.4.2 and Table 5-1), the seismicity in the region and in similar tectonic environments throughout the world suggests that the recurrence intervals of large earthquakes in the back arc regions of subduction zones is long. Thus, earthquakes likely to occur on this feature during the life of the expected facilities would be small. For this study only maximum earthquakes were considered for the seismic sources in the study area. This conservative assumption should be noted when interpreting the results of this study.

5.4.3.2 Peak Ground Accelerations

Only three strong-motion accelerograms recorded in Alaska have been processed (USGS, 1976 and 1978). Two were recorded at the western tip of the Aleutian arc (May 2, 1971, M =7.0); one was recorded in eastern Alaska (July 30, 1972, M_L=7.0). Numerous strong-motion accelerograms recorded during earthquakes originating in the subduction zone along the coast of Japan have been processed and are available. Because similar tectonic conditions exist along the Aleutian arc near the study area, these Japanese records are well suited for estimating ground motions from earthquakes in the Aleutian subduction zone.

A number of the Japanese accelerograms were obtained and processed (Mori and Crouse, 1981), and an attenuation relationship based on these data was developed to estimate peak ground accelerations in the study area from earthquakes originating in the Aleutian subduction zone. The relationship expressed the peak ground acceleration in terms of earthquake magnitude and hypocentral distance. Similar types of attenuation relationships have been developed with western U.S. accelerogram data. These relationships were used to estimate peak ground accelerations for the earthquakes originating within the study area. The implicit assumption in using these attenuation relationships is that the attenuation of ground motion from earthquakes in the Aleutian subduction zone and shallow earthquakes within the study area is very similar to ground-motion attenuation in Japan and in the western U.S., respectively.

The results of these studies indicate that the peak ground acceleration would be approximately 0.1g for all locations within the study area due to either the shallow (M = 8 3/4) or deep (M = 7 3/4) earthquakes postulated for the subduction zone. Therefore, ground motions of long duration, with peaks around 0.1g, should be considered likely during the useful life of the lease areas. These motions also represent the maximum conditions from earthquakes in the Aleutian subduction zone because these postulated earthquakes are also the largest events that could reasonably occur.

The peak ground accelerations due to the occurrence of the maximum earthquake postulated on the seismic sources within the study area (Table 5-1) are shown in Figure 5-5. These accelerations vary from 0.4g to 0.7g for locations near the North Amak Fault Zone and diminish to 0.1g for more distant locations. Ground accelerations on the order of 0.1g to 0.2g can be expected near small magnitude (M=5 1/2) random events, which have been assumed as capable of occurring anywhere within the study area.

5.4.3.4 Time Histories

The accelerograms recommended for the liquefaction analyses are listed in Table 5-2. Because no accelerograms have been recorded during great earth-

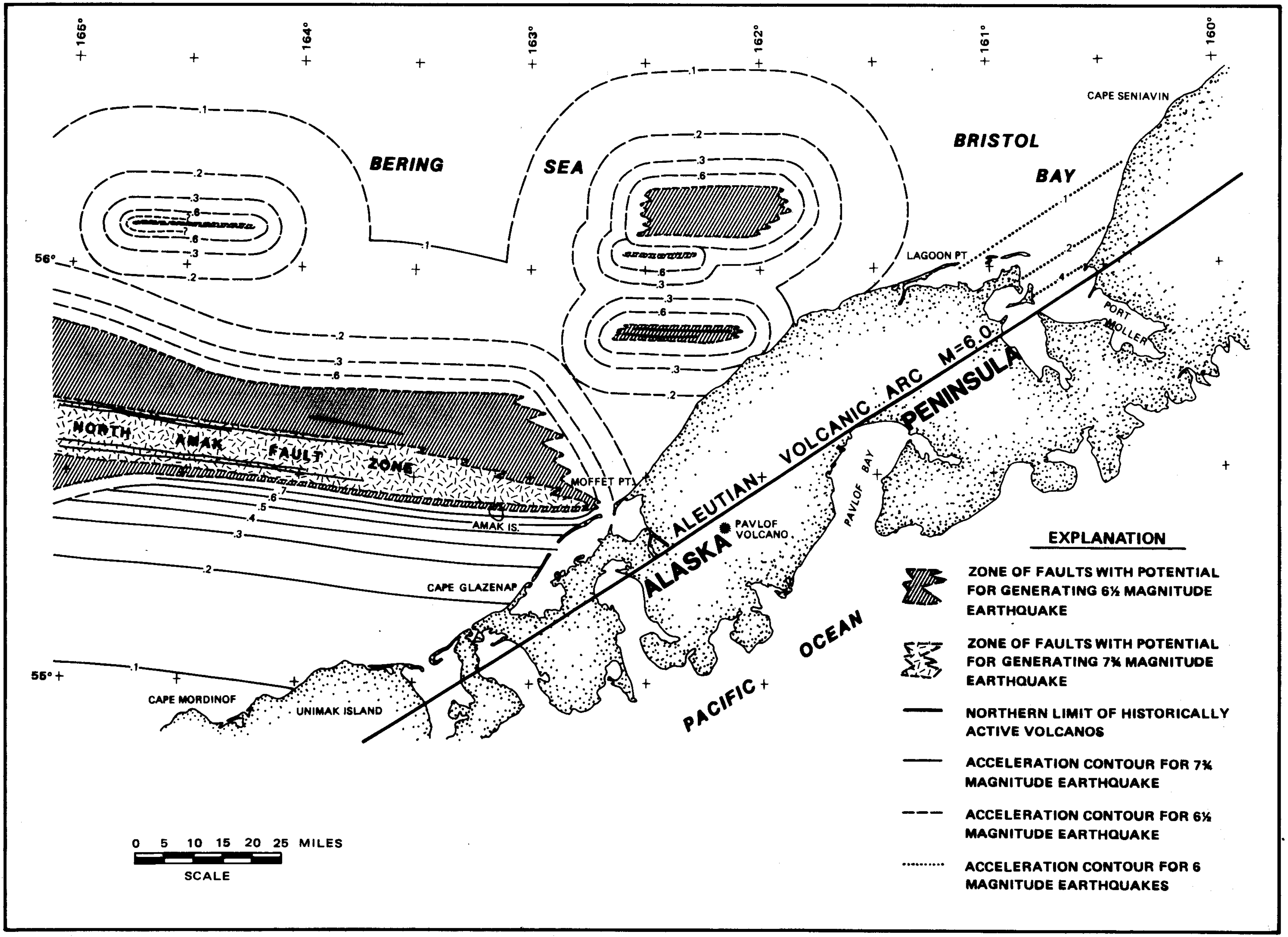

FIGURE 5-5 SOURCES OF POSTULATED MAXIMUM EARTHQUAKES, NORTHERN ALEUTIAN SHELF REGION

Table 5-2 Recommended Time Histories for Earthquake Sources

Earthquake Source	Earthquake Magnitude	Recommended Time History
Aleutian Subduction Zone	8 3/4	A-1 (Jennings and others, 1968)
Major Graben-Bounding	7 3/4	1952 Taft 1940 El Centro
Other Large Back-arc Faults	6 1/2	1971 Holiday Inn 1979 Imperial Valley Array No. 8
Aleutian Arc	6	1966 Parkfield No. 5
Random Event	5 1/2	1957 San Francisco State Bldg. 1941 Long Beach Public Utilities

quakes (M>8), the Caltech artificial earthquake Accelerogram A-1 (Jennings and others, 1968) was selected for the magnitude 8 3/4 event in the Aleutian Subduction Zone. Accelerogram A-1 has frequency characteristics commonly found in motions recorded on deep alluvial sites. Furthermore, its duration is representative of the duration of strong shaking to be expected from an earthquake of this magnitude.

The 1940 El Centro accelerogram, suitably scaled, was selected to approximate shaking near (within about 20 km) magnitude 7 3/4 earthquakes on the North Amak Fault Zone. The properly-scaled 1952 Taft accelerogram which was recorded about 42 km from the White Wolf fault also approximates the shaking at distances greater than about 20 km. Neither accelerogram should be used outside their applicable distance range.

The same criterion applies to the records selected for the magnitude 6 1/2 events for other possible large faults in the back-arc area. The Imperial Valley Array No. 8 accelerogram was recorded approximately 4 km from the fault rupture of the 1979 Imperial Valley earthquake. Therefore, this record is to be used at distances near (within 5 km) the other large back arc faults shown in Figure 5-5. The Holiday Inn accelerogram, recorded about 9 km from the fault rupture of the 1971 San Fernando earthquake, should be used, after scaling, to approximate the shaking at distances greater than 5 km from the fault zones. The records selected for the magnitude 6 and 5 1/2 events can be used at any distance provided they are properly scaled.

As noted above, the recommended accelerograms will have to be scaled to obtain the proper peak accelerations. By definition, the scaling factor for each recommended accelerogram is the ratio of the peak ground acceleration estimated for a particular location in the study area to the peak acceleration of the recommended accelerogram. For example, the peak acceleration estimated at any location in the study area due to the magnitude 8 3/4 earthquakes is 0.1g. Since the peak acceleration for Accelerogram A-1 is 0.385g (Jennings and others, 1968), the scaling factor applied to this record is 0.1/0.385 = 0.26. The peak ground accelerations for the other maximum earthquakes can be obtained from Figure 5-5 and used to obtained the proper scaling factors for the other recommended time histories.

5.5 SEDIMENT CHARACTERISTICS

The results of the geological laboratory studies were used to provide a detailed description of the upper 1 to 2 m of sediment in the study area. Detailed discussions of the cores, as well as grain size, mineralogy, carbon content and engineering properties are provided in the following paragraphs.

5.5.1 Core Descriptions

Radiographs were taken of five vibracores to assess stratigraphic relationships, the presence of bioturbation, location of pebbles, and coring disturbance. Core locations and descriptions are presented in Appendix III.

Cores were generally bioturbated throughout their length and showed minimal bedding. Evidence of bioturbation included numerous discrete burrows, and more commonly, complete homogenization of the sediment with total absence of internal structure. Subrounded, 4-mm-long clasts were commonly observed throughout the cores. Because there is no evidence for significant Holocene glacial activity in the region, it is doubtful that these particles are the result of ice rafting. Rather they probably represent fecal pellets.

Radiographs indicate that the top 5 to 15 cm of sediment in most cores appears less dense and less well compacted than the rest of the core. This may be due to a higher water content in the surficial sediment and to almost annual storm reworking of this upper layer. Sample No. 58 (Station 1270/175) is different from all of the other cores in that its radiograph shows two well-stratified, non-bioturbated units at 15 to 23 cm and 120 to 130 cm. Specific conditions responsible for the preservation of these horizons are unknown.

Four cores have shell layers averaging about 2.5 cm in thickness. Each of these cores was collected from a water depth of approximately 90 m. The shell layers, found 50 to 90 cm beneath the sediment surface, may represent a storm lag deposit. Attempts to date these layers did not result in useable radiometric data.

5.5.2 Grain Size

The results of grain-size analyses indicate that most surficial sediments are silty sands and sands (Figure 5-6). Appendix I contains calculated grain size data and computed Folk (1980) sediment texture parameters. Analyses showed a mean grain size (M_z) distribution similar to that of Sharma (1975, 1979). Close examination of the relationship between individual samples, however, revealed a much more complicated grain-size distribution (Figure 5-7).

The complex sediment texture within the study area is attributed to four factors: 1) water depth, 2) currents, 3) shelf morphology, and 4) modern source areas. The water depth of the area is important in determining the effective wave base. This is the depth at which storm-produced waves can transmit their energy to the sediment. The Bering Sea is one of the stormiest

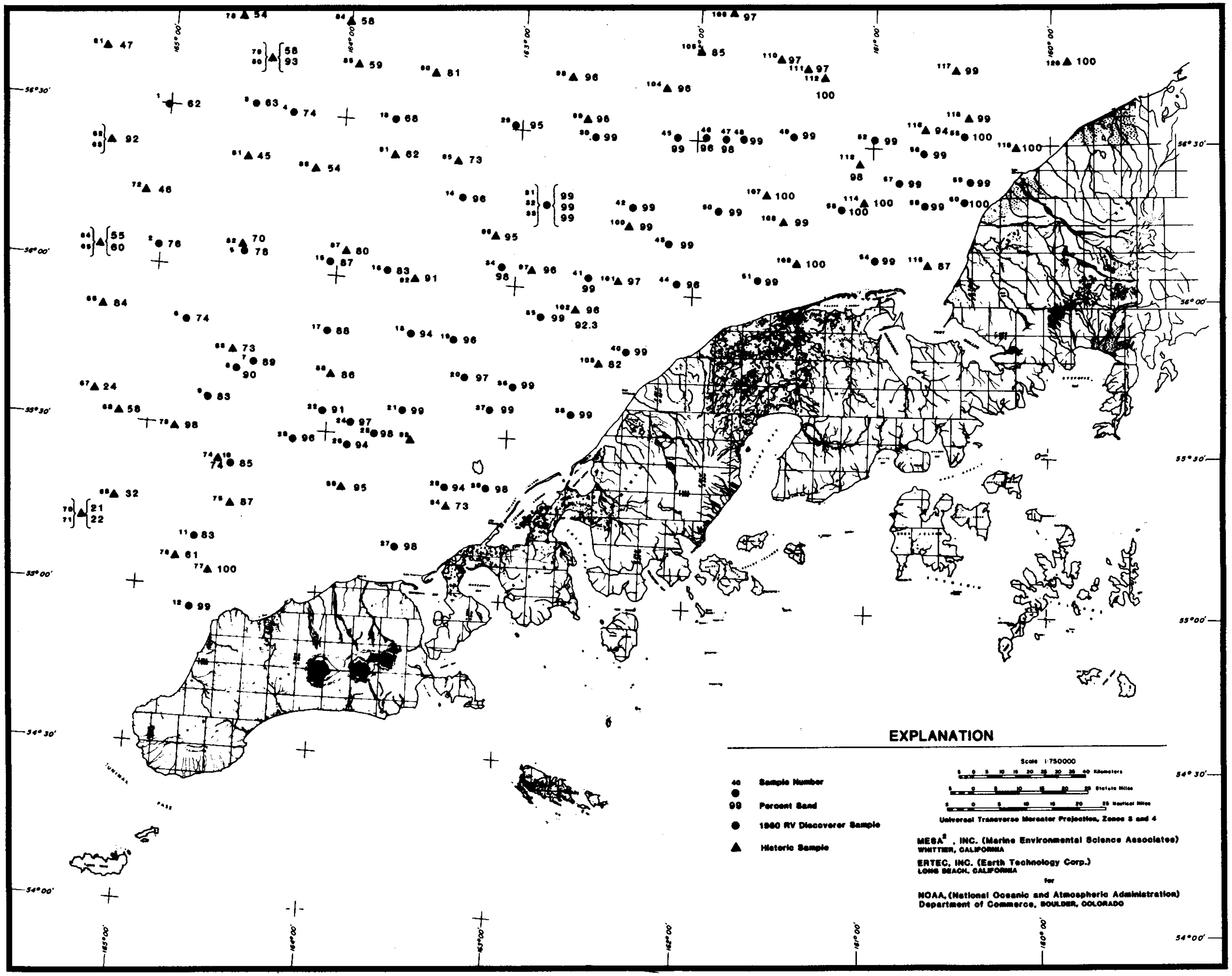

FIGURE 5-6 PERCENT SAND IN SURFACE SEDIMENTS

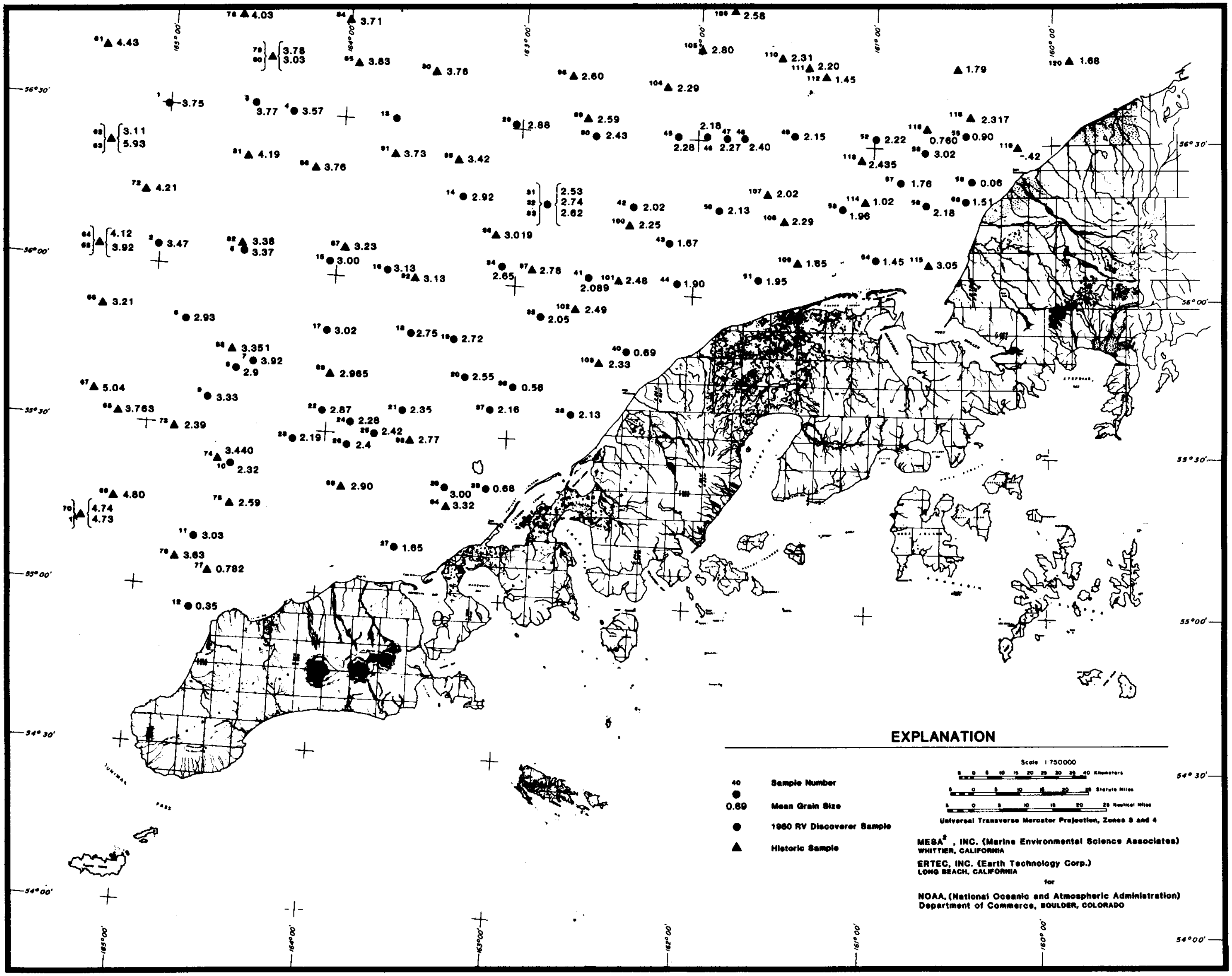

FIGURE 5-7 MEAN GRAIN SIZE OF SURFACE SEDIMENTS

regions of the world. Waves have an average height of 2 m, a period of 6 sec, and lengths of 50 m (Askren, 1972). The annual maximum storm waves predicted from synoptic surface wind charts have a height of 10 m (Sharma and others, 1972). By using Lamb's equation for estimating maximum horizontal bottom current velocity (Lamb, 1879), Askren determined that the maximum depth of wave-induced sediment transport in Bristol Bay is approximately 100 m. This suggests that the entire area is affected by storm-wave agitation.

Storm-wave-generated bottom agitation causes sediments finer than a certain size to erode leaving behind coarser size sediments. After repeated movements and depositions, each grain reaches a theoretical equilibrium position. The effects of this transport can best be seen in the mean grain size distribution within the study area. Sediments within Bristol Bay generally decrease in mean grain size with increase in water depth. This trend suggests that the mean grain size of the sediment has reached a crude textural equilibrium with prevailing conditions. This is in contrast to many other continental shelves throughout the world which still show sediment distribution patterns which indicate that they are relects from times of Pleistocene lower sea level.

Sediment standard deviation (sorting) also reflects the influence of wave activity, plus the modifying influences of currents, shelf morphology, and source area (Figure 5-8). Sediments with a mean grain size of approximately 2.5 phi (equivalent to 0.18 mm) are the best sorted, as would be expected from Inman's predictive hydrodynamic studies (Inman, 1949). The coarser material near-shore (recent sediment input) as well as the finer sediments in deeper water, where less wave influence exists, have the poorest sorting.

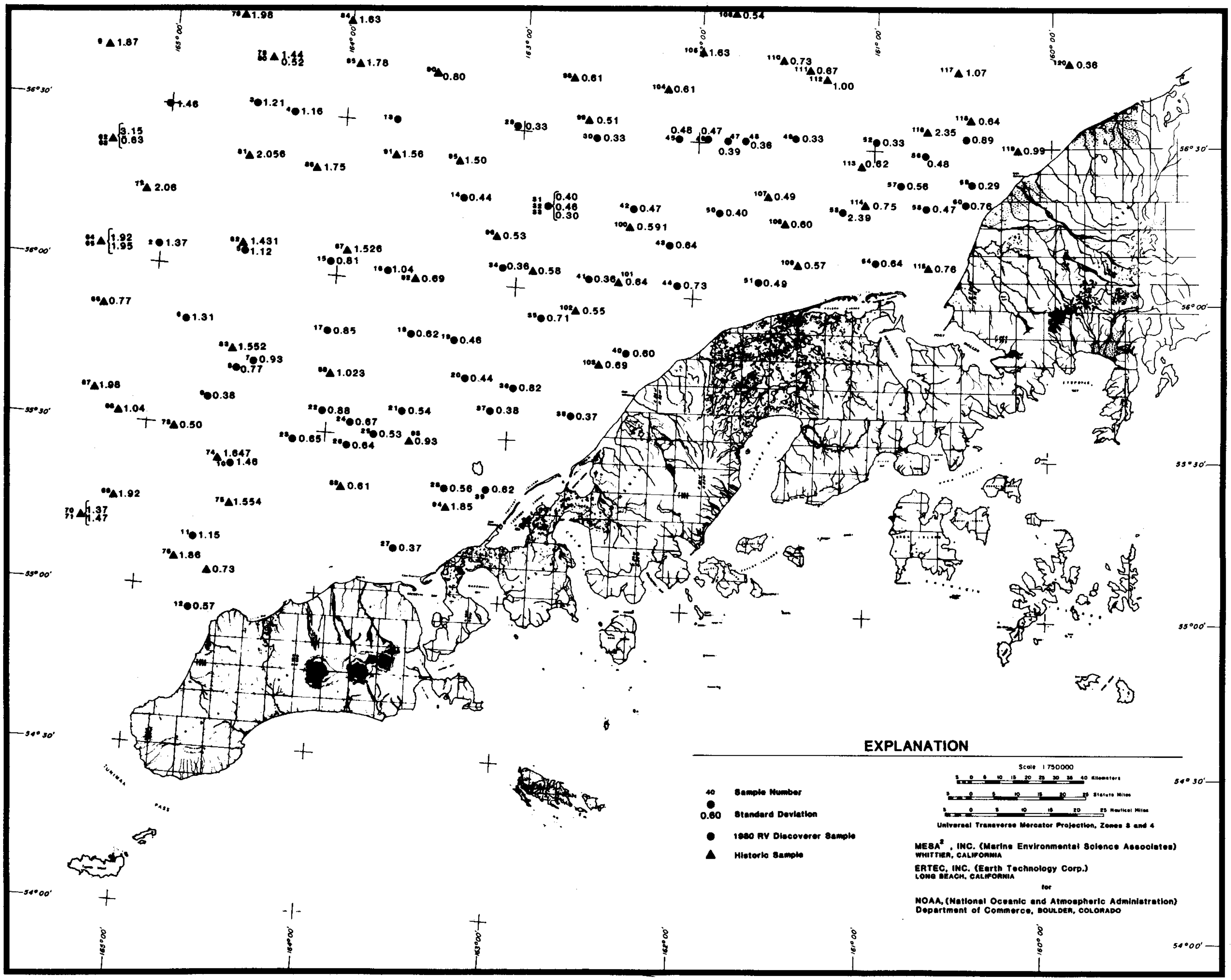

FIGURE 5-8 GRAIN SIZE STANDARD DEVIATION OF SURFACE SEDIMENTS

Skewness (Figure 5-9) reflects the progressive sediment fining offshore. Coarse sediments are located over most of the area sampled during the Discoverer program, whereas fine-skewed sediments are concentrated in samples with mean grain size less than 2.5 . Kurtosis (Figure 5-10) increases and reaches a maximum in sediments with a mean grain size of 3.0 phi (0.125 mm).

5.5.3 Mineralogy

Mineralogic studies indicate that five minerals or mineral groups compose the majority of southeastern Bering Sea sediments. These are quartz, feldspar, hypersthene, hornblende, and the opaque minerals (Figures 5-11 to 5-16). Table 4-1 summarizes results of the microscopic mineral investigations.

Euhedral grains of each mineral were common, causing the sediments to appear angular to sub-angular with poor sphericity. Two types of hornblende were observed: 1) common hornblende, strongly pleochroic in green and brown; and 2) basaltine, a type of hornblende common in basalts or hornblende andesites, pleochroic in brown and dark brown.

The primary source of surface sediment in Bristol Bay appears to be the Alaska Peninsula and Unimak Island. The presence of unworn and unaltered hypersthene and opaque minerals suggests a nearby source of basic and ultrabasic rock. Both the Alaska Peninsula and Unimak Island are composed primarily of volcanic flow and volcanoclastic rocks, which are mostly porphyritic basalts and andesites. Areas of intrusive quartz diorite and hornblende-biotite granite are also present (Kennedy and Waldron, 1955; and Waldron, 1961; Burk, 1965).

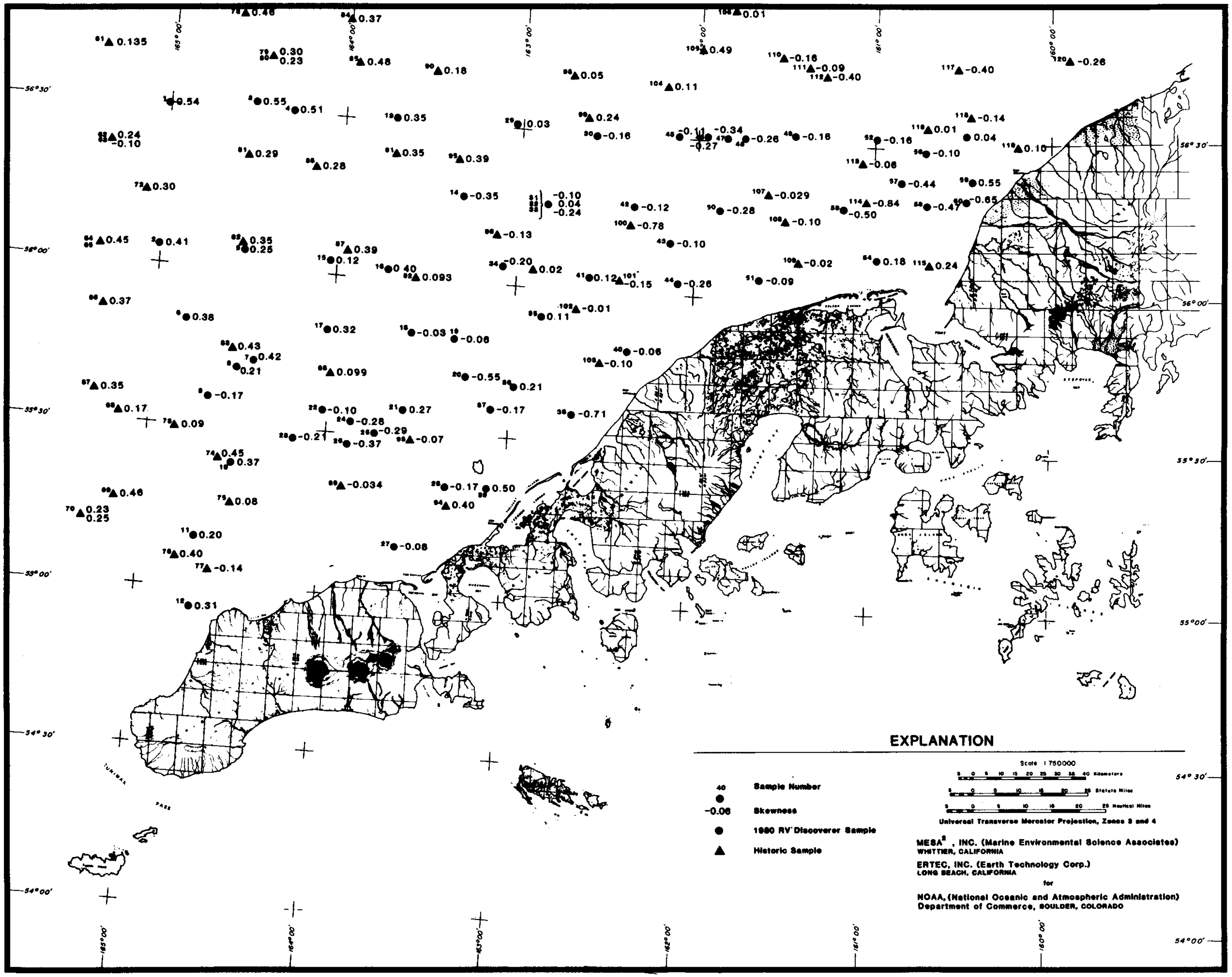

FIGURE 5-9 SEDIMENT SKEWNESS

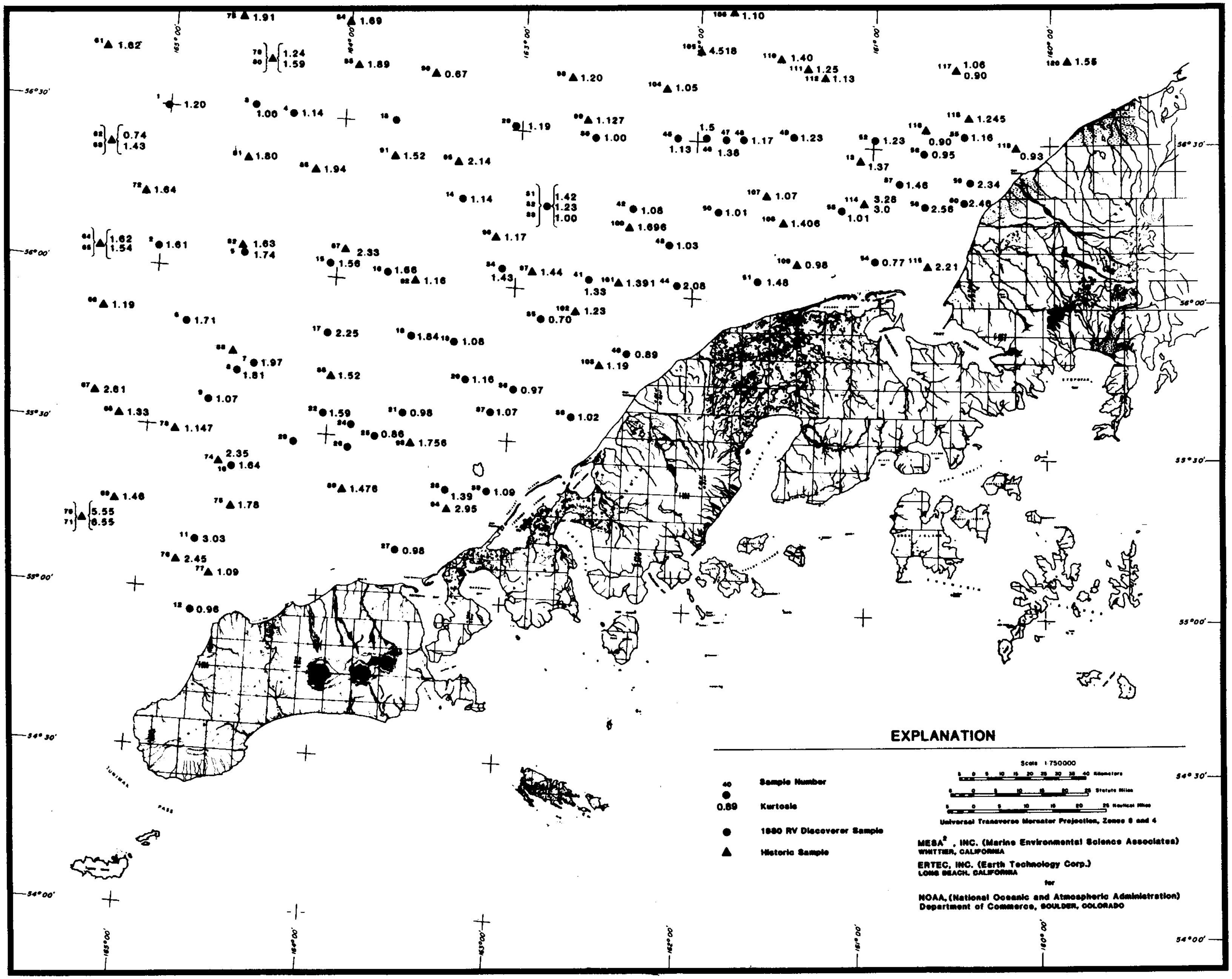

FIGURE 5-10 SEDIMENT KURTOSIS

Table 5-3 Summary of Results From Drop Penetrometer Tests

Corre-sponding Sample Number	Soil[1] Type	Maximum Penetration d_{max} (cm)	Acceleration (g)/Penetration Resistance (kg)[2] at d=0[3]	d=5	d=10	d=15	d=30	Estimated Minimum Friction Angle
2	SM(4)	25	0.8/35	1.0/50	1.2/65	1.1/57	-	39
3	SM(4)	43	0.9/43	1.0/50	1.2/65	1.3/72	1.6/94	36
6	SM(4)	23	0.7/28	1.0/50	1.1/57	1.2/65	-	40
9	SM(4)	20	0.8/35	1.1/57	1.3/72	1.3/72	-	41
9	SM(4)	41	0.8/35	1.3/72	1.5/86	1.4/79	1.4/79	36
11	SM(4)	23	0.8/35	1.1/57	1.5/86	1.5/86	-	40
17	SP/SM(3)	15	0.8/35	1.2/65	2.0/123	1.0/50	-	43
20	SP(2)	13	0.8/35	1.3/72	1.0/50	-	-	43
20	SP(2)	17	0.9/43	1.5/86	1.0/50	4.1/275	-	42
24	SP/SM(3)	11	0.9/43	2.2/137	1.3/72	-	-	44
24	SP/SM(3)	8	0.7/28	2.2/137	-	-	-	46
35	SP(2)	14	0.8/35	1.2/65	1.2/65	-	-	43
40	SP(1)	18	0.8/	1.2/65	1.7/100	1.7/100	-	42
43	SP(1)	6	0.8/35	2.1/130	-	-	-	49
46	SP(2)	4	0.8/35	-	-	-	-	49
59	SP(1)	4	0.8/35	-	-	-	-	49

Notes:

1) Refer to Table 4-3
2) Penetration Resistance (kg)
3) d = Penetration Depth (cm)

The Amak Basin, just north of Unimak Island, has apparently served as a sink for the majority of heavy minerals from Unimak Island, for it is here that the greatest concentration of basaltine and opaque minerals are found. Another concentration of hornblende is found offshore from the Black Hills of the Alaska Peninsula. This hornblende is not basaltine (Figure 5-15), but rather, is from the Naknek Formation, the unit that makes up much of the Black Hills. The Naknek Formation is an arkosic sandstone that is composed of about 5 percent hornblende. The source for the Naknek sandstone is a hornblende-biotite granite (Burk, 1965). Following fluvial transport to shore, sorting by currents and wave action has concentrated the hornblende of the Naknek close to shore, while the remainder of the rock, quartz and feldspar, has been transported farther offshore.

Hypersthene in the area shows a steady decrease in abundance with increase in distance from shore (Figure 5-14), while quartz (Figure 5-11) and feldspar (Figure 5-12) show significant increase in abundance as distance from shore and source area increases. The ratio of quartz and feldspar is nearly uniform throughout the area investigated (Figure 5-13). This suggests that little or no chemical weathering in the source terrain and little post-depositional modification of sediment in the Bristol Bay region.

Opaque minerals are concentrated north of Unimak Island and in the area surrounding Amak Island (Figure 5-16). The percentage of opaques decreases with increase in distance from shore; they are very rare offshore from the Black Hills. The distribution pattern of the heavy mineral fraction in the Bristol Bay region reflects present day sources and suggests that at least the heavy mineral fraction is contemporary.

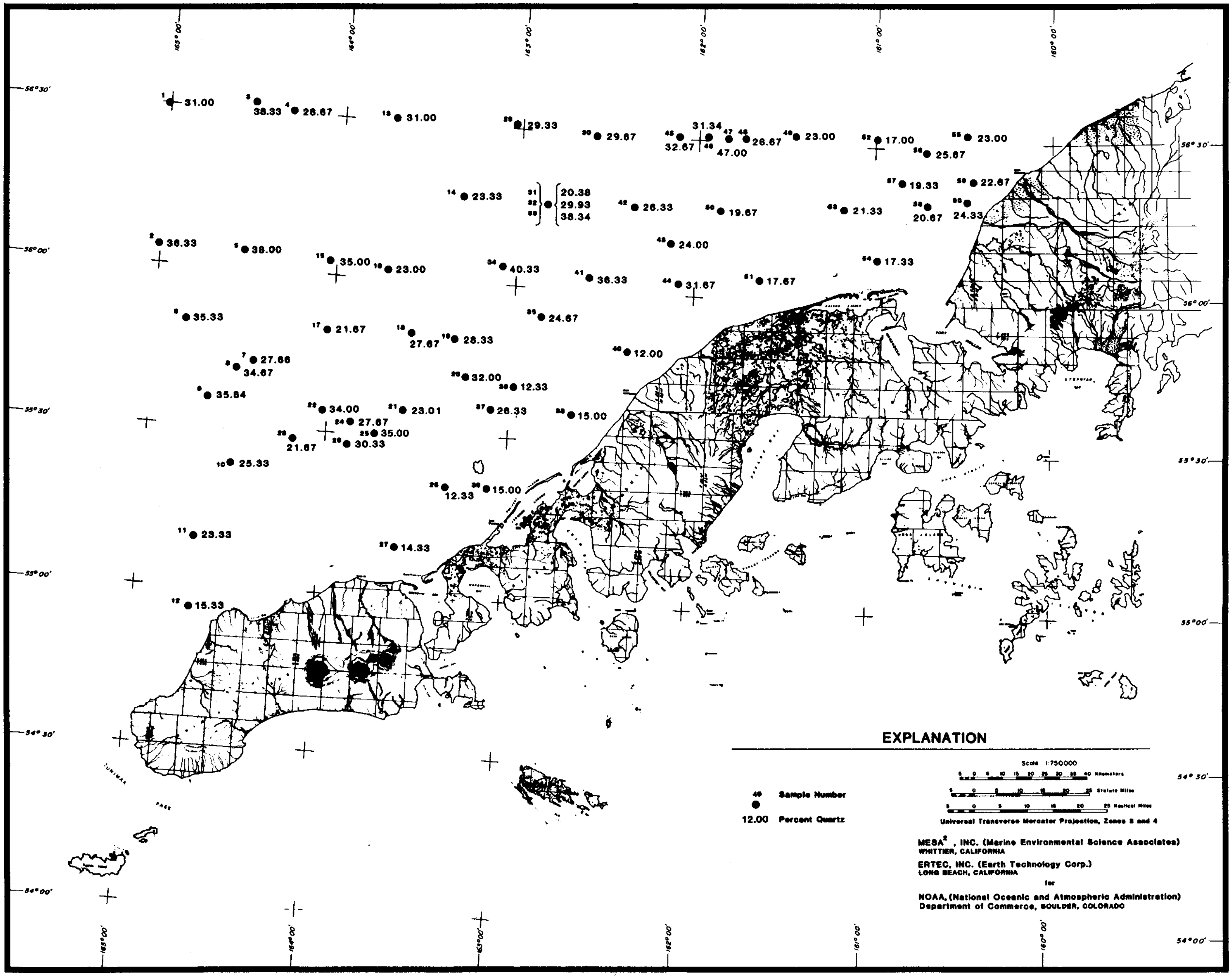

FIGURE 5-11 PERCENT QUARTZ IN SURFACE SEDIMENTS

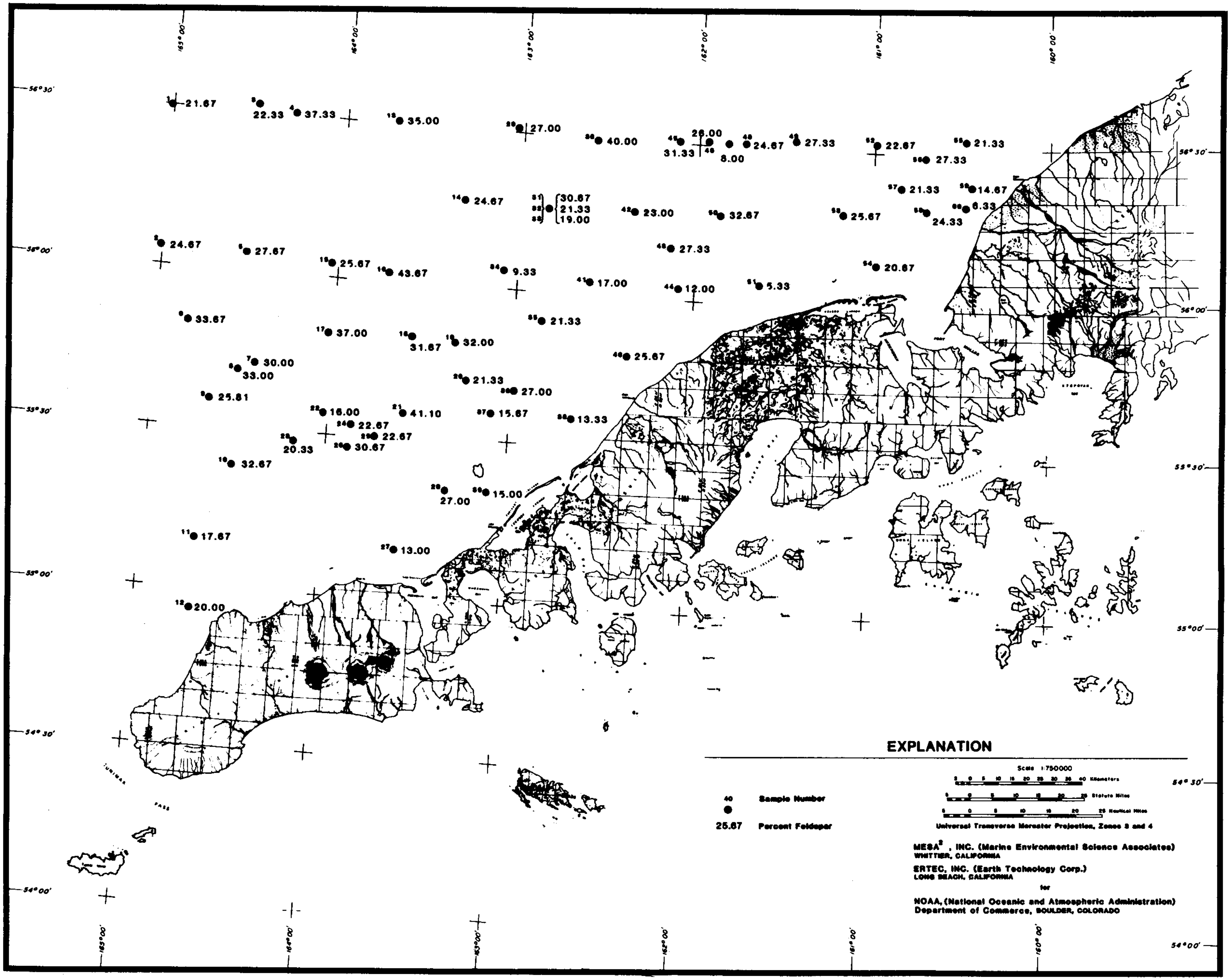

FIGURE 5-12 PERCENT FELDSPAR IN SURFACE SEDIMENTS

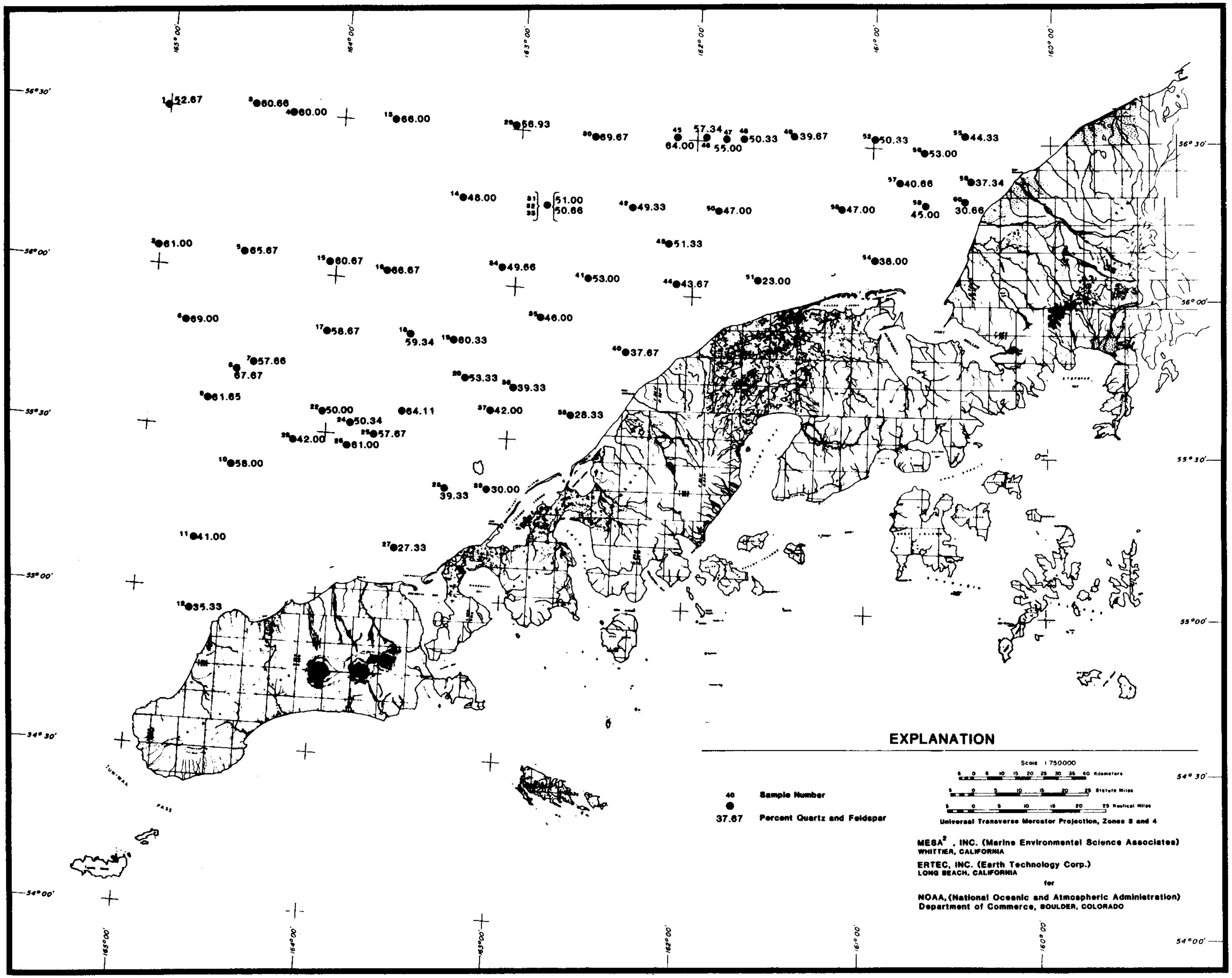

FIGURE 5-13 RATIO OF QUARTZ TO FELDSPAR IN SURFACE SEDIMENTS

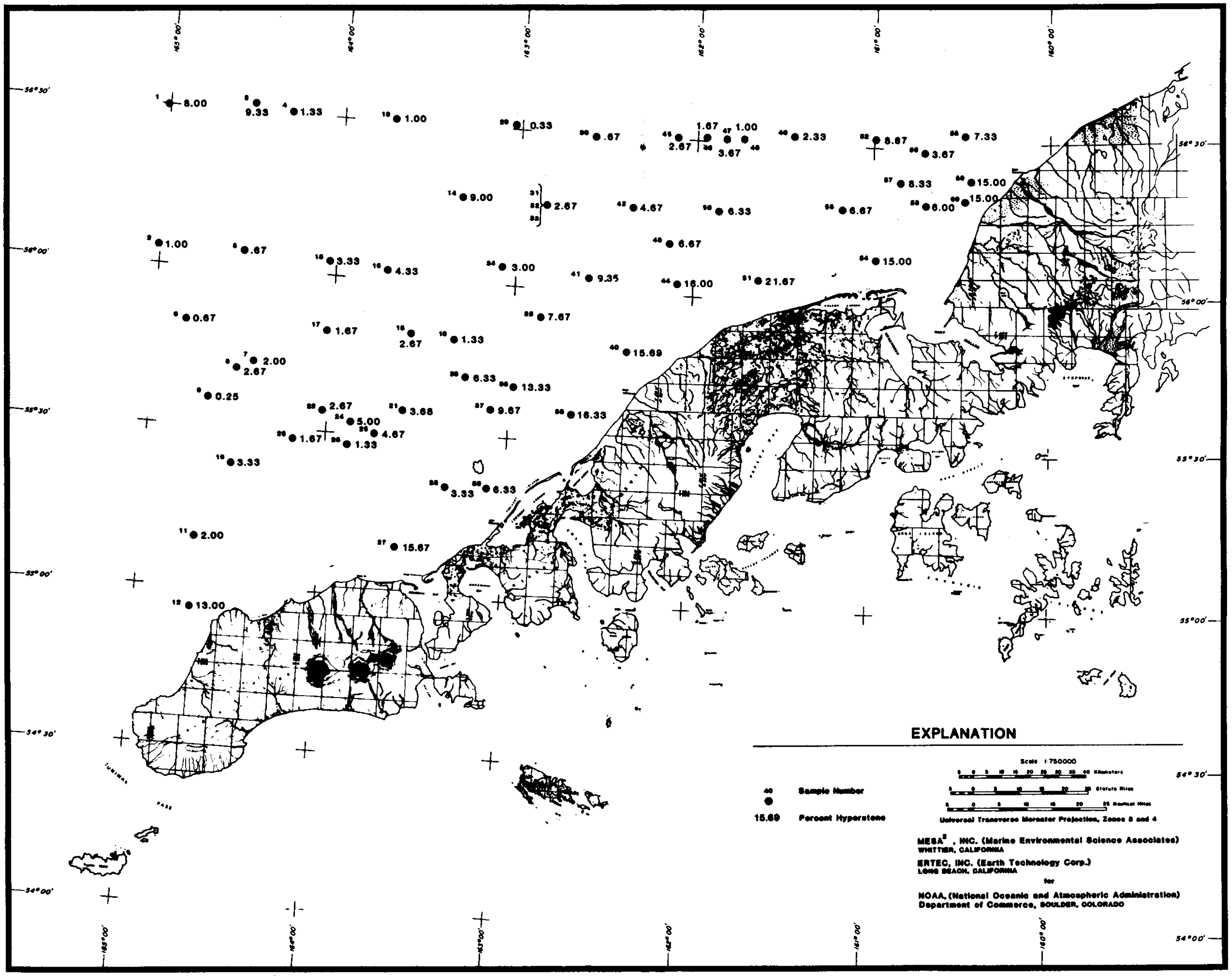

FIGURE 5-14 PERCENT HYPERSTHENE IN SURFACE SEDIMENTS

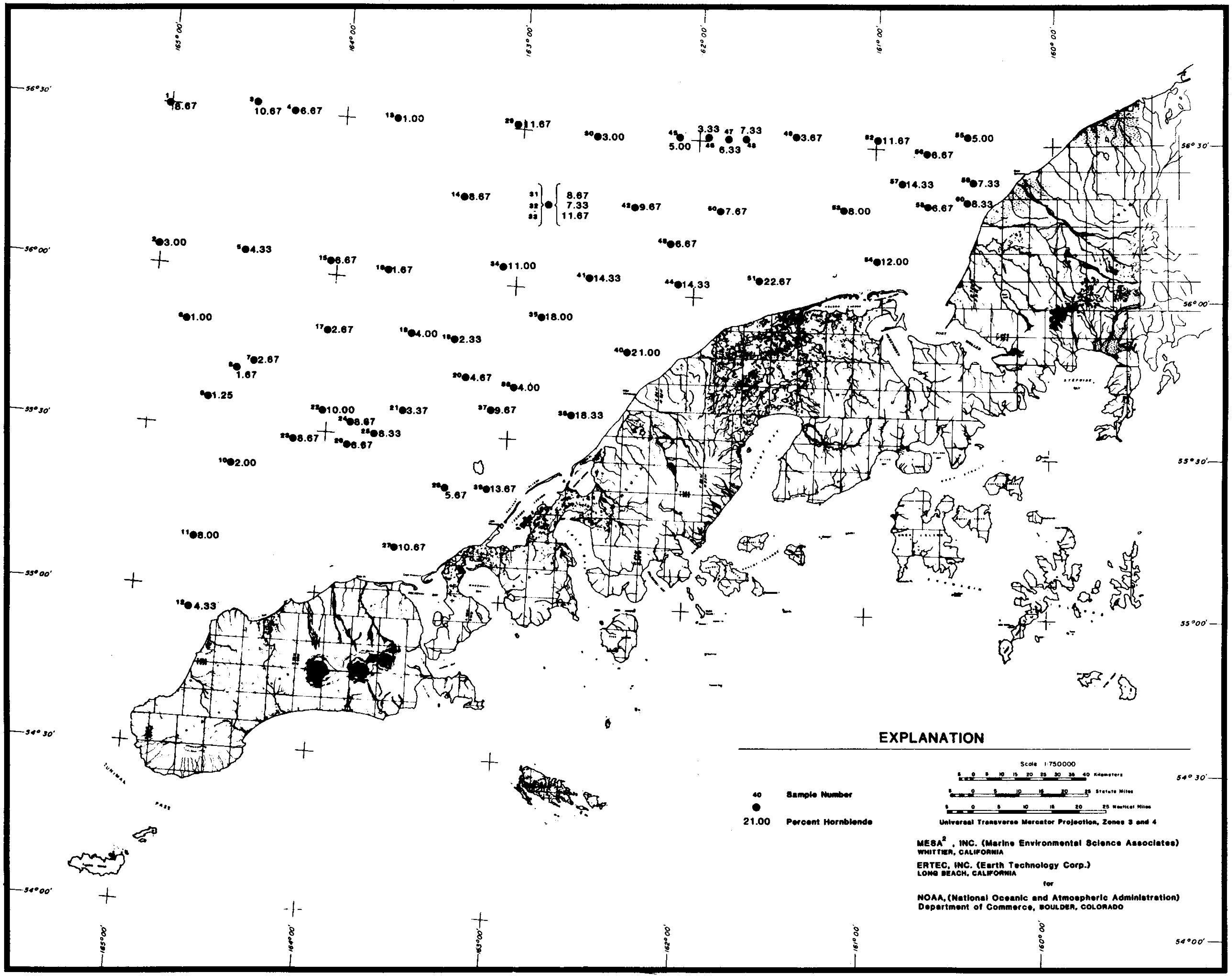

FIGURE 5-15 PERCENT HORNBLENDE IN SURFACE SEDIMENTS

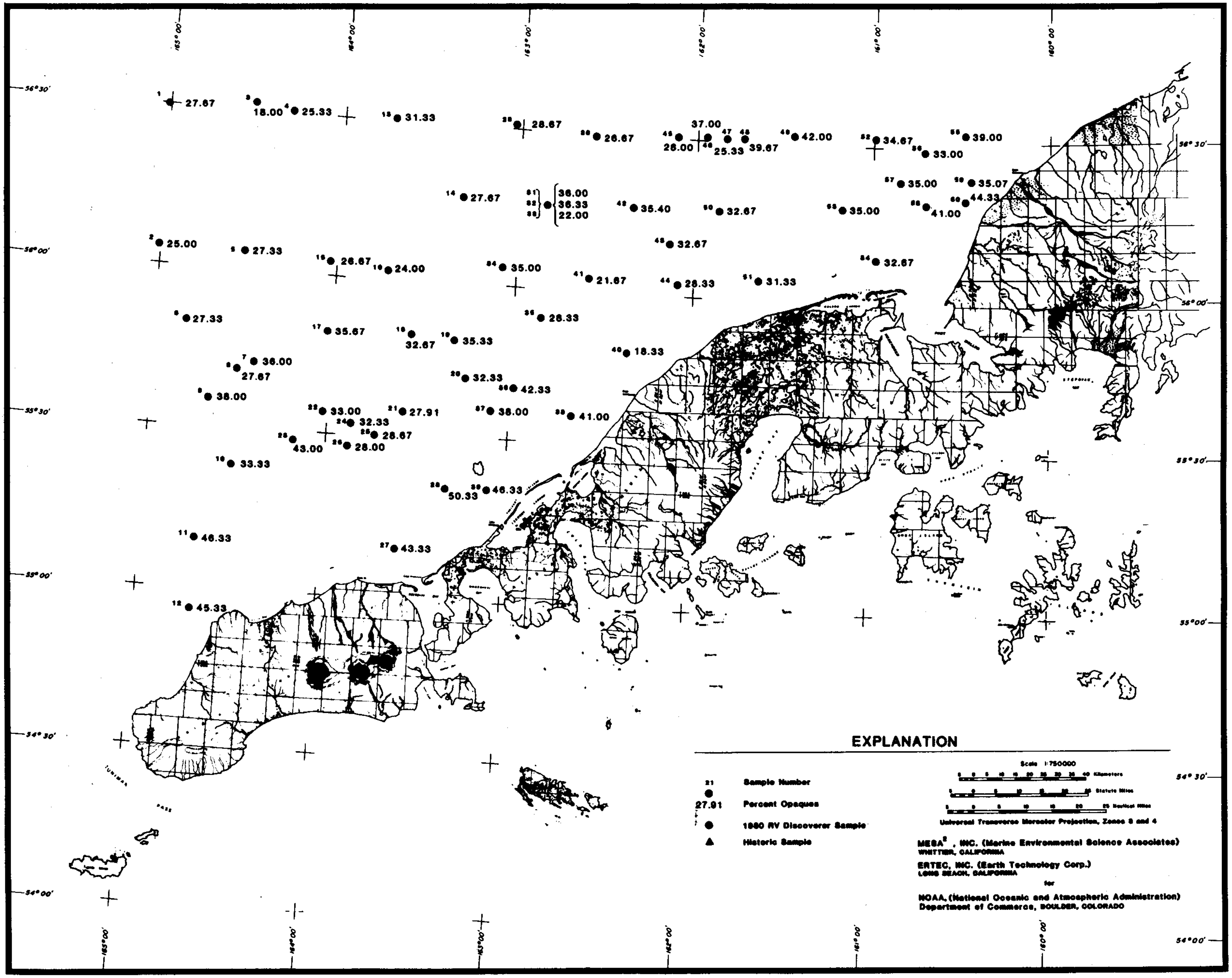

FIGURE 5-16 PERCENT OPAQUES IN SURFACE SEDIMENTS

The depositional pattern for the heavy mineral fraction, which is similar to that described by Sharma, also resembles sediment associations described by Gardner and others (1979) for the adjoining St. George Basin area. By using a Q-mode factor analysis of 58 variables related to sediment size and composition, Gardner and his colleagues determined three main sediment sources. These are the Alaskan mainland, the Aleutian Islands, and the Pribilof Islands. In the Bristol Bay region, the major present day source areas are the Alaska mainland, the Alaska Peninsula, and Amak Island.

5.5.4 Carbon Content

The percentages of total carbon, total inorganic carbon, total organic carbon, and total carbonate were analyzed using a LECO WR-12 induction furnace and a modified Kolpac and Bell apparatus. These analyses were performed for 11 of the surficial sediment grab samples. Test specimens were chosen because of their fine mean grain size, on the assumption that the highest carbon values would be obtained from the samples containing the most clay.

All of the samples show low carbon concentrations when compared to average shelf values. Total organic carbon ranges from about 0.4 percent to 0.3 percent with an average of nearly 0.4 percent (Figure 5-17 and Table 4-2). These values are far below the average of 1.5 percent determined by Trask (1932) for lower latitude shelves, but similar to values displayed by Sharma (1975) for Bristol Bay. Measurements were made of the $CaCO_3$ content from 11 grab samples. The maximum $CaCO_3$ was about 0.3 percent, while the average was about 0.2 percent (Table 4-2).

There is a definite negative correlation between grain size and carbon content. A similar trend is well documented in the St. George Basin area by

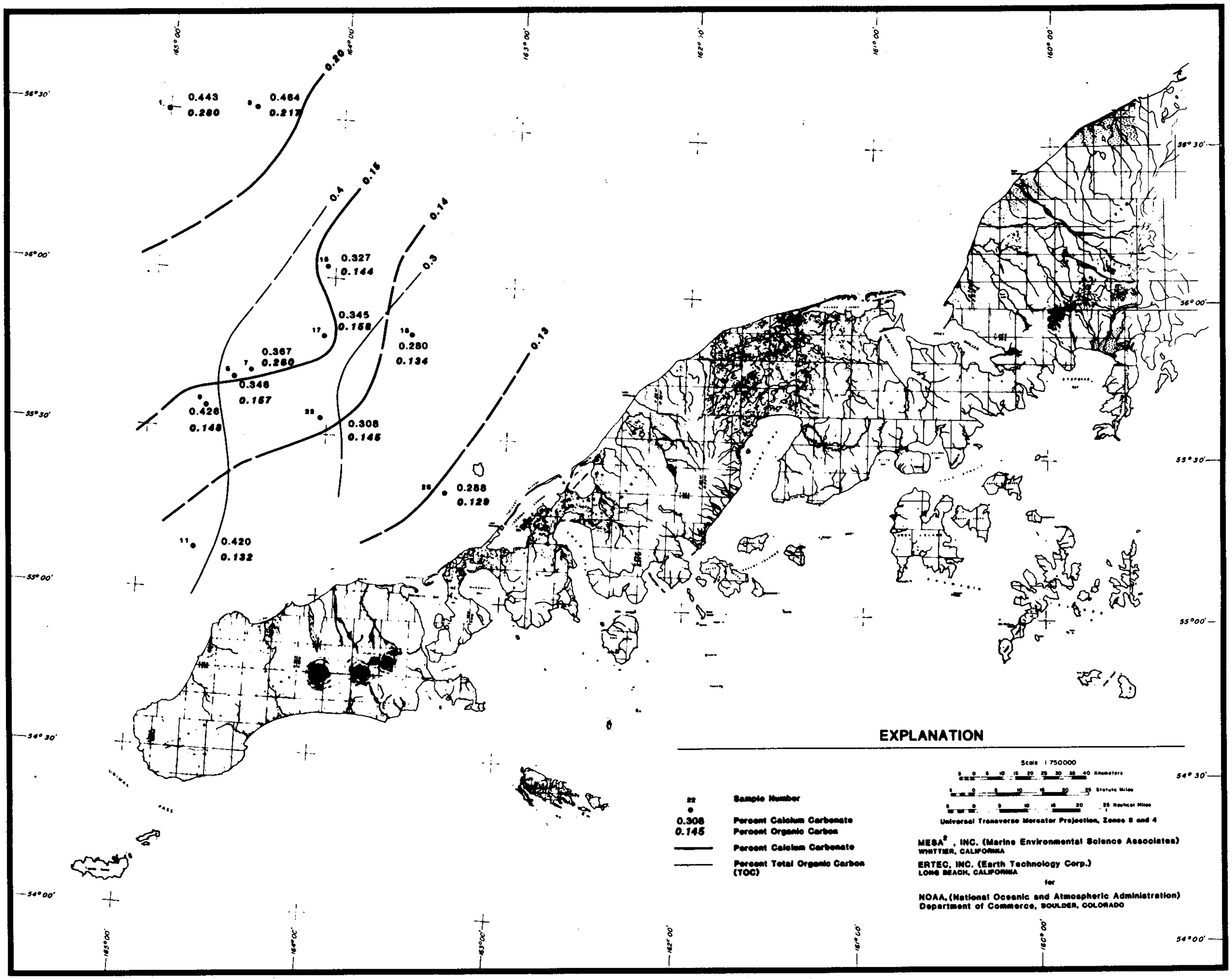

FIGURE 5-17 TOTAL ORGANIC CARBON AND PERCENT CALCIUM CARBONATE IN SURFACE SEDIMENTS

Gardner and others (1979) and by other workers including Kemp (1971), working in Lake Ontario, and Bordovskiy (1965), working on Bering Sea sediments close to the Russian shore. Sharma (1975) suggests this same relationship for Bristol Bay.

Bordovskiy (1965) has explained this association between clay rich sediments and high organic content by identifying the major source of the organic material. The predominant form of carbon in sea water is as dissolved matter. This matter readily forms stable organic mineral compounds with clay particles. In other words, carbon is trapped and incorporated into the clay particles, thereby resulting in clay-size sediment high in carbon.

This mechanism explains the low carbon content observed in most of the sediments of the Bristol Bay area. Bristol Bay sediments contain no more than 11 percent clays, and generally contain 3 percent or less (Sharma, 1975). Similar clay percentages were noted in the analyses of samples collected by this study.

5.5.5 Engineering Properties

The engineering characteristics of sediments on the North Aleutian Shelf were evaluated based on the results of a visual examination of the recovered samples, in situ shear strength measurements, and a series of engineering laboratory tests. Before presenting these data, it is essential that two limitations be noted.

The first limitation is associated with the depth of sampling. In every case these engineering characteristics were deduced from data gathered in the upper 1 to 2 m of the soil profile. Therefore, interpretations based on these data are appropriate only for the same depth range. In a strict sense this restricts use of the data to a limited number of engineering applications such as pipeline stability calculations, small-foundation bearing capacity determinations and scour potential assessments. It is possible to extrapolate surficial properties to greater depths (>1 to 2 m) by judicious application of generalized geotechnical engineering relationships and by careful review of the geologic history for the area. However, this approach is subject to considerable uncertainty and definitely would be inappropriate for final design of key bottom-supported petroleum facilities.

A second limitation deals with the quality of data. The objective of this engineering evaluation was not to define precise engineering properties. Rather it was to obtain a general understanding of conditions over a large area. This philosophy led to use of the vibracore, Van Veen sampler, gravity core and drop penetrometer. The three types of soil sampling tools introduce considerable disturbance to the sediment during sampling; because of induced vibrations in the case of the vibracore, or volume change characteristics in the case of the Van Veen and gravity samplers. Likewise the drop penetrometer involves uncertainty but in its case through the interpretation process. Consequently some discrepancies between actual in-situ properties and the characteristics presented below must be anticipated.

5.5.5.1 Visual Classification

Examination of the recovered surficial sediments determined that the study area is covered by a surficial layer of granular sediments. From the following field observations, it was inferred that these sediments are generally very dense.

1) Penetration of the high resolution seismic profiling system (3.5 kHz) was limited. Typical acoustic penetration depths ranged from 0 to 22 m with average penetration less than 5 m.

2) Results of in situ testing using the drop penetrometer indicated that minimal penetration occurred.

3) Little or no penetration occurred during gravity sampling using either a 140 kg or 360 kg weight stand.

4) Attempts to sample the in situ sediments by vibracorer were not as successful as anticipated. Vibracore penetration was shallow and the core recoveries were short. Although this was partially due to equipment limitations, the dense nature of the sediment was considered to have been a significant contributing factor.

Visual examination of the recovered samples and the results of subsequent index property tests (settling tube and grain-size analyses) indicate that the surficial sediments in the study area can be divided into the following four types with respect to geotechnical engineering characteristics:

1) Soil Type No. 1, SP(1) - dark brown gravelly sand and dark gray coarse to medium sand with little or no fines. The gravelly sand is present near the coastline.

2) Soil Type No. 2, SP(2) - dark gray and relatively uniform fine sand with little or no fines.

3) Soil Type No. 3, SP/SM(3) - gray to brownish gray fine sand with some fine and occasional shell fragments. This is a transitional zone between Soil Type No. 2 sediments and Soil Type No. 4 sediments described below.

4) Soil Type No. 4, SM(4) - Brown gray fine silty sand with an appreciable amount of fine and occasional shell fragments.

The distribution of these sediments is shown in Figure 5-18.

5.5.5.2 In Situ Shear Strength Measurements

As summarized in Section 3.3.3, in situ penetration measurements were performed at 46 locations using a drop penetrometer device (Scott, 1967). Acceleration records obtained by the device were converted to penetration resistance values at various penetration depths by integrating the recorded

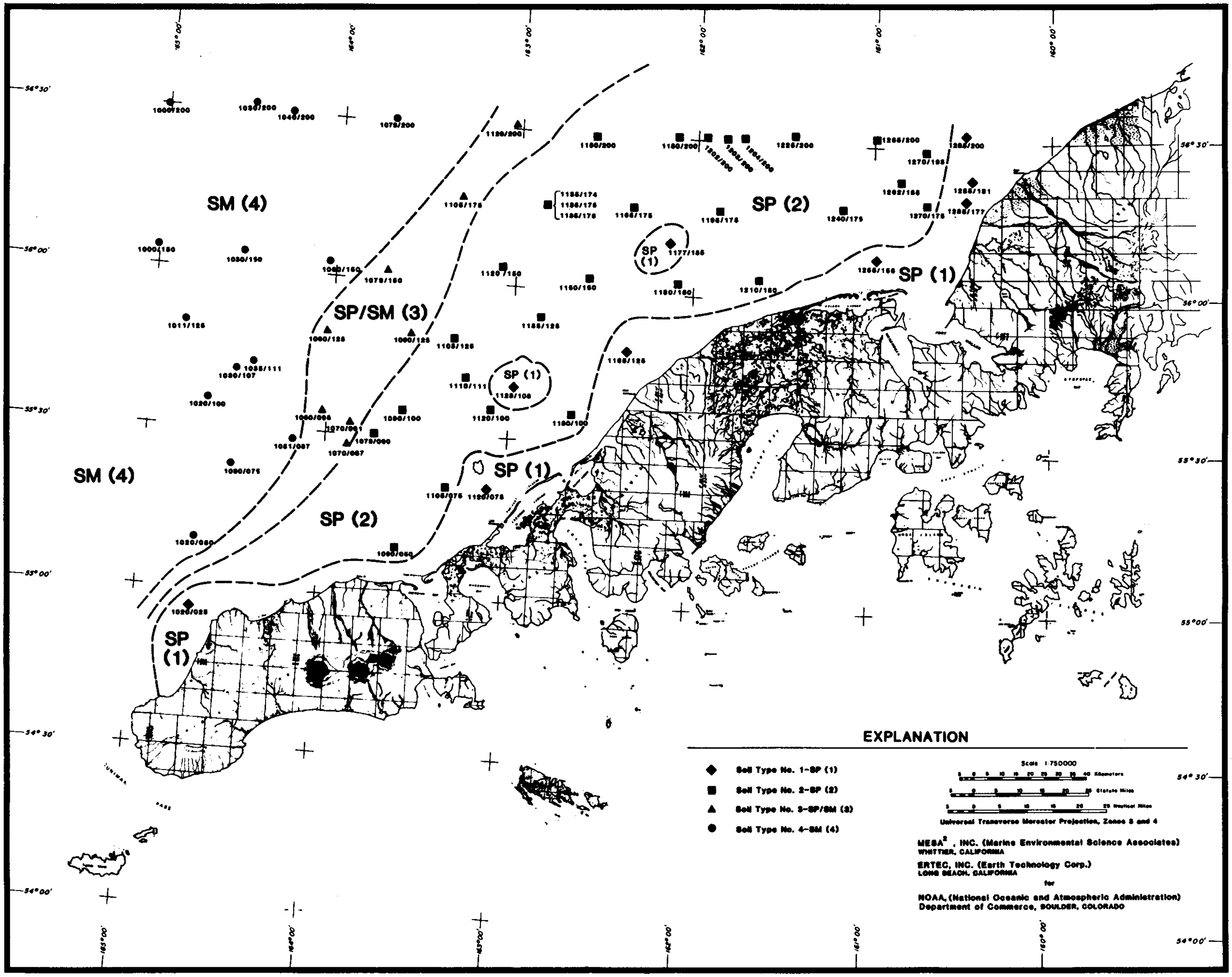

FIGURE 5-18 DISTRIBUTION OF SOIL TYPES

acceleration-time histories using the characteristics of the accelerometer and penetrometer assembly. Results of these analyses were used to obtain a resistance force versus penetration plot.

Sixteen records were selected for detailed evaluations. The remaining records were disregarded for one or more of the following reasons:

1) Illegible records where either the diamond-tipped stylus failed to register on the pressure sensitive paper or the traces were too faint to be accurately interpreted

2) Invalid records where the penetrometer assembly failed to penetrate into the soil due to inclined entry or operational difficulty, and

3) Multiple records of similar order of magnitudes obtained at one station (i.e., only one of the similar records was used).

The selected records were digitized and then double integrated using a computer program developed by Professor Scott. Relevant results are summarized in Table 5-3.

An estimate of the in situ friction angle was made by correlating the penetration resistance results with penetration resistance values calculated analytically using a method developed by Durgunoglu and Mitchell (1975). These individuals determined that penetration resistance depends on the soil type, penetrometer roughness, and the apex angle of the penetrometer cone (60° in this study). One of the major uncertainties in this method is the frictional value between the penetrometer and soil. In this study, an upper bound friction angle was estimated assuming that the penetrometer was completely smooth (i.e., friction at the penetrometer-soil interface was zero). Similarly, a lower bound estimate was made assuming that the penetrometer was completely rough (i.e., friction between the penetrometer and soil equal to the shear strength of the soil). The results of the soil friction angle estimate are shown in Table 5-3.

Table 5-4 Expected Range of Dry Unit Weights

Soil Type[1]	Expected Range of Dry Unit Weight (kN/m^3)	Selected for Test Specimen Preparation (kN/m^3)
SP (1)	15.0 to 17.5	16
SP (2)	15.0 to 17.0	16
SP/SM(3)	15.0 to 17.0	16
SM (4)	13.5 to 15.0	15

Notes:

1) Refer to Table 4-3

Based on the results shown in this table, the following friction angles (ϕ) estimates were made for the four types of surficial sediments in the study area:

1) Soil Type No. 1: ϕ = 43° to 49°
2) Soil Type No. 2: ϕ = 43° to 49°
3) Soil Type No. 3: ϕ = 44° to 47°
4) Soil Type No. 4: ϕ = 36° to 42°

The magnitude of these friction angles indicates that the surficial sediments in the study area are very dense. Equivalent relative densities would be in excess of 90 percent or more. Inasmuch as the above friction angles are representative of surficial sediments and correspond to low confining stress, a decrease in friction angle with depth might be expected, as the friction angle decreases with increasing confinement.

5.5.5.3 Index Properties

The laboratory test program was designed to characterize the sediments at the site and to provide geotechnical engineering properties for use in the geotechnical hazard assessments. The index property tests comprised

	Number	ASTM Designation
Grain Size Analyses	34	422
Unit Weights	46	-
Water Contents	46	216
Specific Gravity of Solids	3	854
Maximum Dry Unit Weights	8	2049
Minimum Dry Unit Weights	8	2049

The results of grain size analyses for the 34 specimens are summarized in Appendix I. Average characteristics are summarized in Figure 5-19. As described above (Section 5.5.5.1), the surficial sediments in the study area can be divided into four types; the spatial distribution of these four sediment types is shown in Figure 5-18. With the exception of Soil Type No. 4, these sediments are relatively uniform with a coefficient of uniformity (D_{60}/D_{10}) ranging from 1.3 to about 3.5.

Unit weight measurements were made on 46 samples. The results of these tests are summarized in Table 4-3. These results were plotted with respect to the mean grain size, D_{50}, and are shown in Figure 5-20. As can be seen from this figure, the results indicate a wide scatter in dry unit weight values. This was due to the varying extent of sample disturbance introduced during sampling and possibly during handling and transporting the samples. Because the sampling methods (gravity core, vibracore, and Van Veen) employed in this study are known to disturb sands and to change their engineering properties, most of these unit weights are suspect.

Moisture content tests were performed on 46 samples. The results of these tests are summarized in Table 4-3. Due to sample disturbance effects, these moisture content values are probably higher than the values representative of in situ conditions.

Specific gravity tests were performed on three bulk-sample specimens in accordance with ASTM D854. As tabulated in Table 4-4, the specific gravity values for Soil Type 1 and 4 are 2.74 and 2.69, respectively, and for Soil Type 2 is about 2.8.

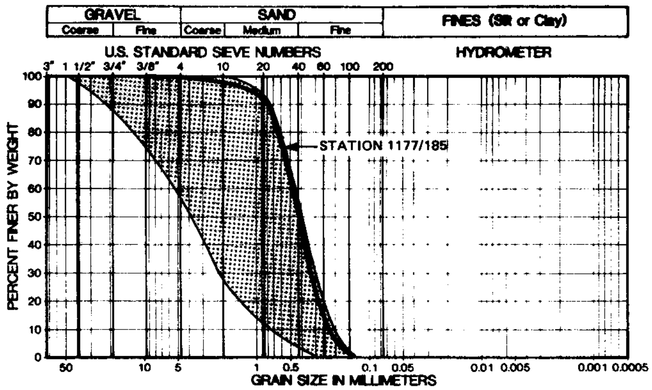

SOIL TYPE NO. 1—SP (1)

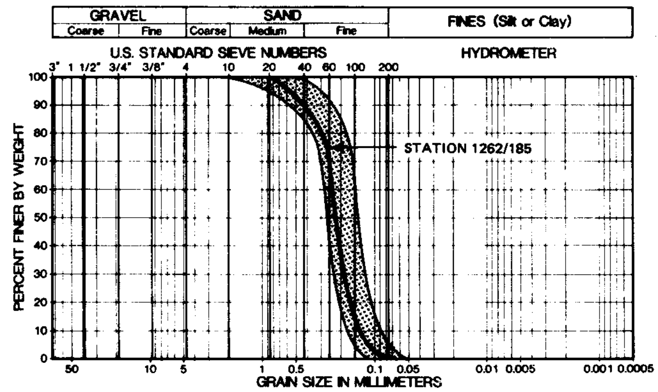

SOIL TYPE NO. 2—SP (2)

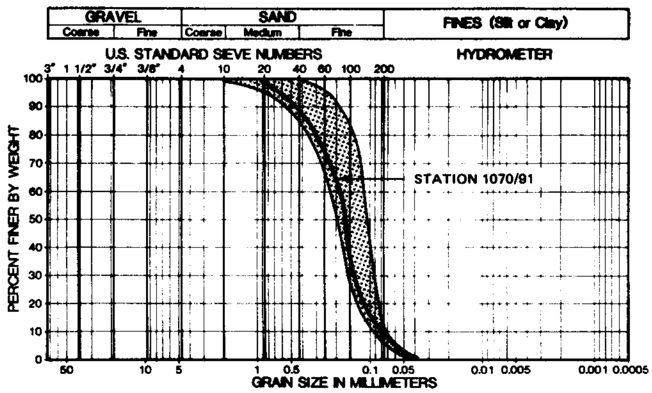

SOIL TYPE NO. 3—SP/SM (3)

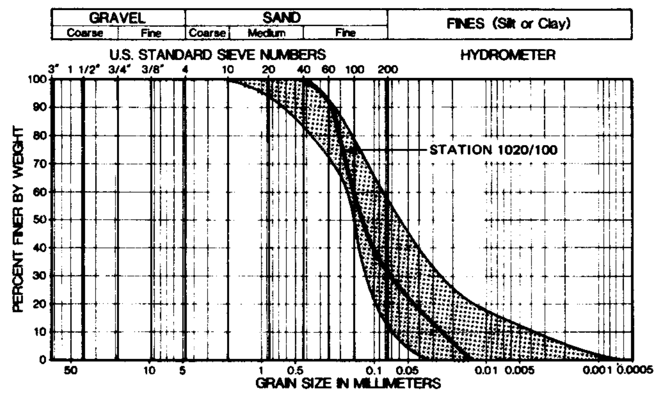

SOIL TYPE NO. 4—SM (4)

FIGURE 5-19 RANGE OF GRAIN-SIZE CONDITIONS

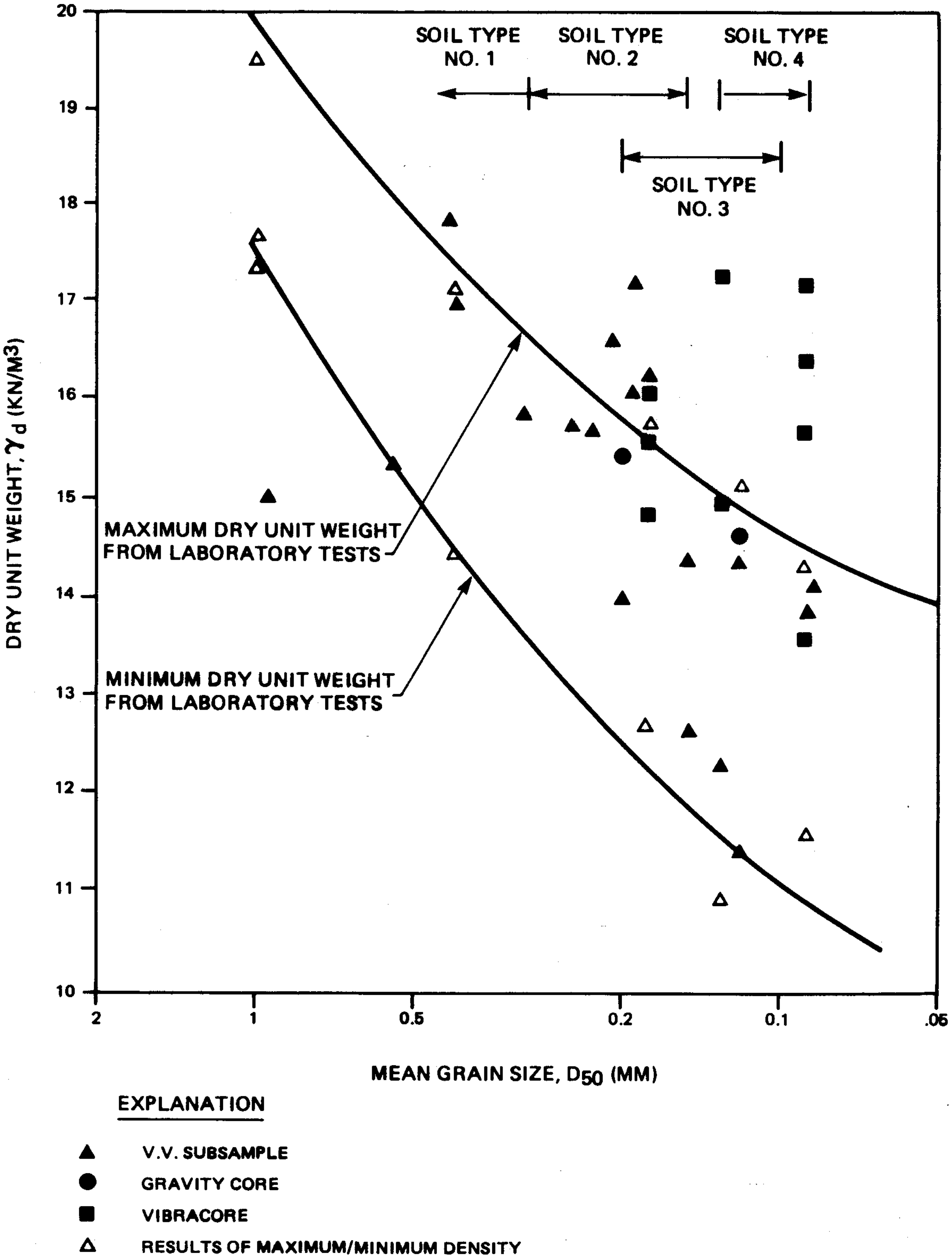

FIGURE 5-20 VARIATION OF DRY UNIT WEIGHT WITH MEAN GRAIN SIZE

Eight sets of maximum and minimum dry unit weight tests were performed in accordance with ASTM D2049. Results of these tests are summarized in Table 4-5. These results indicate that the maximum and minimum dry unit weights are highest for the coarse-grained soils (Soil Type 1) and lowest for the fine-grained soils (Soil Type 4).

5.5.5.4 Geotechnical Engineering Properties Tests

The engineering properties tests were performed on good quality gravity core specimens and on reconstituted specimens. One of the major difficulties in performing tests on reconstituted samples is that it requires a reliable estimate of in situ unit weights of the sediments. The results of in situ shear strength measurements with the drop penetrometer indicate that surficial sediments in the study area are very dense. As shown in Figure 5-21, a comparison of the estimated friction angle values from in situ measurements with the empirical correlation between friction angle and relative density (DM-7, 1971) indicates that the relative densities of sediments in the study are close to 100 percent. Likewise, the plot of dry unit weights versus the mean grain sizes (D_{50}) indicates that the average dry unit weights are very close to the maximum dry unit weights as determined by the laboratory tests. Again, this is indicative of the dense nature of the in situ sediments.

In this study, the 25 kg bulk samples obtained at Stations 1020/100, 1070/91, 1177/185 and 1262/185 (Sample Nos. 9, 24, 43 and 57) were selected to represent the four soil types in the study area. Based on an evaluation of the available in situ test results and index properties as well as engineering judgment, possible ranges of in situ dry unit weights of the sediments were estimated. They are shown in Table 5-4. In this table, the dry unit weights selected for preparing the reconstituted specimens are also indicated. These

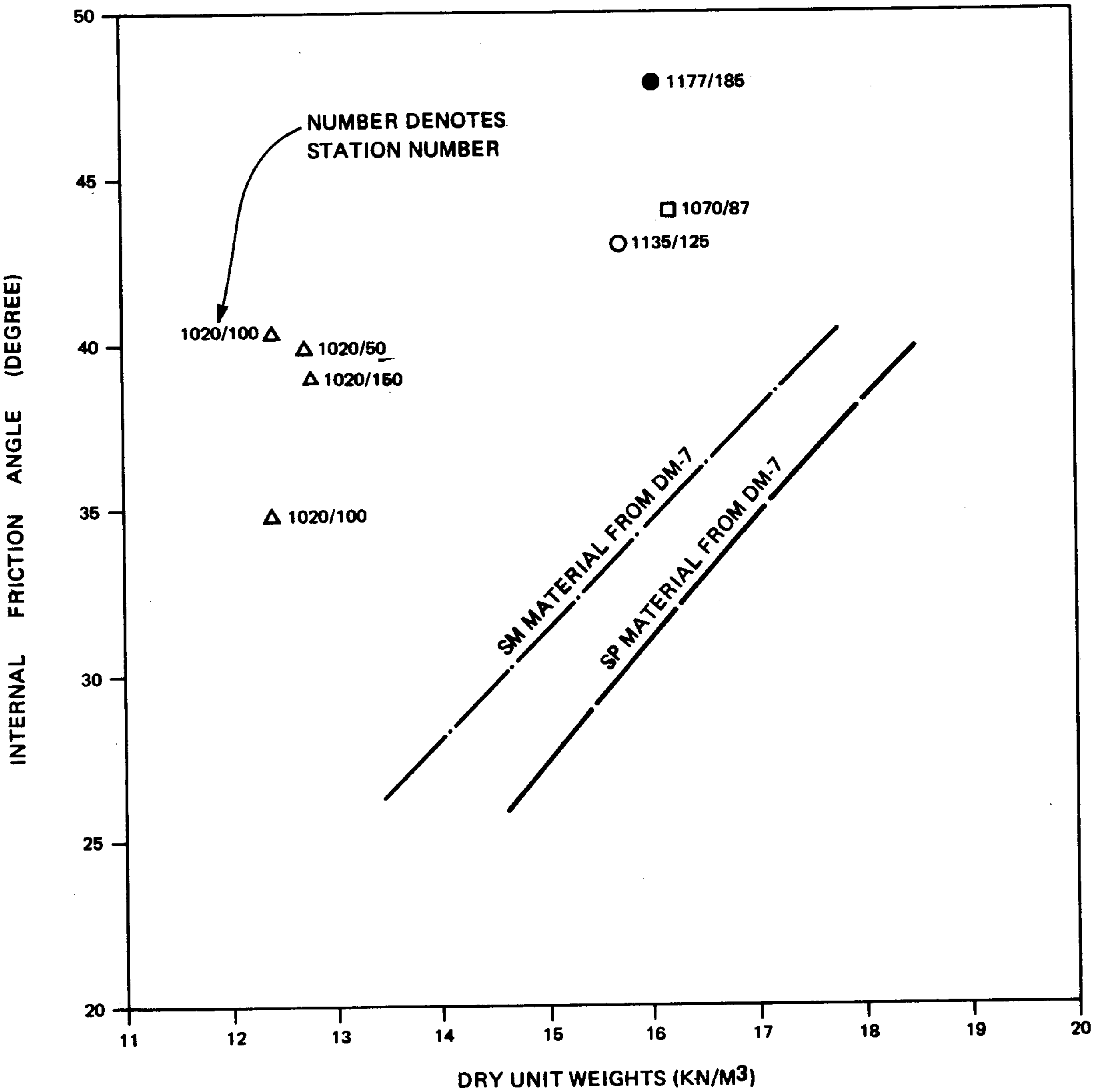

NOTES: DATA POINTS ARE BASED ON:

1. MINIMUM INTERNAL FRICTION ANGLE FROM INTERPRETATION OF PENETROMETER DATA
2. DRY UNIT WEIGHT FROM VAN VEEN SUBSAMPLES (TABLE 4-3)

SYMBOLS

● SOIL TYPE 1 – SP (1)

○ SOIL TYPE 2 – SP (2)

□ SOIL TYPE 3 – SP/SM (3)

△ SOIL TYPE 4 – SM (4)

FIGURE 5-21 VARIATION OF FRICTION ANGLE WITH DRY UNIT WEIGHT

dry unit weights were considered to be best estimates of unit weights for sediments within the study area with the exception of Soil Type No. 1 where the selected dry unit weight probably corresponds to the anticipated lower bound value in situ. Thus, the geotechnical properties obtained from tests on reconstituted specimens may be conservative for Soil Type No. 1, and probably correspond to lower bound values in situ.

Seven oedometer tests were performed on three gravity core specimens and four reconstituted specimens. A summary of the results from these tests is presented in Table 4-6. Plots of voids ratio versus the logarithm of consolidation stress are presented in Appendix II. These plots indicate that the sediments are relatively incompressible except where densities are low.

Six permeability measurements were performed on two gravity core specimens and four reconstituted specimens. The results of these tests are summarized in Table 4-7. As shown in this table, Soil Type Nos. 1 and 2 are relatively permeable with coefficients of permeability ranging from 10^{-3} to about 5×10^{-5} cm/sec. Soil Type Nos. 3 and 4 are less permeable due to the presence of appreciable fines content.

Isotropically consolidated-drained triaxial compression tests were performed on 12 reconstituted specimens and two gravity core specimens. Two of the test series were multistage, the rest were single stage. The results of these tests are summarized in Table 4-8. The Mohr's circles as well as the stress-strain and volumetric-change plots are provided in Appendix II. The results of tests on reconstituted specimen indicated that the effective friction angles are about 39°, 40°, 41°, and 37° for Soil Types Nos. 1, 2, 3, and 4 respectively. The two multistage tests on gravity core specimens indicate that the effective friction angle is about 35° to 38° for Soil Type No. 4.

This range in effective friction angle for Soil Type No. 4 is slightly lower than what was estimated from the in situ shear strength measurements. This may be indicative of sample disturbance and other factors such as the procedures utilized in intepreting the in situ strength measurements.

Cyclic simple shear tests were performed on five gravity core specimens and 12 reconstituted specimens. The results of these tests are summarized in Table 4-9 and in Figure 5-22. An examination of these results indicates that the cyclic shearing strengths determined from the gravity core specimens are either higher than or of the same order of magnitude as the reconstituted specimens, which were prepared at higher unit weights than the gravity core specimens. This apparent contradiction is thought to be indicative of the significant effects of soil grain-structure arrangement in situ that is not accounted for by reconstituted samples duplicating only the dry unit weight. Data presented in Figure 5-22 were subsequently adjusted to likely field conditions based upon the age of the deposits (Seed, 1976). Age dating studies (Section 4.2.4) suggest that sediments at the site below a depth of 0 to 3 m are at least 11,000 years old. A correlation of this information with the data presented by Seed (1976) indicates that the cyclic shearing strengths of the in situ sediments excluding the agitated surficial veneer would be at least 50 percent higher than strengths measured in the laboratory. The cyclic simple shear test results from the gravity core specimens also indicate that limiting shearing strains develop regardless of the magnitude or duration of the applied cyclic shearing stress (Appendix II). This is indicative of dense soils where the effects of dilation prevent a complete loss of shearing resistance.

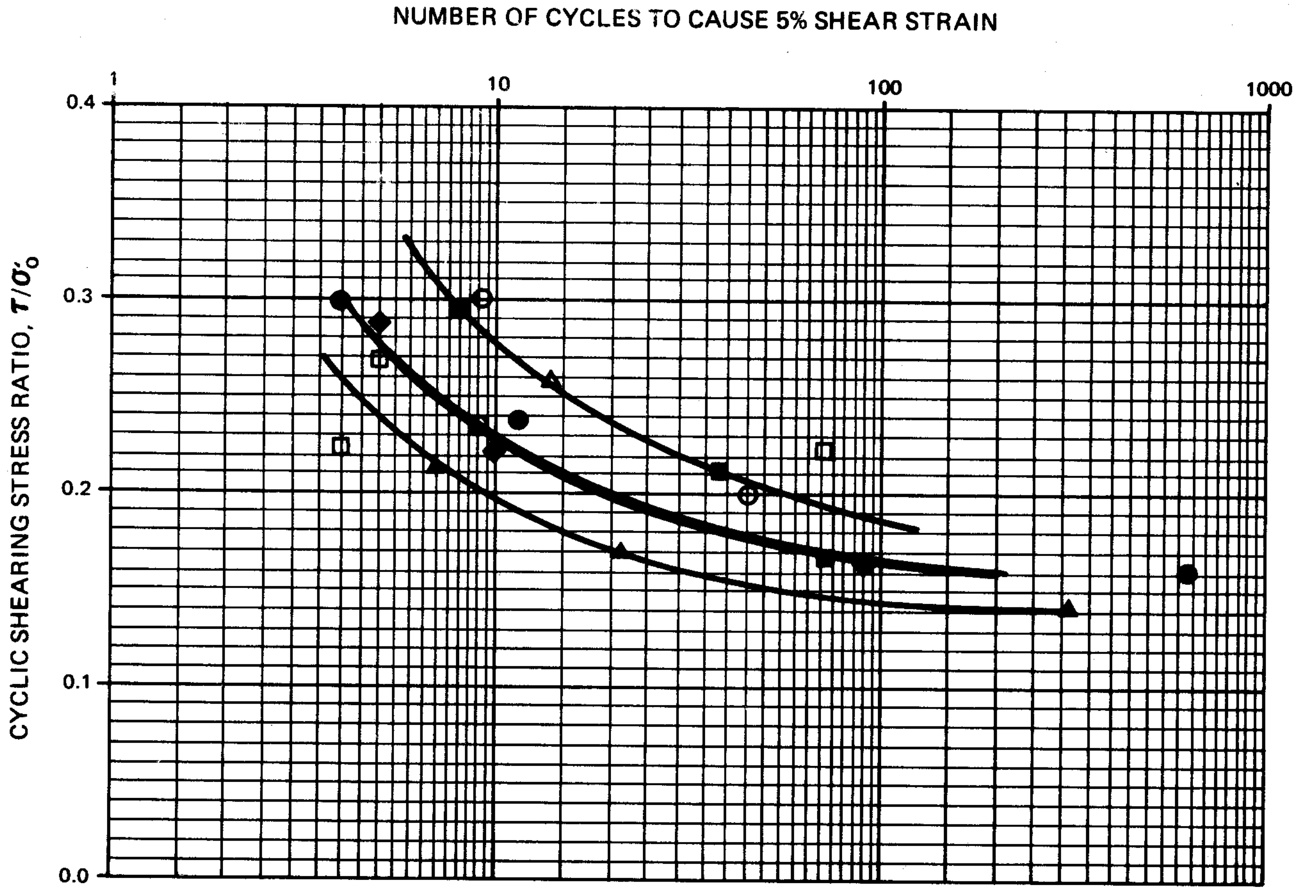

SYMBOL	SAMPLE NO.	SAMPLE TYPE	SOIL TYPE	γ_d KN/M^3	WATER CONTENT (%)
□	2	UNDISTURBED	SM-ML	14.4	31
△	11	UNDISTURBED	SM	15.5	28
○	23	UNDISTURBED	SM	14.7	30
●	9	RECONSTITUTED	SM	15.1	30
■	24	RECONSTITUTED	SP-SM	15.7	27
◆	43	RECONSTITUTED	SP	16.3	24
▲	57	RECONSTITUTED	SP	16.1	23

FIGURE 5-22 RESULTS OF CYCLIC SIMPLE SHEAR TESTS

Modulus and damping characteristics were determined for four reconstituted specimens utilizing a Hardin type resonant column test device for low strain amplitudes (10^{-4} to 10^{-2} percent shearing strain) and an MTS Model 810 cyclic triaxial loading system operating in strain-controlled mode for higher strain applitudes (10^{-2} to 1 percent shearing strain). A summary of test results is provided in Tables 4-10 and 4-11; Appendix II contains individual test data. Based on the same reasoning stated in the previous section, the stiffness of an in situ deposit is expected to be higher than these laboratory data. Data presented by Anderson and Stokoe (1978) suggest that the in situ modulus curves could be best represented by multiplying the laboratory modulus values presented in Appendix II by 1.5 (i.e., a 50 percent increase).

5.6 GEOTECHNICAL ANALYSIS

Information presented in the preceding sections of this chapter were integrated to provide basic site characterization data necessary for an engineering evaluation of soil behavior. This evaluation considered the geotechnical behavior of soils under (1) gravity loading, (2) storm-wave loading, and (3) earthquake loading. Results from these analyses formed the basis for identifying potential geologic hazards on the Northern Aleutian Shelf.

A considerable degree of judgment must be used when interpreting the meaning or significance of the following analyses. These analyses were often based on information which was insufficient or inferred. For example, only surficial sediment data (upper 1 to 2 m) were obtained; hence, soil profiles had to be inferred from existing geologic data and judgment. Despite these limitations, the geotechnical analyses provide a framework for judging the potential severity of certain hazards. Future site-specific studies should address these hazards carefully before installation of any important structure.

5.6.1 Gravity Loading

Gravity loading refers to loading which results from the buoyant weight of the structure or the soil mass. The principal geotechnical considerations associated with gravity loading include vertical bearing capacity and settlement, when the load results from structures, and slope instability in areas where the seafloor slopes substantially. Most geotechnical problems related to gravity loading result where soft sediments exist and as noted in Section 5.5, the limited data available for the study area definitely suggest that soils are dense.

5.6.1.1 Bearing Capacity

Bearing capacities for surficial sediments should be high in view of the high frictional angles characterizing surficial sands. For most locations the effective angle of internal friction will be greater than 36°. The associated design bearing capacity for a surface foundation with this friction angle will be in excess of 150 kN/m^2 for a footing with a 2 m width. Appropriate adjustments must be made to this value if horizontal forces exist concurrent with vertical loading forces.

This bearing capacity estimate is most applicable for the design of pipelines and small mat foundations, with a diameter or width less than 1 to 2 m. The absence of geotechnical information at greater depths creates a degree of uncertainty about the use of friction angles determined in this study to compute bearing capacity for larger foundations, such as might exist with an exploratory jackup rig. Although softer layers were not interpreted from geophysical records, the occurrence of an underlying weaker layer which could cause "punch-through" of a heavily-loaded, large foundation cannot be ruled out. Given this uncertainty, it is evident that more detailed site-specific studies will be warranted when potentially critical structures are being placed on the seafloor.

5.6.1.2 Settlement

The settlement of sandy soils under static (or gravity) loading is generally small, as compared to clayey soils. The results of oedometer tests (Section 5.5.5) confirm this behavior. Compression indices for tests on reconstituted samples were typically an order of magnitude less than the values normally associated with clays. Higher values recorded for gravity-core samples are attributed to sample looseness near the seabottom.

These low compression indices imply that settlements will be small as long as the foundation size is small and loads are within normal limits. Most of the settlement should occur rapidly as immediate (or elastic) compression of the soil structure. Much of the site is covered with relatively fine to medium sands (D_{10} > 0.05 mm); hence, permeability will be relatively high and consolidation will be rapid. Consequently, any time-dependent settlement is expected to occur rapidly.

The uncertainties associated with soil conditions at depth means that the above interpretations are most appropriate for small foundations. Although deeper soils are expected to be either dense sands or stiff clays, site-specific studies will have to be conducted to verify this premise, particularly where critical structures are to be emplaced.

5.6.1.3 Slope Stability

Available bathymetric information indicates that the natural slope of the seafloor in the study area is gentle with a maximum gradient on the order of

0.5 percent near the coastline and with a gradient of about 0.02 percent or less over much of the study area.

The surficial sediments encountered in the study area are characterized by dense sandy materials. These types of materials have adequate shearing resistance so that the potential for slope instability under gravity loading is very low. The sediments below the surficial sediments are expected to have similar or greater shearing resistance. Thus, no unusual slope instability problems are anticipated in the study area unless man-made, large gradients are created. At these locations slope stability should be investigated on a site-specific basis.

5.6.2 Storm-Wave Loading

Storms generated in the Gulf of Alaska and the Bering Sea will occur in the study area at fairly frequent intervals, as noted in Section 2.2.3. The consequence of these storms will be large storm waves having significant wave heights from 15 to 25 m. These large waves potentially can cause scour of fine-grained sands and silts, liquefaction of sands in shallow water, and slope instabilities due to hydrodynamic pressure oscillation. Storm waves can also indirectly affect the soil as they load pipelines and other bottom-supported structures. Treatment of these indirect loading effects is, however, beyond the scope of this regional analysis. Detailed evaluations of wave-structure interaction should be anticipated during site-specific investigations.

5.6.2.1 Scour

Wave-induced currents in combination with local bottom currents acting on fine silts and sands can result in scour of the seafloor (e.g. Kuenen, 1950). As summarized in Section 2.2.4, maximum bottom currents are expected to be on the order of about 100 cm/sec in the coastal region and slightly less in deeper water. In proximity to an offshore structure, these currents would likely be even higher, due to hydrodynamic interaction effects. According to empirical relationships developed by Kuenen (1950), these velocities are sufficiently high to transport surficial sediments in the area. This indicates a potential for scouring in a major portion of the area, particularly along the coastal region and in proximity to an offshore structure.

The possibility of scour presents no significant problem to the design of offshore structures. Various remedial measures can be taken to mitigate the scour effects. These remedial measures should be developed for each specific case taking the type and configuration of the offshore structure into consideration.

5.6.2.2 Wave-Induced Liquefaction

The passage of storm waves can generate a transient pore pressure and a permanent excess pore-water pressure buildup in cohesionless sediments (Finn and others, 1980). The magnitude of the transient and permanent pore pressures depends on a number of factors, including the wave height and length, the water depth, and the soil type. Where conditions are suitable, the transient pore pressures develop instantaneously in a one-to-one relationship with the applied wave loading while the excess pore pressure buildup accumulates in proportion to the number of wave-induced shearing stress reversals. As the pore pressure increases, the effective resistance of cohesionless soil can decrease, which can lead to potential instability of the seafloor.

The interaction of a storm wave with the seafloor sediments and its associated effects on the seafloor stability involve many important individual elements. Rational frameworks for evaluating these types of problems have been provided by various investigators (e.g., Seed and Rahman, 1977; Finn and others, 1980). In this analysis the potential for wave-induced liquefaction within the study area was evaluated using the method recommended by Seed and Rahman, (1977). The following maximum wave characteristics were considered:

- maximum wave height = 30 m
- period = 15 seconds
- water depth = 76 m

This analysis also required use of a wave-height/occurrence histogram. The distribution shown in Table 5-5 was assumed for this study. The values shown in this table were based on engineering judgment and unpublished data for the area. Site-specific information and evaluation are necessary for further refinement of these values.

This analysis involved the following steps:

1. Evaluate the storm-wave-induced shear stress in the soil profile.
2. Establish an equivalent uniform storm.
3. Estimate the excess pore pressure increase.

The induced shear stress for each wave cycle (component) was calculated using the theory of elasticity as formulated by Seed and Rahman (1979). The equivalent uniform storm was then established using their shear stress ratio at the top of soil profile induced and the liquefaction strength curves (Figure 5-23) in accordance with the procedures developed by Lee and Chan (1972).

The third step in the analysis involved an estimate of the excess (or permanent) pore-water pressure increase. In this study, simplified procedures were used to estimate the excess pore pressure in accordance with the following equation given by Seed and Rahman (1977):

Table 5-5 Wave-Height Histogram Used in Liquefaction Studies

Wave Height (m)	Number of Occurrences
30.0	1
28.0 to 29.3	1
26.7 to 28.0	2
25.3 to 26.7	3
24.0 to 25.3	7
22.7 to 24.0	16
21.3 to 22.7	24
20.0 to 22.3	31
18.7 to 20.0.	35
17.3 to 18.7	39
16.0 to 17.3	75
14.7 to 16.0	103
13.3 to 14.7	141
12.0 to 13.3	176
10.7 to 12.0	220
9.3 to 10.1	270
8.0 to 9.3	325

Note: The total storm duration was estimated to be about 6.1 hours assuming an average period of about 15 seconds.

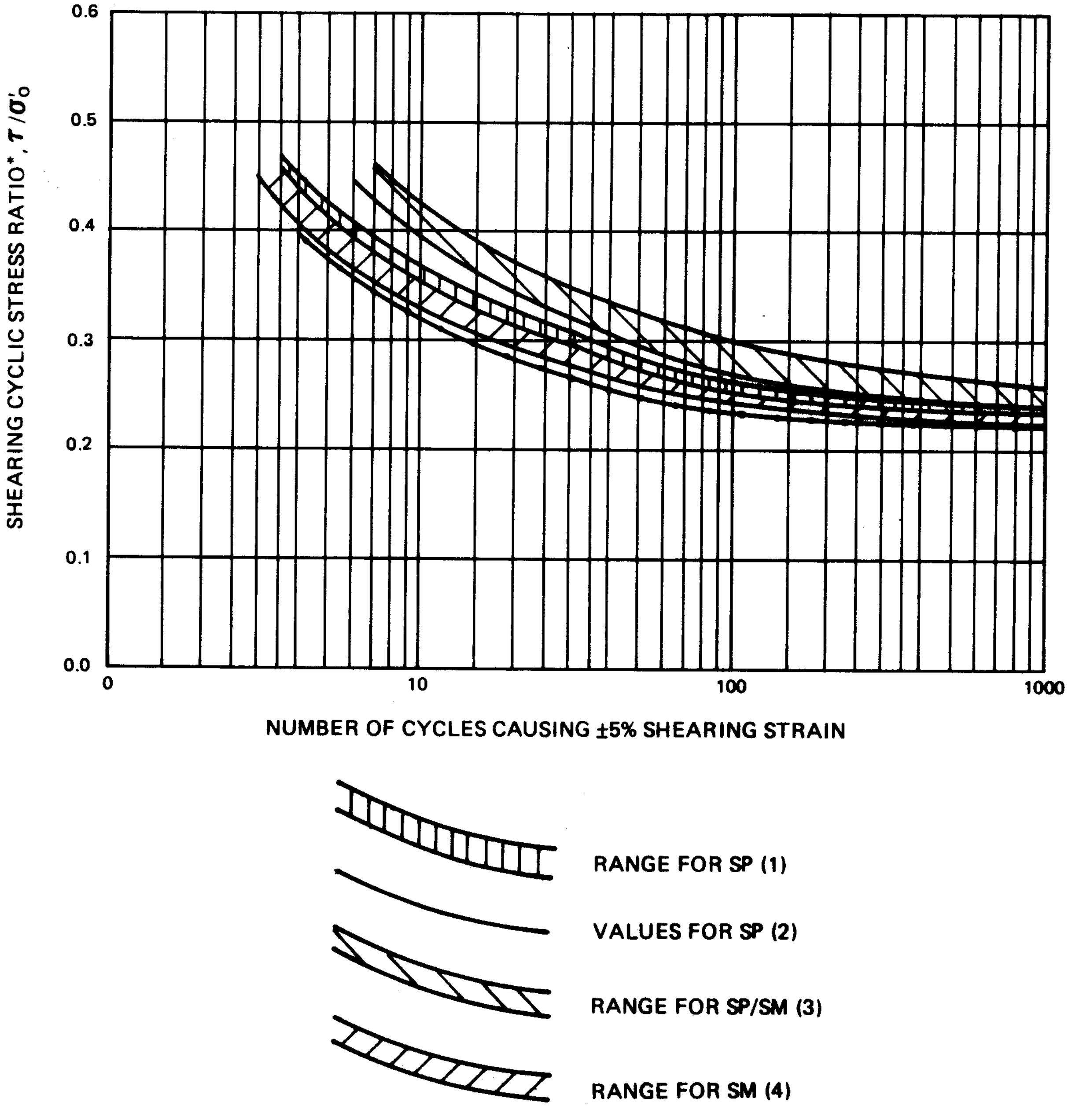

*DEFINED AS RATIO OF CYCLIC SHEARING STRESS (τ) TO INITIAL EFFECTIVE VERTICAL STRESS (σ'_o)

FIGURE 5-23 ESTIMATED LIQUEFACTION STRENGTH IN THE FIELD

$$\frac{\Delta u_g}{\sigma'_{vo}} = \frac{2}{\pi} \sin^{-1} \left(\frac{N}{N_1}\right)^{1/2\Theta} \quad \text{. . . . . (5-2)}$$

where

σ'_{vo} = initial effective vertical stress

Δu_g = excess pore pressure

N = equivalent number of cycles of a specific wave height that produces same effect as the storm wave

N_1 = number of cycles of a given cyclic shearing stress ratio (ratio of cyclic shearing stress to σ'_{vo}) that produces liquefaction of the soil. N_1 can be obtained from liquefaction strength curves.

Θ = empirical factor, a value of $\Theta = 0.7$ is typical (Seed and Rahman, 1977) and was assumed in this study.

The use of Equation 5-2 to estimate the excess pore pressure is conservative inasmuch as the effects of pore pressure dissipation and redistribution are not considered. This equation was adopted in lieu of a more complicated analysis (e.g., Finn and others, 1980; Clukey and Sangrey, 1980). The excess pore pressure values obtained on the basis of the above equation represent conservative upper bound estimates. The calculated excess pore pressure ratio ($\Delta u/\sigma'_{vo}$) was found to be negligible (less than 0.02). Thus, the potential for wave-induced liquefaction is extremely low.

5.6.2.3 Wave-Induced Transient Porewater Pressure

The passage of storm waves also induced transient porewater pressure which imposes transient seepage forces and reduced effective stress in the soils. This must be considered in evaluating the storm-wave-induced instability.

In this study the amplitude of the transient pore pressure (Δu_t) was calculated by the following simplified formula (Liu and others, 1979):

$$\Delta u_t = P_o \frac{\cosh\left[\frac{2}{L}\pi (d_s - Z)\right]}{\cosh\left(\frac{2}{L}\pi d_s\right)} \quad \text{(5-3)}$$

where

P_o = amplitude of wave pressure on the seafloor

$$= \frac{\gamma_w \times H}{2 \cosh\left(\frac{2\pi d}{L}\right)} * \cosh\left(\frac{2}{L} x - \omega t\right)$$

L = wave length

d = water depth

γ_w = unit weight of seawater

H = wave height

d_s = thickness of soil profile overlying an impermeable layer

Z = depth at any point along the soil profile

x = horizontal distance from wave crest

t = time

ω = circular frequency of wave train

The vertical and horizontal hydraulic gradients can be calculated by partial differentiation with respect to z and x. With the given condition, the maximum hydraulic gradient was found to be less than 0.15 $^m/_m$ (meter of water column per meter length). This small transient hydraulic gradient is not critical to the stability of seafloor slope; however, it should be considered in the design of pipelines and man-made slopes in the area.

The results of the above evaluation indicate that the storm-wave induced liquefaction potential is extremely low for locations where the water depth is 76 m or more. More critical conditions potentially develop as the water depth decreases. However, even at a depth of 25 m, the analysis predicts minimal pore pressure buildup. As with any coastal regime, some sediment movements might be anticipated at less than 25 m of water because of the combined action of wave-induced excess and transient pressure. Most sediments in this depth regime are very coarse sands and gravels, and hence, should be very resistant to wave-induced instability. Nevertheless, localized deposits of finer sediments may occur and the bearing support of these materials will be potentially reduced or temporarily lost.

5.6.2.4 Slope Stability Under Wave Loading

As described previously, the natural slopes of the study area are gentle with gradients generally less than 0.5 percent. The preceding pore pressure evaluation indicates that the buildup in pore pressure will be minimal, and hence, the effects of storm-waves on slope stability will be small, i.e., the potential for seafloor slope instability under storm-wave loading will be extremely low.

5.6.3 Earthquake Loading

The Northern Aleutian Shelf study area has a high level of seismic activity. Results presented in Section 5.4.3 indicate that ground accelerations equal to at least 0.1g can be expected throughout the area; peak accelerations between 0.4 and 0.7g are predicted near the North Amak Fault Zone. The consequence of earthquake-induced ground shaking can be liquefaction and settlement of sandy soils, seafloor slumping or inertial loading of any bottom-supported structures. Inertial loading of a structure results in both added forces on structural members and connections as well as added loading to the soil as the structure responds at some damped natural frequency of vibration.

This analysis considered only the "free-field" loading associated with liquefaction, settlement, and slope instability. The inertial response of structures, whether the structure is a platform or pipeline, warrants special consideration on a project-specific basis. Procedures outlined in API RP2A (API, 1982) and ATC (1980) provide guidelines for treating these loading phenomena.

5.6.3.1 Liquefaction and Settlement

For granular soils, earthquake-induced cyclic shearing stresses cause a temporary progressive buildup in pore-water pressure within the soil. For loose sands, when the pore pressure reaches the effective overburden pressure, the sediments temporarily become fluid-like in consistency and are said to have liquefied. In the case of loose sands at or near this condition, the soil may temporarily lose its ability to support a structure or resist lateral loading. However, for medium dense to dense sandy soils such as those in the study area, the tendency of the sand to increase in volume as shear deformations occur (called dilation) increases the undrained shearing resistance of the soil even if the earthquake-induced excess pore presures increase to values approaching effective vertical stresses. This results in a stable, limiting deformation state (or residual undrained strength) which inhibits large shear deformation or failure. Thus, either "seismically-induced pore-pressure buildup" or "cyclic mobility" (e.g., Seed, 1976; Castro and Poulos, 1976) are probably more appropriate terms to describe the earthquake loading effects for the study area even though the term "liquefaction" is widely used in engineering practice. The term "liquefaction" is used in this study to describe the state of earthquake-induced excess pore pressure reaching the initial (prior to seismic loading) effective overburden of the soil.

From the onset of this study, it was recognized that "liquefaction" in the traditional sense of fluid-like failure would be improbable for the study area. Simplified total (undrained) analyses such as those described by Seed and Idriss (1971) and Seed (1976) would not properly describe the effects of earthquake loading. Upon consultation with NOAA representatives a mutual agreement was reached to evaluate the study area using an effective-stress computer program called DESRA II (Martin and others, 1976; Lee and Finn, 1977). This program features an algorithm for estimating the increase in pore-water pressures resulting from earthquake-induced cyclic shearing stresses. The program also models the effects of pore-pressure redistribution and dissipation within the soil deposit during and immediately after earthquake loading. Both features provide improved liquefaction potential evaluations.

To perform the DESRA analyses, a number of specific soil parameters were estimated on the basis of laboratory test data and published empirical soil property correlations. These parameters included the low-strain shear modulus and maximum soil shearing strength, the one-dimensional rebound characteristics, the liquefaction strength and the permeability of the soil. The low-amplitude shear moduli (G_{max}) were estimated using the following relationship (Seed and Idriss, 1971):

$$G_{max} = 1000\ k_2\ \sigma_o'^{0.5} \quad \text{(5-4)}$$

where

k_2 = a constant which varies with soil type and density,

σ_o' = the mean effective confining pressure at the depth of interest.

The k_2 values utilized in this study were based on the results of resonant column tests adjusted to represent closely in situ conditions (Figure 5-24). Values of G_{max} and associated maximum shearing strength, τ_{max}, were used to define a hyperbolic stress-strain relationship (Duncan and Chan, 1970) which characterized the soil response throughout earthquake loading. The τ_{max} values were estimated from the results of static triaxial tests assuming that the effective friction angles of 39°, 41°, 41°, and 37° appropriately represent the four soil profiles at Stations 1177/185, 1262/185, 1070/91, and 1020/100, respectively.

For saturated sands, cyclic loading causes an incremental change (increase) in excess pore pressure of, Δu, in accordance with the following expression of Finn and others (1976):

$$\Delta_u = \overline{E}_r \, \Delta\varepsilon_{vd} \quad \ldots\ldots\ldots\ldots \quad (5\text{-}5)$$

where

$\overline{E}_r$ = one-dimensional rebound modulus

$\Delta\varepsilon_{vd}$ = incremental change in volumetric strain

The rebound modulus, $\overline{E}_r$, is expressed (Martin and others, 1975) as:

$$\overline{E}_r = \frac{(\sigma'_v)^{1-m}}{Mk(\sigma'_{vo})^{n-m}} \quad \ldots\ldots\ldots\ldots \quad (5\text{-}6)$$

where

σ'_{vo} = initial effective vertical stress

σ'_v = effective vertical stress at any time

k,m,n = experimental rebound parameters determined by one-dimensional loading and unloading tests.

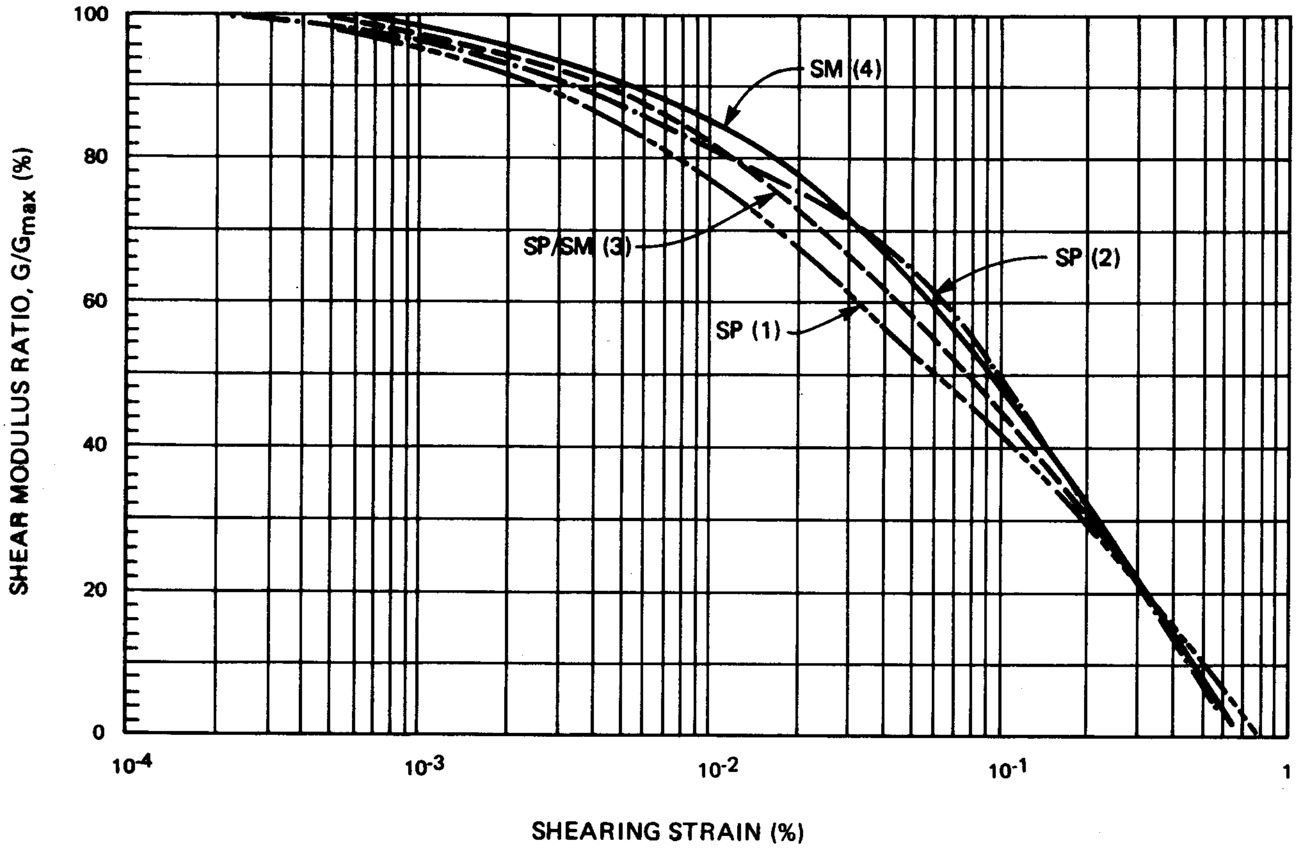

SOIL TYPE	K_2
SP (1)	16
SP (2)	15
SP/SM (3)	14
SM (4)	10

$G_{max} = 1000 * K_2 \sqrt{\sigma_o'}$

WHERE G_{max} = MAXIMUM SHEAR MODULUS (KN/M^2)

G = SHEAR MODULUS (KN/M^2) AT SPECIFIC SHEARING STRAIN LEVEL

σ_o = MEAN EFFECTIVE CONFINING STRESS (KN/M^2)

FIGURE 5-24 SHEAR MODULUS VALUES USED IN LIQUEFACTION ANALYSES

The liquefaction strengths of the four soil profiles were obtained from the results of cyclic simple shear tests with appropriate corrections to account for in situ conditions (Figure 5-23). The permeability characteristics of the site soils were obtained from laboratory data. These characteristics were required to account for pore pressure redistribution and dissipation during earthquake loading. Best-estimate soil properties utilized in this study are presented in Table 5-6.

In this liquefaction evaluation, the earthquake time histories identified in Table 5-2 were utilized as seismic input. These earthquake time histories were scaled to the peak ground acceleration levels shown in Figure 5-5. The seismic record was introduced at the bottom of the soil profile; a transmitting boundary at the base apportions the input motion such that energy radiates upward and downward from the input point in a manner consistent with the relative compliance of the soil column above and below the point of input.

Forty-six liquefaction analyses were performed to evaluate pore pressure buildup in the study area during various earthquake loadings. Table 5-7 provides a summary of the results of various cases analyzed. Appendix IV presents both calculated profiles of maximum earthquake-induced excess pore pressure and selected pore pressure profiles at various time intervals during earthquake loading.

The results presented in Table 5-7 and Appendix IV were plotted to show the potential for earthquake-induced liquefaction within the study area. This interpretation is presented in Figure 5-25. In this figure liquefaction potential is subdivided into the following three categories:

Table 5-6 Soil Properties for Liquefaction Analyses

Geotechnical Properties	Values Used For Soil Type[1)]				
	SP(1)	SP(2)	SP/SM(3)	SM(4)	Remarks
Total Unit Weight (kN/m^3)	20.5	20.0	20.0	19.0	
Effective Friction Angle (Degrees)	39	41	41	37	
Rebound Parameter k	0.043	0.105	0.134	0.051	
Rebound Parameter m	0.464	0.358	0.357	0.415	
Rebound Parameter n	0.067	0.063	0.05	0.067	
Coefficient of Permeability (cm/sec)	10^{-3}	5×10^{-3}	5×10^{-5}	2×10^{-5}	
Shear Modulus Coefficient, K_2	1.5 Times Lab Data	1.5 Times Lab Data	1.5 Times Lab Data	1.5 Times Lab Data	Figure 5-23
Damping Ratio	Figure II-41	Figure II-40	Figure II-42	Figure II-39	
Liquefaction Strength	Figure 5-23	Figure 5-23	Figure 5-23	Figure 5-23	

Note: [1)]Refer to Table 4-3

Table 5-7 Summary of Results from Liquefaction Analyses *

Earthquake Source	Earthquake Record	Maximum Ground Acceleration(g)	Liquefaction Results for Profile in Soil Type[1]			
			SP(1)	SP(2)	SP/SM(3)	SM(4)
Aleutian Subduction Zone	A-1	0.16	No Liq.	No Liq.	No Liq.	No Liq.
		0.19	No Liq.	No Liq.	No Liq.	No Liq.
Major Grabens	Taft, 1952	0.4	No Liq.	No Liq.	No Liq.	No Liq.
		0.5	Liq. in Top 8m	Liq. in Top 8m	No Liq.	Liq. in Top 3m
		0.6	-	-	Liq. in Top 4m	-
		0.7	Liq. in Top 12m	Liq. in Top 14m	Liq. in Top 8m	Liq. in Top 8m
	El Centro, 1940	0.4	No Liq.	No Liq.	No Liq.	No Liq.
		0.5	No Liq.	No Liq. between 2m to 3m	No Liq.	No Liq.
		0.6	-	-	No Liq.	-
		0.7	Liq. in Top 12m	Liq. in Top 14m	Liq. in Top 8m	Liq. in Top 9m
Other Large Back-Arc Faults	El Centro, 1979	0.3	No Liq.	No Liq.	No Liq.	No Liq.
		0.6	No Liq.	No Liq.	No Liq.	No Liq.
Aleutian Arc	Parkfield, 1966	0.4	No Liq.	No Liq.	No Liq.	No Liq.
Random[2] Events	-	-	-	-	-	-

Notes: 1) Refer to Table 4-3 for soil types.
2) Random events were considered least critical and thus, not analyzed. No liquefaction would be expected during these events.

* In this study "liquefaction" refers to the condition when earthquake-induced excess pore pressure equals the initial effective overburden.

1) High potential area where excess pore pressure buildup approaching effective overburden pressures is considered highly likely.

2) Moderate potential area where high pore pressure buildup is possible but is not considered likely.

3) Lower potential area where high pore pressure buildup is considered to be highly unlikely.

The liquefaction potential contours shown in Figure 5-25 were based on broad extrapolations and assumptions necessary for the preliminary and regional nature of this study. It was not intended to provide detailed assessment for a specific structure. Such an analysis requires further detailed site specific evaluations which take into account the possible effects of soil-structure interaction.

The consequence of "liquefaction", should it occur, will be controlled by the denseness of the sands. As noted previously, the surficial sediments in the study area are apparently very dense. Laboratory cyclic simple shear test data on these dense samples indicate that limiting strains develop regardless of the magnitude or duration of the applied cyclic shearing stresses. Thus, even in areas of high liquefaction potential, flow failure such as that experienced by the foundation of Sheffield Dam during the 1926 Santa Barbara earthquake (Seed and others, 1969) is unlikely. However, small permanent deformations during shaking are possible, with additional vertical displacements occurring as excess pore presssures dissipate. The magnitude of this post-earthquake settlement is also expected to be small.

The above liquefaction analyses were performed for a free field stress condition. Past experience indicates that the liquefaction potential for the soil beneath an offshore gravity-base structure is likely to be less than that of the free field. This primarily results from the effect of preshearing

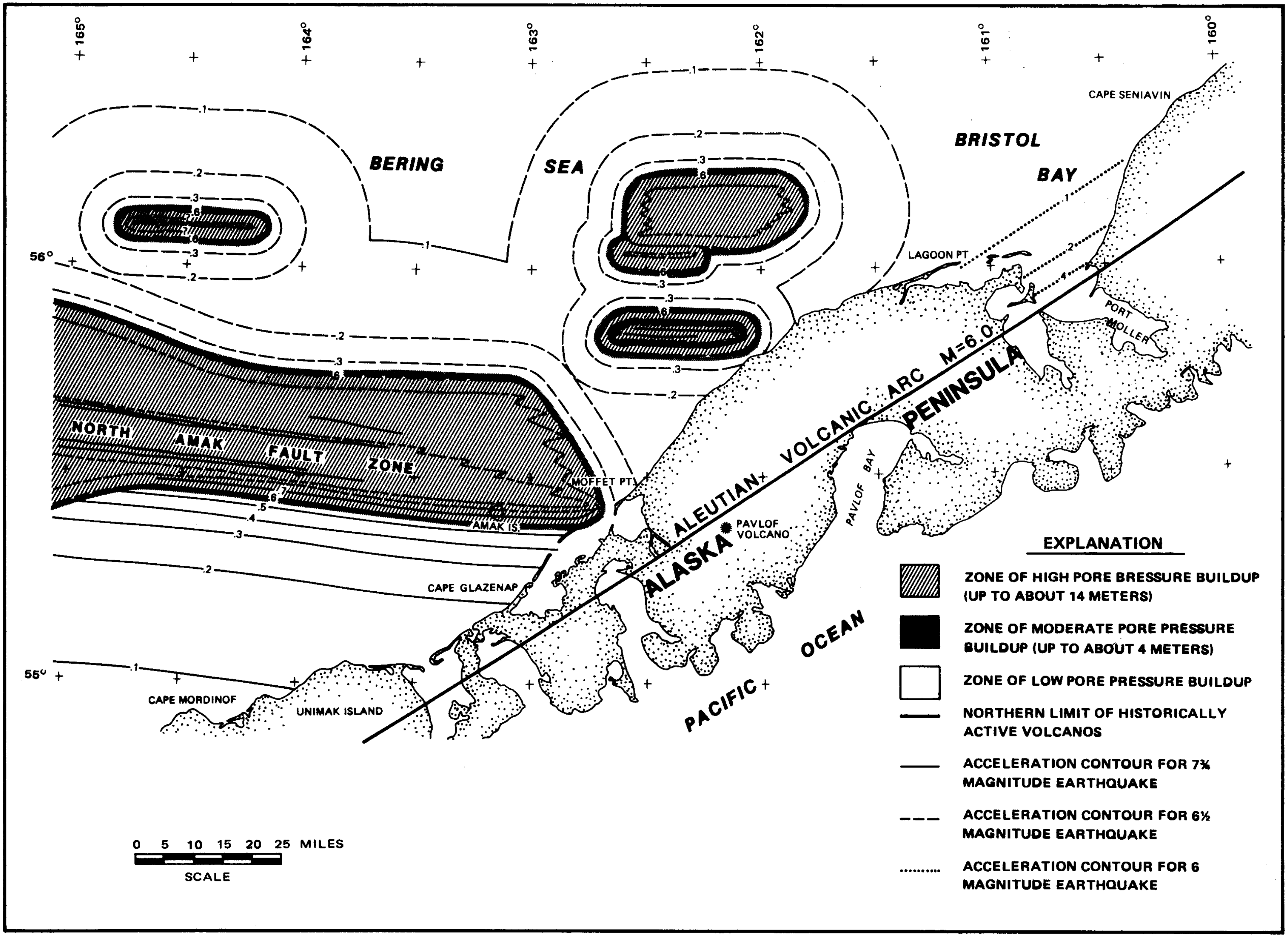

FIGURE 5-25 POTENTIAL FOR EARTHQUAKE-INDUCED PORE PRESSURE BUILDUP

(static horizontal shearing stress) and increases in confining pressure due to the structure loading, which usually more than offset the effects of additional cyclic shearing stresses induced by inertial response of the structure.

5.6.3.2 Slope Stability During Earthquakes

The potential for earthquake-induced slope failures is expected to be very low in most locations because of the relatively flat nature of the seafloor and the denseness of the seafloor sediments. In those areas where high excess pore-water pressures are predicted, some slope deformation might be anticipated during design earthquake accelerations. However the tendency for dilation should preclude any flow-type failures or the initiation of turbidity flows.

These conclusions assume that no local deposits of loose Holocene sands occur. Such materials are susceptible to large movement on slopes with angles less than 0.5 percent. Although such sediments are not anticipated, more detailed site investigations will ultimately be required in the area prior to development to verify this assumption.

6.0 POTENTIAL GEOLOGIC HAZARDS

6.1 EARTHQUAKES

The study region is in proximity to one of the more tectonically active regions of the world with a high rate of seismic activity. The major source of large earthquakes is the Alaska-Aleutian subduction zone which has generated several earthquakes in excess of magnitude 8 in historic times. Earthquakes of similar magnitude can be expected in the future and are capable of causing peak ground accelerations of about 0.1g in the study region.

A less-well known source of possible large earthquakes is the large faults that form the margins of the basins behind (north of) the Aleutian arc such as the North Amak Fault Zone. This fault zone extends westerly through the study region and beyond for a distance of more than 150 km (Plate IV(A)). The largest earthquake possible on this large normal fault zone must be estimated due to the short earthquake records in the area. Empirical data from similar faults throughout the world suggest that an earthquake of up to magnitude M_s 7 3/4 is plausible for this zone, but that such an event would probably have very long recurrence intervals, and hence, would not be very likely during the time span over which oil exploration and recovery are presently envisaged. If such an earthquake were to occur, peak ground accelerations could reach 0.4 to 0.7g in the vicinity of the fault zone (Figure 5-5).

Moderate-magnitude earthquakes could emanate from other faults within the area. Some of these faults extend upward to near the seafloor and a few even have seafloor expression in the form of surficial sags (Plates V(A) and V(B)).

Present data are not of sufficient resolution or density of spacing to completely characterize the nature of these faults; therefore, they are conservatively estimated to be capable of producing magnitude 6 1/2 earthquakes. Still other small faults may exist where geophysical data have not yet been collected. To account for these types of faults, a random earthquake of magnitude 5 1/2 is postulated.

6.2 SURFACE FAULTING

Surface faulting may also be a significant geologic hazard in specific locations. Faults disrupt the seafloor in two areas (Plates VIII(A) and VIII(B)) of the study region and approach the surface to within 150 to 300 m in three other areas (Plates V(A) and V(B)). Engineered facilities in these regions could be subject to vertical fault displacement or tilting of the seafloor and strong earthquake shaking. Data are presently not sufficient to estimate the amount of surface displacement which might be associated with these faults. Empirical fault-displacement/earthquake-magnitude data (Slemmons, 1977) for normal faults indicate that magnitude M_s 7 3/4 earthquakes can generate surface displacements of about 5 to 15 m.

6.3 VOLCANOES

The study area is bounded on the southeast by the volcanically active Aleutian Islands and Alaska Peninsula. Three major potentially active volcanoes are adjacent to the study region: Shishaldin, Pavlof, and Veniaminoff. The primary hazard from these volcanoes appears to be ash fall. The controlling factor in ash dispersal is wind direction. In the summer when the prevailing winds are from the south, volcanic ejecta could be carried into the site region.

Earthquakes associated with volcanic eruptions are generally less than magnitude 6 and thus ground shaking would probably attenuate rapidly enough that peak accelerations would generally be less than about 0.1g in the study region (Figure 5-5). The hazard from volcano-induced earthquakes is, therefore, regarded to be low.

6.4 SOIL INSTABILITY

Geotechnical studies indicate that geologic hazards due to soil instability will generally be related to storm-wave and earthquake loading. Soils appear to be dense or hard, and slopes are relatively flat (less than 0.5 percent); hence, many of the hazards commonly associated with weak sediments or slope instabilities do not exist. This suggests that bearing support for foundations will be acceptable under gravity (or static) loading (no storm-waves or earthquakes) as long as normal geotechnical design procedures are followed.

Wave-induced soil instabilities may be of potential concern at shallow water locations (e.g., water depths less than 25 m) where, during intense storm waves, bearing support for pipelines or other small, bottom supported structures could decrease or be temporarily lost. Whereas a possibility exists for wave-induced instability in shallow water, the likelihood generally appears to be low due to denseness and coarse-particle size of surficial sediment.

A more serious wave-induced instability potentially results from sediment scour. The sandy sediments in the study area have a grain-size distribution which is potentially susceptible to scour. Furthermore, maximum bottom currents on the seafloor in the study area are expected to be on the order of about 100 cm/sec in the coastal region and slightly less in deeper water. Higher velocities may also occur in proximity to a particular offshore structure because of hydrodynamic interaction effects. Published correlations indicate that these currents are sufficiently high to scour and transport the surficial sediment on the shelf.

Earthquake-induced soil instabilities form another potential geologic hazard for the shelf. This hazard was evaluated by conducting laboratory tests to evaluate the cyclic strength of the soil and then using this information to predict analytically the tendency for excess pore-pressure buildup at different locations. Results of these analyses were used to identify three levels of hazard:

1) High-potential area where high excess pore-pressure buildup is considered very likely.

2) Moderate-potential area where high pore-pressure buildup is possible but is not considered likely.

3) Lower-potential area where high pore-pressure buildup is considered very unlikely.

Figure 5-25 identifies areas on the North Aleutian shelf having these rankings.

It should be again noted, that "liquefaction" resulting in fluid-like failure is highly improbable for the study area. The term of "liquefaction" utilized in this report refers to the condition of excess pore pressure reaching the intital effective overburden value. The results of the earthquake-related seismic analysis also indicate that the potential depth of sediment liquefaction is very shallow (less than 15 m) even in zones of high pore-pressure buildup. In addition, the sediments in the study area are apparently quite dense. Data from laboratory cyclic simple shear tests indicate that certain limiting strains developed regardless of magnitudes or duration of the applied cyclic shearing stress. The limiting strain capability as well as the gentle slope gradients of the seafloor in the study area lead to the conclusion that seafloor instability in the form of flow slides as a result of strong earthquake shaking is unlikely even in areas of high pore-pressure buildup or liquefaction. However, seismically-induced permanent settlements or subsidence may be possible.

6.5 SHALLOW GAS AND GAS SEEPS

There is no conclusive seismic evidence for the presence of gas seeps within the area. However, at a few locations bowed reflectors and anomalies in reflector intensity suggest the presence of near-surface shallow gas. No hydrocarbons were reported from any sediment sample locations. "Bright spots" and chaotic reflectors indicative of possible hydrocarbon occurrence were observed on deep-penetration seismic-reflection lines. These areas are located west of Amak Island and north of Unimak Island at depths generally greater than 800 m, Plates V(A) and V(B).

Caution will be required in areas exhibiting a potential for shallow gas or gas-saturated sediments. In addition to the possibility of blowouts from shallow formational gas, accumulations of gas in sediments may result in low to negligible sediment strengths increasing the potential for soil instability. This hazard is important but not considered critical because of the infrequent occurrence.

6.6 SEDIMENT TRANSPORT

Numerous scours were identified from their distinctive signature on the side-scan sonar and 3.5 kHz data sets (Plates V(A) and V(B)). These results suggest that significant sediment transport must be anticipated, particularly in shallow water areas. In some case, these scours are incised up to 5 m into the sandy seafloor.

Generally, most scours have asymmetric cross-sections. The scours often occur in groups with some groups containing more than 200 distinct linear scours. Some individual scours have minimum lengths of 800 m, which is the limit of the side-scan sonar coverage. The width of individual scours ranges from a few meters to more than 250 m. The orientation of the scour sets varies from parallel to shore to perpendicular to shore. Some areas appear to have been influenced by the transverse longitudinal ridge system that covers the southeastern portion of the shelf. Other areas possess individual sets of intersecting scours, or more intricate sets of scours having sinuous or free-form shapes. Many scours have rippled coarse sand or lag gravel in their troughs.

6.7 OTHER POSSIBLE HAZARDS

From intermediate-penetration seismic data, a probable extension of the Black Hills Uplift is noted on the Geologic Hazards Map, Plates V(A) and V(B). This narrow basement rise ascends abruptly from a depth of approximately 1 km near its western edge to 130 m below the sea bottom within 10 km of the Peninsula. The possible effect of the shallow nature of the uplift should be considered during platform and pile design.

7.0 CONCLUSIONS AND RECOMMENDATIONS

7.1 CONCLUSIONS

Geological hazards on the Northern Aleutian Shelf have been evaluated during this study. The area encompassed by the evalution extends from the Alaskan Peninsula and Unimak Island on the south to latitude 57° 00' on the north, and between Port Moller (159° 30' W) and Unimak Pass (165° W) on the east-west boundaries. The evaluation was accomplished by conducting a review of existing literature followed by a field investigation and laboratory studies. The following conclusions were formulated on the basis of information gathered during this evaluation.

Regional Setting.

The regional setting for the area involves

1) a very flat continental shelf with maximum water depths less than 110 m and with maximum slopes of less than 0.5 percent;

2) a dynamic and complex oceanographic environment with salinities from 31 to 33 $^{o}/oo$, water temperatures from 0.5 to 18° C, 100 year significant wave heights from 17 to 23 m, tides from 2 to 7 m, and current velocities up to 100 cm/sec;

3) severe meteorologic conditions where winds approach or exceed 55 knots, where significant accumulations of precipitation occur and where temperatures range +25° C to -25° C

4) complex geologic conditions which have evolved from a complex process of subduction, uplift, sedimentation, glaciation and volcanism and which presently are strongly influenced by active seismic and volcanic environments.

This regional setting governs the potential for geologic hazards either directly as in the case of seismicity and volcanism, or indirectly such as the effects of storm waves on the stability of a bottom-supported platform or pipeline.

Field Program.

The field program was performed from aboard the NOAA ship Discoverer and involved seismic profiling, sediment sampling and in situ testing. Over 4000 km of seismic profile were collected; sediment samples were obtained at 60 stations. From this program it was concluded that

1) high quality geophysical data can be obtained using 3.5 kHz, uniboom, air gun, sparker and sidescan equipment during calm weather periods;

2) extreme care must be used during profiling due to the prevalence of crab pots in the survey area;

3) surficial sediments can be sampled with grab samplers, gravity coring methods and vibracorers, but penetration is limited to the upper 1 to 2 m due to the dense sandy characteristics of the soil; and that

4) drop penetrometer testing provides an efficient means of obtaining information about surficial soil conditions in situ, without necessitating elaborate deployment equipment, but as with sediment sampling, the depths of penetration are limited.

Laboratory Program.

Laboratory testing was conducted in shore-based testing facilities. The scope of these tests ranged from geological descriptions through cyclic testing. Results of this program indicated that

1) sediments on the shelf are silty sands and sands with mean grain sizes which decrease from 1 to 5 phi (0.5 to 0.0625 mm) as water depth increases, and with poorest sorting in shallow and deep waters;

2) the majority of the samples are composed of varying amounts of quartz, feldspar, hypersthene, hornblende and opaque minerals;

3) carbon concentrations are low with total organic carbon ranging from 0.3 to 0.5 percent and $CaCO_3$ averaging 0.2 percent;

4) four general soil types can be delineated from an engineering standpoint with each type being distinguished by decreasing percentages of course material and increasing percentages of silts;

5) the dry unit weight water content of surficial sediments range from 12 to 18 kN/m^3 and 10 to 40 percent, respectively;

6) apparent specific gravities of sediment particles vary from 2.67 to 2.80;

7) maximum and minimum dry unit weights range from 14 to 20 kN/m^3 and 12 to 18 kN/m^3, respectively;

8) compressibility is low with compression indices varying from 0.03 to 0.19 and recompression indices ranging from 0.003 to 0.012;

9) materials are relatively permeable with coefficients of permeability ranging from 1×10^{-3} to 5×10^{-5} cm/sec;

10) frictional characteristics of the sediments are high with effective friction angles from isotropically consolidated-drained triaxial tests ranging from 37° to 41°;

11) liquefaction strengths when normalized by the effective vertical stress during cyclic loading are from 0.32 to 0.40 for 10 cycles of loading and from 0.24 to 0.34 for 30 cycles of loading and exhibit low strain potential due to material denseness; and

12) low amplitude shear moduli vary from 1.1×10^4 kN/m^2 to 1.8×10^5 kN/m^2, damping values range from 2 to 5 percent, and strain effects are similar to those recorded for other sands.

Data Interpretation and Results.

Data gathered during the literature review, field program and laboratory testing were interpreted collectively to develop a regional framework for geological conditions within the study area. The results of this evaluation indicate that

1) bathymetry is flat with maximum slopes near the coastline of 0.5 percent or less and slopes beyond the 90 m isobath equal to 0.02 percent or less;

2) three sediment-filled basins (St. George, Amak and Bristol Bay) dominate the geologic structure within the study area;

3) complex basement-involved faulting occurs in proximity to the edges of St. George Basin and the Amak Basin and some of these faults are associated with surficial sag zones;

4) the upper 0 to 20 m of sediment originated in the late Quaternary (Wisconsinan and Holocene) and have an age of 11,000 to 12,000 years B.P. at a depth of 1 m;

5) The area is seismically active and has a potential for large earthquakes with the most likely sources of strong ground motion being the Alaska-Aleutian subduction zone. A less frequent source of large earthquakes is the major faults bounding the Amak and St. George basins.

6) maximum earthquake magnitudes can range from 8 3/4 for the Aleutian subduction zone down to 5 1/2 for a random event;

7) peak ground accelerations during earthquake loading will likely be equal to 0.1g for the overall study area and could reach 0.4 to 0.7g on a less frequent basis near the North Amak Fault Zone.

8) sediments are sands and silty sands with relative densities near 100 percent and in situ friction angles from drop penetrometer tests of 36° to 50°;

9) geotechnical performance of the sediments under gravity loading will be adequate and conventional analytical methods can be used in establishing foundation design methods;

10) storm-wave loading may create some engineering concerns in shallow-water depths by scour or wave-induced instability and these concerns should be addressed in site specific design; and that

11) surficial sediments may "liquefy" during large earthquakes near the major fault zones but consequences will likely be limited to settlement and inertial loading to the structure.

Potential Geologic Hazards.

Potential geologic hazards on the North Aleutian Shelf which will require special consideration during siting of exploratory and production facilities include:

1) earthquakes which can cause ground accelerations of 0.1 to 0.7g depending on the specific location of the facility;

2) surface faulting which could result in vertical offsets of 5 to 15 m;

3) volcanoes which could inundate a facility with volcanic ejecta if prevailing winds are from the south;

4) soil instability during storm-wave loading as sediments scour or liquefy under the action of hydrodynamic pressure fluctuations or bottom currents;

5) soil instability during earthquake loading as surficial sediments (0 to 15 m) in proximity to the earthquake source liquefy;

6) shallow gas and gas seeps which may cause blowouts or weakened soil conditions; and

7) sediment transport which can either bury, expose or undermine bottom supported structures.

Whereas the potential impact of these hazards is serious, all can generally be handled with existing technology either by relocating the site to avoid the hazard (faults or gas seeps) or by designing the facility to withstand the effects of the hazard. For example, the potentially harmful effects of earthquakes can be mitigated by adequate structural and foundation design followed by judicious use of protection systems.

7.2 RECOMMENDATIONS

This geologic hazards assessment was performed to obtain a regional understanding of geologic conditions on the Northern Aleutian Shelf which may impact lease development. Results of the study indicate that certain geologic hazards exist and must be addressed in any development of the area. It is recommended that these developments be approached on a site-specific basis and that they include as a minimum

1) additional oceanographic and meteorologic studies to enhance present understanding of currents, waves and wind conditions at a site;

2) additional high resolution sub-bottom seismic profiling and side-scan sonar surveying to define surface and near-surface geology in more detail;

3) geotechnical borings to a depth of 100 m or more for the purpose of obtaining high quality soil samples and in situ test data (vane shear or cone penetrometer);

4) specialized laboratory testing of high quality samples to establish design parameters for engineering studies;

5) further engineering studies to evaluate soil and foundation stability under gravity, storm-wave and earthquake loading conditions; and

6) field monitoring of foundation performance to ensure that behavior is consistent with expectation.

8.0 REFERENCES CITED

Alaska Geological Society, 1975, Composite stratigraphic section, Bristol Bay and Alaska Peninsula regions, Alaska: The Alaska Geological Society, 1 sheet.

American Petroleum Institute (API), 1982, RP 2A: Recommended Practice for Planning, Designing, and Constructing Fixed Offshore Platforms, 13th Edition, Dallas, Texas.

Anderson, D. G., and Stokoe, K. H., II, 1978, Shear modulus: A time dependent material property: ASTM Symposium on Dynamic Soil and Rock Testing, Denver, Colorado.

ATC, 1980, Tentative Provisions for the Development of Seismic Regulations for Buildings: Applied Technology Council, San Francisco, California.

Armstrong, R. L. , Harakal, J. E., and Hollister, V. F., 1976, Age determination of late Cenozoic porphyry deposits of the North American Cordillera: in Institution of Mining and Metallurgy: Applied Earth Science, Institution of Mining and Metallurgy Transactions, Section B. V. 85, p. B239-B244.

Arsen'ev, V. S., 1967. The currents and water masses of the Bering Sea: (Transl., 1968 National Marine Fisheries Center, Seattle), 146 p.

Askren, D. R., 1972, Holocene Stratigraphic Framework Southern Bering Sea Continental shelf: Master's Thesis, University of Washington, 104 p.

Baily, K. A., Cooper, A. K., Marlow, M. S., and Scholl, D. W., 1976, Preliminary residual magnetic map of the eastern Bering Shelf and parts of western Alaska: U.S. Geological Survey, Miscellaneous Field Studies Map MF-716.

Baranov. B. V., and Lobkovskii, L. I., 1980, Shallow seismicity in the back-arc of the Kurile Island arc and its connection with the Benioff zone; Dokl. Akad. Nauk. USSR, V. 255, no. 1.

Beikman, H., 1975, Preliminary geologic map of the Alaska Peninsula and Aleutian Islands: U.S. Geological Survey, Miscellaneous Field Studies Map MF-674, 2 sheets.

Berryhill, R. V., 1963, Reconnaissance of beach sands, Bristol Bay, Alaska: U.S. Bureau of Mines, Report of Investigations 6214, 48 p.

Bordovskiy, O. K., 1965, Accumulation and transformation of organic substances in marine sediment: Marine Geology, V. 3, p. 3-114.

Brower, W. A., Jr., Sezrby, H. W., Wise J. L., Davis, H. F., and Prechtel, A. S., 1977, Climatic Atlas of the outer continental shelf waters and coastal regions of Alaska: Arctic Environmental Information and Data Center, Anchorage, 443 p.

Burk, C. A., 1965, Geology of the Alaskan Peninsula Island Arc and Continental Margin: Geological Society of America, Memoir 99, 250 p.

Casagrande, A., 1976, Liquefaction and cyclic deformation of sands - a critical review: Harvard Soil Mechanics Series No. 88, Harvard University, Cambridge, Mass.

Castro, G., and Poulos, S. J., 1976, Factors affecting liquefaction and cyclic mobility: Preprint, ASCE Annual Convention and Exposition, Philadelphia, Pennsylvania, Sept 27-Oct 1.

Clukey, E. C., and Sangrey, D. A., 1980, Evaluating submarine slope instability in Alaska: Paper presented at the ASCE Annual Meeting, Hollywood, Florida, October 27-31.

Cobb, E. H., 1972, Metallic mineral resources of the Cold Bay Quadrangle, Alaska; U.S. Geological Survey, Miscellaneous Field Studies Map MF-441, 1 sheet.

Cooper, A. K., Marlow, M. S., Parker A. W., and Childs, J. R., 1979, Structure-contour map on acoustic basement in the Bering Sea: U. S. Geological Survey, Miscellaneous Field Studies Map MF-1165.

Cooper, A. K., Scholl, D. W., and Marlow, M. S., 1976, Plate tectonic model for the evolution of the eastern Bering Sea Basin: Geological Society of America Bulletin, V. 87, p. 1099-1126.

Curray, J. R., 1965, Late Quaternary history, continental shelves of the United States, in Wright, H. E., and Frey, D. G., (editors). The Quaternary of the United States, Princeton, New Jersey, Princeton University Press, p. 723-735.

Davies, J. N., 1981, Seismic and volcanic risk in the St. George Basin and adjacent Aleutian arc, in Environmental assessment of the Alaskan Continental shelf: Combellick, R. E., and Sackinger, W. M., eds.,; Fairbanks and Juneau, Alaska, U.S. Dept. of Commerce, NOAA, OCS Environmental Assessment Prog., Chap. 3.

DM-7, 1971, Design Manual for Soil Mechanics, Foundations and Earth Structures, U. S. Navy, Bureau of Yards and Docks.

Dodimead, A. J., Favorite, F. and Hirano, T., 1963, Salmon of the North Pacific Ocean, Part II. Review of oceanography of the subarctic Pacific Region: International North Pacific Fisheries Committee, Bulletin No. 13, p. 1-11 and 177-187.

Duncan, J. M., and Chang, Y., 1970, Non linear analysis of stress and strain in soils: ASCE Journal, Soil Mechanics and Foundation Engineering Division, V. 96, No. SM5.

Durgunglu H., and Mitchell, J. K., 1975, Static penetration resistance of soils. I-Analysis, II-Evaluation of Theory and Implications for Practices: In Proceedings, In Situ Measurement of Soil Properties, V. I, Raleigh, North Carolina.

Emery, K. O., 1938, Rapid method of mechanical analysis of sands: Journal of Sedimentary Petrology, V. 8, p. 105-11.

Favorite, F., Ahantz, J. W., and Hebard, C. P., 1961, Oceanographic observations in Bristol Bay and the Bering Sea 1939-1941 (USCGT Redwing): U. S. Fish and Wildlife Service, Special Scientific Report - Fisheries, No. 381.

Felix, F., 1969, Origin and recent history of Newport submarine canyon, California Continental Borderland: Office of Naval Research, Geophysics Branch, Tech. Report NR083-144, 52 p.

Finn, W. D. Lian, Siddharthan, R., and Martin, G. R., 1980, Wave-induced instability in ocean floor sands, Preprint, ASCE Convention and Exposition, Miami, Florida.

Folk, R. L., 1980, Petrology of Sedimentary Rocks: Hemphill Publishing, Austin, Texas, p. 41-45.

Folk, R. L., 1974, Petrology of Sedimentary Rocks: Hemphill Publishing, Austin, Texas, 182 p.

Folk, R. L., and Ward, W. C., 1957, Brazos river bar - a study in the significance of grain-size parameters: Journal of Sedimentary Petrology, V. 27, p. 3-26.

Gardner, J. V., Vallier, T. L., Dean, W. E., Kvenvolden, K. A., and Redden, G. D., 1979, Sedimentology and geochemistry of surface sediments and the distribution of faults and potentially unstable sediments, St. George Basin region of the outer continental shelf, southern Bering Sea: U. S. Geological Survey, Open File Report 79-1562, 88 p.

Gershanovich, D. E., 1968, New data on geomorphology and recent sediments of the Bering Sea and the Gulf of Alaska: Marine Geology, V. 6, p. 281-296.

Gibbs, R. J., 1974, A settling tube system for sand-size analysis, Journal Sedimentary Petrology, V. 44, p. 583-588.

Gibbs, R. J., Mathews, M. D., and Lindk, D. A., 1971, The relationship between sphere size and settling velocity, Journal Sedimentary Petrology, V. 41, p. 7-18.

Grow, J. A., and Atwater, T. A., 1970, Mid-Tertiary tectonic transition in the Aleutian Arc: Geological Society of America Bulletin, V. 81, p. 3715-3722.

Hand, B. M., 1964, Hydrodynamics of beach and dune sedimentation (Ph.D Thesis): Pennsylvania State University, University Park, Pennsylvania, 163 p.

Hebard, J. F., 1961, Currents in the southeastern Bering Sea: International North Pacific Fisheries Committee, Bulletin No. 5, p. 9-15.

Hebard, J. F., 1959, Currents in the southeastern Bering Sea and possible effects upon King Crab Larvae: U. S. Fish and Wildlife Service, Special Scientific Report - Fisheries, No. 293.

Hsui, A. T., and Toksoz, M. N., 1981, Back-arc spreading: trench migration, continental pull or induced convection?: Tectoniphysics, V. 74, p. 89-98.

Hunter, R. E. Sallenger, A. H., and Dupre', W. R., 1979, Maps showing directions of longshore sediment transport along the Alaska Bering Sea Coast: U.S. Geological Survey, Miscellaneous Field Investigations Map, MF-1049.

Inman, D. L., 1949, Sorting of sediments in the light of fluid mechanics: Journal of Sedimentary Petrology, V. 19, p. 51-70.

Jennings, P. C., Housner, G. W., and Tsai, N. C., 1968, Simulated earthquake motions, Earthquake Engineering Research Laboratory Report, California Institute of Technology, April.

Katili, J. A., and Soetadi, 1971, Neotectonics and seismic zones of Indonesia: Proceedings of Royal Society of New Zealand.

Kemp, A. L. W., 1971, Organic carbon and nitrogen in the surface sediments of Lake Ontario, Erie, and Huron: Journal of Sedimentary Petrology, V. 41, p. 537-548.

Kennedy, G. C., and Waldron, H. H., 1955, Geology of Pavlof Volcano and vicinity, Alaska: U.S. Geological Survey Bulletin, 1028-A, p. 1-19.

Kinder, T. H., 1977, The hydrographic structure over the continental shelf near Bristol Bay, Alaska, June 1976: Department of Oceanography of Washington Technical Report, Ref- M77-3, 61 p.

Kinder, T. H., and Schumacher, J. D., 1980, Hydrographic structure over the continental shelf of the southeastern Bering Sea, <u>in</u> Coachman, L. K., and Tripp, R. B., (editors), Fifth annual report Bristol Bay Oceanographic Processes: Pacific Marine Environmental Lab., Environmental Research Laboratory, NOAA, p. 25-79. Also <u>in</u> Hood, D.W., and Calder, J.A., 1981, The eastern Bering Sea shelf: oceanography and resources, NOAA/OMPA, distributed by Univ. Wash. Press, Seattle, pp. 31-52.

Kolpack, R. L., and Bell, S. A., 1968, Gasometric determination of carbon in sediments by hydroxide absorption, Journal Sedimentary Petrology, V. 38, No. 2, p. 617-620.

Komar, P. D., 1976, Beach Processes and Sedimentation: Prentice-Hall Inc., Englewood Cliffs, New Jersey, 429 p.

Kuenen, P. H., 1950, Marine Geology, New York, Wriley.

Lamb, Horace, 1879, Hydrodynamics: Dover Publications, New York, p. 367., 1945.

Lee, R. L., and Chan, K., 1972, Number of equivalent significant cycles in strong motion earthquakes: Proceedings, International Conference on Microzonation, Seattle, Washington, October.

Lee, M. K. W., and Finn, W. D., Liam, 1977, DESRA, Program for the dynamic effective stress response analysis for soil deposits: Soil Mechanics Series No. 36, Dept. of Civil Engineering, University of British Columbia, Vancouver, B. C. Canada.

Lisitzin, A. P., 1972, Sedimentation in the world oceans: Society of Economic Paleontologists and Mineralogists Special Publication No. 17, p. 77.

________, 1966, Recent sedimentation in the Bering Sea (in Russian); Inst. Okenol. Akac. Nauk U.S.S.R., (translated by Israel Program for Scientific Translation), from U.S. Department of Commerce, Clearinghouse for Federal Scientific and Technologic Information, 614 p.

Liu, P. L. F., Timothy, P., and O'Donnell, R., 1979, Wave-induced forces on buried pipelines in permeable seabeds: Proceedings, 4th Conference on Civil Engineering in the Ocean, San Francisco, California.

Marlow, M. W., and Cooper, A. K., 1980a, Mesozoic and Cenozoic structural trends beneath the southern Bering Sea shelf: American Association Petroleum Geologists Bulletin, V. 64, p. 2139-2155.

Marlow, M. S., and Cooper, A. K., 1980b, Multichannel seismic-reflection profiles collected in 1976 in the southern Bering Sea shelf: U.S. Geolgoical Survey, Open File Report OF 80-389.

Marlow, M. S., McLean, Hugh, Cooper, A. K., Vallier, T. L., Gardner, J. V., McMullin, R., and Lynch, M. B., 1980; A preliminary summary of Regional Geology, Petroleum Potential, Environmental Geology, and Technology for Exploration and Development for proposed OCS Lease Sale No. 7, Northern Aleutian Shelf, Bering Sea, Alaska: U.S. Geological Survey, Open File Report, OF 80-653, 53 p.

Marlow, M. S., Gardner, J. V., Vallier, T. L. McLean H., Scott, E. W., and Lynch, M. B., 1979, Resource report for proposed OCS Lease Scale No. 70, St. George Basin, Shelf Area, Alaska: U.S. Geological Survey, Open File Report OF 79-1650, 79 p.

Marlow, M. S., McLean H., Vallier, T. L., School, D. W., Gardner, J. V., and Powers, R., 1976a, Preliminary report on the regional geology, oil and gas potential and environmental hazards of the Bering Sea shelf south of St. Lawrence, Island, Alaska: U. S. Geological Survey Open File Report OF 76-785, 98 p.

Marlow, M. S., Scholl, D. W., Cooper, A. K., and Buffington, E. C., 1976b, Structure and evolution of Bering Sea shelf south of St. Lawrence Island: American Association of Petroleum Geologists Bulletin, V. 60, No. 2, 161-183.

Martin, G. R., Finn, W. D. L., and Seed, H. B., 1975, Fundamentals of liquefaction under cyclic loading, Journal of Geotechnical Engineering Division, ASCE, Vol. 101, No. GT5, pp. 423-438.

Martin G. R., Finn, Liam, W. D., and Seed, H. B., 1976, Fundamentals of liquefaction under cyclic loading, ASCE Journal, Geotechnical Engineering Division, V. 101, No. GT5.

McGeary, S. E., and Ben-Avraham, Z., 1981, Allochthonous terranes in Alaska: Implications for the structure and evolution of the Bering Sea shelf: Geology, v. 9, p. 608-614.

McIntyre, D. D., 1969, The hydraulic equivalence and size distribution of some mineral grains from a beach, Journal of Geology, V. 67, p. 278-301.

McLean, H. 1979, Observations on the geology and petroleum potential of the Cold Bay-False Pass Area, Alaska Peninsula: U.S. Geological Survey Open File Report OF 79-1605.

_______, 1977, Organic geochemistry, lithology and paleontology of Tertiary and Mesozoic rocks from wells on the Alaska Peninsula: U.S. Geological Survey, Open File Report OF 77-813, 62 p.

McLean, H.,, Englehardt, C. L., and Howell, D. G., 1978, Reconnaissance map of the Cold Bay and False Pass quadrangles, Alaska: U.S. Geological Survey, Open File Report OF 78-813, 62 p.

Minerals Management Service (MMS), 1982, St. George Basin final environmental impact statement: U.S. Dept. Interior.

Molnia, B. F., Schwab, W. C., Austin, W. A., and Hoose, P. J., 1982, Map of potential geologic hazards on North Aleutian Shelf (Lease Scale 92), U.S. Geological Survey, Open File Report OF 82- in press.

Moore, D. G., 1972, Reflection profiling studies of the California Continental Borderland: Structure and Quaternary Turbidite Basins: Geological Society of America, Special paper 197, 142 p.

Mori, A. W., and Crouse, C. B., 1981, Strong motion data from Japanese earthquakes: World Data Center A for Solid Geophysics, Report SE-29, NOAA, December.

Nakamura, K., Jacob, K., Daives, J., 1977, Volcanoes as possible indicators or tectonic stress orientations - Aleutians and Alaska, in Island Arcs, Deep Sea Trenches and Back-Arc Basins; American Geophysical Union, Maurice Ewing Series V. 1, p. 1-14.

Nelson, C. H., Hopkins, D. M., and Scholl, D. W., 1974, Cenozoic Sedimentary and Tectonic History of the Bering Sea: in Hood, D. W., and Kelly, E. J., (eds.), Oceanography of the Bering Sea. Institute of Marine Science, University of Alaska Occasional Publication No. 2, p. 485-516.

Ohtani, K., 1973, Oceanographic structure in the Bering Sea: Memoirs of the Faculty of Fisheries, Hokkaido University, V. 21, p. 65-106.

Pearson, C. A., Mofjeld, H. O., and Tripp, R. B., 1981, Tides of the Eastern Bering Sea Shelf: in Hood, D. W. and Calder, J. A., eds., The Eastern Bering Sea Shelf: Oceanography and Resources: Office of Marine Pollution Assessment of the National Oceanic and Atmospheric Administration, V. 1, p. 111-130.

Quayle, R. G., and Fulbright, D. C., 1975, Extreme wind and wave return periods for the U.S. Coast: Mariner's Weather Log, V. 19, p. 67-70.

Reed, W. E., LeFever, R., and Moir, G. 1976, Depositional environment interpretations using settling velocity (Psi) distribution, Geological Society of America Bulletin, V. 87, No. 5.

Sanford, R. B., and Swift, D. J., 1971, Comparison of sieving and settling techniques for size analysis using a Benthos Rapid Sediment Analyzer: Sedimentology, V. 17, p. 257-264.

Schell, B. A., 1982, Distribution and style of faults in the Great Basin and their relationship to the magnitude and frequency of earthquakes: American Geophysical Union, Chapman Conference, Snowbird, Utah.

Schell, B. A., Farley, T., and Muir, S. G., 1981, Fault rupture and earthquake hazards in east-central Nevada and west central Utah: Association of Engineering Geologists, Meeting Program with Abstracts, p. 52.

Schlee, J., 1966, A modified Woods Hole Rapid Sediment Analyzer: Journal of Sedimentary Petrology, V. 36, p. 403-413.

Scholl, D. W., Buffington, E. C., and Hopkins, D. M., 1966, Exposure of basement rock on the continental slope of the Bering Sea: Science, V. 153., p. 992-994.

Schumacher, J. D., Kinder, T.H. Pashinski, D.J., and Charnell, R. L., 1979, A structural front over the continental shelf of the eastern Bering Sea: Journal Physical Oceanography, V. 9, p. 79-87.

Scott, R. S., 1967, In-place measurement of the strength of ocean floor soils by accelerometer: Proceedings, Civil Engineering in the Oceans, ASCE Conference, San Francisco, California, p. 419-444.

Seed, H. B., 1976, Evaluation of soil liquefaction effects on level ground during earthquakes: Preprints, ASCE Annual Convention and Exposition, Philadelphia, PA.

Seed, H. B., Lee, K. L., and Idriss, I. M., 1969, An analysis of the Sheffield Dam failure: ASCE Journal, Soil Mechanics and Foundation Division, V. 95, No. SM6.

Seed, H. B., and Rahman, M. S., 1977, Analysis for wave-induced liquefaction in relation to ocean floor stability: Report No. UCB/TE 77/02, Department of Civil Engineering, Institute of Transportation and Traffic Engineering, University of California at Berkeley.

Seed, H. B., and Idriss, I. M., 1971, Simplified procedures for evaluating soil liquefaction potential: ASCE Journal, Soil Mechanics and Foundation Division, V. 93, No. SM3.

Sengupta, S., and Veenstra, H. J., 1968, On sieving and settling techniques for sand analysis: Sedimentology, V. 11, p. 83-98.

Sharma, G. D., 1979, The Alaska Shelf: Springer-Verlag, New York, 498 p.

Sharma, G. D., 1975, Contemporary epicontinental sedimentation and shelf grading in the southeast Bering Sea: in Forbes, R. B., (editor), Contributions to the Geology of the Bering Sea Basin and Adjacent Regions; Geologic Society of America, Special Paper 151, p. 33-48.

Sharma, G. D., 1974, Contemporary deposition environmental of the eastern Bering Sea: in Hood, D. W., and Kelly, E. J. (editors), Oceanography of the Bering Sea, Institute of Marine Science, University of Alaska Occasional Publication No. 2, p. 517-552.

Sharma, G. D., Naidu, A. S., and Hood, D. W., 1972, Bristol Bay: A model of a contemporary graded shelf, American Association of Petroleum Geologists. Bulletin, V. 56, p. 2000-2012.

Slemmons, D. B., 1977, State-of-the-art for assessing earthquake hazards in the United States, Report 6: Faults and Experiment Station Miscellaneous Paper S-73-1.

Spence, W., 1977, The Aleutian arc: Tectonic blocks, episodic subduction, strain diffusion, and magma generation: Journal of Geophysical Research, V. 82, p. 213-230.

Takenouti, A. Y., and Ohtani, K., 1974, Currents and water masses in the Bering Sea: A review of Japanese Work, in Hood, D. W., and Kelley, E. J. (editors), Oceanography of the Bering Sea, Institute of Marine Science, University of Alaska Occasional Publication 2, p. 39-57.

Thom, E. C., 1973, Extreme wave height distributions over oceans: ASCE Journal, Waterways, Harbors and Coastal Engineering Division, V. 99, p. 355-374.

Trask, P. D., 1932, Origin and environment of source beds of petroleum: Gulf Publishing Company, Houston, 323 p.

U.S. Army, Corps of Engineers, 1974, The Bristol Bay environment, A background study of available knowledge: Arctic Environmental Information and Data Center, University of Alaska, Anchorage, 858 p.

U.S. Department of Commerce, 1979, Coastal Pilot #9, Pacific and Arctic Coasts, U.S. Department of Commerce, National Oceanic and Atmospheric Administration, National Ocean Survey, Washington, D. C.

USGS, 1976, Seismic engineering data report: strong-motion earthquake accelerograms, digitization and analysis, 1971 records: Open File Report No. 76-609, July.

USGS, 1978 Seismic engineering data report: strong-motion earth records: Open File Report No. 78-941, October.

Uyeda, S. 1977, Some basic problems in the trench-arc-back-arc system, in Island Arcs, Deep Sea Trenches and Back-Arc Basins: American Geophysical Union, Maurice Ewing Series, V. 1, p. 1-14.

Uyeda, S., Kanomori, H., 1979, Back-arc opening and the moe of subduction: Journal of Geophysical Research, V. 84, p. 1049-1061.

Von Huene, R. and Shor, G. G., 1969, The structure and tectonic history of the eastern Aleutian Trench: Geologic Society of America Bulletin, V. 80, p. 1889-1902.

Waldron, H. H., 1961, Geologic reconnaissance of Frosty Peak Volcano and vicinity, U.S. Geological Survey Bulletin, 1028-T, p. 677-708.

Wallace, R. E., 1977, Profiles and ages of young fault scarps, north-central Nevada: Geological Society of America Bulletin, V. 88, p. 1267-1281.

Wilcox, R. E., 1959, Some effects of recent volcanic ash falls with special reference to Alaska: U.S. Geological Survey Bulletin, 1028-N, p. 409-476.

Wilson, F. H., 1981, Map and table showing radiometric ages of rocks in the Alaska Peninsula: U.S. Geological Survey Open-File Report OF81-471, 23 p.

Zonenshain, L. P., and Savostin, L. A., 1981, Movement of lithospheric plates relative to subduction zones: formation of marginal seas and active continental margins: Tectonophysics, V. 74, p. 57-87.

9.0 PLATES

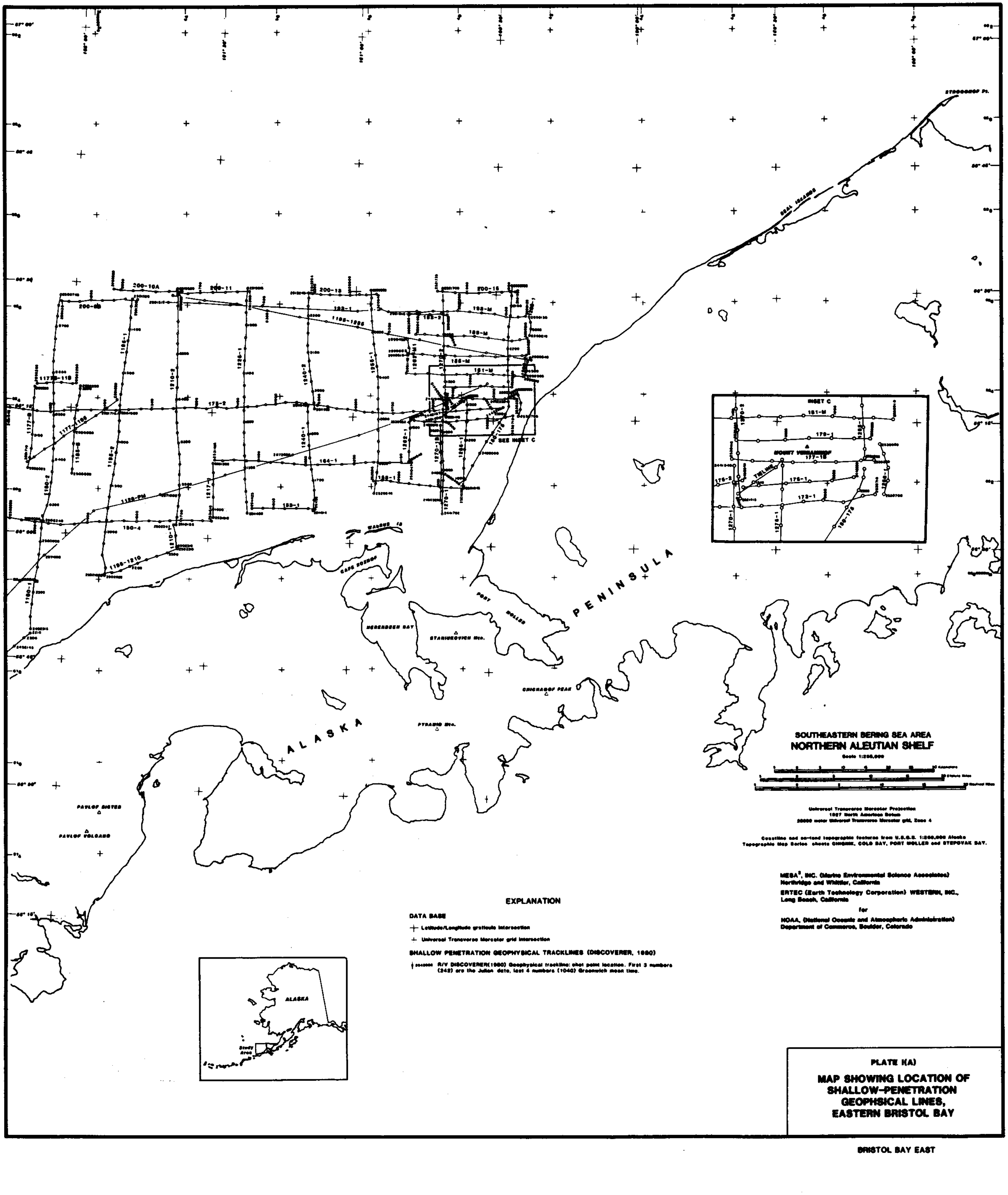

BRISTOL BAY EAST

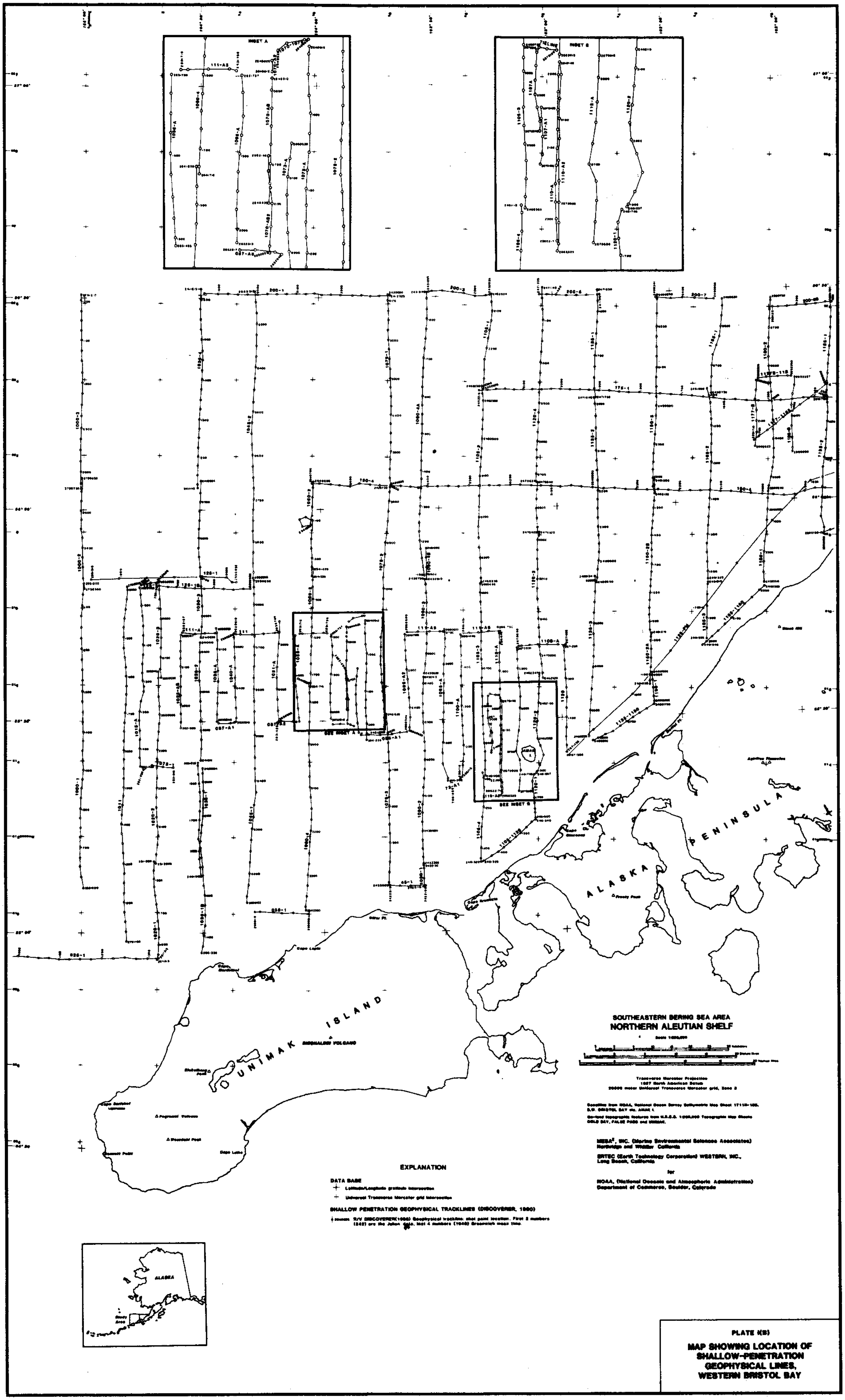

BRISTOL BAY WEST

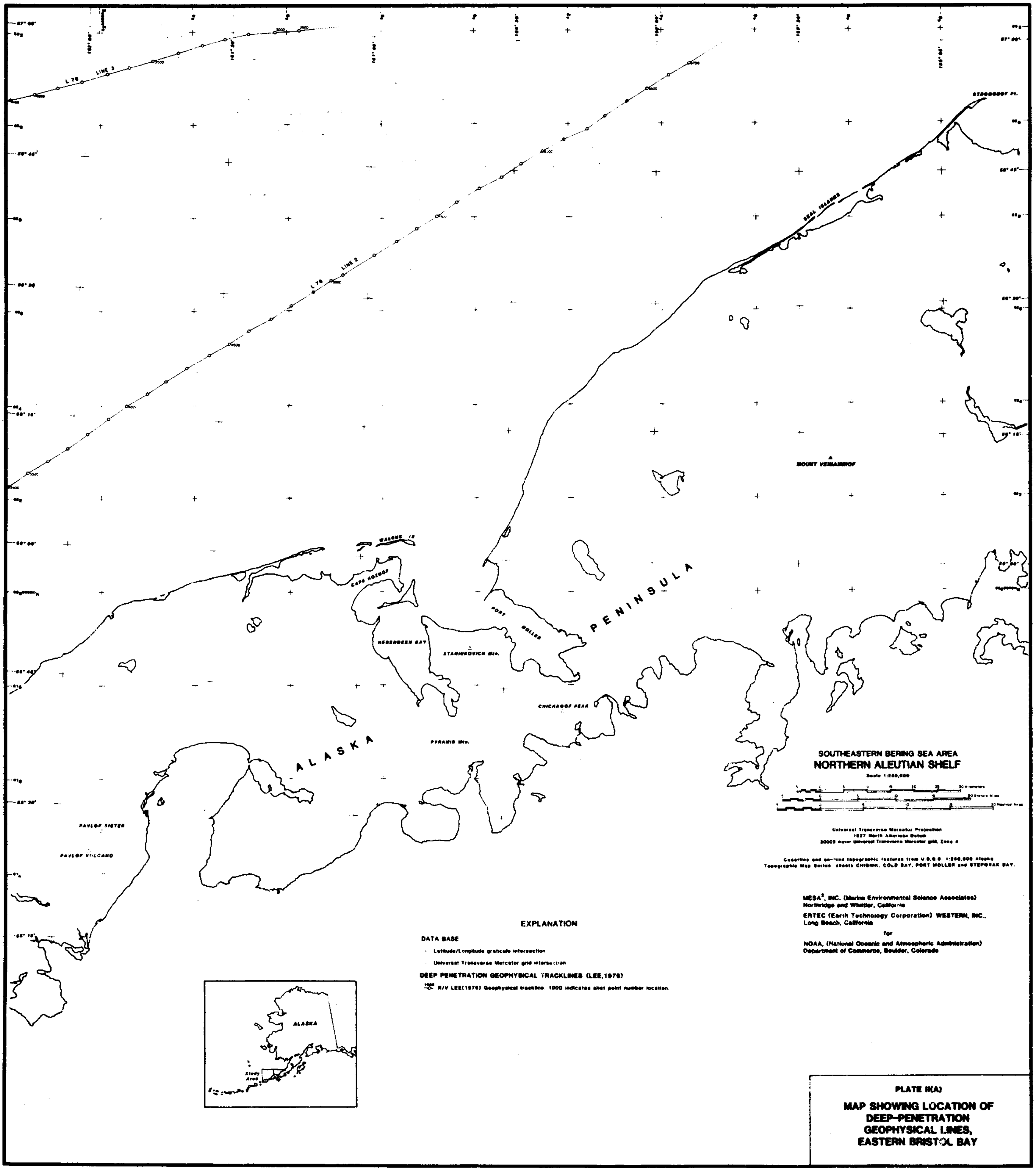

BRISTOL BAY EAST

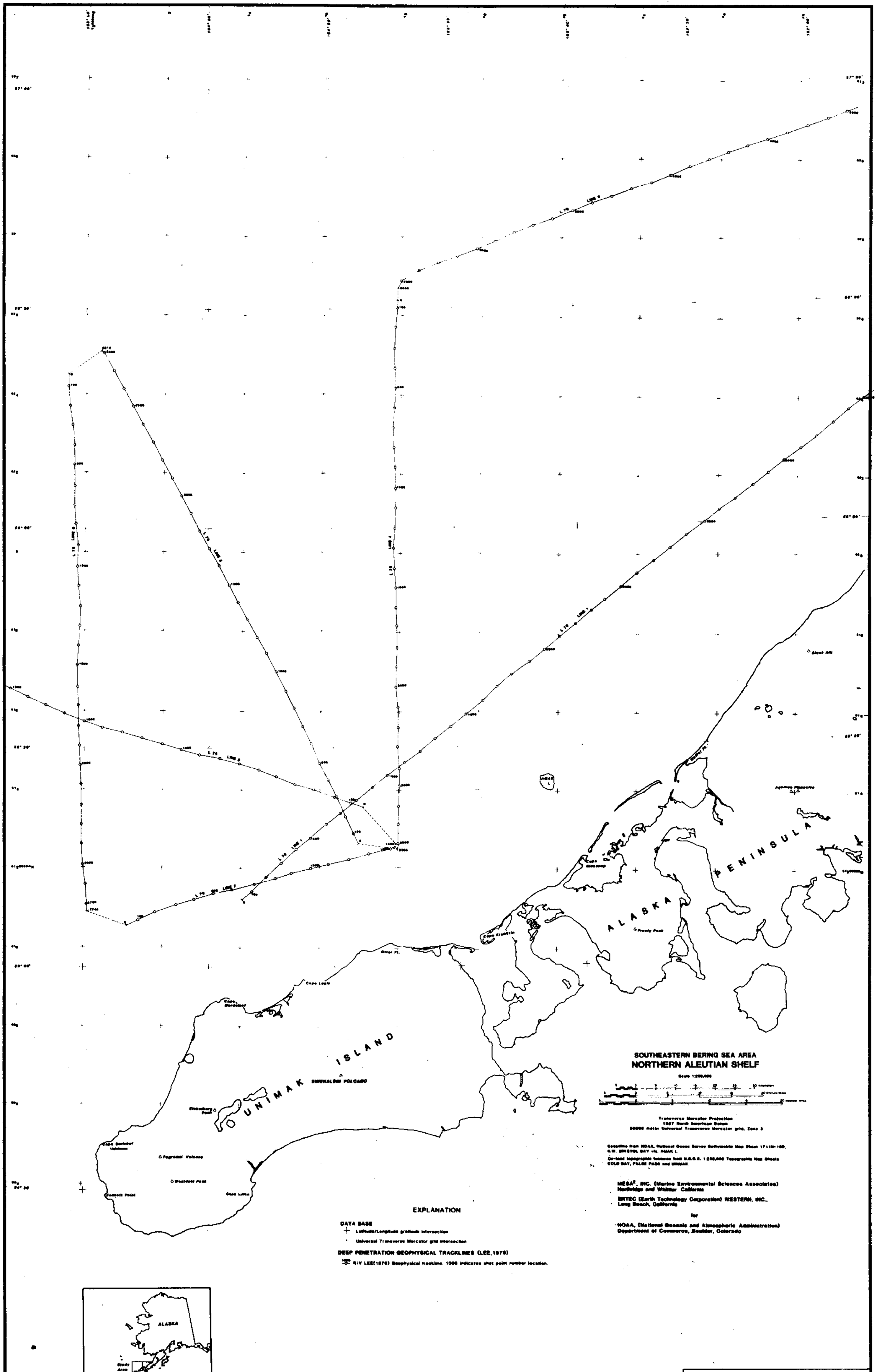

PLATE II(B)

MAP SHOWING LOCATION OF DEEP-PENETRATION GEOPHYSICAL LINES, WESTERN BRISTOL BAY

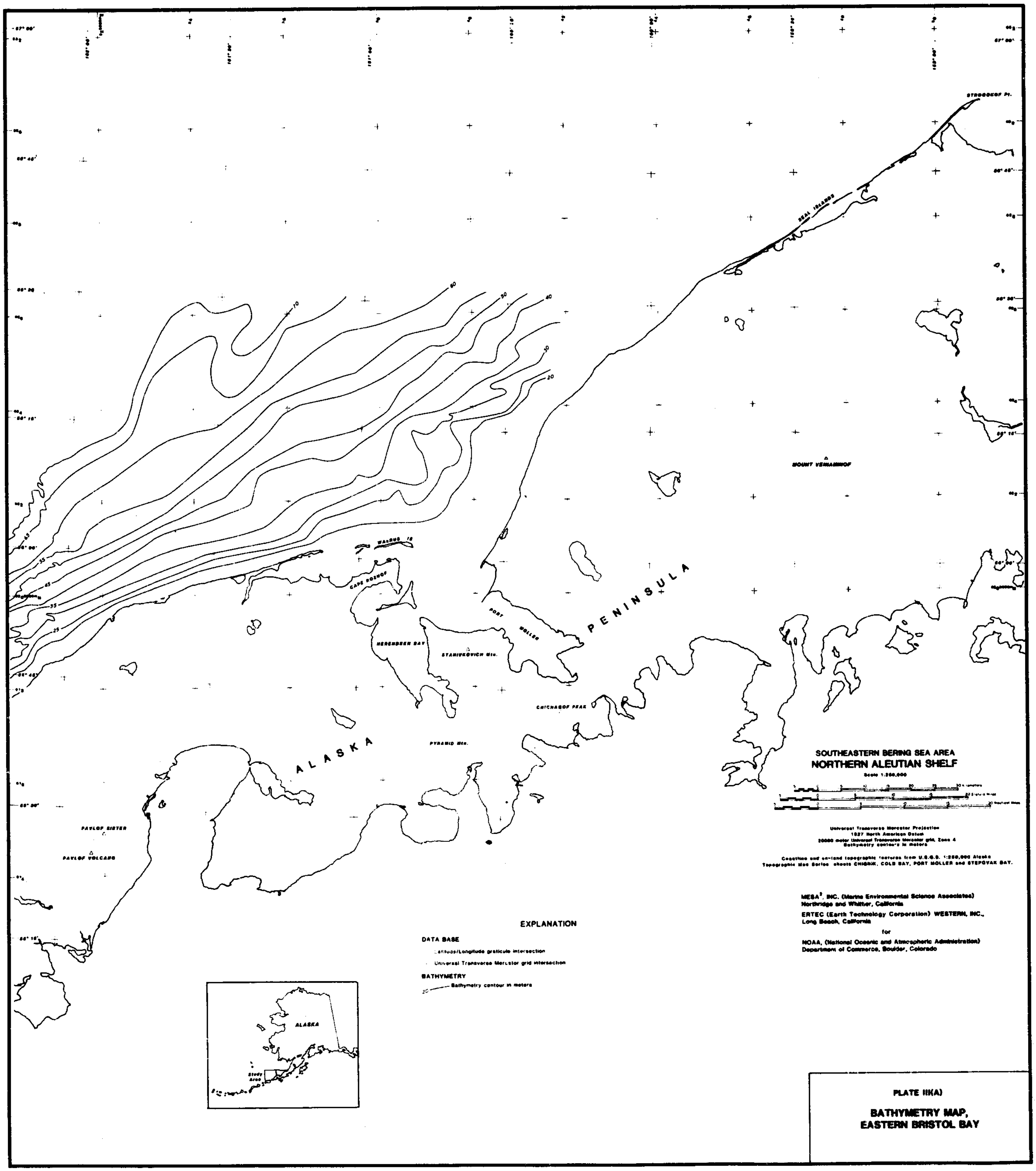

BRISTOL BAY EAST

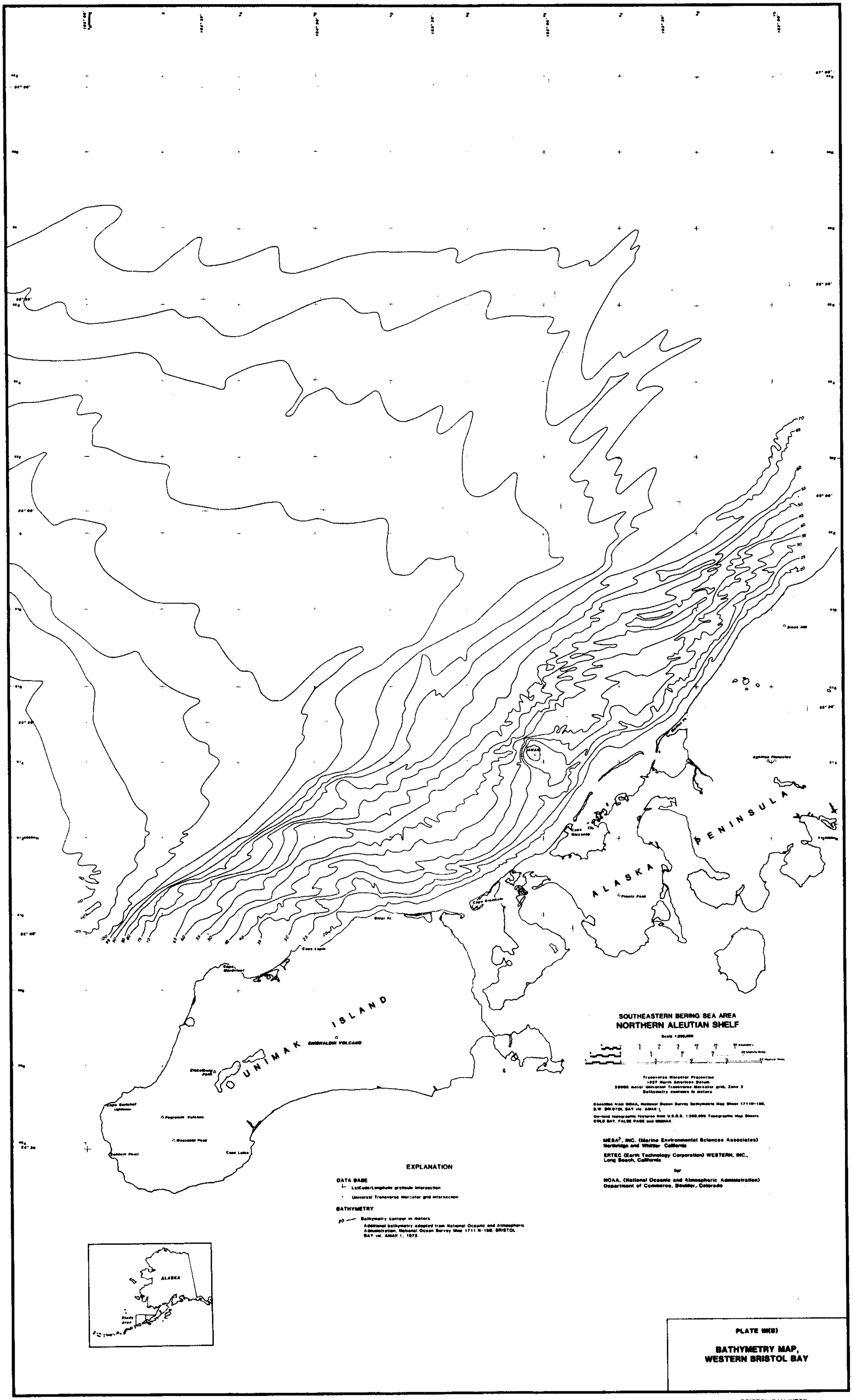

BRISTOL BAY WEST

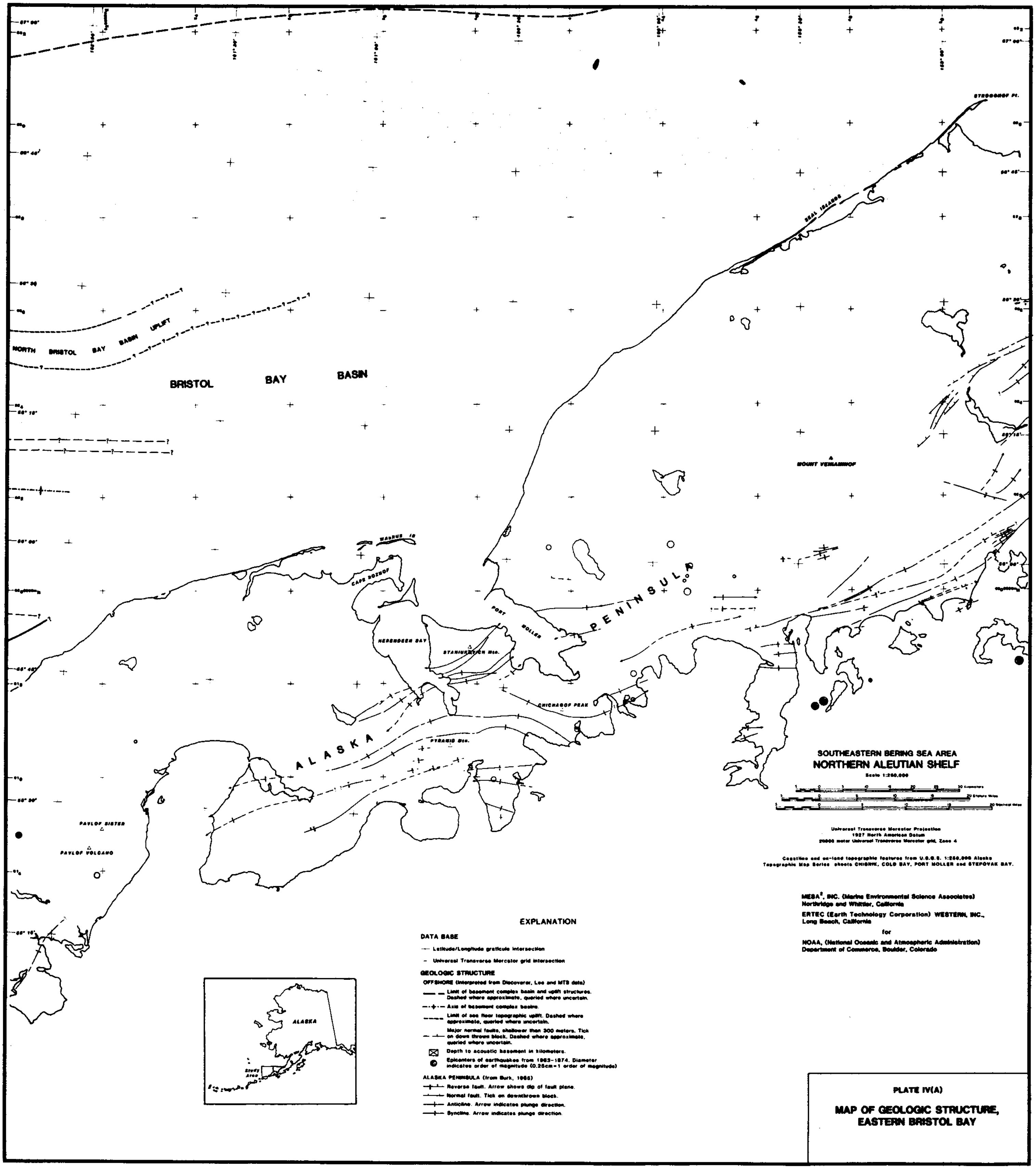

BRISTOL BAY EAST

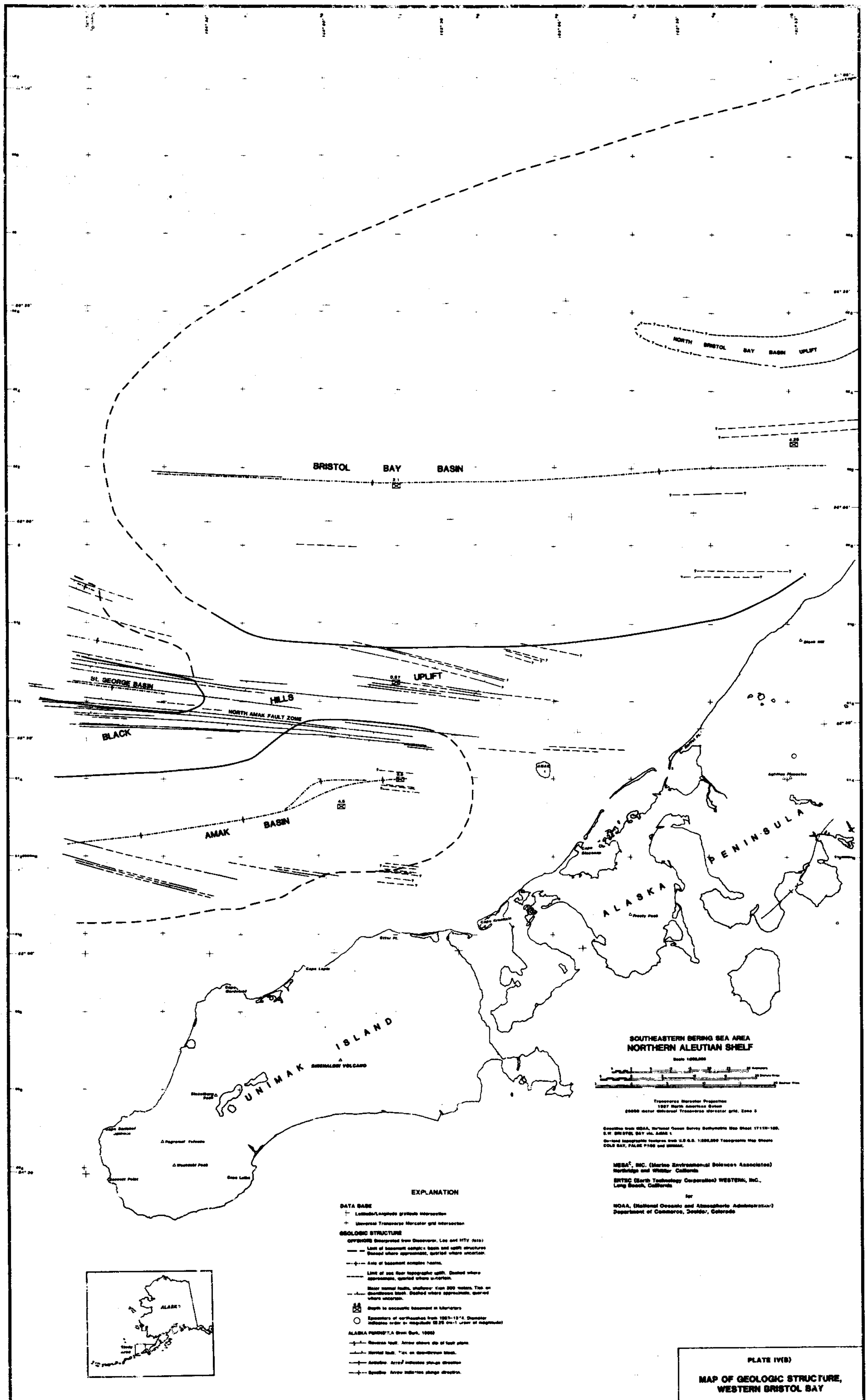

BRISTOL BAY WEST

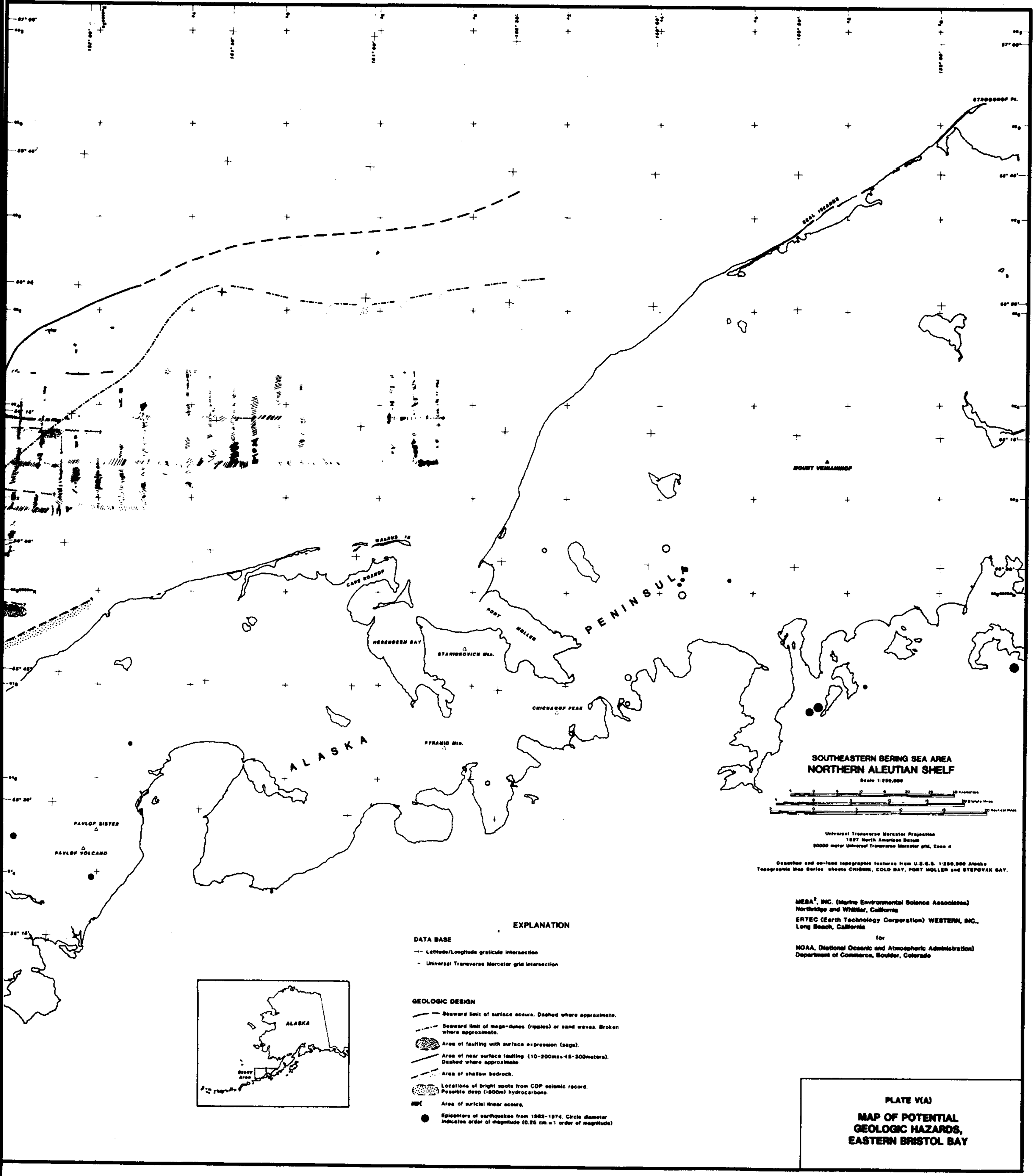

BRISTOL BAY EAST

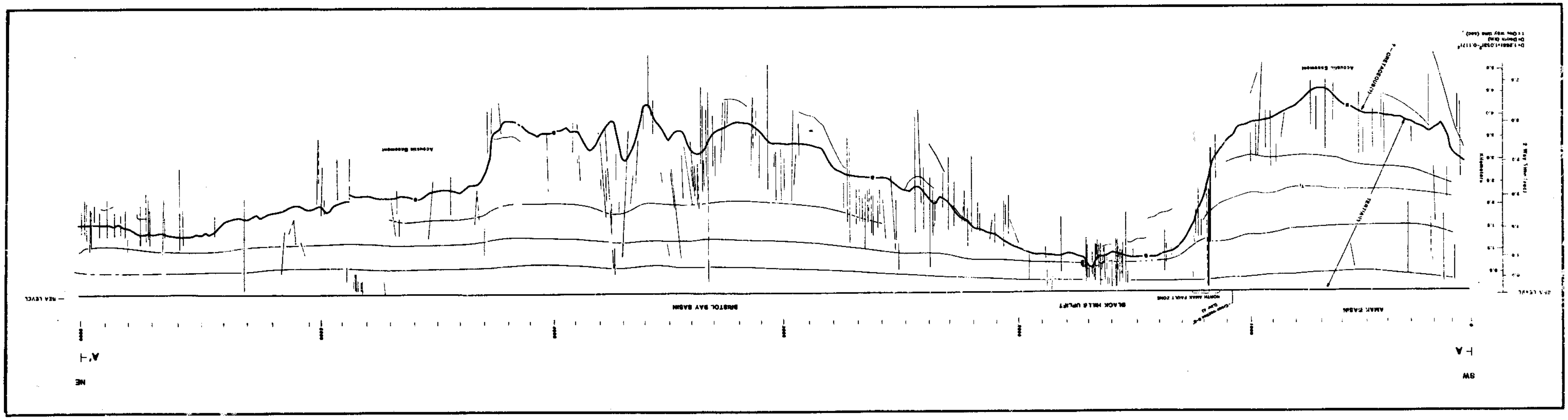

PLATE VI

GEOLOGIC CROSS-SECTION A-A'
ALONG R/V S.P. LEE (1976)
LINES 1 AND 2

MESA², INC (Marine Environmental Science Associates)
Whittier, California

ERTEC (Earth Technology Corporation) WESTERN, INC.,
Long Beach, California

for

NOAA (National Oceanic and Atmospheric Administration)
Department of Commerce, Boulder, Colorado

EXPLANATION

—T_1— Lower Tertiary

—B— Contact of unconformable acoustic basement

R/V S.P. Lee (1976) shot points

Horizontal Scale 1:250,000

Vertical Exaggeration 10:1

0 5 10 15 20 Kilometers

0 5 10 Statute Miles

PLATE VI

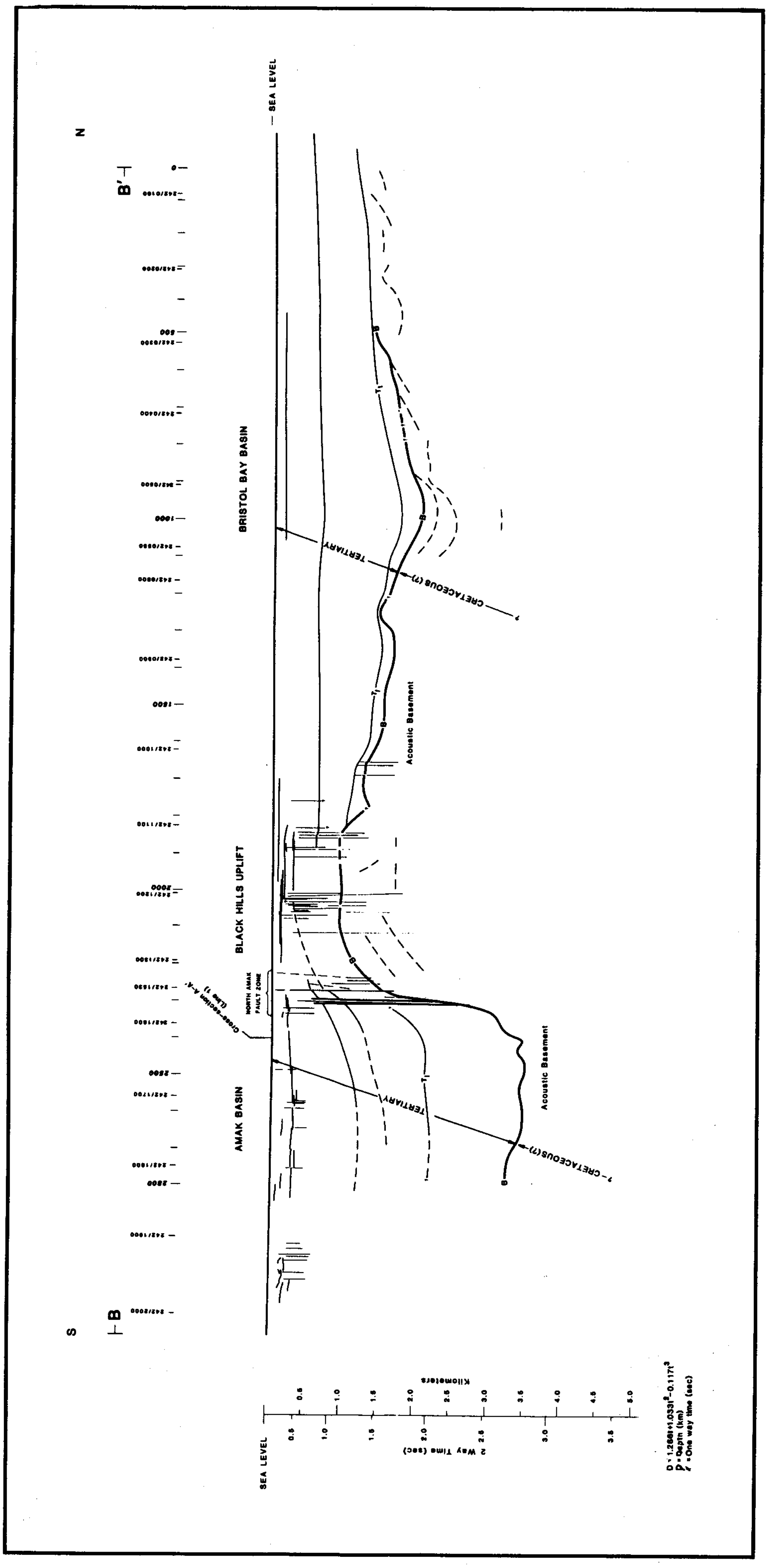

PLATE VII

GEOLOGIC CROSS-SECTION B-B'

ALONG R/V S.P. LEE (1976) LINE 4 AND DISCOVERER (1980) LINE 1079

MESA², INC. (Marine Environmental Science Associates) Whittier, California

ERTEC (Earth Technology Corporation) WESTERN, INC., Long Beach, California

for

NOAA, (National Oceanic and Atmospheric Administration) Department of Commerce, Boulder, Colorado

EXPLANATION

—T_l— Lower Tertiary

—B— Contact of unconformable acoustic basement.

— 242/0200 R/V Discoverer (1980) shot points. First number (242) indicates Julian date, second number (0200) indicates time.

— 500 R/V S.P. Lee (1976) shot points.

Horizontal Scale 1:250,000

Vertical Exaggeration 10:1

5 0 5 10 15 20 Kilometers

5 0 5 10 Statute Miles

PLATE VII

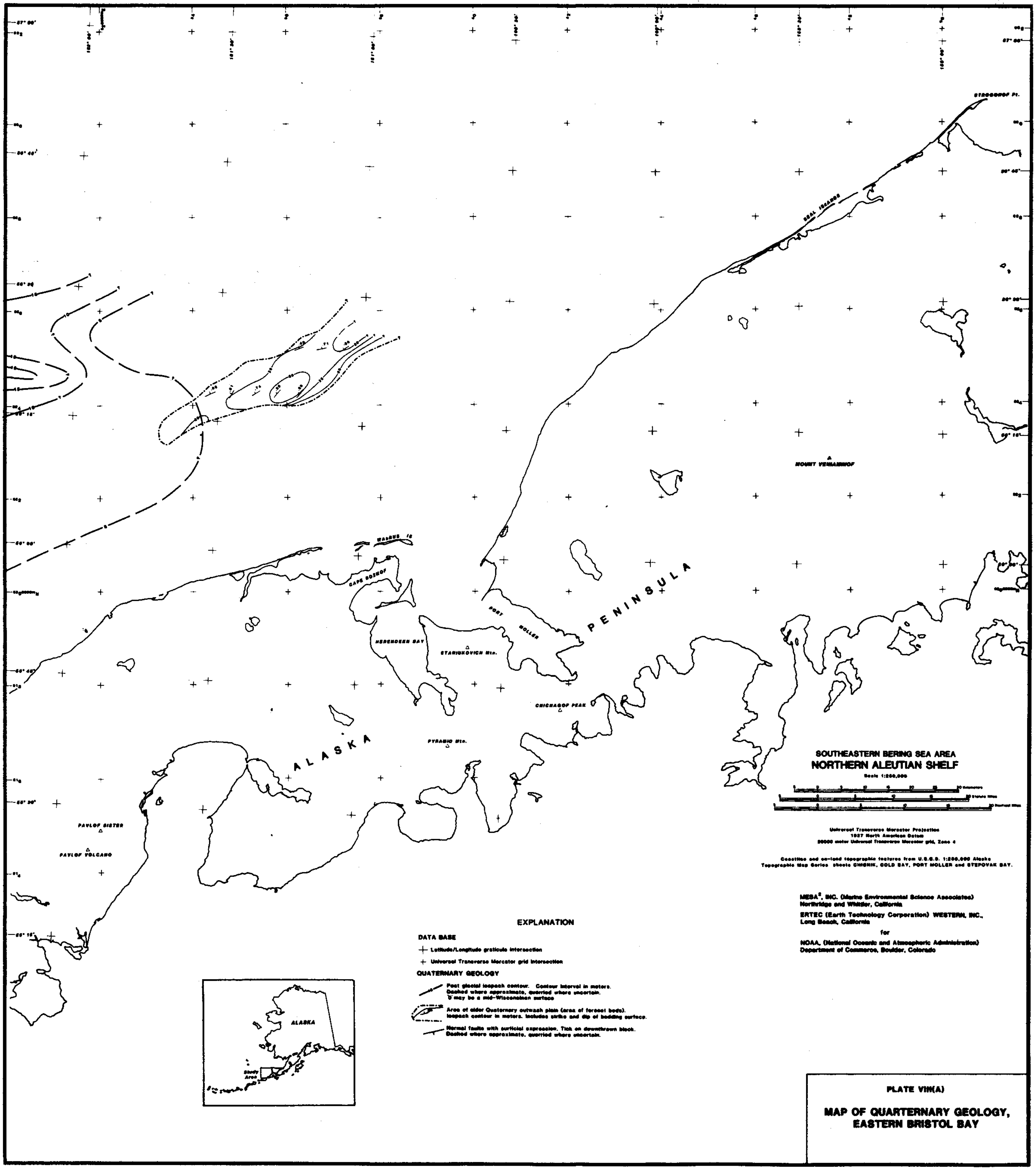

BRISTOL BAY EAST

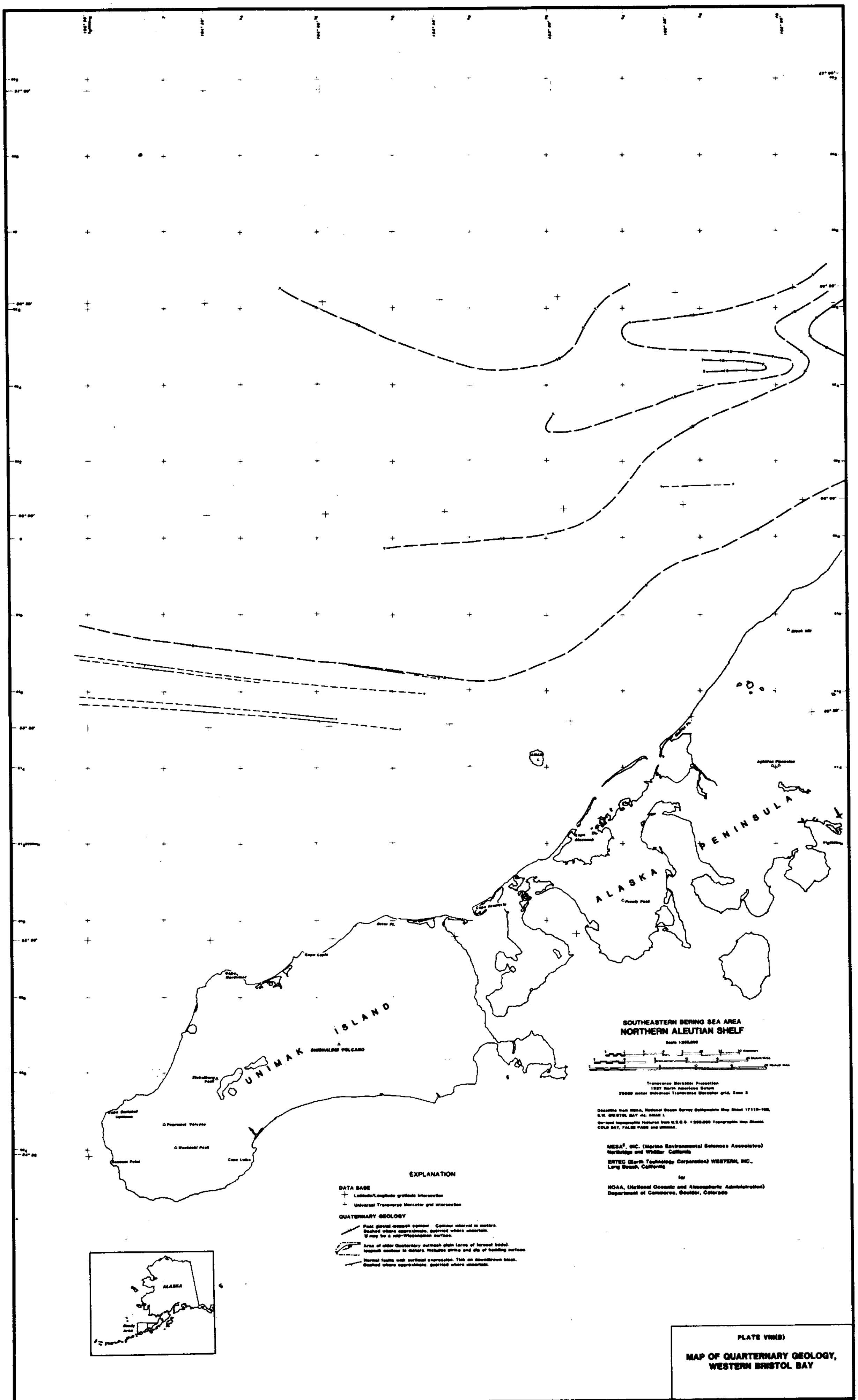

BRISTOL BAY WEST

APPENDIX I

SAMPLE LOCATIONS AND GRAIN-SIZE DISTRIBUTIONS

I.0 DEFINITIONS

Most of the grain size data for sediments obtained during the field program are reported in phi (ϕ) units. The equivalence between phi units and mean grain diameter is shown below.

Millimeters	Phi (ϕ)	Wentworth Size Class
2.4 - 2.0	-1.0	Granule
2.0 - 1.0	0.0	Very coarse sand
1.0 - 0.50	1.0	Medium sand
0.50 - 0.25	2.0	Fine sand
0.25 - 0.125	3.0	Very fine sand
0.125 - 0.0625	4.0	Coarse silt
0.0625 - 0.031	5.0	Medium silt
0.031 - 0.0156	6.0	Fine silt
0.0156 - 0.0078	7.0	Very fine silt
0.0078 - 0.0039	8.0	Coarse clay
0.0039 - 0.0020	9.0	Medium clay
0.0020 - 0.00098	10.0	Fine clay

Results of sediment analyses are also reported in terms of mean grain size, standard deviation, skewness, and kurtosis. These statistical parameters are described by Folk and Ward (1957) in the following manner:

1) Mean Grain Size:

The mean grain size is a measure of the average value of grain diameter as described by the following formula

$$M = \frac{\phi_{16} + \phi_{50} + \phi_{84}}{3}$$

where ϕ indicates a ϕ percentile.

2) Standard Deviation:

The standard deviation is a measure of sediment sorting with 68 percent of the distribution lying within $\pm$ 1 standard deviation of the mean.

3) Skewness and Kurtosis:

Skewness and kurtosis tell how closely the grain size distribution approaches the normal Gaussian probability curve. Skewness defines the asymmetry of a grain size distribution and is determined from the following formula

$$SK = \frac{\phi_{16} + \phi_{84} - 2\phi_{50}}{2(\phi_{84} - \phi_{16})} + \frac{\phi_{5} + \phi_{95} - 2\phi_{50}}{2(\phi_{95} - \phi_{5})}.$$

where ϕ indicates a ϕ percentile. Kurtosis defines the degree of peakedness of sediment size distribution and is determined from the following formula

$$K = \frac{\phi_{95} - \phi_{5}}{2.44\ (\phi_{75} - \phi_{25})}$$

where ϕ indicates a ϕ percentile.

Table I-1. Sample Data

Sample[1] Number	Station Number	Latitude(N)	Longitude(W)	Depth(m)	Sediment Parameters (Folk and Ward) % sand	% silt	% clay	Mean(ϕ)	Standard Deviation(ϕ)	Skewness	Kurtosis
1	1000/200	56° 29.9'	164° 59.3'	82	62	36	2	3.75	1.46	0.54	1.20
2	1000/150	56° 03.5'	164° 59.6'	93	76	22	2	3.47	1.37	0.41	1.61
3	1030/200	56° 31.0'	164° 30.0'	82	63	34	3	3.77	1.21	0.55	1.00
4	1040/200	56° 30.4'	164° 16.7'	82	74	24	2	3.57	1.16	0.51	1.14
5	1030/150	56° 03.0'	164° 31.0'	93	78	10	2	3.37	1.12	0.25	1.74
6	1011/125	55° 50.2'	164° 48.4'	95	74	24	2	3.53	1.31	0.38	1.71
7	1035/111	55° 42.8'	164° 26.5'	95	89	9	2	2.93	0.93	0.42	1.97
8	1030/107	55° 41.0'	164° 31.0'	95	90	8	2	2.90	0.77	0.21	1.81
9	1020/100	55° 36.4'	164° 40.2'	100	83	14	3	2.16	0.38	-0.17	1.07
10	1030/75	55° 23.0'	164° 31.0'	100	85	14	1	2.32	1.46	0.37	1.64
11	1020/50	55° 09.6'	164° 41.4'	99	83	15	2	3.03	1.15	0.20	3.03
12	1020/25	54° 56.5'	164° 41.0'	60	99	1	0	0.35	0.57	0.31	0.96
13	1079/200	56° 30.0'	163° 42.0'	82	--	--	-	----	----	----	----
14	1105/175	56° 16.0'	163° 18.0'	89	96	4	0	2.92	0.44	-0.35	1.14
15	1060/150	56° 03.0'	164° 02.0'	92	87	11	2	3.00	0.81	0.12	1.56
16	1079/150	56° 03.0'	164° 43.0'	93	83	16	1	3.13	1.04	0.40	1.66
17	1060/125	55° 49.6'	164° 02.2'	94	88	10	2	3.05	0.85	0.32	2.25
18	1090/125	55° 50.0'	163° 33.0'	94	94	4	2	2.75	0.62	-0.03	1.84
19	1105/125	55° 49.0'	163° 19.0'	90	96	4	0	2.72	0.46	-0.06	1.08
20	1110/111	55° 42.2'	163° 14.8'	83	97	3	0	2.55	0.44	-0.55	1.16
21	1090/100	55° 35.0'	163° 35.0'	83	99	1	0	2.35	0.54	0.27	0.98
22	1060/98	55° 35.1'	164° 03.0'	98	91	7	2	2.87	0.88	-0.10	1.59
23	1051/87	55° 29.2'	164° 11.1'	97	96	4	0	2.19	0.65	-0.21	0.77
24	1070/91	55° 31.9'	163° 53.9'	84	97	3	0	2.28	0.67	-0.28	1.11
25	1079/90	55° 30.9'	163° 44.1'	84	98	2	0	2.42	0.53	-0.29	0.86
26	1070/87	55° 29.4'	163° 52.2'	89	94	4	2	2.40	0.64	-0.37	1.07
27	1090/50	55° 09.0'	163° 35.0'	39	98	2	0	1.64	0.37	-0.08	0.98
28	1105/75	55° 22.4'	163° 20.3'	51	94	4	2	3.00	0.56	-0.17	1.39
29	1120/200	56° 30.1'	163° 02.3'	81	95	5	0	2.88	0.33	0.03	1.19
30	1150/200	56° 29.1'	162° 33.5'	81	99	1	0	2.43	0.33	-0.16	1.00
31	1135/174	56° 15.0'	162° 49.7'	80	99	1	0	2.53	0.40	-0.10	1.42
32	1135/175	56° 15.0'	162° 49.7'	80	99	1	0	2.74	0.46	0.04	1.23
33	1135/176	56° 15.0'	162° 49.7'	80	99	1	0	2.62	0.30	-0.24	1.00

NOTES: (1) Samples 1 through 60 are from this study; samples 61 through 120 are from previous studies.

Table I-1. Sample Data (Continued)

Sample[1] Number	Station Number	Latitude(N)	Longitude(W)	Depth(m)	Sediment Parameters (Folk and Ward) % sand	% silt	% clay	Mean(ϕ)	Standard Deviation(ϕ)	Skewness	Kurtosis
34	1120/150	56° 03.1'	163° 04.5'	86	98	2	0	2.65	0.36	-0.20	1.43
35	1135/125	55° 49.3'	162° 50.0'	80	99	1	0	2.05	0.81	0.11	0.70
36	1128/108	55° 40.0'	162° 58.7'	62	99	1	0	0.56	0.82	0.21	0.97
37	1120/100	55° 36.0'	163° 06.0'	62	99	1	0	2.16	0.38	-0.17	1.07
38	1150/100	55° 35.5'	162° 37.9'	40	99	1	0	2.13	0.37	-0.71	1.02
39	1120/75	55° 20.8'	163° 07.9'	36	98	2	0	0.68	0.62	0.50	1.09
40	1165/125	55° 48.4'	162° 22.3'	46	99	1	0	0.69	0.60	-0.06	0.89
41	1150/150	56° 01.9'	162° 35.3'	77	99	1	0	2.48	0.36	0.12	1.33
42	1165/175	56° 15.0'	162° 20.7'	82	99	1	0	2.20	0.47	-0.12	1.08
43	1177/185	56° 08.2'	162° 09.7'	80	99	1	0	1.67	0.64	-0.10	1.03
44	1180/150	56° 01.2'	162° 06.4'	72	99	1	0	1.90	0.73	-0.26	2.08
45	1180/200	56° 28.0'	162° 05.1'	72	99	1	0	2.28	0.48	-0.11	1.13
46	1202/200	56° 28.9'	161° 50.7'	81	96	4	0	2.18	0.47	-0.27	2.10
47	1203/200	56° 28.9'	161° 48.1'	93	98	2	0	2.27	0.39	-0.34	1.38
48	1204/200	56° 28.9'	161° 42.8'	91	98	2	0	2.40	0.36	-0.26	1.17
49	1225/200	56° 29.3'	161° 25.8'	75	99	1	0	2.15	0.33	-0.16	1.23
50	1195/175	56° 14.0'	161° 51.4'	72	99	1	0	2.13	0.40	-0.28	1.01
51	1210/150	56° 02.0'	161° 37.9'	40	99	1	0	1.95	0.49	0.09	1.48
52	1255/200	56° 29.7'	160° 57.8'	68	99	1	0	2.15	0.33	-0.16	1.23
53	1240/175	56° 15.8'	161° 09.6'	52	100	0	0	1.96	0.75	-0.50	1.01
54	1255/158	56° 06.9'	160° 55.8'	33	99	1	0	1.45	0.64	0.18	0.77
55	1285/200	56° 30.4'	160° 27.6'	44	100	0	0	0.90	0.89	0.04	1.16
56	1270/193	56° 27.5'	160° 42.0'	55	99	1	0	3.02	0.48	-0.10	0.95
57	1262/185	56° 22.5'	160° 49.5'	49	100	0	0	1.76	0.56	-0.44	1.46
58	1270/175	56° 17.0'	160° 42.0'	33	99	1	0	2.18	0.47	-0.47	2.56
59	1285/181	56° 22.2'	160° 26.1'	34	99	1	0	0.06	0.29	0.55	2.34
60	1285/177	56° 17.5'	160° 28.0'	22	100	0	0	1.57	0.76	-0.65	2.46

NOTES: (1) Samples 1 through 60 are from this study; samples 61 through 120 are from previous studies.

Table I-1. Sample Data (Continued)

Sample[1] Number	Station Number	Latitude(N)	Longitude(W)	Depth(m)	Sediment Parameters (Folk and Ward) % sand	% silt	% clay	Mean(ϕ)	Standard Deviation(ϕ)	Skewness	Kurtosis
61	146	56° 40.3'	165° 22.9'	77	47.0	47.0	6.0	4.431	1.868	0.135	1.615
62	149	56° 23.8'	165° 18.2'	85	30.0	43.0	27.0	5.928	3.148	-0.104	0.739
63	150	56° 23.8'	165° 18.2'	85	92.0	7.0	1.0	3.113	0.626	0.244	1.434
64	152	56° 03.5'	165° 18.9'	97	55.0	38.0	7.0	4.118	1.927	0.446	1.615
65	153	56° 03.5'	165° 18.9'	97	60.0	33.0	7.0	3.921	1.946	0.496	1.540
66	D-5	55° 52.0'	165° 16.0'	--	84.0	13.0	3.0	3.207	0.767	0.365	1.188
67	155	55° 36.0'	165° 17.3'	111	10.0	66.0	10.0	5.037	1.970	0.354	2.613
68	C-5	55° 32.0'	165° 09.0'	--	58.0	39.0	3.0	3.763	1.039	0.166	1.328
69	B-5	55° 16.0'	165° 08.0'	--	31.7	56.9	11.4	4.798	1.923	0.455	1.456
70	156	55° 12.2'	165° 17.9'	114	22.0	71.0	7.0	4.737	1.365	0.231	5.547
71	157	55° 12.2'	165° 17.9'	114	21.0	72.0	7.0	4.726	1.466	0.251	6.548
72	E-5	56° 16.0'	165° 05.0'	--	46.0	47.0	7.0	4.206	2.061	0.302	1.644
73	G-11	55° 30.6'	164° 50.2'	101	-----	----	---	-----	-----	-----	-----
74	B-6	55° 24.0'	164° 35.0'	--	74.2	19.5	6.3	3.440	1.647	0.449	2.351
75	002	55° 16.0'	164° 30.0'	91	87.2	9.5	3.3	2.592	1.554	0.082	1.781
76	13	55° 05.5'	164° 47.0'	102	61.0	30.7	8.3	3.633	1.861	0.400	2.445
77	A-6	55° 03.0'	164° 35.0'	--	99.8	0.2	0.0	0.782	0.733	-0.135	1.089
78	F-6	56° 45.0'	164° 36.0'	--	54.2	35.6	10.1	4.027	1.976	0.463	1.911
79	065	56° 40.3'	164° 26.6'	74	58.0	37.0	5.0	3.778	1.443	0.304	1.242
80	067	56° 40.3'	164° 26.6'	74	93.0	6.0	1.0	3.029	0.523	0.231	1.588
81	E-6	56° 22.0'	164° 32.0'	--	45.1	46.0	8.9	4.186	2.056	0.289	1.803
82	D-6	56° 05.0'	164° 32.0'	--	70.0	25.0	5.0	3.373	1.431	0.353	1.626
83	C-6	55° 45.0'	164° 33.0'	--	73.0	21.0	6.0	3.351	1.552	0.430	1.932
84	F-7	56° 48.0'	164° 00.0'	--	57.7	36.5	5.8	3.714	1.628	0.366	1.687
85	19	56° 40.0'	163° 57.6'	77	59.3	33.3	7.4	3.833	1.777	0.482	1.888
86	E-7	56° 20.0'	164° 08.0'	--	54.0	40.0	6.0	3.763	1.751	0.282	1.936
87	D-7	56° 05.0'	163° 56.0'	--	79.8	14.7	5.5	3.227	1.526	0.391	2.327
88	C-7	55° 42.0'	164° 00.0'	--	86.4	11.0	2.6	2.965	1.023	0.099	1.523
89	B-7	55° 21.0'	163° 54,0'	--	95.3	2.5	2.3	2.895	0.605	-0.034	1.476
90	F-8	56° 39.0'	163° 29.0'	--	80.9	17.5	1.6	3.176	0.804	0.179	0.876

NOTES: (1) Samples 1 through 60 are from this study; samples 61 through 120 are from previous studies.

Table I-1. Sample Data (Continued)

Sample[1] Number	Station Number	Latitude(N)	Longitude(W)	Depth(m)	Sediment Parameters (Folk and Ward) % sand	% silt	% clay	Mean(ϕ)	Standard Deviation(ϕ)	Skewness	Kurtosis
91	068	56° 24.2'	163° 42.0'	83	62.0	33.0	5.0	3.729	1.559	0.345	1.520
92	D-8	56° 00.0'	163° 33.0'	--	91.4	5.9	2.6	3.131	0.689	0.093	1.158
93	003	55° 30.0'	163° 32.0'	64	92.3	5.9	1.8	2.769	0.925	-0.069	1.756
94	1	55° 17.7'	163° 18.9'	48	73.0	19.3	7.7	3.317	1.851	0.401	2.951
95	E-8	56° 20.0'	163° 20.0'	--	5.8	21.1	5.8	3.415	0.504	0.389	1.139
96	070	56° 09.3'	163° 08.2'	86	95.0	3.0	2.0	3.019	0.533	-0.134	1.172
97	D-9	56° 03.0'	162° 54.0'	--	96.0	1.0	3.0	2.778	0.579	0.018	1.444
98	F-9	56° 40.0'	162° 42.2'	--	95.7	1.9	2.4	2.599	0.607	0.054	1.195
99	076	56° 32.2'	162° 37.8'	73	96.0	2.0	2.0	2.593	0.506	0.237	1.127
100	075	56° 11.7'	162° 22.7'	68	99.0	0.0	1.0	2.252	0.591	-0.068	1.696
101	D-10	55° 58.0'	162° 25.0'	--	97.0	1.0	2.0	2.079	0.637	-0.153	1.391
102	072	55° 56.5'	162° 38.0'	75	96.0	3.0	1.0	2.487	0.551	-0.012	1.232
103	004	55° 46.0'	162° 29.5'	57	87.0	1.7	1.3	2.329	0.688	-0.098	1.188
104	F-10	56° 38.0'	162° 12.0'	--	96.0	2.0	2.0	2.290	0.612	0.107	1.048
105	11	56° 45.5'	161° 59.7'	71	84.7	5.7	9.7	2.800	1.625	0.485	4.508
106	118	56° 53.8'	161° 47.1'	72	97.0	1.0	2.0	2.577	0.540	0.010	1.101
107	E-11	56° 17.0'	161° 35.0'	--	99.9	0.1	0	2.018	0.491	-0.029	1.068
108	005	56° 14.0'	161° 30.0'	88	98.6	0.4	1.0	2.287	0.602	-0.098	1.406
109	BB-1	56° 06.0'	161° 25.5'	--	99.9	0.1	0.0	1.647	0.567	-0.022	0.983
110	116	56° 43.9'	161° 31.3'	83	97.0	1.0	2.0	2.317	0.727	-0.157	1.402
111	F-11	56° 43.0'	161° 21.0'	--	97.4	1.0	1.6	2.203	2.667	-0.085	1.245
112	F-13	56° 41.0'	161° 14.0'	--	100.0	0.0	0.0	1.448	1.002	-0.402	1.132
113	114	56° 25.3'	161° 04.0'	63	98.0	1.0	1.0	2.435	0.615	-0.058	1.370
114	3	56° 17.4'	161° 02.3'	52	99.7	0.3	0.0	1.020	2.390	-0.840	3.280
115	111	56° 06.4'	160° 41.0'	19	87.0	10.0	3.0	3.047	0.763	0.239	2.211
116	110	56° 31.5'	160° 41.5'	61	94.0	2.0	4.0	0.760	2.353	0.005	0.895
117	007	56° 43.0'	160° 31.0'	64	99.0	0.0	1.0	1.789	1.070	-0.402	1.063
118	006	56° 34.0'	160° 26.0'	64	99.0	0.7	0.3	2.317	0.639	-0.142	1.245
119	BB-12	56° 28.5'	160° 10.0'	--	100.0	0.0	0.0	-0.423	0.994	0.096	0.928
120	F-14	56° 45.0'	159° 50.0'	--	100.0	0.0	0.0	1.676	0.658	-0.261	1.554

NOTES: (1) Samples 1 through 60 are from this study; samples 61 through 120 are from previous studies.

Table I-2. Engineering Data

Station	Sample Type	Soil Type	D_{10} (mm)	D_{50} (mm)	D_{60} (mm)	CU	%Finer #200
120/200		SP/SM (3)	.08	.10	.11	1.4	10
128/108	Bag	SP (2)	.42	1.00	1.10	2.6	1
135/175		SP (2)	.10	.14	.15	1.5	1
150/100		SP (2)	.12	.18	.19	1.6	1
150/150		SP (2)	.12	.19	.20	1.67	1
165/125		SP (1)	.34	.70	.84	2.47	1
177/185	Bag	SP (1)	.20	.42	.45	2.25	1
180/200		SP (2)	.11	.20	.21	1.91	1
210/150		SP (2)	.16	.25	.27	1.69	1
255/158		SP (1)	.19	.43	.52	2.74	1
255/200		SP (2)	.12	.20	.22	1.83	1
262/185		SP (2)	.17	.28	.30	1.76	2
270/193		SP (2)	.12	.25	.26	2.17	2
285/181		SP (1)	.50	1.20	1.50	3.00	1
285/181		SP (1)	.60	1.00	1.00	0.66	1
285/200		SP (1)	.20	.55	.70	3.50	1

Table I-2. Engineering Data (Continued)

Station	Sample Type	Soil Type	D_{10} (mm)	D_{50} (mm)	D_{60} (mm)	CU	%Finer #200
0/150	Gravity Core @ 22 cm	SM (4)	0.01	0.07	0.09	9.0	51
0/150	Gravity Core @ 50 cm	SM (4)	0.004	0.06	0.08	20.0	59
0/150	Gravity Core @ 64 cm	SM (4)	0.006	0.07	0.09	15.0	53
0/200		SM (4)	-	0.16	0.20	-	20
20/25		SP (1)	0.7	1.4	1.5	-	1
20/50	Gravity Core @ 8 cm	SM (4)	0.05	0.09	0.11	2.2	25
20/100		SM (4)	-	0.13	0.15	-	30
30/200		SM (4)	-	0.10	0.11	-	26
35/111		SM (4)	-	0.11	0.12	-	30
51/87	Gravity Core @ 11 cm	SM (4)	-	0.12	0.15	-	26
51/87	Gravity Core @ 21 cm	SM (4)	0.03	0.14	0.16	5.3	23
51/87	Gravity Core @ 33 cm	SM (4)	0.008	0.12	0.18	22.5	33
51/87	Gravity Core @ 64 cm	SM (4)	0.007	0.09	0.11	15.7	39
70/91		SP/SM (3)	.08	.20	.21	2.6	7
79/200		SM (4)	-	.09	.10	-	32
90/50		SP (2)	.19	.30	.35	1.8	1
90/125		SP/SM (3)	.08	.10	.11	1.4	8
120/100		SP (2)	.12	.19	.20	1.7	1

APPENDIX II

SUMMARY OF LABORATORY TEST RESULTS

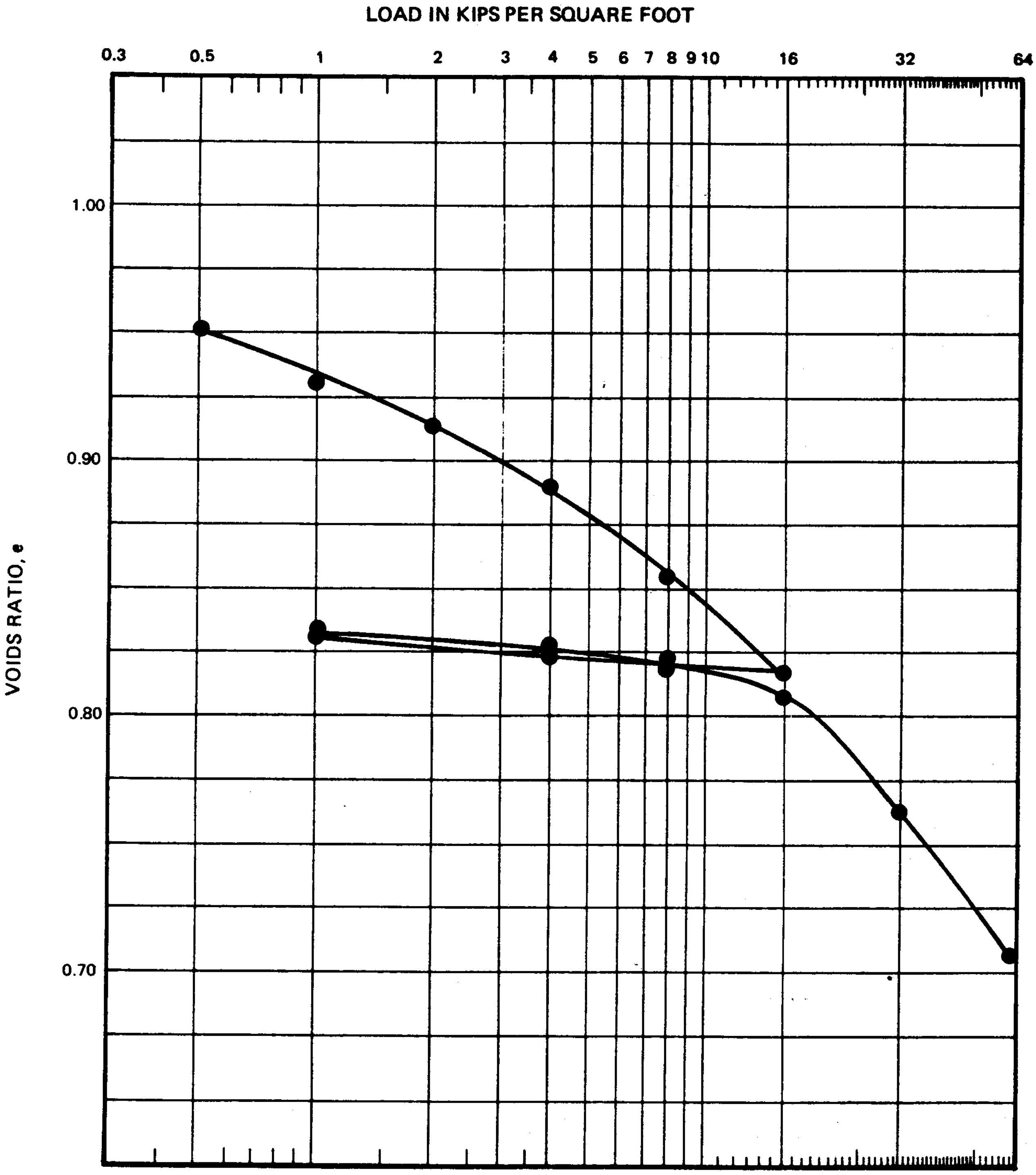

SAMPLE NO.: 2
WATER DEPTH (METERS): 93
DEPTH INTERVAL (CM): 5 - 10
TYPE OF SAMPLE: GRAVITY CORE

INITIAL VOIDS RATIO: 1.0
COMPRESSION INDEX: 0.2
RECOMPRESSION INDEX: 0.01

FIGURE II-1 CONSOLIDATION TEST RESULTS – SAMPLE 2

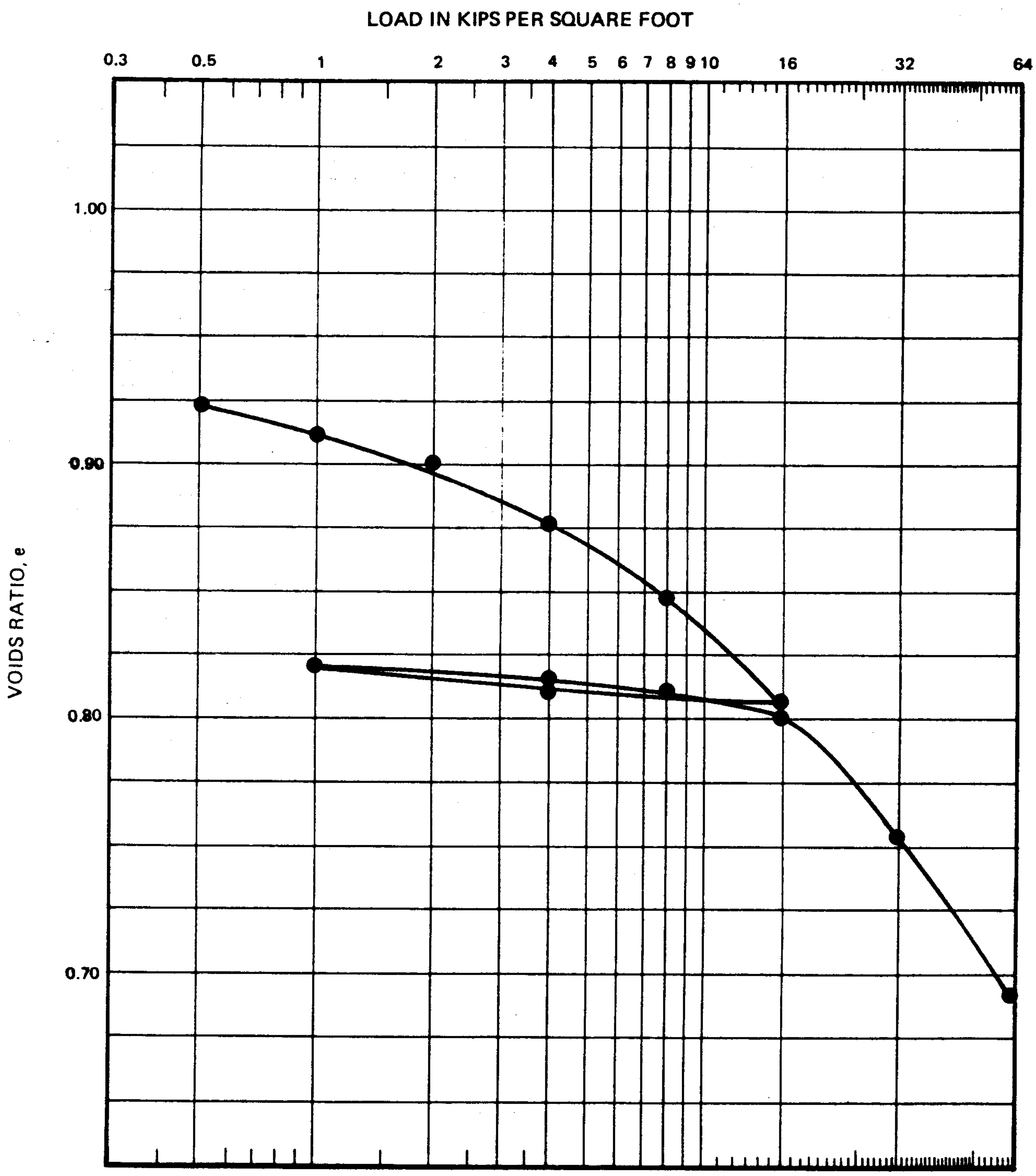

SAMPLE NO.: 2

WATER DEPTH (METERS): 93

DEPTH INTERVAL (CM): 30 - 35

TYPE OF SAMPLE: GRAVITY CORER

INITIAL VOIDS RATIO: 1.0

COMPRESSION INDEX: 0.2

RECOMPRESSION INDEX: 0.01

FIGURE II-2 CONSOLIDATION TEST RESULTS – SAMPLE 2

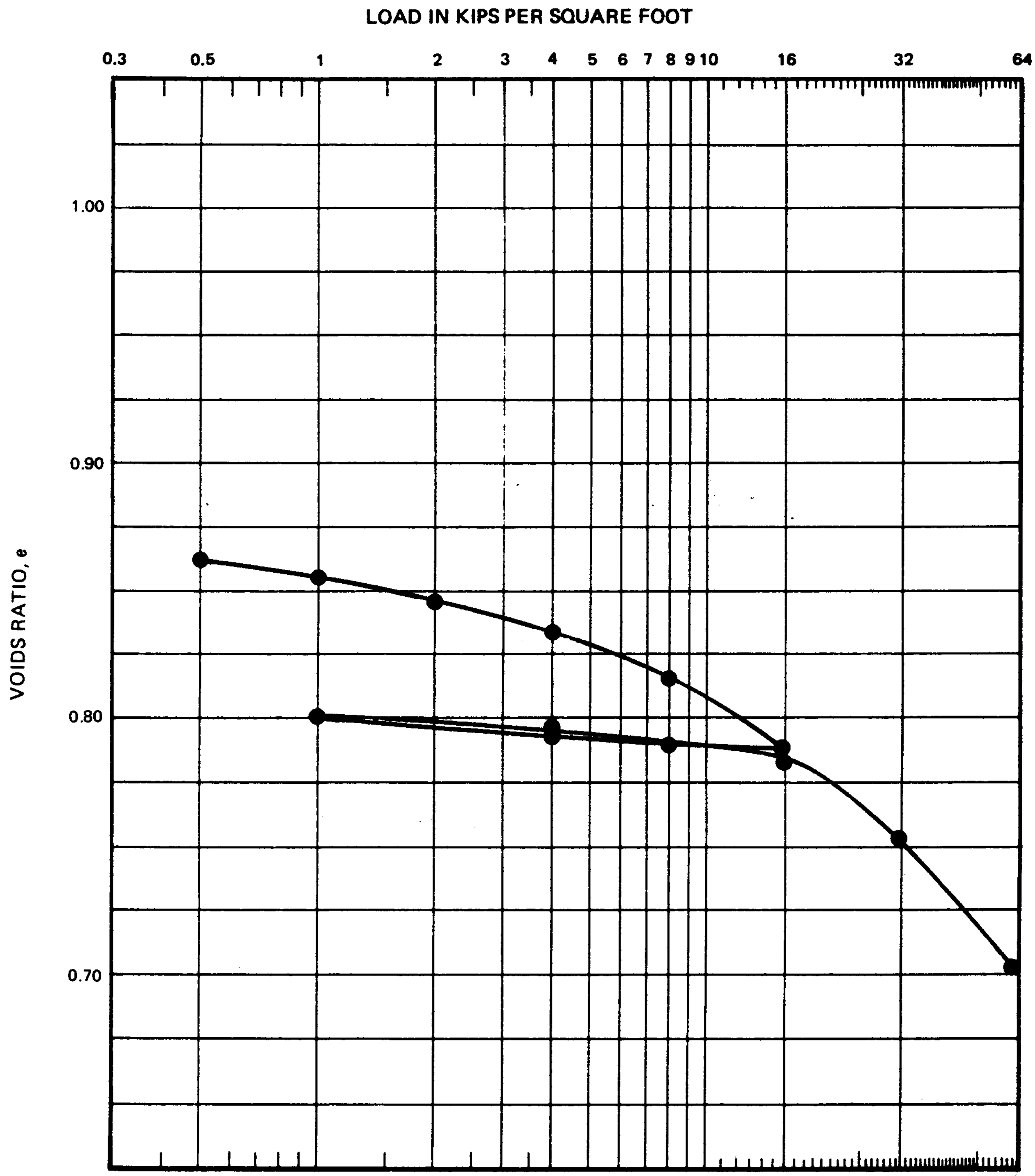

SAMPLE NO.: 23
WATER DEPTH (METERS): 97
DEPTH INTERVAL (CM): 15 - 20
TYPE OF SAMPLE: GRAVITY CORE

INITIAL VOIDS RATIO: 0.9
COMPRESSION INDEX: 0.15
RECOMPRESSION INDEX: 0.008

FIGURE II-3 CONSOLIDATION TEST RESULTS – SAMPLE 23

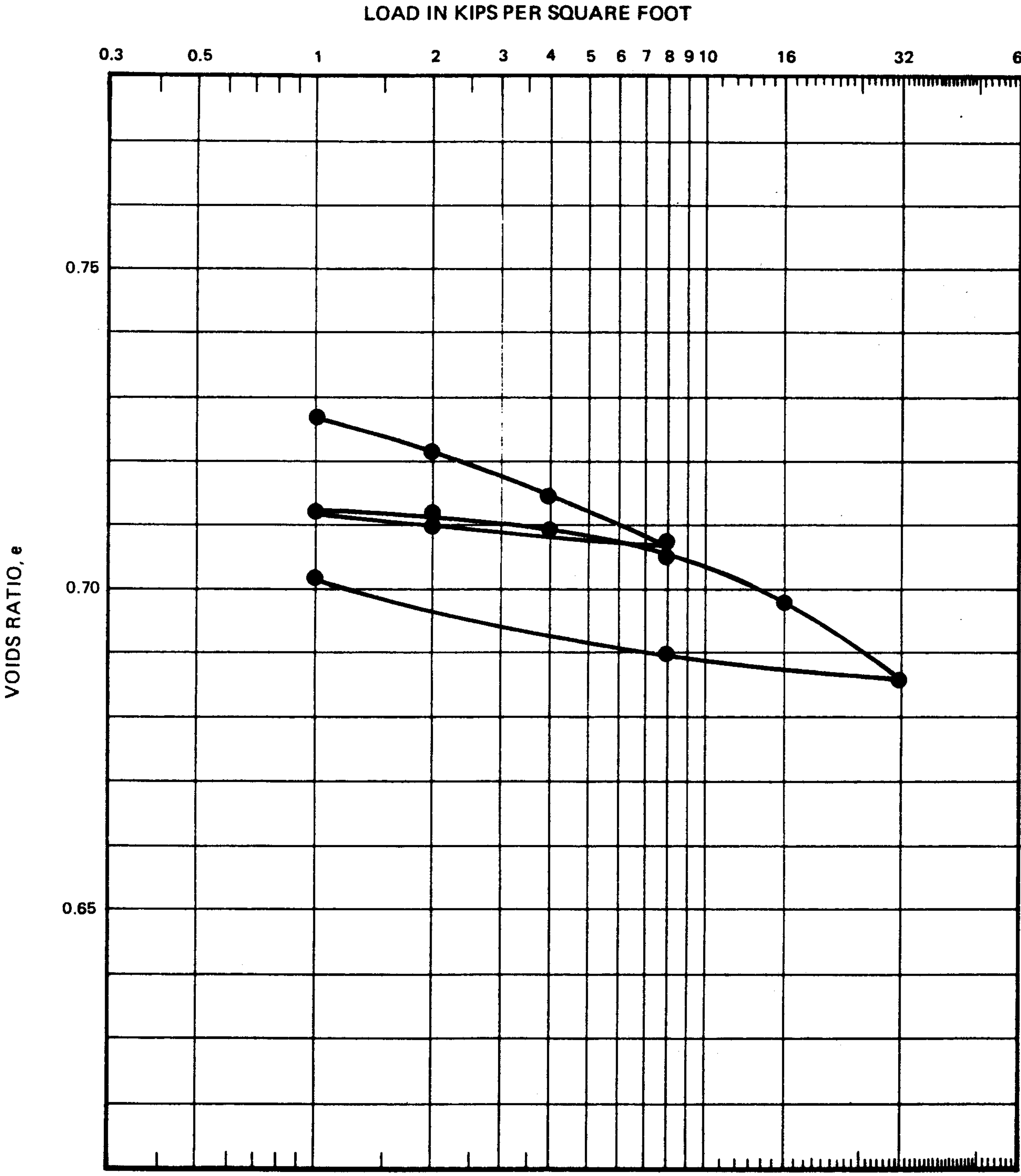

SAMPLE NO.: 9
WATER DEPTH (METERS): 100
DEPTH INTERVAL (CM): SURFICIAL
TYPE OF SAMPLE: RECONSTITUTED

INITIAL VOIDS RATIO: 0.7
COMPRESSION INDEX: 0.035
RECOMPRESSION INDEX: 0.005

FIGURE II-4 CONSOLIDATION TEST RESULTS – SAMPLE 9

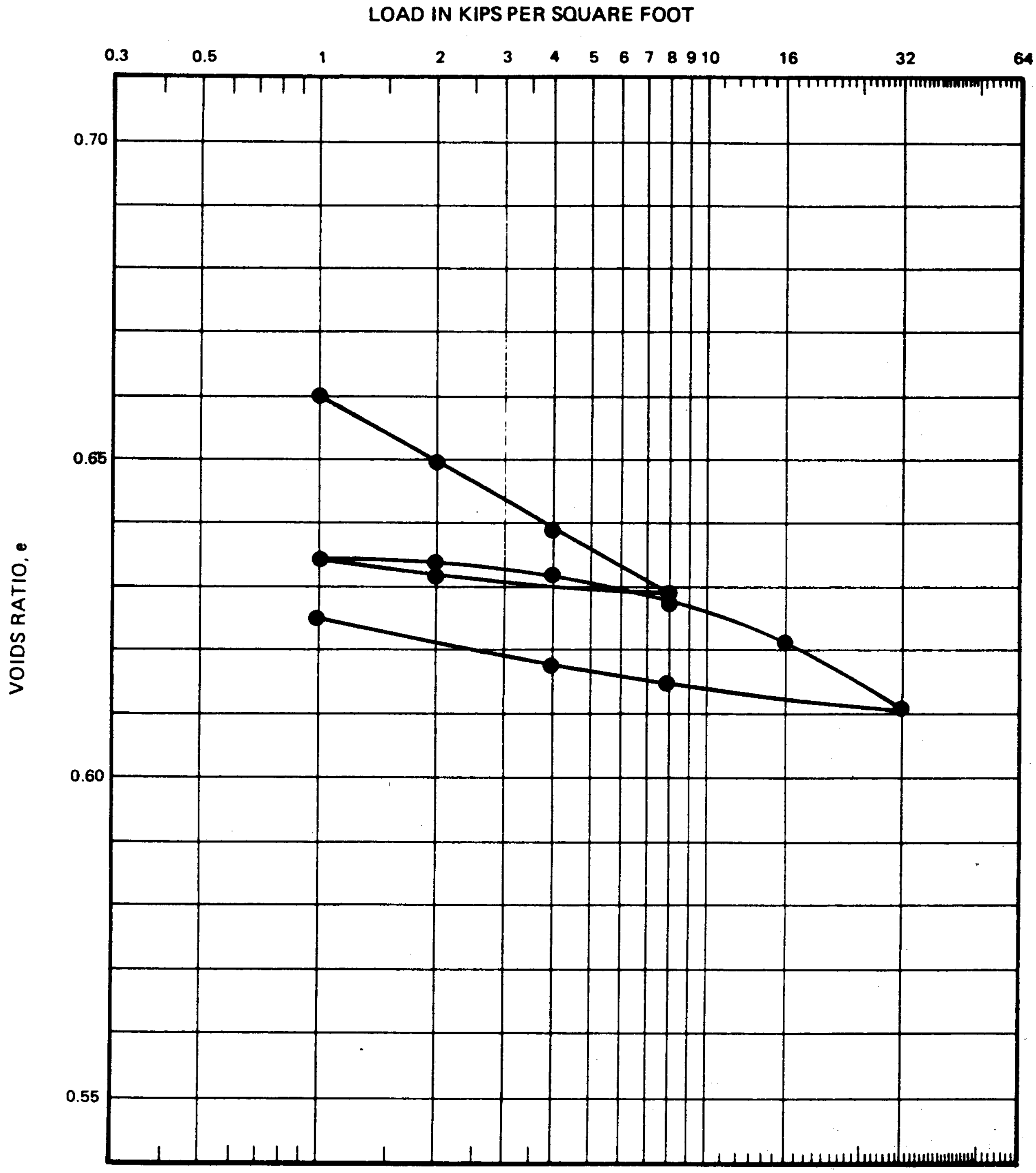

SAMPLE NO.: 24
WATER DEPTH (METERS): 84
DEPTH INTERVAL (CM): SURFICIAL
TYPE OF SAMPLE: RECONSTITUTED

INITIAL VOIDS RATIO: 0.7
COMPRESSION INDEX: 0.03
RECOMPRESSION INDEX: 0.005

FIGURE II-5 CONSOLIDATION TEST RESULTS – SAMPLE 24

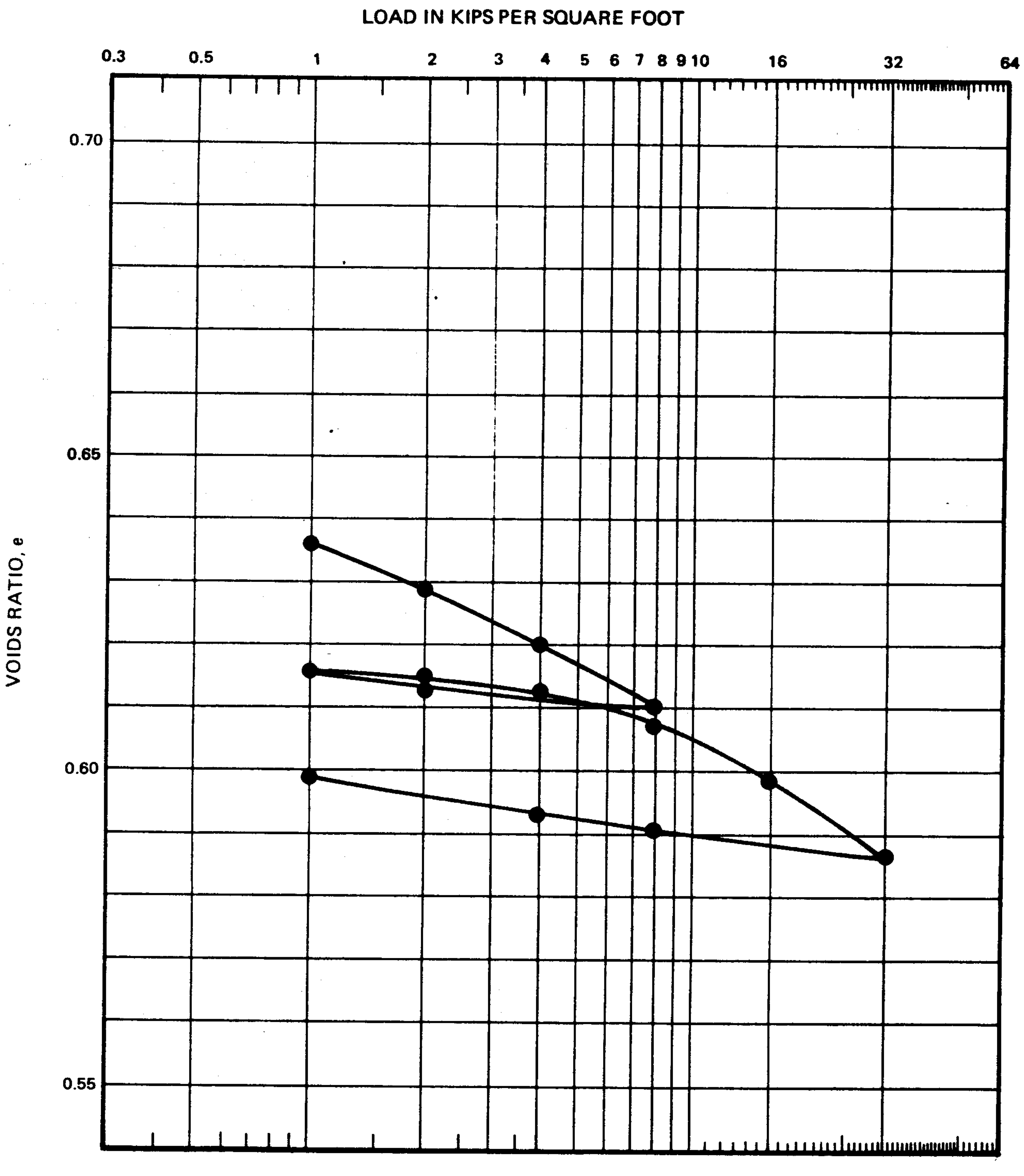

SAMPLE NO.: 43
WATER DEPTH (METERS): 80
DEPTH INTERVAL (CM): SURFICIAL
TYPE OF SAMPLE: RECONSTITUTED

INITIAL VOIDS RATIO: 0.65
COMPRESSION INDEX: 0.04
RECOMPRESSION INDEX: 0.005

FIGURE II-6 CONSOLIDATION TEST RESULTS – SAMPLE 43

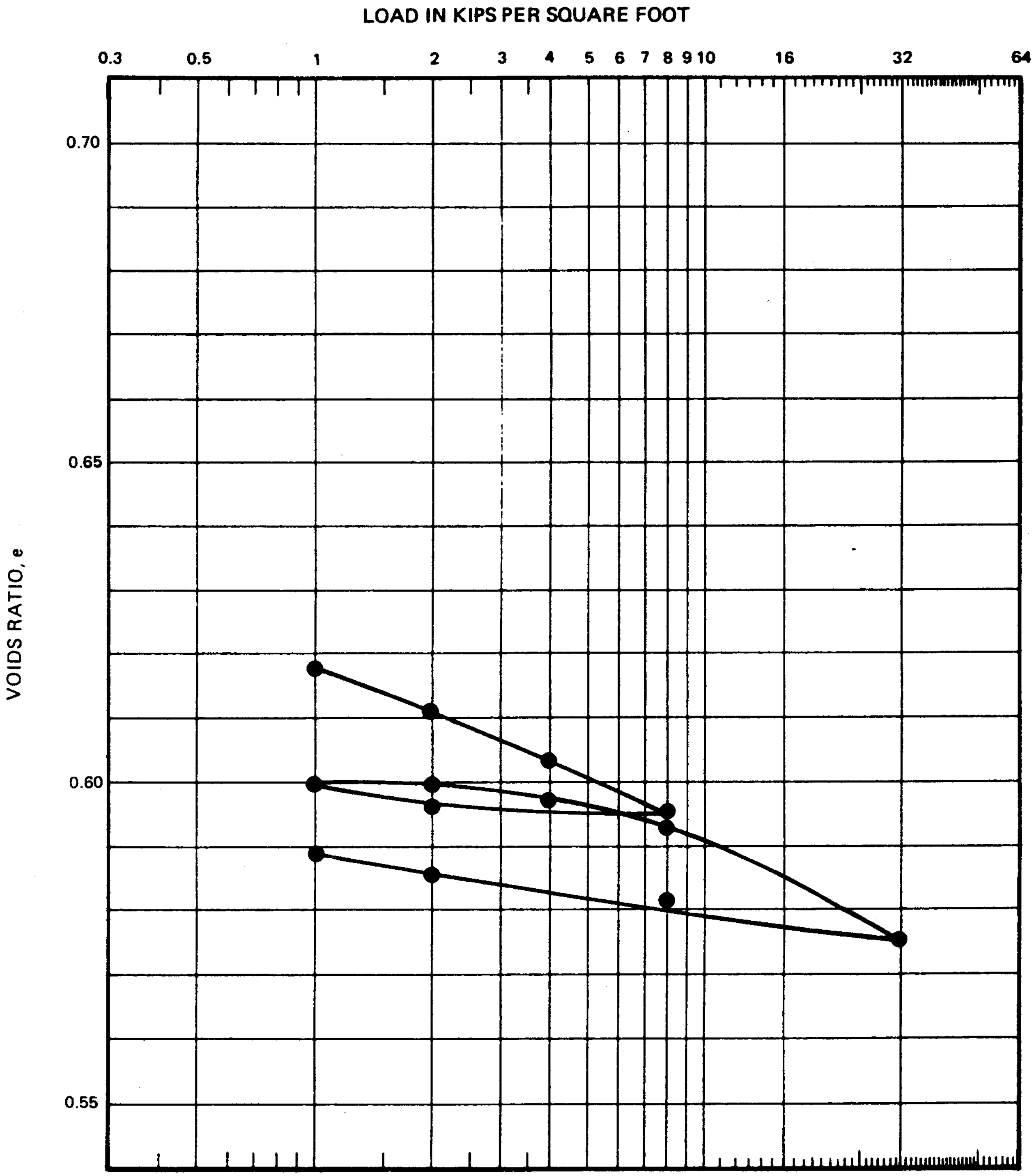

SAMPLE NO.: 57
WATER DEPTH (METERS): 49
DEPTH INTERVAL (CM): SURFICIAL
TYPE OF SAMPLE: RECONSTITUTED

INITIAL VOIDS RATIO: 0.6
COMPRESSION INDEX: 0.03
RECOMPRESSION INDEX: 0.003

FIGURE II-7 CONSOLIDATION TEST RESULTS – SAMPLE 57

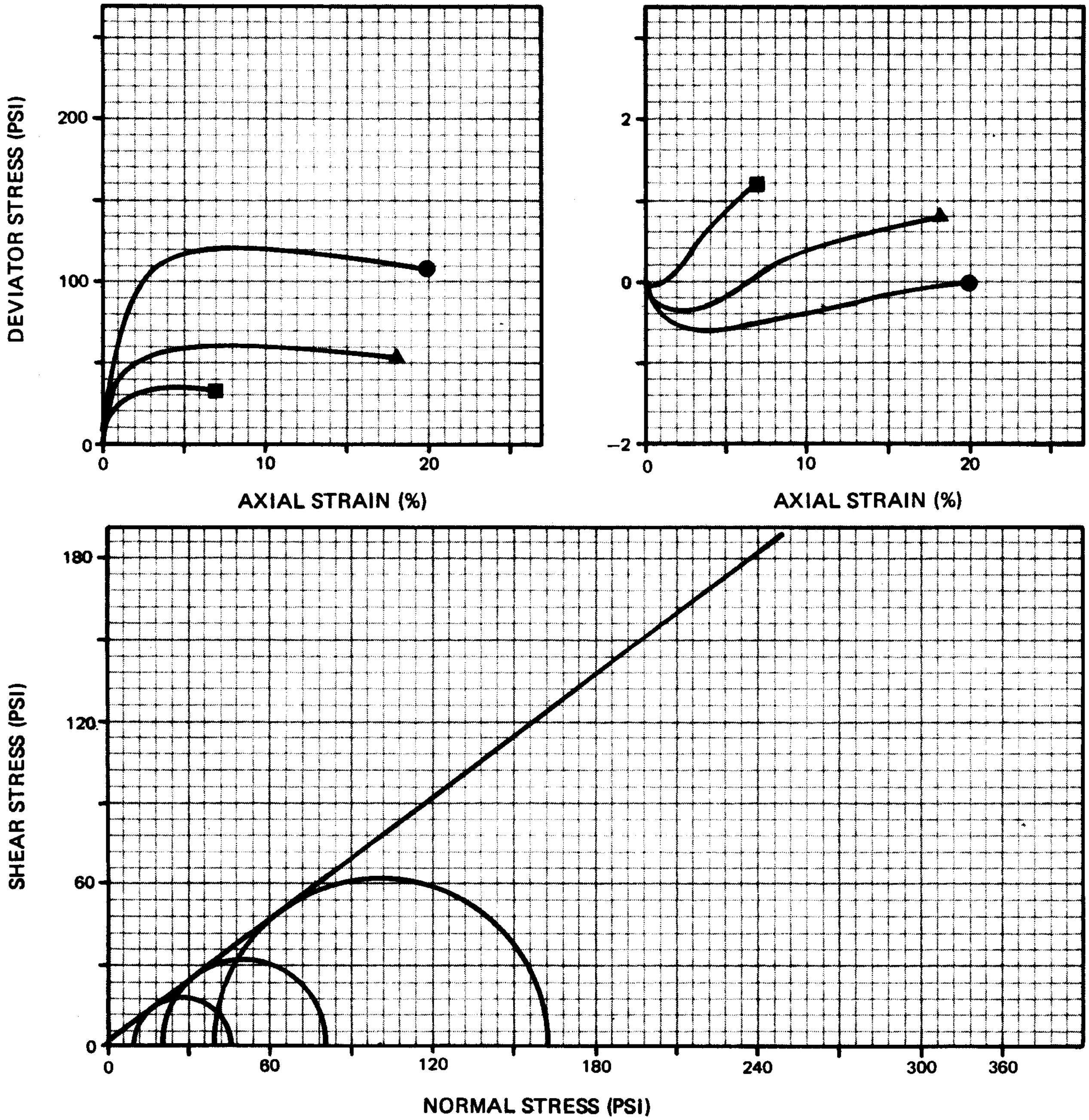

SYMBOL	BORING NUMBER	SAMPLE NUMBER	SAMPLE INTERVAL	TYPE OF SAMPLE	SOIL TYPE	TYPE OF TEST	DRY DENSITY (PCF)	MOISTURE CONTENT (%)	CONFINING PRESSURE (PSI)	MAXIMUM DEVIATOR STRESS $\sigma_1 - \sigma_3$ (PSI)	STRAIN RATE (%/MIN)	BACK PRESSURE
	1020/100	9	N/A	R	SM4	CD	95	15	40	121	0.08	
	1020/100	9	N/A	R	SM4	CD	95	15	20	60	0.08	
	1020/100	9	N/A	R	SM4	CD	95	15	10	35	0.08	

FIGURE II-8 STATIC TRIAXIAL TEST RESULTS FROM RECONSTITUTED TESTS ON SAMPLE 9

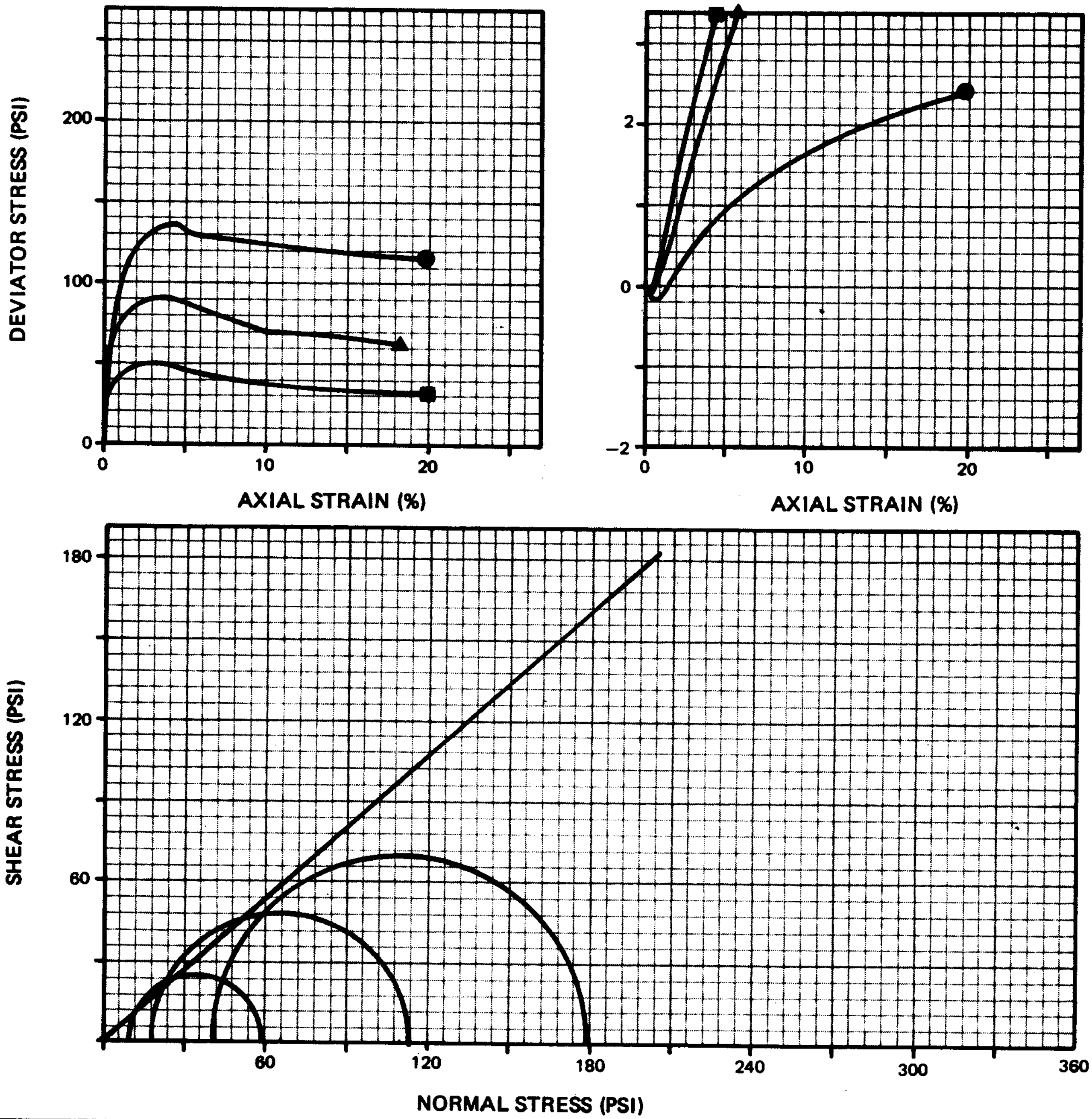

SYMBOL	BORING NUMBER	SAMPLE NUMBER	SAMPLE INTERVAL	TYPE OF SAMPLE	SOIL TYPE	TYPE OF TEST	DRY DENSITY (PCF)	MOISTURE CONTENT (%)	CONFINING PRESSURE (PSI)	MAXIMUM DEVIATOR STRESS $\sigma_1-\sigma_3$ (PSI)	STRAIN RATE (%/MIN)	BACK PRESSURE
	1070/91	24	N/A	R	SP/SM	CD	99	15	40	138	0.08	
	1070/91	24	N/A	R	SP/SM	CD	99	15	20	91	0.08	
	1070/91	24	N/A	R	SP/SM	CD	99	15	10	50	0.08	

FIGURE II-9 STATIC TRIAXIAL TEST RESULTS FROM RECONSTITUTED TESTS ON SAMPLE 24

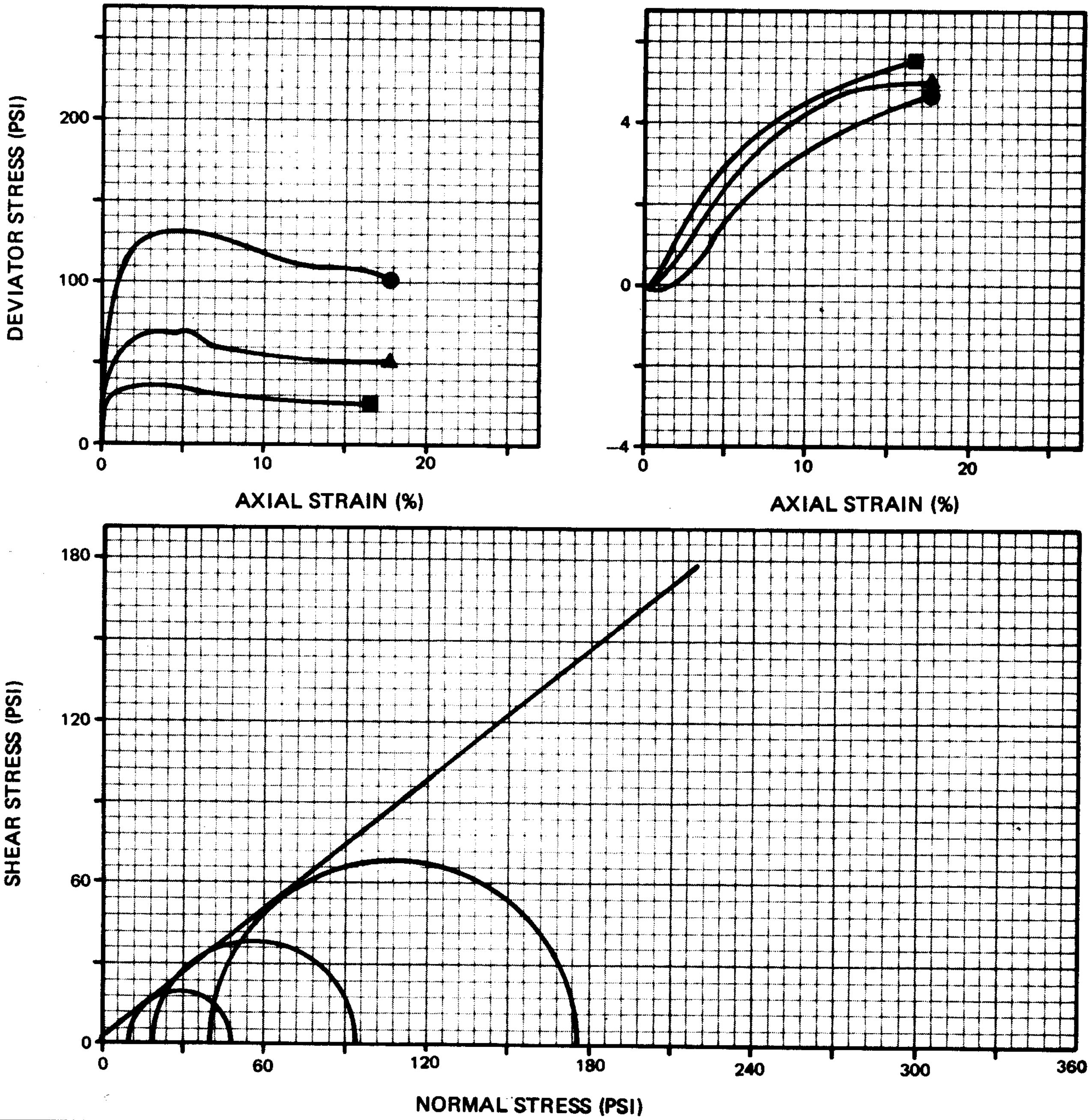

SYMBOL	BORING NUMBER	SAMPLE NUMBER	SAMPLE INTERVAL	TYPE OF SAMPLE	SOIL TYPE	TYPE OF TEST	DRY DENSITY (PCF)	MOISTURE CONTENT (%)	CONFINING PRESSURE (PSI)	MAXIMUM DEVIATOR STRESS $\sigma_1-\sigma_3$ (PSI)	STRAIN RATE (%/MIN)	BACK PRESSURE
	1177/185	43	N/A	R	SP1	CD	103	10	40	136	0.08	
	1177/185	43	N/A	R	SP1	CD	103	10	20	73	0.08	
	1177/185	43	N/A	R	SP1	CD	103	10	10	38	0.08	

FIGURE II-10 STATIC TRIAXIAL TEST RESULTS FROM RECONSTITUTED TESTS ON SAMPLE 43

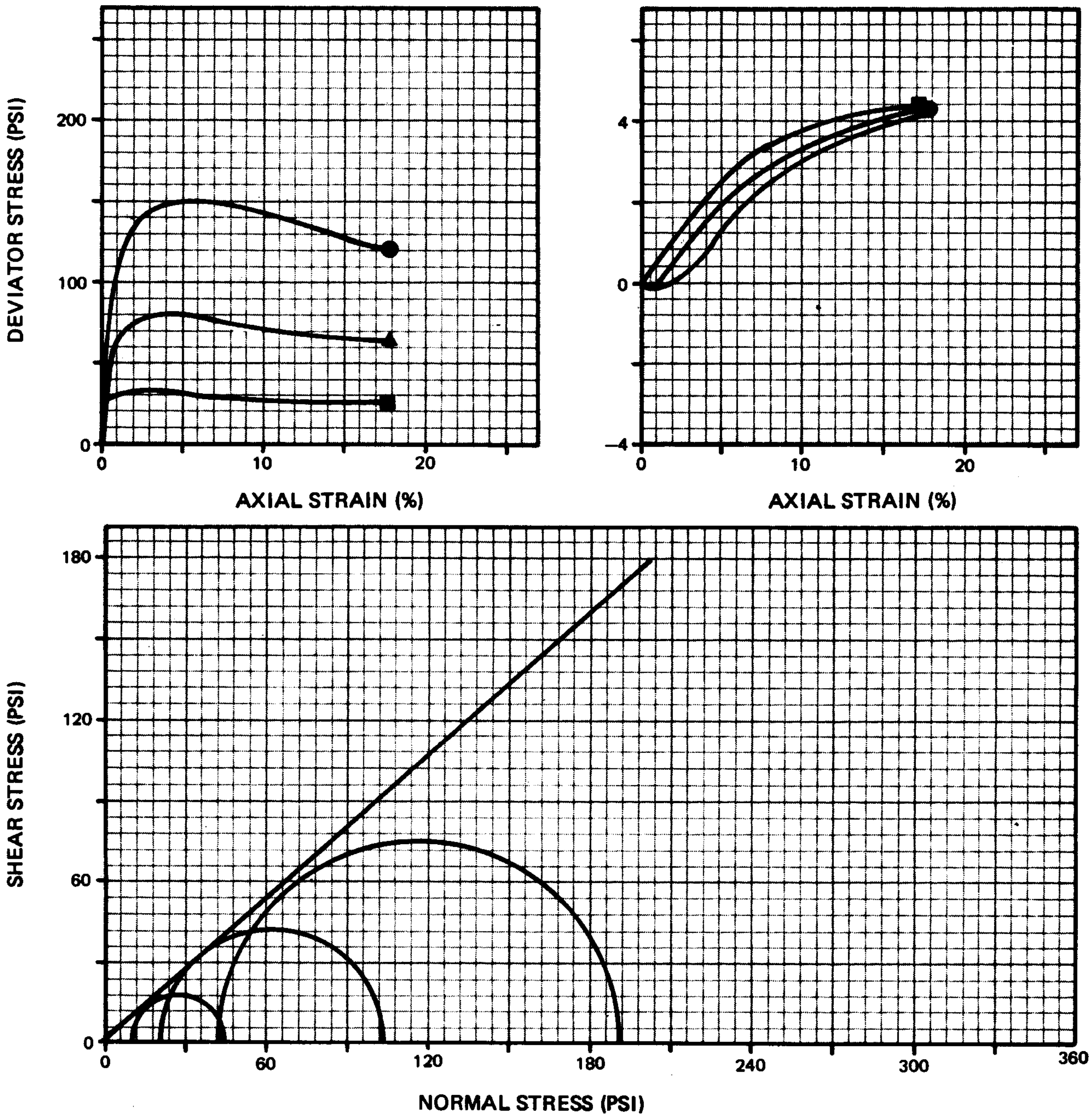

SYMBOL	BORING NUMBER	SAMPLE NUMBER	SAMPLE INTERVAL	TYPE OF SAMPLE	SOIL TYPE	TYPE OF TEST	DRY DENSITY (PCF)	MOISTURE CONTENT (%)	CONFINING PRESSURE (PSI)	MAXIMUM DEVIATOR STRESS $\sigma_1-\sigma_3$ (PSI)	STRAIN RATE (%/MIN)	BACK PRESSURE
	1262/185	57	N/A	R	SP2	CD	102	10	40	151	0.08	
	1262/185	57	N/A	R	SP2	CD	102	10	20	82	0.08	
	1262/185	57	N/A	R	SP2	CD	102	10	10	34	0.08	

FIGURE II-11 STATIC TRIAXIAL TEST RESULTS FROM RECONSTITUTED TESTS ON SAMPLE 57

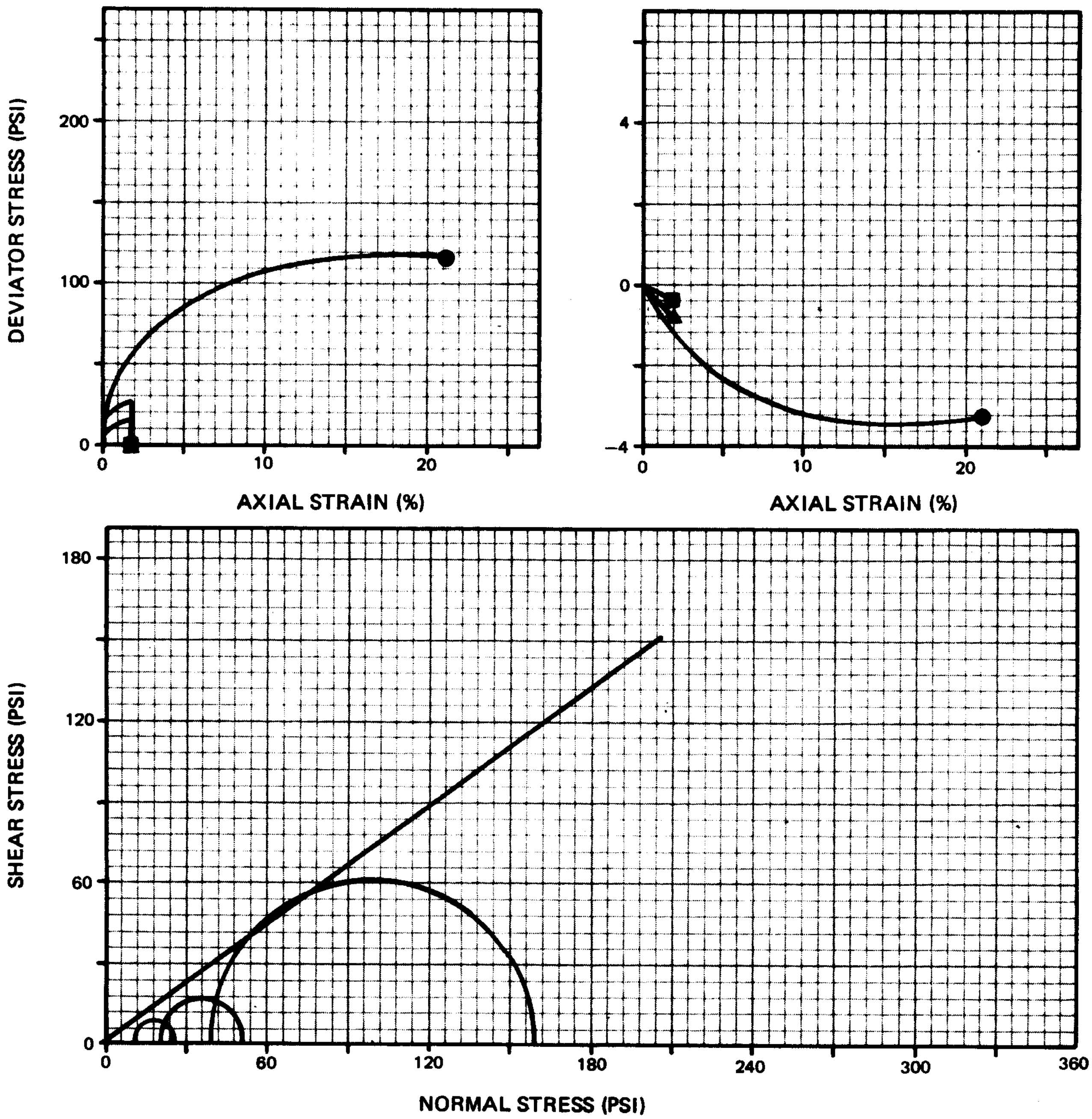

SYMBOL	BORING NUMBER	SAMPLE NUMBER	SAMPLE INTERVAL	TYPE OF SAMPLE	SOIL TYPE	TYPE OF TEST	DRY DENSITY (PCF)	MOISTURE CONTENT (%)	CONFINING PRESSURE (PSI)	MAXIMUM DEVIATOR STRESS $\sigma_1-\sigma_3$ (PSI)	STRAIN RATE (%/MIN)	BACK PRESSURE
	1000/150	2	13 - 19	GC	SM4	CD	88	37	40	118	0.08	
	1000/150	2	13 - 19	GC	SM4	CD	88	37	20	31	0.08	
	1000/150	2	13 - 19	GC	SM4	CD	88	37	10	16	0.08	

FIGURE II-12 MULTISTAGE STATIC TRIAXIAL TEST RESULTS FROM GRAVITY CORE SAMPLE NO. 2

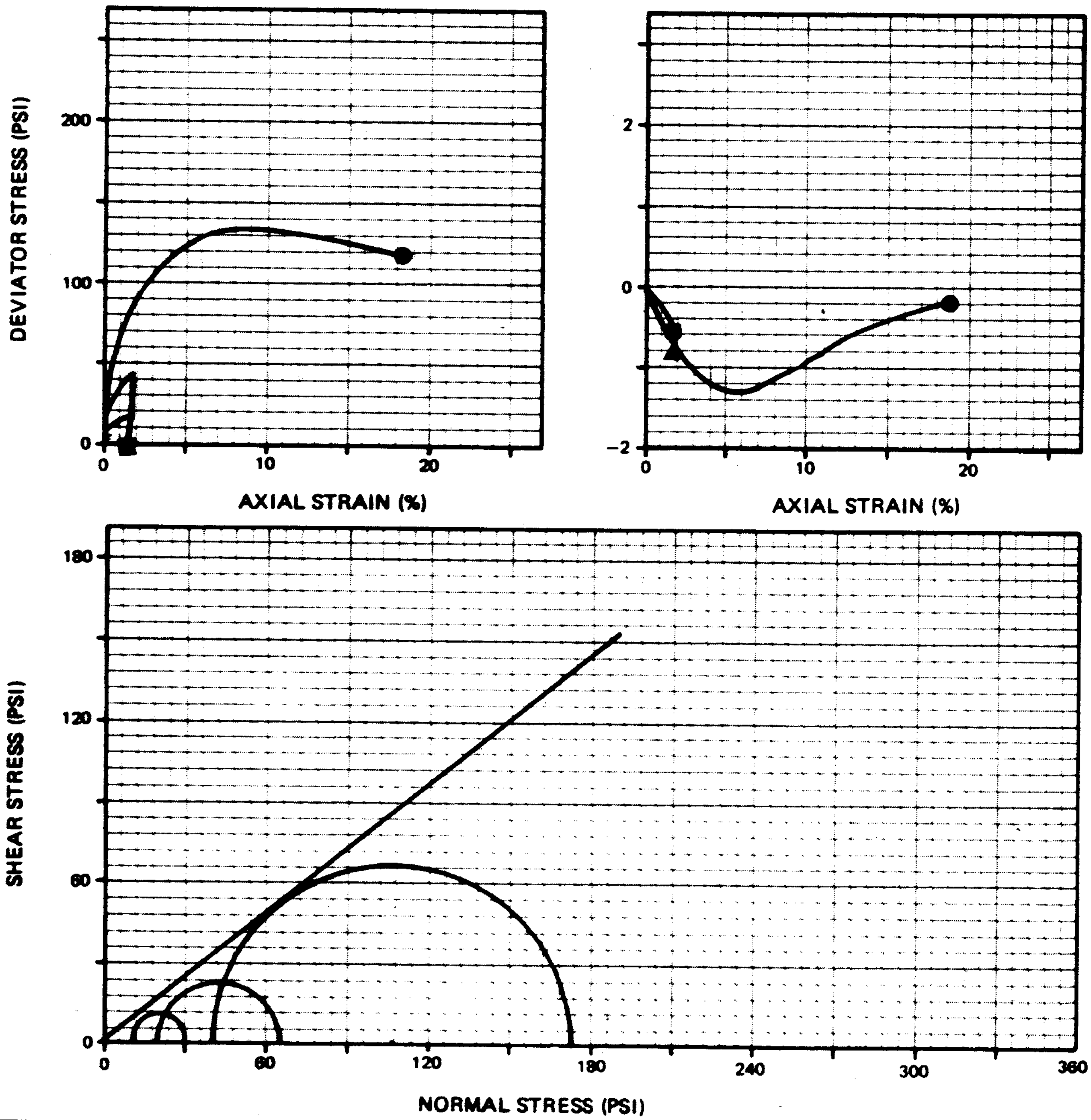

SYMBOL	BORING NUMBER	SAMPLE NUMBER	SAMPLE INTERVAL	TYPE OF SAMPLE	SOIL TYPE	TYPE OF TEST	DRY DENSITY (PCF)	MOISTURE CONTENT (%)	CONFINING PRESSURE (PSI)	MAXIMUM DEVIATOR STRESS $\sigma_1 - \sigma_3$ (PSI)	STRAIN RATE (%/MIN)	BACK PRESSURE
	1051/87	23	14 - 20	GC	SP/SM	CD	93	29	40	133	0.08	
	1051/87	23	14 - 20	GC	SP/SM	CD	93	29	20	45	0.08	
	1051/87	23	14 - 20	GC	SP/SM	CD	93	29	10	21	0.08	

FIGURE II-13 MULTISTAGE STATIC TRIAXIAL TEST RESULTS FROM GRAVITY CORE SAMPLE NO. 23

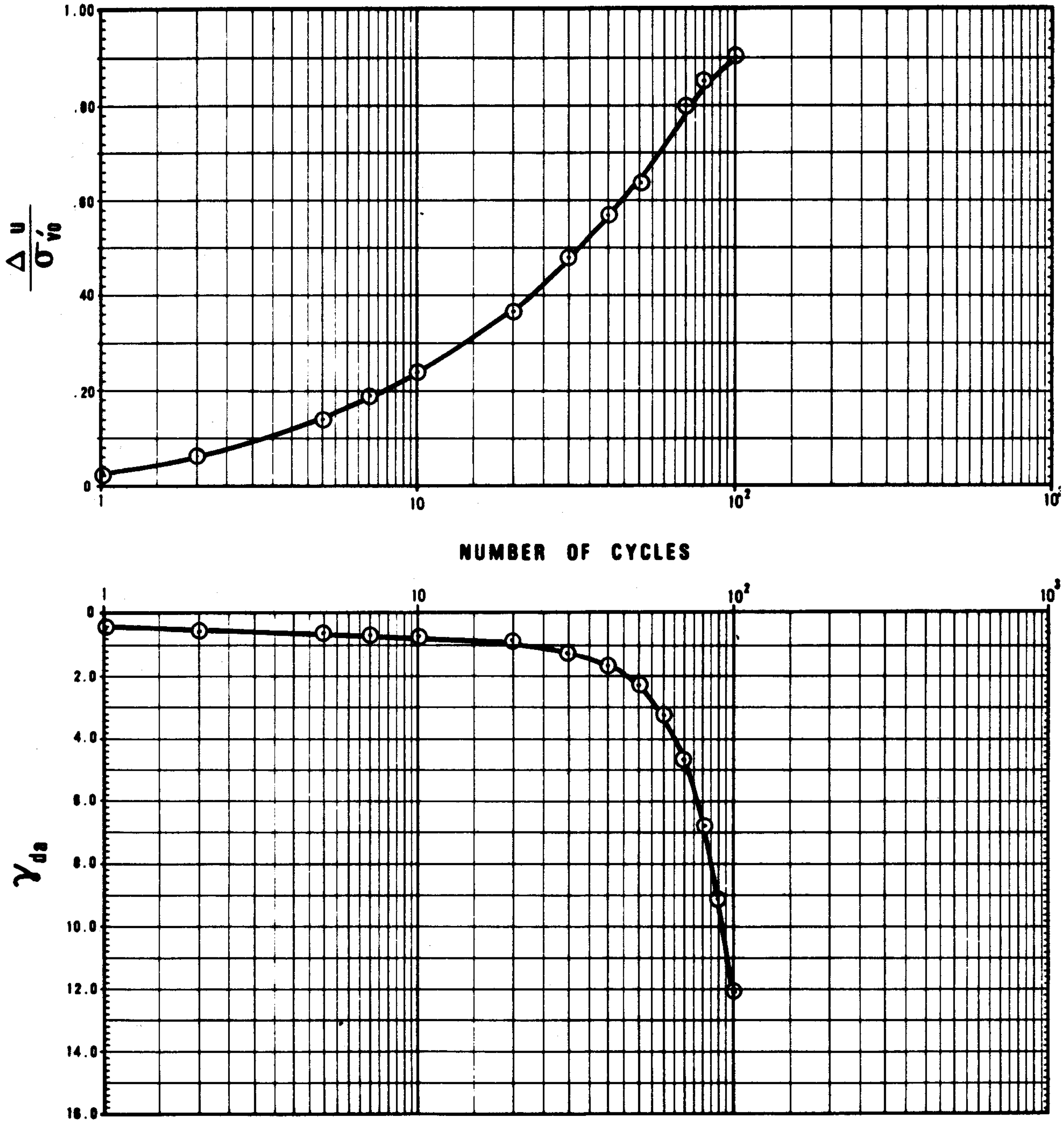

TEST NO.	SAMPLE NO.	SAMPLE DEPTH (cm)	σ'_{vo} *	τ_h/σ'_{vo}	SOIL TYPE
1	2	48 - 51	70	0.22	SM

*KN/M^2

FIGURE II-14 LIQUEFACTION TEST RESULTS FROM GRAVITY CORE – SAMPLE 2-1

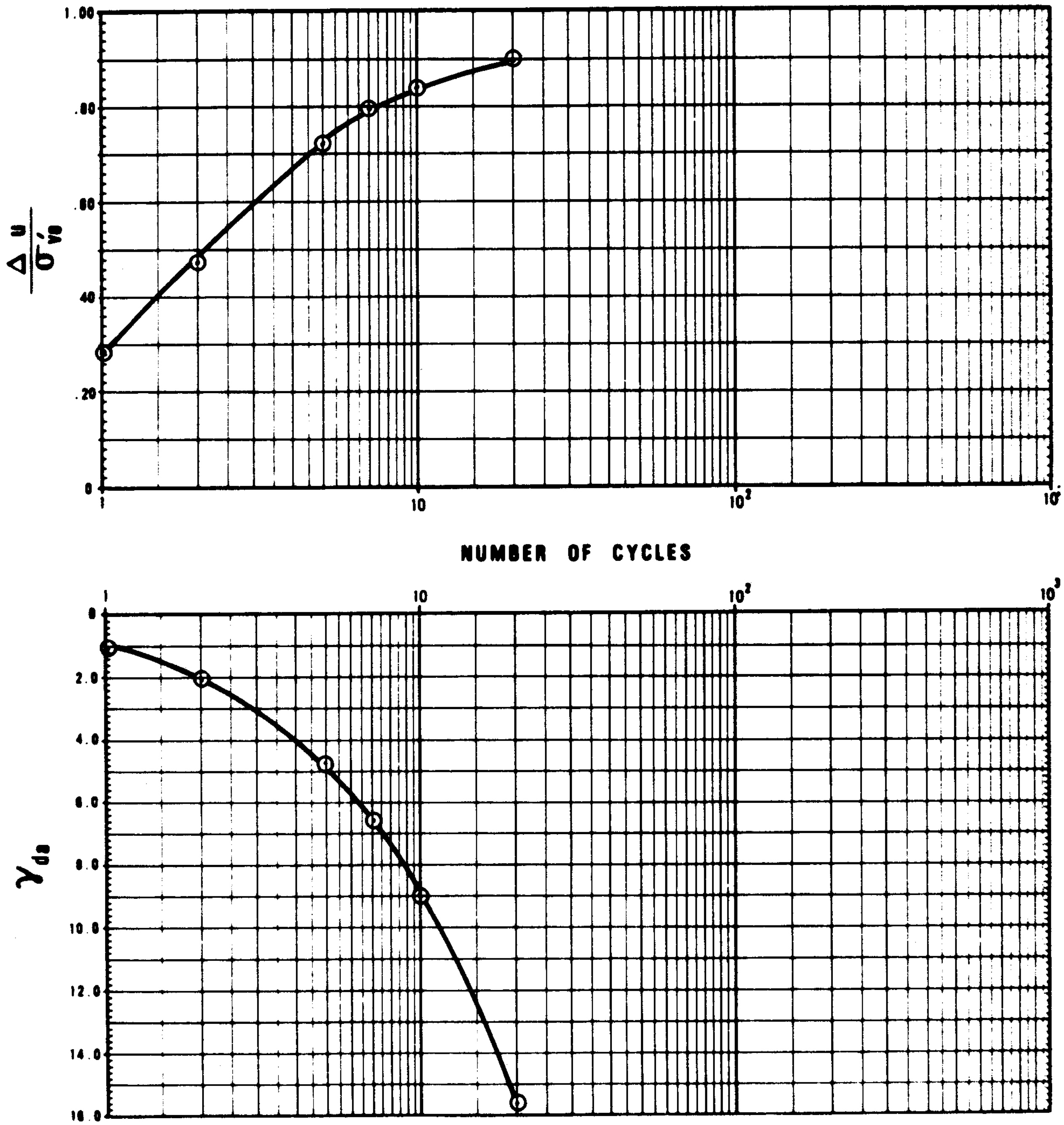

TEST NO.	SAMPLE NO.	SAMPLE DEPTH (cm)	σ'_{vo} *	τ_h/σ'_{vo}	SOIL TYPE
2	2	65 - 68	70	0.27	SM

*KN/M2

FIGURE II-15 LIQUEFACTION TEST RESULTS FROM GRAVITY CORE — SAMPLE 2-2

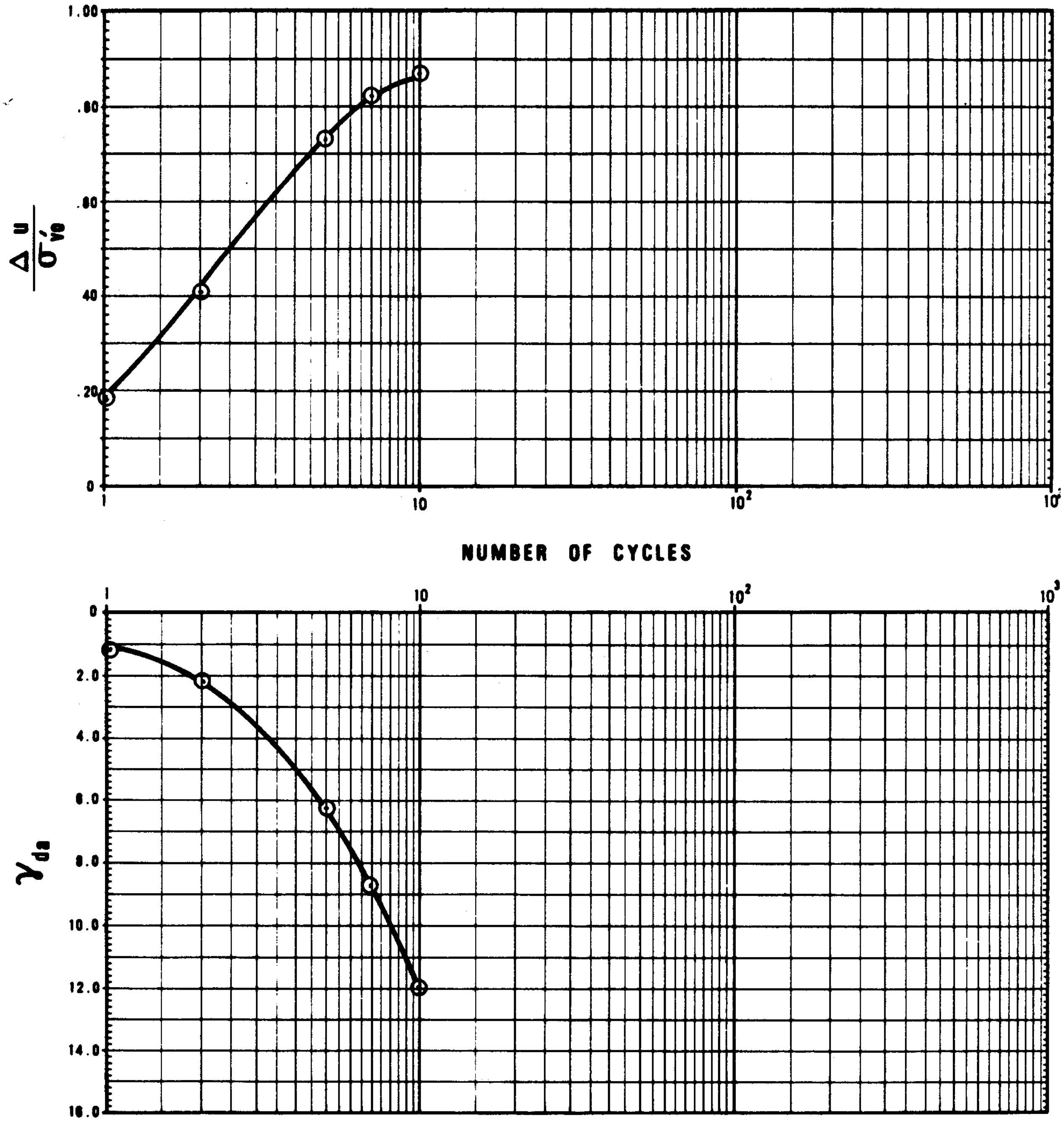

TEST NO.	SAMPLE NO.	SAMPLE DEPTH (cm)	σ'_{vo} *	τ_h/σ'_{vo}	SOIL TYPE
3	2	20 - 23	70	0.22	SM

*KN/M^2

FIGURE II-16 LIQUEFACTION TEST RESULTS FROM GRAVITY CORE – SAMPLE 2-3

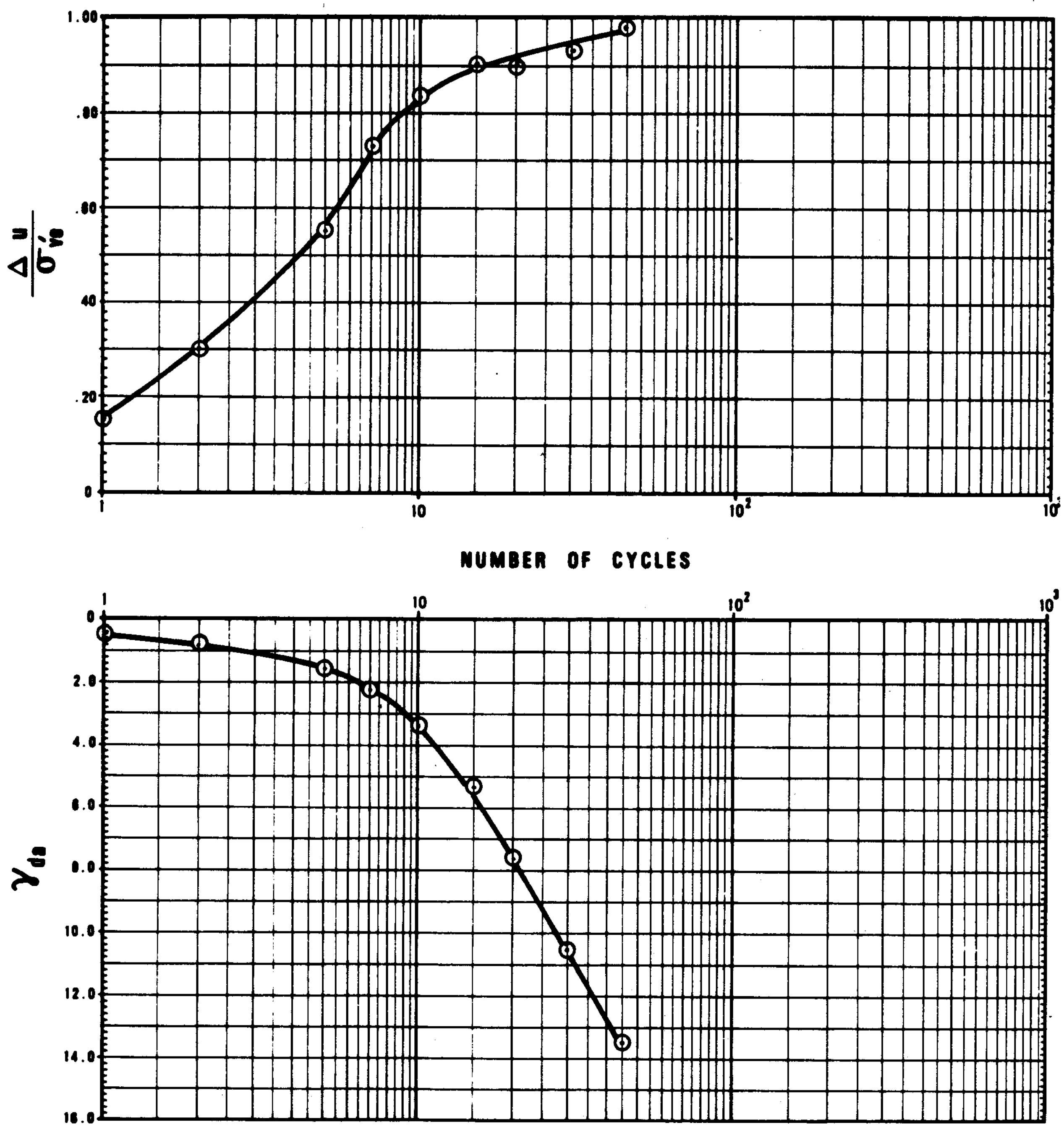

TEST NO.	SAMPLE NO.	SAMPLE DEPTH (cm)	σ'_{vo} *	τ_h/σ'_{vo}	SOIL TYPE
1	11	5 - 8	70	0.26	SM

*KN/M^2

FIGURE II-17 LIQUEFACTION TEST RESULTS FROM GRAVITY CORE – SAMPLE 11-1

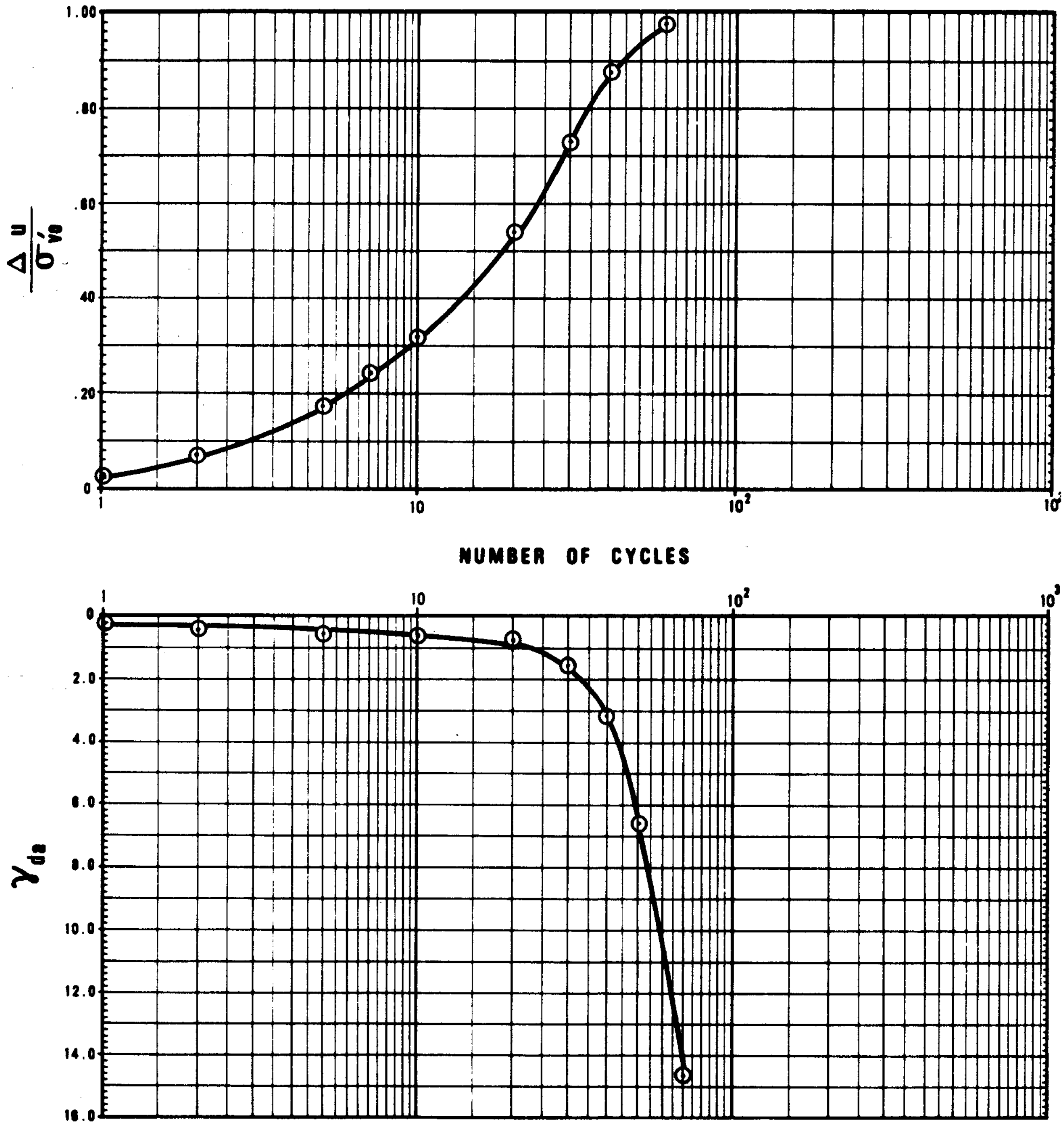

TEST NO.	SAMPLE NO.	SAMPLE DEPTH (cm)	σ'_{vo} *	τ_h/σ'_{vo}	SOIL TYPE
1	23	32 - 35	70	0.20	SM

*KN/M^2

FIGURE II-18 LIQUEFACTION TEST RESULTS FROM GRAVITY CORE – SAMPLE 23-1

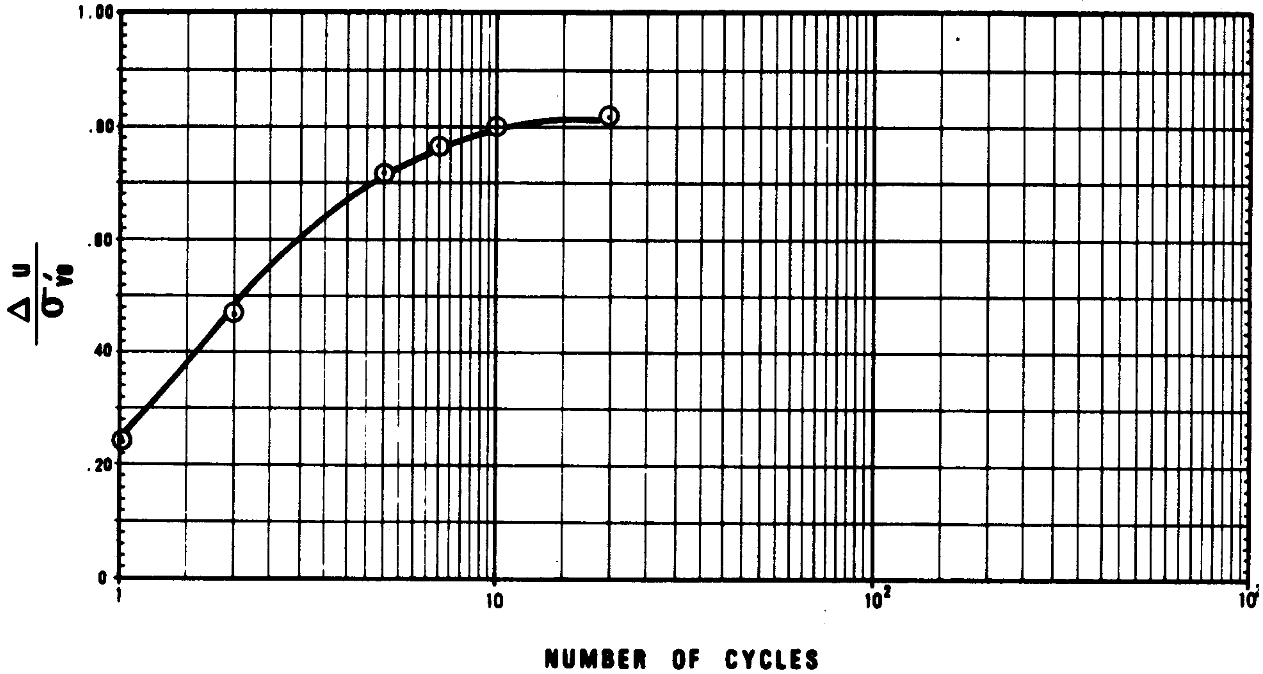

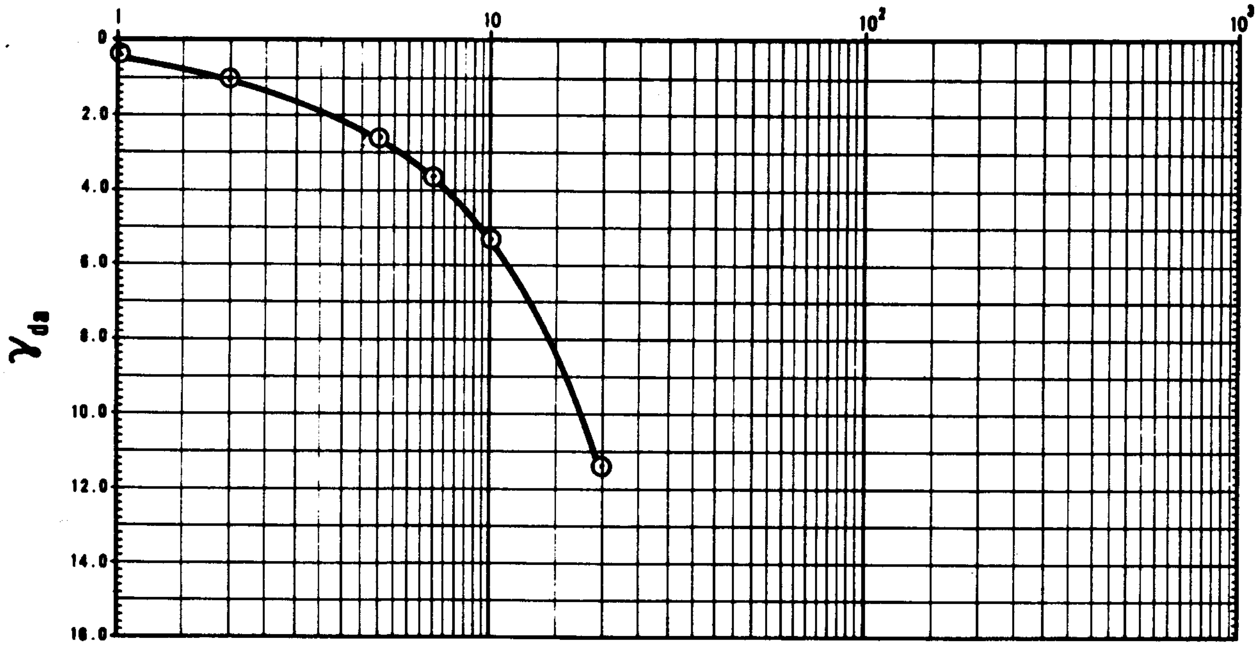

TEST NO.	SAMPLE NO.	SAMPLE DEPTH (cm)	σ'_{vo} *	τ_h/σ'_{vo}	SOIL TYPE
2	23	62 - 65	70	0.23	SM

*KN/M^2

FIGURE II-19 LIQUEFACTION TEST RESULTS FROM GRAVITY CORE — SAMPLE 23-2

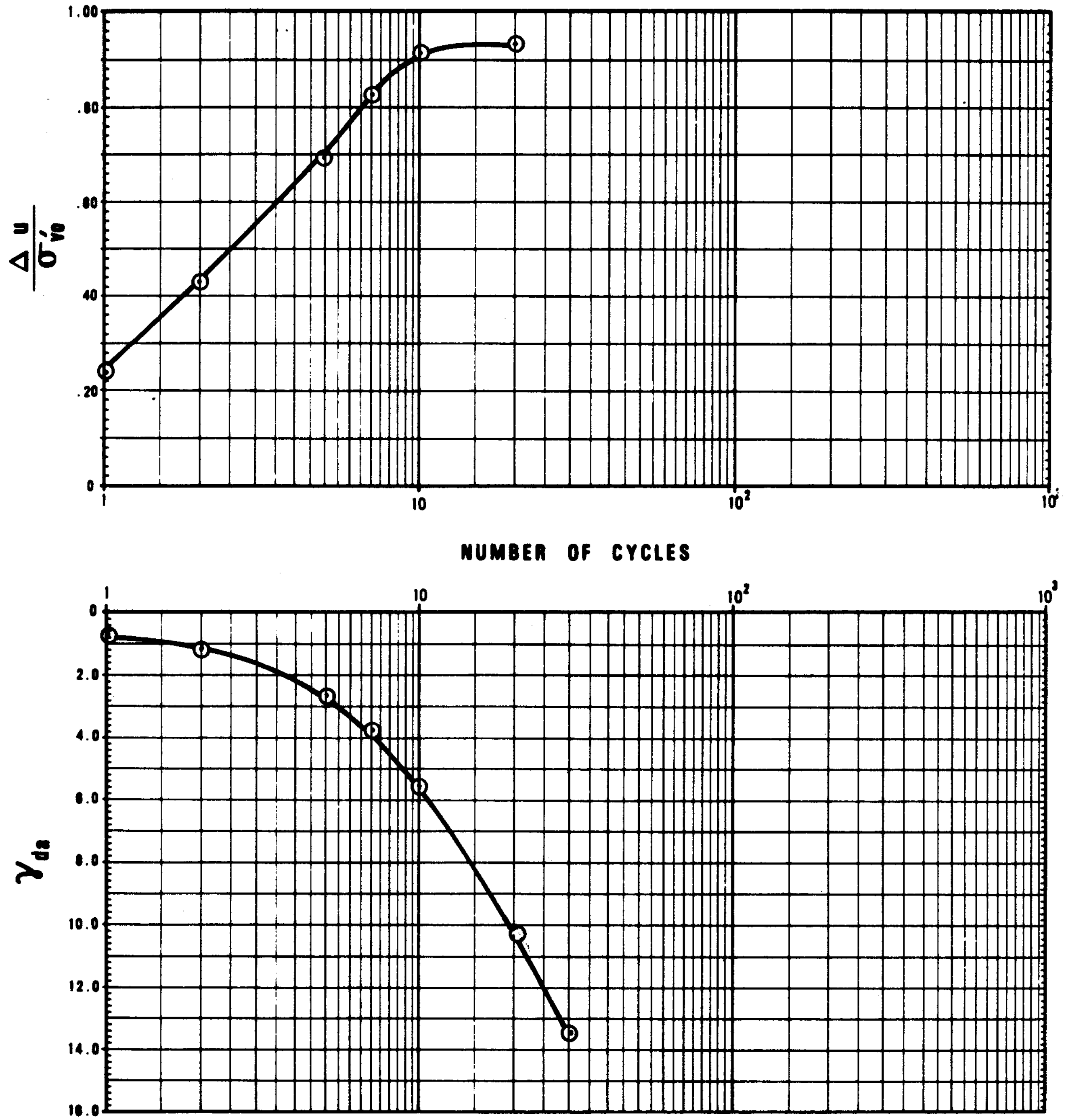

TEST NO.	SAMPLE NO.	SAMPLE DEPTH (cm)	σ'_{vo} *	τ_h/σ'_{vo}	SOIL TYPE
2	3	20 - 23	70	0.30	SM

*KN/M^2

FIGURE II-20 LIQUEFACTION TEST RESULTS FROM GRAVITY CORE – SAMPLE 23-3

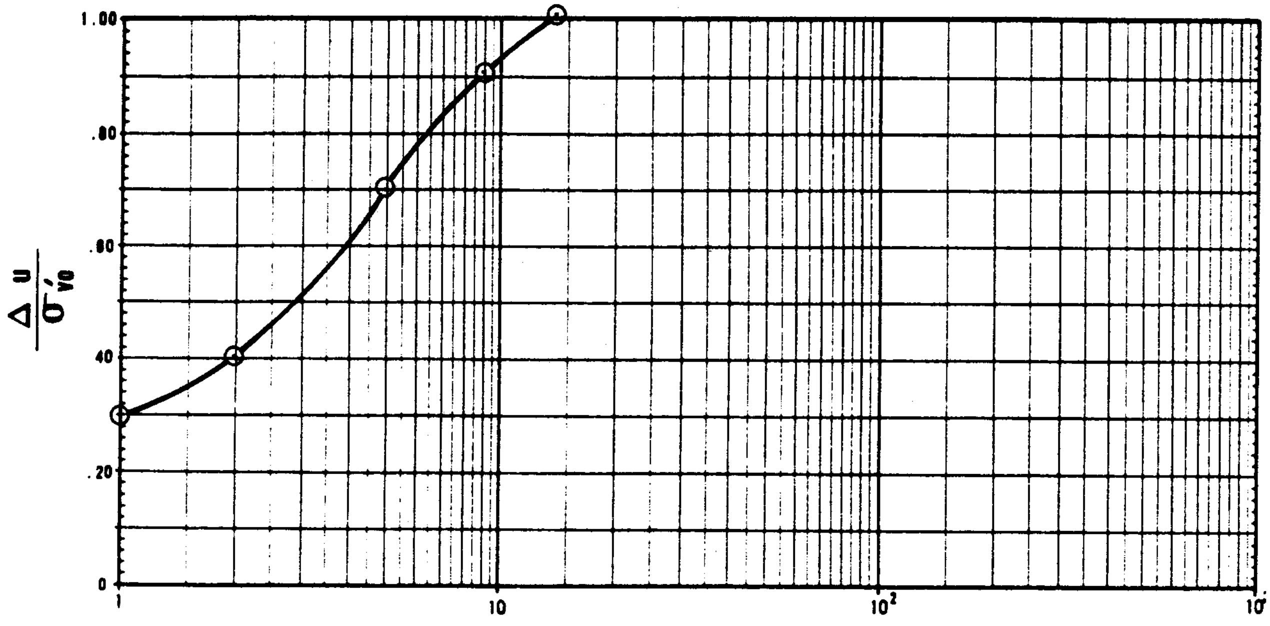

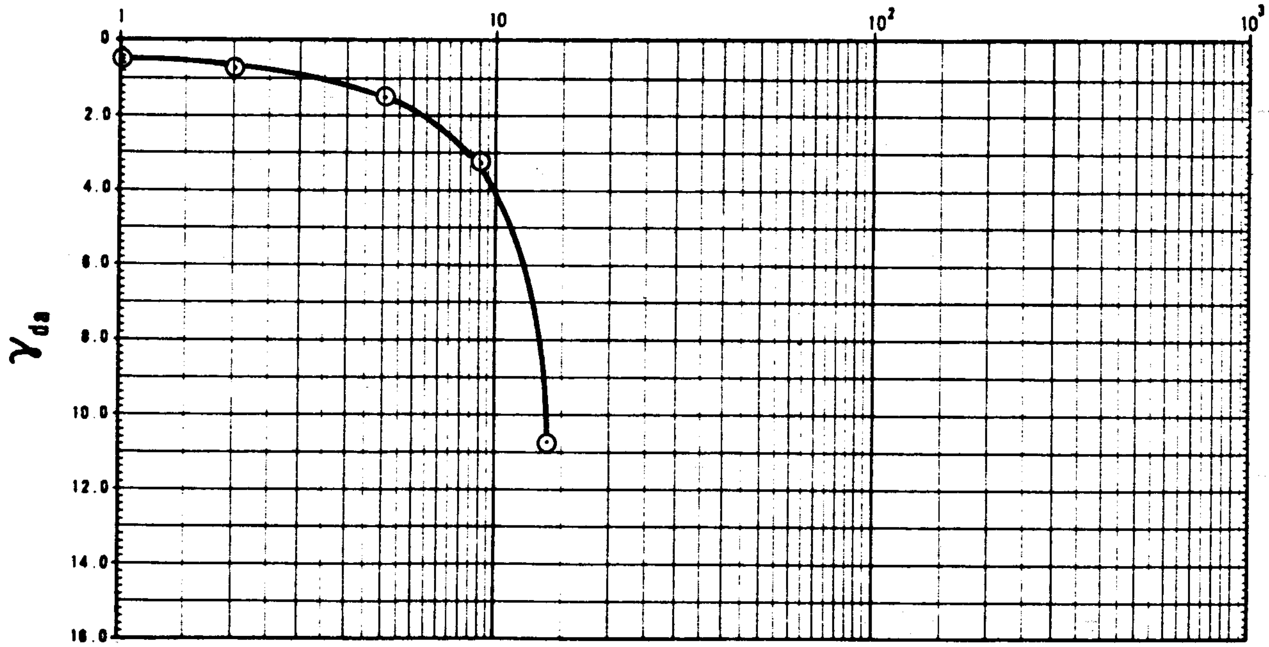

TEST NO.	SAMPLE NO.	SAMPLE TYPE	σ_v*	τ/σ_v	SOIL TYPE
1	9	RECONSTITUTED	70	0.24	SM

*KN/M2

FIGURE II-21 LIQUEFACTION TEST RESULTS FOR RECONSTITUTED SAMPLE 9-1

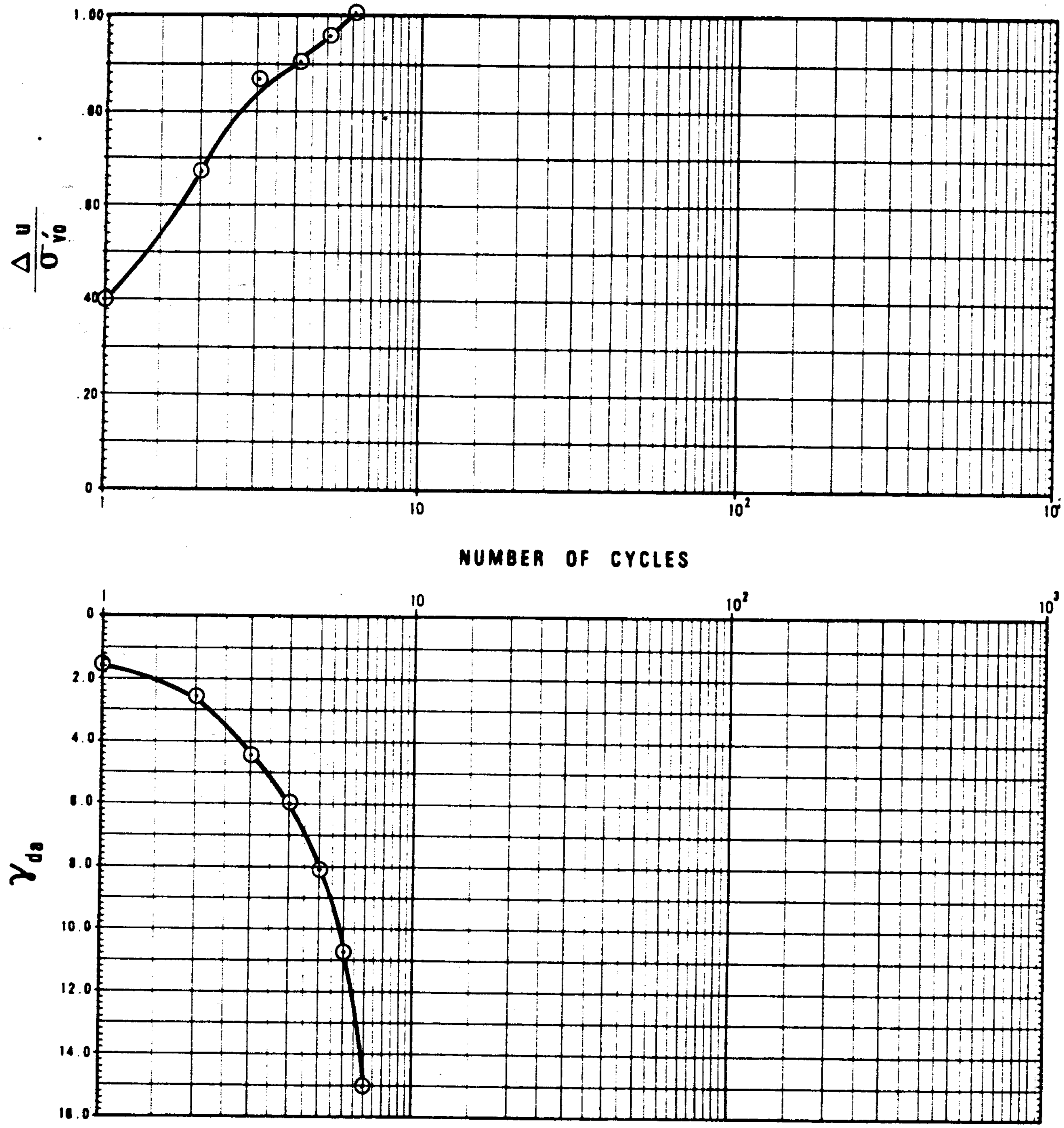

TEST NO.	SAMPLE NO.	SAMPLE TYPE	σ_v*	τ/σ_v	SOIL TYPE
2	9	RECONSTITUTED	70	0.29	SM

*KN/M²

FIGURE II-22 LIQUEFACTION TEST RESULTS FOR RECONSTITUTED SAMPLE 9-2

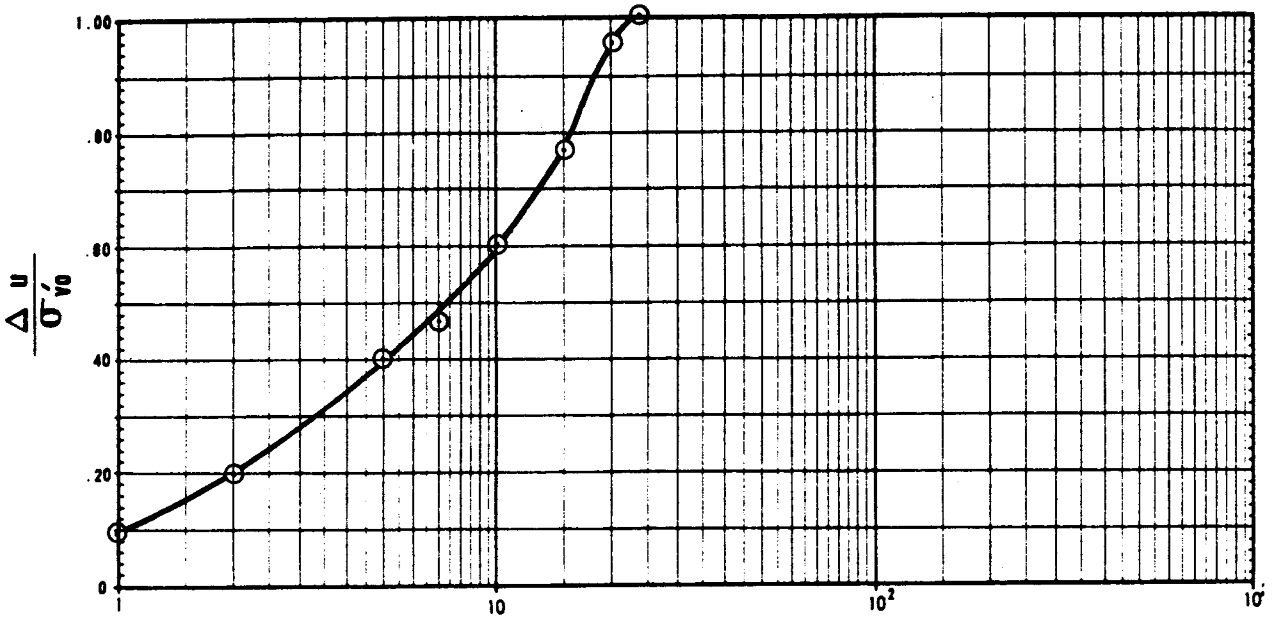

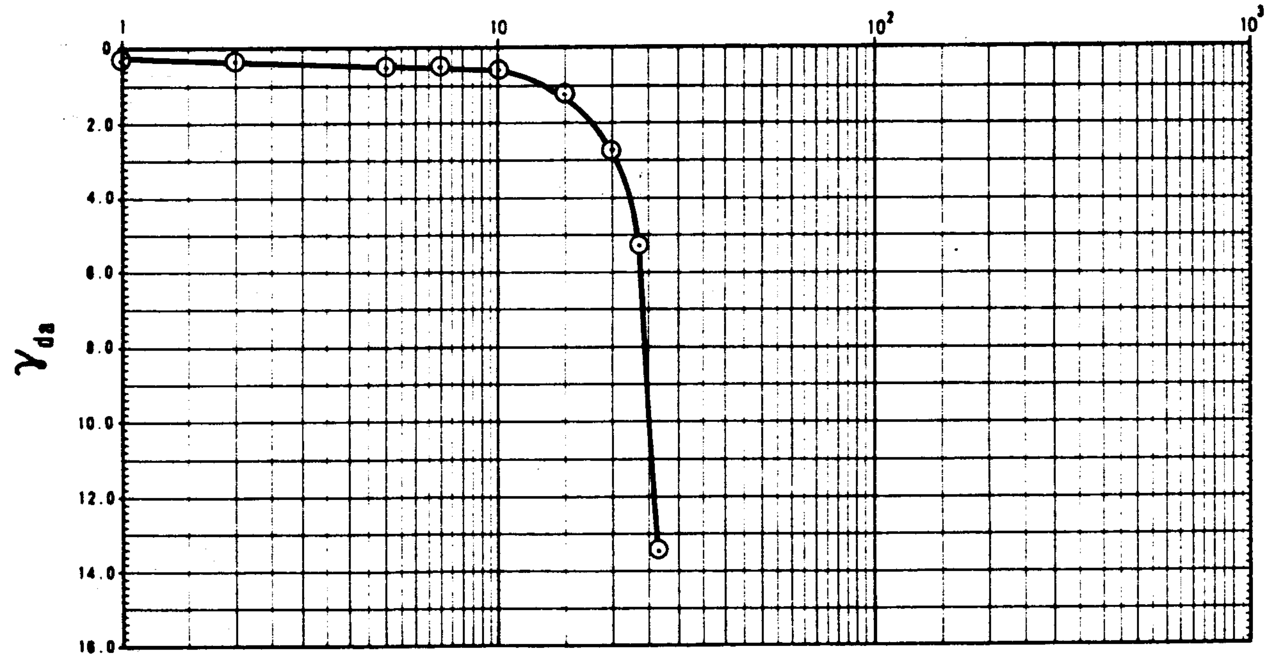

TEST NO.	SAMPLE NO.	SAMPLE TYPE	σ_v*	τ/σ_v	SOIL TYPE
3	9	RECONSTITUTED	70	0.19	SM

*KN/M^2

FIGURE II-23 LIQUEFACTION TEST RESULTS FOR RECONSTITUTED SAMPLE 9-3

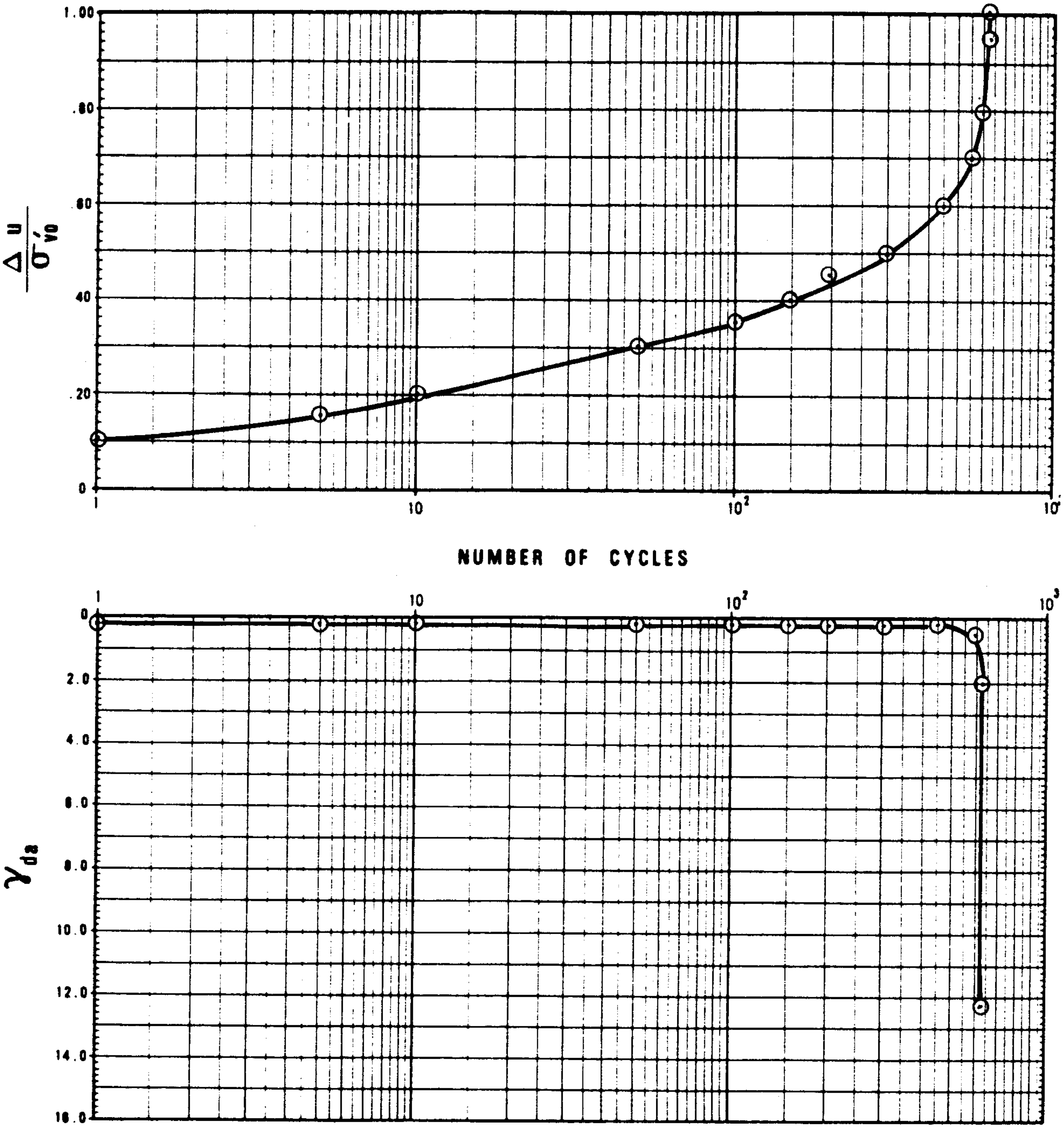

TEST NO.	SAMPLE NO.	SAMPLE TYPE	σ_v*	τ/σ_v	SOIL TYPE
4	9	RECONSTITUTED	70	0.16	SM

*KN/M^2

FIGURE II-24 LIQUEFACTION TEST RESULTS FOR RECONSTITUTED SAMPLE 9-4

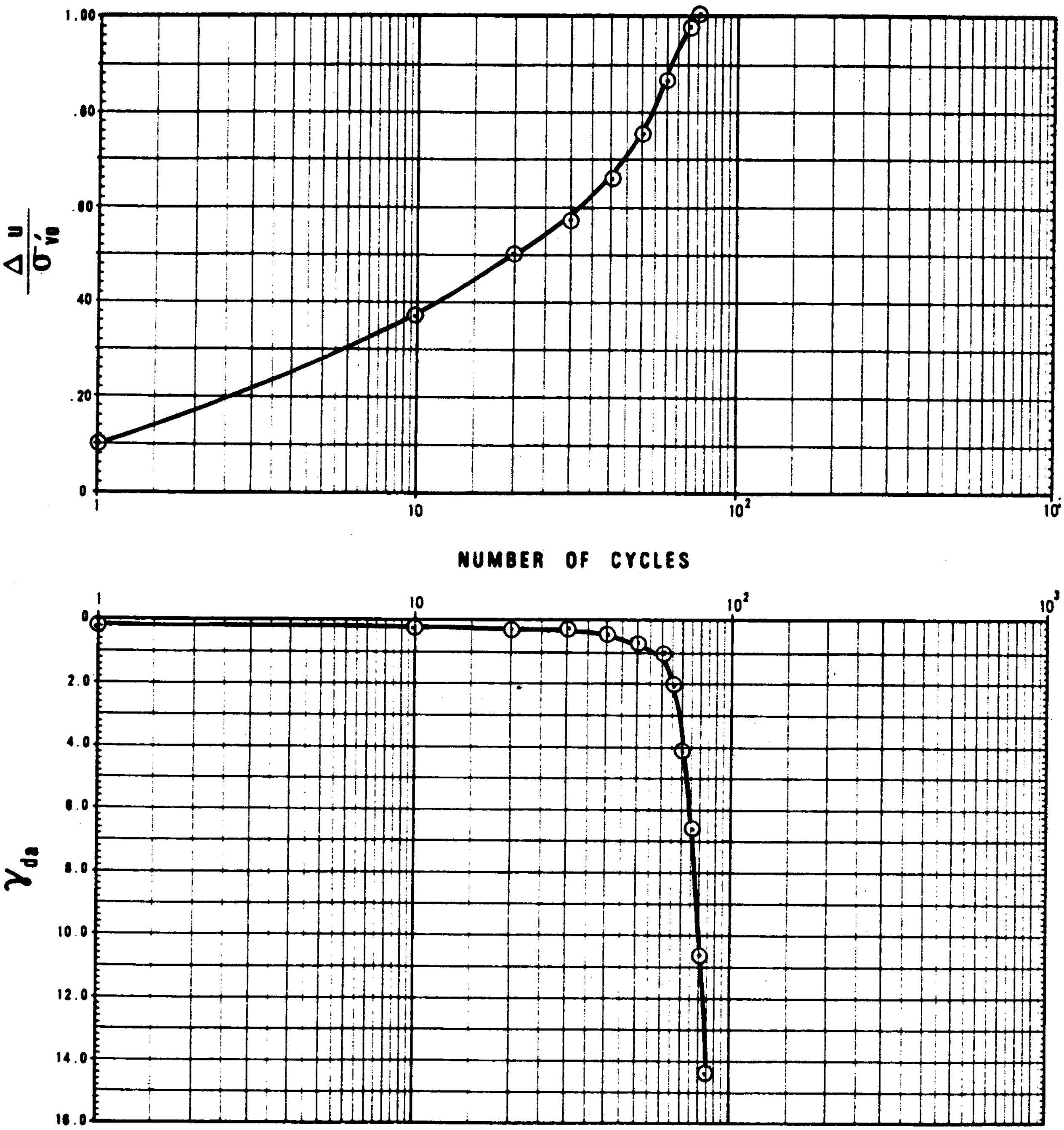

TEST NO.	SAMPLE NO.	SAMPLE TYPE	σ_v*	τ/σ_v	SOIL TYPE
1	24	RECONSTITUTED	70	0.17	SP-SM

*KN/M2

FIGURE II-25 LIQUEFACTION TEST RESULTS FOR RECONSTITUTED SAMPLE 24-1

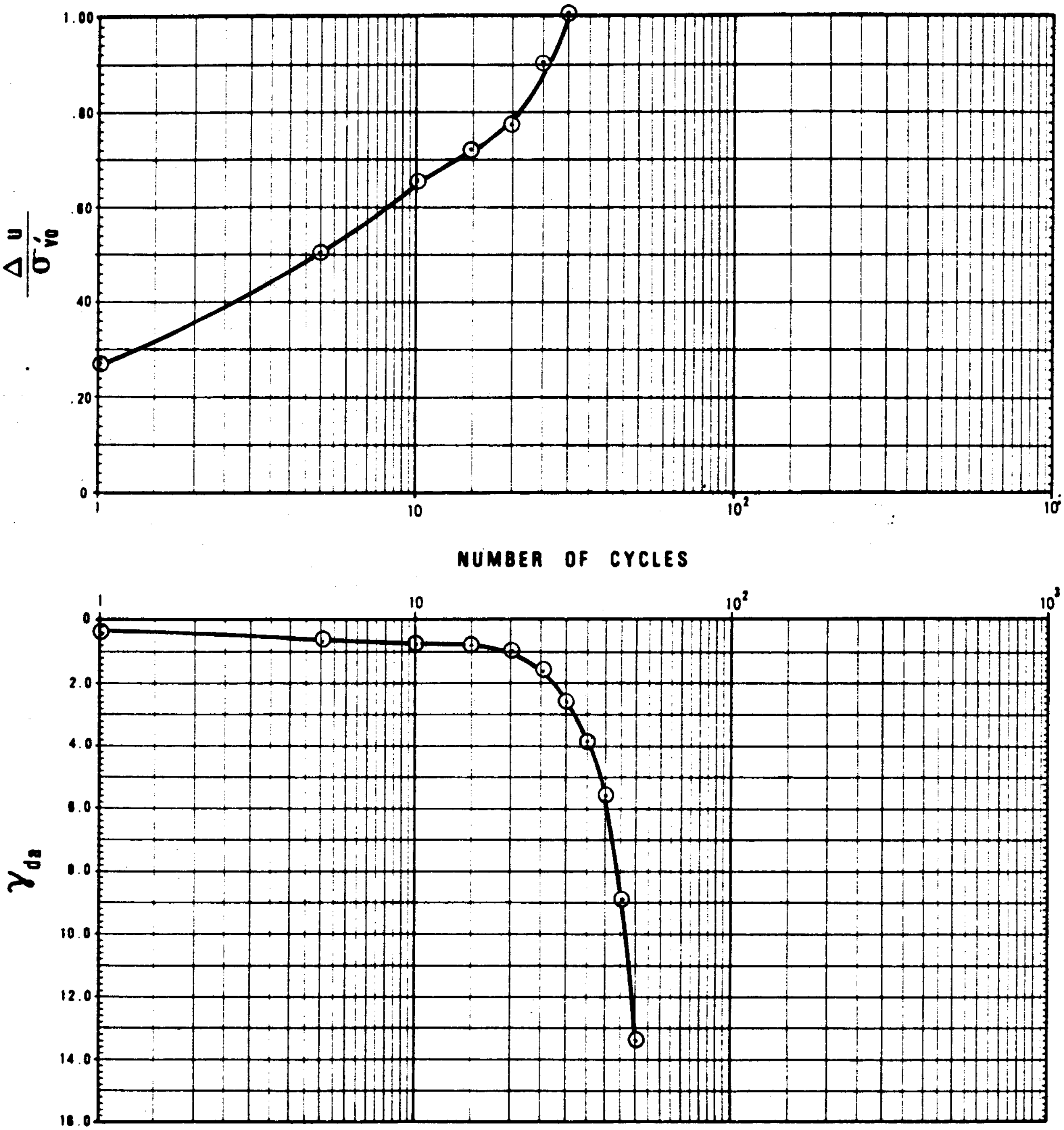

TEST NO.	SAMPLE NO.	SAMPLE TYPE	σ_v*	τ/σ_v	SOIL TYPE
2	24	RECONSTITUTED	70	0.21	SP-SM

*KN/M2

FIGURE II-26 LIQUEFACTION TEST RESULTS FOR RECONSTITUTED SAMPLE 24-2

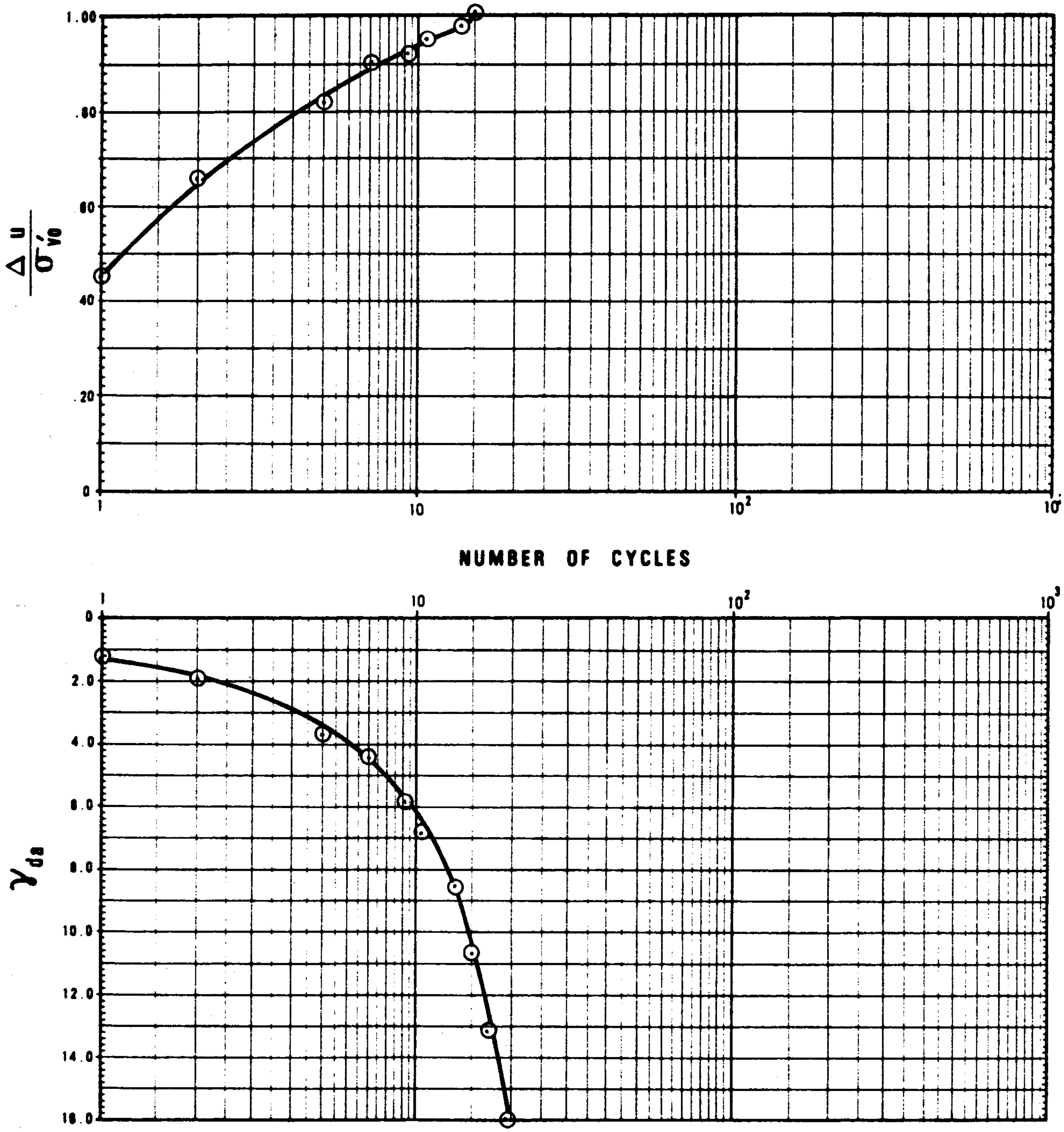

TEST NO.	SAMPLE NO.	SAMPLE TYPE	σ_v*	τ/σ_v	SOIL TYPE
3	24	RECONSTITUTED	70	0.30	SP-SM

*KN/M²

FIGURE II-27 LIQUEFACTION TEST RESULTS FOR RECONSTITUTED SAMPLE 24-3

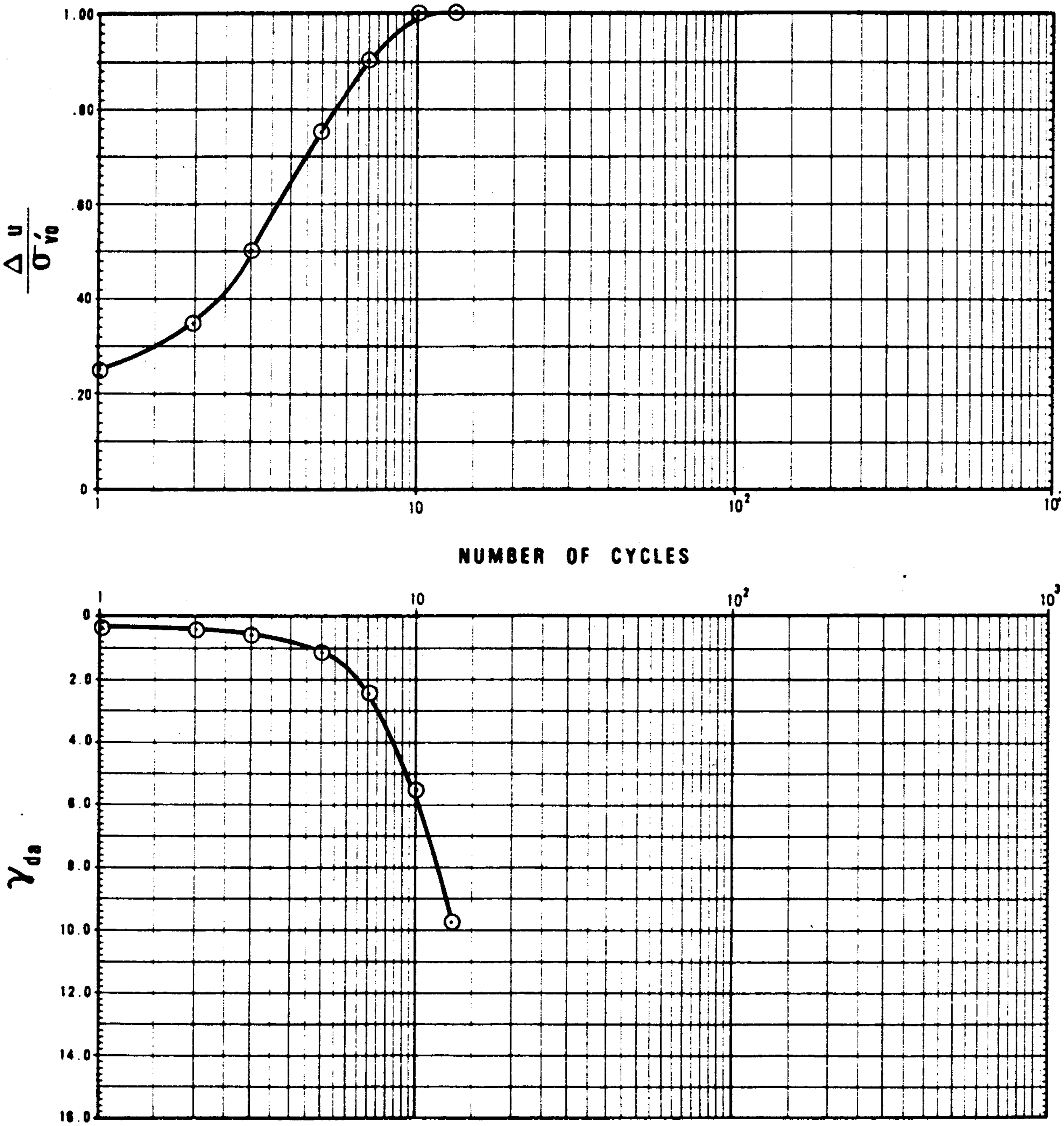

TEST NO.	SAMPLE NO.	SAMPLE TYPE	σ_v*	τ/σ_v	SOIL TYPE
3	43	RECONSTITUTED	70	0.22	SP

*KN/M2

FIGURE II-28 LIQUEFACTION TEST RESULTS FOR RECONSTITUTED SAMPLE 43-3

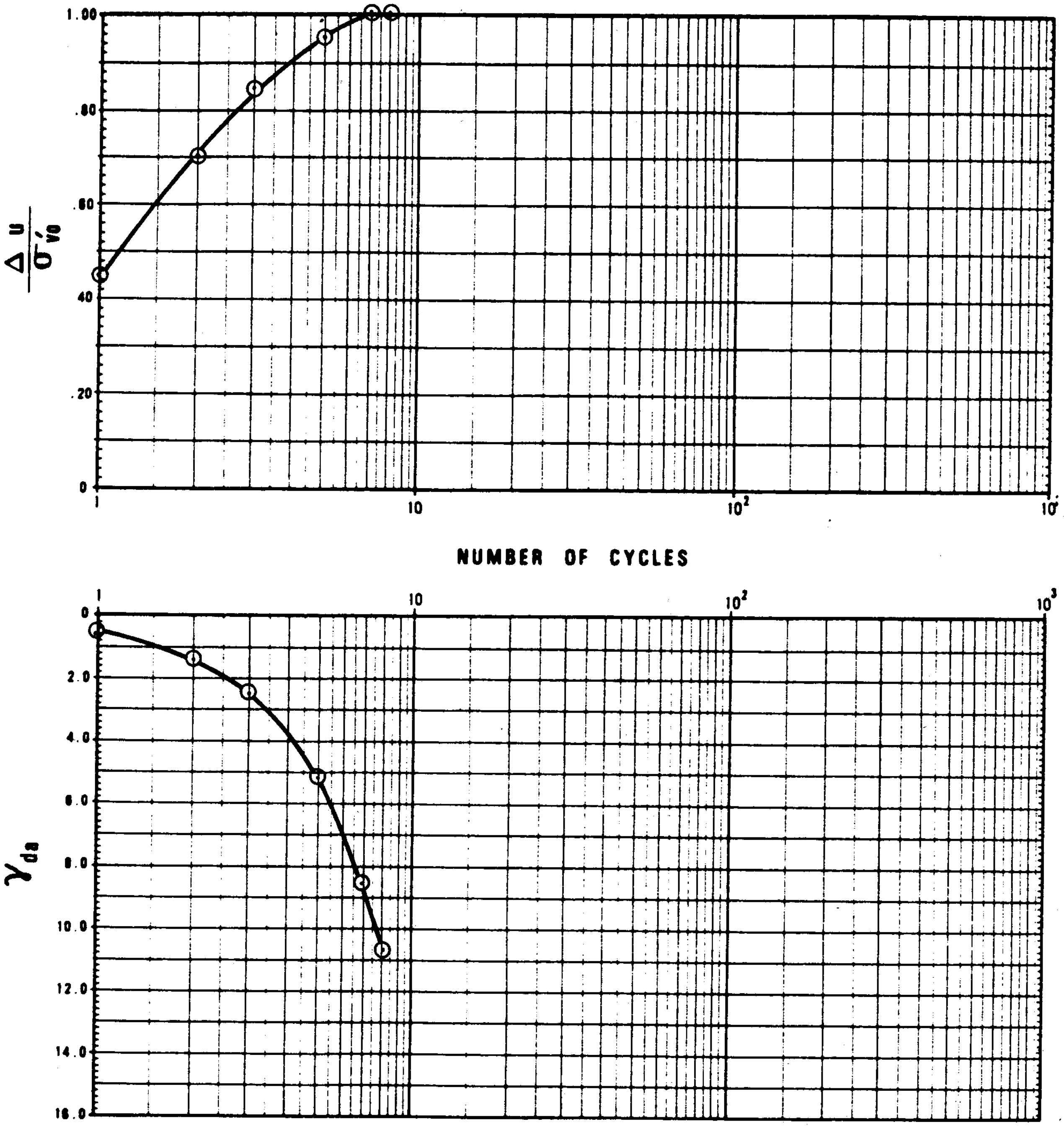

TEST NO.	SAMPLE NO.	SAMPLE TYPE	σ_v*	τ/σ_v	SOIL TYPE
4	43	RECONSTITUTED	70	0.29	SP

*KN/M^2

FIGURE II-29 LIQUEFACTION TEST RESULTS FOR RECONSTITUTED SAMPLE 43-4

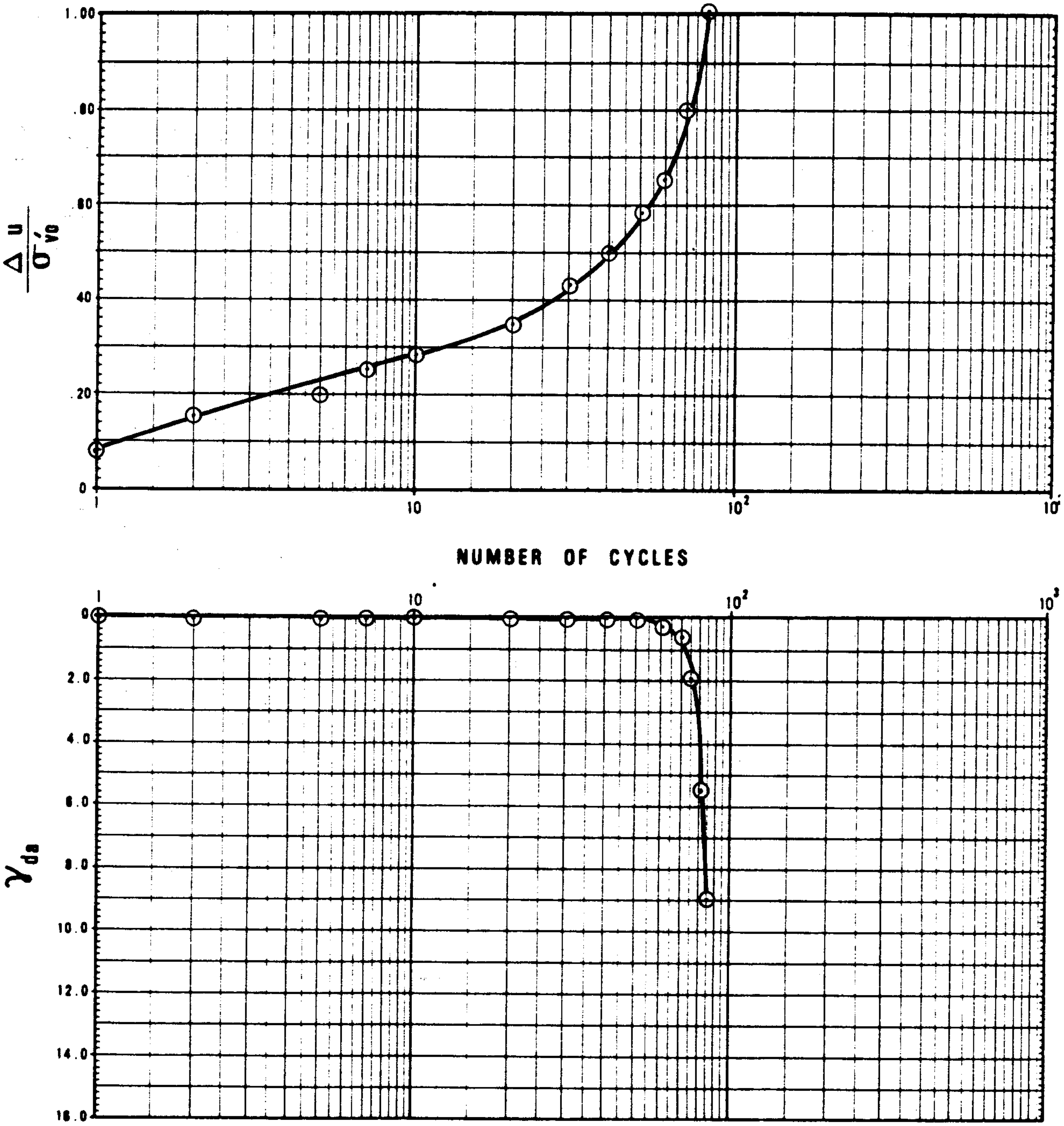

TEST NO.	SAMPLE NO.	SAMPLE TYPE	σ_v*	τ/σ_v	SOIL TYPE
5	43	RECONSTITUTED	70	0.17	SP

*KN/M²

FIGURE II-30 LIQUEFACTION TEST RESULTS FOR RECONSTITUTED SAMPLE 43-5

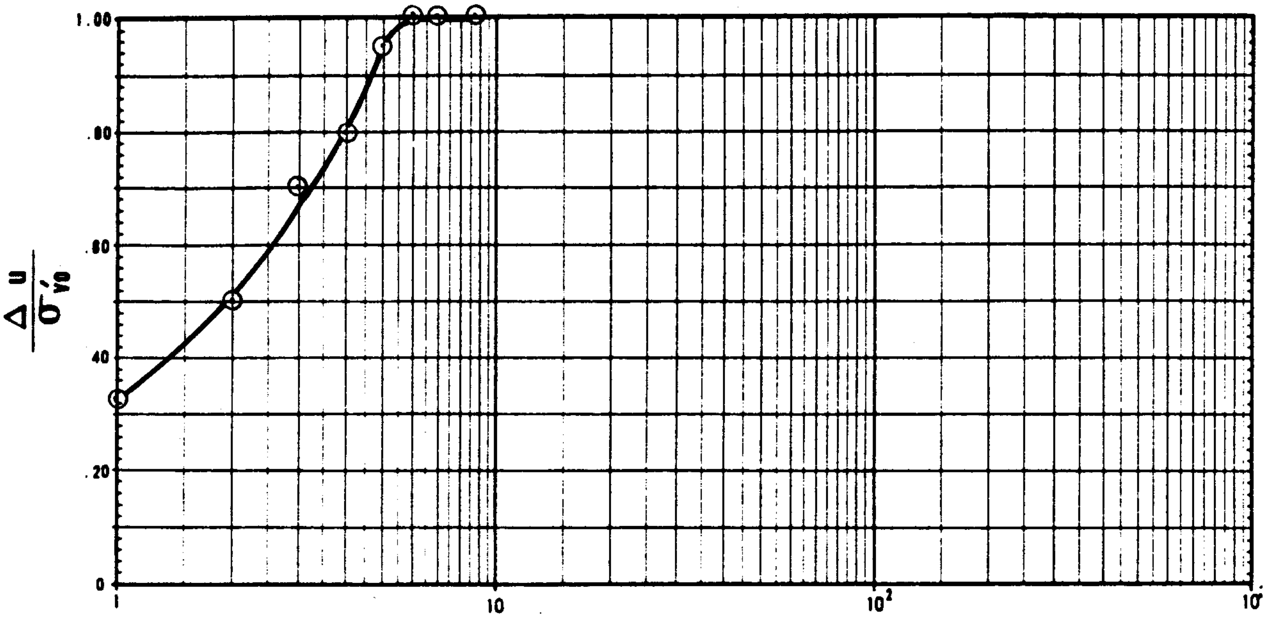

NUMBER OF CYCLES

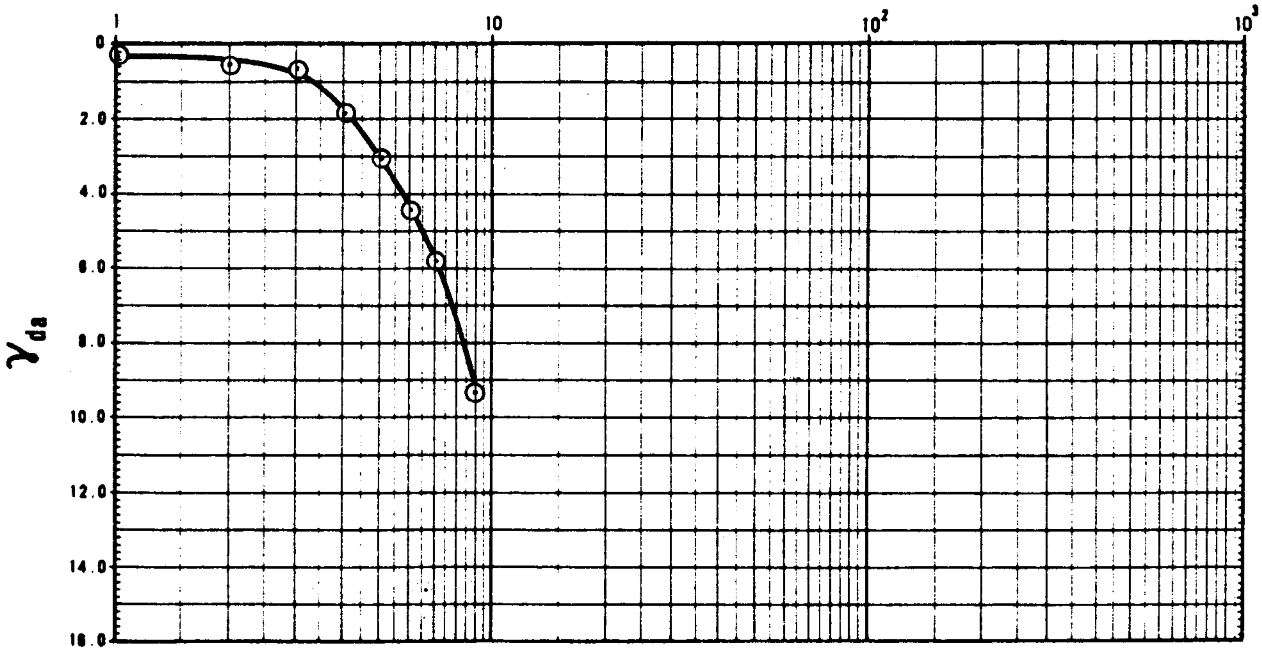

TEST NO.	SAMPLE NO.	SAMPLE TYPE	σ_v*	τ/σ_v	SOIL TYPE
1	57	RECONSTITUTED	70	0.21	SP

*KN/M^2

FIGURE II-31 LIQUEFACTION TEST RESULTS FOR RECONSTITUTED SAMPLE 57-1

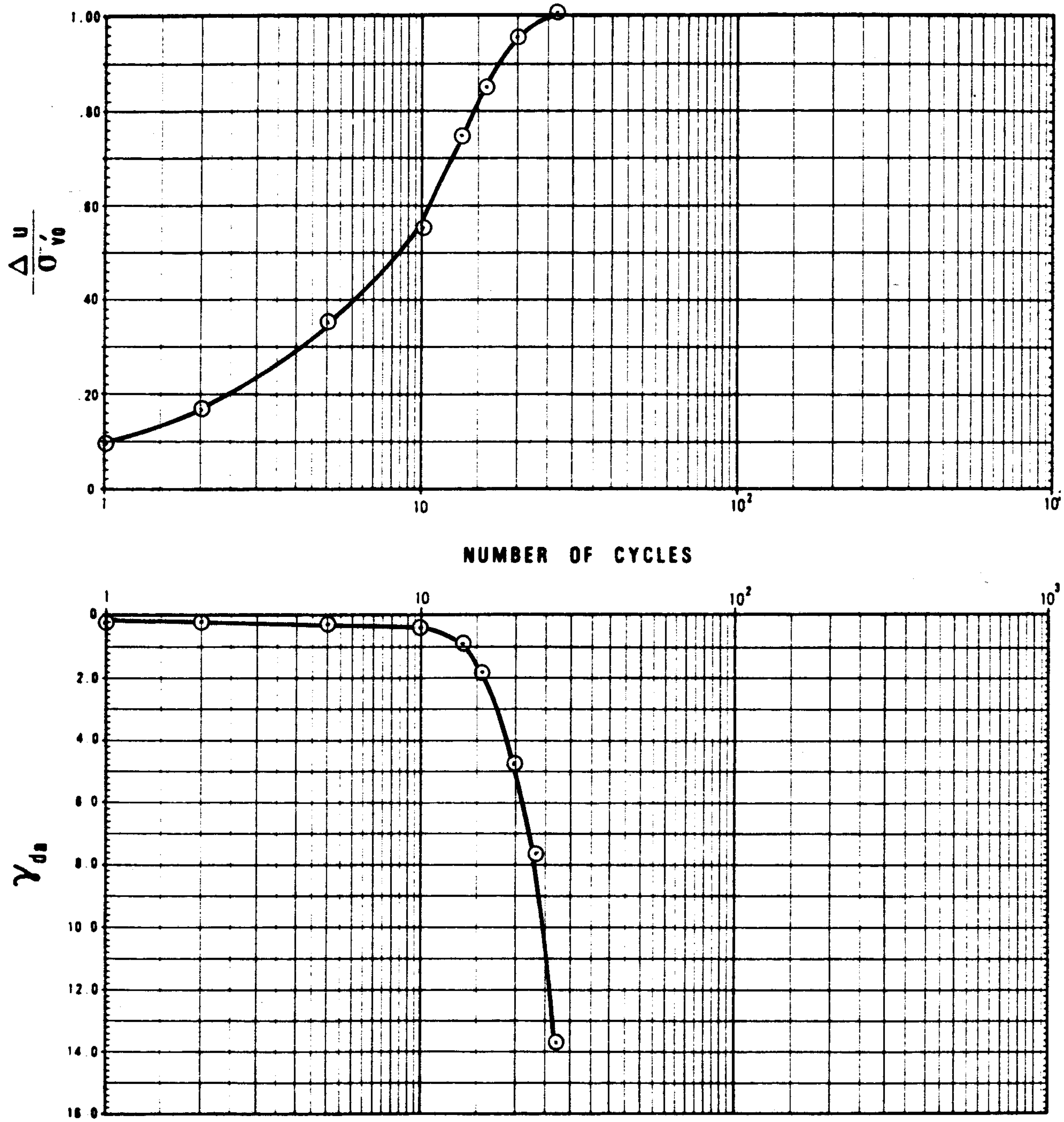

TEST NO.	SAMPLE NO.	SAMPLE TYPE	σ_v*	τ/σ_v	SOIL TYPE
2	57	RECONSTITUTED	70	0.17	SP

*KN/M²

FIGURE II-32 LIQUEFACTION TEST RESULTS FOR RECONSTITUTED SAMPLE 57-2

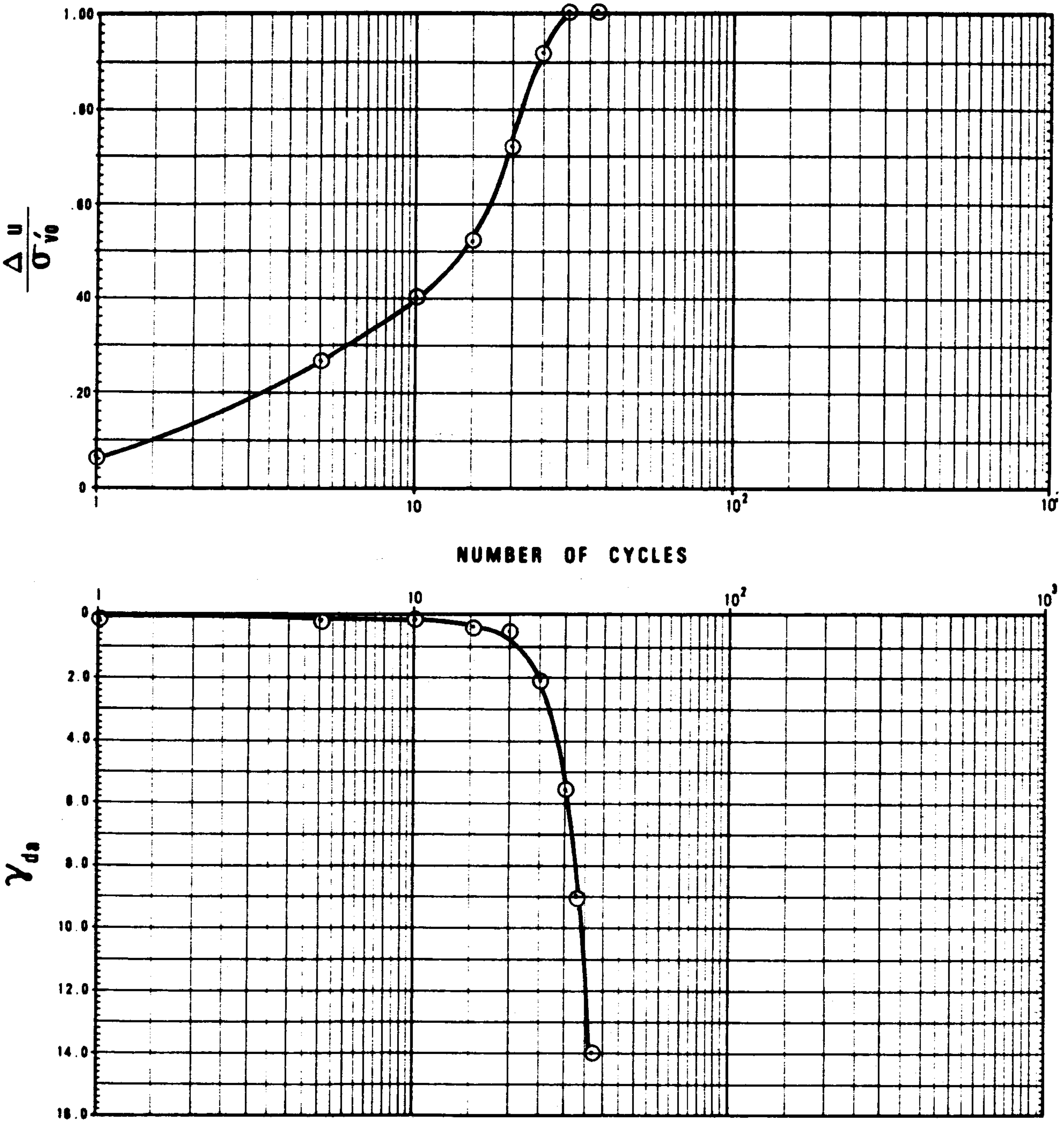

TEST NO.	SAMPLE NO.	SAMPLE TYPE	σ_v*	τ/σ_v	SOIL TYPE
3	57	RECONSTITUTED	70	0.14	SP

*KN/M²

FIGURE II-33 LIQUEFACTION TEST RESULTS FOR RECONSTITUTED SAMPLE 57-3

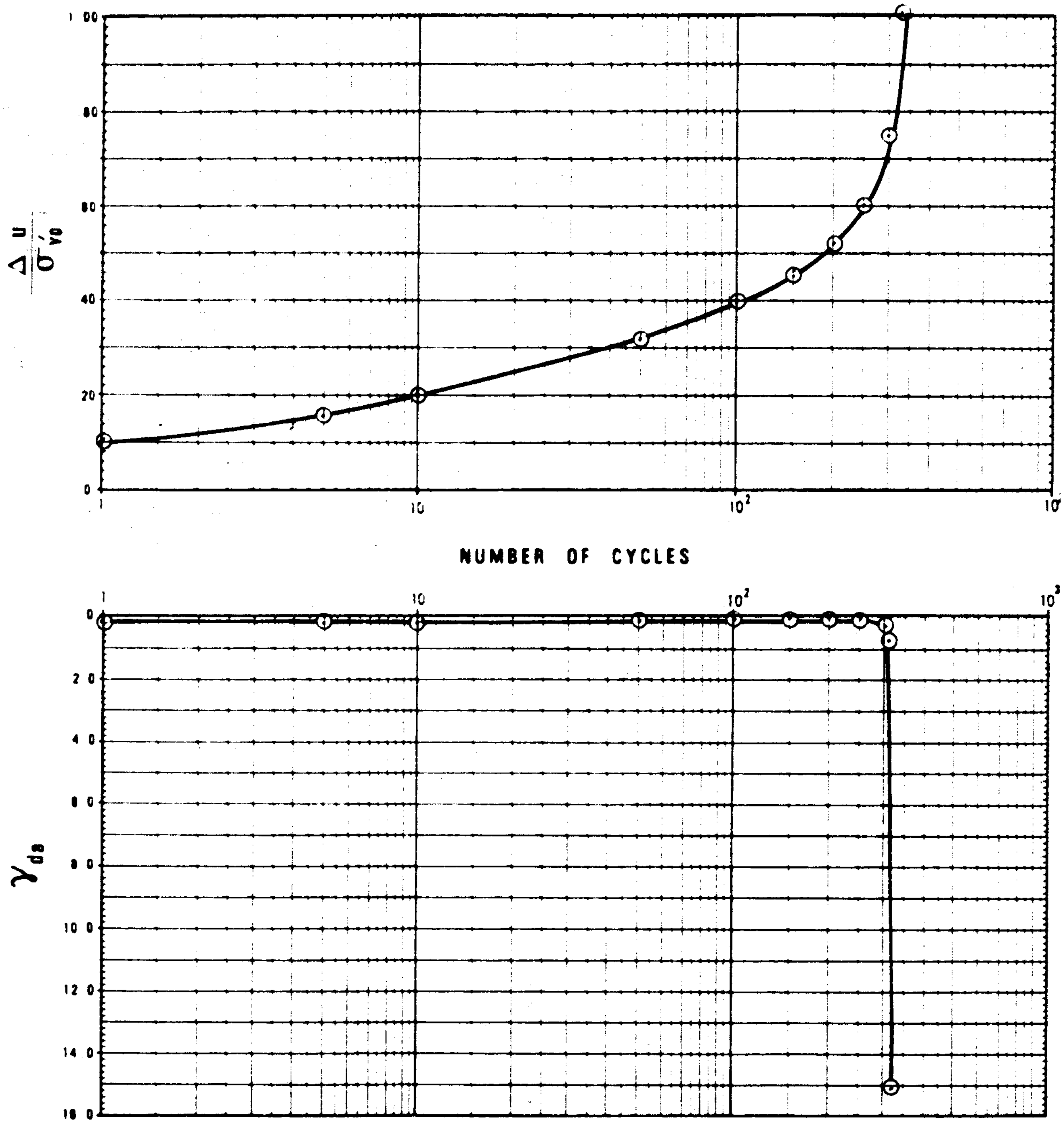

TEST NO.	SAMPLE NO.	SAMPLE TYPE	σ_v*	τ/σ_v	SOIL TYPE
4	57	RECONSTITUTED	70	0.13	SP

*KN/M^2

FIGURE II-34 LIQUEFACTION TEST RESULTS FOR RECONSTITUTED SAMPLE 57-4

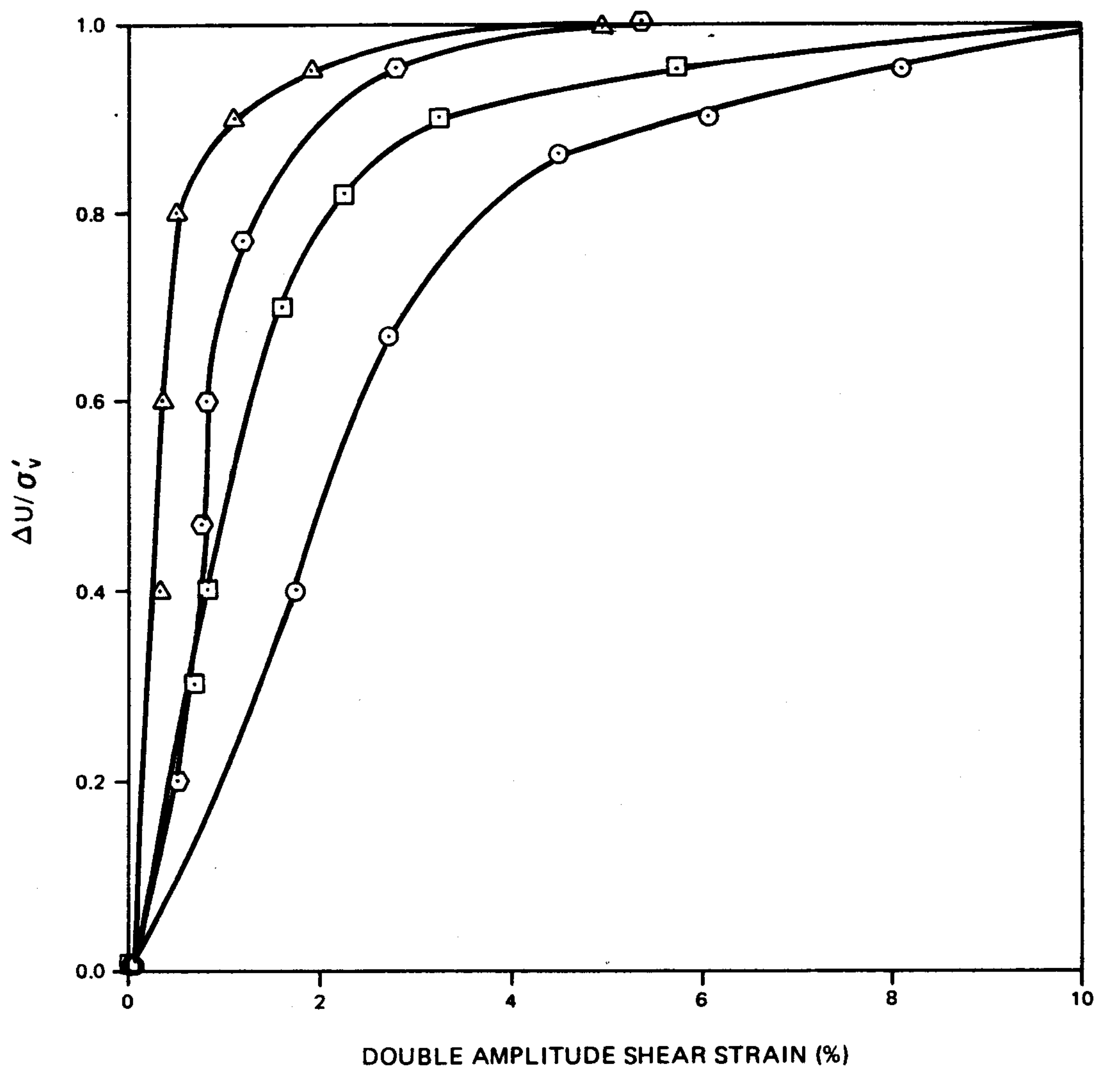

SAMPLE NO.: 9

DRY DENSITY (KN/M^3): 15.1

WATER CONTENT (%): 30

SYMBOL	STRESS RATIO τ/σ'_v
○	0.29
□	0.24
⬡	0.19
△	0.16

FIGURE II-35 PORE PRESSURE/STRAIN RESPONSE CURVES FOR RECONSTITUTED SAMPLE 9

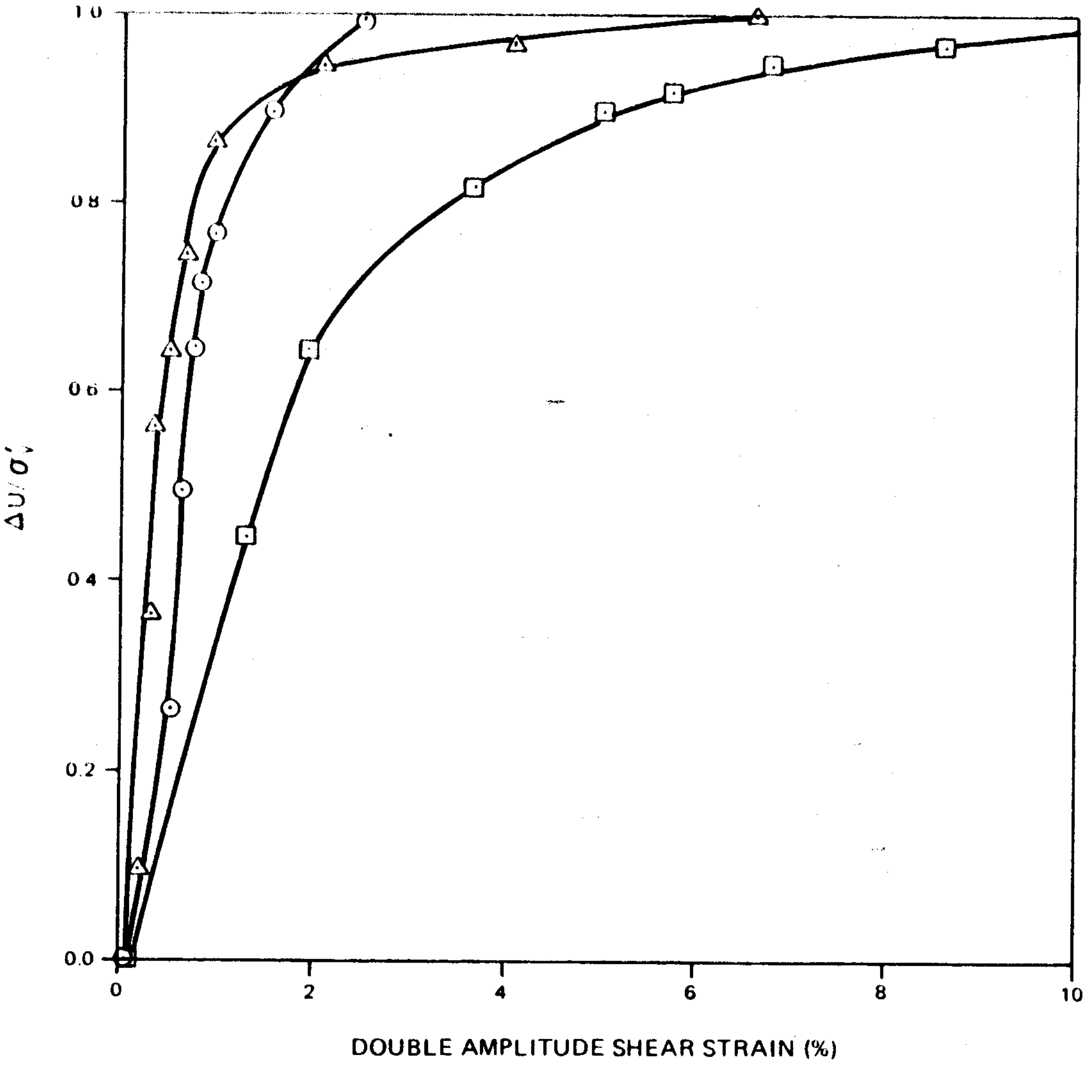

SAMPLE NO.: 24
DRY DENSITY (KN/M^3): 15.7
WATER CONTENT (%): 27

SYMBOL	STRESS RATIO τ/σ'_v
○	0.21
□	0.30
△	0.17

FIGURE II-36 PORE PRESSURE/STRAIN RESPONSE CURVES FOR RECONSTITUTED SAMPLE 24

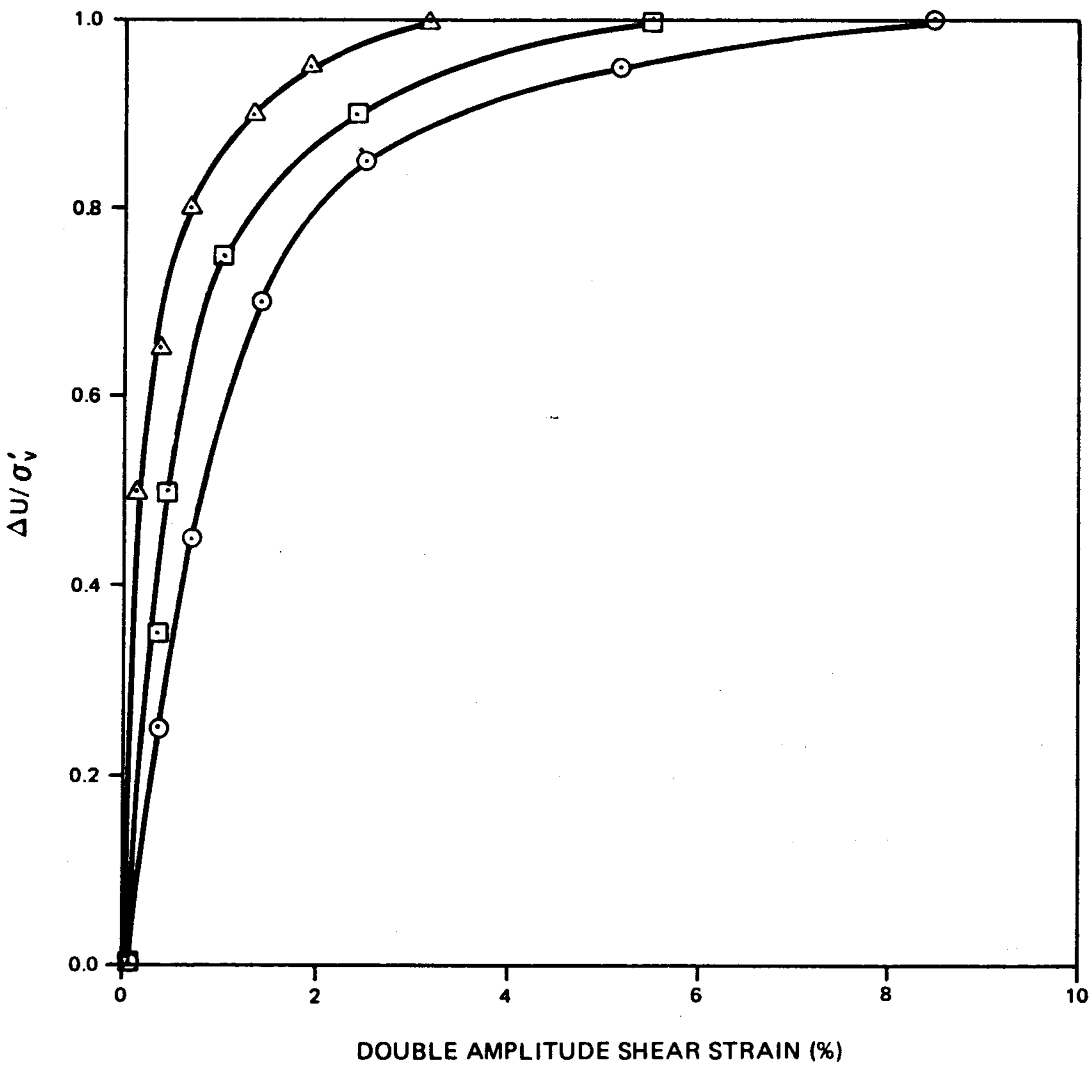

SAMPLE NO.: 43

DRY DENSITY (KN/M³): 16.3

WATER CONTENT (%): 24

SYMBOL	STRESS RATIO τ / σ'_v
○	0.29
□	0.22
△	0.17

FIGURE II-37 PORE PRESSURE/STRAIN RESPONSE CURVES FOR RECONSTITUTED SAMPLE 43

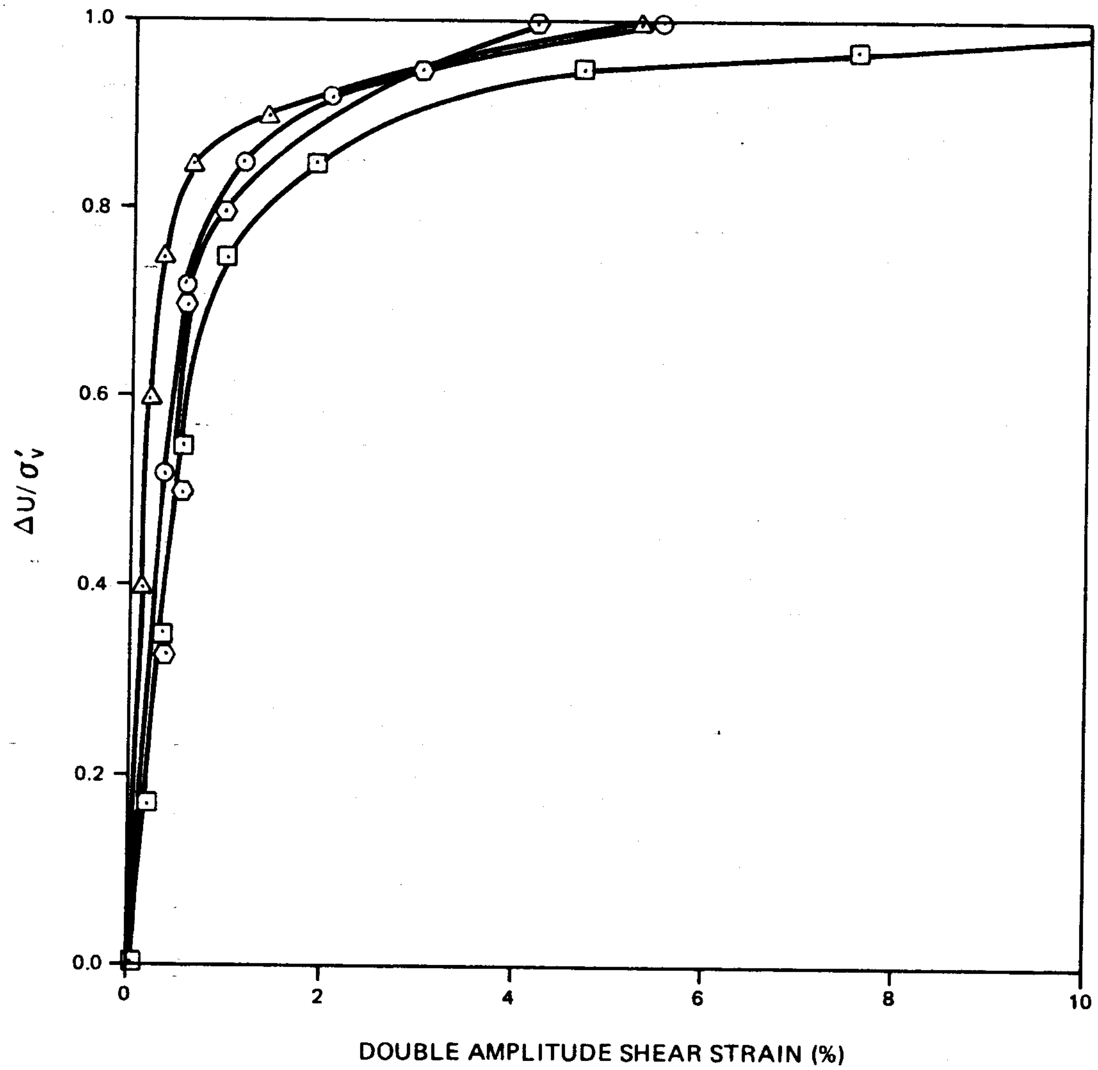

SAMPLE NO.: 57

DRY DENSITY (KN/M³): 16.2

WATER CONTENT (%): 24

SYMBOL	STRESS RATIO τ/σ'_v
⬡	0.21
□	0.17
△	0.14
○	0.13

FIGURE II-38 PORE PRESSURE/STRAIN RESPONSE CURVES FOR RECONSTITUTED SAMPLE 57

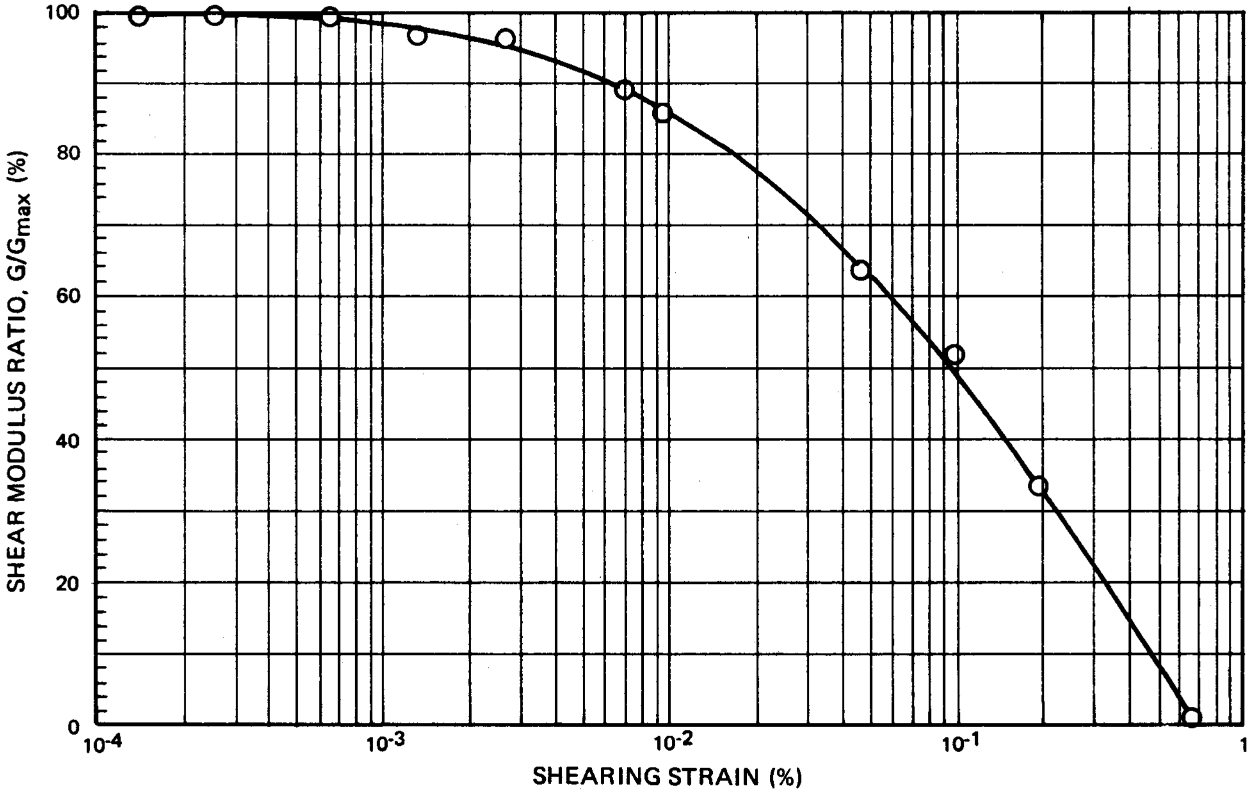

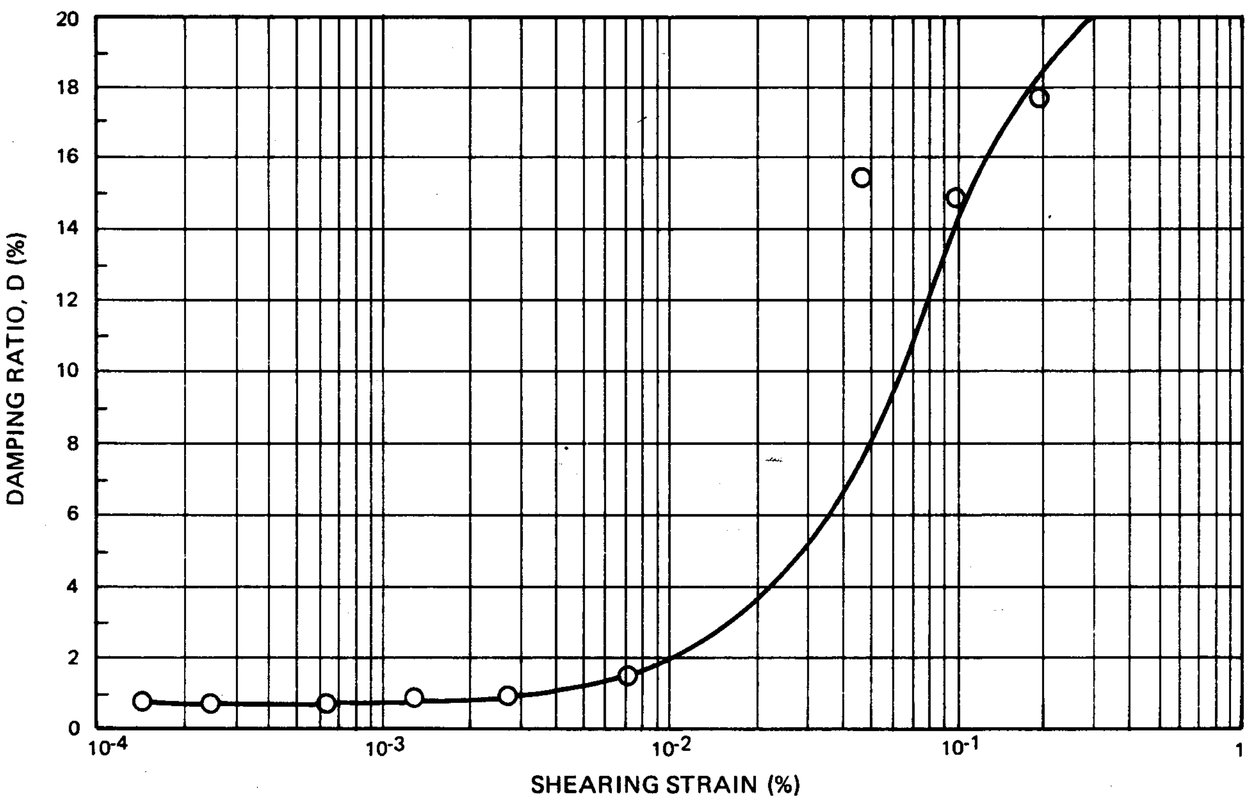

SAMPLE NO.: 9

WATER DEPTH (METERS):100

DEPTH INTERVAL: SURFICIAL

SAMPLE TYPE: RECONSTITUTED (SM)

DRY UNIT WEIGHT (KN/M^3): 15

WATER CONTENT (%): 14

CONFINING PRESSURE (KN/M^2): 140

G_{max} (KN/M^2): 0.8×10^5

FIGURE II-39 MODULUS AND DAMPING RATIO CURVES FOR SAMPLE 9

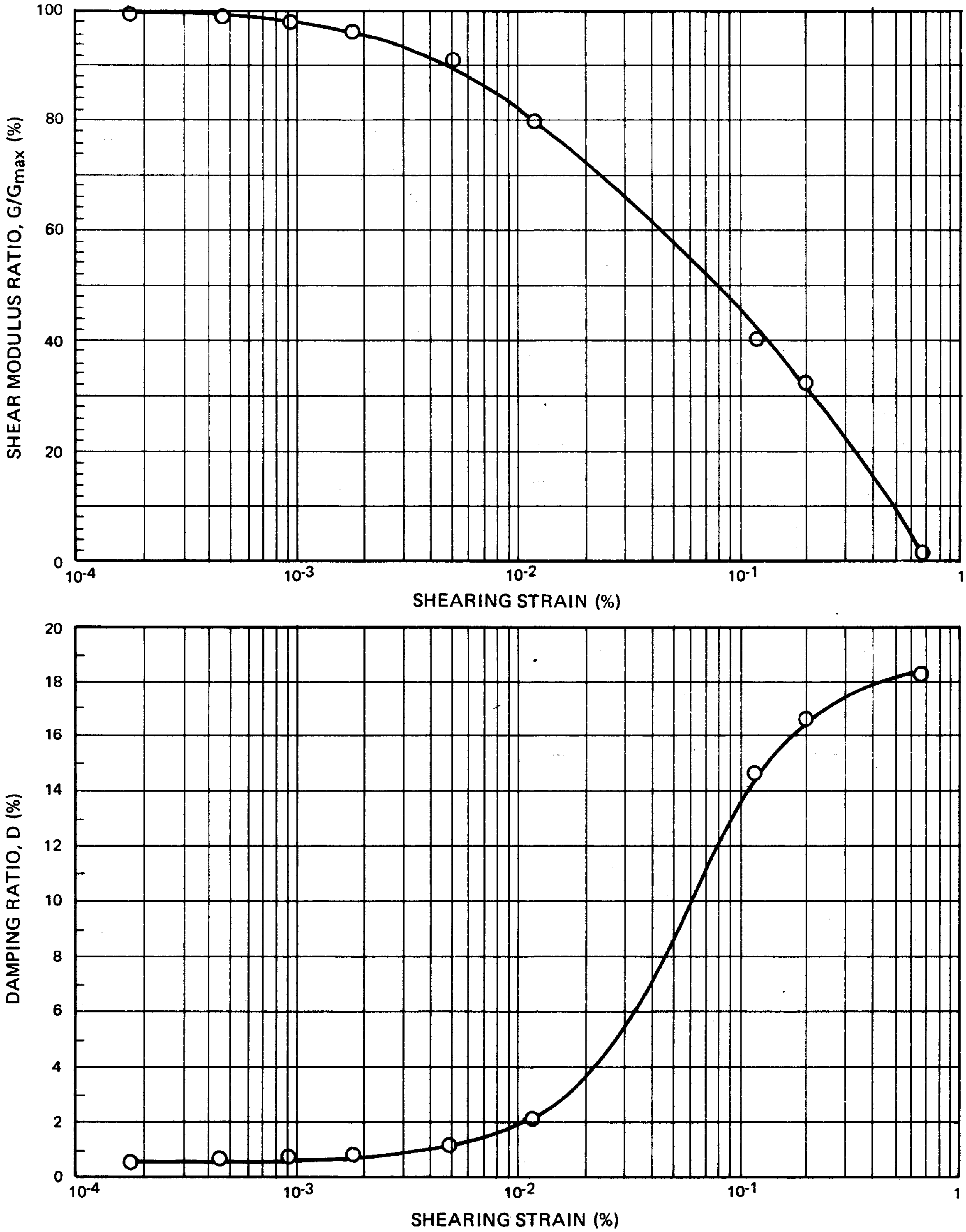

SAMPLE NO.: 24

WATER DEPTH (METERS): 84

DEPTH INTERVAL: SURFICIAL

SAMPLE TYPE: RECONSTITUTED (SP/SM)

DRY UNIT WEIGHT (KN/M^3): 16

WATER CONTENT (%): 15

CONFINING PRESSURE (KN/M^2): 140

G_{max} (KN/M^2): 1.1×10^5

FIGURE II-40 MODULUS AND DAMPING RATIO CURVES FOR SAMPLE 24

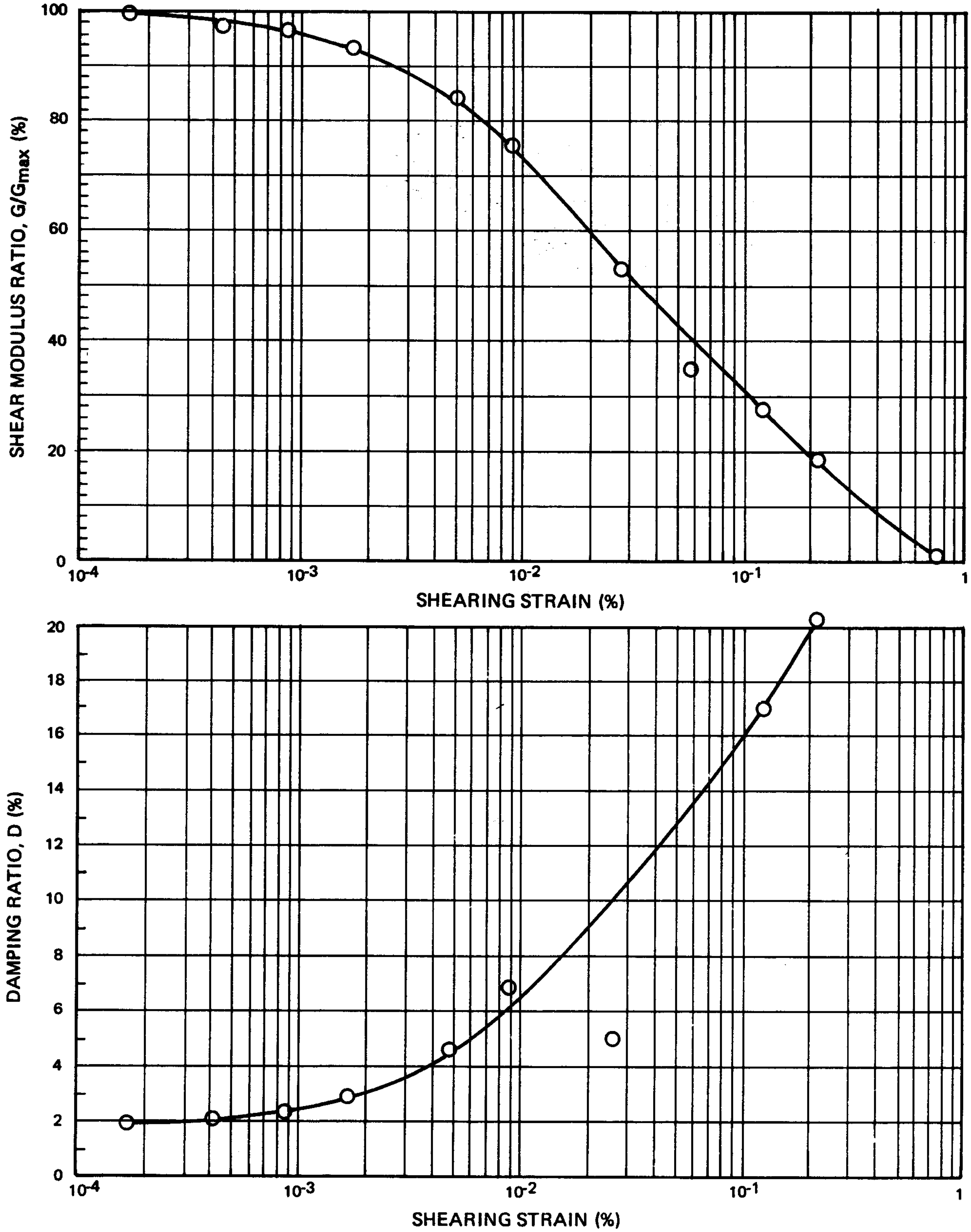

SAMPLE NO.: 43
WATER DEPTH (METERS): 80
DEPTH INTERVAL: SURFICIAL
SAMPLE TYPE: RECONSTITUTED (SP)

DRY UNIT WEIGHT (KN/M^3): 16
WATER CONTENT (%): 10.5
CONFINING PRESSURE (KN/M^2): 140
G_{max} (KN/M^2): 1.2×10^5

FIGURE II-41 MODULUS AND DAMPING RATIO CURVES FOR SAMPLE 43

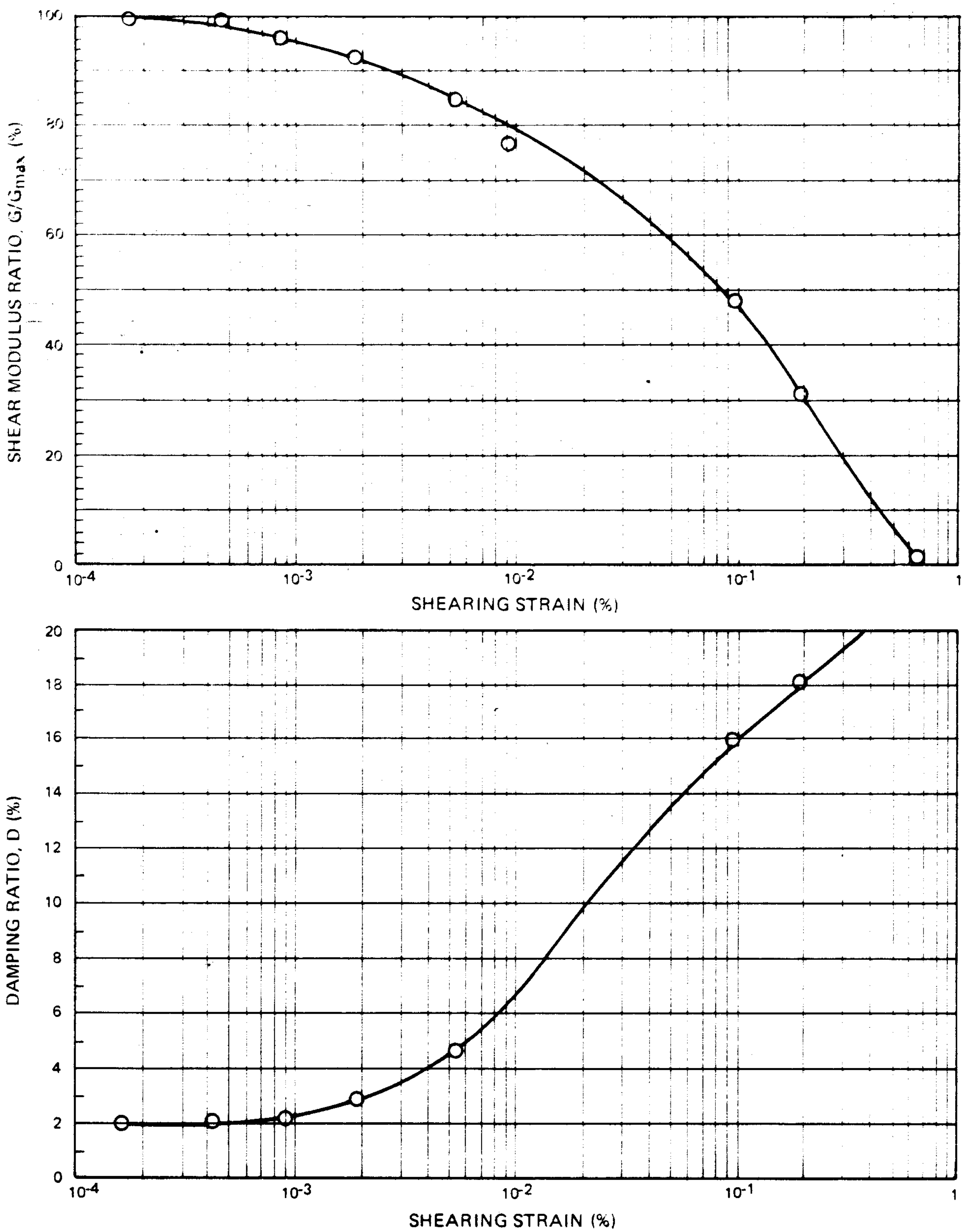

SAMPLE NO.: 57
WATER DEPTH (METERS): 49
DEPTH INTERVAL: SURFICIAL
SAMPLE TYPE: RECONSTITUTED (SP)

DRY UNIT WEIGHT (KN/M^3): 16
WATER CONTENT (%): 9.5
CONFINING PRESSURE (KN/M^2): 140
G_{max} (KN/M^2): 1.2×10^5

FIGURE II-42 MODULUS AND DAMPING RATIO CURVES FOR SAMPLE 57

APPENDIX III

VIBRACORE DESCRIPTIONS

Marine Environmental Science Associates

VISUAL CORE DESCRIPTION

LEGEND

CENTIMETERS

0

COLOR	SUB SAMPLE	DESCRIPTION

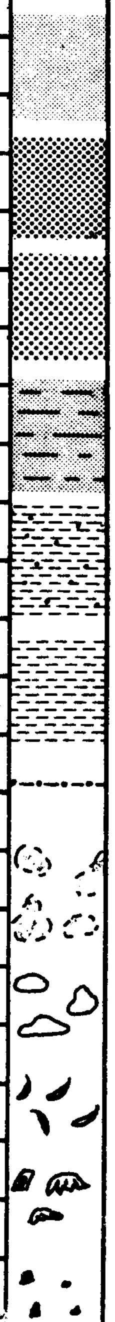

Fine and Very Fine Sand

Medium Sand

Coarse Sand

Silty Sand

Sandy Silt

Silt

Gradational color change

Mottling

Burrows

Pelecypods

Shell fragments

Rock fragments

Marine Environmental Science Associates

VISUAL CORE DESCRIPTION

PROJECT NOAA - Bristol Bay

STATION 0/200 A Section 1 LOGGED BY E. Johnson DATE 15Jan82

LOCATION 56°29.9'N 164°59.3'W LENGTH 86 cm

WATER DEPTH 82 m SECTION 1 OF 2

VESSEL Discoverer DATE 279 JD 1980

LENGTH 86 cm TYPE CORE Vibracore

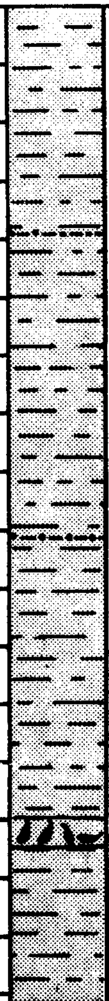

CENTIMETERS	COLOR	SUB SAMPLE	DESCRIPTION
0–10	5y5/2	X (0–8 cm)	0-8 cm: Geotechnical and grain size analysis Light olive grey, silty fine sand
30	5y3/2		Olive grey, silty fine sand mottled with dusky yellow green silty sand
55	5gy3/2		Greyish olive green silty fine sand with slight mottling
73	5y3/2		Olive grey fine sand with scattered whole pelecypod shells, 1 cm in diameter, and a pebble, 1 cm in diameter
80–90	5y3/2	X (78–86 cm)	Olive grey silty sand 78-86 cm: Geotechnical and grain size analysis 86cm: Bottom of section 1.

Scale: 0, 10, 20, 30, 40, 50, 60, 70, 80, 90 CENTIMETERS

Note: Section 2 was lost in shipping from <u>Discoverer</u>.

Marine Environmental Science Associates

mesa2, inc.

VISUAL CORE DESCRIPTION

PROJECT NOAA Bristol Bay

STATION 0/200B Section 1 LOGGED BY E. Johnson DATE 15Jan82

LOCATION 56°29.9'N 164°59.3'W LENGTH 91 cm

WATER DEPTH 82 m SECTION 1 OF 2

VESSEL Discoverer DATE 279JD1980

LENGTH 91cm TYPE CORE Vibracore

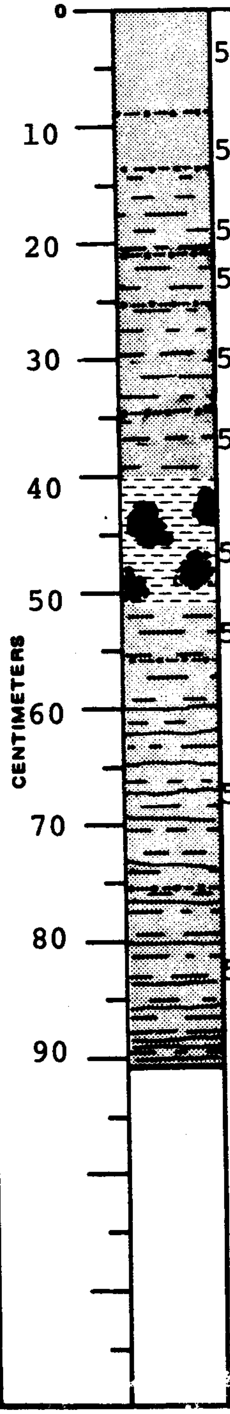

COLOR	SUB SAMPLE	DESCRIPTION
5y5/2	☒	Light olive grey very fine sand 0-8 cm: Geotechnical and grain-size analysis
5y3/2		Olive grey fine sand
5y5/2		Light olive grey silty fine sand
5gy2/1		Greenish Black silty fine sand
5y5/2		Light olive grey silty fine sand
5g2/1		Greenish black silty fine sand
5y5/2		Light olive grey silt mottled with greenish black silt
5g2/1		Greenish black silty fine sand
5b5/1		Bluish grey silty fine sand with thin black silt stringers
5y5/2	☒	Light olive grey silty fine sand with thin black and brown silt stingers 83-91 cm : Geotechnical and grain-size analysis 91 cm: Bottom of section 1

Marine Environmental Science Associates

PAGE 2 OF 2

VISUAL CORE DESCRIPTION

PROJECT NOAA - Bristol Bay

STATION 0/200B section 2 LOGGED BY E. Johnson DATE 15Jan82

LOCATION 56°29.9'N 164°59.3'W LENGTH 71 cm

WATER DEPTH 82 m SECTION 2 OF 2

VESSEL Discoverer DATE 279 JD 1980

LENGTH 71 cm TYPE CORE Vibracore

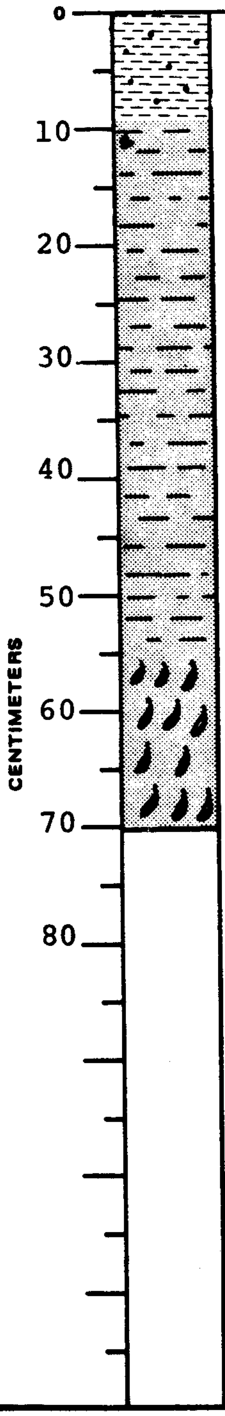

COLOR	SUB SAMPLE	DESCRIPTION
5y5/2	X	Light olive grey sandy silt with scattered coarse sand particles 0-8 cm: Geotechnical and grain-size analysis 11 cm: 1.3 cm rock clast
5gy2/1		Greenish black silty fine sand
5y4/4	X	Moderate olive brown very fine sand with many articulated pelecypods [Cardita (Cyclocardia) crebricostata (Kraus)?] average 3 cm in diameter 63-71 cm: Geotechnical and grain-size analysis 71 cm: Bottom of core Note: To define true depth in core add 91 cm to depth shown in left hand margin.

Marine Environmental Science Associates

VISUAL CORE DESCRIPTION

PROJECT NOAA-BRISTOL BAY

STATION 20/100 LOGGED BY E. Johnson DATE 15Jan82

LOCATION 55°36.4'N 164°40.2'W LENGTH 80 cm

WATER DEPTH 100 m SECTION 1 OF 1

VESSEL Discoverer DATE 282 JD 1980

LENGTH 80 cm TYPE CORE Vibracore

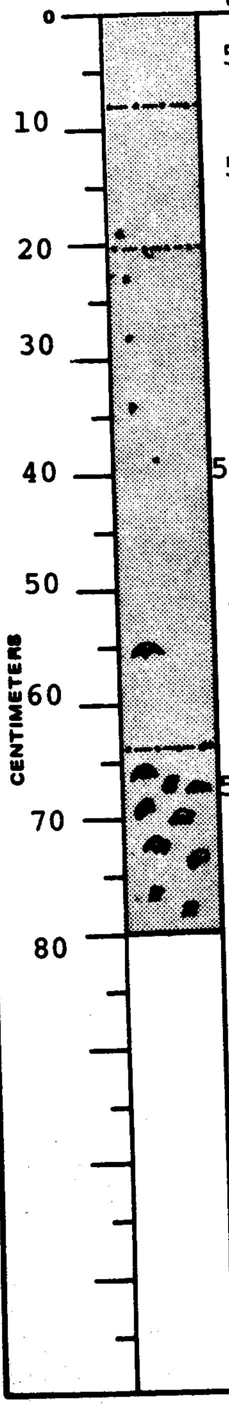

COLOR	SUB SAMPLE	DESCRIPTION
5y5/2	X	Lt.Olive Grey very fine sand 0-8 cm: Geotechnical and grain size analysis
5gy3/2		Grayish olive green fine sand 19cm : .5 cm rounded rock particle 23cm : .3 cm rounded rock particle 27cm : .18 cm rounded rock particle 34cm : .45 cm rounded rock particle
5y2/1		39cm : 1.0 cm rounded rock particle Greenish Black fine sand 55cm : Shell fragment, 3 cm long
5gy3/2	X	Grayish olive green fine sand with shell hash. Shells average length is .5 cm. Fragments decrease in size and frequency downward in core. 72-80 cm: Getechnical and grain size analysis 80 cm: Bottom of core

Marine Environmental Science Associates

VISUAL CORE DESCRIPTION

PROJECT NOAA - Bristol Bay

STATION 70/87 A LOGGED BY E. Johnson DATE 15Jan82

LOCATION 55°29.4'N 163°52.2'W LENGTH 65 cm

WATER DEPTH 89 m SECTION 1 OF 1

VESSEL Discoverer DATE 283 JD 1980

LENGTH 65 cm TYPE CORE Vibracore

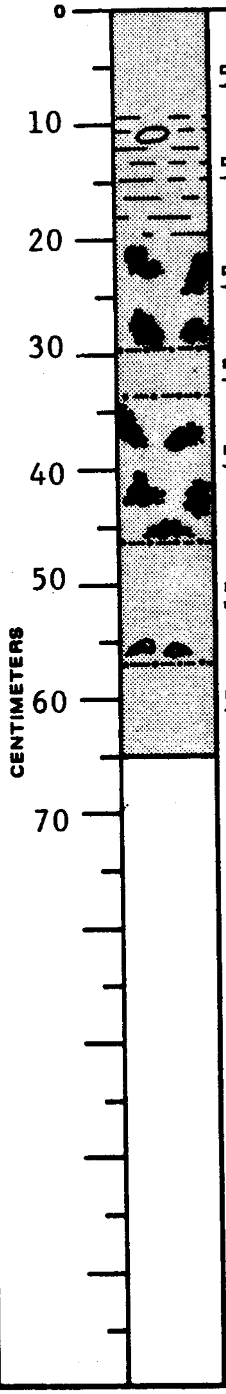

COLOR	SUB SAMPLE	DESCRIPTION
5y5/2		Lt. Olive grey fine sand 0-8 cm :Geotechnical and grain size analysis
5y4/4		11 cm :burrow Moderate olive brown silty sand
5y3/2		Olive grey very fine sand with mottling
5gy2/1		Greenish black very fine sand
5y3/2		Olive grey very fine sand with mottling
5gy2/1		Greenish black very fine sand 56 cm : shell fragments
5gy4/1		Dark greenish grey very fine sand 57-65 cm :Geotechnical and grain size analysis 65 cm Bottom of core

Note: Additional core from catcher not described

Marine Environmental Science Associates

VISUAL CORE DESCRIPTION

PROJECT NOAA - Bristol Bay

STATION 70/87 B　　LOGGED BY E. Johnson　　DATE 15Jan82

LOCATION 55°26.4'N 163°52.2' W　　LENGTH 68 cm

WATER DEPTH 89 m　　SECTION 1 OF 1

VESSEL Discoverer　　DATE 283 JD 1980

LENGTH 68 cm　　TYPE CORE Vibracore

CENTIMETERS: 0, 10, 20, 30, 40, 50, 60, 70

COLOR	SUB SAMPLE	DESCRIPTION
5y5/2	X	Lt. Olive grey fine sand 0-8 cm:Geotechnical and grain size analysis 7 cm:burrow
5y3/2 & 5g2/1		Olive grey and greenish black fine sand 1 cm:volcanic pebble
5y 3/2		Olive grey medium sand unit 1 cm thick .3 cm clast
5g2/1		Greenish black silty sand with mottling 41 cm shell fragments
5y3/2		Olive grey fine sand 56 cm:shell fragment
NI		Black coarse sand 59 cm:rock and shell fragments, 1 cm average length. One shell fragment appears to be. Cardium (Cerastoderma) ciliatum
5gy4/1		Dark greenish grey fine sand 68 cm:Bottom of core

APPENDIX IV

RESULTS OF LIQUEFACTION ANALYSES

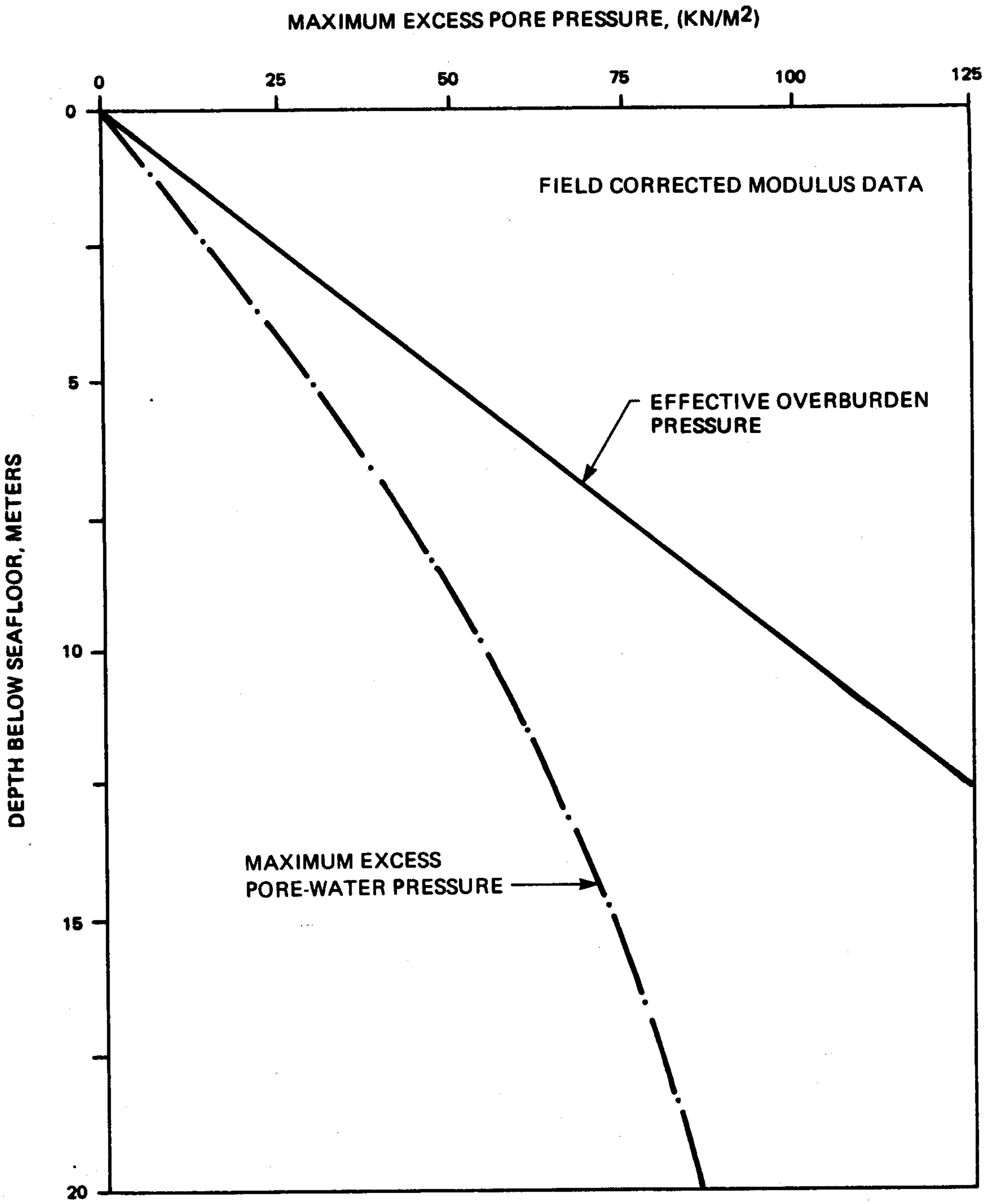

SOIL TYPE SP (1)

EARTHQUAKE SOURCE SUBDUCTION ZONE

EARTHQUAKE RECORD (NORMALIZED TO Amax = 0.16g) CAL TECH A-1

MAXIMUM GROUND ACCELERATION = Amax

CONCLUSION: NO LIQUEFACTION

FIGURE IV-1 MAXIMUM EXCESS PORE PRESSURE RESPONSE CURVE (SP1, SUBDUCTION ZONE, 0.16g)

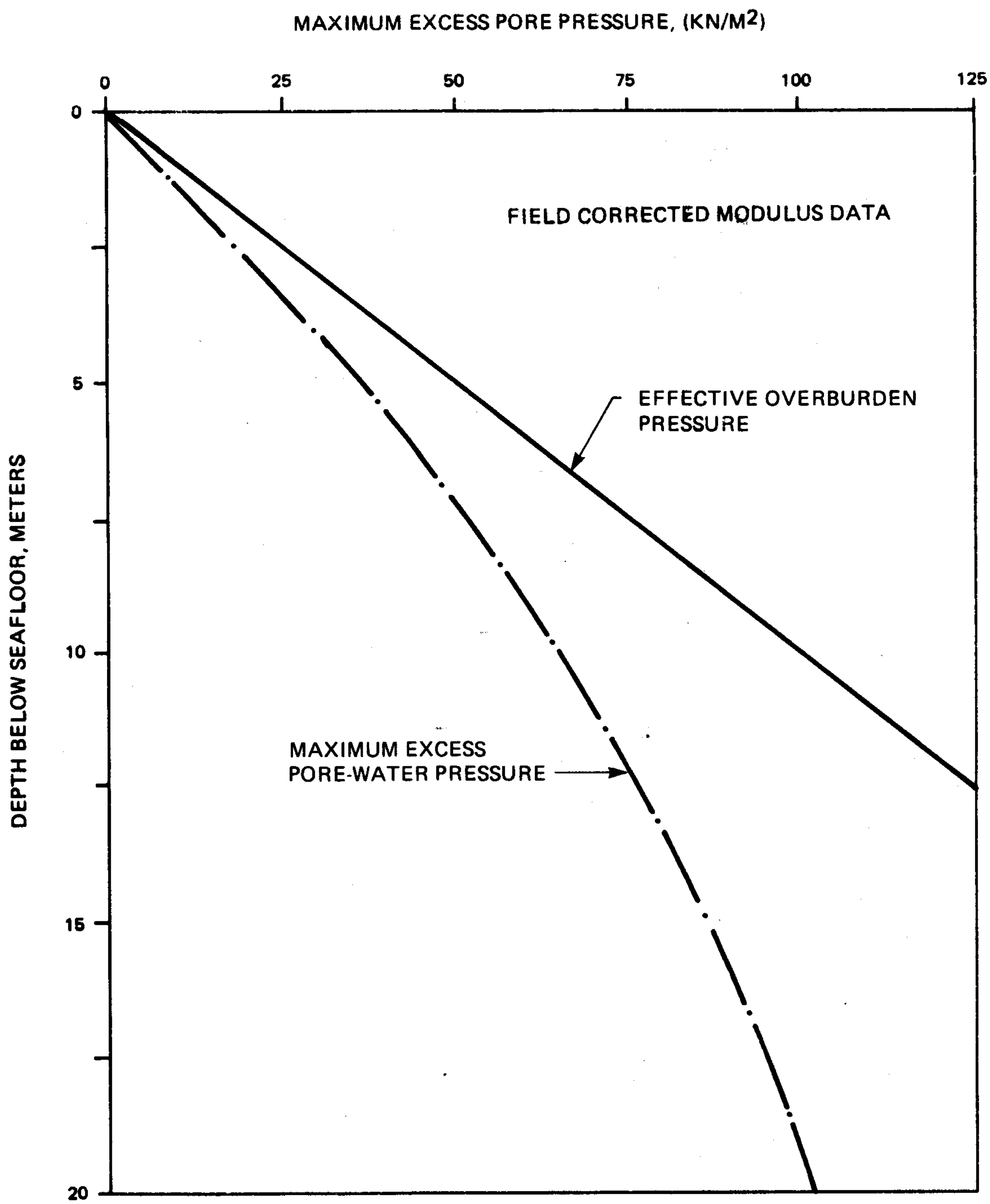

SOIL TYPE SP (1)

EARTHQUAKE SOURCE SUBDUCTION ZONE

EARTHQUAKE RECORD (NORMALIZED TO Amax = 0.19g) CAL TECH A-1

MAXIMUM GROUND ACCELERATION = Amax

CONCLUSION: NO LIQUEFACTION

FIGURE IV-2 MAXIMUM EXCESS PORE PRESSURE RESPONSE CURVE (SP1, SUBDUCTION ZONE, 0.19g)

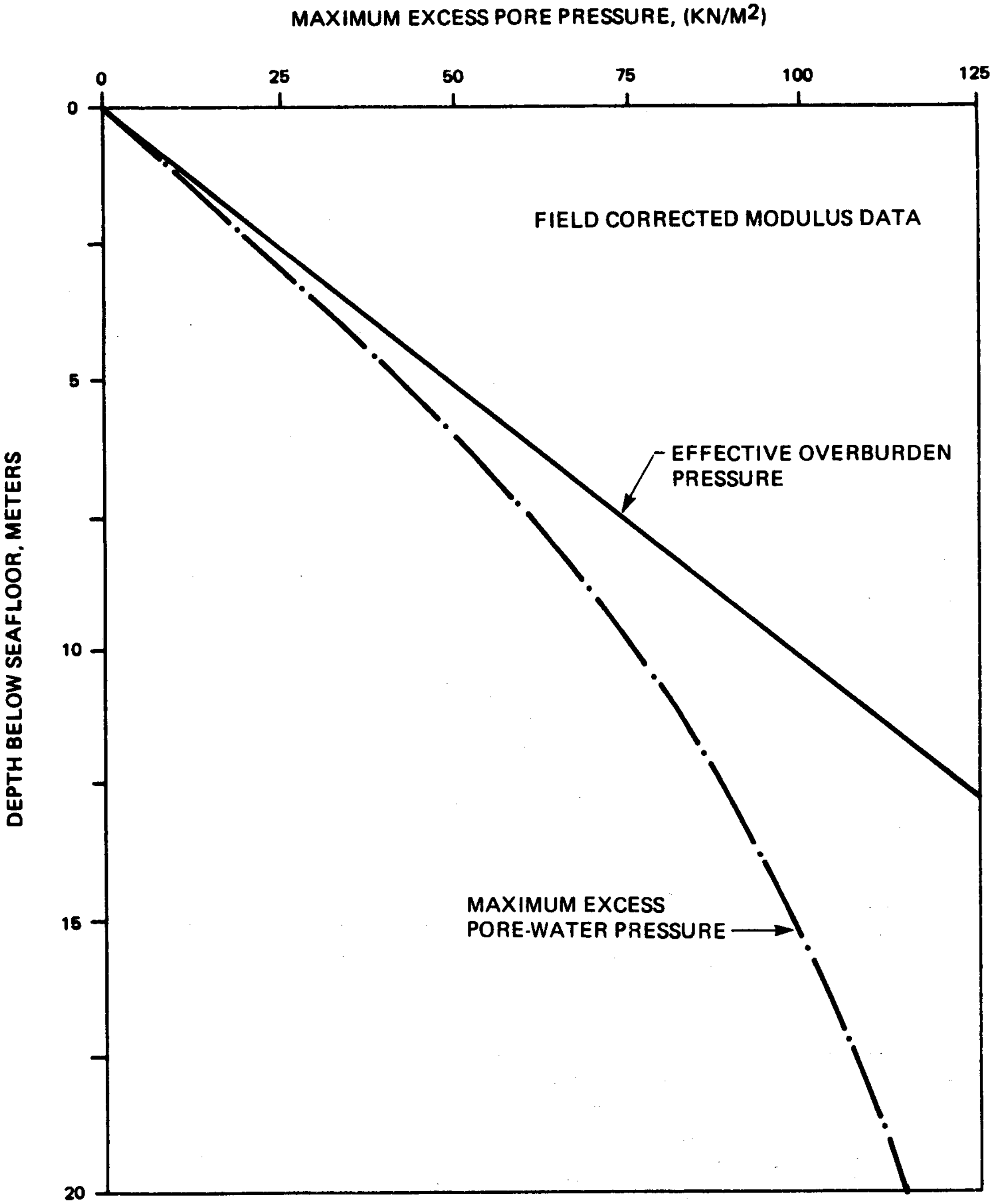

SOIL TYPE SP (1)

EARTHQUAKE SOURCE MAJOR GRABENS

EARTHQUAKE RECORD (NORMALIZED TO Amax = 0.4g) TAFT 1952

MAXIMUM GROUND ACCELERATION = Amax

CONCLUSION: NO LIQUEFACTION

FIGURE IV-3 MAXIMUM EXCESS PORE PRESSURE RESPONSE CURVE (SP1, MAJOR GRABENS, 0.4g)

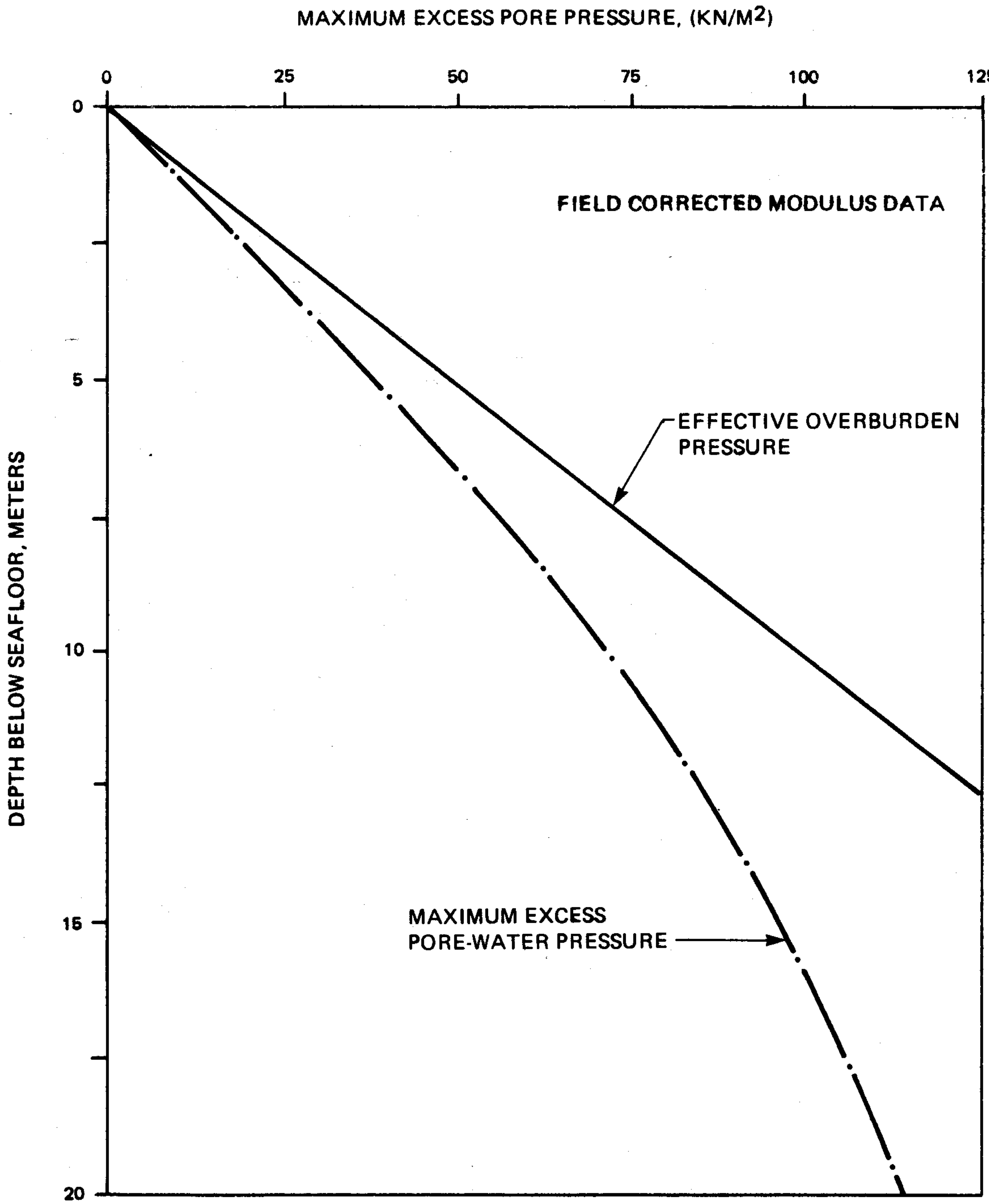

SOIL TYPE SP (1)

EARTHQUAKE SOURCE MAJOR GRABENS

EARTHQUAKE RECORD (NORMALIZED TO Amax = 0.4g) EL CENTRO 1940

MAXIMUM GROUND ACCELERATION = Amax

CONCLUSION: NO LIQUEFACTION

FIGURE IV-4 MAXIMUM EXCESS PORE PRESSURE RESPONSE CURVE (SP1, MAJOR GRABENS, 0.4g)

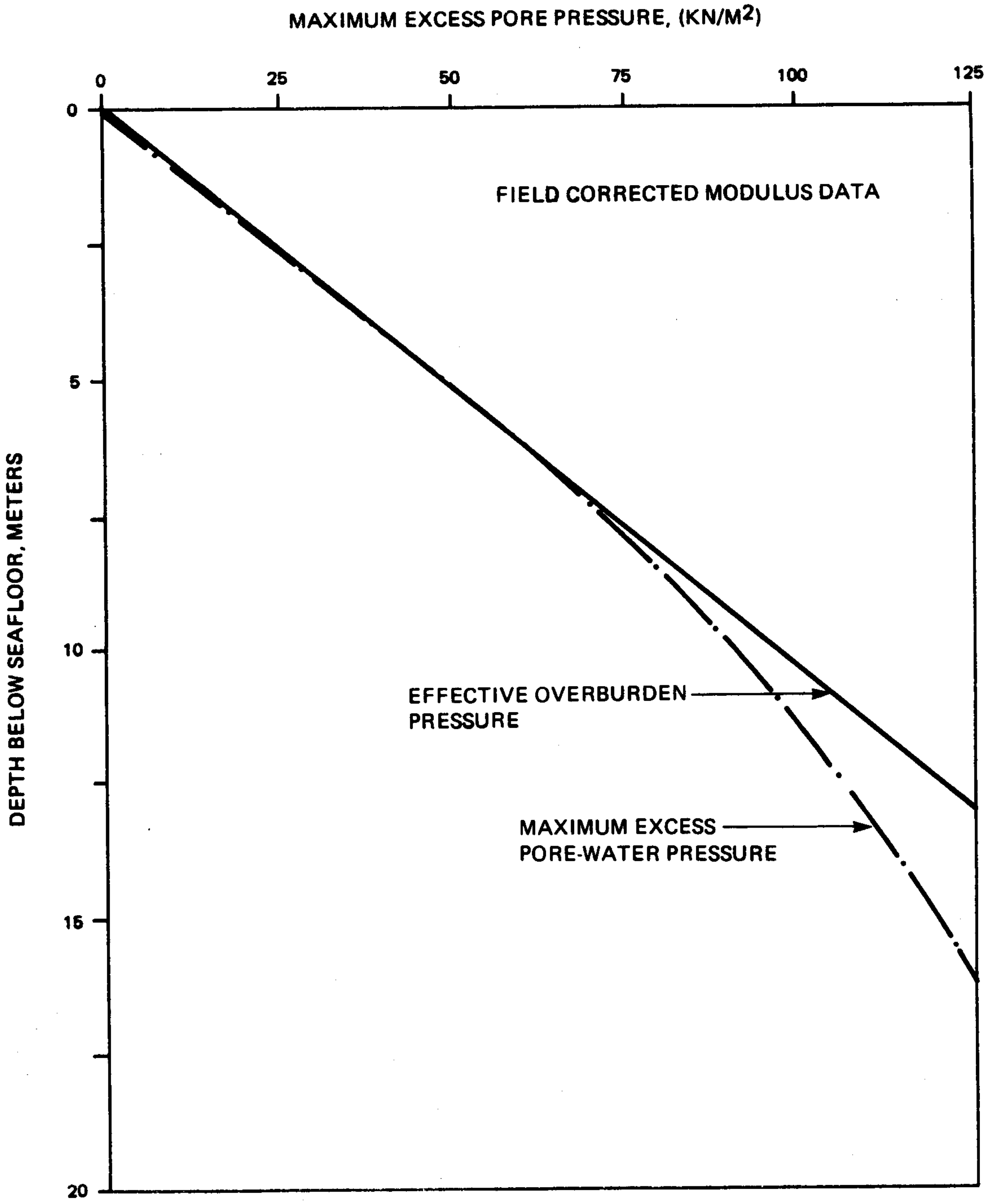

SOIL TYPE SP (1)

EARTHQUAKE SOURCE MAJOR GRABENS

EARTHQUAKE RECORD (NORMALIZED TO Amax = 0.5g) TAFT 1952

MAXIMUM GROUND ACCELERATION = Amax

CONCLUSION: LIQUEFACTION TO 8 M

FIGURE IV-5 MAXIMUM EXCESS PORE PRESSURE RESPONSE CURVE (SP1, MAJOR GRABENS, 0.5g)

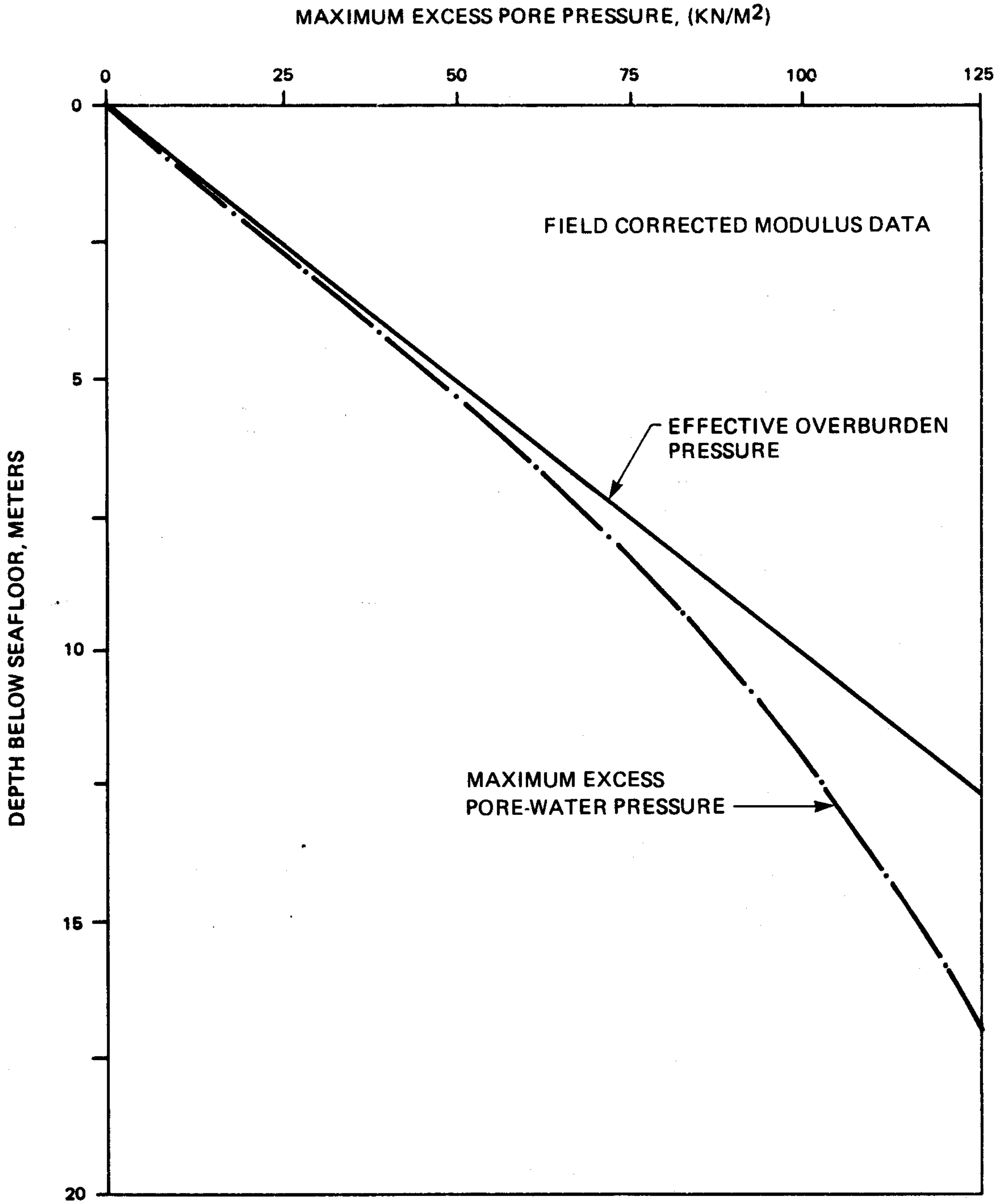

SOIL TYPE SP (1)

EARTHQUAKE SOURCE MAJOR GRABENS

EARTHQUAKE RECORD (NORMALIZED TO Amax = 0.5g) EL CENTRO 1940

MAXIMUM GROUND ACCELERATION = Amax

CONCLUSION: NO LIQUEFACTION

FIGURE IV-6 MAXIMUM EXCESS PORE PRESSURE RESPONSE CURVE (SP1, MAJOR GRABENS, 0.5g)

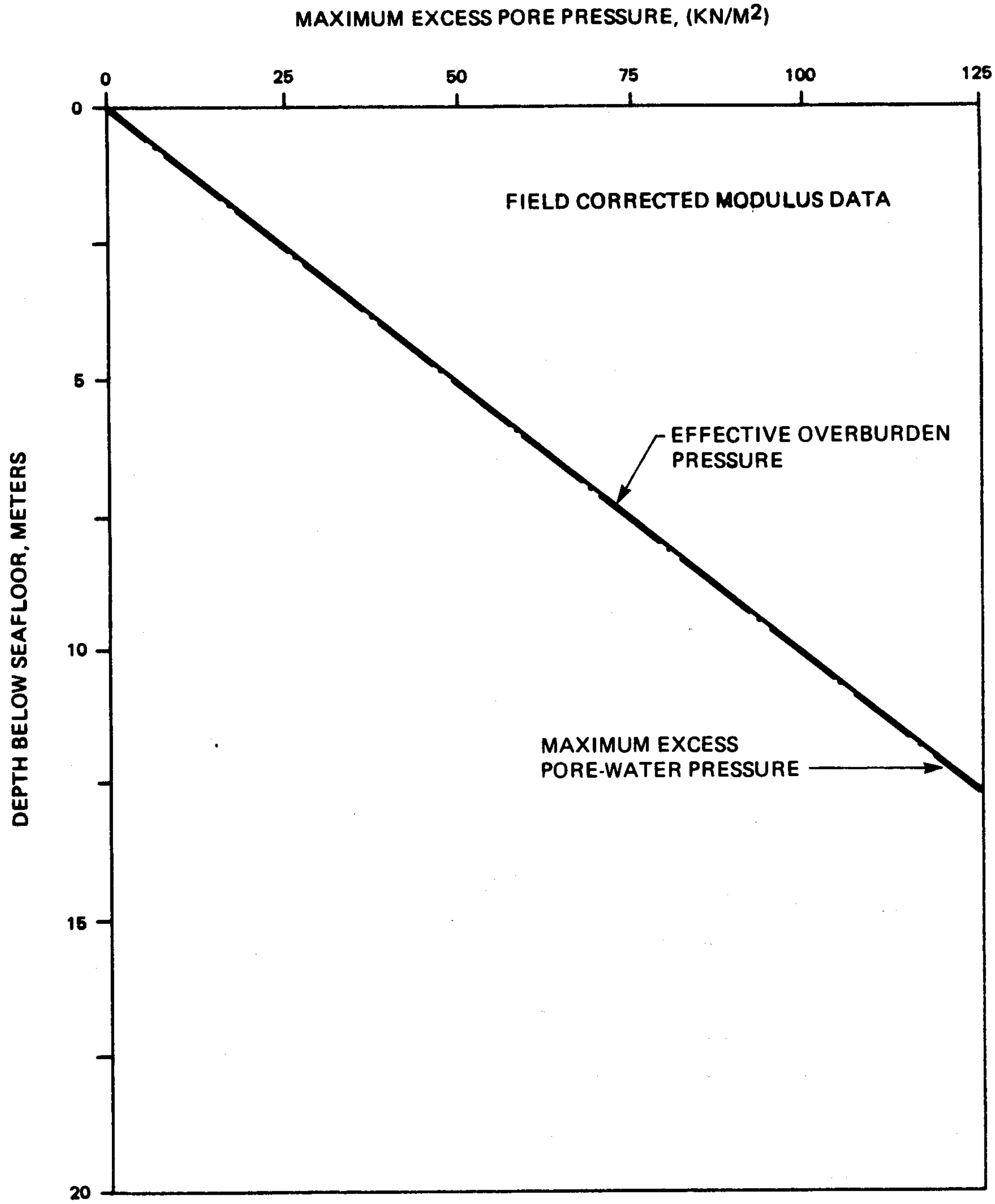

SOIL TYPE SP (1)

EARTHQUAKE SOURCE MAJOR GRABENS

EARTHQUAKE RECORD (NORMALIZED TO Amax = 0.7g) TAFT 1952

MAXIMUM GROUND ACCELERATION = Amax

CONCLUSION: LIQUEFACTION TO 12 M

FIGURE IV-7 MAXIMUM EXCESS PORE PRESSURE RESPONSE CURVE (SP1, MAJOR GRABENS, 0.7g)

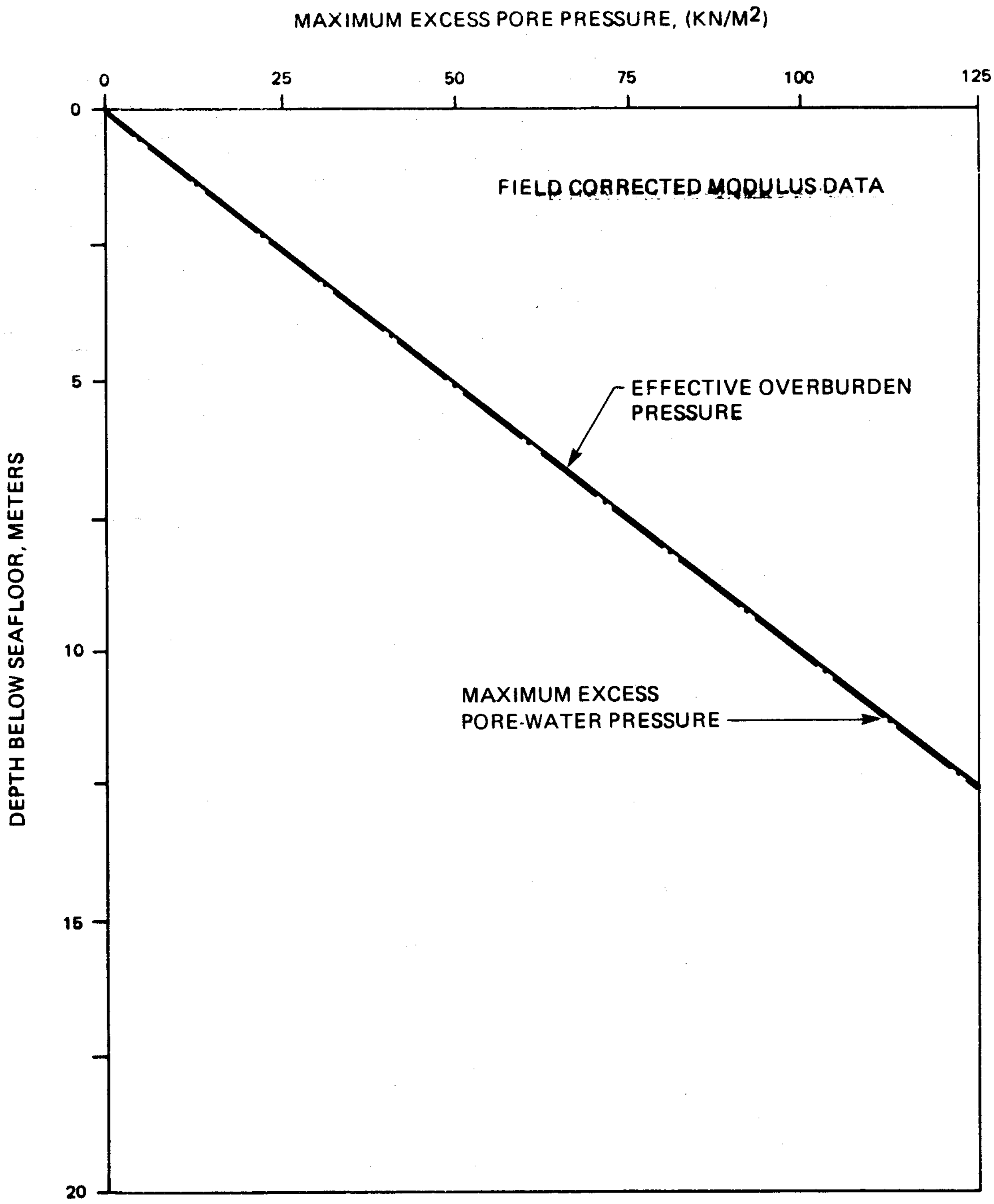

SOIL TYPE SP (1)

EARTHQUAKE SOURCE MAJOR GRABENS

EARTHQUAKE RECORD (NORMALIZED TO Amax = 0.7g) EL CENTRO 1940

MAXIMUM GROUND ACCELERATION = Amax

CONCLUSION: LIQUEFACTION TO 12 M

FIGURE IV-8 MAXIMUM EXCESS PORE PRESSURE RESPONSE CURVE (SP1, MAJOR GRABENS, 0.7g)

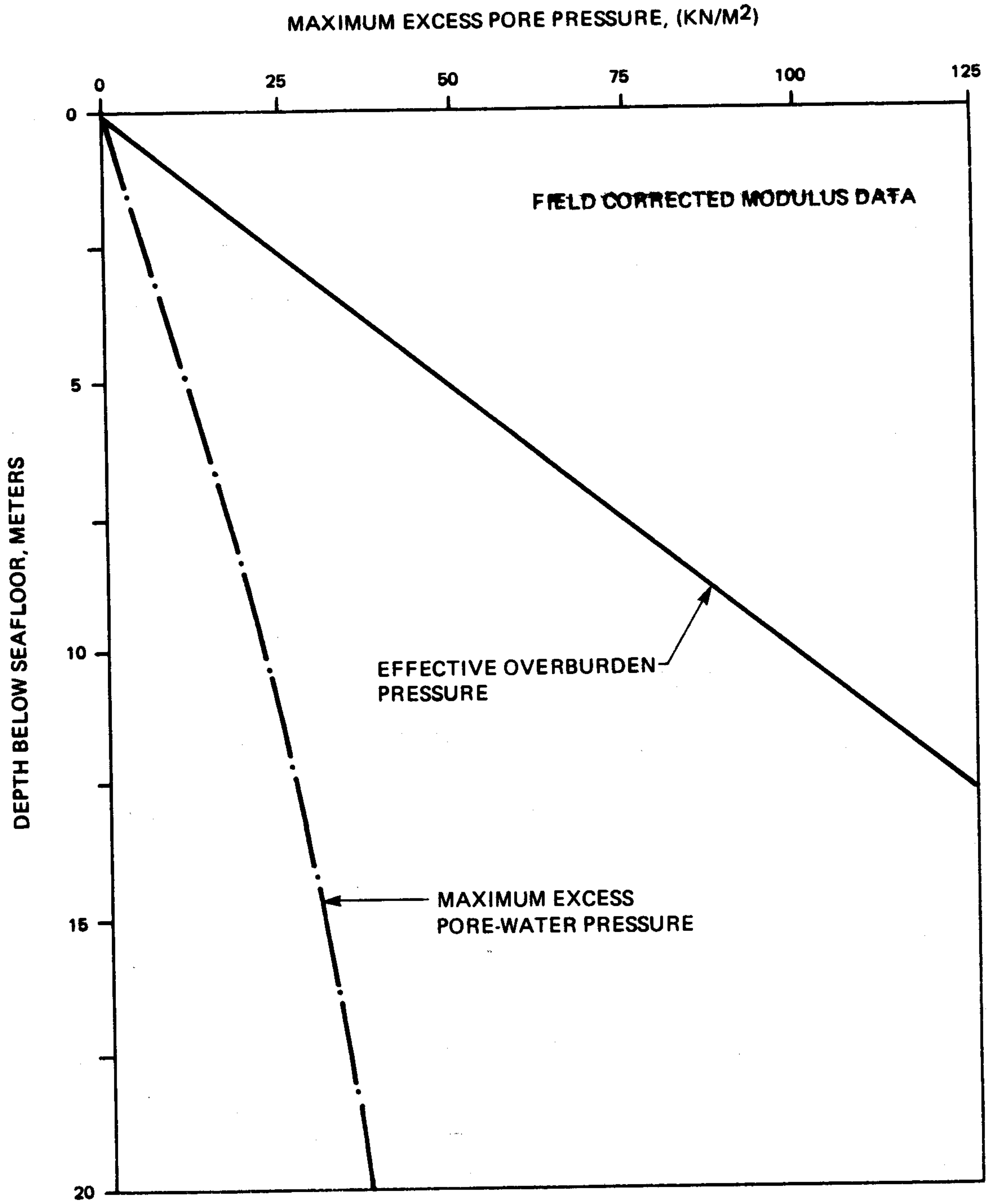

SOIL TYPE SP (1)

EARTHQUAKE SOURCE BACK ARC FAULTS

EARTHQUAKE RECORD (NORMALIZED TO Amax = 0.3g) EL CENTRO 1979

MAXIMUM GROUND ACCELERATION = Amax

CONCLUSION: NO LIQUEFACTION

FIGURE IV-9 MAXIMUM EXCESS PORE PRESSURE RESPONSE CURVE (SP1, BACK ARC FAULTS, 0.3g)

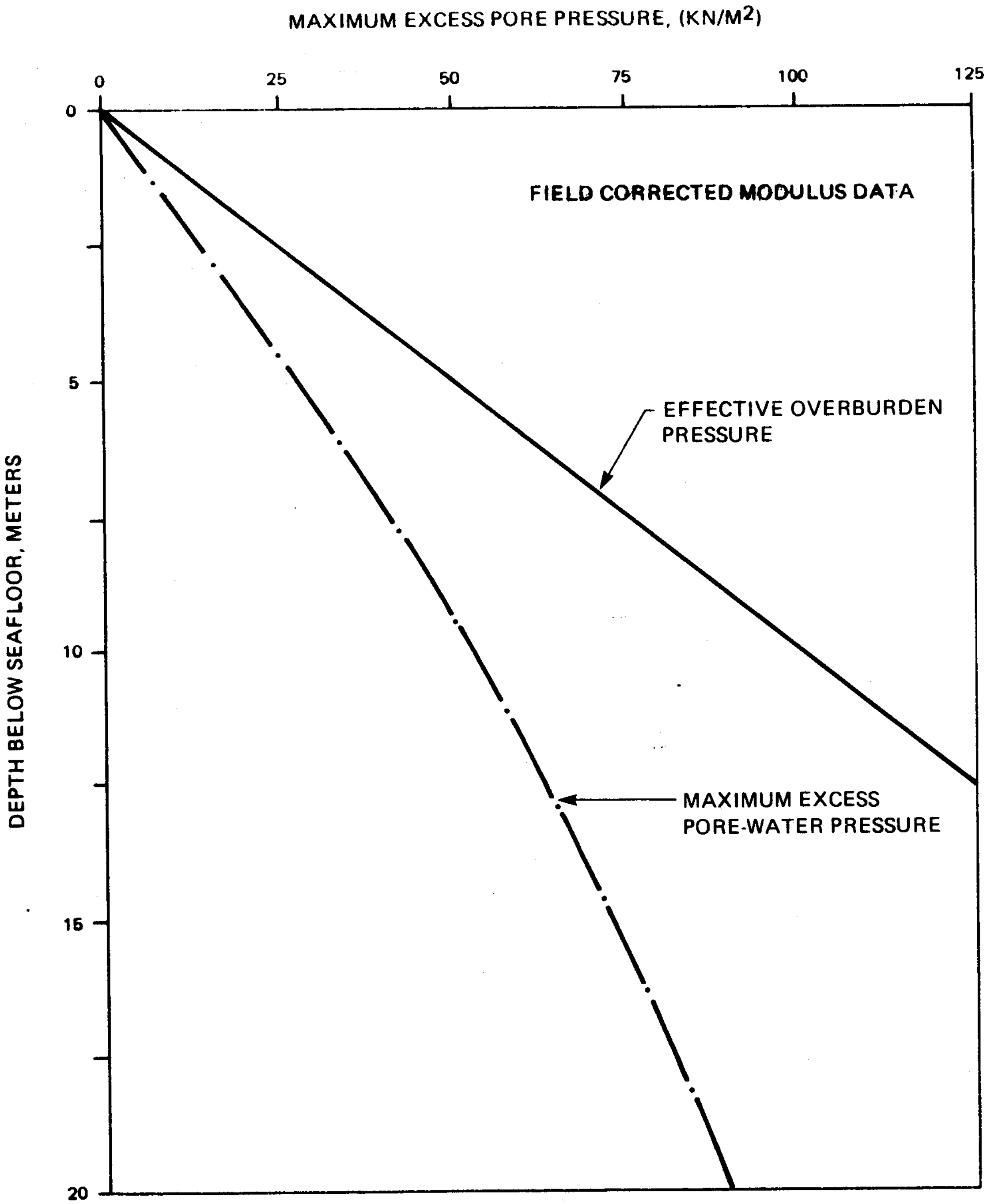

SOIL TYPE SP (1)

EARTHQUAKE SOURCE BACK ARC FAULTS

EARTHQUAKE RECORD (NORMALIZED TO Amax = 0.6g) EL CENTRO 1979

MAXIMUM GROUND ACCELERATION = Amax

CONCLUSION: NO LIQUEFACTION

FIGURE IV-10 MAXIMUM EXCESS PORE PRESSURE RESPONSE CURVE (SP1, BACK ARC FAULTS, 0.6g)

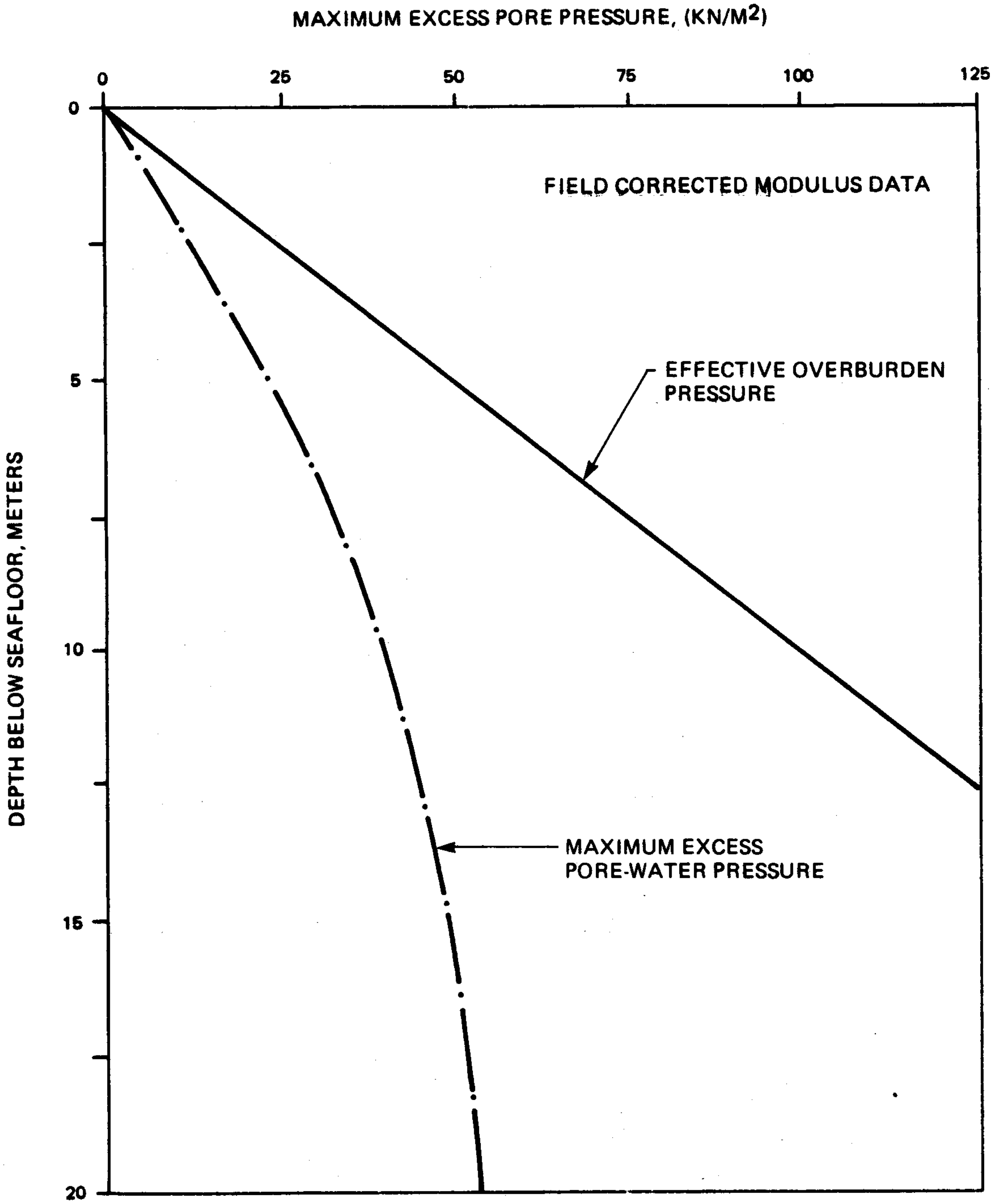

SOIL TYPE SP (1)

EARTHQUAKE SOURCE ALEUTIAN ARC

EARTHQUAKE RECORD (NORMALIZED TO Amax = 0.4g) PARKFIELD 1966

MAXIMUM GROUND ACCELERATION = Amax

CONCLUSION: NO LIQUEFACTION

FIGURE IV-11 MAXIMUM EXCESS PORE PRESSURE RESPONSE CURVE (SP1, ALEUTIAN ARC, 0.4g)

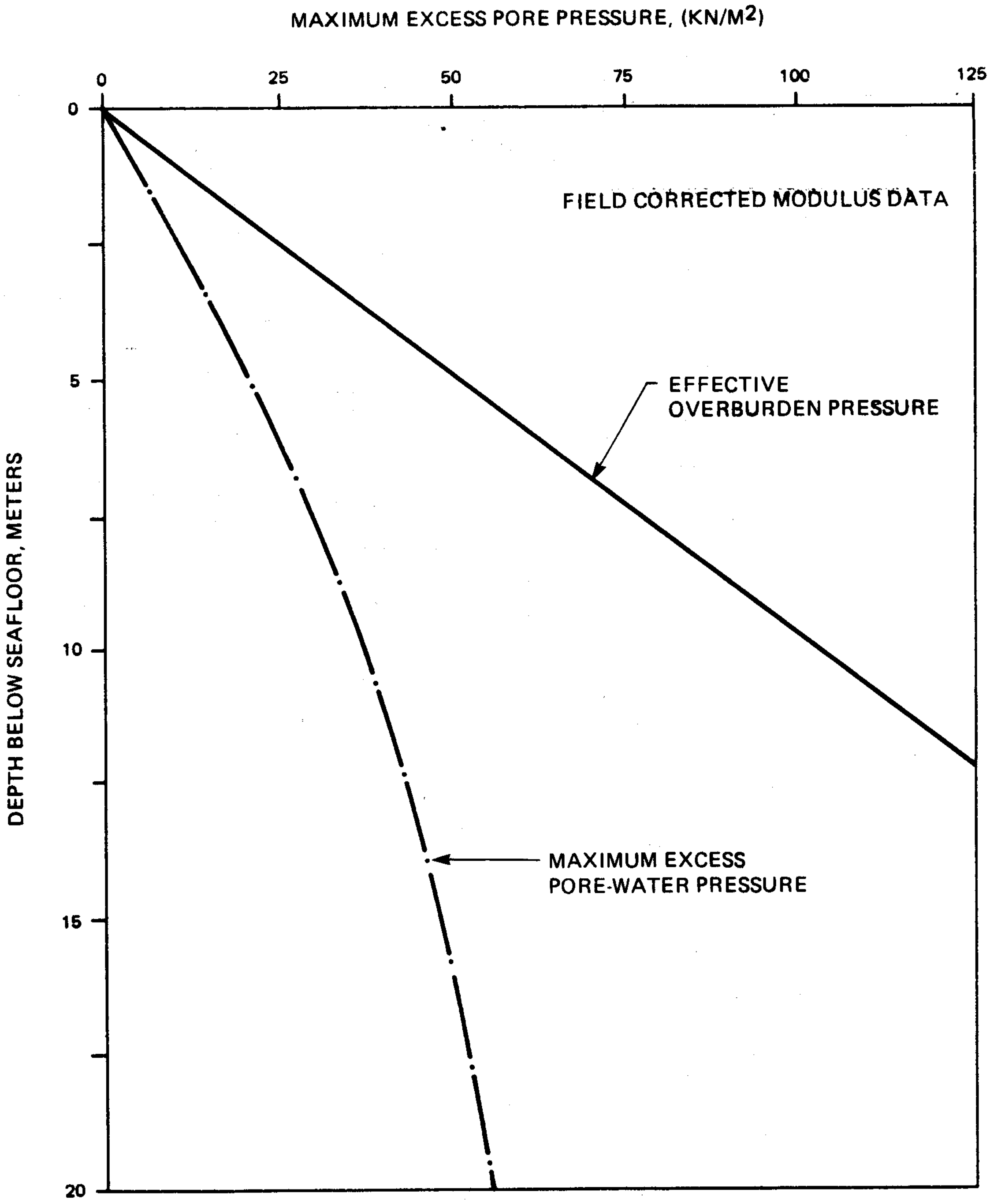

SOIL TYPE SP (2)

EARTHQUAKE SOURCE SUBDUCTION ZONE

EARTHQUAKE RECORD (NORMALIZED TO Amax = 0.16g) CAL TECH A-1

MAXIMUM GROUND ACCELERATION = Amax

CONCLUSION: NO LIQUEFACTION

FIGURE IV-12 MAXIMUM EXCESS PORE PRESSURE RESPONSE CURVE (SP2, SUBDUCTION ZONE, 0.16g)

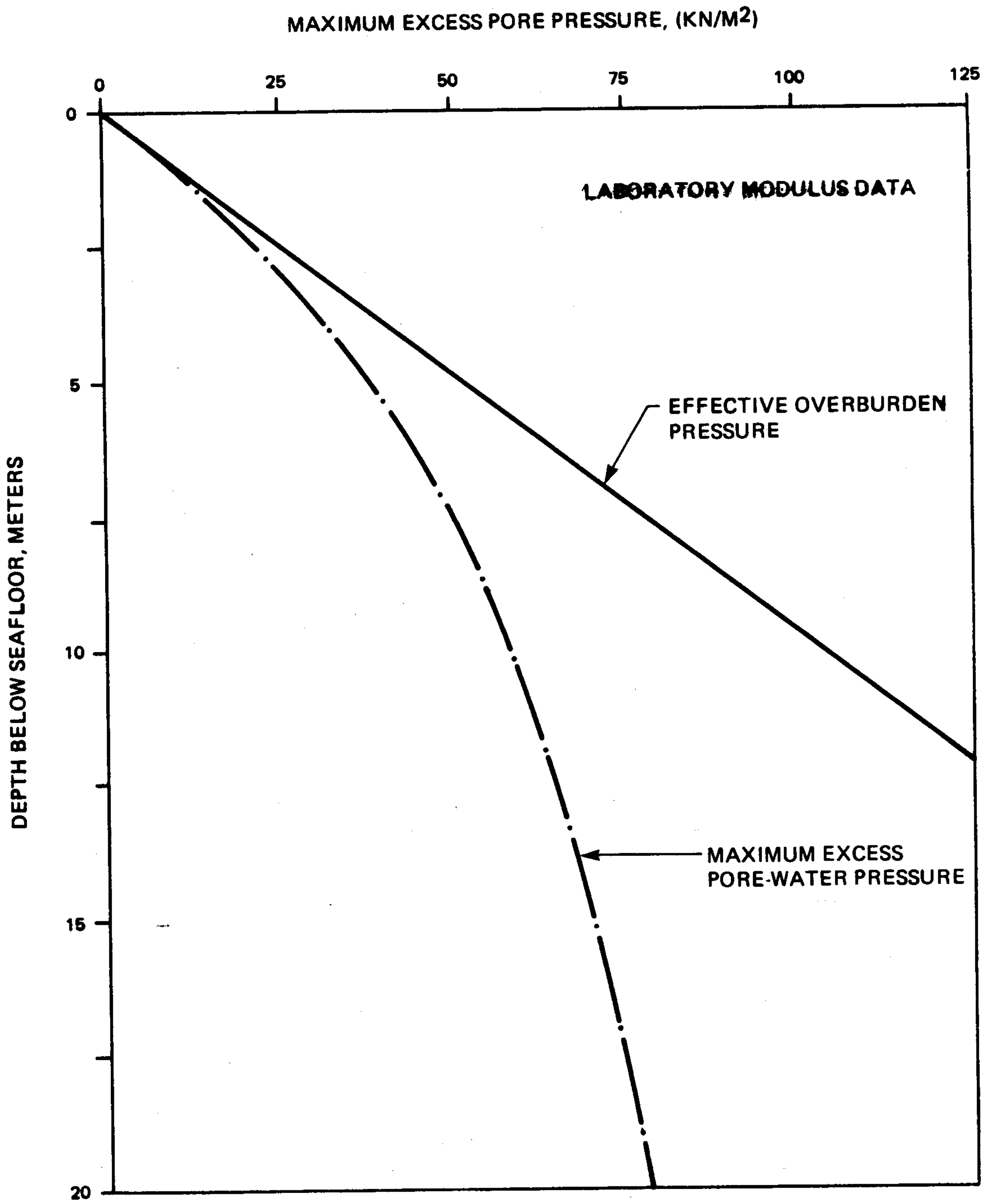

SOIL TYPE SP (2)

EARTHQUAKE SOURCE SUBDUCTION ZONE

EARTHQUAKE RECORD (NORMALIZED TO Amax = 0.16g) CAL TECH A-1

MAXIMUM GROUND ACCELERATION = Amax

CONCLUSION: NO LIQUEFACTION

FIGURE IV-13 MAXIMUM EXCESS PORE PRESSURE RESPONSE CURVE (SP2, SUBDUCTION ZONE, 0.16g)

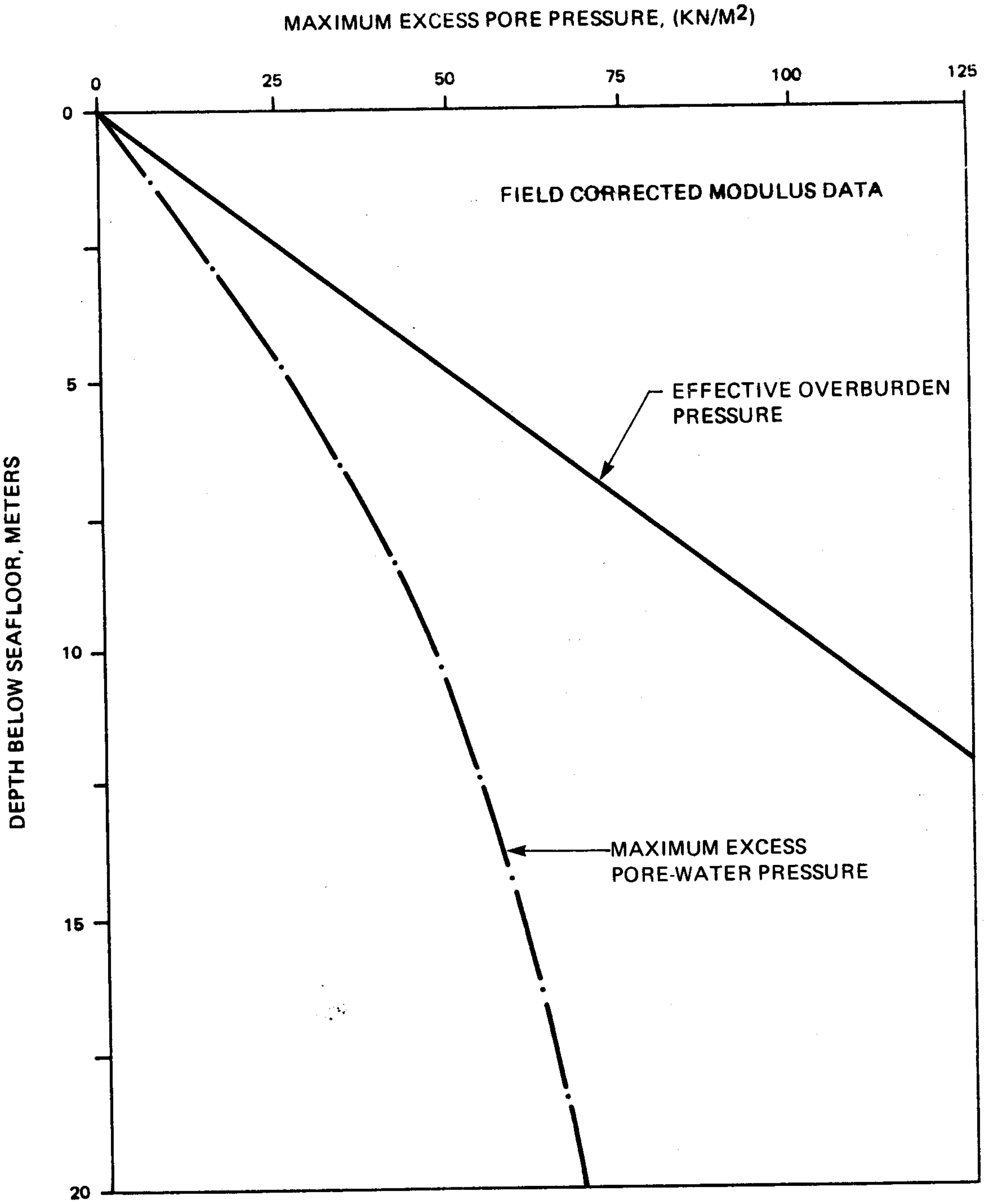

SOIL TYPE SP (2)

EARTHQUAKE SOURCE SUBDUCTION ZONE

EARTHQUAKE RECORD (NORMALIZED TO Amax = 0.19g) CAL TECH A-1

MAXIMUM GROUND ACCELERATION = Amax

CONCLUSION: NO LIQUEFACTION

FIGURE IV-14 MAXIMUM EXCESS PORE PRESSURE RESPONSE CURVE
(SP2, SUBDUCTION ZONE, 0.19g)

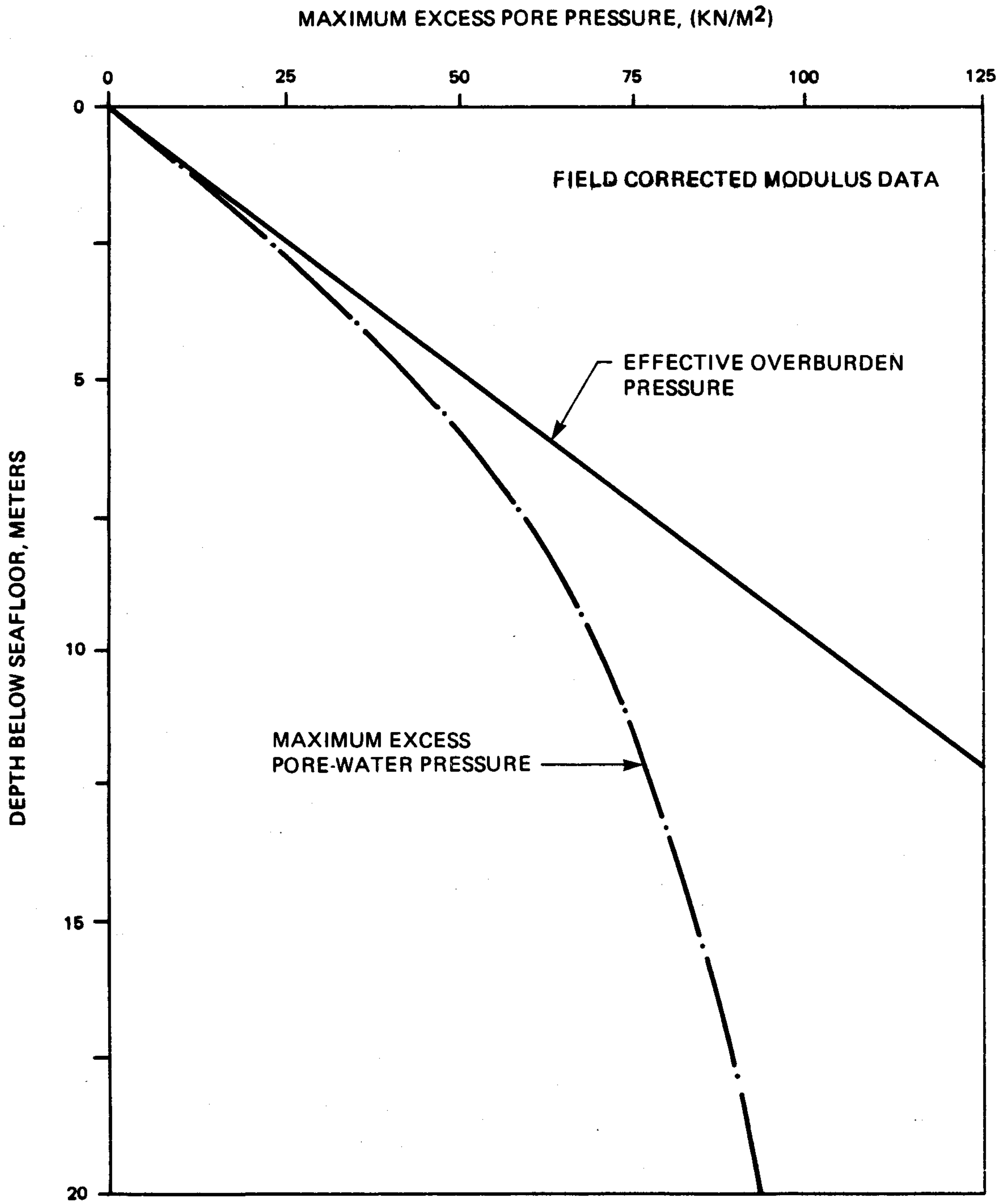

SOIL TYPE SP (2)

EARTHQUAKE SOURCE MAJOR GRABENS

EARTHQUAKE RECORD (NORMALIZED TO Amax = 0.4g) TAFT 1952

MAXIMUM GROUND ACCELERATION = Amax

CONCLUSION: NO LIQUEFACTION

FIGURE IV-15 MAXIMUM EXCESS PORE PRESSURE RESPONSE CURVE (SP2, MAJOR GRABENS, 0.4g)

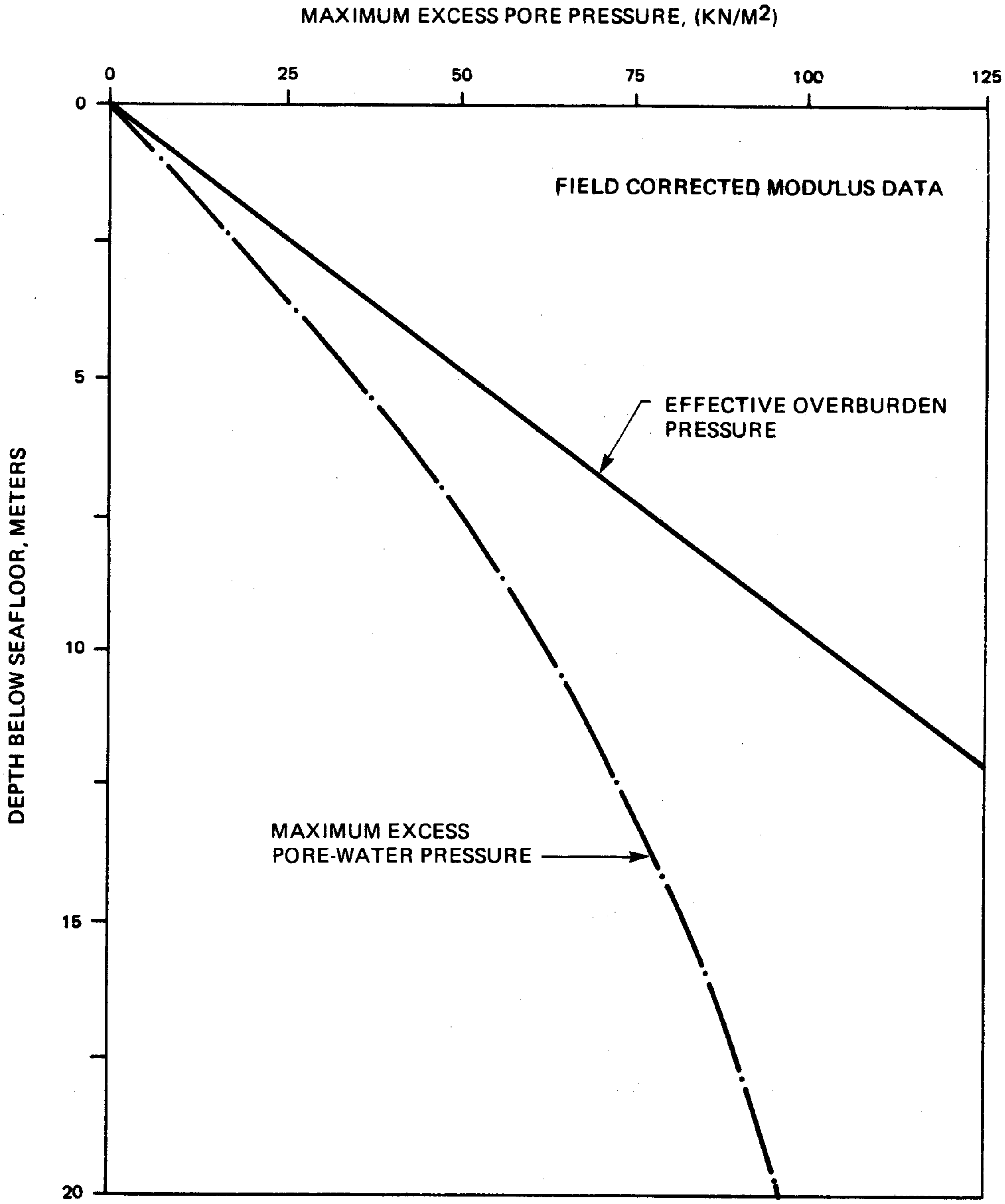

SOIL TYPE SP (2)

EARTHQUAKE SOURCE MAJOR GRABENS

EARTHQUAKE RECORD (NORMALIZED TO Amax = 0.4g) EL CENTRO 1940

MAXIMUM GROUND ACCELERATION = Amax

CONCLUSION: NO LIQUEFACTION

FIGURE IV-16 MAXIMUM EXCESS PORE PRESSURE RESPONSE CURVE (SP2, MAJOR GRABENS, 0.4g)

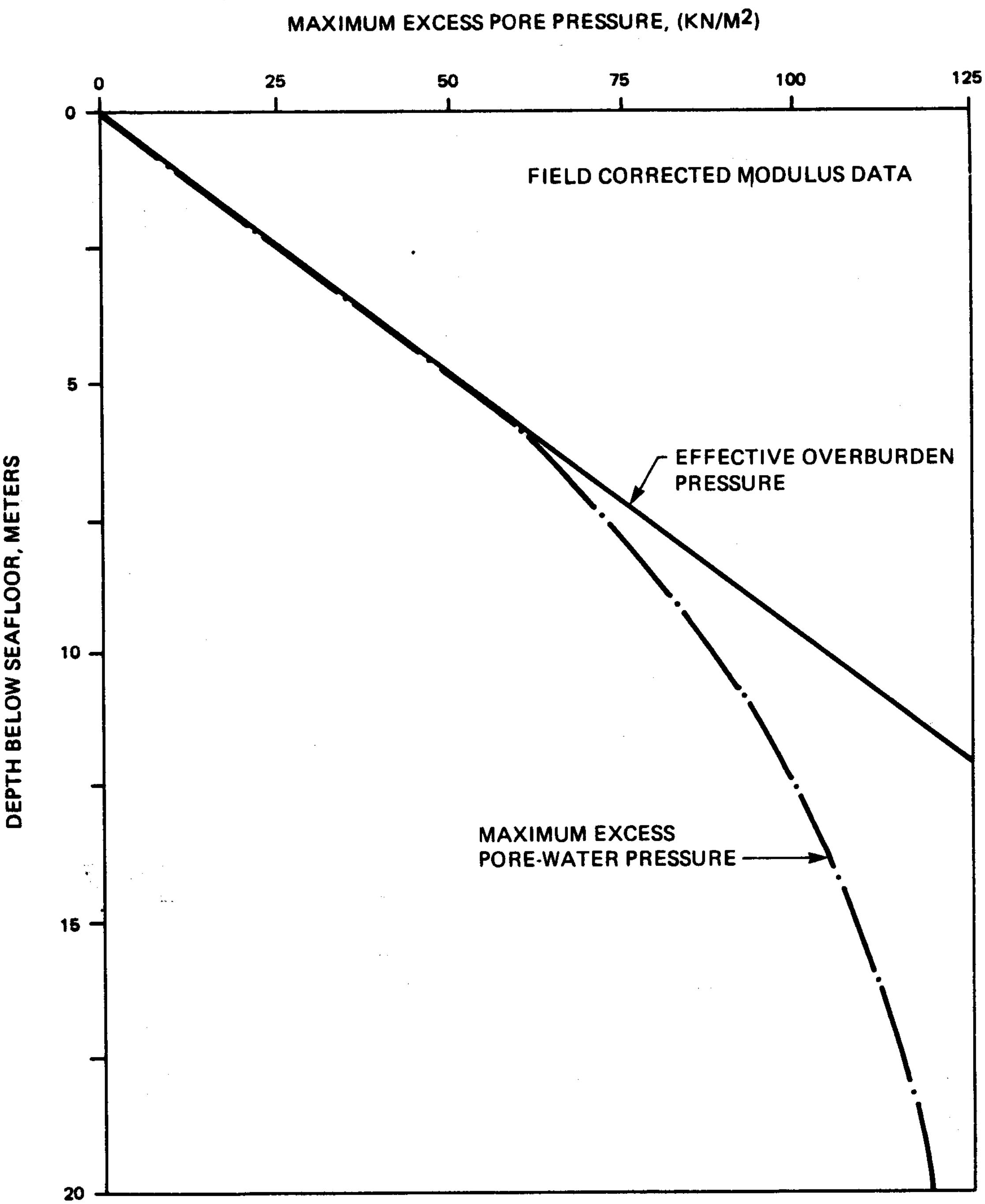

SOIL TYPE SP (2)

EARTHQUAKE SOURCE MAJOR GRABENS

EARTHQUAKE RECORD (NORMALIZED TO Amax = 0.5g) TAFT 1952

MAXIMUM GROUND ACCELERATION = Amax

CONCLUSION: LIQUEFACTION TO 8 M

FIGURE IV-17 MAXIMUM EXCESS PORE PRESSURE RESPONSE CURVE (SP2, MAJOR GRABENS, 0.5g)

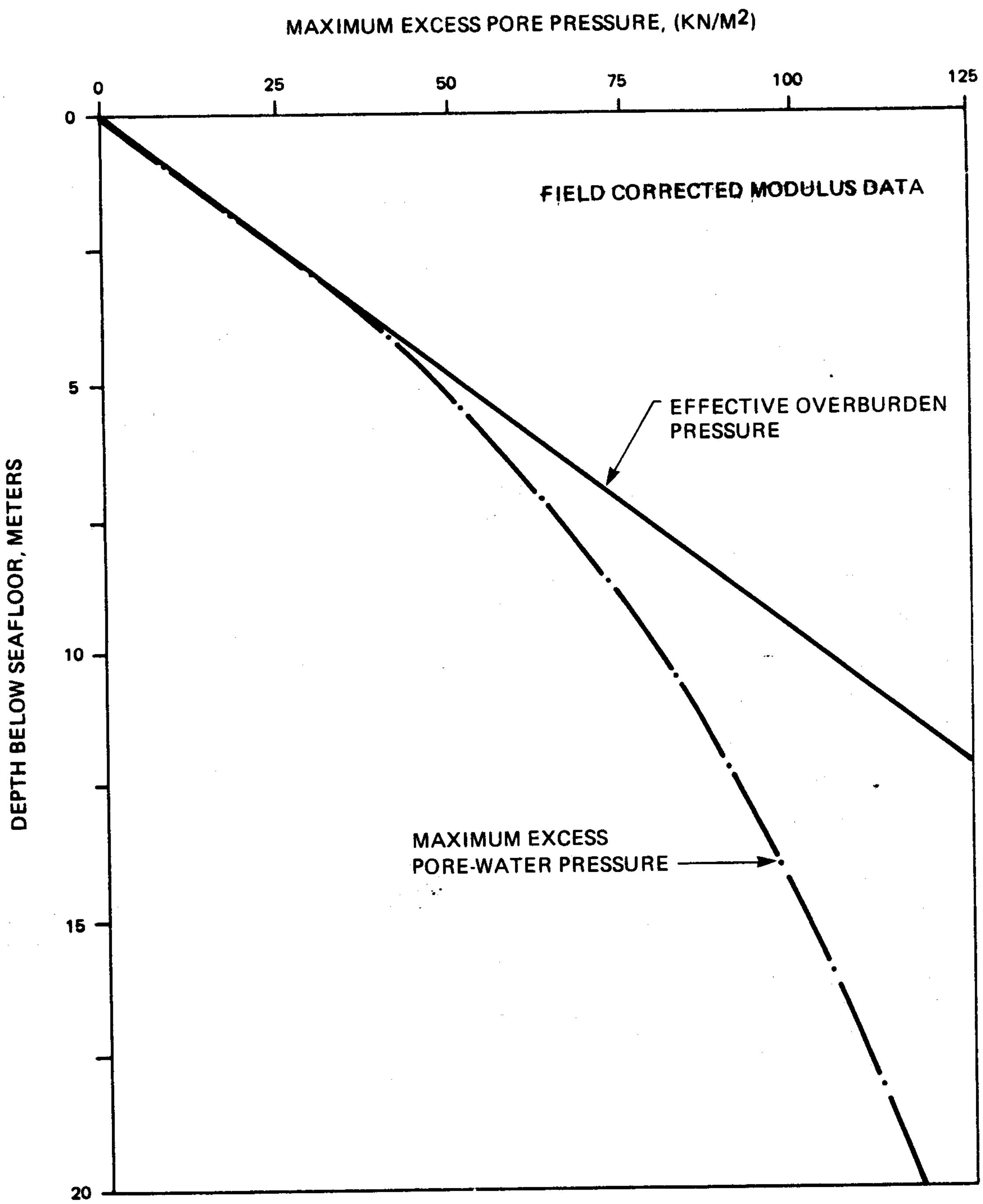

SOIL TYPE SP (2)

EARTHQUAKE SOURCE MAJOR GRABENS

EARTHQUAKE RECORD (NORMALIZED TO Amax = 0.5g) EL CENTRO 1940

MAXIMUM GROUND ACCELERATION = Amax

CONCLUSION: LIQUEFACTION TO 3 M

FIGURE IV-18 MAXIMUM EXCESS PORE PRESSURE RESPONSE CURVE (SP2, MAJOR GRABENS, 0.5g)

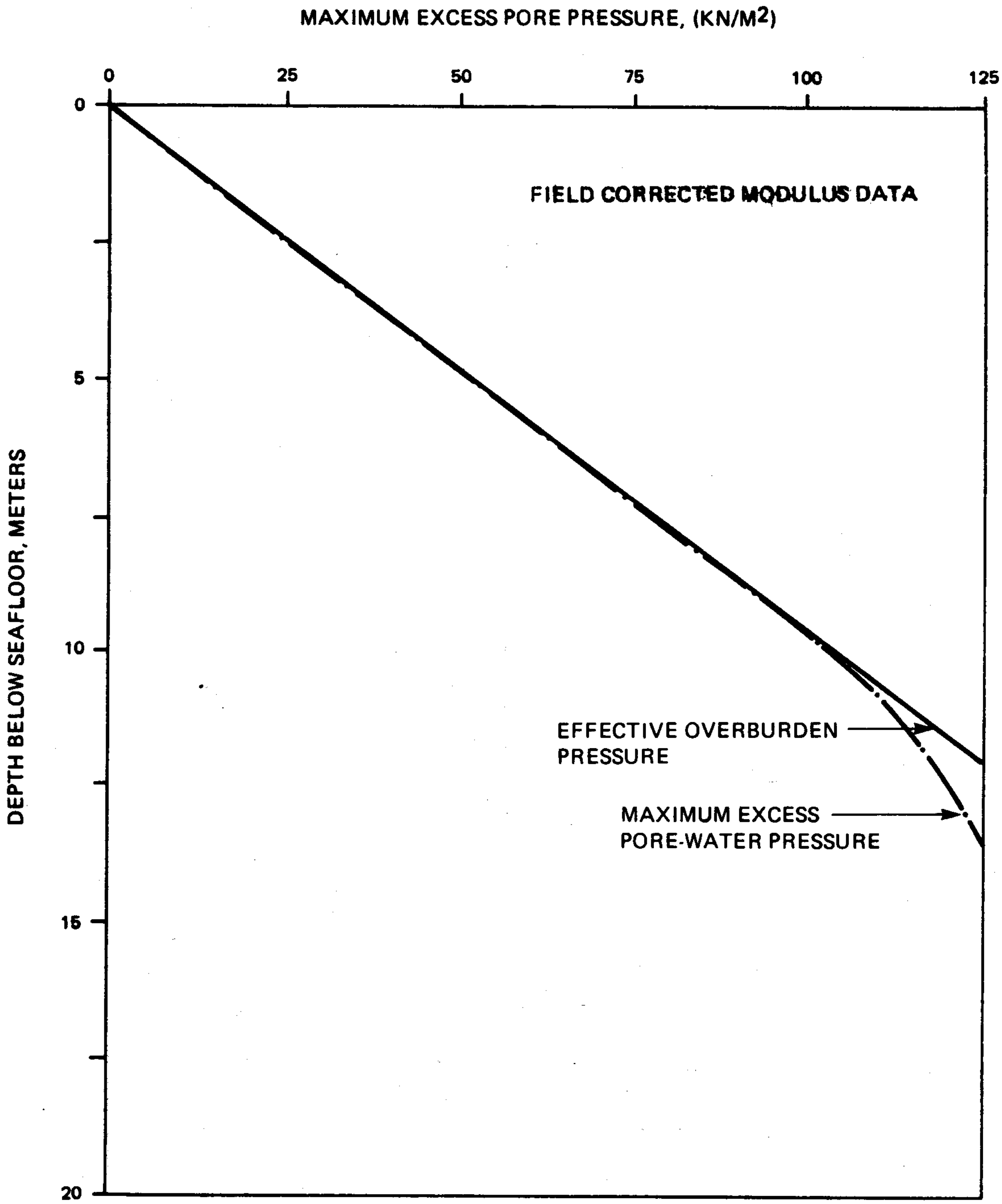

SOIL TYPE SP (2)

EARTHQUAKE SOURCE MAJOR GRABENS

EARTHQUAKE RECORD (NORMALIZED TO Amax = 0.7g) EL CENTRO 1940

MAXIMUM GROUND ACCELERATION = Amax

CONCLUSION: LIQUEFACTION TO 14 M

FIGURE IV-10 MAXIMUM EXCESS PORE PRESSURE RESPONSE CURVE (SP2, MAJOR GRABENS, 0.7g)

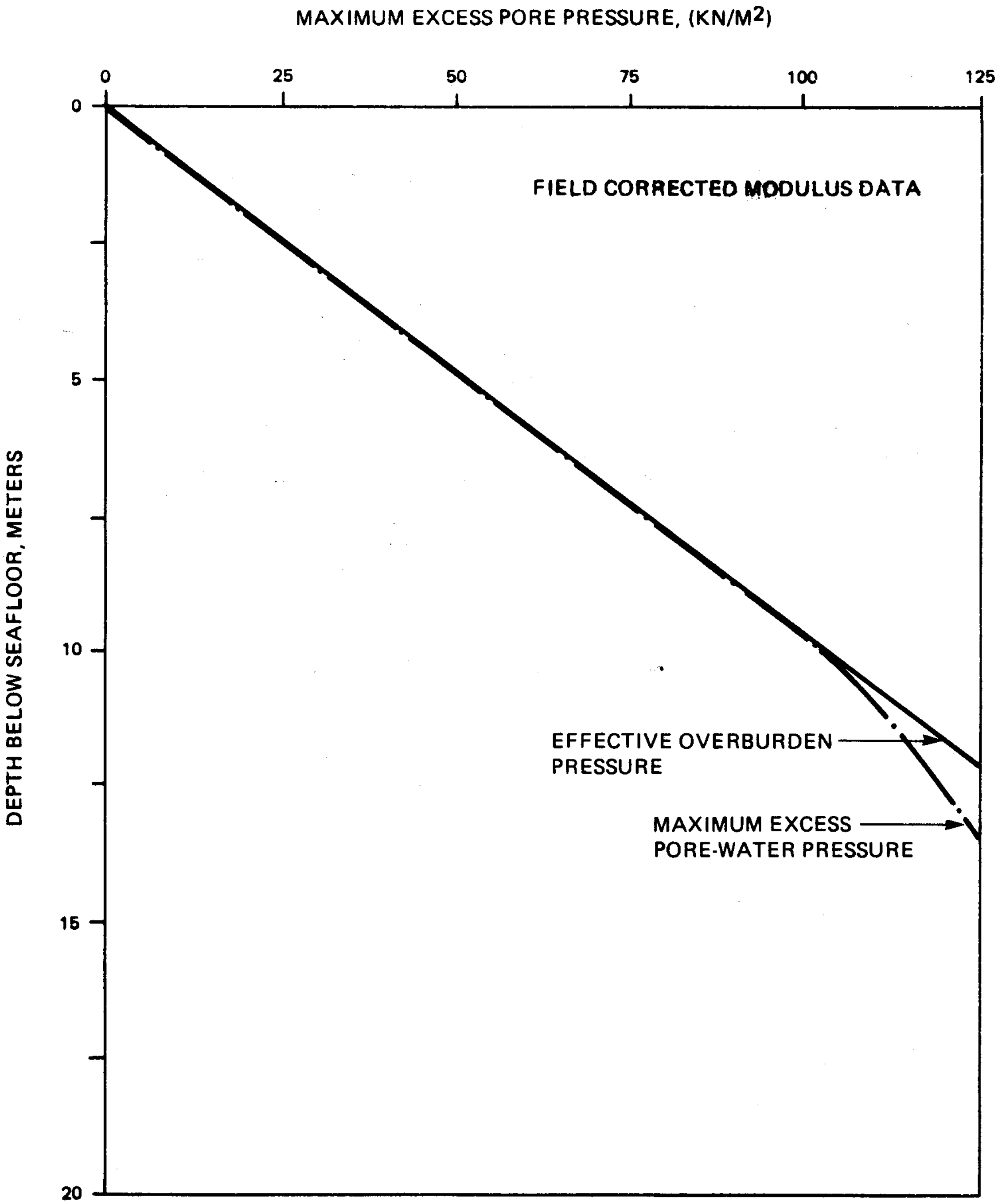

SOIL TYPE SP (2)

EARTHQUAKE SOURCE MAJOR GRABENS

EARTHQUAKE RECORD (NORMALIZED TO Amax = 0.7g) TAFT 1952

MAXIMUM GROUND ACCELERATION = Amax

CONCLUSION: LIQUEFACTION TO 14 M

FIGURE IV-20 MAXIMUM EXCESS PORE PRESSURE RESPONSE CURVE (SP2, MAJOR GRABENS, 0.7g)

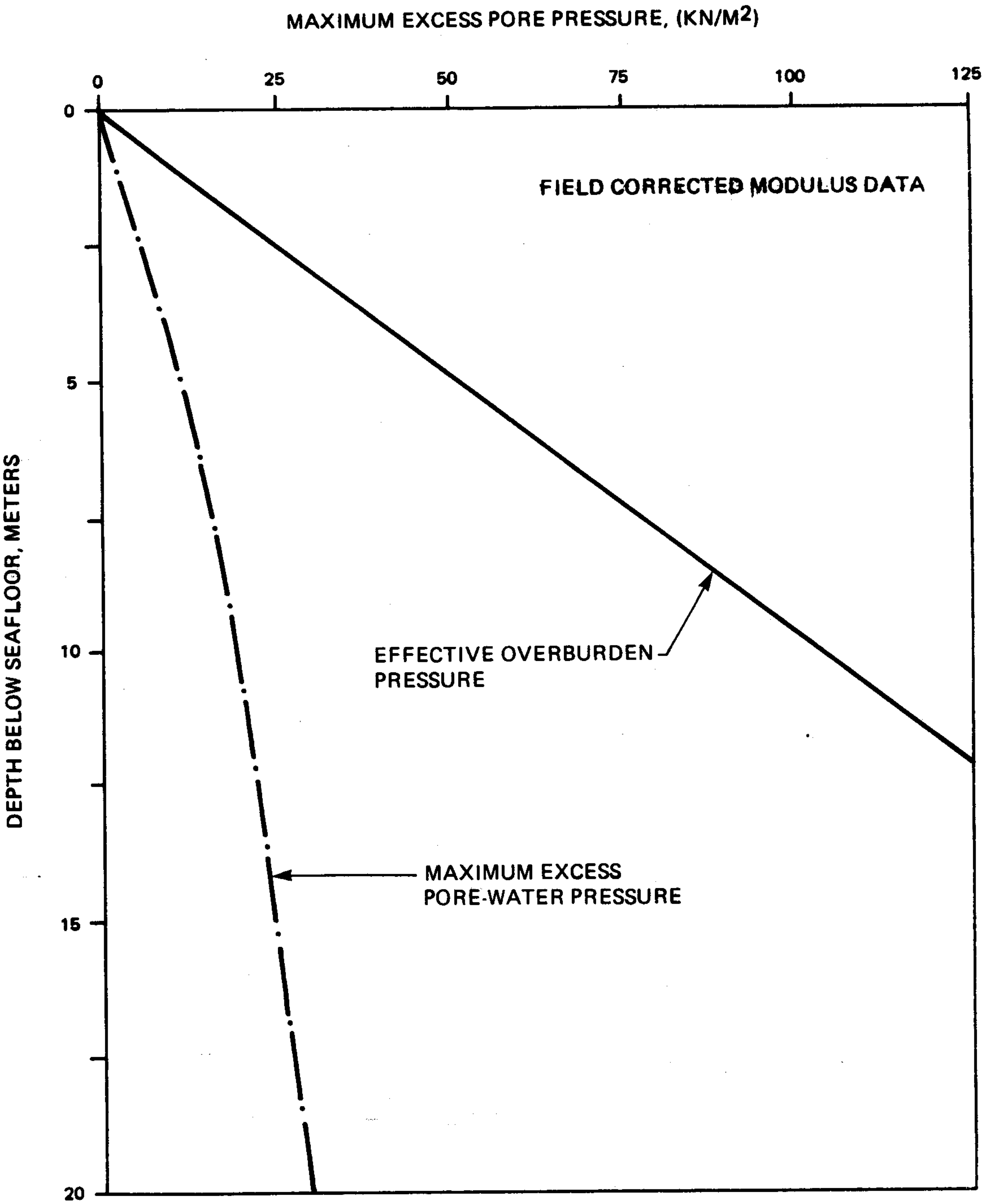

SOIL TYPE SP (2)

EARTHQUAKE SOURCE BACK ARC FAULTS

EARTHQUAKE RECORD (NORMALIZED TO Amax = 0.3g) EL CENTRO 1979

MAXIMUM GROUND ACCELERATION = Amax

CONCLUSION: NO LIQUEFACTION

FIGURE IV-21 MAXIMUM EXCESS PORE PRESSURE RESPONSE CURVE (SP2, BACK ARC FAULTS, 0.3g)

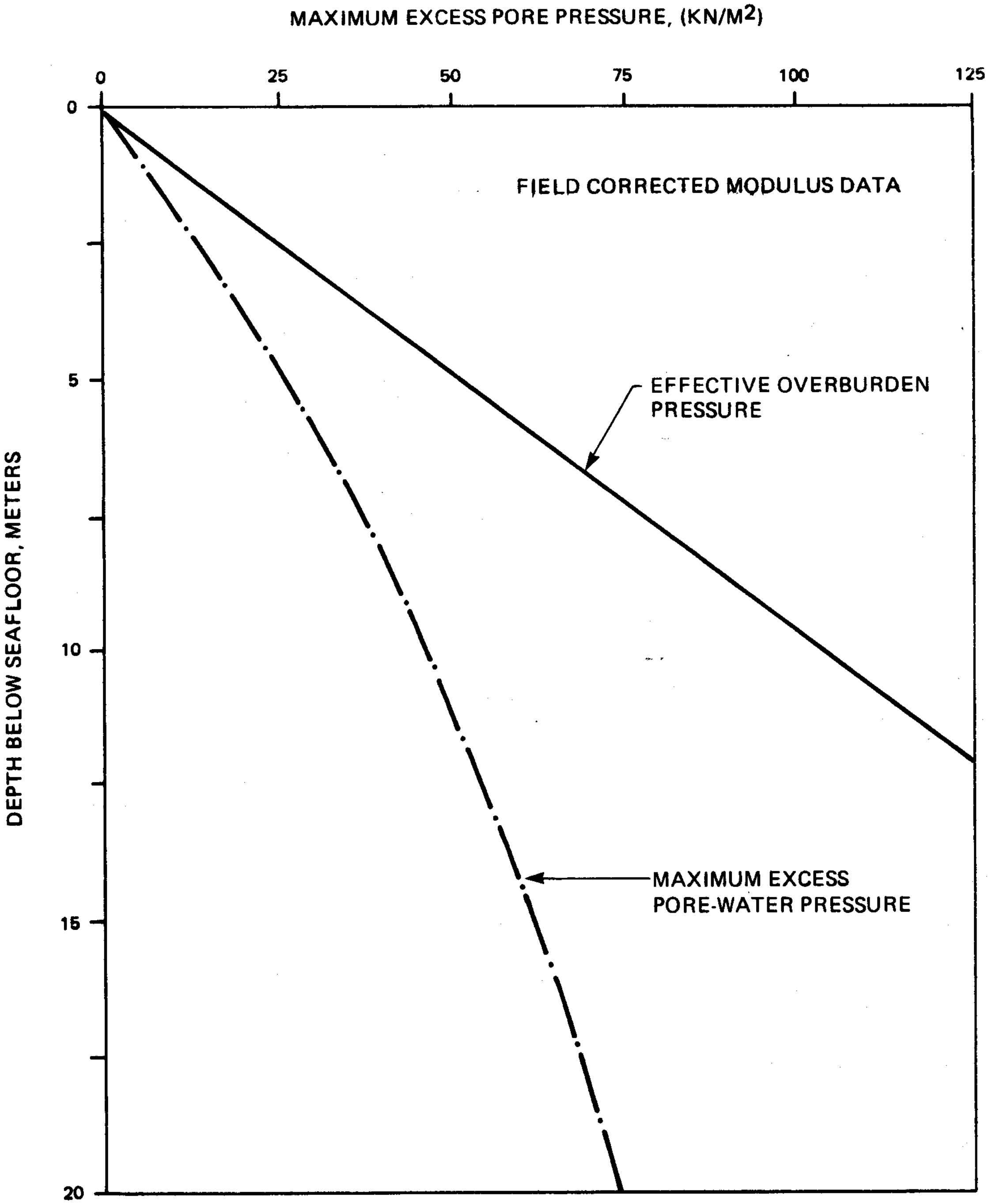

SOIL TYPE SP (2)

EARTHQUAKE SOURCE BACK ARC FAULTS

EARTHQUAKE RECORD (NORMALIZED TO Amax = 0.6g) EL CENTRO 1979

MAXIMUM GROUND ACCELERATION = Amax

CONCLUSION: NO LIQUEFACTION

FIGURE IV-22 MAXIMUM EXCESS PORE PRESSURE RESPONSE CURVE (SP2, BACK ARC FAULTS, 0.6g)

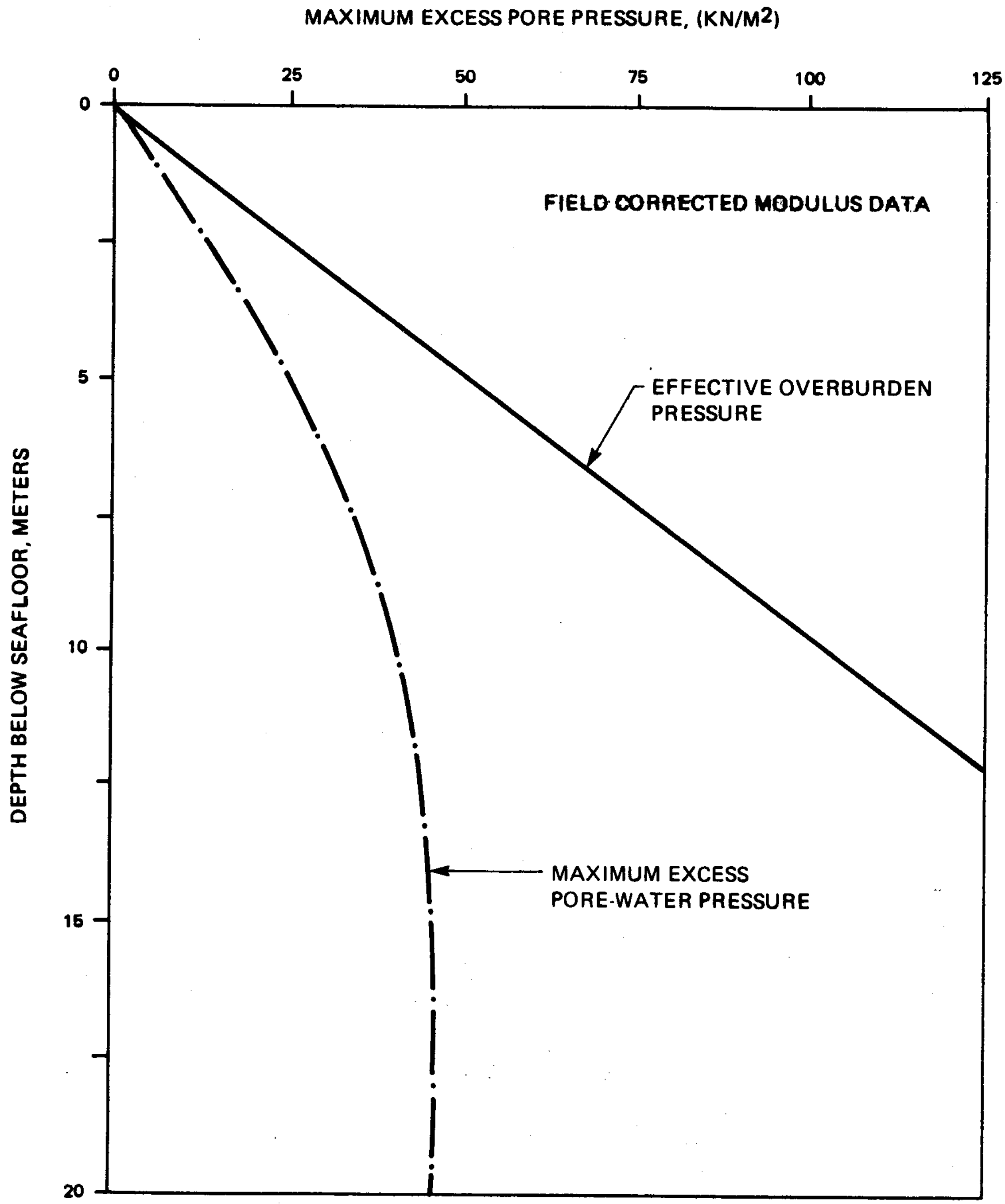

SOIL TYPE SP (2)

EARTHQUAKE SOURCE ALEUTIAN ARC

EARTHQUAKE RECORD (NORMALIZED TO Amax = 0.4g) PARKFIELD 1966

MAXIMUM GROUND ACCELERATION = Amax

CONCLUSION: NO LIQUEFACTION

FIGURE IV-23 MAXIMUM EXCESS PORE PRESSURE RESPONSE CURVE (SP2, ALEUTIAN ARC, 0.4g)

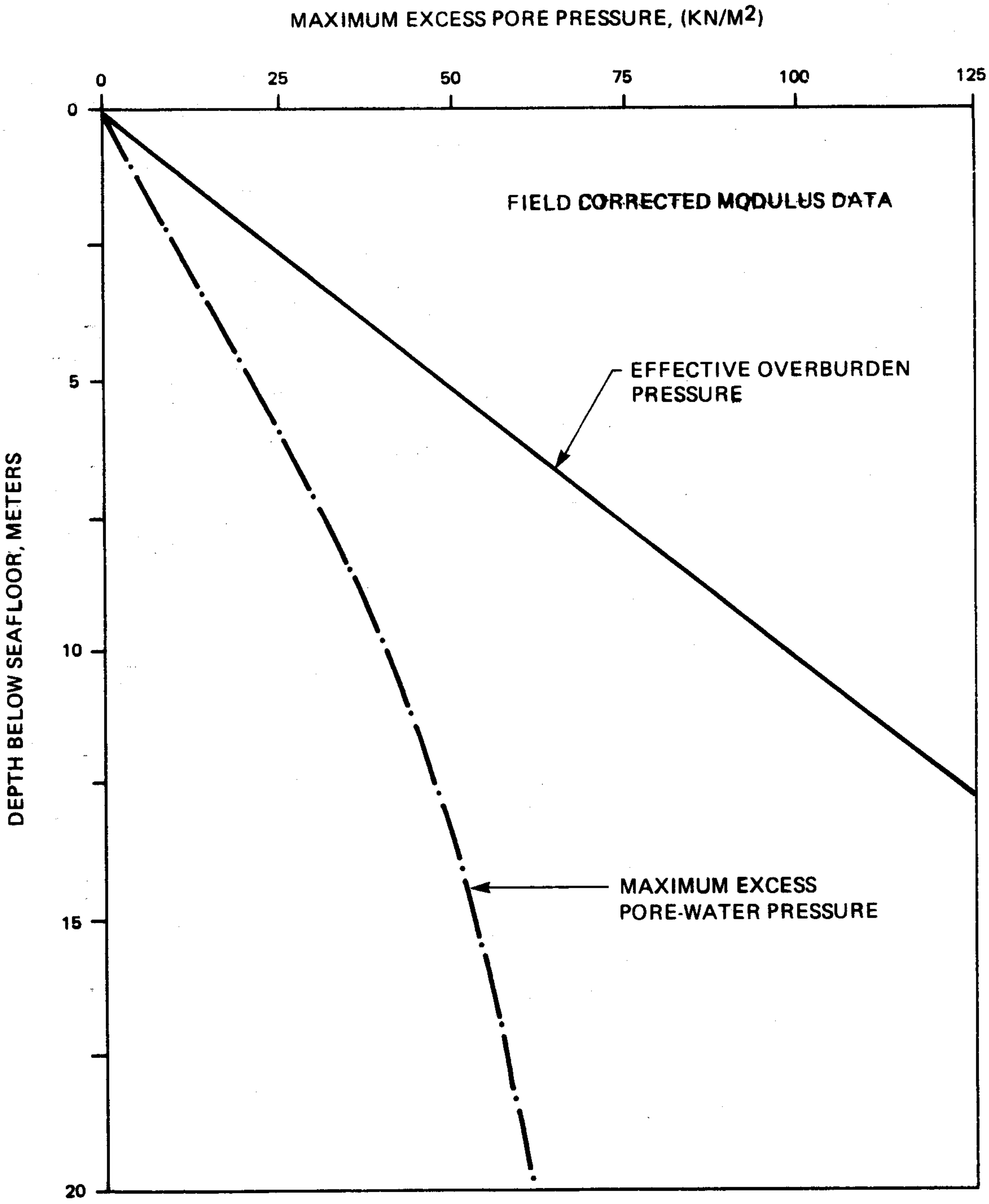

SOIL TYPE SP/SM (3)

EARTHQUAKE SOURCE SUBDUCTION ZONE

EARTHQUAKE RECORD (NORMALIZED TO Amax = 0.16g) CAL TECH A-1

MAXIMUM GROUND ACCELERATION = Amax

CONCLUSION: NO LIQUEFACTION

FIGURE IV-24 MAXIMUM EXCESS PORE PRESSURE RESPONSE CURVE (SP/SM3, SUBDUCTION ZONE, 0.16g)

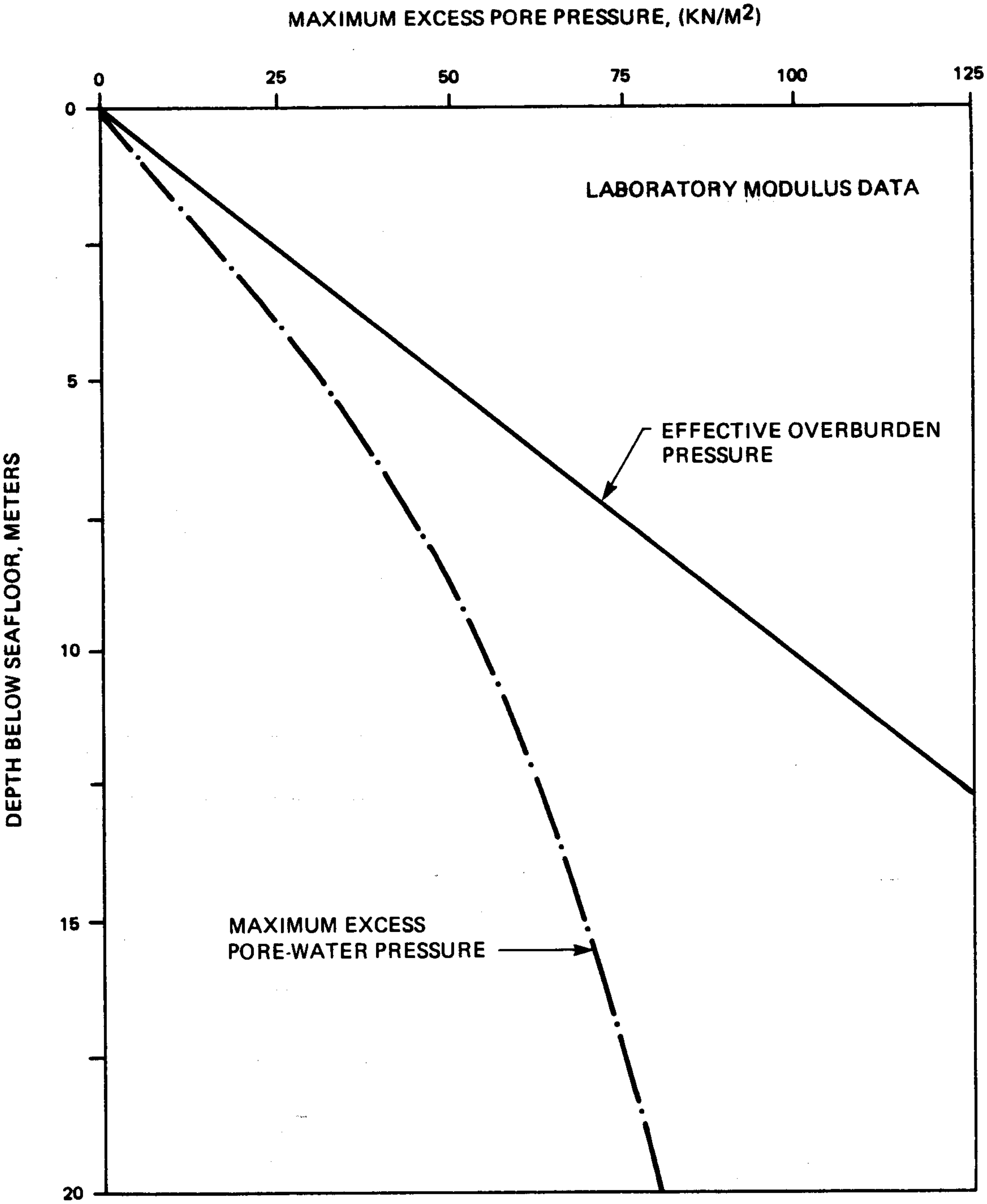

SOIL TYPE SP/SM (3)

EARTHQUAKE SOURCE SUBDUCTION ZONE

EARTHQUAKE RECORD (NORMALIZED TO Amax = 0.16g) CAL TECH A-1

MAXIMUM GROUND ACCELERATION = Amax

CONCLUSION: NO LIQUEFACTION

FIGURE IV-25 MAXIMUM EXCESS PORE PRESSURE RESPONSE CURVE (SP/SM3, SUBDUCTION ZONE, 0.16g)

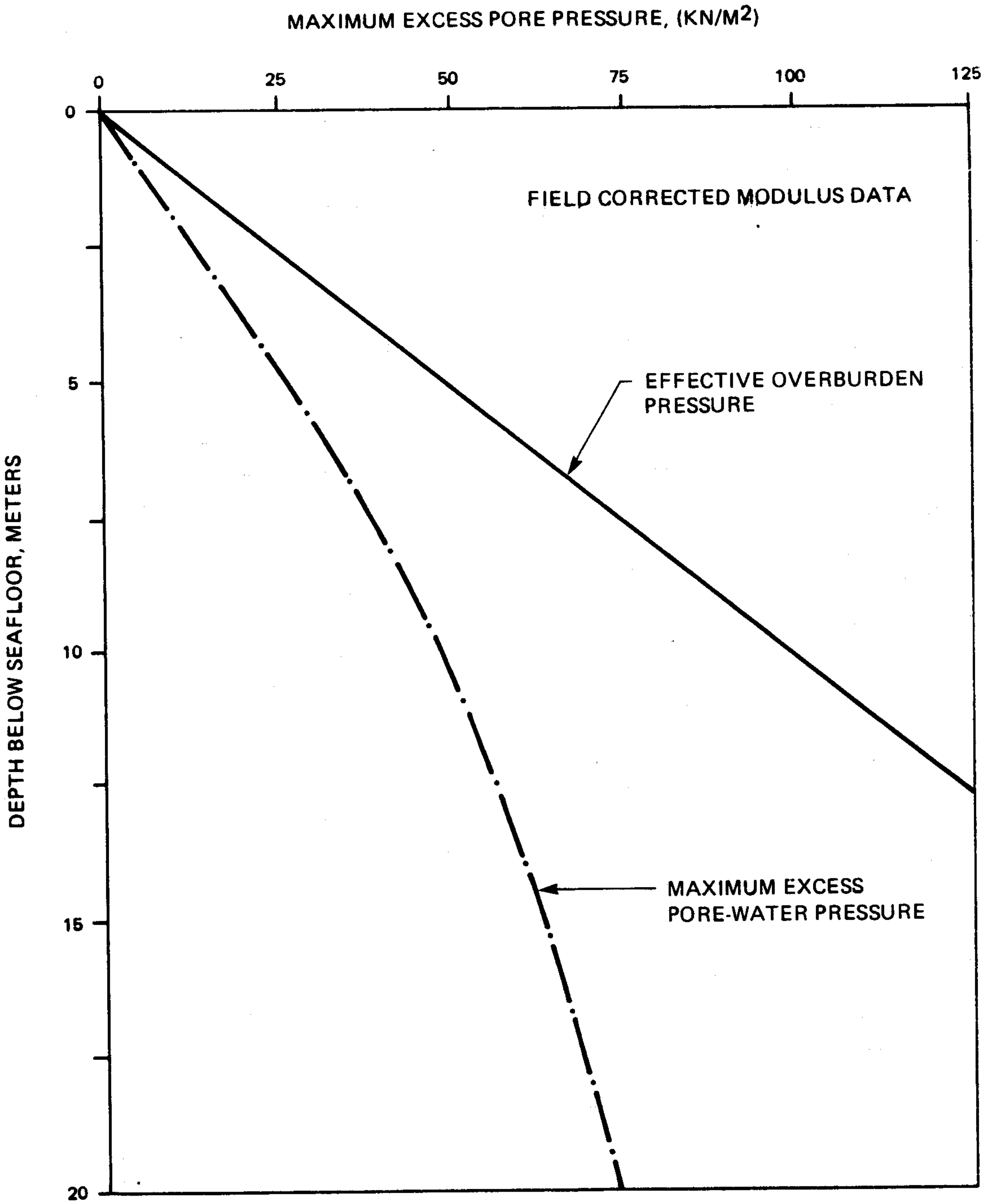

SOIL TYPE SP/SM (3)

EARTHQUAKE SOURCE SUBDUCTION ZONE

EARTHQUAKE RECORD (NORMALIZED TO Amax = 0.19g) CAL TECH A-1

MAXIMUM GROUND ACCELERATION = Amax

CONCLUSION: NO LIQUEFACTION

FIGURE IV-26 MAXIMUM EXCESS PORE PRESSURE RESPONSE CURVE (SP/SM3, SUBDUCTION ZONE 0.19g)

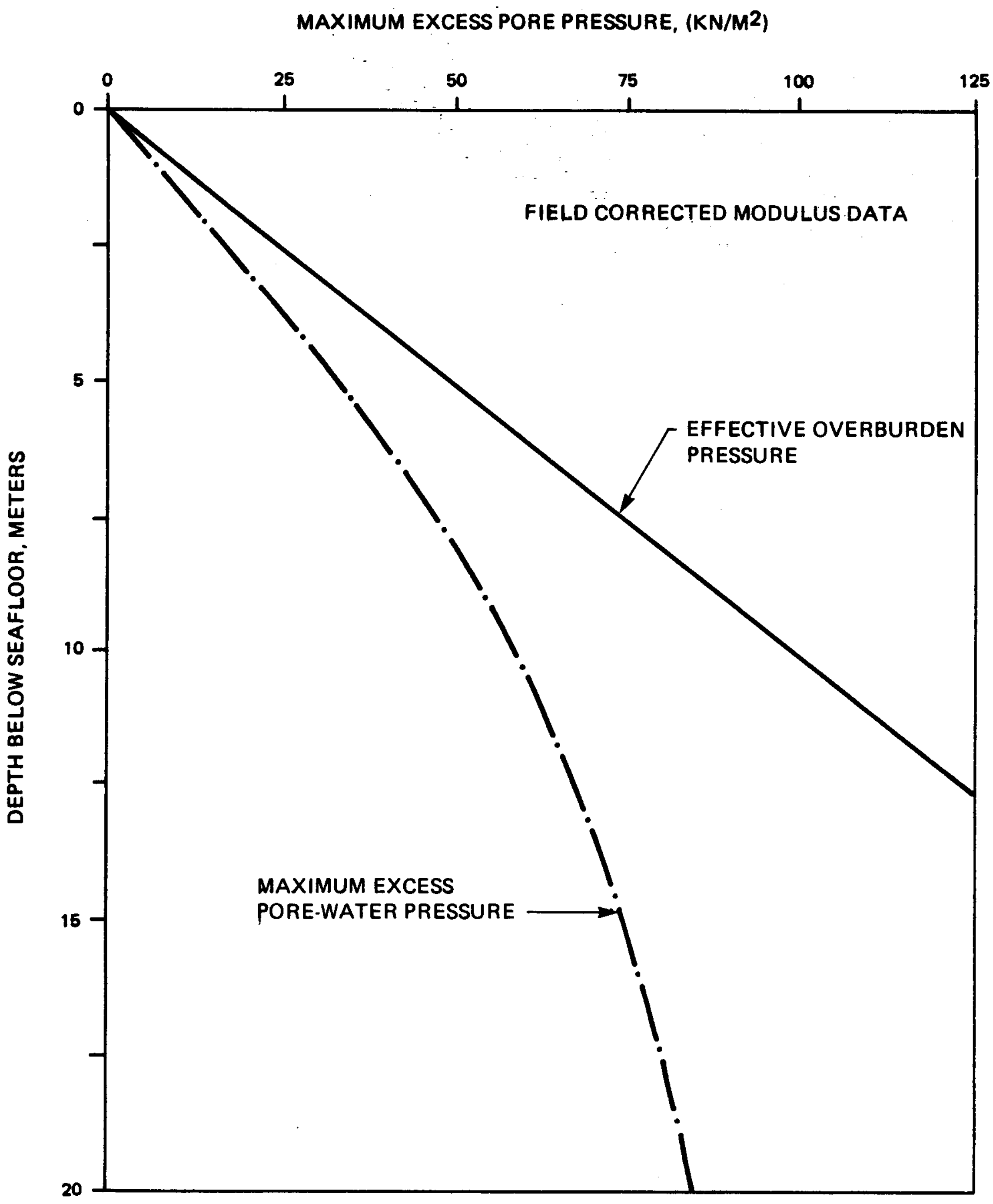

SOIL TYPE SP/SM (3)

EARTHQUAKE SOURCE MAJOR GRABENS

EARTHQUAKE RECORD (NORMALIZED TO Amax = 0.4g) TAFT 1952

MAXIMUM GROUND ACCELERATION = Amax

CONCLUSION: NO LIQUEFACTION

FIGURE IV-27 MAXIMUM EXCESS PORE PRESSURE RESPONSE CURVE (SP/SM3, MAJOR GRABENS, 0.4g)

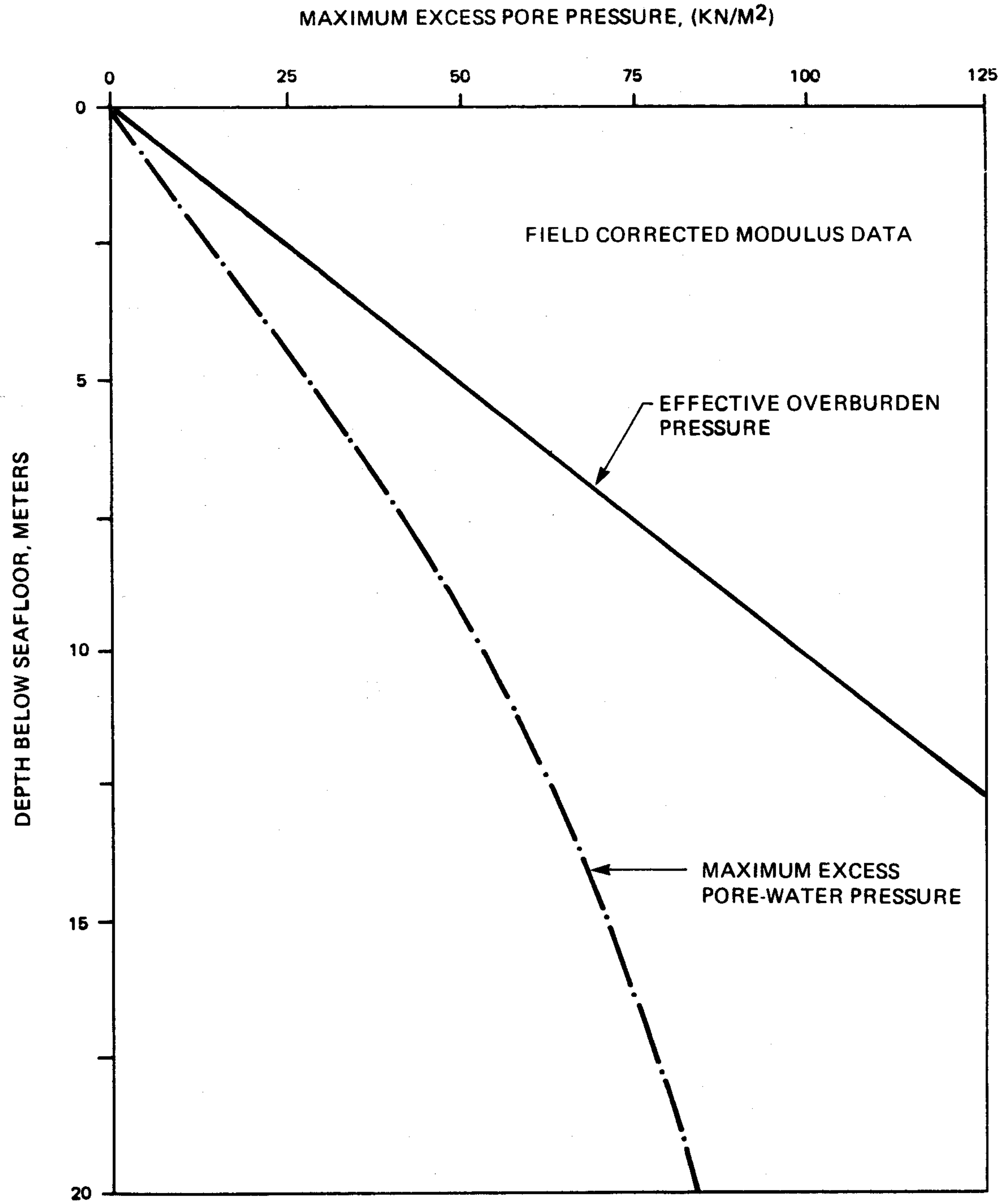

SOIL TYPE SP/SM (3)

EARTHQUAKE SOURCE MAJOR GRABENS

EARTHQUAKE RECORD (NORMALIZED TO Amax = 0.4g) EL CENTRO 1940

MAXIMUM GROUND ACCELERATION = Amax

CONCLUSION: NO LIQUEFACTION

FIGURE IV-28 MAXIMUM EXCESS PORE PRESSURE RESPONSE CURVE (SP/SM3, MAJOR GRABENS, 0.4g)

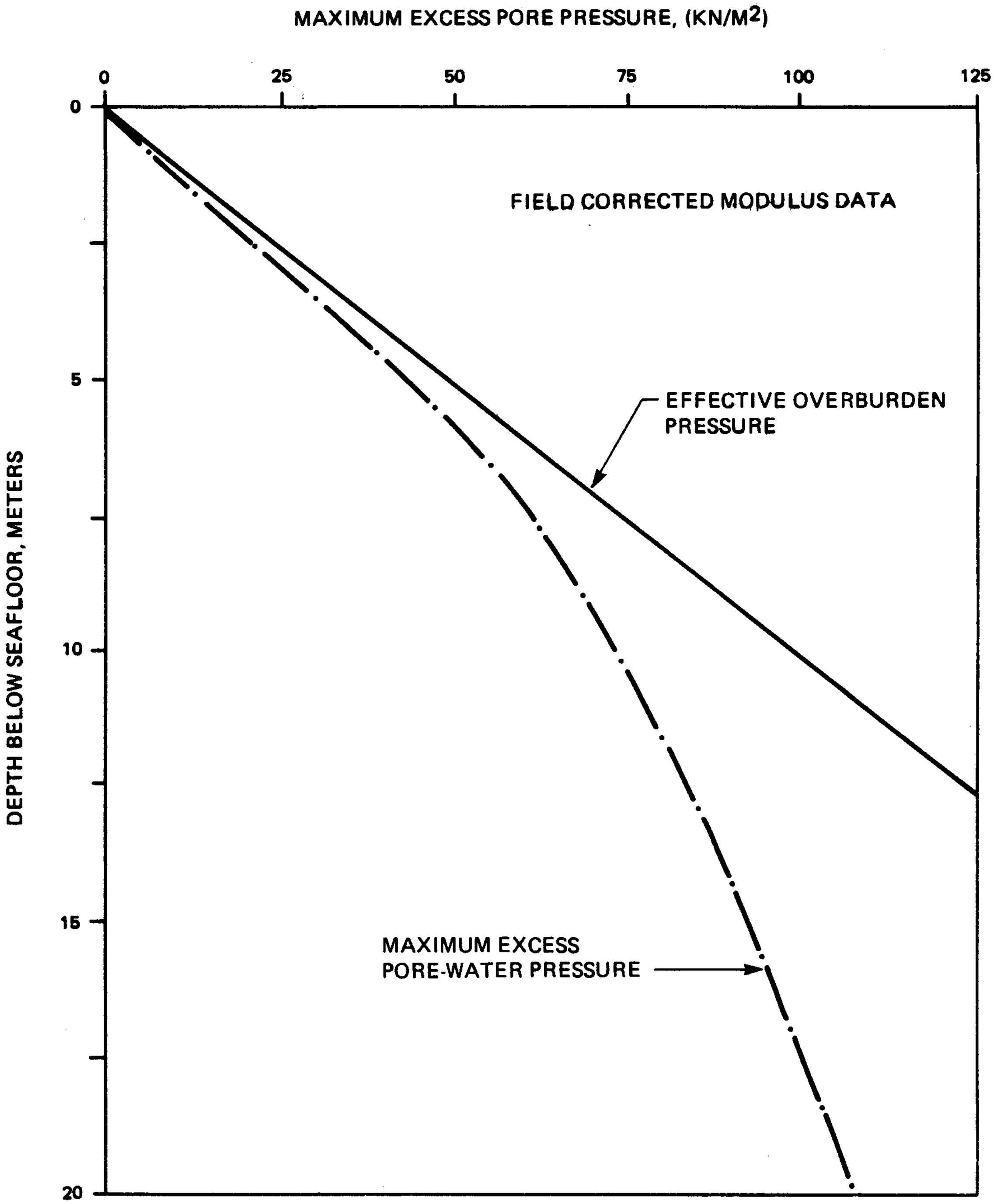

SOIL TYPE SP/SM (3)

EARTHQUAKE SOURCE MAJOR GRABENS

EARTHQUAKE RECORD (NORMALIZED TO Amax = 0.5g) TAFT 1952

MAXIMUM GROUND ACCELERATION = Amax

CONCLUSION: NO LIQUEFACTION

FIGURE IV-29 MAXIMUM EXCESS PORE PRESSURE RESPONSE CURVE (SP/SM3, MAJOR GRABENS, 0.5g)

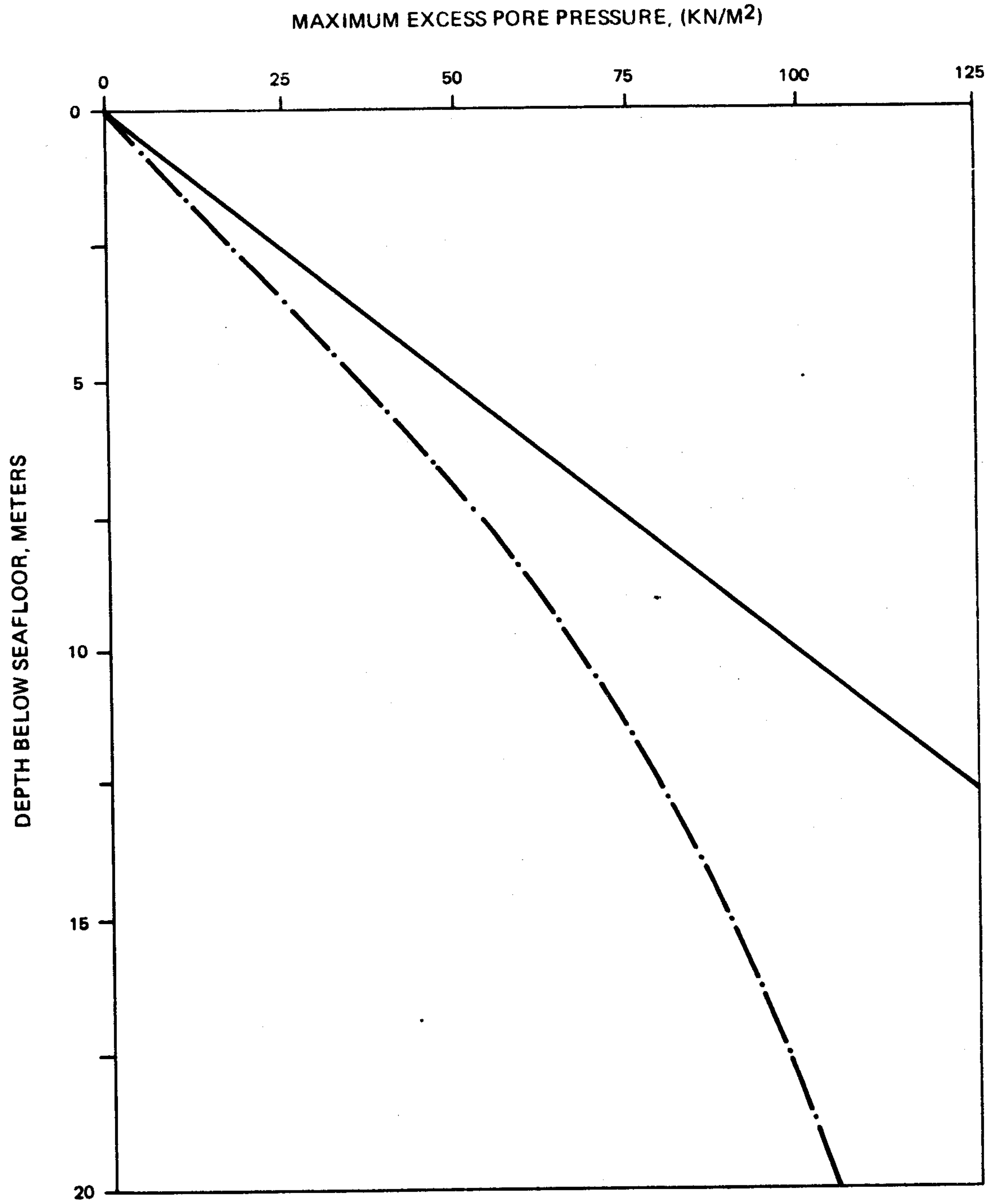

SOIL TYPE SP/SM (3)

EARTHQUAKE SOURCE MAJOR GRABENS

EARTHQUAKE RECORD (NORMALIZED TO Amax = 0.5g) EL CENTRO 1940

MAXIMUM GROUND ACCELERATION = Amax

CONCLUSION: NO LIQUEFACTION

FIGURE IV-30 MAXIMUM EXCESS PORE PRESSURE RESPONSE CURVE (SP/SMS, MAJOR GRABENS, 0.5g)

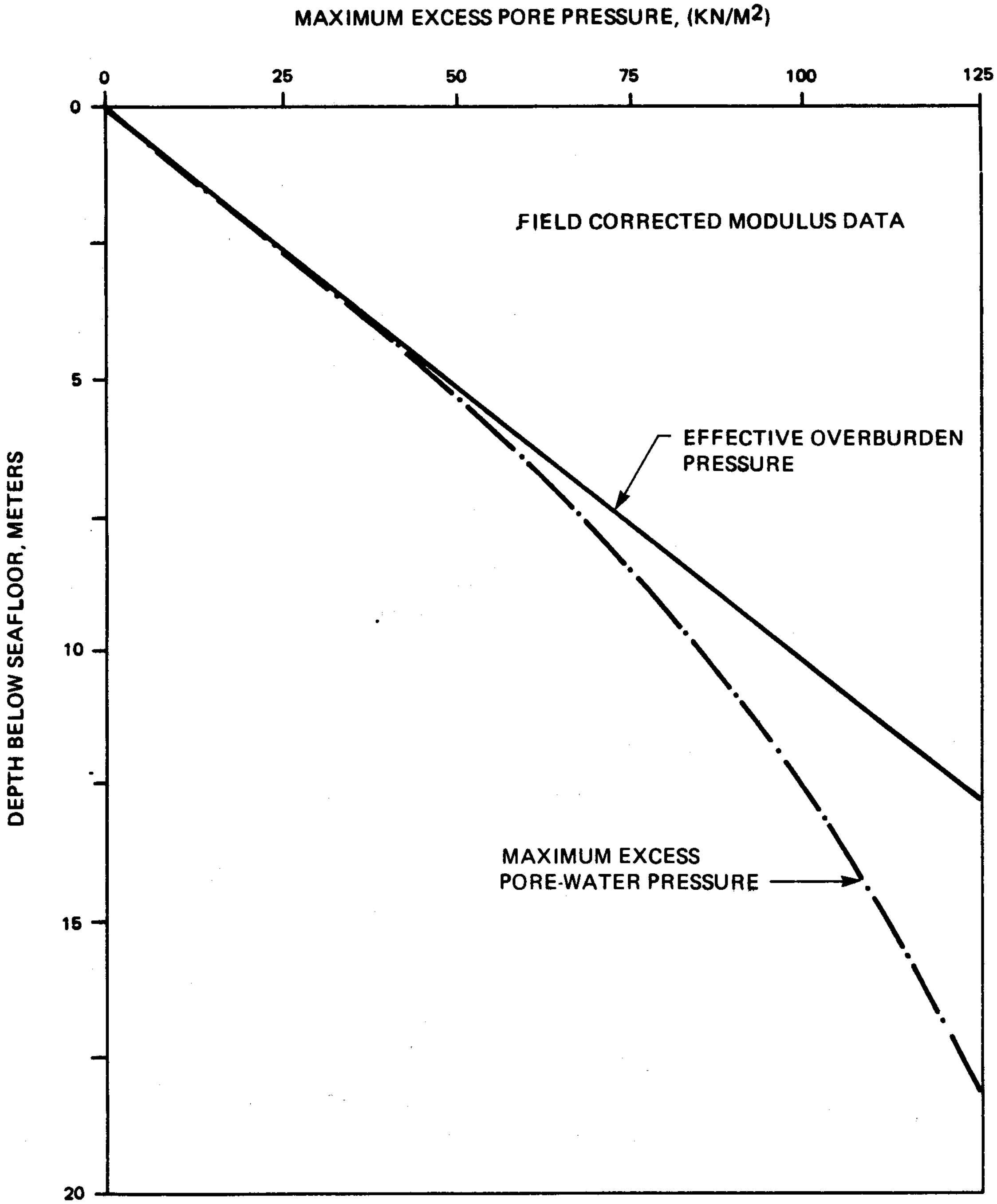

SOIL TYPE SP/SM (3)

EARTHQUAKE SOURCE MAJOR GRABENS

EARTHQUAKE RECORD (NORMALIZED TO Amax = 0.6g) TAFT 1952

MAXIMUM GROUND ACCELERATION = Amax

CONCLUSION: LIQUEFACTION TO 3.8 M

FIGURE IV-31 MAXIMUM EXCESS PORE PRESSURE RESPONSE CURVE (SP/SM3, MAJOR GRABENS, 0.6g)

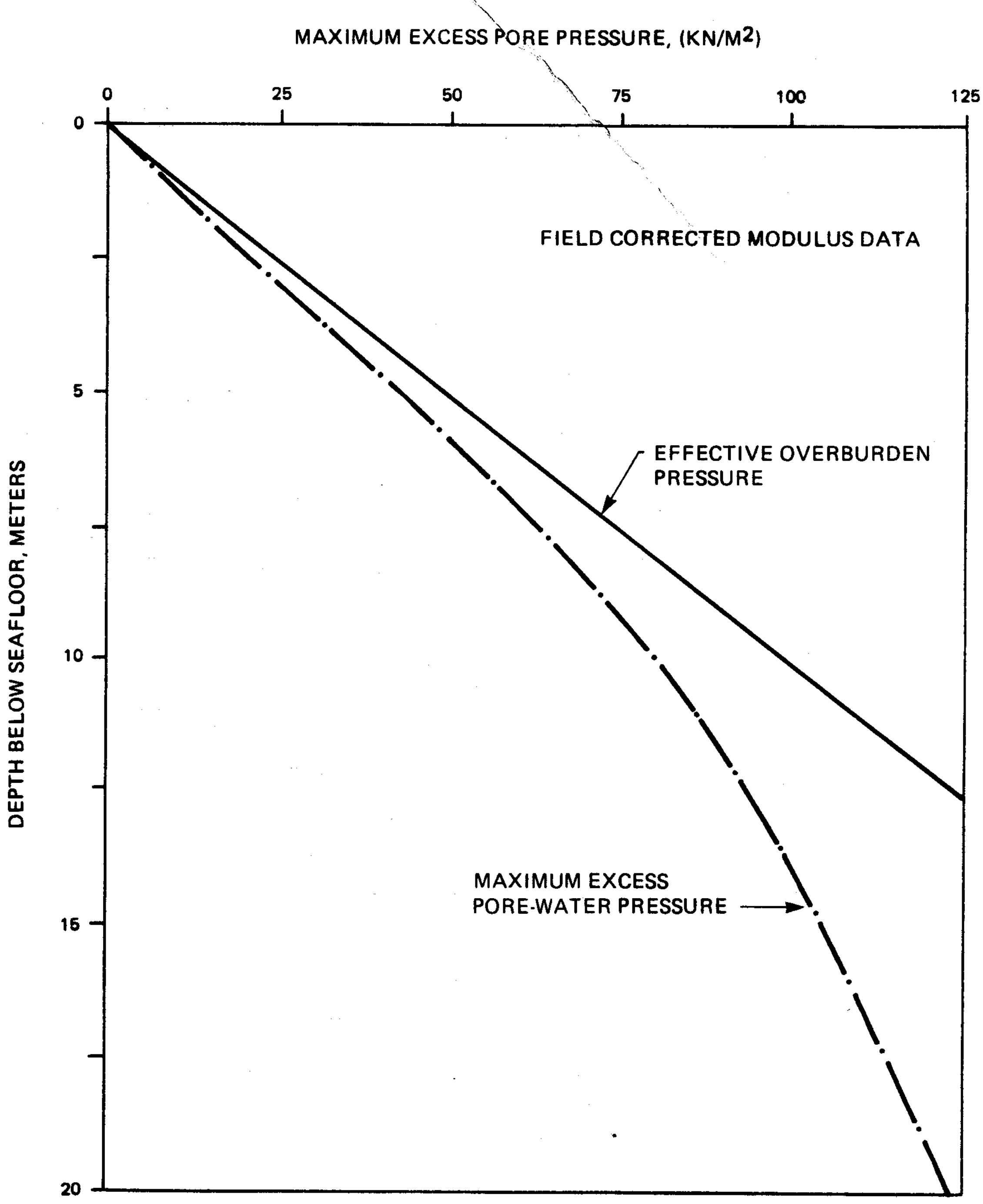

SOIL TYPE SP/SM (3)

EARTHQUAKE SOURCE MAJOR GRABENS

EARTHQUAKE RECORD (NORMALIZED TO Amax = 0.6g) EL CENTRO 1940

MAXIMUM GROUND ACCELERATION = Amax

CONCLUSION: NO LIQUEFACTION

FIGURE IV-32 MAXIMUM EXCESS PORE PRESSURE RESPONSE CURVE (SP/SM3, MAJOR GRABENS, 0.6g)

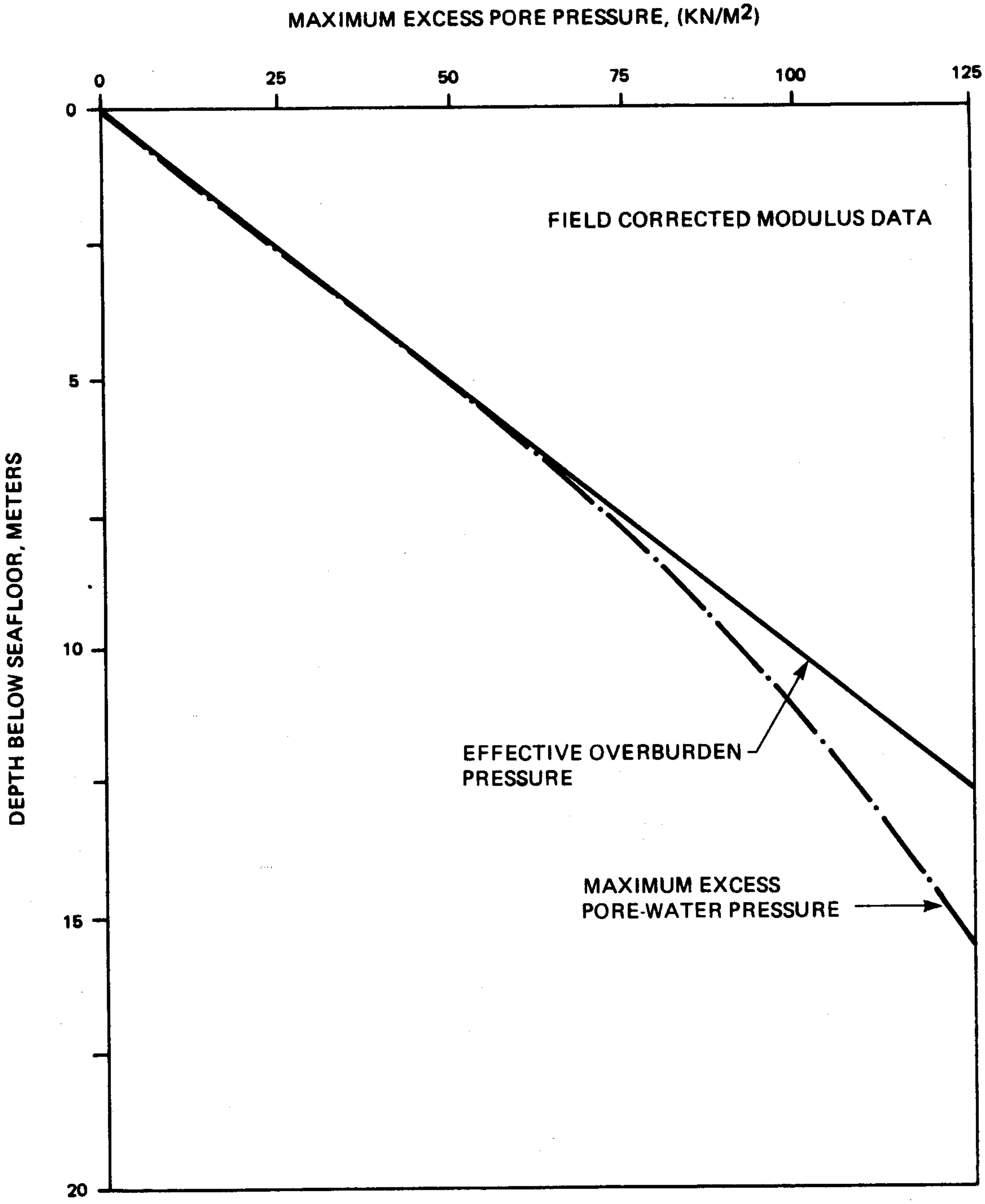

SOIL TYPE SP/SM (3)

EARTHQUAKE SOURCE MAJOR GRABENS

EARTHQUAKE RECORD (NORMALIZED TO Amax = 0.7g) TAFT 1952

MAXIMUM GROUND ACCELERATION = Amax

CONCLUSION: LIQUEFACTION TO 8 M

FIGURE IV-33 MAXIMUM EXCESS PORE PRESSURE RESPONSE CURVE (SP/SM3, MAJOR GRABENS, 0.7g)

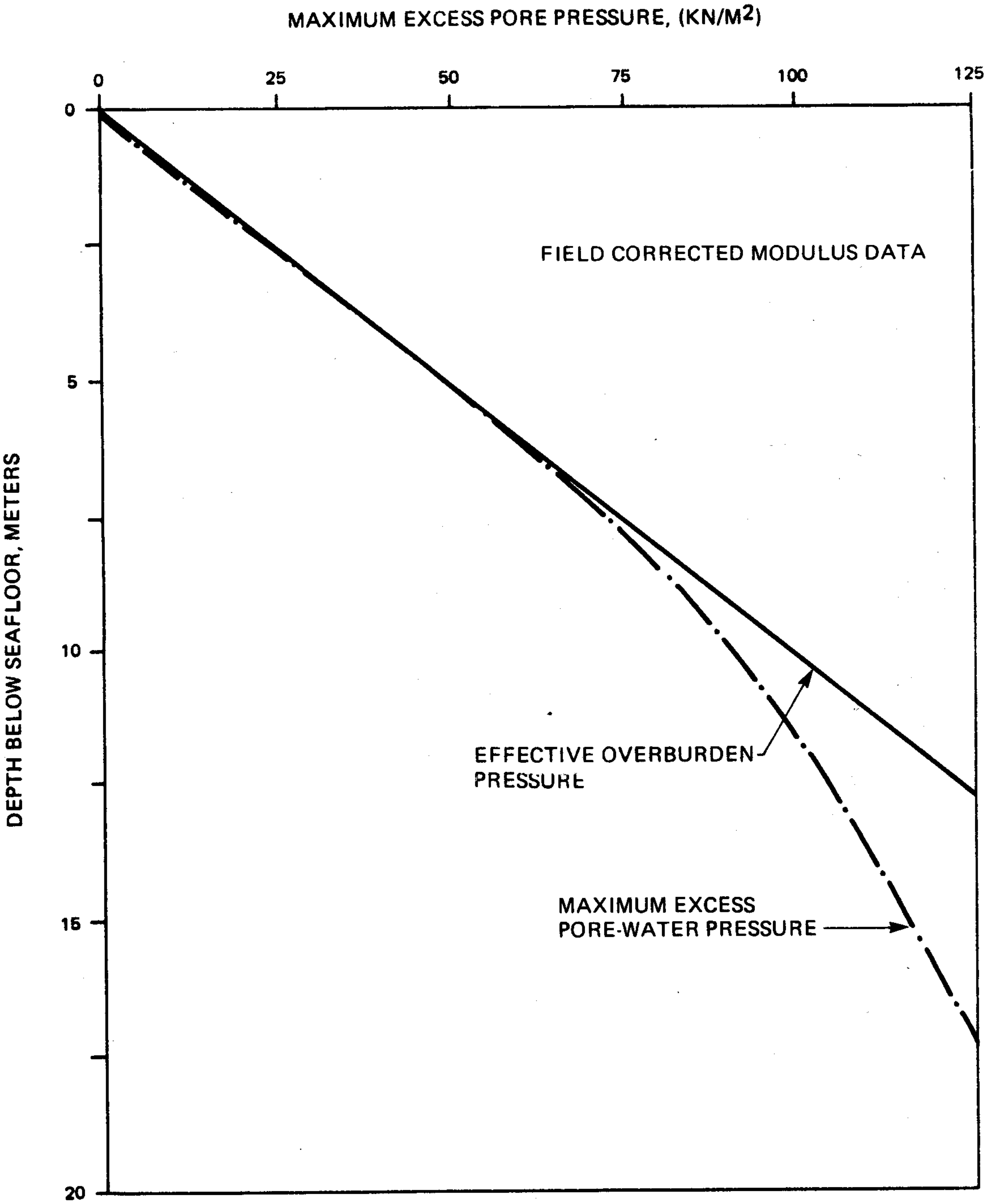

SOIL TYPE SP/SM (3)

EARTHQUAKE SOURCE MAJOR GRABENS

EARTHQUAKE RECORD (NORMALIZED TO Amax = 0.7g) EL CENTRO 1940

MAXIMUM GROUND ACCELERATION = Amax

CONCLUSION: LIQUEFACTION TO 8 M

FIGURE IV-34 MAXIMUM EXCESS PORE PRESSURE RESPONSE CURVE (SP/SM3, MAJOR GRABENS, 0.7g)

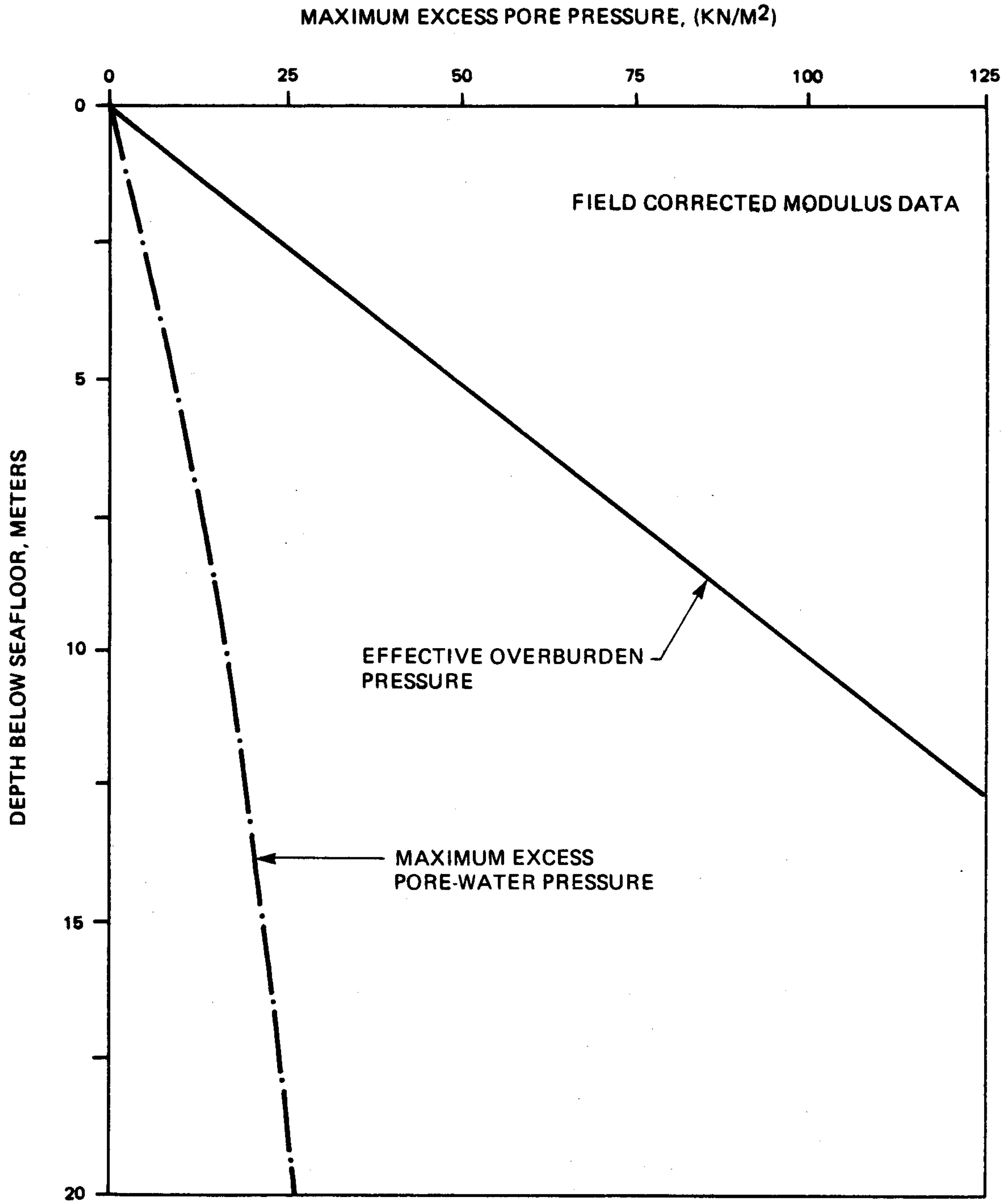

SOIL TYPE SP/SM (3)

EARTHQUAKE SOURCE BACK ARC FAULTS

EARTHQUAKE RECORD (NORMALIZED TO Amax = 0.3g) EL CENTRO 1979

MAXIMUM GROUND ACCELERATION = Amax

CONCLUSION: NO LIQUEFACTION

FIGURE IV-35 MAXIMUM EXCESS PORE PRESSURE RESPONSE CURVE (SP/SM3, BACK ARC FAULTS, 0.3g)

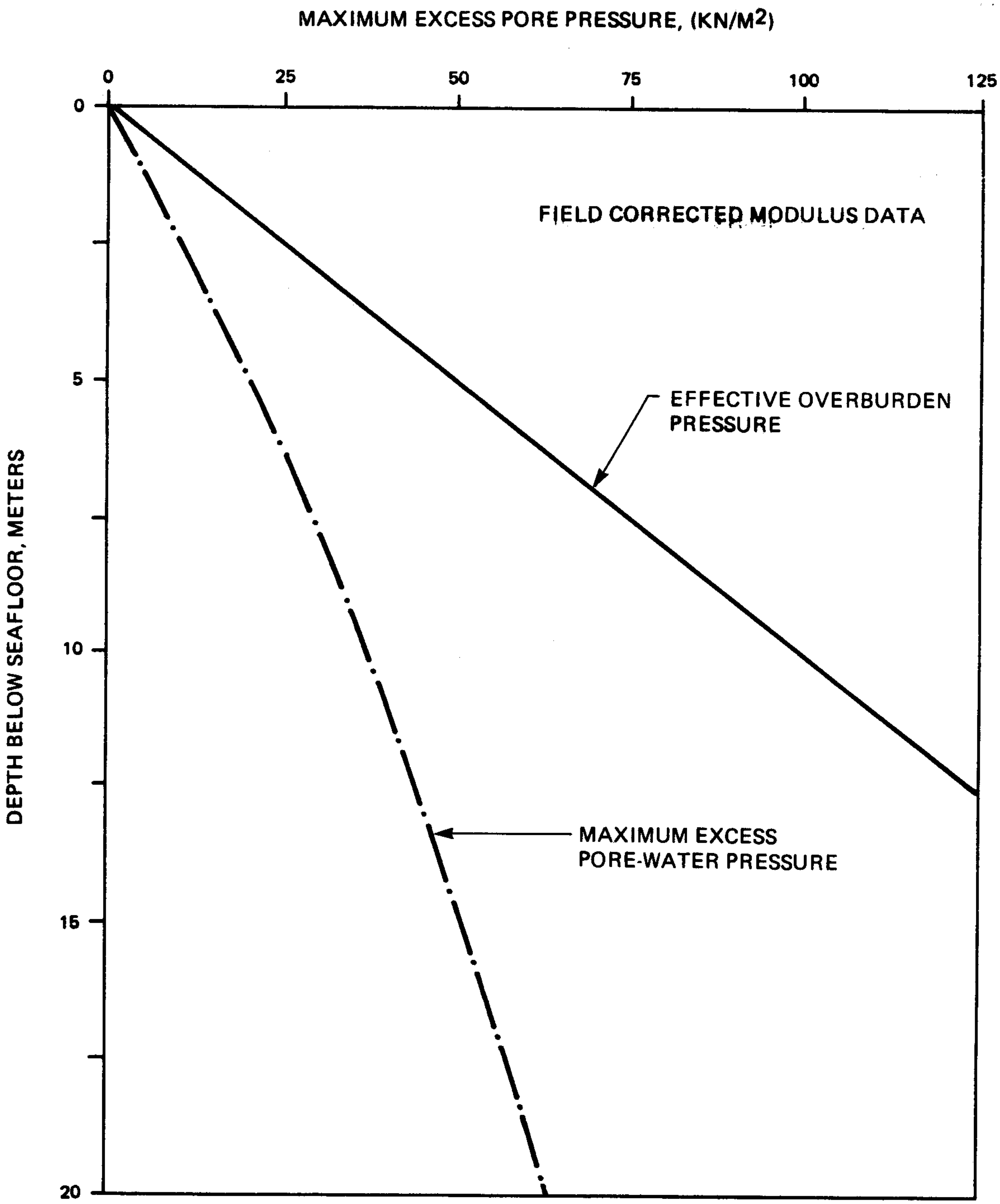

SOIL TYPE SP/SM (3)

EARTHQUAKE SOURCE BACK ARC FAULTS

EARTHQUAKE RECORD (NORMALIZED TO Amax = 0.6g) EL CENTRO 1979

MAXIMUM GROUND ACCELERATION = Amax

CONCLUSION: NO LIQUEFACTION

FIGURE IV-36 MAXIMUM EXCESS PORE PRESSURE RESPONSE CURVES (SP/SM3, BACK ARC FAULTS, 0.6g)

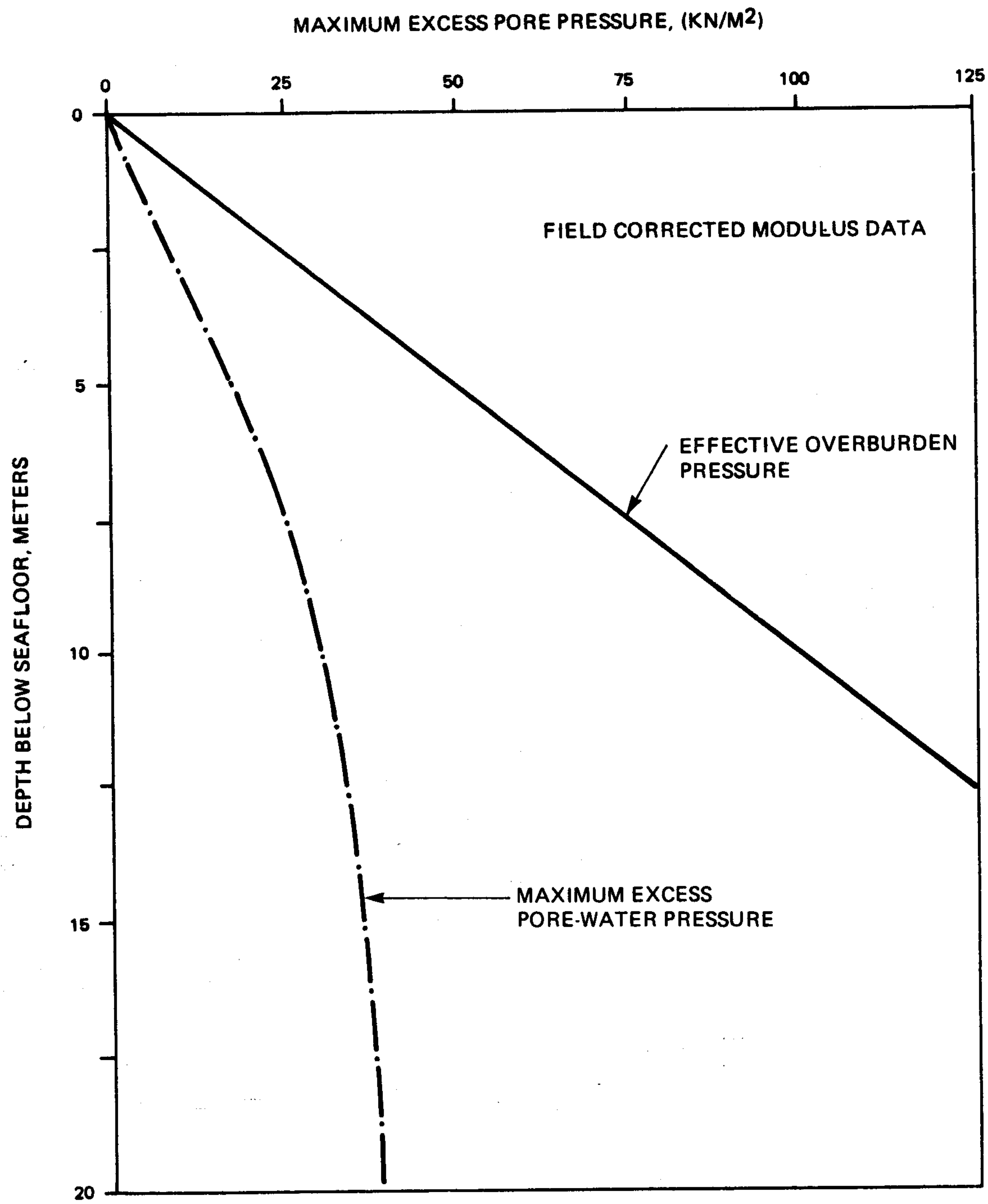

SOIL TYPE SP/SM (3)

EARTHQUAKE SOURCE ALEUTIAN ARC

EARTHQUAKE RECORD (NORMALIZED TO Amax = 0.4g) PARKFIELD 1966

MAXIMUM GROUND ACCELERATION = Amax

CONCLUSION: NO LIQUEFACTION

FIGURE IV-37 MAXIMUM EXCESS PORE PRESSURE RESPONSE CURVE (SP/SM3, ALEUTIAN ARC, 0.4g)

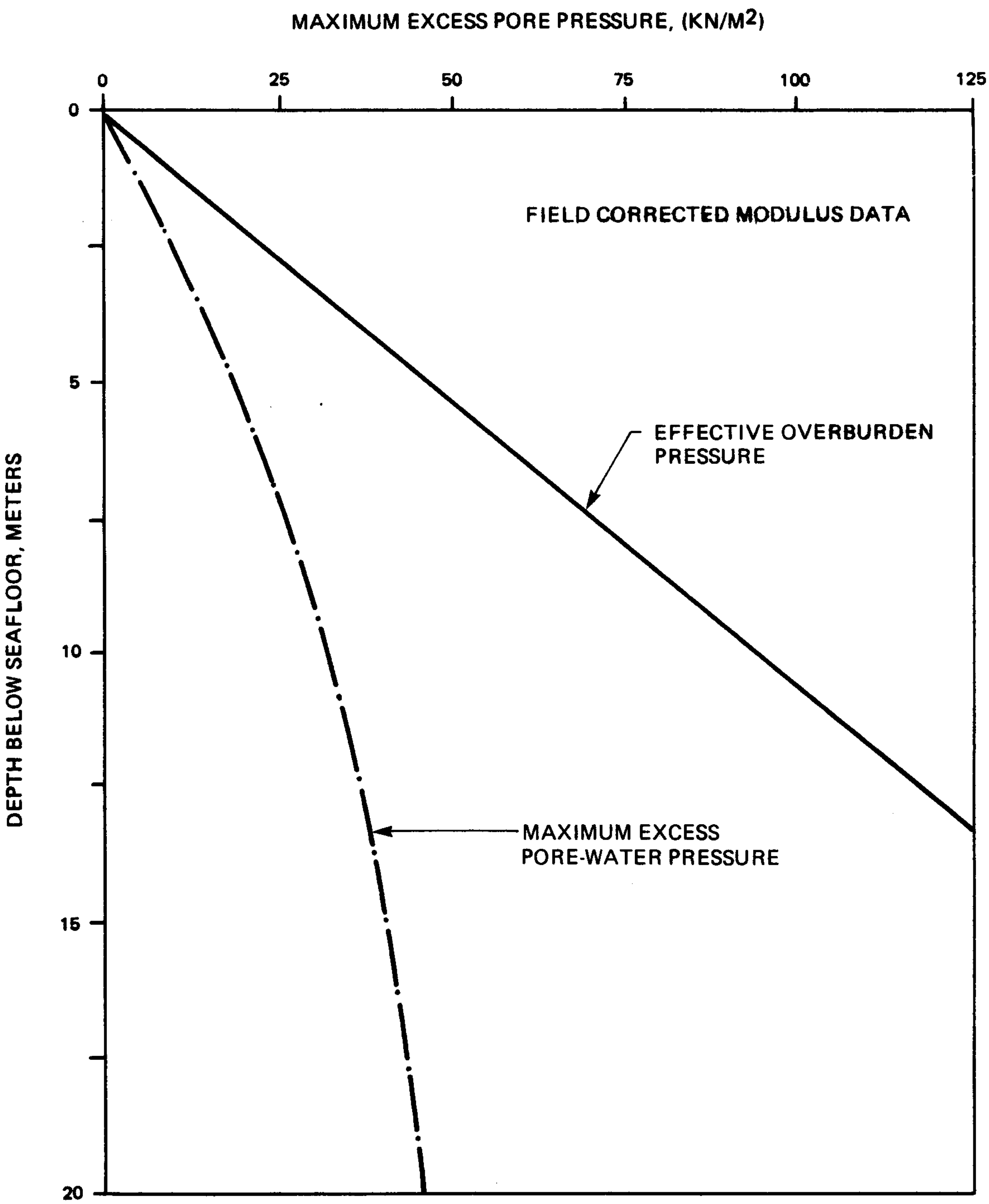

SOIL TYPE SM (4)

EARTHQUAKE SOURCE SUBDUCTION ZONE

EARTHQUAKE RECORD (NORMALIZED TO Amax = 0.16g) CAL TECH A-1

MAXIMUM GROUND ACCELERATION = Amax

CONCLUSION: NO LIQUEFACTION

FIGURE IV-38 MAXIMUM EXCESS PORE PRESSURE RESPONSE CURVE (SM4, SUBDUCTION ZONE, 0.16g)

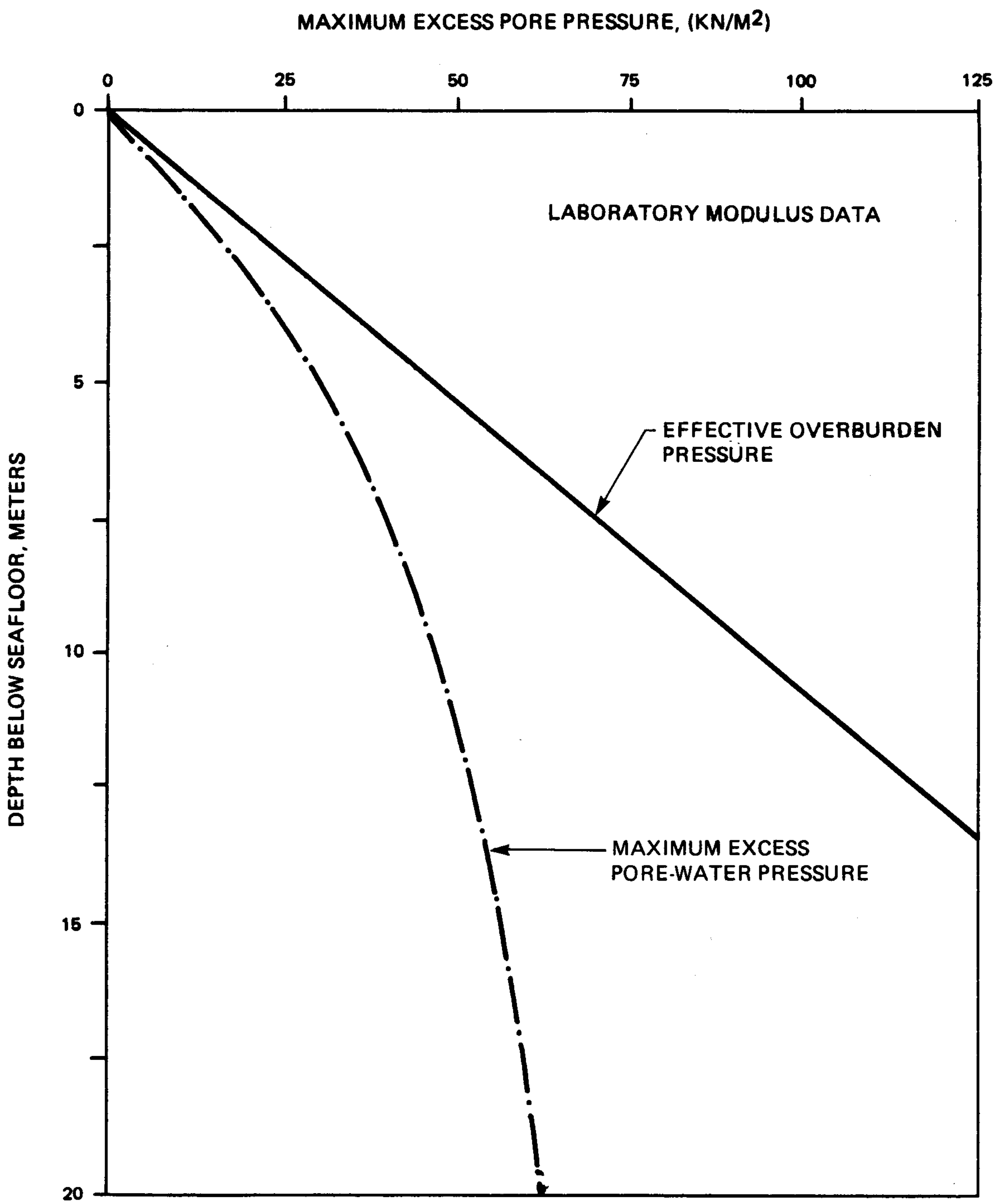

SOIL TYPE SM (4)

EARTHQUAKE SOURCE SUBDUCTION ZONE

EARTHQUAKE RECORD (NORMALIZED TO Amax = 0.16g) CAL TECH A-1

MAXIMUM GROUND ACCELERATION = Amax

CONCLUSION: NO LIQUEFACTION

FIGURE IV-39 MAXIMUM EXCESS PORE PRESSURE RESPONSE CURVE (SM4, SUBDUCTION ZONE, 0.16g)

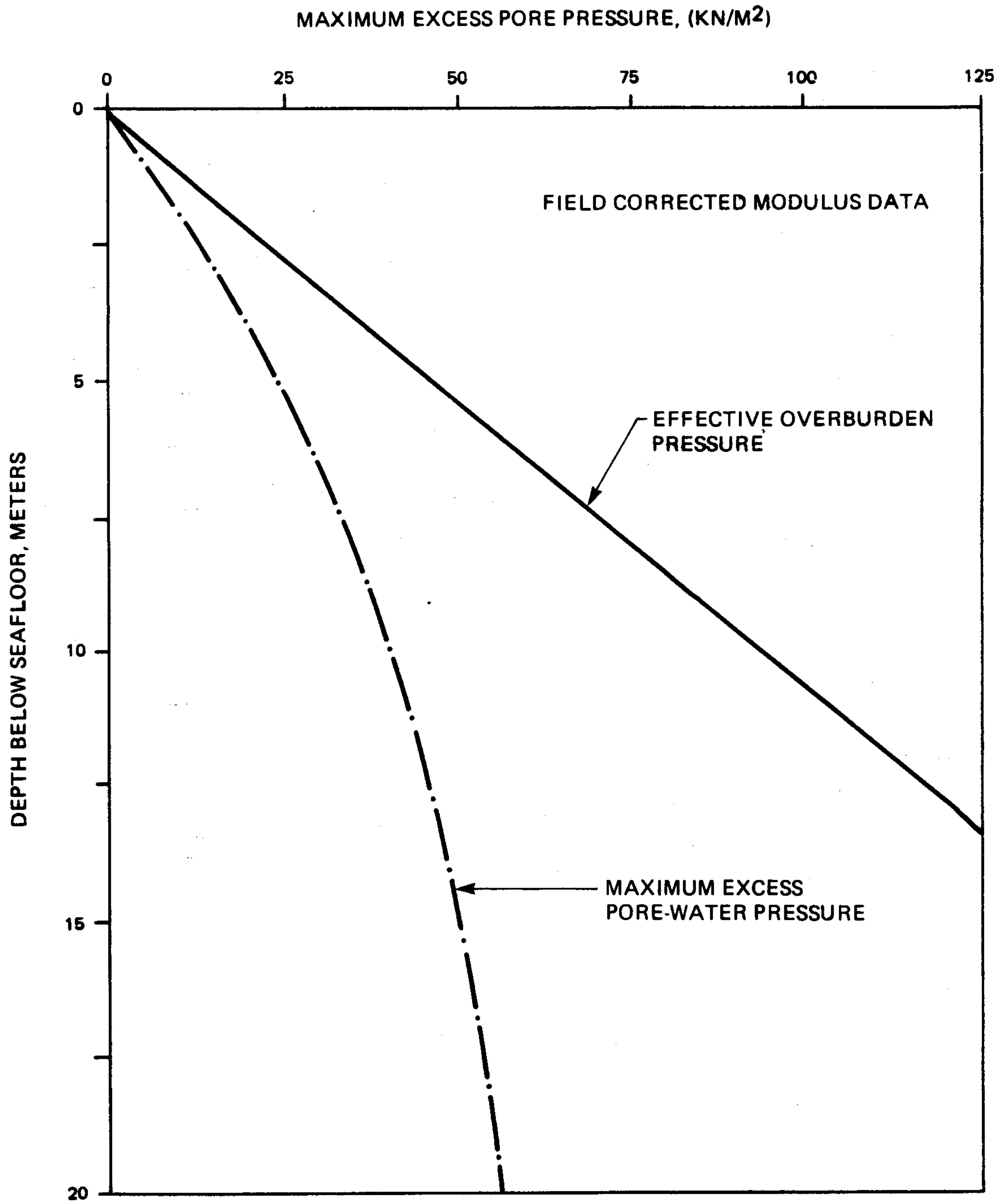

SOIL TYPE SM (4)

EARTHQUAKE SOURCE SUBDUCTION ZONE

EARTHQUAKE RECORD (NORMALIZED TO Amax = 0.10g) CAL TECH A-1

MAXIMUM GROUND ACCELERATION = Amax

CONCLUSION: NO LIQUEFACTION

FIGURE IV-40 MAXIMUM EXCESS PORE PRESSURE RESPONSE CURVE (SM4, SUBDUCTION ZONE, 0.10g)

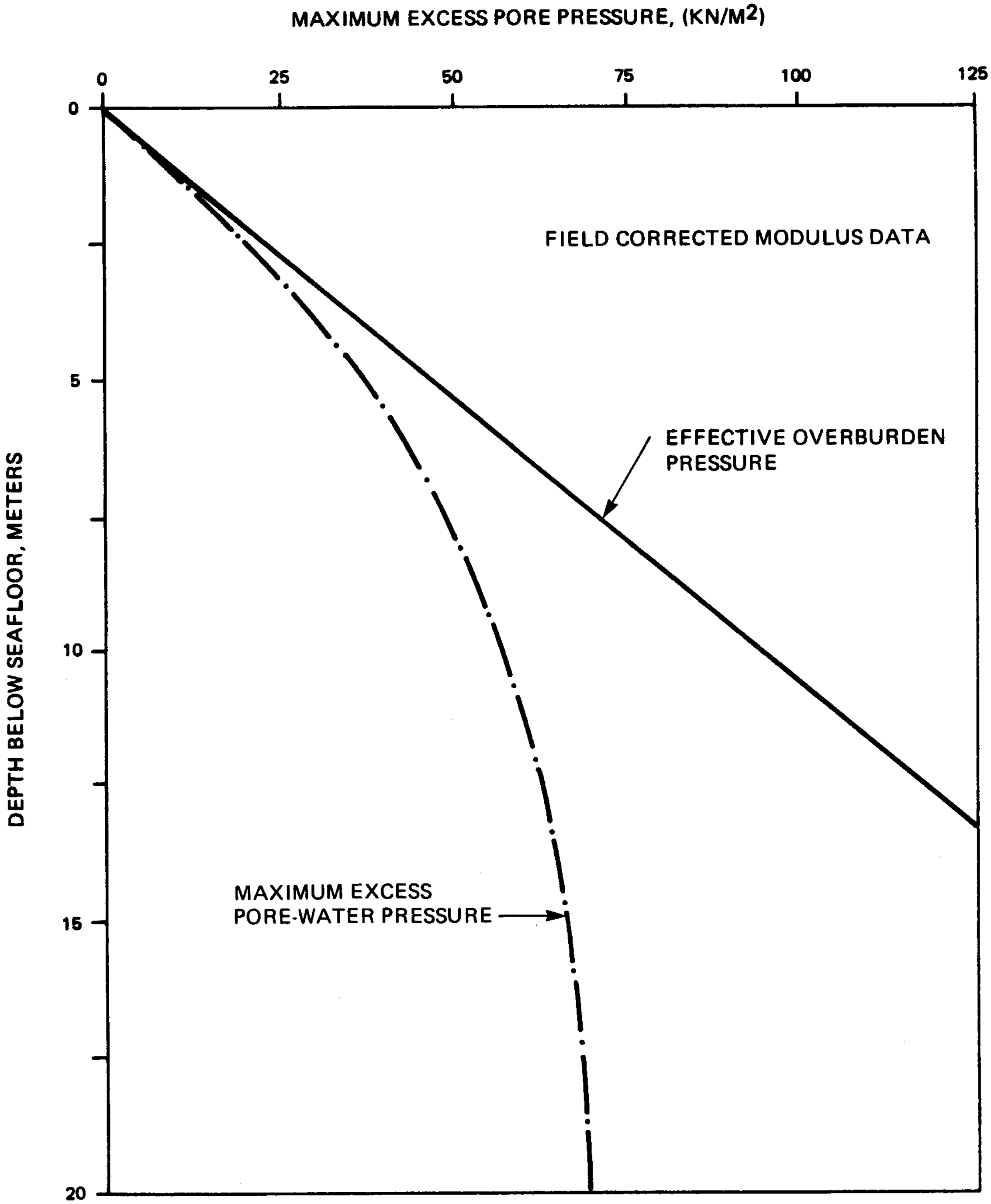

SOIL TYPE SM (4)

EARTHQUAKE SOURCE MAJOR GRABENS

EARTHQUAKE RECORD (NORMALIZED TO Amax = 0.4g) TAFT 1952

MAXIMUM GROUND ACCELERATION = Amax

CONCLUSION: NO LIQUEFACTION

FIGURE IV-41 MAXIMUM EXCESS PORE PRESSURE RESPONSE CURVE (SM4, MAJOR GRABENS, 0.4g)

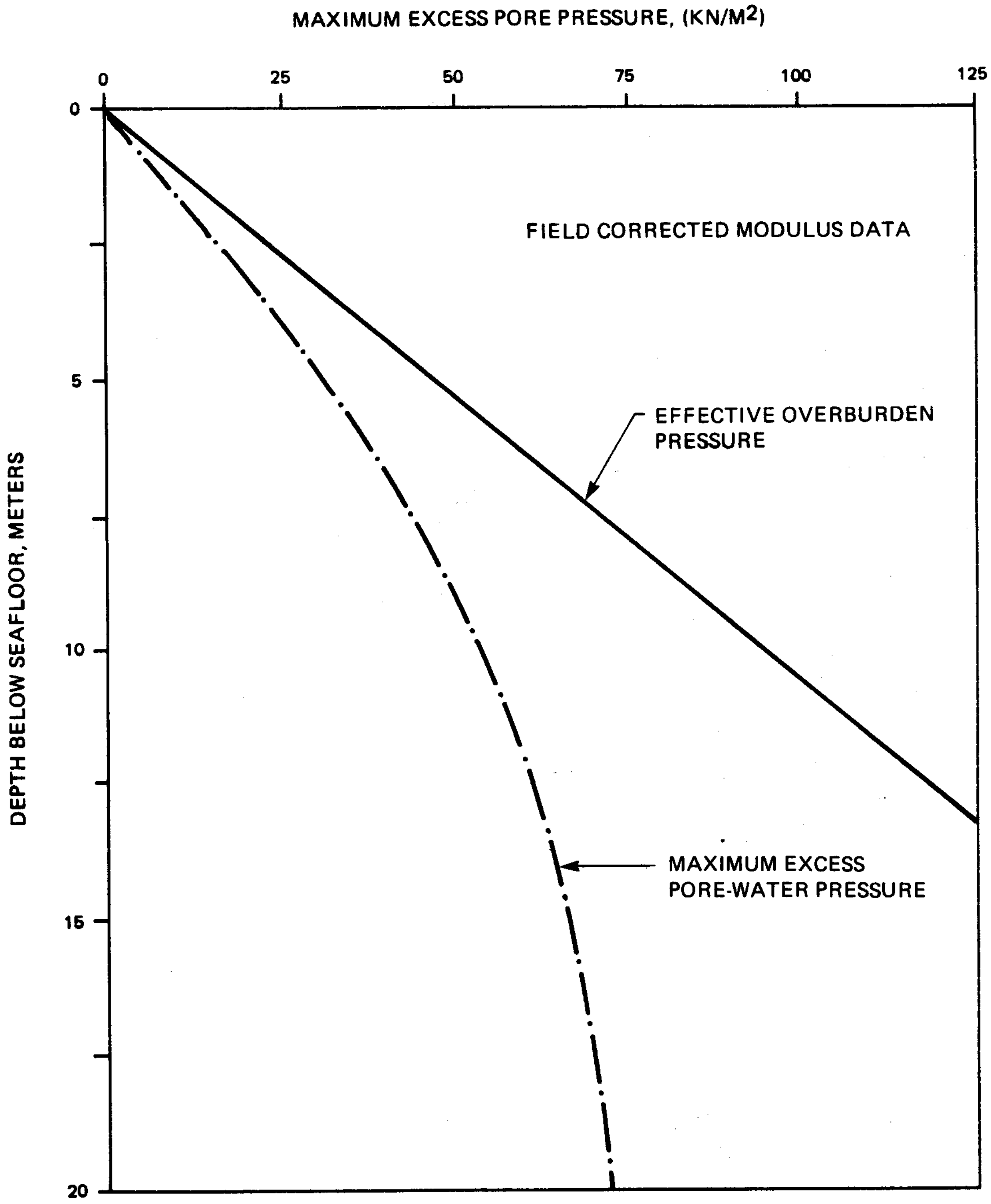

SOIL TYPE SM (4)

EARTHQUAKE SOURCE MAJOR GRABENS

EARTHQUAKE RECORD (NORMALIZED TO Amax = 0.4g) EL CENTRO 1940

MAXIMUM GROUND ACCELERATION = Amax

CONCLUSION: NO LIQUEFACTION

FIGURE IV-42 MAXIMUM EXCESS PORE PRESSURE RESPONSE CURVE
(SM4, MAJOR GRABENS, 0.4g)

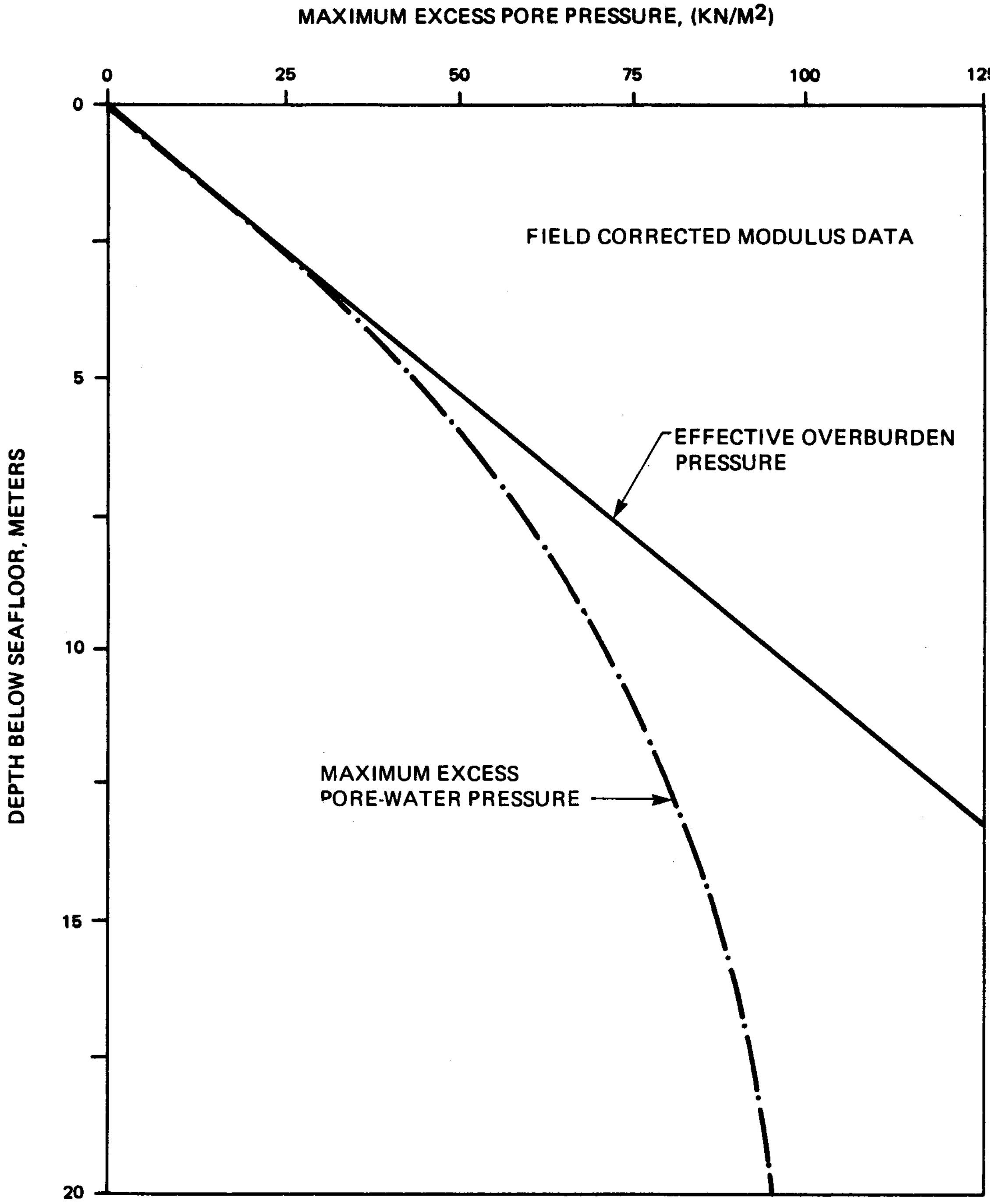

SOIL TYPE SM (4)

EARTHQUAKE SOURCE MAJOR GRABENS

EARTHQUAKE RECORD (NORMALIZED TO Amax = 0.5g) TAFT 1952

MAXIMUM GROUND ACCELERATION = Amax

CONCLUSION: LIQUEFACTION TO 3 M

FIGURE IV-43 MAXIMUM EXCESS PORE PRESSURE RESPONSE CURVE (SM4, MAJOR GRABENS, 0.5g)

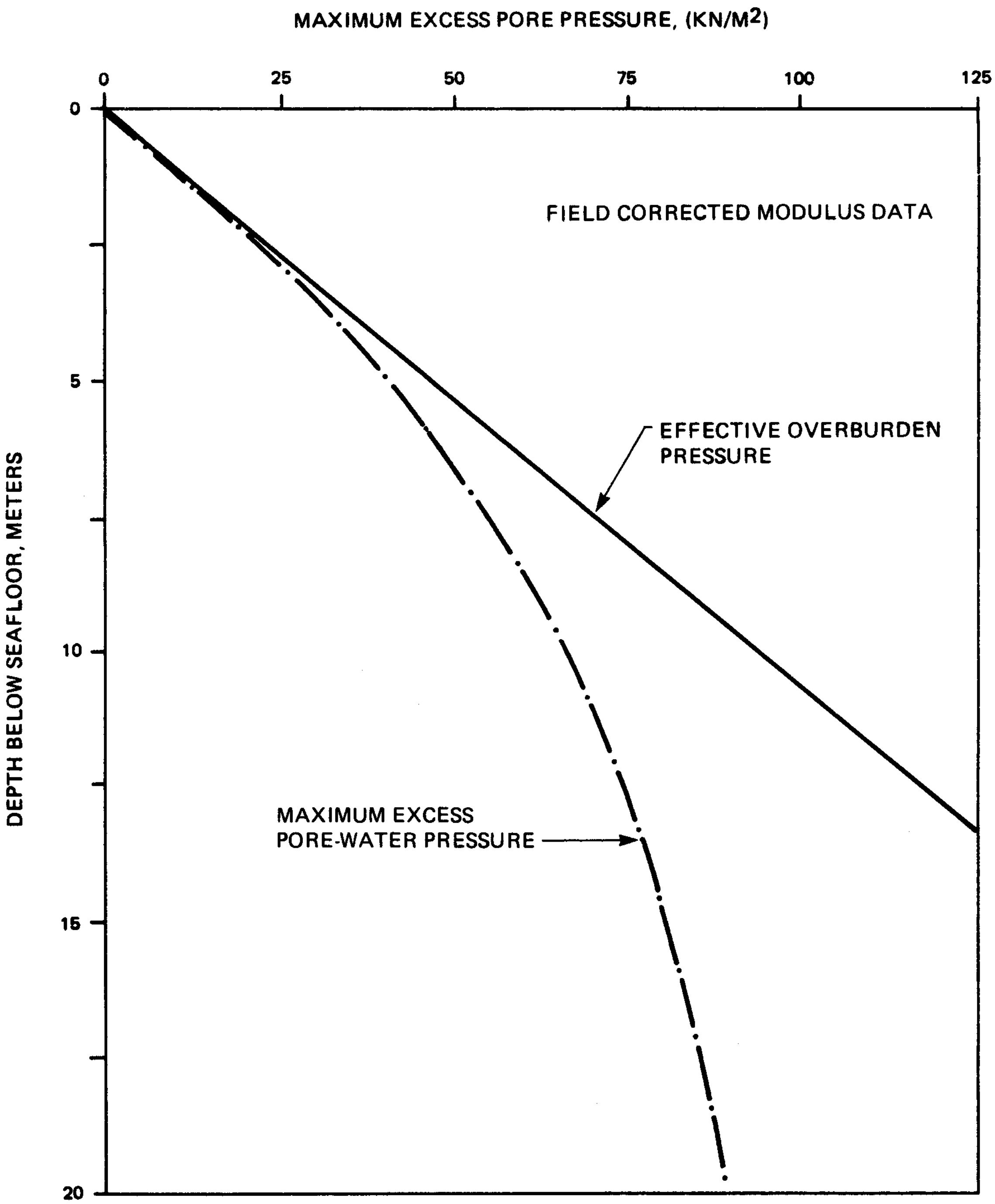

SOIL TYPE SM (4)

EARTHQUAKE SOURCE MAJOR GRABENS

EARTHQUAKE RECORD (NORMALIZED TO Amax = 0.5g) EL CENTRO 1940

MAXIMUM GROUND ACCELERATION = Amax

CONCLUSION: NO LIQUEFACTION

FIGURE IV-44 MAXIMUM EXCESS PORE PRESSURE RESPONSE CURVE (SM4, MAJOR GRABENS, 0.5g)

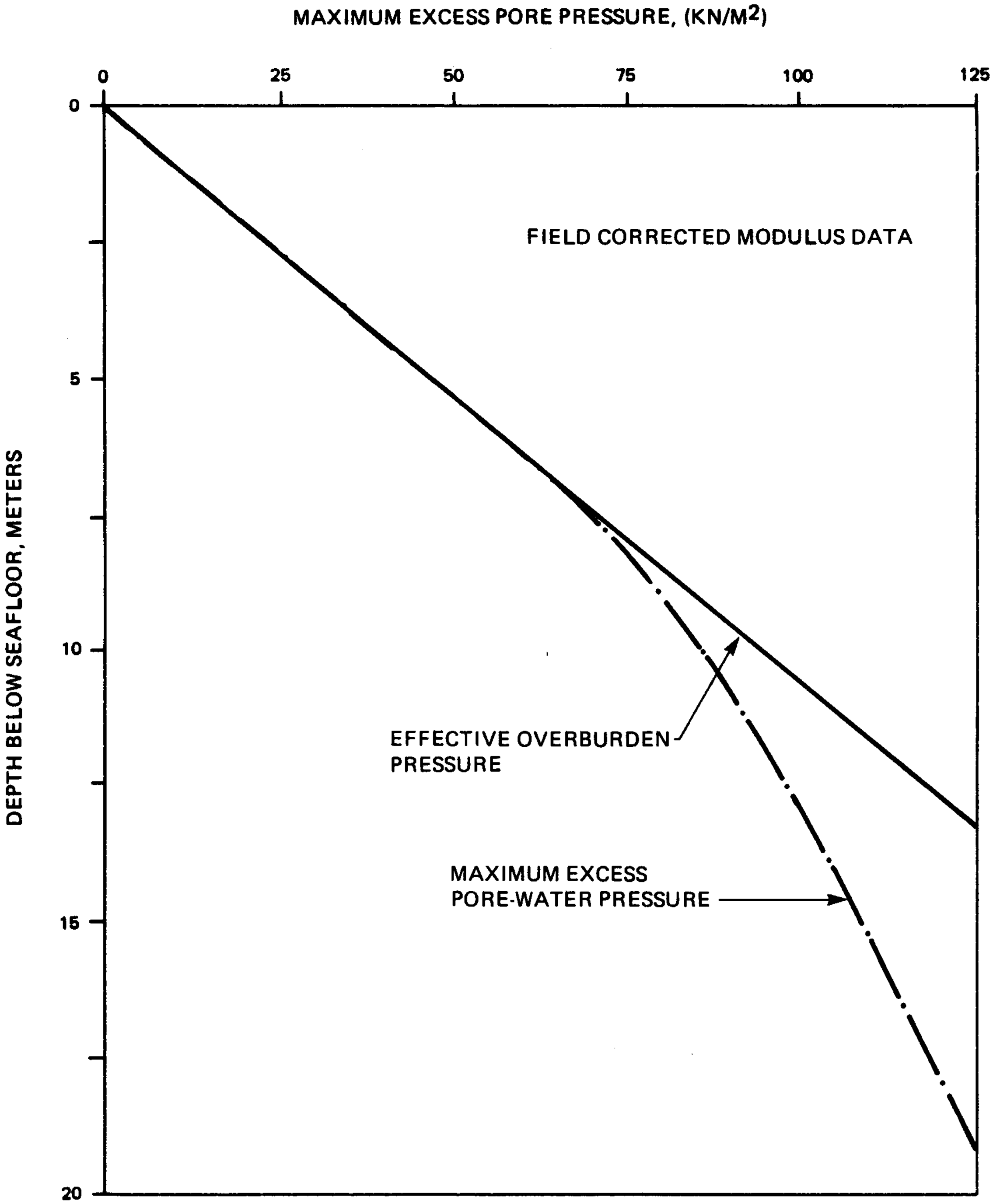

SOIL TYPE SM (4)

EARTHQUAKE SOURCE MAJOR GRABENS

EARTHQUAKE RECORD (NORMALIZED TO Amax = 0.7g) TAFT 1952

MAXIMUM GROUND ACCELERATION = Amax

CONCLUSION: LIQUEFACTION TO 8 M

FIGURE IV-45 MAXIMUM EXCESS PORE PRESSURE RESPONSE CURVE (SM4, MAJOR GRABENS, 0.7g)

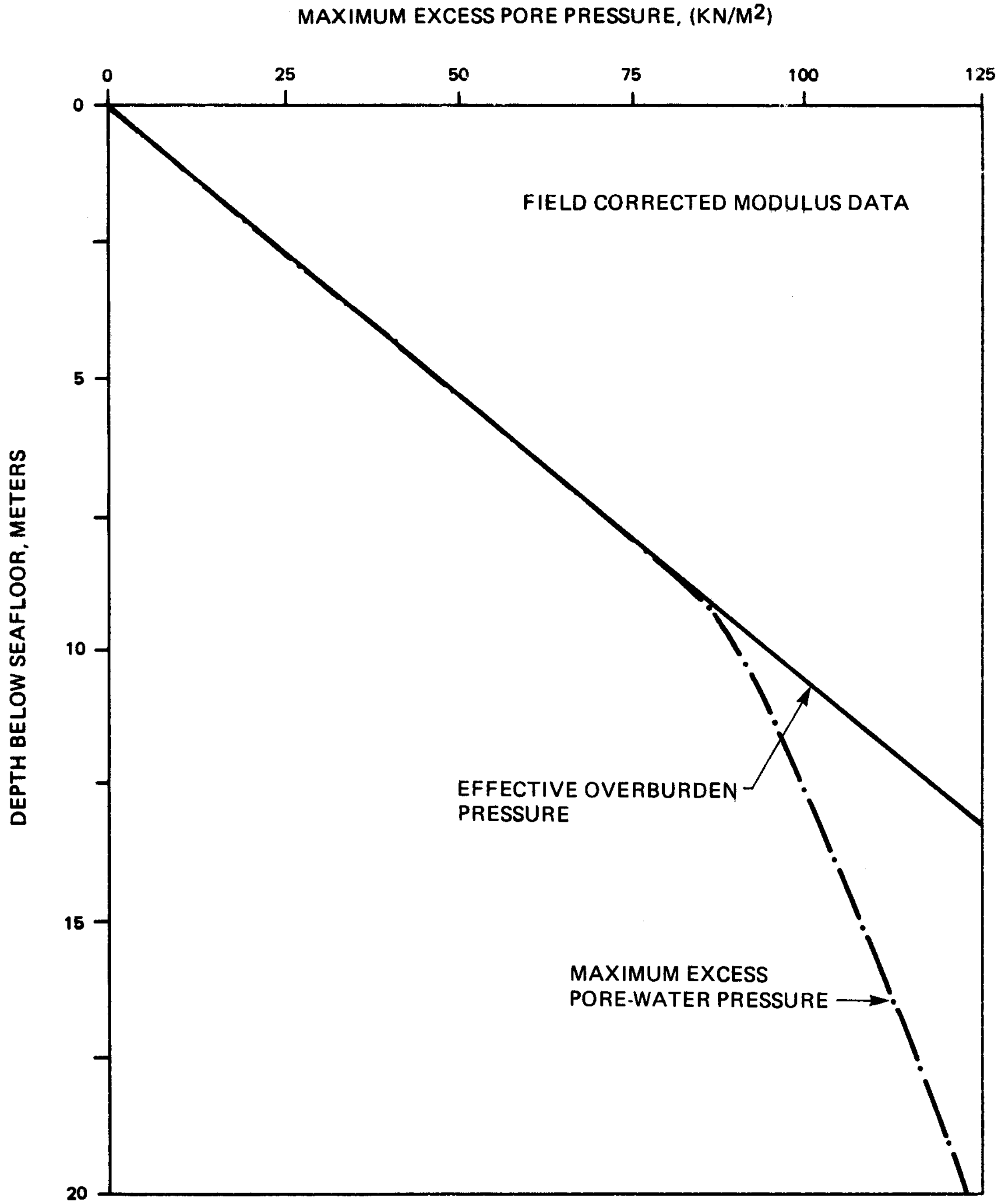

SOIL TYPE SM (4)

EARTHQUAKE SOURCE MAJOR GRABENS

EARTHQUAKE RECORD (NORMALIZED TO Amax = 0.7g) EL CENTRO 1940

MAXIMUM GROUND ACCELERATION = Amax

CONCLUSION: LIQUEFACTION TO 9 M

FIGURE IV-46 MAXIMUM EXCESS PORE PRESSURE RESPONSE CURVE (SM4, MAJOR GRABENS, 0.7g)

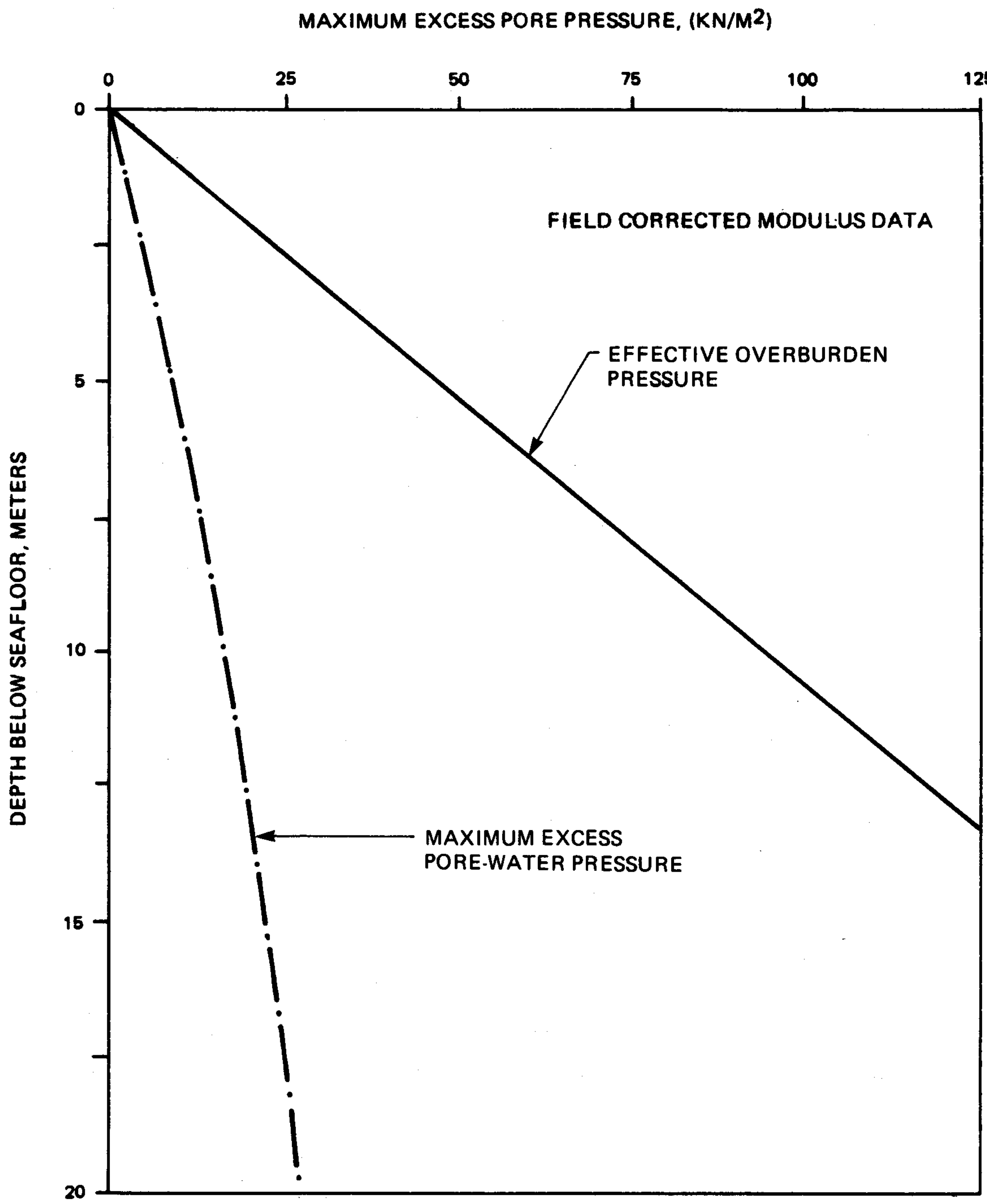

SOIL TYPE SM (4)

EARTHQUAKE SOURCE BACK ARC FAULTS

EARTHQUAKE RECORD (NORMALIZED TO Amax = 0.3g) EL CENTRO 1979

MAXIMUM GROUND ACCELERATION = Amax

CONCLUSION: NO LIQUEFACTION

FIGURE IV-47 MAXIMUM EXCESS PORE PRESSURE RESPONSE CURVE (SM4, BACK ARC FAULTS, 0.3g)

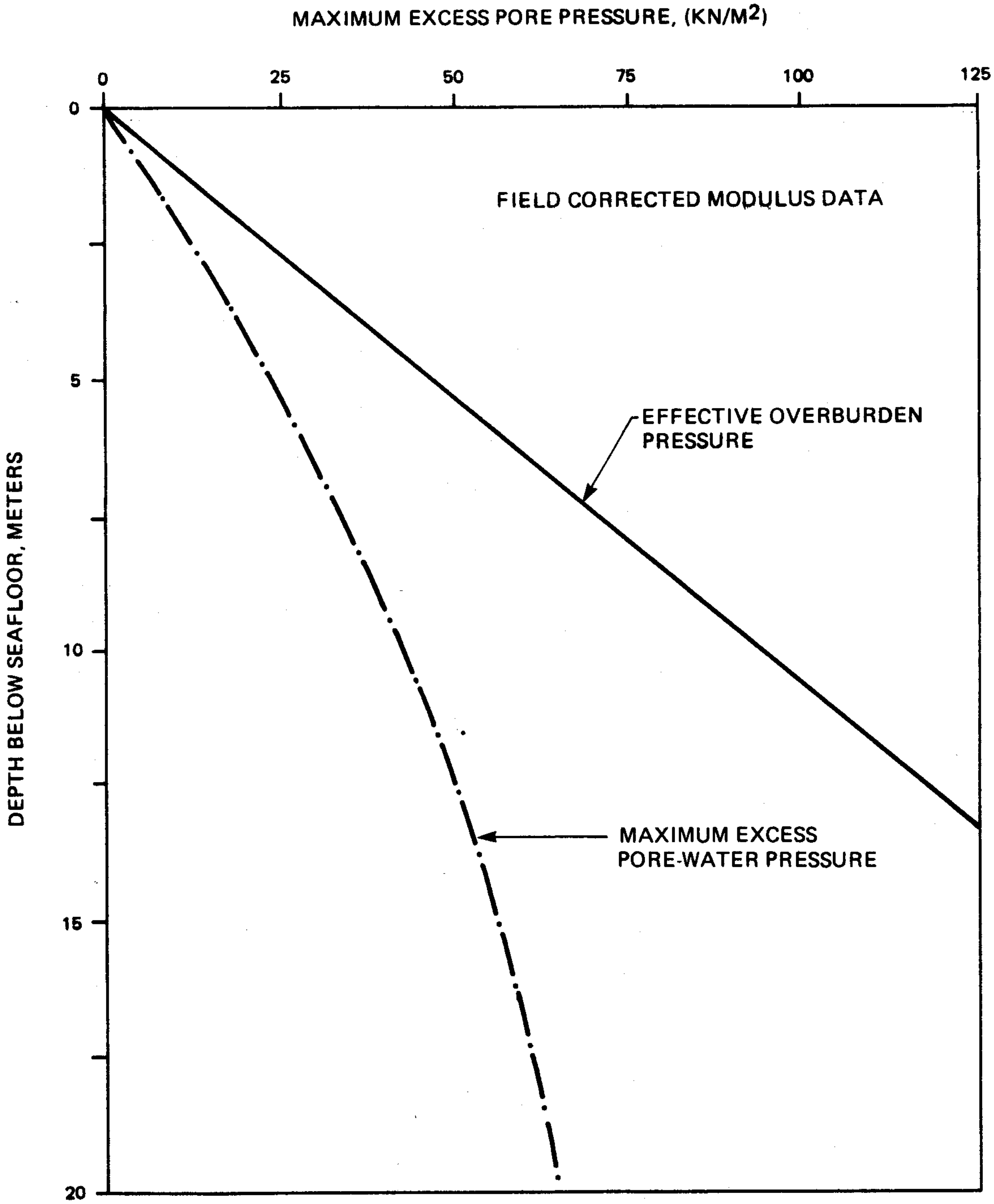

SOIL TYPE SM (4)

EARTHQUAKE SOURCE BACK ARC FAULTS

EARTHQUAKE RECORD (NORMALIZED TO Amax = 0.6g) EL CENTRO 1979

MAXIMUM GROUND ACCELERATION = Amax

CONCLUSION: NO LIQUEFACTION

FIGURE IV-48 MAXIMUM EXCESS PORE PRESSURE RESPONSE CURVE (SM4, BACK ARC FAULTS, 0.6g)

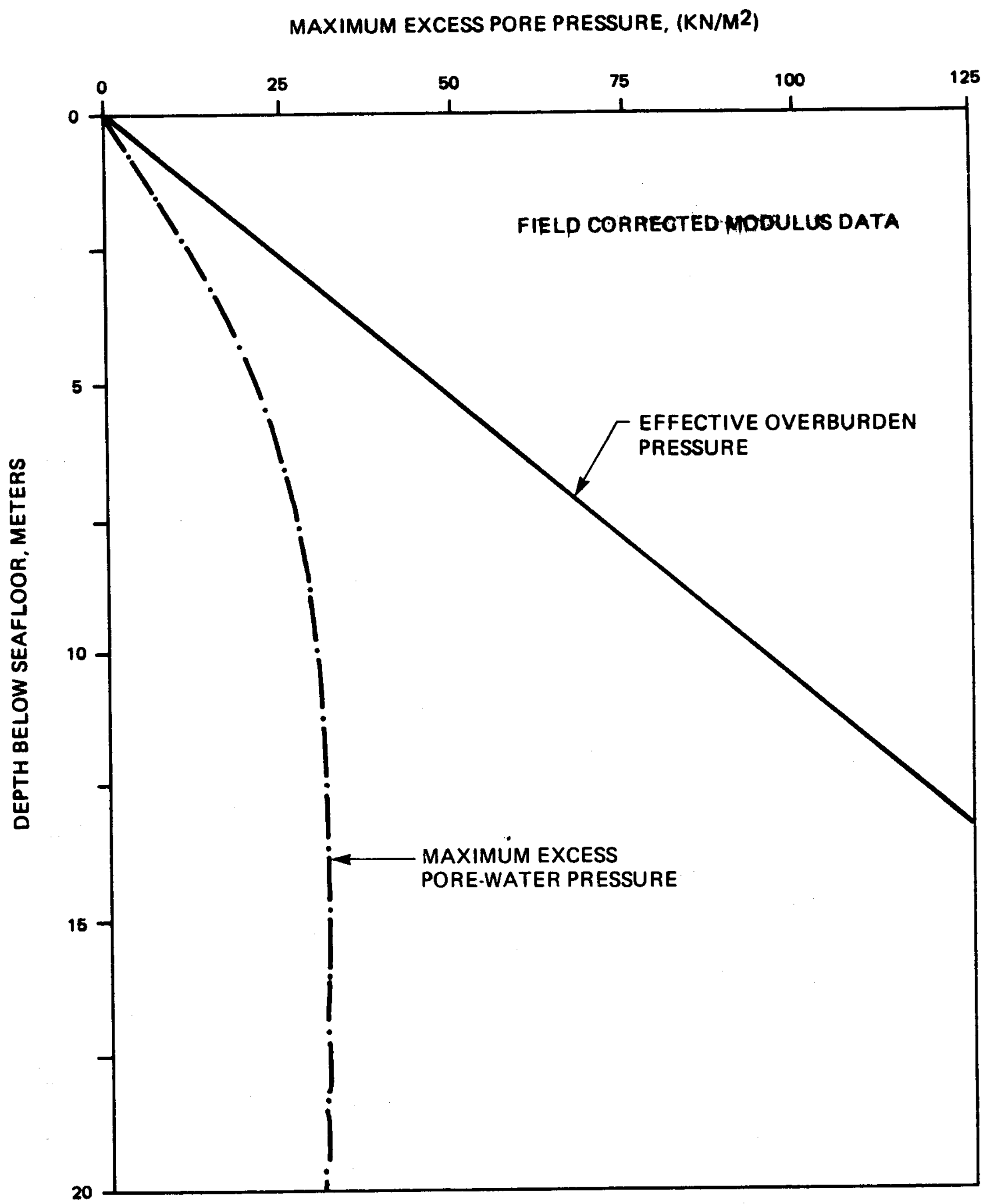

SOIL TYPE SM (4)

EARTHQUAKE SOURCE ALEUTIAN ARC

EARTHQUAKE RECORD (NORMALIZED TO Amax = 0.4g) PARKFIELD 1966

MAXIMUM GROUND ACCELERATION = Amax

CONCLUSION: NO LIQUEFACTION

FIGURE IV-49 MAXIMUM EXCESS PORE PRESSURE RESPONSE CURVE (SM4, ALEUTIAN ARC, 0.4g)

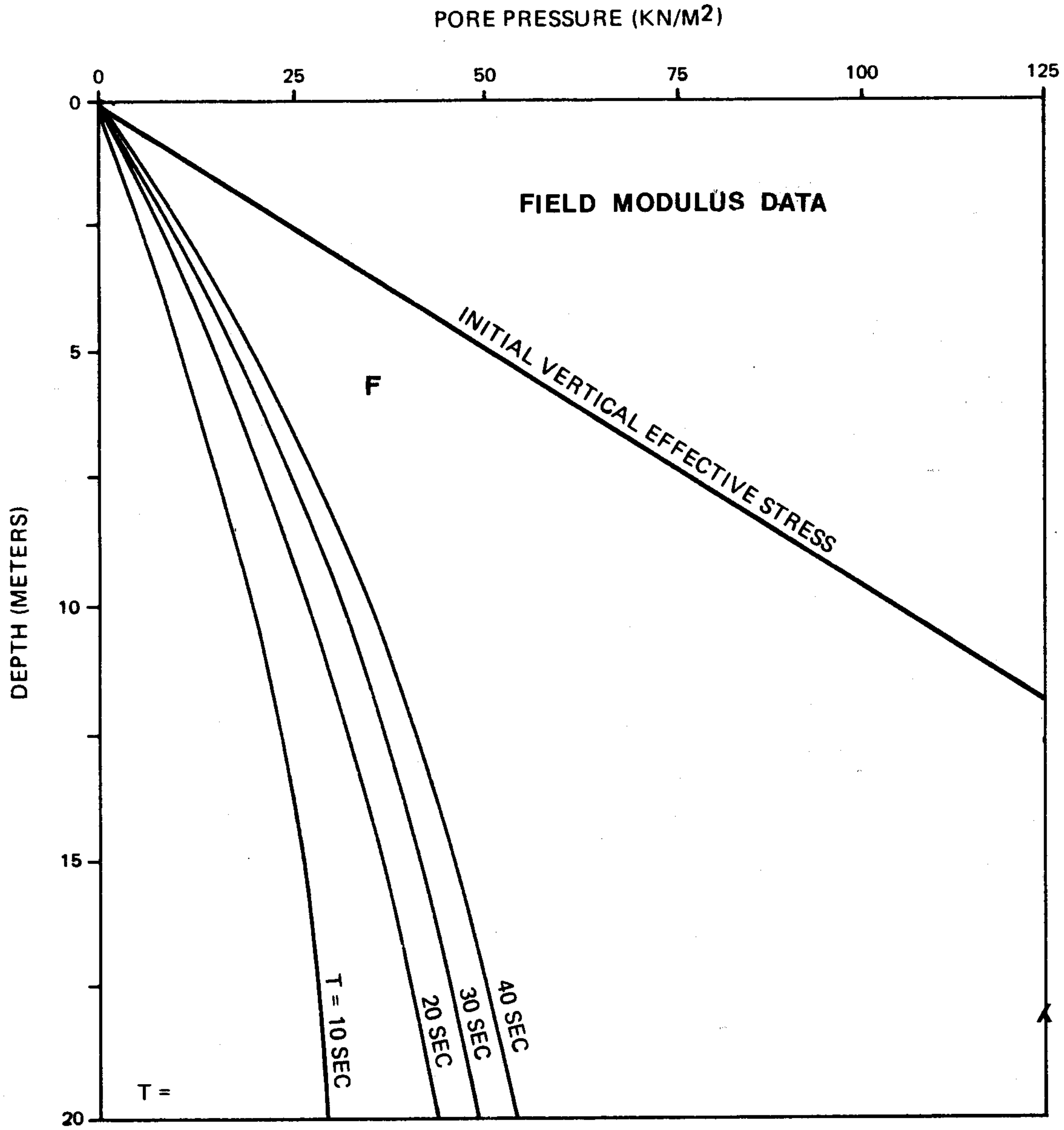

SOIL TYPE (PROFILE) SP (2)

EARTHQUAKE SOURCE SUBDUCTION ZONE

EARTHQUAKE RECORD (NORMALIZED TO Amax = 0.16g) CAL TECH A-1

MAXIMUM GROUND ACCELERATION Amax

CONCLUSION: **NO LIQUEFACTION**

FIGURE IV-50 PORE PRESSURE RESPONSE CURVES (SP2, SUBDUCTION ZONE, 0.16g)

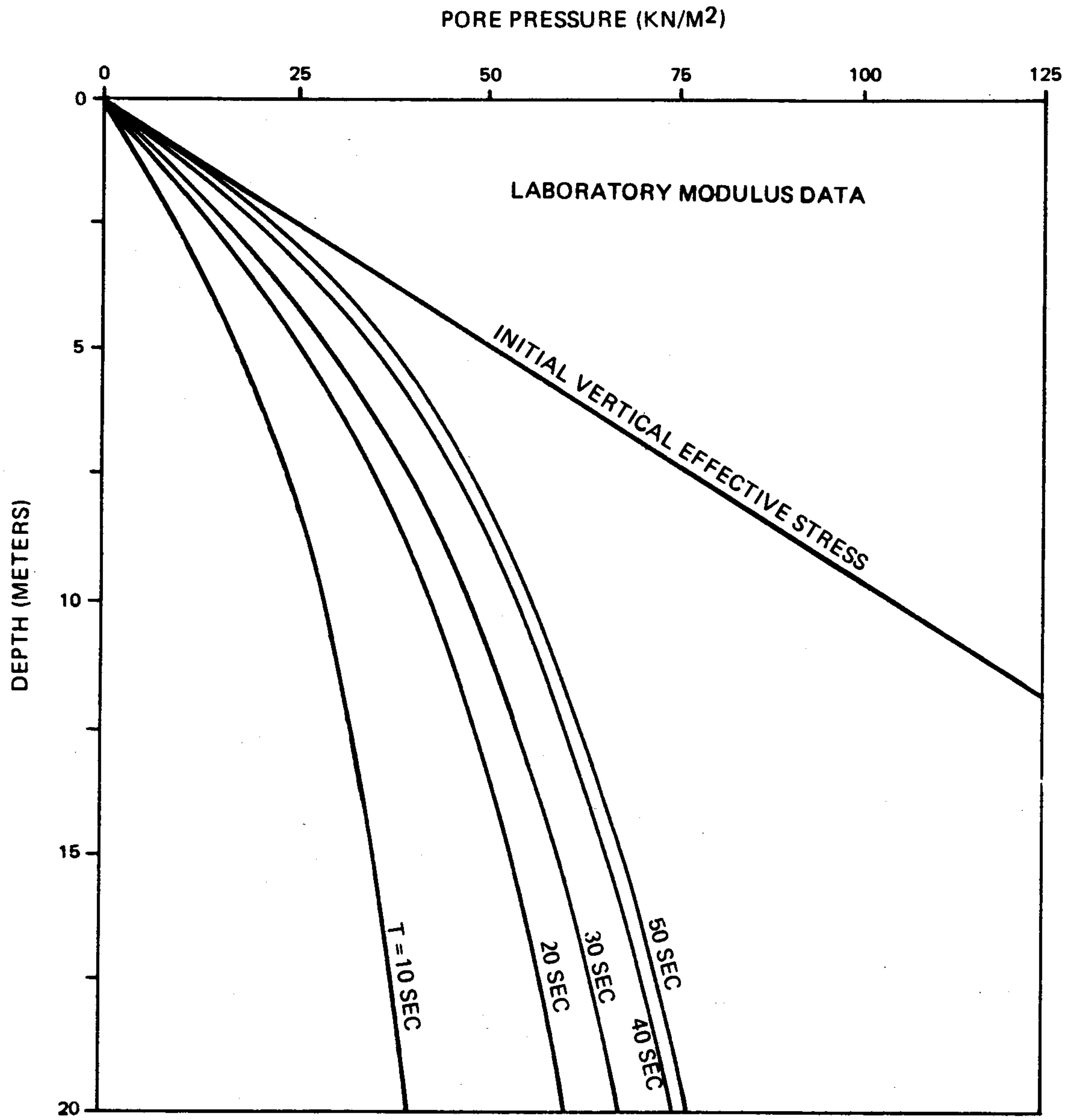

SOIL TYPE (PROFILE) SP (2)

EARTHQUAKE SOURCE SUBDUCTION ZONE

EARTHQUAKE RECORD (NORMALIZED TO Amax = 0.16g) CAL TECH A-1

MAXIMUM GROUND ACCELERATION = Amax

CONCLUSION: LIQUEFACTION TO 1 M

FIGURE IV-51 PORE PRESSURE RESPONSE CURVES (SP2, SUBDUCTION ZONE, 0.16g)

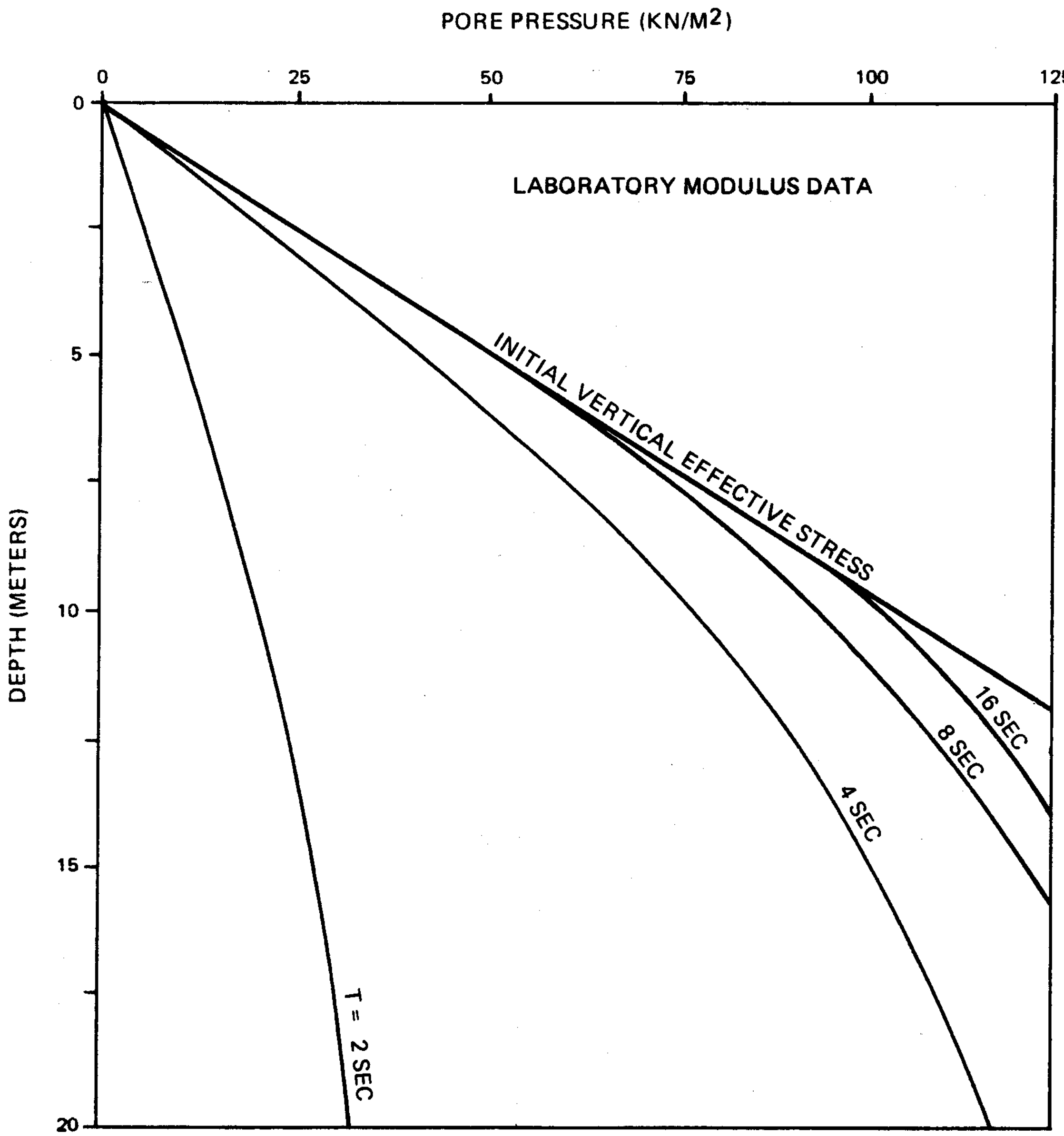

SOIL TYPE (PROFILE) SP (2)

EARTHQUAKE SOURCE MAJOR GRABENS

EARTHQUAKE RECORD (NORMALIZED TO Amax = 0.7g) EL CENTRO 1940

MAXIMUM GROUND ACCELERATION = Amax

CONCLUSION: LIQUEFACTION TO >8 M

FIGURE IV-52 PORE PRESSURE RESPONSE CURVES (SP2, MAJOR GRABENS, 0.7g)

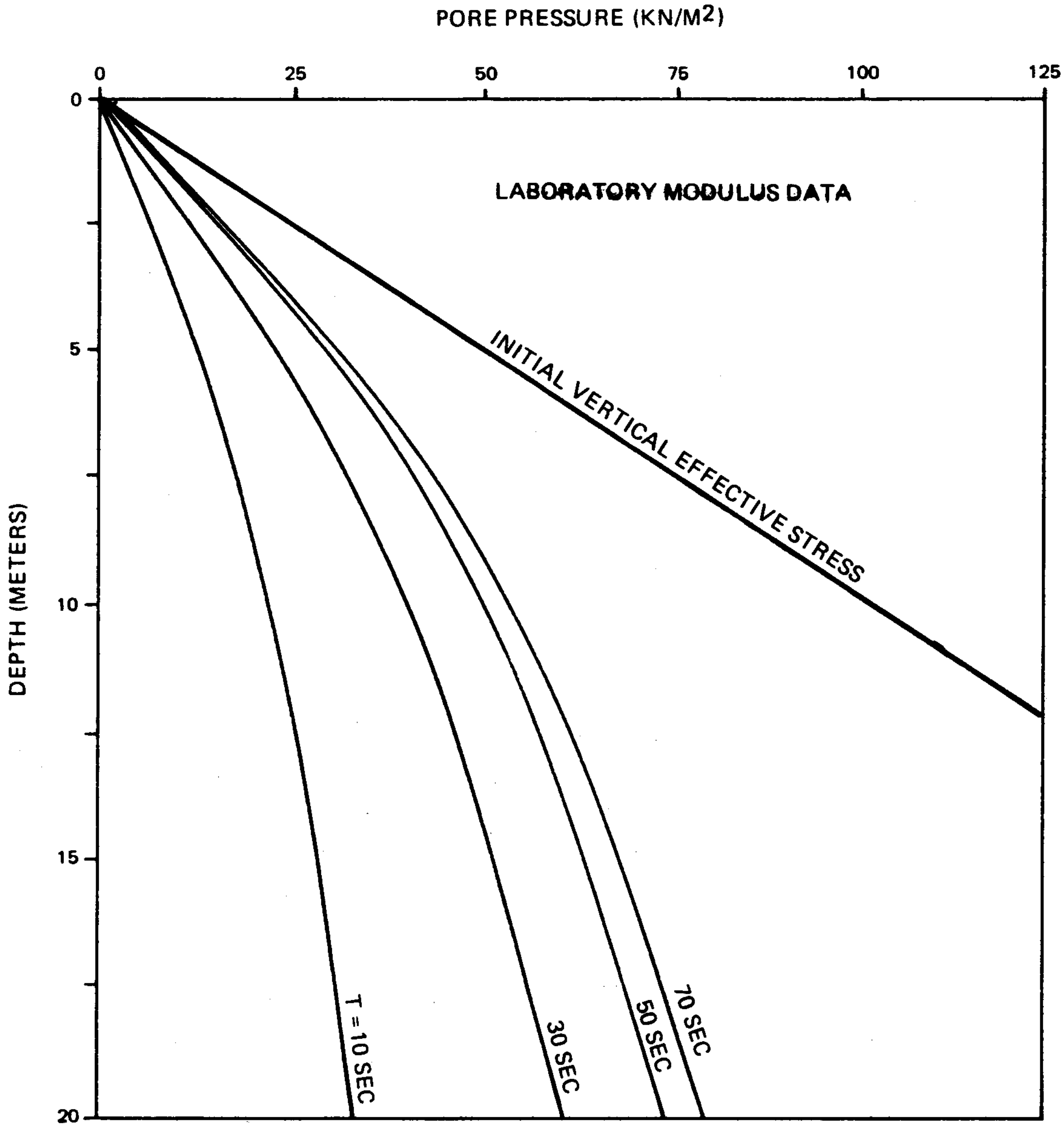

SOIL TYPE (PROFILE) SP/SM (3)

EARTHQUAKE SOURCE SUBDUCTION ZONE

EARTHQUAKE RECORD (NORMALIZED TO Amax = 0.16g) CAL TECH A-1

MAXIMUM GROUND ACCELERATION = Amax

CONCLUSION: NO LIQUEFACTION

FIGURE IV-53 PORE PRESSURE RESPONSE CURVES (SP/SM3, SUBDUCTION ZONE, 0.16g)

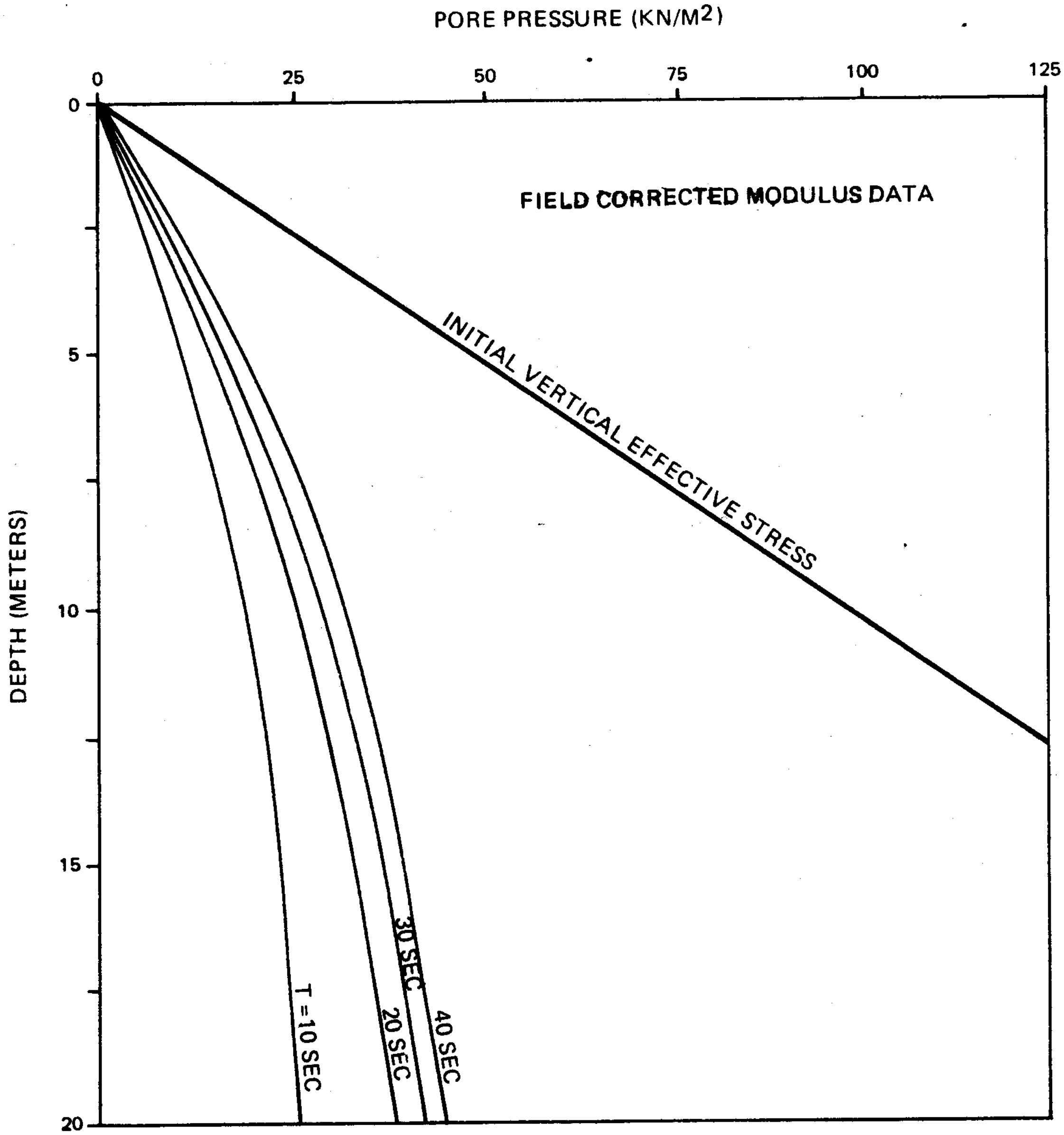

SOIL TYPE (PROFILE) SM (4)

EARTHQUAKE SOURCE SUBDUCTION ZONE

EARTHQUAKE RECORD (NORMALIZED TO Amax = 0.16g) CAL TECH A-1

MAXIMUM GROUND ACCELERATION = Amax

CONCLUSION: NO LIQUEFACTION

FIGURE IV-54 PORE PRESSURE RESPONSE CURVES (SM4, SUBDUCTION ZONE, 0.16g)

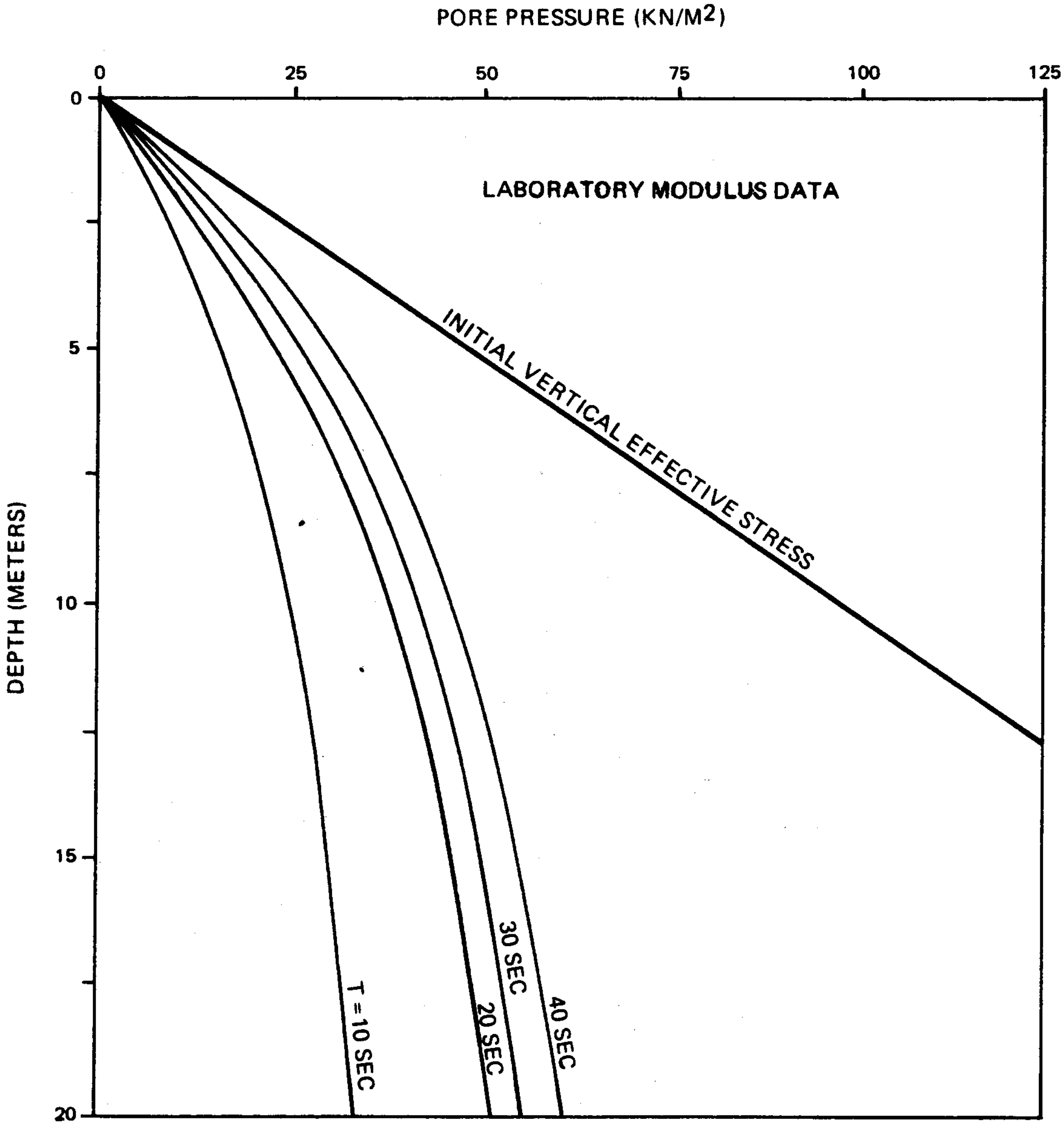

SOIL TYPE (PROFILE) SM (4)

EARTHQUAKE SOURCE SUBDUCTION ZONE

EARTHQUAKE RECORD (NORMALIZED TO Amax = 0.16g) CAL TECH A-1

MAXIMUM GROUND ACCELERATION = Amax

CONCLUSION: NO LIQUEFACTION

FIGURE IV-55 PORE PRESSURE RESPONSE CURVES (SM4, SUBDUCTION ZONE, 0.16g)

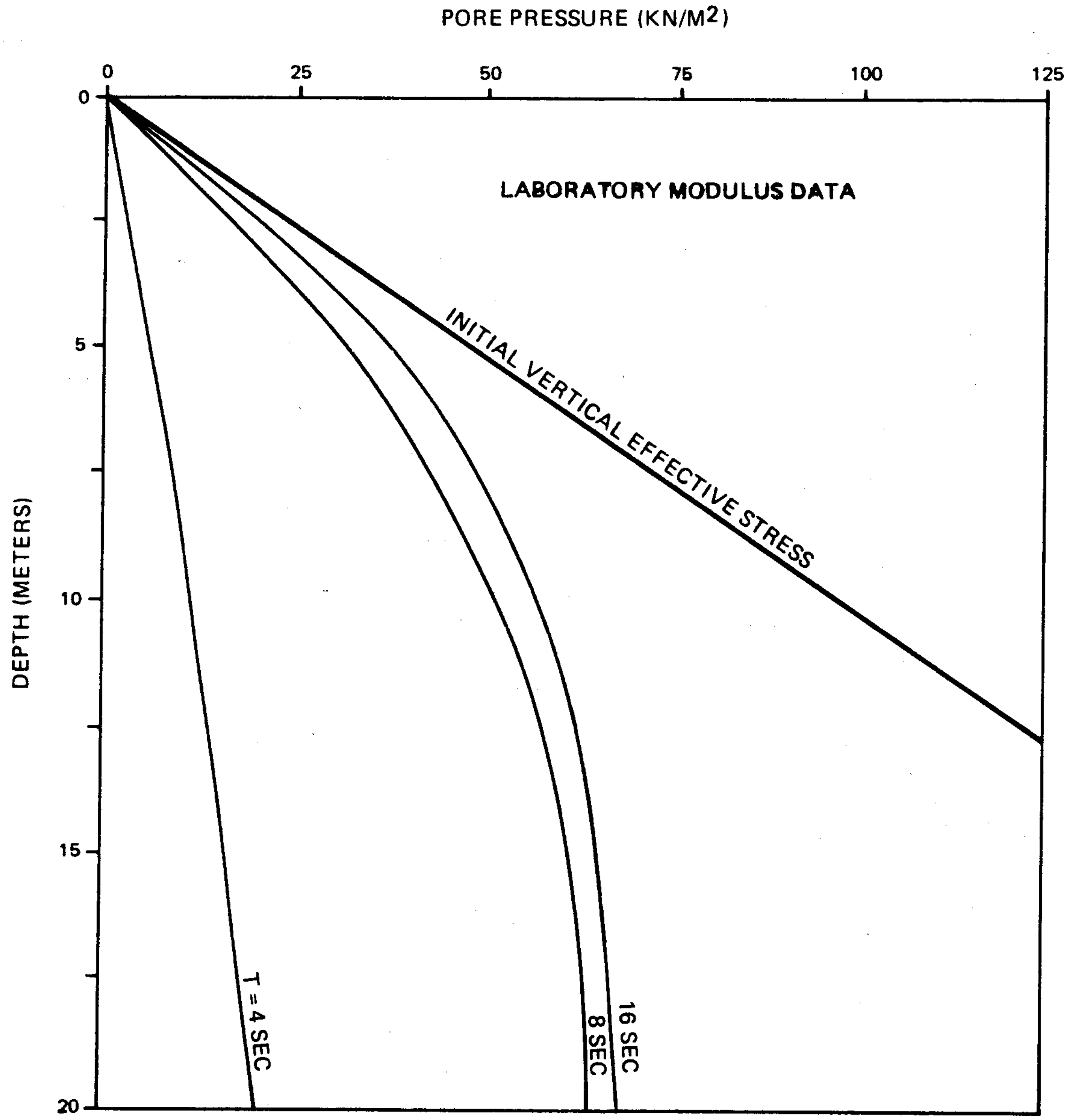

SOIL TYPE (PROFILE) SM (4)

EARTHQUAKE SOURCE MAJOR GRABENS

EARTHQUAKE RECORD (NORMALIZED TO Amax = 0.4g) TAFT 1952

MAXIMUM GROUND ACCELERATION = Amax

CONCLUSION: NO LIQUEFACTION

FIGURE IV-56 PORE PRESSURE RESPONSE CURVES (SM4, MAJOR GRABENS, 0.4g)

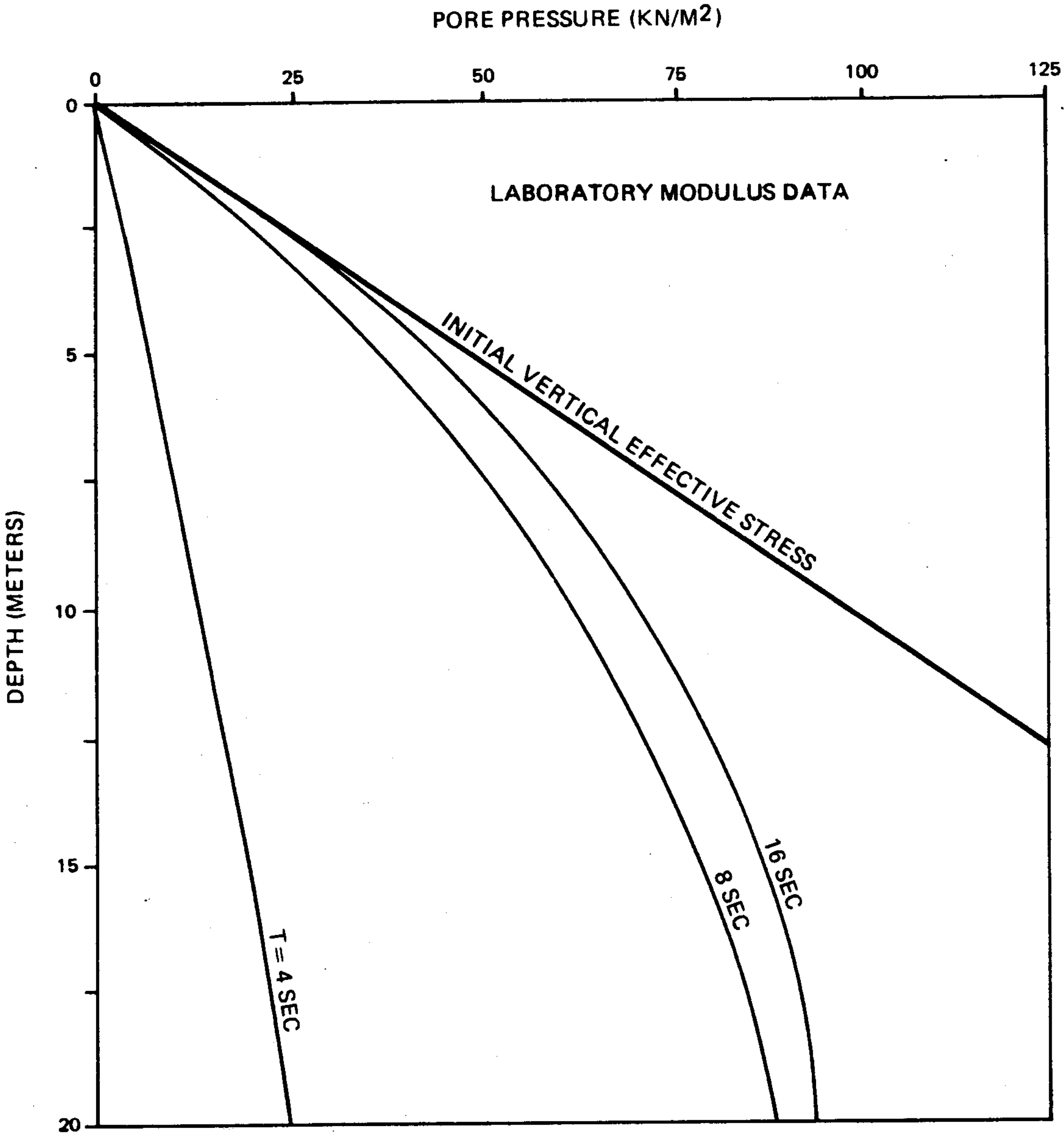

SOIL TYPE (PROFILE) SM (4)

EARTHQUAKE SOURCE MAJOR GRABENS

EARTHQUAKE RECORD (NORMALIZED TO Amax = 0.5g) TAFT 1952

MAXIMUM GROUND ACCELERATION = Amax

CONCLUSION: LIQUEFACTION TO 3 M

FIGURE IV-57 PORE PRESSURE RESPONSE CURVES (SM4, MAJOR GRABENS, 0.5g)

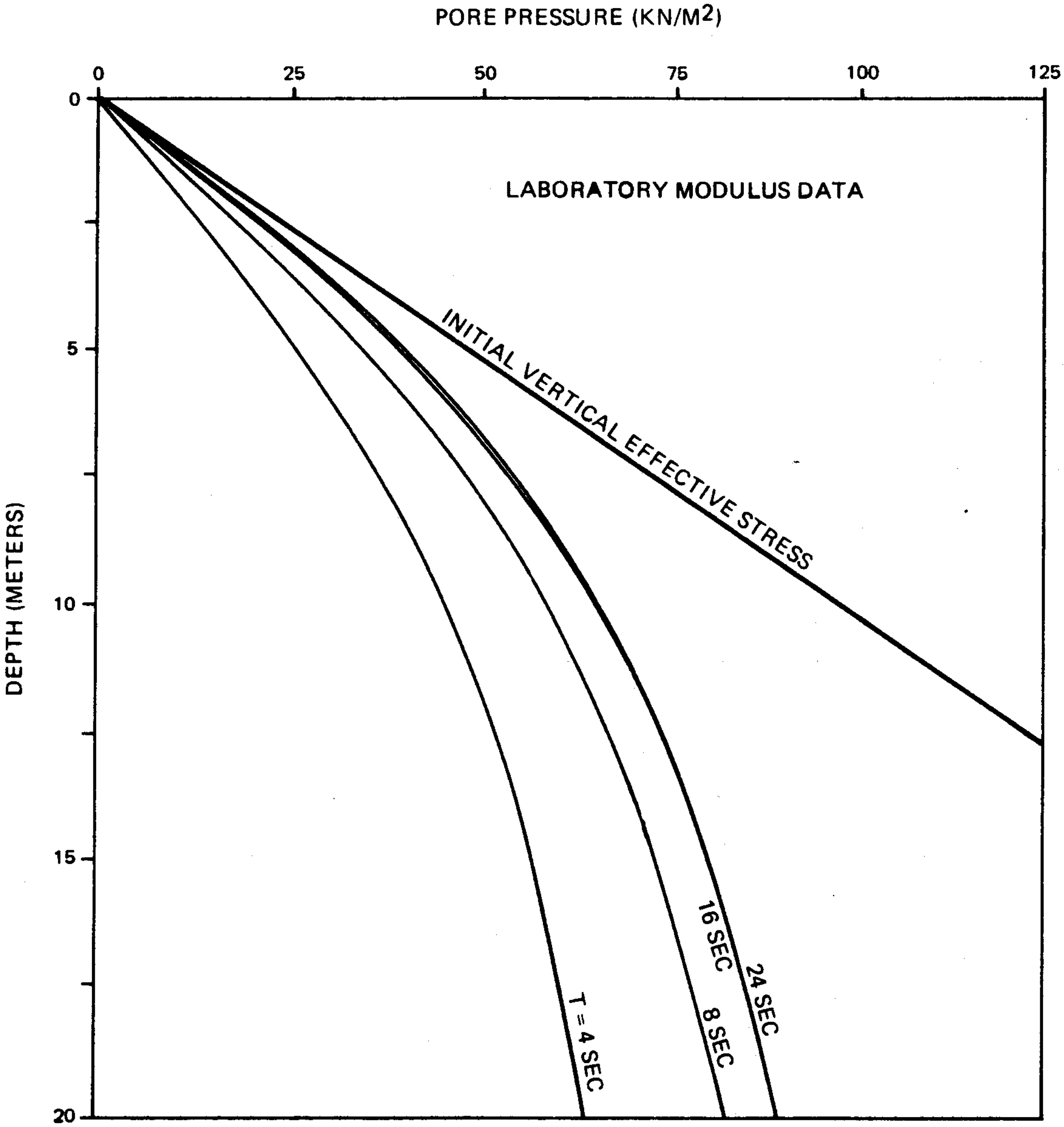

SOIL TYPE (PROFILE) SM (4)

EARTHQUAKE SOURCE MAJOR GRABENS

EARTHQUAKE RECORD (NORMALIZED TO Amax = 0.5g) EL CENTRO 1940

MAXIMUM GROUND ACCELERATION = Amax

CONCLUSION: NO LIQUEFACTION

FIGURE IV-58 PORE PRESSURE RESPONSE CURVES (SM4, MAJOR GRABENS, 0.5g)

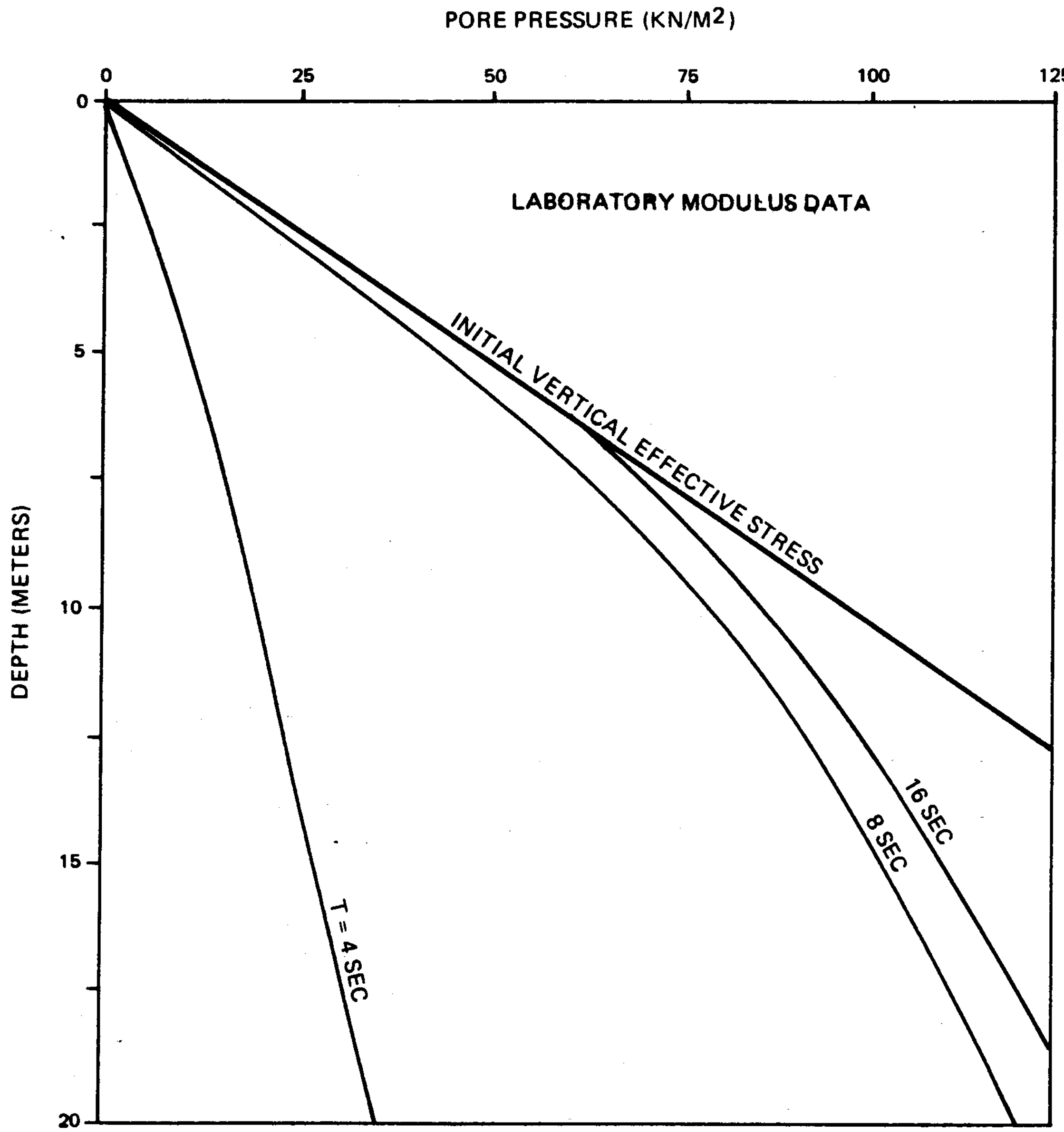

SOIL TYPE (PROFILE) SM (4)

EARTHQUAKE SOURCE MAJOR GRABENS

EARTHQUAKE RECORD (NORMALIZED TO Amax = 0.7 g) TAFT 1952

MAXIMUM GROUND ACCELERATION = Amax

CONCLUSION: LIQUEFACTION TO >7M

FIGURE IV-59 PORE PRESSURE RESPONSE CURVES (SM4, MAJOR GRABENS, 0.7g)

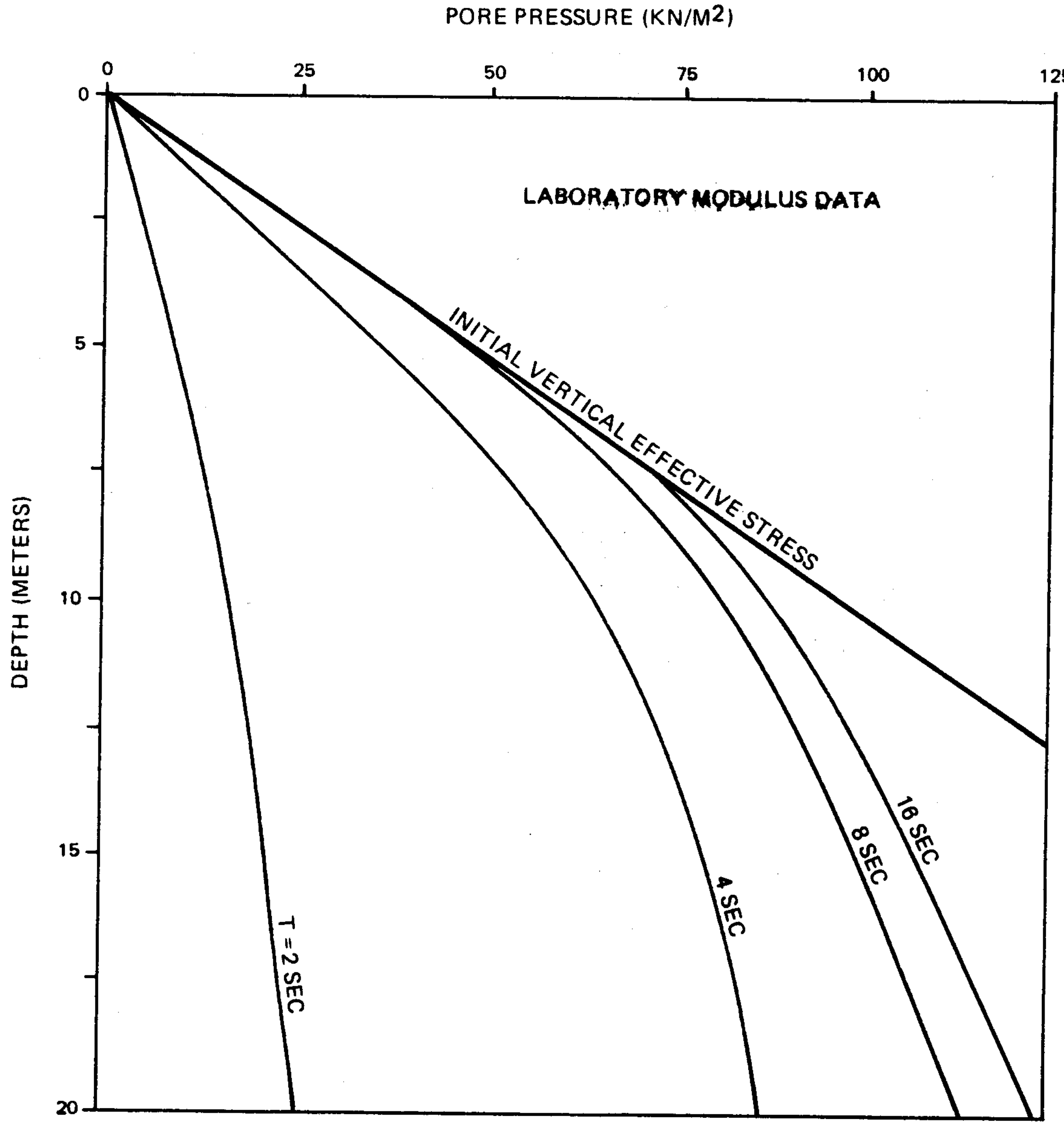

SOIL TYPE (PROFILE) SM (4)

EARTHQUAKE SOURCE MAJOR GRABENS

EARTHQUAKE RECORD (NORMALIZED TO Amax = 0.7g) EL CENTRO 1940

MAXIMUM GROUND ACCELERATION = Amax

CONCLUSION: LIQUEFACTION TO > 7M

FIGURE IV-60 PORE PRESSURE RESPONSE CURVES (SM4, MAJOR GRABENS, 0.7g)

GEOLOGIC PROCESSES AND HAZARDS OF THE BEAUFORT AND CHUKCHI SEA SHELF AND COASTAL REGIONS

by

Larry Phillips
Peter Barnes
Erk Reimnitz
Ralph Hunter

U.S. Geological Survey

Final Report
Outer Continental Shelf Environmental Assessment Program
Research Unit 205

October 1985

TABLE OF CONTENTS

OVERVIEW

I. Summary of objectives, conclusions and implications with respect to OCS oil and gas development.

This study presents a continuation and expansion of our investigations of the arctic marine sedimentary environments off northern Alaska. We have concentrated within this report on understanding shelf processes within the chukchi Sea, correlating the shallow shelf stratigraphy on part of the Beaufort Sea, understanding rates of coastal erosion and shoreline evolution along the Beaufort coast, and on the rates of sediment disruption by sea ice and character of ice gouges in the Beaufort Sea. The observations, conclusions and implications of our studies summarizing these varied arctic environments are included in the following (The letters key to full topic discussions as attachments to this report):

A. Reconnaissance geophysical surveys of the Chukchi Sea show that a thin sediment cover, generally less than 6 m thick, overlies folded bedrock over much of the shelf and that locally on the northwest part of the shelf an extensive filled channel system exists. The channels record a complex fill-history apparently related to multiple sea level changes. Side-scan sonar surveys record abundant ice gouging within the Barrow Sea Valley with decreasing gouge abundance occurring on the western shelf. Currents may rapidly fill in the gouges on parts of the shelf. The side-scan sonar surveys also define areas where both gray whales and walrus are feeding on the sea floor surface. The benthic mammal feeding areas are identified in regions containing sand and gravel along the eastern part of the shelf in areas dominated by the Alaska Coastal Current. Extensive gravel bedform fields also exist on the outer shelf to depths of 49 m suggesting that storm-generated currents do rework the shelf sediments but the periodicity of the storm events is unknown. Box cores show that the shelf surficial sediments on the outer shelf consist of mud or gravelly mud, whereas, the inner shelf is composed of sand and gravel. Bioturbation is abundant in all cores.

B. Gas samples from box cores in the Chukchi Sea contain light hydrocarbons but they are present in low concentations in the surface sediments and are likely the result of biological processes.

C. Coastline erosion for part of the Beaufort Sea Coast records an average rate of 2.5 m/yr. In places the local long-term erosion can be up to 18 m/yr, while accretion rates near the active mouths of the Colville River are as high as 20 m/yr. The texture of the coastal plain sediments apparently control s the erosion rates with fine-grained mud averaging high erosion rates of 5.4 m/yr, whereas, sandy to gravelly deposits erode at 1.4 m/yr. The difference in erosion rates suggests that the grain size of the bluff material exerts the dominate control on the coastal retreat rates.

D. Investigations of the inner shelf seismic stratigraphy between the Canning River and Prudhoe Bay identify four unconformities in the subsurface strata as well as one on the present erosional sea floor surface. Identified seismic horizons within the western study area can be correlated with stratigraphic interpretations of more than 20 offshore boreholes. This then allows correlation of the unconformable surfaces to transgressive events.

E. Observations and measurements on recently formed ice gouges in eastern Harrison Bay indicate significant variability from year to year in ice gouge processes based on their number, size, and distribution. Ice gouge recurrence rates show that 3.7% of the sea floor is disrupted each year. This suggests that approximately 50% of the sea floor can be reworked in 20 years. Within the study area, in water depths of 5-16 m, gouges > 1 m deep occur every 6+ years and account for 0.1-0.2% of all gouges in this area. In water depths > 10 m the sea floor can be completely disrupted to a depth of 1 m in approximately 800 years.

F. Repetitive side-scan sonar surveys between 1975 and 1980 in the Beaufort sea were used to assess sea floor changes due to ice gouging along 8 shore-perpendicular corridors. The percentage of sea floor area impacted annually by ice keels increases from the coast seaward to at least the 25 m isobath. Up to 6.8% of the total sea bed area scanned along the 15 km long corridors was disrupted in a single year. Total sea floor disruption in single km-long segments ranged as high as 60 %. High gouge densities are associated with wide, shallow "multiplet" gouging events, where long sections of pressure-ridge keels raked the bottom. Small annual variations in the amount and intensity of new gouges indicate rather consistent reworking of the inner shelf by this process.

II. Introduction

A. General nature and scope of study

High-latitude continental shelves, where ice is present seasonally, comprise 25 percent of the total world shelf area. Yet the interaction of ice in the region of sedimentary processes and the influence of geology on the ice regime on North American arctic shelves and coasts is poorly understood. Investigations of the continental shelf and shores of the Chukchi and Beaufort Seas was initiated in 1970. The primary goal of this program has been to understand the processes unique to arctic coasts and shelves.

B. Specific objectives

Many questions have been raised on the basis of our past investigations, which apparently hold the key to an understanding of the seasonal cycle in the marine environment. It is these tasks that we address in our current research.

1. Location and extent of sea floor ice gouging, especially the maximum extent and intensity of modern ice gouging, including densities, depths, and directions of gouges, and statistical distribution of ice gouge depths.

2. Recent changes in bathymetry and shelf-edge morphology which may be related to shelf sediment transport by ice or other means.

3. Profiles of shallow sediment structures in selected regions with emphasis on studies that will provide information on past history of ice involvement with the sea floor and the potential for the presence of sand and gravel.

4. Develop cooperative studies with Canadian geoscientists to assess similarities and differences concerning ice seabed interactions on the Alaskan and Canadian Beaufort shelves.

C. Relevance to problems of petroleum development

The character of the arctic continental shelf and coastal area, with year round and seasonal sea ice and with permafrost, faces the developer with many special problems. The interaction of the arctic shelf with the arctic pack ice takes the form of ice gouging and the formation of a large stamukhi zone each winter. Furthermore, ice zonation is determined by sea bed morphology and textural character.

Oil drilling and production during the next several years will probably extend into the stamukhi zone seaward of the seasonal fast-ice zone. Of critical concern are ice gouging, ice zonation, strudel scour, storm-generated currents on the Chukchi shelf, and sand and gravel sources; all related to sea bed morpholgy and sea bed character. These are of concern to the government, in that an adequate understanding of arctic processes is needed to assure safe development and adequate environmental protection. Any structure which is to be mated with the ocean floor requires data concerning the strength and character of the ocean floor and its effect on the ice canopy. Likewise, the strength and effects of storm-generated currents is also unknown. Foundation materials in the form of gravels will be needed for work pads offshore. In addition, the offshore drilling operation may encounter unsupportive sediments with permafrost and associated gas hydrates which could be substantially altered during the process of pumping hot oil up to the sea floor or along the sea floor in gathering and transportation pipe lines.

III. Current state of knowledge

The current state of knowledge for the Beaufort Sea is summarized within this report. The availability of only small boats for the past field efforts has resulted in knowledge biasing the coastal regions, the very inner fringe of the continental shelf rather than the whole outer continental shelf.

On the middle and outer shelf big ship geophysical studies by the USGS provided considerable knowledge on structural framework, the stratigraphy, and certain hazards such as slumping. But very little work has been done here along the lines of research we and others conduct on modern processes and hazards relevant to the seaward thrust of petroleum development.

The current state of knowledge for the Chukchi Sea is increasing and to date approximately 50 percent of the shelf lease areas have been covered in reconnaisance studies. Ice gouging, migrating bedforms and sand banks, strong currents both coastal and storm-generated, and extensive filled paleochannels possibly containing permafrost or gas are hazards identified to date on the Chukchi shelf. North of 71°, however, limited data exists. The northern shelf will contain the most extensive ice gouged terrane on the Chukchi Sea shelf as well as contain extensive slump terranes. Large ship operations and favorable ice conditions are needed to complete the studies of the northern Chukchi Sea shelf.

IV. Study area

A. Chukchi Sea--The Alaska mainland between Cape Lisburne and Point Barrow slopes generally northward. The southern part of the mainland is hilly, whereas the northern part is a gently sloping coastal plain. The edge of the mainland, which faces the open sea in some places and faces lagoons, bays or barrier spits elsewhere, is marked in most places by cliffs or bluffs, which tend to gradually decrease in height northward. Barrier islands and spits are extensive along the Chukchi Sea coast from Point Barrow, Point Franklin, and Icy Cape, three of the major capes along this coastline.

Much of the Chukchi Sea north of Point Hope consists of a broad, nearly flat, shallow shelf. The average depth is 50 m. Herald Shoal, which lies in the central shelf area, rises up to 14 m depth; Hanna Shoal, on the northern part of the shelf, rises to approximately 20 m depth. The Barrow Sea Valley lies near the northern edge of the shelf. Nearshore, in depths less than 25 m, shore-parallel shoals are developed off the capes. Actively migrating longshore bars form adjacent to the beaches.

The high sea cliffs at and near Cape Lisburne are cut in bedrock of Permian and Triassic age. Cretaceous bedrock, mostly sandstone and shale, forms the sea cliffs aroung Ledyard Bay, east of Cape Lisburne. Cretaceous bedrock is exposed in the lower parts of sea cliffs as far north as Skull Cliff, between Peard Bay and Barrow. The upper parts of the sea cliffs at Skull Cliff and elsewhere on the coastal plain are made up of unconsolidated Quaternary deposits.

Tidal currents, storm currents and the offshore, shore-parallel Alaska Coastal Current modify the sea floor along the eastern Chukchi Sea by erosion and transportation of sediment as migrating bedforms. The nearshore currents are generated mostly by winds, and the offshore region is dominated by northeast-directed storm currents and by the northeast-flowing Alaska Coastal Current.

The tides are small in the Chukchi Sea, and the tidal range along the eastern coast is generally less than 10 cm. The tides are of the semi-diurnal type. The tidal wave moves from north to south in the Chukchi Sea. Tide-generated currents can be expected to be of limited velocity along the open coast.

Storms during the summer months usually result in winds from the southwest which move across the Chukchi Sea. The maximum fetch then develops across the open water. The resulting storm waves and storm-generated currents may erode and scour the sea floor as well as result in intense sediment transport on the shelf and on the shoals.

Wind-generated currents are extremely variable both in velocity and in direction of movement for the nearshore region. The predominant summer winds are from the northeast, generating nearshore current velocities of 4 to 20 cm/sec. The wind generated currents generally follow the bottom contours. Daily variations in the current direction are reported for the nearshore region.

The Alaska Coastal Current represents a northeast flowing "warm" water mass derived from the Bering Sea. The current bifurcates at Cape Lisburne, one branch flowing north and the other branch flowing to the northeast parallel to the coast. The current varies in width and can be as narrow as 20 to 37 km. The velocities of the coastal current vary from 50 cm/sec. near Cape Lisburne, to 5 to 87 cm/sec. south of Icy Cape, to 55 cm/sec. north of Wainwright. Surface velocities of up to 200 cm/sec. and mid depth velocities of 70 cm/sec. are reported north of Wainwright. To the northwest of Wainwright near the Barrow Submarine Canyon head, a returning southwest-directed current is reported west of the Alaska Coastal Current with surface velocities of 80 cm/sec. The southwest-flowing current is poorly defined in space and time. Large clockwise rotating spiral currents are reported west of Barrow and may represent interaction between the Alaska Coastal Current and the westward flowing current of the Beaufort Gyre.

B. Beaufort Sea--The primary study area includes the Beaufort Sea shelf between Barter Island on the east and Point Barrow on the west with emphasis on an inshore segment between Flaxman Island and Cape Halkett. The adjacent land is a broad, flat coastal plain composed mainly of Quaternary deposits of tundra silts, sands, and gravels. In much of the area, the coast is being eroded by the sea at a rapid rate forming coastal bluffs as much as 6 m high. The line of bluffs is interrupted by low mud flats at the mouths of major rivers. Much of the coast is marked by islands at varying distances from the shore. Most of the islands are less than 3 m in elevation, narrow, and comprised of sand and gravel. Others are capped by tundra and are apparently erosional remnants of the inundated coastal plain. Coast-parallel shoals are also a feature of the inner shelf.

The shelf is generally rather flat and remains shallow for a considerable distance from shore. Off the Colville River the 2-m isobath is up to 12 km from shore. The width of the shelf is variable, ranging from, 55 km in the east to 110 km in the west. The shelf break lies at depths of 50 to 70 m. The shallowness of the shelf break and the presence of elevated Pleistocene beach lines suggests broad regional uplift. The Holocene marine sediments on the inner shelf are generally 5 to 10 m thick and composed of complex textural and compositional character. Ice and oceanographic factors interact to form a complex sediment section composed of wave and current-bedded sequences intensely churned and disrupted by ice.

The rivers flood in early June, delivering 50 to 80 percent of the yearly runoff in a 2-3 week period. The bulk of sediment input from rivers is associated with this flood. No river gravels presently reach the ocean. Initial flooding seaward of the river delta occurs on top of the unmelted sea ice, although the influx of warmer water eventually leads to ice-free areas off the deltas early in the sea-ice melt season. River drainage basins are located in the Brooks Range and the eastern rivers drain directly into the ocean while the western rivers meander across the broad coastal plain.

Sea ice is a ubiquitous feature in the study area. New ice starts to form in late September and grows to a thickness of 2 m through the winter, welding remnant older ice into more or less solid sheets. Where forces are sufficient, ice fractures and piles into hummocks and ridges. By June, sea-ice melting is well underway and usually sometime in July enough ice has melted so that the protected bays and lagoons are free of ice, and temperate latitude processes of waves and wind-driven currents are active. Ice remains on the shelf in the study area throughout the summer. Its location and concentration depend on the degree of melting and winds. The prevailing northeasterly wind tends to carry drifting summer ice away from the shore while the westerlies pile ice against the coast. Ice commonly remains grounded throughout the summer on many of the shoals on the inner shelf.

Currents and waves are a function of the winds during the open-water season. Waves are generally poorly developed due to the limited fetch which results from the presence of ice during most of the summer. Water circulation is dominated by the prevailing northeasterly winds which generate a westerly flow on the inner shelf. In winter, currents under the ice are generally sluggish although restrictions of the tidal prism by ice, at tidal inlets and on the broad, shallow, 2-m bench cause significantly higher velocities.

V. Sources, methods and rationale of data collection

A. Equipment operated routinely from the R/V KARLUK and other scientific vessels includes box cores, dredges, gravity and vibracores, water salinity, temperature and turbidity sensors, fathometers, a high and medium resolution seismic system, camera and TV system, and a side-scan sonar system. Precision navigation is maintained to 3 m accuracy with a range-range system.

Special techniques include (a) repetitive sonar and fathometer surveys of ice gouges, (b) diving observations and bottom photography, (c) measurements of sediment thicknesses within ice gouges by combined use of narrow beam echo sounder, and (d) a near-bottom tow package incorporating sub-bottom profiler and television, (e) nearsurface stratigraphic studies using a vibracores capable of obtaining 2 and 6 m long sediment cores, and (f) detailed surveys of bathymetry in river and lagoonal channels and in the vicinity of man-made structures. Coastal observations of rates of bluff erosion and the distribution and elevation of storm surge strand lines carried out by helicopters. Winter ice observations involve ice coring, diving observations along with modified system of upward-looking fathometer and side-scan sonar.

VI. Results, discussions and conclusions--(as attachments to this report)

A. Geologic investigations in the Chukchi Sea, 1984, NOAA ship SURVEYOR cruise.

B. Hydrocarbons in surface sediments of the Chukchi Sea.

C. Beaufort Sea coastal erosion, shoreline evolution and sediment flux.

D. Pleistocene and Holocene seismic stratigraphy between the Canning River and Prudhoe Bay, Alaska.

E. Temporal and spatial character of newly formed ice gouges in eastern Harrison Bay, Alaska, 1978-1982.

F. Rates of sediment disruption by sea ice as determined from characteristics of dated ice gouges created since 1975 on the inner shelf of the Beaufort Sea, Alaska.

VII. Needs for further study

As petroleum exploration and develpment continues to press into deeper water and further from shore in both the Beaufort and Chukchi Seas the geologic environment and hazards of these regions will need better defining. In particular the impact of the transportation phase of development is poorly understood. As yet no offshore pipeline or coastal crossing have been attempted except by use of causeways which will become unfeasible at greater distances from shore and at greater depths. From this perspective we see the following needs for additional geologic information within the Beaufort Sea. 1) A definitive study of coastal and barrier island stabilities and the sedimentary dynamics of the nearshore environment. We understand a good deal about this environment, however, there are still major questions such as the fate of river sediments (none are presently deposited off the Sagavanirktok River), 2) Continued studies of ice gouging directed toward understanding the energy expended at the sea floor and the quantities of sediment disturbed and displaced. This would allow us to estimate the relative saftey of various pipeline schemes of seabed structures.

Several other areas of study will be needed to keep abreast of the present state of knowledge. A) Studies of the shelf edge slump and slide terrain and its associated gasses. B) Cooperative studies, including cruises with the Canadian geoscience community will allow for an increased rate of learning and will keep us informed of Canadian advancements (they may be first to develop resources far from shore). C) Studies of the "recovery" rates of offshore drilling sites, such as CIDS, to determine the seabed response to artificial alteration.

Our view of the needs for future study in the Chukchi Sea is based on the present state of knowledge which continually improves and may well raise new questions. As seen at present, the primary emphasis of future work should include the following: (a) investigation of ice gouging on the northern shelf (area north of 71°) as well as slumping along the shelf break and on the west side of the Barrow Sea Valley; (b) using vibracores establish the sediment depth of ice interaction on the present shelf; (c) establish potential sand and gravel resources using vibracores (d) define the Chukcki Sea biofacies in relation to fauna, current regime, sediment texture, and identify major benthic feeding areas of walrus and gray whales; (e) identify processes forming and moving major bedform fields on the shelf; and (f) identify origin and reoccurrence rates of movement of storm-generated (?) gravel waves on the outer shelf.

As our work and the work of others progresses, new thoughts and questions will develop and need to be incorporated into future research.

VIII. Published reports since last annual report

Rearic, D. M., Barnes, P. W., and Reimnitz, Erk, 1981, Ice gouge data, Beaufort Sea, Alaska, 1972-1980; U.S. Geological Survey Open-file Rept. 81-950, 8 microfiche cards.

Reimnitz, Erk and Barnes, P. W., 1981, Depositional complexities in the sea-ice environment of arctic shelves: Example from Harrison Bay, Alaska: American Assoc. Petrol. Geol. Bulletin, San Francisco, California, AAPG-SEPM Annual Convention, May 31-June 2, (abs), v. 65, p.978.

Weeks, W. R., Barnes, P. W., Rearic, D. M., and Reimnitz, Erk, 1981, Statistice of ice gouging on the Alaskan Shelf of the Beaufort Sea: EOS, Transactions of the American Geophysical Union, v. 62, no. 45, p. 902.

Barnes, P. W., and Minkler, P. W., 1982, Sedimentation in the vicinity of a causeway groin Beaufort Sea, Alaska, 1982, U.S. Geol. Survey Open-file Rept. 82-615, p. 12

Barnes, P. W., Rearic, D. M., and Reimnitz, Erk, 1982, Ice gouge characteristics and their relation to ice zonation, Beaufort Sea, Alaska, Abstract vol. 11th International Congress on Sedimentology, Hamilton, Ontario, Canada, p. 75.

Barnes, P. W., Reimnitz, Erk, and Fox, D., 1982, Ice rafting of fine-grained sediment, a sorting and transport mechanism, Beaufort Sea, Alaska, Jour. Sed. Petrol., v. 52, p. 493-502.

Barnes, P. W., and Reimnitz, Erk, 1982, Sediment content of nearshore facies-Fall, 1980, Beaufort Sea, Alaska, U.S. Geol. Survey Open-file Rept. 82-716, 18 p.

Barnes, P. W., and Reimnitz, Erk, 1982, Net flow of near-bottom waters on the inner Beaufort Sea Shelf as determined for sea bed drifters, U.S. Geol. Survey Open-file Rept. 82-717, 9 p.

Barnes, P. W., and Reiss, Tom, 1982, Erosion and migration of an artificial sand and gravel island, NIAKUK III, Beaufort Sea, Alaska, U.S. Geol. Survey Open-file Rept. 82-608, 9 p.

Barnes, P. W., and Ross, C. R., 1982, Marine ice-pushed boulder ridge, Beaufort Sea, Alaska, Arctic, V. 35, p. 312-316.

Dunton, K. H., Reimnitz, Erk, and Schonberg, S., 1982, An arctic kelp community in the Alaskan Beaufort Sea, Arctic, v. 35, no. 4, p. 465-484.

Kempema, E. W., Barnes, P. W., Reimnitz, Erk, Asbury, J. L., and Rearic, D. M., 1982, A summary of U.S. Geological Survey marine geological data collected in the Beaufort Sea, Alaska, 1982, U.S. Geol. Survey Open-file Rept. 83-493, 2 rolls microfilm, 9 p.

Reimnitz, Erk, and Kempema, E. W., 1982, Dynamic ice-wallow relief of northern Alaska's nearshore - a dynamic bedform, Jour. of Sed. Petrol., v. 52, no. 2, p. 451-462.

Minkler, P. W., Reimnitz, Erk, and Barnes, P. W., 1982, A summary of U.S. Geological Survey marine geologic data collected in the Beaufort Sea, Alaska, July through August, 1981, U.S. Geol. Survey Open-file Rept. 82-586.

Reimnitz, Erk, Barnes, P. W., Rearic, D. W., Minkler, P. W., Kempema, E., and Reiss, T., 1982, Marine geological investigations in the Beaufort Sea in 1981 and preliminary interpretations for region from the Canning River to the Canadian border, U.S. Geol. Survey Open-file Rept. 82-974.

Reimnitz, Erk, Kempema, E. W., and Ross, C. R., 1982, Observations on the mode and rate of decay of an artificial ice island in the Alaskan Beaufort Sea, OTC #4310, Offshore Tech. Conf. Proceedings, v. 3, p. 121-132.

Reimnitz, Erk, and Kempema, E. W., 1982, High rates of bedload transport measured from filling rate of large strudel scour craters in the Beaufort Sea, Alaska, U.S. Geol. Survey Open-file Rept 82-588, 22 p.

Barnes, P. W., and Reimnitz, Erk, 1983, Sedimentary facies on an ice dominated shelf, Beaufort Sea, Alaska, U.S. Geol. Survey Circular 917, 37 p.

Reimnitz, Erk, and Kempema, E. W., 1983, High rates of bedload transport measured from infilling rate of large strudel-scour craters in the Beaufort Sea, Alaska, Continental Shelf Reasearch, v. 1, no. 3, p. 237- 251.

Reiss, T., Phillips, R. L., Hunter, R. E., and Barnes, P. W ., 1983, A summary of U.S. Geological Survey marine geologic studies on the inner shelf of the Chukchi Sea, Alaska, 1975 and 1981, U.S. Geol. Survey Open-file Rept. 83-71, 11 p.

Weeks, W. F., Barnes, P. W., Rearic, D. M., and Reimnitz, Erk, 1983, Statistical aspects of ice gouging in the Alaskan shelf of the Beaufort Sea, CRREL Rept. 83-21, Hanover, NH, U.S. Army Corps of Engineers, 34 p.

Barnes, P. W., Rearic, D. M., and Reimnitz, Erk, 1984, Ice gouge characteristics and their relation to ice gouging and ice dynamics, in P. W. Barnes, D. M. Shell, and E. Reimnitz (eds.), The Alaskan Beaufort Sea - Ecosystems and Environment, Academic Press, San Francisco, California, 466 p.

Barnes, P. W., Shapiro, L. and Reimnitz, Erk, 1984, Control concepts for mid-shelf shear zone, in Abstracts, Arctic Energy Technologies Workshop, Nov. 14-15, 1984, U.S. Dept. of Energy, Office of Fossil Energy, Morgantown Energy Technology Center, Morgantown, West Virginia, 5 p.

Graves, S. M., Reimnitz, Erk, and Barnes, P. W., 1984, A summary of U.S. Geological Survey marine geological data collected in the Beaufort Sea, Alaska, 1983, U.S. Geol. Survey Open-file Rept. 84-117, 13 p.

Phillips, R. L., Reiss, T. E., Kempema, E. W., and Reimnitz, Erk, 1984, Nearshore marine geologic investigations, - Wainwright to Skull Cliff, northeast Chukchi Sea, U.S. Geol. Survey Open-file Rept. 84-108, 33 p.

Reiss, T. E., Hunter, R. E., and Phillips, R. L., 1984, A summary of U.s. Geological Survey marine geologic studies on the inner shelf of the Chukchi Sea, Alaska, summer 1982, U.S. Geol. Survey Open-file Rept. 84-116, 12 p.

Phillips, R. L., and Reiss, T. E., 1984, Nearshore marine geologic investigations, Icy Cape to Wainwright, northest Chukchi Sea, U.S. Geol. Survey Open-file Rept. 84-828, 27 p.

Phillips, R. L., and Reiss, T. E., 1984, Nearshore marine geologic investigations, Point Barrow to Skull Cliff, northeast Chukchi Sea, U.S. Geol. Survey Open-file Rept. 85-50, 22 p.

Phillips, R. L., 1984, Current-dominated sedimentation in the northeastern Chukchi Sea, Alaska, in research sysposium, Sedimentology of shelf sands and sandstones, Canadian Soc. of Petrol. Geologists, p. 86.

Reimnitz, Erk, Barnes, P. W., and Phillips, R. L., 1984, Geologic evidence for 60 m deep pressure-ridge keels in the Arctic Ocean, Ice Symposium, August 27-31, 1984, Hamburg, Germany, v. II, p. 189-206.

Reimnitz, Erk, and Barnes, P. W., 1984, Determining the maximum ice keel depth in the Beaufort Sea, in Abstracts, Arctic Energy Technologies Workshop, Nov. 14-15, 1984, U.S.

Dept. Energy, Office of Fossil Energy, Morgantown Energy Tech. Center, Morgantown, West Virginia, 8 p.

Reimnitz, Erk, and Kempena, E. W., 1984, Pack ice interaction with Stamukhi Shoal, Beaufort Sea, Alaska, in P. W. Barnes, D. M. Schell and Erk Reimnitz (eds.), The Alaskan Beaufort Sea - Ecosystem and Environment, Academic Press, San Francisco, California, p. 159-184.

Weeks, W. F., Barnes, P. W., Rearic, D. M., and Reimnitz, Erk, 1984, Some probabilistic aspects of ice gouging in the Alaskan shelf of the Beaufort Sea, in P. W. Barnes, D. M. Schell, and Erk Reimnitz (eds.), The Alaskan Beaufort Sea - Ecosystem and Environment, Academic Press, San Francisco, California, p. 213-236

Barnes, P. W., Reimnitz, Erk, and Rearic, D. M., 1984, Ice gouge characteristics related to sea-ice zonation, Beaufort Sea, Alaska, Montebello, Quebec, Canada, National Research Council of Canada, Ice Scour Workshop, Feb. 15-19, 1982, 32 p.

Barnes, P. W., Ross, C. R., and Reimnitz, Erk, 1984, Correlation between an ice ridge and sea bed geologic boundary, Montebello, Quebec, Canada, National Research Council of Canada, Ice Scour Workshop. Feb. 15-19, 1982, 15 p.

Bea, R. G., Puskar, F. J., Barnes, P. W., and Reimnitz, Erk, 1985, The role of ice gouging in determining global forces on arctic structures, Proceedings, American Soc. of Civil Engineers, Arctic, 85, p. 251-266.

GEOLOGIC INVESTIGATIONS IN THE CHUKCHI SEA, 1984, NOAA SHIP SURVEYOR CRUISE

by

R. L. Phillips
P. Barnes
R. E. Hunter
D. Rearic
T. Reiss
E. Kempema
J. Chin
S. Graves
T. Scott

TABLE OF CONTENTS

LIST OF FIGURES

Figure 13. Seismic profile north of Cape Lisburne. Both profiles (E and F) show thin sediment cover over inclined bedrock which is typical for the southern Chukchi Sea.

Figure 14. Isopachs, in meters, of Holocene-Quaternary sediment in the northeast Chukchi Sea. The nearshore isopachs are from Phillips and Reiss, 1984.

Figure 15. Modern channel trends in the head of the Barrow Sea Valley.

Figure 16. Seismic profile on the west side of the Barrow Sea Valley showing fluvial channel deposits overlying gently inclined bedrock.

Figure 17. B) Seismic profile near the center of the Barrow Sea Valley showing eroded Quaternary deposits overlying gently inclined strata. C) Bottom profile in the Barrow Sea Valley showing either eroded or slumped deposits overlying bedrock (water depth 68.5 m).

Figure 18. Modern channels at the head of Barrow Sea Valley. D) Seismic profile showing channel incised into Quaternary deposits which overlie inclined bedrock. E) Bottom profile of channel.

Figure 19. A) A thin sediment cover, locally containing gravel, overlies inclined bedrock on the outer shelf. B) An angular unconformity separates a lower folded and faulted bedrock sequence from an upper gently inclined (but also faulted) bedrock sequence. A thin sediment cover overlies the bedrock.

Figure 20. Holocene-Quaternary sediment thickness, channel trends and channel-fill deposits on the outer part of the Chukchi Sea.

Figure 21. Major seismic units and interpretative depositional environments for channel-fill deposits, northwest Chukchi Sea. Unit D rests on an erosional surface cut to 63 m into bedrock (116 m below present sea level); Unit C drapes an irregular erosional surface developed on Unit D and represents a probable marine depositional sequence; Unit B contains abundant channels but may also include estuarine to deltaic to terrestrial depositional environments; and Unit A contains fluvial to probable marine environments and would contain Holocene transgressive deposits.

Figure 22. Channel-fill sequence containing 3 seismic units consisting of Unit D fluvial deposits, Unit C draped deposits (marine?) and Unit A deposits which consist of a fluvial to marine sequence.

Figure 23. Channel-fill deposits within a large channel system, northwest Chukchi Sea. Four seismic unit separated by erosional surfaces are identified and consist of a basal fluvial sequence (Unit D), a well-bedded draped sequence of probable marine origin (Unit C), a fluvial-dominated sequence (Unit B), and the uppermost sequence (Unit A) consisting of fluvial to marine beds.

Figure 24. Channel-fill deposits within a large channel system containing a thick basal sequence of fluvial deposits (Unit D), a draped marine sequence (Unit C), a thick fluvial sequence (Unit B), and a thin fluvial-marine sequence (Unit A).

Figure 25. Channel-fill deposits recording a thin and discontinuous basal fluvial sequence (Unit D), a thick draped marine sequence (Unit C), a poorly defined fluvial sequence (Unit B), and a relatively thick fluvial-marine sequence (Unit A).

Figure 26. Phi diagram showing box core textural composition in percent for the outer shelf samples in the Chukchi Sea.

Figure 27. Surficial gravel deposits on the southeast Chukchi Sea determined from samples and side-scan sonar records.

Figure 28. Surficial gravel deposits on the central Chukchi Sea. The distribution of gravel determined from sonographs and box coring.

Figure 29. Continuation of line 25 (Figure 28) showing the surficial gravel deposits identified on sonographs in the outer Chukchi Sea.

Figure 30. Gravel size analyses of coarse=grained fractions of box cores, outer Chukchi Sea.

Figure 31. Gravel deposits northwest of Cape Lisburne, Chukchi Sea.

Figure 32. Gravel bedforms west of Cape Lisburne. A) Northward-trending gravel ribbons at 42 m depth cut by ice gouges. B) Gravel sheet and ribbons at 38 m depth cut by ice gouges. C) Gravel sheet deposit at 34 m depth cut by ice gouges.

Figure 33. Gravel bedforms on the outer shelf, Chukchi Sea. A) Gravel waves at 45.5 m depth migrating to the west. B) Gravel bedforms (?) at 43.5 m depth on flank of a gravel sheet. C) Gravel bedforms at 49 m depth.

Figure 34. Radiographs of outer shelf box cores containing gravel. A) Core 15 (44.4 m) contains abundant gravel throughout core as well as burrows. B) Core 17 (43.2 m) shows both shells and gravel mixed in a mud substrate. C) Core 38 (45.7 m) contains bioturbated mud with gravel as a surficial lag and in burrows.

Figure 35. Ice gouge and gravel bedform trends (gravel ribbons and symmetrical gravel wave crest trends) off Cape Lisburne, Chukchi Sea.

Figure 36. Radiographs of outer shelf box cores. A) Core 36 (53.5 m), B) core 16 (49.5 m), C) core 14 (44.8 m); all cores show bioturbated to disrupted strata, burrows, poorly defined bedding, shells, and scattered pebbles in sandy mud to muddy sand matrix.

Figure 37. Radiographs of outer shelf box cores. A) Core 37 (46.0 m), B) core 32 (41.2 m); both cores consist of bioturbated mud with scattered pebbles and shells.

Figure 38. Sediment components from channel samples of box cores in the northeast part of the Chukchi Sea.

Figure 39. Major surficial sediment facies observed in the northeast part of the Chukchi Sea. The three outer facies contain distinctive fauna dominated by bivalves and gastropods in the Outer Sand; barnacles, bryzoans and brachiopods in the Outer Gravel; and echinoids in the Coastal Current Sand. The greatest faunal abundance and diversity occurs in the Outer Gravel facies.

Figure 40. Outer Sand facies box cores. A) Radiograph of core 11 (42.5) containing scattered gravel and shells as well as abundant bioturbation. B) Radiograph of core 22 (42.1 m) containing abundant gravel with crude bedding. C) Photo of core 10 (42.9 m) which contains bioturbated sand with a few scattered pebbles. D) Photo of core 21 (47.7 m) containing a shell lag, scattered pebbles and abundant bioturbation.

Figure 41. Faunal composition of inner shelf box cores. Includes only material from within the core and not the living fauna on the box core surface.

Figure 42. A) Transition between the Outer Gravel facies (right side of sonograph) and sandwaves in the Coastal Current Sand facies directly west of Wainwright. The depth is 28.5 m. B) Outer Gravel facies west of Point Franklin.

Figure 43. Outer Gravel facies box core 30 (40.2 m). A) Photograph of core top which contains scattered pebbles and cobbles as well as branching bryzoans. Tunicates cover some of the cobbles here. B) Peel of core showing the upper erosional gravel-shell lag deposit and scattered gravel in the lower part of the core.

Figure 44. Outer Gravel facies box core 25 (40.2 m). A) Photograph of top of core showing the surficial gravel lag and biology. Sponges, bryzoans, urchins, and barnacles are common. B) Core peel showing the upper gravel-shell lag and bioturbated sediment. Most biogenic fragments in core are barnacles. The box core is 31 cm in length; the peel is 19 cm wide.

Figure 45. Outer Gravel facies box core 31 (42.0 m) A) Photograph of top of core showing the surface gravel-shell lag with a large worm on the right side of core. B) Core peel showing the gravel-shell lag and bioturbated sediments. C) X-ray of core peel showing the gravel distribution and crude bedding.

Figure 46. Outer Gravel facies. A) Core 2 (45.3 m) peel showing bioturbated sediment and upper gravel-shell lag. B) X-ray of core peel showing the surficial gravel concentration. C) Core 24 (36.6 m) peel contains scattered shells and cobbles. D) Core 1 (43.5 m) with a surficial gravel-shell lag.

Figure 47. Coastal Current Sand facies containing sandwaves at 28 m depth on northwest part of Blossom Shoals off Icy Cape. The sandwaves range up to 0.9 m in height. B) Straight-crested sandwaves at 23 m depth west of Wainright.

Figure 48. Coastal Current Sand facies containing northward migrating sandwaves at 28 to 30 m depth off Point Franklin.

Figure 49. Coastal Current Sand facies. A) Core 29 (35.0 m) taken near the seaward boundary with the Outer Gravel facies. The peel shows a surficial gravel-shell lag overlying bioturbated sand. B) Core 7 (28.7 m) core peel contains bioturbated sand with scattered shells and echinoid fragments. C) Core 8 (24.6 m) photograph of top of core showing the distribution and abundance of echinoids. D) Peel of core 8 which contains bioturbated sand with scattered echinoid and shell fragments.

Figure 50. Inner Gravel facies box core 5 (18.3 m). X-ray of core peel showing bioturbated gravel.

Figure 51. Inner shelf bottom current features. A) Linear furrows at depths of 69 m are erosional bedforms cut into mud. B) Northeast-directed sediment "streaming" from ice gouges indicate bottom current direction in regions where sandwaves are not observed on sonographs.

Figure 52. Major location of gray whale feed traces along the eastern boundary of the Alaska Coastal Current.

Figure 53. Gray whale feeding traces west of Wainwright, Chukchi Sea. A) Founded and elliptical to current-modified feeding traces. B) Current-modified whale feeding traces at 24 m depth.

Figure 54. A) Gray whale feeding traces within an ice gouge off Wainwright. B) Round to elongate scattered feeding traces in coarse sand and pebbles west of Point Franklin.

Figure 55. A) Scattered feeding traces within an area dominated by the Alaska Coastal Current south of Icy Cape. B) Outer shelf feeding traces of unknown origin (possibly walrus) at depth of 48 m.

Figure 56. Rose diagram of ice gouge orientations in the northeast Chukchi Sea. H) Ice gouge trends on the east side of the Barrow Sea Valley. I) Ice gouge trends on the west side of the Barrow Sea Valley.

Appendix D Figures:

Figure 1. High-resolution seismic profile on line 44 where box core 32 was obtained. See Fig. 3 for trackline location and Figure 5 for box core location. Bedrock consists of parallel and gently inclined strata cut by a fluvial channel deposit. Box core 32 taken where seismic record ends on right.

Figure 2. High-resolution seismic profile on line 44 where box core 33 was obtained. Parallel reflectors are present only in the upper part of section. The lower acoustic "turbid" zone may be due to gas-charged sediment as high values of methane were found in box core 33. Box core 33 taken where seismic record ends on right.

LIST OF TABLES

INTRODUCTION

Geologic processes on high latitude shelfs are poorly understood because of the harsh environment, sea ice, and the limited number of previous studies. Studies of the high latitude shelf environment of the Chukchi Sea were initiated to provide the Government and the public with adequate knowledge to safely lease offshore lands. This report presents preliminary findings from a study of the geologic environment of the Chukchi Sea from Point Hope north to 71° 38' on the western part of the shelf and to the vicinity of Point Franklin on the eastern shelf (figure 1).

Data were gathered from the NOAA ship SURVEYOR from August 26 to September 17, 1984. Pack ice conditions limited investigations north of 71 degrees in the eastern part of the study area. The pack ice front was approximately 5 to 7 miles northwest of Point Franklin when studies were started (figure 2). During the latter part of the season investigations were conducted north to 71° 38' in the western part of the Chukchi Sea.

High-resolution seismic profiles, bathymetry and side-scan sonar surveys were collected along approximately 2440 km of trackline (figures 3 and 4). Forty box cores, 4 dredge samples and 2 gravity cores were also obtained (figures 5 and 6). Bottom drifters were deployed at 8 sites. During part of the study bad weather and ice hampered our research. Short period high northeast storm waves seriously interfered with the seismic and side-scanning sonar records and caused the termination of some lines on the outer and inner shelf. However, during periods of high wind and waves the nearshore areas protected by the capes allowed us to continue our investigations.

The objectives of the scientific program include the following: A) determination of the location, density and depth of modern sea floor ice gouging, B) Observe recent changes in bathymetry and sea bed morphology and determine their origins, C) Obtain seismic profiles of the modern sediment cover and of bedrock to determine the history of ice gouging, and D) identify potential sand and gravel resources.

METHODS

On the cruise we obtained analog recordings of side-scan sonar, 3.5 khz sub-bottom profiler, high resolution seismic system, and 12 khz and 3.5 khz bathymetry. A Kline Associates 100 khz and 500 khz side-scan fish towed approximately fifteen meters above the sea-bed was used as the source for the sea-bed

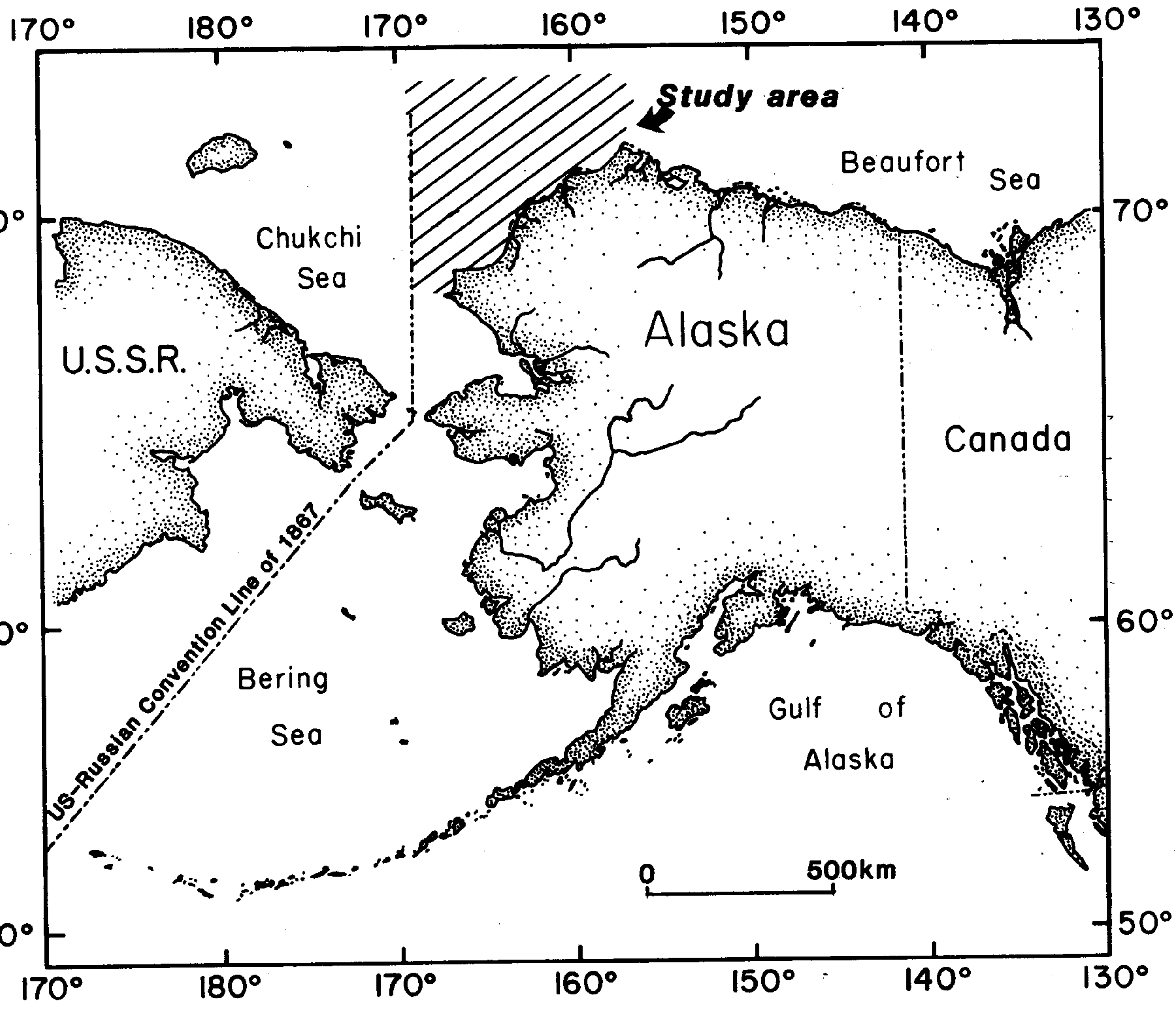

Figure 1. Location of study area in the northeastern Chukchi Sea.

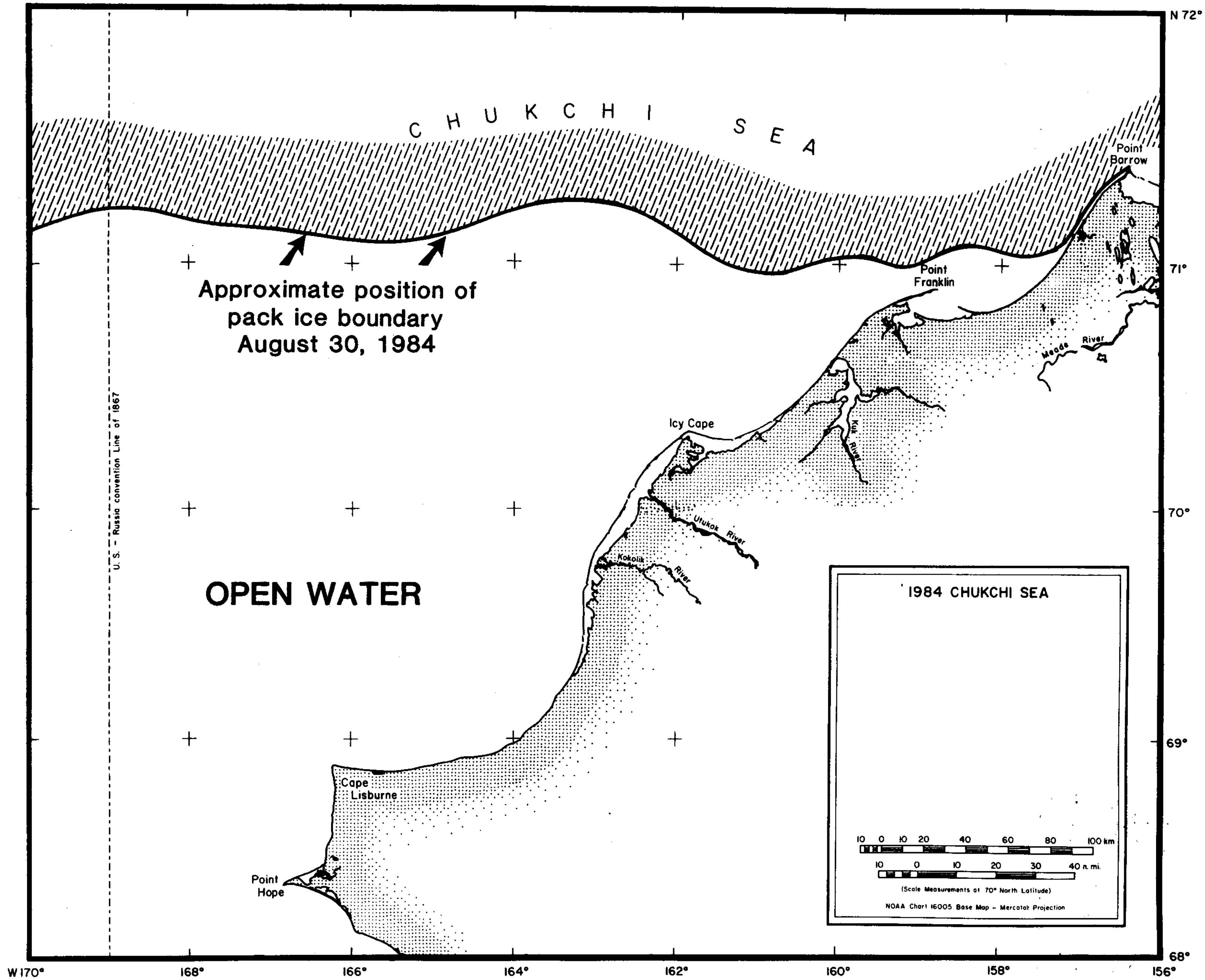

Figure 2. Approximate location of pack ice boundary at the start of the Chukchi Sea study, 1984.

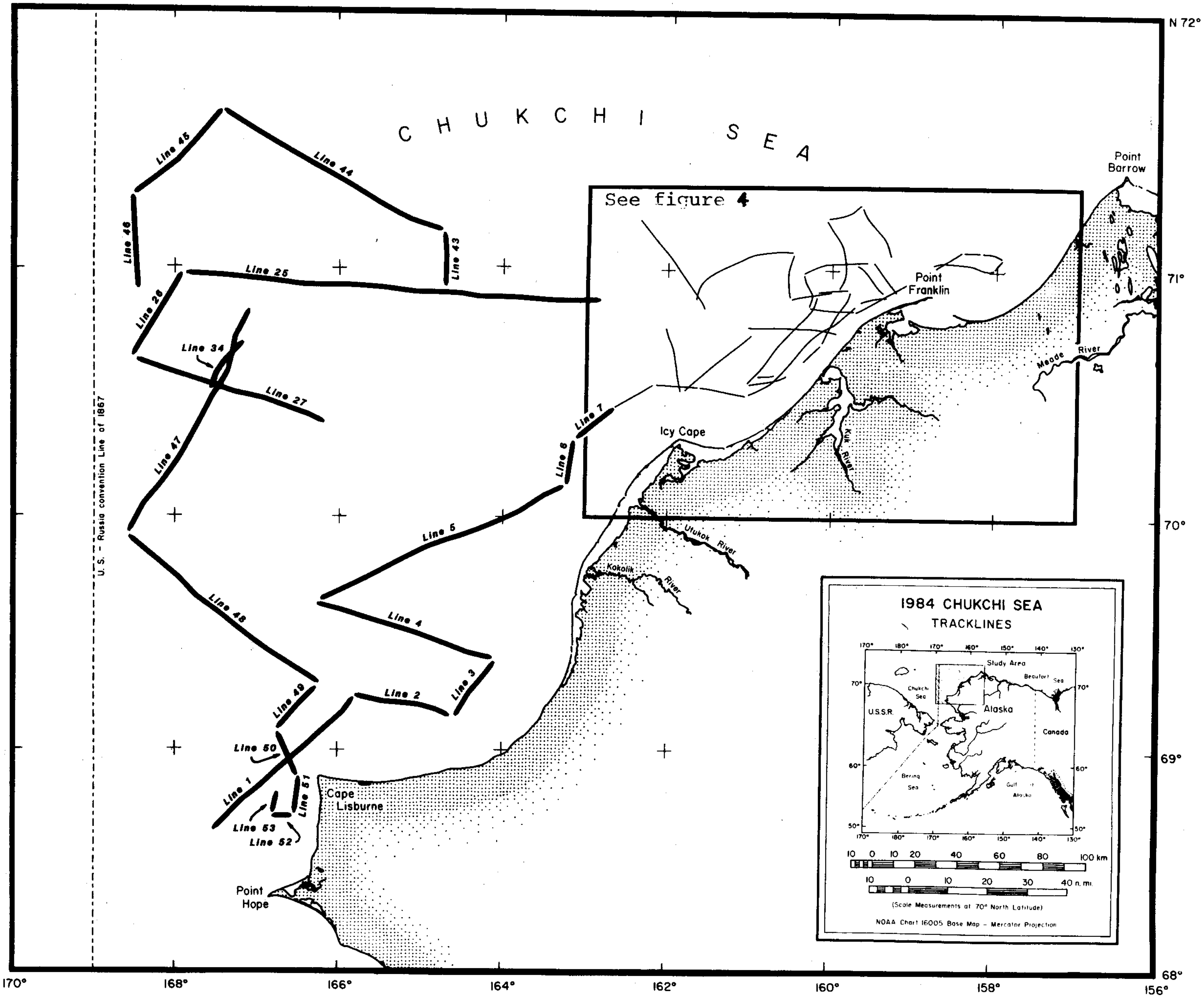

Figure 3. Track lines obtained in the outer part of the study area. See figure 4 for track line numbers in the nearshore region.

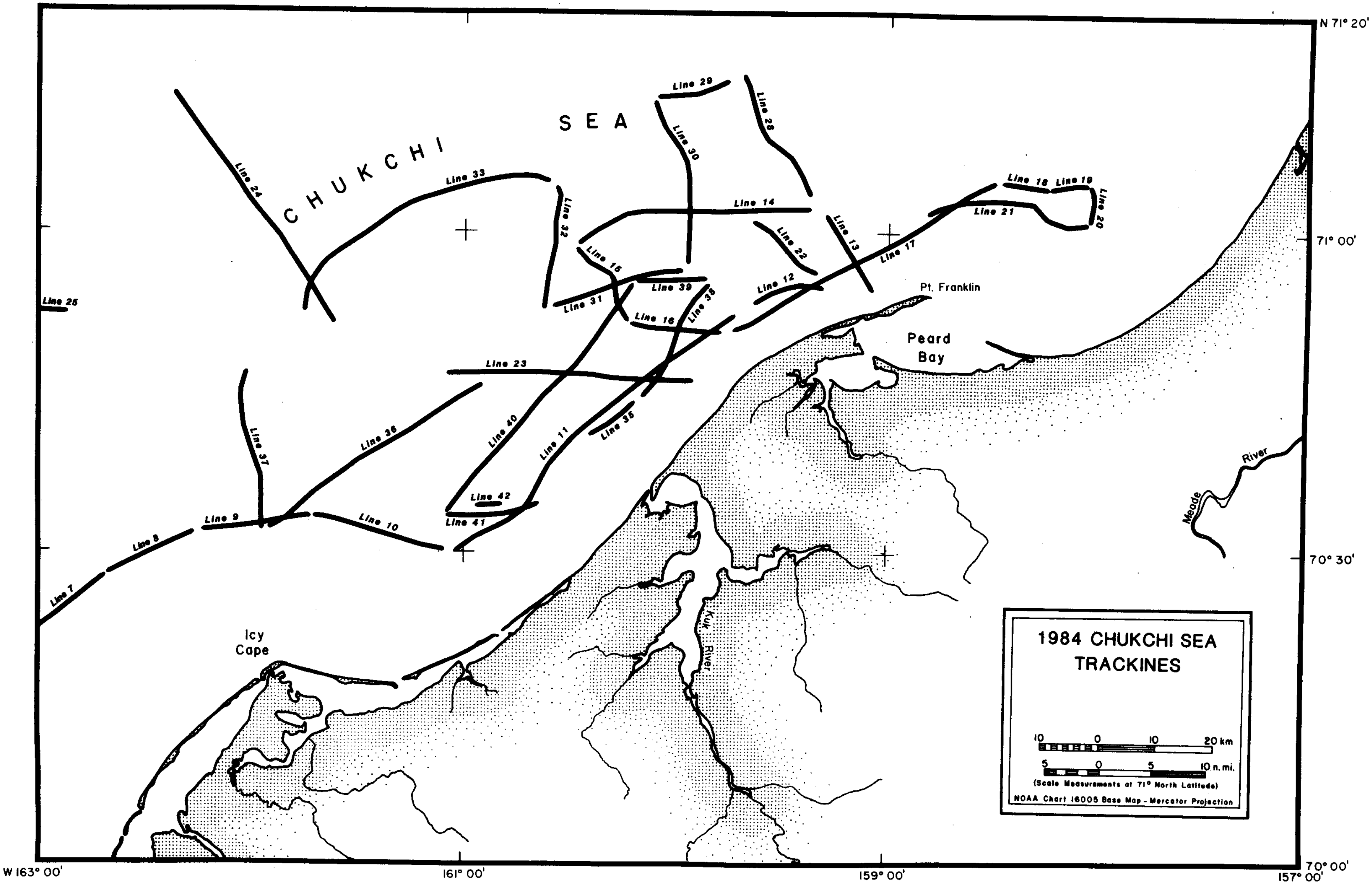

Figure 4. Track lines obtained in the northeastern part of the Chukchi Sea from Icy Cape to north of Point Franklin.

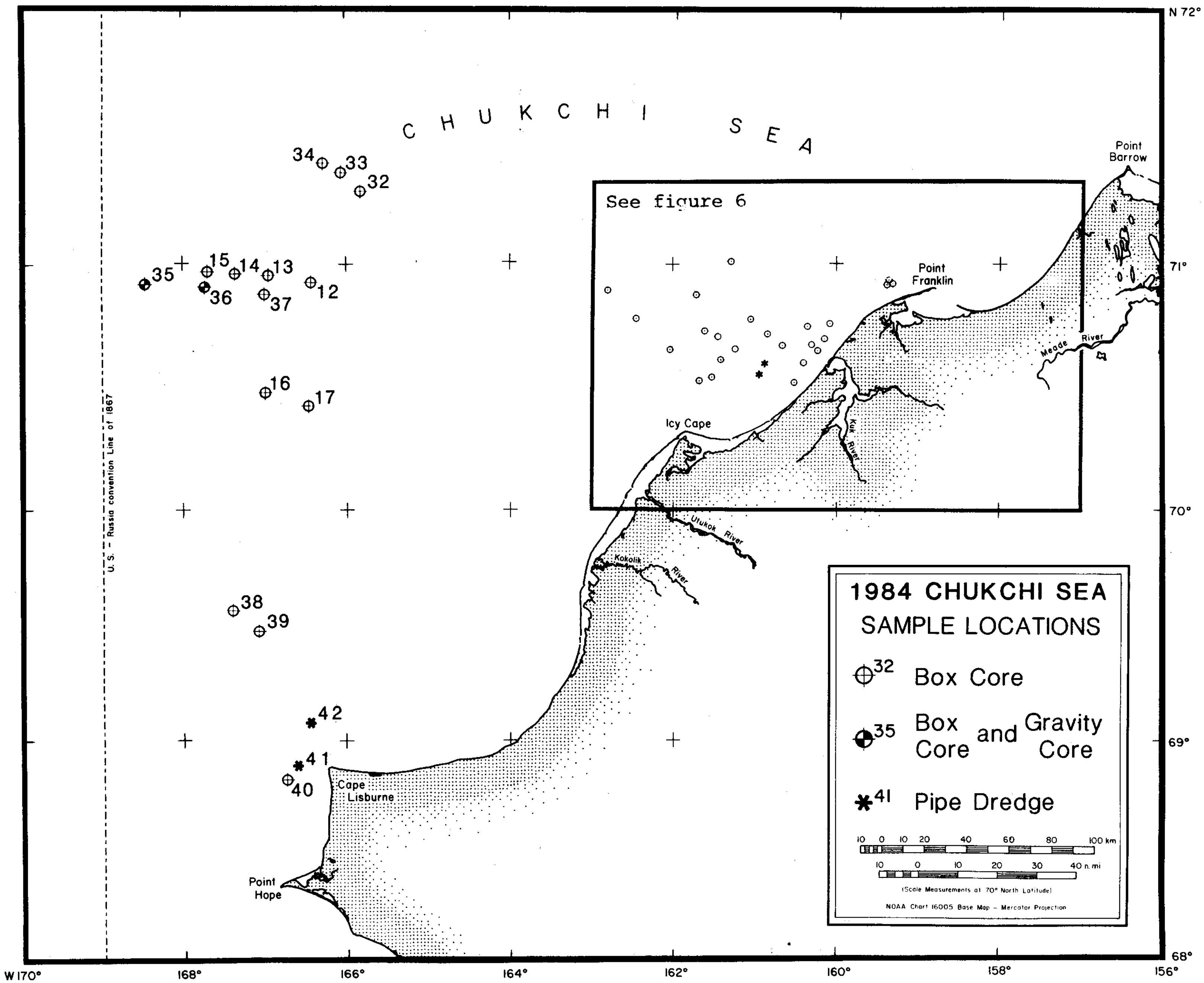

Figure 5. Sediment sample locations in the outer part of the study area. See figure 6 for sample numbers in the nearshore region.

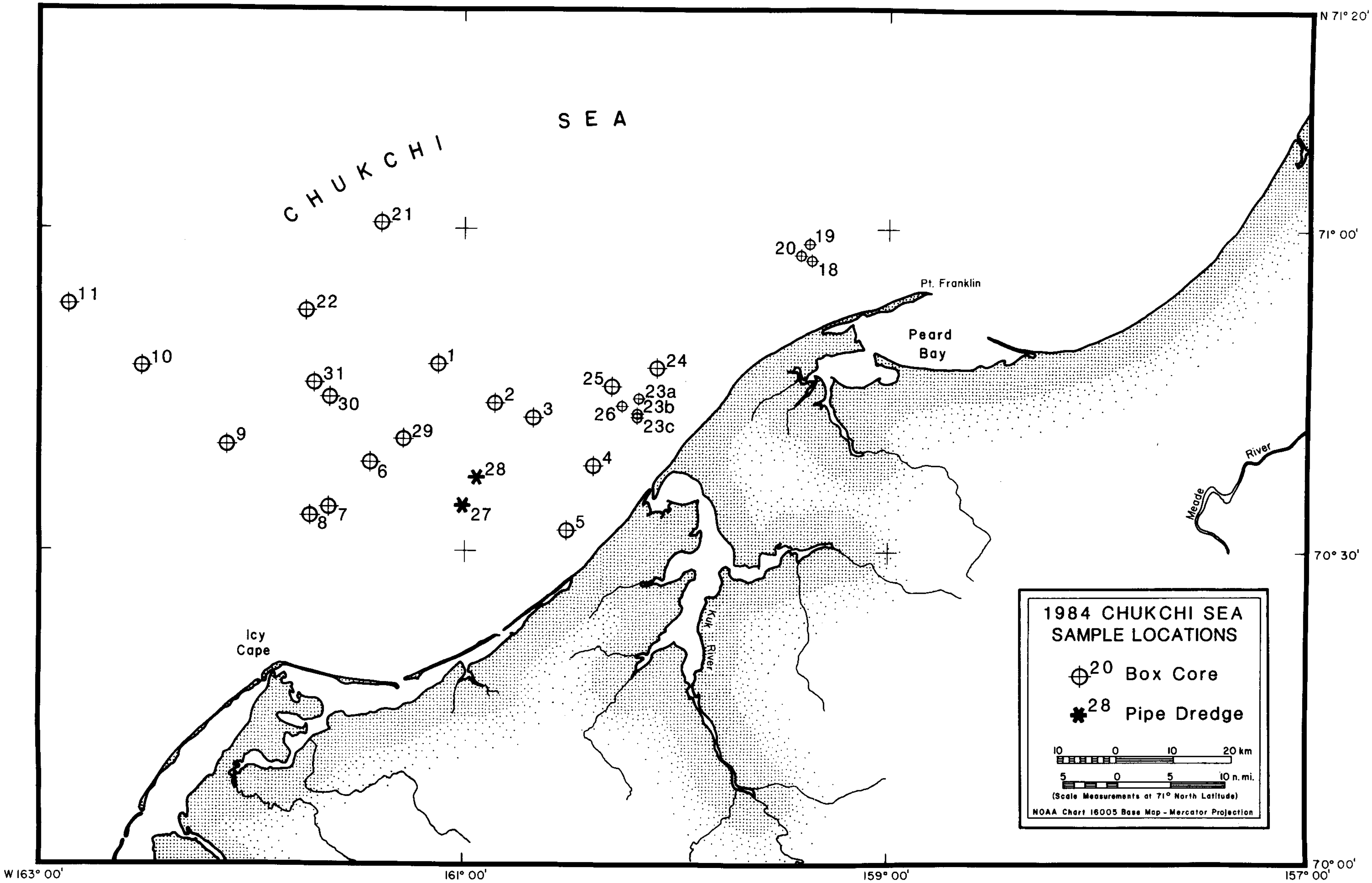

Figure 6. Sediment samples obtained in the northeast Chukchi Sea.

sonar data. The side-scanning fish also contains a 500 khz microprofiler and a a 3.5 khz sub-bottom profiler for viewing expanded sea-floor relief and shallow sub-bottom stratigraphy. Under optimum conditions subsurface reflections were obtained to depths of 15 meters below the sea-floor.

An ORE geopulse sub-bottom profiler was used at 100, 105, and 175 joules of power with the high resolution seismic signal pickup with a single channel, 25 element hydrophone. Under optimum conditions sub-bottom penetrations were obtained to 150 meters. Bathymetry was recorded with a hull-mounted transducer source.

The sea floor was sampled with a 60x31x22 cm box core, a 3 meter gravity core, and a pipe dredge. Recoveries of up to 56 cm were achieved with the box core.

Navigation for tracklines and sample sites consisted of Satelite Navigation, using a Magnavox Omega system, a Del Norte UHF transponder system and deduced reckoning.

BATHYMETRY

Much of the Chukchi Sea floor is relatively flat and shallow with depths averaging between 40 and 50 m. Locally, enclosed depressions and scattered highs contribute as much as 5 m of relief. Two areas contain bathymetric highs; the nearshore area off Icy Cape, Blossom Shoals, where migrating sand banks rise to within 10 m of the sea surface, and on the northern part of the shelf, Hannna Shoal which rises to within 25 m of the sea surface (Hill and others, 1984). Along the northeast part of the Chukchi Sea the Barrow sea valley forms a major erosional incision into the shelf starting west of Point Franklin and trending northeast parallel to shore. The sea floor rapidly drops to over 100 m depth within the sea valley (Hill and others, 1984). On the outer shelf, north of Hanna Shoal and Bank, the sea floor slopes north toward the shelf break where at approximately 60 m depth the shelf slope rapidly increases. Local gulleys and larger erosional features disect the outer shelf edge (figure 7).

CURRENTS

Surface wind-generated currents, the shore-parallel Alaska Coastal Current and shelf currents erode and transport sediment modifying the sea floor of the Chukchi Sea. The nearshore currents are generated mostly by winds, whereas, the offshore region is dominated by northeast- and southwest-directed storm currents and by the northeastward flowing Alaska Coastal Current (figure 8).

During the summer months, storms from the southwest commonly move across the Chukchi Sea. Their maximum fetch then developes across the open water (Wiseman and Rouse, 1980). The resulting storm waves and storm-generated currents erode and scour the sea

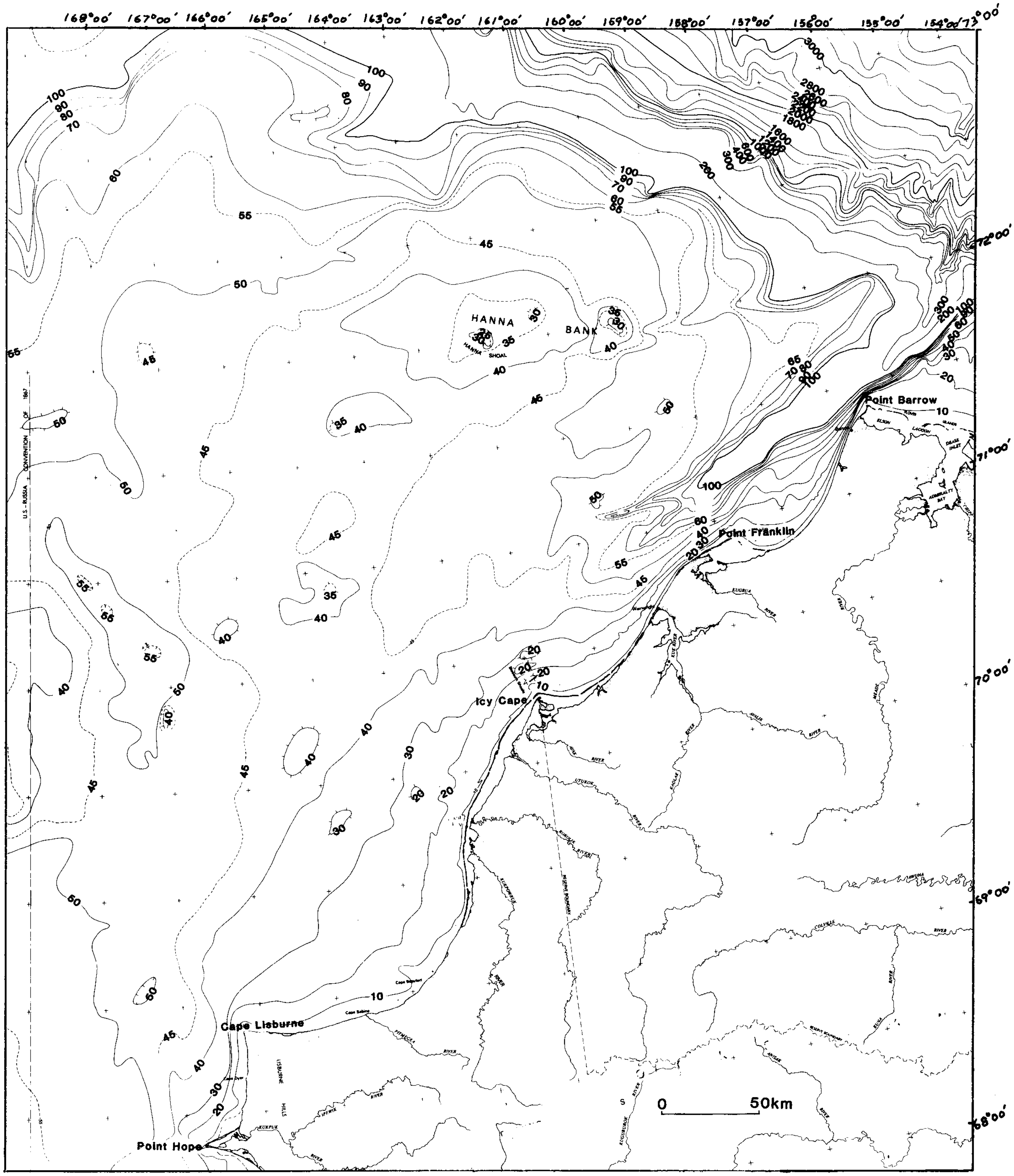

Figure 7. Chukchi Sea bathymetry. Data modified from Hill and others, 1984. Contours in meters.

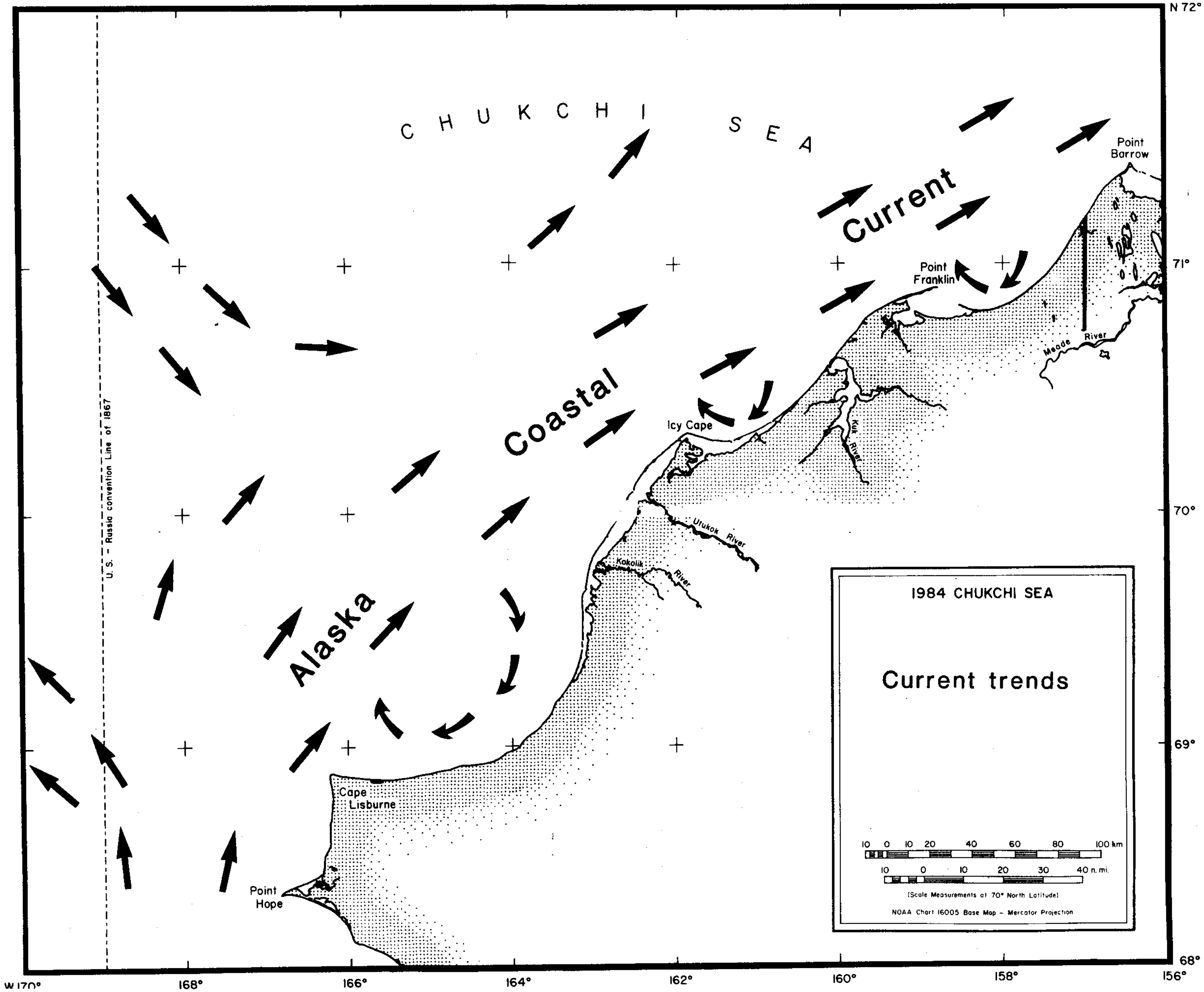

Figure 8. Current trends within the Chukchi Sea. The Alaska Coastal Current parallels the coastal region with clockwise rotating currents developing nearshore behind the capes. Current data modified from Coachman and others, 1975.

floor and transport sediment on the shelf and shoal regions. The storm-generated currents probably reinforce the normal shelf currents resulting in periods of bedform migration and sediment transport.

The Alaska Coastal Current represents a northeastward flowing "warm" water mass derived from the Bering Sea (Paquette and Bourke, 1972). The northward flowing Bering Sea water bifurcates near Point Hope, one part flowing to the northwest around the south side of Herald Shoal and the other forming the Alaska Coastal Current which flows to the northeast parallel to the Alaska Coast (figure 8). The Alaska Coastal Current, which can be as narrow as 37 km, approaches the coast near Wainwright and Barrow. Surface velocities of up to 200 cm/sec. are reported for the Alaska Coastal Current southwest of Point Franklin (Hufford, 1977). Southward flowing clockwise gyres develope east of the Alaska Coastal Current north of the major promatories off Cape Lisburne, Icy Cape and Point Franklin (Fleming and Heggarty, 1966, Sharma, 1979, Lewbel and Gallaway, 1984). West of the Alaska Coastal Current off Point Franklin on the west side of the Barrow Sea Valley a southwest-directed current is reported with surface velocities of up to 80 cm/sec (Hufford, 1977). The southwest flowing currents are poorly defined in space and time. Southeast-directed bottom currents are also identified on the western part of the outer shelf (Coachman and others, 1975). Large clockwise rotating spiral currents are also reported northwest of Barrow and may represent interaction between the Alaska Coastal Current and the westward flowing current of the Beaufort Gyre (Solomon and Ahlmas, 1980).

ICE REGIME

The ice covers the Chukchi Sea for 8 to 10 months every year with 2 to 4 months of open-water during the summer-fall season. During September to early October the Arctic pack ice usually reaches its maximum northern retreat, near 72 to 73 degrees. The pack ice then advances to the south, and by January the entire Chukchi Sea is ice covered (Grantz and others, 1982). Nearshore, fast ice forms and reaches its maximum development in March and April (figure 9). Storms and winds from the northeast will move the pack ice to the west resulting in the formation of the persistent Chukchi Polynya usually by January (Stringer, 1982). However, the overall pack ice movement west of the Chukchi Polynya is to the west and northwest (Stringer, 1978, 1982, Lewbel, 1984) except for short periods during ice breakout when ice movement is to the south through the Bering Straits.

HOLOCENE-QUATERNARY SEDIMENT

Over much of the Chukchi Sea shelf a thin blanket of Holocene-Quaternary sediment overlies inclined and folded bedrock. The surficial sediment cover ranges in thickness from less than 1 m to over 12 m (Creager and McManus, 1967, Moore, 1964, Grantz and others, 1982). Thicker accumulations of

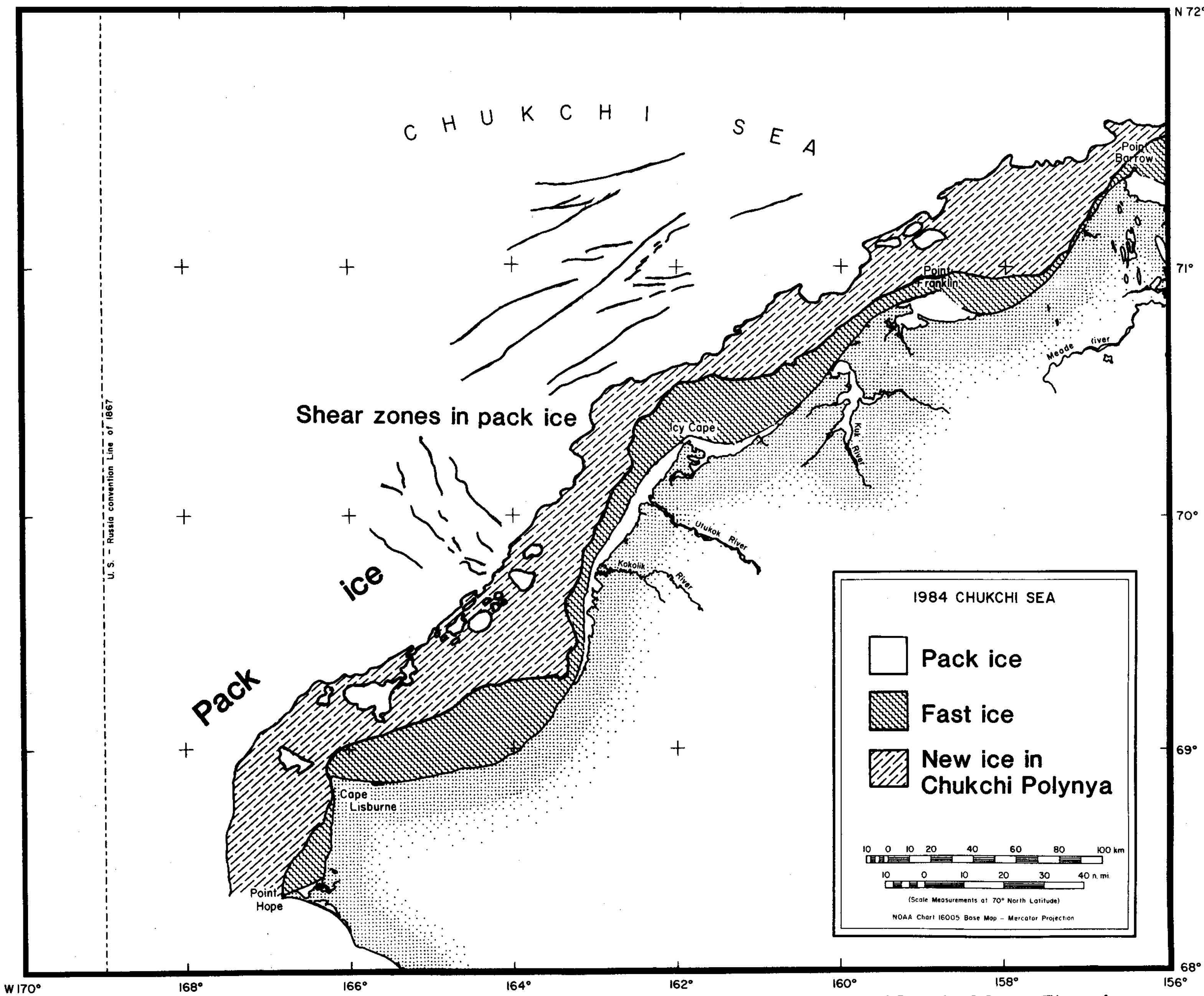

Figure 9. Ice zonation in the northeastern Chukchi Sea March-April, 1983. The ice field boundaries obtained from 1983 satellite photos. The maximum extent and development of shore-fast ice occurs during this time period. Northeast-directed storms form the Chukchi Polynya, separating the fast ice from the offshore pack ice. The large pack ice blocks in the Chukchi Polynya were moving to the south during this period of observation.

Quaternary sediment are reported in channel-fill deposits of paleovalleys that were cut into the shelf during Pleistocene sea level lowstands (Grantz and others, 1982).

High resolution seismic profiles obtained during this study show that: 1) a thin sediment cover, generally less than 4 m thick, overlies folded bedrock over much of the Chukchi Sea; 2) local blanket sediment accumulations, greater than 6 m thick are limited and are only identified on the shelf southwest of Cape Lisburne (14 m sediment thickness), and at the head of Barrow Sea Valley northwest of Point Franklin (over 14 m of Quaternary sediment); and 3) in the northwest part of the Chukchi Sea a series of paleochannels cut into bedrock contain up to 64 m of channel-fill sediment. The age of the channel-fill deposits is uncertain.

In the southern part of the study area, south of 70 degrees N, bedrock is overlain by a thin blanket sediment deposit. Local accumulations of up to 14 m of sediment are found directly west of Cape Lisburne at depths of 32 m (figure 10). Horizontal and parallel almost transparent reflectors overly gently inclined stata under the thick sediment accumulation (figure 11a). This sediment deposit thins toward shore near Cape Lisburne. To the north of Cape Lisburne a wide band of sediment approximately 4 m to 5 m thick trends to the northeast (figure 10). Landward, toward Cape Beaufort, the sediment cover rapidly thins to 1 to 2 m as the water depth shallows to 20 m (figures 11b, 12c). To the northwest of the northeast trending sediment band the Holocene-Quaternary deposits are thin, varying from 1 to 3 m in thickness (figure 10).

The northeast trending sediment band continues toward Icy Cape. Internally the sediment contains horizontal and parallel reflectors overlying inclined strata (figures 12d, 13a, 13b). This sediment band may have formed by sediment transportation and deposition by the northward flowing Alaska Coastal Current in combination with ice groundings and ice push. This sediment band also underlies an area of severe ice ridging (Stringer 1978). To the east in shallow water storm waves have eroded the sea bed removing part of the sediment cover. To the northwest of the sediment band, northeast flowing shelf currents have eroded the surficial sediment leaving a thin sediment cover over bedrock.

Nearshore, north of 70 degrees to Blossom Shoals, the Holocene-Quaternary sediment blanket varies from 2 to 5 m in thickness. Off Icy Cape the outer sand bank contains over 10 m of sediment overlying bedrock (figure 14). Nearshore, between Icy Cape and Point Franklin as well as north of Blossom Shoals, the Holocene-Quaternary sediment cover is also thin varying from less than 2 m to 3 m in thickness.

The thickest Holocene-Quaternary deposits are found at the head of the Barrow Sea Valley west of Point Franklin where the sediment is over 14 m thick. The sediment increases in thickness

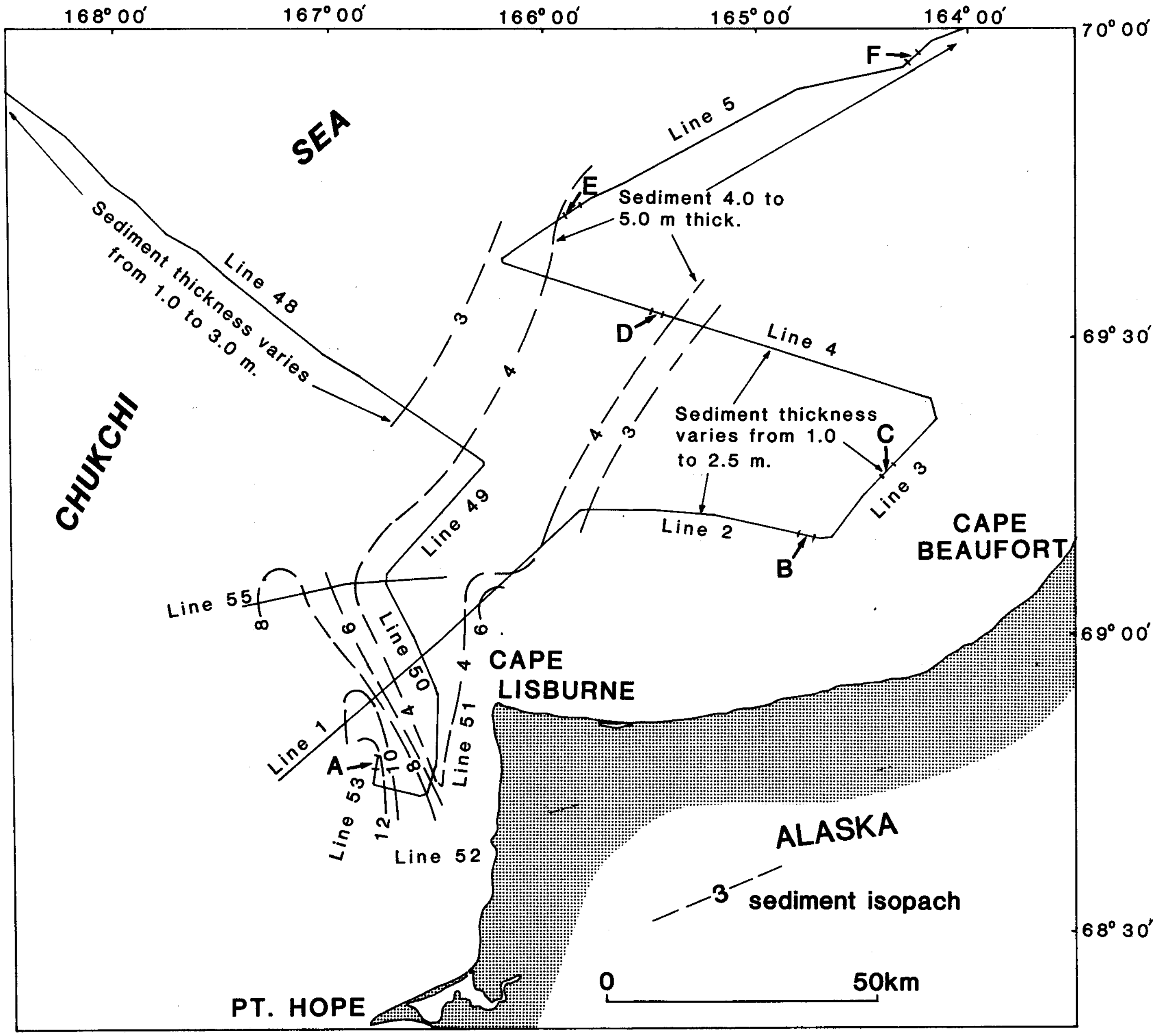

Figure 10. Isopachs of Holocene-Quaternary sediment near Cape Lisburne. The letters indicate seismic profile locations. Isopachs are in meters.

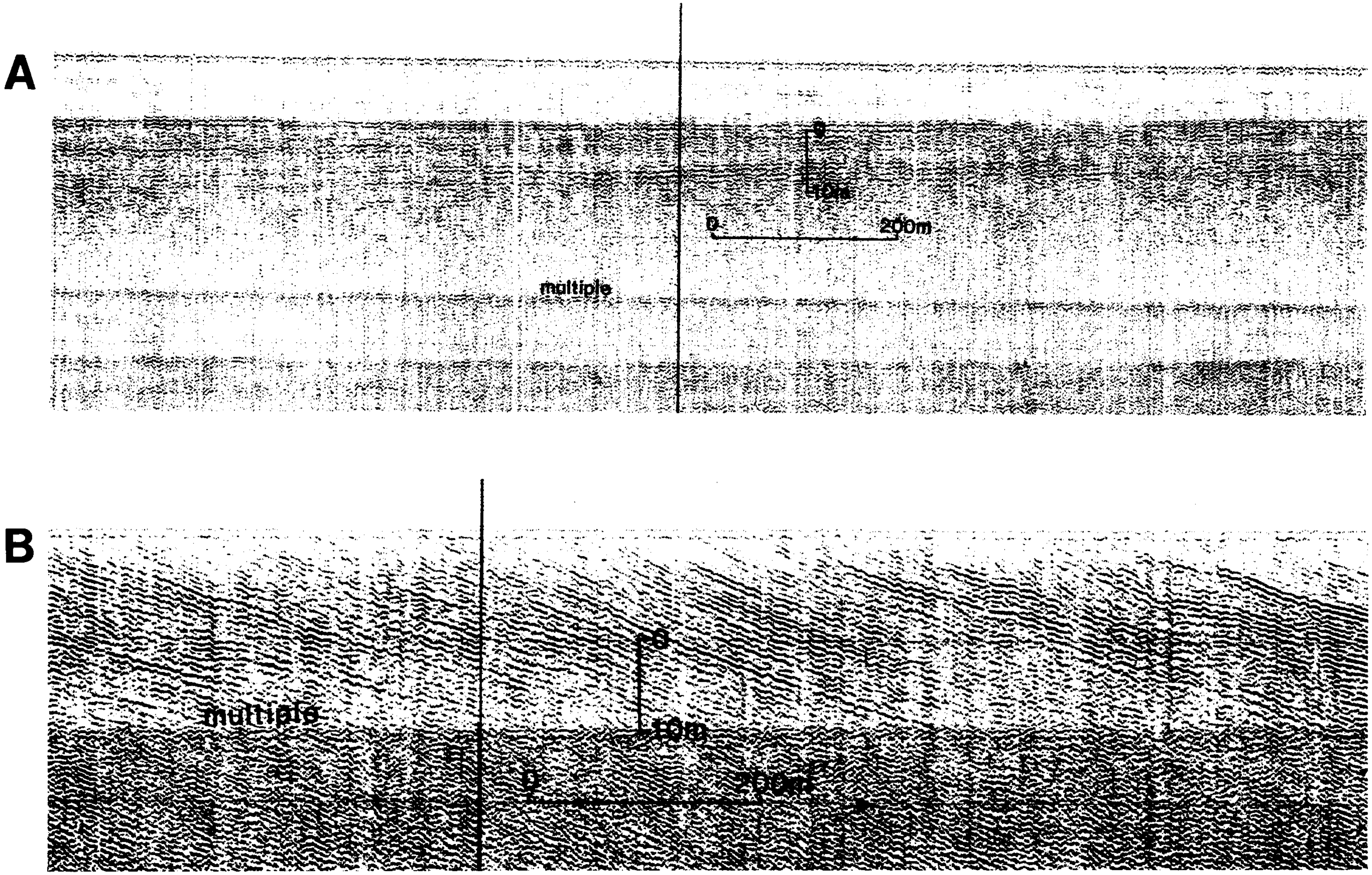

Figure 11. Seismic profiles near Cape Lisburne. A). An upper transparent (sand?) unit overlies slightly inclined strata. B). A thin, less than 2 m thick, sediment cover overlies dipping bedrock. See figure 10 for profile locations.

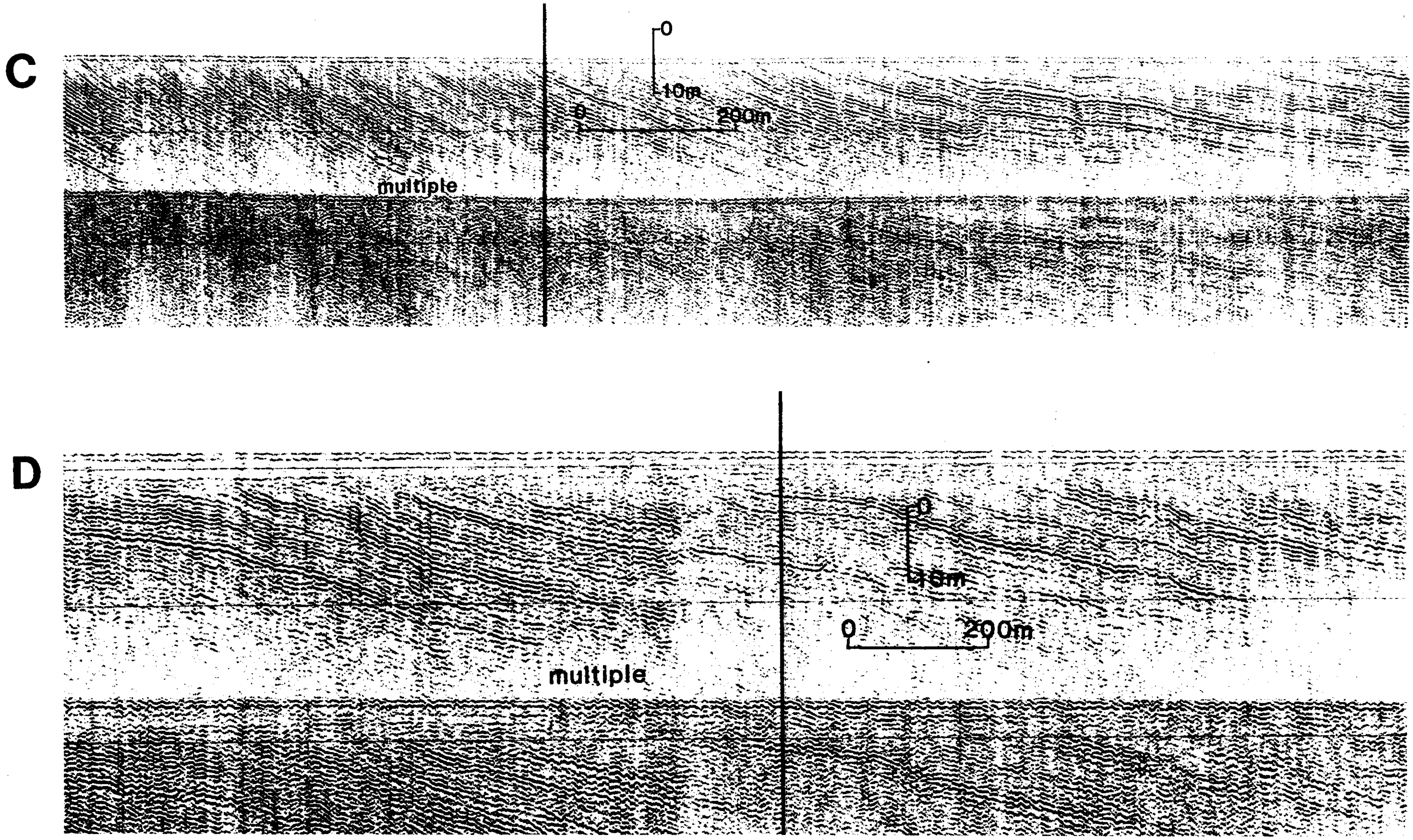

Figure 12. Seismic profiles north of Cape Lisburne. C) A thin sediment cover overlies bedrock west of Cape Beaufort. D). The upper seismic unit containing horizontal strata is approximately 4 m thick and may represent sediment deposited by the northward flowing currents. See figure 10 for profile locations.

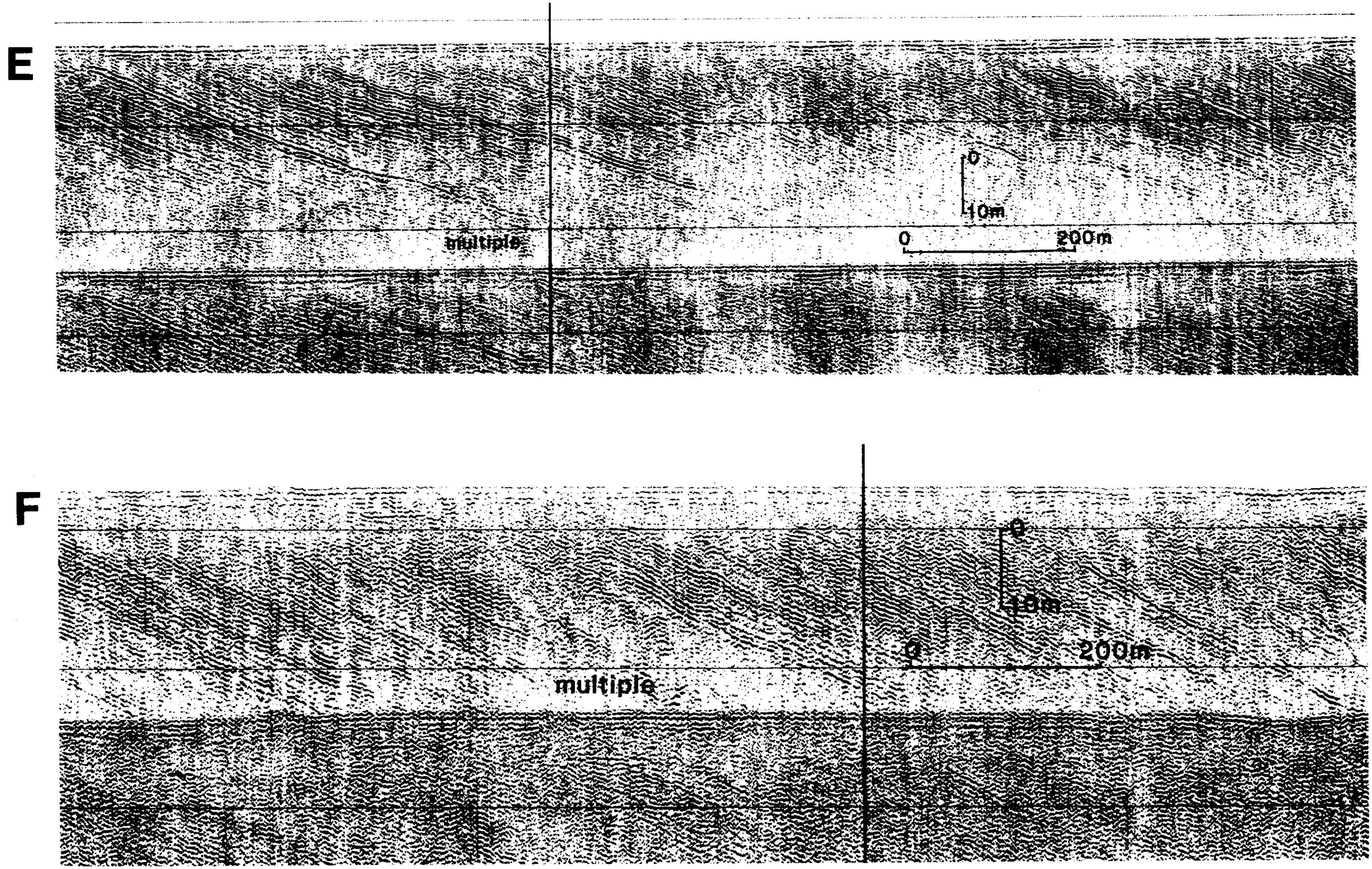

Figure 13 Seismic profile north of Cape Lisburne. Both profiles (E and F) show thin sediment cover over inclined bedrock which is typical for the southern Chukchi Sea. See figure 10 for location for (E) and figure 27 for location for (F).

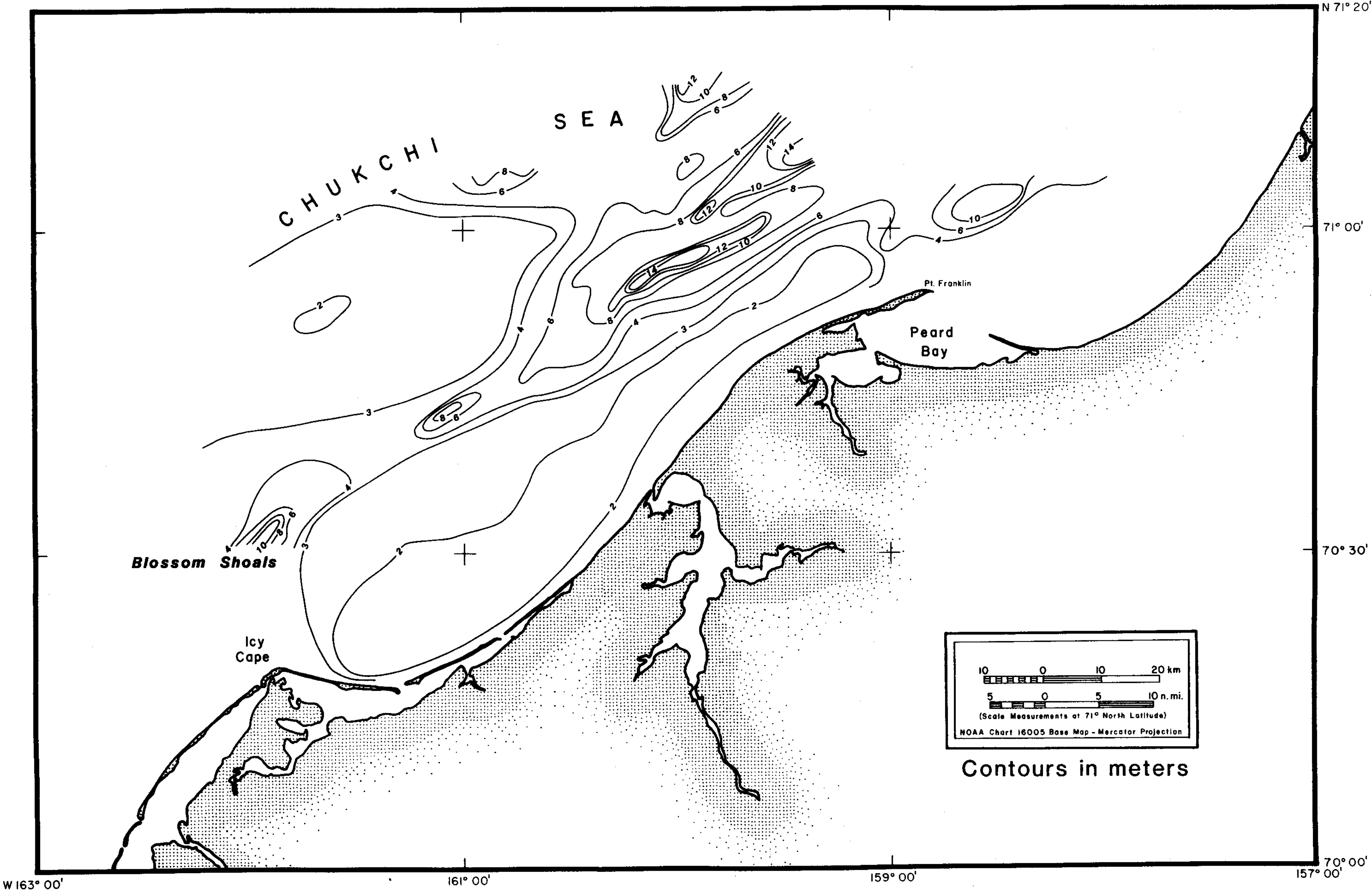

Figure 14. Isopachs, in meters, of Holocene-Quaternary sediment in the northeast Chukchi Sea. The nearshore isopachs are from Phillips and Reiss, 1984.

with increasing depth with most deposits greater than 6 m thick below 55 m. The thickest deposits trend to the northeast in linear bands parallel to the slope of the Barrow Sea Valley (figure 14). Within the sea valley modern channels are eroding the Quaternary deposits (figure 15).

On the west flank of the Barrow Sea Valley a series of paleochannels contain up to 13 m of sediment fill. The channeled sequence forms most of the Holocene-Quaternary sediment cover (figures 15, 16). However, to the east most of the Quaternary deposits within the head of the sea valley rarely contain coherent internal reflectors. The thickest deposits are found within the deeper parts of the sea valley adjacent to modern erosional channels. The Quaternary sediments are apparently being eroded by an internal drainage systems within the head of the sea valley (figures 17b, 17c). Channels cut through the Quaternary deposits down to bedrock (figures 18d, 18e).

To the west on the outer shelf the Holocene-Quaternary sediment blanket, which overlies folded to gently inclined bedrock, is thin varying from less than 1 m up to 5 m in thickness (figures 19a, 19b).

CHANNEL-FILL DEPOSITS (age unknown)

A series of filled paleochannels incised into bedrock are identified in the northwest part of the study area starting at approximately 70 30'N and 167 00' west (figure 20). Based on limited trackline coverage, the largest channel system trends to the northwest. In water depths ranging from 45 to 50 m the channels are cut to depths of 10 m to over 64 m below the sea bed. The channels range up to 13 km in width. The channels may not represent a specific time event (same age) but represent multiple erosional and depositional events during different sea level lowerings. Evidence for different time events producing the channels is preserved in the distinct channel-fill stratigraphy, the superposition of stratigraphic units, and erosional contacts of some seismic units.

Four major seismic units containing distinctive depositional features are identified within the larger channel systems; 2 to 3 seismic units in the shallow channels.

The uppermost depositional sequence, seismic unit A, represents a thin blanket deposit ranging up to 6 m in thickness. This unit overlies all of the channeled and non-channeled deposits. Internally horizontal or gently inclined parallel reflectors characterize this sequence. The lower reflectors may truncate the underlying strata forming an undulatory contact.

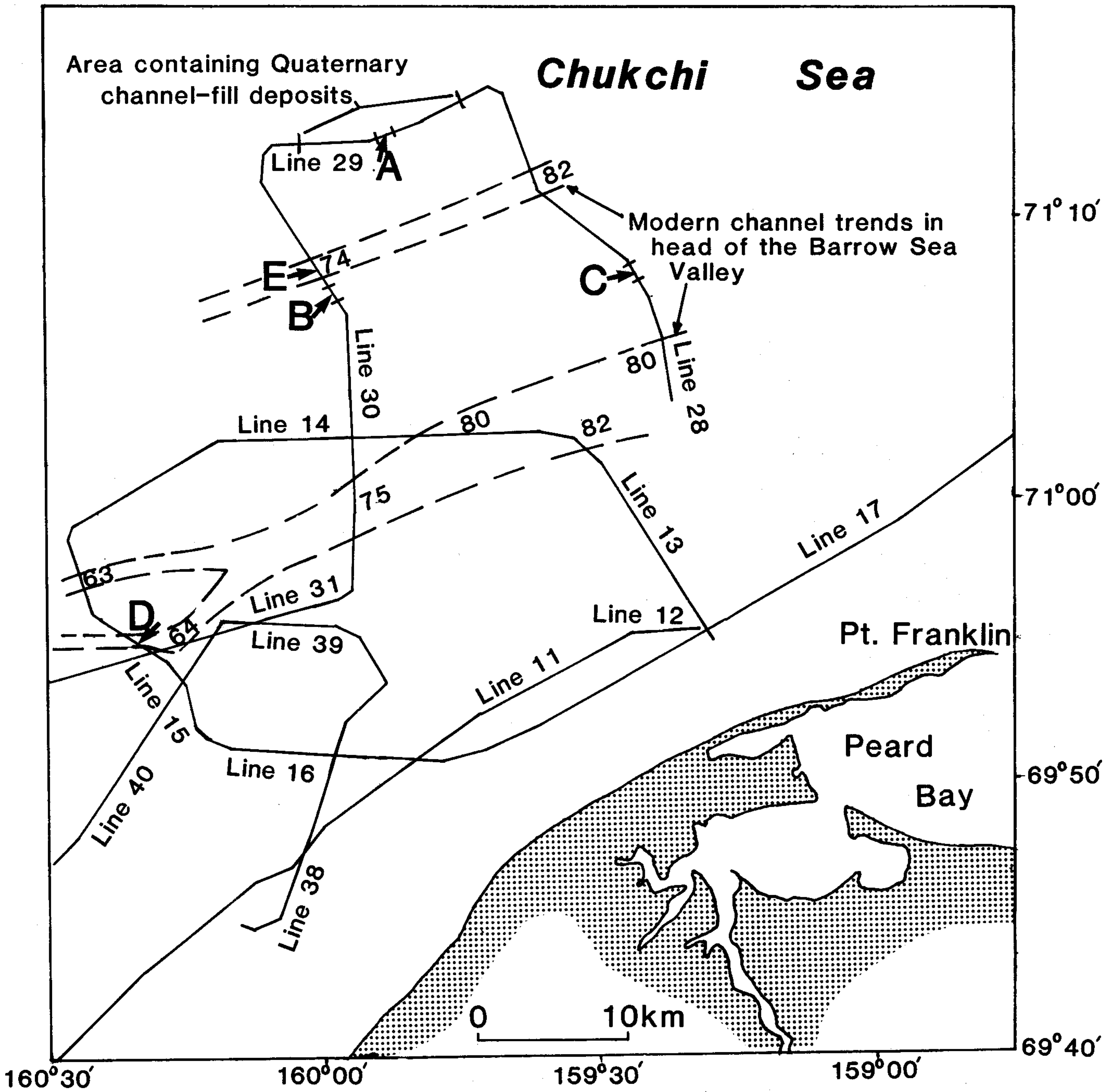

Figure 15. Modern channel trends in the head of the Barrow Sea Valley. The numbers within the channels indicate the maximum water depth in meters; the letters indicate seismic or bottom profile locations.

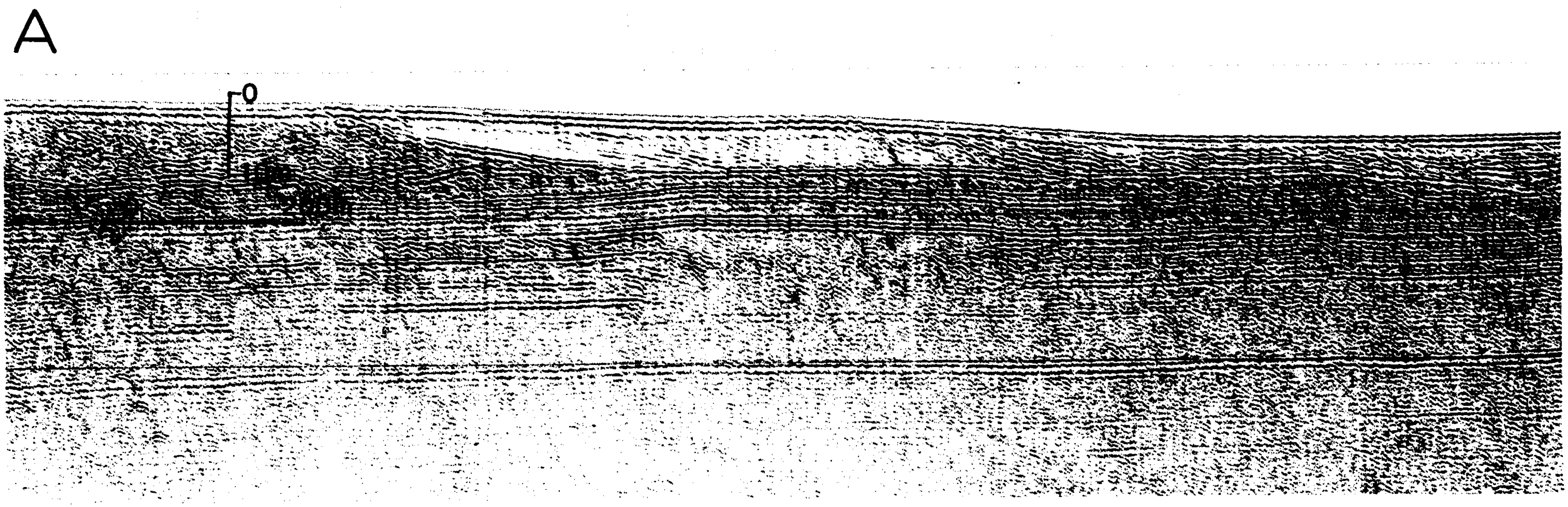

Figure 16. Seismic profile on the west side of the Barrow Sea Valley showing fluvial channel deposits overlying gently inclined bedrock. See figure 15 for profile location.

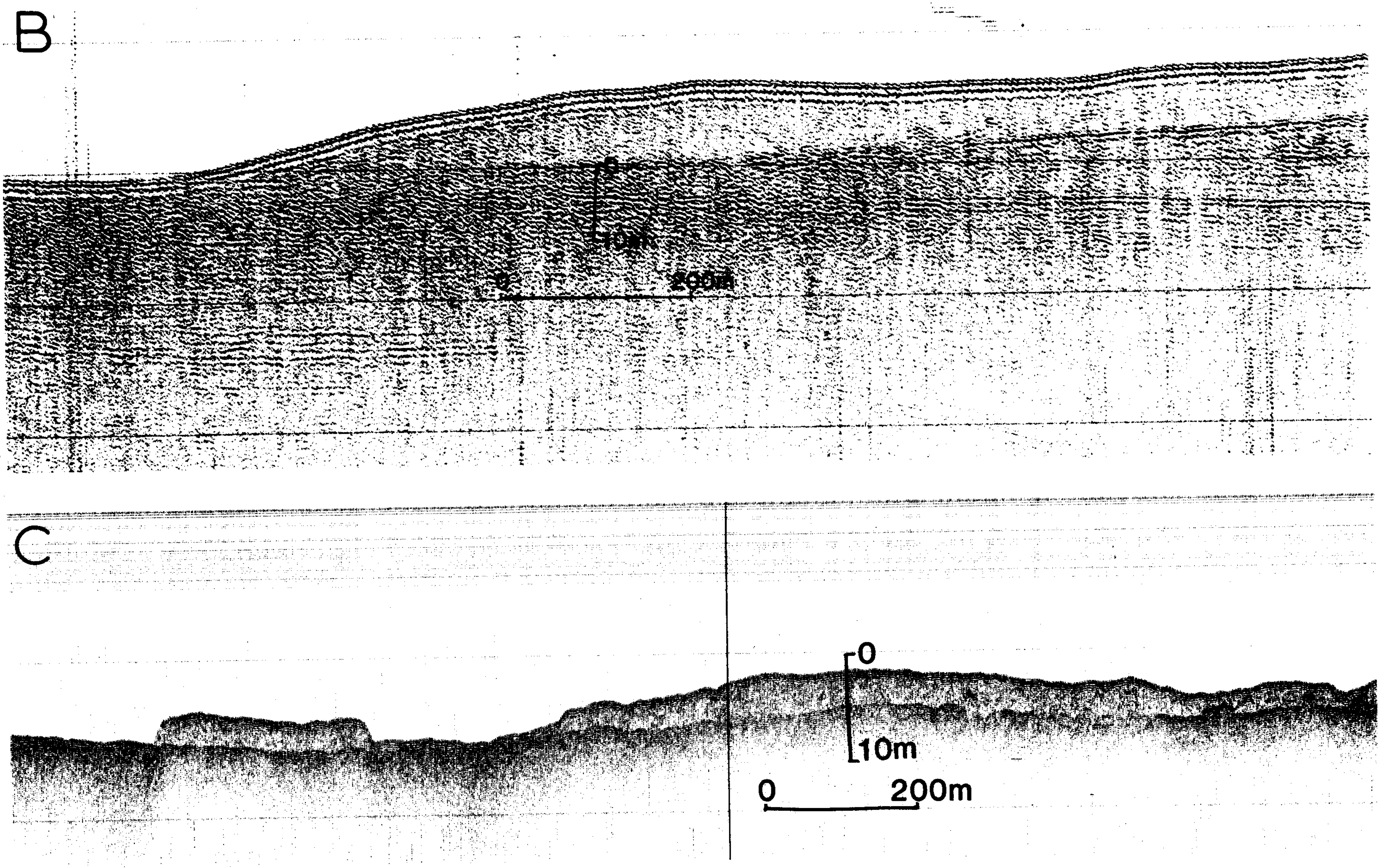

Figure 17. B). Seismic profile near the center of the Barrow Sea Valley showing eroded Quaternary deposits overlying gently inclined strata. A modern channel has cut through the young sediment down to bedrock. C). Bottom profile in the Barrow Sea Valley showing either eroded or slumped deposits overlying bedrock (water depth 68.5 m). See figure 15 for profile locations.

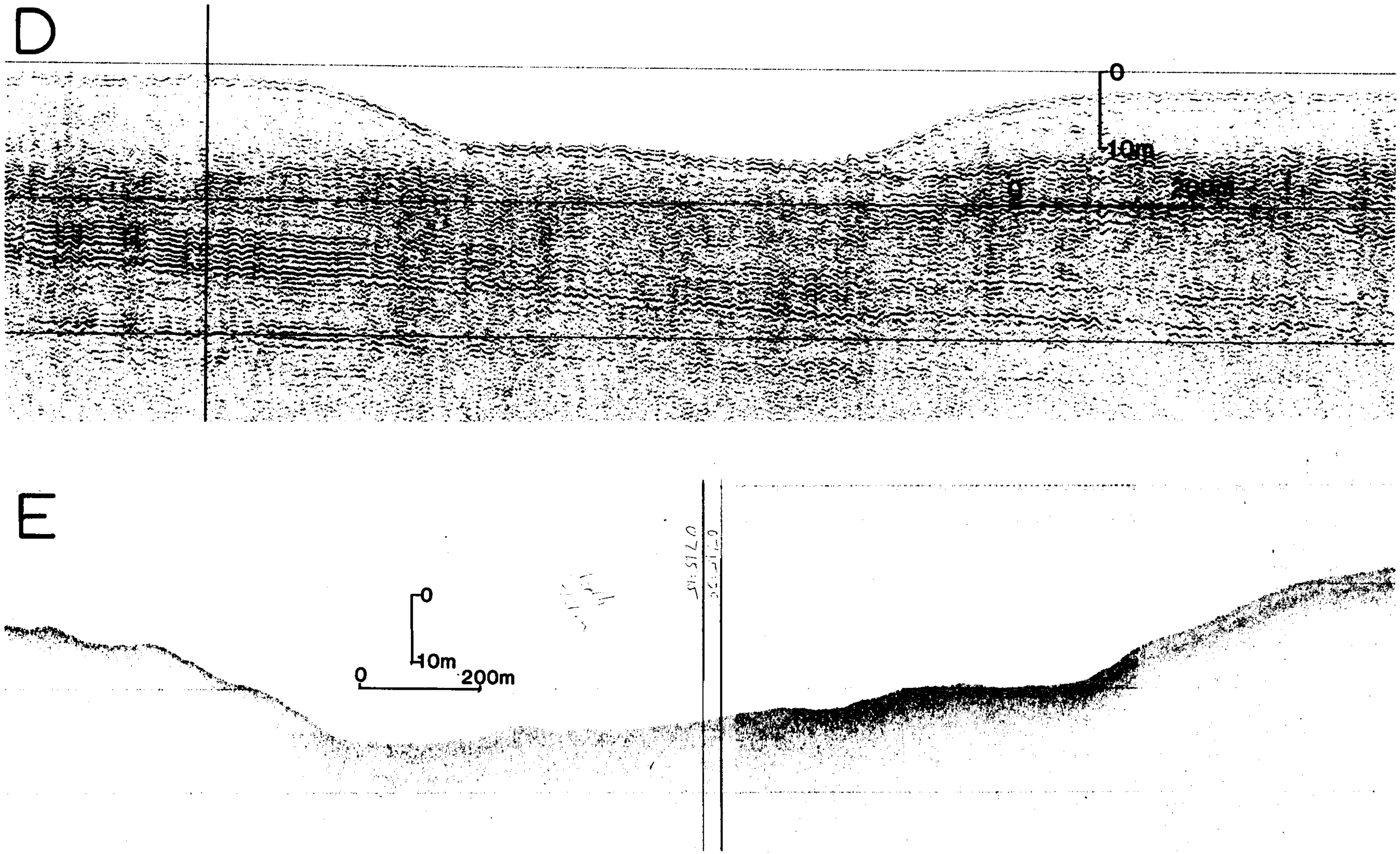

Figure 18. Modern channels at the head of Barrow Sea Valley. D). Seismic profile showing channel incised into Quaternary deposits which overlie inclined bedrock. E). Bottom profile of channel. See figure 15 for profile locations.

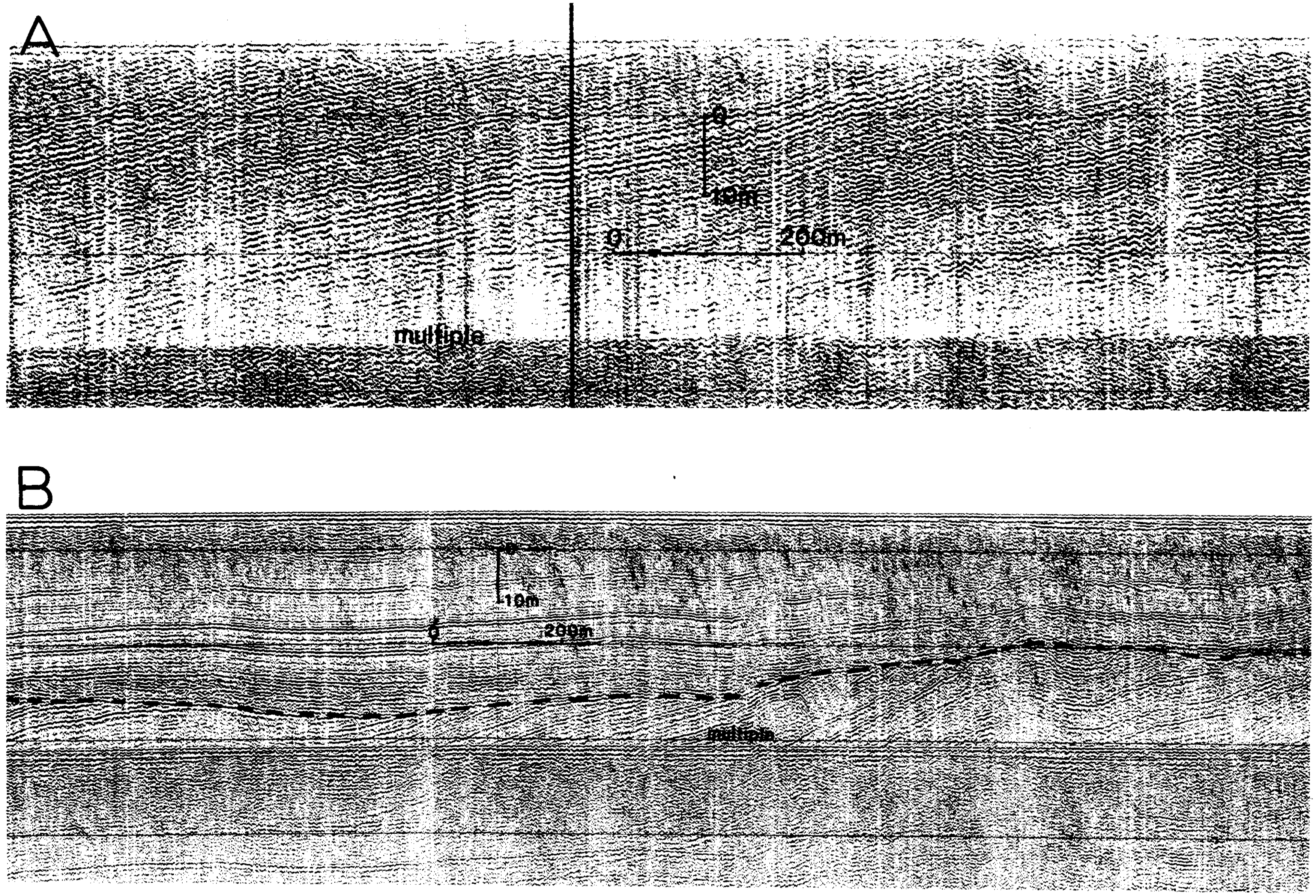

Figure 19. A). A thin sediment cover, locally containing gravel, overlies inclined bedrock on the outer shelf. B). An angular unconformity separates a lower folded and faulted bedrock sequence from an upper gently inclined (but also faulted) bedrock sequence. A thin sediment cover overlies the bedrock. See figure 20 for profile locations.

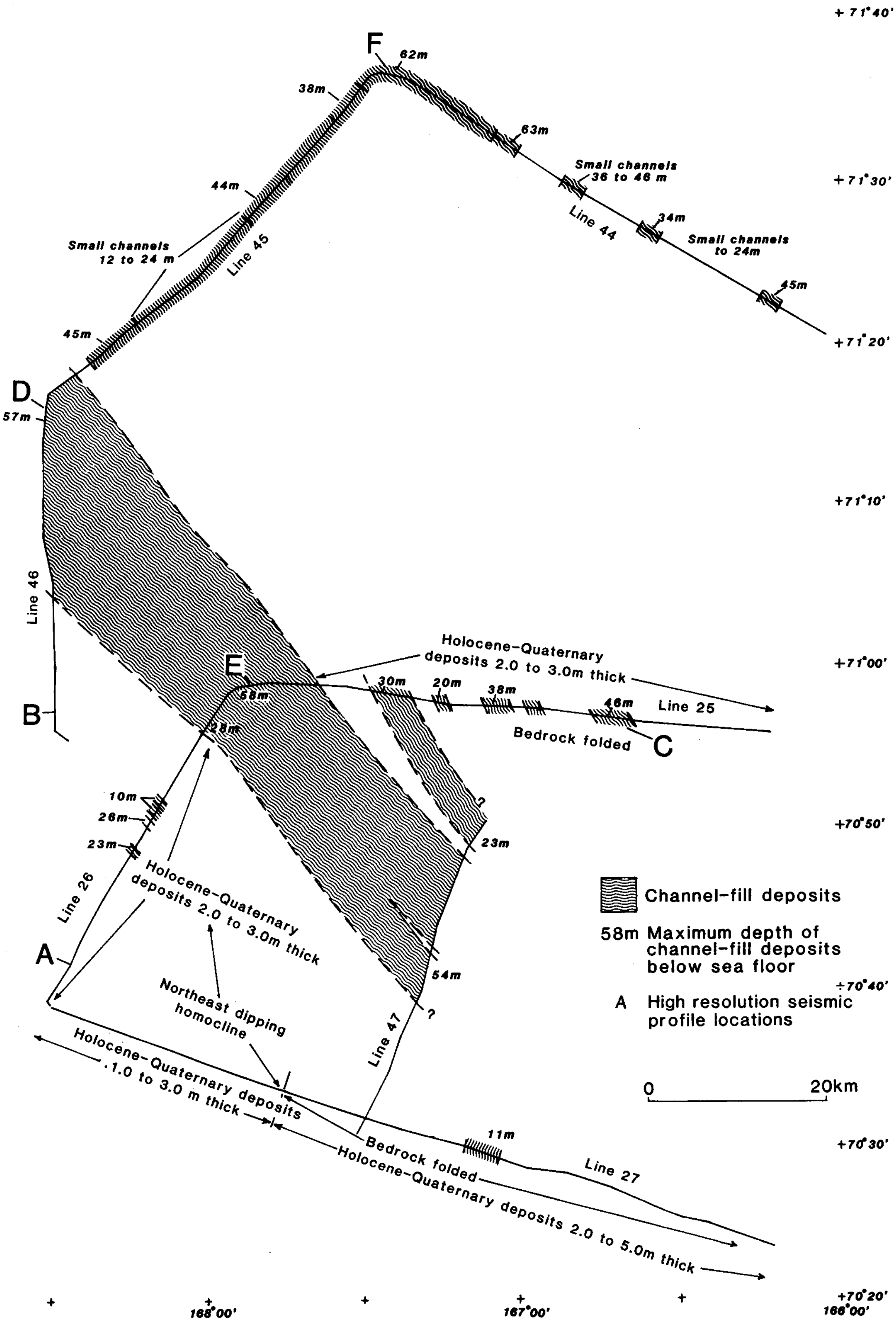

Figure 20. Holocene-Quaternary sediment thickness, channel trends and channel-fill deposits on the outer part of the Chukchi Sea. The maximum depth of channel incision, expressed in meters, determined from seismic profiles.

The underlying sequence, seismic unit B, is also a blanket deposit varying from 14 to 32 m in thickness (averages about 18 m). The thicker depositional sequences represent local deep channels cut into underlying strata. Internally this unit exhibits complex sedimentation patterns. The reflectors can be discontinous, contain abundant defraction hyperboles, or contain well defined parallel inclined reflectors. Truncation of the reflectors (due to channeling) can be locally common. The lower contact is usually undulatory and erosional.

The underlying sequence, seismic unit C, varies in thickness from 2 to over 28 m. Horizontal and parallel or slightly undulatory and parallel reflectors comprise the seismic section. The reflectors are parallel and continous throughout the seismic records. The basal reflectors of this sequence are usually draped over an irregular erosional surface, likewise, the reflectors thin but are also draped over channel flanks or other topographic irregulatories.

The basal seismic sequence, unit D, is usually discontinous and poorly preserved. The strata vary in thickness from erosional pinchouts to over 16 m. Abundant hyperboles, locally inclined and parallel reflectors, or small-scale channeling characterizes the basal unit where preserved (figure 21).

The character of the reflectors within the seismic sequences identifies possible depositional environments. The channels record similar fill-stratigraphy even within multi-cyclic erosional-depositional events. Unit A represents fluvial to marine sedimentation and would include Holocene transgressive deposits. Unit B represents fluvial-dominated sedimentation as indicated by the abundant internal channel deposits but this sequence may also include some marine, estuarine, lagoonal and terrestrial facies. Unit C represents deposition of fine-grained sediment within a quiet low energy environment. Marine conditions most likely prevailed during deposition of this sequence, however, bay or estuarine facies may also produce a similar depositional sequence. The basal sequence, unit D, represents mainly fluvial deposition probably related to the period of bedrock erosion when the deep channels were initially cut.

The channel-fill sequences can vary; most channels record an initial channel down-cutting (to 116 m below present sea level) and deposition of fluvial sediments (unit D). After deposition of the fluvial sediments a period of erosion followed. The draped strata (unit C) overlying the fluvial sediments (unit D) represent marine sediment deposition during a transgression (figures 22, 23, 24, 25). The next depositional sequence, unit B, probably contains a variety of environments including fluvial, lagoonal, barrier island to possible marine (figure 24). Within unit B a large channel over 28 m deep (103 m below sea level) has removed both underlying units C and D. The unit B channel is in

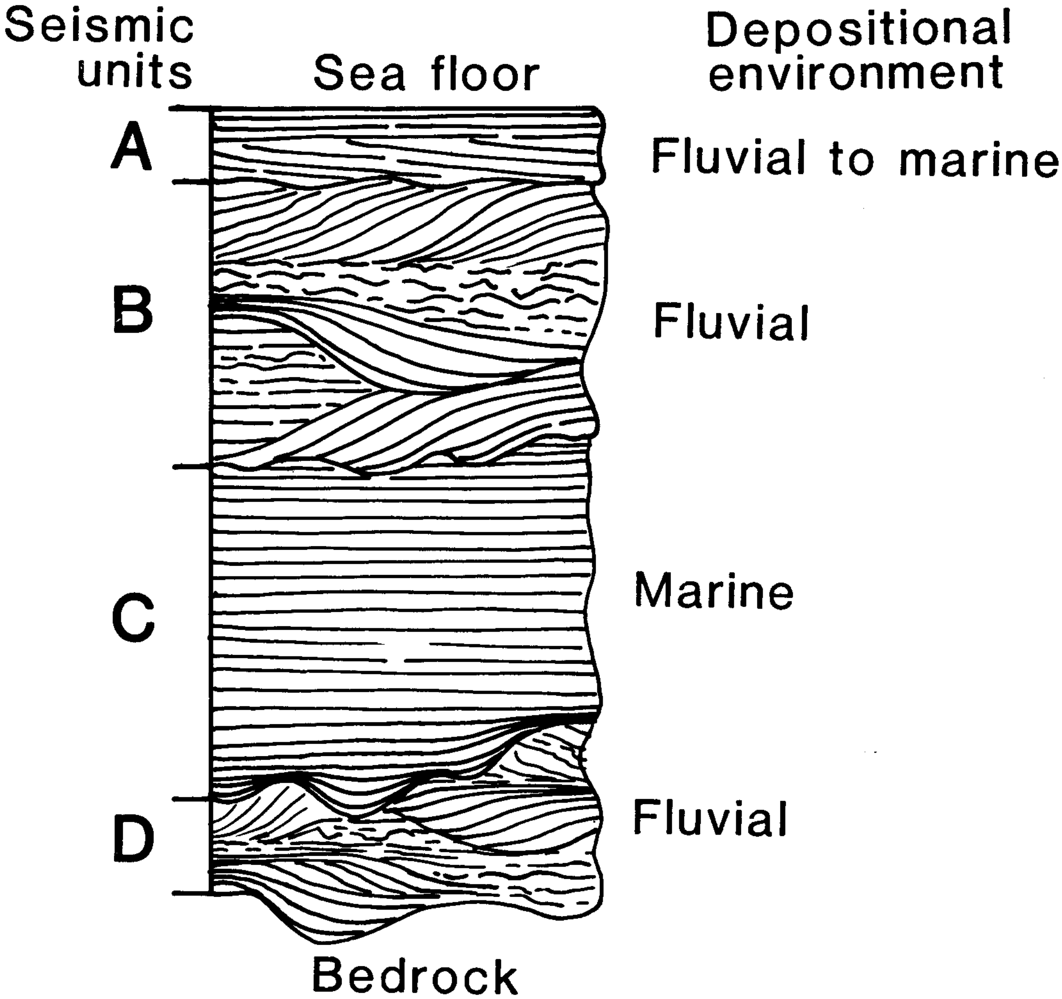

Figure 21. Major seismic units and interpretative depositional environments for channel-fill deposits, northwest Chukchi Sea. Unit D rests on an erosional surface cut to 63 m into bedrock (116 m below present sea level); Unit C drapes an irregular erosional surface developed on Unit D and represents a probable marine depositional sequence; Unit B contains abundant channels but may also include estuarine to deltaic to terrestrial depositional environments; and Unit A contains fluvial to probable marine environments and would contain Holocene transgressive deposits.

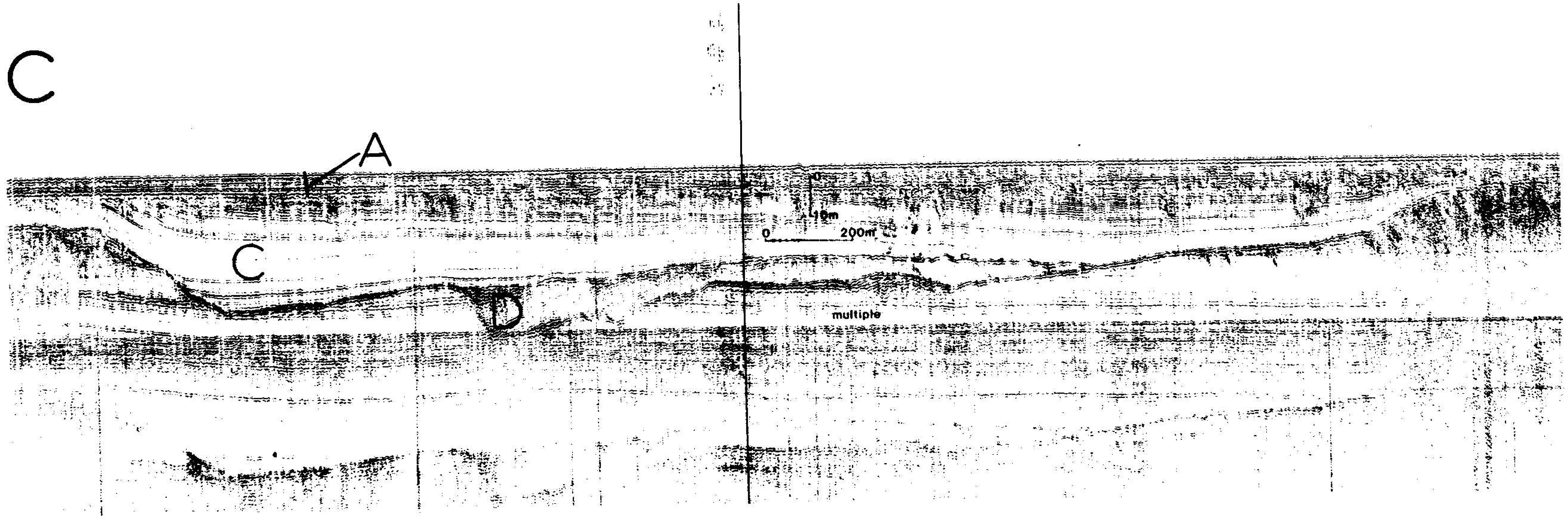

Figure 22. Channel-fill sequence containing 3 seismic units consisting of Unit D fluvial deposits, Unit C draped deposits (marine ?) and Unit A deposits which consist of a fluvial to marine sequence. See figure 20 for profile location C.

D

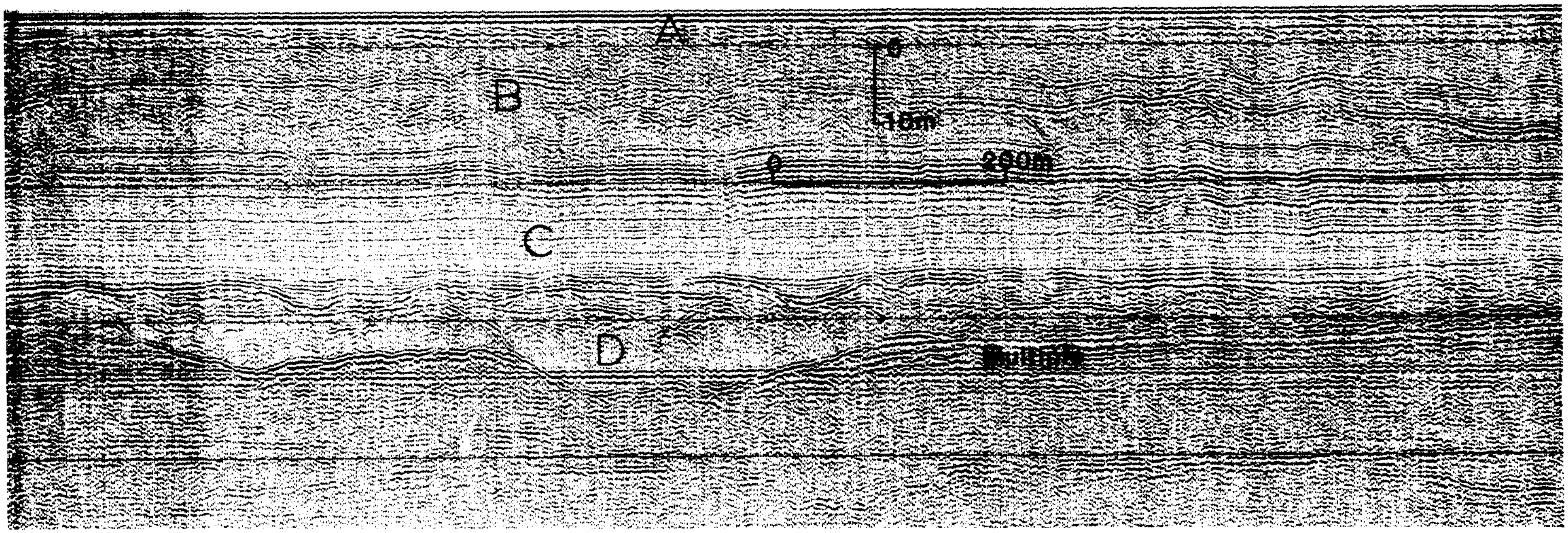

Figure 23. Channel-fill deposits within a large channel system, northwest Chukchi Sea. Four seismic units separated by erosional surfaces are identified and consist of a basal fluvial sequence (Unit D), a well-bedded draped sequence of probable marine origin (Unit C), a fluvial-dominated sequence (Unit B), and the uppermost sequence (Unit A) consisting of fluvial to marine beds. See figure 20 for profile location.

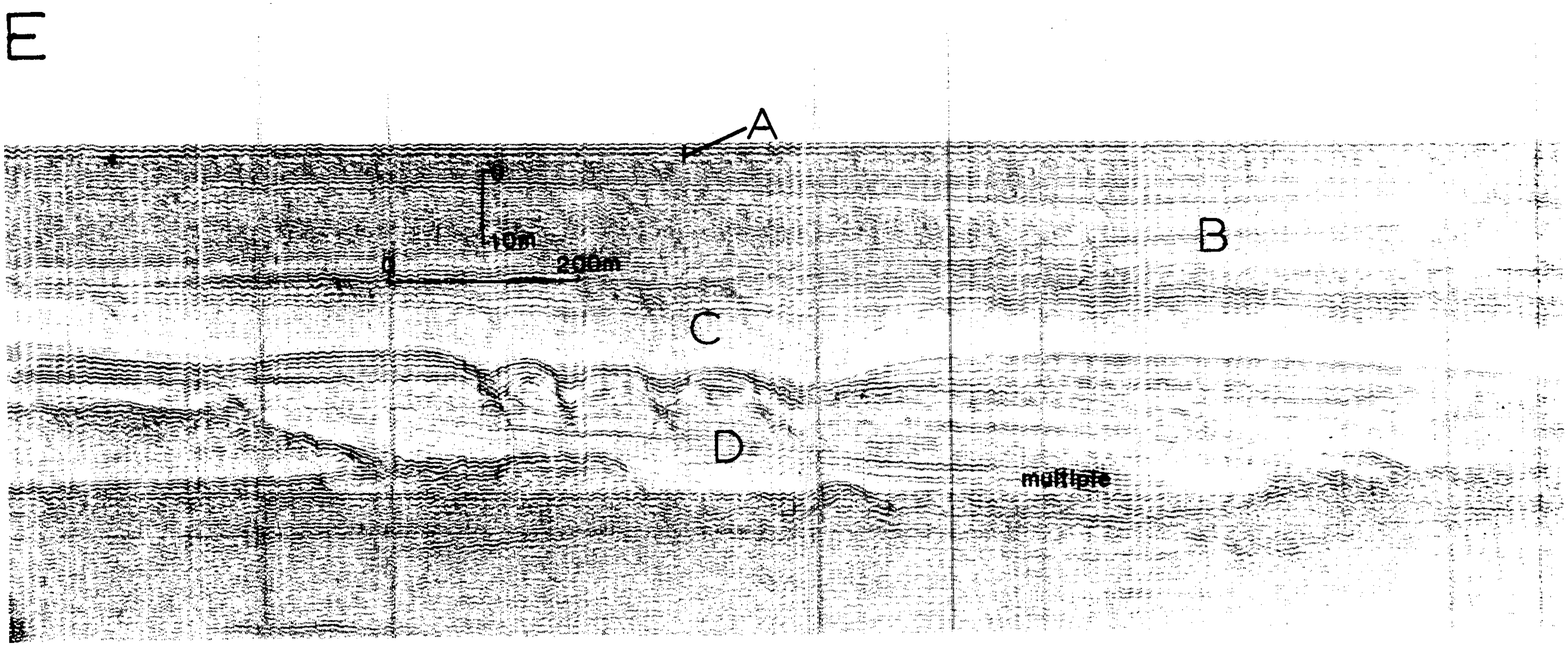

Figure 24. Channel-fill deposits within a large channel system containing a thick basal sequence of fluvial deposits (Unit D), a draped marine sequence (Unit C), a thick fluvial sequence (Unit B), and a thin fluvial-marine sequence (Unit A). See figure 20 for profile location.

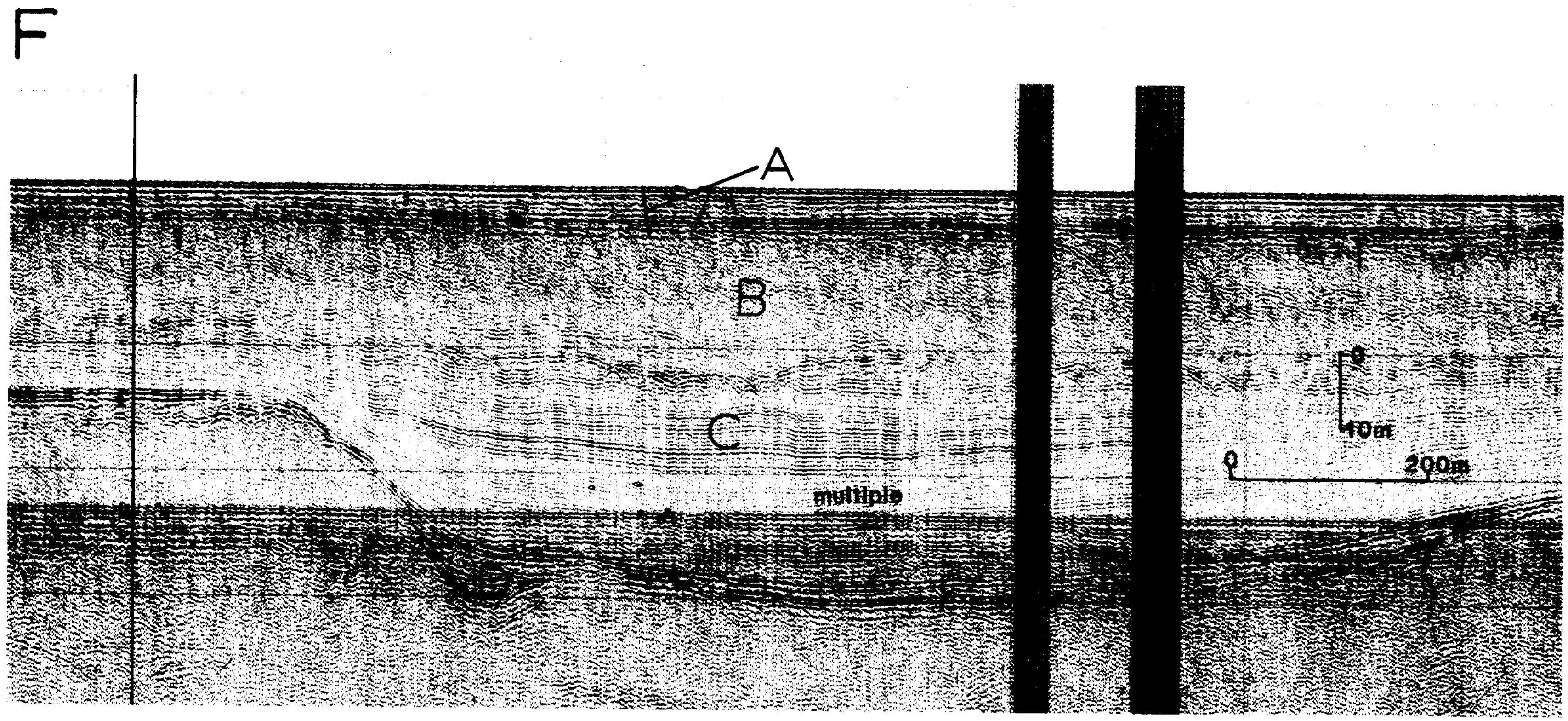

Figure 25. Channel-fill deposits recording a thin and discontinous basal fluvial sequence (Unit D), a thick draped marine sequence (Unit C), a poorly defined fluvial sequence (Unit B), and a relatively thick fluvial-marine sequence (Unit A). See figure 20 for profile location.

turn filled with parallel draped reflectors. In much of this unit numerous shallow channels characterize the depositional sequences. The upper depositional unit contains only shallow, to 6 m thick, isolated channels suggesting fluvial deposition. Lagoonal, barrier island and marine environments may be found within this sequence.

During sea level lowerings multiple channeling events are proposed. At least 3 periods of sea level lowering and cutting of channels are recognized: 1) channels were initially incised to at least 116 m below present sea level, then filled during a transgressive event (deposition of seismic units D and C); 2) sea level lowering again resulted in channels cut to at least 103 m below present sea level (deposition of seismic unit B); and 3) a third sea level lowering event to at least 92 m below present sea level is recorded in channels lacking deposition of seismic unit B. The time relationship of the channels lacking unit B to the channels containing unit B is unknown.

The age of the channeling events is uncertain but may range from Quaternary to Tertiary. A "young" age is suggested for the channel-fill deposits based on the following: 1) the channels are incised into at least two stratigraphic bedrock units which are separated by an angular unconformity, the gently inclined strata of the North Chukchi Basin which overlies older folded bedrock (figure 19b); 2) the channels are not folded suggesting the channel-fill is younger than the folding event; 3) some channels appear to be bedrock controlled following the strike of underlying strata which also suggests the channels are younger than the bedrock they are incised into; 4) the channels must be younger than Late Cretaceous age because paleocurrent data and nonmarine channel trends (early to late Cretaceous age Nanushuk Group sandstones in the North Slope) are to the east to northeast (Bird and Andrews, 1979; Molenaar, 1985) over 90 degrees apart from the Chukchi Sea northwest trending paleochannels; 5) the channels are cut to at least 116 m below present sea level suggesting possible Quaternary sea level lowerings (however the channels may be incised to deeper depths to the north beyond the area of our track lines); and 6) some wide channels underly areas now containing sea floor depressions suggesting either compaction of unconsolidated sediment or the melting of permafrost to produce the sea floor depressions (figure 7).

The above evidence suggests a Quaternary to Tertiary age range for the channel deposits. However, the major problem of this "young" age is the identification of the channel's sediment source, because the major southern Holocene drainage pattern in the Chukchi Sea was to the west through the Chukchi Valley (McManus and others, 1983) (the present Hope Sea Valley located east of Wrangel and Herald Islands), and not where those ancient channels are located. Likewise, the Barrow Sea Valley was probably the major Holocene drainage for streams and rivers from the east to at least south to Wainwright and the Kuk River because paleochannels trend north into the sea valley. The present lack of adequent drainage sources suggest that the outer shelf channels are pre-Holocene in age.

The Chukchi Sea channel deposits may be sources of sand and gravel. However, they may also represent geologic hazards if they contain permafrost or as in some cases where they contain gas (Appendix D). Drilling will be required to evaluate the channel deposits for a source of sand and gravel as well as establish the age of formation.

SURFICIAL SEDIMENTS

Sonographs along with bottom sampling can delineate the Chukchi Sea's major surficial sediment types. The sea floor texture ranges from sandy mud to muddy sandy gravel. Bedforms, current related sea floor processes, and mammal feeding areas can also be identified from sonographs.

The surficial sediment distribution of the southern Chukchi Sea is fairly well defined from previous work (Creager and McManus, 1966, Barnes, 1970) and is summarized in Grantz and others (1982) and Lewbel (1984). This section summarizes new data obtained from box cores, dredges and sea floor sonographs specifically of textures and sedimentalogic processes acting on the sea floor in the Chukchi Sea. The study is discussed in two sections, the outer shelf which includes the area from Cape Lisburne north, and the inner shelf located at the head of Barrow Sea Valley.

OUTER SHELF

The sediment texture in the outer shelf ranges from mud to gravelly muddy sand. Fifteen box cores are texturally classified as: 1) slightly gravelly sandy mud, 7 cores; 2) sandy mud, 4 cores; 3) slightly gravelly muddy sand, 2 cores; and 4) gravelly muddy sand, 2 cores (classification of Folk, 1974). The distribution of gravel, sand and mud components of the outer shelf cores show the areal variation in the sediment fractions on the shelf. The mud content increases to the north (figure 26, Appendix A).

Sonographs in conjunction with sampling defines the sea floor surface textures. Gravel- and sand-floored regions are readily identified by the presence of bedforms. However, mud appears to be the dominant surficial texture followed by slightly gravelly sandy mud on the outer shelf.

Gravel

Gravel is abundant in the southern part of the Chukchi Sea near Cape Lisburne and near Cape Beaufort (figure 27). In the northern shelf gravel patches are scattered and abundant only south of 71 degrees north (figures 28 and 29).

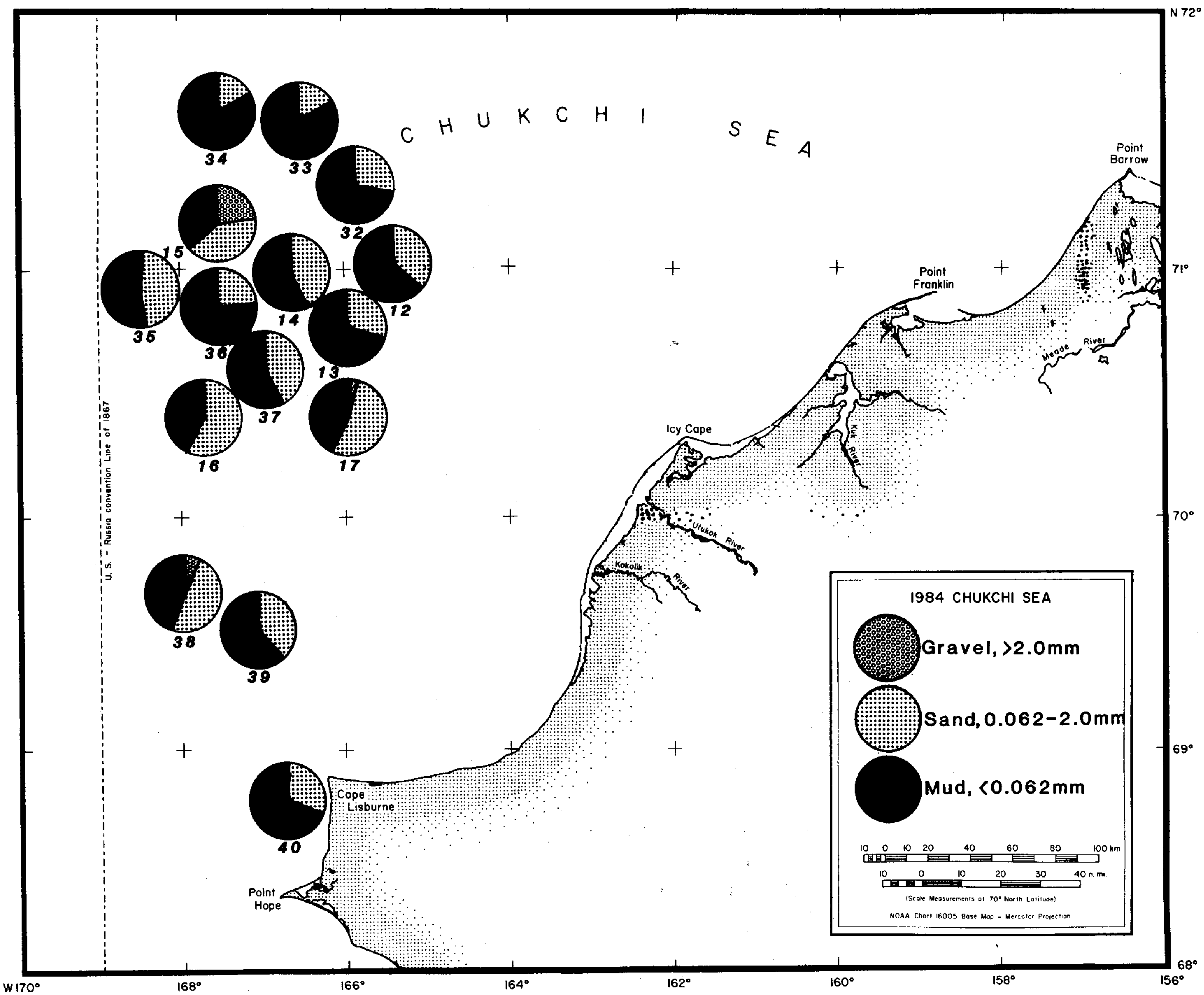

Figure 26. Phi diagram showing box core textural composition in percent for the outer shelf samples in the Chukchi Sea.

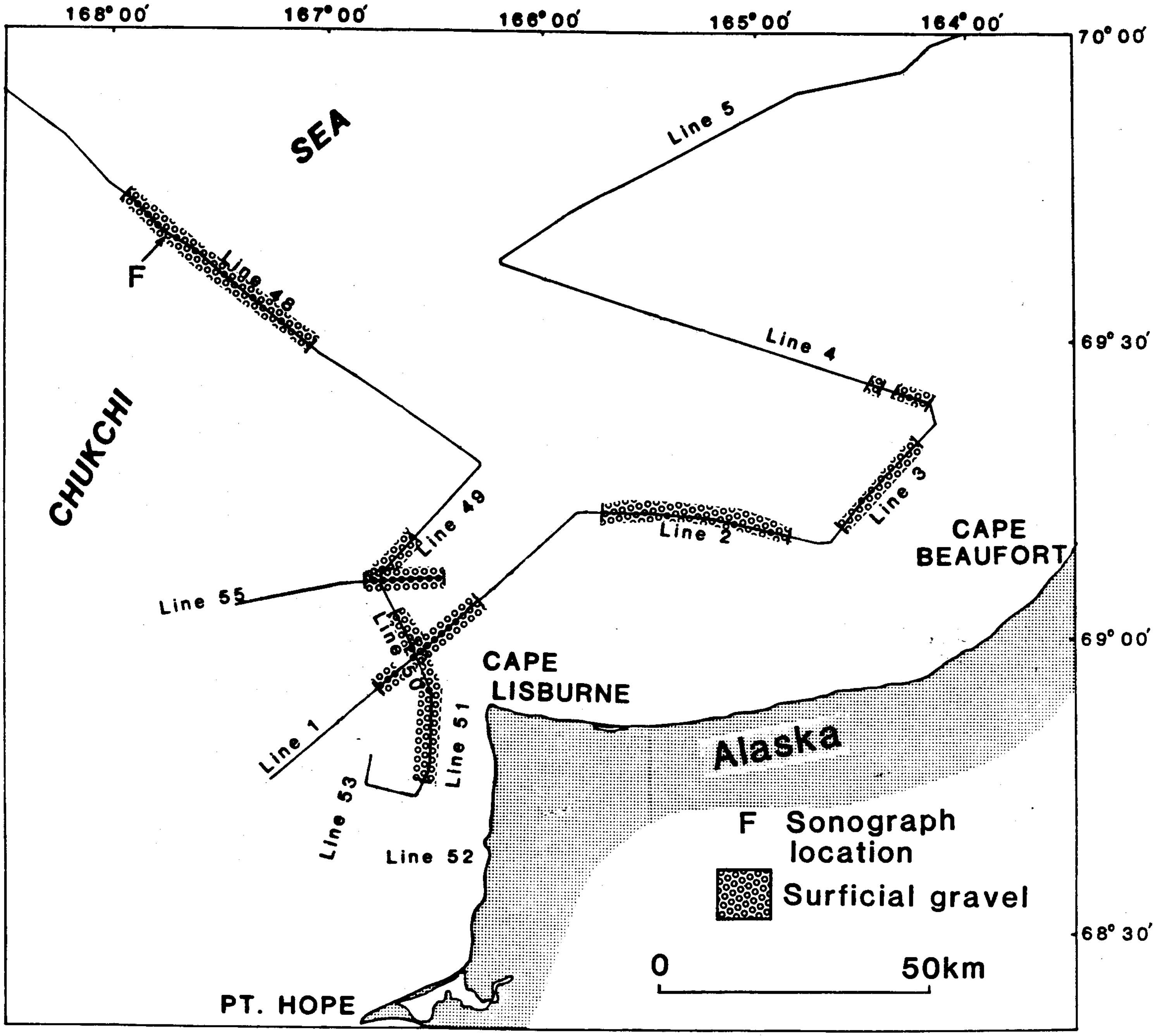

Figure 27. Surficial gravel deposits on the southeast Chukchi Sea determined from samples and side-scan sonar records.

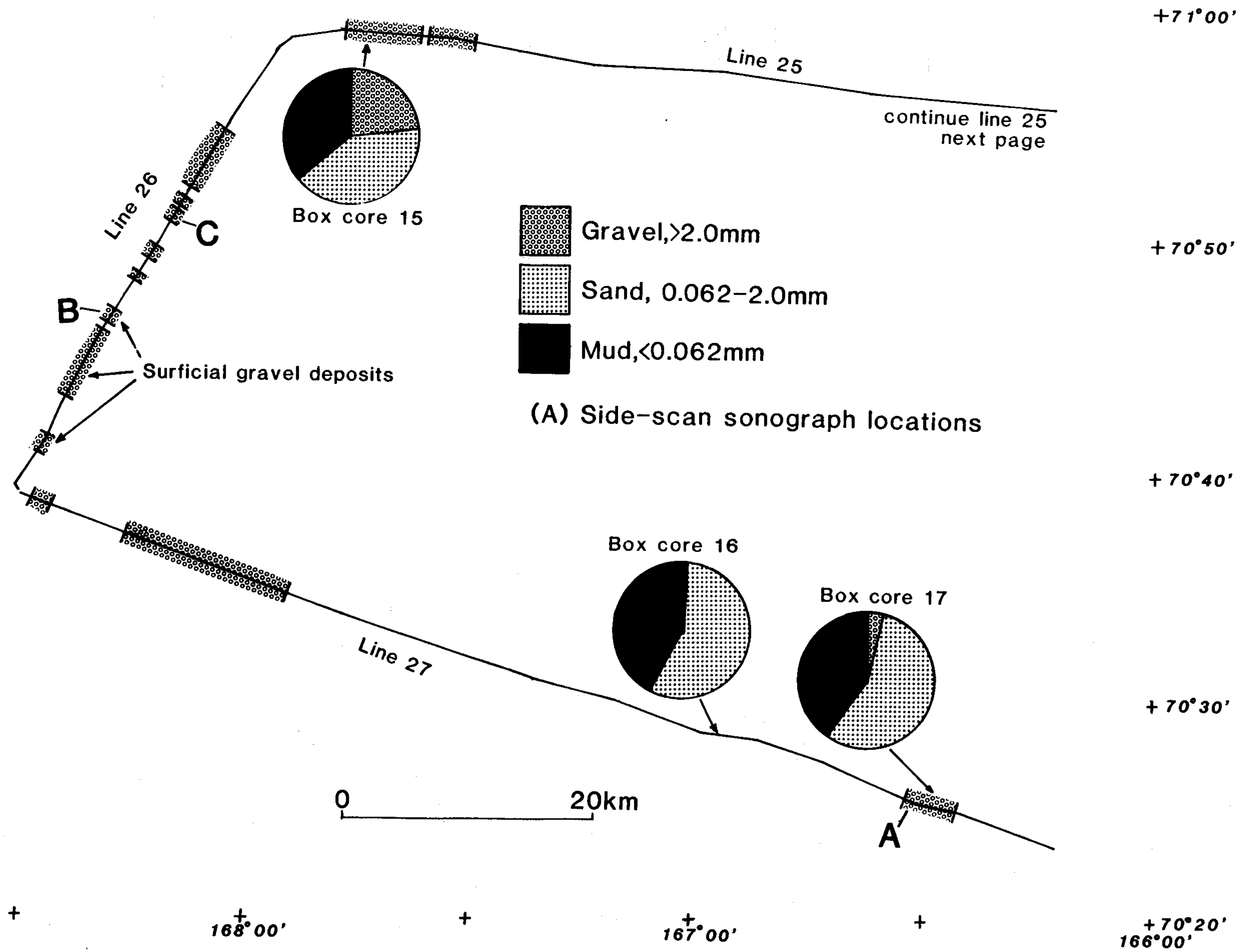

Figure 28. Surficial gravel deposits on the central Chukchi Sea. The distribution of gravel determined from sonographs and box coring. See figure 3 for track line locations.

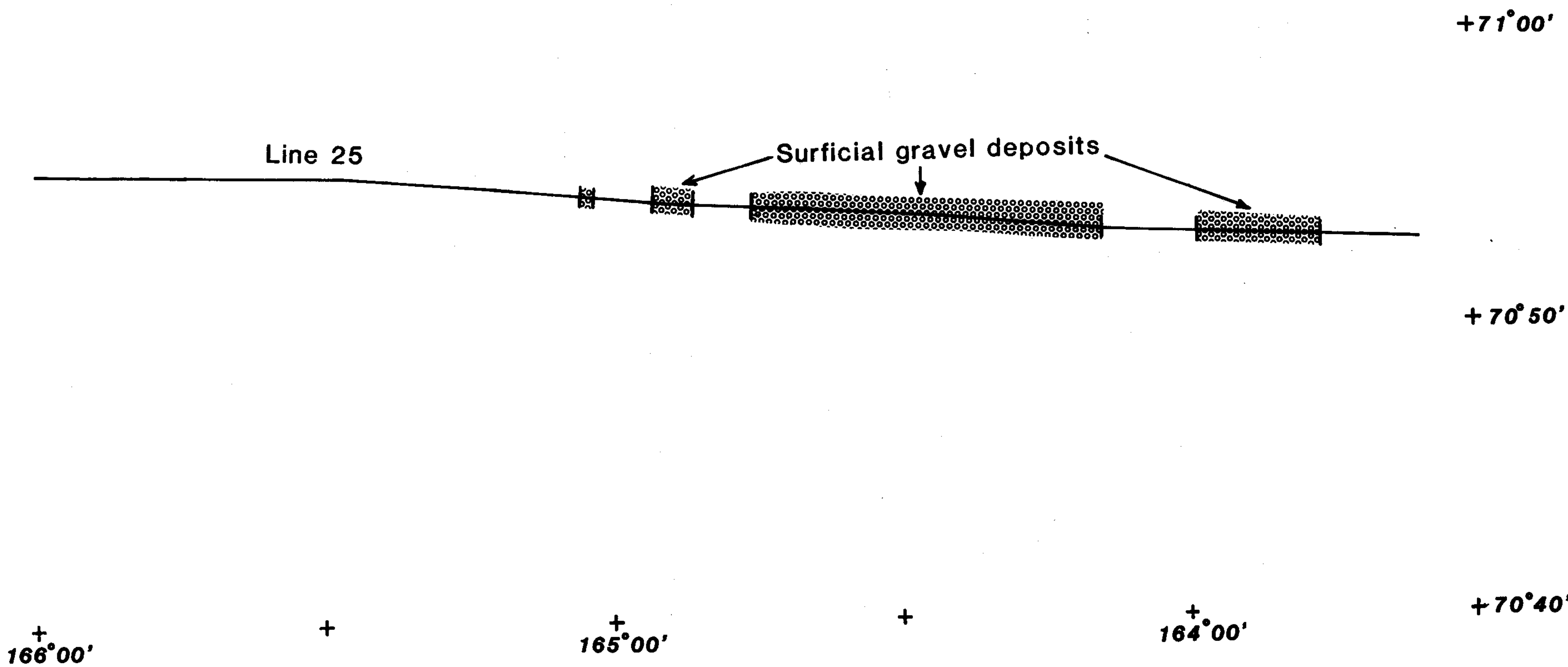

Figure 29. Continuation of line 25 (figure 28) showing the surficial gravel deposits identified on sonographs in the outer Chukchi Sea. See figure 3 for track line locations.

Size analyses of the gravel fraction of 5 box cores and one dredge sample show that the gravel ranges up to 32 mm and falls in the pebble size range. A unimodal size distribution is present in 4 samples and a bimodal distribution in 2 samples (figure 30). The dominant pebble size mode of 5 of the samples is between 4 and 8 mm. The pebbles are either well-rounded (samples 15 and 17) or contain a population of rounded to angular clasts (sample 42). The composition of the pebble fraction varies depending on adjacent bedrock sources and transport distance. Marble and sandstone clasts are abundant near Cape Lisburne, whereas, well-rounded black siliceous clasts dominate in the northwest samples (samples 14,15,16). Sand size mica is abundant in the northern most gravels.

Surficial concentrations of gravel in the Chukchi Sea, reflects regions of active currents and subsequent sea floor erosion. In some examples the gravel is restricted to bathymetric highs. The pebbles occur either as extensive sheets ranging up to 45 km in length or as scattered patches separated by sandy mud. In all gravel-rich areas a thin, usually less than 2 to 4 m thick, Holocene-Quaternary sediment cover overlies bedrock which suggests that the gravels represent an erosional lag deposits.

The surficial gravel deposits exhibit a variety of bedforms. Widespread gravel sheets some covered with symmetrical gravel waves are the most common sea floor feature. Gravel waves also occur in areas where gravel sheets do not exist. Linear gravel ribbons(?) associated with mud or sand are also a common feature on the flanks of gravel sheet deposits especially near Cape Lisburne. The linear gravel ribbons are positive features with relief less than 30 cm, a width ranging from 2 to 4 m, and a spacing of between 5.5 and 6 m (figure 31A). The gravel ribbons usually lie at a slight angle to the ice gouge trend. With decreasing depth, abundant ice gouging can be associated with the gravel ribbons (figure 31B) and at the shallowest depths the gravel ribbons change to gravel sheet deposits. Ice gouging is still common within the gravel sheet deposits (figure 31C).

Near Cape Lisburne besides the linear gravel bedforms nearly parallel to the ice gouge trend, transverse gravel waves oriented perpendicular to the ice gouge trend are common (figure 32D). Shore-parallel bedforms are found on the flanks of the gravel sheets (figure 32E). To the west of Cape Lisburne, at depths of 45 to 49 m, an extensive gravel sheet exists with scattered sand bedforms overlying the gravel (figure 32F). These sand bedforms indicate that active currents exist and are capable of moving sand-size particles at depths greater than 40 m.

In the northwest part of the outer shelf, gravel sheets are restricted to areas of thin sediment cover and to local broad bathymetric highs (less than 4m high). These gravel deposits also exhibit a range of bedform types similar to those observed near Cape Lisburne.

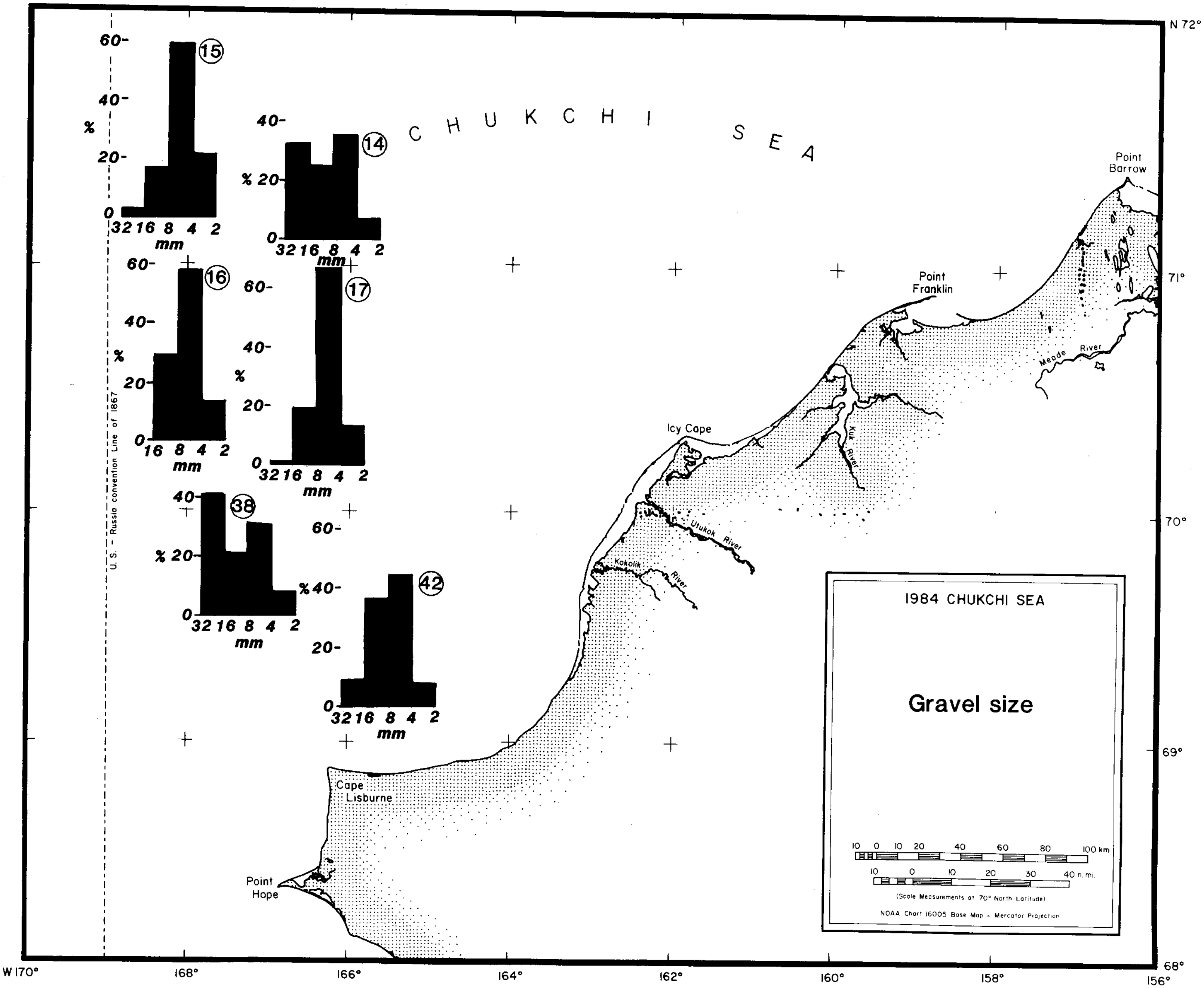

Figure 30. Gravel size analyses of coarse-grained fractions of box cores, outer Chukchi Sea. Sample 42 is a dredge sample. The sample numbers are indicated by circle.

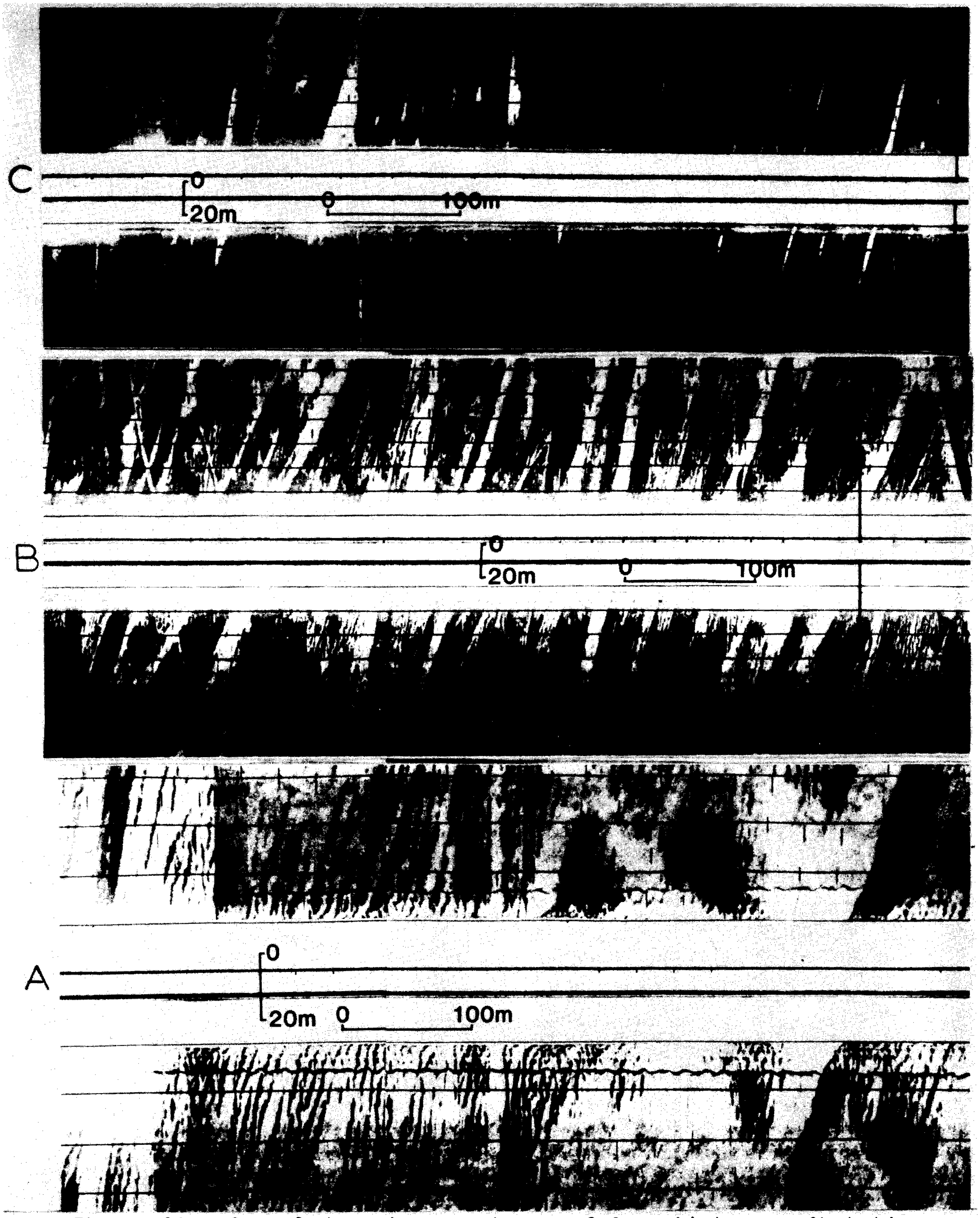

Figure 31. Gravel deposits northwest of Cape Lisburne, Chukchi Sea. A) Northward-trending gravel ribbons at 42 m depth cut by ice gouges. The gravel ribbons are <30 cm high, 2 to 4 m wide and spaced 5.5 to 6 m apart. B) gravel sheet and ribbons at 38 m depth cut by ice gouges. C). Gravel sheet deposit at 34 m depth cut by ice gouges. The transition from A to B to C is typical of gravel deposits in the outer shelf. See figure 35 for sonograph locations.

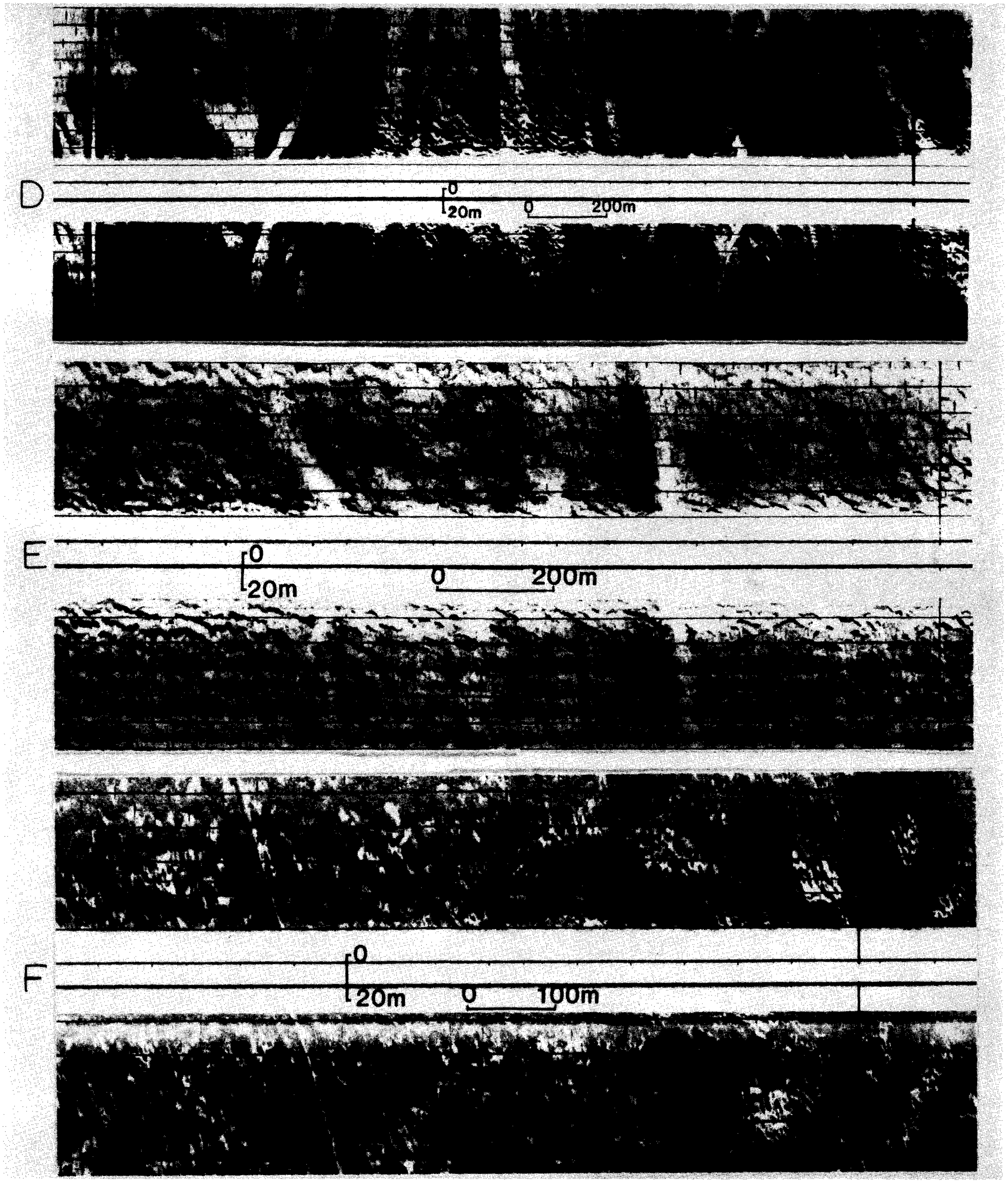

Figure 32. Gravel bedforms west of Cape Lisburne. D) Shore-normal gravel bedforms at 37.5 m depth (center of sonograph) and ice gouges oriented perpendicular to shore. E) Gravel waves at 39 m depth oriented normal to shore. The wave length is aproximately 7 to 8 m. F) Scattered sandwaves on a gravel sheet deposit west of Cape Lisburne. See figure 35 for location of figures D and E and figure 27 for location of figure F.

Gravel ribbons also occur associated with and parallel to ice gouges. Gravel waves, up to 20 to 30 cm high, can be oriented transverse to the ribbons or occur as distint fields (figure 33A). Scattered sand or gravel bedforms without a distinct orientation may be formed on the flanks of the bathymetric highs (figure 33B). The gravel sheet deposits can also exhibit a variety of bedform types (figure 33C). Most of the gravel sheets in the outer shelf contain symmetrical bedforms oriented essentially transverse to the adjacent ice gouge trend.

The gravel deposits in the Chukchi Sea exhibit a variety of bedforms suggesting that active currents exist possibly during storm periods which reinforce the shelf currents. The currents then are capable of moving pebble-size clasts on the sea floor.

Box cores show gravel scattered throughout the cores. A slight increase in gravel content at the top of some cores suggests an erosional lag deposit (figure 34). Bedding is poorly defined within the gravel-rich cores. Vertical and horizontal burrows are also abundant suggesting biological disruption of the substrate.

The gravel deposits identified in the outer shelf represent erosional storm-lag deposits. The gravels are found either where a thin Holocene-Quatenary sediment cover exists, or, especially, on local bathymetric highs. The gravels may represent exposed parts of the Holocene transgressive lag deposit which now is being eroded.

The source of the gravel is uncertain, however, prime candidates are bedrock and ice rafting. However, the well-rounded siliceous pebbles are similar to the suite present on the beaches north of Icy Cape. This may suggest that fluvial transport to the west occurred across the exposed coastal plain during sea level lowstands.

Discussion

The variety of gravel bedforms found to depths of 49 m, are the result of a combination of factors including: 1) current erosion and sediment transport by the northward flowing Alaska Coastal Current (along the east side of the Chukchi Sea) and east or west flowing shelf currents (the northwest part of the shelf), and 2) westward flowing storm-generated currents on both the inner and outer shelf regions. Evidence for currents is best demonstrated in the area of geatest gravel accumulation off Cape Lisburne. Here, the gravel ribbons and symmetric gravel bedforms are oriented north-south, essentially parallel to shore (figure 35) and to the northward flowing coastal current. The dominant ice gouge trend in this same region is northeast-southwest with a secondary component oriented east-west normal to the gravel ribbons and gravel waves. Ice can only move to the west, upslope, when storms come from the west. During periods of open water the symmetric shore-parallel gravel waves may be initially

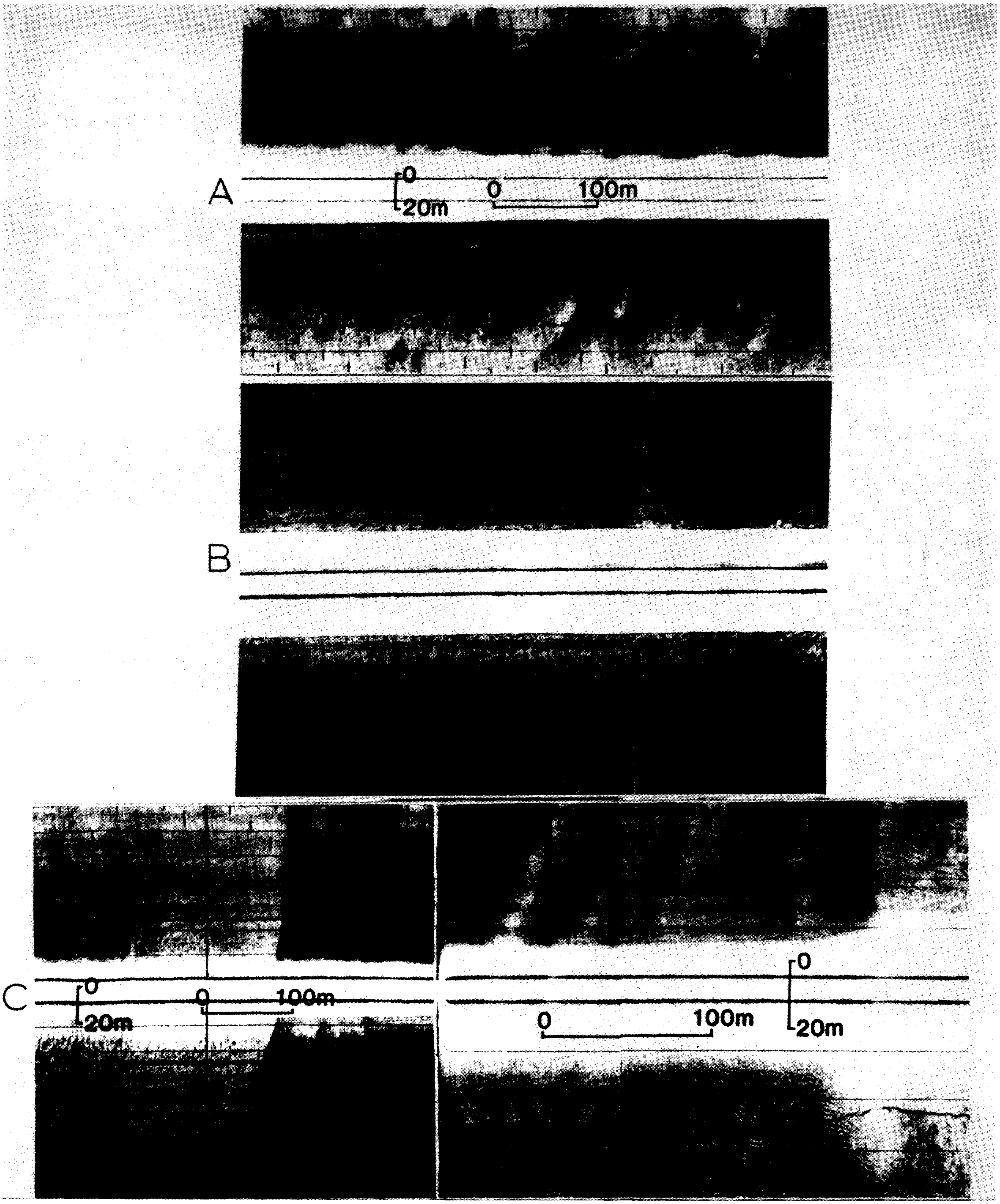

Figure 33. Gravel bedforms on the outer shelf, Chukchi Sea. A) Gravel waves at 45.5 m depth migrating to the west. B) Gravel bedforms (?) at 43.5 m depth on flank of a gravel sheet. The gravel bedforms rise above the sea floor. C) Gravel bedforms at 49 m depth. Scattered gravel bedforms change to gravel sheet deposits with a slight decrease in depth. An expanded view of gravel sheet (right side sonograph) shows symmetrical gravel waves covering the deposit. See figure 28 for profile locations.

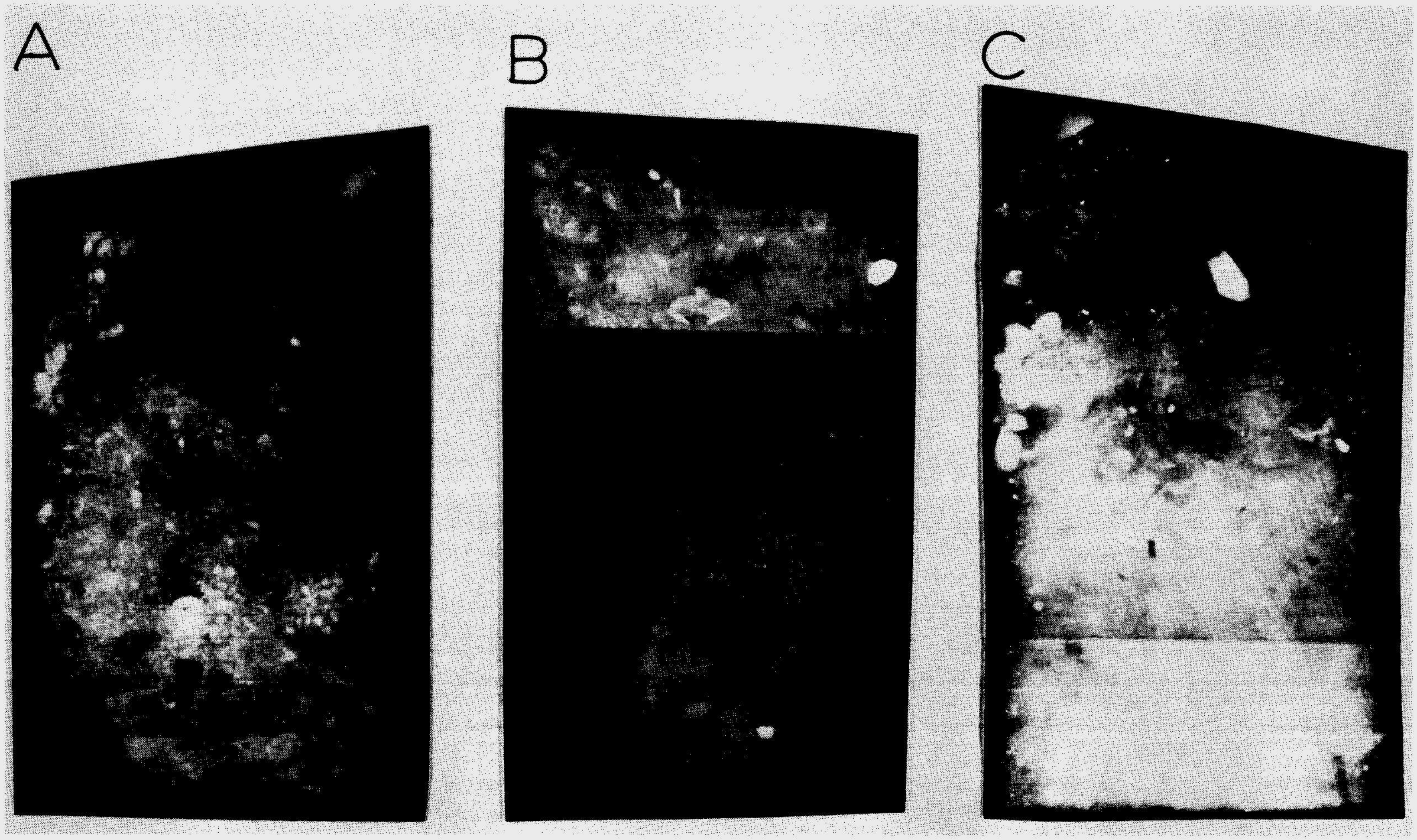

Figure 34. Radiographs of outer shelf box cores containing gravel. A) Core 15 (44.4 m) contains abundant gravel throughout core as well as burrows. B) Core 17 (43.2 m) shows both shells and gravel mixed in a mud substrate. C) Core 38 (45.7 m) contains bioturbated mud with gravel as a surficial lag and in burrows. See figure 26 for core locations. The cores are 19 cm wide.

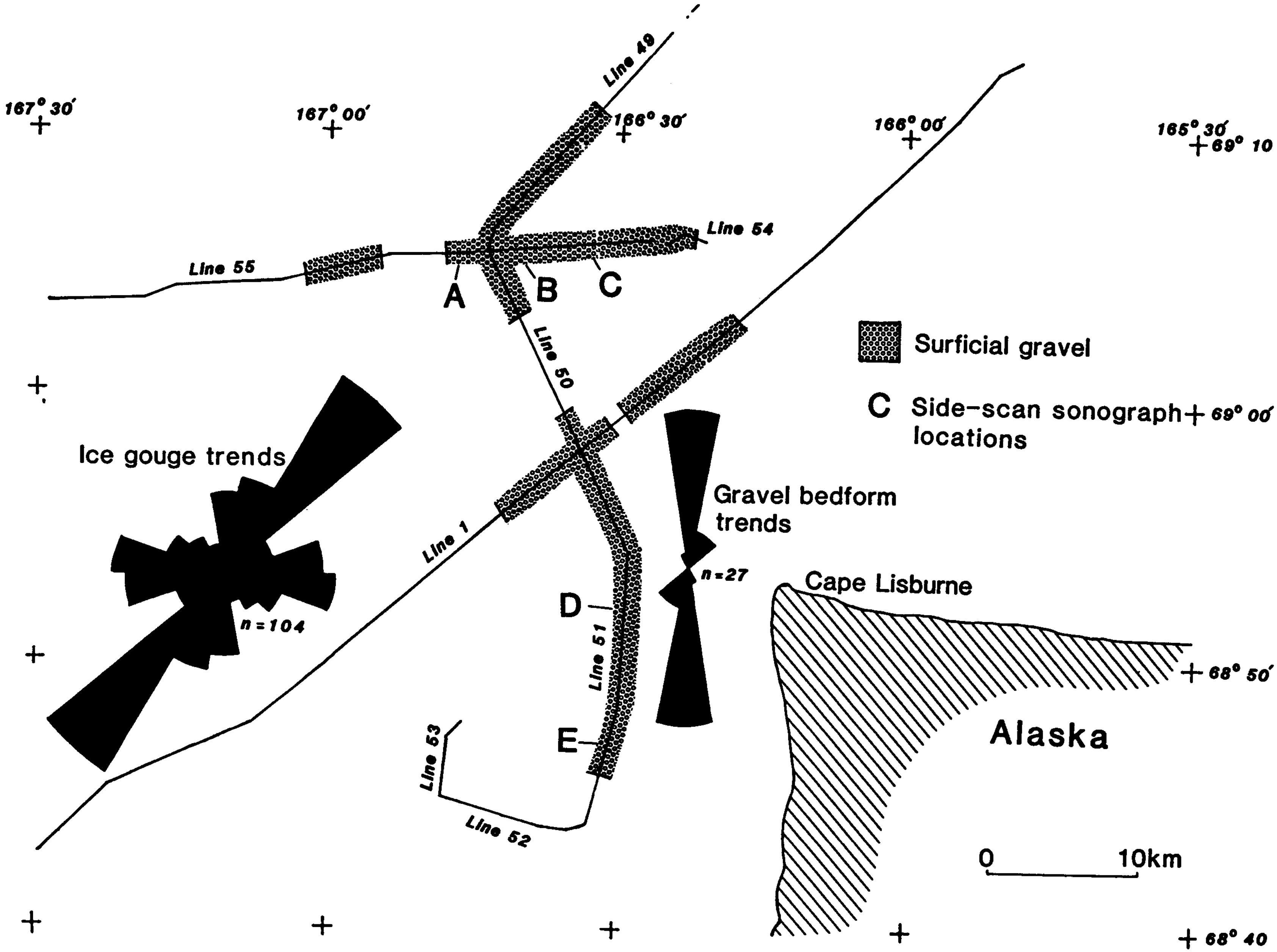

Figure 35. Ice gouge and gravel bedform trends (gravel ribbons and symmetrical gravel wave crest trends) off Cape Lisburne, Chukchi Sea. The gravel bedforms lie at an angle to the ice gouges suggesting a combination of processes produced and maintained the gravel bedforms including storms from the west initially forming the gravel bedforms and the northward flowing Alaska Coastal Current maintaining the bedforms.

produced by storm waves moving from the west to the east (allows maximum fetch). The shore-parallel bedforms are then further maintained by the northward flowing coastal current. The gravel waves in the northwest part of the study area, likewise, are oriented north-south and transverse to the gravel ribbons suggesting currents from the east or west produced the bedforms. Storms from the west may also have reinforced the shelf currents moving gravel on the sea bed.

The reoccurrence interval of the storm events capable of moving pebbles at 49 m depth is unknown, but the presence of gravel bedforms on the shelf indicates bottom currents of up to 150 cm/sec (8 mm quartz clasts at 20° C, Miller and others, 1977) do occur periodically.

Mud

Sandy mud to slightly gravelly sandy mud is the common texture on the outer shelf. The sand fraction contains abundant mica. Internally the box cores record crude bedding, disrupted strata, abundant bioturbation, scattered pebbles, filled clay lined and oxidized burrows, as well as bivalves and gastropod remains (figures 36 and 37). Gravel is rare in the 3 cores north of 71 degrees and the mud fraction increases to 83 percent (Appendix A).

The biological composition of the outer shelf box cores, when compared to the inner shelf cores, show low species diversity and abundance. The living organisms found on the surface and within the cores include brittle stars, anemones, crustaceans (shrimp), a variety of polychaete worms, and a few pelcypods and gastropods. The shell fraction of all cores only contains pelcypod and gastropod remains. In the upper part of cores 33 and 34 the shells are thin and fragile suggesting dissolution of calcium carbonate; where as in the bottom 30 cm pelcypods are leached and are identified by molds. Leached shells within 20 cm of the sea floor surface suggests the deposits are of considerable age.

In all cores bioturbation is abundant. Based on the apparent low abundance of infauna but the presence of intense biotubation suggest that the outer shelf is an area of low sediment input. Biological pocesses dominate over physical processes on the outer shelf.

INNER SHELF

Based on core analyses and grab samples the sediment texture of the inner shelf, at the head of the Barrow Sea Valley west of Icy Cape to Point Franklin, ranges from gravelly muddy sand to gravelly sand to sand to muddy sand to sandy mud (classification of Folk, 1974). The distribution of gravel, sand and mud components of the samples show an abundant sand fraction containing gravel and some mud throughout the inner shelf (figure

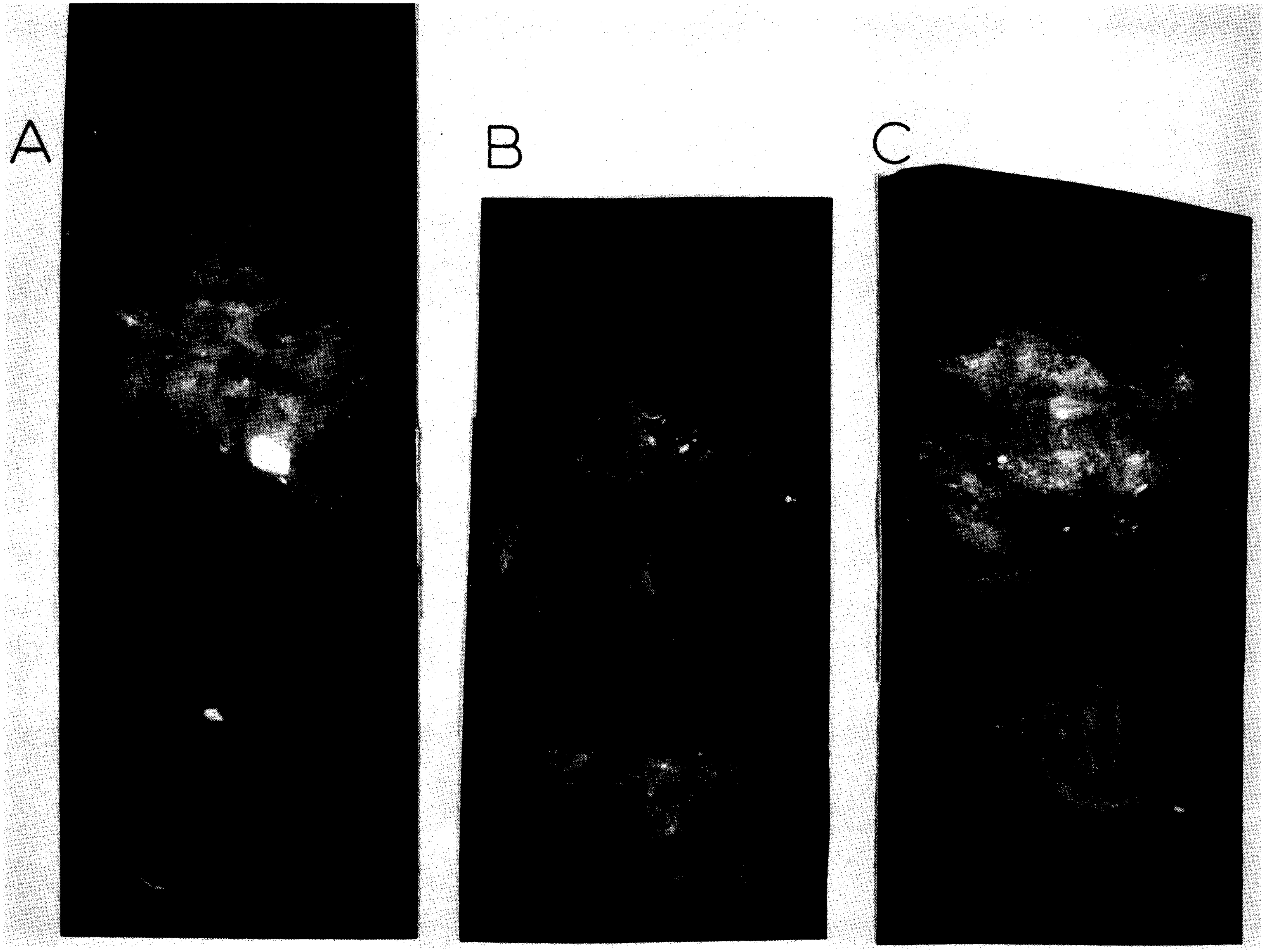

Figure 36. Radiographs of outer shelf box cores. A) Core 36 (53.5 m), B) core 16 (49.5 m), C) core 14 (44.8 m); all cores show bioturbated to disrupted strata, burrows, poorly defined bedding, shells, and scattered pebbles in sandy mud to muddy sand matrix. See figure 26 for core locations. The cores are 19 cm wide.

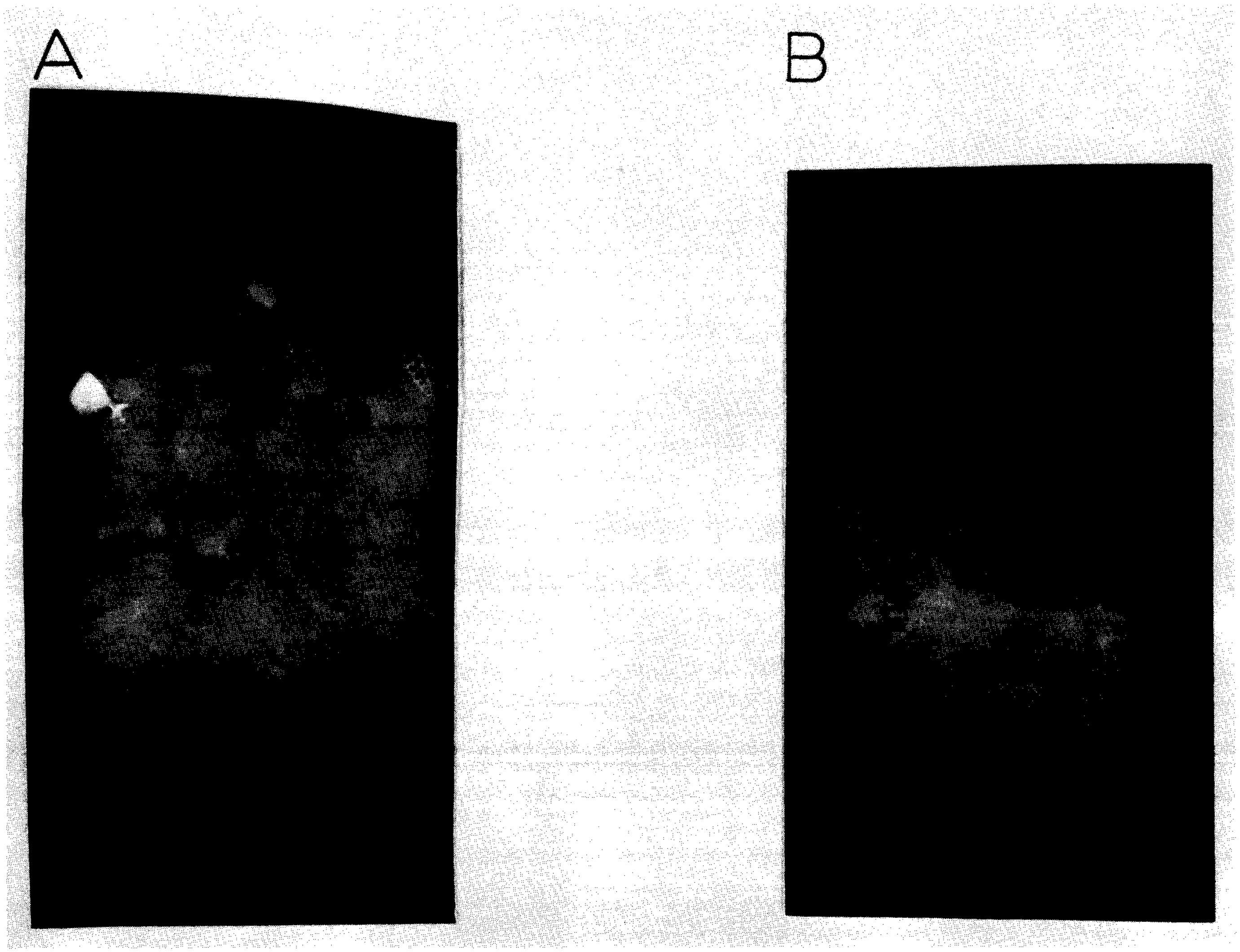

Figure 37. Radiographs of outer shelf box cores. A) Core 37 (46.0 m), B) core 32 (41.2 m); both cores consist of bioturbated mud with scattered pebbles and shells. See figure 26 for core locations. The cores are 19 cm wide.

38, Appendix A). The highest mud content is found off Point Franklin. Sediment analyses of cores found no readily distinct sediment patterns. However, core x-rays, core peels, and sonographs do reveal distinct surficial sediment patterns. The surficial textural distribution defines extensive erosional areas as well as areas of sediment transport within a region influenced by strong shelf currents. Shelf currents and specifically the Alaska Coastal Current has an affect over a 60 km wide area of the sea floor parallel to shore. Within this area at least 4 major textural-biological facies are identified: 1) an outer sand, 2) outer gravel, 3) coastal current sand, and 4) an inner gravel (figure 39).

Outer sand facies

The outer sand facies occupies the western flank of the Barrow Sea Valley. The sea floor is flat in the southern region changing to a gently eastward slope to the north. The depths range from 42 to over 48 m. An extensive gravel field, the outer gravel facies, and overconsolidated mud in the northern part of the sea valley bounds most of the eastern flank of the outer sand facies.

From sonographs and box cores, gravel patches are identified in this facies (figure 39). Gravel is present in the 4 box cores and contributes up to 15 percent of the sediment (sample 22, Appendix A). The texture ranges from slightly gravelly sand to gravelly mud. Micaceous sand is abundant in all cores.

Internally the box cores exhibit abundant bioturbation with scattered pebbles, crude pebble bedding (core 22) or shell layers (core 21) (figure 40).

The fauna of the outer sand facies is dominated by bivalves and gastropods, similar to the composition of the outer shelf fauna (figure 41, Appendix C). Barnacles, bryzoans, echinoids and worm tubes are a minor component of the biological community. The greatest numbers of barnacles occurred in the core containing the highest gravel content (core 22).

Outer gravel facies

The outer gravel facies occurs inshore from the outer sand facies. It represents a surficial gravel-shell lag deposit that is at least 165 km long. The width varies from 11 km at the south to 27 km at its maximum width. The depths of the deposit range from 40 m west of Icy Cape to over 60 m in the north. The eastern flank of this facies southwest of Point Franklin is as shallow as 28 m. The thickness of the gravel varies and can be as thin as 4 cm where it overlies over-consolidated mud (cores 3, 4, 20, and 25) or as thick as 8 to 10 cm over gravelly sand. Within the sea valley over-consolidated mud outcrops at the northwest part of this facies (figure 39). Based on box cores, over-consolidated mud underlies the northern gravel deposits south to near Wainwright.

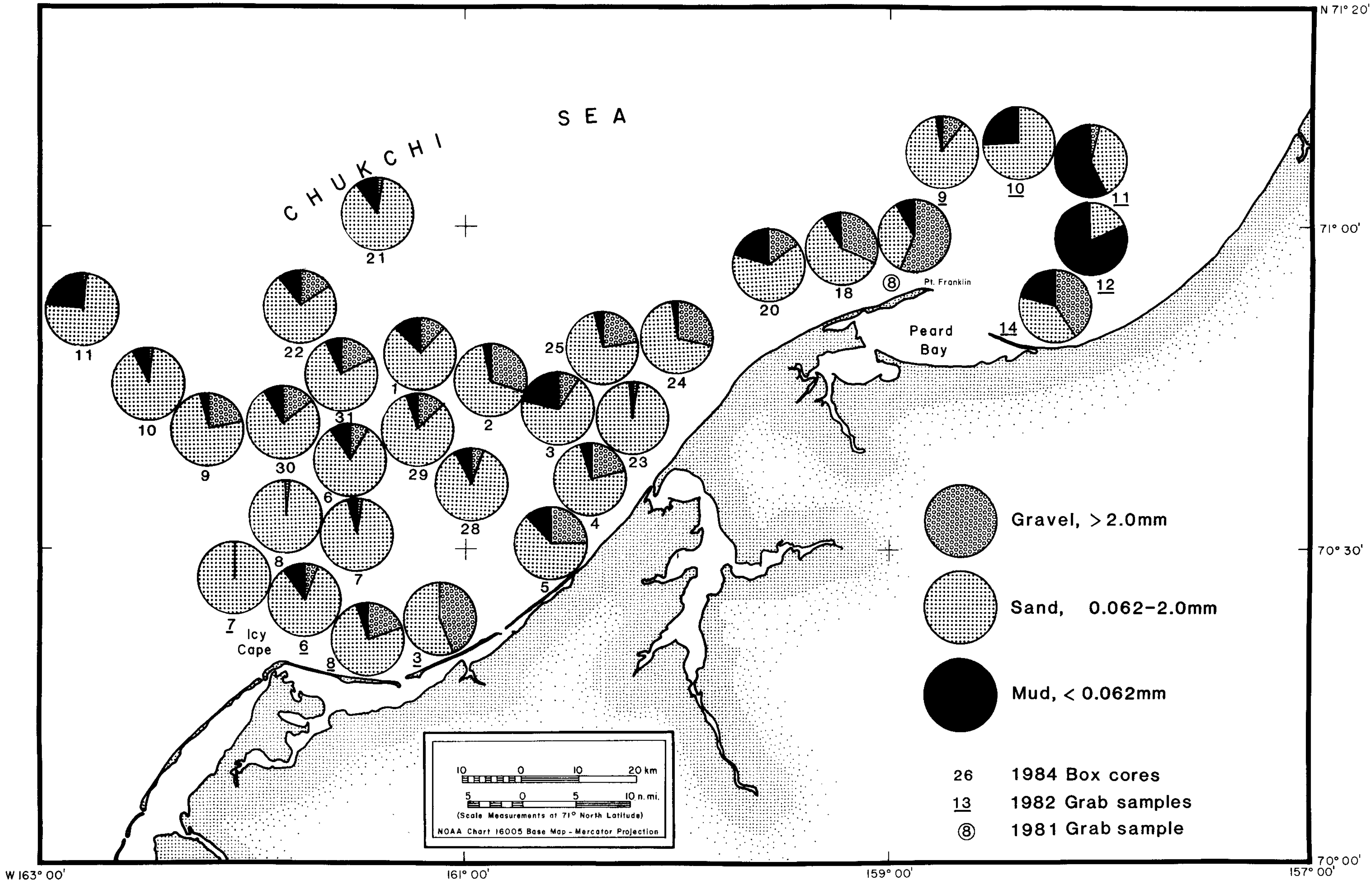

Figure 38. Sediment components from channel samples of box cores in the northeast part of the Chukchi Sea.

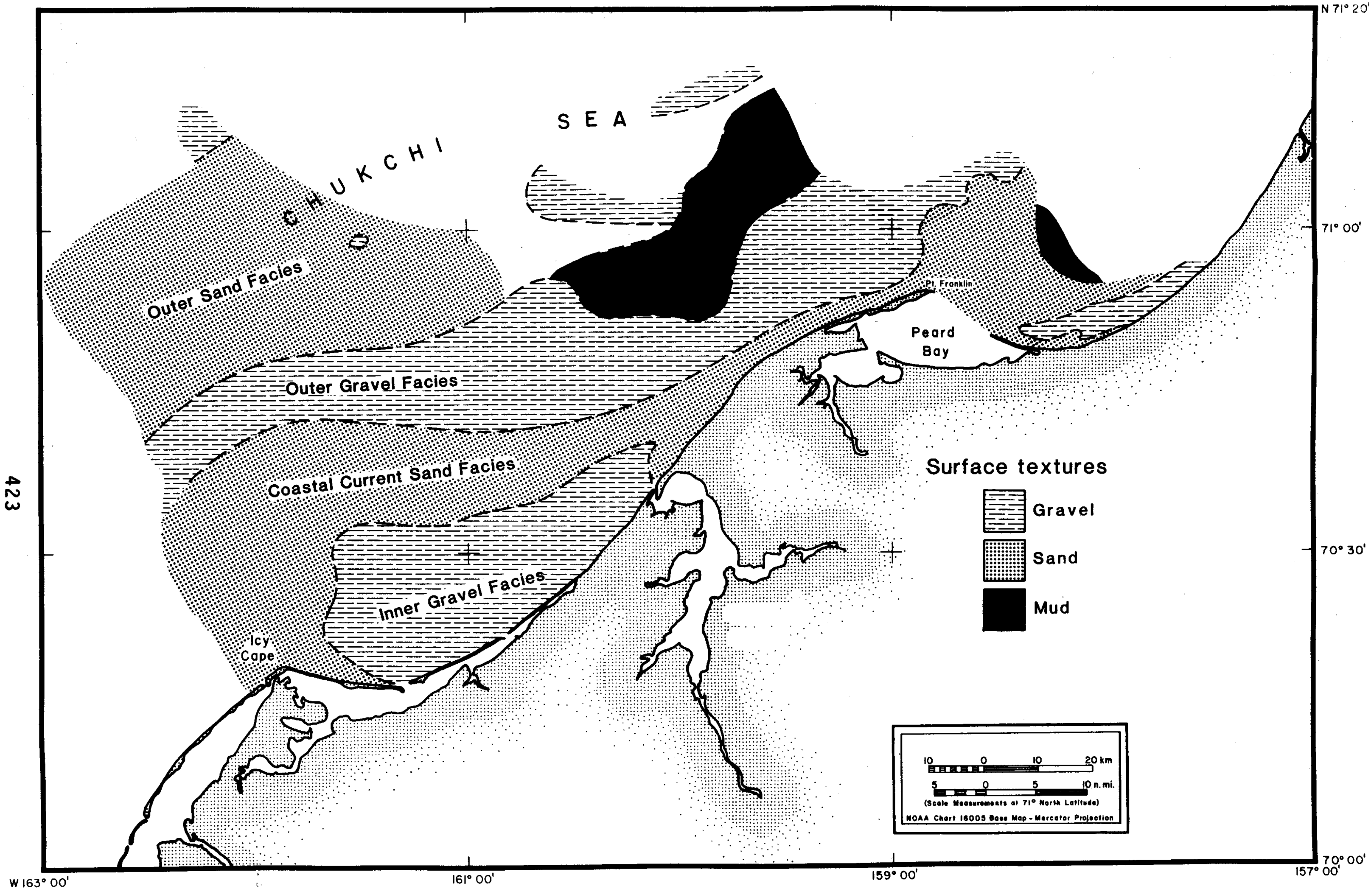

Figure 39. Major surficial sediment facies observed in the northeast part of the Chukchi Sea. The three outer facies contain distinctive fauna dominated by bivalves and gastropods in the Outer Sand; barnacles, bryzoans and brachiopods in the Outer Gravel; and echinoids in the Coastal Current Sand. The greatest faunal abundance and diversity occurs in the Outer Gravel facies.

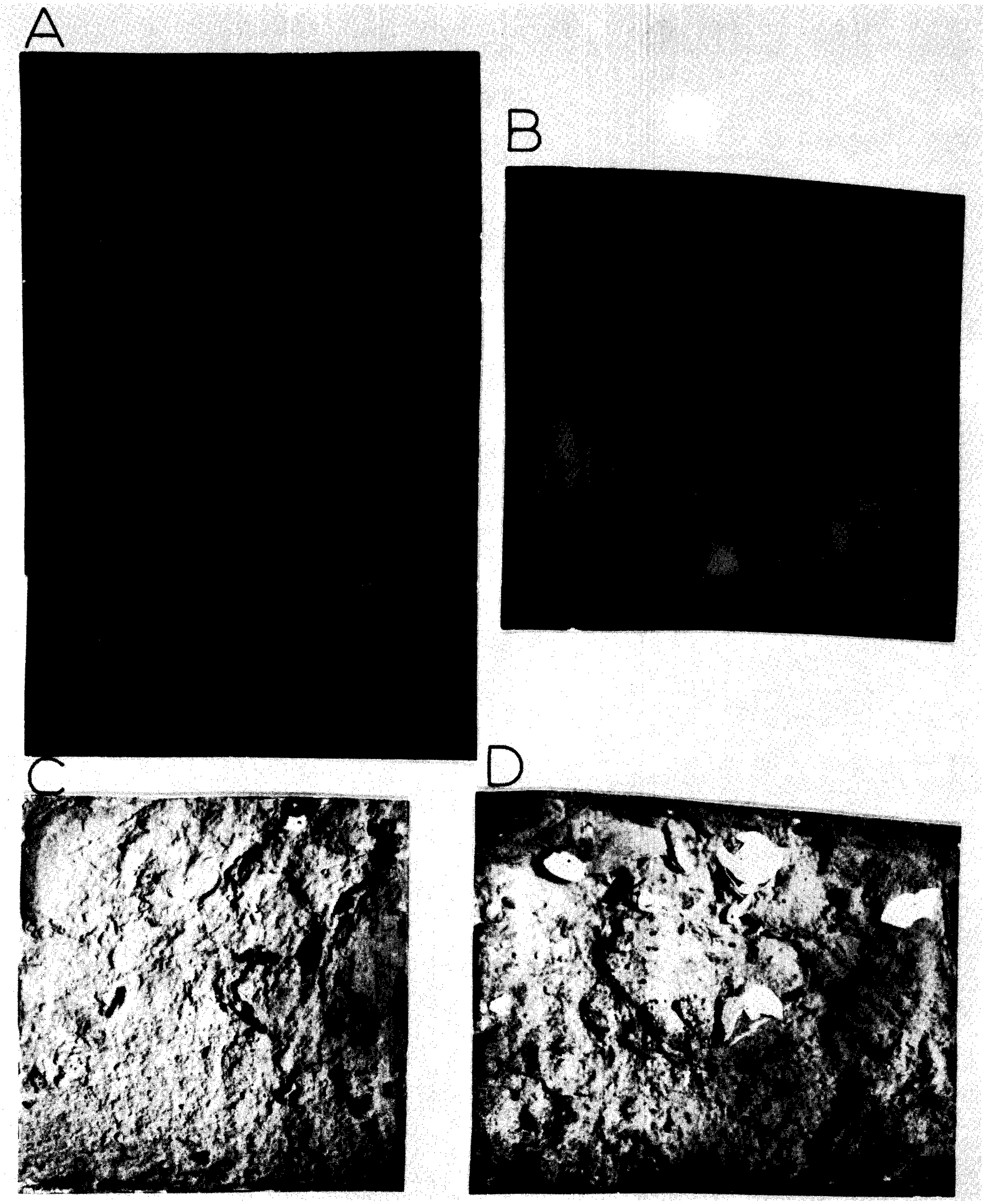

Figure 40. Outer Sand facies box cores. A) Radiograph of core 11 (42.5 m) containing scattered gravel and shells as well as abundant bioturbation; B) radiograph of core 22 (42.1 m) containing abundant gravel with crude bedding; C) photo of core 10 (42.9 m) which contains bioturbated sand with a few scattered pebbles; D) photo of core 21 (47.7 m) containing a shell lag, scattered pebbles and abundant bioturbation. See figure 38 for core locations. The cores are 19 cm wide.

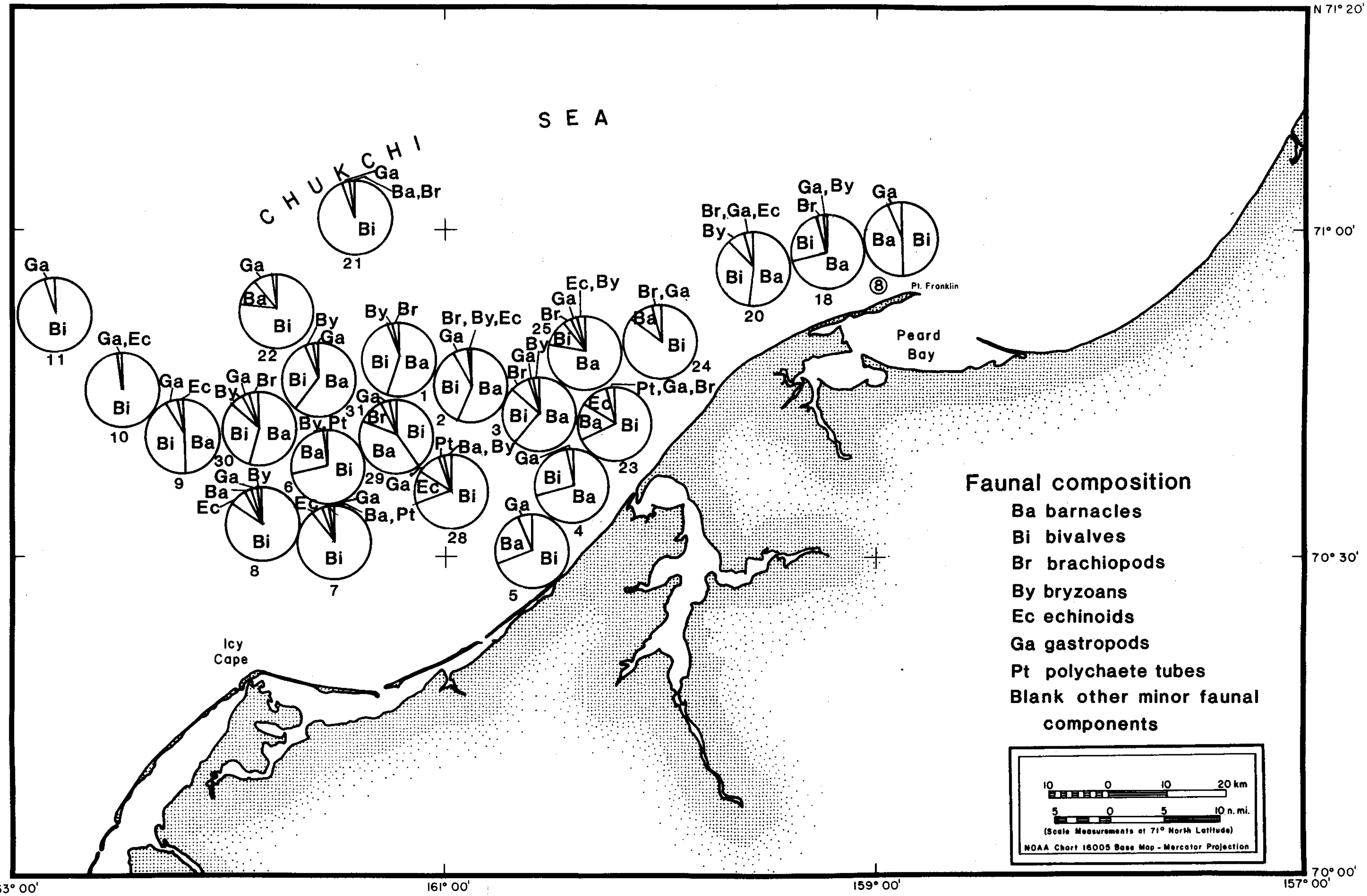

Figure 41. Faunal composition of inner shelf box cores. Includes only material from within the core and not the living fauna on the box core surface. The faunal analyses conducted on the >2.0 mm size fraction of washed samples of most of the core following the method of Wilson, 1979.

In this facies sonographs record either a scattered mottled pattern or distinctive dark patches (figure 42) and box cores confirm the presence of gravel. No gravel bedforms have been identified within this facies.

The gravel content of the box cores ranges from 9.4 to 31.7 percent (Appendix A, figure 38). Of the 10 box cores taken in this facies; 7 are classified texturally as gravelly sand, 3 as gravelly muddy sand and 1 as muddy sandy gravel. Gravel is present in all cores. The gravel clasts range in size up to 24 cm, however, most clasts are less than 10 cm. The clast composition also varies and consists of igneous, sandstone, siltstone and dolomite. Red granite clasts are found in most cores. The gravel clasts vary from well-rounded to angular.

Box cores show both the sea floor surface and the distribution of the clasts, fauna, and internal bedding. The sediment surface can vary in concentrations of shells, clasts, and animals (figures 43a, 44a, 45a). Internally, however, the cores and radiographs show a gravel-shell lag, up to 10 cm thick, in the upper part of the cores (figures 43, 44, 45, 46). Gravel can also be scattered throughout the core sediment. Coarse-grained lag deposits may also be present at the base of some samples. Bedding is usually indistinct. Bioturbation, however, is abundant with preserved burrow structures.

The benthic fauna can be exceedingly rich especially towards the north. The fauna consists of; sponges, barnacles, bryzoans, brittle stars, urchins, brachiopods, sea cucumbers, hermit crabs, shrimp, isopods, and tube worms. Large polychaete worms are also present in some cores (figure 45a). The death assemblage contains in order of decreasing abundance; barnacles, bivalves, gastropods, bryzoans, brachiopods, echinoids, and chiton plates (figure 41, Appendix C). Barnacles, many stained and oxidized, are the most abundant component within the cores. Living barnacles, however, are not common within the samples. The widespread gravel substrate provides a habitat for the extensive epifauna that exists within this facies.

Coastal current sand facies

The coastal current sand facies lies to the east of the outer gravel facies. It forms a northeast trending textural band from Icy Cape to north of Point Franklin. Inshore, northeast of Icy Cape, the facies is bounded by the inner gravel facies. North of Wainwright the coastal current sand facies merges with the nearshore sand. The textural band ranges in width from 20 km to less than 4 km (figure 39). The depths vary from 40 m to less than 20 m. This facies is distint in that it contains abundant echinoids, records active northward sediment transport represented by sand wave fields, and is a major feeding ground for Gray whales.

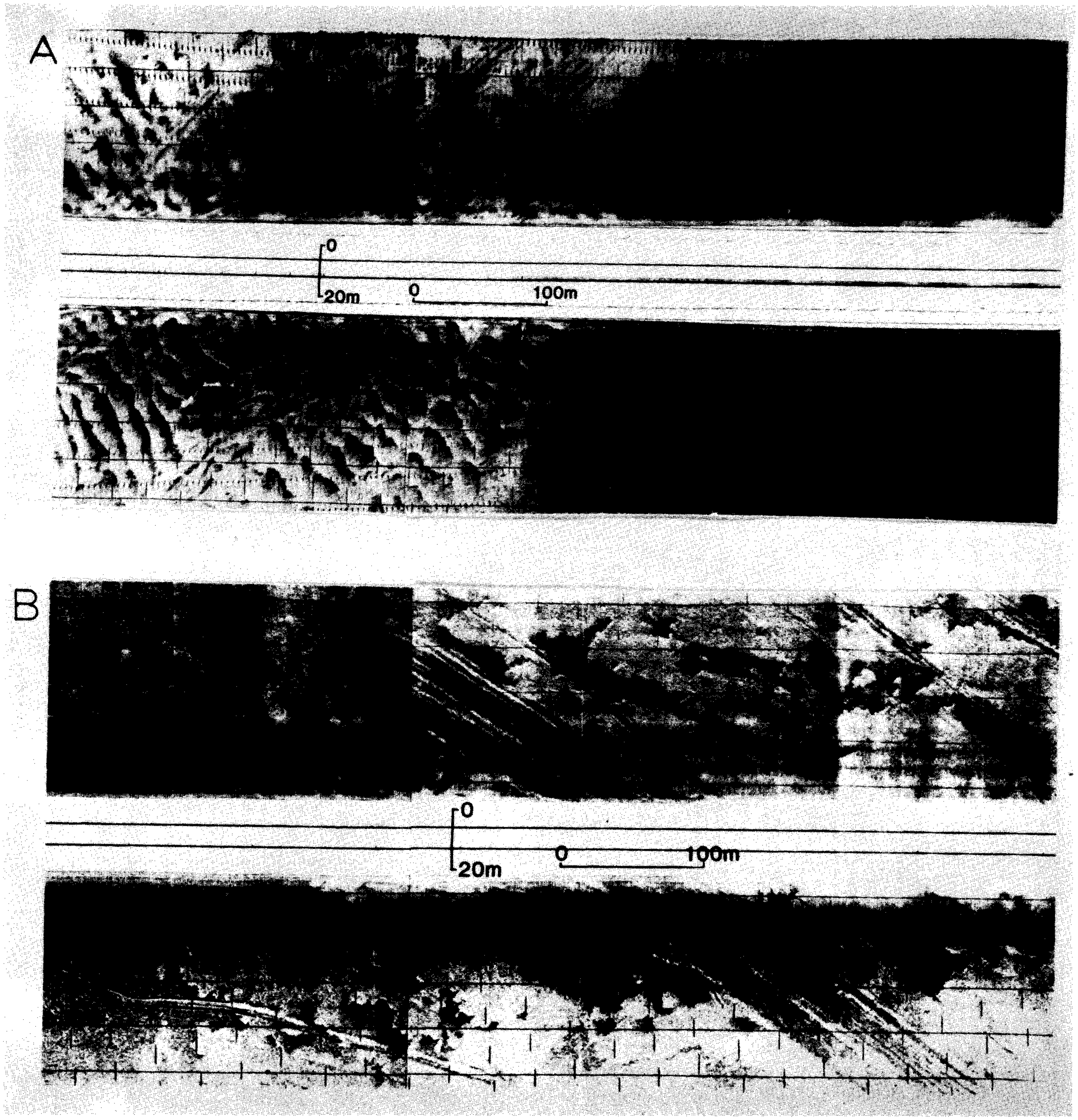

Figure 42. A) Transition between the Outer Gravel facies (right side of sonograph) and sandwaves in the Coastal Current Sand facies directly west of Wainwright. The depth is 28.5 m. B) Outer Gravel facies west of Point Franklin. The gravel sheet (left side of sonograph) changes to scattered gravel deposits locally covered by sand.

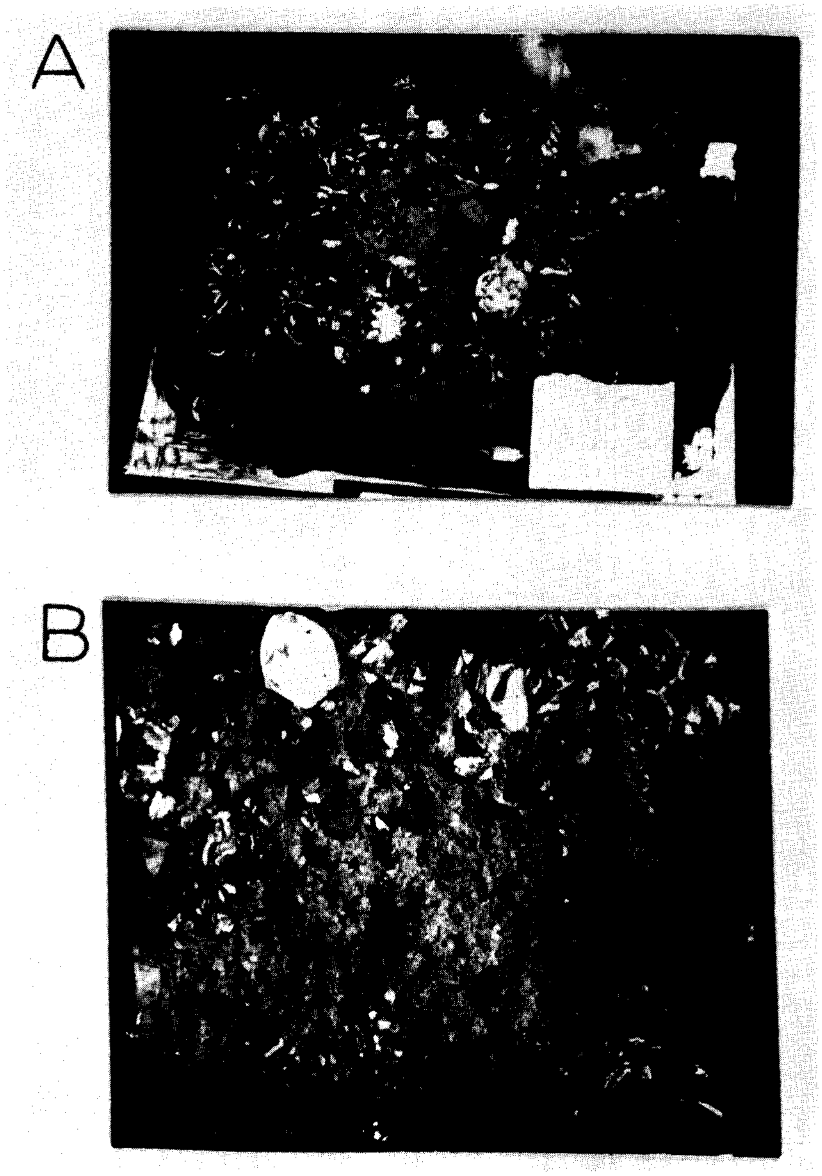

Figure 43. Outer Gravel facies box core 30 (40.2 m). A) photograph of core top which contains scattered pebbles and cobbles as well as branching bryzoans. Tunicates cover some of the cobbles here. B) Peel of core showing the upper erosional gravel-shell lag deposit and scattered gravel in the lower part of the core. The box core is 31 cm in maximum length; the peel is 19 cm wide. See figure 38 for core location.

A

B

Figure 44. Outer Gravel facies box core 25 (40.2 m). A) Photograph of top of core showing the surficial gravel lag and biology. Sponges, bryzoans, urchins, and barnacles are common. B) Core peel showing the upper gravel-shell lag and bioturbated sediment. Most biogenic fragments in core are barnacles. The box core is 31 cm in length; the peel is 19 cm wide. See figure 38 for location.

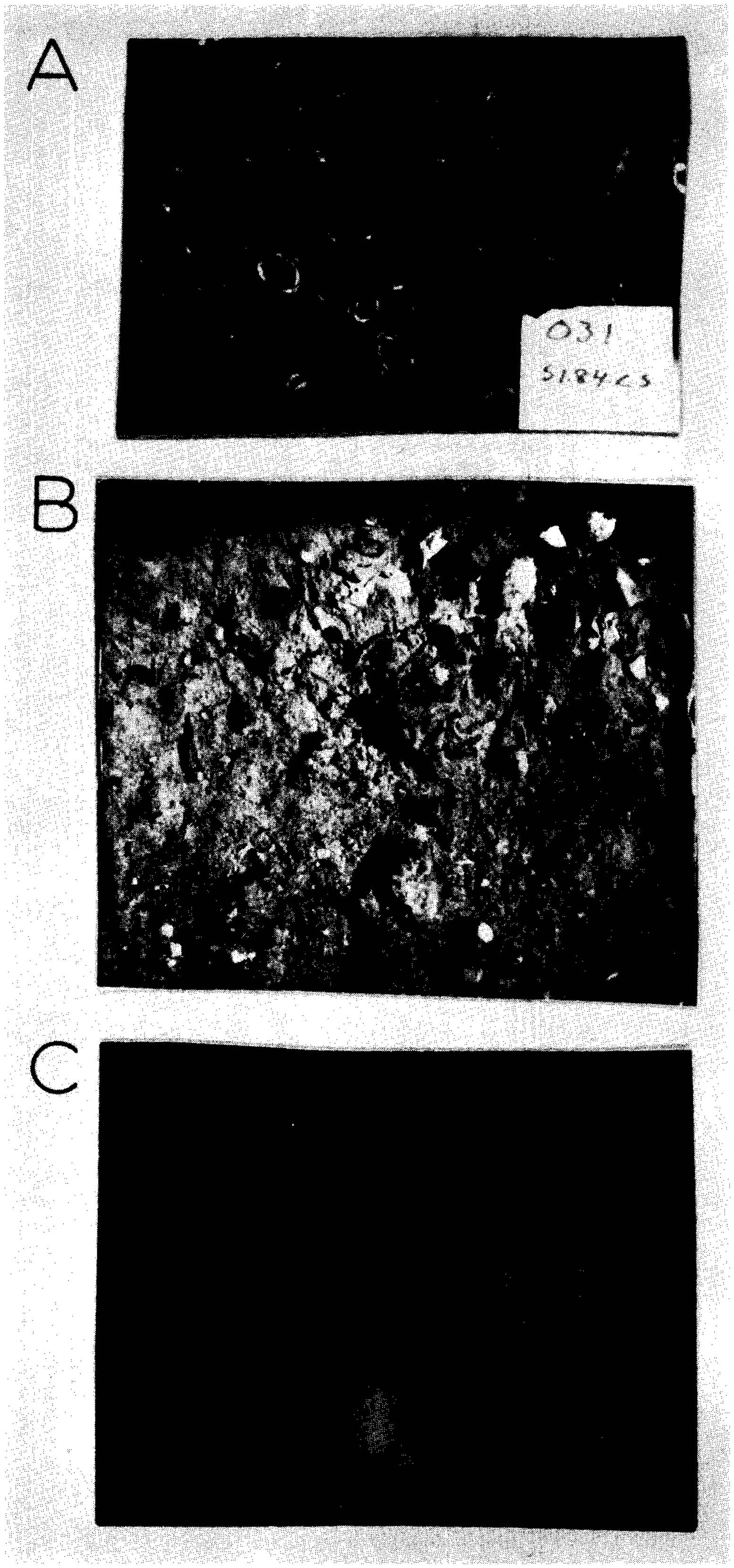

Figure 45. Outer Gravel facies box core 31 (42.0 m). A) Photograph of top of core showing the surface gravel-shell lag with a large worm on right side of core. B) Core peel showing the gravel-shell lag and bioturbated sediments. C) X-ray of core peel showing the gravel distribution and crude bedding.

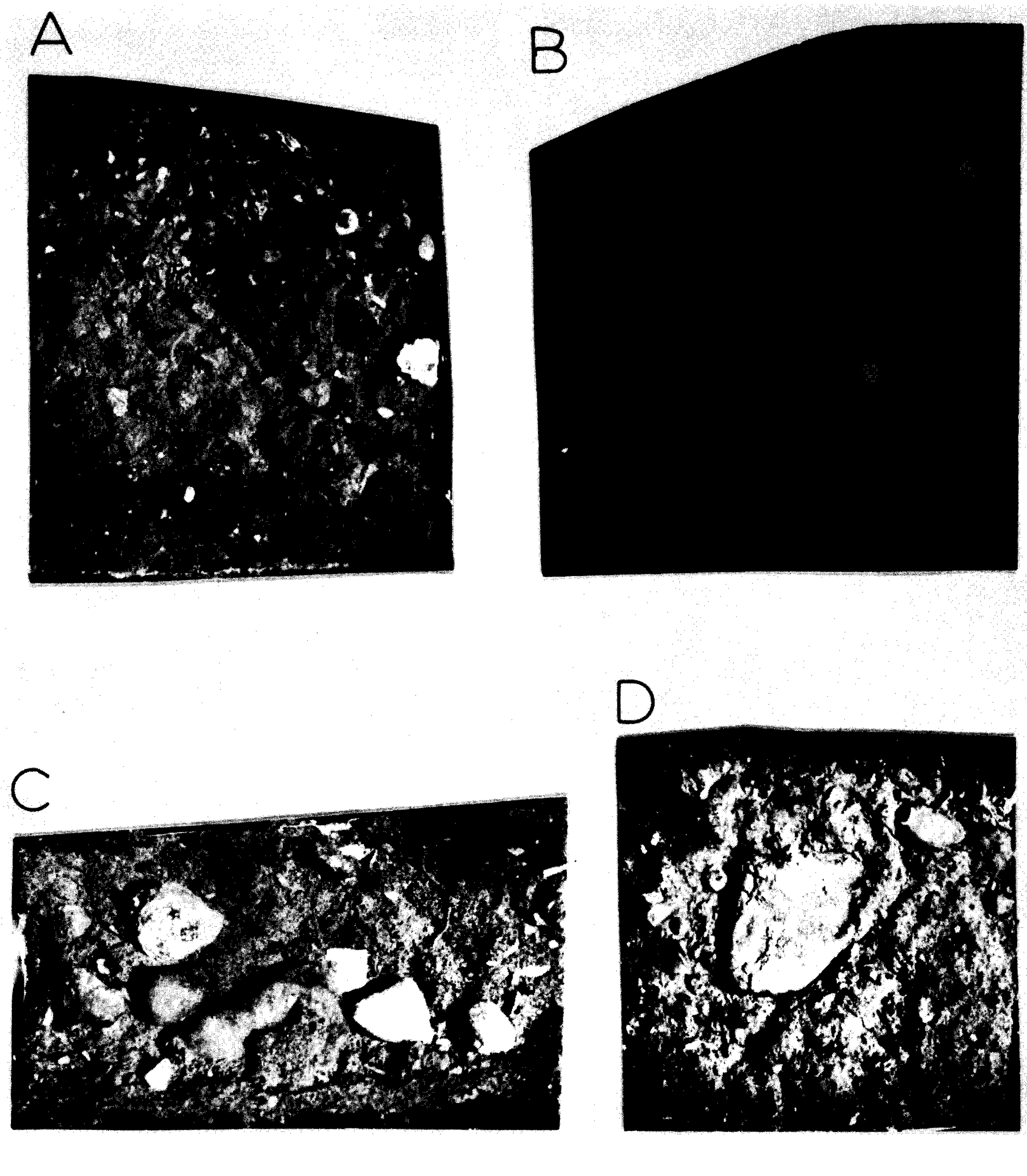

Figure 46. Outer Gravel facies. A) Core 2 (45.3 m) peel showing bioturbated sediment and upper gravel-shell lag. B) X-ray of core peel showing the surficial gravel concentration. C) Core 24 (36.6 m) peel contains scattered shells and cobbles. D) Core 1 (43.5 m) with a surficial gravel-shell lag. The cores are 19 cm wide.

The contact with the outer gravel facies can be abrupt where large-scale sand waves exist (figure 42a) or can be apparently gradational. Sandwave fields occur within this facies off Icy Cape, Wainwright, and Point Franklin (figures 47, 48). Where large bedforms are not evident on the sonographs small-scale bedforms (height less than 5 cm) are expected as ripples were observed on the surface of some box cores. The large-scale bedforms are found to depths of 39 m off Icy Cape, between depths of 23 and 38 m west of Wainwright, and 18 to 30 m off Point Franklin. Most bedforms contain northward facing slip faces indicating northward bedform migration and sediment transport. The sand waves represent straight- to sinuous-crested bedforms ranging in height from 0.5 to 1.3 m (figures 47, 48).

The sand content of the box cores varies from 82 to 98 percent. The texture classification for samples in this facies ranges from slightly gravelly muddy sand, to gravelly muddy sand, to gravelly sand, to sand (figure 38, Appendix A). The high gravel content in core 29, which is located near the western boundary of the coastal current sand facies, may reflect a transition zone between the facies or may represent lateral shifting of the facies because of currents or sediment supply.

All box cores contain abundant bioturbation, scattered invertebrates, and exhibit some crude bedding (figure 49). Echinoids are abundant both on the sea floor surface, as observed on the top of cores 7 and 8, and are also abundant within the cores (figure 49d, Appendix C).

Living echinoids in this facies range in size from 2 mm up to 4 cm. The sea floor surface where box core 7 and 8 were taken contain, respecively, 103 and 110 echinoids per square meter. The echinoid is identified as _Echinarachnius parma_ and has been reported from southwest of Icy Cape at depths of 31 m (Naidu and Sharma, 1970). Bivalves, barnacles, echinoids, gastropods, and polychaete tubes (_Pectinara_) form the major invertebrate members of this community.

The sea bed contains abundant pits that in places cover most of the sea floor. The pits are attributed to benthic feeding by Gray whales (_Eschrichtius robustus_) and will be discussed in a following section.

Inner gravel facies

The inner gravel facies occupies the area east of the coastal current sand facies from northeast of Icy Cape to near Wainwright. The contact with the coastal current sand facies is gradational. The gravel band is over 70 km long and is up to 28 km wide. The depths range from approximately 30 m to less than 5 m nearshore. Most of the gravel is found at depths less than 25 m.

In contrast with the outer gravel facies, gravel bedforms

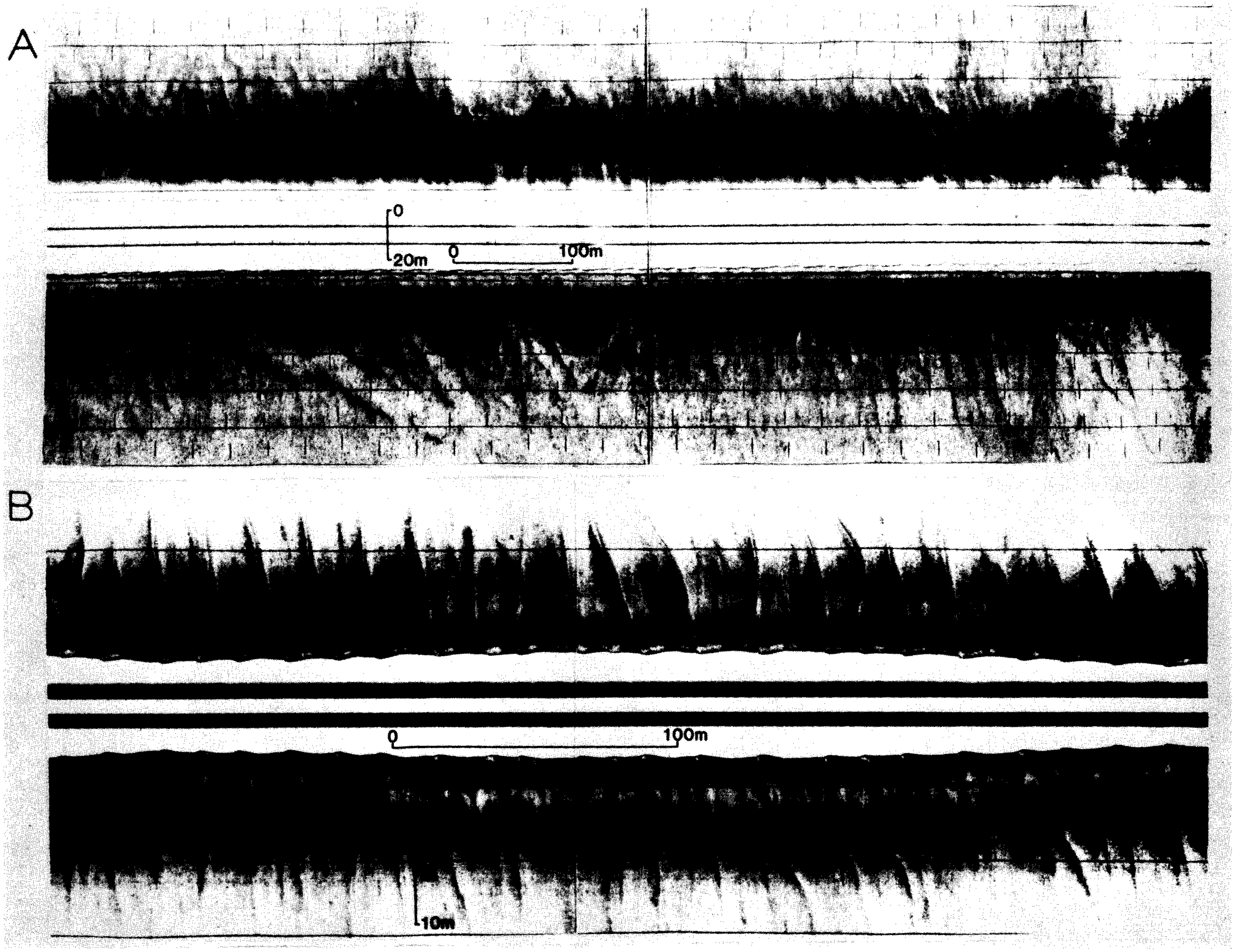

Figure 47. A) Coastal Current Sand facies containing sandwaves at 28 m depth on northwest part of Blossom Shoals off Icy Cape. The sandwaves range up to 0.9 m in height. B) Straight-crested sandwaves at 23 m depth west of Wainwright. The sandwaves range in height from 1.0 to 1.3 m and have a wave length of approximately 38 m.

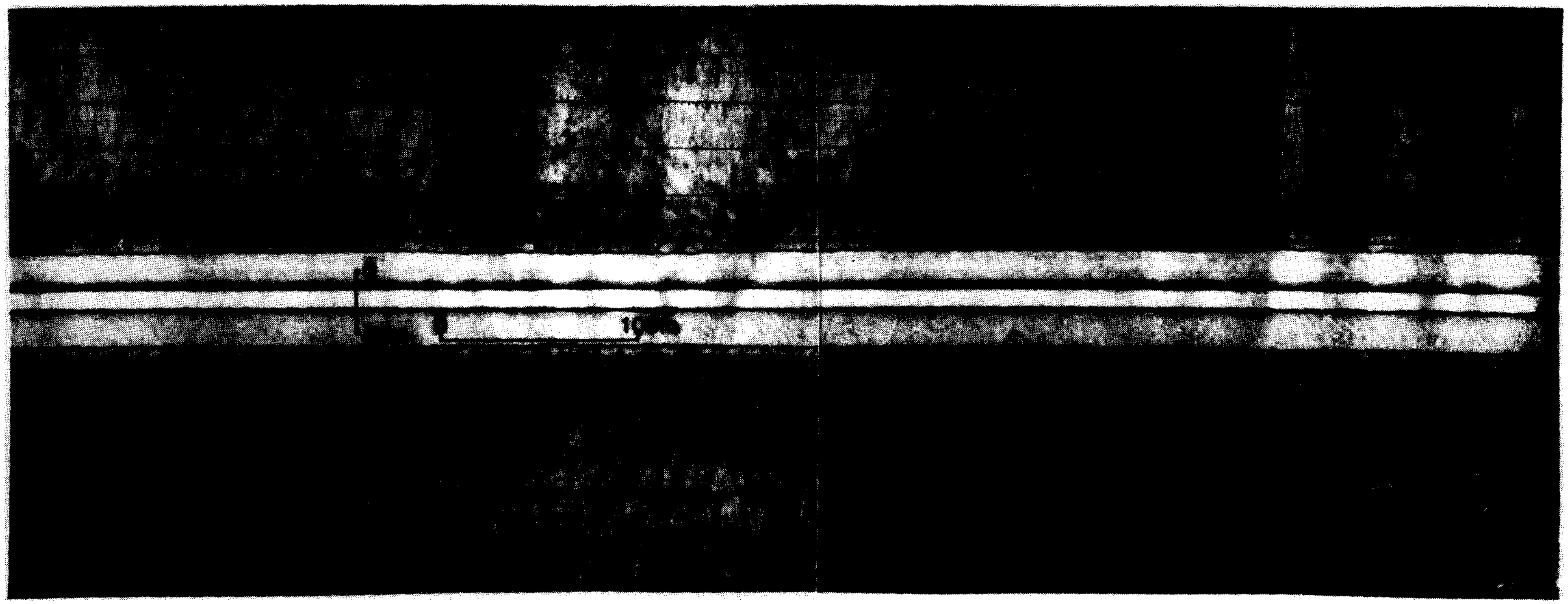

Figure 48. Coastal Current Sand facies containing northward migrating sandwaves at 28 to 30 m depth off Point Franklin. The sandwaves are approximately 0.5 m high.

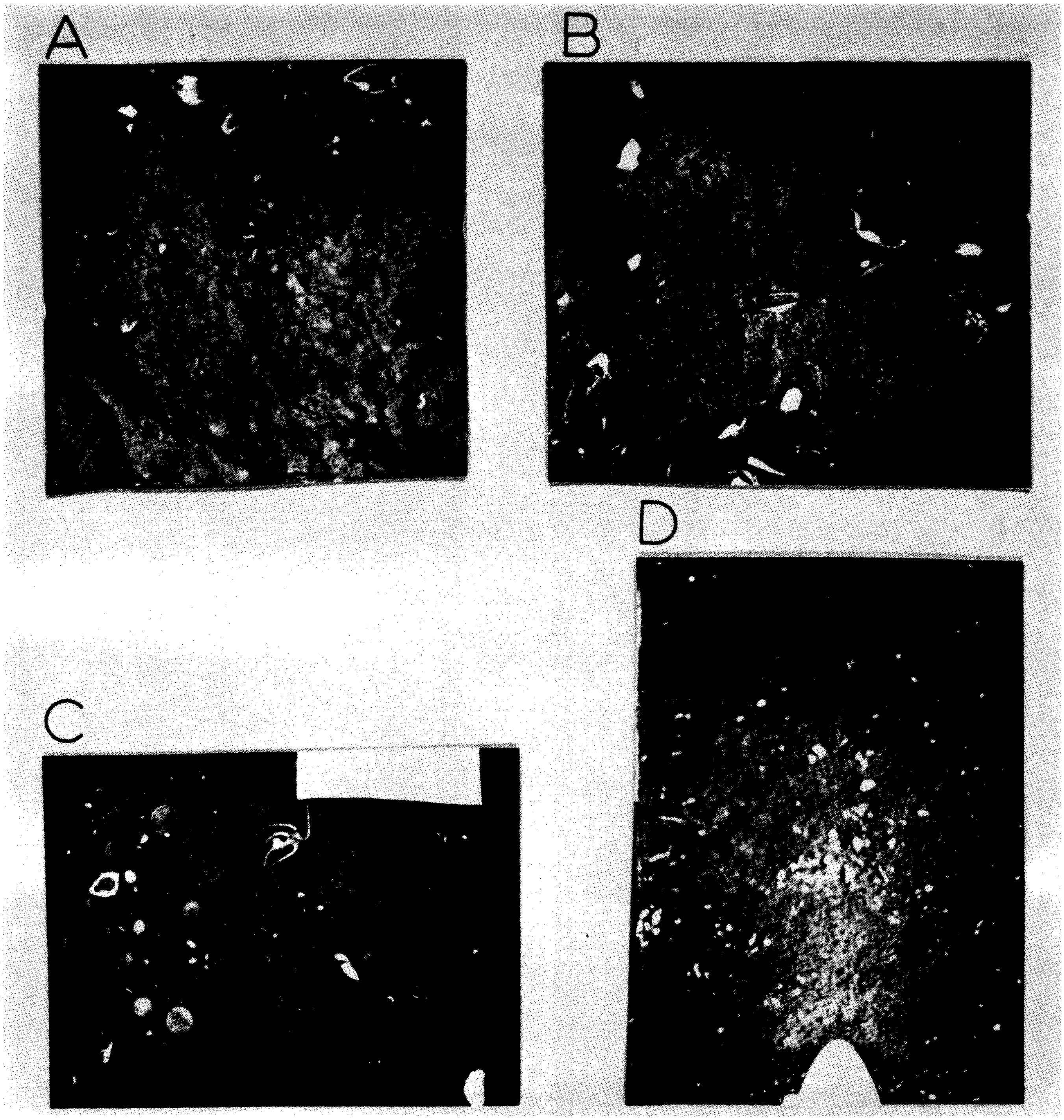

Figure 49. Coastal Current Sand facies. A) Core 29 (35.0 m) taken near the seaward boundary with the Outer Gravel facies. The peel shows a surficial gravel-shell lag overlying bioturbated sand. B) Core 7 (28.7 m) core peel contains bioturbated sand with scattered shells and echinoid fragments. C) Core 8 (24.6 m) photograph of top of core showing the distribution and abundance of echinoids. D) Peel of core 8 which contains bioturbated sand with scattered echinoid and shell fragments. The core peels are 19 cm wide; the box core is 31 cm in length.

are observed on sonographs. Gravel sheets, gravel-sand patches, and shore-normal symmetrical gravel bedforms characterize the sea foor surface in this facies. Irregular shore-parallel gravel-sand patches occur offshore changing to shore-normal gravel bedforms nearshore (Phillips and Reiss, 1984).

Limited box core data record bioturbated gravel, sand and mud (figure 50). The gravel consists of rounded to angular clasts of sandstone, siltstone, coal as well as black siliceous pebbles.

The core fauna is somewhat restricted (based on limited samples) and consists of barnacles, bivalves and gastropods (Appendix C).

Discussion

The inner shelf at the head of the Barrow Sea Valley is greatly influenced by two processes; 1) the northeastward flowing Alaska Coastal Current, and 2) storm-generated currents. The distribution of the surficial sediments in this region is the result of sediment transport and on-going erosion of the sea bed by these currents (figure 39).

The outer sand facies represents an area of thin sediment cover (less than 3 m thick), contains erosional gravel patches, with bioturbation a dominant process. Local storm-generated currents and shelf currents flowing into as well as up the Barrow Sea Valley (Garrison and Becker, 1976; Mountain and others, 1976) erode the sediment.

Within the outer gravel and coastal current sand facies the Alaska Coastal Current and shelf currents flowing into the Barrow Sea Valley erode and transport sediment to the north. The outer gravel facies represents an erosional surficial gravel-shell lag deposit produced by the northward flowing currents. It also overlies areas of thin sediment cover over bedrock and grades laterally to the northeast into apparently erosional deposits within over-consolidated mud. Evidence for erosion and currents is found in the over-consolidated mud where fields of linear, northeast-trending sediment furrows are abundant to depths of at least 80 m (figure 51a). Sediment furrows form in mud between velocities of 20 cm/sec for deep sea sediments to >40 cm/sec for shelf environments (Flood, 1984). Velocities probably with this range most likely produced the sediment furrows in the head of the Barrow Sea Valley. This facies also records low sediment deposition with erosion apparently the major process.

The coastal current sand facies is an area of northward sediment transport. It forms the seaward part of a sediment circulation cell between Icy Cape and Wainwright. Sand bedforms cover a series of arcuate shoals off Icy Cape (Phillips and Reiss, 1984). These shoals migrate seaward where ice groundings and the Alaska Coastal Current erode the banks. Fields of northward migrating large-scale bedforms then form as a result of

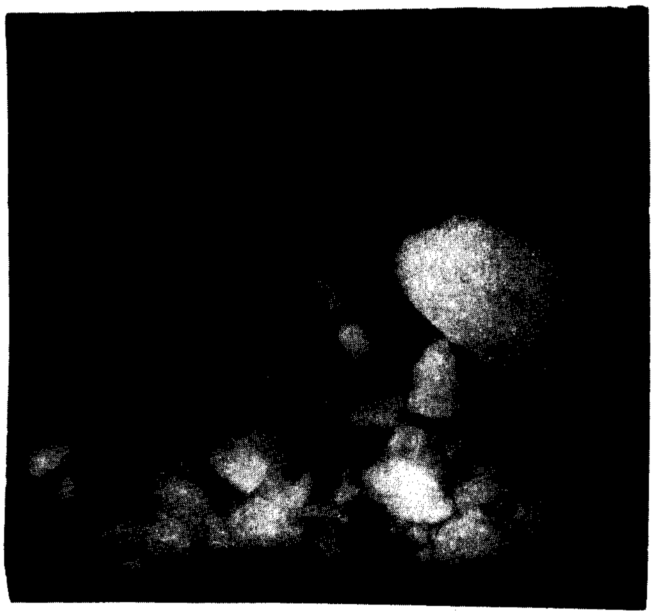

Figure 50. Inner Gravel facies box core 5 (18.3 m). X-ray of core peel showing bioturbated gravel.

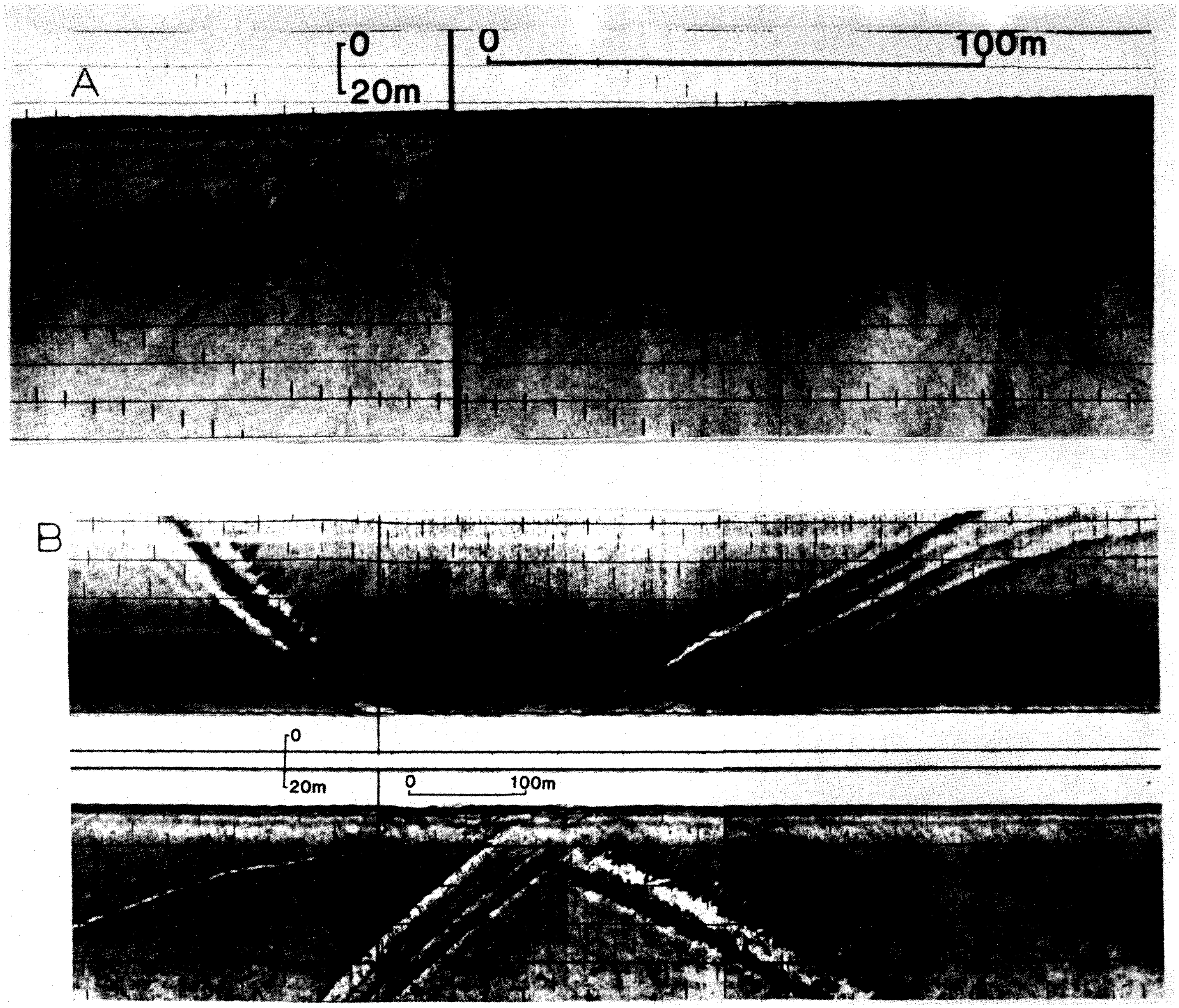

Figure 51. Inner shelf bottom current features. A) Linear furrows at depths of 69 m are erosional bedforms cut into mud. The dark streaks on the sonograph represent the base of the furrow and probably consist of gravel or shell debris. These furrows occuppy most of the region of over-consolidated mud at the north end of the Outer Gravel facies (figure 38). B) Northeast-directed sediment "streaming" from ice gouges indicate bottom current direction in regions where sandwaves are not observed on sonographs.

the coastal currents eroding the shoals. As the water deepens to the north the large-scale sandwaves change to rippled sand. Where the sea floor shallows and the coastal current impinges against the coast off Wainwright and Point Franklin, large-scale sandwave fields occur again. Northward flowing currents are still evident where large-scale bedforms are not observed on sonographs. Ice gouge flanks may also contain northward streaming sediment which are similar to comet marks observed on other non-gouged shelfs (figure 51b). Northward flowing currents form these features.

The inner gravel facies represents an area of erosion by storm-generated waves and currents as well as longshore sediment transport nearshore. The shore-normal symmetrical gravel waves, starting at depths of 10 to 15 m, reflect the direct effects of shoaling waves acting on the sea bed. At deeper depths both wave-generated currents as well as the northward flowing Alaska Coastal Current erode the sea bed producing the surficial gravel lags. Sediment erosion results in a thin sediment cover of 2 m or less. Nearshore, shore-parallel currents transport the finer sediment fractions towards Icy Cape.

BENTHIC MAMMAL FEEDING AREAS

Caifornia gray whales have been observed on the inner shelf for the past 3 summers in the region west of Icy Cape to north of Point Franklin. Gray whales are very abundant throughout this area as individuals and in pods, especially within the region of the Alaska Coastal Current. The gray whales feed on benthic amphipods and isopods in the Coastal Current Sand facies. Gray whales have been observed surfacing surrounded by sediment plumes indicating active benthic feeding. Locally scattered, rounded sea floor pits, attributed to gray whale benthic feeding, characterize parts of the sea floor in the Coastal Current Sand facies. The greatest sea floor disturbance is in the inner shelf west of Wainwright and north to Point Franklin (figure 52). Here, a variety of apparently freshly-produced and current modified feeding pits are observed (figure 53). Elliptical multiple feeding pits to wide elliptical oval pits characterize the sea bed (Type I and Type II feeding pits of Nelson and Johnson, 1984). The pits range in length from 1.0 to 3.8 m and in width from 1.0 to 2.5 m. Near Wainwright the depths where the sea floor pits have been observed vary from 23 to 34 m. A sandwave field bounds the landward flank of the feeding area.

Three box cores (cores 23a, b, c), taken in succession where sediment plumes were observed surrounding surfacing gray whales, record coarse pebbly sand in all cores. Abundant amphipods and some isopods were found in the cores.

The feeding traces also record varying sea foor modification of ice gouges (figure 54a). Fresh gouges did not contain feeding pits whereas some gouges contained scattered feeding traces both in the gouge troughs and on internal ridges within the gouges

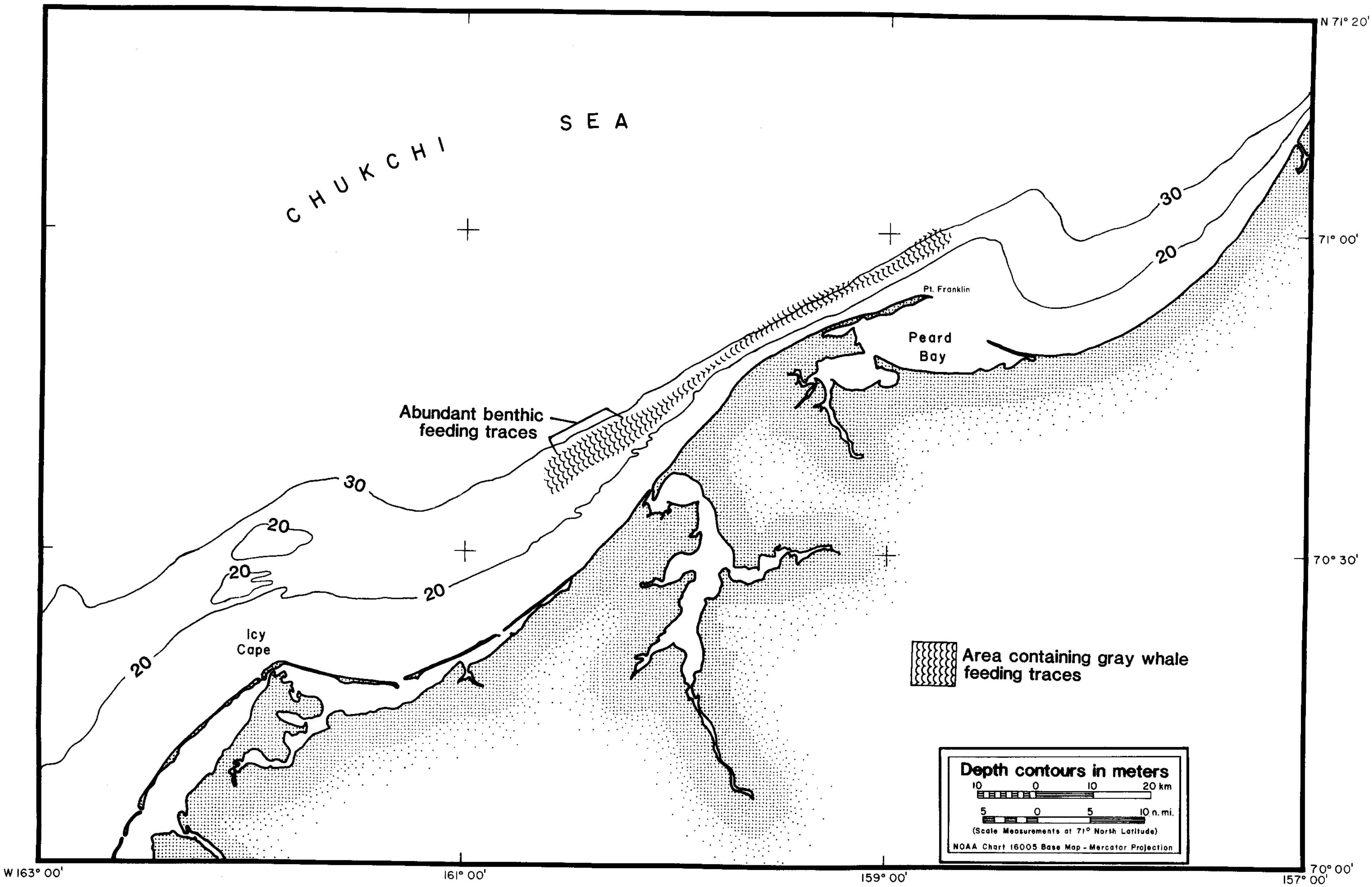

Figure 52. Major location of gray whale feed traces along the eastern boundary of the Alaska Coastal Current. The boundary limits of the feeding areas are only approximate. Scattered sea floor pits are also observed south of Icy Cape between depths of 20 to 35 m as well as east of Point Franklin. Some of the scattered feeding pits may also represent walrus feeding traces.

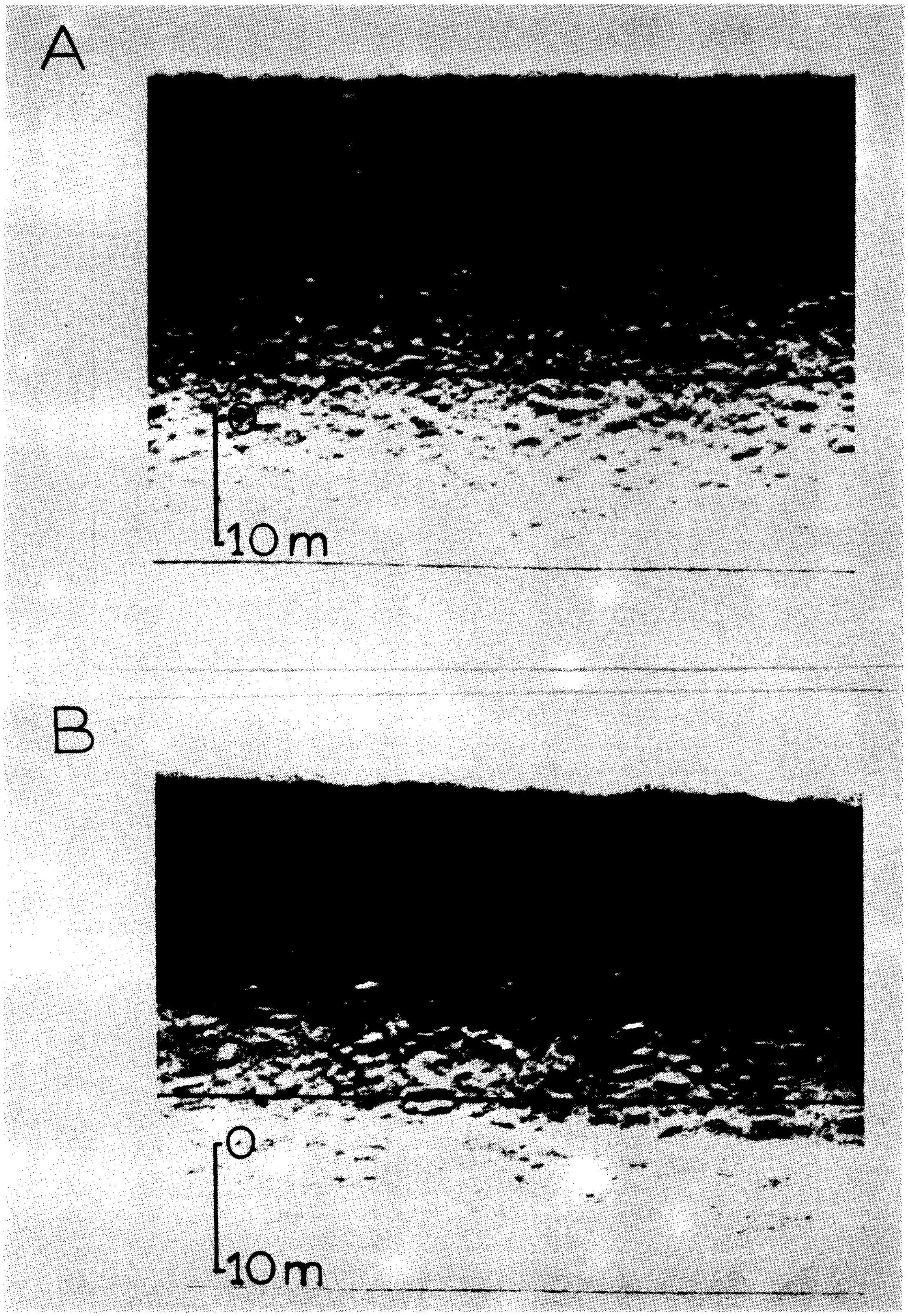

Figure 53. Gray whale feeding traces west of Wainwright, Chukchi Sea. A) Rounded and elliptical to current-modified feeding traces. B) Current-modified whale feeding traces at 24 m depth. A sandwave field bounds the feeding area (sandwaves start off right side of photo). Both sonographs are 500 Khz records.

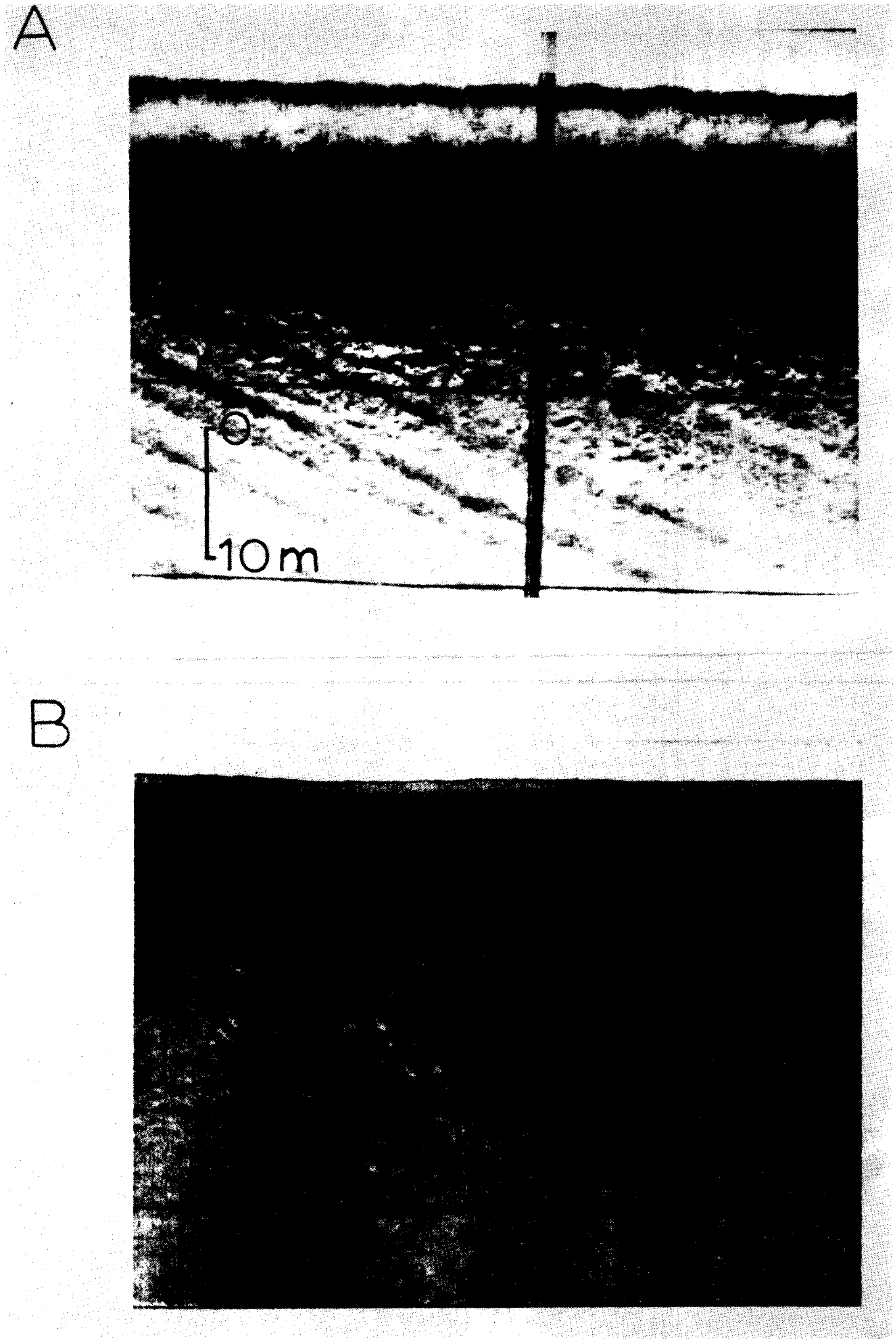

Figure 54. A) Gray whale feeding traces within an ice gouge off Wainwright. B) Round to elongate scattered feeding traces in coarse sand and pebbles west of Point Franklin. Sonographs are 500 Khz (A) and 100 Khz (B) records.

while other gouges were completely pitted. This may suggest that some of the intensely pitted ice gouges are over one season old.

North of Point Franklin adjacent to a sandwave field scattered rounded pits in coarse pebbly sand are also observed in the sonographs (figure 54b). These pits may represent either whale feeding traces in a coarser sediment type then found in the southern feeding area or it may represent possible walrus feeding traces. South of Icy Cape within the area dominated by the Alaska Coastal Current scattered sea floor pits are also observed (figure 55a). These pits may represent areas where gray whales are "test" feeding or they may represent an area of active bottom currents filling in the feeding pits resulting in a low density of feeding traces.

Benthic feeding traces of unknown origin are also observed as scattered patches on the outer shelf (figure 55b). These feeding traces are represented by linear to curved pits and they occur adjacent to gravel patches on the sea bed. These feeding traces may be produced by walrus.

Walrus feeding traces are found in the northeast Chukchi Sea to depths of at least 53 m. Long narrow linear furrows, gently curved furrows, or S-shaped to irregular sea bed furrows characterize the feeding traces. The sea floor furrows are less than 1 m wide and range in length from 10 m to 40 m. The furrows can be solitary features or they may be found as groups of linear parallel traces. The feeding traces generally parallel the Alaska Coastal Current suggesting the walrus use the currents during feeding. The greatest concentration of these feeding traces were preserved within the Outer Gravel Facies.

The reconnaisance surveys on the Chukchi Sea show that gray whale and walrus feeding areas do exist on and adjacent to the region bounded by the Alaska Coastal Current. Other feeding areas can be expected on the outer shelf and on the west side of the Barrow Sea Valley adjacent to Hanna Shoal. The areal distribution of the feeding areas as well as the total sea floor ulitilized by mammals in feeding in the northern Chukchi Sea is unknown.

ICE GOUGING

Sea ice plays an active role in the reworking and transport of sediments on the Chukchi Sea shelf. The seasonal ice canopy can be divided into three distinct zones. Along the coast and extending from promontory to promontory is the quasi-stable, often uniform ice of the fast ice zone. Immediatly seaward of this zone, pressure and shear ridges develop in response to the interaction between the stationary fast ice and moving ice further offshore. The ice ridges in this zone are often grounded. Further offshore pack ice and ice ridges are essentially free to drift guided by winds and currents. Unequal pressures within the yearly ice pack give rise to numerous

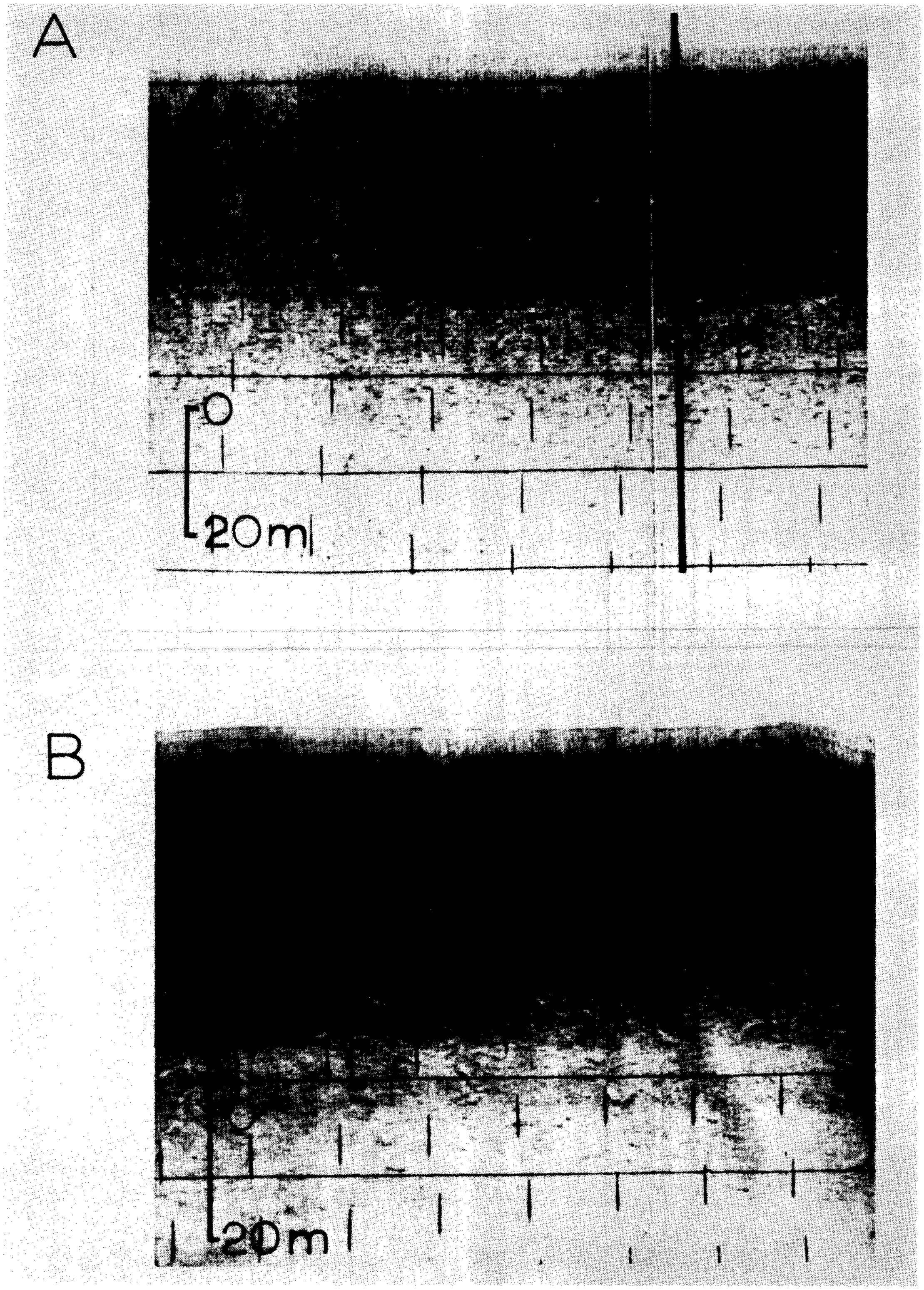

Figure 55. A) Scattered feeding traces within an area dominated by the Alaska Coastal Current south of Icy Cape.
B) Outer shelf feeding traces of unknown origin (possibly walrus) at depth of 48 m. This type of feeding trace commonly occurs adjacent to gravel patches. Sonographs are 100 Khz records.

pressure ridges of varying heights. Ice keels extend to varying depths beneath the shear and pressure ridges in the ice canopy. Ice keels to 50 m have been observed from limited data sets in the Arctic Basin to the north and even deeper keels have been statistically predicted. When keels of sufficient draft to ground are incorporated in a moving ice canopy the sea floor sediment is disrupted and bulldozed forming linear plow marks or gouges.

TERMINOLOGY

An ice gouge is defined as a single sea floor groove or plow mark generated by one protrusion of an ice keel. A single ice keel having more than one protrusion may create many parallel gouges. This results in a multiplet or set of closely spaced gouges generated by the same ice keel. Gouge depth is the measured depth of a gouge below the surrounding sea floor. This measurement does not necessarily indicate the depth of ice incision as sediment may have infilled the gouge since its inception. Ridges usually flank one or both sides of a gouge and represent the plowed debris from the gouge event. Gouge relief refers to the vertical distance from the floor of the gouge to the crest of the ridge. The gouge orientation refers to the trend of linear gouges and, as used here, is the dominant trend within our observational segment on the sonograph. Orientation trends of gouge lineations do not necessarly imply the direction of motion of ice which created the gouge.

RESULTS

A summary of ice gouge trends in the Chukchi Sea record a dominant northeast-southwest orientation (figure 56). Tomil (1978) also notes local dominant ice gouge trends that parallel the bathymetric contours which agrees with our data. The ice gouge trends in the Chukchi Sea apparently reflect the effects of shelf currents, storms and pack ice movement. The northwest-southeast ice gouge trend (C, figure 56) may reflect ice movement by shelf currents as a southeast-directed current is reported for area "C" (figure 8) (Coachman and others, 1975). Likewise, the shore-parallel ice gouge trends along the eastern part of the Chukchi Sea reflect ice movements by the Alaska Coastal Current. Ice generally moves 45 degrees to the right of the wind (Thorndike and Colony, 1982). The winds in the Chukchi Sea region are from the northeast with summer storms generally from the southwest or west which should move ice to the northwest and to the east respectively. The summer storms may account for the onshore trends of gouges off Cape Lisburne (G, figure 56) and on the east side of the Barrow Sea Valley (H, figure 56). However, the dominant northeast-southwest ice gouge trend on the Chukchi Sea shelf must reflect the pack ice movement to the south during the fall as well as the effects of shore parallel shelf currents. Whereas, the dominant pack ice movement to the west and northwest (Stringer, 1978, 1982) apparently does not readily affect the sea floor on the outer shelf.

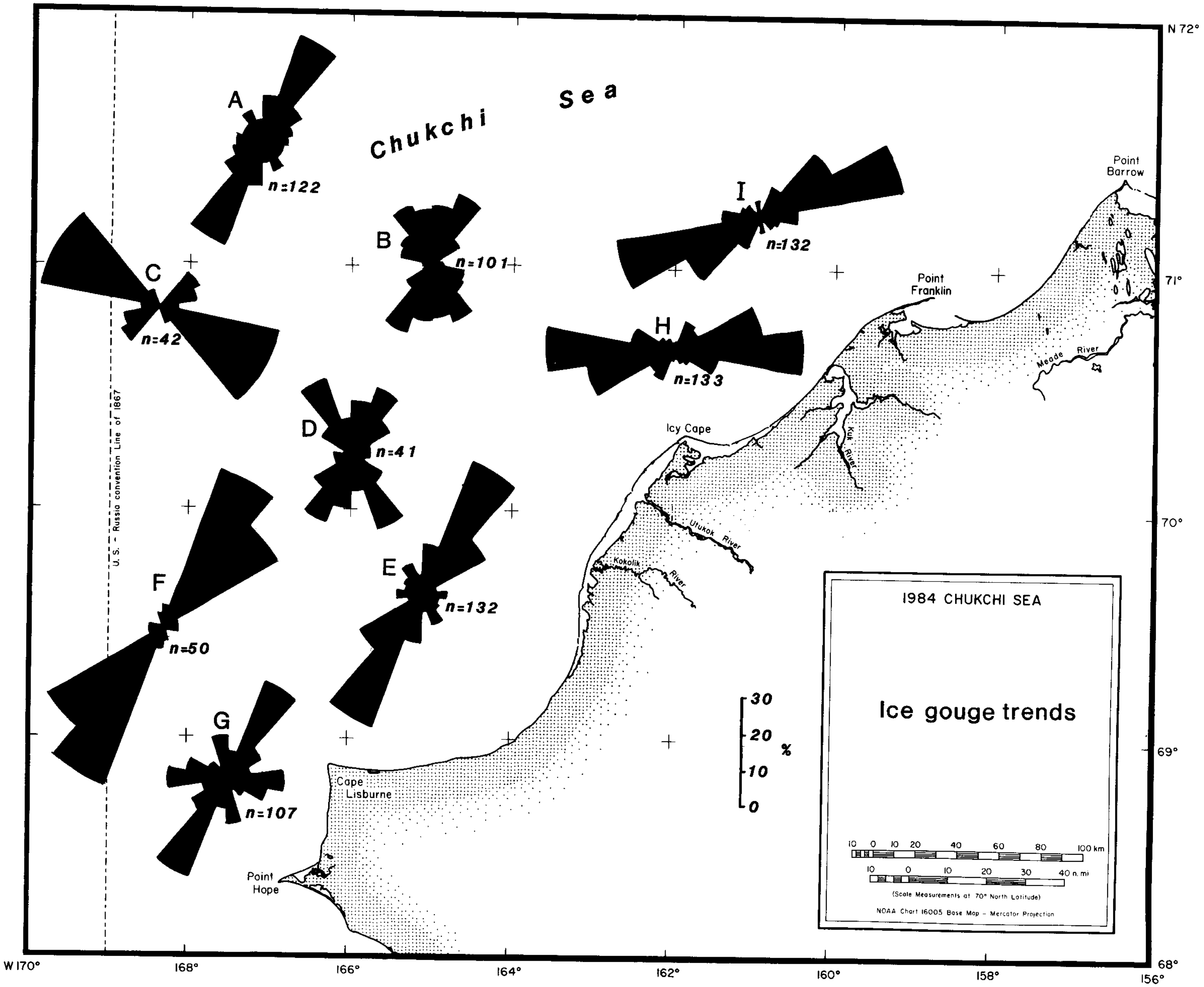

Figure 56. Rose diagram of ice gouge orientations in the northeast Chukchi Sea. H) Ice gouge trends on the east side of the Barrow Sea Valley. I) Ice gouge trends on the west side of the Barrow Sea Valley.

On the outer shelf (northwest part) of the Chukchi Sea the maximum ice gouge incision depth is 1.3 m (table 1). Most of the ice gouges are shallow, 0.3 m of less in depth below the sea floor. The "shallow" gouges may represent "older" gouge events that are now being filled with sediment or they may also reflect the thin sediment cover over bedrock (ice is not cutting into bedrock).

The maximum ice gouge density for lines 25, 26, 27, and 44 (figure 3) are 5 gouges per km with these values only found on gravel-covered bathymetric highs. The adjacent low regions average 1 gouge per km on line 44, 1 gouge per 3 km on line 27, 1 gouge per 4 km on line 26, whereas, line 45 varies from 1 gouge per 3 km to 1 gouge per 7 km. The ice gouge abundance rapidly decreases with increasing depth (table 1).

On the inner shelf (northeast part of the Chukchi Sea) within and adjacent to the Barrow Sea Valley ice gouging is identified to 58 m depth. The maximum ice gouge incision depth, 2.9 m with 3.9 m ice gouge relief, occurs on line 23 (figure 4) at the head of the Barrow Sea Valley. The water depth is 45 m where the maximum ice gouge incision is located. Multiple, parallel ice gouges formed by large ice sheets or ridges account for the abundance of shallow, 0.3 m depth or less, bottom disturbances in shallow water areas (24 to 34 m water depth) (table 2). The ice gouges at deeper depths tend to represent solitary grounding events, especially within the deeper parts of the sea valley.

The maximum ice gouge density within the Barrow Sea Valley ranges from 19 gouges per km at 44 to 46 m depth (line 24, outer sand facies) on the east flank of the sea valley, to 24 gouges per km at 28 m depth (line 17, inner sand facies) directly west of Point Franklin. Low ice gouge densities, 1 gouge in 10 km (35 m depth) to 1 gouge per km (24 to 29 m depth) are recorded on the shoreward part of the outer gravel facies and in the coastal current sand facies respectively. These low gouge densities are apparently the result of active currents filling in the gouge traces within these two facies as at deeper depths and at shallow depths ice gouging ranges from 14 per km to 12 per km respectively.

In the southern part of the Chukchi Sea, north of Cape Lisburne (line 4), ice gouge incision depths are also shallow with most gouges 0.3 m or less. The gouge densities are greatest on the shoreward regions ranging up to 6 gouges per km between 24 to 28 m depth.

DISCUSSION

Although ice gouging is pervasive on the Chukchi shelf, but away from topographic highs and the nearshore slopes, gouging is

Water depth (m) \ Ice gouge depth (m)	0.2–0.3	0.3–0.4	0.4–0.5	0.5–0.6	0.6–0.7	0.7–0.8	0.8–0.9	0.9–1.0	1.0–1.1	1.1–1.2	1.2–1.3	1.3–1.4
50–52	5	4		1								
48–50	10	23	1	1			2		1		1	
46–48	39	36			2	2						
44–46	29	102	1	2		1	1					1
42–44	20	132		1								
40–42	15	65		6			1			1		
38–40	32	196	43	1	3		1		1			1

Table 1. Maximum ice gouge incision depth vs. water depth for the northwest Chukchi Sea. Numbers in boxes represent number of gouges in class. Data from lines 25, 26, 27, 44, 45 and 46 (see Figure 3 for trackline locations). Most of the ice gouge incisions are shallow, 0.3 m or less below the sea floor; however, the shallow gouges may represent "older" gouges that are filling with sediment. The ice gouge abundance also decreases with increasing depth with most of the gouges found between 38 to 44 m on gravel covered bathymetric highs.

Water depth (m) \ Ice gouge depth (m)	0.3–0.4	0.4–0.5	0.5–0.6	0.6–0.7	0.7–0.8	0.8–0.9	0.9–1.0	1.0–1.2	1.2–1.3	1.3–1.4	1.4–1.5	1.5–1.6	1.6–1.7	1.7–1.8	1.8–1.9	1.9–2.0	2.0–2.1
58–60	5																
56–58	11	1															2
54–56	26	1															1
52–54	35	3															
50–52	52	1							1								
48–50	30																
46–48	77	2	4	1	1												
44–46	113	1	1	2	1	2	1	1								2	
42–44	6	2															
40–42	39		1														
38–40	118	2	3														
36–38	49																
34–36	68	1			1	1											
32–34	199	4	1	2	1												
30–32	74																
28–30	299	1			1	1		1									
26–28	203	2	2	3	2	3	1	1	1								
24–26	236	4	3	3		1	1	2	1						1		

One ice gouge to 2.9 m depth.

Table 2. Maximum ice gouge incision depths vs. water depth for the Barrow Sea Valley region. Numbers in boxes represent number of gouges in class. Data obtained from tracklines in figure 4. The maximum ice gouge incision depth is 2.9 m at 45 m water depth near the center of the Barrow Sea Valley. Most of the ice gouges are shallow, 0.3 m or less in depth below the sea floor. Multiple ice gouge incisions are common to 32-34 m water depth; at deeper depths the ice gouges are usually solitary events.

rare and gouge depths are shallow. Furthermore, in the deep water areas gouge relief is commonly subdued indicating that waves, currents and biological activity are perhaps the dominant surface reworking processes, since gouging is less frequent.

The highest gouge intensities (most numerous and deepest) are found on the east facing slopes of bathymetric highs and along the steeper slopes of the coastal margin. The bathymetric highs and inshore areas comprise a relatively small portion of the shelf area yet are subject to higher gouge intensities. Gouging occurs here because a greater number of ice keels exist with shallower draft which interact with the shallow sea floor. The broad flat areas, depths of 40 to 50 m, provide the rarer deep draft ice a large surface to gouge.

Over the broad and generally flat regions of the study area gouging increases northward. This is because of the incursion of ice ridges and ice island fragments from the Arctic Basin to the north and to the greater period of ice cover. Conversely longer periods of open water in the southern parts of the study area allow greater sediment reworking by storm waves and currents. Additionally the shoals and broad expanse of the northern shelf filter out southward moving ice of sufficient draft to gouge the sea floor. This implies that much of the gouging in the study area may be the result of locally generated ice ridges. From studies in the Beaufort Sea we know that gouges from locally generated ice ridges are shallow due to the general incompetence of newly created ridges and their keels.

Ice gouging is a process that is constantly reworking the surface sediment of the Chukchi Sea shelf. However, currents, waves, and biological processes are also active in reworking the this surficial sediment layer at a higher rate in the deeper and southern portion of the study area masking the effects of gouging. Inshore of about 30 m water depth and on the flanks and the crests of bathymetric highs ice gouging dominates the surficial sediment processes except in areas where the Alaska Coastal Current actively impinges on the sea floor.

CONCLUSIONS

1) A thin sediment cover, less than 4 to 5 m thick, overlies folded bedrock over much of the Chukchi Sea shelf.

2) Channel-fill deposits of unknown age occur in the northwest part of the Chukchi shelf. These channel deposits may represent possible hazard if they contain gas or permafrost. They may also represent a potential source of sand and gravel on the outer shelf.

3) The outer shelf surface sediment is composed of micaceous sandy mud with scattered surficial gravel on bathymetric highs.

4) The surface sediment in the southern part of the Barrow Sea Valley can be divided into 4 facies, an outer sand, an outer gravel, a coastal current sand, and an inner gravel. Distinctive benthic biological cummunities inhabit these facies.

5) Storm-generated currents, shelf currents, and biological processes dominate on the outer shelf; storm-generated currents, the shore-parallel Alaska Coastal Current, and biological processes rework the eastern shelf regions.

6) Sand waves, gravel waves, gravel ribbons, extensive gravel sheet deposits, and linear erosional furrows are the common bedforms on the Chukchi shelf that indicate active bottom currents.

7) Gray whale feeding areas are identified within the coastal current sand facies off Wainwright; walrus feeding traces are identified in the outer gravel facies as well as on the outer shelf.

8) Ice gouging, to 58 m water depth, occurs throughout the Chukchi shelf, however, most of the gouges are shallow, less than 0.3 m in depth below the sea floor, and scattered. High ice gouge densities are identified on the northern shelf areas investigated and on the flanks of the Barrow Sea Valley.

REFERENCES

Barnes, P. W., 1970, Preliminary results of geologic studies in the eastern central Chukchi Sea, U. S. Coast Guard oceanographic rept., no. 50,, p87-110.

Bird, K. J., and Andrews, J., 1979, Subsurface studies of the Nanushuk Group, North Slope, Alaska, in Ahlbrandt, T. S., ed., Preliminary geologic, petrologic, and paleontologic results of the study of Nanushuk Group rocks north slope, Alaska, U. S. Geol. Survey circular 794, p. 32-41.

Coachman, L. K., Aagaard, K., and Tripp, R. B., 1975, Bering Strait--the regional physical oceanography, Univ. Wash. Press, Seattle, 172 p.

Creager, J. S., and McManus, D. A., 1966, Geology of the Chukchi Sea, in Wilimovsky, N. J., and Wolf, J. N., eds., Environments of the Cape Thompson region, Alaska, U. S. Atomic Energy Commission, Div. of Technical Information, p. 755-786.

Creager, J. S., and McManus, D. A., 1967, Geology of the floor of the Bering and Chukchi Seas--American studies, in Hopkins, D. M., ed., The Bering land bridge: Stanford Univ. Press, Stanford, Calif., p. 7-31.

Fleming, R. H., and Heggarty, D., 1966, Oceanography of the southeastern Chukchi Sea, in Wilimovsky, N. J., and Wolf, J. N., eds., Environment of the Cape Tompson region, Alaska, U. S. Atomic Energy Commission, Div. of Technical Information, p. 697-754.

Flood, R. D., 1984, Classification of sedimentary furrows and a model for furrow initiation and evolution, Geol. Soc. of America Bull., v. 94, p. 630-639.

Folk, R. L., 1974, Petrology of sedimentary rocks, Hemphill Publishing Co., Austin, Texas, 182 p.

Garrison, G. R., and Becker, P., 1976, The Barrow submarine canyon: a drain for the Chukchi Sea, Jour. of Geophysical Res., v. 81, p. 4445-4453.

Grantz, A., Dinter, D. A., Hill, E. R., Hunter, R. E., May, S. D., McMullin, R. H., and Phillips, R. L., 1982, Geologic framework, hydrocarbon potential, and environmental conditions for exploration and development of proposed oil and gas lease sale 85 in the central and northern Chukchi Sea, U. S. Geol. Survey Open-file rept. 82-1053, 84 p.

Hill, E. R., Grantz, A., May, S. D., and Smith, M., 1984, Bathymetric map of the Chukchi Sea, Miscellaneous investigation series map I-1182-D.

Hufford, G. L., 1977, Northeast Chukchi Sea coastal currents, Geophys. Res. Letters, v. 4, no. 10, p. 457-460.

Lewbel, G. S.,1984, Environmental hazards to petroleum industry development, in Truett, J. C., ed, Proceedings of synthesis meeting: The Barrow Arch environment and planned offshore oil and gas development, NOAA/OCSEAP, p. 31-46.

Lewbel, G. S., and Gallaway, B. J., 1984, Transport and fate of spilled oil, in Truett, J. C., ed, Proceedings of synthesis meeting: The Barrow Arch environment and planned offshore oil and gas development, NOAA/OCSEAP, p. 7-29.

McManus, D. A., Creager, J. S., Echols, R. J., and Holmes, M. L., 1983, The Holocene transgression of the flank of Beringia: Chukchi valley to Chukchi estuary to Chukchi Sea, in Masters, P. M., and Flemming, N. C., eds., Quaternary coastlines and marine archaeology: towards the prehistory of land bridges and continental shelves, Academic Press, p. 365-388.

Miller, M. C., McCave, I. N., and Komar, P. D., 1977, Threshold of sediment motion under unidirectional currents, Sedimentology, v. 24, p. 507-525.

Molenaar, C. M., 1985, Subsurface correlations and depositional history of the Nanushuk Group and related strata, North Slope, Alaska, in Huffman, A. C., ed., Geology of the Nanushuk Group and related rocks, North Slope, Alaska, U. S. Geol. Survey Bull. 1614, p. 37-59.

Moore, D. G., 1964, Acoustic reflection reconnaissance of continental shelves: the Bering and Chukchi Seas, in Miller, R. I., ed., Papers in Marine Geology, Shepard Commemorative Volume, MacMillan press, New York, p. 319-362.

Mountain, D. G., Coachman, L. K., and Aagaard, K., 1976, On the flow through Barrow Canyon, Jour. Phys, Oceanography, v. 6, p. 461-470.

Naidu, A. S., and Sharma, G. D., 1970, Geologic, biological, and chemical oceanography of the eastern central Chukchi Sea, U. S. Coast Guard oceanographic Rept., no. 50, p. 173-195.

Nelson, C. H., and Johnson, K. R., 1984, Gray whales, tillers of the sea floor, in Clarke, S. H., ed., Highlights in Marine Geology, U. S. Geol. Survey circular 938, p. 99-107.

Paquette, R. G., and Bourke, R. H., 1974, Observations on the coastal current of Arctic Alaska, Jour. Marine Res., v. 32, no. 2, p. 195-207.

Phillips, R. L., and Reiss, T. E., Kempema, E., and Reimnitz, E., 1982, Marine geologic investigations, Wainwright to Skull Cliff, northeast Chukchi Sea, U. S. Geol. Survey Open-file rept. 84-108, 33 p.

Phillips, R. L., and Reiss, T. E., 1984, Nearshore marine geologic investigations, Icy Cape to Wainwright, northeast Chukchi Sea, U. S. Geol. Survey Open-file rept. 85-50, 22 p.

Sharma, G. D., 1979, The Alaska shelf: hydrographic, sedimentary and geochemical environment, Springer-Verlag, New York.

Solomon, H., and Ahlnas, K., 1980, Ice spirals off Barrow as seen by satellite, Arctic, v. 33, no. 1, p. 184-188.

Stringer, W. J., 1978, Morphology of Beaufort, Chukchi, and Bering Seas nearshore ice conditions by means of satellite and aerial remote sensing, v. 1, Geophy. Inst. Univ. of Alaska, Fairbanks, 34 p.

Stringer, W. J., 1982, Width and persistence of the Chukchi Polynya, NOAA/OCSEAP Rept., 17 p.

Thorndike, A. S., and Colony, R., 1982, Sea ice motion in response to geostrophic winds, Jour. Geophy. Res., v. 87, no. C8, p. 5845-5852.

Toimil, L. J., 1978, Ice gouge microrelief on the floor of the eastern Chukchi Sea, Alaska: a reconnaissance survey, U. S. Geol. Survey Open-file Rept., 94 p.

Wilson. J. B., 1979, Biogenic carbonate sediments on the Scottish continental shelf and on Rockall Bank, Marine Geol., v. 33, p. M85-M93.

Wiseman, W.J., Jr., and Rouse, L. J., Jr., 1980, A coastal jet in the Chukchi Sea, Arctic, v. 33, no. 1, p. 21-29.

APPENDICES

Appendix A

1984 Chukchi Sea Samples							
Sample #	Sample Type	Latitude (North)	Longitude (West)	Depth (m)	Gravel (%)	Sand (%)	Mud (%)
001	Box Core	70.79330	161.12830	43.5	12.1	75.0	12.9
002	Box Core	70.73330	160.84670	45.3	29.4	66.3	4.3
003	Box Core	70.70830	160.65500	43.9	9.4	69.3	21.3
004	Box Core	70.64170	160.40170	22.3	20.5	74.5	5.0
005	Box Core	70.52670	160.57330	18.3	24.2	63.6	12.1
006	Box Core	70.64670	161.41000	37.0	7.6	82.6	9.7
007	Box Core	70.55170	161.64830	28.7	2.0	94.7	3.2
008	Box Core	70.54330	161.78330	24.6	0.8	98.4	0.8
009	Box Core	70.65830	162.16330	39.2	21.1	74.5	4.4
010	Box Core	70.77170	162.54330	42.9	2.2	89.7	8.0
011	Box Core	70.88330	162.86170	42.5	1.8	74.3	23.9
012	Box Core	70.93330	166.34000	42.1	-----	36.0	64.0
013	Box Core	70.95500	166.94830	45.5	-----	29.2	70.8
014	Box Core	70.97320	167.39670	44.8	-----	42.4	57.6
015	Box Core	70.98000	167.73670	44.4	22.9	40.9	36.1
016	Box Core	70.47170	166.95330	49.5	0.5	57.1	42.4
017	Box Core	70.41000	166.47500	43.2	3.5	53.2	43.3
018	Box Core	70.94500	159.35330	39.2	31.7	60.3	7.9
019	Box Core	70.97500	159.37170	52.2	ROCK	-----	-----
020	Box Core	70.96000	159.42670	49.4	15.7	64.9	19.3
021	Box Core	71.02000	161.36330	47.7	1.7	88.9	9.4
022	Box Core	70.88330	161.75670	42.1	15.1	74.2	10.7
023 A	Box Core	70.72670	160.17500	23.7	3.8	95.3	0.9
023 B	Box Core	70.69670	160.20830	23.7	2.9	96.8	0.3
023 C	Box Core	70.69330	160.20830	23.7	19.3	79.9	0.8
024	Box Core	70.77670	160.09000	36.6	28.0	69.6	2.4
025	Box Core	70.76000	160.33170	40.2	22.7	73.2	4.1
026	Box Core	70.71170	160.27000	29.3	23.4	74.6	1.9
027 START	Pipe Dredge	70.57000	160.98330	31.3	0.7	93.6	5.7
027 END		70.57000	160.99170				
028 START	Pipe Dredge	70.61330	160.93670	35.0	5.3	87.1	7.6
028 END		70.61500	160.93930				
029	Box Core	70.67920	161.26850	40.3	12.8	82.5	4.7
030	Box Core	70.73170	161.57500	40.2	14.3	77.5	8.2
031	Box Core	70.76000	161.70670	42.0	17.3	75.6	7.1
032	Box Core	71.28830	165.72670	41.2	0.3	27.4	72.3
033	Box Core	71.37330	166.12830	42.4	-----	16.7	83.3
034	Box Core	71.40830	166.35330	43.0	1.0	15.9	83.0
035	Box Core	70.91500	168.46670	43.0	1.3	45.7	52.9
035 G	Gravity Core	70.91500	168.46670	43.0			
036	Box Core	70.88000	167.78170	53.5	0.2	23.3	76.5
036 G	Gravity Core	70.88000	167.78170	53.9			
037	Box Core	70.84000	167.10330	46.0	0.6	41.6	57.8
038	Box Core	69.57830	167.41170	45.7	6.3	48.9	44.8
039	Box Core	69.49330	167.06170	45.0	0.1	37.6	62.3
040	Box Core	68.82000	166.74500	40.5	0.5	30.2	69.3
041 START	Pipe Dredge	68.91830	166.56000	36.5			
041 END		68.92130	166.56050				
042 START	Pipe Dredge	69.10170	166.41500	31.1			
042 END		69.10170	166.42183				

Appendix B

1981 Chukchi Sea Samples							
Sample #	Sample Type	Latitude (North)	Longitude (West)	Depth (m)	Gravel (%)	Sand (%)	Mud (%)
008	Grab	70.96104	158.98534	28.6	59.6	34.5	5.5

1982 Chukchi Sea Samples							
Sample #	Sample Type	Latitude (North)	Longitude (West)	Depth (m)	Gravel (%)	Sand (%)	Mud (%)
001	Grab	70.43645	161.31513	22.0	4.1	88.8	6.9
002	Grab	70.57261	160.88451	27.0	9.7	72.5	17.8
003	Grab	70.30769	161.38040	6.7	43.5	55.6	0.8
004	Grab	70.32925	161.44785				
005	Grab	70.36929	161.60620				
006	Grab	70.40710	161.77314	16.7	5.9	84.1	9.9
007	Grab	70.45207	161.96241	16.5	0.1	98.8	1.0
008	Grab	70.35409	161.75108	10.8	19.7	75.7	4.6
009	Grab	70.99737	158.54305	19.0	5.9	90.9	3.1
010	Grab	70.98577	158.38219	21.0	0.1	70.8	28.1
011	Grab	70.95229	158.28459	19.0	4.0	38.3	57.7
012	Grab	70.90994	158.21192	17.0	0.4	18.6	80.7
013	Grab	70.87287	158.19676	14.0	3.7	40.8	55.5
014	Grab	70.84760	158.17605	14.0	40.0	39.6	20.4
015	Grab	70.83480	158.23021				
016	Grab	70.98072	157.42988				
017	Grab	70.93045	157.61289				
018	Grab	70.93518	157.62725				
019	Grab	70.87266	157.87974				

Appendix C

Biological Composition of Inner Shelf Samples

Biological Environment	Sample #	Biological Specimen *								Depth (m)
		Ba	Bi	By	Br	Ec	Cp	Ga	Pt	
Outer Sand Facies	84-10		99.5			0.2			0.2	42.0
	84-11		96.1					3.9		42.5
	84-21	0.4	98.2		0.2			1.2		47.7
	84-22	12.6	78.5					8.9		42.1
Outer Gravel Facies	84-1	54.9	36.7	4.4	2.3			1.7		43.5
	84-2	56.4	34.5	0.9	1.2	0.1	0.1	6.8		45.3
	84-3	61.8	25.0	0.5	9.5	1.7		1.5		43.9
	84-9	50.2	42.1			0.6		6.7		39.2
	84-18	71.3	25.6	0.1	2.5	0.1		0.4		39.2
	84-20	52.0	36.7	9.3	1.3	0.1		0.6		49.4
	84-24	10.8	86.0	2.9				0.3		36.6
	84-25	77.7	16.0	0.2	3.9	0.6	0.1	1.5		40.2
	84-26	19.6	78.3	0.1	0.1	1.2		0.7		29.3
	84-30	55.5	34.5	7.0	0.9			2.1		40.2
	84-31	60.0	33.8	3.7	0.3			2.2		42.0
	81-8	43.9	50.5					5.5		28.6
Coastal Current Sand Facies	84-6	26.4	72.3	1.1					0.2	37.0
	84-7	0.5	90.7			6.0		2.7	0.1	28.7
	84-8	3.5	85.2			8.3		3.0		24.6
	84-23	15.5	68.6		0.3	11.6		1.6	2.5	23.7
	84-28	1.9	69.9	1.3		14.7		10.9	1.9	31.3
	84-29	36.2	45.7	2.6	11.4	0.3		3.7		35.0
Inner Gravel Facies	84-4	70.8	26.9	0.4				1.9		22.3
	84-5	24.9	69.6					5.5		18.3

Biological Composition of Outer Shelf Samples

Biological Environment	Sample #	Biological Specimen *								Depth (m)
		Ba	Bi	By	Br	Ec	Cp	Ga	Pt	
Outer Shelf Facies	84-34		89.1					10.9		43.0
	84-36		100.0							53.5
	84-37		89.9					10.1		46.0
	84-39		28.5					71.5		45.0
Cape Lisburne	84-42	6.4	75.1		0.2			18.3		31.1

* Biological specimens: Percentage (by weight) of biological fraction of sediment sample. Codes used are as follows:
  - Ba - Barnacles
  - Bi - Bivalves
  - By - Bryzoans
  - Br - Brachiopods
  - Ec - Echinoids
  - Cp - Chitons
  - Ga - Gastropods
  - Pt - Polychaete (*Pectinaria* sp.) tubes

APPENDIX D

BOX CORE STATIONS 32-33 IN RELATION TO HIGH-RESOLUTION SEISMIC PROFILES

High-resolution reflection seismic profiles on line 44 on the northwest part of the Chukchi Sea where box cores 32 and 33 obtained show different acoustic signitures. Where box core 32 obtained the sub-bottom reflectors show well-defined parallel strata cut by a fluvial channel deposit (figure 1). In contrast, where box core 33 taken continous reflectors only occur in the upper part of the section with apparently acoustic impenetrable zones throughout the lower part of the section (figure 2). The acoustic "turbid" zone may possible be due to gas within the sediment as high methane values were obtained in box core 33 (see following report). However, the acoustic "turbid" zone may be caused by other physical features as uniform sediment texture or lack of bedding or textural contrasts.

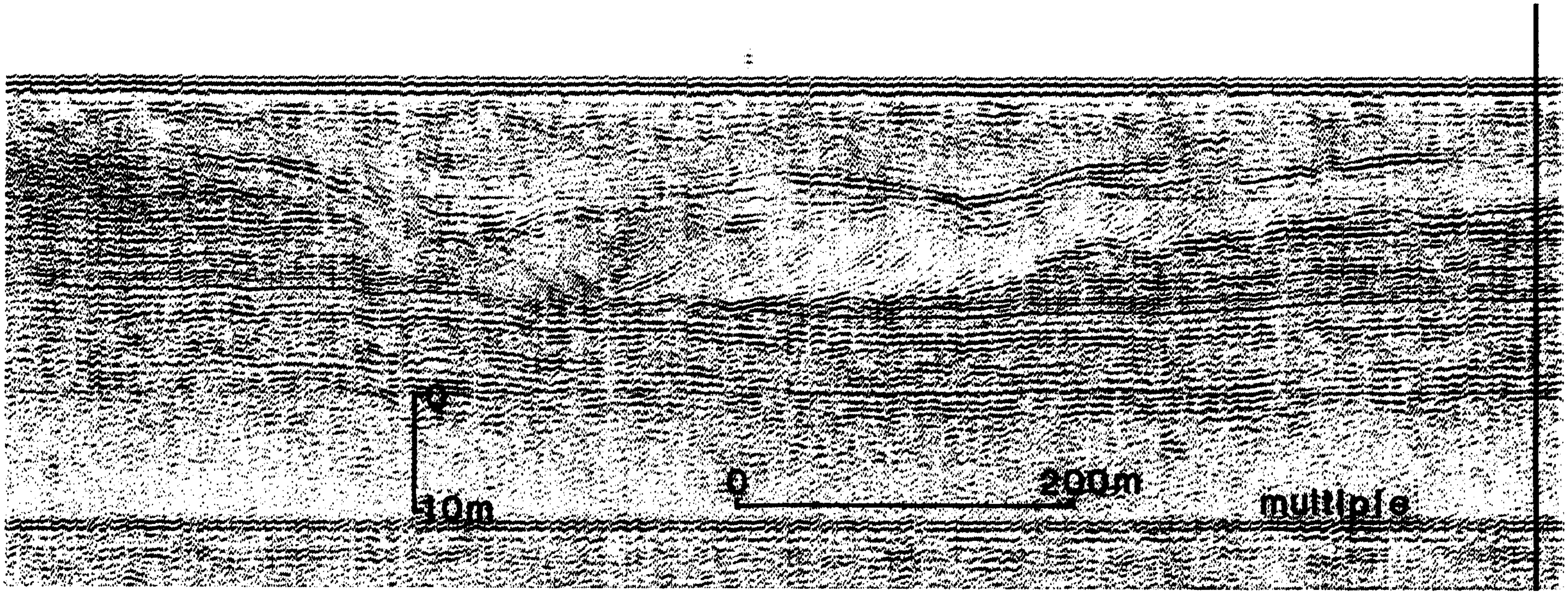

Figure 1. High-resolution seismic profile on line 44 where box core 32 was obtained. See figure 3 for track line location and figure 5 for box core location. Bedrock consists of parallel and gently inclined strata cut by a fluvial channel deposit. Box core 32 taken where seismic record ends on right.

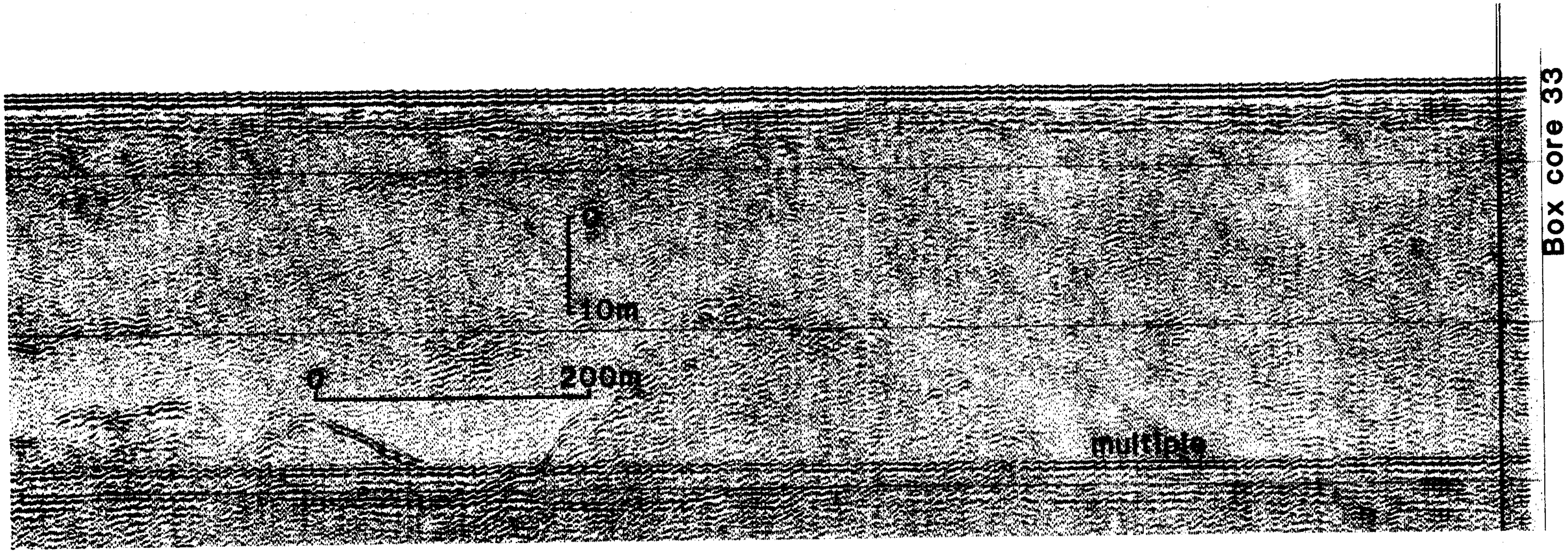

Figure 2. High-resolution seismic profile on line 44 where box core 33 was obtained. Parallel reflectors are present only in the upper part of section. The lower acoustic "turbid" zone may be due to gas-charged sediment as high values of methane were found in box core 33. Box core 33 taken where seismic record ends on right.

HYDROCARBON GAS IN SURFACE SEDIMENTS OF THE CHUKCHI SEA

by

Margaret Golan-Bac

TABLE OF CONTENTS

HYDROCARBON GAS IN SURFACE SEDIMENTS OF THE CHUKCHI SEA

Margaret Golan-Bac

INTRODUCTION

This geochemical study is part of a U.S. Geological Survey investigation in the Chukchi Sea in 1984 on the NOAA Ship SURVEYOR (Phillips et al, this report). During August 26 to Sept. 17, 1984, 40 box cores, 2 gravity cores and 4 dredge samples were collected in the shelf sediments of the Chukchi Sea. Of these, nineteen box cores and one gravity core were sampled for hydrocarbon gas analysis. Gas sample sites are illustrated in Figure 1. Specifically, the hydrocarbon gases examined were methane (C1), ethane (C2), ethene (C2=), propane (C3), propene (C3=), isobutane (iC4) and n-butane (n-C4). The main objective was to sample localities where previous geophysical surveys indicated the possibility of gassy sediments and to ascertain the composition and origin of these gases.

METHODS

The box cores were subsampled for hydrocarbon gas analysis using a steel cylinder (diameter = 7.5 cm). The total length of box core sediment ranged from 18 cm to 56 cm. One gravity core was taken whose total length was 69 cm. A 10 cm section of sediment was removed from the top of the box core (0-10 cm) and from the bottom if possible. One sample (10 cm) was taken from the bottom portion of the gravity core. Each sample was immediately extruded into a can (approximately one liter volume) equipped with two septa covered holes near the top. Seawater was added to the can and 100 ml of this water was removed to establish a headspace before the can was sealed with a double-friction seal lid. Seawater samples were also canned periodically to monitor the composition of the water added to the sediment-filled cans. All cans were turned upside down and frozen until analysis in the shore-based laboratory. The frozen cans were brought to room temperature and shaken to extract the gases from the sediment into the air headspace. About 5 ml of this headspace gas was removed through the septa covered ports with a gas tight syringe. Exactly 1 ml of this mixture was injected into the gas chromatograph equipped with both flame-ionization and thermal conductivity detectors. The gas chromatograph was calibrated with a standard mixture of hydrocarbon gas. Calculations of gas concentrations were made by integrating the areas or measuring heights of the hydrocarbon peaks on the chromatograms. An average composition of the seawater sample headspace that would have contributed to the sediment sample analysis was subtracted from each analysis. Partition coefficients used to correct for differences in gas solubility are as follows: C1 = 0.8; C2, C3, iC4, nC4 = 0.7; C2=, C3= = 0.6. Concentrations are reported as nl/l wet sediment. Results are semi-quantitative but can be compared because all samples were processed in the same manner.

RESULTS

The concentration of hydrocarbon gases recovered from the 19 box cores and one gravity core are reported in Table 1. Hydrocarbon gases were present in all the samples analyzed. C1 is the most abundant hydrocarbon gas, ranging in concentration from 690 to 22,000 nl/l wet sediment. Box core 33 is the sample with the highest concentration of methane. The other hydrocarbon gases were present in much lower concentrations and when detected, ranged in concentration from 4 to 390 nl/l wet sediment. In general, the concentration of ethane is slightly greater than propane which is slightly greater than the butane (iC4 plus nC4) concentration. The alkenes C2= and C3= are in the same range of concentration as C2 and C3, although the concentration of C2= was greater than the concentration of C2 in a majority of the samples, while the concentration of C3 exceeds the concentration of C3= in a majority of the samples.

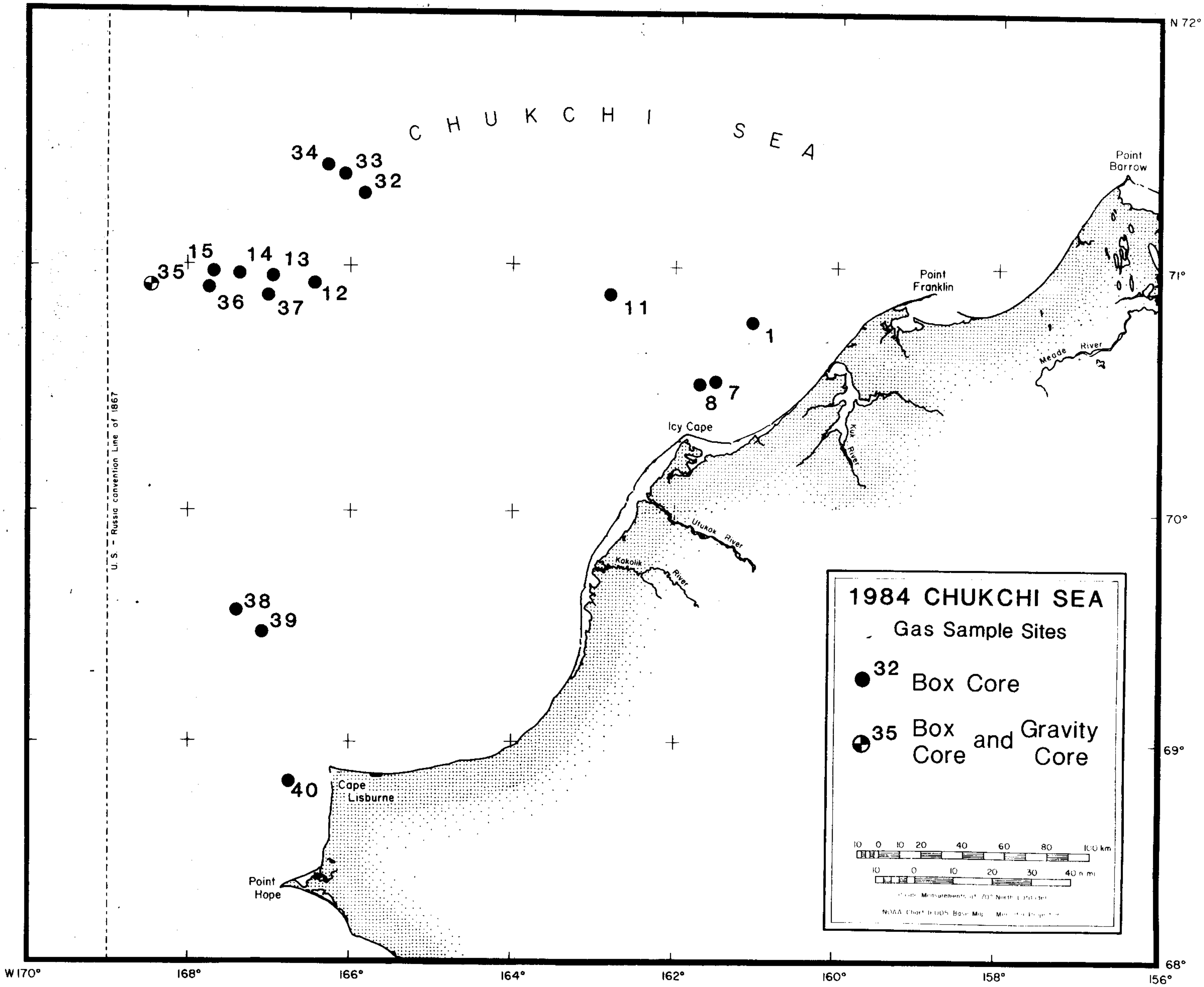

Figure 1. Location of hydrocarbon gas sampling sites in the Chukchi Sea.

Table 1. Hydrocarbon Gas Concentrations in Near-Surface Sediments of the Chukchi Sea.

Station & Int. (cm)	Water Depth (m)	C1	C2	C2=	C3	C3=	iC4	nC4	Location Latitude	Location Longitude
		nanoliters of gas / liter wet sediment								
Box 001 0-10	44	3200	330	350	240	170	23	59	70° 47.6' N	161° 07.7' W
Box 007 0-10	29	2200	130	120	59	50	14	26	70° 33.1' N	161° 38.9' W
Box 008 14-24	25	9400	53	83	31	49	8	20	70° 32.6' N	161° 47.0' W
Box 011 0-10	42	790	170	280	91	73	8	26	70° 53.0' N	162° 51.7' W
Box 011 20-30		1400	100	280	77	73	10	20		
Box 012 0-10	42	3300	220	270	150	70	18	41	70° 56.0' N	166° 20.4' W
Box 012 41-51		2100	72	250	72	74	n.d.	21		
Box 013 0-10	46	690	160	280	92	71	9	25	70° 57.3' N	166° 56.9' W
Box 014 0-10	45	900	220	250	92	58	7	21	70° 58.6' N	167° 23.8' W
Box 014 38-48		2700	110	300	100	87	14	26		
Box 015 0-10	44	2000	250	300	130	91	13	38	70° 58.8' N	167° 44.4' W
Box 015 18-28		7200	210	350	160	100	22	46		
Box 016 0-10	50	2000	130	330	100	92	10	14	70° 28.3' N	166° 57.2' W
Box 016 25-35		4500	130	280	99	78	13	30		
Box 017 0-10	43	3200	140	290	110	91	13	30	70° 24.6' N	166° 28.5' W
Box 017 23-29		3400	190	380	130	100	15	33		
Box 032 0-10	41	1200	170	280	110	69	10	34	71° 17.3' N	165° 43.6' W
Box 032 40-50		4800	73	200	72	68	10	40		
Box 033 0-10	42	2500	150	290	100	75	15	44	71° 22.4' N	166° 07.7' W
Box 033 35-45		22000	77	250	75	95	10	30		
Box 034 0-10	43	1400	150	240	94	90	17	52	71° 24.5' N	166° 21.2' W
Box 034 34-44		9900	89	190	86	56	8	24		
Box 035 0-10	43	2200	150	260	95	68	8	33	70° 54.9' N	168° 28.0' W
Box 035 37-47		7900	84	280	83	89	8	23		
Gravity 035 52-62		3600	72	260	74	86	9	36		
Box 036 0-10	54	2900	200	240	120	71	4	37	70° 52.8' N	167° 46.9' W
Box 036 46-56		4300	70	140	86	50	16	34		
Box 037 0-10	46	4900	210	390	140	72	12	45	70° 50.4' N	167° 06.2' W
Box 037 32-42		13000	92	280	130	91	14	21		
Box 038 0-10	47	2600	130	260	110	75	17	57	69° 34.7' N	167° 24.7' W
Box 038 37-47		4000	160	300	120	120	18	44		
Box 039 0-10	46	1200	160	260	110	75	13	52	69° 29.6' N	167° 03.7' W
Box 039 37-47		1800	85	290	94	78	12	39		
Box 040 0-10	40	2600	150	210	110	63	15	51	68° 49.2' N	166° 44.7' W
Box 040 19-29		8100	85	190	73	55	19	39		

n.d. = not detected

DISCUSSION

A 1982 geophysical survey by the U.S. Geological Survey in the Chukchi Sea (Phillips and Reiss, 1984) revealed the occurrence of acoustically impenetrable zones in the surface sediments. The 1984 geophysical survey revealed a similar phenomena. Figures 1 and Appendix D (Phillips et al, this report) illustrate the extent of occurence of these zones and demonstrate the alternating zones of acoustically penetrable and impenetrable sediments observed in one geophysical transect (line 44). One possible explanation for this phenomena is the presence of interstitial gas bubbles in the sediment, as demonstrated by Schubel (1974). Box 33, where the highest concentration of methane was observed, was taken on a line 44, however, the amount observed is well below the concentration of methane that is indicative of saturation (about 40 ml of C1 per liter of seawater according to Yamamoto et al., 1976). There are several possible explanations for this observation: (1) the geophysical anomaly may not be due to gassy sediments(2) the geophysical anomaly may be due to gassy sediments, but an impervious sediment layer is preventing the diffusion and/or migration of the gas to the surface sediments sampled (3) the sampling station may have been outside the zone of acoustically impenetrable sediments. The hydrocarbon concentrations observed in surface sediments of the Chukchi Sea are in the same range of concentrations observed in for example, the shelf environment of the Bering Sea (Kvenvolden and Redden, 1980). The source of this "background" concentration of hydrocarbon gases likely results from in situ biological and /or very early diagenetic processes (Claypool and Kvenvolden, 1983).

CONCLUSIONS

Light hydrocarbons C1, C2, C2=, C3, C3=, iC4, and nC4 are present in low concentrations in surface sediments of the shelf in the Chukchi Sea and likely result from biological and/or very early diagenetic processes. If the geophysical anomalies are due to gas-charged sediment, the inability to recover samples with high gas concentrations may result from the presence of an impervious layer preventing the diffusion and/or migration of the gas to the surface sediments sampled or the "gassy" sediments may be spotty in distribution, and therefore a more detailed sampling program would have to be pursued in order to recover samples with high gas concentrations.

REFERENCES

Claypool, G.E., and Kvenvolden, K.A. 1983, Methane and other hydrocarbon gases in marine sediment: Annual Reviews of Earth and Planetary Sciences, v, 11, p. 299-327.

Kvenvolden, K.A. and Redden, G.D., 1980, Hydrocarbon gas in sediment from the shelf, slope, and basin of the Bering Sea: Geochemica et Cosmochimica Acta , v. 44, p. 1145-1150.

Phillips, R.L. and Reiss, T.E., 1984, Nearshore marine geologic investigations, Icy Cape to Wainwright, northeast Chukchi Sea. U.S. Geological Survey Open-File Rept. 84-828, 27 p.

Schubel, J.R., 1974, Gas bubbles and the acoustically impenetrable, or turbid, character of some estuarine sediment. In: Natural gases in marine sediments, I.R. Kaplan, ed., 275-298. Plenum Press, N.Y.

Yamamoto, S., Alcauskas, J.B., and Crozier, T.E., 1976, Solubility of methane in distilled water and seawater: Journal of Chemical and Engineering Data, v. 21, no. 1, p. 78-80.

BEAUFORT SEA COASTAL EROSION, SHORELINE EVOLUTION, AND SEDIMENT FLUX

by

Erk Reimnitz, Scot M. Graves,
and Peter W. Barnes

TABLE OF CONTENTS

LIST OF FIGURES

Figure 18. Freshly undercut 3 m high bluff.

Figure 19. Typical summer conditions on seaward-facing beach.

Figure 20. Landsat image (August 1, 1976) of central study area showing: 1) typical summer ice distribution, restricting significant fetch to warm and sheltered waters; 2) absence of protecting barriers along Cape Halkett coast, where most sediment is introduced; 3) tundra-covered older surfaces (including numerous islands), versus recent, active, and barren surfaces (delta flats and barrier islands); 4) deep (over 2 m) ice-covered lakes versus shallow ones; 5) sediment-laden waters around the stagnant Colville Delta.

Figure 21. Index map for the 3 major coastal segments represented on this mapsheet, and for the 15 sectors for which calculations are tabulated in the Appendix.

Figure 22. General geometry used for volume calculations.

Figure 23. Graph of ice content versus depth below tundra surface (after Sellman, et al., 1975).

Figure 24. Special case geometries.

Figure 25. Map of Cape Halkett promontory, showing an old beachline/barrier chain separating two distinct types of surficial deposits; 1000 year hind- and forecast shorelines, lake depths, location of an early 19th century island called Cape Halkett, and the largest shallow lakes which may be candidates for thermal collapse, breaching, and resulting lagoon formation (Wiseman, et al., 1973) are shaded to show their distinction from present lagoons.

Figure 26. Graph of monthly (July, August, and September) mean and seasonal mean sea level measured at Prudhoe Bay West Dock - NOAA tide station #949-7649. Trend line represents least square fit to seasonal mean data. Note sea level usually peaks in August (spring floods) and decreases thereafter (after Inman 1984).

Figure 27. Sequence of lagoon formation and barrier island isolation by thaw-lake coalescence. A) initial tapping, draining, and coalescing of lakes; B) continued coalescing of lakes and thermal erosion of shoreline; C) continued thermal erosion and isolation of offshore tundra remnants; D) erosion of tundra remnants and reworking of sand and gravel into offshore barriers (from Wiseman, et al., 1973).

Figure 28. Comparison of hydrographic surveys repeated after 15 years in the East Siberian Sea (after Klyuyev 1965).

LIST OF TABLES

BEAUFORT SEA COASTAL EROSION, SHORELINE EVOLUTION, AND SEDIMENT FLUX

By

Erk Reimnitz, Scot M. Graves, and Peter W. Barnes

ABSTRACT

Using two 1:50,000-scale NOS charts, from surveys spaced 30 years apart, this study delineates patterns in coastline changes and sediment yields from erosion for 344 kms of Alaska's Beaufort Sea coast. Excluding the large Colville Delta, which advances at an average rate of 0.4 m/yr, the overall coastline is eroding at a rate of 2.5 m/yr. In places the local long-term erosion rates are as high as 18 m/yr, while accretion rates near the active mouths of the Colville River are as high as 20 m/yr. The coastal plain deposits in the western third of the study area are fine-grained mud; here average erosion rates are highest (5.4 m/yr). The rest of the study area is composed of sandy to gravelly deposits, which erode at 1.4 m/yr. This difference suggests that the grain size of bluff material exerts the dominant control on coastal retreat rates. Other important factors include bluff height, ice content and thaw settling, bluff orientation, and degree of exposure to the marine environment. Vertical crustal motion has not played an important role during Holocene time, as evidenced by the constant elevation of 120,000 yr old shoreline deposits traceable for 200 km from Barrow to the Colville River, and by 30 yr observations on tidal benchmarks along the Beaufort Sea coast.

In calculating sediment yield we consider not only the materials in coastal bluffs above sea level, but also the submerged profile to 2m depths. Assuming this profile to be in dynamic equilibrium, we account for material eroded to a depth of 2m below msl as the profile migrates landward. The upper part of this roughly 5 m thick eroded section contains up to 75% ice, and the sediment yield is reduced accordingly in our calculations. The annual yield from coastal retreat thus calculated is 2.5 x $10^6 m^3$, with the offshore contribution slightly higher than the onshore contribution. Based on our evaluation of sparse data on sediment carried by Arctic streams, we estimate the annual sediment yield from the adjacent drainage areas is 2 x $10^6 m^3$, a rate that is slightly less than that from coastal erosion.

Knowledge of recent patterns in coastal retreat, coupled with knowledge of factors controlling this retreat, allows us to estimate the configuration and location of past and future coastlines. We find no support for the theory that the evolution of coastal embayments and lagoons begins with the breaching and coalescing of large lakes, followed by thaw settlement. Rather, the existence of older, coarse-grained, and erosion-resistant barrier-island and beach deposits exerts a strong influence on the locus and shape of some of the newly forming embayments. Others, however, remain unexplained.

If the present coastal-retreat rates have been sustained since sea level approached its present position about 5,000 yr BP, then the corresponding ancient shoreline could have ranged from 7 to 27 km seaward of the present one, in accordance mainly with grain-size variations in coastal bluffs. Furthermore, if erosion occurred only to 2-m water depths, as assumed in our sediment yield calculations, 10-20 km wide and 2m deep platforms should be widespread around the Arctic Ocean. Since such wide platforms do not exist, and since we can show that thaw settling contributes much less to the shape of the marine profile in the Arctic than previously proposed, coastal retreat must be associated with erosion reaching to depths much greater than 2 m. The sediment

yield therefore could be manyfold larger than we calculated. A growing body of evidence from interpretations of boreholes, seismic reflection data, Foraminifera, and soil engineering properties of surficial sediments shows that the seafloor of the inner shelf seaward to at least 20-m depth is indeed an erosional surface truncating older strata. Considering the rapid, and deep-reaching erosion, shallow bays, lagoons, and barrier islands do not provide adequate long-term sediment sinks accommodating materials introduced at the present high rates. Modern deposits found in some of these features may be held there for some time, but are soon re-introduced to the sea as the shelf profile moves through the locality. We therefore conclude that the sediment yield from coastal retreat and rivers largely by-passes the shelf. Part of this sediment flux is seen in form of a 2-3 m thick, transient "Rototill" layer draped over large regions of the open shelf, a result of ice-keels plowing up underlying strata and mixing these sediments with modern materials and fauna.

Within the conterminous United States, the Gulf of Mexico coast has the highest erosion rates. The Texas coast, fringed by a low coastal plain of unconsolidated sediments, marked by vertical crustal stability, and therefore in some respects similar to that of the Beaufort Sea, retreats about 1.2 m/yr, or about half the Beaufort Sea average. Since coastal erosion in Arctic regions is restricted to three summer months when waves and coastal currents are active, erosion rates there must be multiplied by a factor of four for a meaningful comparison with the rates of ice-free low-latitude coasts, which experience waves and currents year round. Accordingly, Arctic erosion rates are 8 times higher than Texas rates. Additionally, Arctic fetches are severely restricted during the navigation season by the ever present polar pack, unlike the long and constant Texas fetch which allows generation of larger and more pervasive waves. Lastly, most of the damage to low latitude coastlines is done by winter storms, when the Arctic coastline is well protected by ice. Classic wave theory therefore can not account for the sediment dynamics of the Arctic coastal zone. We feel that processes here are driven largely by sea ice acting as the most important geologic agent.

Considering the rapid shoreline development by petroleum industry, our inadequate understanding of Arctic coastal processes begs for accelerated research in this region.

INTRODUCTION

Two sets of charts published by the U.S. Hydrographic Service and the National Ocean Survey, showing the shorelines for 1950 and for 1980 respectively, are compared in this study of Alaska's north coast between Drew Point and Prudhoe Bay. The mapping was done in accordance with national standards at a scale of 1:50,000, large enough to allow accurate and comprehensive delineation of changes in the coastline configuration over the 30 year study period (see accompanying mapsheet).

Previous studies (Dygas and Burrell, 1976; Lewellen, 1977; Hopkins and Hartz, 1978; Cannon, 1979; Kovacs 1983; and Naidu 1984), using largely spot measurements from aerial photos and maps (for example fig. 4*) *Footnote: Figures 2 through 21 are found on the mapsheet numbered sequentially in an easterly direction along the coast) have documented rapid rates of coastal retreat. They also point out large regional differences and rapid changes in island configuration and location over various time spans.

The new 30 year comparison entails complete coverage of the coast within the study area (fig. 1) and allows an accurate determination of coastal erosion rate patterns. The coastal erosion rates together with the sediment yield from upland sources are used to estimate the minimum amount of sediment supplied from the study area to the Beaufort Sea. An attempt was also made to interpret trends in coastal evolution in light of what is known about the unique high latitude modern shelf environments. Attempts to extrapolate paleo shorelines from the presently high transgression rates forced consideration of the continental shelf profile, and its evolution through time. These considerations lead to the realization that the arctic marine environment contains elements that are more erosive than its low-latitude counterpart, partly through the abrasive action of sea ice.

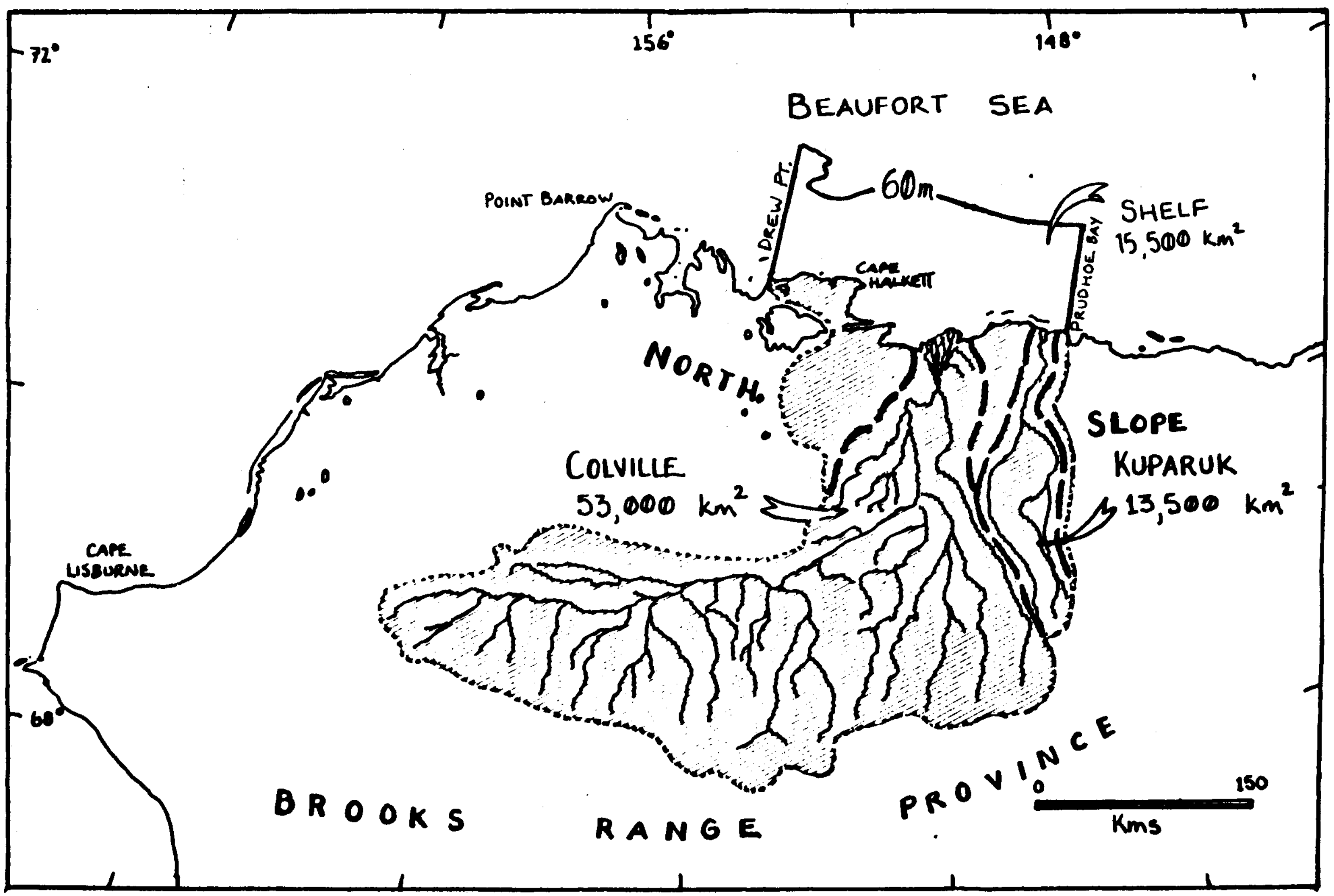

Figure 1. Map of Drainage and Shelf Areas considered in our study.

REGIONAL SETTING

Physiography and Surficial Deposits

The coastal plain in the study area is a vast, flat, tundra-covered surface with thousands of shallow (1-2 m) thaw lakes (figs. 3, 20). Along the coast this surface is only 2 to 6 m above sealevel, and rises imperceptibly to the south (figs. 3, 5, and 17). The tundra surface is underlain by the Quarternary Gubik Formation (Black, 1964) whose marine, alluvial, and glacio-fluvial sediments are mantled by 2-3 m of late Pleistocene and Holocene thaw-lake deposits, consisting mostly of peat and mud (Williams et al, 1977). Except for a seasonal thaw layer (generally up to 30 cm thick), the material underlying the tundra surface is permanently ice bonded to a depth of hundreds of meters. In the upper several meters these materials contain 60% to 70% ice in grain interstices, and in the form of small but pervasive sub-horizontal ice lenses. In addition, these upper sediments contain 10% to 20% ice in the form of massive ice wedges (fig. 9 and 10) (Sellmann, et al., 1975). Coastal bluffs within the study area generally are 2 to 3m, and in a few areas up to 6 m high. Sandy gravel beaches fronting many of the coastal bluffs are generally about 10 m wide (figs. 6, 11, and 18) and only several tens of cm thick. The active mouths of the Kuparuk and the Colville Rivers are marked by very low mud flats (figs. 13 and 20), whereas the inactive distributaries are generally marked by 1 m high tundra covered surfaces (fig. 12). About 5 to 8 km from shore an island chain stretches from Harrison Bay to Prudhoe Bay. The islands are mostly low (1-2 m high) and narrow barriers composed of sand and gravel. Pingok, Bodfish, Bertoncini, and Cottle Islands are exceptions in that they contain remnants of the tundra-covered coastal plain with higher elevations corresponding to adjacent land areas (figs. 18 and 20). Harrison Bay and the stretch of coast from Cape Halkett to Drew Point are not protected by islands, with the exception of the sand bar across the large breached lake at Pogik Bay (fig. 3).

The 2-m isobath, which roughly corresponds to the ultimate thickness of the seasonal fast ice, marks a distinct change from a flat inshore submarine bench to a steeper-sloping seaward profile. The outer edge of this so called "2 m bench" (Barnes and Reimnitz, 1973) is often slightly shallower than the waters some distance landward. We include this feature on the mapsheet and in our sediment budget calculations as it is (1) an important morphologic feature (Reimnitz and Bruder, 1972), (2) the boundary between texturally well sorted sands inshore, and poorly sorted sandy muds offshore (Barnes and Reimnitz, 1973), (3) controls sea ice zonation (Reimnitz et al, 1978), and (4) is the outer boundary to which seasonal bottom freezing occurs (Reimnitz and Barnes, 1974). In Harrison Bay the 2m bench is up to 10 km wide whereas elsewhere it is only 0.5 to 5 km wide.

Wave Exposure

The sea surface is completely ice covered for 9 months each year (fig. 3) and even during the short open-water season fetch and waves are minimized by the abundance of drifting ice (figs. 14B and 20). On any usual summer day a skiff can therefore safely land on a seaward-facing beach (fig. 19), while in the lagoons the relatively ice-free conditions lead to greater wave activity. Even during rare periods when much of the continental shelf is ice free some grounded ice will usually collect and remain in the nearshore zone. Winds from the northeast dominate, and coastal currents, movement of the littoral drift, and ice drift are primarily to the west (U.S. Department of Commerce, 1981, p.57).

Shore Processes

Nummedahl (1979) reviewed available littoral transport estimates and concluded that the average rate of transport is westward at a "a few tens of thousands of cubic meters per year". A more thorough evaluation of Beaufort Sea coastal processes by Owens, et al., (1980) quotes a transport rate of 2,000 to 5,000 m^3/yr. Reimnitz and Kempema (1983) made measurements at a site along the outer part of the 2 m bench, several km from the coast. They determined transport rates similar to littoral transport estimates for bedload material in a several kilometer wide coastal belt. This transport again is mainly to the west due to prevailing easterly winds.

The sediment transport is not driven by waves and currents alone. Grounded ice in the nearshore seems to play a more important role in various ways besides its bulldozing action. When worked by storm waves (fig. 16A), or when under the influence of currents, grounded ice acts to intensify turbulence resulting in increased sediment suspension and transport, and a highly irregular "ice-wallow relief" is imparted to the beach and shoreface (Reimnitz and Kempema, 1983) (figs. 7 and 16). This irregular relief, when in turn attacked by normal waves in the absence of grounded ice, results in increased bottom instability, sediment re-suspension, and transport. During open-water storm conditions these combined processes can act in a coastal belt 1000 meters or more wide, bringing about accelerated bottom erosion and a steepening of the foreshore. This steepening of the foreshore in turn can result in accelerated coastal retreat. Under such conditions as much as 30m of coastal plain deposits can be eroded within a period of several days (Short et al, 1974).

Exclusive to this environment are a number of unique processes. Considering the ice-bonded nature of the coastal deposits, and that air and ocean temperatures are at or near the freezing point, factors other than the energy level of the marine environment affect coastal processes. In most cases retreat of the coastal bluffs involves the process of thermo-erosion which includes the following: a) formation of a thermo-erosional niche, when a turbulent sea is brought in contact with bluffs (figs. 9, 10, 11, and 18), b) collapse of bluff materials (figs. 2 and 5), c) slumping, and d) saturated flow of thawed sediments. The mechanisms are described in detail by Harper (1978). A pre-requisite for initiation of these mechanisms is that sea level overtop the protecting beach. Normal summer storms blowing from northeasterly directions result in a lowering of sea level and exposure of the upper part of the 2 m bench with waves breaking some distance from the bluffs. The development of a thermo-erosional niche therefore is most commonly seen with westerly winds, which raise sealevel in the Beaufort Sea, and particularly with storm surges (Reimnitz and Maurer, 1979). While storm surges are rare, bluff erosion probably contributes the largest amounts of sediment to the sea during these short periods. At these times sediment transport is opposite in direction to the long-term westward movement (Reimnitz and Maurer, 1979). The highest rates of thermo-erosion associated with niche development occur in areas of fine grained, ice rich coastal plain deposits which are widespread in the western third of the study area. In these areas the sparsity of sand and gravel in eroded bluff material does not even permit the formation of beaches (fig. 5).

In the littoral zone and on the beaches along the Canadian Arctic and Chukchi Sea coasts, seasonal variations in the depth to the upper surface of ice-bonded sand and gravel have been monitored (for example, Harper et al, 1978). The bonded and presumably erosion resistant materials are generally less than a meter below the sediment surface both at the beach and at wading depths near the beach. According to theoretical calculations (Harper et al, 1978; Taylor, 1980) maximum thaw rates of only 50 to 70 cm/day are indicated during storm conditions, when thermal diffusivity could be a factor of one thousand by high groundwater flow rates, and when sediments released can be removed at the same rate as the frost table retreats, thereby always maintaining direct seawater contact with ice bonded sediments. Because short-term rates of coastal changes in the Beaufort Sea are higher than theoretical considerations would permit, Harper, et al. (1978) speculated that here ice-bonding may not be as widespread as on the Canadian and Chukchi coasts. However, permafrost studies, for example by Morack and Rogers (1981), and our own probing with rods, indicate shallow ice bonding along the Beaufort Sea coast beaches and in the nearshore. Morack and Rogers (1981) found that the cores of rapidly migrating barrier islands (Reindeer and Cross Island, just east of the study area) contain only sporadic bonding. According to jet drilling on these islands, the non-bonded materials seem to be brine pockets (Osterkamp, oral communication, 1985). Such patchy ice-bonding suggests that the shoreline configuration of these islands during storm erosion should show corresponding irregularities. We have observed these islands under many storm conditions, and never noted irregularities in beach configuration caused by variations in degree of ice bonding and erodability. Therefore, and because of the very high shore retreat rates during single storms, we believe that ice bonding of sediments does not retard beach dynamics during the open-water season.

The onset of winter, with decreasing water temperature, brings about conditions that have received very little study. In many polar regions the formation of an ice foot (Owens, 1982) is an important phenomenon. There are many forms and types of ice foot (Dionne, 1973), and a treatment here is not necessary. Once formed, an ice foot armors the beach, arrests erosion, and in many cases should even result in beach accretion. The fact that sediment layers are interbedded with ice during growth of the ice foot implies sediment movement from inshore areas up onto the beach and foreshore, and consequent steepening of the shoreface. In rare instances, an ice foot does form along the beaches of the Alaskan Beaufort Sea coast (Short et al, 1974). However, our observations over many years during the fall, winter, and spring storms in the Beaufort Sea, with and without adequate fetch for wave generation, lead us to believe that ice foot is of little consequence to Beaufort Sea coastal processes. We have observed sediments on the beach face to be ice bonded during cold storms, but that erosion nevertheless proceeds rapidly by ripping slabs of bonded sand and gravel from the beach (fig. 14C) and moving these in the swash zone, still intact, for some distance along the beach. During such times the back of the active beach generally is defined by a 1 to 1.5 m high vertical cliff of ice bonded sand and gravel (fig. 14C).

Littoral processes previously not documented for polar seas are those related to the formation of underwater ice (Martin, 1981) in the surf zone. Anchor ice is one form of underwater ice produced when water is so agitated at subfreezing temperatures that an ice cover can not form. Under these conditions the water becomes slightly supercooled and ice nucleates on the seabed. This process is well documented in high latitude streams (Arden and Wigle, 1972; Tsang 1982; Osterkamp 1978), but is little understood in the marine environment. Our own observations, made during three different fall storms, each with 25 knot winds and air temperatures of -10 °C, indicate that in marine waters less than 2 m deep bottom sediments become ice bonded. In one instance, a 150 m diving traverse from the beach to 5 m water depth (Reindeer Island, October 1982) revealed ice-bonded sand and gravel interbedded with ice layers in a 30 m wide zone near shore. From the 2-m isobath seaward the seafloor was not ice-bonded but instead covered with pillow-size masses of ice (fig. 8). These ice-pillows consisted of an outer (10 cm thick) rind of fragile ice platelets, and a massive, sediment laden core. These observations were made immediately after a three- day storm, during which the bottom may well have been completely ice covered. The effects of this observed ice bonding and of anchor ice formation on coastal processes during fall storms is a matter of speculation. Our sketchy observations serve to demonstrate how little is actually known about arctic nearshore processes during times of severe fall weather; yet it is during this period that the greatest coastal changes occur. A very different kind of anchor ice, formed from fresh water, is reported in the Canadian Archipelago (Sadler and Serson, 1981) but has not been seen along the Alaskan Beaufort Sea coast.

A final littoral process to consider is that of bulldozing of shoreface materials by ice onto seaward facing beaches and barrier islands (Hume and Schalk, 1964; Barnes, 1982; McLaren, 1982; Kovacs, 1983). In some years the sediment volumes so contributed to arctic beaches are considerable. Thus Hume and Schalk (1964) estimated that in one case up to 10 % of the beach material above sealevel near Barrow had been transported there from offshore by ice push, but that a more typical figure would be 1 to 2 %. In our study area the process occurs mainly on those stretches of coast facing the open ocean and rarely in protected lagoons. The resulting ice/sediment piles normally contain sand and gravel-size material that is left as hummocks after the ice melts (fig. 15). The process was unusually active during the winter of 1982/83, based on more than a decade of our observations in the study area. The chain of islands from Thetis through Cottle Island, a distance of 42 km, was marked by sand and gravel piles with average estimated volumes of at least 1 cubic meter per meter of shoreline. A 6-m high, 20-m wide ice, and 1-km long rubble pile on Spy Island was covered with very large sediment volumes, consisting of sand and gravel. The sediment included pockets of clean sand. Bottom grab samples collected along a transect seaward from the ice pile in the direction from which the ice shove originated showed the first clean sand

Figure 2. Slumping of 2 m bluff following formation of basal niche.

Figure 3. June 20 photograph of Pogik Bay and flat, lake dotted coastal plain prior to breakup of fast-ice.

Figure 4. Aerial photographs comparing the coastline at Esook in 1949 and 1981 demonstrating 410 m of bluff retreat. The near vertical arrows point to the same hut on the two photos (from Kovacs, 1983).

Figure 5. Low altitude oblique photo of last remaining hut at Esook Trading Post (from Kovacs, 1983).

Figure 6. Aerial photograph of a beach transgressing over low tundra with ice wedge polygons (from Kovacs, 1983).

Figure 7. Low altitude oblique photo of seaward side of a barrier island showing ice-wallow relief.

Figure 8. Pillows of anchor ice (underwater ice attached to submerged objects) found widespread in shallow coastal waters during freeze-up storms. The pillow in the foreground is 50cm across and attached to medium grained unfrozen sands at 5m water depths.

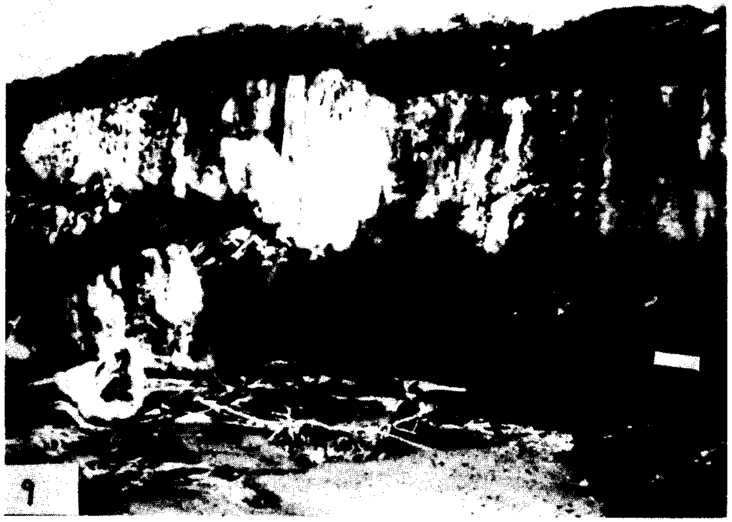

Figure 9.

Fresh exposure of a 2 m high coastal bluff cutting massive ice in longitudinal section.

Figure 10. Cross section of ice wedge in cryoturbated sandy bluff (glove for scale).

Figure 11. Erosional niche at the base of a high bluff in aeolian (dune) sands.

Figure 12. Erosion of low, vegetated, inactive delta front.

Figure 13. Silt flats on prograding part of delta.

Figure 14. Thetis Island: A) gently sloping beach in 1979 after a winter of ice-override; note striated slope B) beach scarp on september 12, 1982 C) and on october 9, 1982 after fall storm.

Figure 15. Gravel-covered ice rubble pile.

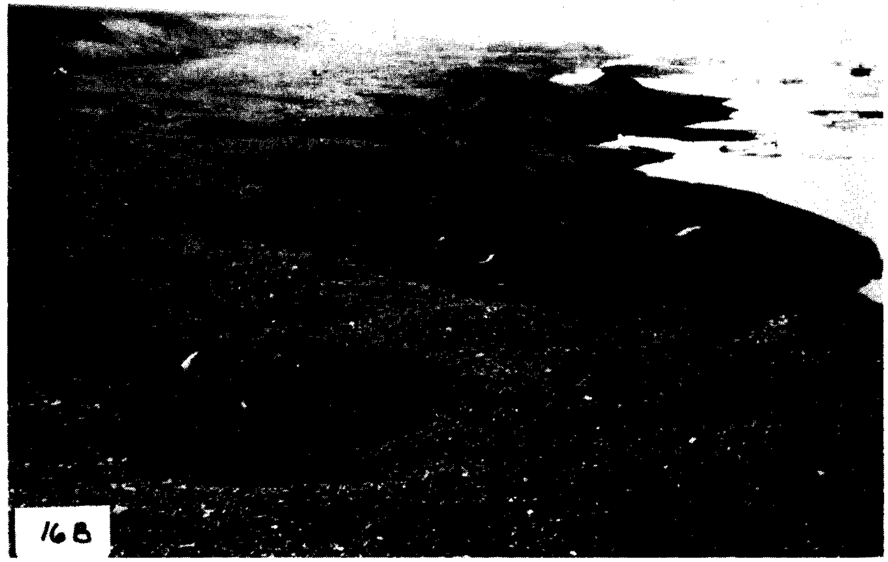

Figure 16. A) ice wallowing in surf zone, and B) the resulting relief.

Figure 17. Low coastal plain marked by two storm surge lines.

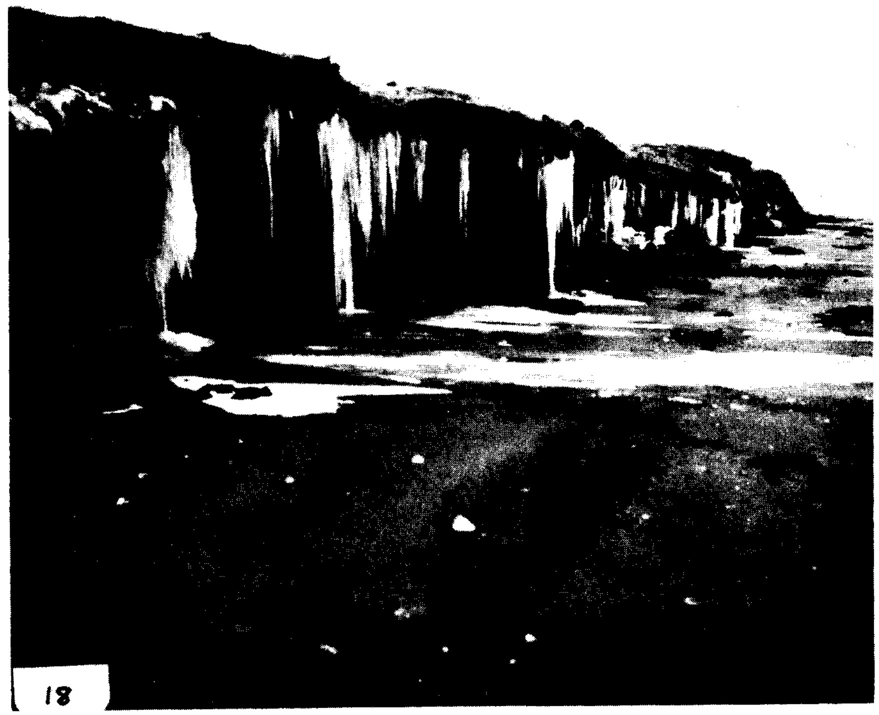

Figure 18. Freshly undercut 3 m high bluff.

Figure 19. Typical summer conditions on seaward-facing beach.

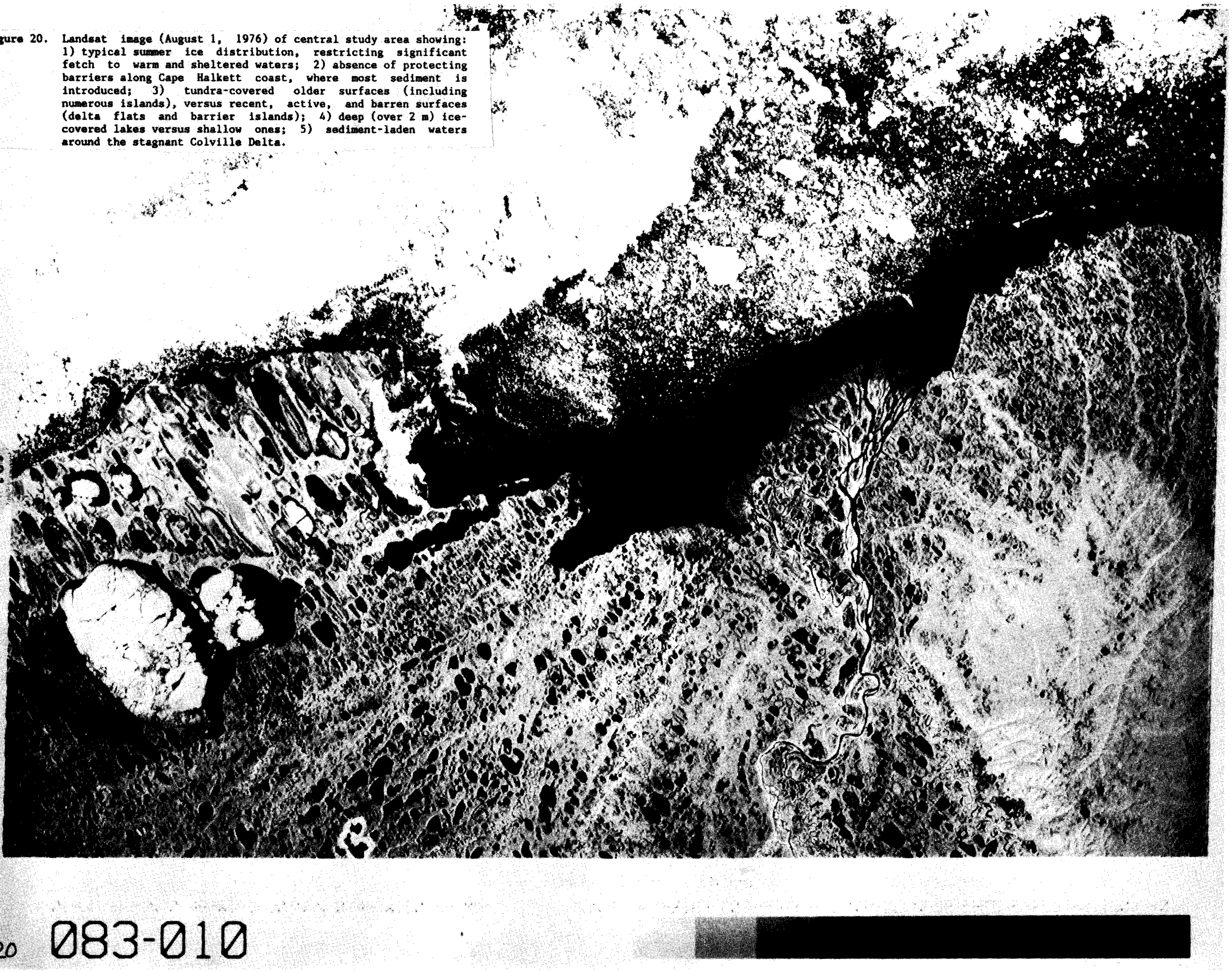

Figure 20. Landsat image (August 1, 1976) of central study area showing: 1) typical summer ice distribution, restricting significant fetch to warm and sheltered waters; 2) absence of protecting barriers along Cape Halkett coast, where most sediment is introduced; 3) tundra-covered older surfaces (including numerous islands), versus recent, active, and barren surfaces (delta flats and barrier islands); 4) deep (over 2 m) ice-covered lakes versus shallow ones; 5) sediment-laden waters around the stagnant Colville Delta.

at a distance of 40 m, and a water depth of 4 m. That point, therefore, gives the minimum distance for the origin of the sand in the ice pile. While ice-bulldozing during some years may help restore to the beach and shoreface a part of what is removed by waves, currents, and other processes, we feel that its overall contribution is small.

METHODS

Retreat rates were obtained for the roughly 344 km of coastline by comparing two sets of charts at a scale of 1:50,000 covering the north coast of Alaska between Drew Pt. and Prudhoe Bay. This comparison shows changes in the position of the shoreline, referenced originally to mean lower low water (MLLW) by the Coast and Geodetic Survey (C&GS), and lately by the National Ocean Survey (NOS).Some previous studies of coastal erosion focused on bluff retreat, which over short time periods is not always the same as shoreline retreat. For this reason our numbers locally differ from previously published ones, but overall show the same pattern.

The study area was divided into three major segments in order to present the overall coastline on the mapsheet at the desired resolution. Figure 21 serves as a key to these three major coastal segments and the 15 subdivisions used in our calculations. The original C&GS charts (numbers 9466 through 9472) represent the coastline configuration in 1949-1952. The new NOS charts depict the coastline as mapped by the State of Alaska in 1980. The seaward extent of the eroding coastal zone considered in our calculations is the position of the 2-m isobath. Since the bathymetry was not resurveyed in connection with the recent mapping effort, but stems from the original 1949-52 charts, we simply shifted the position of the 2-m isobath (mapsheet) landward in tandem with local shoreline retreat. A previously uncharted shallow basin in an embayment off sector 9 was delineated by our own bathymetric surveys in 1980.

A few small areas not covered by the NOS charts were dealt with by comparing the 1949 coastline on USGS topographic maps with the 1980 data. The maps were brought to a common scale and projection, and changes in the coastal configuration registered using the same methods applied elsewhere. Areas treated in this manner (southern part of sector 6, western and eastern borders of sectors 11, and central part of sector 14) are identified on the mapsheet.

For convenience of discussion, we divided the coast into 15 sectors based on morphologic and geologic similarities. To calculate sediment input from coastal erosion, each of these sectors in turn was divided into 500-m long segments numbered from west to east along the coast. The segments were then treated individually using the following geometries.

Generalized nearshore geometry

Quantitative estimates of the sediment introduced by coastal erosion are based on the application of a generalized nearshore geometry (fig. 22) for each 500 m segment. In this model geometry, segment length, bluff height, changes in shoreline position, and distance to the 2-m isobath are measured values; whereas the width, slope, and thickness of the offshore component, and the indicated secondary prism dimensions are calculated values. The general model geometry distinguishes between the two different sources of sediment released to the sea during coastal retreat: 1) The sediment contained in the bluffs between the 1949 and 1980 coastal outlines, and 2) the volume eroded offshore between the new and old nearshore profiles out to the 2-m isobath. For a few particular segments (~ 14% of those studied) alternative geometries were applied. These are described under "Special case geometries" and shown in figure 24. Tabulated in the Appendix are all measured and calculated values, and parameters assumed in determining the sediment contribution from each of the 500m segments comprising the 15 sectors.

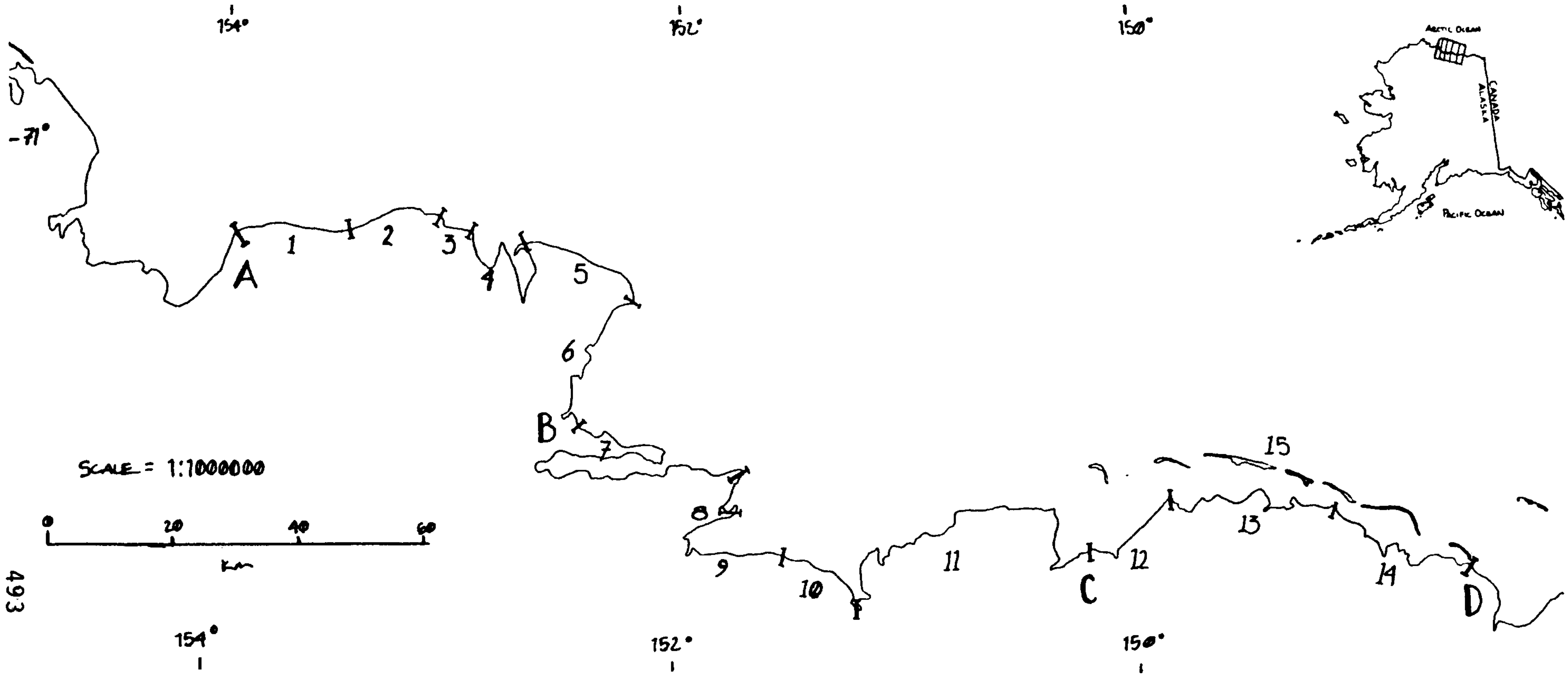

Figure 21. Index map for the 3 major coastal segments represented on this mapsheet, and for the 15 sectors for which calculations are tabulated in the appendix.

Sediment yield from bluff erosion

To calculate the sediment contribution from bluff erosion we use the 30 year coastal retreat distance (assuming bluff and shoreline retreat in tandem), bluff height, and the ice content of the eroded material (figs. 22, 23). Because the topographic elevations presented on published maps generally are several meters too high (Lewellen, 1977) we used in our calculations bluff heights from the field notes of D.M. Hopkins, S. Rawlinson, and Reimnitz, and Barnes. In determining percentage of excess ice for the coastal plain sediments we refered to a data compilation by Sellmann et al (1975), giving excess ice content versus depth below the tundra surface for coastal plain deposits of the Gubik Formation near Barrow, Alaska (fig. 23). The eroded bluff materials in sectors 7 through 15 are coarser grained than those near Barrow, and therefore our assumed ice percentages here are probably too high. However, in the rapidly eroding sectors 1 through 6 the coastal plain deposits are very similar in lithology, and, therefore, presumably ice content, to those at Barrow. Sellmann et al (1975) assume an in situ after-thaw-settlement porosity of 35 to 40%, while we assume that marine dispersal of sediment results in deposits of only 30% porosity.

In progradational or accreting areas of the coast, we calculated volume additions for above sealevel material assuming elevations of 20 cm and 40 cm for delta mud flats, and beaches and spits, respectively. The use of these particular values is based upon estimates from our field observations.

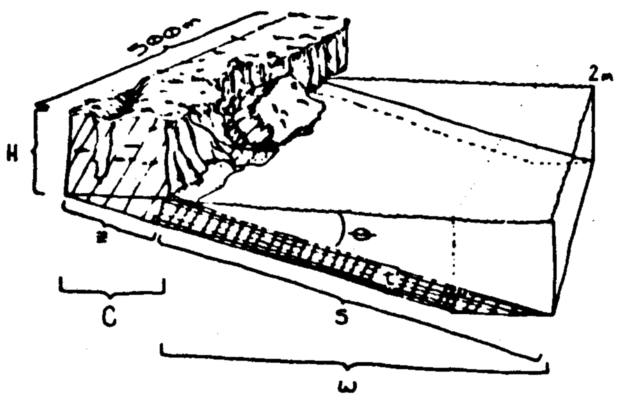

MEASURED PARAMETERS
500m segment length
H bluff height
C change +- in coastline
w distance to 2m isobath

CALCULATED PARAMETERS
Θ offshore slope = (arctan 2/w)
s width of offshore polyhedron = ($2/\sin\Theta$)
t thickness of offshore polyhedron = ($C\sin\Theta$)
z secondary prism width = ($C/\cos\Theta$)

EQUATIONS
vi (initial bluff volume) = 500(HC+0.5zt)
v1 (bluff volume - excess ice%) = vi-excess ice%
v2 (offshore polyhedron volume) = 500(st-0.5zt)
V (total volume input) = v1+v2
T (total weight input in metric tonnes) = 1.89V

Figure 22. General geometry used for volume calculations:

Sediment yield from offshore erosion

To calculate sediment contributions to the sea from the erosion of seafloor material between the shoreline and the 2-m isobath we assume that the slope of the seafloor in this area of the nearshore is in dynamic equilibrium and remains constant as the shoreline retreats. This assumption is based on our local marine surveying experience. The distance of a vessel from the coast and the corresponding water depths, at almost any location, match those indicated on 30 year old published nautical charts. This coincidence, and serious questions concerning the maintenance of such an "equibibrium profile" are discussed in detail later using a site in the western portion of the study area as an example.

Figure 21 shows schematically the geometry of the eroded offshore areas and how we normally calculated the resulting sediment volumes. We assume no excess ice for the reworked offshore layer, which generally is only 10 to 20 cm thick (see sector tabulations 1-15 in Appendix). Assigning excess ice percentages according to the graph in figure 23 for the submerged layer changes our total volume estimates by at most 10%.

Where the 2-m isobath is highly crenulated, we arbitrarily smoothed it for our measurements. In the previously uncharted area off sector 9, where published charts place the 2-m isobath at 11 to 14 km from shore, we attempt to reduce possible errors by introducing bathymetry delineated from our own surveys in 1980.

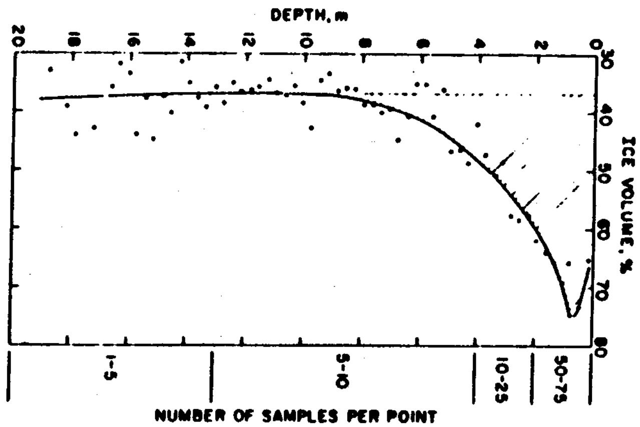

Figure 23 Graph of ice content versus depth below tundra surface (after Sellman et. al. 1975).

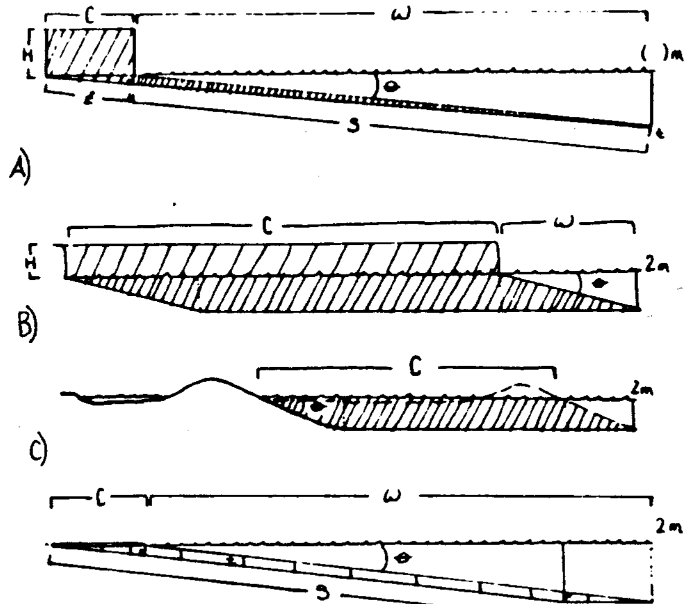

Figure 24. Special case geometries:

A) where segment borders lagoon with a maximum depth < 2 m
 $vi = 500(HC+0.5zt)$, $v1 = vi$-excess ice%, $v2 = 0.5(500st)$
B) where $C > W$
 $vi = 500HC$, $v1 = vi$-excess ice%, $v2 = 500C2$
C) where barrier or spit shifted onshore
 $vi = 0$, $v1 = 0$, $v2 = 500C2$
D) where accretion has occured
 $vi = v1 = +500HC$, $v2 = +500st$

Special case geometries

There are several exceptions to the general approach outlined above. The primary differences lie in deviations from the idealized geometry to more closely approximate the dimensions and resulting volumes for unique local configurations. In all of these instances the special case geometries applied are identified and keyed to the particular segments concerned (sector tabulations in Appendix and figure 24A-D).

In sector 14 (Simpson Lagoon), where maximum water depths are less than 2m, the offshore volume considered takes the form of a triangular prism of lagoon-floor material whose apex is at the deepest central point of the lagoon (fig. 24A). The geometry applied here assumes that as the coastline retreats, there is no corresponding shift of the offshore margin, and its depth remains constant.

Two of the remaining three exceptions to the general geometry depict settings in which the landward shift of a relatively steep nearshore profile results in the removal of a substantially thicker prism of offshore material. In one case (fig. 24B) the distance covered by the retreating coastline is greater than the distance measured from the shore to the position of the 2-m isobath. This situation is common in the Cape Halkett area (sectors 5 and 6). We believe that using the general model here might result in values that are excessive relative to our generally conservative estimates for the offshore sediment yield. The second such case occurs where onshore migration of a spit or barrier and accompanying shift of the adjacent nearshore profile likewise results in the removal of a very thick offshore prism (fig. 24C). Examples of these type areas are Pitt Point and Pogik Bay. In the Jones/Return Island chain (sector 15), we assumed no volume change for the sand and gravel barrier islands (tan colored, in figure 20). Even at the large scale used in this study, we were unable to resolve net volume changes in these barrier islands, and treated them as migrational bodies. Their motion is westward, obliquely onshore, or longshore, thereby adding to the overall westward nearshore sediment transport, but not to the shelf sediment budget. Similarly for the Eskimo Islands (sector 7), which like the cores of certain members of the Jones islands presently are stationary coastal plain remnants, we were unable to resolve net changes in the overall volume. Here erosion of westerly exposed tundra bluffs appeared to be compensated for by accretion on adjacent and leeward beaches and spits.

The last exception to the general model deals with areas of actively accreting or prograding shorelines. Here we assumed a seaward shift of the shoreface and offshore profile, with prograding mud flats and beaches at respective elevations of 20cm and 40cm (fig. 24D). In the overall summary of volumes and weights, the net gain calculated for these areas was subtracted to arrive at the final sediment yield.

RESULTS

For each of the 15 sectors a tabulation appears in the Appendix showing both measured and calculated values used to determine the sediment yield from coastal retreat. These appendices are identified by sector numbers, and are keyed to locations along the coast (figure 21 on the mapsheet). Table 1 is a summary of sediment yields for the entire area.

The average rate of coastal retreat for the 344 km of coastline studied is 2.1 m/yr. This rate includes accretionary shoreline changes along the large Colville River system where 48 km of coastline have advanced an average of 0.4 m/yr. Excluding the delta, the erosion rate is 2.5 m/yr. After subtracting excess ice from the eroded bluffs, we calculate the total annual sediment contribution from subaerial erosion from the entire study area to be $1.2 \times 10^6 m^3$. This number represents the sum of the sediment yields from all segments and divided by 30 years. Using the same approach we estimate the annual sediment contribution from erosion in the offshore (submarine) to be $1.3 \times 10^6 m^3$. The total annual sediment yield from coastal erosion

TABLE 1

SUMMARY OF ANNUAL SEDIMENT YIELD

FROM COASTAL EROSION:

Overall Erosion Rate = 2.1 m/yr
without Colville Delta sector = 2.4 m/yr

		Per Kilometer	Total
Bluffs	volumes =	$3500m^3$	$1200000m^3$
	weights =	6600tm	2300000tm
Offshore	volumes =	$3800m^3$	$1300000m^3$
	weights =	7200tm	2500000tm
Total	volumes =	$7300m^3$	$2500000m^3$
	weights =	13800tm	4700000tm

FROM RIVER INPUT:

Combined Drainage Area	$74000km^2$
Average Denudation Rate	$50tm/km^2$
volumes =	$1950000m^3$
weights =	3700000tm

therefore is 2.5 x 10^6m^3. To help visualize the significance of this sediment volume one can prorate this for the Holocene period (10,000 yrs) and spread it over the immediate continental shelf adjoining the study area (15,500 km^2, see fig.1). The resulting sediment layer would be 1.6 m thick. As discussed below, however, offshore erosion associated with the present transgression is not restricted to coastal waters of less than 2 m depth. The inner and midshelf areas are a surface undergoing erosion and therefore, overall sediment yields may be many times larger than our calculations indicate.

Table 2 lists available sediment textures for coastal plain deposits exposed in bluffs along the Beaufort Sea. Two of the bluff sections listed, Christie Point (155°, 35'W) and Tigvariak Island (147°, 15'W), lie outside of the study area. The former is considered representative of the fine-grained deposits found in sectors 1 through 6. The latter, an abnormally coarse grained section and as far as we know without counterpart in the study area, is included to suggest the variability of coastal plain deposits along the Beaufort. The only information on the amount of organic matter contained in bluffs comes from S. Rawlinson's extensive work around Simpson Lagoon. The figure of 40 % he obtained probably is roughly representative of bluff compositions for the entire region.

TABLE 2

CLASTIC COMPONENT OF BLUFFS

Sample Location	Grain Size % gravel	sand	mud	Reference
Oliktok Pt. & Kavearak Pt.	0	69	31	R. Lewellen 1973 writ. comm. (average of 2 smpls.)
*Simpson Lagoon	0	85	15	S. Rawlinson 1983 writ. comm. (average of 60 smpls.)
!#Tigvariak Isl.	2.6	62.9	34.5	Reimnitz & Barnes unpub.
	2.5	61.9	35.6	(average of 2 smpls.)
Atigaru Pt.	0	85	15	R. F. Black 1964
Drew Pt.	0	8	92	
Teshekpuk L.	0	42	58	
!Christie Pt.	0	32	68	

* organic component up to 41% of overall bluff composition
! chosen for its unusually rich accumulation of gravels
\# location outside of study area

DISCUSSION

Regional patterns in coastline recession

There are large regional variations in the rate of shoreline retreat from the 30 yr average of 2.1 m/yr. Extremes range from a retreat rate of 18 m/yr near Cape Halkett, to an accretion rate of 20 m/yr near the active mouths of the Colville drainage system (mapsheet). There is a pronounced disparity in erosion rates between the western and eastern parts of the study area. The western portion is entirely composed of fine grained coastal plain deposits extending north from the Pelukian beachline (fig. 25). Retreat rates of bluffs here (sectors 1-6, but exclusive of Pogik bay with its unique setting), average 5.4m/yr. The remaining part of the study area lies east and to the south of the Pelukian beachline where coarser grained materials make up the bluffs. The average retreat rate for this section of coastline, exclusive of the Colville River Delta sector is 1.4 m/yr.

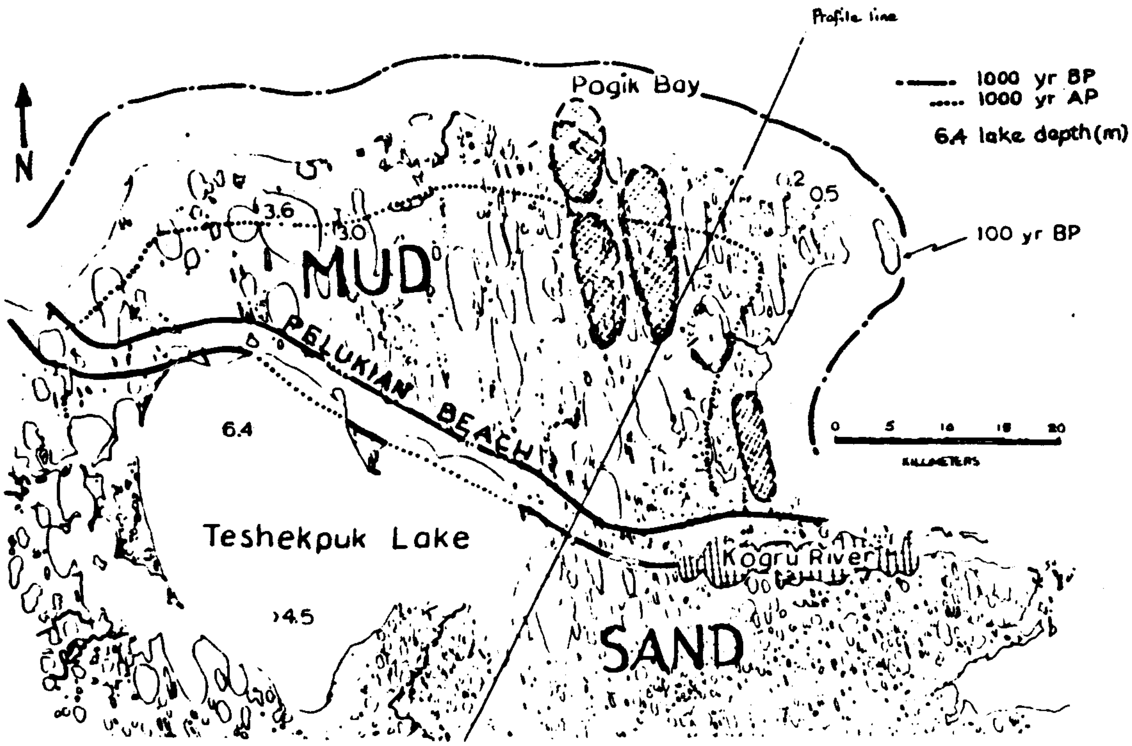

Figure 25. Map of Cape Halkett promontory, showing an old beachline/barrier chain separating two distinct types of surficial deposits; 1000 year hind- and forecast shorelines, lake depths, location of an early 19th century island called Cape Halkett and the largest shallow lakes which may be candidates for thermal collapse, breaching, and resulting lagoon formation (Wiseman, et al., 1973) are shaded to show their distinction from present lagoons.

Long term changes in the configuration of coastlines are dependent on a combination of various climatic and oceanographic factors, as well as on the composition and geometry of the coastal plain transgressed. Severe short-term episodes of coastal erosion may locally play a significant role in the overall evolution of the coastline. An example is the single storm event of several days duration in 1972 (Short, 1973), in which almost 30 m of bluff was removed from the seaward facing shores of Pingok Island. During intervening years bluffs may locally appear entirely stabilized.

An understanding of regional differences in erosion rates in terms of geologic and oceanographic setting allows for the reconstruction of past shorelines, and the prediction of future trends in coastal evolution. Certain factors known to influence erosion rates along the Beaufort Sea coast are discussed next.

Vertical movement of the earth crust is important in some parts of Alaska for coastal evolution, and will be analyzed first for the study area. The consistent altitude (7 m +/-3 m) of the Pelukian shoreline from Barrow to the Colville River (Hopkins and Carter, 1980) are strong evidence that this stretch of coast has been stable for the last 120,000 years. Thus Dease Inlet and Smith Bay, two of northern Alaska's most pronounced embayments, cannot have been produced by differential vertical motion during that time period. According to Hopkins and Hartz (1978) the coarse-grained coastal plain deposits cropping out in the Jones Islands may also be Pelukian beach deposits. If true, such deposits would extend at a uniform level throughout the entire study area, except for a gap in eastern Harrison Bay. From examination of our seismic records of the region, industry borehole data, and from onland studies of the Quaternary geology (David Carter, oral communication, 1985), there seems no evidence for Holocene subsidence and this break in the supposed continuous Pelukian beachline remains unexplained.

Mean sealevels for the summer months from 1975 to 1984, measured by the NOS at the east end of sector 14 are shown in figure 26. The best- fit line for that data indicates a sealevel rise of 2 cm/yr or 2 m/100 yrs. This is much higher than the 0.1 to 0.15 m/100yr worldwide sealevel rise and therefore suggests subsidence of that area. The configuration of shallow subbottom seismic reflectors in the region, in particular that of the post-Pelukian unconformity offshore, does not support local subsidence. Furthermore, the modern coastal retreat rates in the area of the tide gauge are among the lowest of the entire study area. Thus we can find no support for the 9-year sealevel trend shown by summer tidal data. The gauge has been operated for only 2 to 3 months each summer, and is located on a recently constructed gravel causeway. On this causeway are the reference benchmarks used to re-establish the gauge each summer. Most of these are lost each year due to causeway maintenance work. Moreover, the causeway serves for the transport of single modules weighing 1,000 tons or more. For these reasons we regard the tide gauge data unreliable.

An important data set on relative sealevel changes was obtained during the recent mapping project, when tidal bench marks from the original 1950 work were re-occupied. At five locations between Lonely (Mapsheet) and the Canadian border a total of sixteen benchmarks were referenced to a new tidal datum obtained from one and a half year observations near Prudhoe Bay. Table III shows the suggested changes in benchmark elevations, and notes on the length of observations and problems encountered. Most measurements suggest an increase in elevation relative to sealevel, except for the Demarcation Bay site, where submergence of 3 to 5 cm is suggested for the 29-yr period. The indicated elevation increases may be attributed to the fact that the new sealevel information is based on over one year of data, while the old datum stems from relatively short summer observations, when sealevel in the Beaufort Sea is universally higher (Sames Spargo, State of Alaska Coastal and Marine Boundary Section, oral communication, 1985). Thus there is no indication of significant vertical crustal movement of Alaska's north coast during the study period.

All information available to us therefore suggests that irregularities in coastline configuration within the study area have not been produced by differential vertical crustal motion during Holocene time.

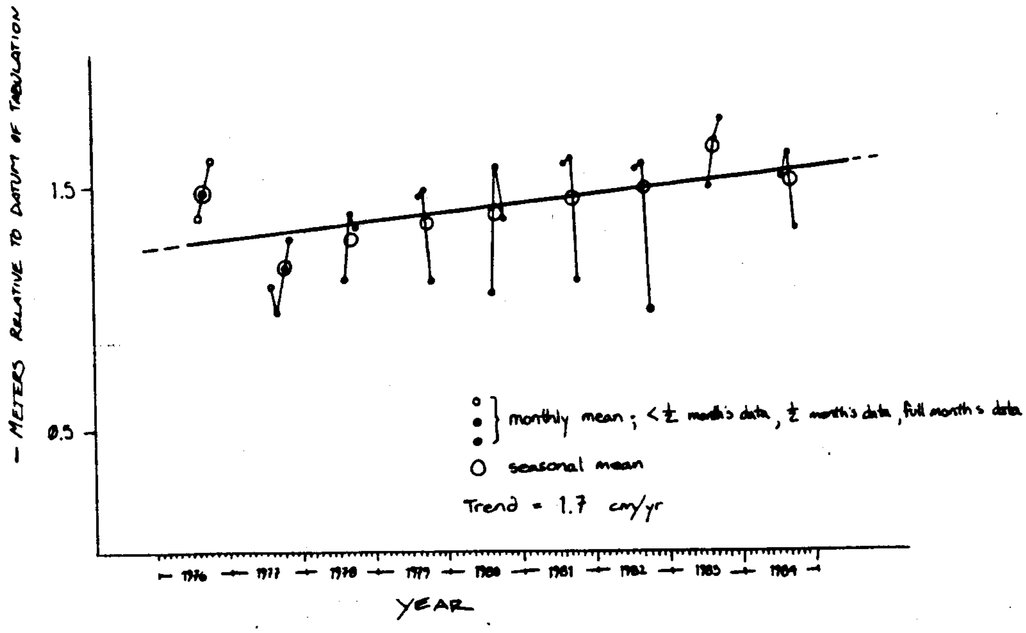

Figure 26. Graph of monthly (july, august, and september) mean and seasonal mean sea level measured at Prudhoe Bay West Dock - NOAA tide station #949-7649. Trend line represents least square fit to seasonal mean data. Note sea level usually peaks in august (spring floods) and decreases thereafter. (after Inman 1984)

TABLE III

CHANGES IN TIDAL BENCHMARK ELEVATUIONS OVER 30 YEARS

Location Longitude W	Station Identification	Years Observed	Changes Relative to MLLW
Lonely	Camp	1951 - 1981	-.01
153°05.0'	rm1	1951 - 1981	+.21
	rm2	1951 - 1981	+.07

1951 data: 2 weeks observation (July); later adjusted for up to .4m frost heave
1951 data: 4 week observation (late Aug.-Sept.) synchronous with Cross Island datum

Flaxman Island	1	1950 - 1981	+.06
146°2.8'	2	1950 - 1981	-.01
	3	1950 - 1981	-.01

1950 data: 1 month automatic gauge records (Aug.)
1981 data: 3 days observations (late Aug.) synchronous with Cross Island datum

Simpson Cove	A	1981 - 1982	+.10
144°49.0'	B	1981 - 1982	+.06
	C	1981 - 1982	+.07
	D	1981 - 1982	+.05
	E	1981 - 1982	+.06

1981 data: 31 day observation (mid-Aug.-Sept.) synchronous with Cross Island datum
1982 data: 11 day observation (mid-July) synchronous with Prudhoe Bay datum
Historical records indicate BM1 was .48 m above ground level, now it is .66 m up due to erosion?
(See "Arctic Tides" by Rollin Harris, C&GS, 1911)

Barter Island	2	1951 - 1981	+.14
143°36.5'	4	1951 - 1981	+.05

1951 data: adjusted for up to .92 m frost heave
1981 data: 3 day observation (late Aug.)

Demarcation Bay	1	1952 - 1981	-.03
141°12.0'	2	1952 - 1981	-.04
	3	1952 - 1981	-.05

1952 data: 1 month observation (Aug.)
1981 data: 24 day observation (late Aug.-Sept.) synchronous with Cross Island datum

From Alaska Photogrametric Consultants Group, 1982 and 1983.

Bluff height is one of the dominant factors controlling rates of erosion (Owens et al, 1980). In areas of high bluffs, where large sediment volumes are made available by melting, the marine energy in some seasons simply is inadequate to remove material at the rate at which it is introduced into the nearshore. The introduced materials are seen on beaches and in the swash zone in various forms, waiting for a surge and wave action to remove them. Areas as in figure 6 that lack bluffs, on the other hand, are quickly inundated upon contact with the sea due to the extremely large amounts of ice in the upper 2 m of coastal plain deposits and the resulting thaw collapse. Here little lateral transport of sediment, or 'marine energy', is required to inundate the coastal plain. High bluffs along the Chukchi coast are partly responsible for the much lower erosion rates there than along the Beaufort Sea coast (Harper,1978). Similarly, high bluffs in the Kogru River area are probably in part responsible for the lower erosion rates there than at Cape Halkett, although in this case the degree and direction of exposure and especially bluff lithology are perhaps the dominant factors.

The presence or absence of a beach, and its volume, strongly affect the coastal retreat process. Broad and high beaches are rarely overtopped by the sea. Their presence therefore reduces thermal processes to ineffective atmospheric summer warming, and eliminates the effects of the sea. One such area is the north coast of Pingok Island, where for reasons not well understood the beach broadened, even advanced, during the study period, yet the bluff continued to retreat. As discussed later, and shown in figure 32, the eroding offshore profile has cut into massive underlying gravel. Since the local bluffs on the island contain almost no gravel size material, the submerged offshore gravels may be the source for the beach materials. This in turn would call for ice-bulldozing as transport agent to supply the beach. Because this study compares shorelines, while others may have considered the changes in the bluffline only, our erosion rates differ from previously published values. The Pingok Island retreat rates shown in figure 32 are from Naidu (1984), and serve as example.

Variation in coastal plain composition (sediment grainsize) is an extremely important parameter. Coastal plain deposits containing pebbles and cobbles in a sandy matrix erode much slower than those composed mostly of silt and clay with their higher ice contents (Hopkins and Hartz, 1978). Areas with fine grained coastal plain deposits are also marked by a lack of protective beaches (fig. 5), due to a scarcity of sand and gravel size particles. The importance of grainsize is evidenced by the dramatic differences in coastal retreat rates between the eastern and western portions of the study area. From Oliktok Point eastward, where the coastal plain is composed of a series of coalescing alluvial and glacial outwash fans extending northward from the Brooks Range (Hopkins and Hartz, 1978), retreat rates are nearly an order of magnitude less than in the area between Cape Halkett and Drew Point north of the Pelukian barrier chain (fig. 26) where bluffs are composed of marine mud (Carter and Robinson, 1980). These differences are partly responsible for the more stable coasts in sectors 12 through 14 (1.3 m/yr) than those of sectors 1 through 6 (5.4 m/yr). The coarse Pelukian beach deposits north of Kogru River (sector 7), and possibly also exposed to the east in a number of the Jones Islands in form of high tundra-covered coastal plain remnants (fig. 18, and 20) (Hopkins and Hartz, 1978) are more resistant to erosion and control coastline evolution. Thus, the rapidly retreating promontory between Cape Halkett and Drew Point will likely stabilize at the ancient Pelukian barrier chain on the north shore of Teshekpuk Lake (fig. 25) in a few thousand years.

Degree and direction of exposure to the various climatic and oceanographic processes affect erosion rates. Open water conditions with waves and currents are needed to remove the materials introduced by bluff erosion. Simpson Lagoon is ice free for a greater part of the summer than the "open ocean" waters north of the Jones Islands (see typical ice distribution in fig. 19). The increased fetch in lagoons affords greater potential for erosive processes and consequently retreat rates in the lee of these islands are commonly higher than on the ocean-facing side (sector 15). Water temperature also affects erosion rates, partly owing to more effective niche development, and partly due to the extended open water season near river mouths. The coastal plain remnants in that part of the Jones Islands chain equidistant from the warming effects of the Colville and

Kuparuk Rivers may be testimony to this influence. Such old remnants may have long since disappeared in the islands directly off the Kuparuk River, leaving barriers composed only of a thick sand and gravel lag atop residual tundra cores. Cannon (1978) pointed out that southfacing bluffs, those exposed to the sun for the greater part of the day, erode faster than north-facing bluffs. An example of the results of this difference in orientation is partly reflected in the higher erosion rate of bluffs on the south side of Pingok Island. Reimnitz and Maurer (1979) pointed out that storm surges, and, therefore, westerly winds in general, should be those most effective in producing significantly elevated tide and wave conditions, and thought that for this reason west-facing promontories retreat faster than those facing east. The resulting pattern, as best exemplified by the coastal configuration and retreat rates in sectors 13 and 14, is indicative of processes acting in a direction contrary to those responsible for the westward orientation of the small coastal spits trailing off the mainland promontories. This pattern however does not hold elsewhere in the study area.

Formation of embayments and lagoons by thermal collapse

Wiseman et al (1973) showed how thermal collapse of lakes breached by the transgressing sea results in formation of embayments and lagoons (fig. 27). They envisioned a 4-phase evolution beginning with an area of large lakes similar to the Cape Halkett region. The coalescence of such lakes and the breaching and inundation by marine waters to form Kogru River type inlets is their second phase. This is followed by a widening of the inlet, and eventual stranding of coastal plain remnants to form an island-protected lagoon setting similar to that of Simpson Lagoon, as phase 3. The scenario is concluded by citing Leffingwell Lagoon (east of study area) as an example of maturity in phase 4. Reimnitz and Maurer (1979) have pointed out problems with this model, presenting Kogru River and Prudhoe Bay as examples. The lakes in these two regions are currently perched several meters above sealevel. Thus the anticipated amounts of thermal collapse of existing lake beds without subsequent deepening by erosion, could not create the 3 to 4 m water depths found in the two embayments. Also, enlarging the types of lakes found north of Teshekpuk Lake (fig. 25) as in phase two of Wiseman et al (1973) would result in water bodies oriented at right angles to the existing major embayments and lagoons we are trying to explain.

The lakes deeper than 2 m in the area north of Teshekpuk can be recognized by their persisting seasonal ice cover in figure 20 (Sellmann et al, 1975). Figure 25 indicates actual lake depths according to Holmquist (1978); C. Sloan, USGS (oral communication, 1980) and J.Helmericks, bush pilot (oral communication, 1984). The figure also shows three lakes that have been recently breached by the advancing sea to form very shallow NW-SE oriented embayments. Pogik Bay is one such embayment. The 2-m isobath, perhaps marking the northern part of this former lake basin, juts seaward by about a kilometer beyond the general trend of that isobath on either side (see sector 4, Sheet 1). Thus the lake basin is a submerged promontory, more resistant to erosion than the surrounding terrain. Perhaps this can be attributed to the former existence of a deep lake underlain by a thaw bulb lacking excess ice. Upon breaching and inundation such lake bed would be dense and stable, and therefore not subject to further thermal collapse. A similar setting and evolution is described by Tomirdiaro (1975) for a cape in the East Siberian Sea. The cape marks a deep lake basin breached by the transgressing sea. Pogik Bay, however, is generally too shallow for use by even light float planes. The resistance to erosion here may alternatively be due to a thick accumulation of fibrous organic matter on the former lake bed.

The NE coast of present Cape Halkett may mark the west shore of a former large lake breached about 200 years ago. According to Leffingwell (1919, p.170), Dease and Simpson in 1837 mention a passage inside of a tundra-covered island which they named as the original Cape Halkett. Some 19th century charts (for example H.O.Chart no. 68, 1893 edition) show this island elongated parallel to the regional trend of lake axes. On figure 25 we stipled the outline of this former island. The last tundra remnants of the island disappeared by about 1945, and in 1952 it was charted as a shoal (sheet 7991). The water depth over the presumed former lake between the

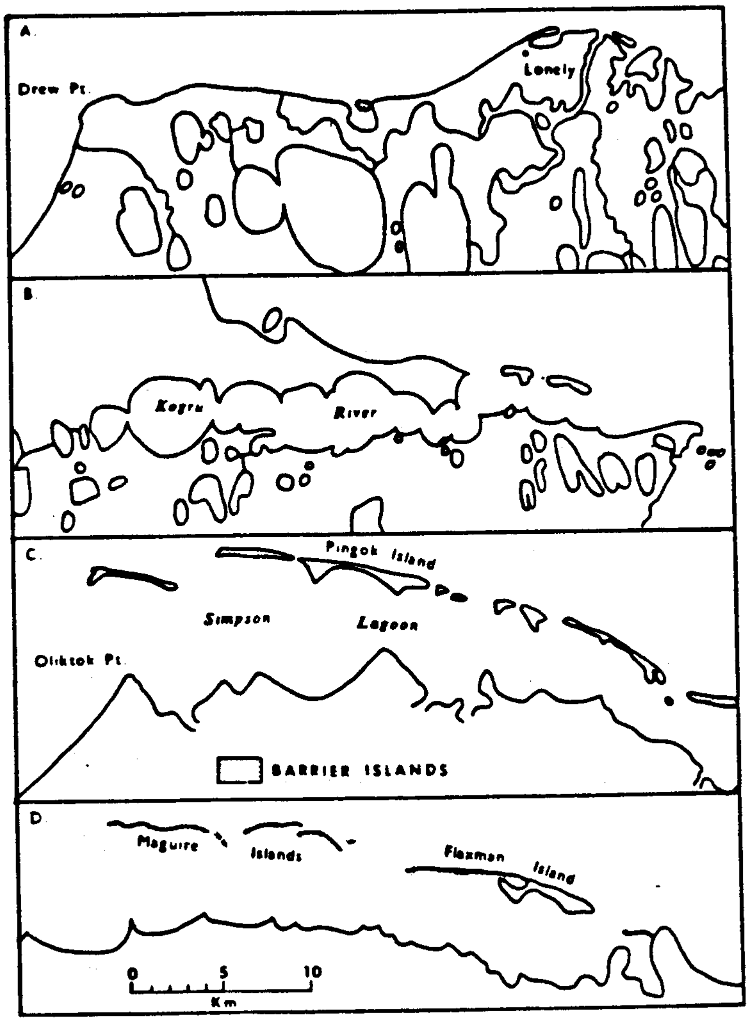

Figure 27. Sequence of lagoon formation and barrier island isolation by thaw-lake coalescence. A) initial tapping, draining, and coalescing of lakes, B) continued coalescing of lakes and thermal erosion of shoreline, C) continued thermal erosion and isolation of offshore tundra remnants, D) erosion of tundra remnants and reworking of sand and gravel into offshore barriers (from Wiseman, et.al., 1973).

cape and the shoal is now less than 2 m. High resolution seismic records across that area show no sub-bottom evidence for a filled lake basin. The above considerations and facts suggest that we have to search for other mechanisms to explain the formation of bays and lagoons than that hypothesized by Wiseman, et al. (1973).

Thermal collapse resulting in the development of coastal sediment sinks

According to our tabulations the sediment contribution from erosion in the offshore is slightly larger than that from the onshore. But the absolute reliability of the calculated values for this contribution is questionable due to the possibility of thermal collapse in the offshore zone. Harper (1978) in fact stated that "thaw subsidence causes a continual steepening of the offshore profile and provides a sediment sink for eroded sediments." The following section will pursue the question of offshore thaw settlement by first analyzing the Russian studies from the Laptev and East Siberian Seas commonly referred to in western literature (e.g. National Research Council, Marine Board, 1982) and then an example profile from our study area for evidence on thermal collapse.

Example from the East Siberian Sea

Russian workers have attributed the most important role in the shaping of the arctic continental shelf profile to thermal processes. Thus Tomirdiaro (1975) states "The eastern Arctic seas are largely young Holocene bodies of water formed by thermo-abrasional processes; it is thermo-abrasion, and not the usual abrasion processes, that has formed the socalled Arctic continental-oceanic zone here in such a short time." His interpretation relies heavily on the marine studies reported on by Klyuyev (1965). The data Klyuyev presents are hydrographic surveys repeated over time intervals of 15 to 20 years, off coasts that are retreating as fast as the coast in sectors 1 through 6 in our study. One of these surveys repeated after 15 years (fig. 28) suggests a maximum lowering of the seafloor by 0.6 to 0.7 m in the depth range from 2 to 4 m, or a shoreward shift of the 2-, 4-, and 6-m isobaths by 0.5 to 1.2 km. The seafloor lowering was least adjacent to the coast, and on the outer end of the profile at 6 to 7 m depth. Klyuyev claims that the possibility of errors in navigation or in sealevel datum were definitely excluded in these surveys. We note that the 0-m isobath, which should represent the shoreline, remained stationary while the bluff had retreated by 170 m. This seems a doubtful and highly unlikely event, and detracts from the validity of his conclusions. The following considerations cast further doubt on his conclusions.

Klyuyev (1965) apparently attributes the depth changes entirely to thermal collapse, and presents evidence that the upper surface of the ice bonded section is at or immediately below the seafloor. The evidence he presents also can be interpreted differently. He reports that short cores may contain several millimeter long ice crystals. We have observed that small ice crystals form in fine grained sediments during fall storms, triggered by a rise in water salinity and a drop in water temperature to slightly below its freezing point. The sediment interstitial water still retains a slightly lower salinity acquired from summer river flow. The ice platelets seem to decay within a month into winter. Klyuyev (1965) also reports ice in sediments and bonded sediments in the normally submerged littoral zone when it lies exposed during strong winds. Ice bonded sediments in the Alaskan Arctic are also near the surface on the 2m bench, where the fast ice rests on the bottom at winter's end. The thickness of the unbonded sediment layer in shallows, however, is not an indicator of the thickness of unbonded sediments offshore. He further cites as indirect confirmation of the existence of permafrost on the seafloor the following fact: "Vessels drift during a storm even with two anchors. The anchors slip over the solid bottom, and when the depth is slight a characteristic knocking can be heard." He states that the bottom is not rocky where these observations were made. Such observations have also been made during fall storms in the Alaskan Arctic (Jim Adams, tug boat operator, oral communication, 1984). Our own work has shown that shallow water sand and coarser deposits during freeze-up storms become ice bonded

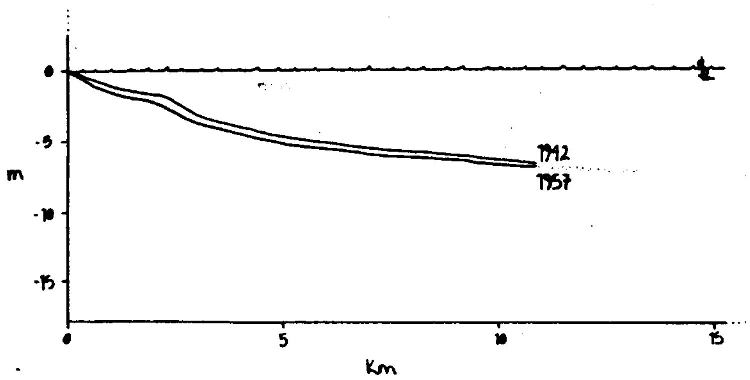

Figure 28. Comparison of hydrographic surveys repeated after 15 yrs in the East Siberian Sea (after Klyuyev 1965).

and form anchor ice, as discussed earlier. Ice bonding, however, apparently forms only a surface crust, which disappears after the ocean has a new ice canopy. The annual formation of a seafloor crust can not result in net thermal collapse. The principal evidence for submarine thermal settlement brought forth by Klyuyev is the presence in the Laptev and East Siberian Seas of wedge-shaped depressions with peaked flanking ridges, which he interprets to be thermokarst features, resulting mainly from the melting of ice wedges. These are subdued in shallow waters, become best defined with increasing water depth (15 to 20 m), and are found seaward to 50 m water depth. This distribution pattern, with better preservation at increased water depth where sediments are more cohesive than on the inner shelf, and also the shapes of the features in fathograms, match exactly those of ice gouges on the Beaufort Sea shelf (Reimnitz and Barnes, 1974; Barnes et al, 1984). The features are much too large (120 m wide) to be produced from the melting of ice wedges (Footnote: * There is a large discrepancy between the 8 and even 12 m depression depth he quotes, and the maximum 5 m we measure from his figures). Lastly, we note that thaw settlement in the coastal zone should result in the trapping of most sediments introduced. There should be little chance for sediment sorting, and underlying ice-bonded materials should become buried by sedimentary accumulations. Yet the local bluffs in the Siberian studies reported on introduce silt and clay-size materials, while offshore deposits are sandy. To us this indicates that mechanical, rather than pure thermal energy is at work, winnowing the sediments introduced. This also indicates that steep-sided depressions with flanking ridges shown by Klyuyev (1965) are short-lived, and that the sedimentary environment is not unlike that of the Beaufort Sea.

Analysis of a North Slope profile

The following is an analysis of a coastal plain/continental shelf profile in our most dynamic region near Cape Halkett, to shed light on this question of offshore thermal collapse. Figure 29 is the overall profile compiled from published topographic maps and charts. Over the first five km inland the profile represents all elevations given at specific distances from the coast into one line. As this part of the land-surface profile is important in the following discussion, we prefer to eliminate any distractions produced by local irregularities. A line on Figure 26 indicates the precise location and trend of the profile. This particular line was chosen as an onshore continuation of an offshore profile which we have re-surveyed repeatedly for monitoring the rate of ice gouging from 1977 through 1980.

The coastal plain from the beach for a distance of 35 km inland has slightly undulating relief ranging between 5 and 12 meters above sea level. The last 5 km to the beach are marked by generally decreasing elevations, with a general slope that matches that of the seafloor for a few kilometers onto the continental shelf. The coastal zone is a pronounced niche in this profile, as amplified in figures 29B, 30A and B, and 31.

Unfavorable geometry of the shore stations with respect to the inshore end of the survey line (fig. 25) introduces possible north-south position errors of plus or minus 23 m for our own surveys. The western shore station is located at the corner of the hut at Esook (fig. 5), which has not been surveyed accurately. Thus there is an additional unknown error that affects the comparison between the 1950 and 1980 profiles. Our fathograms show slight local depth differences from one season to another during the 1977 to 1980 interval. But in view of the possible position errors, the overall bottom profiles are similar enough to be shown as a single solid line in figure 29B. This line is relative to a sealevel average for all survey periods, and has a likely error of 20 cm relative to the true datum. The shoreward end of our survey lines lies at the bar marking the seaward edge of the 2m bench; the missing part of the profile from there to the beach is shown as a straight line. The dotted line in figure 29B is taken from a dense set of soundings made by the U.S. Coast and Geodetic Survey in 1952.

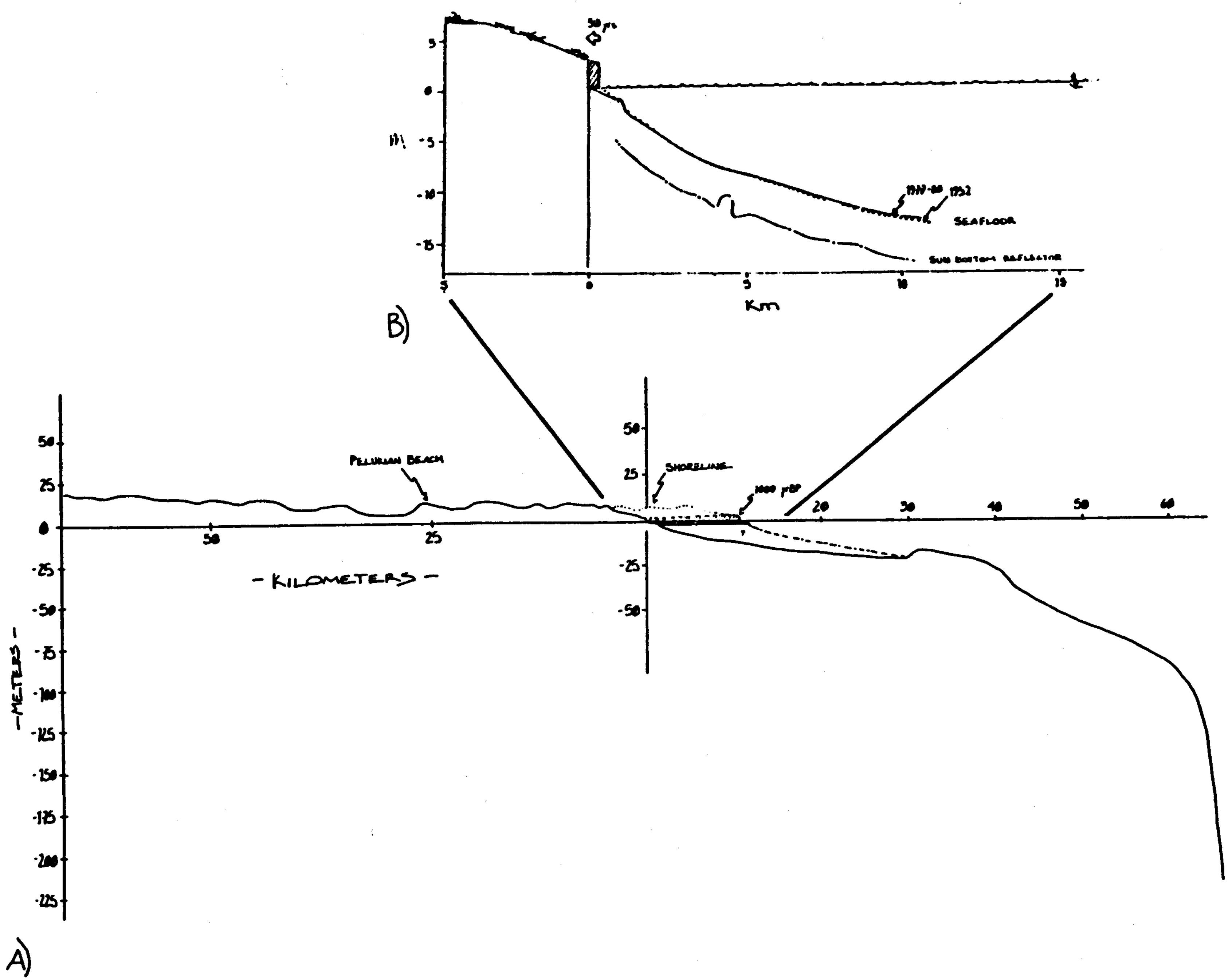

Figure 29 Coastal plain/shelf profile along line indicated on figure 25
A) present profile and 1000 yr hindcast with accounted and unaccounted volumes indicated, B) detailed coastal zone profile showing a 30 year comparison of bluff and seafloor, and a shallow seismic reflector.

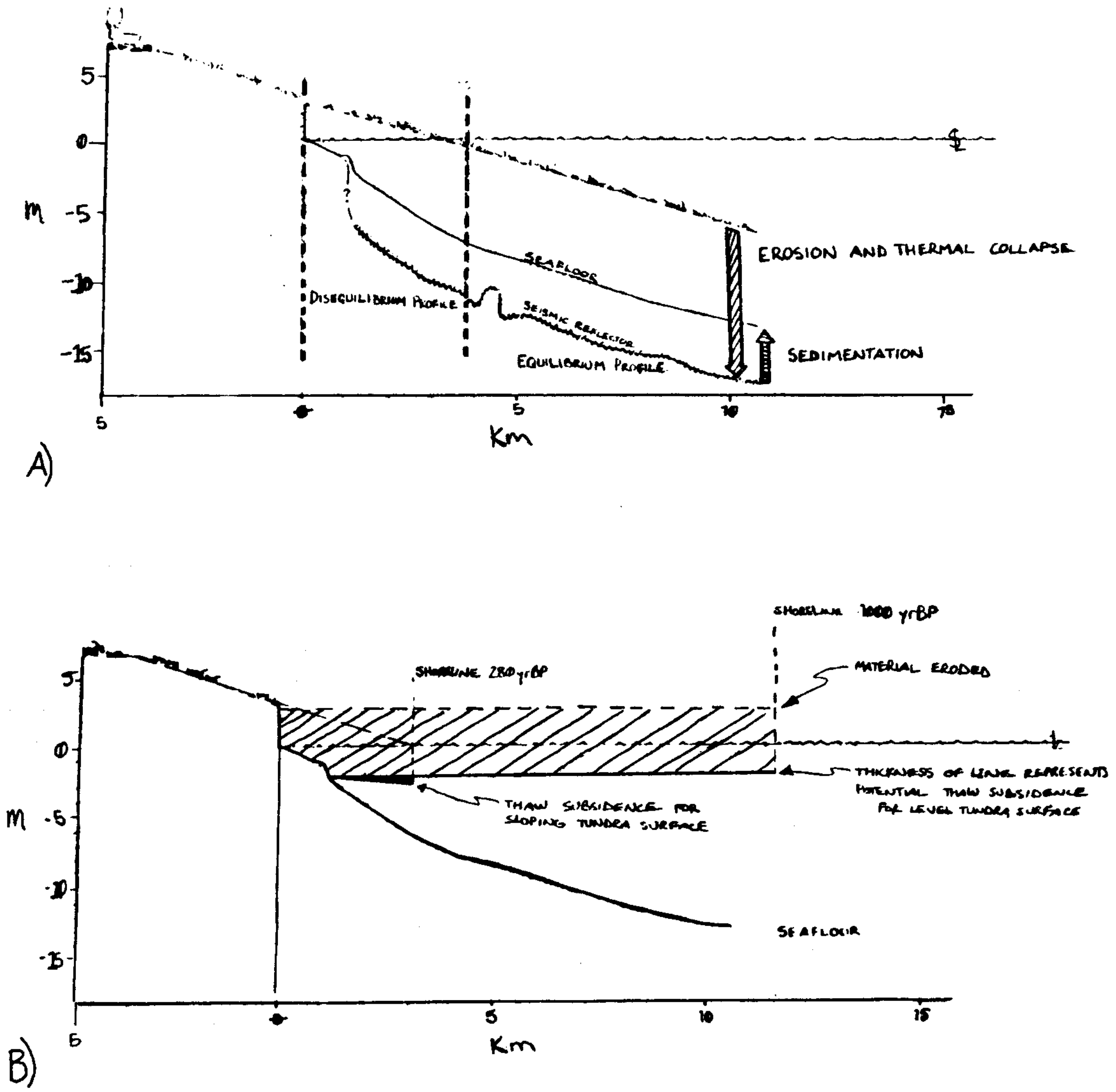

Figure 30. Same profile as figure 29.B with hypothetical tundra surfaces, A) possible origin of the seismic reflector as the old land surface after erosion, thaw subsidence and Holocene sedimentation, and B) potential thaw settlement below the -2m truncation surface for both level and sloping tundra surfaces assuming deep thaw.

The 30 year comparison of the inner shelf bottom profile shown in figure 29B suggests slight buildup (5-20 cm) at a distance of 5 to 10 km from the coast, and deepening (10 cm) in the first kilometer seaward of the 2m bench. This comparison also suggests that the seaward edge of the 2m bench maintained its position, while the coastline retreated. This is in conflict with the model we used for calculating sediment input by erosion. We have no data on any depth changes across the 2m bench, from where according to our methods and calculations the major part of the sediment budget is derived. The suggested widening of the 2-m bench at this site during the last 30 years should be verified by increased navigational accuracy. But in the meanwhile an analysis of the offshore extension of the profile in light of the extremely rapid transgression is informative.

Figure 29B shows the shallowest seismic sub-bottom reflector below the shelf surface, as delineated by a 7 kHz profiling system used in conjunction with the depth recorder. This reflector is characterized by jagged relief of 2 to 3 m amplitude, indicated here schematically. The reflector is smooth only across the 2 m high, 500 m wide mound at 4.5 km from the coast.

In our Beaufort Sea geophysical studies we have generally taken the shallowest, continuous, sub-bottom reflector to represent the base of Holocene marine sediments, for reasons discussed by Reimnitz et al (1982). In numerous instances this interpretation has been confirmed by coring and other work. In the area off Cape Halkett, however, we have no such ground truth. If we assume this reflector is the base of the Holocene as elsewhere, then it may mark the former land surface, having been slightly modified by the bevelling action of the transgressing sea, which reworks just the upper few meters of coastal plain deposits. As the transgression proceeds, material below sealevel may for a time experience additional thaw collapse, and this may explain the different slope of the inshore 5 km of the seafloor and sub-bottom reflector. As thaw settlement is complete and all material reaches equilibrium with the thermal regime, the slope of the seafloor flattens out at an attitude parallel the slope of the old tundra surface. Following this line of reasoning the vertical distance separating the trace of the old tundra surface bevelled to sealevel and the position of the first sub-bottom reflector is explained by 8 m of erosion and thaw settlement, followed by re-deposition of 4 m of bluff and nearshore material. This hypothesis is illustrated in figure 30A and is shown to be unlikely later on.

The jagged sub-bottom reflector is characteristic of several extensive regions in the Beaufort Sea. In one such area industry soil borings showed the reflector to conform to the top of ice bonded sediments. At two sites several km west of our profile Harrison and Osterkamp (1981) investigated the depth to ice bonded permafrost. At 2.7 m and at 5.5 m water depth, the first signs of ice were seen at 4 and 5 m, respectively, below the seafloor. At the latter hole, the phase change from partial to solid bonding occurs between 5 and 7 m, and Osterkamp believes that the boundary from which seismic energy is reflected should be very irregular under these conditions (oral communication, 1984). Alternatively then the sub-bottom reflector in figures 29B and 30A may more likely mark the upper surface of bonded subsea permafrost. From the point where the reflector terminates on our records in shallow water, it probably rises beneath the 2m bench, to conform to the seafloor from there to the beach, and rises sharply to the land surface at that point. If so, this reflector can not also be the former coastal plain surface, or the interface between older and Holocene sediments.

Figure 29A shows where the inner shelf profile would have been 1000 years before the present, assuming the maintenance of a profile of dynamic equilibrium. Even if the seafloor slope was much steeper at that time, this reconstruction implies a large wedge of material unaccounted for in our calculations of sediment removed during the transgression. Our tabulations account only for the hachured portion of this cross section. In figure 30B, we indicate how much of the implied missing wedge can be reasonably attributed to thaw settlement. We again use data from Sellmann et al (1975), and assume that sediments in situ retain a porosity of 40% after thaw collapse. Sellmann's data from the Barrow area shows that most excess ice, and therefore thaw settlement occurs in the upper 7 m of the coastal plain. We apply that data to two hypothetical cases where both assume a constant sealevel. In the first case the coastal plain extended seaward horizontally at a level 3 m above the present sea, and has been removed to the -2 m level by erosion and deposited elsewhere. This slab is shown in a stippled pattern. The thickness of the line at the base of this slab represents the amount of thaw settlement possible for that erosion surface (about 5 cm). In the second case the old tundra surface intersects sealevel 3 km from the present shore, and again is truncated down to the -2 m level. We can only make reasonable estimates of thaw settlement for this erosion surface from the edge of the 2m bench to the point where the coastal plain dips below sealevel. The possible thaw settlement is indicated as a wedge, with a maximum thickness of 39 cm at a point where todays water depth is 7.5 m. At this point, the discrepancy between the eroded slab we account for in our sediment-yield calculations plus thaw settlement and the actual seafloor is about 5 m. Using available data the maximum thaw settlement that could have occured anywhere along this profile is about 1.5 m.

Although we do not know the distribution of excess ice in the offshore, our analysis of the profile strongly suggests that the niche in the coastal zone must be due either to (a) erosion by lateral transport through a combination of processes involving ice, waves and currents; or (b) was produced over a long time period in a somehow different setting, in which the coast was stable. We rule out the latter, as analyses of temperature profiles in 5 boreholes offshore from Pitt Point (sector 2) indicate a retreat rate of several meters per year for the last 1000 years (Harrison and Osterkamp, 1981). Furthermore, Lachenbruch (1985) states "the absence of a thermal disturbance in coastal wells along the Beaufort Sea implies the shoreline has been transgressing rapidly" (1-2m/yr).

The transgression is rapid along the entire Beaufort Sea coast from Barrow to the Mackenzie Delta in Canada (Hopkins and Hartz, 1978). The profile discussed above is not unusual for this coast, except for the areas off the two largest rivers, the Colville and the Mackenzie. The bluff retreat is not associated with the formation of a platform near sealevel. This implies that the entire inner shelf should be an erosional surface, with possibly several tens of meters removed since the transgression.

There is indeed strong evidence that much of the Beaufort Sea inner shelf is an erosional unconformity. Reimnitz et al (1982) showed a sparsity of Holocene marine sediments for the region between 146°W and the Canadian border, and presented seismic evidence indicating that the inner and mid-shelf surface truncates older strata. Isopach maps of Holocene sediments prepared since show that such materials are restricted to bays and lagoons in that region. Similarly, the inner shelf surface between 146°W and the present study area, from the island chains to about 30 m water depth, truncates seaward dipping older strata (S.C. Wolf et al, 1985, and on-going work by Wolf and the authors). These findings are supported by studies of over 20 boreholes in that area. Overconsolidated silt and clay cover much of the Alaskan Beaufort Sea shelf. Lee and Winters (in press) studied the consolidation properties and mechanisms for surficial sediments and conclude that subaerial freezing during periods of lowered sea level was probably the principal cause. Only the lagoons contain local accumulations of soft Holocene marine sediments (Wolf et al, 1985; and Smith, 1985). But even here some areas are marked by ongoing erosion. Thus, Dunton et al (1982) presented supporting evidence for vertical erosion at 6 m depth in the sheltered waters of Stefansson Sound, directly off the Sagavanirktok River. This ongoing erosion resulted in the Boulder Patch as a modern lag deposit. Analysis of seismic records from Prudhoe to Harrison Bay has not been completed, but the data indicate a similar setting.

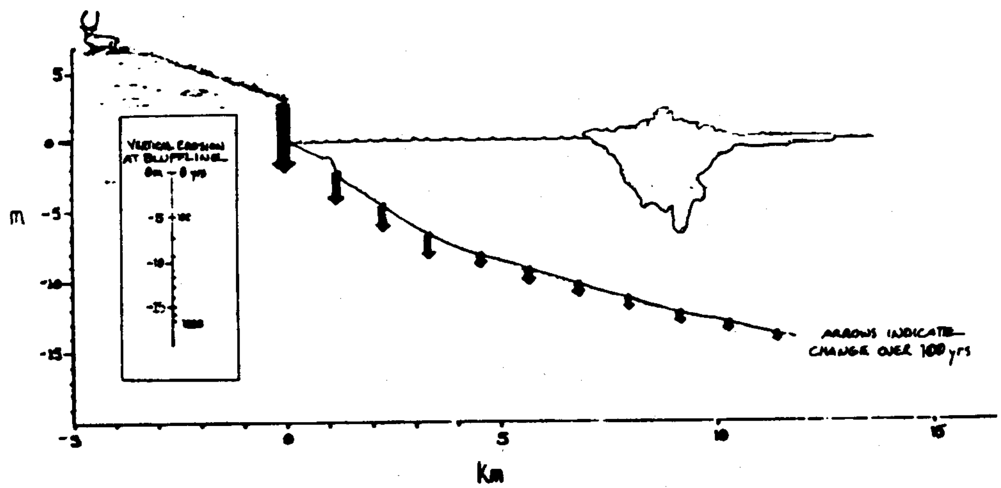

Figure 31. Present land and seafloor surface with arrows indicating vertical erosion predicted for the next hundred years at 1 km intervals along the profile; inset shows thousand year vertical erosion predicted for a point at the present shore.

Vertical shelf erosion by a shifting "equilibrium profile"

In seas not dominated by ice, the inner shelf apparently maintains a profile of dynamic equilibrium, by some referred to as "Bruun's Rule" (Bruun, 1962; Schwartz, 1967; Swift, 1968; and Rosen, 1978). Winant et al (1975) show that seasonal changes in the profile across the beach and out to 10 m water depth can be described using empirical eigenfunctions. While the year round presence of drifting pack strongly affects processes and very likely also the shape of the profile, we can nevertheless assume that the profile is maintained and shifted landward as the sea transgresses. Let us consider the implications of a dynamic equilibrium profile through the last thousand years for the Cape Halkett area.

As depicted in figure 29A, sea level likely was constant while the coast retreated about 10 km. This reconstruction has two important implications: (1) the amount of sediment supplied to the sea by erosion is increased by at least a factor of four over that calculated from bluff and shallow nearshore erosion alone, and (2) we can calculate vertical erosion rates for any point on the inner shelf. The latter is shown in figure 31, and should be of particular value for ongoing arctic coastal development and construction projects. The length of arrows along the profile in this figure indicate the depth to which erosion would lower specific points on the seafloor during the next 100 years by a simple landward shift of our assumed "equilibrium profile". The scale to the right of the profile shows the expected vertical erosion over time for a point originating on the tundra surface at time zero. While the arrows along the profile will not serve as actual measures of seafloor erosion to be expected in the design of buried offshore pipelines, they do indicate a situation of considerable import to the development of the offshore oil fields.

Total sediment yield from rivers and from coastal erosion

To obtain the sediment yield for that portion of the North Slope feeding the shelf within our study area, we must first evaluate what is known about the river input to the sea. Milliman and Meade (1983), using 5.8 millions tons as the annual suspended sediment load of the Colville River (Arnborg et al, 1967), with a drainage basin of 50,000 km^2, estimate northern Alaska's sediment supply from rivers at 120 tons/km^2/yr. For the following reasons we believe that number is an order of magnitude too large: Vast regions in the Eurasian Arctic with similar settings as that of the Colville River drainage area yield 8 tons/km^2/yr according to the compilations by Milliman and Meade (1983). They use that same number as an estimate for northeastern Canada, where no actual measurements have been made. The Mackenzie drainage basin yields only 55 tons/km^2/year (Milliman and Meade, 1983). The Babbage River (between the Mackenzie and the Alaskan border) according to two years of measurements by Forbes (1981) yields 42 tons/km^2/yr. The yield for these two rivers should be much higher than that of the flat Colville River drainage area. The Sagavanirktok River immediately east of our study area (draining 14,500 km^2) according to our own sketchy measurements yields about 5 tons/km^2/yr, and according to one summer of stream gauging by NORTEC yields 7.4 tons/km^2/yr (R.P. Britch, written communication, 1984). Even the Sagavanirktok River, judging by its steeper gradient and braided nature, should have a higher sediment yield per unit area than the Colville River.

In view of the above considerations, we estimate 10 tons/km^2/yr as the sediment yield from 74,000 km^2 drainage areas adjoining the coastal sector studied here (fig. 1). Upland sources accordingly yield 740,000 tons of sediment per year. This compares to about 5 million tons per year, contributed by coastal erosion. Previous studies estimated that streams supply four times more sediment to the Beaufort Sea than coastal erosion (Owen et al, 1980). According to our own calculations the sediment yield from coastal erosion is seven times higher than that from streams, and we believe that factor is very conservative.

Based on the geometry assumed in our study, the thickness of the sediment layer removed between the shoreline and the 2-m isobath during the 30 year period of coastal retreat typically is less than 20 cm. In reality the layer very likely is many times thicker, and also extends seaward far beyond the 2 m isobath. Thus the sediment yield resulting from the erosive transgression is many times larger than we calculated. If this is true, then the rate of coast transgression is influenced not only by the lithology of bluff materials, but by the lithology of sediments underlying the inner continental shelf. As discussed earlier, some of these subsea deposits may find their way to the beaches, and in turn affect their lithologies.

From the above considerations it follows that the several meter thick blanket of Holocene marine sediments found locally on the actively eroding part of the profile represents sediment in transit, or in flux. Over large areas this layer is about as thick as the maximum ice gouge incision depth (Barnes et al, 1984), or roughly one tenth of the water depth out to the 40-m isobath. Off certain deltas the layer is about as thick as the depth to which strudel scour reworks the section, or about 6 m (Reimnitz and Kempema, 1983). These processes excavate underlying, older sediments and admix them into the flux. The resulting layer may be viewed as a roto-till, or better "gouge-till" unit. These sea ice-related, erosive processes explain why the surface sediments contain mixtures of modern Foraminifera together with iron-oxide stained, old forms that are outside their depth range and habitat (Kristin A. McDougall, oral communications, 1984). The processes also explain why clay mineral suites in surface sediments, unlike patterns on other Alaskan shelf regions, do not reveal patterns that can be traced back to their continental source regions. The distribution of suites instead is patchy, and has been attributed to relict nature of surface sediments (Naidu and Mowatt, 1983). The materials probably are derived to a large extent from erosion of local sources on the shelf, and are incorporated into the surficial "gouge-till" unit.

Given the sediment input from coastal erosion and streams, and published estimates of littoral transport in the Beaufort Sea, one is led to attempt completing the sediment budget by considering the sinks. Placing the sediment budget within the constraints of the concept of a littoral cell, including sources, pathways, and sinks (e.g. Inman and Chamberlain, 1960; Inman and Brush, 1973) has proven useful in studies elsewhere. The concept requires a dominant source at one end, and a major sink somewhere off the other end of the cell. This concept seems to break down where the system is not dominated by a point source, as in our case. Rather evenly distributed input from erosion of the Beaufort Sea coast far outweighs the riverine input. Average littoral transport is capable of passing about ten thousand tons past a point along the shore (e.g. Short et al, 1974). The average sediment input resulting from coastal retreat is 7,300 m^3/km of shoreline. As reported earlier, the above-sealevel part of the coastal plain in the study area is composed of about 50% sand with less than 1% of gravel, the material considered in littoral transport estimates. This implies that the littoral transport system at any specific point will choke from the sand introduced from only about 3 km of updrift coastline. This further implies that either the sediment sinks are closely spaced, or other transport agents than those considered at low latitudes dominate the arctic sedimentary environment.

A lack of sediment sinks on the exposed inner shelf, and the restricted occurence of Holocene sediments within the shelter of certain lagoons, has already been discussed. Can the sediments collecting with the lagoons, and those contained within the island chains, account for the sediment input to the Beaufort Sea over geologic time scales? We take a look at Simpson Lagoon in an attempt to shed light on that question. Crude calculations comparing the present volume of the lagoon with its sediment supply indicate the basin would fill to sealevel within several hundred years. That obviously is not occuring, and therefore the lagoon over long time spans can not accomodate the sediment introduced, but is by-passing large amounts of material. The fact that the lagoon is being enlarged by erosion greatly complicates any attempts to predict even its immediate future. The lower part of figure 32 views the development of Simpson Lagoon paleo-shorelines during the last five thousand years, as interpreted by Naidu et al (1984) from bluff retreat rates. We noted previously that measurements of bluff retreat rates over short time periods are not expected to parallel shoreline retreat rates exactly, and in this case do differ from our values. The upper part of figure 32 is a present-day profile of the area, together with hypothetical profiles 1,000 yrs ago and predicted for the year 3,000, based on the regional average erosion rate of 2 m/yr. This profile evolution is intended to depict a lagoon, rather than Simpson Lagoon specifically. The profile also shows the generalized upper surface of a thick underlying unit of massive gravel specific to Simpson Lagoon. We constructed this profile from 12 soil borings in the area, as shown.

The information contained in figure 32 leads to the following observations: Even during the last five thousand years, since worldwide sealevel rise reached its present position and the transgression ended elsewhere, it continued at such a rapid rate in the arctic that lagoons must be considered as ephemeral features only. Thus even the modern deposits contained in arctic lagoon/barrier island systems can not serve as long term sediment sinks. These deposits are a flux, to be re-mobilized by the advancing sea within several thousand years. More importantly, the modern lagoon/barrier island morphology and deposits are only thin surficial features in the predicted deep-reaching profile evolution during two thousand years. This profile seaward of the islands apparently has cut a deep notch into the underlying fluvial gravel.

Since even the outer shelf is presently an area of sediment by-passing (Reimnitz et al, 1984), the ultimate depository should be the Arctic Basin floor. While deposition rates in the deep Arctic Ocean have in the past been thought to be very low, recent work by Sejrup et al (1984) suggests values many times higher.

Surficial sedimentary deposits of the coastal plain north of the Pelukian shoreline (fig. 26) are tentatively interpreted as inner shelf deposits laid down during the last marine transgression (Carter and Robinson, 1980). Similar interglacial units of up to 15 m thickness underly much of the present inner shelf (Smith, 1985), where they are being truncated by the current transgression. Thus the Holocene transgressive and erosional environment seems to contrast with depositional environments of past interglacial periods. One known difference between the last interglacial period and the present is that sealevel was 7 to 8 m higher than now. We feel that higher water level alone can not explain why marine sediments accreted in shallow water during past transgressions and were preserved. There is, however, a growing body of evidence indicating that the last interglacial transgression had warmer air and sea temperatures than today. This implies there was less sea ice. Thus Carter (1980) states the "straightness of a 250 km long barrier chain and presence of microfauna now endemic to the North Atlantic indicates that Pelukian deposits of northern Alaska formed at a time when the Beaufort Sea and channels between the Canadian Arctic islands were more open than now" (Carter, 1980). Also, studies of over 20 offshore boreholes suggest that marine deposits of Pelukian age were not disrupted by ice gouging (Peggy Smith, oral communication, 1984). Conditions during the last transgression, when glaciomarine sediments of the Flaxman Formation were deposited, are less clear. Carter (written communication, 1985) feels that Flaxman deposits may originate from a time when enormous volumes of floating glacial ice were produced by the rapid break-up of a large part of the Laurentide ice sheet. The presence of much glacial ice, and findings of fossil ribbon seal and gray whale very rarely found in the Beaufort Sea today, might also indicate warmer conditions, and possibly again less sea ice growth than at present.

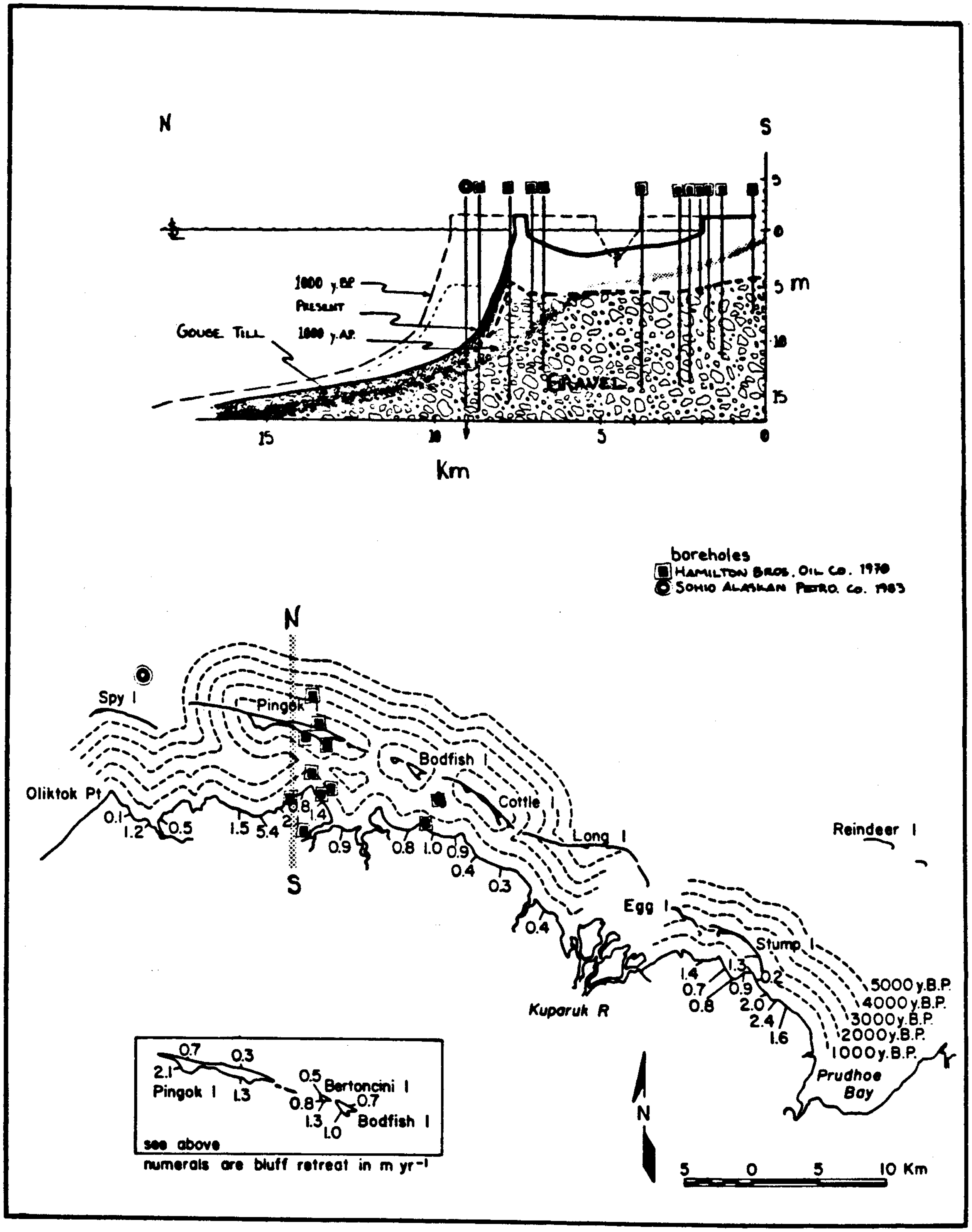

Figure 32. Simpson Lagoon paleoshorelines (after Naidu et al. 1984) and our interpretation of lagoon profile evolution. Depths to massive fluvial gravel generalized form soil borings.

Comparison with Gulf Coast erosion rates

May et al (1983) compiled information on the erosion rates for the United States shorelines. They state "the Gulf coast states have the distinction of having the most rapid average erosion rates (1.8 m/yr) on a national scale." The Texas coast is marked by lagoons bordering a flat coastal plain of poorly consolidated deposits, and recent crustal stability. This coast, eroding at an average rate of 1.2 m/yr, in many respects has a setting similar to that of the North Slope. The Beaufort Sea coast retreats at a rate almost twice that high, and average rates in the Soviet Arctic seem to be still higher (Tomirdiaro, 1975).

When considering the actual time frame in which dynamic nearshore processes act in the two different environments, a major discrepancy in erosion rates becomes evident. At lower latitudes the marine forces attacking the coasts are at work for 12 months of the year, while the arctic shoreline retreats only during three summer months. For the majority of the year, and including the period with the severest weather, the arctic shoreline is frozen and stable under a protective coat of snow and ice. Elsewhere during this period the greatest coastal damage is done. Using a common denominator in our comparisons of Texas and North Slope erosion rates, we find that the latter is a minimum of 8 times higher. This raises the fundamental question: What mechanisms or forces make the arctic coastal environment more erosive than that of lower latitudes?

Sea ice as erosion agent?

Some workers have attributed the high erosion rates, and even the characteristic shelf profile of the arctic largely to thermal processes. In this study we have shown that besides thaw settlement, much mechanical energy is required to transport away large sediment volumes to account for the maintenance of the present shelf profile with coastal retreat.

Wave energy in the classical sense can not account for the rapid erosion of the coast and shelf. Published sediment transport estimates for the littoral zone do not account for the action of ice. Floating ice wallowing in a wave train and currents along the shoreface results in sediment movement. Reimnitz and Kempema (1982) have demonstrated the formation of large, irregular hydraulic bedforms resulting from the interaction of waves and currents with ice touching the seafloor to at least 10 m water depth. But net sediment transport has not been quantified. Computations of toe protection required around a hypothetical cone drilling structure under assumed wave and current conditions in the Arctic predict the erosion of gravel size sediment out to 20 m water depth (Kobayashi, 1981). The effects of ice keels in bottom contact or even barely skimming the sea bed without actually going aground should be similar. Thus sediment erosion from hydraulic processes as a result of flow interaction with ice keels probably extends far beyond the 20-m isobath. In two separate studies we have shown that bedload movement is rapid far beyond the surf zone. In one study bedload transport at 9 m^3 yr^{-1} was measured at a distance of about 4 km from shore (Reimnitz and Kempema, 1983). This was assumed shore-parallel, but may have an offshore component. In another study, involving repetitive surveys to monitor ice gouging rates in Harrison Bay, Barnes and Reimnitz (1979) report fall storms obliterated all gouges from the shore to 13 m water depth, at a distance of 15 km from land. Here also, extensive sand movement occured. The mechanism by which the sediments were moved are unclear, but we suspect that not storm waves but rather underwater ice formation (frazil and anchor ice) may play a role. Frazil ice formation during fall storms certainly is involved in the incorporation of large volumes of fine sediment into the seasonal ice canopy in some years Barnes et al (1982); Osterkamp and Gosink (1984). During the winters 1978 and 1979 the sediment-laden ice extended out to the stamukhi zone, with concentrations of 243 t/km^2 and 800 t/km^2 respectively (Barnes et al, 1982). According to rough calculations the area between the coast and the stamukhi zone, as mapped by Reimnitz et al (1978), covers 3,290 km^2 in the study region. Thus the ice canopy held .79 x 10^6 tons in 1978, and 2.6 x 10^6 in 1979. In the first of the two winters the sediment was composed mainly of silt and clay, but sediment samples collected from the ice in 1979 contained up to 30 % sand. Sediment weights held suspended by the winter ice canopy therefore are significant in terms of the overall sediment budget. However, since most of the sediment is released locally to the water column during the following summer melt, rafting of sediment introduced into the fast ice by fall storms can not account for all of the sediment eroded. During fall storms and the actual production of frazil ice the inner shelf waters may be flowing at a rate of over two knots for several days. We believe this may be the time when most sediment is transported away from the region.

CONCLUSION

The effects of wave base on the dynamic equilibrium profile (Moore and Curray, 1964) are probably unimportant in this environment of drifting pack and short fetches. The over-riding controls most likely are "ice-base" and related processes. Our findings, however, do not help explain the problem of widespread occurrence of erosional platforms in wave-protected, rocky, cold-climate shorelines (Trenhaile, 1983). We believe that the effects of pack ice on the shaping of the shelf profile probably is restricted to weakly consolidated sediments, where each ice impact, however light, loosens material and produces a visible surface expression. The loosened material is winnowed by waves and currents, aided by such unique arctic processes as strudel scour, ice wallowing, and rafting by frazil- and anchor-ice. Lastly, there is the bulk displacement of sediment by the bulldozing action of ice, directed mainly westward and slightly onshore. But much work needs to be done, under conditions which man has not yet learned to cope with, before a basic understanding of arctic erosion and transport mechanisms can be achieved.

ACKNOWLEDGEMENTS

We received much information and help from S. Rawlinson in the initial stages of this study, and thank him for sharing his data. Personal insights of P. Sellmann broadened the scope of this investigation. His constructive criticism and review, together with those by D. Inman and D. Hopkins are gratefully acknowledged. L. Gaydos and W. Acevedo were instrumental in providing us with enhanced Landsat imagery for figure 20. J. Dailey helped to determine the vintage of data sets used in delineation of the coastline in the original base maps. A. Kovacs provided us with several photos from key localities in the study area.

This study was funded in part by the Minerals Management Service through interagency agreement with the National Oceanic and Atmospheric Administration, as part of the Outer Continental Shelf Environmental Assessment Program.

REFERENCES

Arden, R.S. and Wigle, T.S., 1972, Dynamics of ice formation in the upper Niagara River, *in* International Symposium on the Role of Snow and Ice in Hydrology, Banff, Alberta: v. 2, UNESCO-WMO- IHAS, p. 1296-1313.

Arnborg, L., Walker, H.J., and Peippo, J., 1967, Suspended load in the Colville River, Alaska, 1962: Geografiska Annaler, v. 49 Series A, no. 2-4, p. 131-144.

Barnes, P.W., McDowell, D., and Reimnitz, Erk, 1978, Ice gouging characteristics: Their changing patterns from 1975-1977, Beaufort Sea, Alaska: U.S. Geological Survey Open-File Report 78-730, p. 42.

Barnes, P.W., Rearic, Douglas M., and Reimnitz, Erk, 1984, Ice gouging characteristics and processes, *in* Barnes, P.W., Schell, D.M., and Reimnitz, Erk (eds.) The Alaskan Beaufort Sea: Ecosystems and Environments: Academic Press Inc., Orlando, Florida, p. 185-212.

Barnes, P.W., Reimnitz, Erk, Smith, G., and Melchior, J., 1977, Bathymetric and shoreline changes, northwestern Prudhoe Bay, Alaska: U.S. Geological Survey Open-File Report 77-167, p. 15.

Barnes, P. W. and Reimnitz, Erk, 1973, The shore fast ice cover and its influence on the currents and sediment along the coast of northern Alaska: EOS, American Geophysical Union, v. 54, p. 1108.

Barnes, P. W. and Reimnitz, Erk, 1974, Sedimentary processes on arctic shelves off the northern coast of Alaska, *in* Reed, J.C. and Slater, J.E (eds.) The Coast and Shelf of the Beaufort Sea: The Arctic Institute of North America, Arlington, Va, p. 439-476.

Barnes, P. W. and Reimnitz, Erk, 1979, Ice gouge obliteration and sediment redistribution event; 1977-1978, Beaufort Sea, Alaska: U.S. Geological Survey Open-File Report 79-848, p. 28.

Barnes, P. W., 1982, Marine ice-pushed boulder ridge: Arctic, v. 35, no. 2, p. 312-316.

Black, R.E. and Barksdale, W.E., 1949, Oriented lakes of northern Alaska: Journal of Geology, v. 57, p. 105-118.

Black, R.F., 1964, Gubik Formation of Quaternary age in northern Alaska: U.S. Geological Survey, Professional Paper 302-C, p. 59- 91.

Brigham, J. K., Hopkins, D. M., Carter, L. D., and Miller, G. H., 1980, Application of amino acid geochronology to deposits of the arctic coastal plain, Alaska: preliminary results and implications, *in* Proceedings of the ninth annual Arctic Workshop, April 4 and 5, 1980: INSTAAR, University of Colorado, Boulder, Co., p. 34-35.

Bruun, Per, 1962, Sea level rise as cause of shore erosion: American Society of Civil Engineers Proceedings, Journal of the Waterways and Harbors Division, v. 88, no. WW1, p. 117-130.

Cannon, P.J. and Rawlinson, S.E., 1978, The environmental geology and geomorphology of the barrier island-lagoon system along the Beaufort Sea coastal plain from Prudhoe Bay to the Colville River: U.S. Department of Commerce, National Oceanic and Atmospheric Administration, Boulder, Co, .

Cannon, P.J., 1979, The environmental geology and geomorphology of the barrier island-lagoon system along the Beaufort Sea coastal plain, *in* Environmental Assessment of the Alaskan Continental Shelf, Annual Reports: v. 10, p. 209-248.

Carson, C.E. and Hussey, K.M., 1959, The multiple-working hypothesis as applied to Alaska's oriented lakes: Proceedings of the Iowa Academy of Sciences, v. 66, p. 334-349.

Carson, C.E and Hussey, K.M., 1962, The oriented lakes of arctic Alaska: Jounal of Geology, v. 70, p. 417-439.

Carter, David L., 1983, Cenozoic glacial and glaciomarine deposits of the central north slope, Alaska, *in* Thorson, R.M. and Hamilton, T.D. (eds.) Glaciation in Alaska: extended abstracts from a workshop, Occasional Paper: Alaskan Quaternary Center, University of Alaska Museum, Fairbanks, Alaska, p. 17-21.

Carter, L. David and Robinson, Stephen W., 1980, Minimum age of beach deposits north of Teshekpuk Lake, Alaskan arctic coastal plain: U.S. Geological Survey in Alaska, Accomplishments during 1979, Geological Survey Circular 823-B, p. B8-B9.

Curray, J.R., 1964, Transgressions and regressions, *in* Miller, R.L. (ed.) Papers in marine geology-Shepard Commemorative Volume: McMillan Company, New York, p. 175-203.

Dionne, J.C., 1973, La notion de pied de glace (icefoot), en particulier dans l'estuaire du Saint-Laurent: Cahiers de Geographie de Quebec, v. 17, no. 41, p. 221-250.

Dunton, Kenneth H., Reimnitz, Erk, and Schonberg, Susan, 1982, An arctic kelp community in the Alaskan Beaufort Sea: Arctic, v. 35, no. 4, p. 465-484.

Dygas, J.A. and Burrell, D.C., 1976, Dynamic sedimentological processes along the Beaufort Sea coast of Alaska, *in* Assessment of the Arctic Marine Environment: Selected Topics: Institute of Marine Sciences, University of Alaska, Fairbanks, Alaska, p. 189-203.

Dygas, J.A., Tucker, R., and Burrell, D.C., 1972, Geologic report of the heavy minerals, sediment transport, and shoreline changes of the barrier islands and coast between Oliktok Point and Beechey Point, *in* Kinney, P.J. and others (eds.), Baseline Data Study of the Alaskan Arctic Aquatic Environment; University of Alaska International Marine Sciences Report R-72-3: p. 62-121.

Forbes, D.L., 1981, Babbage River delta and lagoon: hydrology and sedimentology of an arctic estuarine system (unpublished Ph.D. dissertation): Department of Geography, University of British Columbia, Vancouver B.C., 554 p.

Harper, J.R., Owens, E.H., and Jr., W.J. Wiseman, 1978, Arctic beach processes and the thaw of ice-bonded sediments in the littoral zone, *in* Proceedings of the 3rd International Permafrost Conference: National Academy of Sciences, Washington, D.C., p. 195-199.

Harper, J.R., 1978, The physical processes affecting the stability of tundra cliff coasts (unpublished Ph.D. thesis): Department of Marine Sciences, Louisiana State University, Baton Rouge, LA., 212 p.

Harrison, W. D. and Osterkamp, T. E., 1981, Subsea permafrost: probing, thermal regime and data analysis: Environmental Assessment of the Alaskan Continental Shelf, Annual Reports of Principal Investigators for the year, U.S. Department of Commerce, v. 7: Hazards, p. 291-350.

Hartz, R.W., 1978, Erosional hazards map of the arctic coast of the National Petroleum Reserve, Alaska: U.S. Geological Survey Open-File Report 78-406, 8 p.

Hodel, Karen, 1985, Microfeatures of quartz grains from modern Arctic terrestrial and subaqueous environments, North Slope, Alaska: (unpublished Master's Thesis), University of California, Berkeley, 69 p, .

Holmquist, Charlotte, 1978, Lakes of polar regions: age, complexity, and trophic state: Proceedings of the International Association of Theoretical and Applied Limnologists, v. 20, no. 1, p. 615-617.

Hopkins, D.M. and Carter, L.D., 1980, Discrepancy in correlation of transgressive marine deposits of Alaska and the eastern arctic, *in* Proceedings of the 9th Annual Arctic Workshop: INSTAAR, University of Colorado, Boulder, Colorado, p. 12-13.

Hopkins, D.M. and Hartz, R.W., 1978, Coastal morphology, coastal erosion and barrier islands of the Beaufort Sea, Alaska: U.S. Geological Survey Open-File Report 78-1063, 54 p.

Hume, J.D. and Schalk, M., 1964, The effects of ice push on Arctic beaches: American Journal of Science, v. 262, p. 267-273.

Inman, D. L. and Brush, B. M., The coastal challenge: Science, v. 181, p. 20-32.

Inman, D. L. and Chamberlain, T. K., 1960, Littoral sand budget along the southern California coast, *in* Report of the Twenty-first International Geological Congress abstracts: Copenhagen.

Klyuyev, Ye. V., 1965, The role of permafrost factors in the dynamics of bottom topography in polar seas: Oceanology of the Academy of Sciences of the U.S.S.R., v. 5, no. 1, p. 78-83.

Kobayashi, Nobuhisa, Vivatrat, Vitoon, Watt, Brian, Madsen, Ole S., and Boaz, Irvin B., 1981, Erosion prediction for exploration and production structures in the arctic: Offshore Technology Conference, 13th annual meeting, Houston, Texas, v. OTC paper 4114.

Kovacs, Austin, 1983, Shore ice ride-up and pile-up features, Part I: Alaska's Beaufort Sea coast: CRREL Report 83-9, U.S. Army Corp of Engineers, Hanover, New Hampshire, 59 p.

Kovacs, Austin, 1984, Shore ice ride-up and pile-up features, Part II: Alaska Beaufort Sea coast - 1983 and 1984: CRREL Report 84-26, U.S. Army Corps of Engineers, Hanover, New Hampshire, 29 p.

Lachenbruch, Arthur T., Sass, J.H., Marshall, B.V., and Moses, T.H. Jr., 1982, Permafrost, heat flow, and the geothermal regime at Prudhoe Bay, Alaska: Journal of Geophysical Research, v. 87, no. B11, p. 9301-9316.

Lachenbruch, Arthur T., 1985, Temperature and Depth of Permafrost on North Slope, Alaska: American Association of Petroleum Geologists, Bulletin, v. 69, no. 4, p. 667-668.

Lee, Homa J. and Winters, William J., 1984, Strength and consolidation properties of stiff Beaufort Sea sediment, *in* Proceedings, Arctic Energy Technologies Workshop, November 14-15, 1984: U.S. Department of Energy, Office of Fossil Energy Morgantown Energy Technology Center, Morgantown, West Virginia, 10 p, .

Leffingwell, E. deK., 1919, The Canning River region, northern Alaska: U.S. Geological Survey Professional Paper 109, 251 p.

Lewellen, R.I., 1977, , A study of Beaufort Sea coastal erosion, northern Alaska; Published by the author: , P.O. Box 2435, Littleton Co.

Livingstone, D.A., 1954, On the orientation of lake basins: American Journal of Science, v. 252, p. 547-554.

Martin, Seelye, 1981, Frazil ice in rivers and oceans, *in* Annual Reviews of Fluid Mechanics: v. 13, Annual Reviews Inc., p. 379- 397.

Matthews, J.B., 1981, Circulation in the Sale 71 area, *in* Norton, D.W and Sackinger, W.M. (eds.), Beaufort Sea Sale 71 Synthesis Report: U.S. Department of Commerce, National Oceanic & Atmospheric Administration, Boulder, Co, p. 71-178.

May, S. Kimball, Dolan, Robert, and Hayden, Bruce P., 1983, Erosion of U.S. shorelines: EOS, Transactions, American Geophysical Union, p. 521-522.

McDonald, B.C. and Lewis, C.P., 1973, Geomorphic and sedimentologic processes of rivers and coasts, Yukon coastal plain: Environmental-Social Communication, Northern Pipeline, Task Force on Northern Oil Development, Report 73-79, 245 p.

McLaren, Patrick, 1982, The coastal geomorphology, sedimentology and processes of eastern Melville and western Byam Martin Islands, Canadian Arctic archipelago: Geological Survey of Canada, Commission Geologique du Canada, Bulletin, no. 333.

Moore, David G. and Curray, Joseph R., 1964, Wave-base, Marine Profile of Equilibrium and Wave-built Terraces: Discussion: Geological Society of America Bulletin, no. 75, p. 1267-1273.

Moore, J. Robert, Buck, Beaumont, Gerwick, Ben C. Jr., Judge, Alan S., Lewis, C. F. Michael, Runge, Karl H., Sellmann, Paul V., and Watt, Brian J., 1982, Understanding the arctic sea floor for engineering purposes: Committe on Arctic Seafloor Engineering, Marine Board Commission on Engineering and Technical Systems, National Research Council, National Academy Press, Washington, D.C.

Morack, J.L. and Rogers, J.C., 1981, Seismic evidence of shallow permafrost beneath islands in the Beaufort Sea, Alaska: Arctic, v. 34, no. 2, p. 169-174.

Naidu, A. S., Mowatt, T. C., Rawlinson, Stuart E., and Weiss, Herbert V., 1984, Sediment characteristics of the lagoons of the Alaskan Beaufort Sea coast and evolution of Simpson Lagoon, *in* Barnes. P.W., Schell, D.M., Reimnitz, Erk (eds.), The Alaskan Beaufort Sea: Ecosystems and Environments: Academic Press Inc., Orlando, Florida, p. 275-292.

Naidu, A. S. and Mowatt, T. C., 1983, Sources and dispersal patterns of clay minerals in surface sediments from the continental shelf areas off Alaska: Geological Society of America Bulletin, v. 94, p. 841-854.

Nummedal, D., 1979, Coarse-grained sediment dynamics - Beaufort Sea, Alaska., *in* Proceedings of port and ocean engineering under arctic conditions: Norwegian Institute of Technology, p. 845-858.

Osterkamp, T.E. and Gosink, Joan P., 1984, Observations and analyses of sediment laden sea ice, *in* Barnes, P.W., Schell, D.M., and Reimnitz, Erk (eds.), The Alaskan Beaufort Sea: Ecosystems and Environments: Acadaemic Press Inc., Orlando, Florida, p. 73-94.

Osterkamp, T.E., 1978, Frazil ice formation: a review: Journal of the Hydraulics Division, ASCE, v. 104, no. HY9, p. 1239-1255.

Owens, E. H., Harper, J. R., and Nummedal, D., 1980, Sediment transport processes and coastal variability on the Alaskan North Slope, *in* Proceedings of the 17th International Coastal Engineering Conference: ASCE, Sydney, Australia, p. 1344-1363.

Owens, E.H. and Harper, J.R., 1977, Frost-table and thaw depth in the littoral zone near Peard Bay, Alaska: Arctic, v. 30, no. 3, p. 155-168.

Owens, E.H., 1982, Ice foot, *in* Schwarts, M.L. (ed.), Encyclopedia of Beaches and Coastal Environments: Hutchinson Ross Publishing Co., Stroudsburg, Pa., p. 480-481.

Reimnitz, Erk and Barnes, P.W., 1974, Sea ice as a geologic agent on the Beaufort Sea shelf of Alaska, *in* Reed. J.C. and Slater, J.E. (eds.), The Coast and Shelf of the Beaufort Sea. Proceedings of the Arctic Institute of North America Symposium on Beaufort Sea and Shelf Research: Arctic Institute of North America, Arlington, Va., p. 301-353.

Reimnitz, Erk and Bruder, K.F., 1972, River discharge into an ice-covered ocean and related sediment dispersal, Beaufort Sea, coast of Alaska: Geological Society of America Bulletin, v. 83, no. 3, p. 861-866.

Reimnitz, Erk and Kempema, E.W., 1982, Dynamic ice-wallow relief in northern Alaska's nearshore: Journal of Sedimentary Petrology, v. 52, no. 2, p. 451-462.

Reimnitz, Erk and Kempema, E.W., 1983, High rates of bedload transport measured from the infilling rate of large strudel-scour craters in the Beaufort Sea, Alaska: Continental Shelf Research, v. 1, no. 3, p. 237-251, plus erratum in next issue for missing page.

Reimnitz, Erk and Maurer, D.K., 1979, Effects of storm surges on the Beaufort Sea coast, northern Alaska: Arctic, v. 32, no. 4, p. 329-344.

Reimnitz, Erk, Toimil, L.J., and Barnes, P.W., 1978, Arctic continental shelf morphology related to sea-ice zonation, Beaufort Sea, Alaska: Marine Geology, v. 28, p. 179-210.

Rex, R.W., 1961, Hydrodynamic analysis of circulation and orientation of lakes in northern Alaska: Geol. Arct., v. 2, p. 1021-1043.

Rosen, Peter S., 1978, A regional test of the "Bruun Rule" on shoreline erosion: Marine Geology, v. 26, p. M7-M16.

Rosen, Peter S., 1978, Predicting beach erosion as a function of rising water level: Discussion: Journal of Geology, v. 86, no. 6, p. 763-764.

Schwartz, Maurice L., 1967, The "Bruun Theory" of sea-level rise as a cause of shore erosion: Journal Of Geology, v. 75, no. 1, p. 76-92.

Sejrup, Hans Peter, Miller, Gifford H., Brigham-Grette, Julie, Lovlie, Reidar, and Hopkins, David, 1984, Amino acid epimerization implies rapid sedimentation rates in Arctic Ocean cores: Nature, v. 310, p. 772-775.

Sellmann, P. V., Brown, J., Lewellen, R., McKim, H., and Merry, C., 1975, The classification and geomorphic implications of thaw lakes on the arctic coastal plain, Alaska: CRREL Research Report 344, U.S. Army Corp of Engineers, Hanover, New Hampshire, 21 p.

Sellmann, P.V., Weeks, W.F., and Campbell, W.J., 1975, Use of side-looking airborne radar to determine lake depth on the Alaskan North Slope, *in* Cold Regions Research and Engineering Laboratory, Special Report 230, 6 p: .

Short, A. D., Coleman, J. M., and Wright, L. D., 1974, Beach dynamics and nearshore morphology of the Beaufort Sea coast, Alaska, *in* Reed, J.C. and Sater, J.E. (eds.) The Coast and Shelf of the Beaufort Sea,: The Arctic Institute of North America, Arlington, Va, p. 477-488.

Smith, Peggy, 1985, Late Quaternary Geology of the Beaufort Sea Inner Shelf near Prudhoe Bay, *in* Bartch-Winkler, S. and Reed, K.M. (eds.), U.S. Geological Survey Circular 945, Accomplishments during 1983, p 100-103.

Swift, Donald J. P., 1968, Coastal erosion and transgressive stratigraphy: Journal of Geology, v. 76, p. 444-456.

Taylor, R.B., 1980, Beach thaw depth and the effect of ice-bonded sediment on beach stability, *in* Proceedings of the Canadian Coastal Conference, Burlington, Ontario, April 22-24, 1980: p. 103-121.

Tedrow, J.C.F., 1969, Thaw lakes, thaw sinks and soils in northern Alaska: Biuletyn Peryglacjalny, v. 20, p. 337-344.

Tomirdiaro, S.V., 1975, Thermo abrasion-induced shelf formation in the eastern arctic seas of the USSR during the Holocene: DOKLADY, Earth Science Sections, v. 219, no. 1-6, p. 23-26.

Trenhaile, A.S., 1983, The development of shore platforms in high latitudes, in Smith, D.E. and Dawson, A.G. (eds.), Shorelines and Isostacy: Academic Press Inc., New York, NY, p. 77-93.

Tsang, Gee, 1982, Frazil and anchor ice: a monograph: NRC Subcommittee on hydraulics of ice covered rivers, Ottawa, Ontario, Canada, 90 p.

Weeks, W.F. and Weller, G., 1984, Offshore oil in the Alaskan Arctic: Science, v. 225, no. 4660, p. 371-378.

Weller, M.W. and Derksen, D.V., 1979, The geomorphology of Teshekpuk Lake in relation to coastline configuration of Alaska's coastal plain: Arctic, v. 32, no. 2, p. 152-160.

Williams, J.R., Yeend, W.E., Carter, L.D., and Hamilton, T.D., 1977, Preliminary surficial deposit map of National Petroleum Reserve: U.S. Geological Survey Open-File Report 77-868.

Winant, Clinton D., Inman, Douglas L., and Nordstrom, Charles E., 1975, Description of seasonal beach changes using empirical eigenfunctions: Journal of Geophysical Research, v. 80, no. 15, p. 19-79.

Wiseman, W.J., Coleman, J.M., Gregory, A., Short, A.D., Suhayda, J.N., Walters, C.D., and Wright, L.D., 1973, Alaskan arctic coastal processes and morphology: Techical Report, 149, Louisiana State University, Baton Rouge, LA., 171 p.

Wolf, S.C., Reimnitz, Erk, and Barnes, P.W., 1985 (in press), Pleistocene and Holocene Seismic Stratigraphy between the Canning River and Prudhoe Bay, Alaska: U.S. Geological Survey Open-File Report, 26 p.

APPENDIX (individual sector tabulations)

SECTOR # 1 Length: 19 km Average Retreat Rate: 8.3 m/yr

Segment	Onshore				Offshore				Totals	
No.	H	C	vi	v1	θ°	w	t	v2	volume	tons
1	4.0	150	300000	246000	0.23	500	0.60	128000	374000	707000
2	4.0	230	460000	380000	0.19	600	0.77	186000	566000	1070000
3	4.0	240	480000	394000	0.14	800	0.60	204000	598000	1130000
4	4.0	230	460000	380000	0.14	800	0.57	197000	577000	1090000
5	4.0	230	460000	380000	0.13	850	0.54	199000	579000	1094000
6	4.0	220	440000	360000	0.13	850	0.52	191000	551000	1041000
7	4.0	210	420000	344000	0.14	800	0.52	182000	526000	994000
8	4.0	220	440000	360000	0.15	750	0.59	188000	548000	1036000
9	4.0	300	600000	492000	0.16	700	0.86	236000	728000	1376000
10	4.0	350	700000	574000	0.19	600	1.17	248000	822000	1554000
11	4.0	380	760000	623000	0.29	400	1.90	199000	822000	1554000
12	4.0	300	600000	492000	0.25	450	1.33	200000	692000	1308000
13	4.0	280	560000	459000	0.29	400	1.40	182000	641000	1211000
14	4.0	230	460000	377000	0.25	450	1.00	171000	548000	1036000
15	4.0	300	600000	492000	0.25	450	1.33	200000	692000	1308000
16	4.0	350	700000	574000	0.25	450	1.56	214000	788000	1489000
17	4.0	400	800000	656000	0.23	500	1.60	240000	896000	1693000
18	4.0	480	960000	787000	0.25	450	2.13	224000	1011000	1911000
19	4.0	450	900000	738000	0.33	350	2.57	161000	899000	1699000
20	4.0	350	700000	574000	0.36	320	2.19	159000	733000	1385000
21	3.5	360	630000	498000	0.33	350	2.06	175000	673000	1272000
22	3.0	330	495000	376000	0.29	400	1.65	194000	570000	1077000
23	3.0	300	450000	342000	0.25	450	1.33	200000	542000	1024000
24	2.0	280	280000	196000	0.22	510	1.10	203000	399000	754000
25	2.0	280	280000	196000	0.19	600	0.93	215000	411000	777000
26	2.0	200	200000	140000	0.18	650	0.62	169000	309000	584000
27	2.0	210	210000	147000	0.18	650	0.65	176000	323000	610000
28	2.0	200	200000	140000	0.16	700	0.57	171000	311000	588000
29	2.0	160	160000	112000	0.16	700	0.46	142000	254000	480000
30	2.0	180	180000	124000	0.19	600	0.60	153000	277000	524000
31	2.0	270	270000	189000	0.25	450	1.20	189000	378000	714000
32	2.0	270	270000	189000	0.29	400	1.30	179000	368000	696000
33	2.0	190	190000	133000	0.23	500	0.76	154000	287000	542000
34	2.0	170	170000	119000	0.19	600	0.57	146000	265000	501000
35	2.0	140	140000	98000	0.20	580	0.48	123000	221000	418000
36	2.0	120	120000	84000	0.19	600	0.40	108000	192000	363000
37	2.0	50	50000	35000	0.19	600	0.17	48000	83000	157000
38	2.0	0	0	0	0.20	580	0	0	0	0
TOTALS ($x10^3$) :			16095	12800				6654	19454	36767

SECTOR # 2   Length: 12.5 km   Average Retreat Rate: 1.3 m/yr

Segment No.	Onshore H	C	vi	v1	Offshore θ°	w	t	v2	Totals volume	tons
1	1.5	0	0	0	0.23	500	0	0	0	0
2	1.5	20	15000	10000	0.29	400	0.10	19000	29000	55000
3	1.5	50	38000	25000	0.38	300	0.33	46000	71000	134000
4	1.5	100	75000	49000	0.46	250	0.80	80000	129000	244000
5	1.5	110	82000	53000	0.57	200	1.10	80000	133000	251000
6	1.5	90	68000	44000	0.55	210	0.86	71000	115000	217000
7	1.5	30	22000	14000	0.55	210	0.29	28000	42000	79000
8	1.5	30	22000	14000	0.67	170	0.35	27000	41000	77000
9	3.0	0	0	0	0.57	200	0	0	0	0
10	1.5	20	15000	10000	0.55	210	0.19	19000	29000	55000
11	0.4	60	12000	8000	0.88	130	0.92	46000	54000	102000
12	0.4	100	0	0	2.29	50	4.00	25000	25000	47000
13	0.4	80	0	0	1.64	70	2.29	24000	24000	45000
14	0.4	100	20000	13000	3.81	30	6.65	15000	28000	53000
15	1.5	60	45000	29000	3.81	30	3.99	15000	44000	83000
16	1.5	0	0	0	0.95	120	0	0	0	0
17	0.4	20	4000	3000	1.15	100	0.40	18000	21000	40000
18	0.4	120	24000	16000	3.81	30	7.98	15000	31000	59000
C 19	0.4	0	0	0	1.60	270	7.54	270000	270000	510000
C 20	0.4	0	0	0	1.60	270	7.54	270000	270000	510000
C 21	0.4	0	0	0	1.60	270	7.54	270000	270000	510000
C 22	0.4	0	0	0	1.60	270	7.54	270000	270000	510000
C 23	0.4	0	0	0	1.60	270	7.54	270000	270000	510000
24	1.5	20	15000	10000	0.36	150	0.13	19000	29000	55000
D 25	0.4	+20	0	0	0.36	320	0.06	+21000	+21000	+40000
TOTALS ($x10^3$) :			457	298				1876	2174	4106

SECTOR # 3   Length: 6 km   Average Retreat Rate: 7.8 m/yr

Segment No.	Onshore H	C	vi	v1	Offshore θ°	w	t	v2	Totals volume	tons
1	3.0	100	150000	114000	0.11	1000	0.20	95000	209000	395000
2	1.5	300	270000	176000	0.11	1000	0.60	255000	431000	815000
3	1.5	450	422000	274000	0.09	1200	0.75	366000	640000	1210000
4	1.5	280	240000	156000	0.09	1300	0.43	250000	406000	767000
5	1.5	40	30000	20000	0.07	1500	0.05	395000	415000	784000
6	1.5	100	76000	49000	0.05	2200	0.09	98000	147000	278000
7	1.5	220	166000	108000	0.05	2200	0.02	209000	317000	599000
8	1.5	270	167000	109000	0.04	2400	0.18	200000	309000	584000
9	1.5	300	245000	159000	0.05	2200	0.27	280000	439000	830000
10	1.5	190	152000	99000	0.06	2000	0.19	181000	280000	529000
11	1.5	310	245000	159000	0.05	2200	0.28	288000	447000	845000
12	1.5	200	160000	104000	0.06	2000	0.20	190000	294000	556000
TOTALS ($x10^3$) :			2323	1527				2807	4334	8192

SECTOR # 4   Length: 11 km   Average Retreat Rate: Pogik Bay ~0.4 m/yr, barrier ~7.3 m/yr

Segment	Onshore				Offshore				Totals	
No.	H	C	vi	vl	$\theta°$	w	t	v2	volume	tons
D 1	1.5	+70	+52000	+52000	0	0	0	0	+52000	+98000
D 2	1.5	+100	+75000	+75000	0	0	0	0	+75000	+142000
D 3	1.5	+80	+60000	+60000	0	0	0	0	+60000	+113000
D 4	1.5	+120	+90000	+90000	0	0	0	0	+90000	+170000
5	1.5	0	0	0	0	0	0	0	0	0
D 6	2.0	+60	+60000	+60000	0	0	0	0	+60000	+113000
7	2.0	0	0	0	0	0	0	0	0	0
8	2.0	0	0	0	0	0	0	0	0	0
9	2.0	20	20000	14000	0	0	0	0	14000	26000
10	1.5	70	52000	34000	0	0	0	0	34000	64000
11	1.5	100	75000	49000	0	0	0	0	49000	93000
12	1.5	130	98000	64000	0	0	0	0	64000	121000
13	1.5	120	90000	59000	0	0	0	0	59000	112000
14	1.5	120	90000	59000	0	0	0	0	59000	112000
15	1.5	130	98000	64000	0	0	0	0	64000	121000
16	1.5	170	127000	83000	0	0	0	0	83000	157000
17	1.5	200	150000	98000	0	0	0	0	98000	185000
18	1.5	200	150000	98000	0	0	0	0	98000	185000
D 19	0.2	+100	+10000	+10000	0.06	2000	0.10	+95000	+105000	+198000
D 20	0.2	+300	+30000	+30000	0.05	2200	0.26	+298000	+328000	+620000
21	0.2	0	0	0	0.05	2200	0	0	0	0
D 22	0.2	+200	+20000	+20000	0.06	2000	0.21	+201000	+221000	+418000
C Offshore input for migrating barrier at bay mouth :								1972000	1972000	3727000
TOTALS ($x10^3$) :			553	225				1378	1603	3030

SECTOR # 5 Length: 22.5 km Average Retreat Rate: 7.4 m/yr

Segment No.	Onshore H	C	vi	v1	Offshore θ°	w	t	v2	Totals volume	tons
D 1	0.2	+80	+8000	+8000	0.07	1600	0.10	+78000	+86000	+163000
2	2.0	100	100000	70000	0.08	1500	0.13	97000	167000	316000
3	2.0	70	70000	49000	0.06	2000	0.07	69000	118000	223000
4	2.0	100	100000	70000	0.05	2100	0.10	98000	168000	318000
5	2.0	250	250000	175000	0.05	2200	0.23	236000	411000	777000
6	2.0	500	500000	350000	0.07	1600	0.63	422000	772000	1459000
7	2.0	480	480000	366000	0.08	1500	0.64	403000	769000	1453000
8	3.0	300	450000	342000	0.08	1500	0.40	270000	612000	1157000
9	2.0	160	160000	122000	0.08	1400	0.23	151000	273000	516000
10	2.0	120	120000	84000	0.08	1500	0.16	115000	199000	376000
11	2.0	110	110000	77000	0.08	1500	0.15	106000	183000	346000
12	2.0	140	140000	98000	0.10	1200	0.23	132000	230000	435000
13	3.0	60	90000	68000	0.09	1300	0.09	59000	127000	240000
14	2.0	110	110000	77000	0.11	1000	0.22	104000	181000	342000
15	3.0	100	150000	114000	0.13	860	0.23	95000	209000	395000
16	2.0	180	180000	126000	0.16	700	0.51	157000	283000	535000
17	4.0	210	420000	344000	0.11	1000	0.42	188000	532000	1006000
18	2.0	340	340000	238000	0.10	1100	0.62	287000	525000	992000
19	2.0	410	410000	287000	0.11	1000	0.88	326000	613000	1159000
20	2.0	400	400000	280000	0.11	1000	0.80	320000	600000	1134000
21	2.0	280	280000	196000	0.15	980	0.57	240000	436000	824000
22	4.0	300	600000	492000	0.13	900	0.67	250000	742000	1402000
23	2.0	260	260000	182000	0.13	900	0.58	222000	404000	764000
24	2.0	250	250000	175000	0.13	900	0.56	215000	390000	737000
25	3.0	130	195000	148000	0.10	1100	0.24	122000	270000	510000
26	3.0	110	165000	125000	0.10	1100	0.20	104000	229000	433000
27	2.0	120	120000	84000	0.10	1100	0.22	113000	197000	372000
28	2.0	250	250000	175000	0.11	1000	0.50	219000	394000	745000
29	2.0	300	300000	210000	0.12	960	0.62	253000	463000	875000
30	3.0	300	450000	342000	0.12	980	0.61	254000	596000	1126000
31	3.0	300	450000	342000	0.16	990	0.60	255000	597000	1128000
32	2.0	260	260000	182000	0.12	970	0.54	225000	407000	769000
33	2.0	310	310000	217000	0.13	900	0.69	257000	474000	896000
34	2.0	400	400000	280000	0.16	720	1.11	289000	569000	1075000
35	3.0	400	600000	456000	0.19	600	1.33	267000	723000	1367000
36	2.0	300	300000	210000	0.19	600	1.00	225000	435000	822000
37	2.0	250	250000	175000	0.24	480	1.04	185000	360000	680000
38	2.0	120	120000	84000	0.23	500	0.48	106000	190000	359000
39	3.0	80	120000	91000	0.16	700	0.23	75000	166000	314000
40	3.0	70	105000	80000	0.13	900	0.16	67000	147000	278000
41	3.0	100	150000	114000	0.11	1000	0.20	95000	209000	395000
42	1.0	100	50000	30000	0.09	1300	0.15	96000	126000	238000
43	1.0	200	100000	60000	0.08	1500	0.27	187000	247000	467000
44	1.0	370	185000	111000	0.08	15000	0.50	324000	435000	822000
45	1.0	400	200000	120000	0.06	2000	0.40	360000	480000	907000
TOTALS ($x10^3$) :			11042	8010				8562	16572	31321

SECTOR # 6 Length: 24 km Average Retreat Rate: 2.9 m/yr

Segment	Onshore				Offshore				Totals	
No.	H	C	vi	v1	$\theta°$	w	t	v2	volume	tons
1	2.0	100	100000	70000	0.14	800	0.25	94000	164000	310000
2	3.5	130	227000	179000	0.14	820	0.32	120000	299000	565000
3	3.5	100	175000	138000	0.11	1000	0.20	95000	233000	440000
4	3.5	100	175000	138000	0.11	1000	0.20	95000	233000	440000
5	3.5	90	158000	124000	0.11	1000	0.18	86000	210000	397000
6	3.5	100	175000	138000	0.13	900	0.22	94000	232000	438000
7	3.5	110	192000	151000	0.16	700	0.31	101000	252000	476000
8	3.5	120	210000	166000	0.16	700	0.34	110000	276000	522000
9	2.0	110	110000	77000	0.14	800	0.27	102000	179000	338000
10	2.0	130	130000	91000	0.13	850	0.31	120000	211000	399000
11	2.0	140	140000	98000	0.13	850	0.33	1128000	1226000	2317000
12	3.0	110	165000	125000	0.13	900	0.24	103000	228000	431000
13	3.0	100	150000	114000	0.12	940	0.21	95000	209000	395000
14	3.5	80	140000	111000	0.12	920	0.17	77000	188000	355000
15	3.5	50	88000	70000	0.13	910	0.11	49000	119000	225000
16	3.5	0	0	0	0.10	1100	0	0	0	0
17	3.5	20	35000	28000	0.10	1200	0.03	20000	48000	91000
18	3.5	40	70000	55000	0.09	1250	0.06	39000	94000	178000
19	3.5	30	52000	41000	0.07	1700	0.04	89000	130000	246000
20	3.5	100	175000	138000	0.07	1700	0.12	97000	235000	444000
21	2.0	100	100000	70000	0.08	1400	0.14	96000	166000	314000
22	2.0	100	100000	70000	0.07	1600	0.12	97000	167000	316000
23	1.0	150	75000	45000	0.07	1700	0.18	143000	188000	355000
24	1.0	110	55000	33000	0.09	1250	0.18	105000	138000	261000
25	2.0	100	100000	70000	0.08	1350	0.15	96000	166000	314000
26	3.0	110	165000	125000	0.09	1250	0.18	105000	230000	435000
27	3.0	110	165000	125000	0.13	900	0.24	120000	245000	463000
28	3.0	80	120000	91000	0.08	1500	0.11	78000	169000	319000
29	3.0	60	90000	68000	0.08	1500	0.08	59000	127000	240000
30	3.0	100	150000	114000	0.08	1500	0.13	97000	211000	399000
31	3.0	150	225000	171000	0.08	1500	0.20	143000	314000	593000
32	3.0	130	195000	148000	0.08	1500	0.17	124000	272000	514000
33	3.0	110	165000	125000	0.08	1500	0.15	106000	231000	437000
34	3.0	110	165000	125000	0.09	1300	0.17	105000	230000	435000
35	3.0	100	150000	114000	0.07	1600	0.12	97000	211000	399000
36	3.0	100	150000	114000	0.06	2000	0.10	98000	212000	401000
37	3.0	100	150000	114000	0.04	3000	0.07	98000	212000	401000
38	3.0	100	150000	114000	0.04	3000	0.07	98000	212000	401000
39	3.0	120	185000	140000	0.03	3300	0.07	118000	258000	488000
40	3.0	110	165000	125000	0.03	3600	0.06	108000	233000	440000
41	3.0	80	120000	91000	0.03	3500	0.05	79000	170000	321000
42	3.0	40	60000	46000	0.03	3400	0.02	40000	86000	162000
43	3.0	20	30000	23000	0.03	3400	0.01	20000	43000	81000
44	3.0	20	30000	23000	0.03	3400	0.01	20000	43000	81000
45	3.0	20	30000	23000	0.03	3400	0.01	20000	43000	81000
46	3.0	20	30000	23000	0.03	3400	0.01	20000	43000	81000
47	3.0	40	60000	46000	0.03	3400	0.02	40000	86000	163000
48	4.0	70	140000	115000	0.03	3400	0.04	69000	184000	348000
TOTALS ($x10^3$) :			5987	4543				5113	9656	18250

SECTOR # 7 Length: 24.5 km Average Retreat Rate: 1.4 m/yr

Segment No.	Onshore H	C	vi	v1	Offshore θ°	w	t	v2	Totals volume	tons
1	3.0	90	135000	103000	0.03	4000	0.05	89000	192000	363000
2	3.0	110	165000	125000	0.03	4000	0.06	108000	233000	440000
3	3.0	100	150000	114000	0.04	3000	0.07	98000	212000	401000
4	3.0	60	90000	68000	0.04	2800	0.04	59000	127000	240000
5	3.0	0	0	0	0.04	2600	0	0	0	0
6	3.0	100	150000	114000	0.05	2500	0.08	98000	212000	401000
7	3.0	90	135000	103000	0.06	2000	0.09	88000	191000	361000
8	3.0	180	270000	205000	0.08	1400	0.26	168000	373000	705000
9	3.0	0	0	0	0.10	1200	0	0	0	0
10	3.0	140	210000	160000	0.15	750	0.37	127000	287000	543000
11	3.0	130	195000	148000	0.79	600	0.43	116000	264000	499000
12	3.0	100	150000	114000	0.23	500	0.39	90000	204000	386000
13	4.0	20	40000	33000	0.23	500	0.08	20000	53000	100000
14	4.0	20	40000	33000	0.21	550	0.07	20000	53000	100000
15	4.0	0	0	0	0.23	500	0	0	0	0
16	4.0	0	0	0	0.79	600	0	0	0	0
17	3.0	20	30000	23000	0.13	850	0.05	20000	43000	81000
18	3.0	20	30000	23000	0.12	950	0.04	20000	43000	81000
19	3.0	50	75000	57000	0.11	1050	0.10	49000	106000	200000
20	3.0	50	75000	57000	0.10	1150	0.10	49000	106000	200000
21	3.0	30	90000	68000	0.10	1150	0.10	49000	117000	221000
22	5.0	0	0	0	0.10	1100	0	0	0	0
23	5.0	0	0	0	0.10	1100	0	0	0	0
24	5.0	30	75000	57000	0.10	1150	0.05	30000	87000	164000
25	3.0	60	90000	68000	0.10	1200	0.10	59000	127000	240000
26	3.0	60	90000	68000	0.09	1250	0.10	59000	127000	240000
27	5.0	70	175000	148000	0.09	1300	0.11	68000	216000	408000
28	5.0	50	125000	108000	0.08	1350	0.15	96000	204000	386000
29	1.0	100	50000	30000	0.08	1350	0.15	96000	126000	238000
30	4.0	0	0	0	0.05	2500	0	0	0	0
31	4.0	0	0	0	0.05	2500	0	0	0	0
32	4.0	0	0	0	0.05	2500	0	0	0	0
33	4.0	0	0	0	0.05	2500	0	0	0	0
34	4.0	0	0	0	0.05	2500	0	0	0	0
35	4.0	0	0	0	0.05	2500	0	0	0	0
36	4.0	0	0	0	0.05	2500	0	0	0	0
37	4.0	0	0	0	0.05	2500	0	0	0	0
38	4.0	0	0	0	0.05	2500	0	0	0	0
39	4.0	0	0	0	0.05	2500	0	0	0	0
40	4.0	0	0	0	0.05	2500	0	0	0	0
41	4.0	0	0	0	0.05	2500	0	0	0	0
42	2.0	0	0	0	0.05	2500	0	0	0	0
43	2.0	0	0	0	0.05	2500	0	0	0	0
44	2.0	30	30000	21000	0.04	3200	0.02	30000	51000	96000
45	2.0	70	70000	49000	0.04	2600	0.05	69000	118000	223000
46	2.0	60	60000	42000	0.05	2300	0.05	59000	101000	191000
47	2.0	100	100000	70000	0.06	1900	0.10	97000	167000	316000
48	1.0	100	50000	30000	0.07	1600	0.12	97000	127000	240000
49	1.0	20	50000	30000	0.08	1450	0.03	20000	50000	95000

Input not calculated for Eskimo Islands; no significant net change.

TOTALS ($x10^3$) :	2295	2269	2048	4317	8159

SECTOR # 8 Length: 8.5 km Average Retreat Rate: 1.7 m/yr

Segment No.	Onshore				Offshore				Totals	
	H	C	vi	v1	θ°	w	t	v2	volume	tons
1	2.0	70	70000	49000	0.05	2400	0.06	69000	118000	223000
2	2.0	70	70000	49000	0.04	3000	0.05	69000	118000	223000
3	2.0	50	50000	35000	0.03	3500	0.03	49000	84000	159000
4	2.0	0	0	0	0.03	3300	0	0	0	0
5	2.0	0	0	0	0.03	3500	0	0	0	0
6	2.0	0	0	0	0.03	3600	0	0	0	0
7	2.0	0	0	0	0.03	3800	0	0	0	0
8	2.0	20	20000	14000	0.03	4000	0.01	20000	34000	64000
9	2.0	50	50000	35000	0.03	4000	0.03	50000	85000	161000
12	2.0	0	0	0	0.03	4000	0	0	0	0
11	2.0	0	0	0	0	0	0	0	0	0
12	2.0	0	0	0	0	0	0	0	0	0
13	2.0	0	0	0	0	0	0	0	0	0
14	2.0	0	0	0	0	0	0	0	0	0
15	2.0	0	0	0	0	0	0	0	0	0
16	2.0	0	0	0	0	0	0	0	0	0
17	2.0	30	30000	21000	0.05	2500	0.20	30000	51000	96000
18	2.0	20	20000	14000	0.05	2500	0.20	20000	34000	64000
19	2.0	0	0	0	0.05	2300	0	0	0	0
Total of Offshore spits, bars, flats :									126000	23814000
TOTALS ($x10^3$) :			562	469				433	902	1705

SECTOR # 9 Length: 23 km Average Retreat Rate: 0.7 m/yr

Segment	Onshore				Offshore				Totals	
No.	H	C	vi	v1	θ°	w	t	v2	volume	tons
1	3.0	0	0	0	0.08	1500	0	0	0	0
2	4.0	0	0	0	0.08	1500	0	0	0	0
3	3.0	0	0	0	0.08	1500	0	0	0	0
4	3.0	0	0	0	0.08	1500	0	0	0	0
5	4.0	0	0	0	0.10	1200	0	0	0	0
6	2.0	0	0	0	0.09	1300	0	0	0	0
7	3.0	0	0	0	0.10	1200	0	0	0	0
8	2.0	0	0	0	0.09	1300	0	0	0	0
9	5.0	0	0	0	0.09	1300	0	0	0	0
10	3.0	0	0	0	0.07	1600	0	0	0	0
11	2.0	20	20000	14000	0.07	1600	0.03	20000	34000	64000
12	3.0	0	0	0	0.07	1600	0	0	0	0
13	3.0	20	30000	23000	0.07	1600	0.03	20000	43000	81000
14	4.0	20	40000	33000	0.07	1700	0.02	20000	53000	100000
15	2.0	20	20000	14000	0.07	1700	0.02	20000	34000	64000
16	2.0	40	40000	28000	0.08	1500	0.05	39000	67000	127000
17	4.0	40	80000	66000	0.08	1500	0.05	39000	105000	198000
18	2.0	100	100000	70000	0.08	1500	0.13	97000	167000	316000
19	2.0	20	20000	14000	0.08	1400	0.29	20000	34000	64000
D 20	0.2	+130	+13000	+13000	0.08	1400	0.18	+129000	+142000	+268000
21	2.0	100	100000	70000	0.10	1200	0.17	96000	166000	314000
22	2.0	80	80000	56000	0.08	1500	0.11	78000	134000	253000
23	2.0	60	60000	42000	0.06	2000	0.06	59000	101000	191000
24	2.0	70	70000	49000	0.06	2000	0.07	69000	118000	223000
25	2.0	70	70000	49000	0.07	1700	0.08	69000	118000	223000
26	3.0	60	90000	68000	0.08	1400	0.09	59000	127000	240000
27	3.0	0	0	0	0.08	1500	0	0	0	0
28	3.0	20	20000	15000	0.06	1800	0.02	20000	35000	66000
29	4.0	50	100000	82000	0.06	1800	0.06	49000	131000	248000
30	3.0	110	165000	125000	0.06	1800	0.12	107000	232000	438000
31	3.0	30	45000	34000	0.06	1900	0.03	30000	64000	121000
32	3.0	40	60000	46000	0.05	2300	0.03	40000	86000	163000
33	2.0	40	40000	28000	0.05	2300	0.03	40000	68000	129000
34	2.0	20	20000	14000	0.05	2300	0.02	20000	34000	64000
35	3.0	30	45000	34000	0.05	2300	0.03	30000	64000	121000
36	4.0	20	40000	33000	0.05	2300	0.02	20000	53000	100000
37	3.0	0	0	0	0.05	2300	0	0	0	0
38	3.0	20	30000	23000	0.05	2300	0.02	20000	43000	81000
39	4.0	20	40000	33000	0.05	2300	0.02	20000	53000	100000
40	4.0	20	40000	33000	0.05	2300	0.02	20000	53000	100000
41	3.0	0	0	0	0.05	2300	0	0	0	0
42	3.0	0	0	0	0.05	2300	0	0	0	0
43	3.0	0	0	0	0.05	2300	0	0	0	0
44	4.0	0	0	0	0.05	2300	0	0	0	0
45	2.0	0	0	0	0.06	2300	0	0	0	0
46	2.0	0	0	0	0.06	2300	0	0	0	0
TOTALS	($x10^3$) :		1452	1083				992	2075	3922

SECTOR # 10   Length: 15.5 km   Average Retreat Rate: 2.5 m/yr

Segment	Onshore				Offshore				Totals	
No.	H	C	vi	v1	θ	w	t	v2	volume	tons
1	1.5	50	38000	25000	0.01	12000	0.01	50000	75000	142000
2	1.5	30	22000	14000	0.01	11000	0.005	30000	44000	83000
3	1.5	20	15000	10000	0.01	11000	0.003	20000	30000	57000
4	1.5	20	15000	10000	0.01	11000	0.003	20000	30000	57000
5	1.5	0	0	0	0.01	11400	0	0	0	0
6	3.0	0	0	0	0.01	11400	0	0	0	0
7	1.5	20	15000	10000	0.01	11000	0.003	20000	30000	57000
8	1.5	60	45000	29000	0.01	11000	0.01	60000	89000	168000
9	1.5	100	75000	49000	0.01	10700	0.02	99000	148000	280000
10	1.5	130	98000	64000	0.01	10500	0.02	129000	193000	365000
11	1.5	90	68000	44000	0.01	10500	0.02	90000	134000	253000
12	1.5	100	75000	49000	0.01	10000	0.02	99000	148000	280000
13	1.5	90	68000	44000	0.01	10000	0.02	90000	134000	253000
14	1.5	80	60000	39000	0.01	10000	0.02	80000	119000	225000
15	1.5	90	68000	44000	0.01	10200	0.02	90000	134000	253000
16	1.5	120	90000	59000	0.01	10100	0.02	119000	178000	336000
17	1.0	20	10000	6000	0.01	10200	0.004	20000	26000	49000
18	1.0	40	20000	12000	0.01	9900	0.01	40000	52000	98000
19	1.0	60	30000	18000	0.01	10000	0.01	60000	78000	147000
20	1.0	100	50000	30000	0.01	10500	0.02	99000	129000	244000
21	1.0	140	70000	42000	0.01	10700	0.03	139000	181000	342000
22	1.0	200	100000	60000	0.01	10700	0.04	198000	258000	488000
23	1.0	100	50000	30000	0.01	11200	0.02	99000	129000	244000
24	1.0	90	45000	27000	0.01	11600	0.02	90000	117000	221000
25	1.0	90	45000	27000	0.01	12000	0.02	90000	117000	221000
26	1.0	80	40000	24000	0.01	12200	0.01	80000	104000	197000
27	1.0	90	45000	27000	0.01	12600	0.01	90000	117000	221000
28	1.0	60	30000	18000	0.01	13000	0.01	60000	78000	147000
29	1.5	70	53000	34000	0.01	13400	0.01	70000	104000	196000
30	1.5	100	75000	49000	0.01	13700	0.01	100000	149000	282000
31	1.5	50	38000	25000	0.01	13800	0.01	50000	75000	142000
TOTALS ($x10^3$) :			1453	919				2281	3200	6048

SECTOR # 11 Length: 48 km Average Retreat Rate: +.4 m/yr

Segment No.	Onshore H	C	vi	v1	Offshore θ°	w	t	v2	Totals volume	tons
1	0.5	40	10000	6000	0.01	14000	0.006	40000	46000	87000
2	0.5	20	5000	3000	0.01	13600	0.003	20000	23000	43000
3	0.5	40	10000	6000	0	0	0	0	6000	11000
4	0.5	30	7000	4000	0	0	0	0	4000	8000
5	0.5	20	5000	3000	0	0	0	0	3000	6000
6	0.5	50	12000	7000	0	0	0	0	7000	13000
7	0.5	50	12000	7000	0	0	0	0	7000	13000
8	0.5	20	5000	3000	0	0	0	0	3000	6000
D 9	0.2	+60	+6000	+6000	0	0	0	0	+6000	+11000
10	0.5	0	0	0	0.1	3500	0	0	0	0
11	0.5	100	25000	14000	0.01	12400	0.10	70000	84000	159000
12	0.5	80	20000	11000	0	0	0	0	11000	21000
13	0.5	20	5000	3000	0	0	0	0	3000	6000
14	0.5	0	0	0	0.01	11000	0	0	0	0
15	0.5	30	7000	4000	0.01	10450	0.01	50000	54000	102000
16	0.5	80	20000	11000	0	0	0	0	11000	21000
17	0.4	100	20000	20000	0.01	9700	0.02	99000	119000	225000
18	0.4	70	14000	14000	0.01	8900	0.02	70000	84000	159000
19	0.4	90	18000	18000	0.01	8600	0.02	90000	108000	204000
20	0.4	110	22000	22000	0.01	8000	0.03	110000	132000	249000
21	0.4	230	46000	46000	0.02	7400	0.06	226000	272000	514000
22	0.4	160	32000	32000	0.02	7200	0.04	158000	190000	359000
D 23	0.2	+110	+11000	+11000	0.02	7200	0.03	+109000	+120000	+227000
24	0.4	140	28000	28000	0.02	7200	0.04	139000	167000	316000
D 25	0.2	+220	+22000	+22000	0.02	7100	0.06	+217000	+239000	+452000
26	0.5	0	0	0	0.01	8200	0	0	0	0
D 27	0.2	+150	+15000	+15000	0.01	8700	0.03	+149000	+164000	+310000
D 28	0.2	+110	+11000	+11000	0.01	8600	0.02	+109000	+120000	+227000
D 29	0.2	+20	+2000	+2000	0.01	8500	0.004	+20000	+22000	+42000
30	0.5	200	50000	29000	0.01	8100	0.04	197000	226000	427000
31	0.5	300	75000	43000	0.01	7900	0.07	294000	337000	637000
32	0.5	0	0	0	0.01	8300	0	0	0	0
33	0.5	210	52000	30000	0.01	9480	0.04	208000	238000	450000
34	0.5	200	50000	29000	0.01	10000	0.04	198000	227000	429000
35	1.0	0	0	0	0.01	10000	0	0	0	0
36	1.0	80	40000	24000	0.01	9500	0.02	80000	104000	197000
37	1.0	20	20000	12000	0.01	9650	0.004	20000	32000	60000
D 38	0.2	+100	+10000	+10000	0.01	10100	0.02	+99000	+109000	+206000
D 39	1.0	70	70000	42000	0.01	10300	0.01	70000	112000	212000
40	1.0	100	100000	60000	0.01	9800	0.02	99000	159000	301000
41	1.0	110	110000	66000	0.01	9300	0.02	109000	175000	331000
D 42	0.2	+20	+2000	+2000	0.01	9200	0.004	+20000	+22000	+42000
43	1.0	40	40000	24000	0.01	9100	0.01	40000	64000	121000
44	1.0	30	30000	18000	0.01	9000	0.006	30000	48000	91000
45	1.0	40	40000	24000	0.01	8900	0.01	40000	64000	121000
46	1.0	0	0	0	0.01	9300	0	0	0	0
47	1.0	100	100000	60000	0.01	9750	0.02	10000	70000	132000
48	1.0	200	200000	120000	0.01	10000	0.04	198000	318000	601000
49	1.0	100	100000	60000	0.01	10100	0.02	99000	159000	301000
50	0.5	110	28000	16000	0.01	10150	0.02	11000	27000	51000
51	0.5	120	30000	17000	0.01	10200	0.02	119000	136000	257000
52	0.5	120	30000	17000	0.01	10300	0.02	119000	136000	257000
53	0.5	100	25000	14000	0.01	10000	0.02	99000	113000	214000
54	0.5	120	30000	17000	0.01	9700	0.02	119000	136000	257000
D 55	0.2	+30	+3000	+3000	0.01	9400	0.006	+30000	+33000	+62000
D 56	0.2	+220	+22000	+22000	0.01	8800	0.05	+217000	+239000	+452000
57	0.2	90	9000	9000	0.01	8300	0.02	90000	99000	187000
58	0.2	320	32000	32000	0.01	7700	0.08	313000	345000	652000
59	0.2	280	28000	28000	0.02	7250	0.08	274000	302000	571000
60	0.2	160	16000	16000	0.02	7200	0.04	160000	176000	333000

(sector 11 continued)

61	0.2	200	20000	20000	0.02	7200	0.05	197000	217000	410000
62	0.2	0	0	0	0.02	7200	0	0	0	0
63	0.2	0	0	0	0.01	7700	0	0	0	0
64	0.2	0	0	0	0.01	7850	0	0	0	0
D 65	0.2	+300	+30000	+30000	0.01	7900	0.08	+290000	+320000	+605000
D 66	0.2	+410	+41000	+41000	0.01	7700	0.10	+399000	+440000	+832000
D 67	0.2	+400	+40000	+40000	0.01	7400	0.11	+389000	+429000	+811000
68	0.2	0	0	0	0.01	7600	0	0	0	0
69	0.2	0	0	0	0.01	7400	0	0	0	0
70	0.2	100	10000	10000	0.02	7100	0.02	99000	109000	206000
71	0.2	200	20000	20000	0.02	6950	0.05	197000	217000	410000
72	0.2	200	20000	20000	0.02	6900	0.06	197000	217000	410000
73	0.2	210	21000	20000	0.02	6700	0.06	207000	227000	429000
74	0.2	160	16000	16000	0.02	6250	0.05	158000	174000	329000
D 75	0.2	+60	+6000	+6000	0.02	5700	0.02	+60000	+66000	+125000
D 76	0.2	+500	+50000	+50000	0.02	5400	0.18	+477000	+527000	+996000
D 77	0.2	+600	+60000	+60000	0.02	5320	0.22	+566000	+626000	+1183000
D 78	0.2	+400	+40000	+40000	0.02	5400	0.15	+385000	+425000	+803000
D 79	0.2	+220	+22000	+22000	0.02	5500	0.08	+216000	+238000	+450000
D 80	0.2	+300	+30000	+30000	0.02	5300	0.11	+291000	+321000	+607000
D 81	0.2	+300	+30000	+30000	0.02	5100	0.12	+291000	+321000	+607000
D 82	0.2	+350	+35000	+35000	0.02	5000	0.14	+338000	+373000	+705000
D 83	0.2	+300	+30000	+30000	0.02	5400	0.11	+292000	+322000	+609000
D 84	0.2	+200	+20000	+20000	0.02	5100	0.08	+196000	+216000	+408000
85	0.2	0	0	0	0.02	6700	0	0	0	0
86	0.2	20	2000	2000	0.02	6550	0.006	20000	22000	42000
D 87	0.2	+200	+20000	+20000	0.01	8500	0.02	+80000	+100000	+189000
D 88	0.2	+100	+10000	+10000	0	0	0	0	+10000	+19000
89	0.2	100	10000	10000	0	0	0	0	10000	19000
90	0.2	120	12000	12000	0	0	0	0	12000	23000
91	0.2	80	8000	8000	0	0	0	0	8000	15000
92	0.2	60	6000	6000	0	0	0	0	6000	11000
93	0.2	100	10000	10000	0	0	0	0	10000	19000
94	0.2	90	9000	9000	0	0	0	0	9000	17000
D Total of Offshore spits, bars, flats :								+68000	+680000	+1285000
TOTALS ($x10^5$) :			624	664				+777	+113	+214

SECTOR # 12 Length: 16.5 km Average Retreat Rate: 1.6 m/yr

Segment	Onshore				Offshore				Totals	
No.	H	C	vi	vl	θ°	w	t	v2	volume	tons
1	1.0	40	20000	12000	0.02	6000	0.01	40000	52000	98000
2	1.0	40	20000	12000	0.02	6000	0.01	40000	52000	98000
3	1.0	20	10000	6000	0.02	5500	0.01	20000	26000	49000
4	1.0	60	30000	18000	0.02	5500	0.02	60000	78000	147000
5	1.0	30	15000	9000	0.02	4500	0.01	30000	39000	74000
6	1.0	20	10000	6000	0.02	4700	0.01	20000	26000	49000
7	1.0	20	10000	6000	0.02	4700	0.01	20000	26000	49000
8	1.0	80	41000	25000	0.03	3500	0.05	79000	104000	197000
9	1.0	80	42000	25000	0.01	1300	0.12	78000	103000	195000
10	1.0	70	37000	22000	0.11	1100	0.13	68000	90000	170000
11	1.5	100	90000	59000	0.15	750	0.29	102000	161000	304000
12	1.5	100	82000	53000	0.16	700	0.29	93000	146000	276000
13	1.5	100	83000	54000	0.19	600	0.33	92000	146000	276000
14	2.0	100	110000	77000	0.23	500	0.40	92000	169000	319000
15	2.0	110	111000	78000	0.23	500	0.44	98000	176000	333000
16	2.0	80	84000	57000	0.14	800	0.20	76000	133000	251000
17	2.0	80	80000	56000	0.10	1100	0.14	77000	133000	251000
18	2.5	40	50000	37000	0.17	650	0.12	39000	76000	144000
19	2.0	70	70000	49000	0.19	600	0.23	66000	115000	217000
20	2.0	30	30000	21000	0.19	600	0.10	29000	50000	95000
21	2.25	20	22000	16000	0.16	700	0.06	20000	36000	68000
22	2.25	20	22000	16000	0.19	600	0.07	20000	36000	68000
23	1.0	0	0	0	0.19	600	0	0	0	0
24	1.25	0	0	0	0.19	600	0	0	0	0
25	2.0	0	0	0	0.19	600	0	0	0	0
26	2.0	0	0	0	0.19	600	0	0	0	0
27	1.0	0	0	0	0.23	500	0	0	0	0
28	2.0	20	20000	14000	0.19	600	0.07	20000	34000	64000
29	2.0	20	20000	14000	0.19	600	0.02	20000	34000	64000
30	1.0	20	10000	6000	0.16	700	0.02	20000	26000	49000
31	1.0	20	10000	6000	0.16	700	0.02	20000	26000	49000
32	1.0	110	65000	39000	0.16	700	0.11	101000	140000	265000
33	1.0	100	50000	30000	0.19	600	0.33	92000	122000	231000
TOTALS ($x10^3$) :			1244	823				1532	2355	4450

SECTOR # 13   Length: 32 km   Average Retreat Rate : 1.2 m/yr

Segment	Onshore				Offshore				Totals	
No.	H	C	vi	v1	θ°	w	t	v2	volume	tons
1	1.0	20	10000	6000	0.38	300	0.13	19000	25000	47000
2	2.0	20	20000	14000	0.16	700	0.06	20000	34000	64000
3	1.5	40	30000	20000	0.13	900	0.09	39000	59000	111000
4	1.5	50	38000	25000	0.11	1000	0.10	49000	74000	140000
5	1.5	0	0	0	0.07	1600	0	0	0	0
6	1.75	20	17000	11000	0.07	1700	0.02	20000	31000	59000
7	2.0	0	0	0	0.07	1700	0	0	0	0
D 8	0.2	+100	+10000	+10000	0.05	2300	0.09	+103000	+113000	+214000
D 9	0.2	+20	+2000	+2000	0.06	2000	0.02	+19000	+21000	+40000
10	1.75	0	0	0	0.07	1600	0	0	0	0
D 11	0.2	+120	+12000	+12000	0.08	1400	0.17	+122000	+134000	+253000
12	1.0	100	50000	30000	0.08	1400	0.14	96000	126000	238000
13	0.75	100	38000	22000	0.10	1200	0.17	96000	118000	223000
14	0.75	60	22000	13000	0.08	1500	0.08	59000	72000	136000
D 15	0.2	+40	+4000	+4000	0.37	3100	0.26	+40000	+44000	+83000
16	0.75	0	0	0	0.03	3300	0	0	0	0
17	0.75	0	0	0	0.03	3100	0	0	0	0
18	1.0	80	40000	24000	0.04	2900	0.06	79000	103000	195000
19	1.0	100	50000	30000	0.04	2700	0.07	98000	128000	242000
D 20	0.2	+20	+2000	+2000	0.04	260	0.01	+14000	+16000	+30000
21	1.0	20	10000	6000	0.04	2800	0.01	20000	26000	49000
22	1.0	30	15000	9000	0.04	3000	0.02	30000	39000	74000
23	1.5	70	52000	34000	0.04	3200	0.04	69000	103000	195000
24	1.0	80	40000	24000	0.03	3300	0.05	79000	103000	195000
25	2.0	30	30000	20000	0.03	3500	0.02	30000	50000	94000
26	1.0	80	40000	24000	0.03	3700	0.04	79000	103000	195000
D 27	0.4	+20	+4000	+4000	0.03	3700	0.01	+19000	+23000	+43000
28	0.75	0	0	0	0.03	3500	0	0	0	0
D 29	0.4	+20	+4000	+4000	0.03	3400	0.01	+19000	+23000	+43000
D 30	0.4	+20	+4000	+4000	0.03	3300	0.01	+19000	+23000	+43000
31	1.5	60	45000	29000	0.04	3200	0.04	59000	88000	166000
32	1.5	80	60000	39000	0.04	2800	0.06	79000	118000	223000
33	1.0	70	35000	21000	0.06	2000	0.07	69000	90000	170000
34	1.75	40	35000	21000	0.08	1400	0.06	39000	60000	113000
35	1.75	20	12000	8000	0.11	1000	0.04	20000	28000	53000
D 36	0.4	+40	+8000	+8000	0.09	1300	0.06	+38000	+46000	+87000
37	1.75	30	26000	18000	0.06	1800	0.03	30000	48000	91000
38	1.0	0	0	0	0.05	2300	0	0	0	0
39	1.0	20	10000	6000	0.04	2700	0.01	20000	26000	49000
40	1.5	20	15000	9000	0.04	3000	0.01	20000	29000	55000
41	1.0	20	10000	6000	0.03	3500	0.01	20000	26000	49000
42	1.5	30	22000	14000	0.03	3300	0.02	30000	44000	83000
43	1.0	90	45000	27000	0.03	3400	0.05	89000	116000	219000
44	1.75	100	75000	51000	0.04	3000	0.07	98000	149000	282000
45	1.75	120	90000	61000	0.03	3500	0.07	118000	179000	338000
46	1.5	110	82000	53000	0.03	3500	0.06	108000	161000	304000
D 47	0.4	+20	+4000	+4000	0.03	3300	0.01	+19000	+23000	+43000
48	1.5	0	0	0	0.03	3300	0	0	0	0
49	2.0	100	110000	77000	0.05	2200	0.10	107000	184000	348000
50	1.0	90	45000	27000	0.10	1100	0.16	86000	113000	214000
D 51	0.4	+30	+6000	+6000	0.06	1900	0.03	+29000	+35000	+66000
52	1.25	40	25000	16000	0.05	2200	0.04	40000	56000	106000
53	1.75	90	79000	53000	0.05	2300	0.08	88000	141000	266000
54	1.25	90	56000	35000	0.05	2300	0.08	88000	123000	232000
55	1.25	90	56000	35000	0.05	2300	0.08	88000	123000	232000

(sector13 continued)

56	1.25	100	62000	39000	0.06	2000	0.10	98000	137000	259000
57	1.25	120	75000	47000	0.09	1300	0.18	114000	161000	304000
58	1.25	100	62000	39000	0.10	1100	0.18	95000	134000	253000
59	1.5	0	0	0	0.06	1800	0	0	0	0
60	1.5	20	15000	10000	0.05	2200	0.02	20000	30000	57000
61	1.0	30	15000	9000	0.05	2100	0.03	30000	39000	74000
62	1.5	40	30000	20000	0.06	1900	0.04	39000	59000	111000
63	1.5	20	15000	9000	0.08	1500	0.03	20000	29000	55000
64	1.75	70	61000	41000	0.19	600	0.23	66000	107000	202000
TOTALS ($x10^3$) :			1710	1072				2219	3291	6220

SECTOR # 14 Length: 28 km Average Retreat Rate : 1.7 m/yr

Segment No.	Onshore H	C	vi	vl	Offshore $\theta°$	w	t	v2	Totals volume	tons
1	1.75	20	17000	11000	0.08	1400	0.03	20000	31000	59000
2	1.75	0	0	0	0.08	1500	0	0	0	0
3	1.5	0	0	0	0.06	1800	0	0	0	0
4	1.25	20	12000	8000	0.06	1900	0.02	20000	28000	53000
5	1.75	30	26000	18000	0.07	1700	0.04	30000	48000	91000
6	2.25	0	0	0	0.07	1600	0	0	0	0
7	2.25	20	22000	16000	0.06	1800	0.02	20000	36000	68000
8	1.75	30	26000	18000	0.06	1800	0.03	30000	48000	91000
9	1.75	0	0	0	0.07	1700	0	0	0	0
10	1.75	20	17000	11000	0.06	1800	0.02	20000	31000	59000
11	1.5	0	0	0	0.06	1900	0	0	0	0
12	1.25	0	0	0	0.05	2200	0	0	0	0
13	1.25	20	12000	8000	0.04	2700	0.01	20000	28000	53000
D 14	0.4	+30	+6000	+6000	0.03	3300	0.02	+38000	+44000	+83000
D 15	0.4	+40	+8000	+8000	0.03	3500	0.02	+38000	+46000	+87000
16	2.25	20	22000	16000	0.03	4000	0.01	20000	36000	68000
17	2.25	20	22000	16000	0.02	4100	0.01	20000	36000	68000
18	1.25	60	37000	23000	0.03	3700	0.03	59000	82000	155000
19	1.25	40	25000	16000	0.03	4300	0.02	40000	56000	106000
20	2.25	0	0	0	0.02	5000	0	0	0	0
21	1.25	0	0	0	0.02	5400	0	0	0	0
22	0.75	0	0	0	0.02	5000	0	0	0	0
23	0.75	20	7000	4000	0.02	4600	0.01	20000	24000	45000
24	0.75	20	7000	4000	0.03	4500	0.01	20000	24000	45000
25	0.75	100	38000	22000	0.03	4200	0.05	99000	121000	229000
26	0.75	200	75000	44000	0.03	3700	0.11	194000	238000	450000
27	0.75	220	83000	49000	0.03	3400	0.13	213000	262000	495000
28	0.75	70	26000	15000	0.03	4000	0.04	69000	84000	159000
29	0.75	40	15000	9000	0.03	3500	0.02	40000	49000	93000
30	0.75	0	0	0	0.04	3000	0	0	0	0
31	0.75	70	26000	15000	0.04	3000	0.05	69000	84000	159000
32	0.75	100	38000	22000	0.04	3200	0.06	98000	120000	227000
A 33	0.75	50	19000	11000	0.03	3000	0.03	39000	50000	94000
A 34	0.75	200	75000	44000	0.02	3100	0.07	147000	191000	361000
A 35	0.75	210	79000	46000	0.03	2700	0.11	152000	198000	374000
A 36	0.75	180	68000	40000	0.03	2300	0.10	11000	51000	96000
A 37	0.75	0	0	0	0.03	2600	0	0	0	0
A 38	1.25	30	26000	16000	0.03	2600	0.01	11000	27000	51000
A 39	1.75	0	0	0	0.03	2500	0	0	0	0
A 40	1.75	20	17000	11000	0.03	2000	0.01	11000	22000	41000
A 41	1.75	0	0	0	0.04	1700	0	0	0	0
A 42	1.25	0	0	0	0.04	1500	0	0	0	0
A 43	0.75	0	0	0	0.05	1400	0	0	0	0
A 44	1.5	40	30000	20000	0.05	1300	0.03	20000	40000	76000
A 45	1.25	0	0	0	0.04	1700	0	0	0	0
A 46	1.75	0	0	0	0.03	2000	0	0	0	0
A 47	1.75	20	17000	11000	0.03	1700	0.01	9000	20000	38000
A 48	0.75	20	7000	4000	0.04	1400	0.01	7000	11000	21000
A 49	1.0	20	10000	6000	0.04	1300	0.01	7000	13000	24000
A 50	1.25	0	0	0	0.04	1500	0	0	0	0
A 51	1.25	0	0	0	0.03	1900	0	0	0	0
A 52	1.25	0	0	0	0.03	2000	0	0	0	0
A 53	1.25	0	0	0	0.03	1900	0	0	0	0
A 54	1.0	20	10000	6000	0.05	1200	0.02	11000	17000	32000
A 55	1.25	0	0	0	0.07	800	0	0	0	0
A 56	1.25	0	0	0	0.14	400	0	0	0	0
TOTALS ($x10^3$) :			897	546				1470	2016	3811

SECTOR # 15 Length: 36.5 km Average Retreat Rate : 1.0 m/yr

Pingok Island : segments measured clockwise around island from west end.

Segment No.	Onshore H	C	vi	v1	Offshore θ°	w	t	v2	Totals volume	tons
1	2.25	0	0	0	0.57	200	0	0	0	0
D 2	0.4	+20	+10000	+10000	0.67	170	0.59	+43000	+53000	+100000
D 3	0.4	+30	+6000	+6000	3.81	30	2.00	+15000	+21000	+40000
4	1.25	0	0	0	1.64	70	0	0	0	0
D 5	0.4	+130	+26000	+26000	2.29	50	5.19	+130000	+156000	+295000
D 6	0.4	+120	+24000	+24000	2.29	50	4.79	+120000	+144000	+272000
7	0.75	0	0	0	1.43	80	0	0	0	0
D 8	0.4	+20	+4000	+4000	1.43	80	0.50	+20000	+24000	+45000
D 9	0.4	+30	+6000	+6000	1.43	80	0.75	+30000	+36000	+68000
D 10	0.4	+40	+8000	+8000	1.04	110	0.73	+40000	+48000	+91000
11	1.75	40	35000	24000	1.43	80	1.00	30000	54000	102000
12	1.75	20	18000	12000	1.15	100	0.40	18000	30000	57000
13	1.75	80	70000	47000	0.95	120	1.33	53000	100000	189000
B 14	0.5	100	25000	14000	2.29	50	2.00	100000	114000	215000
15	0.5	100	25000	14000	0.10	1200	0.17	96000	110000	208000
16	1.75	100	88000	59000	0.10	1200	0.17	96000	155000	293000
17	1.75	100	88000	59000	0.13	900	0.22	94000	153000	289000
18	1.75	110	96000	65000	0.23	500	0.44	98000	163000	308000
19	1.75	100	88000	59000	0.16	700	0.29	93000	152000	287000
20	1.75	100	88000	59000	0.15	750	0.27	93000	152000	287000
21	1.75	100	88000	59000	0.14	800	0.25	94000	153000	289000
22	1.75	100	70000	47000	0.11	1000	0.20	95000	142000	268000
23	2.0	80	70000	49000	0.08	1400	0.11	78000	127000	240000
24	1.75	90	79000	53000	0.07	1750	0.10	88000	141000	266000
25	1.75	60	52000	35000	0.06	1950	0.06	59000	94000	178000
26	1.25	80	50000	31000	0.06	1950	0.08	78000	109000	206000
27	1.25	80	50000	31000	0.06	1900	0.08	78000	109000	206000
28	1.25	100	63000	39000	0.07	1650	0.12	97000	136000	257000
29	2.25	80	90000	64000	0.06	1850	0.09	78000	142000	268000
30	2.25	100	112000	80000	0.06	1800	0.11	97000	177000	335000
31	2.25	30	34000	24000	0.05	2500	0.02	30000	54000	102000
Offshore input from removal of bar :								17000	17000	32000

//

(sector 15 continued)

Bertoncini and Bodfish Islands : segments measured clockwise from west end.

Segment No.	Onshore H	C	vi	v1	Offshore θ°	w	t	v2	Totals volume	tons
B 1	1.75	120	105000	71000	0.95	40	2.00	120000	191000	361000
B 2	1.75	100	88000	59000	1.14	50	2.00	100000	159000	301000
B 3	2.25	120	135000	97000	0.95	40	2.00	120000	217000	410000
B 4	2.25	100	112000	80000	1.14	90	2.00	100000	180000	340000
5	1.75	70	61000	41000	0.57	200	0.70	58000	99000	187000
D 6	0.4	+50	+10000	+10000	0.14	775	0.12	+49000	+59000	+112000
7	1.75	40	0	0	2.86	0	0	0	0	0
D 8	0.4	+20	+4000	+4000	0.14	800	0.05	+20000	+24000	+45000
D 9	0.4	+20	+4000	+4000	0.13	900	0.04	+18000	+22000	+42000
D 10	0.4	+60	+12000	+12000	0.09	1300	0.01	+6000	+18000	+34000
D 11	0.4	+20	+4000	+4000	0.06	1800	0.02	+19000	+23000	+43000
D 12	0.4	+110	+22000	+22000	0.07	1700	0.13	+106000	+128000	+242000
13	2.25	0	0	0	0.09	1200	0	0	0	0

//

(sector 15 continued)

Cottle Island : segments measured clockwise from west end.

Segment No.	Onshore H	C	vi	v1	Offshore θ°	w	t	v2	Totals volume	tons
1	1.75	0	0	0	0.76	150	0	0	0	0
2	1.75	20	17000	11000	1.15	100	0.40	18000	29000	55000
3	1.75	40	35000	24000	1.15	100	0.80	32000	56000	106000
4	1.75	0	0	0	0.72	160	0	0	0	0
5	1.75	50	44000	30000	1.15	100	1.00	37000	67000	127000
6	1.75	50	44000	30000	2.3	50	2.00	25000	55000	104000
7	1.75	60	52000	35000	1.64	70	1.71	34000	69000	130000
8	1.75	90	79000	53000	1.27	90	2.00	45000	98000	185000
9	1.75	60	52000	35000	1.64	70	1.70	34000	69000	130000
10	1.75	40	35000	24000	0.76	150	0.53	35000	59000	112000
11	1.75	0	0	0	0.52	220	0	0	0	0
12	1.75	20	17000	11000	0.57	200	0.20	19000	30000	57000
13	1.75	0	0	0	0.38	300	0	0	0	0
14	1.75	0	0	0	0.10	1100	0	0	0	0
15	1.75	100	88000	59000	0.08	1400	0.14	96000	155000	293000
16	1.75	50	44000	30000	0.08	1500	0.07	49000	79000	149000
17	1.75	0	0	0	0	0	0	0	0	0
D 18	0.4	+70	+7000	+7000	0.10	1100	0.12	+69000	+76000	+144000
19	1.75	0	0	0	0.13	900	0	0	0	0
20	1.75	80	88000	59000	0.10	1200	0.13	77000	136000	257000
21	1.75	50	44000	30000	0.08	1500	0.07	49000	79000	149000
22	.1.75	0	0	0	0.08	1400	0	0	0	0
23	1.75	0	0	0	0.08	1300	0	0	0	0
D 24	0.4	+20	+4000	+4000	0.08	1400	0.03	+21000	+25000	+47000
25	1.75	20	17000	11000	0.07	1600	0.03	20000	31000	59000
26	1.75	30	26000	18000	0.08	1500	0.04	30000	48000	91000
27	1.75	0	0	0	0.07	1600	0	0	0	0
28	1.75	0	0	0	0.07	1600	0	0	0	0
29	1.75	0	0	0	0.07	1600	0	0	0	0

Input not calculated for Thetis, Spy, Leavitt, Stump, Egg, and Long islands; no net change.

TOTALS ($x10^3$) :	2428	1581	2052	3633	6866

PLEISTOCENE AND HOLOCENE SEISMIC STRATIGRAPHY BETWEEN THE CANNING RIVER AND PRUDHOE BAY, ALASKA

by

S. C. Wolf, Erk Reimnitz,
and P. W. Barnes

TABLE OF CONTENTS

LIST OF FIGURES

Pleistocene and Holocene Seismic Stratigraphy between the Canning River and Prudhoe Bay, Alaska

by

S.C. Wolf, Erk Reimnitz, and P.W. Barnes

INTRODUCTION

Petroleum development along the shores of the Beaufort Sea, Alaska, particularly in the vicinity of Prudhoe Bay, has led to an increased awareness and concern for the marine and coastal plain environments, for geohazards and engineering problems, for the geologic history, for arctic processes of sediment erosion and deposition, for sea ice movement and its effects, and for permafrost, to mention but a few. This report is primarily concerned with the shallow stratigraphy of the inner shelf between Flaxman Island in the east and Prudhoe Bay, some 50 km to the west. The Branch of Pacific Marine Geology of the U.S. Geological Survey has acquired a large amount of seismic, side-scan sonar and bathymetric data in the region since 1970. These data form the basis for this study. Additionally, bottom samples, cores, temperature and salinity data, and diving programs have provided much information complementary to the research program. Twenty boreholes drilled throughout the study area by Harding-Lawson Associates under contract to the Conservation Division of the U.S. Geological Survey in 1979, (Fig. 1), and several additional ones drilled under the OCSEAP, provide ground truth for the seismic stratigraphy. The stratigraphic and environmental record from these boreholes have been interpreted by David Hopkins, Roger Hartz and Peggy Smith of the U.S. Geological Survey (Hopkins and others, 1978; Hartz and others, 1979; Smith and Hopkins, 1979; and Smith, in press).

The seismic data available for this study are a combination of high resolution geophysical records, obtained with such systems as boomers, minisparkers, and fixed frequency transducers within the range of 3.5 to 7 kHz. The side-scan sonar provided seafloor imagery and the transducers provided bathymetric data. The purpose of the study leading to this report has been to obtain and interpret all available geophysical data, to relate the findings to borehole data both onshore and offshore, to develop an understanding of the geologic framework that operated during Quaternary time, and to describe the recent geologic history of the area.

REGIONAL SETTING

The study area is **encompassed** by the Canning River fan delta on the east and the Sagavanirktok delta on the west. The coastal plain in the area is underlain by a series of coalescing alluvial and glacial-outwash fans extending northward from the Brooks Range (Hopkins and Hartz, 1978). The tundra surface is dotted by thousands of shallow thaw lakes, and crossed by shallow river channels both abandoned and presently active. Coastal bluffs along the plain gradually rise in height from 2 m to 6 m to the south, where the plain merges with the Brooks Range. An offshore island chain sub-parallel to the coastline consists of islands that appear to be true constructional barrier islands, whereas the eastern one (Flaxman Island, Fig. 1) is really a coastal plain remnant, capped by tundra as much as six meters above sea level. Seismic data suggest that some of the other islands may have origins similar to Flaxman Island. Although they may appear as true barrier islands, they may in fact consist of erosional debris resulting from destruction of a coastal **remnant**, later shaped by modern currents to appear surficially as a classical barrier island.

Between the islands and the coastline are lagoons which receive sediment supplied by rivers and coastal erosion. The lagoons are generally protected from large pack ice by the island chain and shallow passes, whereas the shelf seaward of the island chain is severely gouged by sea ice. Sedimentation appears to be low or non-existent and is influenced by coastal currents and by ice drifting from east to west. Coastal erosion, dominated by thermokarst processes, proceeds at an

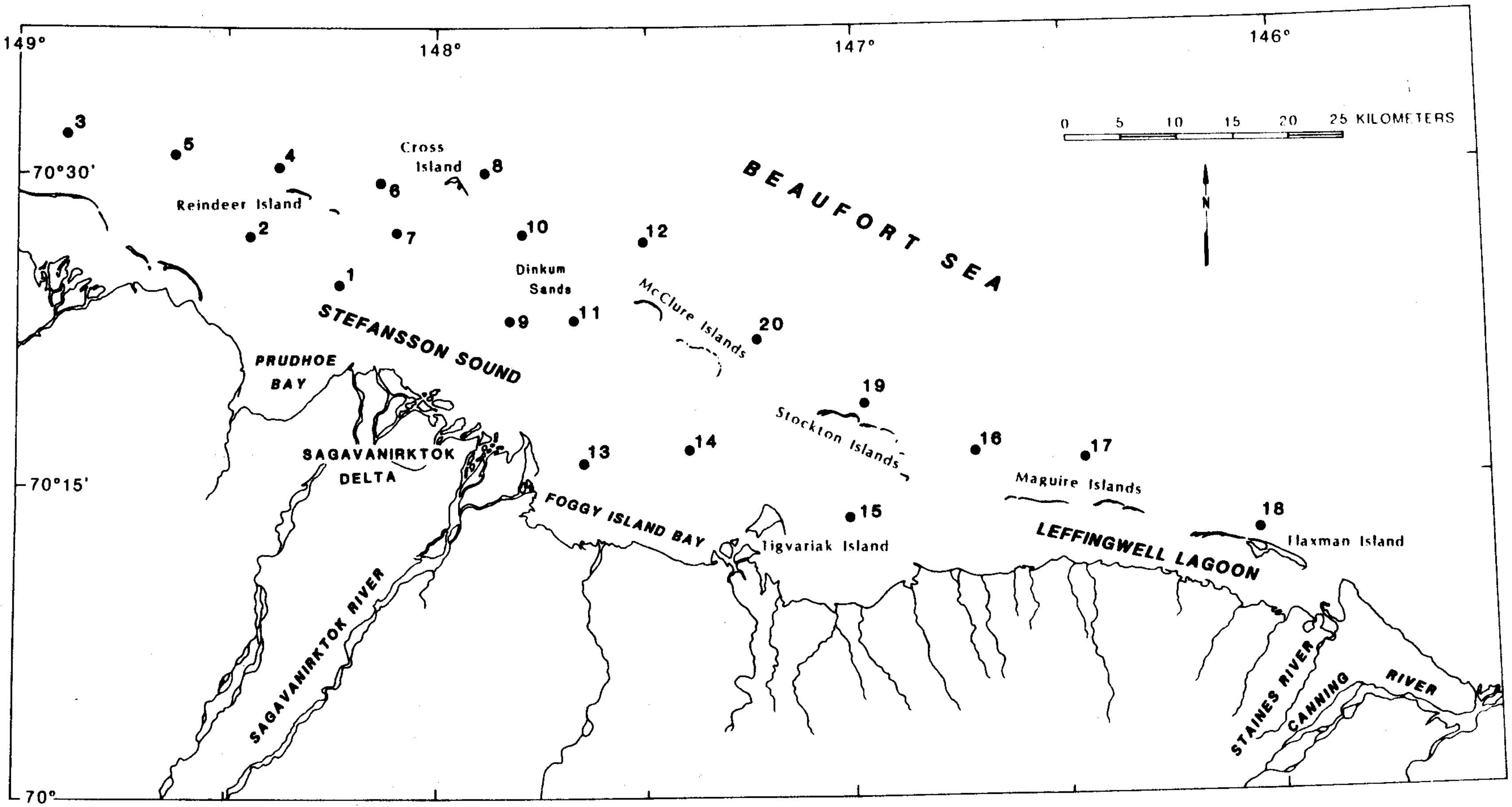

FIGURE 1. Map showing location of study area. Numbers refer to boreholes drilled in 1979 (Harding-Lawson Associates - USGS Conservation Division). Map is composed of Beechey Point to Flaxman Island Quadrangles (USGS).

average rate of 1.6 m/yr (Hopkins and Hartz, 1978). But the high-standing areas of Flaxman Island actually are retreating at a rate of 3.5 m/yr (Lewellen, 1977), demonstrating that the island also will appear as a barrier island in a few hundred years.

Topographic maps and LANDSAT images indicate that the Canning River in the past has shifted back and forth across its subaerial fan, as evidenced by the well developed radial channel pattern. The river's most recent shift has been from discharge points in Leffingwell Lagoon to the eastern fan boundary in Camden Bay .

The acoustic response of the sedimentary sequence to high resolution seismic profiling techniques in the Beaufort Sea is inferior to that of any other Quaternary to Holocene sediments we have studied with similar techniques in other parts of the world. We attribute this poor seismic resolution to a combination of factors unique to high latitudes:

1) Subaerial exposure of a soft sediment section to the cold atmosphere during glacial periods results in permafrost agradation, which in turn results in the formation of large masses of ground ice, in the form of ice wedges and ice lenses, that can be several meters thick. Besides this massive ice, there is excess interstitial ice in the sediments, totaling as much as 80% or more ice by volume in the upper 5 m of the section (Sellmann, et al., 1975). This ice does not necessarily conform to bedding planes in stratified sections. Thus, where preserved since the last glacial transgression, the ice results in discontinuous or irregular acoustic reflectors where good stratification may actually have existed.

2) Where glacial regression results in the disappearance of the ice in sediments, thaw collapse, small scale slumping, and sediment deformation may result.

3) Transgressive beach sedimentation, during periods of glacial regression, may replace the ice within ice wedges with sand and gravel. In this case, the basal transgressive unit will not be a distinct and continuous unit separating pre-transgressive sediments from post-transgressive ones.

4) The growth process of massive ice results in sediment deformation (cryoturbation). Thus the sediments exposed in coastal bluffs 2 m to 7 m high in the area generally appear unstratified or exhibit small scale crenulated folding.

5) The processes of formation of strudel scour craters to a sub-seafloor depth of 6 m to 7 m, and rapid filling of such craters (Reimnitz and Kempema, 1983), result in deposits at modern delta fronts consisting largely of strudel scour fill. These steep sided sediment pockets can not be resolved with presently available seismic reflection techniques.

6) Slow deposition on a jagged shelf surface that has been rapidly reworked by ice gouging (Reimnitz and Barnes, 1974; Barnes and others, 1984) results in the formation of complex, interfingering shoestring-shaped deposits (Reimnitz and Barnes, 1981). The resulting sediment package appears unstratified in seismic reflection profiles.

7) The presence of permafrost itself, whether partly or fully ice bonded, results in large sound velocity inhomogeneities within the section. A non-homogeneous velocity structure adds further complexities to the seismic stratigraphy. In the Canadian part of the Beaufort Sea, work with high resolution profiles has led to the concept of acoustically defined permafrost with its own, sporadic reflectors of several types (O'Connor, 1981).

8) Gas charged sediments are widespread in the study area (Harding-Lawson Assoc., 1979). Essentially vertically bonded non-stratified acoustic anomalies are produced (Boucher and others, 1981).

BACKGROUND INFORMATION

The first studies of the inner shelf stratigraphy in the study area were those reported on by Reimnitz and others (1972), who used interpretion of mini-sparker data to map the depth to the base of Holocene marine sediments and several underlying reflectors. Although they suspected the presence of offshore permafrost in certain shallow areas, their data did not confirm it. Since then more than 25 widely spaced boreholes have been drilled and numerous probe penetrations were made in the study area, mainly to study offshore permafrost (Harding-Lawson Associates, 1979; Osterkamp and Harrison, 1976, 1982; Osterkamp and Payne, 1981; Miller and Bruggers, 1980; Blouin and others, 1979; Harrison and Osterkamp, 1981; Sellman and Chamberlain, 1979). The information so obtained was extended considerably by the analyses of seismic data (Boucher and others, 1981; Neave and Sellman, 1982, 1983, 1984; Morack and Rogers, 1982, 1984; Rogers and Morack, 1980). From these studies we know that ice bonded permafrost is widespread within 5 to 10 meters or more of the seafloor. But this permafrost is patchy, and the depth to the top of ice bonded materials very irregular. In thick deposits of sand and gravel off Prudhoe Bay the top of ice bonded sediments drops sharply to 100 m or more. This feature has been interpreted as a major paleo-valley emerging from Prudhoe Bay and turning west out of Stefansson Sound. (Hopkins and others, 1979). An area of scattered boulders with prolific kelp growth was mapped from geophysical data, cores, surface samples, and diving off the Sagavanirktok River (Reimnitz and Ross, 1979). Beyond some speculation on the existence of three major paleo-valleys, one east of Flaxman Island, one between the Maguire and Stockton Island, and one off Prudhoe Bay (Hopkins and others, 1979), no stratigraphic interpretation of the borehole data has been published to date. While all inner shelf data, including a recent study of sediment geotechnical properties (Lee and Winters, in press), indicate a thin and patchy cover of Holocene marine sediments, a thick wedge of such Holocene materials has been defined on the central and outer shelf (Dinter, 1982).

SURVEY METHODS

Seismic work by the USGS in this area began in 1970, utilizing an ORE towed vehicle transducer system operating at 3.5 kHz. Data were poor, probably as a result of a combination of factors, such as, poor sediment response, poor equipment performance, and poor environmental conditions. In 1971 the 12 m R/V LOON, the first U.S. Geological Survey arctic vessel, began operating in the area using a 500 joule minisparker with an electrode designed by the first author. Data were recorded on a Gifft Model 4000 graphic recorder. The receiver consisted of a Teledyne model 20 high-resolution hydrostreamer and preamplifier, and a Khronhite passive filter. Data in most cases were acceptable to marginal. Degraded records were often due to marginal sea states for high-resolution profiling, but in particular due to the fine to coarse grained sediments with minimal internal reflectors. Much of the work occurred in shallow water and, therefore, produced multiples which obscured the actual data. A Simrad recorder provided bathymetric data. The acquired data resulted in a report on the surficial stratigraphy of the region between Tigvariak Island and the Colville Delta (Reimnitz and others, 1972). The 1972 operating season utilized the same fathometer, but replaced the sparker with an EG&G Model 230 Uniboom and an EG&G Model 265 Hydrostreamer. We also added an EG&G Model 259, 100 kHz side-scan sonar to record seafloor imagery. Seismic records were greatly improved in resolution, but with some loss of penetration. The side-scan sonar was towed from the bow of the boat off an "A" frame, rather than off the stern, as the vessel commonly surveyed in very shallow water (1m). This towing arrangement also facilitated the towing of other equipment off the narrow stern. Side-scan data, even in very shallow water, were excellent. Additionally, an EDO Model 324, 12 kHz transducer was mounted on the Uniboom catamaran to supplement bathymetric as well as some sub-bottom data in 1972. This bathymetry was recorded on a Gifft 4000 graphic recorder and the seismic data on an EPC 4100 graphic recorder. The 1973 field season operated with the same equipment as in 1972 with the exception of the 12 kHz transducer, and the addition of a second boomer plate to the Uniboom catamaran. This addition resulted in insignificant improvements of penetration and signal to noise ratio, and therefore was discontinued in succeeding field efforts.

In 1975 the R/V LOON was replaced by the newly constructed 13 m R/V KARLUK. No data were taken in this area during the 1974 field season. Aboard the KARLUK , the surveys from 1975 through 1982 were accomplished utilizing the Uniboom and side-scan sonar systems, and occasionally a sparker for site-specific studies. Additionally, a Raytheon RTT 1000, sub-bottom profiling system was added to the instrumentation in 1975. This system operates at 3.5, 7.0 and 200 kHz. Most data were taken at 7 and 200 kHz. A Del Norte Model 502 seismic amplifier and 12-20 hydrostreamer provided improved seismic data quality during this period. An EPC 3200 dual channel graphic recorder replaced the EPC 4100 in 1982. New program requirements and state of the art equipment development brought about instrumentation changes in 1983. The EG&G side-scan sonar system was replaced with a Klein Hydroscan system, consisting of a 531T, three-channel tape-compatible recorder, 100 kHz and 500 kHz side-scan sonars, and a combined sub-bottom (3.5 kHz) and micro profiler (500 kHz) attachment. Expansion of microprofiler data and recording of 7 kHz data were accomplished with the use of an EPC 1600 graphic recorder. The Uniboom was replaced by an ORE Model 5810A (Geopulse) sound source. Seismic data were tape recorded analog through a TSS Model 307 TVG amplifier for processing of the data, such as removal of sea swell distortion and stacking. The Klein 500 kHz side-scan sonar improved the resolution of seafloor images, but at the expense of range capability compared to the 100 kHz system. Bathymetric detail was greatly improved with the microprofiler, as was sub-bottom penetration with the 3.5 kHz transducer.

In general terms, data acquisition can be divided into groups of instrumentation as follows:

1. Seismic data

   a. EG&G minisparker
   b. EG&G Uniboom
   c. ORE (Geopulse)
   d. RTT 1000 at 7 kHz

2. Seafloor imagery

   a. EG&G side-scan sonar (100 kHz)
   b. Klein Hydroscan (100 and 500 kHz)

3. **Bathymetric data**

   a. Simrad recording fathometer (38 kHz)
   b. EDO (12 kHz)
   c. RTT 1000, (200 kHz)
   d. Klein Hydroscan, (100/500 kHz, 3.5 kHz)

EQUIPMENT CHARACERISTICS AND DATA QUALITY

Typically minisparkers operate at a dominant frequency of approximately 500 Hz within a filter bandpass of 350-900 Hz. The first 1 m to 2 m of sub-bottom data are lost due to the pulse length and reverberation of the outgoing signal. Penetration depths of 100 m and more can generally be achieved with resolution on the order of 1 m to 1.5 m. The dominant frequency of the Uniboom is about 2.5 kHz, with most data recorded between 900 and 2000 Hz. Typically the first .5 m to 1 m of sub-bottom is lost, expected penetration depths of 50 m to 100 m and resolution better than .5 m are appropriate for the uniboom. The ORE Geopulse System has a broader dominant frequency, dependent on power output, but lies generally between 2 and 7 kHz. Tests show that the ORE system has a higher output signal level, a higher frequency content, and can achieve better penetration and resolution than the Uniboom. The better performance of the ORE system in the Beaufort Sea may also be partly due to the common occurrence of sand and gravel, materials in which the ORE gives superior performance. Bandpass filter settings of 1-3 kHz are commonly used. Test runs by the first author have shown that by carrying two uniboom transducers on the same catamaran and pulsing both simultaneously, signal level outputs and broad frequency spectrum similar to those of the Geopulse system can be achieved. However, on small vessels where space is limited, this technique becomes impractical.

Quality of seismic data acquired is also dependent on towing configuration and technique for the source and receiver. In the case of small vessel operations, the source and receiver are towed on opposite sides of the vessel with the hydrophone (receiver) streaming as close to the sea surface as possible. The latter should be short hauled in shallow water and farther from the source in deep water. Degradation of the data often results from rough seas which causes "acoustic noise", from improper towing arrangements, and from inexperience of technical personnel. For example, towing the hydrostreamer too far behind the vessel in shallow water leads to incorrect water depth measurements and placement of multiples on the record. This can make analyses of the records very difficult and reduce the confidence of the interpretation. Quality of the seismic data acquired over the past thirteen years, in this area, has been degraded periodically due to a combination of the preceding causes. Additionally, the data have been degraded more often than not by poor sediment responsiveness to acoustic profiling. Overall, the data are acceptable to marginal, making interpretation and correlation difficult. Level of confidence in interpretation is good between Flaxman and Tigvariak Islands but decreases to questionable north of Prudhoe Bay, largely due to poor profiling conditions in that area. As will be seen later, that area has presented problems in preliminary interpretations of seismic data. The surfical layer of most Holocene sediment does not thicken eastward from Prudhoe Bay into Stefansson Sound, as erroneously interpreted by Reimnitz and others (1972), but rather thins to zero over the area of the Boulder Patch (Reimnitz and Ross, 1979).

Bathymetric and side-scan sonar data are good to excellent, and already have been used extensively for other program objectives.

TRACKLINE COVERAGE

A compilation of all track charts for the 13-year period is shown in Figures 2, 3, and 4 revealing a pattern which appears only partially systematic. However, for the purposes of the present investigation, the line spacing and orientation are adequate. Profiles used to measure depths to different seismic horizons in the study area are labeled with the line number and year on each of the Figures. Almost all of the data recorded along the remaining lines were viewed and used as guides to ensure that our regional correlation of major seismic horizons is correct. A complete listing of seismic lines from 1971 through 1982, including the time of operation of the different geophysical survey equipment and the data roll numbers, is given in the APPENDIX.

The primary reason for the apparently random line patterns is that field work objectives and priorities varied from one year to another, as did the sea ice distribution. The latter is a factor that commonly dictates where and how a particular line can be run. Furthermore, seismic profiles represent only a fraction of the data gathered. Often specific study topics were pursued, involving such additional techniques as underwater photography and video recording, diving operations, sediment and water sampling, coring, ice gouge studies and repetitive surveys of certain lines with side scan and 7 kHz equipment. Furthermore, many tracklines simply represent transit lines from one study site to another, on which only bathymetric data were taken. These factors have resulted in overlapping coverage with minisparker, Uniboom or Geopulse data in certain areas. For example, in 1979 Uniboom and minisparker lines were specifically placed over each of the 20 HLA boreholes drilled during the preceeding winter for the purpose of tying each hole to the seismic survey net. This use of different survey tools from one line to another, and the low

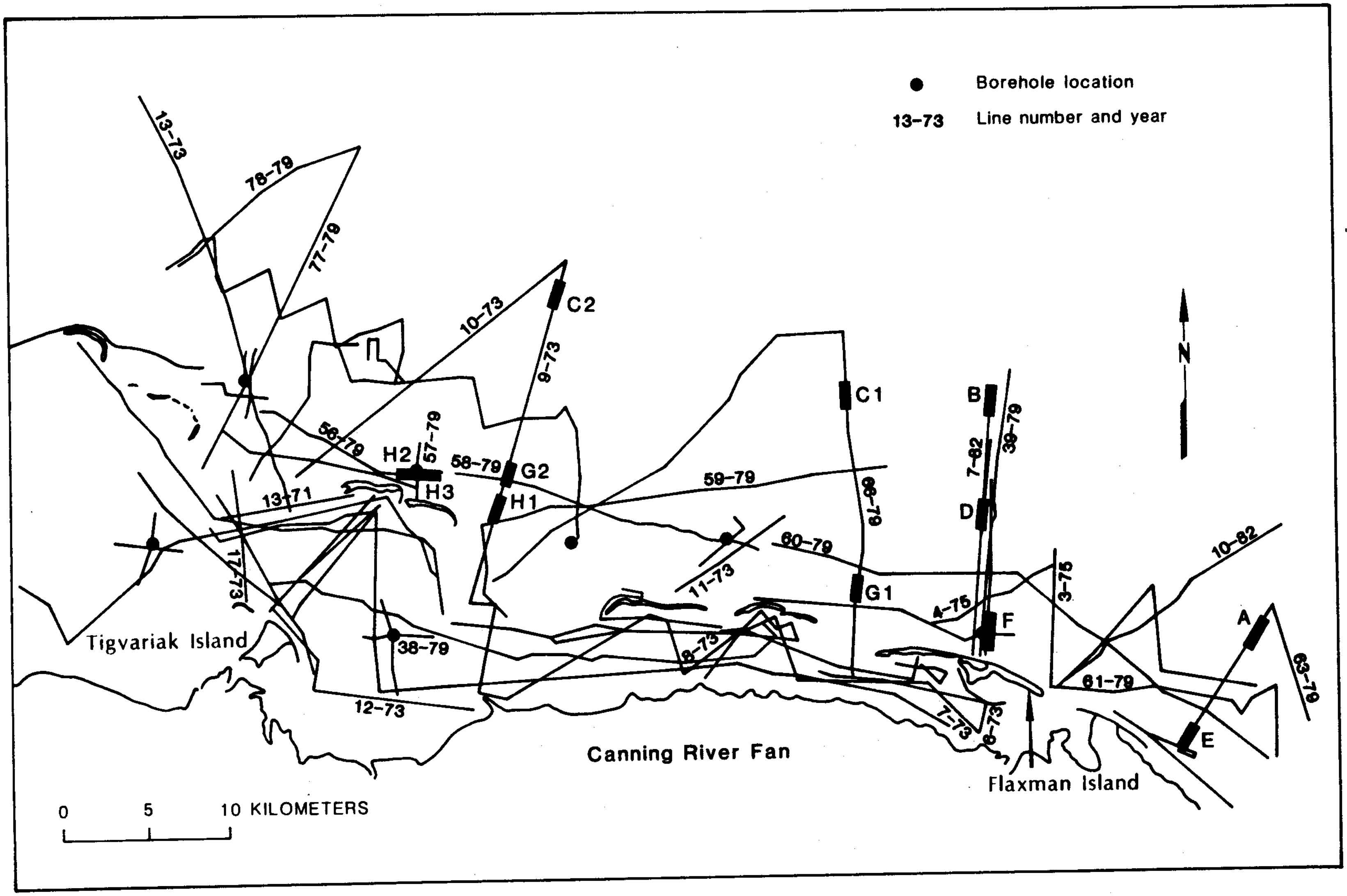

FIGURE 2. Trackline map - Tigvariak Island to Flaxman Island showing tracklines for 1971 - 1982. Tracklines labeled are those along which seismic interpretation was made. Lettered boxes are locations of seismic sections referred to in this report.

558

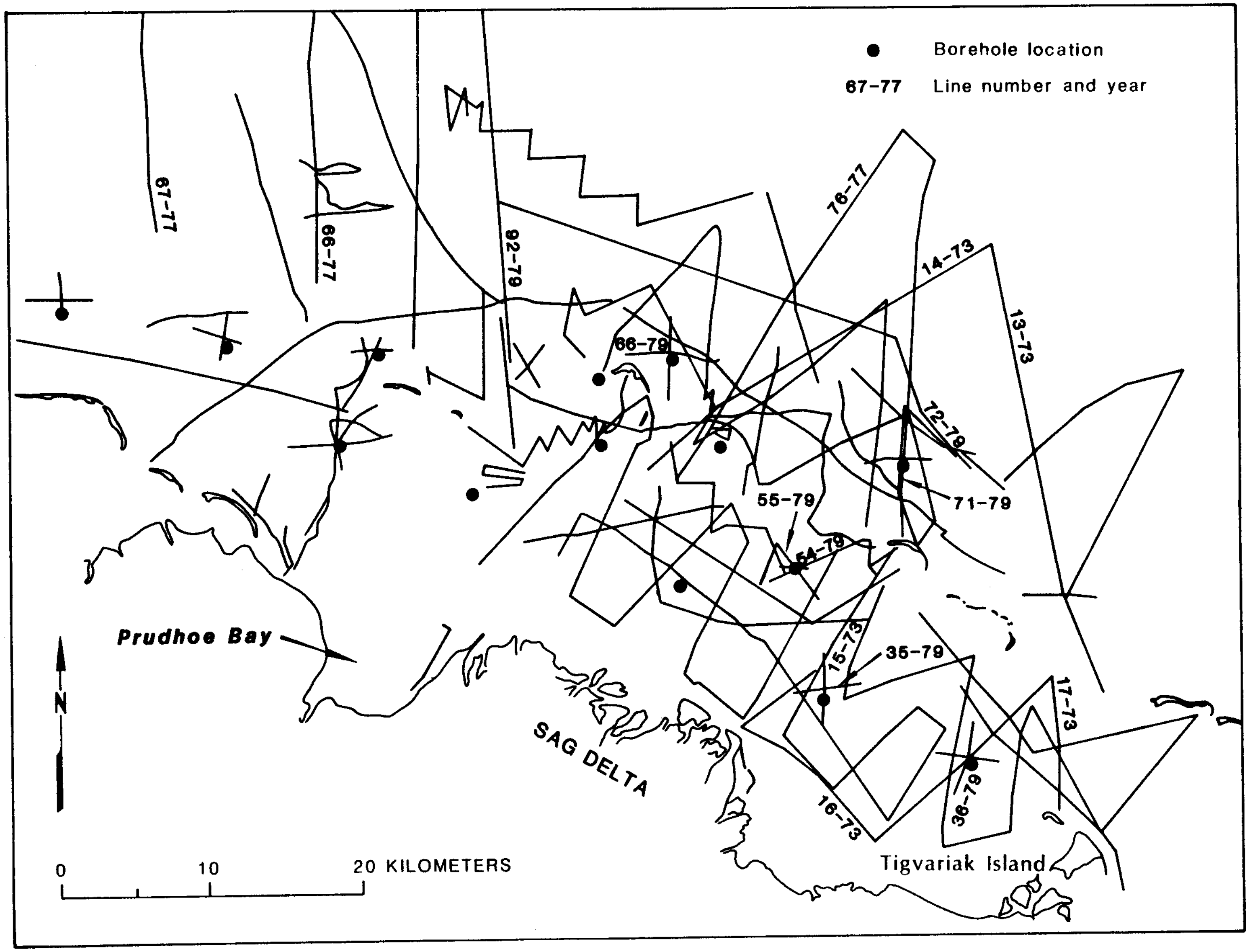

FIGURE 3. Trackline map - Prudhoe Bay to Tigvariak Island showing tracklines for 1973 - 1982. Tracklines labeled are those along which seismic interpretation was made and referenced in this report.

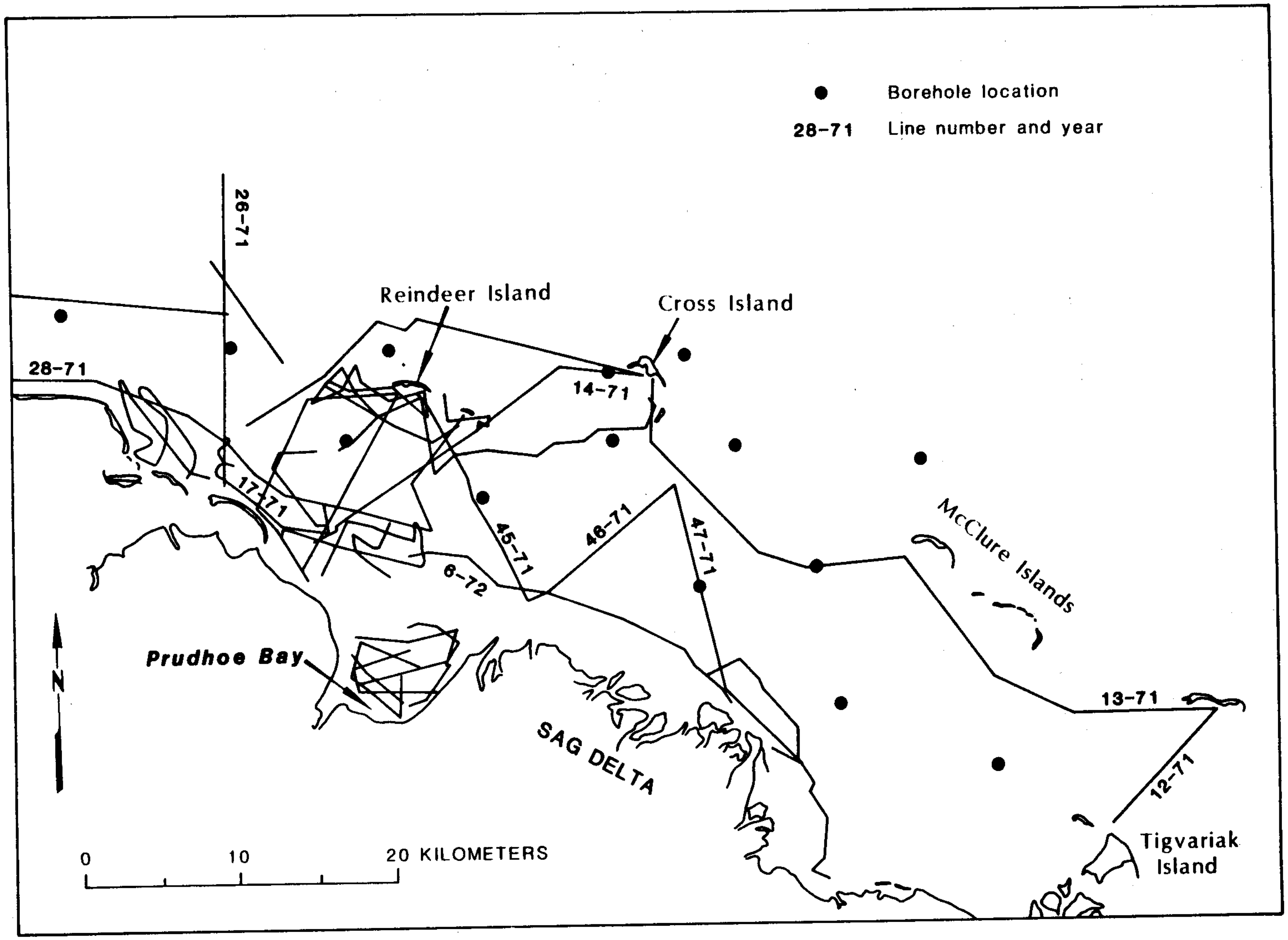

FIGURE 4. Trackline map - Prudhoe Bay to Tigvariak Island showing tracklines for 1971 - 1972. Tracklines labeled are those along which seismic interpretation was made and referenced in this report.

data quality in many places, made correlation between the 20 boreholes a long and difficult project. Lithologic and paleontologic data from the boreholes show a wide variety of sediments and sediment sequences. Prior to the seismic data interpretation, correlation of boreholes was tenuous at best, but a combination of stratigraphic, lithologic, paleontologic, and seismic studies has led to reasonable success in delineating the shallow Pleistocene and Holocene geology throughout most of the area.

SEISMIC DATA ANALYSIS AND RESULTS

Description of Acoustic Reflectors

Eleven seismic profiles, representive of data from the region between Flaxman and Tigvariak Islands are lettered and keyed to Figure 2. The discussion of these samples will serve to introduce the different acoustic surfaces recognized, their characteristics, overall relationships to each other, and their spatial distribution. Seismic sections west of Tigvariak Island are not shown as the data are of poor quality, and the regional seismic stratigraphy is relatively flat lying.

Excluding a very shallow horizon at the base of modern sediment accumulation, we identified seven distinct reflectors, and numbered them 1 through 7. The oldest is number 1. No single profile shows all seven major surfaces as strong reflectors. The key to assigning numbers to these reflectors with a high degree of confidence is a combination of a) traceability from one line to another, b) assumption of an orderly sequence where a particular reflector is not traceable over a long distance, and c) recognition of a strongly developed layer cake stratigraphic model that lacks complexities produced by faulting, tectonic deformation, or interaction of strongly different sediment regimes.

Reflectors 3, 4, and 7 can be traced east-west throughout much of the area, but number 7 occurs only seaward of the barrier islands. It top laps into the present seafloor, dips offshore, and is most likely overlain by additional younger reflectors on the outer shelf beyond the area of our data. Within the lagoons we can trace a shallow reflector, which stratigraphically seems to overlie 7, through the entire region. Because it is so shallow, this surface is traceable only with the 7 kHz records supplemented in places with uniboom where the surface is more than 1 m to 1.5 m below sea floor.

On a regional basis, reflectors 3, 4 and 7 are generally flat lying, whereas intermediate reflectors have slight NE dips. Seaward of the island chain in the central part of the study area, these intermediate reflectors steepen significantly.

Seismic Section A.

This profile (Fig. 5) illustrates surfaces 3 and 4, both with approximately the same reflectivity. Surface 4 is flat lying and conformable to sediments above and below. Surface 3 is overlain by conformable sediments, but truncates a channel-like depression below. On the left side of the profile is a seafloor feature that appears to be a shoal with the steep side to the south. The seafloor on either side of the feature can be traced as a nearly horizontal datum. The orientation of the feature is not known, but it is in all respects, including the water depths of surrounding terrain, so similar to shoals of the stamukhi zone (Reimnitz and Maurer, 1978; Reimnitz and others 1978; Reimnitz and Kempema, 1984), that we interpret the feature as a shore-parallel shoal constructed since the last transgression, and migrating southwestward. Based on acoustic reflectivity, sediments between the sea floor and surface 4 and between 4 and 3 appear to be similar in lithology, and may be sand and silt interbeds.

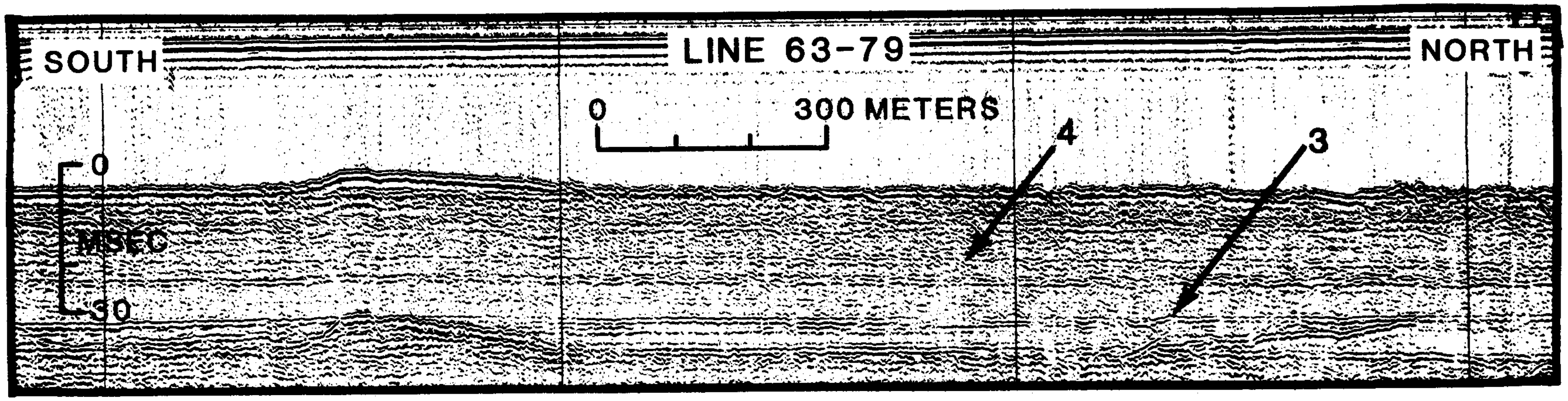

FIGURE 5. Seismic profile near the eastern border of the area taken in approximately 20 m water depth.

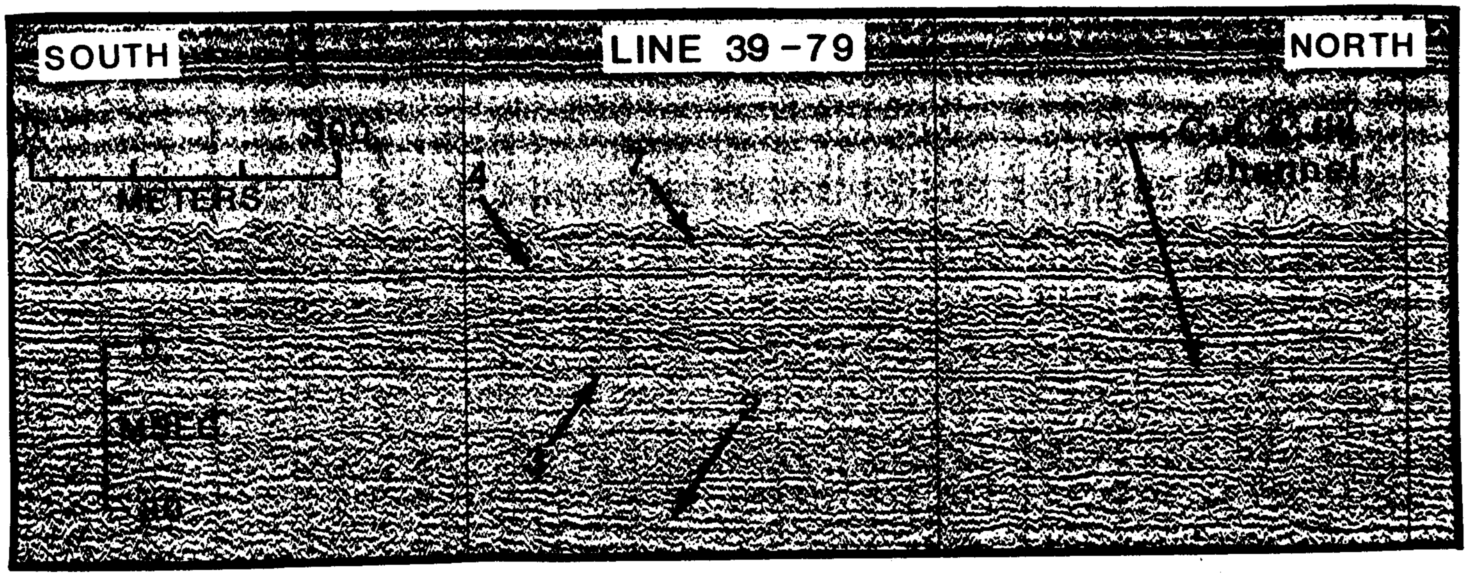

FIGURE 6. Seismic profile taken in 30 m water depth north of Flaxman Island.

Seismic Section B.

This profile (Fig. 6) depicts reflectors 2 and 7 in addition to 3 and 4. All four reflectors are generally conformable to each other. Sediments below 2 and between 3 and 4 appear to be irregularly stratified, with a slight seaward dip. Internal bedding exhibits characteristics of thickening, thinning, pinch outs, and channeling. The irregular seafloor is characteristic of an intensely ice-gouged surface, and in some places, the gouging has cut deeply enough to penetrate surface 7 and remove it entirely. To the south (left) surface 7 outcrops at the seafloor. Surface 3 truncates what may be a small cut-and-fill channel. Sediments between the major surfaces indicated appear less similar in nature and exhibit more varied acoustic reflectivity than those in Figure 5. This might suggest a sediment sequence containing occasional gravel and more sand.

Seismic Section C.

Seismic section C composes two profiles, C-1 and C-2 in which reflectors 3, 4, and 7 can be seen (Fig. 7). In C-1, the acoustic reflectivity of sediments above surface 4 is so similar to that of the sediments below, that it is difficult to differentate. Surface 3 in places is much stronger than it appears laterally. This discontinuous character might be assumed to result from lithologic similarites of the sedimentary facies above and below, and, therefore, the acoustic impedance of the surface is markedly reduced locally. Below this surface, pinch outs and channeling can be observed as in Figure 5. Sediments between 3 and 4, on the basis of acoustic reflectivity, appear to grade upward from sands to interbeds of sand and fine-grained materials. Surface 7 is buried sufficiently deep below ice gouge incision depth to escape reworking. It deepens to the south (left).

In profile C-2, surface 7 is very shallow, weak, and discontinuous. It has been severely destroyed by ice gouging, which suggests that the present seafloor in this part of the offshore region of the area has undergone and is undergoing mechanical reworking. Also, deposition of sediments is not occurring, and the shelf surface may be undergoing erosion. The unit between 3 and 4 shows better seismic stratification in the upper part, suggesting that the sediments may be fining upward as in C-1. However, it should be noted that the upper sediments dip seaward and top lap into reflector 4. Surface 3 is even more discontinuous than in C-1 and most likely for the same reasons.

Reflectors 3 and 4 can be traced westward through the area for which we show no samples to the region off Prudhoe Bay. Reflectors are generally flat lying and have similar characteristics as the examples shown in Figures 5 - 7. However, the two reflectors rarely truncate channels in the western part of the the study area except for an area NE of the Sagavanirktok River where channeling again is observed at similar distances seaward of the island chain.

Seismic Section D.

Two additional reflectors, 1 and 6 can be observed on section D (Fig. 8). Reflector 1 is conformable to surfaces 2, 3, and 4 but has a slight seaward dip. This is the deepest reflector observed throughout the area and was observed only on this seismic trackline. It is important to note that the entire stratigraphic sequence from reflector 1 to the sea floor exhibits relatively flat lying to slightly seaward dipping units and are generally conformable to each other. Surface 6, although difficult to impossible to see in some regions, downlaps onto 4 farther to the north. On many seismic profile crossings, surface 6 apparently top laps or crops out to the south at the juncture of the smooth and heavily gouged seafloor, as seen in this profile. Few profiles show surface 6 extending landward beyond the heavily gouged area and cropping out under the smooth floor. When viewed with side scan sonar, gouges are seen south of the juncture between smooth and jagged seafloor (Barnes and Asbury, in press). This pronounced boundary has been noted in numerous publications and has been described as the "18 meter bench" (Barnes and Reimnitz, 1974; Reimnitz and Barnes, 1974; Reimnitz and others, 1978; Barnes and others, 1980; Reimnitz

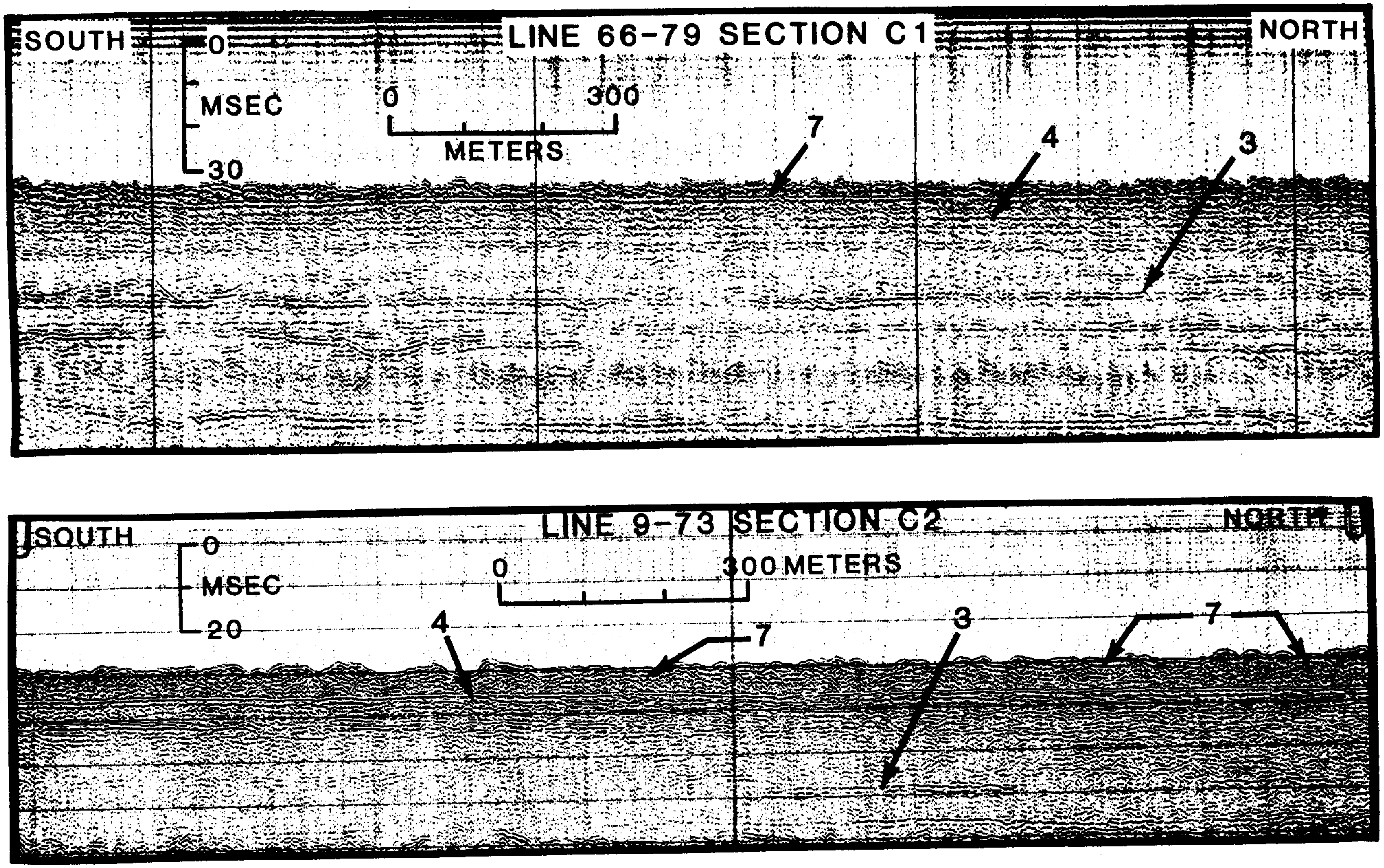

FIGURE 7. Seismic profile taken in 30 m water depth north of the Maguire Islands.

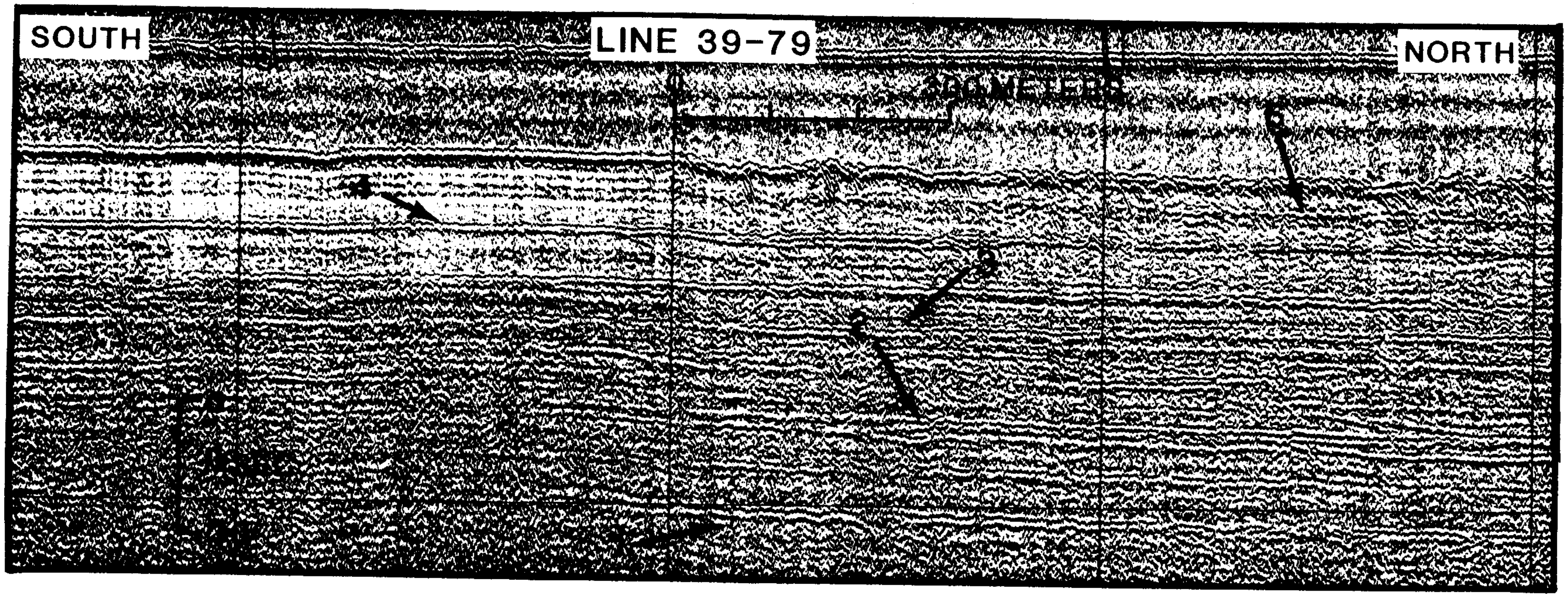

FIGURE 8. Seismic profile taken in approximately 20 m water depth north of Flaxman Island.

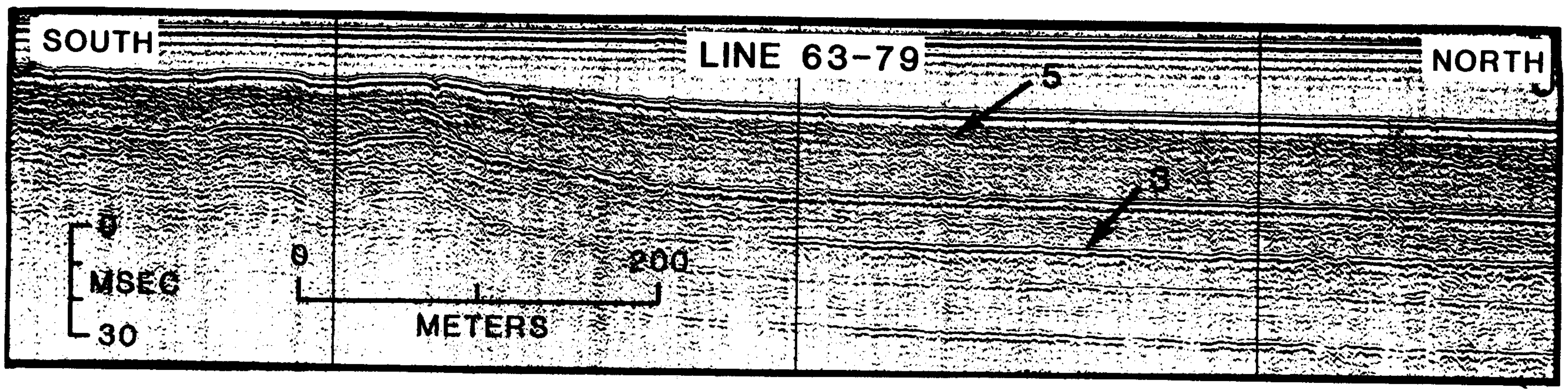

FIGURE 9. Seismic profile taken in approximately 10 m water depth at the eastern margin of the area.

and Kempema, 1984), but a total understanding of its nature, or origin still is lacking.

As is the case with remnants of surface 7, the 2 m to 3 m relief between the smooth seafloor surface and the gouged areas may also represent a combination of mechanical destruction of the sediments by gouging and removal of sediments by currents. In essence the "18 meter bench" is slowly retreating shoreward as intense gouging continues. Sediments below surface 3 and 4 show evidence of pinch-outs and channeling.

Seismic Section E.

Surface 5 can be observed on section E (Fig. 9). This surface has a hummocky, irregular appearance. This characteristic is best seen on the 7 kHz subbottom profiler data. Other profiles show 5 bottom lapping offshore onto 4, and it generally crops out at the sea floor near the barrier islands. Analysis of the 7 kHz records shows the surface to have relief of 2-4 meters, with peak-to-peak distances of 20 to 40 meters. In Figure 9, and elsewhere near the barrier islands, reflector 5 is the first reflector below the sea floor. This stratigraphic postion suggests a possible basal transgressive origin and a Holocene age for the overlying sediments. However, due to its top- and bottom-lapping nature, the overall geometry rules out an early Holocene age. Surface 4 is difficult to see in Figure 9, primarily due to interference by seafloor and underlying multiples. Surface 3 is very pronounced and can be seen to rise slowly to the south, somewhat independent of the present sea floor gradient. Sediments between 5 and what we interpret as 4 have slight seaward dips toward the south end of the seismic profile.

Seismic Section F.

This profile (Fig. 10) passes directly over borehole 18 and illustrates surface 5 and 3. In Figure 9, and other profiles, surface 3 gradually rises to the south and passes under the shoal region surrounding Flaxman Island, unaffected by the stratigraphy and seafloor morphology above. This lack of relationship to the present island chain is characteristic for both surfaces 3 and 4 throughout much of the study area. Surface 5 crops out at the seafloor between borehole 18 and Flaxman Island, and dips in a seaward direction. Also in Figure 9, the internal stratification of the unit between 4? and 5 dip seaward near the island. The internal structures also are very irregular, suggesting disruption by such processes as mass wasting, slumping, or sliding during deposition, particularly at the base of the unit. The seaward dip of this unit seen in Figure 10 is characteristic for units seen in other seismic profiles as far west as the Stockton Islands (Figure 11).

Seismic Section G.

Surface 4 is clearly defined on profile G-1 seaward of the point where it is obscured by multiples, and less well defined on profile G-2 (Fig. 11), an example from a still more westerly region. The bedded, and seaward dipping sedimentary sequence above 4 is truncated at the sea floor. This is analogous to the setting off Flaxman Island shown in Figure 10.

Seismic Section H.

Cut-and-fill channels can be observed on many seismic profiles in the vicinity of the island chain. These old channels all have been filled by sediment in transit on the inner shelf, thereby smoothing over the originally rough seafloor. Section H-1 (Fig. 12) is a profile across the shallow water region in the western half of the island chain. Multiple sequences of cut-and-fill channels can be seen. The smaller, narrow features could be tributary channels feeding into a larger system. This sequence has been truncated, the channels filled, and a very thin younger sequence was deposited on top. The relief of the erosional surface is quite varied and suggests incomplete planation before a following transgression deposited new sediment. Profile H-2 (Fig. 12) is another example, a transverse section across one of the larger channels, in which borehole 19 was sited

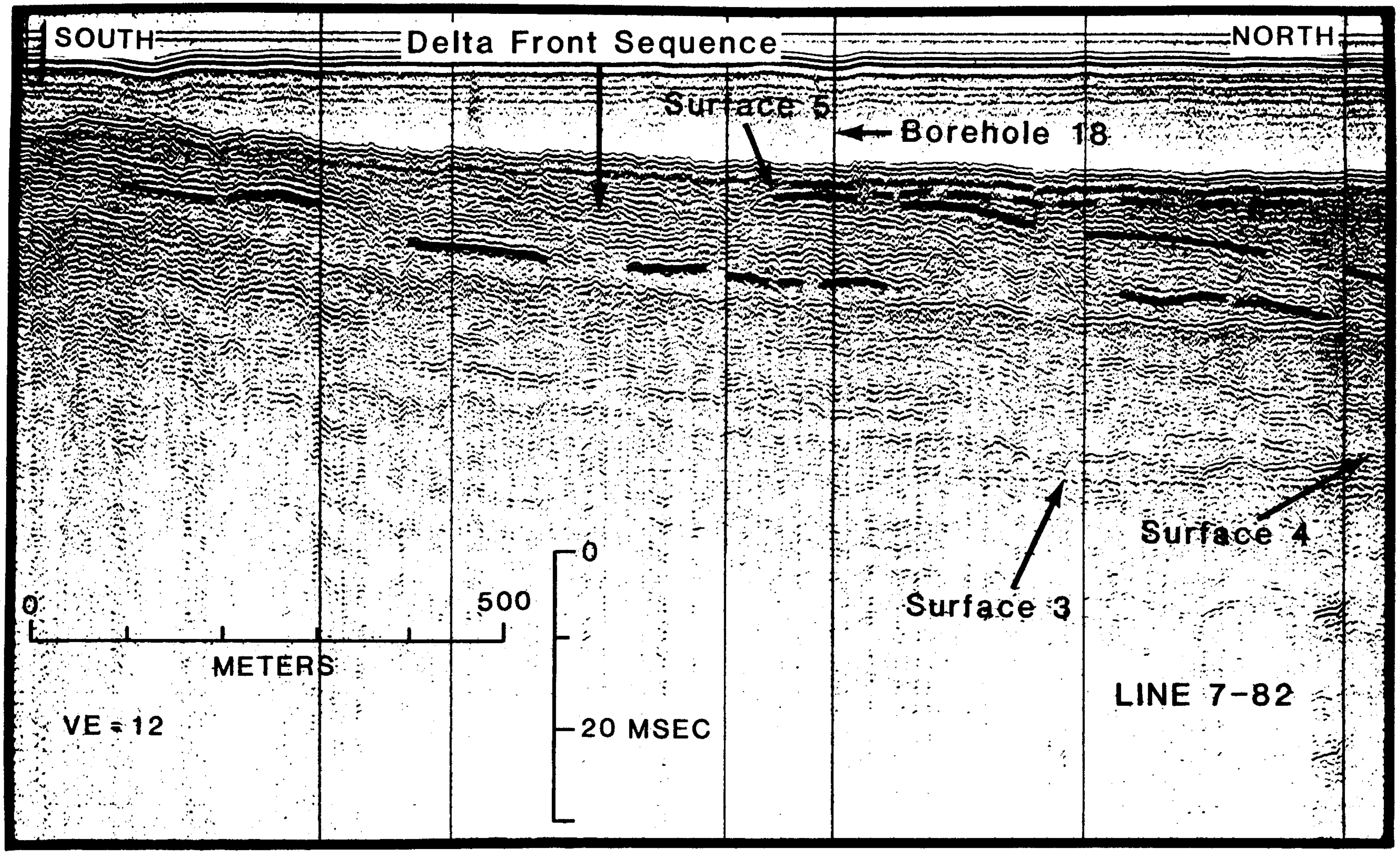

FIGURE 10. Seismic profile taken north of Flaxman Island through borehole 18.

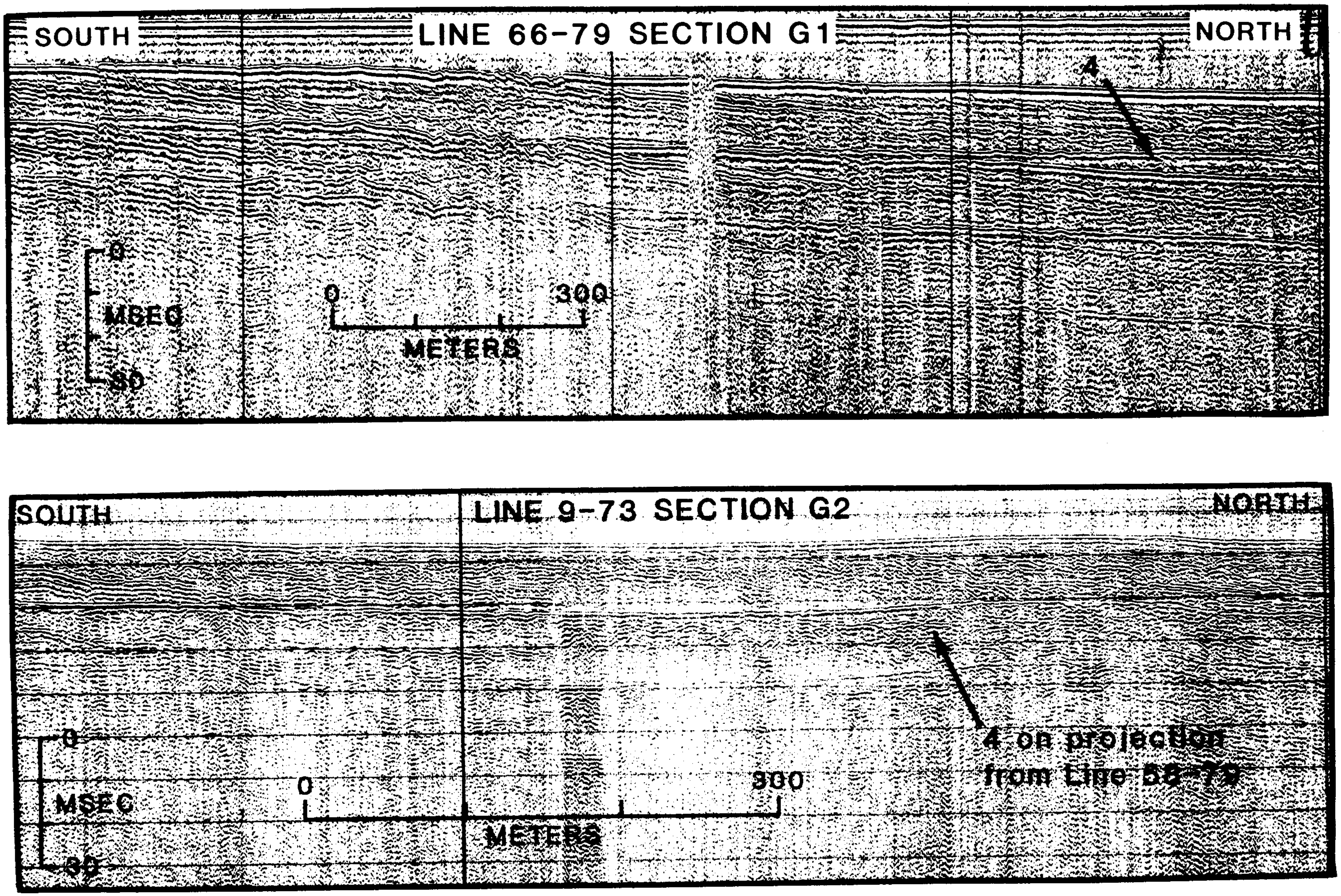

FIGURE 11. Seismic profiles taken on the seaward edge of the barrier island shelf (G1, north of Maguire Island; G2, north of Stockton Islands).

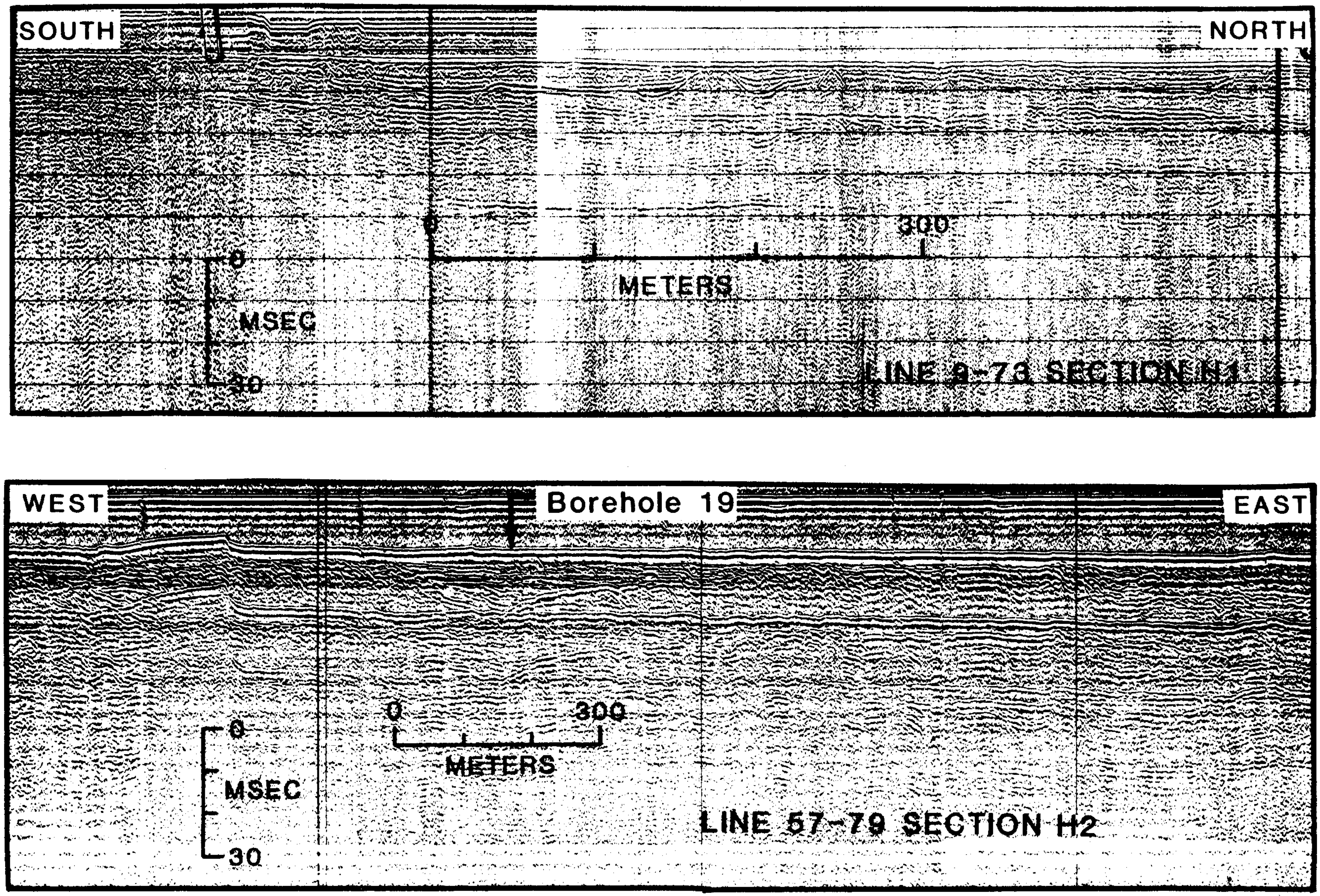

FIGURE 12. Seismic profiles taken in shallow water north of the Stockton Islands.

(Fig. 2). As in profile H-1 (Fig. 12), a shallow erosional surface can be seen east of the channel. The seafloor was again smoothed by sediments filling depressions. An enlargement of the channel is shown on section H-3 (Fig. 13). This channel was approximately 12 meters deep and 600 meters wide, and seems to trend NE-SW. Successive cutting and filling can be seen, with sediment supply originating from the west or south, as indicated by the apparent bedding plane dip of channel fill. This fill possibly originated from erosion in the Stockton Islands area. The materials below the uncomformity into which the channel was cut are nondescript and may consist of sands and gravels intermixed. The knowledge gained from borehole 19 provides ground truth for seismic records that penetrate similar channel fill in other areas. These combined data were very important for the interpretation of the geologic history during Quaternary time in the study area..

Seismic Section I.

Seismic profiles crossing the locations of boreholes 16 and 17 (Fig. 2) reveal that these also were inadvertently drilled into channel fill. The profile in Figure 14 shows that at the precise location of borehole 17, a channel more than 10 meters deep and 800 meters wide is located. This channel, like the one in borehole 19, also is positioned between two present day islands. Although less obvious, this channel reflects several periods of cut-and-fill prior to smoothing of the present surface by movement of recent sediments on the seafloor. In each case, the channel apparently maintained its position through successive transgressions and regressions, spanning considerable time. Seismic data do not suggest additional channels north of the subaerial portions of the Maquire and Stockton Islands. One might speculate that these channels were confined to their positions as a result of the presence of the islands during cutting and filling. This also suggests that the barrier islands are relatively stationary and not moving in time nor constructional in nature.

SUMMARY OF ACOUSTIC REFLECTORS

Seven distinct surfaces have been identified on the high resolution seismic records and described. The essential features of the seven surfaces are:

Surface 7: Seen in seaward, deeper region only. Partially destroyed by ice gouging, slight seaward dip.

Surface 6: Central parts of study region, in places downlaps onto 4, top laps at the smooth shelf shoreward of the 18 m bench, may in part be equivalent to a mechanically formed surface which represents maximum incision depth of ice gouges over long term as the "18 meter bench" retreats shoreward.

Surface 5: Central parts of study region and near the island chain, hummocky relief, downlaps seaward onto 4, crops out at or near the island chain.

Surface 4: Erosional surface, relatively flat in outer regions, rises in attitude near and under the island chain.

Surface 3: Same description as surface 4, but deeper.

Surface 2: Deep reflector in middle and outer portions of eastern area.

Surface 1: Same description as for surface 2, except that it lies deeper in the section.

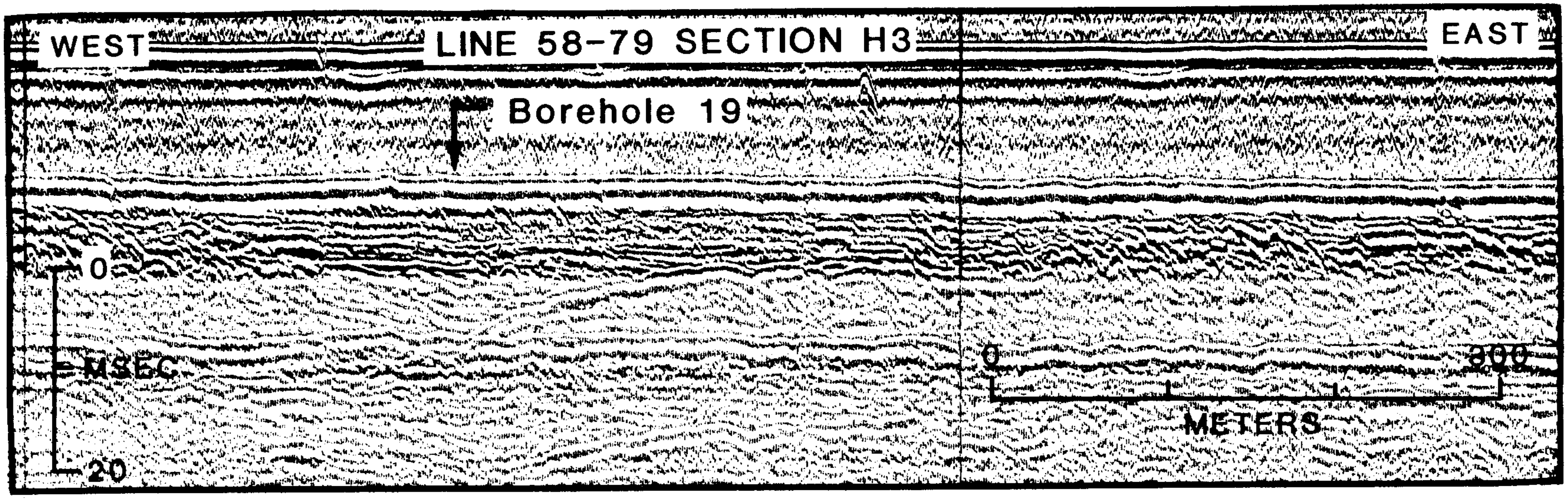

FIGURE 13. Seismic profiles taken through a cut and fill channel located at borehole 19 north of Stockton Islands.

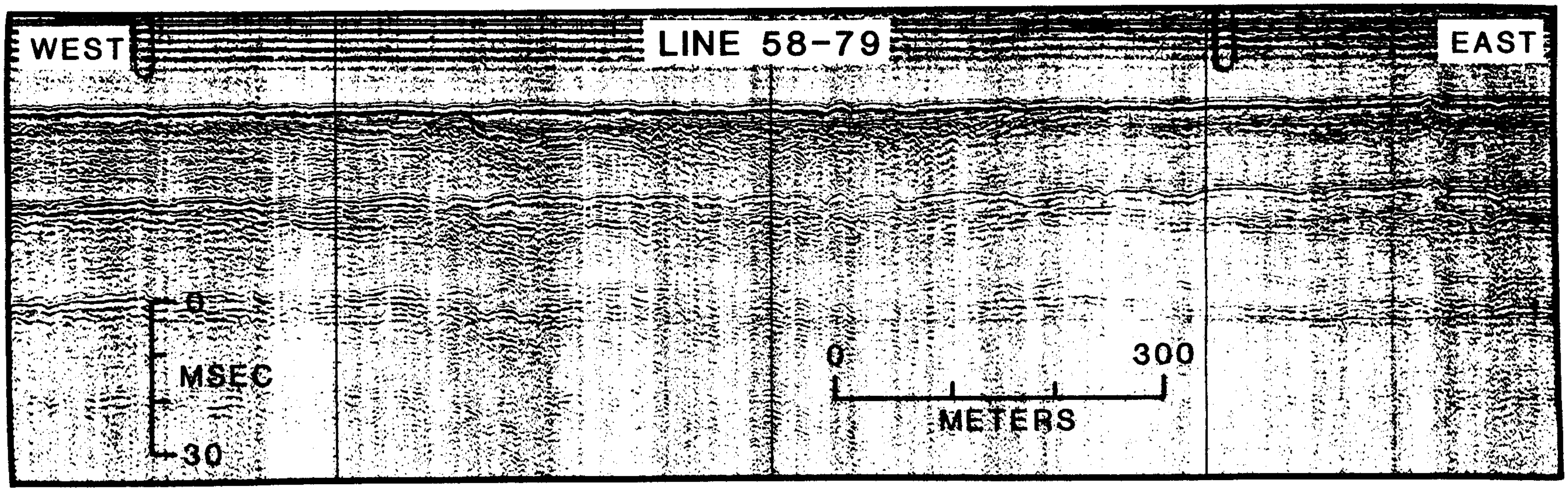

FIGURE 14. Seismic profile taken through a cut and fill channel located at borehole 17 north of Maguire Islands.

AREAL DISTRIBUTION OF MAJOR SEISMIC REFLECTORS AND INTERVENING SEDIMENT PACKAGES

Surfaces 1, 2, 6, and 7

Seismic reflectors 1 and 2 are observed north of Flaxman Island along seismic line 39-79 and reflector 2 alone on the seaward end of line 66-79 north of the Maguire Islands. The significance of these reflectors is that when projected southward into the Alaska State A-1 drill hole on Flaxman Island they lie within a non-marine sequence of sediments. Also, in both areas of occurrence these surfaces have a slight seaward dip, suggesting sediment sources in the Brooks Range, perhaps in a setting similar to that of the present Canning River Fan onshore. Little else can be said about these reflectors, as additional data are lacking. Surfaces 6 and 7 are not significant enough to warrant lengthy discussions of each. However, one should keep in mind their stratigraphic positions relevant to the surfaces discussed below, their seaward dip, and the fact that each crops out at the sea floor.

Sufficient data and seismic line intersections permit contouring of surfaces 3 and 4 and also a "pre-Holocene" reflector from Flaxman Island to Prudhoe Bay.

Surface 3

Figures 15 and 16 define the depth of surface 3, and show the spatial characteristics of sediments which overlie the surface. The contours are dashed where questionable. There is a dominant WNW-ESE trend which generally subparallels the present coastline and island chains. The hachured area north of Prudhoe Bay and southeastward to Tigvariak Island across the Sagavanirktok delta (Fig. 16) represents an area where surface 3 is equal to surface 4. Reflector 3 probably was removed during the erosional cycle which formed surface 4 The area defined as PBT (Fig. 16) refers to a region where seismic records exhibit numerous hyperbolics throughout the section. The significance of these hyperbolics, already mapped and discussed by Reimnitz and others (1972) is still in question; but the restricted occurrence of the hyperbolics in the area near Prudhoe Bay and the "Sag" delta is rather striking. This pattern may represent a broad topographic low that was filled by a sedimentary sequence near the surface and at depth similar to the formation of the Prudhoe Bay area and the subsequent infilling of perhaps an ancestral "Sag" River channel. This topographic low would be a much broader feature than the Paleo Valley postulated by Hopkins to exit from the present Prudhoe Bay and turning westward away from the present "Sag" Delta (Hopkins and others, 1979). Some hyperbolics have also been observed on seismic records around Cross Island to the northeast.

The NE-SW trend of surface 3 contour lines (Fig. 15, 16) may suggest the past existence of a broad flood plain of which the old "Sag" River was a part. Insufficient data exist to substantiate coexistence of an old channel, thus the existence of a low relief flood plain is more appropriate. The convex curvature of the contours north of the Canning fan-delta is also striking. The gradient of that surface steepens as it nears the coast and suggests that surface 3 may crop out south of the shoreline on the present Canning River fan. Two embayments with NE-SW linear trends can be observed on surface 3, one through borehole 17 (Fig. 15) north of the Maguire Islands and the other north of the McClure Islands near borehole 12 (Fig. 16). These embayments may mark an old Canning River drainage in the former case and old "Sag" River drainage in the latter. But the relief across the features is only four meters, and their side slopes are gentle.

The configuration of surface 3 suggests that these two major river systems may have played a part in forming the erosional unconformity during a period of lowered sea level. As transgression resumed, sediments were apparently distributed more or less conformably to surface 3 over the area. However, dips of 8 and 13 minutes can be observed in the outer region between the two embayments previously mentioned. These dips suggest that deposition may have first occurred in this area during the first stages of transgression followed by wider distribution as topographic

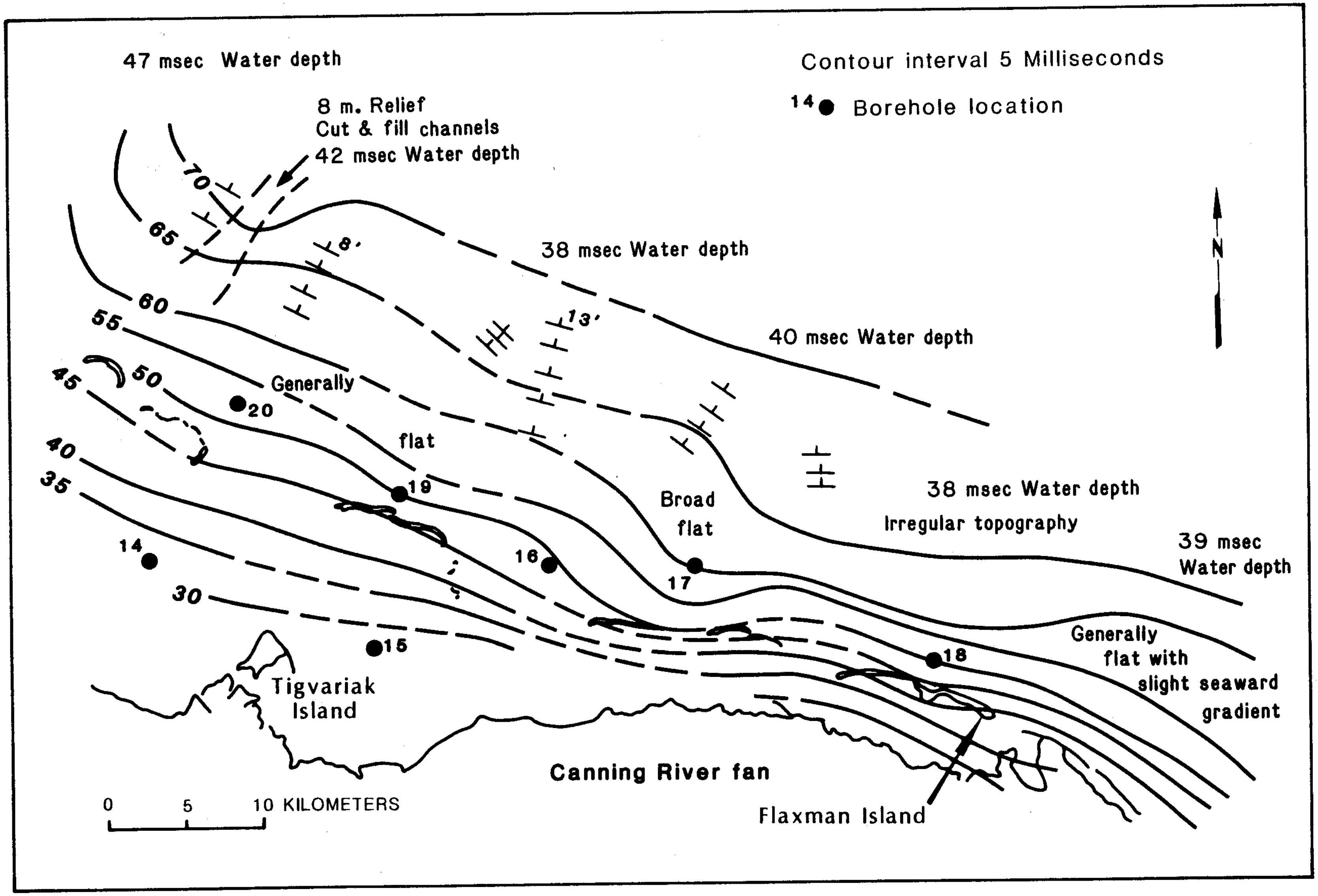

FIGURE 15. Contour map showing depth of surface 3 between Tigvariak and Flaxman Islands.

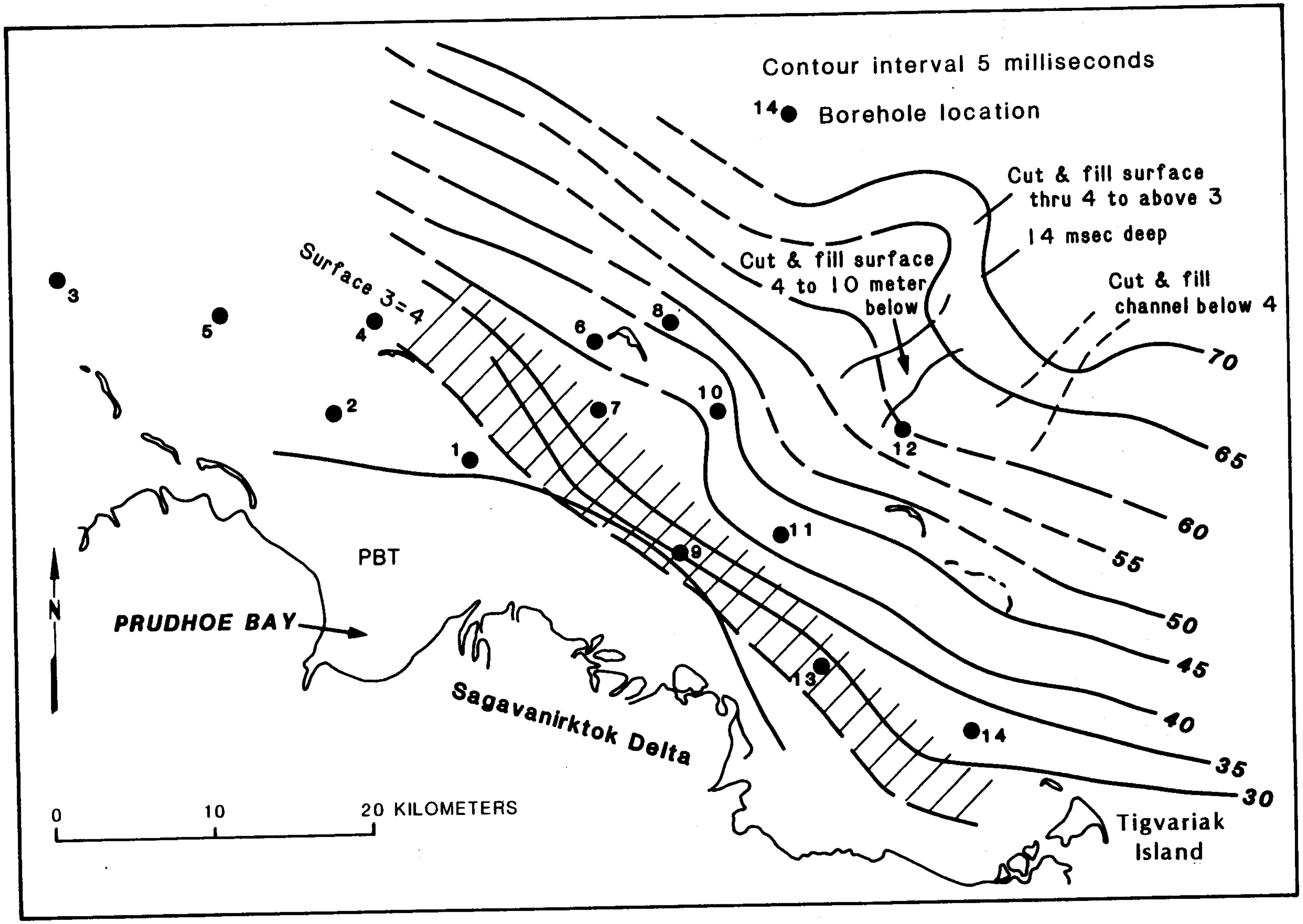

FIGURE 16. Contour map showing depths of surface 3 between Prudhoe Bay and Tigvariak Island.

irregularities were reduced. The cut-and-fill channels in the central region probably were cut at the close of this depositional transgression and at the initiation of the next erosional cycle, which led to the formation of surface 4.

Data from the West Mikkelsen Unit 2 drill hole on Tigvariak Island show loose gravel, sands, and conglomerates of non-marine origin below surface 3. Borehole 15 (Fig. 15) also shows sand and gravel of a non-marine origin below surface 3 in conjunction with fresh water fossils and gravel in the sediments above surface 3 and below surface 4 (Peggy Smith, Oral Commun. 1984). Alaska State A-1 drillhole on Flaxman Island also shows the non-marine characteristics of the sediments below surface 3. The presence of (marine?) shell fragments near surface 3 suggests close proximity to a beach-like environment. Seaward in borehole 18 (Fig. 15), nearshore and beach sediments are indicated above and below surface 3 (Peggy Smith, Oral Commun. 1984). These data suggest that an ancestral shoreline lay somewhat north of the present shoreline at the time of initiation of surface 3. Using a sound velocity of 1600 m/sec for the sediments penetrated acoustically, approximately 10-25 meters of sediment remain between surfaces 4 and 3 in the outer central region, little to none near Prudhoe Bay and approximately 10 m along the Flaxman-Maquire Island chain.

Surface 4

The depth to surface 4 is contoured in Figures 17 and 18, dashed where the surface cannot be clearly seen on the seismic profiles as was the case with surface 3 contours. Those of surface 4 strikes WNW-ESE, and have a gentle offshore slope. The previously existing embayment north of the McClure Islands is no longer evident. The embayment north of the Maquire Islands still existed at the time of surface 4 erosion; but the present embayment is somewhat larger than its predecessor and has shifted somewhat west of its previous position. This suggests that the old Canning River continued to play a role throughout the depositional cycle between surfaces 3 and 4 and was an active agent in forming surface 4 topography. We see no evidence for the existence of an old "Sag" River at this time. A topographic high now exists north of Flaxman Island, where underlying surface 3 had only slight topographic irregularities.

The convex curvature of the contours nearest the coastline of the Canning fan-delta is again evident. Surface 4 is at or near the sea floor near Prudhoe Bay and like surface 3, may crop out south of the coastline on the modern Canning River fan. North and west of Tigvariak Island, sediments overlying surface 4 are conformable, are relatively flat lying, and have a slight seaward dip. A region of cut-and-fill channels and more steeply dipping internal strata than noted above surface 3 exist along the island chain between Stockton and Flaxman Islands (Fig. 17). Direction of dips suggest a crenulated, prograding delta front cut by small channels. This delta-like subsurface feature is clearly related to the present Canning River fan-delta. The 35 to 45 minute dips are, in fact, in agreement with dips characteristic of classic low-latitude "delta front sediments" of other delta systems (Coleman and Prior, 1980). They are, however, much steeper than those of modern Arctic deltas. The position of channels near the modern Canning River suggests that an old Canning River played an active role in the progradation of the postulated delta across erosional surface 4. The orientation of small channels between the Stockton and McClure Islands suggest increased activity of the Shaviovik River, south of Tigvariak Island, during the same time. Most of the larger channels, including those along a NE-ward extension from the "Sag" delta exhibit repeated cycles of cutting and filling. These data suggest that the old Canning and "Sag" Rivers have been maintaining positions throughout the depositional/erosional cycles from pre-surface 3 to post-surface 4 time.

Our interpretation also suggests that following surface 3 time, both the old Canning and old "Sag" Rivers have shifted eastward to new positions as indicated on figures 17 and 18. Currently available data indicate that all channels are located on the seaward side of the present islands, between groups of islands, or between islands within a group. The present island chain and associated zone of shoal water extending as an almost continuous ridge from Flaxman Island to Cross

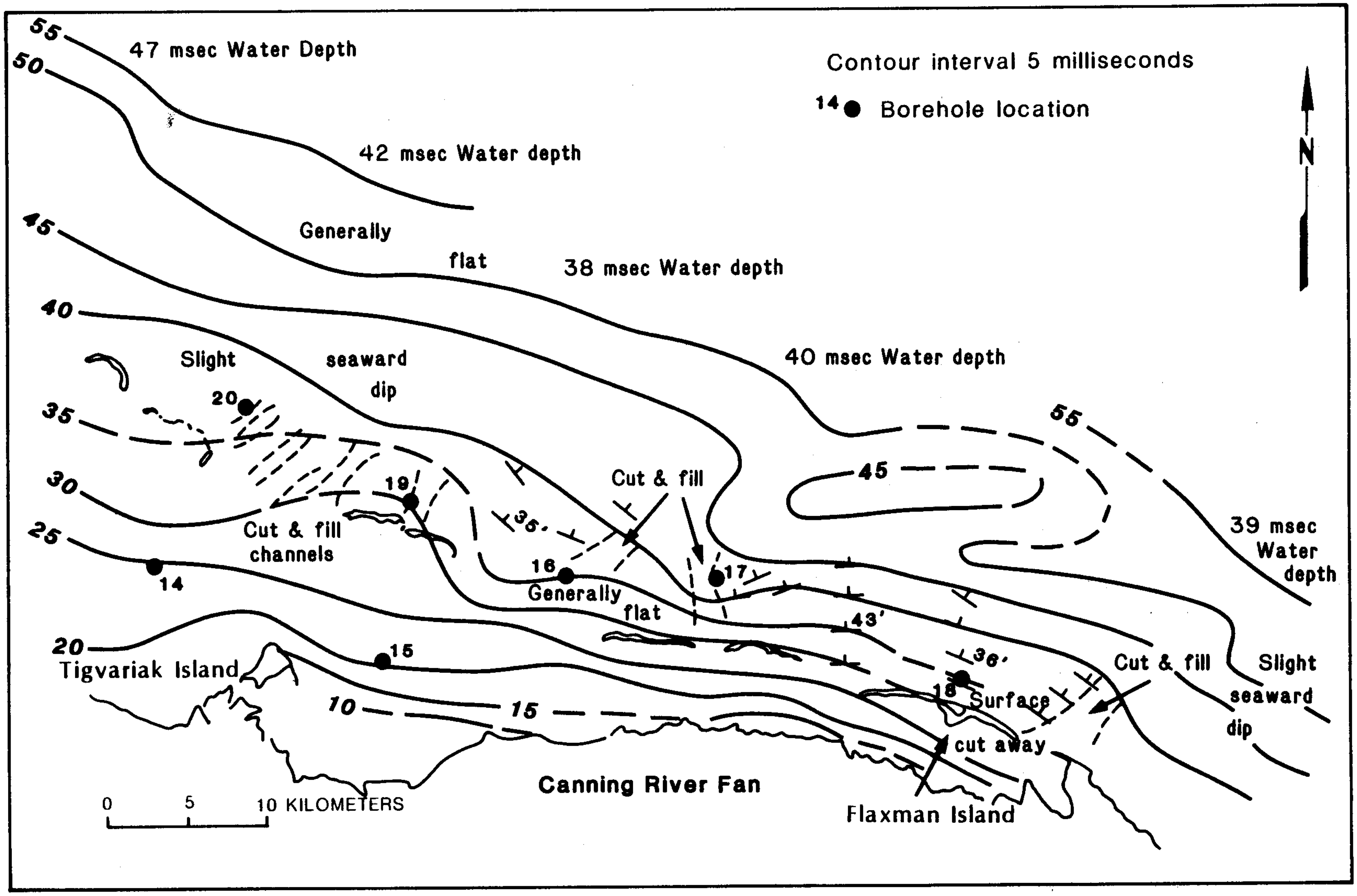

FIGURE 17. Map showing contours drawn on surface 4 between Tigvariak and Flaxman Islands.

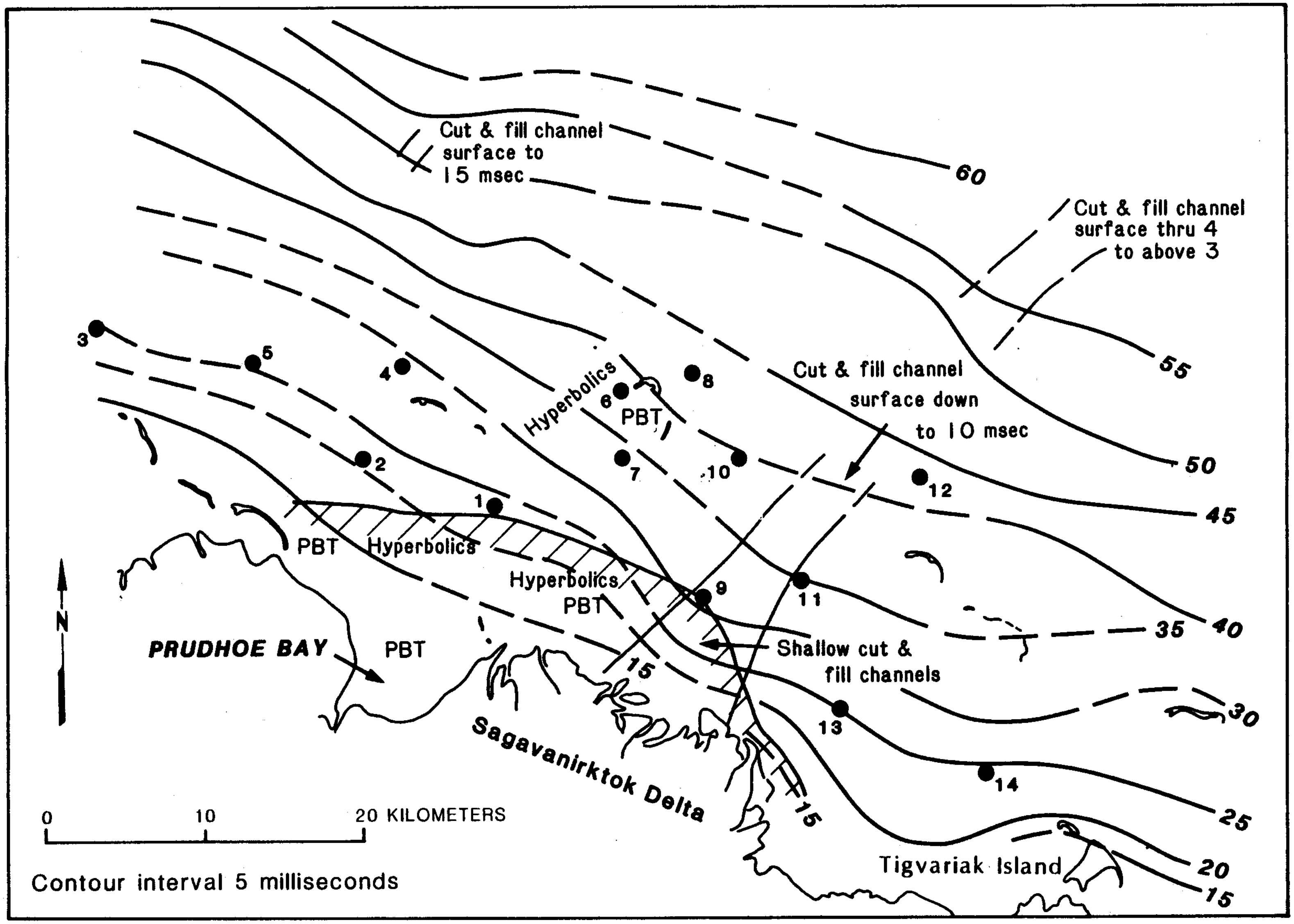

FIGURE 18. Map showing contours drawn on surface 4 between Prudhoe Bay and Tigvariak Island. Numbers by dots indicate borehole number and location.

Island mark a major break in the underlying stratigraphy. Landward of this ridge are flat lying strata, whereas offshore strata dip seaward, implying progradation. The overall geometry is similar to that of a classical delta sequence with topset and foreset beds. The channels in this sequence mark the positions of river distributaries along the delta front.

Borehole data indicate that most sediments between surfaces 3 and 4 are of marine origin (Peggy Smith, Oral Commun., 1984) suggesting that deposition of these sediments was in a predominantly subaqueous shallow water environment. The position of the shoreline at that time is somewhat in doubt, but areas of subaerial depositon most likely existed along the island chains and southward. Sediments seaward of the delta front have slight seaward dips which are comparable to those of pro-delta sediments in other delta systems. Overall, sedimentation in the "Sag" River region was relatively slow and quiet during the period when active deltaic progradation was occurring off the Canning River fan-delta. Although sediments are sand size and finer, boulders have been found in the Flaxman Formation in coastal bluffs from Prudhoe Bay to the Canning River, in adjacent shallow water regions, and in an area defined as the "Boulder Patch" (Reimnitz and Ross, 1979). This Boulder Patch covers extensive areas off the "Sag" River delta between Cross and the McClure Islands, suggesting that these boulders were introduced into this area by ice rafting during accumulation of the fine-grained marine sediments and became incorporated in the sediments as the ice melted.

The location of the Boulder Patch suggests that a shallow open embayment existed during that time, thus allowing ice to enter and become stranded. The islands and parts of the coastline acted as obstacles to penetration of ice into the upper reaches of the then existent delta system. Ice grounding and daming may also account for the fixed positions of some cut-and-fill channels, particularly those between islands and island groups.

Surface 5

Surface 5 is not a continuous surface similar to surfaces 3 and 4. Offshore it downlaps onto surface 4 and crops out near the island chain. Seven kHz, bommer seismic records and side-scan sonographs were obtained along identical tracks across borehole 20 in two different years (1980 and 1981). Partial sections of these records were analyzed and compared to learn about the nature of the hummocky relief so typical of surface 5 (Wolf and others, in press). The side-scan sonographs made possible the relocation of identical targets on the seafloor and confirmed the nearly precise match of the two lines. An example of such targets is shown in Figure 19-I, point B. This analysis revealed lateral trackline offset of approximately 20 meters. The 7 kHz subbottom reflector appears as a very jagged surface with broad highs and lows (Fig. 19-II). The sawtooth pattern has an approximate relief of one to three meters and as much as four to five meters when measurements on both profiles are combined. However, removal of the 20:1 vertical exaggeration inherent in these records shows the subbottom surface to represent "swells and swales" of 20 to 40 meters wavelengths from peak to peak. Superimposing the two profiles, and considering the up to 20 m lateral offset between the two records, revealed no clear match of individual peaks and troughs. This demonstrates that the hummocky relief is not elongated at right angles to the two semi-parallel tracklines. However. this does suggest that broad scale highs and lows with wavelengths possibly of hundreds to thousands of meters, and the general distribution of jagged relief, does match. For different reasons, neither the 7 kHz nor the boomer system permits tracing the details of the hummocky surface to the seafloor.

Both the boomer and the 7 kHz records (Fig. 19-II) show a transparent, nonreflective sediment layer above surface 5. The transparency of the sediment may be a result of intensive mixing by ice gouging, making the unit entirely homogeneous to seismic methods. Thus, the reflector, like surface 6 farther offshore, may in places represent maximum depth of ice gouging nearer shore. This in turn implies that the term "Holocene sediments" may be improper to use to describe the thin surficial sediment layer that consists of intermixed older Pleistocene materials with Holocene fauna in an area believed to nondepositional.

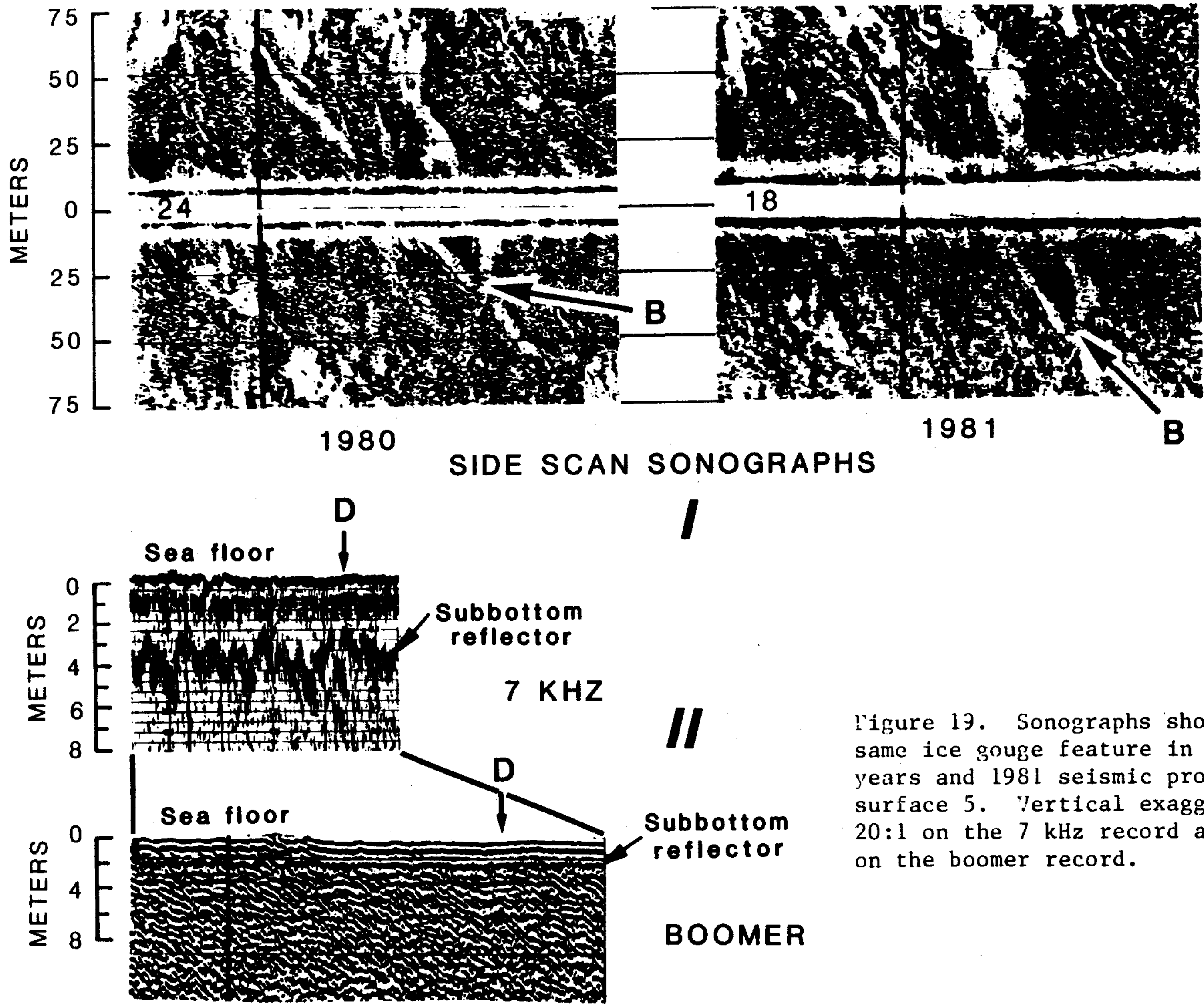

Figure 19. Sonographs showing the same ice gouge feature in succeeding years and 1981 seismic profiles for surface 5. Vertical exaggeration 20:1 on the 7 kHz record and 6.6:1 on the boomer record.

Certain trends of features on surface 5 are, however, notable. Near the island chain, reflector 5 crops out at a sharp boundary between heavily gouged seafloor to the north and an irregularly rough seafloor with scattered boulders and ledges of stiff silty clay to the south. This latter bottom type has been studied with side scan sonar, television, and direct diving observations. The outcrop extends landward through the opening between Karluk and Narwhal Islands north of Foggy Bay (Fig. 1). A similar type of bottom has been identified by similar techniques in an area about 30 km to the east, seaward of Flaxman Island and exhibits the same hummocky reflector. North of Flaxman Island, a 7 kHz seismic profile passes directly over borehole 18, whose stratigraphy has been studied (Hartz and others, 1979; Smith, in press). Stratigraphic and paleontologic data from borehole 18 indicate a boundary at the level of reflector 5, with Holocene above and the Flaxman Formation below (Wolf and others, in press). The Flaxman Formation is generally described as a bedded sandy silt and clay unit containing ice rafted boulders up to 3 m in diameter (Hopkins and others, 1978). This correlation suggests that reflector 5 may identify the top of the Flaxman Formation and the occurrence of seafloor boulders may reflect a non-depositional, perhaps an erosional surface at the present-day seafloor. The boulders, therefore, may represent a lag deposit of the Flaxman Formation which lies below and/or a unit that which has already been eroded away.

The more regional morphology of surface 5 may have analogs in the present day coastal plain and island chains. The broad highs may be buried counterparts of the high areas presently seen as islands and raised areas of the present tundra surface. Inshore from some of the islands are shallow lagoons. Broad lows on the profiles perhaps represent similar features offshore.

The small scale hummocky morphology of reflector 5 could be ascribed to a number of causes, as listed below:

1) The present coastal plain surfaces have similar, although somewhat lower, relief features largely related to the pattern of tundra polygons in permafrost. At times when the advancing sea of the last transgression moved across the coastal plain rapidly enough to prevent the formation of erosional bluffs, the underlying surface may have been buried by the younger sediment and preserved. Because of the different scales of the two relief types, but mainly because of the destructive action of ice keels plowing inro the sea floor, we discard this theory as a cause.

2) The reflector could represent a modified former onshore tundra surface as it would appear after thaw collapse of massive ice, particularly ice wedges, that occur in the upper 5 m of coastal plain deposits. We discard this theory as a cause mainly because the spacing is not right, and because our analysis indicates the depressions are not linear features.

3) The reflector could represent an erosional surface with cut-and-fill features, such as incised delta front channels. We discard this theory as a cause because the scale of the relief is too small.

4) The surface could represent the former land surface modified by ice gouging (Reimnitz and Barnes, 1974; Barnes and others, 1984). However, as in 2 above, the features are not linear, and the features under question are too large.

5) The relief in surface 5 could represent the effects of strudel scour in a deltaic environment (Reimnitz and Kempema, 1983) during the last transgression. We do not favor this interpretation because such a process generates only depressions and could not account for the peaks seen in the relief on the 7kHz record (Fig. 19-II).

6) The relief may not be related to a stratigraphic unit but to a gas boundary within the section, or to sound velocity inhomogeneities in the transition zone between non-

bonded surficial sediments and ice bonded underlying sediments. Elevation changes in the top of the bonded permafrost over short distances have been reported from the Canadian Beaufort Shelf, but we do not have enough information to properly evaluate this possibility.

At this stage of the analysis, we are as yet unprepared to ascribe a cause for the hummocky relief, but it does appear that this regional reflector may be one of many reflectors which are part of the large subsurface old Canning delta described earlier. There are sufficient data to suggest that the present seafloor is an erosional surface. Thus, parts of the top-set units above surfaces 5 and 6 are most likely missing from the section due to erosional processes still operating.

As outlined above, surface 5 crops out along the seaward margin of the island chain. From this point of outcrop to the islands themselves, we have not seen other shallow reflectors that would indicate the islands are constructional features on top of an older surface. This suggests to us that not only Flaxman, but also Maguire, Stockton, McClure, and possibly even Cross Islands are remnant highs of a once very broad, fluvial plain or larger deltaic system consisting of the Canning and "Sag" Rivers as the major sources of sediment supply. Ongoing destruction of these islands will eventually lead to the formation of shoals and small "moving islands" such as Dinkum Sands and Reindeer Island. Tigvariak and Flaxman Islands on the east end of the chain are the least advanced in this cycle, whereas Reindeer Island, north of Prudhoe Bay at the west end of the island chain is the oldest and most nearly destroyed. Many of the islands between the ends of the chain have curved spits and other beach-nearshore features which are concentrations of sands and gravels resulting from erosion of the island cores. As discussed earlier, there are many large and small buried channels with histories of cutting and filling along the island chain, some cut as deeply as 15 m. Thus, the channels have remained in place for extended periods of time and their positions may in fact be due to confinement by the islands.

Surface 5? - Lagoonal Areas

Shoreward of the island chain another surface, about as shallow below the seafloor as reflector 5 can be widely traced on the 7 kHz records. Although this surface may not be equivalent to surface 5 seaward of the island chain, for discussionary purposes, it will be referenced to as surface 5? Lagoonal Areas. Figures 20 and 21 are isopach or maps of the overburden thickness contoured from the 7 kHz data inshore of the island chain. These figures also show the locations and incision depths of buried channels. Surface 5 was selected on the basis of being the deepest, most continuous and acoustically strongest reflector on the 7 kHz records. Many less obvious, discontinuous reflectors, some of which crop out at the seafloor are seen above this surface. In those areas where borings are available, the isopached surface for the most part, matches with the base of Holocene marine sediments. This trend combined with a variety of background information from the area (see for example the section titled, Sea Floor Characteristics) gives us considerable confidence that the sediments isopached in figures 20 and 21 are Holocene marine sediments. The pattern suggests a possible connection between the presumably erosional surface along the island chain and the buried channels. This correlation may be further evidence that the paleogeography of the region was rather similar to the present configuration of the island chain and lagoons, and that the location of the island chain marks a topographic ridge made up of older fluvial or deltaic deposits. Between Flaxman and Tigvariak Islands (Fig. 20), the isopach pattern shows a convex trend very similar to that of surfaces 3 and 4. Westward toward Prudhoe Bay (Fig. 21), the Holocene sediments are thinnest. That area may have been too shallow for sediment accumulation during the time when deposition predominated in the eastern part of the area. Areally restricted accumulations occur only locally between Reindeer and Cross Islands and NW of Tigvariak Island at borehole 14 (Fig. 1). Slightly landward of the Reindeer-Argo Island topographic ridge, and parallel to it, is what appears to be a buried remnant of an older island. Internal structures of that feature consist of steep foreset bedding dipping south, implying southward migration during the island's last stages. Data are sketchy, but we believe that this feature is not part of the Holocene marine section but lies below it. The base of the Holocene(?) section shows

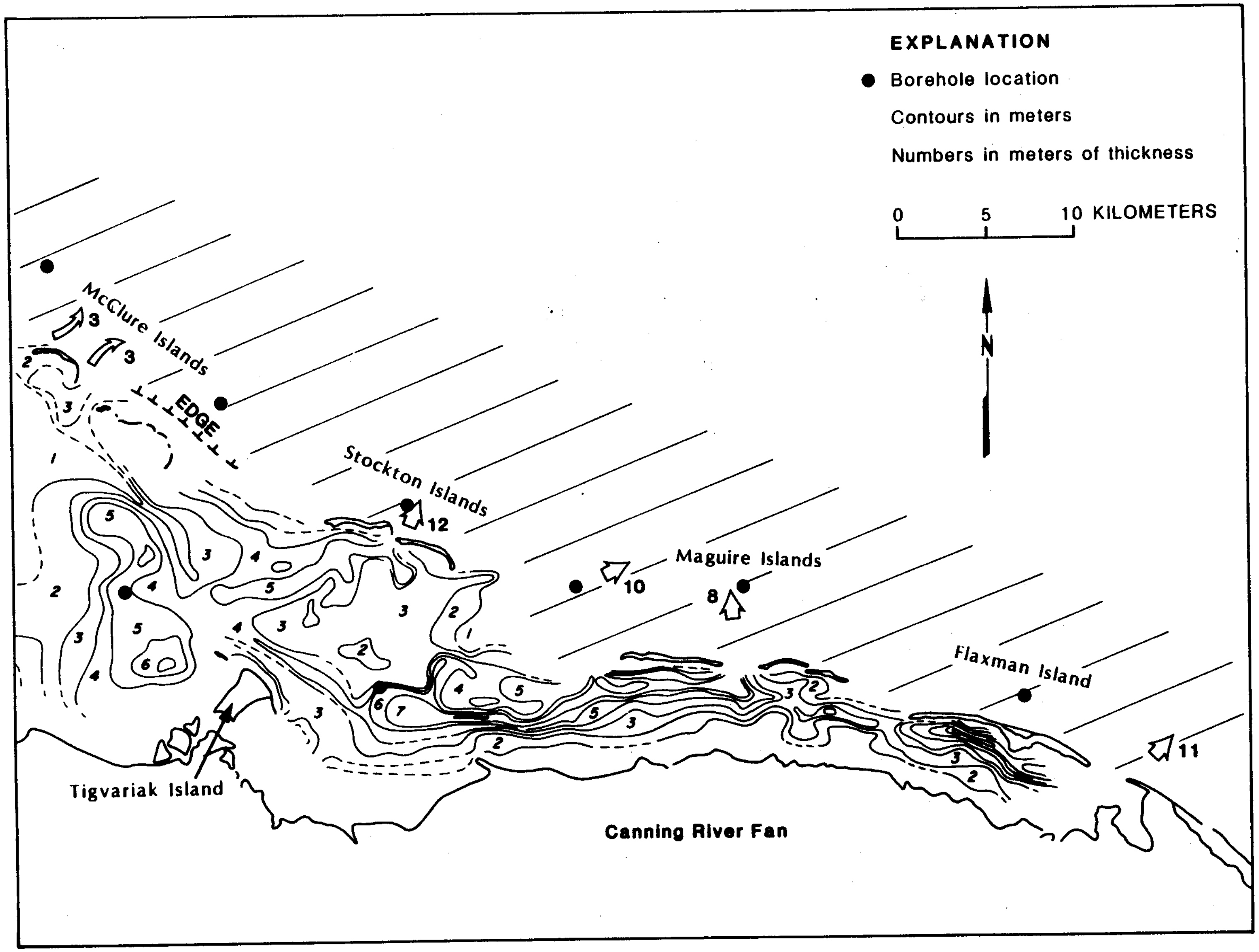

FIGURE 20. Isopach map of thickness of sediment between surface 5? and the seafloor in Leffingwell Lagoon between Tigvariak and Flaxman Islands.

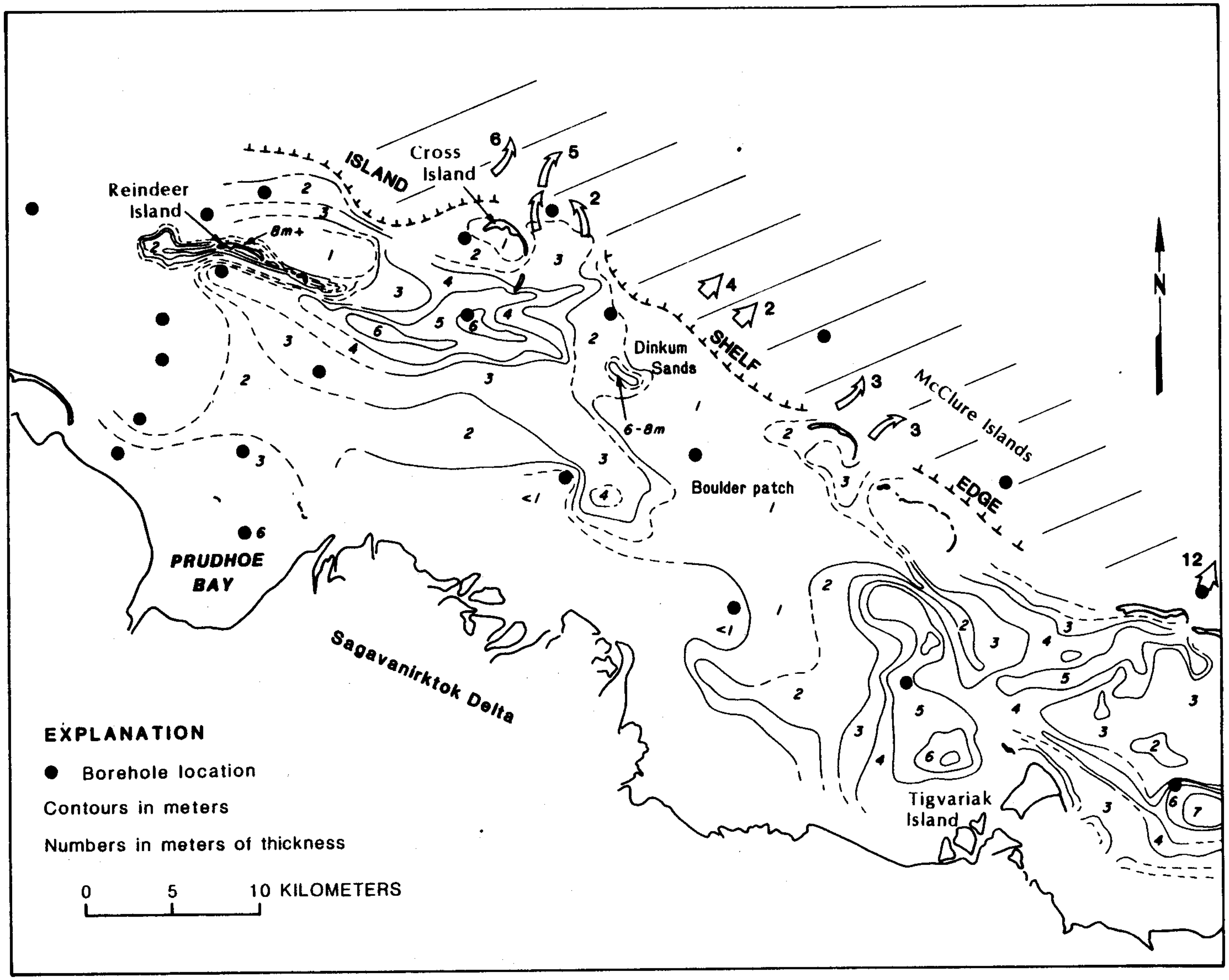

FIGURE 21. Isopach map of thickness of sediment between surface 5? and the seafloor between Prudhoe Bay and Tigvariak Island.

up as a rather widespread, flat reflector, 8 to 10 m below the top of Reindeer Island. The reflector extends to Argo Island and beyond. Thus Reindeer Island today is migrating southwestward (Reimnitz and Kempema, 1982) over the old island which seems to have migrated in a similar direction. The fate of these two islands suggests that the sediment source is to the NE, and that during the wasting away of one island, a new island may again be formed, and the cycle will repeat itself. Similar to Reindeer and Argo Islands, but possibly different from Cross Island, Dinkum Sands to the E of the latter also seems to represent a constructional feature that rests on top of a flat reflector that crops out landward at the Boulder Patch.

The thinning of Holocene sediment from the center of Stefansson Sound toward the delta front of the "Sag" River is notable. As pointed out by Reimnitz and others (1979), a Holocene lack of delta accretion is an arctic enigma. This is strongly supported by the isopachs of Holocene sediment thicknesses at the "Sag" River delta (Fig. 21), fed by the second largest river of the North Slope (Reimnitz and others, 1979).

Sea Floor Characteristics

Areas without Holocene sediment cover should be marked by outcrops of older sediments that possibly differ from modern ones and therefore give the seafloor a different texture. In an attempt to verify the isopach maps of Holocene sediment thickness (Figs. 20, 21), we made a brief analysis of side-scan sonar records obtained along most of the lines in the eastern half of the study area where seismic coverage is available. In the western half of the study area, delineation of the Boulder Patch (Reimnitz and Ross, 1979) involved an analysis of all available data to define the windows in Holocene sediment cover. The results for the eastern half are discussed here.

Figure 22 is a composite of all side-scan sonar data and illustrates seafloor characteristics from Flaxman Island to Tigvariak Island. The line along which reflector 7, present only in the seaward part of the study area, terminates at the seafloor is shown by the heavy line with slashes on the seaward side. Seaward of the 10 meter isobath, the seafloor is jagged from ice plowing, but shows little evidence of the presence of ledges of overconsolidated sediments. Within the lagoons, the floor is generally smooth, indicative of quiet water deposition and ponding of Holocene sediments. The seaward flank of the topographic ridge underlying the island chain, however, has a mottled seafloor with streaks and patches due probably to alternating sand and gravel accumulations. Scattered boulders are recognized near Tigvariak and Flaxman Islands, and along the coast east of the eastern entrance to Leffingwell Lagoon. The somewhat convex trend of the mottled seafloor parallels that of the present coastline. It also coincides with a belt in which we interpret the Flaxman Formation to crop out or a zone that reflects a lag deposit of the Flaxman Formation.

The deflection in trend of the mottled seafloor area to the northwest , i.e., north of Tigvariak Island, suggests the influence of the Sag delta to the west. The overall trend of outcropping reflector (7) , of the 10 m isobath, and the NW-SE trend of ice gouges support the interpretation that the present seafloor is undergoing mechanical destruction and erosion, and that the seaward flank of the topographic ridge marking the island chain is not being spared from destruction. Whatever originally formed the lagoons, the Holocene sediments they presently contain can only be temporary accumulations to be removed, at least in part, as the sea advances in the present erosive cycle. The present seafloor will become the next surface in the sequence of unconformities on the inner shelf, above surfaces 3 and 4.

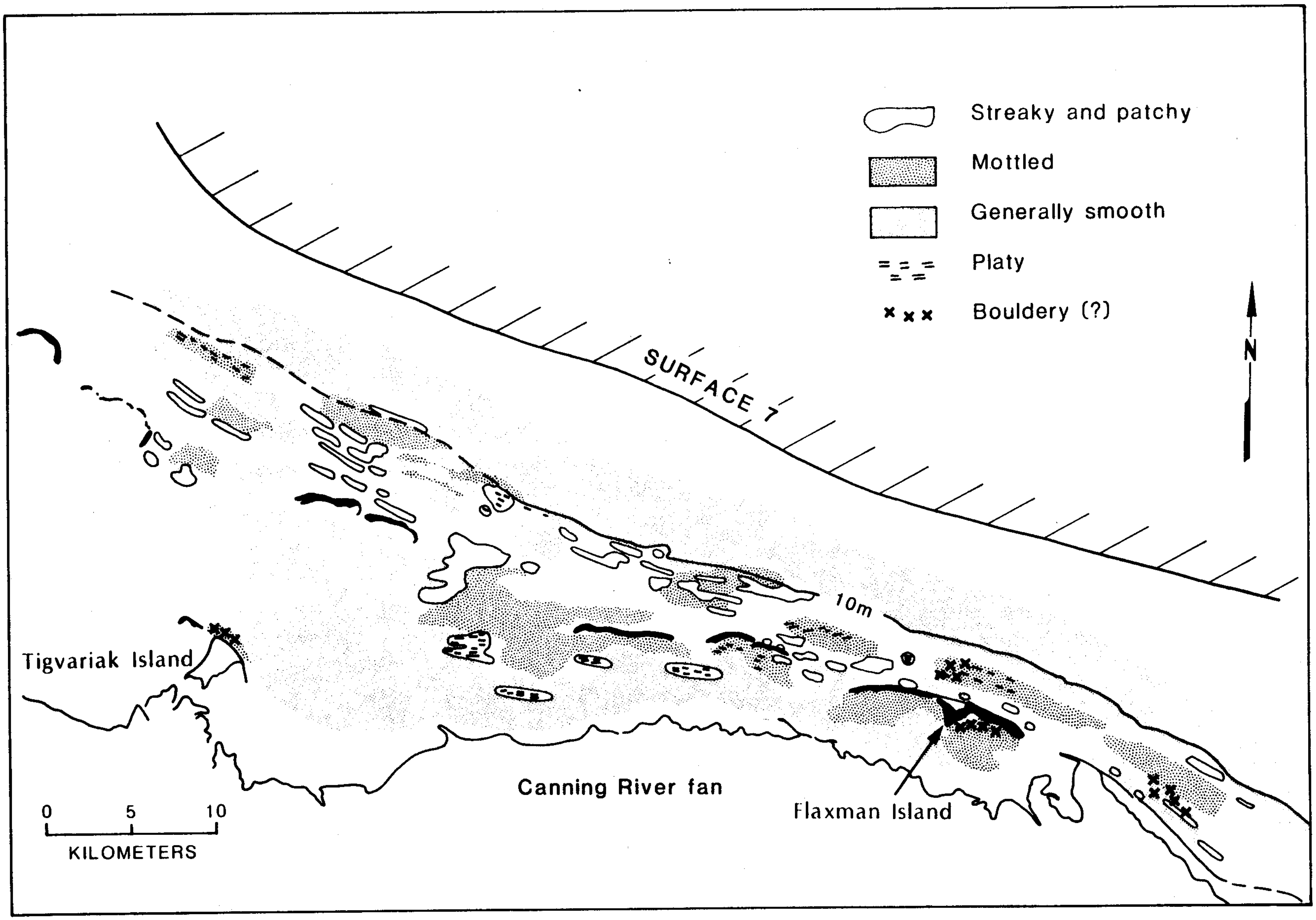

FIGURE 22. Seafloor textural characteristics between Tigvariak and Flaxman Islands.

RELATIONSHIP OF THE CANNING FAN-DELTA TO OFFSHORE STRATIGRAPHY

To understand the relationship between the offshore seismic stratigraphy and the modern Canning fan-delta, we refer to the topographic map of the latter (Fig. 23). This map shows the locations of 5 topographic profiles (Fig. 24) that delineate the fan-delta system. North-south profiles A, B, and C delineate the fan-surface from the Brooks Range to the coast, and the slight relief northward across the lagoon, island chain, and beyond. Profile D is a transverse profile across the main body of the fan, and Profile E defines the floodplain of the Canning River where it exits from the Brooks Range. The subsurface expression of surfaces 3 and 4, angles of dip along section, and attitude of intermediate reflectors are shown below the seafloor.

The NS profiles of the fan surface show two pronounced steps or knickpoints, one at about 7-1/2 meters and another at 50 meters elevation. Traced on the map (Fig. 23) these two steps delineate small lobes between the radial channel pattern on the fan surface. Fan growth occurs as lobes and channel beds agrade at a site until sufficient elevation is achieved to shift the drainage to a lower level area on the fan. Judging from the large overall transverse relief of the fan shown by profile D (Fig. 24) when compared to that of individual channels and lobes, these channels must have switched back and forth numerous times during the construction of the fan. The apex of the radial channel pattern is approximately at the point where the Canning River emerges from the Brooks Range. The regionally convex seaward pattern of the fan contours, as delineated by the two heavy lines that mark the knickpoints in figure 23, the arcuate shape of the present-day coastline, the positions of the barrier islands and shelves, and the arcuate shape of the subsurface stratigraphy all seem to be related to the Canning River as the sediment source. This drainage system, therefore, has been active in the same area through several transgressions and regressions of the sea.

The locus of most recent progradation may have been in the very eastern part of Leffingwell Lagoon, where the lower contour in figure 23 defines a major topographic bulge at the Staines River. Since Leffingwell Lagoon is sediment starved by an eastward shift of the river into Camden Bay, the front of the fan is retreating by coastal erosion at a rate of 1 to more than 4 m/yr (Lewellen, 1977). This retreat is revealed by the highly crenulated coastline (Fig. 25) and erosional bluffs. The shift into Camden Bay must have occurred long enough in the past to allow construction of a small delta bulge at its present mouth (Fig. 25, Point A).

The radial stream pattern, shape, and relief of the present Canning Fan-Delta can be best observed with LANDSAT imagery (Fig. 25). On this image, the eastern 1/3 of the surface has few lakes compared to the western 1/3. This probably reflects more recent flood plain development on the eastern part of the fan. Also evident are the masses of sea ice which come into contact with the island chain and continue to cut into and erode away the Islands and associated topographic ridges. Although somewhat obscured by thin clouds, a westerly drift of suspended sediment emerging from Leffingwell Lagoon is evident.

This entire fan-delta system and its relationship to the marine and non-marine environment is not uncommon to the coastline of northern Alaska. Figure 26 illustrates a LANDSAT image of a series of fan deltas near Demarcation Bay well to the east. Note the head locations of the major rivers, the radial distribution and in particular the sediment being trapped in the lagoon behind the barrier islands. Small amounts of sediment escaping between the islands is picked up by longshore currents and can become attached to the ice which in turn takes it out of the area. Perhaps, as is the case with the Canning fan-delta, there are subsurface deltaic sequences here also.

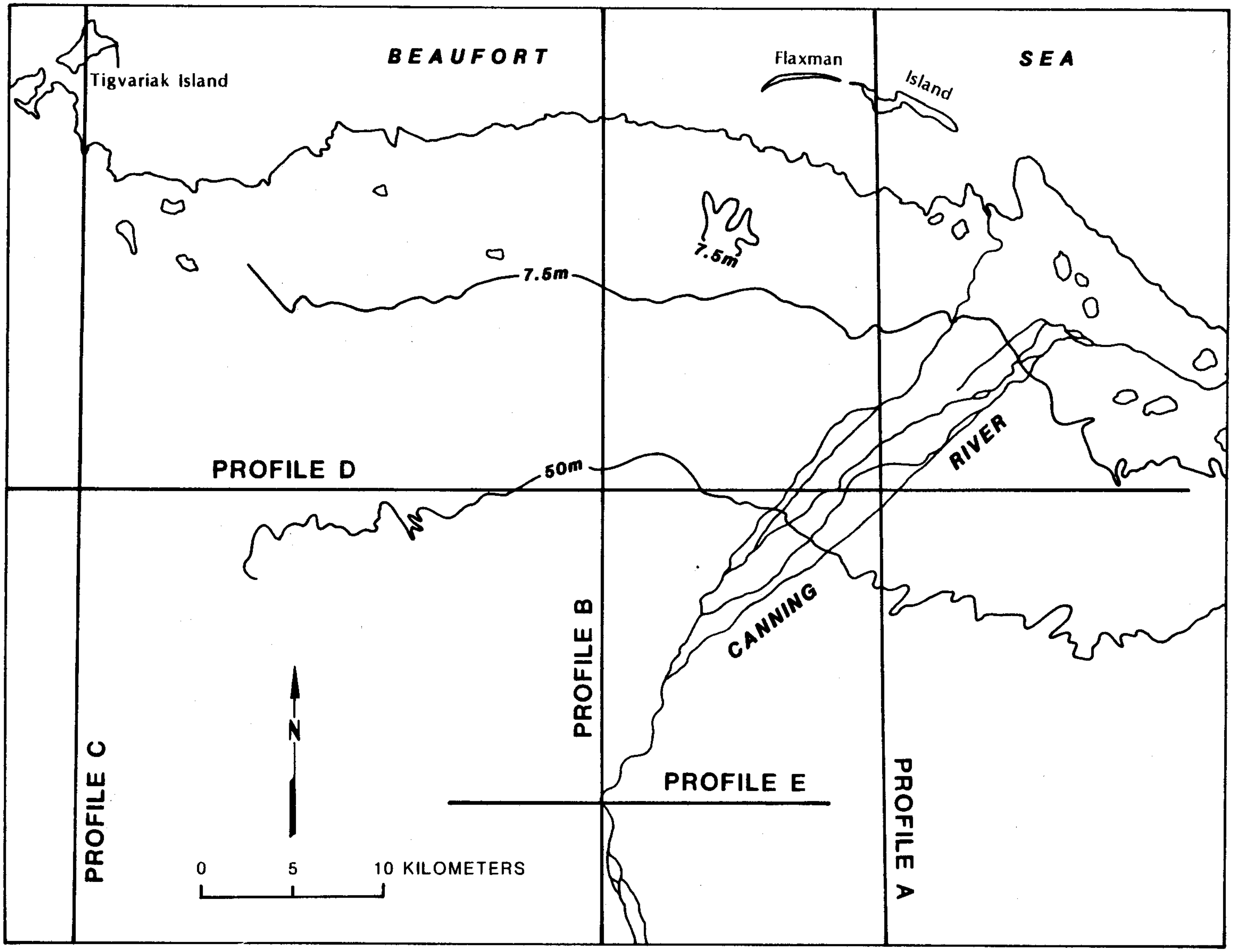

FIGURE 23. Topographic map of the Canning River Fan-Delta showing the location of profiles A through E (Fig. 24).

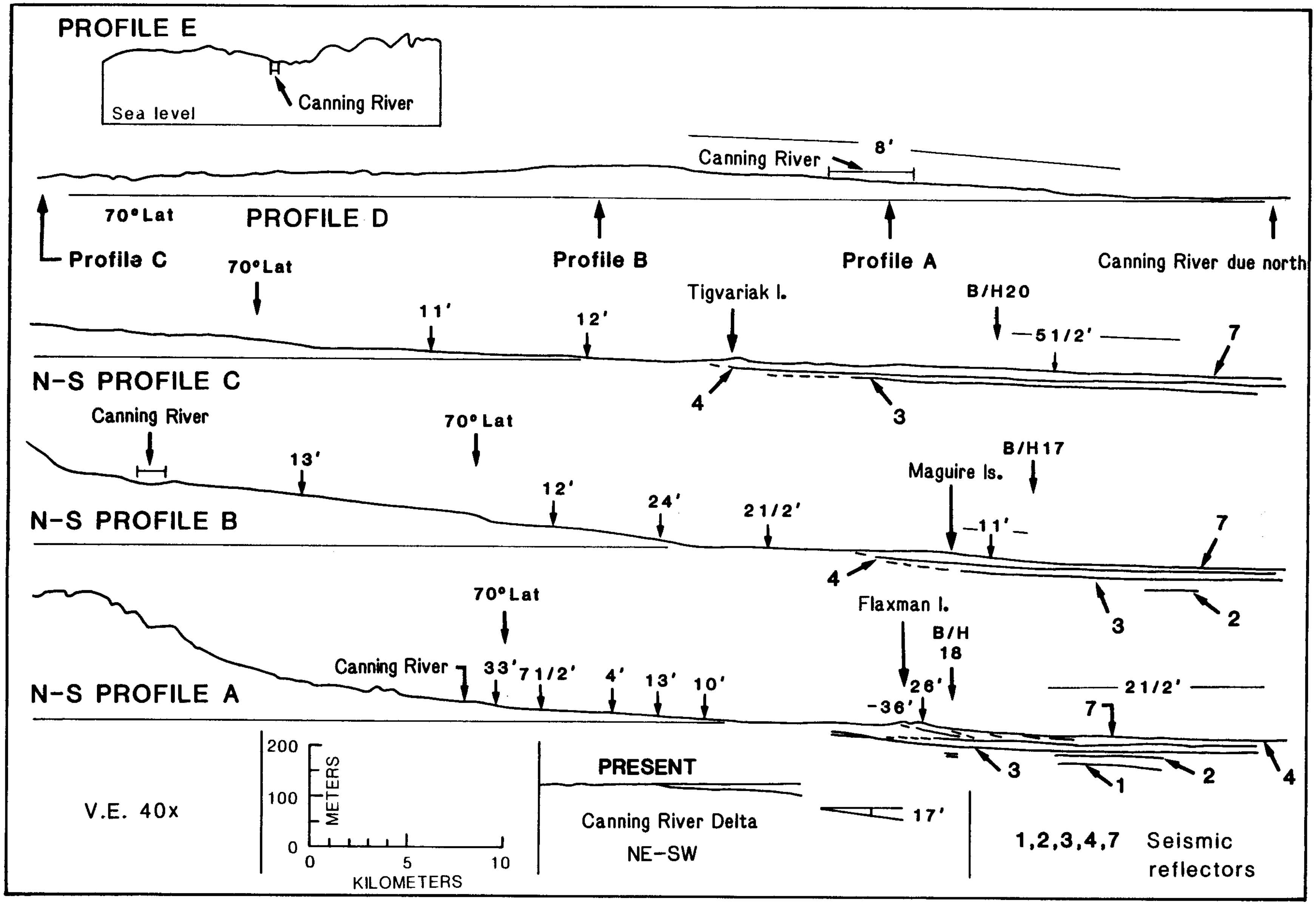

FIGURE 24. Profiles A through E across the Canning River Fan-Delta and seaward.

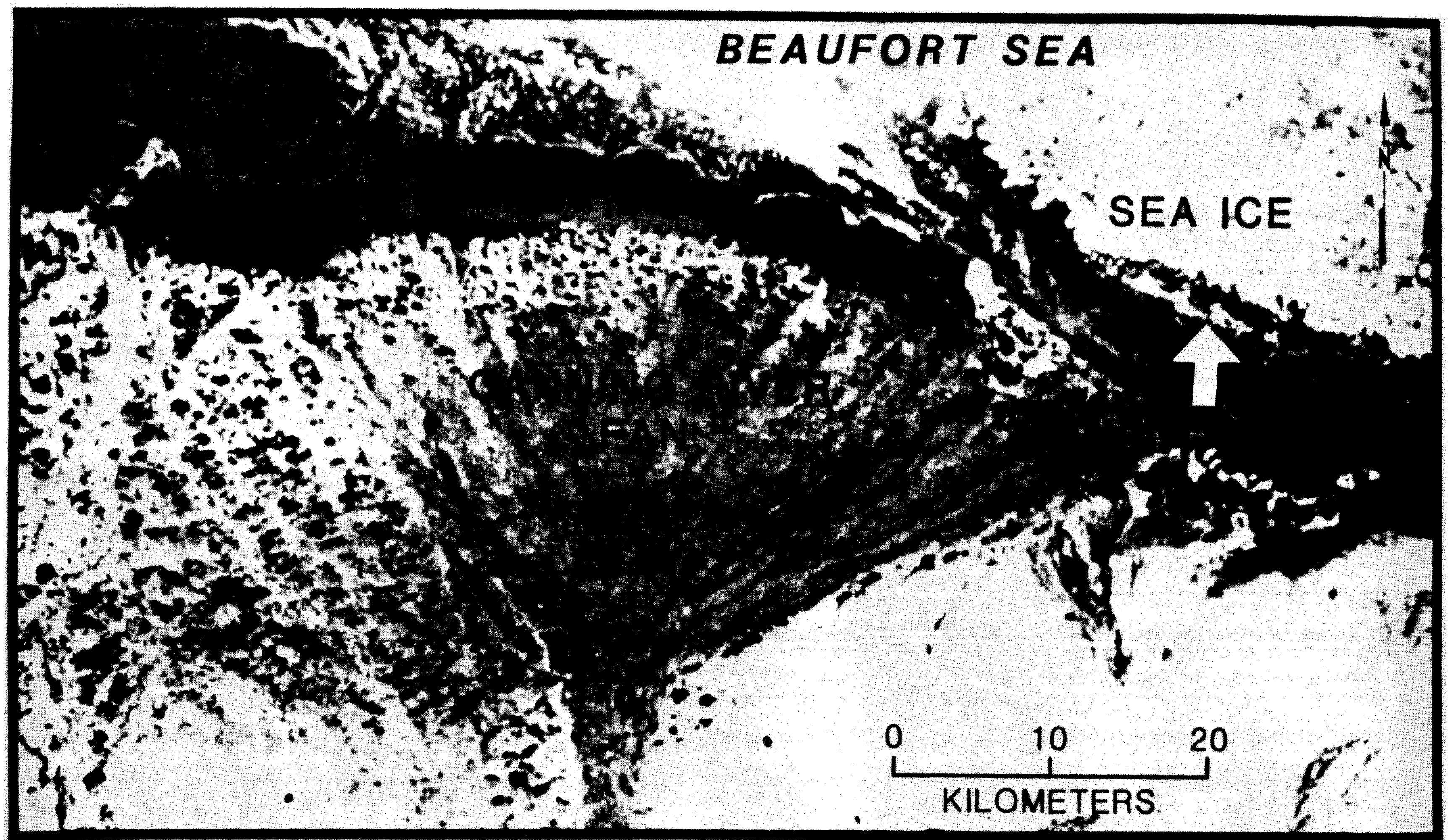

FIGURE 25. LANDSAT imagery of the Canning River Fan-Delta system.

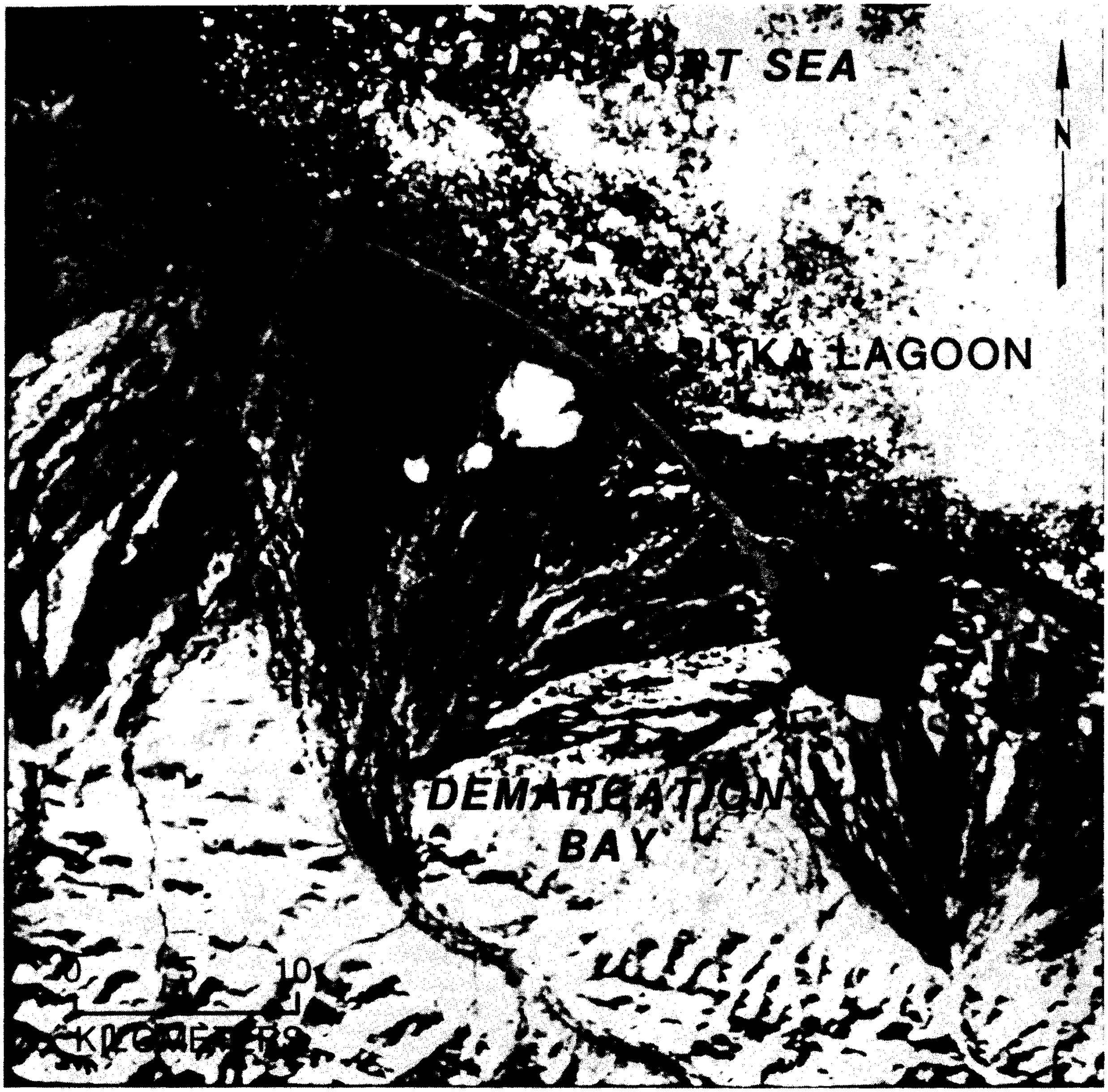

FIGURE 26. LANDSAT imagery of Demarcation Bay, adjacent fans, and barrier islands.

Computer enhancement of LANDSAT data reveals an old rather wide river floodplain on the Canning River fan, following a line from the apex toward Flaxman Island, where subsurface reflector 4 was eroded away at some time prior to accumulation of Holocene sediment. These data suggest that at a lower stand of sea level, the Canning River incised into the fan-delta, cut away at the old erosion surface, and then backfilled as sea level rose.

Surfaces 1 through 4 all have seaward dips. Fan slopes and features that appear to be delta top-set beds in the subsurface from the coast to beyond the island chain have dips varying from 2 to 13 minutes (Fig. 24). Foreset slopes in the subsurface, and surface slopes near the knickpoint have dips of 24 to 36 minutes whereas slopes in the pro-delta sequences offshore are approximately 2 to 5 minutes. These slopes are similar to those of other deltas (Coleman and Prior, 1980). Even the 17 minute delta front slope of the modern Canning River delta bulge in Camden Bay fits well.

In the three north-south profiles of figure 24, landward projections of surfaces 3 and 4 would intercept the present fan surface. This suggests that the present surface may be a very old surface that has experienced multiple cycles of erosion and progradation. The knickpoints themselves, suggest that perhaps at least three major episodes of progradation have occurred, one of which is the subsurface delta defined by seismic stratigraphy.

Commonality of the approximately 7-1/2 meters altitude of Tigvariak and Flaxman Islands, the isolated high areas on the present coastal plain, and the 7-1/2 meter knickpoints just described are a rather striking set of data points. If meaningful, this correlation implies that there may have been a regional fluvial or deltaic plain at a 7-1/2 m elevation and that the relief we see today is all that is left after severe periods of excessive erosion and little deposition. In fact, it appears that the only deposition occurring today is in the quiet lagoons and at the mouths of some rivers.

Figure 27 is a generalized cross section from the Canning fan-delta northward through Flaxman Island and borehole 18. Sedimentary sequences between the fan-delta and Flaxman Island are rather flat lying whereas those north of the island steepen seaward toward borehole 18. The section illustrates the flat lying sequences as topset units and the seaward sequence as delta-front units in a deltaic system. The loose gravels under Flaxman Island are overlain by micaceous shales and siltstones whereas corresponding sediments throughout borehole 18 are mixtures of sandy and clayey silts. The fine-grained sequence that overlies the gravels suggests a depositional history of low terrigenous influx during a transgressive rise in sea level (Vail and others, 1977). The Flaxman Formation likewise is flat lying and rests on the fine-grained topset sequence. Overlying the Flaxman Formation is a non-marine sequence consisting of eolian and coastal plain sediments which contain thaw lake deposits (L. David Carter, oral commun., 1985). The dashed line connecting the top of Flaxman Island with the coastal plain to the south represents the surface of the hypothetical, formally broad fluvial-deltaic plain. Excessive erosion has, for the most part, destroyed this surface leaving Flaxman and Tigvariak Islands, coastal plain highs, and the low relief barrier islands as remnants. Based on all data presented, this illustration depicts one large fluvial-deltaic system consisting of the Canning fan-delta, associated barrier islands, and the subsurface delta.

Earlier discussion focused on the Flaxman Formation, as identified in borehole 18, projecting southward and equivalent to the Flaxman Formation outcrop on Flaxman Island and in the coastal bluffs to the south. The top of the Flaxman Formation is bounded by an unconformity and the base of the unit is thought to be likewise (L. David Carter, oral commun., 1985). In all areas where the formation is known to outcrop, it does so at or near sea level and is thought to be only a few meters thick. This suggests that the unit was deposited on a very broad, nearly horizontal, erosional surface. Assuming this to be true, it would be theoretically impossible to project the Flaxman Formation from Flaxman Island into borehole 18 because to do so would require that the Flaxman extends as a continuous unit diagonally through an unconformity. The unit described in borehole 18 as "Flaxman," (Kris McDougal, 1982) has been shown to be a part of the subsurface delta described earlier and thus rests below the unconformity at the base of the "Flaxman" on Flaxman Island. This line of reasoning suggests that the "Flaxman" cannot be found in borehole 18 and that the topographic highs and barrier islands are

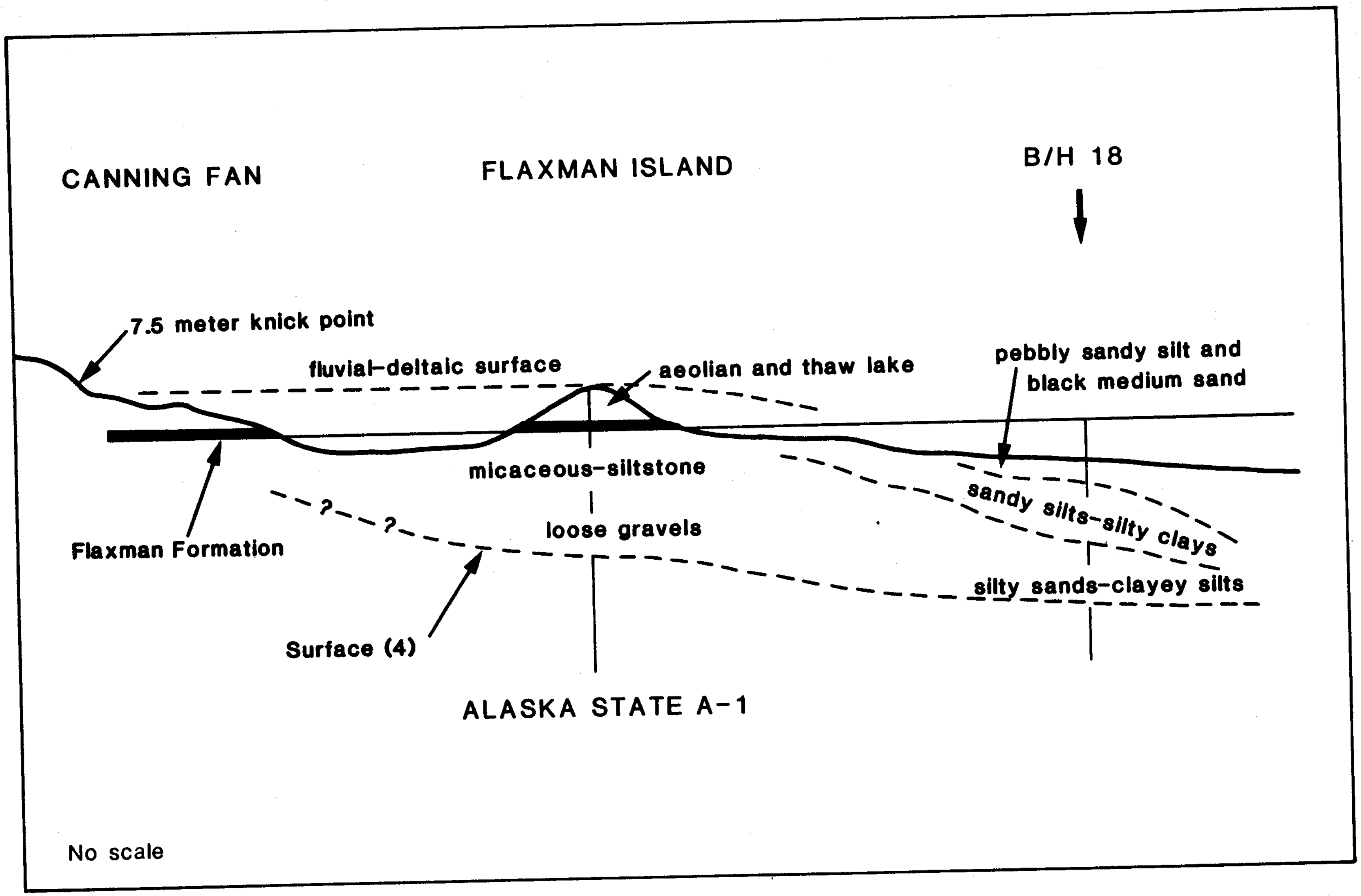

FIGURE 27. Generalized cross section from Canning River Fan-Delta through Flaxman Island to borehole 18.

remnants of a fluvial or deltaic plain which is not related to the subsurface delta. In essence two progradational sequences are separated by the Flaxman Formation. Additionally, it is suggested that no "Flaxman" will be found below the lagoonal floors or offshore because the "Flaxman" at or near sea level has been eroded away.

The Boulder Patch, the pebbly unit at the top of borehole 18, and other similar deposits are essentially lag deposits of the eroded Flaxman Formation. These lag deposits will continue to be located near the seafloor as the finer grained sediments below them are removed from the area by erosion.

Based on this analysis and data described earlier, there appear to be five unconformities, 1) surface 3; 2) surface 4; 3) bottom of the Flaxman Formation; 4) top of the Flaxman Formation; and 5) the present sea floor and isolated areas within the lagoons. Transgressive sequences are represented by the large progradational subsurface delta and the Flaxman Formation. The uppermost fluvial-deltaic plain (?) represents a non-marine progradation over "Flaxman" deposits perhaps occurring during a period of high terrigenous influx (Vail and others, 1977) to the area followed by an excessive erosional cycle. An important consideration is that the "Flaxman" is a marine mud accumulation into which "Flaxman boulders" have been deposited and should not be considered to be of deltaic origin (L. David Carter, oral commun., 1985). This point supports reasoning that discounts the presence of "Flaxman" in borehole 18, except perhaps as a lag deposit at or near the sea floor, and provides an environment for quiet deposition of a marine mud, represented by "Flaxman," upon a flat erosional surface which caps an older deltaic sequence which abuts into an ancestral subaerial Canning fan to the south of present Flaxman outcrops along the coast.

Other conclusions can be drawn from all the data presented in this report. They are as follows:

(1) Bonded permafrost throughout the area was not observed on the seismic records. Borehole data indicated permafrost at, above , or below surfaces 3 and 4 at various locations (Harding-Lawson Assoc., 1979). Using a sound velocity of approximately 1800 m/sec made reasonable correlation of acoustic reflectors with borehole stratigraphy possible. One can conclude therefore that if permafrost does exist in the stratigraphic section described, it has little or no influence on the seismic interpretations.

(2) Geohazards related to slumping and faulting are essentially nonexistent. On seismic records, internal deformation was noted during deposition of what was thought to be the "Flaxman Formation" in borehole 18. This unit and other possible slumping occurrences are at subsurface depth and are related to pre-Holocene deposition and, therefore, are considered to be inactive. Unstable sediments may be encountered in the lagoonal accumulations interpreted to be Holocene deposits. The relatively uniform seaward gradients of surfaces 3 and 4 and the regional parallelism of surface contours to the present coastline suggest that the entire area has been relatively stable throughout the period since the formation of surface 3 and, therefore, deformation or warping of the stratigraphic section is minimal to nonexistent. Gas anomalies were not readily observed throughout the area, but this should not rule out the presence of gas.

(3) Economic gravel deposits probably do not exist. Gravel deposits are known to be present below the Maguire and Flaxman Islands and below the Canning River Fan onshore. These deposits, however, are subsurface and not readily accessible. For the most part, the superficial sediments are fine-grained sands and silts. Gravels or pebbly units near the sea floor are more than likely lag deposits and do not reflect gravel accumulations below. Cut and fill channels described in the area characteristically contain sands and fine-grained deposits associated with minor amounts of gravel.

(4) Historically it appears that after each transgression, i.e., the subsurface delta and the "Flaxman," an extended period of erosion occurred that destroyed much of the sediments that were deposited. If the non marine fluvial-deltaic plain at the top of the stratigraphic

sequence had marine depositional counterparts on the inner shelf, the present erosional cycle has removed them completely, is destroying the fluvial-deltaic plain, is incising into the subsurface delta, and reflects a period of erosion of greater intensity than most previous cycles.

(5) Holocene deposits in the lagoons contain reflectors within the section above the pre-Holocene surface. Holocene sediment offshore, if present, should also have reflectors like those on other shelves, however, ice gouging and intermixing by ice processes may destroy their basic characteristics. As an end result, offshore Holocene sediment may actually appear to be homogenous and acoustically transparent. The base of this homogenous sequence may reflect the maximum depth to which ice gouging has been active in Holocene time. This basal surface may in fact be, in part, a mechanically formed surface as a result of subsurface smearing by ice keels as they passed through the area.

REFERENCES

Barnes, P.W. and Reimnitz, Erk, 1974, Sedimentary processes on Arctic shelves off northern coast of Alaska; in Reed, J.C., and Sater, J.E. (eds.), The Coast and Shelf of the Beaufor Sea. Proceedings of the Arctic Institute of North America Symposium on Beaufort Sea Coast and Shelf Research, Arctic Institute of North America, Arlington, VA, p. 439-476.

Barnes, P.W., Ross, Robin, and Reimnitz, Erk, 1980, Break in gouge character related to ice ridges, *in* National Oceanic and Atmospheric Administration, Environmental Assessment of the Alaskan Continental Shelf; Annual Reports of Principal Investigators for the year ending March, 1980, v. 4, p. 333-343.

Barnes, P.W., Rearic, D.M., and Reimnitz, Erk, 1984, Ice gouge characteristics and processes, *in* Barnes, P.W., Schell, D.M. and Reimnitz, Erk (eds.), The Alaskan Beaufort Sea - Ecosystem and Environment, Academic Press: San Francisco, CA., p. 185-212.

Blouin, S.E., Chamberlain, E.J., Sellmann, P.V., and Garfield, D.E., 1979, Determining subsea permafrost characteristics with a cone penetrometer - Prudhoe Bay, Alaska: Cold Regions Science and Technology, v. 1, no. 1.

Boucher, Gary, Reimnitz, Erk, and Kempema, E.W., 1981, Seismic evidence for an extensive gas-bearing layer at shallow depth offshore from Prudhoe Bay, Alaska: Cold Regions Science and Technology, no. 4, p. 63-71.

Coleman, J.M. and Prior, D.B., 1980, Deltaic Sand Bodies, A 1980 short course, Education Course note series #15, AAPG, Tulsa, OK, p. 171.

Dinter, D.A., 1982, Holocene marine sediments on the middle and outer continental shelf of the Beaufort Sea north of Alaska: U.S. Geological Survey Miscellaneous Investigations Series, Map I-1182-B.

Harding-Lawson Assoc., 1979 Geotechnical investigation of the Beaufort sea, under U.S. Geological Survey contract, #AK 17718: 3 vols., supporting documents.

Harrison, W.D., and Osterkamp, T.E., 1981, Subsea permafrost: Probing, thermal regime and data analysis, in Environmental Assessment of the Alaskan Continental Shelf, Annual Reports v. 7, p. 291-401.

Hartz, R.W., Holden, K., Hopkins, D.M., and Shearer, G., 1979, Location map and summary logs for the Geological Survey's 1979 Beaufort Sea Over-the-ice drilling program. U.S. Geological Survey Open-File Report 79-1303.

Hopkins, D.M. and Hartz, R.W., 1978, Coastal morphology, coastal erosion and barrier islands of the Beaufort Sea, Alaska; U.S. Geological Survey Open-File Report 78-1063.

Hopkins, D.M., McDougall, K., and Nelson, R.E., 1978, The Flaxman Formation of Northern Alaska - evidence of an arctic ice shelf, [Abs.] Fifth American Quat. Association Meeting, Edmonton, Canada.

Hopkins, D.M., Sellmann, P.V., E. Chamberlain, R.E. Lewellen, and S.W. Robinson, 1979, Buried valleys as a possible determinant of the distribution of deeply buried permafrost on the continental shelf of the Beaufort Sea, in NOAA, Environmental Assessment of the Alaskan continental shelf, Annual Reports of Principal Investigators for the year ending march 1979, vol. IX (Hazards): p. 135-141.

Lee, H.J. and Winters, W.J., in press, Strength and consolidation properties of stiff Beaufort Sea silt: Arctic Energy Technologies, volume produced by Department of Energy.

Lewellen, R.I., 1977, A study of Beaufort Sea coastal erosion, northern Alaska: in U.S. National Oceanic and Atmospheric Administration,Environmental Assessment of the Alaskan Continental Shelf: Annual Reports of Principal Investigators for the year ending March 1977, v. 15, p. 491-527.

Miller, D.L. and Bruggers, D.E., 1980, Soil and permafrost conditions in the Alaskan Beaufort Sea: Proceedings of the 12th Annual Offshore Technology conference, Houston, Texas, p. 325-338.

Morack, J.L. and Rogers, J.C., 1982, Marine seismic refraction measurement of near-shore subsea permafrost, in Proceedings of the Fourth Canadian Permafrost Conference, Calgary: National Research Council of Canada, Ottawa, p. 249-255.

Neave, K.G. and Sellmann, P.V., 1982, Subsea permafrost in Harrison Bay, Alaska: An interpretation from seismic data: U.S. Army Cold Regions Research and Engineering Laboratory, Hanover, NH, CRREL Report 82-24.

Neave, K.G. and Sellmann, P.V., 1983, Seismic velocities and subsea permafrost in the Beaufort Sea, Alaska, Proceedings of the Fourth International Conference on Permafrost at Fairbanks: Washington, D.C., National Academy of Sciences, p. 894-898.

Neave, K.G. and Sellmann, P.V., 1984, Determining distribution patterns of ice-bonded permafrost in the U.S. Beaufort Sea from seismic data, in Barnes, P.W., Schell, D.M., and Reimnitz, Erk, (eds.), The Alaskan Beaufort Sea - Ecosystem and Environment, Academic Press, San Francisco, CA, p. 237-258.

O'Conner, J.J., 1981, Distribution of shallow acoustic permafrost in the southern Beaufort Sea: Geological Survey of Canada, Open File Report 953.

Osterkamp, T.E. and Harrison, W.D., 1976, Subsea Permafrost at Prudhoe Bay, Alaska: Drilling report and data analysis: Geophysical Institute, University of Alaska, Fairbanks, Report UAG R-247.

Osterkamp, T.E. and Harrison, W.D., 1982, Temperature measurements in subsea permafrost off the coast of Alaska: Proceedings of the Fourth Canadian Permafrost conference, Calgary: National Research Council of Canada, Ottawa, p. 238-248.

Osterkamp, T.E. and Payne, M.W., 1981, Estimates of permafrost thickness from well logs in northern Alaska: Cold Regions Science and Technology, v. 5, p. 13-27.

Reimnitz, Erk, Wolf, S.C., and Rodeick, C.A., 1972, Preliminary interpretation of seismic profiles in the Prudhoe Bay area, Beaufort Sea, Alaska: U.S. Geological Survey Open-File Report 72-548.

Reimnitz, Erk and Barnes, P.W., 1974, Sea ice as a geologic agent on the Beaufort Sea shelf of Alaska: in Reed, J.C. and Sater, J.E., eds., The Coast and Shelf of the Beaufort Sea. Proceedings of the Arctic Institute of North America Symposium on the Beaufort Sea coast and shelf research, Arctic Institute of North America, Arlington, VA, p. 301-353.

Reimnitz, Erk and Maurer, D.K., 1978, Stamukhi shoals of the Arctic - some observations from the Beaufort Sea: U.S. Geological Survey Open-File Report 78-666, 11 p.

Reimnitz, Erk, Toimil, L.J., and Barnes, P.W., 1978, Arctic continental shelf morphology related to sea-ice zonation, Beaufort Sea, Alaska: Marine Geology, v. 28, p. 179-210.

Reimnitz, Erk, Dunton, Kenneth, and Barnes, P.W., 1979, Anchor ice and lack of delta accretion in the Arctic - A possible link: Geological Society of America, Abstracts with Programs, v. 11, no. 7, p. 501.

Reimnitz, Erk, and Ross, C.R., 1979, Lag deposits of boulders in Stefansson Sound, Beaufort Sea, Alaska: U.S. Geological Survey Open-File Report 79-1205, 26 p.

Reimnitz, Erk and Barnes, P.W., 1981, Depositional complexities in the sea-ice environment of Arctic shelves: Examples from Harrision Bay, Alaska: AAPG SEPM Annual Convention, San Francisco, May 31-June 3 [abs.]: American Association of Petroleum Geologists Bulletin, v. 65, p. 978.

Reimnitz, Erk and Kempema, E.W., 1982, Dynamic ice-wallow relief of northern Alaska's nearshore - a dynamic bedform: Journal of Sedimentary Petrology, v. 52, no. 2, p. 451-462.

Reimnitz, Erk and Kempema, E.W., 1983, High rates of bedload transport measured from infilling rate of large strudel-scour creaters in the Beaufort Sea, Alaska: Continental Shelf Research, v. 1, no. 3, p. 237-151.

Reimnitz, Erk and Kempema, E.W., 1984, Pack ice interaction with Stamukhi Shoal, Beaufort Sea,Alaska, *in* Barnes, P.W., Schell, D.M. and Reimnitz, Erk, (eds.), The Alaskan Beaufort Sea - Ecosystem and Environment, Academic Press, San Francisco, CA, p. 159-184.

Rogers, J.C. and Morack, J.L., 1980, Geophysical evidence of shallow near-shore permafrost, Prudhoe Bay, Alaska: Journal of Geophysical Research, v. 85, no. 89, p. 4815-4853.

Sellmann, P.V., Brown, J., Lewellen R. McKim, H., and Merry, C., 1975, The classification and geomorphic implications of thaw lakes on the Arctic coastal plain, Alaska; CRREL Research Report 34421, U.S. Army Corp of Engineers, Hanover, NH, 31 p.

Sellmann, P.V. and Chamberlain, E.J., 1979, Permafrost beneath the Beaufort Sea near Prudhoe Bay, Alaska: Proceedings of the 11th Annual Offshore Technology Conference, Houston, Texas, p. 1481-1493.

Smith, P.A. and Hopkins, D.M., 1979, Offshore permafrost studies and shoreline history as an aid to predicting offshore permafrost conditions, *in* NOAA, Environmental Assessment of the Alaskan Continental Shelf, Annual Reports of Principle Investigators for the year ending, March 1979, vol. XI (Hazards), p. 116-163.

Smith, P.A. (in press), Late Quaternary Geology of the Beaufort Inner Shelf near Prudhoe Bay, *in* U.S. Geological Survey, Alaska accomplishments during 1983.

Vail, P.R., Mitchum, R.M., Todd, R.G., Widmier, J.M., Thompson, S. III, Sangree, J.B., Bubb, J.N., and Hatlelid, W.G., 1977, *in* Payton, C.E. (ed.), Seismic stratigraphy and global changes of sea level in Seismic stratigraphy - Applications to hydrocarbon exploration, Payton, C.E., ed.: AAPG Mem. 26, Tulsa, OK, 516 p.

Wolf, S.W., Barnes, P.W., and Reimnitz, Erk, (in press), Analysis of hummocky subbottom relief from repetitive observations north of Tigvariak Island, Beaufort Sea, Alaska.

APPENDIX:

TRACKLINE DATES, 1971 - 1982

APPENDIX - Trackline dates, 1971 - 1982

Year	Month	Day	JD	Line	Uniboom (Minisparker)	Roll #	7 kHz	Roll #
1982	Sept	18	261	20	--	--	1102-1126	11
1982	Sept	1	244	6	1147-1520	1	1302-1520	3
1982	Sept	2	245	7	1404-1533	2	--	--
1982	Sept	5	248	10	1545-1855	3	--	--
1982	Sept	7	250	12	1500-1815	3	--	--
1981	July	19	200	5	1335-1740	1	1335-1740	2
1981	July	19	200	6	--	--	1757-1830	2
1981	July	20	201	7	--	--	0013-0830	3
1981	July	20	201	8	--	--	0830-1150	3
1981	July	27	208	16	1153-1415	5	1153-1415	12
1981	July	28	209	17	--	--	1509-1640	12
1981	July	29	210	18	1250-1520	5	1250-1520	13
1981	July	30	211	20	--	--	0845-1110	14
1980	July	19	201	1	--	--	1245-1530	2
1980	July	27	209	12	--	--	0819-1115	8-9
1980	July	28	210	13	1130-1520	4	1220-1520	9
1980	July	28	210	14	1520-1630	4	1520-1630	9-10
1980	July	30	212	15	--	--	0850-1435	10-11
1980	Aug	9	222	24	--	--	1659-1814	17
1980	Aug	11	224	25	--	--	1618-1701	17
1980	Aug	12	225	26	0923-1332	5	0923-1332	18
1979	July	23	204	1	(1709-1752)	1	1709-1752	1
1979	July	29	210	5	--	--	1259-1450	3
1979	Aug	1	213	8	--	--	1526-1558	5
1979	Aug	9	221	14	1600-1727	1	--	--
1979	Aug	9	221	15	(1810-1900)	1	--	--
1979	Aug	9	221	17.	(2043-2130)	1	--	--
1979	Aug	10	222	19	1323-1505	1	--	--
1979	Aug	10	222	20	(2126-2206)	2	--	--
1979	Aug	12	224	26	0714-0835	3	--	--
1979	Aug	12	224	27	0916-1052	3	--	--
1979	Aug	12	224	28	1127-1155	3	--	--
1979	Aug	12	224	29	1536-1800	4	--	--
1979	Aug	13	225	30	1401-2100	4	--	--
1979	Aug	15	227	35A	--	--	1523-1618	10b-11
1979	Aug	16	228	35B	1430-2146	5	--	--
1979	Aug	17	229	36	1209-1444	5	--	--
1979	Aug	18	230	38	1935-2145	5	--	--
1979	Aug	19	231	39	1613-2040	5-6	1613-2000	12

APPENDIX - Trackline dates, 1971 - 1982

Year	Month	Day	JD	Line	Uniboom (Minisparker)	Roll #	7 kHz	Roll #
1982	Sept	18	261	20	--	--	1102-1126	11
1982	Sept	1	244	6	1147-1520	1	1302-1520	3
1982	Sept	2	245	7	1404-1533	2	--	--
1982	Sept	5	248	10	1545-1855	3	--	--
1982	Sept	7	250	12	1500-1815	3	--	--
1981	July	19	200	5	1335-1740	1	1335-1740	2
1981	July	19	200	6	--	--	1757-1830	2
1981	July	20	201	7	--	--	0013-0030	3
1981	July	20	201	8	--	--	0030-1150	3
1981	July	27	208	16	1153-1415	5	1153-1415	12
1981	July	28	209	17	--	--	1509-1640	12
1981	July	29	210	18	1258-1520	5	1250-1520	13
1981	July	30	211	20	--	--	0045-1110	14
1980	July	19	201	1	--	--	1245-1530	2
1980	July	27	209	12	--	--	0819-1115	8-9
1980	July	28	210	13	1130-1520	4	1220-1520	9
1980	July	28	210	14	1520-1630	4	1520-1630	9-10
1980	July	30	212	15	--	--	0850-1435	10-11
1980	Aug	9	222	24	--	--	1659-1814	17
1980	Aug	11	224	25	--	--	1618-1701	17
1980	Aug	12	225	26	0923-1332	5	0923-1332	18
1979	July	23	204	1	(1709-1752)	1	1709-1752	1
1979	July	29	210	5	--	--	1259-1450	3
1979	Aug	1	213	8	--	--	1526-1550	5
1979	Aug	9	221	14	1600-1727	1	--	--
1979	Aug	9	221	15	(1818-1900)	1	--	--
1979	Aug	9	221	17	(2043-2130)	1	--	--
1979	Aug	10	222	19	1323-1505	1	--	--
1979	Aug	10	222	20	(2126-2206)	2	--	--
1979	Aug	12	224	26	0714-0835	3	--	--
1979	Aug	12	224	27	0916-1052	3	--	--
1979	Aug	12	224	28	1127-1155	3	--	--
1979	Aug	12	224	29	1536-1800	4	--	--
1979	Aug	13	225	30	1401-2100	4	--	--
1979	Aug	15	227	35A	--	--	1523-1618	10b-11
1979	Aug	16	228	35B	1430-2140	5	--	--
1979	Aug	17	229	36	1209-1434	5	--	--
1979	Aug	18	230	38	1935-2145	5	--	--
1979	Aug	19	231	39	1613-2030	5-6	1613-2000	12

1979	Aug	20	232	40	--	--	0827-0850	12
1979	Aug	20	232	41	--	--	1139-1235	12
1979	Aug	25	237	43	--	--	1239-1345	13
1979	Aug	26	238	44	--	--	1505-1730	13
1979	Aug	26	238	45	--	--	2049-2146	14
1979	Aug	27	239	46	--	--	1229-1345	14-15
1979	Aug	27	239	47	--	--	1353-1500	15
1979	Aug	27	239	48	--	--	1535-1647	15
1979	Aug	29	241	50	--	--	1044-1154	16
1979	Sept	1	244	54	0853-1026	7	0853-1026	18
1979	Sept	1	244	55	(1027-1125)	7	1027-1125	18
1979	Sept	1	244	56	1321-1520	7	1321-1520	18
1979	Sept	1	244	57	(1545-1616)	7	1545-1616	18
1979	Sept	1	244	58	1645-1452	7	1645-1452	18-19
1979	Sept	1	244	59	(2010-2055)	7	2010-2055	19
1979	Sept	2	245	60	0824-1440	7-8	0824-1440	19-20
1979	Sept	2	245	61	1445-1713	8	1445-1713	20
1979	Sept	3	246	62	1447-1535	8	1447-1535	20
1979	Sept	3	246	63	1617-2037	8	1617-2037	21
1979	Sept	5	248	66	1120-1010	9-10	1120-1010	22-23
1979	Sept	6	249	67	0830-1520	10	0830-1520	23
1979	Sept	8	251	69	0816-1440	10	0816-1440	24
1979	Sept	9	252	71	0734-0930	10	0734-0930	24
1979	Sept	9	252	72	0942-1027	10	0942-1027	25
1979	Sept	10	253	77	0920-1215	11	0920-1215	27
1979	Sept	10	253	78	1215-1402	11	1215-1402	27
1979	Sept	10	253	79	1431-1614	11	1431-1614	28
1979	Sept	11	254	82	(1220-1257)	12	1220-1257	29
1979	Sept	11	254	83	(1313-1726)	12	1313-1726	29-30
1979	Sept	11	254	84	(1727-1937)	12	1727-1937	30
1979	Sept	11	254	85	(1937-2110)	12	1937-2110	30
1979	Sept	18	261	88	--	--	1213-1310	32
1979	Sept	20	263	92	1414-1910	13	1414-1910	33
1979	Sept	20	263	93	--	--	1930-2135	34
1979	Sept	21	264	94	--	--	0905-1515	34-35
1979	Sept	21	264	95	--	--	1521-1614	35
1979	Sept	21	264	96	--	--	1630-1720	35
1979	Sept	23	266	99	--	--	0750-1000	36-37
1979	Sept	23	266	100	--	--	1116-1452	37
1978	Aug	29	241	21	--	--	1557-1730	11
1978	Aug	30	242	24	--	--	0715-1230	11-12
1978	Aug	30	242	25	--	--	1510-1625	12
1978	Aug	31	243	27	1100-1255	3	1100-1255	12-13
1978	Aug	31	243	28	1345-1437	3	1345-1437	13
1978	Aug	31	243	29	--	--	1754-1915	13
1978	Sept	1	244	30	--	--	0055-1130	13
1978	Sept	13	256	37	--	--	0040-2000	18-19
1978	Sept	14	257	38	--	--	0724-0930	20
1978	Sept	14	257	39	--	--	1252-1435	20

1978	Sept	14	257	40	--	--	1540-2015	20
1978	Sept	15	258	41	--	--	0730-1240	21
1978	Sept	16	259	43	--	--	0954-1046	23
1977	Sept	19	262	74	--	--	0737-1145	31
1977	Sept	19	262	75	--	--	1430-1745	31
1977	Sept	21	264	76	0913-1933	9-10	0913-1933	32-33
1977	Aug	23	235	53	--	--	1400-1509	17
1977	Aug	23	235	54	--	--	1700-1025	10
1977	Aug	24	236	55	--	--	1557-1625	10
1977	Sept	8	251	66	1441-2040	5-6	1441-2040	24-25
1977	Sept	9	252	67	1140-2020	6-7	1140-2020	25-26-27
1976	July	24	205	1	--	--	1340-1450	1
1976	July	24	205	2	--	--	1500-1610	1
1976	July	24	205	3	--	--	1615-1730	2
1976	July	27	208	15	--	--	0940-1310	3
1976	July	27	208	16	--	--	1540-1727	3
1976	Aug	14	226	34-17	West Dock Sur. 7 kHz	--	0742-0844	12
1976	Aug	16	228	40	--			
1975	Sept	2	245	2	1205-1020	11	--	--
1975	Sept	8	251	7	--	--	1240-1340	10
1975	Sept	11	254	8	--	--	1101-1456	11
1975	Sept	5	248	3	1155-1730	11	1155-1730	9
1975	Sept	5	248	4	1753-2000	12	1753-2000	9
1973	Aug	20	232	6	1642-1730	--	--	--
1973	Aug	20	232	7	1735-1915	--	--	--
1973	Aug	20	232	8	1923-2240	--	--	--
1973	Aug	21	232	9	0850-1215	--	--	--
1973	Aug	21	232	10	1217-1500	--	--	--
1973	Aug	21	232	11	1734-1837	--	--	--
1973	Aug	22	233	12	0752-1100	--	--	--
1973	Aug	22	233	13	1224-1619	--	--	--
1973	Aug	22	233	14	1619-1926	--	--	--
1973	Aug	23	234	15	0720-0920	--	--	--
1973	Aug	23	234	16	0920-1340	--	--	--
1973	Aug	23	234	17	1340-1455	--	--	--
1972	July	17	198	1	1415-1600	--	--	--
1972	July	17	198	2	1700-1655	--	--	--
1972	July	18	199	3	1121-1222	--	--	--
1972	July	18	199	4	1700-2150	--	--	--
1972	July	19	200	5	1333-1625	--	--	--
1972	July	19	200	6	1740-2155	--	--	--
1972	July	20	201	7	1003-1250	--	--	--
1972	July	20	201	8	1743-1650	--	--	--
1972	July	21	202	10	1240-1607	--	--	--

1972	July	22	203	11	0935-1235	--	--	--
1972	July	22	203	12	1341-1506	--	--	--
1972	July	23	204	13	0950-1105	--	--	--
1972	July	23	204	14	1400-1013	--	--	--
1972	July	23	204	15	0920-1315	--	--	--
1972	July	24	205	16	0842-1615	--	--	--
1972	July	27	208	17-20	Nav. chart missing			
1972	July	--	--	21	1745-2045	--	--	--
1972	July	31	212	22	1000-1527	--	--	--
1972	Aug	1	213					
1971	Sept	2	245	12	(0610-0722)	--	--	--
1971	Sept	2	245	13	(1605-2025)	--	--	--
1971	Sept	4	247	14	(0610-0940)	--	--	--
1971	Sept	4	247	15	(1602-1732)	--	--	--
1971	Sept	4	247	16	(1740-1904)	--	--	--
1971	Sept	4	247	17	(1905-1937)	--	--	--
1971	Sept	5	248	18	(1654-1725)	--	--	--
1971	Sept	5	248	19	(1729-1737)	--	--	--
1971	Sept	5	248	20	(1738-1822)	--	--	--
1971	Sept	5	248	21	(1823-1836)	--	--	--
1971	Sept	5	248	22	(1836-1910)	--	--	--
1971	Sept	6	249	25	(0030-0904)	--	--	--
1971	Sept	6	249	26	(1217-1420)	--	--	--
1971	Sept	6	249	28	(1553-1925)	--	--	--
1971	Sept	6	249	29	(1936-2029)	--	--	--
1971	Sept	12	255	45	(0712-0050)	--	--	--
1971	Sept	12	255	46	(0056-1030)	--	--	--
1971	Sept	13	256	47	(1031-1305)	--	--	--

TEMPORAL AND SPATIAL CHARACTER OF NEWLY FORMED ICE GOUGES IN EASTERN HARRISON BAY, ALASKA, 1978 - 1982

by

Douglas M. Rearic

TABLE OF CONTENTS

LIST OF FIGURES

Figure 9. Graph of the deepest gouge found in each 1 m water depth interval over the entire course of the study. Again, as in Figure 8, deep gouges are restricted to the outer areas of testline 2. Inshore of 15 m water depth the deepest gouges found were consistently 20 cm or less. On testline 1 deep gouging can occur in shallower water depths (note the 70 cm gouge in only 8 m of water).

Figure 10. Graph of the mean gouge depth in each 1 m water depth interval averaged over the entire course of the study. As with Figures 8 and 9, mean gouge depths are very low (about 10 cm) on testline 2 inshore of 15 m water depth, while on testline 1 the mean gouge depths are consistently greater than those of testline 2 for equivalent water depths. In water greater than 15 m deep, average gouge depths are similar for both testlines.

Figure 11. Frequency distributions plotted on similog paper for three gouge characteristics measured in this study: A) gouge depth, B) disruption width, and C) ridge height. Note that the characteristics fall on an approximate straight line indicating a negative exponential distribution. Of special interest are the large values of all three characteristics which do not fit the distribution. The reader is referred to the text for suggestions as to why the fit is so poor for the high-end members of the distributions.

Figure 12. Gouge depth frequency distributions from the studies of A) Weeks et al. (1984), B) Barnes et al. (1984), and Barnes and Rearic (in press). Note that in all these studies, as with the present one, a negative exponential distribution is indicated. The same problem exists in these studies as occurred in the present with the high values failing to fit the distribution. See the text for possible explanations.

Figure 13. Graph of the percent of the seafloor disturbed each year on each testline. For comparison, the 1976 and 1977 values of Barnes et al. (1978) are included. Seafloor disruption is seen to vary yearly between about 1 and 6 percent on the testlines. Note the apparent inverse relationship between the two testlines in yearly percent disturbed.

Figure 14. Graph of the average minimum volume of sediment disturbed each year on the testlines in each 1 m water depth interval. The influence of the shoals is again noted, as with gouge depth, in that values inshore of 15 m water depth are relatively low on testline 2. Testline 1 demonstrates a consistent increase in disruption volume between 7 and 14 m water depth of about 1000 cubic meters per 1 m of water depth increase.

Figure 15. Gouge orientations plotted as rose diagrams for the two testlines. Note that the orientations of testline 1 are subparallel to the bathymetry contours with an approximate east-west orientation. Orientations on testline 2 are more NW-SE, indicating the possible influence of the shoals on the direction of ice movement.

Figure 16. Gouge terminations plotted as rose diagrams for the two testlines. Note the similarity between the two testlines with the dominant trends either onshore in a southeasterly direction or alongshore in a westerly direction. Although gouging is believed to be an upslope process, some gouges are seen to move in an offshore direction. See text for possible explanations.

Figure 17. Gouge terminations by years. (A) Most gouges in the years shown approached from the northwest and terminated in single incisions. (B) Most gouges in the year shown approached from the northeast and produced multiplet terminations.

Figure 18. Plot of the disruption percentages from the present study and that of Barnes et al. (1978) and Reimnitz et al. (1977).

Figure 19. Plot of the percent of seafloor gouged over time from Barnes et al. (1978). The plot is from a model considering yearly replow of previously gouged areas as well as non-gouged areas. The increased percentages of gouging with time determined from this study indicate that the entire seafloor (98%) could be reworked in about 100 years, while in 50 years there is still considerable gouging of the bottom (about 85%). Figures from the curve of Barnes et al. (1978) indicate values on the order of 80% and 55% for these same time spans.

LIST OF TABLES

Temporal and Spatial Character of Newly Formed Ice Gouges in Eastern Harrison Bay, Alaska, 1978 - 1982

by

Douglas M. Rearic

INTRODUCTION

Interaction between the dynamic elements of wind, water, ice and seafloor sediment is recorded on the continental shelf of the Alaskan Beaufort Sea in the form of ice gouges. Gouging of the seafloor by ice keels causes a ridge and furrow microtopography with accompaning horizontal and vertical movement of the sediments (Barnes et al., 1984). Sea-ice forces are responsible for large volumes of sediment disruption and redistribution across the shelf (Barnes et al., 1984), while hydraulic forces from waves and currents further redistribute this sediment, in many cases filling depressions and smoothing the bottom (Barnes and Reimnitz, 1979; Reimnitz and Kempema, 1982).

The sea-ice canopy formed over the inner shelf in winter is broken by zones of ice ridging caused by shear and compressional forces between permanent rotating polar pack ice and seasonal stable shore fast ice (Hibler et al., 1974; Reimnitz et al., 1978; Stringer, 1978; Prichard, 1980). The formation of ice ridges causes ice blocks to be forced under the ice surface to form ice keels which may come into contact with the seafloor. When mobile ice keels in contact with the seafloor plow through the sediments ice gouges are formed (Figure 1).

Recurrence rates for ice gouging of the seafloor as well as the yearly size variation of the features is of major importance today due to petroleum development activities now taking place in the Alaskan Beaufort Sea (Oil and Gas Journal, 1983). Development plans are dependent upon knowledge of yearly gouge rates, depths, widths, and areal distributions in order to protect subsea pipelines from ice impact and bottom founded structures from excessive point source loads and stresses. Sea-ice also has a significant geologic effect on the seafloor through the destruction of sedimentary features such as bedding structure (Figure 2) and biological borings, the building and/or maintaining of shoals (Reimnitz and Kempema, 1984), the bulldozing of shelf sediment onto the beaches by ice ride-up (Barnes, 1982; Kovacs, 1983; Kovacs, 1984), the creation of sedimentary traps by the plowing of ice gouge furrows (Reimnitz and Kempema, 1982), and the transport of sediment by actual bulldozing and resuspension of sediment during ice gouging (Barnes and Rearic, in press). Data on yearly ice gouge characteristics is unfortunately very sparse and an increase in the understanding of this marine process will lead to greater knowledge about the environment of high latitude continental shelves and their hazards. The presence of sea ice and extreme low winter temperatures creates an environment that is affected by forces not usually found in low latitude marine environments. Ice contact with the seafloor, permafrost in the offshore sediments, the draining of the rivers in spring through holes in the ice canopy, and ice ride up and piling on the beaches are dynamic conditions unique to the high latitude environment.

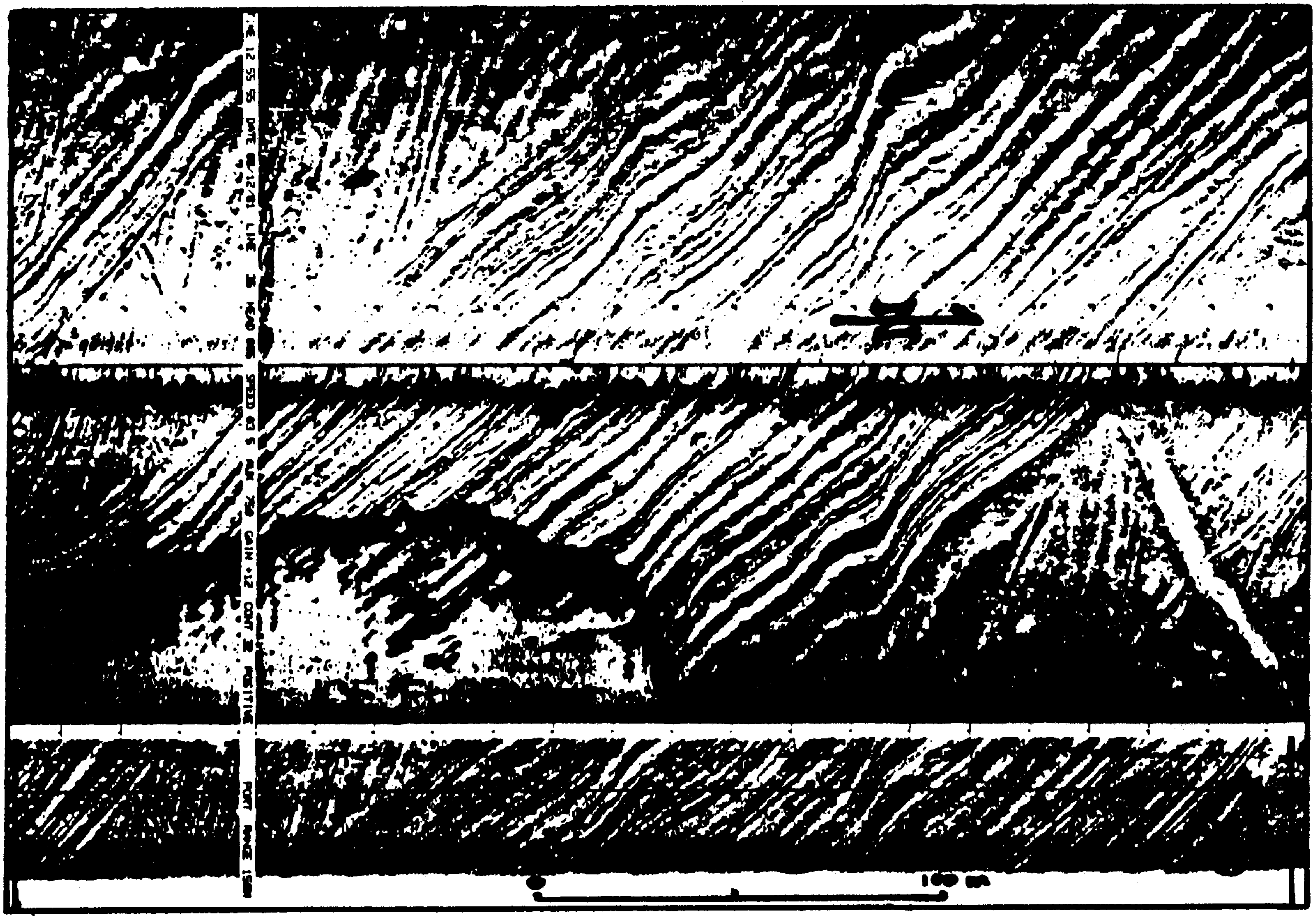

Figure 1. Sonograph record of a multiplet gouge east of Barter Island. Ice floe along bottom margin of record is grounded in about 25m of water. North is to the right and gouging took place in a southeasterly onshore direction.

Figure 2. Sonograph record of an ice gouge produced in a ripple field. Note the destruction to the bedding. The gouge is about 5m wide and 20cm deep.

Ice gouges that are dated as less than one year old have been studied in the Alaskan Beaufort Sea and the results are presented here. The characteristics of these relatively newly formed ice gouges are presented and an interpretation as to the significance of the information is discussed. In some cases the data speaks for itself by allowing the reader to observe variations in the characteristics over time and between shelf environments, while in other cases further interpretation of the data in the form of graphs, figures, and discussion **enhances** the importance of the study in relation to sedimentary processes now occuring in the Alaskan Beaufort Sea.

BACKGROUND

The influence exerted by sea-ice on high latitude and glacial seafloor sediments has been known for some time (Kindle, 1924; Carsola, 1954; Rex, 1955). Early studies centered on qualitative description of ice gouge features (Pelletier and Shearer, 1972; Kovacs and Mellor, 1974; Reimnitz and Barnes, 1974; Lewis, 1977a), while recent studies have attempted to quantify ice gouge chartacteristics (Toimil, 1979; Wahlgren, 1979a; Rearic et al., 1981; Thor and Nelson, 1981; Reimnitz et al., 1981; Barnes et al., 1984; Weeks et al., 1984). The above studies have centered on the total population of ice gouges of all ages existing on the seafloor at any one time.

The rate at which ice gouges are added annually to this record is not fully understood although studies to determine the ice gouge recurrence rate on the shelf have recently been reported (Lewis, 1977b; Reimnitz et al., 1977; Barnes et al., 1978; Pilkington and Marcellus, 1981; Weeks et al., 1983; Barnes and Rearic, in press). Assessing the rate of ice gouge reccurence is difficult. To determine recurrence rates in this study two tracklines were reoccupied on a yearly basis and the gouges less than one year old were measured. Comparing one years record to the next allows a good approximation of the gouges which are added to the seafloor over the previous year. This technique requires precision navigation and for optimum survey conditions, open water free of floating ice.

The first attempt to assess yearly ice gouging rates in the Alaskan Beaufort Sea was by Reimnitz et al. (1977). Preliminary rates were determined for the years 1972-1973. In a latter study estimates for the years 1975-1977 were calculated by Barnes et al. (1978). Gouge rate estimates from both of these studies agreed favorably with each other. They found that approximately 2% of the seafloor was gouged yearly in eastern Harrison Bay with a mean gouge depth of about 20 cm. Although they suggested that many gouges shallower than 20 cm existed, the resolution of their equipment precluded enumeration of the smallest gouges. Rapid infilling of the smallest gouges also increases the difficulty in recording these features. Another problem in these studies has been the lack of an extended data base in order to determine long term and regional variability in the ice gouge rates.

Environmental Setting

Harrison Bay is a large shallow embayment of the Alaskan Beaufort Sea coast (Figure 3). The embayment is influenced by outflow from the Colville River in the south which has created a delta in the southeast portion of the bay. Other characteristics of Harrison Bay include a barrier island system in the eastern part of the bay and sand and gravel shoals in the east and northern parts of the bay (Reimnitz and Maurer, 1978). The northern extent of the bay is marked by shoals at a distance of 50 km from shore in 20 m of water. The shoals attain a height of about 10 m above the surrounding seafloor.

The floor of the bay consists of patchy sand and mud deposits interspersed with layers of stiff silty clay which are highly consolidated and create resistant ledges in the troughs of some ice

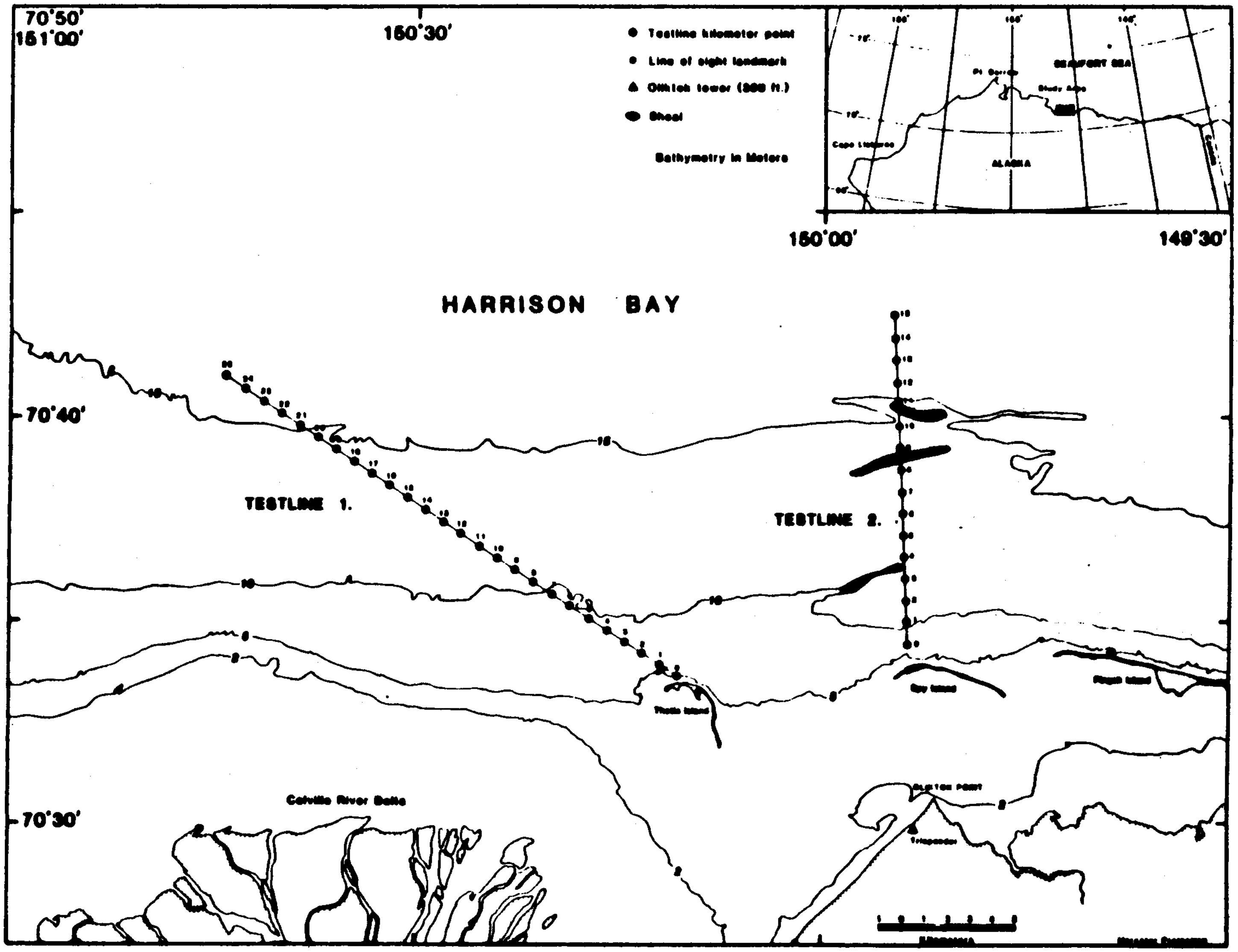

Figure 3. Location map of the study area. Note the location of the shoals along testline 2 and the lack of these features along testline 1. Bathymetry is in meters.

gouges (Reimnitz et al., 1980). Annual suspended sediment imput to the bay from the Colville River is about 5.8 millon metric tons and consists mostly of fine grained inorganic material erroded from river banks, mud bars and the thalweg of the river channels (Arnborg et al., 1967). During the time of greatest sediment transport, usually early June, the mouth of the Colville River and Harrison Bay are covered by ice. The sediment discharged at this time flows over the ice and is eventually either deposited on the bottom through holes erroded in the ice or is carried away on the ice during spring breakup by wind and current (Walker, 1974). Thus, sedimentation in this area is highly non-uniform and differs from deltaic processes of temperate climates.

Freeze up in Harrison Bay begins in late October or early November and is initiated by the formation of slush and frazil ice. As the sea-ice thickens a shore fast ice canopy is formed over the bay and the influence of hydraulic processes is minimized (Matthews, 1981). Ice motions within the ice canopy caused by wind and current create a zone of grounded ice ridges wherever the ice motion is met by resistance from the shore fast component of the canopy. In Harrison Bay this ridge zone, termed the stamukhi zone, occurs in water depths of between 8 and 12 meters (Reimnitz et al., 1978; Stringer, 1978). Further seaward, in water depths of approximately 20 meters, another stamukhi zone occurs and is associated with the shoals of the northern boundary of the bay. Ice keels created during ice ridge formation are responsible for ice gouging throughout the winter. Isolated multi-year ice trapped in the seasonal ice canopy during freeze up may also account for a significant amount of ice gouging (Barnes et al., 1984).

In May and June the Colville River thaws prior to the break up of the sea-ice canopy and floods the canopy with fresh water in the near shore areas. The flooding increases the rate of sea-ice break up and melting. Throughout the summer isolated ice remnants from the previous winter may remain grounded until the next winter freeze up. During the summer open water conditions allow wind forces to create waves and currents that may rework seafloor sediments (Reimnitz and Maurer, 1979). Shoal crests in particular are reworked yearly by these hydraulic processes (Reimnitz and Kempema, 1984). Summer ice conditions can vary and at times can be severe enough to affect navigation by causing excessive deviation from desired courses.

In the southeastern portion of the bay are two barrier islands from which the tracklines of this study initiate (Figure 3). The tracklines are here after termed testlines in that they have been reoccupied yearly with precision navigation techniques since 1972. Testline 1 extends from Thetis Island in a northwesterly direction and has been surveyed to a maximum length of 25 km and a maximum water depth of 16.5m when ice conditions have been favorable. The seafloor covered by testline 1 is relatively smooth with a gentle slope of approximately 0.05 degree. Testline 2 extends north from Spy Island and has been surveyed to a maximum length of 15 km and a maximum water depth of 18.5 m under favorable conditions. The seafloor covered by testline 2 has a slope about the same as testline 1, however, the seafloor here contains 3 successive 2 to 3 meter high shoals, trending east-west, subparallel to the bathymetric contours, in water depths of between 8 to 15 meters. Because of variable ice conditions from year to year the distances covered on the testlines varied yearly.

Study Objectives and Terminology

The objective of this study is intended to extend our understanding of gouge rate variability in both time and areal distribution and to compliment the previous studies of Reimnitz et al. (1977) and Barnes et al. (1978). The variability in gouge size and shape which occur yearly are an important part of this understanding (Figure 4). A thorough description of ice gouge terminology can be found in Barnes et al. (1984) and consists of essentially the following elements:

1) Gouge Event - The passing of a grounded ice keel, leaving one or more furrows, through the bottom sediments of any ice influenced body of water.

2) Gouge - Furrow left on the seafloor whether caused by a single or multiplet event.

3) Single Gouge - The furrow left on the seafloor after the passing of a grounded ice keel having only one projection contacting the bottom.

4) Multiplet - The furrows left on the seafloor after the passing of a grounded ice keel having two or more projections contacting the bottom.

5) Gouge Depth - The depth of a gouge measured vertically from the average level of the surrounding seafloor to the deepest point in the gouge. Only the deepest incision of a multiplet is measured.

6) Gouge Width - The width of a gouge measured horizontally at the average level of the surrounding seafloor. This measurement pertains only to single gouges and does not include the ridges of sediment often found bounding a gouge.

7) Ridge Height - The height of the ridge of sediment bounding a gouge measured vertically from the average level of the surrounding seafloor to the highest point on the ridge. The ridge sediments are primarily made up of material plowed from the corresponding gouge.

8) Gouge Orientation - The orientation of an ice gouge relative to true north. Orientations are reported as a vector between 0 and 180 degrees but do not imply a direction of movement for the ice keel which created the ice gouge.

9) Number of Incisions - The total number of ajoining furrows created by a multiplet event. In some calculations each furrow is treated as an individual gouge while in others the event itself is only considered.

10) Disruption Width - The total horizontal width of a gouge measured at the average level of the surrounding seafloor and including the ridges bounding the gouge. The disruption width of single gouges is estimated to be approximately 25% greater than the gouge width measurement. The width measurements of all multiples are reported as disruption widths.

11) Gouge Termination - The terminous of a gouge on the sonograph record. Generally associated with the terminous is a push moraine of sediment surrounding the final grounding area. The gouge termination is a reliable indicator of the true direction of ice keel movement.

12) Gouge Length - The length of a gouge or multiplet. This measurement is the most difficult to obtain because most gouges do not start and end on the sonograph records. For the purposes of this study all gouges which do not start and end on the sonograph record

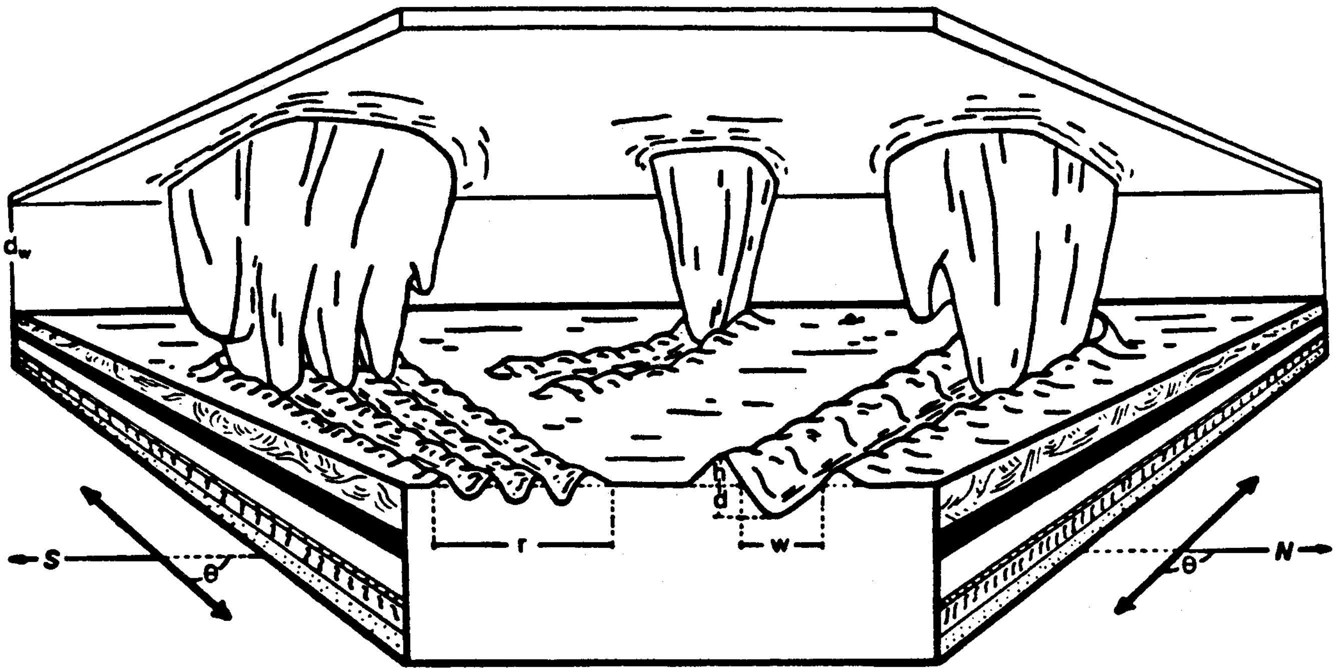

d - Gouge Depth

w - Gouge Width

h - Ridge Height

r - Disruption Width

θ - Gouge Orientation

d_w - Water Depth

Figure 4. Idealized sketch of an ice gouge and gouge multiplet and the terms used to describe the characteristics measured in this study.

are considered to be in excess of 250 meters long (the width of the sonograph record) for the calculations in which they are used.

Methods of Data Collection

Two tracklines in Eastern Harrison Bay (figure 3), 50 km west of Prudhoe Bay, were resurveyed each year between 1977 and 1982 in order to determine the recurrence rate of ice gouging, ice gouge characteristics, and the resultant effects to the seafloor. Five years of data exist for testline 1 and four years of data for testline 2. The data analyzed in this study were collected from onboard the USGS research vessel Karluk. Data collection techniques involved the towing of a side scan sonar fish above the seafloor and recording the reflection returns on a wet paper recorder. The side scan sonar system presents a map view of the seafloor (Belderson et al., 1972) and the slant range (width of the record) was generally 125 m on either side of the ships track. Sonar coverage was accomplished using a model 259-3 EG & G side scan sonar recorder and a model 272 EG & G sonar fish with a 105 kHz pulse. Measurements of number of gouges, width, orientation, termination and length were made from the sonographs (Figure 4). It is estimated that the maximum resolution of the sonographs is 10 cm.

Bathymetry data were recorded on a high-resolution fathometer using a dry paper recording system. A Raytheon RTT-1000 recording fathometer with a 200 kHz transducer allowed resolution of features as small as 15 cm under ideal conditions. Measurements from the fathograms included water depth, gouge depth, and ridge height (Figure 4).

Navigation of the tracklines was accomplished using a combination of trisponder ranges (acoustic pingers with an accuracy of about +-5 m), line of sight, and copies of previously recorded sonographs for comparison with the copies being recorded at that time. This system under ideal conditions will give an accuracy of position to within 5 meters. In the worst cases ice in the path of the boat will cause detours in the testline direction which may cause a loss of coverage dependent on the size and amount of ice encountered. Poor weather and sea state as well as system failure may also degrade the record quality.

Testline 1 navigation consists of line of sight visuals between Oliktok tower and a hut (the only structure) on Thetis Island (Figure 3). The distance from Oliktok tower, on which the range trisponder is located, to the begining of the testline is 12557 meters. The testline is run on a course of 305 degrees true from this point. Deviation from the course can be noted by nonalignment of the tower and hut. The begining of testline 2 lies 7520 meters from Oliktok tower and 9670 meters from a trisponder located on Thetis Island. The testline is then run due true north from this location. Line of sight visuals between a day beacon on Spy Island and the tower on Olikok Point are also used to keep the trackline alignment accurate. On both testlines, photographs of testline sonographs obtained in previous years were used to verify accuracy of trackline possition by comparing bottom features with those previously recorded (Figure 5).

Methods of Data Analysis

The tracklines were plotted on navigation charts in the field each year. Navigation was initially divided into one kilometer segments beginning one kilometer from the barrier island coast and continuing in an offshore direction. The time for each kilometer way point was determined and these points located on the records by interpolation between time marks on the sonograph and fathogram records. The records were then compared to the preceeding years recordings in order to determine new gouges and their characteristics. The measurements were recorded on data sheets and are included as an appendix to this study.

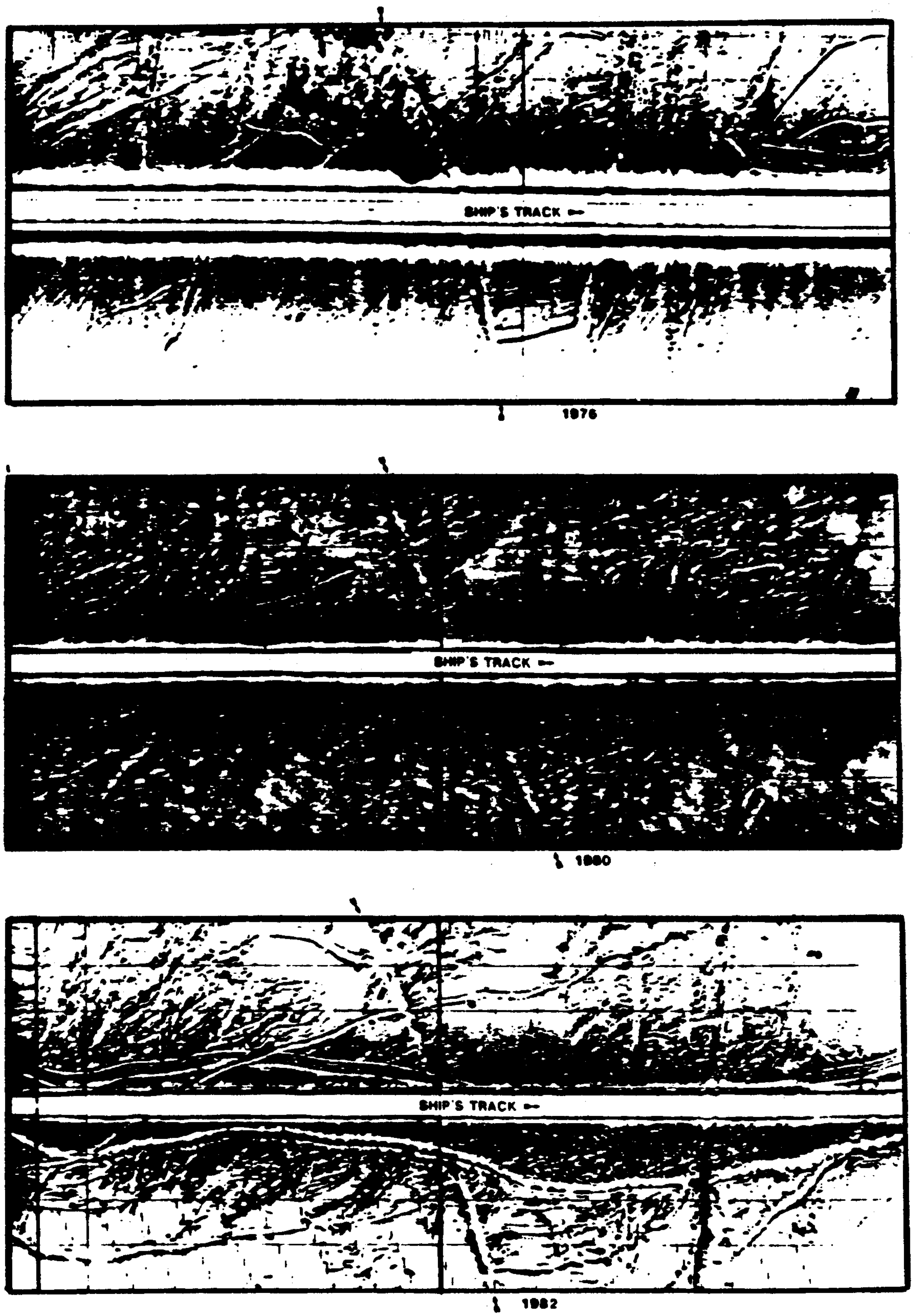

Figure 5. Three sonographs of the same areal coverage from testline 1 for the years 1976, 1980, and 1982. A reference gouge created in 1976 is identified by the arrows on the sonographs. Note the changes to the seafloor over time as gouges are created and subsequently infilled.

RESULTS

The results of this study are based on the observation and measurement of 1292 ice gouges formed between 1977 and 1982. For the purposes of this study these gouges will be termed 'new' gouges. This is done in order to distinguish post 1977 gouges from gouges formed prior to 1977. The gouge characteristic measurements extracted from the records include depth, width, ridge height, length, orientation, and in the case of gouge multiplets, the number of incisions created by a multiplet event and disruption width (Figure 4). The data are described by variations in the total new gouge occurance, yearly variations, and variation between tracklines.

Means and Maximums

All data from both testlines over all years were combined. The data are contained in the data sheets included as the Appendix and in Table I. One of the major observations noted from this study is the high variability in the number of gouges formed from year to year (Table 1). Although having differing seafloor morphologies, both areas averaged about 8-9 new gouges per 1 km segment per year over the course of this study. The number of gouges created over a years time did go as high as 64 in a 1 km segment on testline 1 and 44 on testline 2. However, the highly gouged segments were generally found in water depths greater than 10m.

Most gouges are shallow, 20 cm deep or less. Deep gouges occur only rarely and are relegated to the deeper water depths of the two areas. Gouge depths ranged from a minimum of 10 cm to a maximum of 1.4 m. Segments containing the deepest gouges were in water depths greater than 10 m, much the same as occured with high gouge densities.

The formula for calculation of a distribution mean is dependent upon the type of distribution the data assume when plotted. Most distribution means are calculated based upon the formula for the normal (Gaussian) distribution which is:

$$M = \frac{x_1 + x_2 + x_3 + \cdots x_n}{n}$$

where x is a particular value in the distribution and n is the number of x values in the distribution. When the means of the new gouge depths are calculated using the normal distribution formula, they are 16 cm for testline 1, 14 cm for testline 2, and 15 cm for the total study. These means are approximately 25% shallower than those found in previous studies in this same area (Reimnitz et al., 1977; Barnes et al., 1978). In these earlier studies those gouges less than 20 cm were not included in the calculation of mean gouge depth, which may partially account for the differences noted.

Because the gouge depth data from most ice gouge studies fits an exponential distribution (Barnes et al., 1984; Lewis, 1977a; Weeks et al., 1984) the formula which could be used for the

TESTLINE 1.

Kilometers	0	1	2	3	4	5	6	7	8	9	10	11	12	13	14	15	16	17	18	19	20	21	22	23	24	25		
Water Depth (m)	4.9	5.8	8.3	8.5	9.6	10.1	10.0	10.4	10.9	11.5	12.0	12.4	12.8	13.1	13.6	13.8	14.2	14.6	14.9	15.1	15.2	15.5	15.4	16.0	16.5	16.7		
No. of Gouges																											Total	
1977-1978	0	2	6	0	0	6	0	0	1	18	5	4	15	21	18	8	4	0	0	0	0	10	4	5	0		127	
1978-1979	4	4	13	20	12	0	1	4	9	7	15	9	2	2	6	24	8	3	8	1	-	-	0				142	
1979-1980	-	-	16	30	4	64	51	14	10	5	2	8	0	1	3	40	4	-	13	13	0						278	
1980-1981	-	-	9	15	16	9	2	12	14	15	6	11	15	15	22	30	7	9									207	
1981-1982	1	0	2	8	10	7	3	2	20	20	6	6	3	3													91	
Max. Gouge Depth (m)																											Deepest	
1977-1978	0	.1	.1	0	0	.1	0	0	.3	.2	.1	.1	.1	.3	.2	.3	.5	0	0	0	0	.5	.3	.3	0		.5	
1978-1979	.1	.1	.1	.1	.1	0	.1	.1	.1	.2	.4	.2	.1	.1	.1	.1	.2	.1	.2	.2	-	-	0				.4	
1979-1980	-	-	.1	.8	.1	.1	.1	.1	.1	.1	.4	.3	0	.1	.2	.4	.2	-	.3	.3	0						.4	
1980-1981	-	-	.3	.7	.4	.2	.1	.1	.3	.3	.6	.1	.6	.3	.2	.3	.3	.2									.7	
1981-1982	.1	0	.1	.1	.3	.3	.1	.2	.4	.3	.4	.2	1.0	.5													1.0	
Total Disruption Width (m)																											Total	% Dist.
1977-1978	0	18	20	0	0	9	0	0	4	70	3	29	102	92	46	60	37	0	0	0	0	49	24	46	0		609	2.4
1978-1979	8	8	42	59	45	0	3	25	50	24	60	25	6	5	23	101	30	12	33	4	-	-	0				563	2.7
1979-1980	-	-	71	123	14	174	214	31	43	33	31	62	0	10	27	146	21	0	82	82	0						1164	~~6.5~~ 6.1
1980-1981	-	-	30	70	58	36	8	64	62	96	71	51	74	62	105	113	35	40									975	6.1
1981-1982	1	0	10	31	31	29	4	5	58	62	25	42	22	28													348	2.5

Total No. of New Gouges: 845 Deepest New Gouge: 1.0m Total Disruption Width: 3659m Mean Annual Percent Disturbed: 4.0

TESTLINE 2.

Kilometers	0	1	2	3	4	5	6	7	8	9	10	11	12	13	14	15	16	17	18	19	20	21	22	23	24	25		
Water Depth (m)	6.9	10.0	11.4	11.5	12.2	13.3	14.2	14.9	14.4	14.3	15.1	15.4	16.3	17.2	17.9	18.5												
No. of Gouges																											Total	
1977-1978	12	4	1	22	1	30	17	4	23	0	8	13	11	17	7												170	
1978-1979	0	1	25	44	12	1	0	0	20	0	9	0	1														113	
1979-1980	0	0	0	21	0	1	2	1	14	0	2	1	4														46	
1980-1981	2	5	2	25	7	6	2	0	14	7	7	14	19	8													118	
Max. Gouge Depth (m)																											Deepest	
1977-1978	.1	.1	.1	.1	.1	.2	.2	.1	.1	0	.1	.2	.4	.7	.5												.7	
1978-1979	0	.1	.1	.2	.1	.1	0	0	.1	0	.2	0	.1														.2	
1979-1980	0	0	0	.2	0	.1	.1	.1	.2	0	.1	.1	.3														.3	
1980-1981	.1	.1	.1	.1	.1	.1	.1	0	.2	.4	.2	1.4	.3	.3													1.4	
Total Disruption Width (m)																											Total	% Dist.
1977-1978	72	19	3	97	9	134	65	20	50	0	44	58	56	139	60												826	5.5
1978-1979	0	4	97	149	30	3	0	0	53	0	18	0	4														358	2.8
1979-1980	0	0	0	82	0	3	15	3	48	0	4	1	15														171	1.3
1980-1981	11	13	5	121	21	14	4	0	64	28	49	88	88	34													540	3.9

Total No. of New Gouges: 447 Deepest New Gouge: 1.4m Total Disruption Width: 1895 Mean Annual Percent Disturbed: 3.4

Table I. Condensed data from the Appendix, showing annual variations in gouge characteristics and distribution.

calculation of the mean is as follows (Miller and Kahn, 1962):

$$E = \log_b \left(\frac{b^{x_1} + b^{x_2} + b^{x_3} + \cdots b^{x_n}}{n} \right)$$

$$b = \text{log base} = 10$$

When this formula is used to calculate the mean, the average new gouge depth for testline 1, testline 2, and the total study is 18 cm. This value agrees more favorably with the new gouge depth mean (20 cm) determined from other studies of this area (Barnes et al., 1978).

The area of the seafloor disrupted can be considerable over short time spans. The total width of disruption over the course of this study was 5554 m over an average total trackline length of 34 km. This is an average of 37 m/km/year of disruption occurring in the two areas. As with the above gouge characteristics, the largest disruptions occurred in water depths greater than 10 m. In 1980 a maximum of 214 m of disruption occurred in a 1 km segment and was mostly due to scouring of the seafloor during 5 multiplet events. Single gouges are generally responsible for narrow disruptions in the study area.

Most gouges that were formed had no measureable sediment ridge associated with them. This is due in part to the resolution of the fathograms but also to the shallow depth of most gouges, allowing little sediment to be available to form the ridges. The ridges are also most susceptible to errosion by waves, currents and further ice gouging. The shallow water depths of the two areas subject the seafloor to wave and current reworking and, therefore, may also have an effect on the length of time a sediment ridge is in existance. Only 4 ridges of the 384 measured exceeded 50 cm. Mean ridge height was 14 cm with a maximum height of 90 cm.

Gouge length is the most difficult measurement to obtain and we, therefore, have the least data on this characteristic. Some new gouges begin or end off the record while most travel across the entire width of the record. Few gouges begin and end on the sonograph records and these are generally very shallow, narrow, and short. For these reasons, ranges and the mean for this characteristic have not been calculated.

Yearly Variations In New Gouge Characteristics

Although new ice gouge occurrence is ubiquitous in the study area, both consistancy and variation are noted between years and areas. New gouge frequency curves for testline 2 show a yearly consistancy in the peaks of frequency which correlate with the areas and water depths of the shoals (Figure 6). Seaward of the outer most shoal the new gouge frequencies increase rapidly with increasing water depth. On testline 1 new gouge frequency curves do not exhibit consistency in areal distribution other than a general increase in gouge frequency with an increase in water depth and a peak that shows up at 16m depth particularly in the years 1979 through 1981.

Total disruption width in a segment is a function of the number of gouges in that segment (Barnes et al., 1984) and, therefore, the total disruption width curves (Figure 7) reflect the same peaks in the data as the frequency curves (Figure 6). Disruption width curves of testline 1 data

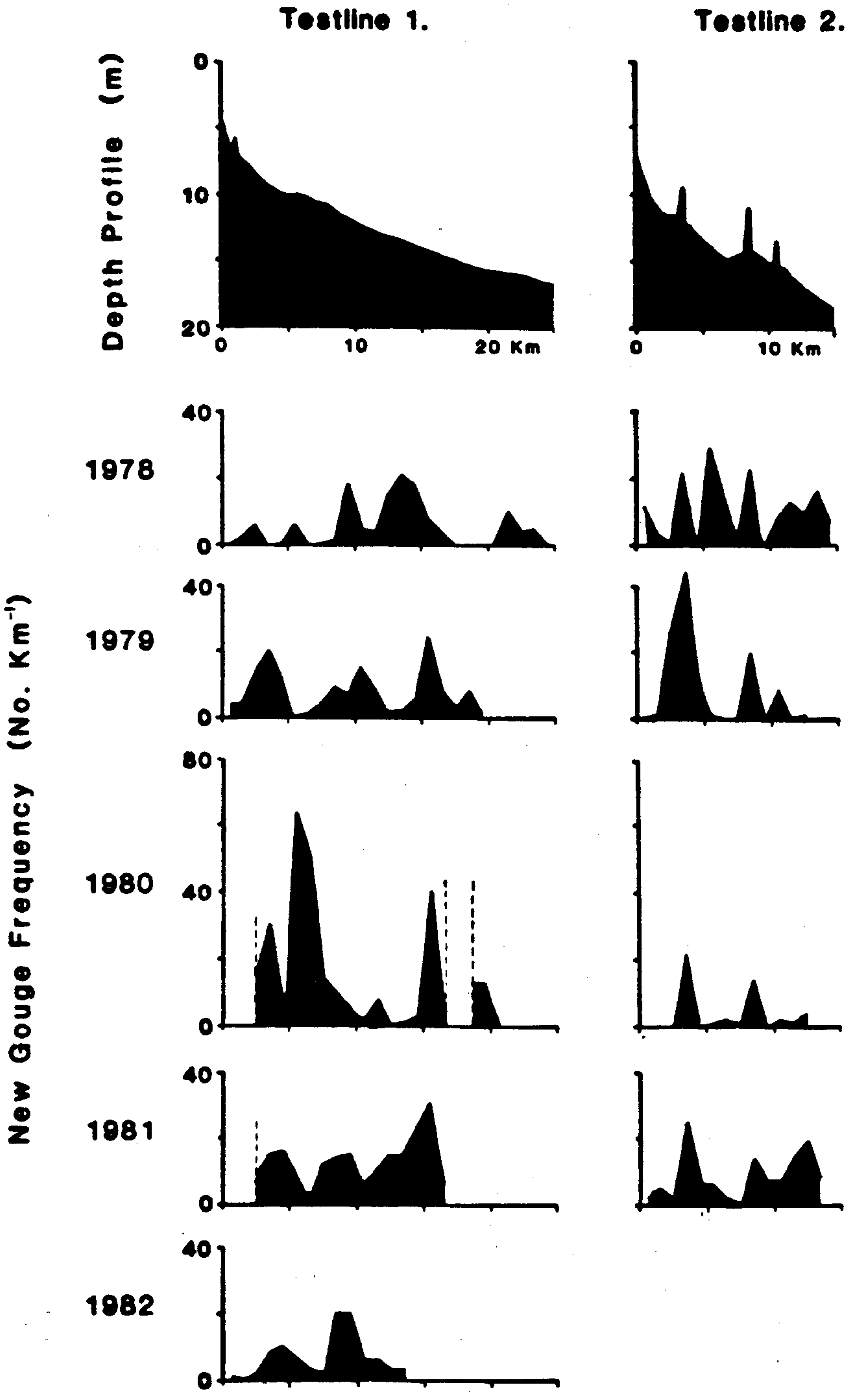

Figure 6. Graph of yearly gouge frequency along both testlines. Note the correspondence of the major peaks of the testline 2 graphs to the shoal locations on the depth profile. In 1978 high frequency gouging also took place between the inner two shoals. Gouge frequency along testline 1 is more variable in its location on the seafloor with very high frequencies often found in shallow water such as occurred in 1980.

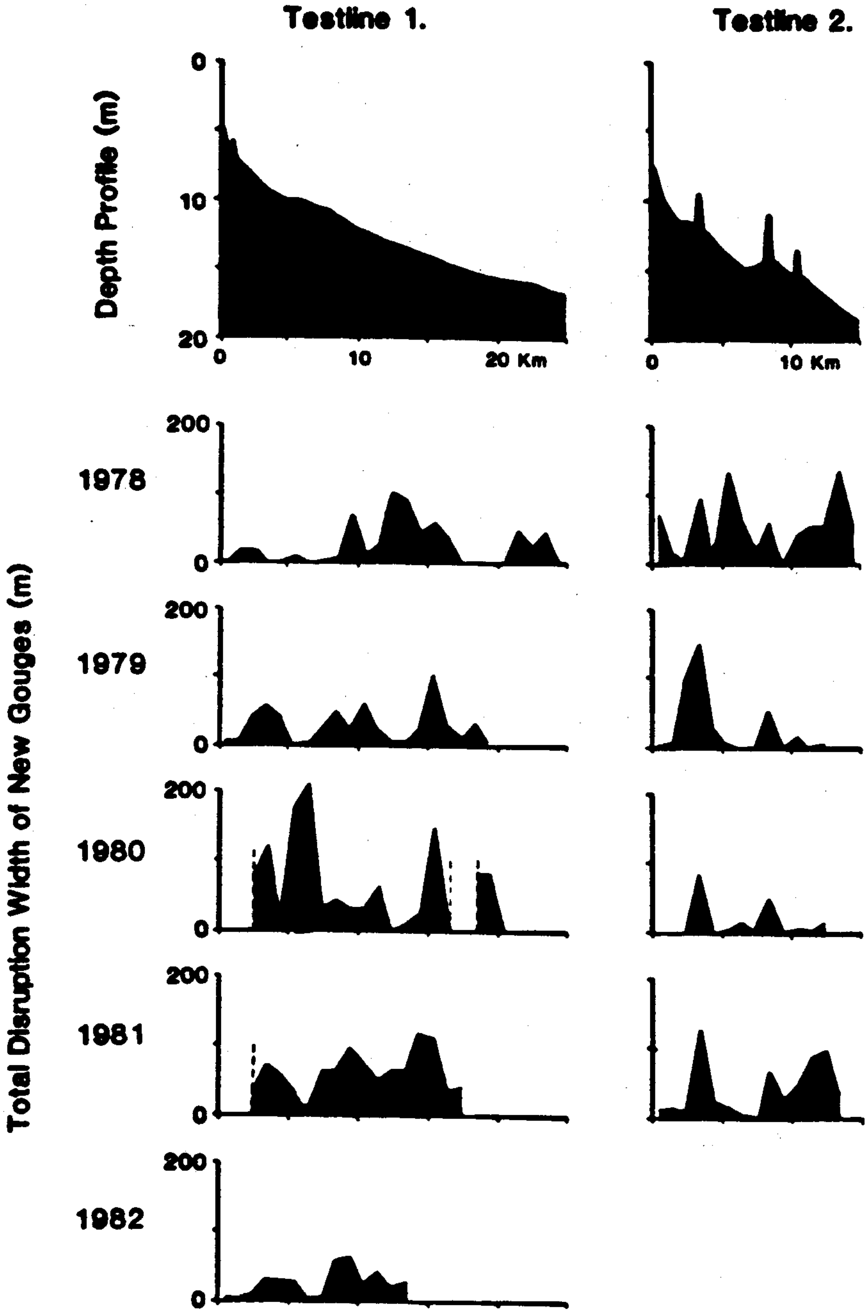

Figure 7. Graph of the total yearly disruption width in each 1km segment along both testlines. Note the similarity of these graphs to those of gouge frequency. Peaks in the disruption values correspond to the peaks of gouge frequency for both testlines indicating a close relationship between the number of gouges created in a segment and the amount of the bottom disturbed by the passing of ice keels through the sediments.

show that disruptions in excess of 100 m/km/year occur in water depths as shallow as 8 m. Testline 2 disruption width curves show that disruptions in excess of 100 m/km/year generally occur on shoal crests or in water depths greater than 11 m. Relatively large disruptions can occur between the shoals as happened between 1977 and 1978 (Figure 7).

The maximum depth of new gouges was determined for each 1 km segment. On testline 1 maximum depths increase with increasing water depth and show a significant increase at a water depth of 10 m (Figure 8). On testline 2, the yearly consistancy of the peaks in new gouge frequency are again noted in the curves of maximum gouge depth. However, although there are peaks inshore of the seaward most shoal of testline 2 these peaks are low values (20 cm or less) and the deepest gouges (>50 cm) occur offshore of the most seaward shoal in 15 m or more of water.

Maximum gouge depth and mean gouge depth for each 1 m water depth interval, averaged over the 5 and 4 years of data, demonstrate the effects of the shoals of testline 2 in controlling the depth of gouging (figures 9 and 10). On testline 1, both the maximum and mean values of gouge depth are greater than those of testline 2 for equivalent water depths. On testline 1, gouges as deep as 70 cm have occurred in water depths as shallow as 8 m and gouge depth averages steadily increase towards deeper water. On testline 2, inshore of 15 m water depth, the deepest gouges found were consistantly 20 cm or less and the mean gouge depth was approximately 10 cm. Seaward of 15 m water depth the mean gouge depths begin to approximate those of testline 1.

Frequency Distributions

Frequency distribution curves of the new gouge depths, widths and ridge heights (Figure 11) fit a negative exponential distribution (Benjamin and Cornell, 1970; Miller and Freund, 1977; Weeks et al., 1981). There are many more small gouges than there are large ones. In studies by Barnes et al. (1984), Barnes and Rearic (in press), and Weeks et al. (1984) the gouge depth distributions of the 'total' gouge population and the 'new' gouge population were also found to be a negative exponential (Figure 12), although gouge depth means were greater (56 cm and 19 cm) than in the present study (18 cm) due to differences in water depths and areas surveyed. Similar gouge distributions were calculated for gouge depths in the Canadian Beaufort Sea by Lewis (1977a,b) and Wahlgren (1979a,b). The deepest and widest gouges and highest ridges of this study do not fit the negative exponential distribution and in fact appear to occur more often than the distribution would call for. Examination of gouge frequency distributions from other studies shows a similar excess at the maximal end of the distributions.

The semilog plots of disruption width frequency vs. water depth and ridge height frequency vs. water depth (Figure 11) are similar in shape to the gouge depth frequency and suggest a negative exponential might also best describe the distribution of this data. Again, as with the gouge depths, the widest gouges and the highest ridges do not fit the distribution. It should be noted that part of this problem may be due to the short time over which the observations were made as it can be seen that there is only one observation for each width interval over 50 m (with the exception of two at 60 m) and each ridge height interval over 50 cm. Figure 11 suggests, therefore, that most gouges are shallow, narrow features having either a very small ridge of excavated material bordering the furrow or, as is often seen on the records, no disernable ridge at all. The most notable problem with attempting to relate the gouge characteristic frequency curves to a negative exponential distribution is the lack of fit in the high value range (gouges >80 cm deep and >50 m wide, and ridges >50 cm high).

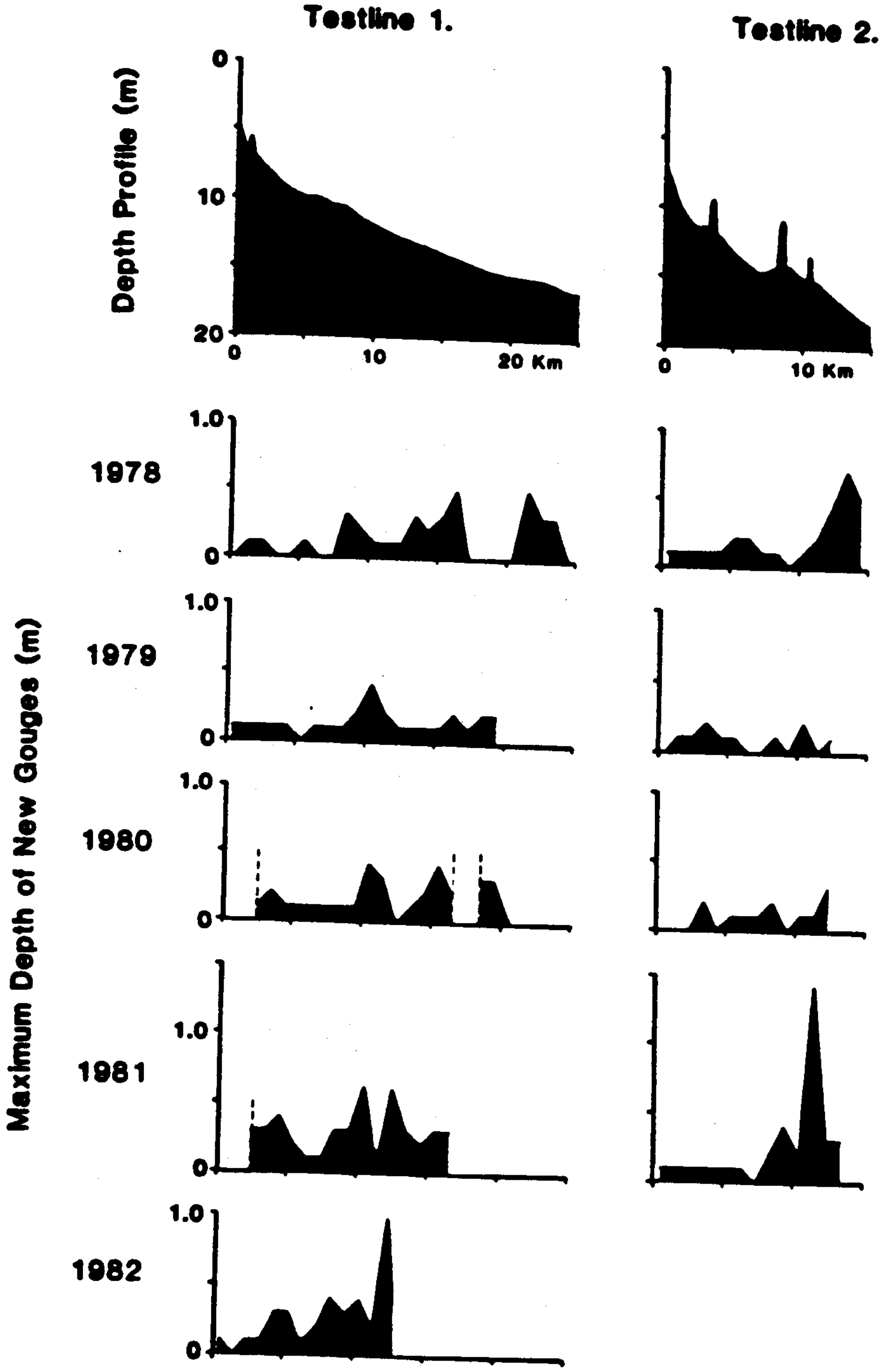

Figure 8. Graph of the deepest gouge in each 1km segment each year. Note that there is no similarity to the graphs of gouge frequency and disruption width. Deep gouges (>50cm) on testline 2 are restricted to areas seaward of the outer most shoal (water depths >15m) while on testline 1 gouges of this depth can occur in water depths less than 10m.

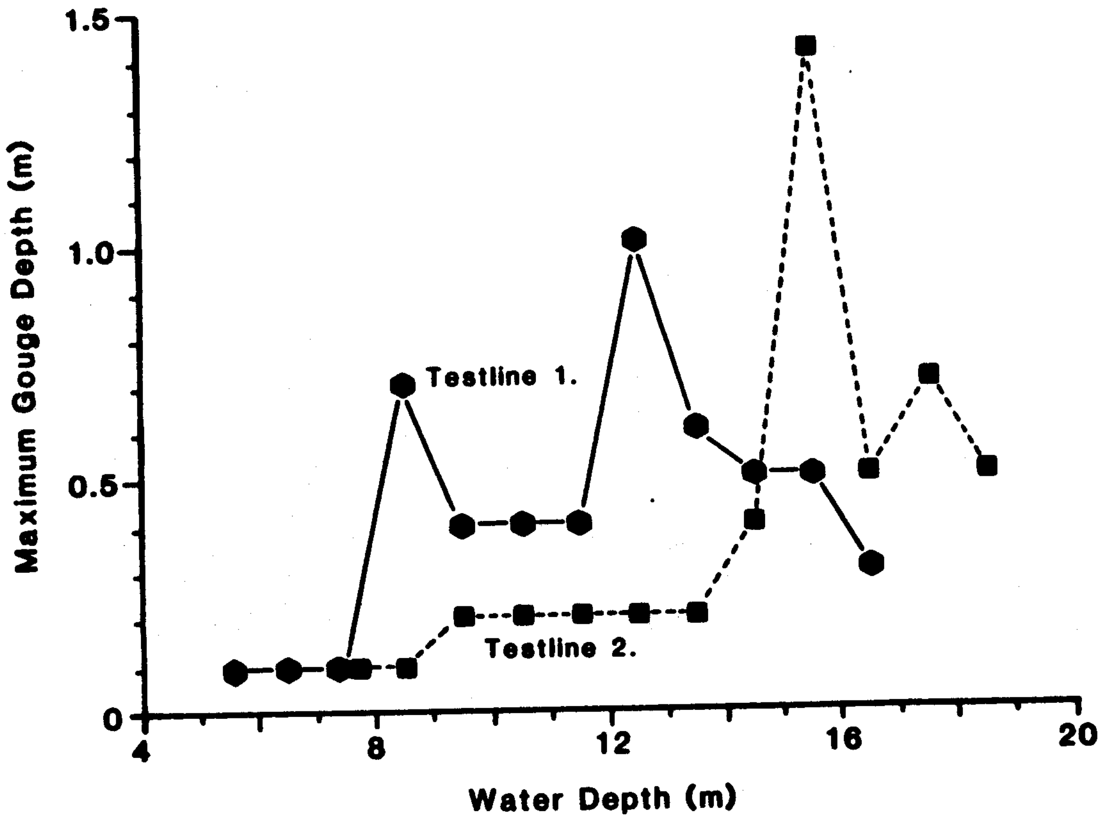

Figure 9. Graph of the deepest gouge found in each 1m water depth interval over the entire course of the study. Again, as in figure 8, deep gouges are restricted to the outer areas of testline 2. Inshore of 15m water depth the deepest gouges found were consistently 20cm or less. On testline 1 deep gouging can occur in shallower water depths (note the 70cm deep gouge in only 8m of water).

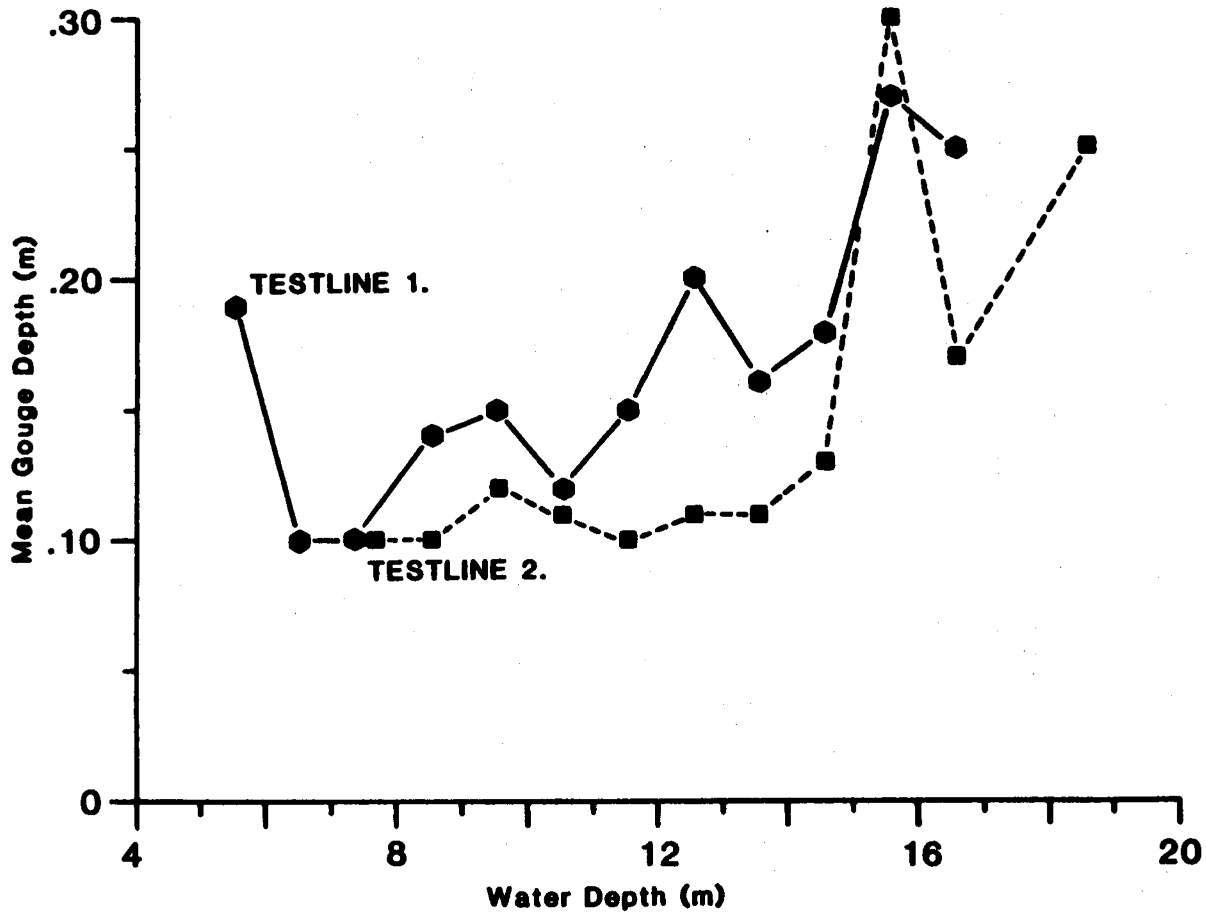

Figure 10. Graph of the mean gouge depth in each 1m water depth interval averaged over the entire course of the study. As with figures 8 and 9, mean gouge depths are very low (about 10cm) on testline 2 inshore of 15m water depth while on testline 1 the mean gouge depths are consistently greater than those of testline 2 for equivalent water depths. In water greater than 15m deep average gouge depths are similar for both testlines.

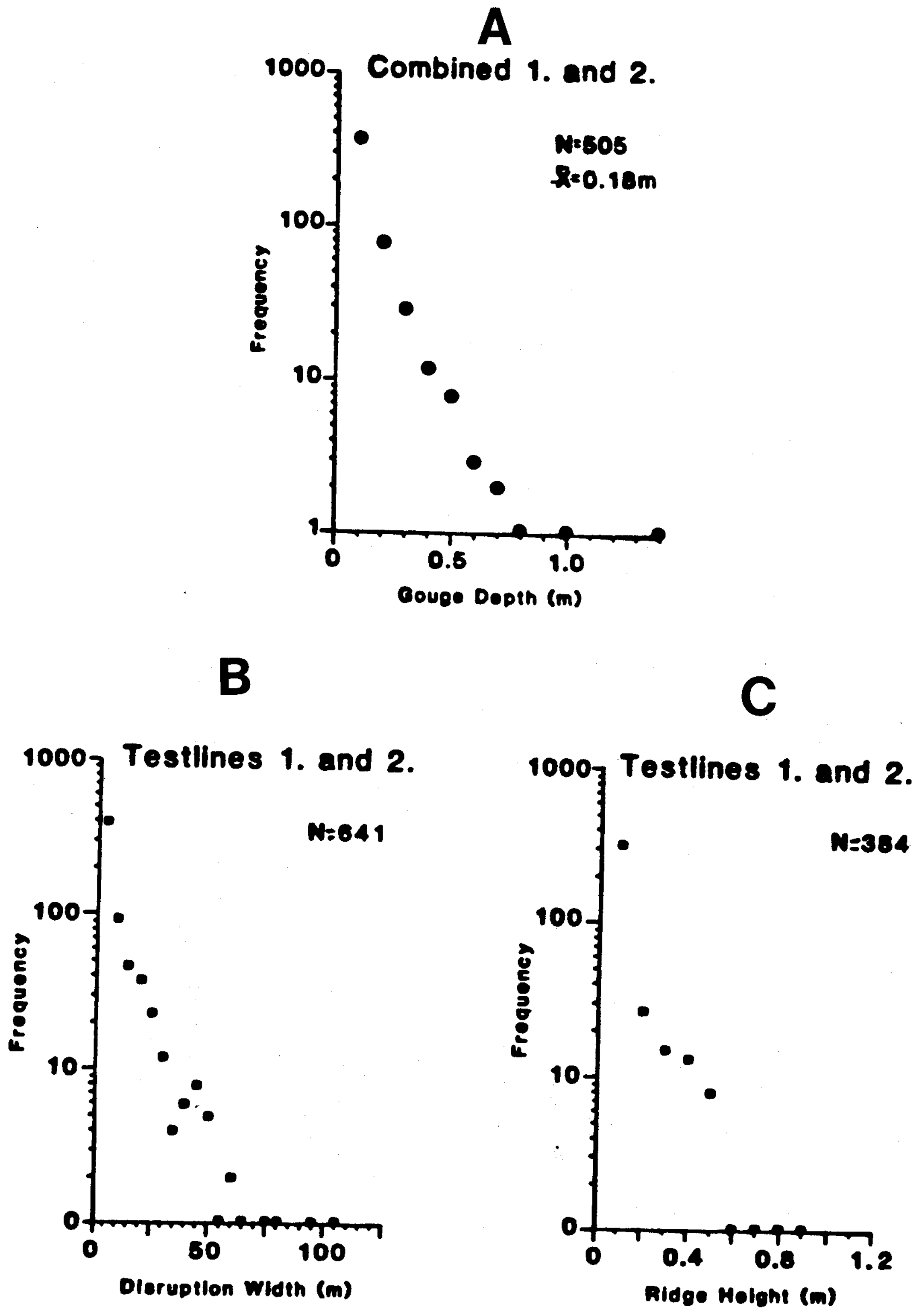

Figure 11. Frequency distributions plotted on similog paper for three gouge characteristics measured in this study; A) gouge depth, B) disruption width, and C) ridge height. Note that the characteristics fall on an approximate straight line indicating a negative exponential distribution. Of special interest are the large values of all three characteristics which do not fit the distribution. The reader is referred to the text for suggestions as to why the fit is so poor for the high end members of the distributions.

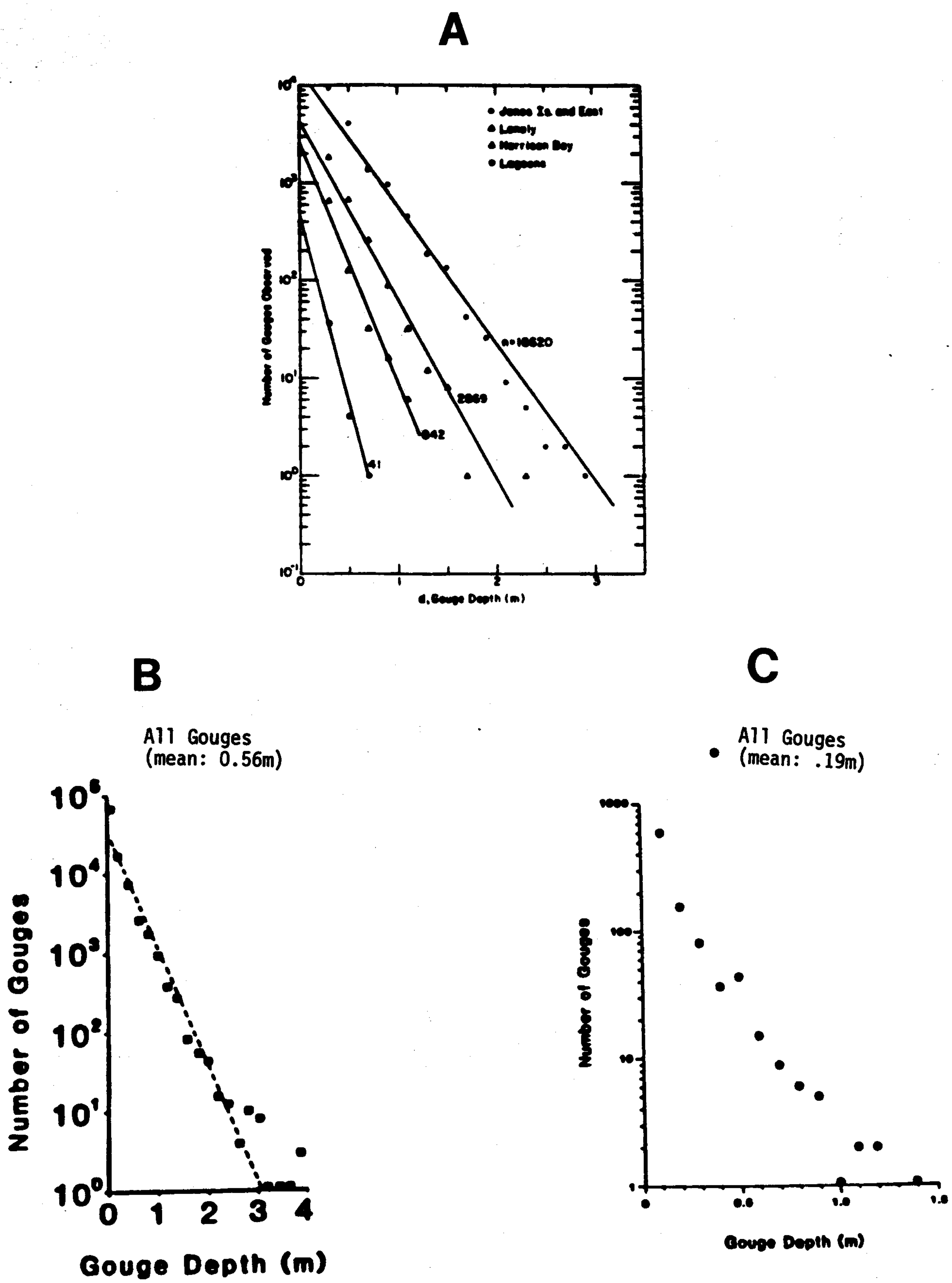

Figure 12. Gouge depth frequency distributions from the studies of A) Weeks et al. (1984), B) Barnes et al. (1984), and Barnes and Rearic (in press). Note that in all these studies, as with the present one, a negative exponential distribution is indicated. The same problem exists in these studies as occurred in the present with the high values failing to fit the distribution. See the text for possible explanations.

Percent Of Seafloor Disrupted

Seafloor disruption by ice gouging can be calculated as a percent of the trackline gouged in any one year. This is accomplished by adding up all the disruption widths (assuming that in the case of gouge width the disruption width is approximately 25% greater) over the length of the trackline and determining what percentage of the total trackline length was gouged.

The amount of seafloor disturbed each year was variable and ranged from a maximum of 6.1% to a minimum of 1.3%. The mean percent of seafloor disruption over the study period was 3.7% (Table II and Figure 13). Mean disruption was simular on both testlines when averaged over the length of the study even though their bottom morphologies are different. Data from Barnes et al. (1978) is included in the plot of Figure 13 as a reference for values calculated from earlier work, although they did not distinguish between disruption widths of multiplets and single gouges. The new mean values that are calculated for seafloor disruption (3.9% and 3.4%) are almost double the 2% value found in the previous studies. Although seafloor disruption percentages exhibit a wide range of values the amount of disruption occurring most often (in 45% of the surveys) is in the 2-3% range (Table II).

Minimum Volume Of Sediment Disrupted

The above discussion was concerned with the area of the seafloor that is being gouged each year. However, it would also be of value to determine the volume of sediment involved in the disruption. This requires the incorporation of gouge depth and length in addition to width measurements. A minimum value for the mean volume of sediment disrupted annually (V) was calculated as follows (Table III). The mean annual gouge depth (X) and mean annual disruption width (Y) were calculated for one meter water depth intervals. The measured length of the gouges was used wherever possible to calculate mean length (Z). The remaining gouges on the sonograph record were assigned a length of >250 m (the width of the sonograph record). For this reason these values represent a minimum length (Table III). The mean values (X,Y,Z) for each one meter water depth interval were multiplied together ($V = X \times Y \times Z$) to give a minimum value of the volume of sediment disturbed within that depth interval.

The following results are calculated for a corridor 0.25 km wide extending through the water depth interval(s) being discussed. On testline 1 an increasing volume of sediment disruption corresponds to increasing water depths from 7 m water depth seaward (Figure 14). Approximately 2000 cubic meters of sediment were disrupted annually in 10 m of water and 7000 cubic meters of sediment in 15 m of water. The slope of this graph indicates that,starting in 10 m of water, for every 1 m increase in water depth there will be a corresponding increase of an additional 1000 cubic meters of disruption per year. If this correspondence holds true, at least to the inner edge of the stamukhi zone, we could expect about 12000 cubic meters of disturbed sediment per year in 20 m water depths. The stamukhi zone values will undoubtedly increase at a greater rate due to the greatly increased intensity of the ice gouge process in this zone (Reimnitz and Barnes, 1974; Barnes and Reimnitz, 1974; Barnes et al., 1984; Barnes and Rearic, in press). On testline 1, in water depths of between 7 and 15 m (a trackline length of about 17 km) a total of about 25000 cubic meters of sediment will be disrupted yearly. The area of the corridor in which this occurs is approximately 4.25 square kilometers. This gives a disruption value of 5800 cubic meters of sediment disturbed per square kilometer.

The shoal dominated profile of testline 2, inshore of 15 m water depth, is disrupted annually on the shoal crests and on their seaward slopes at a rate of about 2000 cubic meters per year in each 1 m water depth interval while in the lee of the shoals volumes on the order of 200-300 cubic meters of sediment are disturbed yearly. Seaward of the shoals in water 15 m or more deep the disruption volumes increase rapidly with increasing water depth and begin to aproximate the slope of the testline 1 graph. In water depths between 7 and 15 m on testline 2 (a trackline length of about 10 km) about 7500 cubic meters of sediment will be disrupted yearly. The area of the corridor in which this occurs is approximately 2.5 square kilometers. This gives a disruption

Testline	Year	Total Disruption Width (m)	Testline Length (x 1000m)	Percent Seafloor Disrupted
1.	1978	609	25	2.4
2.	1978	826	15	5.5
1.	1979	563	21	2.7
2.	1979	358	13	2.8
1.	1980	1164	18	6.~~5~~ /
2.	1980	170	13	1.3
1.	1981	975	16	6.1
2.	1981	540	14	3.9
1.	1982	348	14	2.5
			Means	
1.	5 yrs.	732	18.8	3.9
2.	4 yrs.	474	13.8	3.4

Table II. Annual variations in seafloor disruption for eastern Harrison Bay.

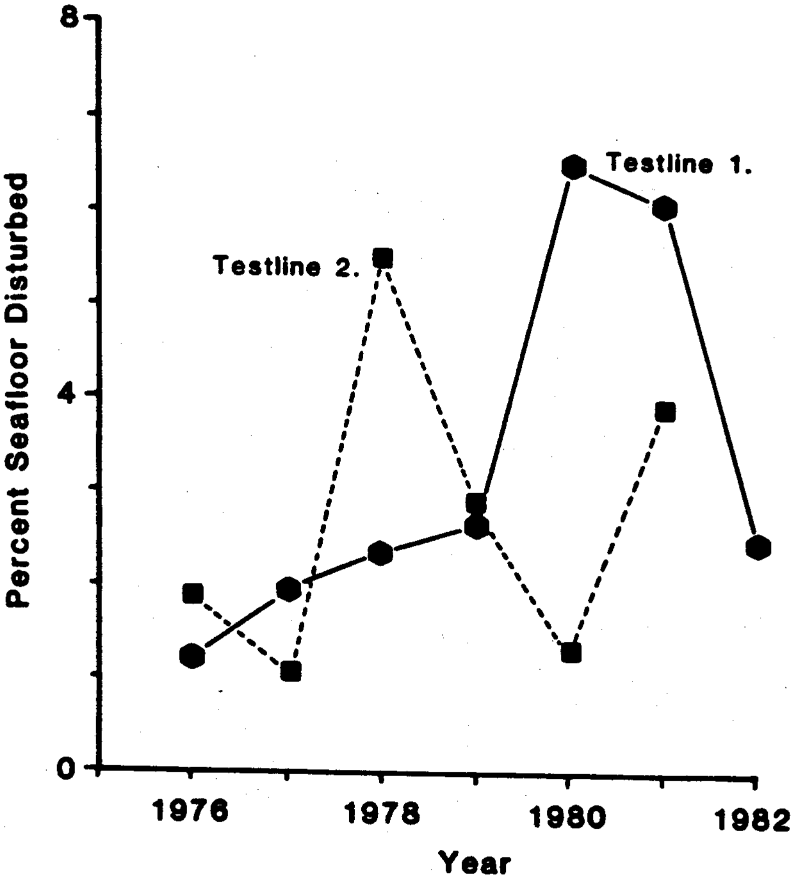

Figure 13. Graph of the percent of the seafloor disturbed each year on each testline. For comparison, the 1976 and 1977 values of Barnes et al. (1978) are included. Seafloor disruption is seen to vary yearly between about 1 and 6 percent on the testlines. Note the apparent inverse relationship between the two testlines in yearly percent disturbed.

Water Depth (m)	TESTLINE 1. X (depth) (m)	Y (width) (m)	Z (length) (m)	V (volume) (m^3)	TESTLINE 2. X (depth) (m)	Y (width) (m)	Z (length) (m)	V (volume) (m^3)
5-6	.19	4	46	35.0				
6-7	.10	2	76	15.2				
7-8	.10	14	>110	> 154.0	.10	15	>250	> 375.0
8-9	.14	49	>204	>1399.4	.10	9	>250	> 225.0
9-10	.15	61	>209	>1912.4	.12	79	>180	>1706.4
10-11	.12	118	>181	>2563.0	.11	26	>142	> 406.1
11-12	.15	87	>233	>3040.7	.10	70	>245	>1715.0
12-13	.20	101	>217	>4383.4	.11	11	>229	> 277.1
13-14	.16	133	>231	>4915.7	.11	27	>216	> 641.5
14-15	.18	164	>236	>6966.7	.13	78	>214	>2170.0
15-16					.30	21	>250	>1575.0
16-17					.17	59	>240	>2407.2
17-18					.20	102	>241	>4916.4

Table III. Volume of disrupted sediment by 1m water depth intervals averaged over the course of this study.

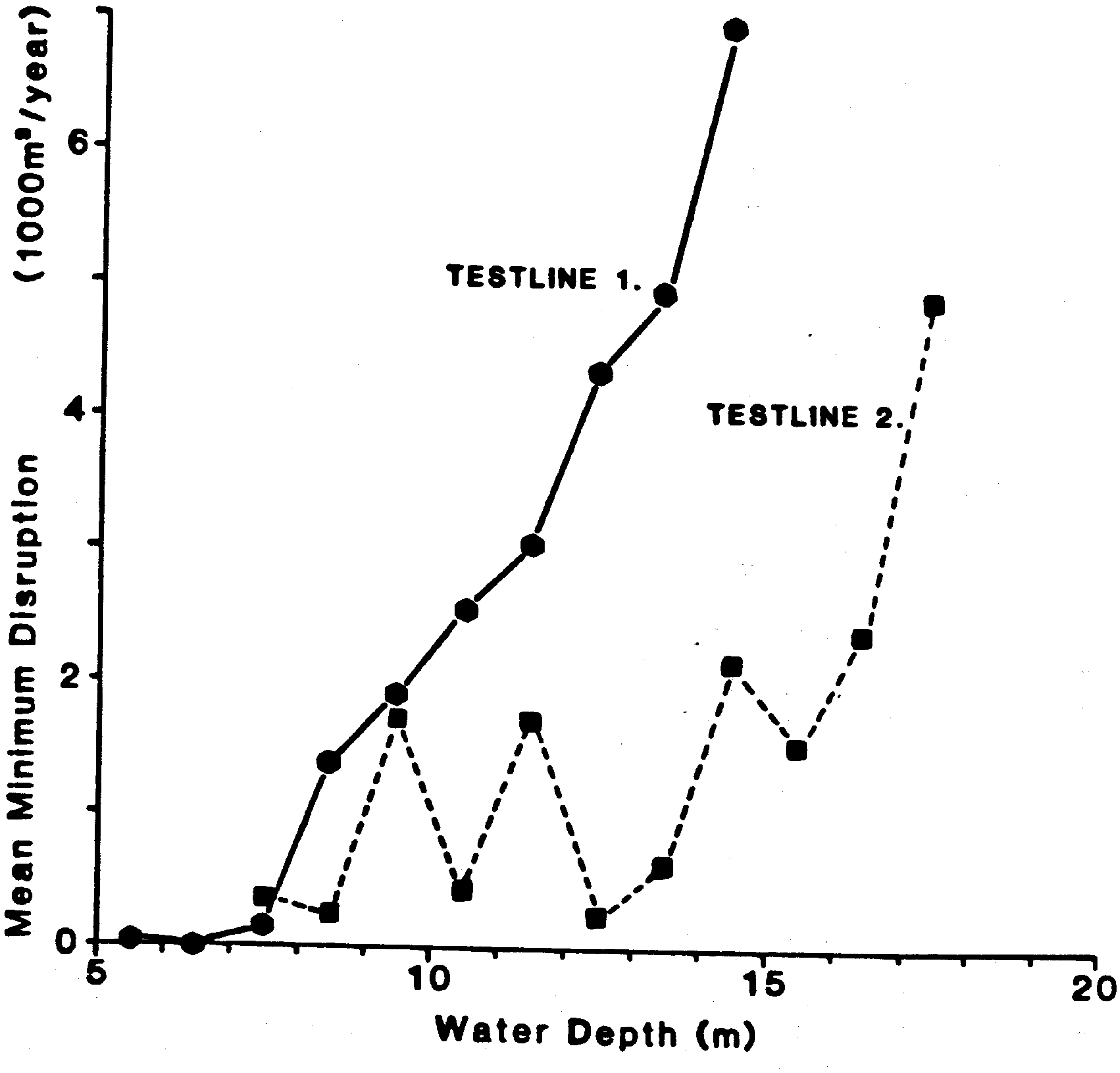

Figure 14. Graph of the average minimum volume of sediment disturbed each year on the testlines in each 1m water depth interval. The influence of the shoals is again noted, as with gouge depth, in that values inshore of 15m water depth are relatively low on testline 2. Testline 1 demonstrates a consistent increase in disruption volume between 7 and 14m water depth of about 1000 cubic meters per 1m of water depth increase.

value of 3000 cubic meters per square kilometer. Of this volume 75% (5500 cubic meters) will occur in the vicinity of the shoals. An additional 7500 cubic meters is disrupted between water depths of 15 m and 18 m (a corridor length of about 5 km). This gives a disruption value of 6000 cubic meters per square kilometer, similar to the value determined for testline 1 in shallower water depths. On testline 2, in water depths of 17 m, 5000 cubic meters of bottom sediments can be disrupted annually while on testline 1 this volume can be disrupted in water depths as shallow as 13 m.

New Gouge/Old Gouge Ratios

The number of new gouges in relation to the total gouge population at the time of survey could be important as a tool for determining relative infilling rates and length of gouge life span on the seafloor. If we compare two areas having equal yearly disruption rates from gouging and we determine that the new gouge to total gouge ratio is higher at one site than at the other then it could imply that infilling occurs at a higher rate at this site.

All the gouges observed on the sonographs were counted and the percent of new gouges of this total was calculated (Table IV). Because of differences in record quality between years the number of new gouges when added to the previous years total did not equal the current years total as might be expected. The same problem was also noted in a study by Barnes et al. (1978). Ideally, on a yearly basis, this should not affect the ratio values because the quality of the records will equally affect both old and new gouge resolution.

On testline 1 new gouges make up 8.6% to 21.1% of the total number of gouges observed. On testline 2, 49.1% to 76.6% of the total gouge population was new. New gouges on testline 1 averaged 14.8% of the total and on testline 2 averaged 59.4%. Apparently, infilling of the older gouges on testline 2 is occurring at a greater rate than on testline 1 particularly since the average rate of new gouge production on testline 2 (3.4%) is not as great as that of testline 1 (3.9%).

New Gouge Orientations and Terminations

The orientation of an ice gouge depicts a track along which ice motion occurred. After delineating the track we can determine the probable direction of approach and estimate what areas of the shelf may be more susceptible to ice gouges and which areas, such as the lee of shoals, may offer protection from gouging ice keels.

Orientations were taken on all new gouges and plotted as rose diagrams (Figure 15). The orientation to the ships track was measured and then the orientation to true north was calculated by correcting for the ships course. Multiplet orientations were counted as only one occurrence of that orientation, and as such, the diagrams are a record of the orientation of ice motion during ice gouging events.

On testline 1 the orientations of new ice gouges are essentially east-west and subparallel to the bathymetry contours. Previous studies of other areas of the shelf have documented the parallel orientation of ice gouges to bathymetry contours when unaffected by seafloor morphology or other factors (Barnes et al. 1984). Testline 2 orientations are generally northwest-southeast and more variable than those of testline 1. This is possibly due to the influence of the shoals deflecting the motion of the ice canopy during winter and interfering with the normal flow of the sea-ice regime.

Gouge orientations tell us that the ice motion was along a particular track but do not give us actual direction of motion. Gouge terminations indicate the direction the ice keel was traveling during its disruption of the seafloor.

Testline	Year	Total Number of Gouges	Total Number of New Gouges	Percent New Gouges
1.	1978	1484	127	8.6
2.	1978	346	170	49.1
1.	1979	886	152	17.2
2.	1979	167	113	67.7
1.	1980	1551	278	17.9
2.	1980	85	46	54.1
1.	1981	979	207	21.1
2.	1981	154	118	76.6
1.	1982	894	91	10.2
		MEANS		
1.	all	1159	171	14.8
2.	all	188	112	59.6

Table IV. Percent new gouges of the total gouge record observed on the seafloor in eastern Harrison Bay. We would expect the sum of the new gouges and the previous year's total gouges to equal this year's total gouge count; however, because of infilling of older gouges, record quality, and deviation from course this is rarely the case. Barnes et al. (1978) noted the same problem in their studies of this area.

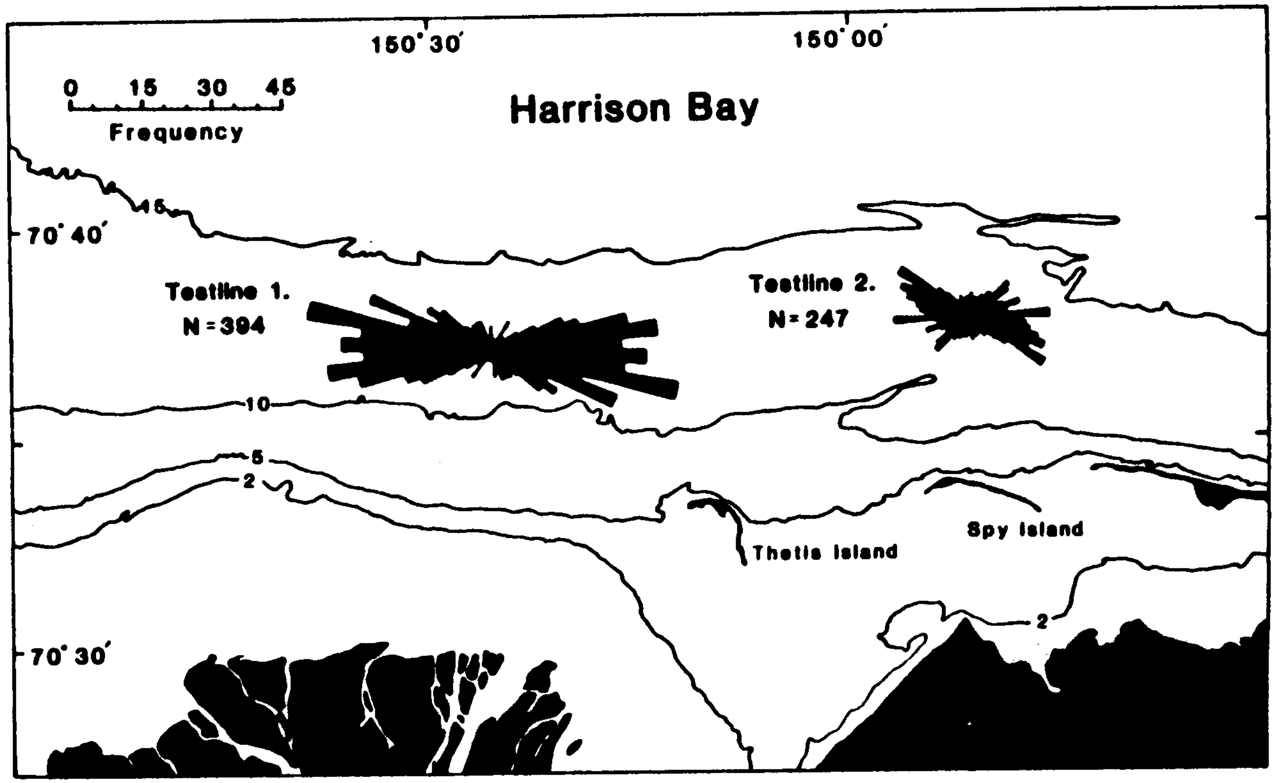

Figure 15. Gouge orientations plotted as rose diagrams for the two testlines. Note that the orientations of testline 1 are subparallel to the bathymetry contours with an approximate east-west orientation. Orientations on testline 2 are more nw-se indicating the possible influence of the shoals on the direction of ice movement.

Gouge terminations for both testlines were plotted as rose diagrams for analysis of direction of ice keel movement during formation of a gouge (Figure 16). Only 0.05% of the 1292 gouges terminated on the sonographs. Of the 64 new gouge terminations 34 (53%) terminated in a southeast direction. Westerly movement of the ice keels is also indicated in the rose diagrams by the termination of 15 gouges (23%) in a southwest to west direction. Fifteen new gouges (23%) terminated in either an offshore or northeasterly direction.

Gouge terminations, when compared by year, indicate that ice approaching from the northwest generally creates gouge terminations with only one incision (Figure 17). This type of termination dominated the data set for four of the five years of comparisons. In the 1979-80 comparison it was noted that the gouge terminations were mostly multiplet in nature and the ice creating these terminations approached from the northeast.

New Gouge Multiplets And New Gouge Events

Multiplet gouging creates a distinguishable gouge pattern formed by several downward projecting keels (Figure 1). Multiplet gouging itself can fall into two catagories depending on the number of incisions and their depths. Multiplets with only a few incisions and deeper than 0.5 m are considered to have been formed from multiyear ice and are possibly related more to the processes involved in the formation of single gouges. Multiplet gouges having more than 3 to 4 incisions and depths less than 0.5 m are generally considered to be the result of first year pressure ridge gouging (Barnes et al., 1984). As a gouge event, the second type of multiplet is responsible for the widest disruption of the seafloor and greatest number of gouges formed. Table V shows that although only 28% of all gouge events are shallow multiplet events at least 65% of all ice gouge furrows and 67% of the disruption is accounted for by these events. (Table VI)

DISCUSSION

The data in this study are the result of the measurement of horizontal and vertical sediment transport caused by the passing of a grounded ice keel through the bottom sediments. Determining the volume and direction of transport will help resolve the role of ice gouging in sediment transport on the Beaufort Sea shelf during winter. Hydraulic influence on the environment is minimal during the 9 months of winter ice cover and sub-ice ocean currents play only a minor roll, if any, in winter sediment transport (Barnes, 1981; Matthews, 1981; Barnes and Reimnitz, 1982).

The results of this study need to be placed in perspective with previous studies of the same area (Reimnitz et al., 1977; Barnes et al., 1978; and Table VII). The differences noted in the gouge character values and in particular the higher rates of reworking are considered to be the effects of better record quality in recent years, allowing a more accurate count of the small gouges. Reimnitz et al. (1977) noted that only disruptions from gouges 20 cm deep or greater were used in estimating their rates of reworking by ice. Barnes et al. (1978) observed in their study an increase in record quality over previous study records. A further increase in record quality is noted in the present study and ice gouges less than 20 cm were routinely observed.

Frequency Distributions

The frequency distribution of ice gouge depths, widths and ridge heights is a negative exponential and similar to that found in previous studies (Barnes et al., 1984; Barnes and Rearic, in press; Weeks et al., 1984). There are many more small gouge depths, gouge widths and ridge

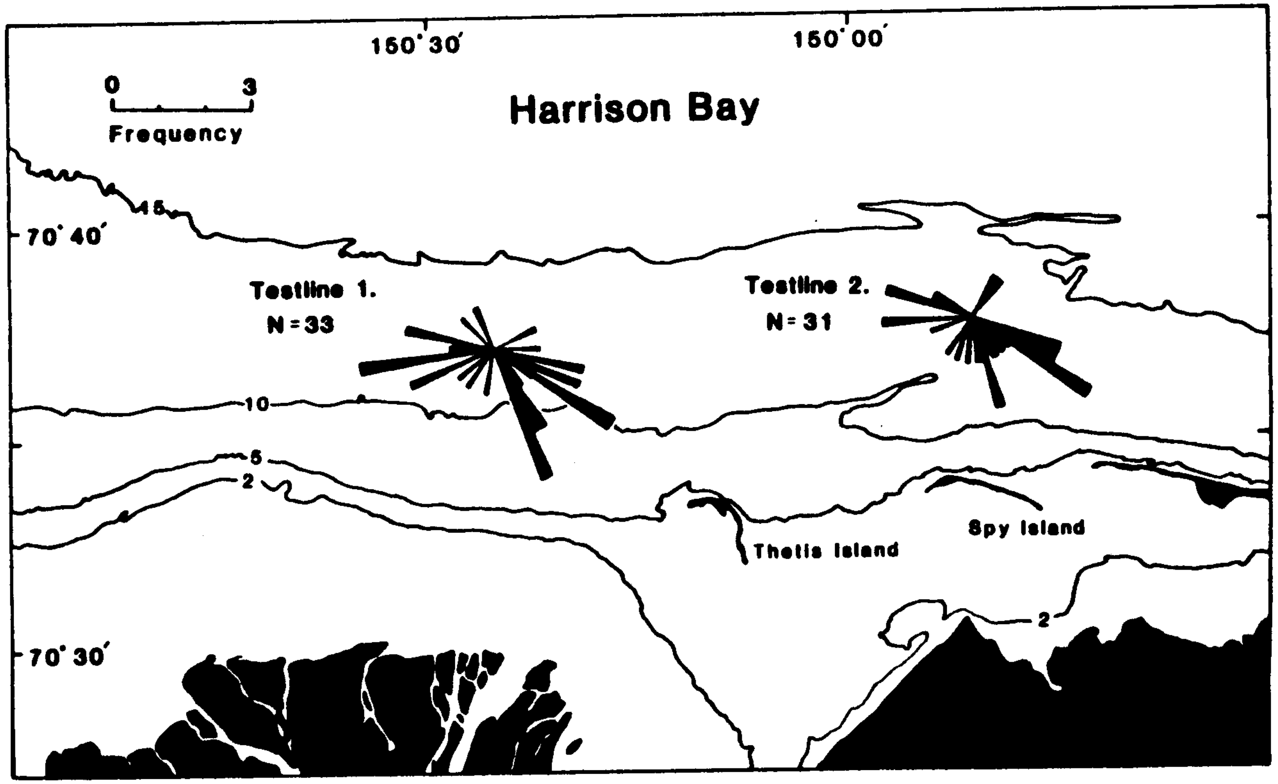

Figure 16. Gouge terminations plotted as rose diagrams for the two testlines. Note the similarity between the two testlines with the dominant trends either onshore in a southeasterly direction or along shore in a westerly direction. Although gouging is believed to be an upslope process some gouges are seen to move in an offshore direction. See text for possible explanations.

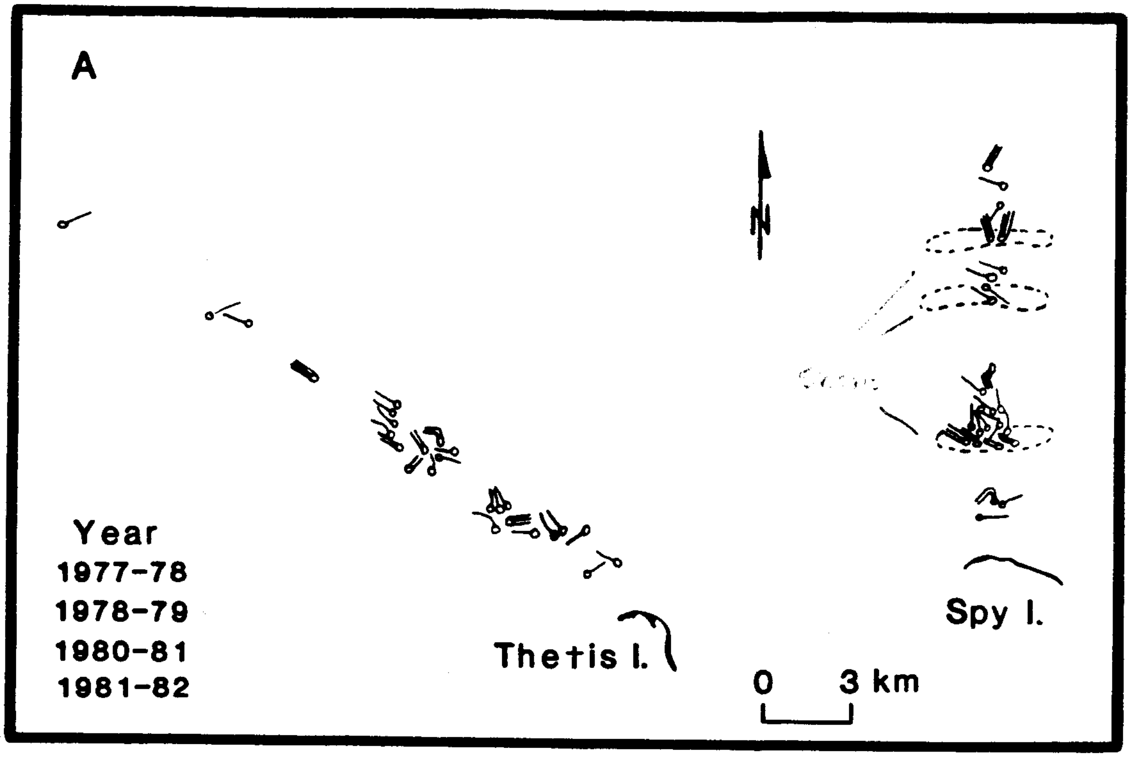

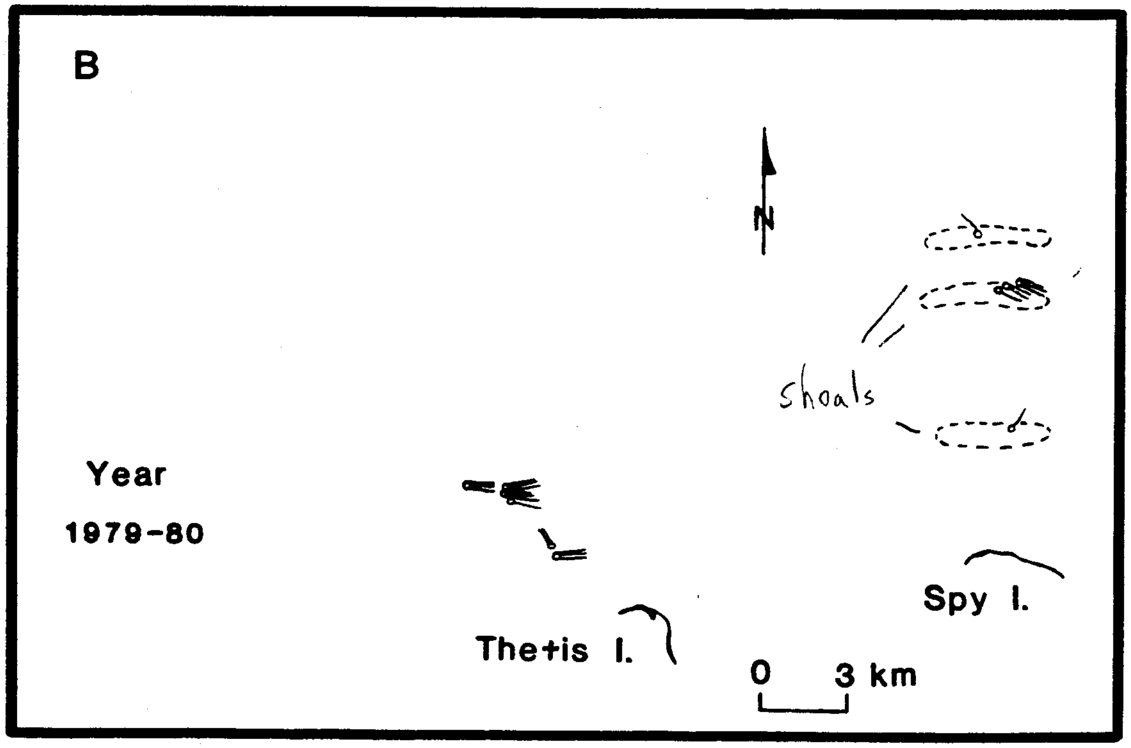

Figure 17. Gouge terminations by years. (A) Most gouges in the years shown approached from the northwest and terminated in single incisions. (B) Most gouges in the year shown approached from the northeast and produced multiplet terminations.

Testline	Year	Single Gouge Events	Multiplet Gouge Events	Percent Multiplet Events	Number of Gouges From Single Events	Number of Gouges From Mult. Events	Percent of Gouges From Mult. Events
1.	1978	24	25	51	24	103	81
2.	1978	61	24	28	61	109	64
1.	1979	59	18	23	59	92	61
2.	1979	24	12	33	24	89	79
1.	1980	34	38	53	34	243	88
2.	1980	22	5	19	22	24	52
1.	1981	93	35	27	93	114	55
2.	1981	87	12	12	87	31	26
1.	1982	56	13	19	56	35	38
				TOTALS			
1.	all	266	129	33	266	587	69
2.	all	194	53	21	194	253	57
Both	all	460	182	28	460	840	65

Calculations are based on 1292 new gouges from 642 new gouge events.

Table V. Testline comparisons between multiplet and single gouge events and the number of new gouges accounted for by the events.

TOTAL DISRUPTION WIDTH (m)

	TESTLINE 1.		TESTLINE 2.	
YEAR	Multiplet	Single	Multiplet	Single
1978	512	97	602	221
1979	383	180	292	66
1980	1004	160	100	70
1981	567	408	201	339
1982	146	202		
Mean	522	209	299	174
Percent of Total	71	29	63	37

Table VI. Comparison of the amount of seafloor disruption accounted for by multiplet and single gouges.

	survey line length (km) TL1	survey line length (km) TL2	number of new gouges TL1	number of new gouges TL2	maximum gouge depth (cm) TL1	maximum gouge depth (cm) TL2	mean gouge depth (cm) TL1	mean gouge depth (cm) TL2	total gouge width (m) TL1	total gouge width (m) TL2	percent of seafloor disturbed TL1	percent of seafloor disturbed TL2
Reimnitz et al (1977)												
1973-1975	16	--	11	--	75	--	*37	--	263	---	1.9	---
Barnes et al (1977)												
1975-1976	16	16	39	41	120	80	31	21	161	268	1.2	1.9
1976-1977	26	18	63	42	60	40	19	12	271	169	1.9	1.1
Rearic (this study)												
1977-1978	25	15	127	170	50	70	17	14	609	826	2.4	5.5
1978-1979	23	13	142	113	40	20	11	11	563	358	2.7	2.8
1979-1980	21	13	278	46	40	30	15	11	1164	171	6.~~5~~1	1.3
1980-1981	18	14	207	118	70	140	18	16	975	540	6.1	3.9
1981-1982	14	--	91	--	100	--	17	--	348	---	2.5	---

* - Note: This value comes from the raw data. Gouges less than 20cm deep on the 1973 record were unresolvable, while on the 1975 record they were easily resolved. Reimnitz et al. (1977) did not use gouges less than 20cm deep in their calculations but estimated that if the smaller gouges were included in the calculations the mean gouge depth would be in the 20cm range.

Table VII. Gouge characteristic comparisons between three studies of the same area in eastern Harrison Bay.

heights than large ones (Figure 11).

The negative exponential distribution, however, fails to fit the extreme high values in this study and in all previous studies. The very largest values (gouges >80 cm deep and >75 m wide and ridges >50 cm high in the present study) do not fit this distribution. In most calculations there are more large gouges on the seafloor than the distribution would account for. Weeks et al. (1984) ascribed this lack of fit to the short time span of ice gouge record that is represented on the seafloor. Infilling of gouges from storms such as occurred in the fall of 1977 (Barnes and Reimnitz, 1979) may occur at short enough time intervals that the occasional deep and/or wide gouge may survive while most of the shallower/narrower gouges are obliterated before a true representative distribution can accumulate on the seafloor. Another possible explanation may be that there are two distributions contained in the data. First year ice (pressure ridges) may account for numerous shallow gouges while the deepest features are created by older, more consolidated ice keels and, therefore, fail to fit the same distribution.

Gouge depth distributions vary across the shelf (Figure 12). In deeper water (the stamukhi zone) there are fewer shallow gouges (Rearic et al., 1981) while in the shallow waters (<20 m) of the present study very few deep gouges were found (Figure 11). In other words, there may be an inshore distribution containing many shallow gouges and a few large gouges and an offshore distribution containing many relatively large gouges and fewer small gouges.

The sea ice environment differs between the offshore and inner shelf. Inshore, ice keels reaching the seafloor are smaller and will leave shallow, narrow gouges in their wake while offshore, in the stamuki zone, many large, competent ice keels are available for gouging. In the offshore areas one deep, wide gouge can obliterate many smaller gouges during one gouge event leaving a trough that is too deep for many of the shallower keels to reach. This effectively limits the area of seafloor available for creation of small gouges.

Maximum Depth of Gouging

The return interval for deeper gouges (>1 m) can be calculated. Barnes et al. (1978) in a 3 year study of new gouges formed in the same area between 1975 and 1977 noted only one new gouge on testline 1 in 1976 that was >1 m deep; none were noted on testline 2 during this period. In the present study one gouge deeper than 1 m was found on each testline. By combining these data a return interval of about 6 years is calculated for gouges greater than 1 m deep. At this rate, in water depths of between 10 and 16 m, the seafloor could be reworked to a depth of 1 m in about 800 years. In 20 years of surveying this environment only 6-8 new gouges >1 m deep will occur. When this number is compared to the more than 5000 new gouges that would be formed over the 20 year period only 0.1 - 0.2% of the new gouges would be >1 m deep.

The return interval can also be calculated as kilometers of trackline covered before a gouge less than one year old and greater than 1 m deep is encountered. Data from Table VII indicates that Barnes et al. (1978) found 1 new gouge greater than 1 m deep in 76 km of trackline coverage. In this study 2 new gouges >1 m deep were found in 156 km of trackline, an average of one every 78 km. Combining the data from both studies we can estimate that in eastern Harrison Bay and in water less than 18 m deep, for every 77 line kilometers of seafloor one gouge greater than 1 m deep will be plowed each year.

Figures 8 and 9 describe the distribution of maximum gouge depths with respect to water depth. Both figures suggest a general increase in maximum gouge depths with an increase in water depth. This seems reasonable when we consider that there are larger ice keels available in deeper water to produce the deeper gouges. A survey of data from other recent ice gouge studies (Barnes et al., 1978; Rearic et al., 1981) as well as the data from this study (Table I) suggests that there may be a maximum depth to which gouging can occur at any given water depth (Table VIII).

gouge depth (m)	water depth (m)	percent of water depth (%)	
0.7	8.7	8.0	Present Study
1.0	12.3	8.1	" "
1.4	15.8	8.9	" "
1.2	13.2	9.1	Barnes et al (1978)
1.8	19.0	9.5	" "
3.8	37.5	10.1	Rearic et al (1981)
4.0	36.2	11.0	" "
4.0	31.4	12.7	" "
	Mean = 9.7%		

Table VIII. The deepest gouges and the water depths they were found in from 3 studies in eastern Harrison Bay and on the Beaufort Sea shelf, Alaska.

X - Current Study B - Barnes et al. (1978) R - Reimnitz et al. (1977)

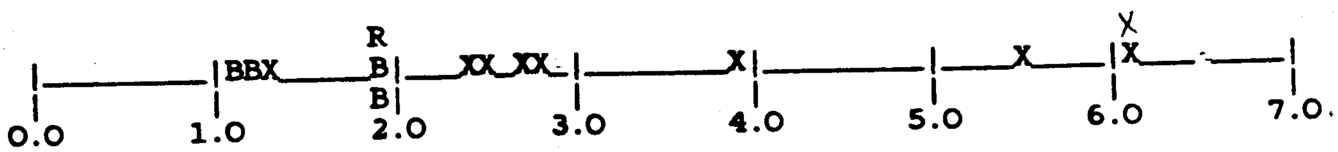

PERCENT DISTURBED

Mean of all studies = 3.2% (seafloor disruption per year)

Figure 18. Plot of the disruption percentages from the present study and that of Barnes et al. (1978) and Reimnitz et al. (1977).

These data show that in any given water depth the maximum gouge depth will be approximately 10% of the water depth (±2%) at least to water depths of about 40 m. However, in areas sheltered by shoals this value will be in the range of only 2-3% of the water depth. This occurs because the larger ice keels capable of deeper gouging are intercepted by the shoals before they can ground on the shelf inshore of the shoals.

Seafloor Disruption

Previous studies have shown that approximately 2% of the seafloor is reworked yearly by sea-ice (Barnes et al., 1978). This is probably the low end of the yearly reworking rates (Figure 18). Rates as great as 6.1% per year were noted during the current study and rates >5% were calculated for 3 of the 9 yearly data sets, although many values are in the 2-3% range and agree favorably with the earlier studies (Figure 18). The approximate doubling in mean rate of seafloor disruption from the 2% of earlier studies to 3.7% in the present study also points out the year to year variability in the ice gouge process.

Barnes et al. (1978) developed a formula to determine the fraction of seafloor disrupted over time (Figure 19). The formula incorporates the concept of proportional replow of previously gouged areas of the seafloor. This assumes that each year new gouges are proportionally divided between ungouged and previously gouged areas. A description the method for calculating this curve can be found in Barnes et al. (1978). The formula is as follows:

$$G_T = 1 - (1-k)^T$$

where:

G_T = *Fraction of the seafloor impacted after T years*

T = *Time in years from an arbitrary* T_o *initiation of new gouging*

k = *Fraction of the seafloor impacted in 1 year*

Using the data from the current study the proportional curve indicates less time is required to gouge the seafloor. From the study of Barnes et al. (1978) the amount of seafloor disturbed in eastern Harrison Bay after 10, 20, 50, and 100 years is 13, 25, 52, and 77 percent. Almost doubling the disruption rate from 2.0 to 3.7 percent increases the amount of seafloor impacted for these same time periods to 32, 52, 84, and 98 percent (Figure 19). The change is considerable as for example the time needed to rework 50% of the seafloor drops from 50 years to only 20 years. Essentially the entire seafloor (98%) is reworked every 100 years to an average depth of 18 cm with most areas reworked many times during this period.

Effects Of Seafloor Morphology On Ice Gouging

Although ice gouges may occur anywhere along either testline, the shoals exhibit some control of gouging on testline 2 (Figures 6, 7, and 8). The peaks in the graphs of the gouge data for testline 2 are a result of the high impact rate on shoal crests due to positive relief of the shoals. Inshore of the seaward most shoal the peaks in the data curves do not reflect high volumes of

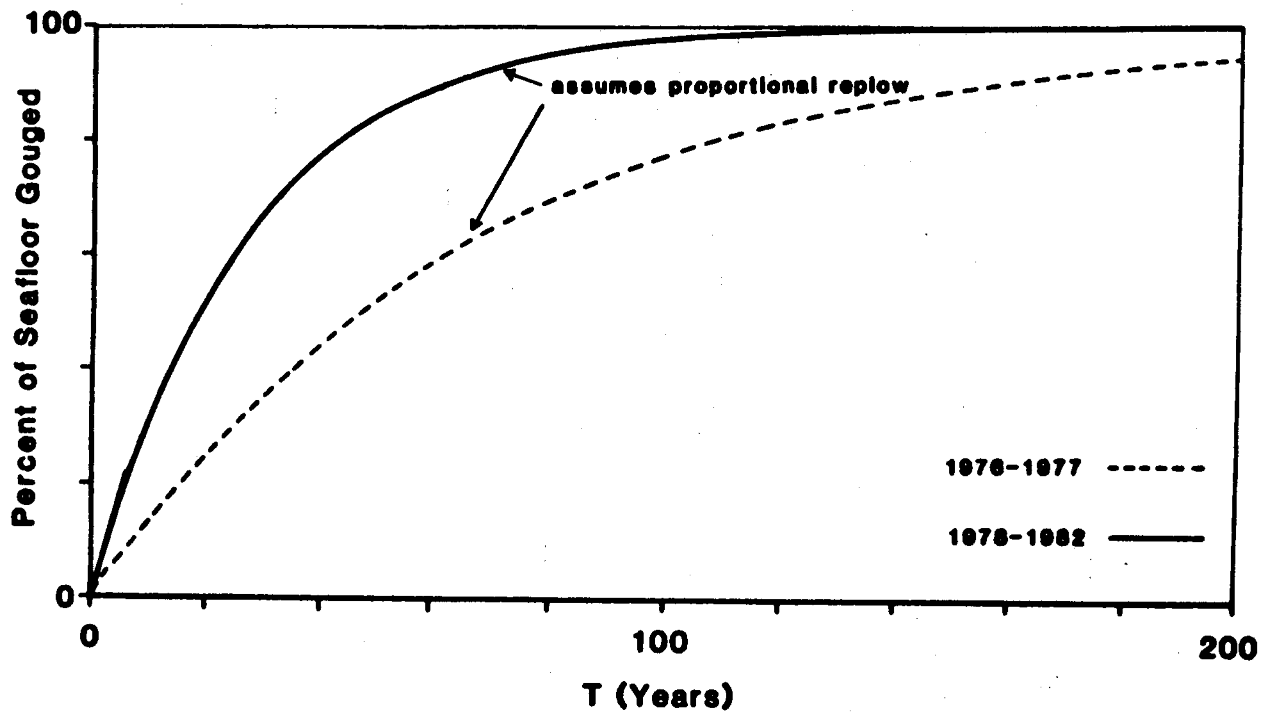

Figure 19. Plot of the percent of seafloor gouged over time from Barnes et al. (1978). The plot is from a model considering yearly replow of previously gouged areas as well as non-gouged areas. The increased percentages of gouging with time determined from this study indicate that the entire seafloor (98%) could be reworked in about 100 years while in 50 years there is still considerable gouging of the bottom (about 85%). Figures from the curve of Barnes et al. (1978) indicate values on the order of 80% and 55% for these same time spans.

sediment disruption (Figure 14) because the deepest gouges occur offshore and these gouges apparently have the greatest affect on the volume of sediment disrupted on testline 2. The mean gouge lengths and widths remain fairly constant throughout the water depth intervals. The shelf inshore of the seaward most shoal on testline 2 can be subjected to a high frequency of gouging but is apparently protected from ice capable of deep gouging.

The inner shelf (water depth <15 m) of testline 1, not having the protection of the shoals, can be subjected not only to high frequency gouging (50+ gouges/km) but also to deep gouging (>.5 m) of the sediments. As the water depth increases on the inner shelf so do the values for all the volume parameters (mean gouge length, width and depth) leading to higher disruption volumes for equivalent water depths when comparing testline 1 to testline 2.

Orientations, Terminations, And Sediment Transport

On a smoothly sloping bottom the movement of ice keels parellels the coast and bathymetric contours (Barnes et al., 1984; Barnes and Rearic, in press). In the present study, the gouges occur on a gently sloping seafloor and are essentially east-west, parallels the bathymetric contours, although the shoals of testline 2 affect the movement of sea-ice in their vicinity (Barnes et al., 1978; Reimnitz and Maurer, 1978). Barnes et al. (1978) observed that gouge trends on testline 2 were northwest-southeast on the outer parts of the testline and northeast-southwest on the inner part. In the present study it was found that about 76% of the gouge directions measured (gouge terminations) were in the southeast (53%) or southwest (23%) quadrants with only 23% divided between the two northern quadrants. Using these figures as a base for estimating sea-ice movement in the nearshore environment, most sea-ice would seem to be approaching the coast from the northwest through northeast quadrants (Figure 17). Ice keels contacting the bottom should bulldoze sediment in an onshore to alongshore direction with only a minor amount of sediment moved offshore during gouging.

Because most gouging is believed to take place in an upslope direction (Barnes et al., 1984) it is difficult to determine the causes for the termination of gouges in an offshore direction. Some of these gouges are associated with the shoals of testline 2 and have terminated on the inshore side of the shoals possibly as the ice was driven offshore by winds, currents, ice pack motion, or a combination of these forces (Figure 17). However, not all of the seaward terminating gouges can be explained by the shoals. Another possible answer may be that the encompassing ice pack has driven a ice bound floe into water that is to shallow to float the floe and as it moves back offshore by a change in ice motion the floe continues to settle into the bottom sediments until release from ice pack pressure causes further movement to cease.

Since most ice gouging takes place in the winter under the seasonal ice-pack when ocean currents are small (Barnes, 1981; Matthews, 1981; Barnes and Reimnitz, 1982) sediment transport by ice gouging plays a signifcant roll in winter (Harper and Penland, 1982). Barnes (1982), in a study of an ice pushed coastal boulder ridge in Camden Bay, suggested that sand, gravel and boulders were moved onshore by direct contact with the sea-ice. The direction of sediment transport suggested by gouge terminations in the present study (Figures 16 and 17) is essentially southeasterly through southwesterly. Because sea-ice is driven by ocean currents and winds, sediment that is resuspended during ice gouging will also be driven along the coast or onshore (Barnes and Reimnitz, 1982).

The distance of transport by ice gouging is difficult to assess. To date no data exist on the actual distance covered by sediment grains during gouging although it seems reasonable to assume that the distances are small. The suspending of fine grained sediments during gouging may allow any existing currents to transport the sediments greater distances. The most significant sediment sinks for this sediment (transported either by actual ice shove or from resuspension by currents) may be the adjacent gouges themselves as well as other seafloor depressions such as strudel scours (Reimnitz and Kempema, 1982).

Hydraulic Reworking

The sand and gravel shoals of testline 2 are less cohesive than the sediments of testline 1 and the gouges are generally shallower for equivalent water depths (Figures 9 and 10). These conditions are conducive to high infilling rates. In the present study an average of about 60% of all observed gouges on testline 2 are new gouges while an average of about only 15% of the observed gouges on testline 1 are new gouges. These figures suggest that testline 2 has higher rate of hydraulic reworking which infills and obliterates ice gouges (Table V). Hydraulic forces are focused on the shoal crests (areas where most of the gouging on testline 2 takes place) and gouges infill at a greater rate than that of the gentler slope of testline 1. On testline 1, hydraulic energy is lower per unit area and the energy is dissipated over a area of more cohesive shelf sediments allowing gouges to withstand reworking for a longer period of time although occasional large storms may cause unusually high rates of infilling (Barnes and Reimnitz, 1979). Ice gouges are preserved for a longer period of time on testline 1 than on testline 2 and the seafloor of testline 1, therefore, records a longer time span of ice gouging.

Multiplet Gouges - Old Ice and New Ice

Barnes et al. (1984) theorized from their data that wide, shallow multiplet gouges were created by newly formed ice ridges and the many ice blocks forming the ice ridges conform at equivalent depths to the bottom topography before consolidation and gouging occur. These gouges are usually responsible for the widest disruptions of the seafloor by a gouge event but they are also the shallowest gouge events. The deepest gouges are created by ice ridges with generally only one or two keels often of unequal depth (Barnes et al., 1984) that have undergone more than one years incorporation into the winter ice canopy, resulting in a welding of the ice blocks together, which creates coherent ice keels with sufficient strength to cause deep ice gouges.

Tables V and VI of the present study show that 65% of the new gouges and 67% of the seafloor disruption occurring in eastern Harrison Bay is caused by multiplet gouging. These multiplets are of both the shallow many keeled type and also the deeper fewer keeled type. Multiplet gouges make up only 28% of the gouge events while the remaining 72% are single gouge events. Reimnitz et al. (1977) noted in their studies of testline 1 that 70% of the disruption between 1973 and 1975 was from 3 multiplet gouges while the remaining 30% of seafloor disruption was from individual gouges.

Given the above, we postulate two ice gouge populations which have distinctive characteristics and create gouges with different depth and width characteristics. The first population is caused by many keeled ice. These wide and shallow multiplet gouges result in large horizontal disruptions of the seafloor. The second population is caused by ice ridges with few or only one keel and results in gouges which are relatively narrow and may be shallow or deep although the deepest gouges are associated with this type.

On testline 1, in 1978 and 1980, multiplets accounted for over 50% of all gouge events and an average of about 85% of the seafloor disruption (Tables V and VI). In contrast, in 1981 on testline 1 and 2 and in 1982 on testline 1 multiplet gouges accounted for only about 10 to 30% of the gouge events and 40% of the seafloor disruption in each area. It is interesting to note that 1981 and 1982 were the years in which the deepest gouges (>1 m) were formed and again suggests that two types of ice gouging are occuring on the shelf today.

In 1981 there was very little multi-year ice on the shelf at freeze-up (Kovacs, 19__). This is also a year in which we find the least amount of disruption on the shelf floor and also one in which we find one of the deepest new gouges. It may be that in the years in which there are significant amounts of multiyear ice grounded on the inner shelf at freeze-up will be years in which there will be less chance of a very deep gouge. This occurs because the grounded multiyear floes act as a barrier to the onshore and alongshore movement of the newly formed winter ice canopy causing sea-ice to pile up behind the barrier of grounded multi-year ice. The ice ridges thus formed are young and relatively unconsolidated and will be responsible for the wide, shallow disruptions that will occur over the winter. Conversely, when there is no multi- year ice on the shelf at freeze-up a solid ice canopy can form with very little ridging occurring on the inner shelf. The multi-year ice that becomes incorporated into the ice canopy will do so in the deeper waters of Harrison Bay and will not be grounded at freeze-up. As the winter progresses, however, the sea-ice containing the older, consolidated keels can move onshore causing the older ice to ground with the results being deeper, narrower single and multiplet gouge events.

CONCLUSIONS

Observations and measurements made on recently formed ice gouges in eastern Harrison Bay, Alaska combined with those of previous studies (Reimnitz et al., 1977; Barnes et al., 1978) indicate significant variability from year to year in ice gouge processes based on their number, size, and distribution. The additional following conclusions can be drawn from the results of this study:

1) Gouge recurrence rates are higher than previously reported when the smallest gouges (<20 cm deep) are included in the calculations. The average rate of of seafloor disruption of 3.7% per year from the present study means that approximately 50% of the seafloor can be reworked in 20 years when using the proportional replow model of Barnes et al. (1978). A rate of 3% is suggested when the earlier work of Reimnitz et al. (1977) and Barnes et al. (1978) are included in the calculation of the average disruption rate.

2) Frequencies of new ice gouge characteristics have negative exponential distributions similar to that determined for the total ice gouge population on the shelf (Weeks et al., 1984). The slope of the distribution curves varies from area to area and is an indication of the intensity of ice gouging and the major distinction between the ice gouge populations discussed here.

3) In the study area, in water depths of 5-16 m, gouges >1 m deep occur every 6+ years and account for 0.1-0.2% of all gouges in this area. In water depths >10 m the seafloor can be completely disrupted to a depth of 1 m in approximately 800 years. One gouge >1 m deep and plowed this year will be crossed for every 77km of trackline coverage of the seafloor.

4) In areas unaffected by the influence of shoals the maximum depth of gouging can be approximately 10% of the water depth (+- 2%) at least to water depths of about 40 m.

5) Seafloor morphology affects the areal distribution and size of ice gouges and the direction of gouging.

6) Most sediment transport by ice gouging is onshore to alongshore which is suggested from the southwesterly through southeasterly ice gouge terminations.

7) On testline 1, in a corridor about 17 km long and 250 m wide, between 7 and 15 m water depth, at least 5800 cubic meters of sediment per square kilometer is disrupted

yearly. In water depths >10 m cumulative disruption volume increases about 1000 cubic meters per 1 m of increased water depth. On testline 2, in a corridor about 10 km long and 250 m wide, between 7 and 15 m water depth, at least 3000 cubic meters of sediment per square kilometer is disrupted, however, 75% of the disruptions occurs on the crests and seaward slope of the shoals of this testline so that the amount of sediment disrupted is more likely to be concentrated in these areas. Offshore of the most seaward shoal about 6000 cubic meters of sediment per square kilometer is disrupted.

8) Ice gouges on testline 2 are hydraulically reworked and infilled at a faster rate than those on testline 1. The shoals of testline 2 contain most of the gouges that are formed each year. High rates of gouge obliteration on these shoals suggest the shoals are a focal point for the energy expended by waves and currents on the ocean floor during summer.

9) Although multiplet events occur less frequently than single gouge events they account for most of the seafloor area impacted by ice. The most frequent and often the deepest gouge events are single gouges and multiplets with few incisions and these account for the greatest vertical displacement of seafloor sediments.

The conclusions reached in this study derive from one area of the Beaufort Sea shelf. However, we believe the processes operating in other areas are the same, although the number, size, frequency, and distribution of new ice gouges will differ. These conclusions form a basis upon which ice gouge processes in areas of similar water depth and seafloor morphology may be estimated.

REFERENCES CITED

Anonymous, 1983, Chances good for federal arctic research unit: Oil and Gas Journal, June 13, 1983, p. 59.

Arnborgi, Lennart, Walker, H.J., and Peippo, Johan, 1967, Suspended load in the Colville River, Alaska, 1962: Geografiska Annaler, v. 49, Ser. A, p. 131-144.

Barnes, P.W., 1981, Physical characteristics of the Sale 71 Area: United States Geological Survey Open-File Report 82-615, 34 p.

Barnes, P.W., 1982, Marine ice-pushed boulder ridge, Beaufort Sea, Alaska: Arctic, v. 35, no.2, p.312-316.

Barnes, P.W., McDowell, D.M., and Reimnitz, Erk, 1978, Ice gouging characteristics: their changing patterns from 1975-1977, Beaufort Sea, Alaska: United States Geological Survey Open-File Report 78-730, 42 p.

Barnes, P.W., and Rearic, D.M., 1985, Rates of sediment disruption as determined from characteristics of dated ice gouges created since 1975 on the inner shelf of the Beaufort Sea, Alaska: United States Geological Survey Open-File Report 85-463, 35 p.

Barnes, P.W., Rearic, D.M., and Reimnitz, Erk, 1984, Ice gouging characteristics and processes, in, Barnes, P.W., and others, eds., The Alaskan Beaufort Sea, ecosystems and environments: Orlando, Florida, Academic Press, inc., p. 185-212.

Barnes, P.W., and Reimnitz, Erk, 1974, Sedimentary processes on the arctic shelves off the north coast of Alaska, in, Reed, J.C., and Sater, J.E., eds., The coast and shelf of the Beaufort Sea: The Arctic Institute of North America, Arlington, Virgina, p. 439-576.

Barnes, P.W., and Reimnitz, Erk, 1979, Ice gouge obliteration and sediment redistribution event; 1977-1978, Beaufort Sea, Alaska: United States Geological Survey Open-File Report 79-848, 22 p.

Barnes, P.W., and Reimnitz, Erk, 1982, Net flow of near-bottom waters on the inner Beaufort Sea shelf as determined for sea bed drifters: U.S. Geological Survey Open-File Report 82-717, 9 p.

Belderson, R.H., Kenyon, N.H., Stride, A.H., and Stubbs, A.R., 1972, Sonographs of the seafloor: New York, Elsevier Press, 185 p.

Benjamin, J.R., and Cornell, C.A., 1970, Probability, statistics and decision for civil engineers: New York, McGraw-Hill, 684 p.

Carsola, A.J., 1954, Microrelief on arctic sea floor: American Association of Petroleum Geologists Bulletin, v. 38, p. 1587-1601.

Harper, J.R., and Penland, Shea, 1982, Beaufort Sea Sediment Dynamics: Final Report prepared for the Geological Survey of Canada, Woodward-Clyde Consultants, Victoria, Canada, 187 p.

Hibler, W.D., Ackley, S.F., Crowder, W.K., McKim, H.L., and Anderson, D.M., 1974, Analysis of shear zone ice deformation in the Beaufort Sea using satellite imagery, in, Reed, J.C., and Sater, J.E., eds., The coast and shelf of the Beaufort Sea: The Arctic Institute of North America, Arlington, Virgina, p. 285-296.

Kindle, E.M., 1924, Observations on ice-borne sediments by the Canadian and other arctic expeditions: American Journal of Science, v. 7, p. 251-286.

Kovacs, Austin, 1983, Shore ice ride-up and pile-up features, Part I: Alaska's Beaufort Sea coast: United States Army Corps of Engineers, CRREL Report 83-9, 51 p.

Kovacs, Austin, 1984, Shore ice ride-up and pile-up features, Part II: Alsaka's Beaufort Sea coast - 1983 and 1984: United States Army Corps of Engineers, CRREL Report 84-26, 29 p.

Kovacs, Austin, and Mellor, Malcom, 1974, Sea ice morphology and ice as a geologic agent in the southern Beaufort Sea, in, Barnes, P.W., and others, eds., The Alaskan Beaufort Sea, ecosystems and environments: Orlando, Florida, Academic Press, Inc., p. 113-161.

Lewis, C.F.M., 1978, The frequency and Magnitude of drift ice groundings from ice-scour tracks in the Canadian Beaufort Sea: in, Proceedings, Port and Ocean Engineering Under Arctic Conditions, 1977, Memorial University, St. Johns, Newfoundland, v. 1, p. 568-579.

Matthews, J.B., 1981, Observations of surface and bottom currents in the Beaufort Sea near Prudhoe Bay, Alaska: Journal of Geophysical Research, v. 86, p. 6653-6660.

Miller, I., and Freund, J.E., 1977, Probability and statistics for engineers: New York, Prentice-Hall, 529 p.

Miller, R.L., and Kahn, J.S., 1962, Statistical analysis in the geological sciences: New York, John Wiley and Sons, Inc., p. 70-72.

Pelletier, B.R., and Shearer, J.M., 1972, Sea bottom scouring in the Beaufort Sea of the Arctic Ocean, in, Marine Geology and Geophysics, Proceedings of the 24th International Geological Congress, Section 8, p. 251-261.

Pilkington, G.R., and Marcellus, R.W., 1981, Methods of determining pipeline trench depths in the Canadian Beaufort Sea: in, Proceedings, Port and Ocean Engineering Under Arctic Conditions, 6th International Conference, v. 2, p. 674-687.

Prichard, R.S., 1980, A simulation of nearshore winter ice dynamics in the Beaufort Sea, in, Prichard, R.S., ed., Sea ice processes and models: University of Washington Press, Seattle, Washington, p. 49-61.

Rearic, D.M., Barnes, P.W., and Reimnitz, Erk, 1981, Ice gouge data, Beaufort Sea, Alaska, 1972-1980: U.S. Geological Survey Open-File Report 82-950, 8 microfiche cards.

Reimnitz, Erk, and Barnes, P.W., 1974, Sea ice as a geologic agent on the Beaufort Sea shelf of Alaska, in, Reed, J.C., and Sater, J.E., eds., The coast and shelf of the Beaufort Sea: The Arctic Institute of North America, Arlington, Virgina, p. 301-351.

Reimnitz, Erk, Barnes, P.W., Rearic, D.M., Minkler, P.W., Kempema, E.W., and Reiss, T.E., 1982, Marine geological investigations in the Beaufort Sea in 1981 and preliminary interpretations for regions from the Canning River to the Canadian border: United States Geological Survey Open-File Report 82-974, 63 p.

Reimnitz, Erk, Barnes, P.W., Toimil, L.J., and Melchoir, John, 1977, Ice gouge recurrence and rates of sediment reworking, Beaufort Sea, Alaska: Geology, v. 5, p. 405-408.

Reimnitz, Erk, and Kempema, E.W., 1983, High rates of bedload transport measured from the filling rate of large strudel scour craters in the Beaufort Sea, Alaska: Continental Shelf Research, v. 1, no. 3, p. 237-251.

Reimnitz, Erk, and Kempema, E.W., 1984, Pack ice interaction with Stamukhi shoal, Beaufort Sea, Alaska: in, Barnes, P.W., and others, eds., The Alaskan Beaufort Sea, ecosystems and environments: Orlando, Florida, Academic Press, Inc., p. 285-296.

Reimnitz, Erk, Kempema, E.W., Ross, C.R., and Minkler, P.W., 1980, Overconsolidated surficial deposits on the Beaufort Sea shelf: United States Geological Survey Open-File Report 80-2010, 37 p.

Reimnitz, Erk, and Maurer, D.K., 1978, Stamukhi shoals of the Arctic - some observations from the Beaufort Sea: United States Geological Survey Open-File Report 78-666, 11 p.

Reimnitz, Erk, and Maurer, D.K., 1979, Effects of storm surges on the Beaufort Sea coast, northern Alaska: Arctic, v. 32, no. 4, p. 329-344.

Reimnitz, Erk, Toimil, L.J., and Barnes, P.W., 1978, Arctic continental shelf morphology related to sea-ice zonation, Beaufort Sea, Alaska: Marine Geology, v. 28, p. 179-210.

Rex, R.W., 1955, Microrelief produced by sea ice grounding in the Chukchi Sea near Barrow, Alaska: Arctic, v. 8, no. 3, p. 177-186.

Stringer, W.J., 1978, Morphology of Beaufort, Chukchi, and Bering Seas nearshore ice conditions by means of satellite and aerial remote sensing: Geophysical Institute, University of Alaska, Fairbanks, Alaska, v. 2, 794 p.

Thor, D.R., and Nelson, C.H., 1981, Ice gouging on the subarctic Bering Sea shelf, in, Hood, D.W., and Calder, J.A., eds., The eastern Bering Sea shelf: oceanography and resources: National Oceanic and Atmospheric Administration, University of Washington Press, Seattle, Washington, v. 1, p. 279-292.

Toimil, L.J., 1978, Ice-gouged microrelief on the floor of the eastern Chukchi Sea, Alaska; a reconnaissance survey: United States Geological Survey Open-File Report 78-693, 48 p.

Walker, H.J., 1974, The Colville River and the Beaufort Sea: some interactions, in, Reed, J.C., and Sater, J.E., eds., The coast and shelf of the Beaufort Sea: The Arctic Institute of North America, Arlington, Virgina, p. 513-540.

Weeks, W.F., Barnes, P.W., Rearic, D.M., and Reimnitz, Erk, 1984, Some probabilistic aspects of ice gouging on the Alaska shelf of the Beaufort Sea, in, Barnes, P.W., and others, eds., The Alaskan Beaufort Sea, ecosystems and environments: Orlando, Florida, Academic Press, Inc., p. 285-296.

Whalgren, R.V., 1979, Ice-scour tracks in eastern Mackenzie Bay and north of Pullen Island, Beaufort Sea: in, Current Research, Part B, Geological Survey of Canada, Paper 79-1B, p. 51-62.

APPENDIX

TESTLINE: 1	JULIAN DATE: 238	YEAR: 1977-1978	TEMPLATE IDENTIFICATION: 1:1.860

TRACKLINE NUMBER: 14, 19

SEGMENT	WATER DEPTH (M)	TOTAL GOUGES	TOTAL NEW GOUGES	%	SINGLE GOUGES: Length NEW SINGLE GOUGES	GOUGE DEPTH (M)	GOUGE WIDTH (M)	RIDGE HEIGHT (M)	Ø (°T)	MULTIPLE GOUGES: Length NEW MULTI. GOUGES	NUMBER OF INCIS.	DEEPEST INCISION (M)	DISRUPT WIDTH (M)	Ø (°T)	COMMENTS CS = 305°T
AB/0	4.2	0	0	0											
															SS # 5 Bots # 8,10
BC/1	7.5	8	2	25.0											Beginning of trackline
1.50	7.8									73	2	NOT CROSSED	18	110/55	totally reworked (hydraulic).
															3m shoal at pt. B.
CD/2	7.7	8	6	75.0											Termination at 1.5 direction - 235°T
2.30	8.0									NL	2	<.2	5	145/90	
2.80	8.5									NL	4	<.2	15	140/85	
DE/3	8.8	2	0	0											sed. ripples (New)
EF/4	9.6	8	0	0											sed. ripples([illegible])
FG/5	10.0	8	6	75.0											Sed ripples (heavy concentrat
5.40	10.0				175	<.2	1	<.2	160/105						orien. = 100°T λ = 2 m
5.65	10.0				63	<.2	2	<.2	160/105						
5.85	9.9				41	<.2	1	<.2	25/160						termination direction - 160°T
5.85	9.9				35	<.2	1	<.2	35/160						termination direction - 160°T
5.85	10.1				32	<.2	1	<.2	35/160						termination direction - 160°T
5.91	10.0				127	<.2	1	<.2	170/115						
GH/6	10.0	3	0	0											reworked bottom - smoothed (hydraulic) sed. waves(f
HI/7	10.5	5	0	0											sed. waves - many orien = 175°T λ = ~100m
IJ/8	10.7	17	1	5.9											
8.60	11.5				NL	.3	3	<.2	25/150						gouge terminates with hooked end upslope
															direction - 150°T

2

TESTLINE: 1	JULIAN DATE: 238	YEAR: 1977-1978	TEMPLATE IDENTIFICATION: 1:1.860

TRACKLINE NUMBER: 14,19

SEGMENT	WATER DEPTH (M)	TOTAL GOUGES	TOTAL NEW GOUGES	%	Length SINGLE GOUGES: NEW SINGLE GOUGES	GOUGE DEPTH (M)	GOUGE WIDTH (M)	RIDGE HEIGHT (M)	Ø (°T)	Length MULTIPLE GOUGES: NEW MULTI. GOUGES	NUMBER OF INCIS.	DEEPEST INCISION (M)	DISRUPT WIDTH (M)	Ø (°T)	COMMENTS CS = 305°T
JK/9	11.5	75	18	24.0											on all [illegible] gouges
9.25	11.6									NL	3	NC	17	155/100	have been smoothed
9.25	11.6									NL	2	NC	11	155/100	by hydrolic reworking.
9.35	11.7				NL	.2	.3	<.2	130/75						
9.40	11.7									NL	2	.2	14	130/75	
9.65	11.9				280	<.2	2	<.2	00/125						
9.85	11.9									105	4	<.2	13	20/145	
9.99	12.0									831	4	NC	9	05/130	continues to next segment.
KL/10	12.0	76	5	6.6											
10.25	12.1									same as above	4	NC	9	05/130	
10.55	12.3				25	<.2	2	<.2	60/05						
LM/11	12.5	91	4	4.3											
11.30	12.6				50	<.2	7	<.2	120/65						START Trackline 19
11.60	12.7				108	NC	3	NC	170/115						terminates upslope with hooked end 115°T
11.80	12.8				138	<.2	11	<.2	160/105						
11.80	12.8				NL	<.2	2	<.2	160/105						terminates direction - 315°T
MN/12	12.8	94	15	16.0											
12.30	13.0				NL	<.2	2	<.2	170/115						
12.45	13.0									NL	4	<.2	23	55/00	
12.45	13.0				117	<.2	5	<.2	55/00						
12.45	13.0									NL	7	NC	65	55/00	
12.65	13.0				163	NC	2	NC	175/120						
12.75	13.0				43	NC	2	NC	05/130						

TESTLINE: 1		JULIAN DATE: 241			YEAR: 1977-1978					TEMPLATE IDENTIFICATION: 1:1.860					
TRACKLINE NUMBER: 14,19					Length SINGLE GOUGES					Length MULTIPLE GOUGES					
SEGMENT	WATER DEPTH (M)	TOTAL GOUGES	TOTAL NEW GOUGES	%	NEW SINGLE GOUGES	GOUGE DEPTH (M)	GOUGE WIDTH (M)	RIDGE HEIGHT (M)	Ø (°T)	NEW MULTI. GOUGES	NUMBER OF INCIS.	DEEPEST INCISION (M)	DISRUPT WIDTH (M)	Ø (°T)	COMMENTS
NO/13	13.2	141	21	14.9											
13.01	13.2									NL	4	<.2	14	00/125	
13.60	13.4									NL	5	NC	40	170/115	terminates direction - 125° T
13.60	13.4									NL	2	.3	13	140/85	
13.70	13.4				NL	<.2	3	.4	160/105						
13.90	13.5									Nl	9	.2	21	160/105	Continues to next segment.
OP/14	13.5	137	18	13.1											
14.10	13.8				35	<.2	2	<.2	130/75						
14.15	13.8									NL	9	.2	21	160/105	
14.25	13.5									NL	3	<.2	8	155/100	
14.50	13.9									NL	4	<.2	12	155/100	
14.80	13.8				NL	NC	2	NC	05/130						
PQ/15	14.0	61	8	13.1											seafloor smoothed from reworking. North of line.
15.80	14.3									NL	8	.3	60	154/99	
QR/16	14.3	71	4	5.6											Reworked seafloor North of line.
16.05	14.3									NL	2	.2	20	151/96	
16.65	14.5									NL	2	.5	17	144/89	
RS/17	14.7	69	0	0.0											Reworked seafloor North of line.
ST/18	15.0	64	0	0.0											Reworked seafloor. Most older gouges infilled and gone.
TU/19	15.3	102	0	0.0											Reworked seafloor. NORTH OF LINE.

4

TESTLINE: 1	JULIAN DATE: 241	YEAR: 1977-1978	TEMPLATE IDENTIFICATION: 1:1,860

TRACKLINE NUMBER: 14, 19					Length SINGLE GOUGES					Length MULTIPLE GOUGES					CS: 305°T
SEGMENT	WATER DEPTH (M)	TOTAL GOUGES	TOTAL NEW GOUGES	%	NEW SINGLE GOUGES	GOUGE DEPTH (M)	GOUGE WIDTH (M)	RIDGE HEIGHT (M)	Ø (°T)	NEW MULTI. GOUGES	NUMBER OF INCIS.	DEEPEST INCISION (M)	DISRUPT WIDTH (M)	Ø (°T)	COMMENTS
UV/20	15.5	118	0	0.0											Reworked seafloor.
VW/21	15.7	108	10	9.3											
21.30	15.6									NL	5	.4	21	149/94	
21.50	15.6									NL	5	.5	28	164/109	
WX/22	15.8	81	4	4.9											
22.40	15.9				NL	<.2	2	<.2	96/131						
22.99	16.0									NL	3	.3	21	152/97	Continues into next segment.
XY/23	16.0	79	5	6.3											
23.01	16.0									NL	3	.3	21	152/97	
23.55	16.0				NL	<.2	2	<.2	142/107						
23.55	16.0				NL	.3	18	.3	124/69						Termination: 249°T
YZ/24	16.5	58	0	0.0											
Z/end	16.7														

TESTLINE: 1	JULIAN DATE: 220	YEAR: 1978-1979	TEMPLATE IDENTIFICATION: 1:1.860

TRACKLINE NUMBER: 13

SEGMENT	WATER DEPTH (M)	TOTAL GOUGES	TOTAL NEW GOUGES	%	SINGLE GOUGES: (LENGTH) NEW SINGLE GOUGES	GOUGE DEPTH (M)	GOUGE WIDTH (M)	RIDGE HEIGHT (M)	ø (°T)	MULTIPLE GOUGES: (LENGTH) NEW MULTI. GOUGES	NUMBER OF INCIS.	DEEPEST INCISION (M)	DISRUPT WIDTH (M)	ø (°T)	COMMENTS CS = 304 °T
AB/0	4.7	8	4	50.0											
0.30	5.1									92	2	<.2	5	00/124	SSS # 8 Pads # 9
0.30	5.1				24	<.2	1	<.2	32/152						
0.30	5.1				21	<.2	1	<.2	157/101						
BC/1	5.7	6	4	66.7											Shoal height = 1.9m at Pt. B
1.75	6.9				52	<.2	1	<.2	11/135						
1.75	6.9				50	<.2	1	<.2	176/120						Terminates direction - 120°T
1.75	6.9				125	<.2	1	<.2	170/114						
1.90	7.5				165	<.2	3	<.2	06/130						
CD/2	8.2	28	13	46.4											
2.05	8.2				42	<.2	2	<.2	20/144						
2.30	7.8				37	<.2	2	<.2	00/124						
2.65	8.2				45	<.2	2	<.2	140/84						
2.60	8.0				20	<.2	1	<.2	140/84						
2.60	8.0				27	<.2	2	<.2	170/114						
2.75	7.9									NL	5	<.2	18	10/134	
2.85	8.1									NL	3	<.2	13	162/106	
DE/3	8.2	20	20	100.0											gouge // to TL
3.30	8.5									NL	5	<.2	12	10/134	and runs length of seg.
3.50	9.0									NL	15	<.2	47	175/119	continues into next segment.
EF/4	9.3	15	12	80.0											
4.15	9.4									NL	12	<.2	45	175/119	
FG/5	10.0	3	0	0											

TESTLINE: 1	JULIAN DATE: 220	YEAR: 1978-1979	TEMPLATE IDENTIFICATION: 1:1.860

TRACKLINE NUMBER: 13

					Length SINGLE GOUGES					Length MULTIPLE GOUGES					
SEGMENT	WATER DEPTH (M)	TOTAL GOUGES	TOTAL NEW GOUGES	%	NEW SINGLE GOUGES	GOUGE DEPTH (M)	GOUGE WIDTH (M)	RIDGE HEIGHT (M)	Ø (°T)	NEW MULTI. GOUGES	NUMBER OF INCIS.	DEEPEST INCISION (M)	DISRUPT WIDTH (M)	Ø (°T)	COMMENTS
GH/6	9.8	1	1	100.0											
6.1	10.0				NL	<.2	2	<.2	150/94						
HI/7	10.1	5	4	80.0											
7.70	10.2				35	<.2	3	<.2	28/152						
7.80	10.8									NL	2	<.2	19	158/102	continues into next segment
7.85	10.5				22	<.2	2	<.2	135/79						sediment waves
IJ/8	10.6	11	9	81.8											
8.01	10.6				30	<.2	2	<.2	158/102						
8.01	10.6									NL	2	<.2	13	158/102	
8.25	11.0				NL	<.2	2	<.2	159/102						Terminates direction - 102°T
8.40	11.1									221	3	<.2	20	157/101	
8.80	11.2									46	2	<.2	12	132/76	
JK/9	11.2	34	6	20.6											
9.05	11.3				NL	.2	8	<.2	132/76						
9.05	11.3				123	<.2	1	<.2	152/96						
9.15	11.4				NL	<.2	3	<.2	140/84						
9.15	11.4				NL	<.2	2	<.2	140/84						
9.80	11.7				NL	<.2	2	<.2	126/70						
9.95	11.7				NL	<.2	3	<.2	11/135						
KL/10	11.8	86	15	17.4											
10.30	11.9				NL	.4	7	.7	92/36						
10.40	12.0				NL	<.2	2	<.2	155/99						
10.60	12.0									375	4	<.2	20	70/124	
10.70	12.0				NL	NC	3	NC	148/92						

TESTLINE: 1 | JULIAN DATE: 220 | YEAR: 1978-1979 | TEMPLATE IDENTIFICATION: 1:1.860

TRACKLINE NUMBER: 13

					Length SINGLE GOUGES					Length MULTIPLE GOUGES					
SEGMENT	WATER DEPTH (M)	TOTAL GOUGES	TOTAL NEW GOUGES	%	NEW SINGLE GOUGES	GOUGE DEPTH (M)	GOUGE WIDTH (M)	RIDGE HEIGHT (M)	ø (°T)	NEW MULTI. GOUGES	NUMBER OF INCIS.	DEEPEST INCISION (M)	DISRUPT WIDTH (M)	ø (°T)	COMMENTS
10.75	12.0				NL	NC	2	NC	148/92						
10.75	12.0				62	<.2	2	<.2	114/58						
10.80	11.8				NL	NC	5	NC	05/129						
10.90	12.3				NL	<.2	2	<.2	140/84						
10.90	12.3				NL	<.2	2	<.2	140/84						
10.90	12.3				NL	<.2	2	<.2	140/84						
10.95	12.2				NL	<.2	2	<.2	142/86						continues into next segment
10.95	12.2				NL	.2	3	<.2	148/92						
LM/11	12.2	51	9	17.6											
11.15	12.3				NL	.2	3	<.2	148/92						
11.15	12.3				72	NC	3	NC	140/84						
11.20	12.3				58	<.2	2	<.2	144/88						
11.75	12.4				130	<.2	1	<.2	161/105						Terminates direction - 127°T
11.80	12.4				150	NC	2	NC	03/127						
11.90	12.5				105	<.2	2	<.2	167/111						
11.90	12.5				127	<.2	2	<.2	167/111						Terminates - direction - 124°T
11.90	12.5				190	NC	2	NC	00/124						
11.95	12.6				117	<.2	3	<.2	131/75						
															START Trackline 33 SSS#12 BATS#106
MN/12	12.7	51	2	3.9											JD 227
12.20	12.9				75	NC	3	NC	143/87						
12.25	12.9				30	<.2	2	<.2	162/106						
NO/13	13.1	68	2	2.9											
13.30	13.1				NL	<.2	2	<.2	55/179						
13.35	13.2				NL	<.2	2	<.2	42/166						

TESTLINE: 1 | JULIAN DATE: 227 | YEAR: 1978-1979 | TEMPLATE IDENTIFICATION: 1:1.860

TRACKLINE NUMBER: 33

					Length SINGLE GOUGES					Length MULTIPLE GOUGES					
SEGMENT	WATER DEPTH (M)	TOTAL GOUGES	TOTAL NEW GOUGES	%	NEW SINGLE GOUGES	GOUGE DEPTH (M)	GOUGE WIDTH (M)	RIDGE HEIGHT (M)	Ø (°T)	NEW MULTI. GOUGES	NUMBER OF INCIS.	DEEPEST INCISION (M)	DISRUPT WIDTH (M)	Ø (°T)	COMMENTS
OP/14	13.2	73	6	8.2											
14.05	13.5									53	2	NC	7	14/138	
14.45	13.4				60	NC	5	NC	19/143						
14.50	13.2				206	<.2	2	<.2	19/143						
14.50	13.2				NL	<.2	3	<.2	159/103						
14.90	13.8				NL	NC	3	NC	170/114						continues into next segment
PQ/15	13.8	64	24	37.5											
15.20	13.8				NL	NC	3	NC	170/114						
15.50	14.0									NL	22	NC	95	110/124	multi-gouge extends length of TL and is ‖.
15.80	14.2				25	<.2	2	<.2	148/92						
QR/16	14.1	85	8	9.4											
16.35	14.2				NL	<.2	2	<.2	05/129						
16.55	14.4									NL	4	.2	9	168/112	
16.60	14.2									NL	2	<.2	15	148/92	
16.95	14.4				200	NC	3	NC	168/112						continues into next segment - Terminates direction - 112° T
															Quality of sonar only fair
RS/17	14.4	45	3	6.7											
17.05	14.5				same as above	NC	3	NC	168/112						
17.20	14.6									NL	2	NC	8	168/112	
ST/18	14.7	76	8	10.5											
18.15	14.9									NL	3	<.2	18	134/78	
18.20	14.8				NL	.2	2	.3	140/84						
18.25	14.7									NL	2	NC	9	14/138	
18.30	14.8				NL	NC	2	NC	167/104						
18.30	15.0				NL	<.2	1	<.2	159/103						

TESTLINE: 1 | JULIAN DATE: 227 | YEAR: 1978-1979 | TEMPLATE IDENTIFICATION: 1:1.860

TRACKLINE NUMBER: 33

					Length SINGLE GOUGES					Length MULTIPLE GOUGES					
SEGMENT	WATER DEPTH (M)	TOTAL GOUGES	TOTAL NEW GOUGES	%	NEW SINGLE GOUGES	GOUGE DEPTH (M)	GOUGE WIDTH (M)	RIDGE HEIGHT (M)	ø (°T)	NEW MULTI. GOUGES	NUMBER OF INCIS.	DEEPEST INCISION (M)	DISRUPT WIDTH (M)	ø (°T)	COMMENTS
TU/19	15.0	85	1	1.1											
19.55	15.0				NL	.2	3	<.2	140/84						
UV/20	15.2	—	—	—											ICE DETOUR
VW/21	15.3	—	—	—											ICE DETOUR
WX/22	15.4	71	0	0											
X/end	15.8														

TESTLINE: 1		JULIAN DATE: 216		YEAR: 1979-1980						TEMPLATE IDENTIFICATION: 1:1.379					
TRACKLINE NUMBER: 17					Length SINGLE GOUGES					Length MULTIPLE GOUGES					
SEGMENT	WATER DEPTH (M)	TOTAL GOUGES	TOTAL NEW GOUGES	%	NEW SINGLE GOUGES	GOUGE DEPTH (M)	GOUGE WIDTH (M)	RIDGE HEIGHT (M)	Ø (°T)	NEW MULTI. GOUGES	NUMBER OF INCIS.	DEEPEST INCISION (M)	DISRUPT WIDTH (M)	Ø (°T)	COMMENTS CS = 305°T
AB/0	5.5	—	—	-											NO RECORD
BC/1	6.1	—	—	-											NO RECORD
															Shoal height = 1.6 m at Pt. B
CD/2	8.2	40	16	40.0											SSS # 6 BATS # 12
2.75	8.1				68	NC	2	NC	163/108						
2.75	8.1									22	3	NC	10	80/125	
2.80	8.4				37	NC	3	NC	125/70						
2.80	8.4									NL	9	NC	50	137/82	unique gouge termination. direction = 262°T
2.95	8.5				NL	NC	3	NC	150/95						continues into next segment
2.95	8.5				NL	<.2	1	<.2	137/82						continues into next segment
DE/3	8.6	48	30	62.5											
3.01	8.6				NL	NC	3	NC	150/95						
3.05	8.6				NL	<.2	2	<.2	137/82						
3.20	8.7				NL	<.2	2	<.2	137/82						
3.25	8.8				NL	<.2	2	<.2	125/70						
3.40	9.0									NL	8	.2	35	134/79	
3.50	9.3									120	5	NC	17	172/117	
3.65	9.4									NL	3	NC	33	28/153	
3.70	9.4									35	.2	NC	8	21/145	direction = 145°T (termination)
3.85	9.7				NL	<.2	2	<.2	147/92						
3.90	9.6									NL	8	<.2	16	145/90	
EF/4	9.8	28	4	14.3											
4.01	9.8				94	NC	2	NC	146/91						
4.25	9.7				37	NC	3	NC	143/88						
4.35	9.8				118	NC	4	NC	158/103						

2

TESTLINE: 1	JULIAN DATE: 216	YEAR: 1979-1980	TEMPLATE IDENTIFICATION: 1.1.379

TRACKLINE NUMBER: 17					Length SINGLE GOUGES					Length MULTIPLE GOUGES					
SEGMENT	WATER DEPTH (M)	TOTAL GOUGES	TOTAL NEW GOUGES	%	NEW SINGLE GOUGES	GOUGE DEPTH (M)	GOUGE WIDTH (M)	RIDGE HEIGHT (M)	ø (°T)	NEW MULTI. GOUGES	NUMBER OF INCIS.	DEEPEST INCISION (M)	DISRUPT WIDTH (M)	ø (°T)	COMMENTS
4.35	9.8				46	NC	2	NC	139/79						
FG/5	10.1	96	64	66.7											
5.10	10.2									181	3	<.2	11	136/81	
5.25	10.0				NL	<.2	2	<.2	148/93						
5.30	10.0				33	<.2	1	<.2	135/80						
5.30	10.0				NL	<.2	2	<.2	140/85						
5.35	10.0				176	<.2	1	<.2	149/94						
5.35	10.0				118	<.2	1	<.2	147/92						
5.35	10.0				NL	<.2	3	.2	130/75						
5.45	10.1				59	NC	3	NC	159/104						direction = 281°T (Termination)
5.55	10.0									NL	25	<.2	80	150/95	direction = 275°T (Termination)
5.85	10.0									NL	13	<.2	24	150/95	(older triplet grounds 293°T and then moves off at 95°T)
5.85	10.0									NL	5	<.2	18	155/100	
5.95	10.2									NL	11	<.2	25	137/82	direction = 262°T Termination - See 6.05
GH/6	10.3	61	51	83.6											Beginning of sand wave field
6.05	10.1									NL	13	<.2	45	137/82	circular - See 5.95
6.40	10.0									68	2	<.2	8	151/96	
6.65	10.5				32	<.2	2	<.2	133/78						
6.75	11.0									NL	7	NC	25	35/160	funny bottom in sand wave troughs?
6.85	10.1									93	7	NC	42	34/159	
6.85	10.1									35	6	NC	17	149/94	
6.90	10.7									NL	2	NC	20	40/165	
6.95	10.1									34	8	NC	43	142/87	direction = 267°T
6.95	10.1									82	5	<.2	11	22/147	continues into next segment

TESTLINE: 1		JULIAN DATE: 216			YEAR: 1979-1980					TEMPLATE IDENTIFICATION: 1:1.379					
TRACKLINE NUMBER: 17					SINGLE GOUGES					MULTIPLE GOUGES					
SEGMENT	WATER DEPTH (M)	TOTAL GOUGES	TOTAL NEW GOUGES	%	Length NEW SINGLE GOUGES	GOUGE DEPTH (M)	GOUGE WIDTH (M)	RIDGE HEIGHT (M)	Ø (°T)	Length NEW MULTI. GOUGES	NUMBER OF INCIS.	DEEPEST INCISION (M)	DISRUPT WIDTH (M)	Ø (°T)	COMMENTS
HI/7	10.2	32	14	43.8											Sand waves; ht: .8 m λ: ~100m
7.01	10.2									82	5	<.2	11	22/147	
7.05	10.9									67	3	NC	12	18/143	
7.80	10.4									NL	6	NC	8	174/119	
IJ/8	11.1	45	10	22.2											
8.30	11.2									NL	10	<.2	43	149/94	
JK/9	11.6	41	5	12.2											
9.45	11.8									37	3	NC	27	117/62	
9.55	11.9				275	NC	2	NC	02/127						Continues into next segment
9.95	12.0				NL	NC	3	NC	145/90						
KL/10	12.1	117	2	1.7											Total gouges may be low due to machine malfunction
10.01	12.1				NL	NC	3	NC	145/90						Orientation suspect due to ice detour.
10.40	12.3				NL	.4	22	.2	63/08						
LM/11	12.6	130	8	6.2											large amount of sediment infilling of gouges -
11.15	12.6									NL	2	.2	30	116/61	many smooth patches on seafloor
11.65	12.6									NL	5	NC	22	166/111	
11.70	12.8				NL	.3	8	<.2	117/62						
MN/12	12.7	123	0	0											sediment infilling of gouges
NO/13	12.8	151	1	0.7											Sediment infilling of most gouges
13.35	13.2				NL	<.2	8	<.2	140/85						

TESTLINE: 1	JULIAN DATE: 216	YEAR: 1979-1980	TEMPLATE IDENTIFICATION: 1:1.379

TRACKLINE NUMBER: 17					Length SINGLE GOUGES					Length MULTIPLE GOUGES					
SEGMENT	WATER DEPTH (M)	TOTAL GOUGES	TOTAL NEW GOUGES	%	NEW SINGLE GOUGES	GOUGE DEPTH (M)	GOUGE WIDTH (M)	RIDGE HEIGHT (M)	ø (°T)	NEW MULTI. GOUGES	NUMBER OF INCIS.	DEEPEST INCISION (M)	DISRUPT WIDTH (M)	ø (°T)	COMMENTS
OP/14	13.7	128	3	2.3											sediment infilling
14.75	14.0				NL	.2	8	<.2	143/88						
14.80	14.0									NL	2	<.2	17	143/88	
PQ/15	13.8	171	40	23.4											Sediment infilling
15.15	14.0									NL	4	NC	16	167/112	
15.25	14.0									NL	7	.2	29	150/95	
15.25	14.0									NL	5	NC	25	132/77	
15.45	14.1				NL	.4	3	.5	160/105						
15.50	14.2									50	6	NC	19	158/103	
15.60	14.3				NL	.2	4	<.2	135/80						
15.65	14.0									NL	16	NC	48	150/95	
QR/16	14.3	104	4	3.8											sonar shutdown makes Total count unreliable -
16.55	14.5									NL	2	.2	15	148/93	Sediment infilling
16.75	14.7				NL	<.2	3	<.2	151/96						
16.75	14.8				NL	<.2	2	<.2	151/96						
RS/17	14.8	—	—	—											Sonar shutdown -
ST/18	15.0	76	13	17.1											
18.99	15.1									NL	6	.2	36	159/104	all continue into
18.99	15.1				NL	.3	8	.4	145/90						next
18.99	15.1									NL	6	NC	36	152/97	segment
TU/19	15.1	77	13	16.9											
19.01	15.1									NL	6	.2	36	59/104	sediment infilling
19.01	15.1				NL	.3	8	.4	145/90						

TESTLINE: 1		JULIAN DATE: 216		YEAR: 1979-1980						TEMPLATE IDENTIFICATION: 1:1.379					
TRACKLINE NUMBER: 17					Length SINGLE GOUGES					Length MULTIPLE GOUGES					
SEGMENT	WATER DEPTH (M)	TOTAL GOUGES	TOTAL NEW GOUGES	%	NEW SINGLE GOUGES	GOUGE DEPTH (M)	GOUGE WIDTH (M)	RIDGE HEIGHT (M)	Ø (°T)	NEW MULTI. GOUGES	NUMBER OF INCIS.	DEEPEST INCISION (M)	DISRUPT WIDTH (M)	Ø (°T)	COMMENTS
19.01	15.1									NL	6	NC	36	52/97	
UV/20	15.6	83	0	0											heavy sediment infilling of gouges
V/END	15.6														

TESTLINE: 1 | JULIAN DATE: 216 | YEAR: 1980-1981 | TEMPLATE IDENTIFICATION: 1:1633

Trackline Number 27					Length SINGLE GOUGES					Length MULTIPLE GOUGES					
SEGMENT	WATER DEPTH (M)	TOTAL GOUGES	TOTAL NEW GOUGES	%	NEW SINGLE GOUGES	GOUGE DEPTH (M)	GOUGE WIDTH (M)	RIDGE HEIGHT (M)	ø (°T)	NEW MULTI. GOUGES	NUMBER OF INCIS.	DEEPEST INCISION (M)	DISRUPT WIDTH (M)	ø (°T)	COMMENTS CS: 305° T
AB/0	5.1	3	—	—											NO 1980 DATA
															SS#14 BATS#18
BC/1	6.3	3	—	—											NO 1980 DATA
															Shoal height = 1.7 m at Pt. B
CD/2	8.5	23	9	39.1											
2.25	8.1				NL	.3	4	.2	155/100						
2.35	7.8				NL	<.2	2	<.2	114/59						
2.55	8.1				NL	<.2	2	<.2	162/107						
2.65	8.5				NL	<.2	3	<.2	145/90						
2.80	8.3				NL	<.2	2	<.2	152/97						
2.85	8.4				NL	<.2	1	<.2	145/90						
2.85	8.4				NL	<.2	2	<.2	74/139						
2.95	8.5				NL	NC	5	NC	116/61						Termination-direction = 61° T
2.95	8.5				NL	<.2	3	<.2	140/85						continues into next segment
DE/3	8.5	47	15	31.9											
3.01	8.5				NL	<.2	3	<.2	140/85						
3.05	8.5				NL	<.2	1	<.2	135/80						
3.15	8.6				NL	<.2	1	<.2	126/71						
3.20	8.6				NL	<.2	2	<.2	122/67						
3.20	8.6									NL	4	NC	34	03/128	
3.20	8.6				NL	<.2	2	<.2	159/104						
3.25	8.7				97	.7	6	<.2	132/77						
3.30	8.7				NL	.3	2	.3	123/68						
3.35	8.9				NL	.2	3	<.2	151/102						
3.60	9.3				42	NC	2	NC	26/151						Termination direction = 151° T
3.65	9.3				45	NC	3	NC	22/150						Termination direction = 150° T
3.85	9.5				NL	.2	4	.3	133/78						

TESTLINE: 1 | JULIAN DATE: 216 | YEAR: 1980-1981 | TEMPLATE IDENTIFICATION: 1:1,633

Trackline Number 27					Length SINGLE GOUGES					Length MULTIPLE GOUGES					
SEGMENT	WATER DEPTH (M)	TOTAL GOUGES	TOTAL NEW GOUGES	%	NEW SINGLE GOUGES	GOUGE DEPTH (M)	GOUGE WIDTH (M)	RIDGE HEIGHT (M)	ø (°T)	NEW MULTI. GOUGES	NUMBER OF INCIS.	DEEPEST INCISION (M)	DISRUPT WIDTH (M)	ø (°T)	COMMENTS
EF/4	9.7	27	16	59.3											
4.10	9.7				NL	.3	3	.4	146/91						
4.20	9.7									NL	2	.2	10	157/102	
4.20	9.7				NL	<.2	1	<.2	169/114						
4.25	9.7				NL	<.2	3	<.2	98/43						
4.30	9.7				NL	.2	3	.4	135/80						
4.45	9.7				NL	.2	2	.2	129/74						
4.50	9.7				NL	.2	2	.2	124/69						
4.50	9.7				NL	.4	3	.2	120/65						
4.55	9.8				NL	.2	3	.2	137/82						
4.65	9.8				NL	<.2	4	<.2	133/78						
4.70	9.8				NL	<.2	2	<.2	130/75						
4.75	10.0									NL	3	<.2	12	139/84	Termination direction - 264°T
4.99	10.1				NL	<.2	3	<.2	130/75						
FG/5	10.1	43	9	20.9											
5.05	10.0				NL	<.2	2	<.2	134/79						
5.20	10.0				NL	<.2	5	<.2	136/81						
5.30	10.0				NL	.2	3	.3	136/81						
5.35	10.0									NL	2	<.2	6	135/80	
5.35	10.0				NL	.2	2	<.2	113/58						
5.70	10.1				NL	<.2	3	<.2	133/78						
5.99	10.0									NL	2	<.2	11	168/113	
GH/6	10.0	13	2	15.4											
6.15	10.3				NL	<.2	3	<.2	130/75						
6.50	10.4				NL	<.2	3	<.2	176/121						

TESTLINE: 1 | **JULIAN DATE:** 216 | **YEAR:** 1980-1981 | **TEMPLATE IDENTIFICATION:** 1:1633

Trackline Number 27

					Length SINGLE GOUGES					Length MULTIPLE GOUGES					
SEGMENT	WATER DEPTH (M)	TOTAL GOUGES	TOTAL NEW GOUGES	%	NEW SINGLE GOUGES	GOUGE DEPTH (M)	GOUGE WIDTH (M)	RIDGE HEIGHT (M)	ø (°T)	NEW MULTI. GOUGES	NUMBER OF INCIS.	DEEPEST INCISION (M)	DISRUPT WIDTH (M)	ø (°T)	COMMENTS
HI/7	10.7	22	12	54.5											Sediment waves: .8 m high λ = 100 m continues throughout segment
7.10	10.2				28	<.2	2	<.2	160/105						
7.20	10.3				NL	NC	8	NC	148/93						
7.60	10.5				110	NC	7	NC	160/105						Termination direction - 285°T
7.75	11.0				40	NC	4	NC	155/100						
7.80	10.8				NL	<.2	2	<.2	124/69						
7.85	10.8				NL	<.2	2	<.2	77/22						
7.85	10.5				NL	NC	3	NC	95/40						
7.95	11.2									NL	2	NC	11	150/95	Termination direction - 220°T
7.95	11.2									95	2	NC	14	145/90	68/13 movement: 90°T then 195°T
7.95	11.2				NL	<.2	3	<.2	68/13						
IJ/8	11.1	38	14	36.8											
8.10	11.0				NL	NC	6	NC	21/146						
8.50	11.2				NL	.3	3	.2	115/60						
8.60	11.5				NL	NC	3	NC	135/80						
8.60	11.5									NL	5	<.2	23	153/98	14/113 160/105 : Shape 98°T then 113°T then 1[illegible]
8.65	11.5				NL	NC	4	NC	163/108						
8.80	11.7				NL	<.2	2	<.2	158/163						
8.80	11.7									44	3	NC	10	27/152	Termination direction - 152°T
8.90	11.8				NL	NC	5	NC	145/90						
JK/9	11.6	48	15	31.3											
9.10	11.6									NL	2	.3	10	161/106	
9.20	11.7				NL	.2	3	<.2	112/57						
9.60	12.0									NL	2	<.2	5	164/109	
9.65	12.0				NL	NC	5	NC	130/75						
9.70	12.1									NL	2	<.2	6	126/71	

TESTLINE: 1		JULIAN DATE: 216			YEAR: 1980 -1981					TEMPLATE IDENTIFICATION: 1:1.633					
Trackline Number 27					Length SINGLE GOUGES					Length MULTIPLE GOUGES					
SEGMENT	WATER DEPTH (M)	TOTAL GOUGES	TOTAL NEW GOUGES	%	NEW SINGLE GOUGES	GOUGE DEPTH (M)	GOUGE WIDTH (M)	RIDGE HEIGHT (M)	Ø (°T)	NEW MULTI. GOUGES	NUMBER OF INCIS.	DEEPEST INCISION (M)	DISRUPT WIDTH (M)	Ø (°T)	COMMENTS
9.70	12.1				NL	<.2	2	<.2	130/75						
9.75	12.1									NL	3	.2	12	136/81	
9.85	12.1				NL	.2	6	<.2	115/60						
9.90	12.2									NL	2	NC	43	00/125	continues into next segment - terminates (125°
KL/10	12.2	87	6	6.9											
10.30	12.5									NL	2	.6	41	170/115	from above - single turns to double incision at mid-seg.
10.60	12.3				NL	NC	2	NC	25/150						
10.75	12.3				NL	.3	3	.4	126/71						
10.80	12.4				NL	.6	11	.5	162/107						Very large gouge - disruption width of 30+ m. (con't to next)
10.90	12.6				NL	NC	8	NC	172/117						large gouge continues to next segment
LM/11	12.5	84	11	13.1											
11.05	12.5				70	<.2	2	<.2	149/94						
11.25	12.5				NL	NC	11	NC	166/111						Very large from above (10.8)
11.50	12.8				75	NC	2	NC	168/113						
11.50	12.8									NL	3	NC	12	175/120	triple that turns to a single (see 10.9) con't's length of sngl
11.50	12.8				NL	NC	5	NC	175/120						continues into next segment
11.85	13.1				NL	NC	3	NC	180/85						
11.85	13.1									NL	3	NC	10	163/108	changes to single in next segment
MN/12	13.0	86	15	17.4											Start roll (Bals) 19
12.15	13.0									NL	2	NC	10	08/133	
12.25	13.2				NL	.3	3	.5	162/107						(Same as 11.85b)
12.50	13.2				NL	<.2	8	<.2	52/177						
12.50	13.2				NL	NC	5	NC	157/102						
12.50	13.2									NL	3	NC	18	176/121	runs parallel along center line (same as 11.50)
12.85	13.1				NL	NC	4	NC	176/121						(same as 11.50 a)

TESTLINE: 1			JULIAN DATE: 216			YEAR: 1980 -1981				TEMPLATE IDENTIFICATION: 1:1633					
Trackline Number 27					Length SINGLE GOUGES					Length MULTIPLE GOUGES					
SEGMENT	WATER DEPTH (M)	TOTAL GOUGES	TOTAL NEW GOUGES	%	NEW SINGLE GOUGES	GOUGE DEPTH (M)	GOUGE WIDTH (M)	RIDGE HEIGHT (M)	ø (°T)	NEW MULTI. GOUGES	NUMBER OF INCIS.	DEEPEST INCISION (M)	DISRUPT WIDTH (M)	ø (°T)	COMMENTS
12.95	13.4									NL	5	.5	13	152/97	single [illegible] turns into multiplet
12.95	13.4				NL	.6	6	.6	118/63						
NO/13	13.4	88	15	17.0											
13.05	13.3									NL	3	NC	15	159/104	(from 12.50c)
13.05	13.3				NL	NC	5	NC	160/105						(from 12.95a)
13.10	13.3				NL	.2	3	<.2	120/65						
13.25	13.5				NL	NC	3	NC	172/117						
13.50	13.5				NL	<.2	2	<.2	158/103						
13.50	13.5				NL	.3	3	<.2	125/70						
13.55	13.4				NL	.3	3	.4	118/63						
13.85	13.7				NL	<.2	3	<.2	166/111						continued into next segment
13.85	13.7									NL	5	.2	19	166/111	
OP/14	13.8	109	22	20.2											
14.05	13.7				NL	NC	3	NC	167/112						
14.05	13.7				178	NC	3	NC	[illegible]8/133						
14.50	13.8									NL	4	.2	26	171/116	
14.60	13.7				NL	<.2	2	<.2	130/75						
14.80	14.0									NL	4	.2	27	171/116	continues into next segment
14.85	13.8				NL	<.2	5	<.2	128/73						
14.99	13.9									NL	7	NC	32	163/108	continues into next segment
14.99	13.9									NL	3	NC	17	164/109	continues into next segment
PQ/15	13.9	106	30	28.3											
15.05	14.0									NL	3	NC	13	166/111	
15.20	14.0									NL	10	.3	30	167/112	
15.30	14.1									NL	2	.3	10	124/69	

TESTLINE: 1			JULIAN DATE: 216			YEAR: 1980–1981				TEMPLATE IDENTIFICATION: 1:1633					
Trackline Number 27					Length SINGLE GOUGES					Length MULTIPLE GOUGES					
SEGMENT	WATER DEPTH (M)	TOTAL GOUGES	TOTAL NEW GOUGES	%	NEW SINGLE GOUGES	GOUGE DEPTH (M)	GOUGE WIDTH (M)	RIDGE HEIGHT (M)	ø (°T)	NEW MULTI. GOUGES	NUMBER OF INCIS.	DEEPEST INCISION (M)	DISRUPT WIDTH (M)	ø (°T)	COMMENTS
15.30	14.1				NL	.2	4	.5	127/67						
15.30	14.1									NL	3	<.2	12	167/112	
15.45	14.3									NL	3	<.2	11	162/107	
15.50	13.7									NL	2	.2	8	140/85	
15.65	14.4									NL	5	NC	18	160/105	
15.95	14.2				NL	<.2	5	<.2	140/85						continues into next segment
QR/16	14.1	83	7	8.4											
16.01	14.1				NL	<.2	5	<.2	140/85						
16.10	14.4				88	NC	2	NC	75/130						directional changes
16.20	14.2				NL	<.2	8	<.2	59/04						
16.55	14.7				NL	<.2	3	<.2	136/81						
16.75	14.6									NL	3	.3	12	147/92	
RS/17	14.7	75	9	12.0											
17.30	14.8				NL	NC	3	NC	120/65						
17.30	14.8				NL	NC	4	NC	120/65						
17.40	14.9				NL	<.2	3	<.2	124/69						Termination – direction • 249 °T
17.45	14.9									NL	3	.2	12	150/95	
17.65	15.0				NL	NC	7	NC	162/107						
17.70	15.0				NL	<.2	2	<.2	127/72						
17.85	15.0				NL	NC	3	NC	145/90						
S/END	15.0														

TESTLINE: 1	JULIAN DATE:	YEAR: 1981-1982	TEMPLATE IDENTIFICATION: 1:1.379

TRACKLINE NUMBER: 16					Length SINGLE GOUGES					Length MULTIPLE GOUGES					CS: 310°T
SEGMENT	WATER DEPTH (M)	TOTAL GOUGES	TOTAL NEW GOUGES	%	NEW SINGLE GOUGES	GOUGE DEPTH (M)	GOUGE WIDTH (M)	RIDGE HEIGHT (M)	Ø (°T)	NEW MULTI. GOUGES	NUMBER OF INCIS.	DEEPEST INCISION (M)	DISRUPT WIDTH (M)	Ø (°T)	Range 100 m * COMMENTS SS# 8 BATS#10
AB/0	5.4	4	1	25.0											1982 BATS RECORD READS ONE METER SHALLOW. ALL
0.55	7.7				25	<.2	1	<.2	129/79						MEASUREMENTS ADJUSTED BY adding 1m to depths.
															Shorter range may effect total gouge counts. *
BC/1	6.6	3	0	0.0											Pt. B on crest of shoal Shoal ht = 1.5m
															100m range may also affect resolution of smaller gouges.
CD/2	8.1	26	2	7.7											
2.99	8.5									NL	2	<.2	10	151/101	Continues into next segment.
DE/3	8.5	64	8	12.5											
3.01	8.5									NL	2	<.2	10	151/101	
3.45	9.0				NL	<.2	1	<.2	142/92						
3.85	9.4				NL	<.2	2	<.2	158/108						
3.90	9.4									NL	2	<.2	9	127/77	
3.95	9.4									NL	2	<.2	8	123/73	
EF/4	9.5	50	10	20.0											
4.01	9.5				NL	NC	4	NC	137/87						Termination: 87°T
4.15	9.5				NL	.2	3	<.2	120/70						
4.25	9.5				NL	.3	3	<.2	98/48						
4.30	9.5									NL	2	<.2	7	116/66	
4.75	9.7				NL	<.2	3	<.2	62/12						
4.75	9.7				62	NC	1	NC	157/107						
4.80	9.8				NL	<.2	2	<.2	137/87						
4.85	9.8				NL	<.2	2	<.2	146/90						
4.90	9.8				NL	<.2	1	<.2	124/71						

683

2

TESTLINE: 1	JULIAN DATE:	YEAR: 1981-1982	TEMPLATE IDENTIFICATION: 1:1.379

TRACKLINE NUMBER: 16					Length SINGLE GOUGES					Length MULTIPLE GOUGES					CS: 310°T
SEGMENT	WATER DEPTH (M)	TOTAL GOUGES	TOTAL NEW GOUGES	%	NEW SINGLE GOUGES	GOUGE DEPTH (M)	GOUGE WIDTH (M)	RIDGE HEIGHT (M)	Ø (°T)	NEW MULTI. GOUGES	NUMBER OF INCIS.	DEEPEST INCISION (M)	DISRUPT WIDTH (M)	Ø (°T)	Range = 100 M * COMMENTS
FG/5	9.8	53	7	13.2											10-20 cm. swell
5.05	9.8				NL	<.2	4	<.2	130/80						
5.10	9.8				NL	.2	3	<.2	130/80						
5.20	9.7				NL	<.2	2	<.2	150/100						
5.20	9.7				NL	.3	5	.3	90/40						
5.30	9.8				NL	<.2	3	<.2	86/36						
5.40	9.8				NL	.2	3	<.2	93/43						
5.50	9.7				NL	<.2	3	<.2	155/105						Termination : 333°T 105 333
GH/6	9.8	22	3	13.6											much movement of sediment. troughs of sand wave field may
6.20	10.2				NL	<.2	1	<.2	165/115						have funny bottom exposed. water depth at trough of sand wave.
6.35	9.7				NL	<.2	1	<.2	140/90						water depth at crest of sand wave
6.80	9.6				NL	<.2	1	<.2	149/99						water depth at crest of sand wave.
HI/7	10.3	31	2	6.5											Extensive sediment movement. troughs have funny bottom.
7.01	10.3				NL	<.2	2	<.2	130/80						
7.65	10.5				NL	.2	2	<.2	138/88						
IJ/8	10.8	64	20	31.3											
8.05	11.1				NL	<.2	2	<.2	145/95						
8.15	10.5									NL	4	.4	16	137/87	shape
8.30	10.9				NL	<.2	3	<.2	144/94						
8.35	10.8				NL	<.2	3	<.2	128/78						
8.40	11.3				NL	<.2	2	<.2	130/80						
8.45	10.8				NL	<.2	1	<.2	116/66						
8.55	11.3				NL	NC	2	NC	172/127						
8.70	11.2				NL	NC	2	NC	141/97						
8.70	11.2				NL	NC	2	NC	178/129						

684

TESTLINE: / | JULIAN DATE: | YEAR: 1981–1982 | TEMPLATE IDENTIFICATION: 1:1.379

TRACKLINE NUMBER: 16

SEGMENT	WATER DEPTH (M)	TOTAL GOUGES	TOTAL NEW GOUGES	%	Length SINGLE GOUGES: NEW SINGLE GOUGES	GOUGE DEPTH (M)	GOUGE WIDTH (M)	RIDGE HEIGHT (M)	Ø (°T)	Length MULTIPLE GOUGES: NEW MULTI. GOUGES	NUMBER OF INCIS.	DEEPEST INCISION (M)	DISRUPT WIDTH (M)	Ø (°T)	CS: 310°T Range = 100m * COMMENTS
8.70	11.2									NL	2	NC	3	174/124	
8.90	11.3				NL	NC	5	NC	07/137						shape
8.95	11.2				NL	NC	1	NC	172/122						
8.99	11.2				NL	<.2	2	<.2	23/153						continues into next segment
8.99	11.2	.								NL	2	<.2	6	137/87	
8.99	11.2				NL	<.2	1	<.2	147/97						
JK/9	11.2	85	20	23.5											
9.01	11.2				NL	<.2	2	<.2	23/153						continued from previous segment
9.01	11.2									NL	2	<.2	6	137/87	
9.01	11.2				NL	<.2	1	<.2	147/97						
9.05	11.3				NL	<.2	1	<.2	135/85						
9.10	11.2				NL	<.2	2	<.2	141/91						
9.15	11.2				NL	<.2	2	<.2	126/76						
9.20	11.2									NL	9	<.2	20	173/123	
9.25	11.2				NL	<.2	2	<.2	151/101						
9.30	11.3				NL	.2	3	.2	131/81						
9.35	11.4									NL	2	.3	20	98/48	
KL/10	11.7	119	6	5.0											100 m Range increases resolution and accounts
10.05	11.5				NL	.3	7	.2	92/42						for high total gouge count.
10.15	11.6				NL	.2	3	.2	153/103						
10.25	11.6				NL	.2	3	.2	105/55						
10.40	11.8				NL	.4	4	.5	40/170						
10.75	11.7				NL	<.2	2	<.2	150/100						
10.80	11.8				NL	<.2	1	<.2	172/122						

TESTLINE: 1 | JULIAN DATE: | YEAR: 1981 -1982 | TEMPLATE IDENTIFICATION: 1: 1,379

TRACKLINE NUMBER: 16

SEGMENT	WATER DEPTH (M)	TOTAL GOUGES	TOTAL NEW GOUGES	%	SINGLE GOUGES (Length) NEW SINGLE GOUGES	GOUGE DEPTH (M)	GOUGE WIDTH (M)	RIDGE HEIGHT (M)	Ø (°T)	MULTIPLE GOUGES (Length) NEW MULTI. GOUGES	NUMBER OF INCIS.	DEEPEST INCISION (M)	DISRUPT WIDTH (M)	Ø (°T)	CS: 310 °T Range = 100 M COMMENTS
LM/11	12.1	128	6	4.7											100 m range increases resolution and accounts for
11.25	12.1				NL	.2	3	<.2	118/68						high total gouge count.
11.35	12.1				NL	<.2	3	<.2	130/80						
11.40	12.2									NL	2	.2	17	148/98	
11.75	12.2				NL	<.2	1	<.2	132/82						
11.85	12.2				NL	.2	13	.4	128/78						
MN/12	12.4	129	3	2.3											
12.50	12.6									NL	2	.4	13	97/47	
12.85	12.3				NL	1.0	7	.4	102/52						
NO/13	12.6	116	3	2.6											
13.85	12.9				NL	<.2	6	<.2	90/40						
13.95	12.9				NL	.5	11	.5	90/40						
13.99	12.9				NL	.2	5	<.2	90/40						
O/end	12.9														

TESTLINE: 2		JULIAN DATE:			YEAR: 1977-1978					TEMPLATE IDENTIFICATION: 1: 1.633					
TRACKLINE NUMBER: 11					Length SINGLE GOUGES					Length MULTIPLE GOUGES					CS: 358°T
SEGMENT	WATER DEPTH (M)	TOTAL GOUGES	TOTAL NEW GOUGES	%	NEW SINGLE GOUGES	GOUGE DEPTH (M)	GOUGE WIDTH (M)	RIDGE HEIGHT (M)	Ø (°T)	NEW MULTI. GOUGES	NUMBER OF INCIS.	DEEPEST INCISION (M)	DISRUPT WIDTH (M)	Ø (°T)	Range: 125 M COMMENTS SS# 5 Rats# 9
AB/0	7.3	39	12	30.8											Bottom r[illegible] for entire line. Most older gouges gone.
0.10	7.8				NL	<.2	2	<.2	140/138						Very small gouges
0.15	7.9									NL	4	<.2	42	27/25	gouge spaced far apart (~5m)
0.25	8.6									NL	7	<.2	27	45/43	
BC/1	10.2	8	4	50.0											
1.20	10.5									NL	3	<.2	16	44/42	Termination: 154°T
1.99	11.5				NL	<.2	2	<.2	17/15						continues into next segment
CD/2	11.5	5	1	20.0											fields of sand waves where many gouges used to be - [illegible]
2.01	11.5				NL	<.2	2	<.2	17/15						continued from previous seg.
DE/3	11.7	24	22	91.7											2.3 m shoal. New gouges on shoal crest. Sed. waves seaward of shoal. / on inside of shoal
3.50	10.9				24	<.2	1	<.2	113/111						Termination: 111°T
3.65	9.5									NL	13	<.2	75	114/112	Pressure ridge on shoal crest. Most gouges on crest
3.65	9.5				31	<.2	1	<.2	40/38						Termination: 38°T
3.70	10.1									38	2	<.2	6	149/147	Termination: 147°T
3.70	10.1				48	<.2	2	<.2	163/161						Termination: 161°T
3.70	10.1				45	NC	3	NC	165/163						Termination: 163°T
3.70	10.1				NL	<.2	2	<.2	38/36						
3.70	10.1				23	<.2	2	<.2	177/175						Termination: 175°T
3.90	12.1				NL	<.2	2	<.2	19/17						seaward of shoal
EF/4	12.4	3	1	33.3											asymmetrical dunes - current direction onshore (~)
4.85	13.1				NL	<.2	7	<.2	85/83						Sed. dune complex (seen [illegible] in same place)
															orientation of crests: 01°T (funny bottom?)(window?)
															gouge appears as a [illegible] scrape

TESTLINE: 2 | JULIAN DATE: | YEAR: 1977-1978 | TEMPLATE IDENTIFICATION: 1:1.633

TRACKLINE NUMBER: 17 | CS: 358°T

Range 125 m

SEGMENT	WATER DEPTH (M)	TOTAL GOUGES	TOTAL NEW GOUGES	%	Length SINGLE GOUGES: NEW SINGLE GOUGES	GOUGE DEPTH (M)	GOUGE WIDTH (M)	RIDGE HEIGHT (M)	Ø (°T)	Length MULTIPLE GOUGES: NEW MULTI. GOUGES	NUMBER OF INCIS.	DEEPEST INCISION (M)	DISRUPT WIDTH (M)	Ø (°T)	COMMENTS
FG/5	13.5	62	30	48.4											older shallow (infilled) gouges Normal to line and can not
5.05	13.5									NL	5	<.2	30	120/118	be resolved. Count may be higher of total gouges.
5.30	13.6				40	NC	2	NC	57/55						
5.50	14.0									94	5	NC	22	09/07	
5.50	14.0									200	7	NC	30	28/26	Termination: 264 26 170
5.95	14.2									NL	2	<.2	16	146/144	
5.99	14.3				NL	.2	7	.4	28/26						con't into next segment
5.99	14.3									NL	9	NC	25	150/148	148 25
GH/6	14.3	32	17	53.1											
6.01	14.3				NL	.2	7	.4	28/26						Poor resolution of gouges normal to trackline.
6.01	14.3									NL	9	NC	25	150/148	
6.10	14.4				NL	<.2	2	<.2	55/53						
6.20	14.4									NL	2	<.2	16	65/63	
6.40	14.5				NL	<.2	5	.2	52/50						
6.40	14.5				NL	<.2	1	<.2	42/40						
6.65	14.6				NL	<.2	2	<.2	52/50						
6.80	14.8				NL	<.2	2	<.2	85/83						
HI/7	15.1	13	4	30.8											sediment waves and other traction features.
7.35	14.7									NL	4	<.2	20	61/59	
IJ/8	14.5	51	23	45.1											3.6 m shoal at mid segment NEW GOUGES ON SHOAL CREST
8.50	11.4				NL	<.2	1	<.2	90/88						MAJOR CHANGE [illegible] Between years
8.50	11.4				NL	<.2	1	<.2	125/123						
8.50	11.4				NL	<.2	1	<.2	135/133						
8.50	11.4				NL	<.2	2	<.2	136/134						
8.50	11.4				NL	<.2	1	<.2	110/108						

TESTLINE: 2 | JULIAN DATE: | YEAR: 1977-1978 | TEMPLATE IDENTIFICATION: 1:1.633

TRACKLINE NUMBER: 17 | CS: 358°T

SEGMENT	WATER DEPTH (M)	TOTAL GOUGES	TOTAL NEW GOUGES	%	Length NEW SINGLE GOUGES	GOUGE DEPTH (M)	GOUGE WIDTH (M)	RIDGE HEIGHT (M)	ø (°T)	Length NEW MULTI. GOUGES	NUMBER OF INCIS.	DEEPEST INCISION (M)	DISRUPT WIDTH (M)	ø (°T)	125 M [illegible] COMMENTS
8.50	11.4				NL	<.2	2	<.2	115/113						
8.50	11.4				46	<.2	1	<.2	02/00						
8.50	11.4				NL	<.2	2	<.2	132/130						
8.50	11.4									NL	2	<.2	5	03/01	
8.50	11.4				NL	<.2	2	<.2	55/53						
8.50	11.4				NL	NC	5	NC	125/123						Termination: 303°T
8.50	11.4				NL	<.2	2	<.2	135/133						
8.50	11.4				NL	<.2	1	<.2	100/98						
8.50	11.4				NL	<.2	1	<.2	115/113						
8.50	11.4				NL	<.2	2	<.2	140/138						
8.50	11.4				NL	<.2	1	<.2	158/156						
8.50	11.4				NL	<.2	1	<.2	01/179						
8.50	11.4				NL	<.2	2	<.2	115/113						
8.50	11.4				NL	<.2	1	<.2	176/174						
8.50	11.4				NL	<.2	1	<.2	50/48						
8.50	11.4				NL	<.2	1	<.2	151/149						
8.50	11.4				NL	<.2	2	<.2	158/156						
JK/9	14.4	18	0	0.0											old gouges are very faint in new profiles due to
															shoal lee?
KL/10	15.3	13	8	69.2											1.8 m shoal at mid segment sed. waves on shoal crest.
10.55	14.3				34	NC	3	NC	17/15						Gouges on seaward side of shoal.
10.55	14.3				12	NC	2	NC	15/13						
10.55	14.3									NL	2	<.2	18	[illegible]/101	
10.60	14.7				22	NC	3	NC	[illegible]/149						
10.65	14.9									NL	2	<.2	12	[illegible]/102	
10.75	15.0				NL	<.2	3	<.2	[illegible]						

3

688

TESTLINE: 2 | JULIAN DATE: | YEAR: 1977-1978 | TEMPLATE IDENTIFICATION: 1:1.633

TRACKLINE NUMBER: 17 | Length SINGLE GOUGES | Length MULTIPLE GOUGES | CS: 358°T

SEGMENT	WATER DEPTH (M)	TOTAL GOUGES	TOTAL NEW GOUGES	%	NEW SINGLE GOUGES	GOUGE DEPTH (M)	GOUGE WIDTH (M)	RIDGE HEIGHT (M)	Ø (°T)	NEW MULTI. GOUGES	NUMBER OF INCIS.	DEEPEST INCISION (M)	DISRUPT WIDTH (M)	Ø (°T)	Range 125 M COMMENTS
LM/11	15.7	19	13	68.4											sed. dunes - / [illegible]
11.60	16.4				75	NC	2	NC	22/20						
11.70	16.2									105	5	NC	13	33/31	
11.80	16.6				NL	<.2	2	<.2	48/46						
11.85	16.7									NL	4	NC	27	90/88	
11.90	16.3				NL	<.2	2	<.2	112/110						
11.99	16.7				NL	.2	8	.3	87/85						
MN/12	16.7	15	11	73.3											
12.10	16.9				NL	.4	3	<.2	77/75						
12.15	16.9									NL	3	<.2	17	115/113	
12.15	16.9				NL	<.2	1	<.2	99/97						
12.15	16.9				NL	<.2	2	.2	62/60						
12.20	16.8				NL	.2	3	.3	89/86						
12.45	16.9				NL	<.2	2	<.2	90/88						
12.50	17.0									NL	3	<.2	25	90/88	
NO/13	17.5	27	17	60.7											
13.05	17.5				NL	.5	20	.3	90/88						
13.15	17.5				NL	<.2	2	<.2	127/125						
13.25	17.5									35	3	NC	16	27/25	Termination: 205°T
13.30	17.5				NL	.7	10	.8	93/91						
13.35	17.6				NL	.2	4	<.2	103/101						
13.35	17.6				NL	<.2	2	<.2	88/86						
13.35	17.6				NL	.4	8	.2	100/98						
13.40	17.7									NL	2	<.2	8	160/158	
13.95	18.0									NL	6	.5	57	92/90	

5

TESTLINE: 2	JULIAN DATE:	YEAR: 1977-1978	TEMPLATE IDENTIFICATION: 1:1,633

TRACKLINE NUMBER: 17					Length SINGLE GOUGES					Length MULTIPLE GOUGES					CS: 358°T
SEGMENT	WATER DEPTH (M)	TOTAL GOUGES	TOTAL NEW GOUGES	%	NEW SINGLE GOUGES	GOUGE DEPTH (M)	GOUGE WIDTH (M)	RIDGE HEIGHT (M)	Ø (°T)	NEW MULTI. GOUGES	NUMBER OF INCIS.	DEEPEST INCISION (M)	DISRUPT WIDTH (M)	Ø (°T)	Range 125m COMMENTS
OP/14	18.3	17	7	41.2											sed. dunes
14.25	18.3				NL	<.2	2	<.2	89/87						
14.65	18.4				NL	<.2	2	<.2	93/91						
14.99	18.5									NL	5	.5	55	98/96	
P/end	18.5														

TESTLINE: 2 | JULIAN DATE: | YEAR: 1978-1979 | TEMPLATE IDENTIFICATION: 1:1.633

TRACKLINE NUMBER: 31 | CS: 358°T

SEGMENT	WATER DEPTH (M)	TOTAL GOUGES	TOTAL NEW GOUGES	%	Length NEW SINGLE GOUGES	SINGLE GOUGES: GOUGE DEPTH (M)	GOUGE WIDTH (M)	RIDGE HEIGHT (M)	Ø (°T)	Length NEW MULTI. GOUGES	MULTIPLE GOUGES: NUMBER OF INCIS.	DEEPEST INCISION (M)	DISRUPT WIDTH (M)	Ø (°T)	Range = 125 M COMMENTS SS#10 Bots #10a.
AB/0	6.5	9	0	0.0											Poor [illegible] edges of sonar.
BC/1	9.9	6	1	16.7											Ribbons of sediment reworking?
1.15	10.2				NL	<.2	3	<.2	48/46						Sand Ribbons (darker return) with ripples: Trough θ = 64°T
															2m wave length, ht = <.2 m reworking indicated.
CD/2	11.3	25	25	100.0											
2.95	11.4									NL	11	<.2	50	22/20	
2.99	11.3									NL	14	<.2	47	20/18	
DE/3	11.3	44	44	100.0											
3.55	10.1				NL	<.2	3	<.2	57/55						2.5 m shoal at end of segment. Most gouging
3.55	10.1				NL	<.2	2	.3	65/63						on shoal crest Sed waves on seaward side of shoal.
3.60	9.2									25	6	<.2	15	19/17	
3.60	9.2				62	<.2	2	<.2	146/144						
3.65	9.1				NL	<.2	2	<.2	108/106						
3.65	9.1				NL	<.2	1	<.2	125/123						
3.65	9.1				NL	<.2	1	<.2	135/133						
3.70	9.5									NL	27	.2	103	147/145	Pressure Ridge scour
3.75	10.2				NL	.2	3	.2	98/96						
3.75	10.2									NL	2	<.2	7	50/48	Gouges on seaward side of shoal
3.80	11.6				NL	<.2	2	<.2	52/50						
3.85	11.8				NL	<.2	3	<.2	42/40						
EF/4	12.1	12	12	100.0											
4.10	12.3				NL	<.2	2	<.2	73/71						
4.25	12.5				NL	<.2	2	<.2	17/15						
4.25	12.5				NL	<.2	3	<.2	60/59						
4.40	11.8				NL	<.2	2	<.2	109/107						Termination · 287°T
															Sand wave Field.

TESTLINE: 2 | JULIAN DATE: | YEAR: 1978 - 1979 | TEMPLATE IDENTIFICATION: 1: 1.633

TRACKLINE NUMBER: 31 | CS: 358°T

SEGMENT	WATER DEPTH (M)	TOTAL GOUGES	TOTAL NEW GOUGES	%	Length SINGLE GOUGES: NEW SINGLE GOUGES	GOUGE DEPTH (M)	GOUGE WIDTH (M)	RIDGE HEIGHT (M)	Ø (°T)	Length MULTIPLE GOUGES: NEW MULTI. GOUGES	NUMBER OF INCIS.	DEEPEST INCISION (M)	DISRUPT WIDTH (M)	Ø (°T)	COMMENTS
4.40	11.8				NL	<.2	2	<.2	94/92						
4.40	11.8				NL	<.2	2	<.2	130/128						Termination: 128°T
4.50	11.9									NL	4	<.2	10	133/131	
4.50	11.9									NL	2	<.2	4	128/126	
FG/5	13.2	20	1	5.0											reworking of seafloor.
5.60	14.0				NL	<.2	2	<.2	74/72						
GH/6	14.1	6	0	0.0											ICE DETOUR AT END OF LINE
HI/7	15.0	1	0	0.0											Sed. waves indicate reworking of seafloor. θ=195°T λ=2m
IJ/8	14.4	23	20	87.0											3.7 m shoal mid segment. MOST GOUGING on shoal
8.50	13.1				NL	<.2	2	<.2	88/86						Sed. Reworking of old gouges indicated.
8.55	12.0				18	<.2	2	<.2	124/122						Termination: 122°T
8.55	12.0				NL	<.2	3	<.2	164/162						
8.60	11.3									NL	6	<.2	12	03/01	
8.60	11.3				NL	<.2	2	<.2	118/116						
8.60	11.2				NL	<.2	1	<.2	120/118						
8.65	11.6									NL	2	<.2	11	126/124	
8.75	13.1									NL	7	<.2	17	170/168	
JK/9	14.6	1	0	0.0											reworking.
KL/10	15.1	14	9	64.3											1.8 m shoal mid segment.
10.55	13.9									15	5	<.2	7	168/166	Termination: 166°T
10.60	14.2									30	3	NC	7	[illegible]/66	Termination: 156°T
10.95	15.3				NL	.2	3	<.2	113/111						

TESTLINE: 2	JULIAN DATE:	YEAR: 1978-1979	TEMPLATE IDENTIFICATION: 1:1.633

TRACKLINE NUMBER: 31					Length SINGLE GOUGES					Length MULTIPLE GOUGES					CS: 358 °T
SEGMENT	WATER DEPTH (M)	TOTAL GOUGES	TOTAL NEW GOUGES	%	NEW SINGLE GOUGES	GOUGE DEPTH (M)	GOUGE WIDTH (M)	RIDGE HEIGHT (M)	Ø (°T)	NEW MULTI. GOUGES	NUMBER OF INCIS.	DEEPEST INCISION (M)	DISRUPT WIDTH (M)	Ø (°T)	COMMENTS
LM/11	15.5	2	0	0.0											
MN/12	16.3	4	1	25.0											
12.50	16.6				NL	NC	3	NC	115/113						Termination: 113 °T
N/end	NMP														loss of fathogram

1

TESTLINE: 2	JULIAN DATE: 215	YEAR: 1979-1980	TEMPLATE IDENTIFICATION: 1:1.379

TRACKLINE NUMBER: 16

SEGMENT	WATER DEPTH (M)	TOTAL GOUGES	TOTAL NEW GOUGES	%	SINGLE GOUGES: Length NEW SINGLE GOUGES	GOUGE DEPTH (M)	GOUGE WIDTH (M)	RIDGE HEIGHT (M)	Ø (°T)	MULTIPLE GOUGES: Length NEW MULTI. GOUGES	NUMBER OF INCIS.	DEEPEST INCISION (M)	DISRUPT WIDTH (M)	Ø (°T)	CS: 358 °T Range: 125 m COMMENTS SS # 5 Bots # 116
AB/0	6.9	5	0	0.0											
BC/1	9.9	0	0	0.0											
CD/2	11.3	1	0	0.0											Sand waves - Bottom [illegible] crest orien: 160°T λ = 2m
DE/3	11.5	26	21	80.8											2m shoal at midsegment; most gouging on shoal crest
3.15	11.6									NL	4	<.2	27	87/85	
3.45	10.8									32	3	<.2	.8	176/176	
3.45	10.8				20	<.2	1	<.2	174/172						
3.60	9.2									NL	9	.2	36	110/108	Pressure ridge scouring
3.70	10.1				NL	<.2	2	<.2	47/45						
3.70	10.1				37	<.2	1	<.2	128/126						
3.70	10.1				NL	<.2	2	.2	80/78						
3.75	10.9				44	<.2	3	<.2	05/03						
EF/4	12.2	9	0	0.0											
FG/5	13.3	1	1	100.0											
5.45	13.7				NL	<.2	2	<.2	40/38						Termination: 218°T
GH/6	14.1	7	2	28.6											Tick Marks - λ = 2m
6.60	14.5				NL	<.2	7	<.2	71/69						Tick Marks - λ = 2m
6.75	14.7				NL	<.2	5	<.2	79/77						
HI/7	15.0	7	1	14.3											change template 1:1.633
7.70	14.4				NL	<.2	2	<.2	140/138						sand waves [illegible] 68°T λ = 2m

694

TESTLINE: 2 | **JULIAN DATE:** 215 | **YEAR:** 1979-1980 | **TEMPLATE IDENTIFICATION:** 1:1.633

TRACKLINE NUMBER: 16 | **CS:** 358 °T

					Length SINGLE GOUGES					Length MULTIPLE GOUGES					
SEGMENT	WATER DEPTH (M)	TOTAL GOUGES	TOTAL NEW GOUGES	%	NEW SINGLE GOUGES	GOUGE DEPTH (M)	GOUGE WIDTH (M)	RIDGE HEIGHT (M)	Ø (°T)	NEW MULTI. GOUGES	NUMBER OF INCIS.	DEEPEST INCISION (M)	DISRUPT WIDTH (M)	Ø (°T)	COMMENTS
IJ/8	14.2	17	14	82.4											3.7 m shoal at mid segment gouging on shoal.
8.45	13.0				NL	<.2	2	<.2	110/108						Termination: 288°T
8.50	12.5				NL	<.2	2	<.2	91/89						
8.50	12.0									NL	4	.2	14	115/113	Termination: 293°T
8.55	11.5									NL	4	<.2	15	120/118	Termination: 298°T
8.60	11.3				NL	<.2	4	<.2	93/91						
8.65	12.2				NL	<.2	3	<.2	109/107						
8.65	12.2				NL	<.2	2	<.2	72/70						
8.75	14.2				NL	<.2	2	<.2	55/53						
JK/9	14.2	0	0	0.0											
KL/10	15.0	3	2	66.7											2 m shoal at mid segment 1 new gouges seaward side.
10.60	14.4				NL	<.2	1	<.2	124/122						
10.65	14.7				NL	<.2	2	<.2	138/136						Termination: 136°T
LM/11	15.1	3	1	33.3											
11.05	15.1				NL	<.2	1	<.2	122/120						
MN/12	16.2	6	4	66.7											
12.40	16.5				NL	<.2	4	<.2	127/125						
12.70	16.4				NL	<.2	2	<.2	58/56						
12.80	16.7				NL	.3	3	.3	73/71						
12.95	17.2				NL	<.2	3	<.2	66/64						
															end of 1979 records
N/end	16.9														

TESTLINE: 2	JULIAN DATE: 216	YEAR: 1980-1981	TEMPLATE IDENTIFICATION: 1:1,633

TRACKLINE NUMBER: 26					Length SINGLE GOUGES					Length MULTIPLE GOUGES					CS: 358°T
SEGMENT	WATER DEPTH (M)	TOTAL GOUGES	TOTAL NEW GOUGES	%	NEW SINGLE GOUGES	GOUGE DEPTH (M)	GOUGE WIDTH (M)	RIDGE HEIGHT (M)	Ø (°T)	NEW MULTI. GOUGES	NUMBER OF INCIS.	DEEPEST INCISION (M)	DISRUPT WIDTH (M)	Ø (°T)	Range = 125 m COMMENTS SS #14 Bots #18
AB/0	7.0	8	2	25.0											Fathogram malfunction until segment 7 (HI).
0.10	7.3				NL	<.2	5	<.2	83/81						Better resolution on 1981 sonar than 1980. Accounts for gouge total difference.
0.60	—				NL	<.2	4	<.2	50/88						Termination: 266°T
CC/1	—	8	5	62.5											
1.05	—				NL	<.2	2	<.2	77/75						Termination: 255°T
1.15	—				NL	<.2	2	<.2	66/64						
1.35	—				NL	<.2	2	<.2	47/44						
1.35	—				NL	<.2	2	<.2	75/73						
1.70	—				NL	<.2	2	<.2	53/51						
CD/2	—	4	2	50.0											
2.10	—				NL	<.2	2	<.2	69/67						
2.99	—				NL	<.2	2	<.2	77/75						
DE/3	—	29	25	86.2											2.3 meter shoal at midsegment. Most
3.05	—				NL	<.2	2	<.2	97/95						gouging on shoal crest.
3.45	—									NL	2	—	23	[illegible]/88	
3.50	—									NL	5	<.2	15	128/126	
3.60	—				NL	<.2	3	<.2	47/45						
3.50	—				NL	<.2	3	<.2	127/125						
3.50	—									NL	3	NC	20	127/125	Termination: 125°T
3.65	—									NL	2	NC	15	119/117	Termination: 117°T
3.60	—									NL	4	NC	17	125/123	Termination: 123°T
3.60	—									NL	2	<.2	9	102/100	
3.60	—									NL	2	<.2	8	115/113	
3.65	—				NL	<.2	3	<.2	125/123						
3.70	—				NL	<.2	3	<.2	69/67						

TESTLINE: 2	JULIAN DATE: 216	YEAR: 1980-1981	TEMPLATE IDENTIFICATION: 1:1,633

TRACKLINE NUMBER: 26 — CS: 358°T

SEGMENT	WATER DEPTH (M)	TOTAL GOUGES	TOTAL NEW GOUGES	%	Length SINGLE GOUGES: NEW SINGLE GOUGES	GOUGE DEPTH (M)	GOUGE WIDTH (M)	RIDGE HEIGHT (M)	Ø (°T)	Length MULTIPLE GOUGES: NEW MULTI. GOUGES	NUMBER OF INCIS.	DEEPEST INCISION (M)	DISRUPT WIDTH (M)	Ø (°T)	COMMENTS
EF/4	—	9	7	77.8											
4.05	—				NL	<.2	1	<.2	95/93						
4.15	—				NL	<.2	2	<.2	32/30						
4.25	—				NL	—	4	—	106/104						
4.35	—				NL	NC	4	NC	170/168						Termination: 168°T
4.60	—				NL	<.2	2	<.2	83/81						
4.60	—				NL	<.2	2	<.2	107/105						
4.85	—				NL	<.2	2	<.2	92/90						
FG/5	—	8	6	75.0											
5.05	—				NL	<.2	3	<.2	120/118						Termination: 118°T
5.15	—				NL	<.2	2	<.2	124/122						
5.15	—				NL	<.2	2	<.2	117/115						
5.20	—				NL	<.2	2	<.2	115/113						
5.95	—				NL	<.2	1	<.2	55/53						
5.99	—				NL	<.2	1	<.2	105/103						Continues into next segment.
GH/6	—	6	2	33.3											
6.01	—				NL	<.2	1	<.2	105/103						
6.65	—				NL	<.2	2	<.2	107/105						
HI/7	14.6	0	0	0.0											
IJ/8	14.3	14	14	100.0											3.5 meter shoal at mid segment. Most gougings on shoal crest.
8.40	12.3				NL	<.2	3	.2	125/123						
8.45	11.5				NL	<.2	4	<.2	88/86						
8.45	11.5				NL	.2	3	.2	132/130						
8.45	11.5				NL	<.2	3	.2	135/133						

TESTLINE: 2			JULIAN DATE: 216			YEAR: 1980 - 1981				TEMPLATE IDENTIFICATION: 1: 1.633					
TRACKLINE NUMBER: 26					Length SINGLE GOUGES					Length MULTIPLE GOUGES					CS: 358°T
SEGMENT	WATER DEPTH (M)	TOTAL GOUGES	TOTAL NEW GOUGES	%	NEW SINGLE GOUGES	GOUGE DEPTH (M)	GOUGE WIDTH (M)	RIDGE HEIGHT (M)	Ø (°T)	NEW MULTI. GOUGES	NUMBER OF INCIS.	DEEPEST INCISION (M)	DISRUPT WIDTH (M)	Ø (°T)	COMMENTS
8.50	11.1				NL	.2	3	.2	35/36						
8.50	11.1				NL	<.2	1	<.2	52/50						
8.55	11.5				NL	<.2	3	<.2	56/54						
8.70	13.0									NL	2	.2	9	124/122	
8.75	13.3				NL	<.2	2	<.2	58/56						
8.75	13.3				NL	<.2	1	<.2	50/48						
8.80	13.4				NL	<.2	1	<.2	123/121						
8.80	13.4									NL	2	<.2	19	128/126	
JK/9	14.0	7	7	100.0											
9.05	14.0				NL	.2	3	.2	90/88						
9.10	14.0				NL	<.2	3	<.2	82/80						
9.10	14.0				NL	.4	5	.5	112/110						Termination: 110 °T
9.15	14.5				NL	<.2	3	<.2	48/46						
9.25	14.6				15	<.2	2	<.2	128/126						
9.40	14.8				NL	.2	2	<.2	95/93						
9.45	14.7				NL	<.2	4	<.2	110/108						Termination: 108°T
KL/10	15.0	7	7	100.0											1.4 m Shoal at mid segment.
10.50	14.1				NL	.2	5	.3	53/51						
10.50	14.1				NL	<.2	6	.2	118/116						
10.50	14.1				NL	<.2	6	<.2	117/115						
10.75	15.0									NL	2	<.2	23	110/108	
10.85	15.3				NL	<.2	2	<.2	174/172						
10.90	15.3				NL	<.2	2	<.2	168/176						

TESTLINE: 2 | JULIAN DATE: 216 | YEAR: 1980-1981 | TEMPLATE IDENTIFICATION: 1:1.633

TRACKLINE NUMBER: 26 | Length SINGLE GOUGES | Length MULTIPLE GOUGES | CS: 358°T

SEGMENT	WATER DEPTH (M)	TOTAL GOUGES	TOTAL NEW GOUGES	%	NEW SINGLE GOUGES	GOUGE DEPTH (M)	GOUGE WIDTH (M)	RIDGE HEIGHT (M)	Ø (°T)	NEW MULTI. GOUGES	NUMBER OF INCIS.	DEEPEST INCISION (M)	DISRUPT WIDTH (M)	Ø (°T)	COMMENTS
LM/11	15.3	15	14	93.3											
11.15	15.6				NL	<.2	3	<.2	95/93						
11.30	15.5				NL	NC	4	NC	168/166						Termination: 034°T (186 38)
11.35	15.5				NL	.3	10	.3	119/117						
11.55	16.0				NL	.2	13	<.2	112/110						
11.60	16.0				NL	.5	10	.4	100/98						
11.65	16.0				NL	.2	2	<.2	100/98						
11.70	16.4				NL	<.2	1	<.2	118/116						
11.80	16.0				NL	.4	5	.5	101/99						
11.85	16.0				NL	<.2	3	<.2	102/100						
11.90	15.3				NL	<.2	2	<.2	103/101						
11.90	15.5				NL	.8	3	<.2	113/111						
11.95	15.8				NL	1.4	8	.9	69/67						
11.95	15.9				NL	.3	4	.3	106/104						
11.95	15.9				NL	.2	2	.4	109/107						
NW/12	16.0	23	19	82.6											
12.01	16.0				NL	.2	2	<.2	122/120						
12.20	16.4				NL	<.2	2	<.2	111/109						
12.25	16.8				NL	.2	5	<.2	66/64						
12.25	16.8				NL	.2	3	.2	133/131						
12.30	16.7				NL	<.2	2	<.2	135/133						
12.35	16.6				NL	.2	3	.2	70/72						
12.35	16.6				NL	<.2	3	<.2	123/121						
12.35	16.6				NL	.2	2	<.2	74/72						
12.40	16.6				NL	.2	2	.2	36/34						
12.45	16.6				NL	<.2	2	<.2	163/161						
12.50	16.4				NL	<.2	2	<.2	00/178						maintains length of segment.

700

TESTLINE: 2 | **JULIAN DATE:** 216 | **YEAR:** 1980-1981 | **TEMPLATE IDENTIFICATION:** 1: 1.633

TRACKLINE NUMBER: 26 | **CS:** 358°T

SEGMENT	WATER DEPTH (M)	TOTAL GOUGES	TOTAL NEW GOUGES	%	SINGLE GOUGES (Length): NEW SINGLE GOUGES	GOUGE DEPTH (M)	GOUGE WIDTH (M)	RIDGE HEIGHT (M)	ø (°T)	MULTIPLE GOUGES (Length): NEW MULTI. GOUGES	NUMBER OF INCIS.	DEEPEST INCISION (M)	DISRUPT WIDTH (M)	ø (°T)	COMMENTS
12.80	17.2				NL	<.2	3	<.2	114/112						
12.85	17.0									NL	3	<.2	25	107/105	
12.90	17.0				NL	<.2	2	<.2	107/105						
12.90	17.0				NL	.2	5	<.2	70/68						
12.99	17.2									NL	2	.3	25	80/78	
NO/13	17.2	16	8	50.0											
13.01	17.2				NL	<.2	4	<.2	103/101						
13.25	17.4				NL	.2	4	.2	92/90						
13.30	17.5				NL	.3	5	.3	116/114						
13.50	17.5				NL	<.2	2	<.2	121/119						
13.65	17.8				NL	.2	3	<.2	129/127						
13.80	18.0				NL	<.2	3	<.2	98/96						
13.90	17.8				NL	<.2	4	<.2	97/95						
13.95	17.7				NL	.2	2	<.2	120/118						
0/end	17.4														

RATES OF SEDIMENT DISRUPTION BY SEA ICE AS DETERMINED FROM CHARACTERISTICS OF DATED ICE GOUGES CREATED SINCE 1975 ON THE INNER SHELF OF THE BEAUFORT SEA, ALASKA

by

Peter W. Barnes and Douglas M. Rearic

TABLE OF CONTENTS

LIST OF FIGURES

LIST OF TABLES

RATES OF SEDIMENT DISRUPTION BY SEA ICE AS DETERMINED FROM CHARACTERISTICS OF DATED ICE GOUGES CREATED SINCE 1975 ON THE INNER SHELF OF THE BEAUFORT SEA, ALASKA

by Peter W. Barnes and Douglas M. Rearic

ABSTRACT

Repetitive sidescan sonar and precision bathymetric surveys made between 1975 and 1980 were used to assess seafloor changes due to ice gouging along 8 shore-perpendicular corridors, and to gain insight into the question of when, where, and how gouges are produced on the inner shelf of the Beaufort Sea. The percentage of seafloor area impacted annually by ice keels increases from the coast seaward to at least the 25-m isobath, the offshore limit of repeated surveys. Up to 6.8 % of the total seabed area scanned along the roughly 15 km-long corridors was disrupted in a single year. Total seafloor disruption in single km-long segments ranged as high as 60 %. The maximum new gouge incision depth measured is 1.4 m. High gouge densities are associated with wide, shallow "multiplet" gouging events, where long sections of pressure-ridge keels raked the bottom. Small annual variations in the amount and intensity of new gouges indicate rather consistent reworking of the inner shelf by this process. Where shoals occur within survey corridors our seafloor monitoring has documented the predicted sheltering of seafloor areas on the landward side.

INTRODUCTION

Ice interaction with the seafloor forms gouges which influence the sedimentarty structures, morphology and sediment transport on the shelves off northern Alaska (Reimnitz and Barnes, 1974, Toimil, 1978, Barnes and others, 1984). Ice gouges and the gouging process are important considerations for the safty and design of pipelines (Weeks and others, 1984) and for foundations relying on the seabed for stability (Bea and others, 1985). Pipelines will have to be protected from the impact of ice on the seabed either by burial or by defensive strategies such as berms or armor. Seafloor morphology influences the lateral shear resistance of bottom founded structures such as mobile exploration islands as the bond with the seafloor may occur through discontinuous sediment contact points formed by ice gouge ridges and troughs. The intensity of ice gouging is also an important indication of the rate and intensity of ice/seafloor interaction on the shelf. The size, shape and frequency of gouging is reflected in the size shape and frequency of ice contacts with the bottom. In addition the gouge parameters reflect the creation of ice keels of sufficient draft and strength to form gouges.

In this report we present data on the rate and character of ice gouging in the fast ice and inner stamukhi zone (Reimnitz and others, 1978), from a series of repetitive seabed observations extending over 8 years at 8 different sites (Figure 1 and Table 1).

We detail their numbers, depth, width and orientation. These repetitive observations have allowed us to document the year to year variability of ice gouge processes and to determine the relationship to changes in ice zonation that occur from year to year. The results are discussed in light of sediment reworking and in relation to the ice regime. We also present preliminary speculations on the rates of gouging in relation to other sedimentary processes acting on arctic shelves.

Our data are from the inner shelf where open water conditions are most common and where the limited range of our precise navigation equipment is most useful. Thus our observations are biased toward shallow water by the data base (average water depth-15m). We would expect different results when repetitive data are gathered from deeper water where ice and sediment conditions will certainty be different (Reimnitz and others, 1978, Barnes and Reimnitz, 1974).

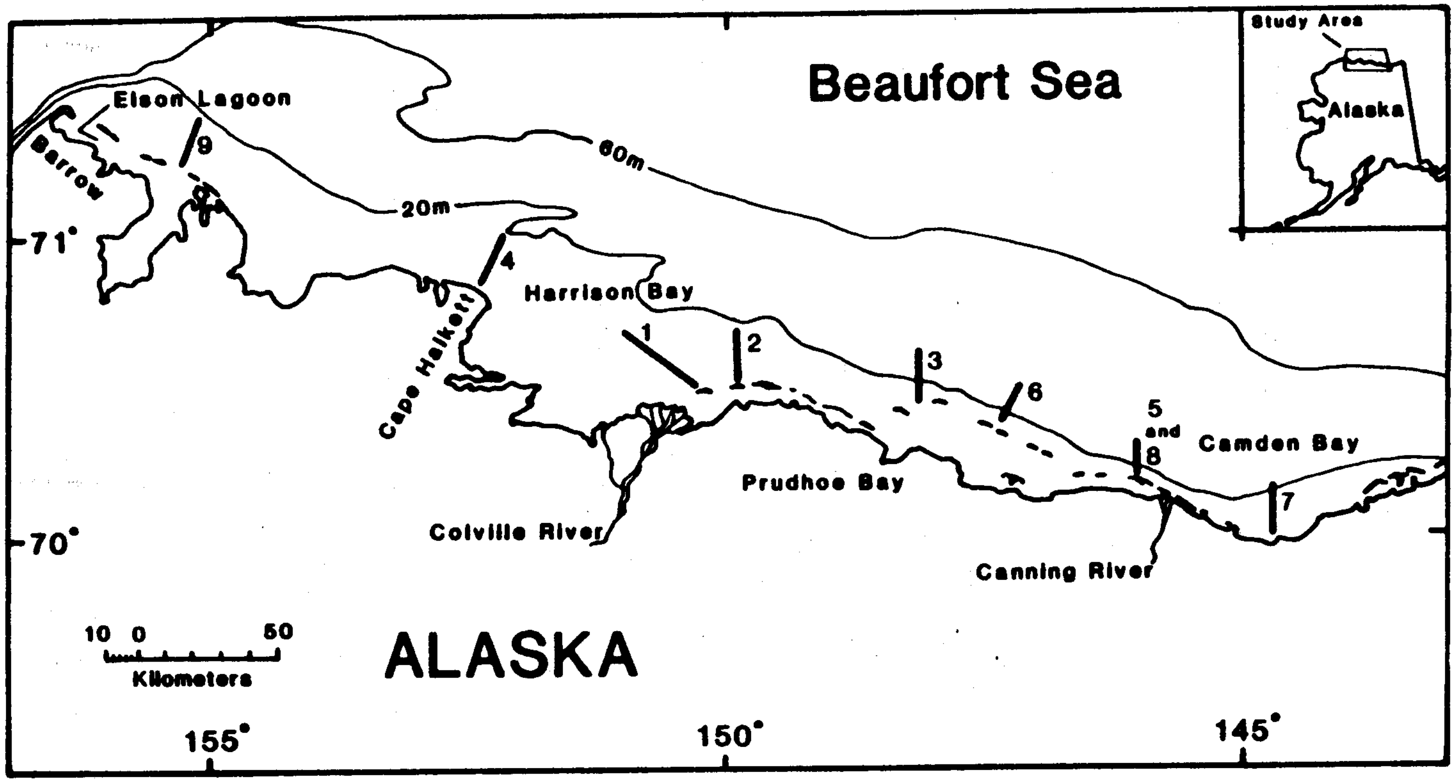

Fig. 1 Location map indicating corridor locations and generalized bathymetry for the Alaskan Beaufort Sea.

TABLE 1.

Location and timing of corridor surveys - Data documentation

Corridor	Baseline Length*	Geographical Name	Survey Year	Time Between Surveys	Trackline Number	Sidescan Roll #	Fathometer Roll #
1	None	Thetis Is.	1975	Base Year			
			1976	1			
			1977	1	35	8	7
			1978	1	14,19	5	8,10
			1979	1	13,33	8,12	9,10b
			1980	1	17	6	12
			1981	1	27	14	18,19
			1982	1	16	8	10
2	None	Spy Is.	1975	Base Year			
			1976	1			
			1977	1	31	6	6
			1978	1	17	5	9
			1979	1	31	10	10a
			1980	1	16	5	11b
			1981	1	26	14	18
3	14936m	Cross Is.	1975	Inadequate data			
			1979	Base Year	92	27	33
			1982	3	12	6	8
4	12622m	Cape Halkett	1977	Base Year	39	12	10
			1978	1	10,11	4	7
			1980	2	20	7	14,15
			1982	2	4	2	2
5	16744m	Flaxman Is.	1979	Base Year	44	15	14
			1980	1	25	9	17
6	21926m	Karluk Is.	1979	Base Year	77	23	27
			1980	1	24	9	17
			1981	1	18	10	13
			1982	1	6	3	3
7	13544m	Camden Bay	1981	Base Year	15	9	11
			1982	1	8	4	5
8	18430m	Flaxman Is.	1981	Base Year	16	9	12
			1982	1	7	3	4
9	17639m	Cooper Is.	1978	Base Year	8	3	5
			1982	4	1	1	1

* Baseline distance is measured between the two shore based navigations stations.

Data Sources (Table 1 continued)

Reports containing data, locations, log sheets, and methodology (records often on microfilm).

Year Collected	Open-File Report No.	Authors
1975	none	
1976	79-766	Reimnitz, Barnes, and Maurer
1977	78-1066	Maurer, Barnes, and Reimnitz
1978	79-384	Reimnitz, Barnes, and Kempema
1979	80-603	Barnes, Reimnitz, Kempema, Minkler, and Ross
1980	81-241	Kempema, Reimnitz, and Barnes
1981	82-586	Minkler, Reimnitz, and Barnes
1982	83-493	Kempema, Barnes, Reimnitz, Asbury, and Rearic

Copies of the Open-files are available at Open Files Services Section, Branch of Distribution, Box 25425, Federal Center, Denver, CO 80225.

Complete microfilm copies of all geophysical records, ships log and computer listings of navigational way ponts, can be obtained from the National Geophysical and Solar-Terrestrial Data Center, NOAA, Boulder CO, 80303.

The original records are archived at the U.S. Geological Survey, Branch of Pacific Marine Geology, 3475 Deer Creek Road, Palo Alto, CA 94304.

Background -

Earlier studies of the rates of ice gouging based on repetitive observations of the seafloor inshore of 20 meters indicated that sea ice presently interacts with the sea bed forming gouges (Lewis, 1977, Reimnitz and others, Barnes and others, 1978). In these previous studies gouging was ubiquitous in the areas studied although data from one study suggested that sediment reworking by waves and currents is important to gouge morphology on the inner shelf inshore of 13m (Barnes and Reimnitz, 1979).

Most ice gouges form in winter when a semi-ridged ice sheet integrates atmospheric and oceanic energy over a large area and allows this energy to be transmitted through the ice canopy and focused on the continental shelf. Here the energy is expended in forming ice ridges and in gouging the sea floor (Barnes and others, 1978; Thomas and Pritchard, 1980). The semi-ridged winter ice sheet allows more energy to be focused at grounded ice keels in winter than would be available during the summer when a discontinuous ice sheet diffuses atmospheric and oceanic energy over smaller areas and distances. In the summer waves and currents are often the only forces acting on isolated grounded ice blocks.

The earlier repetitive surveys mentioned above have shown the rates of seabed reworking by ice for the Canadian shelf and the shelf off northern Alaska to be on the order of 2% each year with depths of incision ranging up to 120 cm but averaging less than 20cm.

The ice regime in the study area is discussed by Kovacs and Mellor (1974) and by Reimnitz and others (1978). Briefly, the ice environment is composed of a relatively stable winter 'fast' ice sheet up to 2m thick inshore of a zone of discontinuously grounded shear and pressure ridges called the stamukhi zone. The outer edge of the fast ice and the inner edge of the stamukhi zone form in water depths of 15 to 25m. The boundary is typically composed of linear ridges which parallel the isobaths. Isolated grounded ridges and grounded ice blocks may occur inside of the stamukhi zone. In particular, a stamukhi zone boundary has, on occasions, developed along the 10 meter isobath in Harrison Bay (Reimnitz and others, 1978).

The stamukhi zone is significant in that the atmospheric and oceanic energies imparted to moving offshore polar ice pack are, primarily expended against the continent within this zone. In this regard the stamukhi zone could be thought of as the winter "surf" zone of the Beaufort Shelf. The expenditure of energies results in higher numbers of pressure and shear ridges than elsewhere in the Beaufort (Weeks and others, 1980) and an intensely gouged seafloor (Barnes and others 1984). Inshore of the stamukhi zone, gouging is expected to be less intense and less frequent due to the expenditure of energy by ridge building and gouging processes within the stamukhi zone. Our study is focused primarily on the area inshore of the stamukhi zone and provides only a glimpse of the rates and character of gouging at the inner margin of the zone. The expenditure of energy and rate of ice gouging is expected to drastically increase seaward of our data set in the stamukhi zone (Barnes and others, 1978, 1984).

METHODS

A 42 foot research vessel was used to run repetitive surveys. The basic objective was to establish tracklines which could be reoccupied in subsequent years. The subsequent trackline observations or line sets from the same or nearly the same corridor forms the basic data for this report. The navigation and depth observations were correlated with sidscan sonar data (Belderson and others, 1972) which covered a swath of seafloor 125 meters wide on either side of the trackline. This resulted in a "corridor" of the seafloor which was resurveyed in subsequent years. We have arbitrarily numbered these corridors depending on the year in which the initial data were collected (Figure 1 and Table 1).

Navigation

The location of the survey vessel for the initial two survey corridors (1 & 2) was determined by aligning the vessel with two in line range marks several kilometers apart and measuring the vessels distance from one of the ranges (Figure 2). With this technique we were able to carry the line seaward from the islands in excess of 20 kilometers achieving position accuracies of better than 20 meters. The technique was occasionally aided by a thermal inversion which created a "mirage" causing the range markers to appear higher above the horizon and thus visible at greater distances. The common summer fog has made the routine re-occupation of corridors one and two difficult and time consuming. As a result of this problem and the lack of appropriate range marks, the remainder of the corridors were navigated using precision range-range electronic navigation alone (Table 2). These navigation systems typically give precision ranges to a few meters and repeatable locations within about 10 meters. For simplicity we chose benchmarks and survey lines such that the corridors could be run equidistant from the two shore stations. This meant that the boat operator and navigator were required to keep the vessel equidistant from both shore stations by maintaining the same range from each station.

Ice gouge measurements

The enumeration of new gouges was accomplished through the comparison of sonograph records and fathograms in one kilometer intervals. The starting point for counting began either on

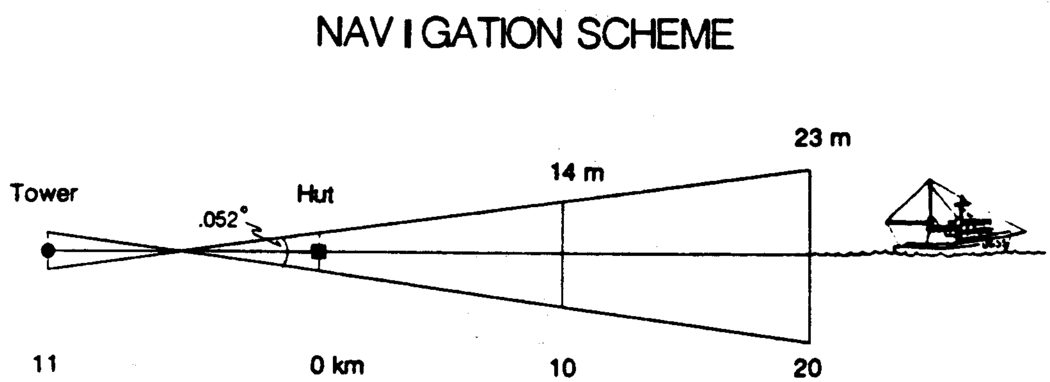

Fig. 2 Navigation scheme used on corridors 1 & 2 indicating the errors likely to be experienced in aligning the ranges with good visibility.

Table 2

Ranges and benchmarks used for navigating along corridors

Corridor	Course	Navigation (Shore Stations)	Remarks
1	305 T	1) Thetis Is. Benchmark (˜ 10m south of hut) 2) Oliktok Pt. 300ft. Tower	Range alignment of Oliktok tower and Thetis Island hut. Distance along line is measured from Thetis Is. or Oliktok.
2	358 T	1) Spy Is. benchmark (under 1950's wooden tower) 2) Oliktok Pt. 300ft. Tower	Range alignment of Oliktok tower and tower over Spy Island bench mark. Distance along line measured from Spy Island or Oliktok.
3	000 T	1) Reindeer Is. tower (USGS tower at Humbolt C-1 well- (lat. 79 29'12"; long. 148 20' 25") 2) Cross Is. (top of USCG RACON tower)	Line is run equidistant from Reindeer and Cross Island.
4	027 T	1) Cape Halkett RACON tower 2) Northeast corner of the sod hut at Esook.	Line is run equidistant offshore from the two stations.
5			One shore location has been lost and the corridor has not been resurveyed.
6	028 T	1) Pole Is. (USGS 50ft. tower) 2) Narwhal Is. (150ft. tower)	Line is run equidistant from Pole and Narwhal Island stations.
7	000 T	1) "Collinson Point" benchmark	Line is run equidistant from the two stations.

		2) Benchmark "Koganak" (~ 13.2km east of "Collinson Point")	
8	006 T	1) Brownlow Point RACON tower 2) Benchmark "Roda" near Point Thompson	Line is run equidistant from the two stations.
9	020 T	1) Cooper Is. NOS benchmark 2) Igilik Is. NOS benchmark	Line is run equidistant from the two stations.

the range/range baseline or one kilometer offshore from a barrier island or coast. One kilometer intervals were scaled off seaward on the navigation charts and the time the vessel crossed the kilometer points was determined. These times were then used to correlate the sonographs and fathograms with the navigation at the established intervals. As pointed out in Wolf and others (1983) systematic errors did occur. Therefore, seabed ice gouge "matches" on sonographs were used wherever possible to establish comparisons between records.

Side-scan sonar records from sequential years were used to determine the number of new (datable) gouges occurring during the year or more interval since the previous survey. The total number of gouges in each segment was also determined. The percent of new gouges to the total was calculated for each interval. Other measurements taken from the sonographs included gouge orientation, gouge width, disruption width of multiplet gouges, and length of gouges (See Barnes and others, 1984, for explanation). The location of each new gouge along the trackline was determined (+/-50 meters) and will allow us to monitor sedimentary processes in the vicinity of the gouge in future years.

Fathogram records were used to determine the maximum depth of the new gouges below the seafloor, maximum height of ridge of plowed sediments from the new gouge, and the water depth at which the new gouge occurred. In the case of multiplet gouges only the deepest incision was measured.

The problem of small gouges

In many cases we were able to resolve individual gouge features on the sonographs that we could not resolve on the fathograms, except to note that the gouge was smaller than we could resolve on most of our fathograms (20 cm). For the large percentage of the new gouges (>60%) that fell into this unresolvable category, we assumed a depth of 10 cm for purposes of our statistical calculations. The assumed depth is probably less than the actual gouge depth for these gouges as the limit of resolution of the sonographs is also near 10cm (based on wavelength), thus the incision depths of the gouges observed on the sonographs and not resolved on the fathograms should fall between 10 and 20cm. From the above it follows that there also exist gouges that are smaller than the 10 to 20 cm resolution of our instruments. These gouges are not accounted for in our data.

Other observations

Observations of interest were noted in the comments column of the data sheets (Appendix). Ice gouge termination directions were determined which indicate the direction of ice keel movement during a gouging event. Sediment wave orientations were determined whenever observed on the sonographs as these have a direct application to sediment movement and infilling. On some corridors, older gouges formed in cohesive sediments are reexposed when non-cohesive sediment cover is redistributed by waves and currents (Barnes and Reimnitz, 1979). These gouges could be misinterpreted as new gouges and counted in the datable gouge population.

Subjectivity of analysis

Due to many factors, such as record quality, navigational accuracy, ice conditions, etc., enumeration of ice gouge data is a subjective task varying significantly between individuals. In this study, we found that new gouges in water depths of less than about 15 m were generally easy to resolve on the sonograph records and thus least subjective. Dated gouges in water depths greater than 15 m required more subjective decisions due to increased gouge densities (>100/km) on the seafloor and resultant complexity of seafloor morphology at these depths.

To keep the subjectivity consistent throughout the data set , the second author enumerated all of the gouge records. Even with this precaution the data exhibit some inconsistencies, particularly with regard to the number of gouges. Examination of the appendix will show segments where the total number of gouges increases from one year to the next by a number greater than the "new" gouge count.

Occasionally assumptions were made regarding what constituted a datable gouge. Areas exist where there were poor "matches" between sequential sonographs due to deviations from trackline, an extended time between resurveys (generally 2 years or more), or extensive hydraulic reworking of the bottom. In these areas, other criteria were used to determine what gouges could be dated. Superposition of gouges on older gouges, the fresh or crisp appearance of gouge trough and ridge morphology, and gouge orientation parallel to other gouges of the same age were used in determining whether a gouge was considered to have been formed since the last survey of the trackline and was, thus, datable. We estimate that these criteria were used in less than 10% of the 1 km segments and that only 30% of the dated gouges within these segments were accounted for by this method.

Reality of Year-to-year differences in ice gouge parameters

In addition to the year to year variability of ice gouge interaction with the seafloor due to the variability of natural processes, artificial factors based on the survey techniques and data quality enter into the comparative analysis. Ice conditions varied from year to year influencing the length of the survey lines and the ability to reoccupy these lines without "ice detours". In addition some datable gouges may have gone uncounted due to poor record quality, or to rapid infilling or to deviations from the desired trackline. Data summarized for entire tracklines are not strictly comparable area to area or year to year as differing line lengths represent unequal portions of the ice gouge environment.

Variable record quality leads to uncertain correlation from year to year which may have resulted in calling gouges "new" and datable when in reality they may have been poorly defined on previous records. We estimate that at most about 25% overcounting of the gouges may have resulted but that these gouges would consist primarily of the small short and shallow gouges which are the least clear on the sonographs and fathograms in all water depths. We also note that since the initiation of the repetitive surveys in 1975 the quality of our records has improved due to growing skills with the equipment and to advances in equipment design. Thus in recent years seabed morphology was visible in greater detail. This means that the number of "new" features may have increased due to this artificial factor.

RESULTS - OBSERVATIONS and DISCUSSION

The morphologic environments for each of the corridors varied considerably. The corridors were resurveyed during the open water seasons from 1977 to 1982, although only a few years of record are available in some corridors (Table 1). As other workers may wish to reoccupy these corridors the methods of navigation and the location of the shore stations used in surveying each of the lines is given in Table 2. The corridors are described from west to east (Figure 1). The raw data are given in the appendix, and data summaries are shown in Table 3 and Figures 3 through 11.

Corridor 9 - This corridor extends northeast from a chain of sand and gravel islands stretching east from Point Barrow (Figure 1). Depths quickly increase to 5m seaward of the islands then steadily increase seaward such that the 20 m contour is crossed more than 12 km from the islands (Figure 3). There are no noticeable shoals or steps along this trackline. The bottom sediments in this area are muds and muddy sands with the coarser sediments generally occurring further inshore.

Corridor 4 - Another northeast trending corridor which starts in shallow water offshore from a coastline with 1 to 2 meter high tundra bluffs. The waters gradually increase in depth to about 15m where a 1to 2m high shoal exists(Fig. 4a & b). The seafloor continues to deepen seaward from here to depths of 19m, 24 km from shore, then rises a few meters over a broad shoal at the outer end. The sediments along this corridor are characterized as muddy sands and sandy muds, although there is no onshore/offshore pattern.

Corridor 1 - One of our oldest corridors, originally established in 1973 (Reimnitz, and others, 1977), and one for which we have the most repetitive surveys (Table 2). The trackline extends northwest from Thetis Island on the eastern side of Harrison Bay (Figure 1). The bottom drops quickly to 7 m seaward of the island, then gently and rather uneventfully to water depths of 15 or more meters in the central part of Harrison Bay (Figure 5 and 6). The sediments along this corridor are sands and muddy sand inshore; offshore the porportion of muds increases.

Corridor 2 - Extending north from Spy Island in the northeast corner of Harrison Bay, this older corridor (established in 1975) is marked by 2 to 3m high sand shoals in water depths of 12 to 15m (Figure 6 and 7) before reaching its seaward limit at water depths near 20m. Except for the sand shoals the sediments along this corridor are sandy muds which generally become finer in a seaward direction.

Corridor 3 - Although also established in 1975, this corridor has been seldom repeated due to the persistence of ice in this area. The corridor extends north equidistant from Cross and Reindeer Islands, offshore of the Prudhoe Bay area (Figure 1). The bottom profile in this corridor is steeper than on the corridors to the west (above), as are the profiles from here eastward to Camden bay (Figure 8). Proceeding seaward, corridor 3 crosses a mound 4 m high in 13m of water then drops to about 19 m before rising gradually to a small shoal or bench between 18 and 22m water depth (Barnes and Asbury, 1985). The mound is composed of sands and gravels while the sediments elsewhere along the corridor are sandy muds and muds. Just inshore of the break in slope at 18 to 22m the bottom sediments are an over consolidated mud, which is common here and elsewhere on the shelf (Reimnitz and others, 1980).

Corridor 6 - Extending northeasterly from the chain of islands north and east of Prudhoe Bay (Figure 1), this corridor's steep profile crosses a bench at 18m and continues dropping to water depths of more than 25m (Figure 9). The sediments in this area are quite varied and are commonly over- consolidated. Sediment descriptions include pebbly clays and stiff sandy muds. At the innermost end of the corridor boulders up to 50cm in diameter have been observed on underwater TV.

Testline 9-COOPER ISLAND

Kilometers	0	1	2	3	4	5	6	7	8	9	10	11	12	13	14	15	16			
Water Depth (m)	6.0	7.7	8.5	9.3	10.0	10.9	11.8	12.4	13.0	13.5	14.0	14.6	15.4	16.2	17.0	18.2	18.7			
No. of New Gouges (m)																		Total	avg/Km	
1978-1982	7	10	16	1	7	5	23	18	12	2	11	4	7	12	16	7	.	158	9.9	
Maximum Gouge Depth (m)																		Deepest		
1978-1982	.1	.3	.3	.3	.6	1.1	1.1	.7	.9	x	.2	x	x	x	x	x		.1		
Total Disruption Width (m)																		Total	avg/Km	% disturbed (in 4 yr)
1978-1982	19	53	71	13	49	51	159	147	132	23	83	43	72	107	142	86		1250	78.1	7.8

Total No. of New Gouges = 158 Deepest New Gouge = 1.1 m Total Disruption Width = 1250 m Mean % disturbed = 2.0

Testline 4-CAPE HALKETT

Kilometers	0	1	2	3	4	5	6	7	8	9	10	11	12	13
Water Depth (m)	x	3.2	5.1	6.8	7.8	8.7	9.5	10.4	11.0	11.9	12.5	13.1	14.0	14.7
No. of New Gouges														
1977-1978	x	4	6	7	4	4	6	5	4	6	11	24	5	19
1978-1980	x	5	3	0	4	4	5	9	x	x	52	20	10	21
1980-1982	x	x	0	0	3	1	1	6	x	x	8	13	8	17
Maximum Gouge Depth (m)														
1977-1978	x	.3	.2	.2	.1	.4	.1	.2	.1	.2	.4	.4	.2	.5
1978-1980	x	.1	.2	0	.1	.4	.1	.1	x	x	.5	.6	.5	.4
1980-1982	x	x	0	0	.1	.1	.1	.2	x	x	.9	.6	.5	.9
Total Disruption Width (m)														
1977-1978	x	16	16	13	13	19	16	24	18	36	46	134	24	96
1978-1980	x	11	13	0	22	14	16	22	x	x	223	77	79	101
1980-1982	x	x	0	0	6	4	5	20	x	x	46	76	61	134

Kilometers	14	15	16	17	18	19	20	21	22	23	24	25	26	27			
Water Depth (m)	15.0	15.4	16.2	16.6	17.5	18.2	18.7	19.0	19.3	19.6	19.9	19.7	19.7	18.5			
No. of New Gouges															Total	avg/Km	
1977-1978	98	45	11	21	13	0	6	7	2	0	6	5	5		322	12.4	
1978-1980	31	x	x												164	13.7	
1980-1982	19														76	6.9	
Maximum Gouge Depth (m)															Deepest		
1977-1978	1.2	.5	.4	.5	.5	0	.4	.3	1.2	0	.1	.3	.5		1.2		
1978-1980	.8	x	x												.8		
1980-1982	.9														.9		
Total Disruption Width (m)															Total	avg/Km	%disturbed
1977-1978	398	321	122	200	68	0	33	34	13	0	29	39	28		1756	67.5	6.8
1978-1980	212	x	x												790	65.8	6.6 (2 yrs.)
1980-1982	144														496	45.1	4.5 (2 yrs.)

Total No. of New Gouges = 562 Deepest New Gouge = 1.2 m Total Disruption Width = 3042 m Mean % disturbed = 3.6 per year

Table 3. Summaries of gouge data by trackline.

Testline 1 - Thetis Island

Kilometers	0	1	2	3	4	5	6	7	8	9	10	11	12	13	14	15	16	17	18	19	20	21	22	23	24	25			
Water Depth (m)	4.9	5.8	8.3	8.5	9.6	10.1	10.0	10.4	10.9	11.5	12.0	12.4	12.8	13.1	13.6	13.8	14.2	14.6	14.9	15.1	15.2	15.5	15.4	16.0	16.5	16.7			
No. of New Gouges																											Total	avg/km	
1977-1978	0	2	6	0	0	6	0	0	1	18	5	4	15	21	18	8	4	0	0	0	0	10	4	5	0		127	5.1	
1978-1979	4	4	13	20	12	0	1	4	9	7	15	9	2	2	6	24	8	3	8	1	x	x	o				142	6.8	
1979-1980	x	x	16	30	4	64	51	14	10	5	2	8	0	1	3	40	4	x	13	13	0						278	15.4	
1980-1981	x	x	9	15	16	9	2	12	14	15	6	11	15	15	22	30	7	9									207	12.4	
1981-1982	1	0	2	8	10	7	3	2	20	20	6	6	3	3													91	6.5	
	5	6	46	73	42	86	57	32	54	65	34	30	35	42															
Maximum Gouge Depth (m)																											Deepest		
1977-1978	0	.1	.1	0	0	.1	0	0	.3	.2	.1	.1	.1	.3	.2	.3	.5	0	0	0	0	.5	.3	.3	0		.5		
1978-1979	.1	.1	.1	.1	.1	0	.1	.1	.1	.2	.4	.2	.1	.1	.1	.1	.2	.1	.2	.2	x	x	0				.4		
1979-1980	x	x	.1	.2	.1	.1	.1	.1	.1	.1	.4	.3	0	.1	.2	.4	.2	x	.3	.3	0						.4		
1980-1981	x	x	.3	.7	.4	.2	.1	.1	.3	.3	.6	.1	.6	.3	.2	.3	.3	.2									.7		
1981-1982	.1	0	.1	.1	.3	.3	.1	.2	.4	.3	.4	.2	1.0	.5													.0		
Total Disruption Width (m)																											Total	avg/km	% disturbed
1977-1978	0	18	20	0	0	9	0	0	4	70	3	29	102	92	46	60	37	0	0	0	0	49	24	46	0		609	24.4	2.4
1978-1979	8	8	42	59	45	0	3	25	50	24	60	25	6	5	23	101	30	12	33	4	x	x	0				563	26.8	2.7
1979-1980	x	x	71	123	14	174	214	31	43	33	31	62	0	10	27	146	21	0	82	82	0						1164	61.3	6.1
1980-1981	x	x	30	70	50	36	8	64	62	96	71	51	74	62	105	113	35	40									975	60.9	6.1
1981-1982	1	0	10	31	31	29	4	5	58	62	25	42	22	28													348	24.9	2.5
	9	26	173	283	148	248	229	125	217	285	190	209	204	197	201	420	123	52	115	86	0	49	24	46					

Total No. of New Gouges = 845 Deepest New Gouge = 1.0 m Total Disruption Width = 3659 m Mean % disturbed = 4.0

Testline 2. - Spy Island

Kilometers	0	1	2	3	4	5	6	7	8	9	10	11	12	13	14	15			
Water Depth (m)	6.9	10.0	11.4	11.5	12.2	13.3	14.2	14.9	14.4	14.3	15.1	15.4	16.3	17.3	17.9	18.5			
No. of New Gouges																	Total	avg/Km	
1977-1978	12	4	1	22	1	30	17	4	23	0	8	13	11	17	7		170	11.3	
1978-1979	0	1	25	44	12	1	0	0	20	0	9	0	1				133	10.2	
1979-1980	0	0	0	21	0	1	2	1	14	0	2	1	4				46	3.5	
1980-1981	2	5	2	25	7	6	2	0	14	7	7	14	19	8			118	8.4	
Maximum Gouge Depth (m)	14	10	28	112	20	38	21	5	71	7	26	28	35	25	7		Deepest		
1977-1978	.1	.1	.1	.1	.1	.2	.2	.1	.1	0	.1	.2	.4	.7	.5		.5		
1978-1979	0	.1	.1	.2	.1	.1	0	0	.1	0	.2	0	.1				.2		
1979-1980	0	0	0	.2	0	.1	.1	.1	.2	0	.1	.1	.3				.3		
1980-1981	.1	.1	.1	.1	.1	.1	.1	0	.2	.4	.2	1.4	.3	.3			1.4		
Total Disruption Width (m)																	Total	avg/Km	% disturbed
1977-1978	72	19	3	97	9	134	65	20	50	0	44	58	56	139	60		826	55.1	5.5
1978-1979	0	4	97	149	30	3	0	0	53	0	18	0	4				358	27.5	2.8
1979-1980	0	0	0	82	0	3	15	3	48	0	4	1	15				171	13.1	1.3
1980-1981	11	13	5	121	21	14	4	0	64	28	49	88	88	34			540	38.6	3.9
	83	36	105	449	60	154	84	23	215	28	115	147	163	173	60				

Total No. New Gouges = 447 Deepest New Gouge = 1.4 m Total Disruption Width = 1895 m Mean % disturbed = 3.4

Table 3 continued.

Testline 3-CROSS ISLAND

Kilometers	0	1	2	3	4	5	6	7	8	9	10	11	12	13	14			
Water Depth (m)	11.5	12.5	12.3	12.0	15.0	17.8	20.5	21.6	22.4	22.7	22.5	22.2	21.7	21.0	24.1			
No. of New Gouges Depth (m)																Total	avg/Km	
1979-1982	6	7	6	11	9	2	5	3	0	4	0	22	8	134		217	15.5	
Maximum Gouge Depth (m)																Deepest		
1979-1982	.1	.1	.1	.1	.1	.2	.2	.1	0	.1	0	.2	.3	.8		8		
Total Disruption Width (m)																Total	avg/Km	%disturbed (in 3 yrs.)
1979-1982	23	22	15	30	25	13	15	9	0	50	0	169	71	600		1042	74.4	7.4

Total No. of New Gouges = 217   Deepest New Gouge = .8   Total Disruption Width = 1042 m   Mean % disturbed = 2.5

Testline 6-KARLUK ISLAND

Kilometers	0	1	2	3	4	5	6	7	8	9	10	11	12	13	14	15	16			
Water Depth (m)	5.8	8.0	9.5	10.2	11.1	12.0	13.5	14.6	15.7	16.2	19.3	21.7	23.2	25.2	26.0	26.5	27.4			
No. of New Gouges																		Total	avg/Km	
1979-1980	x	x	x	x	3	x	5	4										12	4.0	
1980-1981	0	0	2	5	1	2	0	0										10	1.3	
1981-1982	1	5	1	0	1	10	1	1	1	15	19	0	6	0	0	1		66	4.1	
Maximum Gouge Depth (m)																		Deepest		
1979-1980	x	x	x	x	.1	x	.1	.1										.1		
1980-1981	0	0	.1	.1	.1	.1	0	0										.1		
1981-1982	.1	.7	.5	0	.1	.1	.1	.1	.1	.1	.2	0	.2	0	0	.1		.7		
Total Disruption Width (m)																		Total	avg/Km	% disturbed
1979-1980	x	x	x	x	11	x	16	0										35	11.7	1.2
1980-1981	0	0	3	16	3	4	0	0										26	3.3	0.3
1981-1982	3	15	4	0	6	83	1	5	3	57	96	0	25	0	0	6		264	16.5	1.7

Total No. of New Gouges = 88   Deepest New Gouge .7 m   Total Disruption Width = 325 m   Mean % disturbed = 1.1

Table 3 continued.

Testline 5 & 8-FLAXMAN ISLAND

Kilometers	0	1	2	3	4	5	6	7	8	9	10	11			
Water Depth (m)	7.1	10.6	11.9	14.1	16.8	19.8	20.5	22.5	24.3	25.8	27.0	27.7			
No. of New Gouges													Total	avg/Km	
1979-1980 (TL5)	1	0	12	12	x								25	6.3	
1981-1982 (TL8)	0	0	12	1	12	2	2	4	1	5	x		39	3.9	
Maximum Gouge Depth (m)													Deepest		
1979-1980 (TL5)	.1	0	.1	.1	x								.1		
1981-1982 (TL8)	0	0	.1	.1	.1	.1	.1	.3	.1	.8	x		.8		
Total Disruption Width (m)													Total	avg/Km	% disturbed
1979-1980 (TL5)	.1	0	29	25	x								55	13.8	1.4
1981-1982 (TL8)	0	0	54	4	58	10	6	10	4	29	x		175	17.5	1.8

(TL5) Total No. of New Gouges = 25 Deepest New Gouge = .1m Total Disruption Width = 55m Mean % disturbed = 1.4
(TL8) Total No. of New Gouges = 39 Deepest New Gouge = .8m Total Disruption Width = 175m Mean % disturbed = 1.8

Testline 7-CAMDEN BAY

Kilometers	0	1	2	3	4	5	6	7	8	9	10	11	12	13	14	15	16	17			
Water Depth (m)	5.5	6.7	7.1	7.4	8.2	9.0	9.5	10.2	10.8	11.7	12.5	13.0	14.3	15.0	15.9	16.8	17.7	18.6			
No. of New Gouges																			Total	avg/Km	
1981-1982	2	2	2	7	2	15	8	8	4	9	14	23	15	9	18	12	1		151	8.9	
Maximum Gouge Depth (m)																			Deepest		
1981-1982	.1	.1	.1	.1	.1	.2	.1	.3	.1	.1	.1	.1	.3	.2	.7	.4	.1		.7		
Total Disruption Width (m)																			Total	avg/Km	% disturbed
1981-1982	4	9	4	20	5	50	30	40	14	38	32	60	71	28	95	66	3		577	33.9	3.4

Total No. of New Gouges = 151 Deepest New Gouge = .7 m Total Disruption = 577 m Mean % disturbed = 3.4

Table 3 continued.

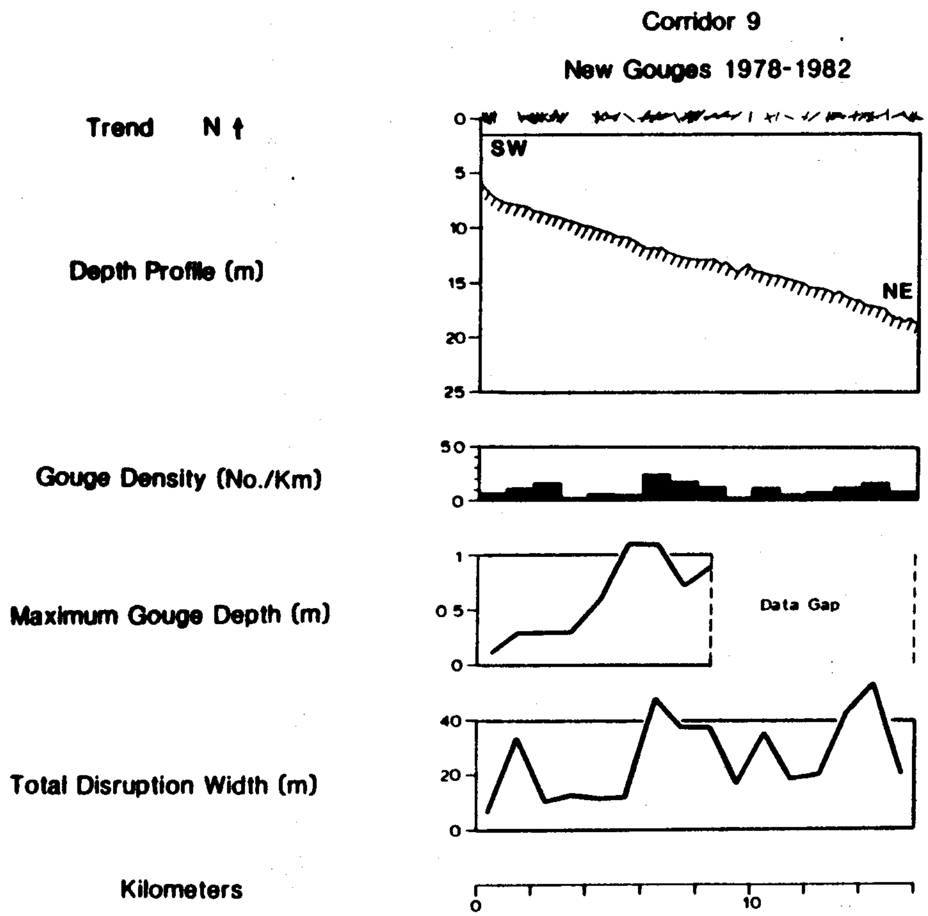

Fig. 3 Graph of dated gouge characteristics and bathymetry profile vs. length of trackline for corridor 9. Vertical exaggeration is 1:400 for figures 3 through 11, except Figure 6. There is a 4 year time span between the compared data sets. See Figure 1 for corridor location.

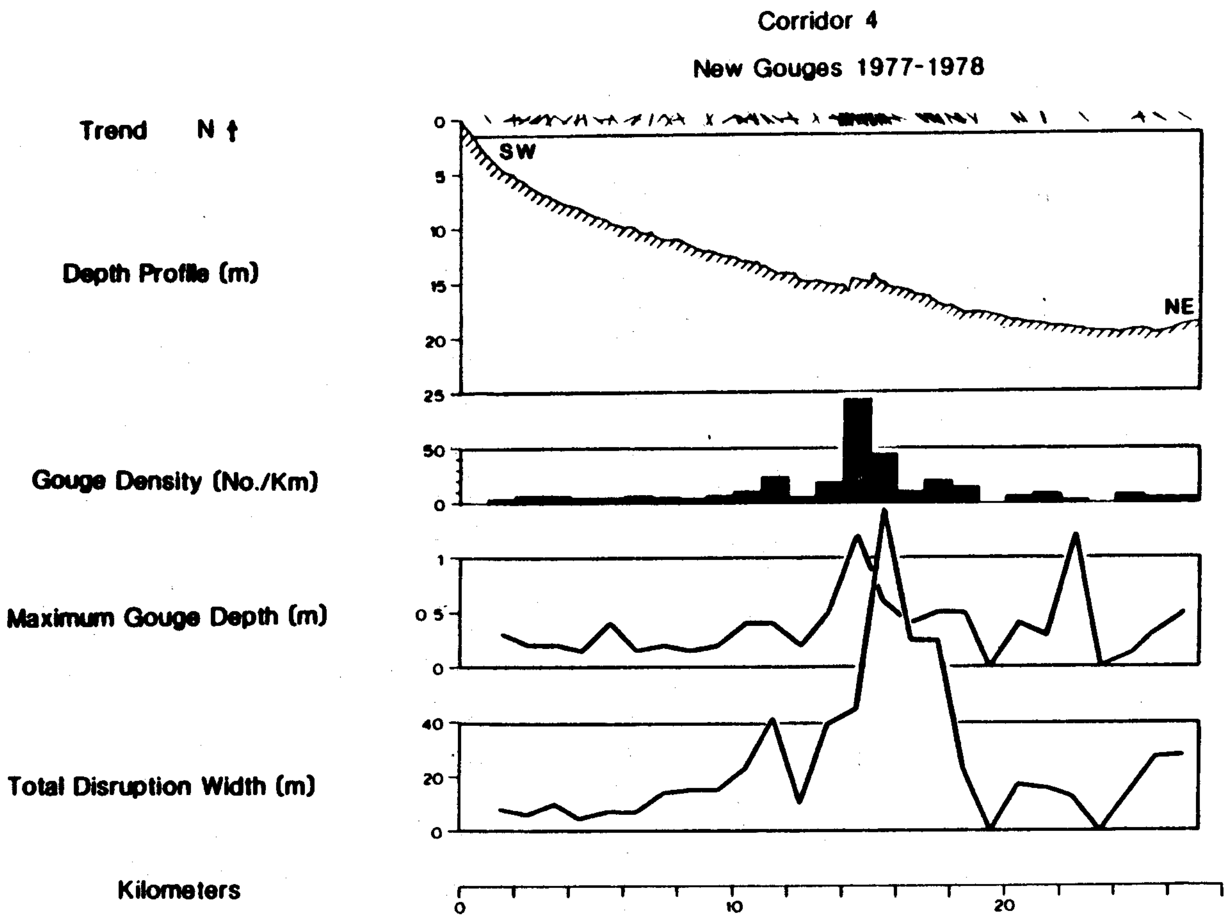

Fig. 4 a. Graph of dated gouge characteristics and bathymetry profile vs. length of trackline for corridor 4 (1 year span between surveys). See Figure 1 for corridor location.

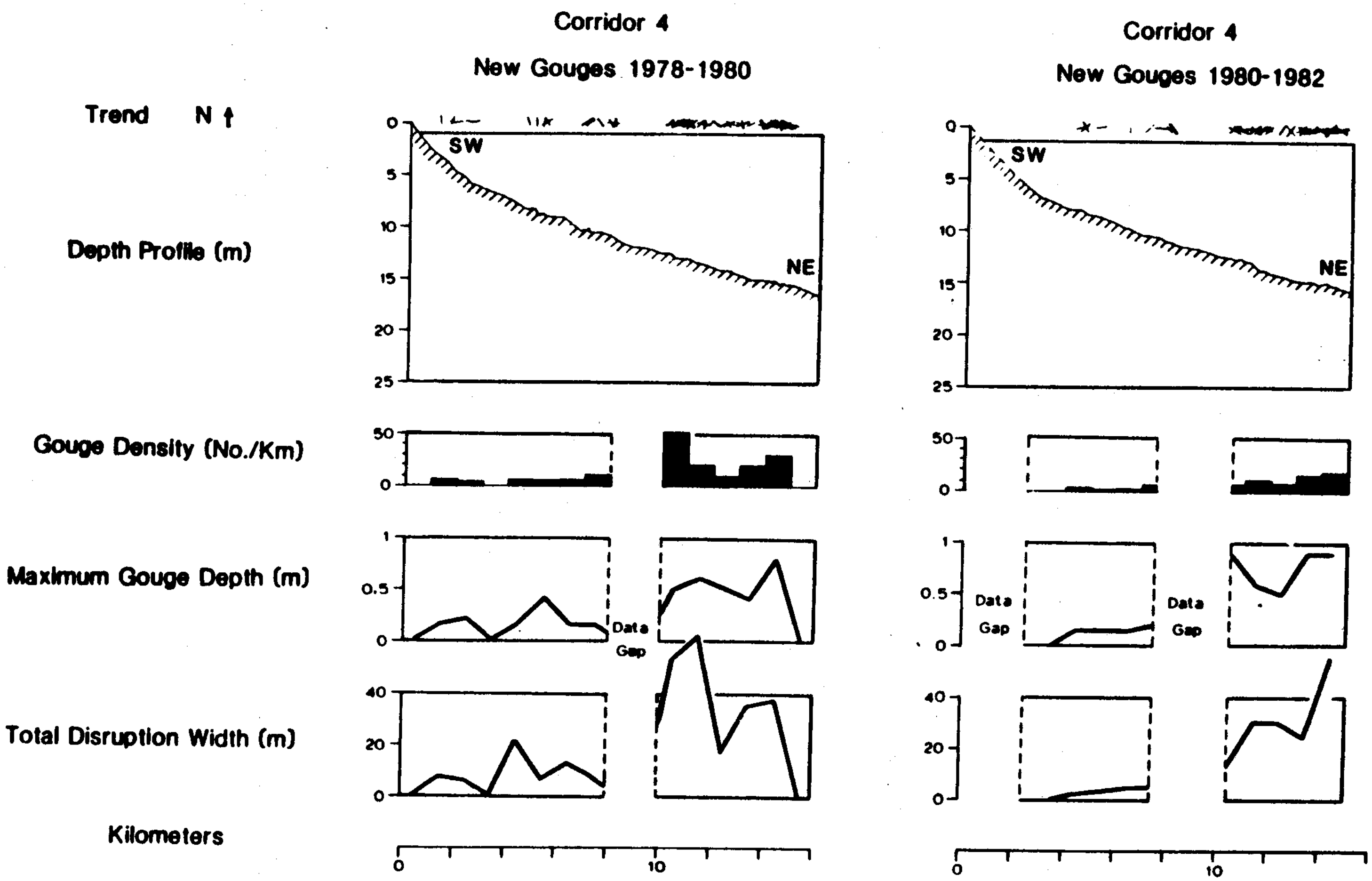

Fig 4 b. Graph of dated gouge characteristics and bathymetry profile vs. length of trackline for corridor 4 (2 year spans between surveys).

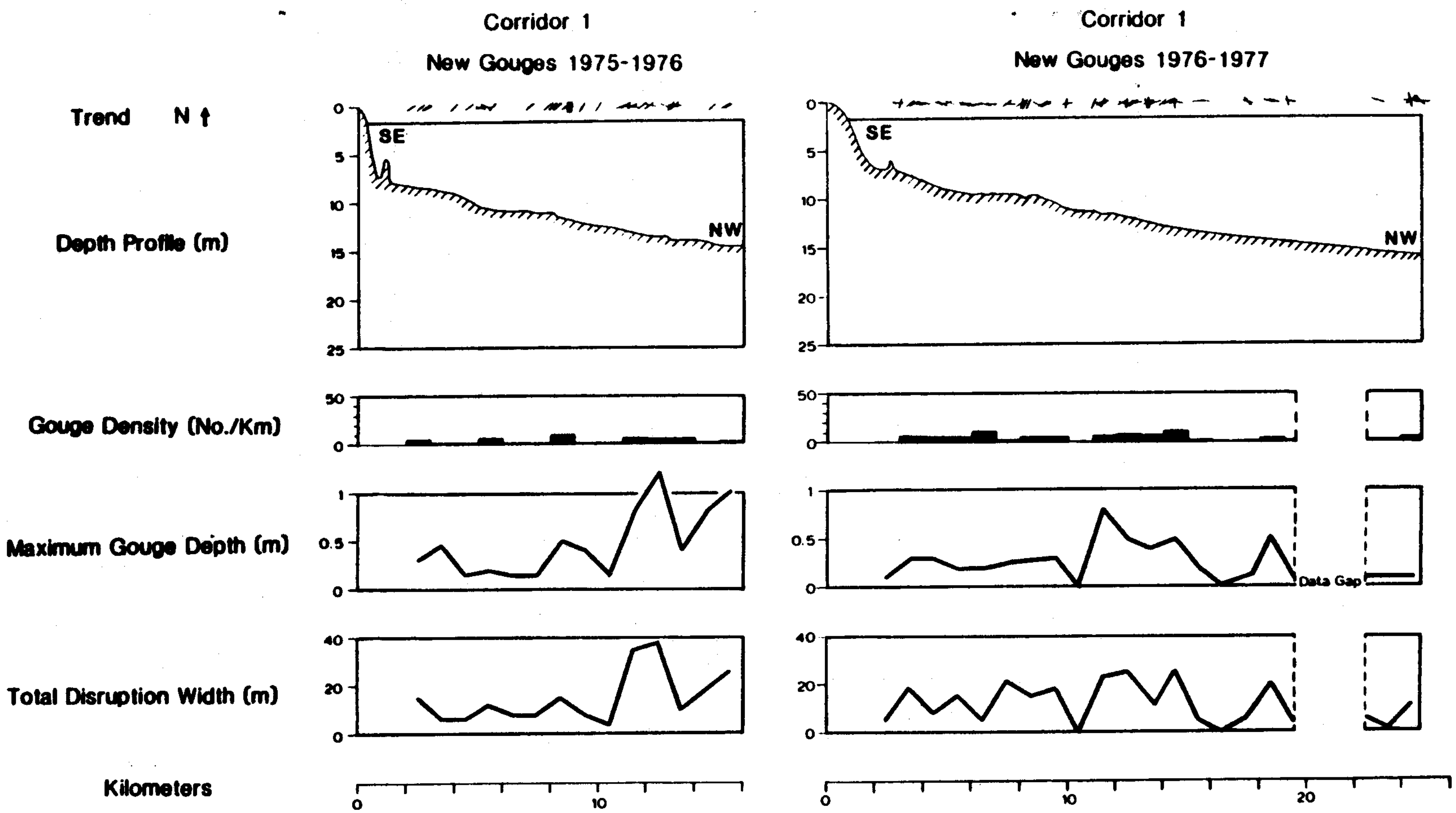

Fig. 5 Graph of dated gouge characteristics and bathymetry profile vs. length of trackline for corridor 1 between 1975 and 1977 (1 year spans between surveys). See USGS Open-File Report #78-730 for data tables for these survey years.

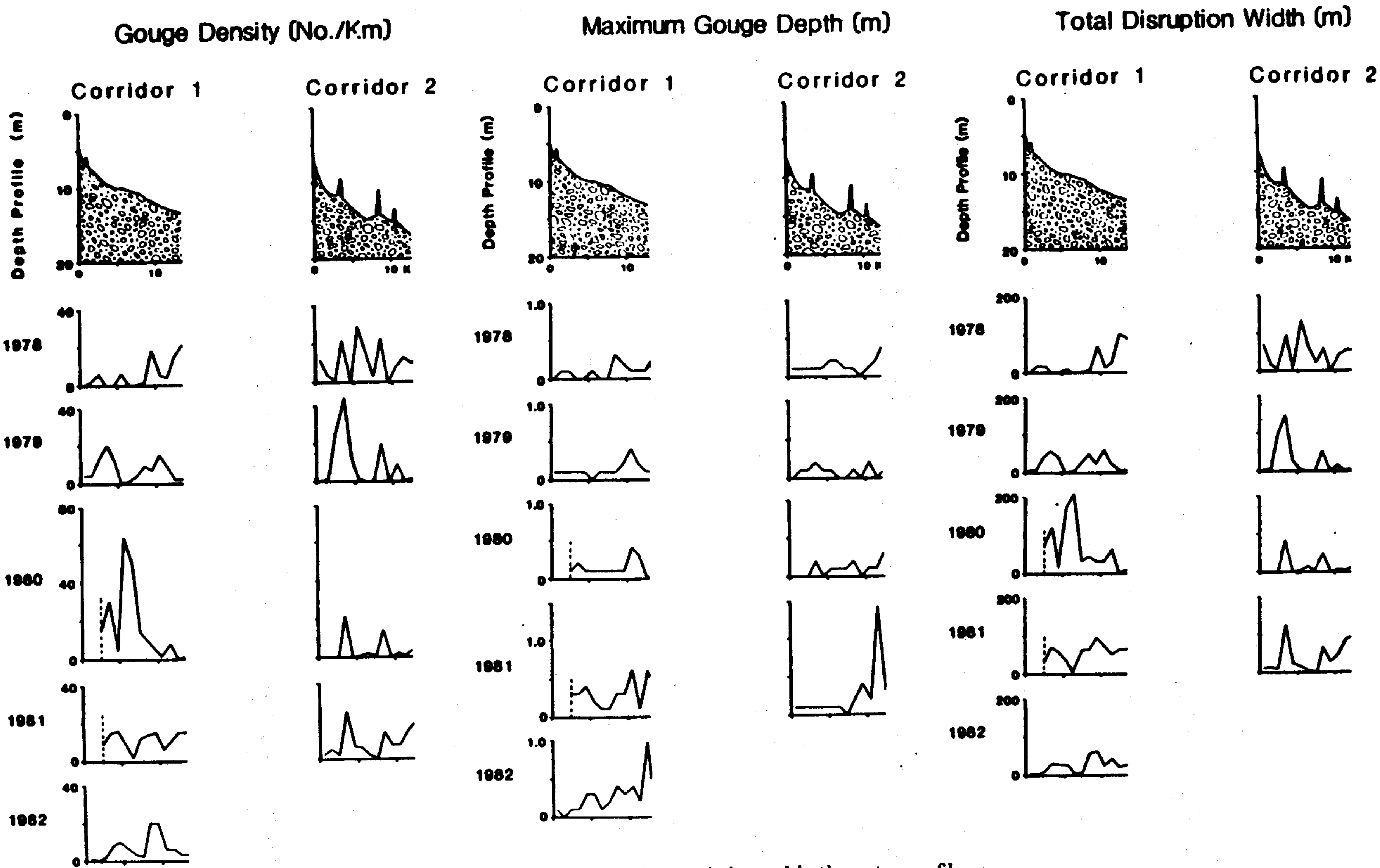

Fig. 6 Graph of dated gouge characteristics and bathymetry profile vs. length for corridors 1 and 2 between 1978 and 1982 (1 year time span between surveys). See Figure 1 for location of corridor. Vertical exaggeration is 1:1000 in this figure.

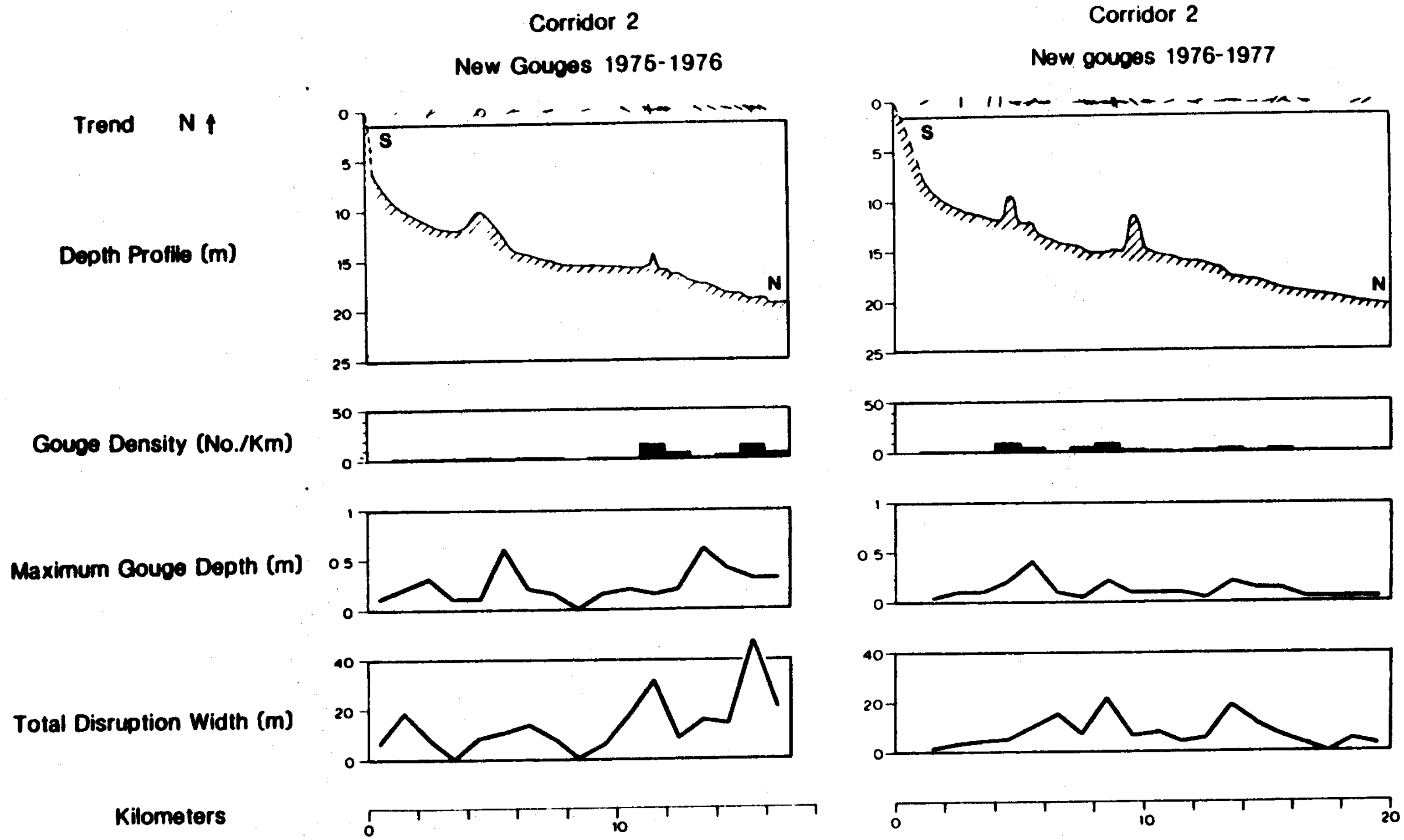

Fig. 7 Graph of dated gouge characteristics and bathymetry profile vs. length of trackline for corridor 2 between 1975 and 1977 (1 year spans between surveys). See Figure 1 for corridor location and USGS Open-File Report #78-730 for data tables for these survey years.

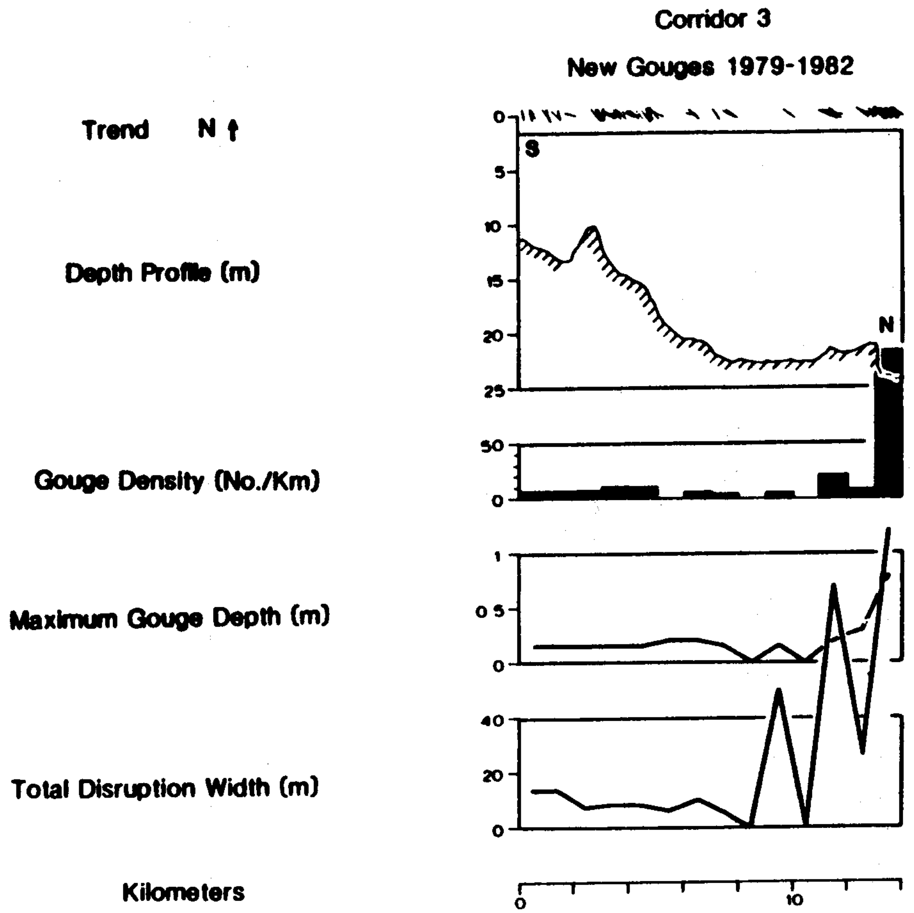

Fig. 8 Graph of dated gouge characteristics and bathymetry profile vs. length of trackline for corridor 3 (3 year spans between surveys). See Figure 1 for corridor location.

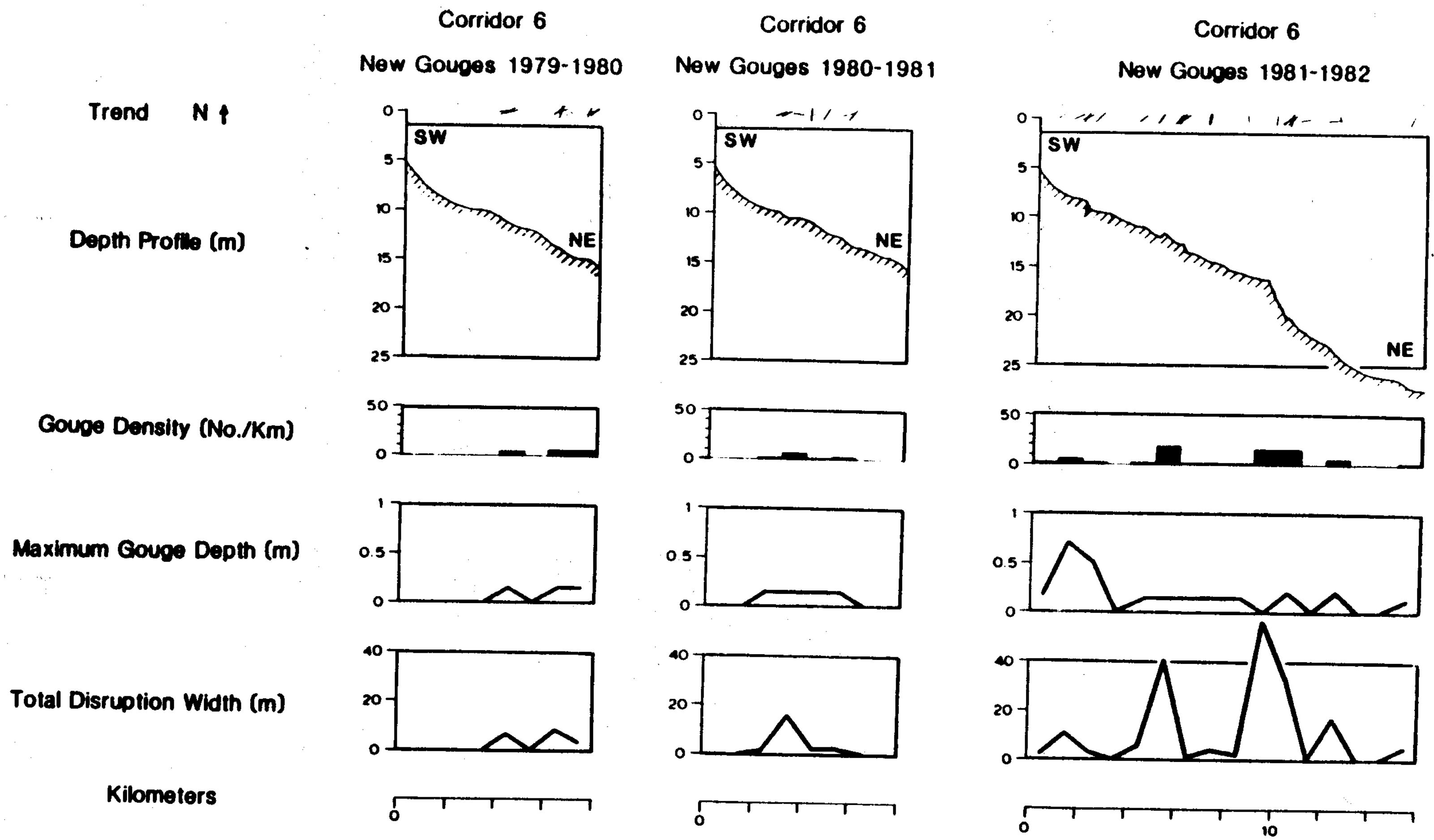

Fig. 9 Graph of new gouge characteristics and bathymetry profile vs. length of trackline for corridor 6 (1 year spans between surveys). See Figure 1 for corridor location.

Corridors 5 and 8 - Corridor 5 was established using navigation stations that ultimately could not be reoccupied and thus we subsequently established corridor 8 nearby using more permanent benchmarks (Figure 1 and Table 2). The bottom profile of these two corridors is steeper in comparison to those further west and show an irregular profile so that a bench or shoal at 18 to 22m is difficult to discern (Figure 10). Inshore sediments are sands and gravels while at about 20 meters and seaward over consolidated sandy muds and pebbly sandy muds are found.

Corridor 7 - Located in the eastern part of Camden Bay, corridor 7 extends northward from a coast of tundra bluffs (Figure 1). Starting in water depths of about 6m the profile gradually drops to depths of more than 16m (Figure 11) similar to the profiles from Harrison Bay westward (Figure 4). Sediments are sands and muddy sands on the inner part of the line while in water depths of about 18m overconsolidated sandy muds and clays are found.

DATED GOUGES

General Characteristics

The present data set consists of 146 kilometers of corridor. Because many of the corridors have been resurveyed more than twice, 308 one kilometer segments of repetitive observations are compared. The observations consist of over 2500 dated sea bed gouges. These gouges accounted for over 12 km of seabed disruption, to a maximum depth of 1.4 meters. Over 85% of these gouges were less than one year old when entered into the data set.

An "average" dated gouge can be defined using the data. We wish to stress that this gouge is not representative of the undated gouge population because of erosion and infilling of the older gouges. Nor is this average gouge representative of the group of datable gouges that exist in toto on the Beaufort shelf as the data set is limited to the inner shelf inshore of 25m. Barnes and others (1984) have suggested that the highest intensity of gouging occurs within the stamukhi zone in water depths of 30 to 40 meters. Thus, the "average" gouge we describe is representative of the gouges less than a year old inshore of the stamukhi zone. This average gouge occurred in water 14.3m deep and incised the bottom to a depth of 19cm. An average of 8.2 datable gouges occurred per kilometer, disrupting 27m or almost 3% of the seabed. The data set indicate that this 3% is a major portion of the the gouges present on the seafloor in the corridors at any one time. Eighteen percent of the 56 gouges per kilometer in the corridors were less than a year old (Table 4).

Considering a larger gouge population (Barnes and others, 1984) from slightly deeper water (18 m) gives an average gouge density of 70 per kilometer or roughly 9 times the average number of datable gouges. This suggests that on the average something more than 10% of the gouges observed on the inner shelf are less than a few years old.

Gouge depth

The logarithmic distribution of dated gouge frequency versus gouge depth is similar to the distribution shown by the entire gouge population (Barnes and others, (1984). There are very few deep gouges and very many shallow ones (Figure 12). The set of dated multiplet gouge depths are deeper than the population of all dated gouges which is contrary to the suggestion by Barnes and others (1984) that multiplet gouging is associated with first year ice ridges in contact with the seafloor which results in shallow gouge features. Possibly multiplet gouging forms the deeper gouges inshore of the stamukhi zone where our data on gouges is concentrated.

There does not appear to be a relationship between the number of datable gouges and the depth of those gouges. In one case a few gouges were deep (Corridor 9; Figure 3), elsewhere there were many new shallow gouges (Corridors 1,2,& 7; Figures 5,6,7 & 11), while in corridor 4 in 1978 there were many new datable gouges and many of these were deep (Figure 4).

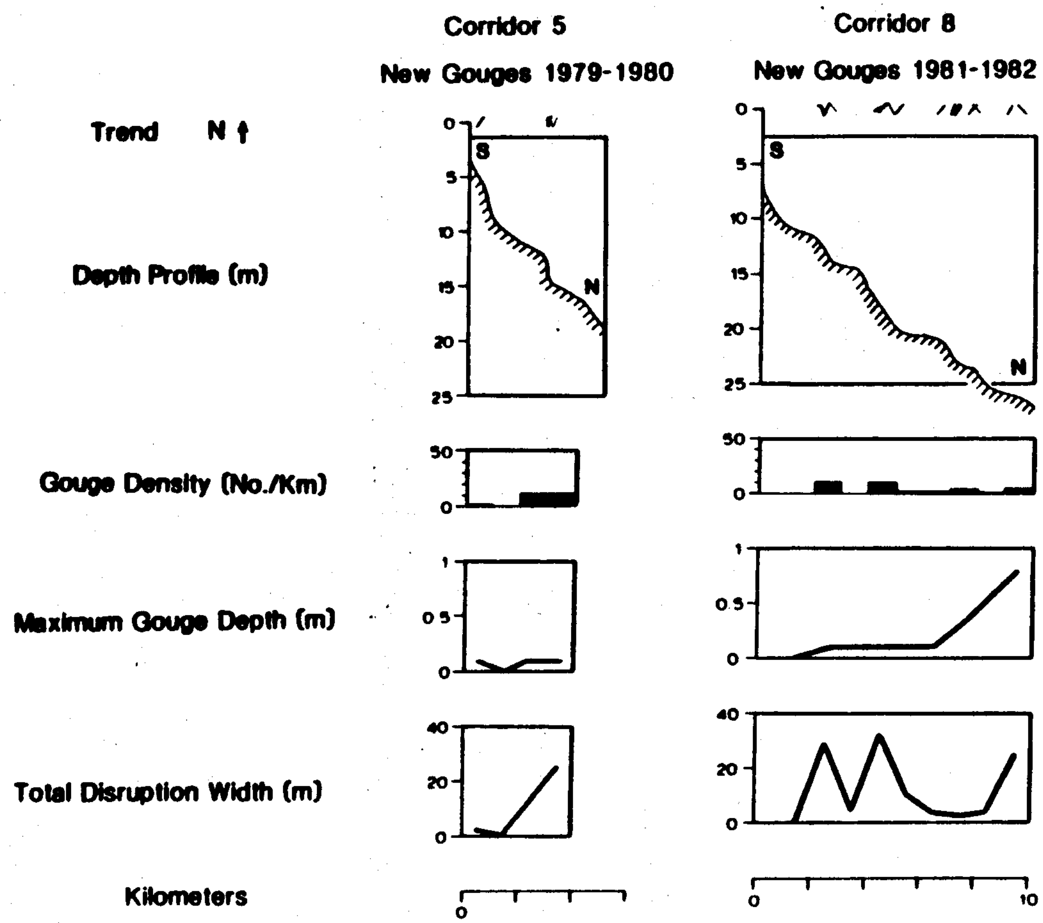

Fig. 10 Graph of new gouge characteristics and bathymetry profile vs. length of trackline for corridors 5 and 8 (1 year spans between surveys). See Figure 1 for corridor location.

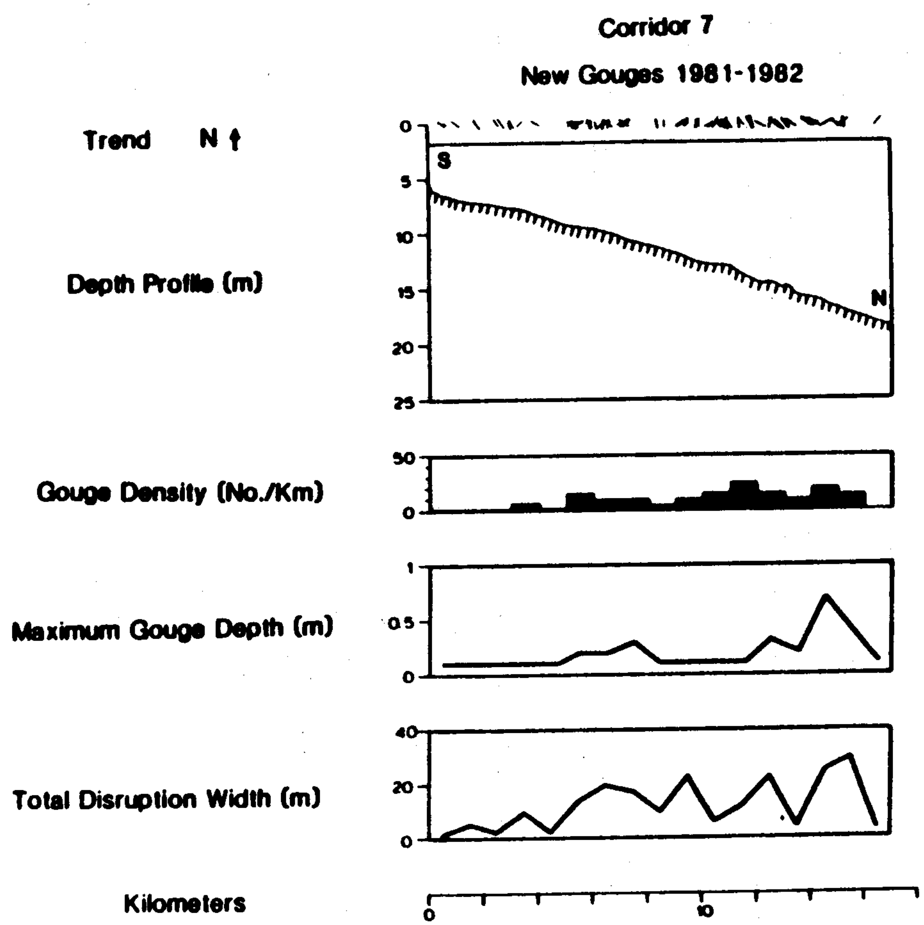

Fig. 11 Graph of new gouge characteristics and bathymetry profile vs. length of trackline for corridor 7 (1 year spans between surveys). See Figure 1 for corridor location.

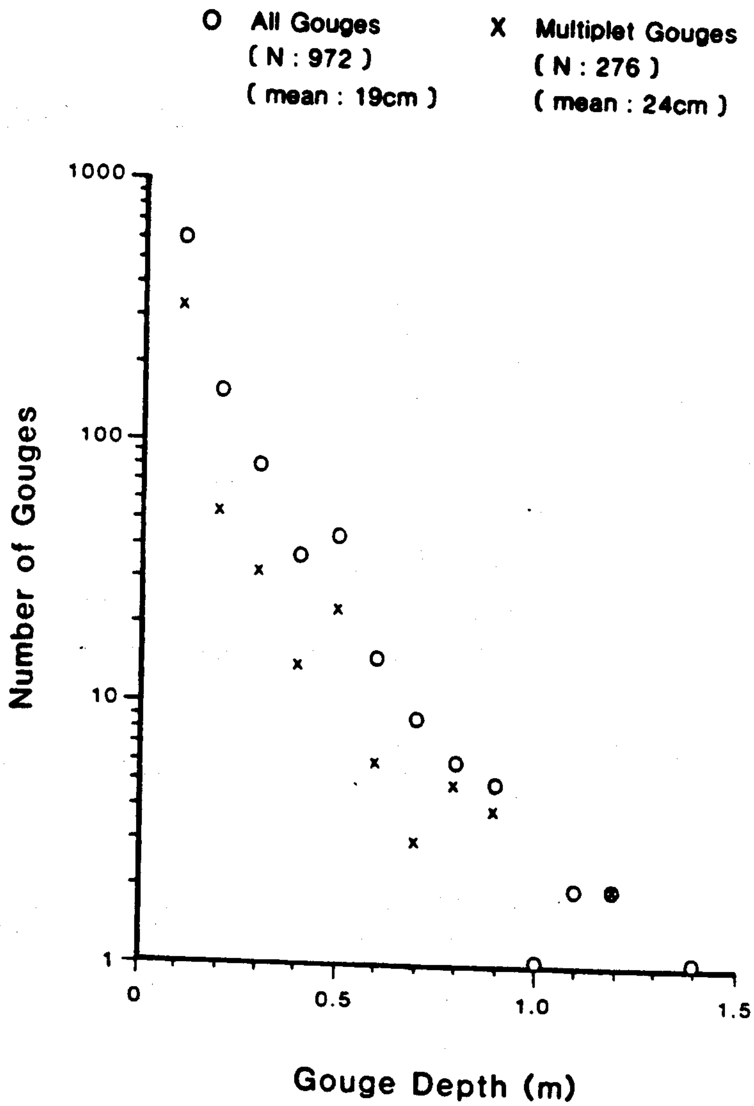

Fig. 12 Distribution of dated gouges versus the observed depth of those gouges. N is the number of gouges in the population.

TABLE 4

Number Of Gouges

Line Number	Water Depth (m)	Average no. Gouges	Seafloor Disruption % per year	Percent of Gouges less than 1 yr. old
1	4-16	64	4.0	22
2	7-17	14	3.4	47
3	11-21	62	2.5	14
4	3-20	81	3.6	10
5 & 8	7-26	76	1.6	11
6	5-26	63	1.1	13
7	6-20	76	3.4	12
9	6-18	13	2.0	18
		56 ave.	2.7 ave.	18 ave.

Age

The data for this study was gathered during the open water season, usually in August. This means that nominally a year passes between successive surveys. We have suggested that most gouging occurs during the winter ice covered period (Barnes and others, 1978, and Barnes and others, 1984). Thus the age of "new" gouges on our records is dependent on the number of winter seasons between successive surveys. In most cases this is 1 year and most of the datable gouges were less than one year old when detected. In a few cases 2,3 and 4 years elapsed between surveys in which case we can only say that the gouging occurred sometime during the 2,3 or 4 years since the last survey.

In addition to the age at time of detection, dated gouges can be assigned to time interval during which they were formed. Thus the gouges that occurred during the winter of 1980-81 can be said to be 4 years old in 1985.

The ratio of the dated gouge population to the total population was computed for each corridor. These data indicate that the dated gouges commonly make up a major percentage of the gouges present on the seafloor, particularly on the inshore segments of the corridors (Table 5). This is best illustrated on corridor 1 where we have the longest dated gouge record (Figure 13). There is also some indication that the decrease is reversed at the inner edge of the stamukhi zone in 20m of water(Corridor 3, in Table 5). We believe this distribution is due to the higher rates of wave and current reworking infilling gouges and obliterating their surface expression (Barnes and Reimnitz, 1978).

TABLE 5. PROPORTION OF GOUGE POPULATION THAT IS DATABLE

KILOMETERS	0	1	2	3	4	5	6	7	8	9	10	11	12	13	14	15	16	17	18	19	20	21	22	23	24	Mean
CORRIDOR 1 (5-1 yr. Data Sets)																										
Avg. No. Gouges/km	4	5	25	36	26	41	19	19	35	56	97	94	97	113	112	101	86	63	72	86	101	108	76	79	58	64
% Datable/Km	38	31	41	42	35	35	43	37	43	22	8	9	8	8	11	26	7	6	9	6	0	9	5	6	0	22
CORRIDOR 2 (4-1 yr Data Sets)																										
Avg. No. Gouges/km	15	6	9	31	8	23	13	5	26	7	9	10	12	22												14
% Datable/Km	14	33	43	90	53	57	29	11	79	25	75	49	62	56												47
CORRIDOR 3 (1-3 yr Data Set)																										
No. Gouges/Km	6	7	6	15	9	7	70	67	87	72	41	124	86	268												62
% Datable	33	33	33	24	33	10	2	2	0	2	0	6	3	17												14
CORRIDOR 4 (1-1 yr Data Set and 2-2 yr Data Sets)																										
Avg. No. Gouges/km	--	42	33	19	23	23	37	23	47	63	122	102	75	127	156	157	110	125	127	97	120	117	93	97	112	81
% Datable	--	9	7	17	11	12	9	18	9	10	10	13	7	10	21	29	17	10	10	0	5	6	2	0	5	10
CORRIDORS 5 and 8 (2-1 yr Data Sets)																										
Avg. No. Gouges/km	3	0	18	44	69	72	134	163	132	125																76
% Datable	17	0	88	51	17	3	2	2	1	4																11
CORRIDOR 6 (3-1 yr Data Sets)																										
Avg. No. Gouges/km	2	36	40	37	39	23	16	13	11	126	132	125	133	85	84	98										63
% Datable	13	6	5	7	5	21	15	13	9	12	11	0	5	0	0	1										13
CORRIDOR 7 (1 yr Data Set)																										
No. Gouges/km	70	37	54	76	41	53	61	76	46	43	46	82	138	140	125	108	91									76
% Datable	3	5	5	9	5	22	14	10	10	19	25	28	10	6	15	12	1									12
CORRIDOR 9 (1-4 yr Data Set)																										
No. Gouges/km	7	10	16	1	10	9	30	19	13	9	16	13	17	20	26	12										13
% Datable	25	25	25	25	17	14	19	24	23	5	17	8	10	15	16	15										18

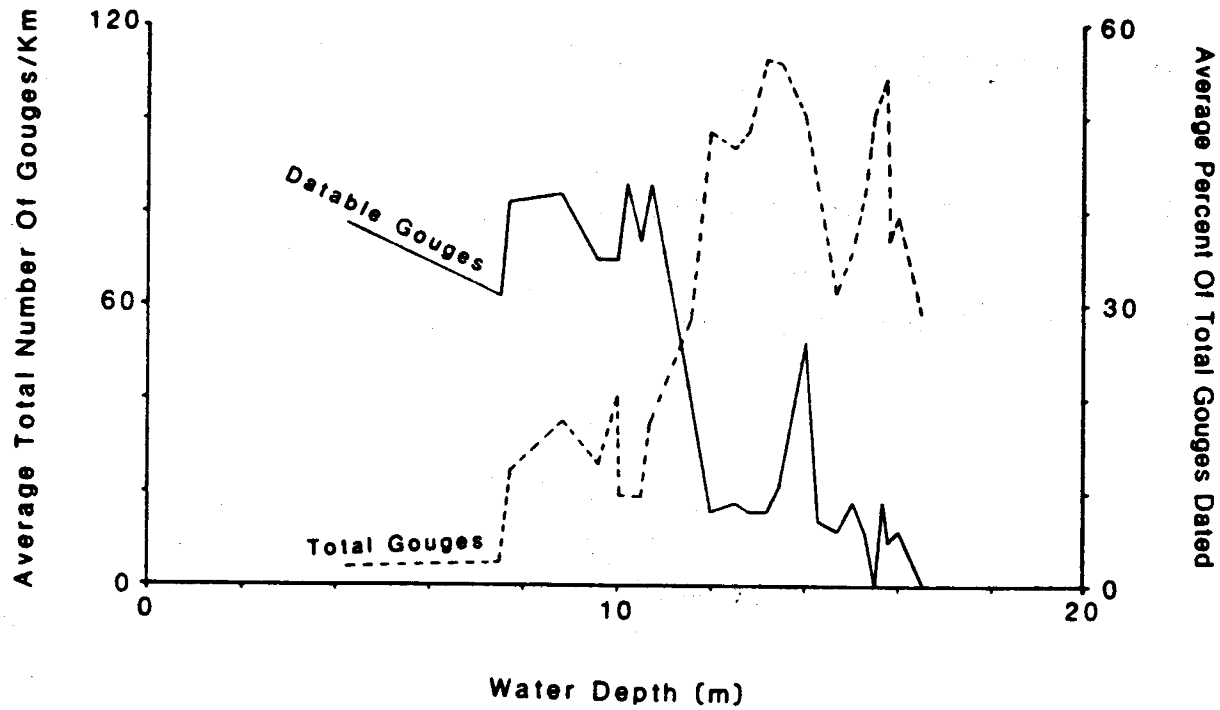

Fig. 13 Comparison of the total gouge population with the percent of that population that was dated (ie. that was generally less than a year old) for corridor 1. Data from Table 5. See Figure 1 for location of corridor 1.

AREAL VARIABILITY

Despite the variability in geographic, sedimentologic, and ice environments of the different corridors, ice gouging occurs ubiquitously in all areas and in all water depths studied. Ice gouging is uniformly distributed inside the 15 meter contour (Figures 3 to 11 and Table 3). Given a random distribution of ice keels in the ice canopy inside the stamukhi zone, a steep rather than gently sloping bottom should be impacted by more ice keels per unit distance. This is not borne out in the overall profiles of the corridors, but is seen where shoals interrupt the profiles (corridor 2, Figure 6 & 7). The steeper profiles of the corridors near Prudhoe Bay (3, 6, 5 and 8 and Figures 8, 9 & 10) do not have noticeable increases in the number of gouges when compared to the more gently sloping corridors to the east and west.

On a smaller scale the concentration and size of newly formed ice gouges is controlled by bottom morphology. Where seafloor slopes are gradual and unbroken by shoals, gouging appears to be evenly distributed in all water depths along the corridors (Corridors 1,7,& 9; Figures 3,5,6, & 11). When shoals occur within the corridor, their abrupt increase in seafloor slope concentrates newly formed gouges on the seaward flanks of these features and partially shelters the inshore areas from gouging (Corridors 2,3,4, & 6; Figures 4,6,7,8 & 9).

Gouge depths and disruption widths of the dated gouges increase slightly in deeper water, although this trend is not clear cut (see corridors 6 and 9; Figures 3 & 9). An increase in disruption widths with increasing water depths is ascribed to the presence and/or development of larger and more massive ice ridges.

The average disruption per kilometer of corridor for different water depths is a further indicator of the increase in amount of disruption in an offshore direction (Figure 14). These data also show a decrease in the amount of disruption between 17.5 and 22.5m. A similar decrease in this gouge parameter was noted by Barnes and others(1984) at these water depths and was linked to the fact that the inner boundary of the stamukhi zone and an associated step or shoal are located here and serve to protect the seafloor inshore for some distance.

Areas that contain higher numbers of dated, shallow gouges and large disruption widths are associated with multiplet gouge events (See for example corridor 1, 1978 and 1979, Figure 6; Table 3). As multiplet gouging has been associated with first year ice ridging (Barnes and others, 1984) the areas of high multiplet density should mark areas of frequent first year ridging of sea ice.

At water depths of 15 to 20 meters, almost all of the records show a sharp increase in all parameters - numbers of gouges, disruption widths, and incision depths (See especially corridor 3; Figure 8). The inner edge of the stamukhi zone commonly occurs in these water depths each year (Kovacs, 1976; Reimnitz, and others, 1978). The increase in new gouging in this zone is in keeping with the vastly increased ice ridging that occurs here (Tucker and others, 1979) and confirms our earlier postulations that gouging would be more intense in this zone (Reimnitz and Barnes, 1974; Barnes and others, 1978; and Barnes and others, 1984). In contrast to the data of corridor 3 and Figure 14, corridors 6 and 8 cross the inner edge of the stamukhi zone and do not reflect the increase in gouging we expect in this region. Either gouging in the stamukhi zone is episodic and intense or the boundary does not mark a major change of ice gouge recurrence rates. At present we prefer to believe the former.

TIME VARIABILITY

The year to year variability of the movement and vigor of deep keeled ice ridges should be reflected in the intensity of fresh seafloor gouging. Ice conditions on the inner shelf can vary from season to season due to timing and intensity of storm events and to ice distribution patterns at

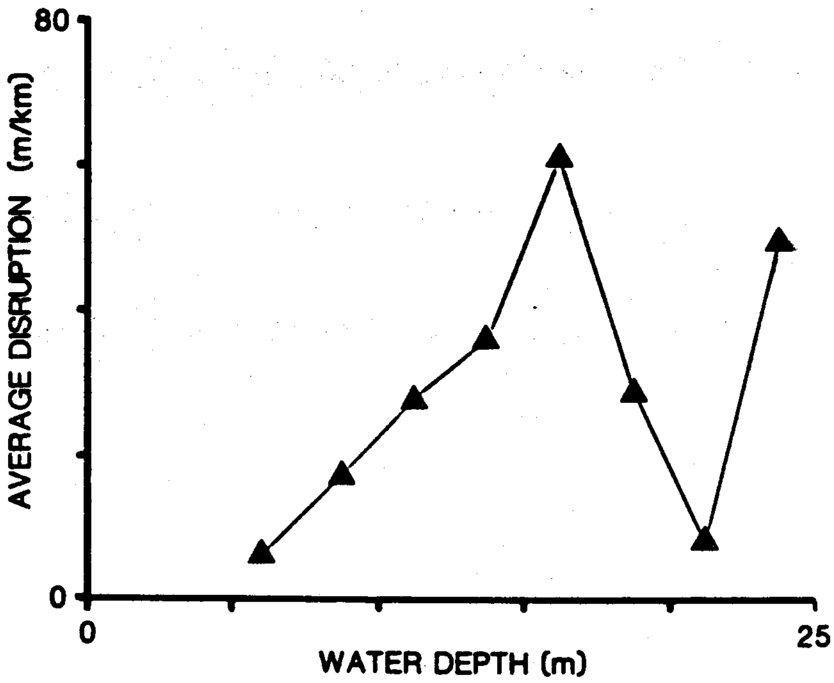

Fig. 14 Comparison of the average amount of seafloor disruption per kilometer and water depth. All corridors were divided into 2.5m depth increments, and the average computed.

freeze up. In 1975, at the end of summer, a large percentage of ice from the previous winter remained on the inner shelf which was incorporated in the 1976 ice canopy. These older "welded" ice blocks (Kovacs and Mellor, 1974) would carry solid ice keels within a moving ice canopy and could form a nucleus for grounded ice ridges (Kovacs, 1976). Gouges formed under such an ice canopy could be dominated by individual gouges and by the 2 to 4 keel multiplets from the "welded" keels. Furthermore these gouges should be deeper due to the more competent older ice keels.

In contrast the inner shelf during the summer of 1980 was essentially free of older ice by the time of freeze up and the 1981 ice canopy in the study area was formed primarily from first year ice. As first year ice is dense, keels will be deeper for first year ridges than multiyear ridges with sails of equal height (Kovacs and Mellor, 1974). However, first year keels would be less competent in their ability to gouge not having undergone extensive welding from successive freeze-thaw cycles, although, they may be responsible for extensive shallow multiplet gouging, commonly with many more than 5 gouges per multiplet (Barnes, and others, 1984). Thus we might expect gouging from the winter of 1980-81 to result in a dominance by shallow multiplet gouges.

The time series data we have to examine is rather limited, consisting of 7 years of records in one corridor and 6 and 2 years of records at only two other corridors (Table 3). The remainder of the data are averaged over several years or represent only a single year. The data indicate no obvious correlation exists between corridors from year to year when comparing trends in average number of dated gouges (Figure 15) or average disruption width (Figure 16). The data do show that the number and width of datable gouges in any year vary by a factor of 5 or more. An attempt to correlate the ice gouge variability with the severity of winter ice conditions by examining the wind record at Barrow has thus far been unsuccessful. The lack of correlation is perhaps due to the short length of record we have in light of the fact that the bottom is only gouged a few percent per year and on the fact that the severity of ice ridging and the seasonality of ridging is poorly known.

CONCLUSIONS

1. The intensity of new gouging is related to water depth and bottom morphology, and indistinctly increases offshore at least to water depths of about 25m. Inshore of the stamukhi zone the amount of gouging and the depth of gouging is rather uniform even into waters less than 10 m deep.
2. No correlation exists between the numbers of new gouges and the depth to which new gouges have penetrated the sea floor. This results because large numbers of new gouge are associated with wide shallow multiplet gouging (first-year pressure ridges)
3. Areas that have high gouge densities and large disruption widths are due to multiplet events. A few large multiplet events may account for extensive but shallow disruption of the seafloor.
4. Annual variations in the number of individual verses multiplet gouges may be related to the presence or absence of multi-year ice ridges on the inner shelf during winter.
5. The annual variations in the data indicate that year to year gouging on this part of the Beaufort shelf is ubiquitous. The year to year intensity of gouging can vary by a factor of 5.

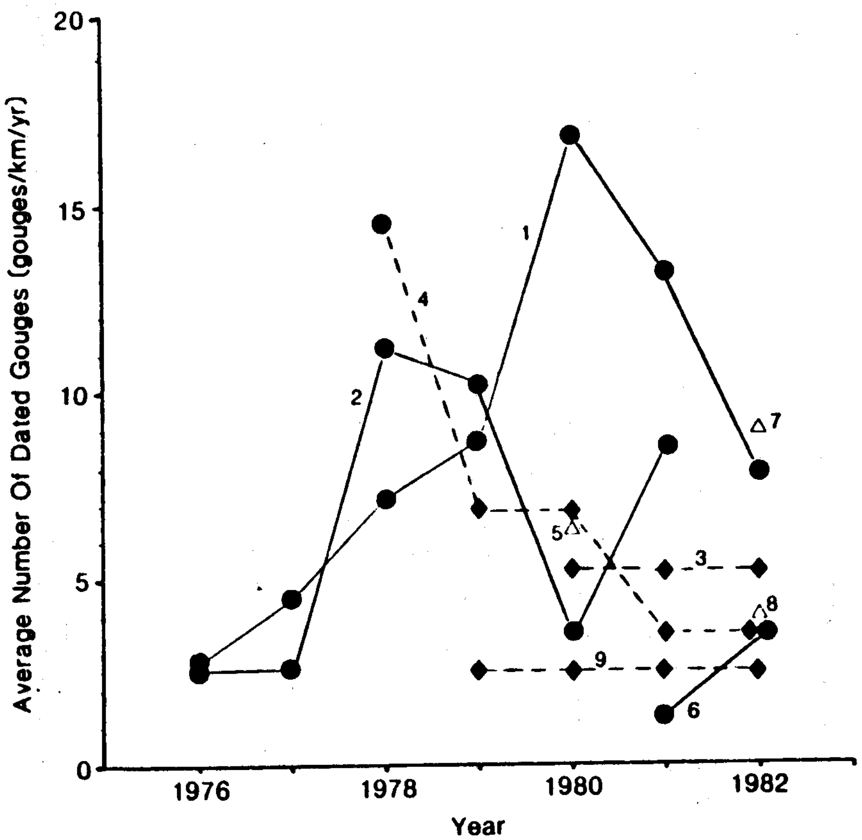

Fig. 15 The yearly variation in the average number of dated gouges per kilometer observed in each of the corridors.

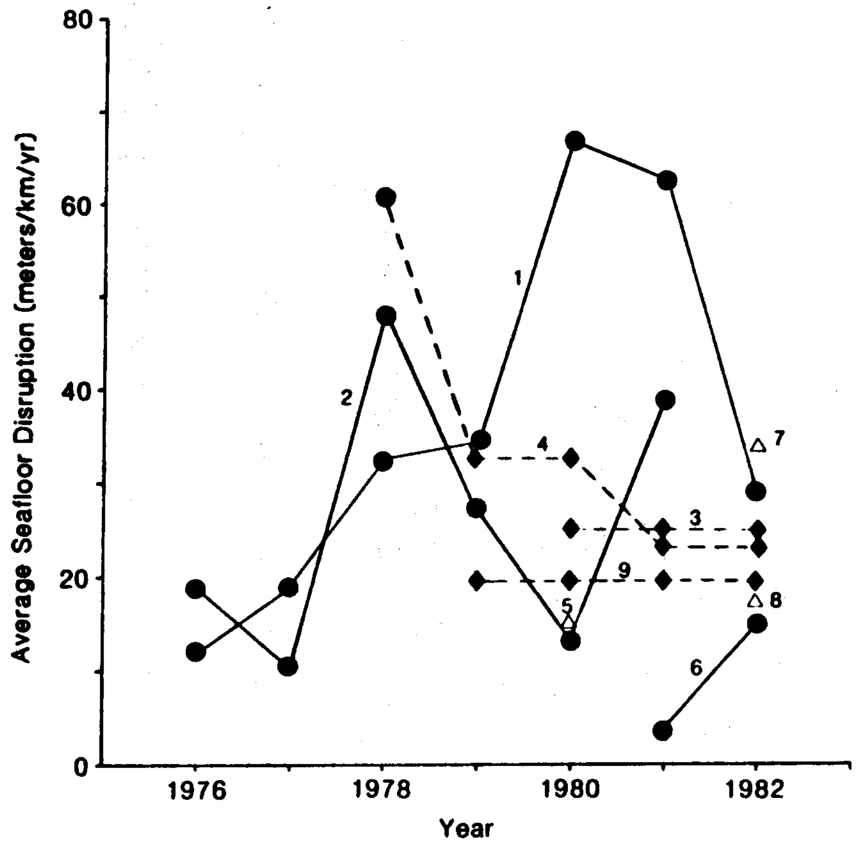

Fig. 16 The yearly variation in the average disruption width per kilometer observed in each of the corridors.

REFERENCES

Barnes, P.W., and Asbury, J., 1985, Detailed morphology of the seafloor at the inner edge of the stamukhi zone, Beaufort Sea, Alaska; proceeding Arctic Workshop, Dept. of Energy, Morgantown Energy Technology Center Morgantown, West Virginia.

Barnes, P.W., McDowell, D.M., and Reimnitz, Erk, 1978, Ice gouging characteristics: their changing patterns from 1975-1977, Beaufort Sea, Alaska: U.S. Geological Survey Open-File Report 78-730, 42 p.

Barnes, P.W., Rearic, D.M. and Reimnitz, Erk, 1984, Ice gouge characteristics and processes: in Barnes, P.W., Schell, D.M. and Reimnitz, Erk, (eds.), The Alaskan Beaufort Sea - Ecosystem and Environment, Academic Press, New York, p. 159-184.

Barnes, P.W., and Reimnitz, Erk, 1974, Sedimentary processes on arctic shelves off the northern coast of Alaska, in, Reed, J.C. and Sater, J.E. eds, The Coast and Shelf of the Beaufort Sea, The Arctic Institute of North America, Arlington, VA, p. 439-476.

Barnes, P.W., and Reimnitz, Erk, 1979, Ice gouge obliteration and sediment redistribution event; 1977-1978, Beaufort Sea, Alaska: U.S. Geological Survey Open-File Report 79-848, 22 p.

Bea, R.G., Puskar, F.J., Barnes, P.W., and Reimnitz, Erk, 1985, The role of ice gouging in determining global forces on arctic structures: Proceedings, American Society of Civil Engineers, Arctic '85, p. 251-266.

Belderson, R.H., Kenyon, N.H. Stride, A.H. and Stubbs, A.R., 1972, Sonographs of the seafloor; A picture atlas, Elsevier Publishing, Co., New York, 185p.

Kovacs, A., 1976, Grounded ice in the fast ice zone along the Beaufort Sea coast of Alaska. US Army Cold Regions Research and Engineering Laboratory, CRREL Report 76-32, 21p.

Kovacs, A. and Mellor, M., 1974, Sea ice morphology and ice as a geological agent in the southern Beaufort Sea, in: Reed, J.C., and Sater, J.E., (eds.), The Coast and Shelf of the Beaufort Sea, Arctic Institute of North America, Arlington, Virginia, p. 1132-161.

Lewis, C.F.M. 1977, The frequency and magnitude of drift ice groundings from ice-scour tracks in the Canadian Beaufort sea, in: Proceedings, Fourth International Conference on Port and Ocean Engineering under Arctic Conditions, 1977, Muggeridge, D.B., (ed.), Memorial University, St. Johns Newfoundland, v. 1, p. 568-576.

Reimnitz, Erk, and Barnes, P.W., 1974, Sea ice as a geologic agent on the Beaufort Sea shelf of Alaska, in, Reed, J.C., and Sater, J.E., eds., The Coast and Shelf of the Beaufort Sea, The Arctic Institute of North America, Arlington, Virginia p. 301-351.

Reimnitz, Erk, Barnes, P.W., Toimil, L.J. and Melchior J., 1977, Ice gouge recurrence and rates of sediment reworking, Beaufort Sea, Alaska: Geology v. 5, p. 405-408.

Reimnitz, Erk,. Kempema, E.W., Ross, C.R. and Minkler, P.W., 1980, Overconsolidated Surficial deposits on the Beaufort Sea Shelf: U. S. Geological Survey Open-File Report No. 80-2010, 38 p.

Reimnitz, Erk, Toimil, L.J., and Barnes, P.W., 1978, Arctic continental shelf morphology related to sea-ice zonation, Beaufort Sea, Alaska; Marine Geology, v.28, p 179-210.

Thomas, D.R., and Pritchard, R.S., 1980, Beaufort Sea ice mechanical energy budget, 1975-76, Flow Research Report No. 165, Flow Industries Kent, Washington, 37p.

Toimil, L.J., 1978, Ice-gouged microrelief on the floor of the eastern Chukchi Sea, Alaska; a reconnaissance survey, U.S. Geological Survey, Open File Report number 78-693, 48p. plus Appendix.

Tucker, W.B., W.F. Weeks, and M.D. Frank, 1979, Sea ice ridging over the Alaskan Continental shelf, Jour. Geophys. Res. v. 84, p. 4885-4897.

Weeks, W.F., Barnes, P.W., Rearic, D.M. and Reimnitz, Erk, 1984, Some probabilistic aspects of ice gouging on the Alaska Shelf of the Beaufort Sea, in Barnes, P.W., Schell, D.M. and Reimnitz, Erk (eds.), The Alaskan Beaufort Sea - Ecosystem and Environment, Academic Press, New York, p. 213-236.

Weeks, W.F., Tucker, W.B. III, Frank, M., and Fungchoroen, S., 1980, Characterization of surface roughness and floe geometry of sea ice over the continental shelfs of the Chukchi and Beaufort Seas, in, R.S. Pritchard, ed., Sea Ice Processes and Models, U. of

Washington Press, Seattle, Washington, p 300-312.

Wolf, S., Barnes, P.W., and Reimnitz, E., 1983, Analysis of hummocky subbottom from repetitive observations north of Tigvariak Island, Beaufort Sea, Alaska; in Annual Reports of Principal Investigator to NOAA's Outer Continental Shelf Environmental Assessment Program: NOAA Juneau, Alaska, 8 pages.

APPENDIX

ICE GOUGE DATA SHEETS

KEY TO APPENDIX

Testline - refers to corridor number to which the data apply

Julian Date, Year - Year and date of survey

Template Identification - Template used to correct orientation distortion cause by variable ship speed and recorder paper speeds - expressed as the ratio of the along track distance to the slant range distance.

Trackline Number - Field number used to organize field data within each years field effort - not used in analysis.

Additional explanation and usage of many of the following terms is given in Barnes and others, (1984) and in Figure A1 taken from that reference.

Single Gouges - Gouges generated by a single tool indenting the bottom leaving a single furrow.

Multiple gouges - Gouges generated by a tool with 2 or more indenters leaving one or more adjoining furrows on the seafloor.

Segment - Corridors were divided into 1 kilometer segments starting at A, thus the first segment is AB with a starting point at 0km (AB/0). Further along the corridor segment DE starts at 3km (DE/3). Within a segment the distance from the inshore end of the corridor to the occurrence of a dated gouge is given in hundreths of a kilometer (eg. within segment BC/1 a dated gouge was located at 1.50km from A).

Water Depth - Water depth at the inner end of a segment at the location of each dated gouge.

Total Gouges - Total number of seafloor furrows observed in a segment. Each furrow in a multiple gouge is counted separately.

Total New Gouges - Total number of dated seafloor gouges in a segment. Each furrow in a dated multiple gouge is counted separately.

Length of new single gouges - Total length in meters of the dated gouges as observed on the sonographs. NL - gouge traversed the entire sonograph and the length was not ascertained: usually a gouge length greater than 250m is indicated based on the scan width of the sonographs.

Gouge depth - The distance in meters from the "average" seafloor to the bottom of a gouge as measured on the fathograms. This depth is entered as $<.2$m when the gouge was not resolvable on the fathogram.

Gouge width - The distance in meters across the width of a gouge at the measured at the level of the "averaged" seafloor measured on the fathogram.

Ridge height - The distance in meters from the "average" seafloor to the top of the highest ridge flanking a dated gouge. This height is assumed to be $<.2$m when the ridge is not resolvable on the fathogram.

Φ ($^{\circ}$ T)- refers to the uncorrected and corrected orientations of the dated gouges relative to true north. The orientations are uniformly reported entered as an angle between 0 and 180° and should not be read as the direction of ice motion during gouging. 160/105 is a gouge oriented at 160° to the right of a ships course of 305° which results in a 105° orientation for the gouge relative to true north.

Length of new Multi. gouges - See Length of single gouges above.

Number of incisions - Refers to the number of parallel adjoining furrows that comprise a multiple gouge feature.

Deepest incision - The distance in meters from the "average" seafloor to the bottom of the deepest furrow in each multiple gouge as measured from the fathograms.

Disruption Width - The distance im meters measured at right angle to a multiple gouge from one bounding ridge to the other. ie the total width of seafloor disrupted by a multiple gouge.

Φ (° T) - Refers to the orientation of the multiple gouges. See this same entry above.

Comments - Includes additional observations on sonographs and fathograms. Note - CS= Ships course, SS# - Side scan sonar roll numbers, Bats# - Fathogram roll number, Termination direction - direction of implied ice motion determined from the termination of an ice gouge and could have an orientation from 0 to 360°

TESTLINE: 1	JULIAN DATE: 220	YEAR: 1978-1979	TEMPLATE IDENTIFICATION: 1:1.860

TRACKLINE NUMBER: 13

SEGMENT	WATER DEPTH (M)	TOTAL GOUGES	TOTAL NEW GOUGES	%	SINGLE GOUGES: NEW SINGLE GOUGES	GOUGE DEPTH (M)	GOUGE WIDTH (M)	RIDGE HEIGHT (M)	Ø (°T)	MULTIPLE GOUGES: NEW MULTI. GOUGES	NUMBER OF INCIS.	DEEPEST INCISION (M)	DISRUPT WIDTH (M)	Ø (°T)	COMMENTS [illegible] = 304 °T
AB/0	4.7	8	4	50.											
0.30	5.1									92	2	<.2	5	00/124	SSS# 8 Rats# 9
0.30	5.1				24	<.2	1	<.2	22/156						
0.30	5.1				21	<.2	1	<.2	157/101						
BC/1	5.7	6	4	66.7											Shoal height = 1.4m at Pt. B
1.75	6.9				52	<.2	1	<.2	11/135						
1.75	6.9				50	<.2	1	<.2	176/120						Terminates direction - 120°T
1.75	6.9				125	<.2	1	<.2	170/114						
1.90	7.5				165	<.2	3	<.2	06/130						
CD/2	8.2	28	13	46.4											
2.05	8.2				42	<.2	2	<.2	20/144						
2.30	7.8				37	<.2	2	<.2	00/124						
2.65	8.2				45	<.2	2	<.2	140/84						
2.60	8.0				20	<.2	1	<.2	140/84						
2.60	8.0				27	<.2	2	<.2	170/114						
2.75	7.9									NL	5	<.2	18	10/134	
2.85	8.1									NL	3	<.2	13	162/106	
DE/3	8.2	20	20	100.											gouge // to TL
3.30	8.5									NL	5	<.2	12	[illegible]/124	and runs length of seg.
3.50	9.0									NL	15	<.2	47	175/119	continues into next segment.
EF/4	9.3	15	12	80.											
4.15	9.4									NL	12	<.2	45	175/11[illegible]	
[illegible]	[illegible]	3	-	-											

TESTLINE: 1	JULIAN DATE: 220	YEAR: 1978-1979	TEMPLATE IDENTIFICATION: 1:1.860

TRACKLINE NUMBER: 13

					Length SINGLE GOUGES					Length MULTIPLE GOUGES					
SEGMENT	WATER DEPTH (M)	TOTAL GOUGES	TOTAL NEW GOUGES	%	NEW SINGLE GOUGES	GOUGE DEPTH (M)	GOUGE WIDTH (M)	RIDGE HEIGHT (M)	Ø (°T)	NEW MULTI. GOUGES	NUMBER OF INCIS.	DEEPEST INCISION (M)	DISRUPT WIDTH (M)	Ø (°T)	COMMENTS
GH/6	9.8	1	1	100.0											
6.1	10.0				NL	<.2	2	<.2	153/74						
HI/7	10.1	5	4	80.0											
7.70	10.2				35	<.2	3	<.2	29/152						
7.80	10.8									NL	2	<.2	19	158/102	continues into next segment
7.85	10.5				22	<.2	2	<.2	135/77						sediment waves
IJ/8	10.6	11	9	81.8											
8.01	10.6				30	<.2	2	<.2	158/102						
8.01	10.6									NL	2	<.2	13	158/102	
8.25	11.0				NL	<.2	2	<.2	159/102						Terminates direction - 102°T
8.40	11.1									221	3	<.2	20	157/101	
8.80	11.2									46	2	<.2	12	132/76	
JK/9	11.2	34	6	20.6											
9.05	11.3				NL	.2	8	<.2	132/76						
9.05	11.3				123	<.2	1	<.2	152/96						
9.15	11.4				NL	<.2	3	<.2	140/84						
9.15	11.4				NL	<.2	2	<.2	140/84						
9.80	11.7				NL	<.2	2	<.2	126/70						
9.95	11.7				NL	<.2	3	<.2	11/135						
KL/10	11.8	86	15	17.4											
10.30	11.9				NL	.4	7	.4	92/36						
10.40	12.0				NL	<.2	2	<.2	[illegible]/99						
10.60	12.0									375	4	<.2	20	[illegible]/124	
10.[illegible]	12.0				NL	NC	3	NC	149/72						

TESTLINE: 1 | JULIAN DATE: 220 | YEAR: 1978-1979 | TEMPLATE IDENTIFICATION: 1:1.R60

TRACKLINE NUMBER: 13

SEGMENT	WATER DEPTH (M)	TOTAL GOUGES	TOTAL NEW GOUGES	%	Cont. SINGLE GOUGES: NEW SINGLE GOUGES	GOUGE DEPTH (M)	GOUGE WIDTH (M)	RIDGE HEIGHT (M)	Ø (°T)	Cont. MULTIPLE GOUGES: NEW MULTI. GOUGES	NUMBER OF INCIS.	DEEPEST INCISION (M)	DISRUPT WIDTH (M)	Ø (°T)	COMMENTS
10.75	12.0				NL	NC	2	NC	148/92						
10.75	12.0				62	<.2	2	<.2	114/58						
10.80	11.8				NL	NC	5	NC	05/121						
10.90	12.3				NL	<.2	2	<.2	140/84						
10.90	12.3				NL	<.2	2	<.2	140/84						
10.90	12.3				NL	<.2	2	<.2	140/84						
10.95	12.2				NL	<.2	2	<.2	142/86						
10.95	12.2				NL	.2	3	<.2	148/92						continues into next segment
LM/11	12.2	51	9	17.6											
11.15	12.3				NL	.2	3	<.2	148/92						
11.15	12.3				72	NC	3	NC	140/84						
11.20	12.3				58	<.2	2	<.2	144/88						
11.75	12.4				130	<.2	1	<.2	161/105						
11.80	12.4				150	NC	2	NC	03/127						Terminates direction - 127°T
11.90	12.5				105	<.2	2	<.2	171/111						
11.90	12.5				127	<.2	2	<.2	161/111						
11.90	12.5				190	NC	2	NC	00/124						Terminates - direction - 124°T
11.95	12.6				117	<.2	3	<.2	131/75						
MM/12	12.7	51	2	3.9											START Trackline 33 SSS#12 BATS#136
12.20	[illegible]				75	NC	3	NC	142/87						JL 227
12.25	12.4				30	<.2	2	<.2	162/106						
NO/13	13.1	[illegible]	2	2.9											
13.30	13.1				NL	<.2	2	<.2	55/179						
13.35	13.2				NL	<.2	2	<.2	112/166						

748

TESTLINE: 1 | JULIAN DATE: 227 | YEAR: 1978-1979 | TEMPLATE IDENTIFICATION: 1.1.860

TRACKLINE NUMBER: 33

					Length SINGLE GOUGES					Length MULTIPLE GOUGES					
SEGMENT	WATER DEPTH (M)	TOTAL GOUGES	TOTAL NEW GOUGES	%	NEW SINGLE GOUGES	GOUGE DEPTH (M)	GOUGE WIDTH (M)	RIDGE HEIGHT (M)	Ø (°T)	NEW MULTI. GOUGES	NUMBER OF INCIS.	DEEPEST INCISION (M)	DISRUPT WIDTH (M)	Ø (°T)	COMMENTS
OP/14	13.2	73	6	8.2											
14.05	13.5									53	2	NC	7	14/138	
14.45	13.4				60	NC	5	NC	19/143						
14.50	13.[illegible]				20in	<.2	2	<.2	19/143						
14.50	13.[illegible]				NL	<.2	3	<.2	159/103						
14.90	13.8				NL	NC	3	NC	170/14						continues into next segment
PQ/15	13.8	64	24	37.5											
15.20	13.8				NL	NC	3	NC	[illegible]/111						
15.50	14.0									NL	22	NC	95	[illegible]/121	multi-gouge extends length of TL and is ‖.
15.80	14.2				25	<.2	2	<.2	178/92						
QR/16	14.1	85	8	9.4											
16.35	14.2				NL	<.2	2	<.2	05/121						
16.55	14.4									NL	4	.2	9	168/112	
16.60	14.2									NL	2	<.2	15	148/92	
16.95	14.4				200	NC	3	NC	168/112						continues into next segment - Terminates direction - 112°T
															Quality of sonar only fair
RS/17	14.4	45	3	6.[illegible]											
17.05	14.5				same as above	NC	3	NC	[illegible]						
17.20	14.6									NL	2	NC	8	168/112	
ST/18	14.7	76	8	10.5											
18.15	14.9									NL	3	<.2	18	[illegible]/78	
18.20	14.8				NL	.2	2	.3	140/84						
18.25	14.7									NL	2	NC	9	14/138	
18.30	14.[illegible]				NL	NC	2	NC	[illegible]						
18.[illegible]	15.0				NL	<.2	1	<.2	15[illegible]/[illegible]						

TESTLINE: 1 | JULIAN DATE: 227 | YEAR: 1978-1979 | TEMPLATE IDENTIFICATION: 1: 1.860

TRACKLINE NUMBER: 33

					Length SINGLE GOUGES					Length MULTIPLE GOUGES					
SEGMENT	WATER DEPTH (M)	TOTAL GOUGES	TOTAL NEW GOUGES	%	NEW SINGLE GOUGES	GOUGE DEPTH (M)	GOUGE WIDTH (M)	RIDGE HEIGHT (M)	Ø (°T)	NEW MULTI. GOUGES	NUMBER OF INCIS.	DEEPEST INCISION (M)	DISRUPT WIDTH (M)	Ø (°T)	COMMENTS
TU/19	15.0	85	1	1.1											
19.55	15.0				NL	.2	3	<.2	170/84						
UV/20	15.2	—	—	—											ICE DETOUR
VW/21	15.3	—	—	—											ICE DETOUR
WX/22	15.4	71	0	0											
X/end	15.8														

750

TESTLINE: 1 | JULIAN DATE: 216 | YEAR: 1979-1980 | TEMPLATE IDENTIFICATION: 1:1.379

TRACKLINE NUMBER: 17

SEGMENT	WATER DEPTH (M)	TOTAL GOUGES	TOTAL NEW GOUGES	%	SINGLE GOUGES: NEW SINGLE GOUGES (Length)	GOUGE DEPTH (M)	GOUGE WIDTH (M)	RIDGE HEIGHT (M)	ø (°T)	MULTIPLE GOUGES: NEW MULTI. GOUGES (Length)	NUMBER OF INCIS.	DEEPEST INCISION (M)	DISRUPT WIDTH (M)	ø (°T)	COMMENTS CS = 325°T
AB/0	5.5	—	—	–											NO RECORD
BC/1	6.1	—	—	–											NO RECORD
															Shoal [illegible] = 7.6 m at [illegible]
CD/2	8.2	40	16	40.0											SSS = 6 EPTS = 12
2.75	8.1				68	NC	2	NC	163/108						
2.75	8.1									22	3	NC	10	[illegible]/125	
2.80	8.4				37	NC	3	NC	125/70						
2.80	3.4									NL	9	NC	50	137/82	unique gouge termination direction = 262°T
2.95	8.5				NL	NC	3	NC	150/95						continues into next segment
2.95	8.5				NL	<.2	1	<.2	[illegible]/82						continues into next segment
DE/3	8.6	48	30	62.5											
3.01	8.6				NL	NC	3	NC	150/95						
3.05	8.6				NL	<.2	2	<.2	137/82						
3.20	8.7				NL	<.2	2	<.2	137/82						
3.25	8.8				NL	<.2	2	<.2	125/70						
3.40	9.0									NL	8	.2	35	134/79	
3.50	9.3									120	5	NC	17	172/117	
3.65	9.4									NL	3	NC	33	28/153	
3.70	9.4									35	2	NC	8	21/145	direction 145°T (termination)
3.85	9.7				NL	<.2	2	<.2	147/92						
3.90	9.6									NL	8	<.2	16	145/90	
EF/4	9.8	28	4	14.3											
4.01	9.8				74	NC	2	NC	[illegible]/91						
4.25	9.7				37	NC	3	NC	[illegible]/88						
4.35	9.8				118	NC	4	NC	[illegible]/103						

TESTLINE: 1		JULIAN DATE: 216		YEAR: 1979-1980						TEMPLATE IDENTIFICATION: 1.1.379					
TRACKLINE NUMBER: 17					Length SINGLE GOUGES					Length MULTIPLE GOUGES					
SEGMENT	WATER DEPTH (M)	TOTAL GOUGES	TOTAL NEW GOUGES	%	NEW SINGLE GOUGES	GOUGE DEPTH (M)	GOUGE WIDTH (M)	RIDGE HEIGHT (M)	Ø (°T)	NEW MULTI. GOUGES	NUMBER OF INCIS.	DEEPEST INCISION (M)	DISRUPT WIDTH (M)	Ø (°T)	COMMENTS
4.35	9.8				46	NC	2	NC	134/79						
FG/5	10.1	96	64	66.7											
5.10	10.2									181	3	<.2	11	136/81	
5.25	10.0				NL	<.2	2	<.2	143/93						
5.30	10.0				33	<.2	1	<.2	135/80						
5.30	10.0				NL	<.2	2	<.2	140/85						
5.35	10.0				176	<.2	1	<.2	149/94						
5.35	10.0				118	<.2	1	<.2	1??/42						
5.35	10.0				NL	<.2	3	.2	130/75						
5.45	10.1				59	NC	3	NC	159/104						direction = 284°T (Termination)
5.55	10.0									NL	25	<.2	80	150/95	direction = 275°T (Termination)
5.85	10.0									NL	13	<.2	24	150/95	([illegible] grounds 243°T and then moves off at 95°T)
5.85	10.0									NL	5	<.2	18	155/100	
5.95	10.2									NL	11	<.2	25	137/82	direction = 262°T Termination - See 6.05
GH/6	10.3	61	51	83.6											Beginning of sand wave field
6.05	10.1									NL	13	<.2	45	137/82	circular [illegible] See 5.95
6.40	10.0									68	2	<.2	8	151/96	
6.65	10.5				32	<.2	2	<.2	133/78						
6.75	11.0									NL	7	NC	25	??/160	[illegible] sand wave troughs?
6.85	10.1									93	7	NC	42	34/159	
6.85	10.1									35	6	NC	17	149/94	
6.90	10.7									NL	2	NC	20	4?/?5	
6.95	10.1									34	8	NC	43	142/87	direction = 267°T
6.95	10.1									82	5	<.2	11	22/?11	[illegible] into next segment

TESTLINE: 1	JULIAN DATE: 216	YEAR: 1979-1980	TEMPLATE IDENTIFICATION: 1:1,379

TRACKLINE NUMBER: 17

SEGMENT	WATER DEPTH (M)	TOTAL GOUGES	TOTAL NEW GOUGES	%	Length SINGLE GOUGES: NEW SINGLE GOUGES	GOUGE DEPTH (M)	GOUGE WIDTH (M)	RIDGE HEIGHT (M)	Ø (°T)	Length MULTIPLE GOUGES: NEW MULTI. GOUGES	NUMBER OF INCIS.	DEEPEST INCISION (M)	DISRUPT WIDTH (M)	Ø (°T)	COMMENTS
HI/7	10.2	32	14	43.8											[illegible] λ = ~100 m
7.01	10.2									82	5	<.2	11	22/147	
7.05	10.9									67	3	NC	12	18/143	
7.80	10.4									NL	6	NC	8	174/119	
IJ/8	11.1	45	10	22.2											
8.30	11.2									NL	10	<.2	43	149/94	
JK/9	11.6	41	5	12.2											
9.45	11.8									37	3	NC	27	117/62	
9.55	11.9				275	NC	2	NC	02/127						continues into next segment
9.95	12.0				NL	NC	3	NC	145/90						
															Total gouges maybe low due to machine malfunction
KL/10	12.1	117	2	1.7											
10.01	12.1				NL	NC	3	NC	145/97						orientation suspect due to ice detour
10.40	12.3				NL	.4	22	.2	63/08						
															large amount of sediment infilling of gouges -
LM/11	12.6	130	8	6.2											many smooth [illegible] on seafloor
11.15	12.6									NL	2	.2	30	116/61	
11.65	12.6									NL	5	NC	22	06/111	
11.70	12.8				NL	.3	8	<.2	117/62						
MN/12	12.7	123	0	0											Sediment infilling of gouges
NO/13	12.8	151	1	0.7											[illegible] infilling of [illegible]
13.35	13.2				NL	<.2	8	<.2	14/[illegible]						

TESTLINE: 1	JULIAN DATE: 216	YEAR: 1979-1980	TEMPLATE IDENTIFICATION: 1:1.379

TRACKLINE NUMBER: 17

					Length SINGLE GOUGES					Length MULTIPLE GOUGES					
SEGMENT	WATER DEPTH (M)	TOTAL GOUGES	TOTAL NEW GOUGES	%	NEW SINGLE GOUGES	GOUGE DEPTH (M)	GOUGE WIDTH (M)	RIDGE HEIGHT (M)	Ø (°T)	NEW MULTI. GOUGES	NUMBER OF INCIS.	DEEPEST INCISION (M)	DISRUPT WIDTH (M)	Ø (°T)	COMMENTS
OP/14	13.9	128	3	2.3											Sediment infilling
14.75	14.0				NL	.2	8	<.2	143/88						
14.80	14.0									NL	2	<.2	17	143/88	
PQ/15	13.8	171	40	23.4											Sediment infilling
15.15	14.0									NL	4	NC	16	167/112	
15.25	14.0									NL	7	.2	29	150/95	
15.25	14.0									NL	5	NC	25	132/77	
15.45	14.1				NL	.4	3	.5	160/105						
15.50	14.2									50	6	NC	19	158/103	
15.60	14.3				NL	.2	4	<.2	135/80						
15.65	14.0									NL	16	NC	48	150/95	
QR/16	14.3	104	4	3.8											sonar shutdown makes Total count unreliable -
16.55	14.5									NL	2	.2	15	148/93	Sediment infilling
16.75	14.7				NL	<.2	3	<.2	151/96						
16.75	14.8				NL	<.2	2	<.2	151/96						
RS/17	14.8	—	—	—											Sonar shutdown -
ST/18	15.0	76	13	17.1											
18.99	15.1									NL	6	.2	36	159/104	[illegible]
18.99	15.1				NL	.3	8	.4	145/90						[illegible]
18.99	15.1									NL	6	NC	36	[illegible]	sediment
TU/19	15.1	77	13	16.9											
19.01	15.1									NL	6	.2	[illegible]	[illegible]/104	sediment infilling
19.01	15.1				NL	.3	8	.1	145/90						

TESTLINE: 1		JULIAN DATE: 216			YEAR: 1979-1980					TEMPLATE IDENTIFICATION: 1:1.379					
TRACKLINE NUMBER: 17					Length SINGLE GOUGES					Length MULTIPLE GOUGES					
SEGMENT	WATER DEPTH (M)	TOTAL GOUGES	TOTAL NEW GOUGES	%	NEW SINGLE GOUGES	GOUGE DEPTH (M)	GOUGE WIDTH (M)	RIDGE HEIGHT (M)	Ø (°T)	NEW MULTI. GOUGES	NUMBER OF INCIS.	DEEPEST INCISION (M)	DISRUPT WIDTH (M)	Ø (°T)	COMMENTS
19.01	15.1									NL	6	NC	36	152/97	
UV/20	15.6	83	0	0											[illegible] sediment infilling of gouges
V/END	15.6														

TESTLINE: 1		JULIAN DATE: 216			YEAR: 1980-1981					TEMPLATE IDENTIFICATION: 1:1633					1
Tracking Number 27					Length SINGLE GOUGES					Length MULTIPLE GOUGES					
SEGMENT	WATER DEPTH (M)	TOTAL GOUGES	TOTAL NEW GOUGES	%	NEW SINGLE GOUGES	GOUGE DEPTH (M)	GOUGE WIDTH (M)	RIDGE HEIGHT (M)	Ø (°T)	NEW MULTI. GOUGES	NUMBER OF INCIS.	DEEPEST INCISION (M)	DISRUPT WIDTH (M)	Ø (°T)	COMMENTS CS: 325°T
AP/0	5.1	3	—	—											NO 1980 DATA
															SS#14 BETS#18
BC/1	6.3	3	—	—											NO 1980 DATA
															Shoal height = 1.7 m at Pt. B
CD/2	8.5	23	9	39.1											
2.25	8.1				NL	.3	4	.2	155/100						
2.35	7.8				NL	<.2	2	<.2	[illegible]/59						
2.55	8.1				NL	<.2	2	<.2	162/107						
2.65	8.5				NL	<.2	3	<.2	145/90						
2.80	8.3				NL	<.2	2	<.2	152/97						
2.85	8.4				NL	<.2	1	<.2	145/90						
2.85	8.4				NL	<.2	2	<.2	14/139						
2.95	8.5				NL	NC	5	NC	116/61						Termination-direction = 61°T
2.95	8.5				NL	<.2	3	<.2	140/85						continues into next segment
DE/3	8.5	47	15	31.9											
3.01	8.5				NL	<.2	3	<.2	143/85						
3.05	8.5				NL	<.2	1	<.2	135/80						
3.15	8.6				NL	<.2	1	<.2	120/71						
3.20	8.6				NL	<.2	2	<.2	122/67						
3.20	8.6									NL	4	NC	34	03/128	
3.20	8.6				NL	<.2	2	<.2	15/101						
3.25	8.7				97	.4	6	<.2	135/77						
3.30	8.7				NL	.3	2	.3	123/65						
3.35	8.9				NL	.2	3	<.2	[illegible]/102						
[illegible].60	9.3				42	NC	2	NC	[illegible]/151						Termination direction = 151°T
[illegible].65	9.3				45	NC	3	NC	[illegible]/150						Termination direction = 155°T
[illegible].85	9.5				NL	.2	4	.3	[illegible]						

TESTLINE: 1 | JULIAN DATE: 216 | YEAR: 1980-1981 | TEMPLATE IDENTIFICATION: 1:1,633

Trackline Number [illegible]

					Length SINGLE GOUGES					[illegible] MULTIPLE GOUGES					
SEGMENT	WATER DEPTH (M)	TOTAL GOUGES	TOTAL NEW GOUGES	%	NEW SINGLE GOUGES	GOUGE DEPTH (M)	GOUGE WIDTH (M)	RIDGE HEIGHT (M)	Ø (°T)	NEW MULTI. GOUGES	NUMBER OF INCIS.	DEEPEST INCISION (M)	DISRUPT WIDTH (M)	Ø (°T)	COMMENTS
EF/4	9.7	27	16	59.3											
4.10	9.7				NL	.3	3	.4	146/91						
4.20	9.7									NL	2	.2	10	157/102	
4.20	9.7				NL	<.2	1	<.2	169/114						
4.25	9.7				NL	<.2	3	<.2	98/43						
4.30	9.7				NL	.2	3	.4	[illegible]						
4.45	9.7				NL	.2	2	.2	129/71						
4.50	9.7				NL	.2	2	.2	124/69						
4.50	9.7				NL	.4	3	.2	[illegible]/85						
4.55	9.8				NL	.2	3	.2	137/82						
4.65	9.8				NL	<.2	4	<.2	[illegible]/78						
4.70	9.8				NL	<.2	2	<.2	[illegible]/75						
4.75	10.0									NL	3	<.2	12	139/84	Termination direction - 264°T
4.99	10.1				NL	<.2	3	<.2	130/75						
FG/5	10.1	43	9	20.9											
5.05	10.0				NL	<.2	2	<.2	134/79						
5.20	10.0				NL	<.2	5	<.2	136/81						
5.30	10.0				NL	.2	3	.3	136/81						
5.35	10.0									NL	2	<.2	6	135/[illegible]	
5.35	10.0				NL	.2	2	<.2	113/[illegible]						
5.70	10.1				NL	<.2	3	<.2	133/[illegible]						
5.99	10.0									NL	2	<.2	11	168/113	
GH/6	10.0	13	2	15.4											
6.15	10.3				NL	<.2	3	<.2	130/[illegible]						
6.50	10.4				NL	<.2	3	<.2	[illegible]						

TESTLINE: 1		JULIAN DATE: 216			YEAR: 1980-1981					TEMPLATE IDENTIFICATION: 1:1633					
Trackline Number 27					Length SINGLE GOUGES					Length MULTIPLE GOUGES					
SEGMENT	WATER DEPTH (M)	TOTAL GOUGES	TOTAL NEW GOUGES	%	NEW SINGLE GOUGES	GOUGE DEPTH (M)	GOUGE WIDTH (M)	RIDGE HEIGHT (M)	ø (°T)	NEW MULTI. GOUGES	NUMBER OF INCIS.	DEEPEST INCISION (M)	DISRUPT WIDTH (M)	ø (°T)	COMMENTS
HI/7	10.7	22	12	54.5											Sediment waves: .8 m or h = 10 m continues throughout segment
7.10	10.2				28	<.2	2	<.2	160/105						
7.20	10.3				NL	NC	8	NC	148/93						
7.60	10.5				110	NC	7	NC	160/105						Termination direction - 285°T
7.75	11.0				40	NC	4	NC	155/100						
7.80	10.8				NL	<.2	2	<.2	124/69						
7.85	10.8				NL	<.2	2	<.2	77/22						
7.85	10.5				NL	NC	3	NC	95/40						
7.95	11.2									NL	2	NC	11	150/95	Termination direction - 220°T
7.95	11.2									95	2	NC	14	145/90	68/13 movement: 90°T then 193°T
7.95	11.2				NL	<.2	3	<.2	68/13						
IJ/8	11.1	38	14	36.8											
8.10	11.0				NL	NC	6	NC	21/146						
8.50	11.2				NL	.3	3	.2	115/60						
8.60	11.5				NL	NC	3	NC	135/80						
8.60	11.5									NL	5	<.2	23	153/98	19/143 102/105 : Shape 98°T then 143°T then 1[illegible]
8.65	11.5				NL	NC	4	NC	163/108						
8.80	11.7				NL	<.2	2	<.2	158/103						
8.80	11.7									44	3	NC	10	27/152	Termination direction - 152°T
8.90	11.8				NL	NC	5	NC	145/90						
JK/9	11.6	48	15	31.3											
9.10	11.6									NL	2	.3	10	161/106	
9.20	11.7				NL	.2	3	<.2	112/57						
9.60	12.0									NL	2	<.2	5	164/109	
9.65	12.0				NL	NC	5	NC	130/75						
9.70	12.1									NL	2	<.2	6	126/71	

TESTLINE: 1 | JULIAN DATE: 21[illegible] | YEAR: 1980 - 1981 | TEMPLATE IDENTIFICATION: 1:1.633

Tracking [illegible] 27

SEGMENT	WATER DEPTH (M)	TOTAL GOUGES	TOTAL NEW GOUGES	%	Length SINGLE GOUGES: NEW SINGLE GOUGES	GOUGE DEPTH (M)	GOUGE WIDTH (M)	RIDGE HEIGHT (M)	Ø (°T)	Length MULTIPLE GOUGES: NEW MULTI. GOUGES	NUMBER OF INCIS.	DEEPEST INCISION (M)	DISRUPT WIDTH (M)	Ø (°T)	COMMENTS
9.70	12.1				NL	<.2	2	<.2	130/75						
9.75	12.1									NL	3	.2	12	125/81	
9.85	12.1				NL	.2	6	<.2	115/60						
9.90	12.2									NL	2	NC	43	00/125	continues into next segment - terminates (125°)
KL/10	12.2	87	6	6.9											
10.30	12.5									NL	2	.6	41	170/115	from above - single turns to double incision at mid-seg.
10.60	12.3				NL	NC	2	NC	25/150						
10.75	12.3				NL	.3	3	.4	12[illegible]/71						
10.80	12.4				NL	.6	11	.5	162/127						Very large gouge - disruption width of 30+ m (con't to next)
10.90	12.6				NL	NC	8	NC	172/117						large gouge continues to next segment
LM/11	12.5	84	11	13.1											
11.05	12.5				70	<.2	2	<.2	149/94						
11.25	12.5				NL	NC	11	NC	166/111						Very large from above (10.8)
11.50	12.8				75	NC	2	NC	1[illegible]8/113						
11.50	12.8									NL	3	NC	12	175/120	triple [illegible] turns to a single. (see 12.9) con't to next seg.
11.50	12.8				NL	NC	5	NC	175/120						continuing into next segment
11.85	13.1				NL	NC	3	NC	103/85						
11.85	13.1									NL	3	NC	10	1[illegible]3/109	changes to single in next segment
MN/12	13.0	86	15	17.4											Start roll (Fats) 19
12.15	13.0									NL	2	NC	10	[illegible]/133	
12.25	13.2				NL	.3	3	.5	1[illegible]/101						(Same as 11.85b)
12.50	13.2				NL	<.2	8	<.2	[illegible]/111						
12.50	13.2				NL	NC	5	NC	15[illegible]/[illegible]						
12.50	[illegible]									NL	3	NC	19	1[illegible]/121	[illegible] (Same as 11.50)
12.85	13.1				NL	NC	4	NC	17[illegible]/1[illegible]1						(Same as 11.50 a)

TESTLINE: 1			JULIAN DATE: 216		YEAR: 1980 -1981					TEMPLATE IDENTIFICATION: 1:1633					
Trackline Number 27					SINGLE GOUGES					MULTIPLE GOUGES					
SEGMENT	WATER DEPTH (M)	TOTAL GOUGES	TOTAL NEW GOUGES	%	NEW SINGLE GOUGES	GOUGE DEPTH (M)	GOUGE WIDTH (M)	RIDGE HEIGHT (M)	Ø (°T)	NEW MULTI. GOUGES	NUMBER OF INCIS.	DEEPEST INCISION (M)	DISRUPT WIDTH (M)	Ø (°T)	COMMENTS
12.95	13.4									NL	5	.5	13	[illegible]/97	[illegible] multiplet
12.95	13.4				NL	.6	6	.6	118/63						
ND/13	13.4	88	15	17.0											
13.05	13.3									NL	3	NC	15	159/104	(from 12.50c)
13.05	13.3				NL	NC	5	NC	100/105						(from 12.95a)
13.10	13.3				NL	.2	3	<.2	120/65						
13.25	13.5				NL	NC	3	NC	112/117						
13.50	13.5				NL	<.2	2	<.2	158/[illegible]						
13.50	13.5				NL	.3	3	<.2	125/70						
13.55	13.4				NL	.3	3	.4	118/63						
13.85	13.7				NL	<.2	3	<.2	166/111						continues into next segment
13.85	13.7									NL	5	.2	19	166/111	
OP/14	13.8	109	22	20.2											
14.05	13.7				NL	NC	3	NC	161/112						
14.05	13.7				178	NC	3	NC	08/133						
14.50	13.8									NL	4	.2	26	171/116	
14.60	13.7				NL	<.2	2	<.2	131/7[illegible]						
14.80	14.0									NL	4	.2	27	171/116	continues into next segment
14.85	13.[illegible]				NL	<.2	5	<.2	128/73						
14.99	13.9									NL	7	NC	32	163/108	[illegible] into next segment
14.99	13.9									NL	3	NC	17	[illegible]	[illegible] next segment
PQ/15	13.9	106	30	28.3											
15.05	14.0									NL	[illegible]	NC	13	[illegible]/11	
15.20	14.0									NL	10	.5	30	[illegible]/12	
15.30	14.1									NL	2	.3	10	124/67	

TESTLINE: 1					JULIAN DATE: 216				YEAR: 1980-1981			TEMPLATE IDENTIFICATION: 1:1633			
Transition Number 2[illegible]					Length SINGLE GOUGES					Length MULTIPLE GOUGES					
SEGMENT	WATER DEPTH (M)	TOTAL GOUGES	TOTAL NEW GOUGES	%	NEW SINGLE GOUGES	GOUGE DEPTH (M)	GOUGE WIDTH (M)	RIDGE HEIGHT (M)	Ø (°T)	NEW MULTI. GOUGES	NUMBER OF INCIS.	DEEPEST INCISION (M)	DISRUPT WIDTH (M)	Ø (°T)	COMMENTS
15.30	14.1				NL	.[illegible]	4	.5	[illegible]/6[illegible]						
15.30	14.1									NL	3	<.2	12	167/112	
15.45	14.3									NL	3	<.2	11	162/107	
15.50	13.7									NL	2	.2	8	143/85	
15.65	14.4									NL	5	NC	18	160/105	
15.95	14.2				NL	<.2	5	<.2	140/85						continues into next segment
QR/16	14.1	83	7	8.4											
16.01	14.1				NL	<.2	5	<.2	140/85						
16.10	14.4				88	NC	2	NC	[illegible]/130						directional changes
16.20	14.2				NL	<.2	8	<.2	59/04						
16.55	14.7				NL	<.2	3	<.2	1[illegible]0/81						
16.75	14.6									NL	3	.3	12	147/92	
RS/17	14.7	75	9	12.0											
17.30	14.8				NL	NC	3	NC	120/65						
17.30	14.8				NL	NC	4	NC	120/65						
17.40	14.9				NL	<.2	3	<.2	124/[illegible]						Termination – direction = 249 °T
17.45	14.9									NL	3	.2	12	150/95	
17.65	15.0				NL	NC	7	NC	162/107						
17.70	15.0				NL	<.2	2	<.2	127/72						
17.85	15.0				NL	NC	3	NC	145/90						
S/END	15.0														

TESTLINE: 1	JULIAN DATE:	YEAR: 1981-1982	TEMPLATE IDENTIFICATION: 1:1.379

TRACKLINE NUMBER: 16 — CS: 310°T

SEGMENT	WATER DEPTH (M)	TOTAL GOUGES	TOTAL NEW GOUGES	%	SINGLE GOUGES: Length NEW SINGLE GOUGES	GOUGE DEPTH (M)	GOUGE WIDTH (M)	RIDGE HEIGHT (M)	Ø (°T)	MULTIPLE GOUGES: Length NEW MULTI. GOUGES	NUMBER OF INCIS.	DEEPEST INCISION (M)	DISRUPT WIDTH (M)	Ø (°T)	[illegible] 100m * COMMENTS SS * 8 PMS * 10
AB/0	5.4	4	1	25.0											1982 EF : [illegible] THREE METER SHALLOW. ALL
0.55	7.7				25	<.2	1	<.2	129/79						measurements adjusted by adding .8m to depths.
															[illegible] range must affect total gouge counts. *
BC/1	6.6	3	0	0.0											[illegible] Shoal ht: 1.5m
															100m range may also affect resolution of smaller gouges.
CD/2	8.1	26	2	7.7											
2.99	8.5									NL	2	<.2	10	151/101	continues into next segment
DE/3	8.5	64	8	12.5											
3.01	8.5									NL	2	<.2	10	151/101	
3.45	9.0				NL	<.2	1	<.2	142/92						
3.85	9.4				NL	<.2	2	<.2	158/108						
3.90	9.4									NL	2	<.2	9	127/77	
3.95	9.4									NL	2	<.2	8	123/73	
EF/4	9.5	50	10	20.0											
4.01	9.5				NL	NC	4	NC	137/87						Termination: 87°T
4.15	9.5				NL	.2	3	<.2	120/70						
4.25	9.5				NL	.3	3	<.2	98/48						
4.30	9.5									NL	2	<.2	7	[illegible]/66	
4.75	9.7				NL	<.2	3	<.2	62/12						
4.75	9.7				62	NC	1	NC	[illegible]/101						
4.80	9.8				NL	<.2	2	<.2	137/87						
4.85	9.8				NL	<.2	2	<.2	14[illegible]/9[illegible]						
4.90	9.8				NL	<.2	1	<.2	1[illegible]4/[illegible]1						

2

TESTLINE: 1 | JULIAN DATE: | YEAR: 1981-1982 | TEMPLATE IDENTIFICATION: 1:1,369

TRACKLINE NUMBER: 16

CS: 310°T

Purge = 1?? ft

					Length SINGLE GOUGES					Length MULTIPLE GOUGES					
SEGMENT	WATER DEPTH (M)	TOTAL GOUGES	TOTAL NEW GOUGES	%	NEW SINGLE GOUGES	GOUGE DEPTH (M)	GOUGE WIDTH (M)	RIDGE HEIGHT (M)	Ø (°T)	NEW MULTI. GOUGES	NUMBER OF INCIS.	DEEPEST INCISION (M)	DISRUPT WIDTH (M)	Ø (°T)	COMMENTS
FG/5	9.8	53	7	13.2											1?-20 cm [illegible]
5.05	9.8				NL	<.2	4	<.2	120/80						
5.10	9.8				NL	.2	3	<.2	30/8[illegible]						
5.20	9.7				NL	<.2	2	<.2	150/100						
5.20	9.7				NL	.3	5	.2	90/40	—					
5.30	9.8				NL	<.2	3	<.2	86/36						
5.40	9.8				NL	.2	3	<.2	13/43						
5.50	9.7				NL	<.2	3	<.2	155/105						Termination : 323°T 105 335
GH/6	9.8	22	3	13.6											much movement of sediment. troughs of sand wave field may
6.20	10.2				NL	<.2	1	<.2	165/115						have funny bottom exposed. water depth at trough of sand wave
6.35	9.7				NL	<.2	1	<.2	14[illegible]/9[illegible]						water depth at crest of sand wave
6.80	9.6				NL	<.2	1	<.2	149/99						water depth at crest of sand wave
HI/7	10.3	31	2	6.5											extensive sediment movement. troughs have funny bottom.
7.01	10.3				NL	<.2	2	<.2	130/80						
7.65	10.5				NL	.2	2	<.2	138/88						
IJ/8	10.8	64	20	31.3											
8.05	11.1				NL	<.2	2	<.2	145/95						
8.15	10.5									NL	4	.4	16	137/87	shape
8.30	10.9				NL	<.2	3	<.2	144/94						
8.35	10.8				NL	<.2	3	<.2	128/78						
8.40	11.3				NL	<.2	2	<.2	13[illegible]/8[illegible]						
8.45	10.6				NL	<.2	1	<.2	116/66						
8.55	11.3				NL	NC	2	NC	177/127						
8.70	11.2				NL	NC	2	NC	[illegible]/71						
8.7[illegible]	11.2				NL	NC	2	NC	178/12[illegible]						

TESTLINE: /	JULIAN DATE:	YEAR: 1981–1982	TEMPLATE IDENTIFICATION: 1:1.379

TRACKLINE NUMBER: 16					Length SINGLE GOUGES					Length MULTIPLE GOUGES					CS: 310°T
SEGMENT	WATER DEPTH (M)	TOTAL GOUGES	TOTAL NEW GOUGES	%	NEW SINGLE GOUGES	GOUGE DEPTH (M)	GOUGE WIDTH (M)	RIDGE HEIGHT (M)	Ø (°T)	NEW MULTI. GOUGES	NUMBER OF INCIS.	DEEPEST INCISION (M)	DISRUPT WIDTH (M)	Ø (°T)	Range = 100m * COMMENTS
8.70	11.2									NL	2	NC	3	[illegible]/124	
8.90	11.3				NL	NC	5	NC	87/137						~ slope
8.95	11.2				NL	NC	1	NC	172/122						
8.99	11.2				NL	<.2	2	<.2	23/[illegible]						continues into next segment
8.99	11.2									NL	2	<.2	6	137/87	
8.99	11.2				NL	<.2	1	<.2	147/[illegible]						
JK/9	11.2	85	20	23.5											
9.01	11.2				NL	<.2	2	<.2	23/153						continued from previous segment
9.01	11.2									NL	2	<.2	6	[illegible]/87	
9.01	11.2				NL	<.2	1	<.2	147/97						
9.05	11.3				NL	<.2	1	<.2	135/85						
9.10	11.2				NL	<.2	2	<.2	141/91						
9.15	11.2				NL	<.2	2	<.2	126/76						
9.20	11.2									NL	9	<.2	20	173/123	
9.25	11.2				NL	<.2	2	<.2	151/101						
9.30	11.3				NL	.2	3	.2	131/81						
9.35	11.4									NL	2	.3	20	98/48	
KL/10	11.7	119	6	5.0											100 m Range increases resolution and accounts for high total gouge count.
10.05	11.5				NL	.3	7	.2	92/42						
10.15	11.6				NL	.2	3	.2	153/103						
10.25	11.6				NL	.2	3	.2	[illegible]						
10.40	11.8				NL	.4	4	.5	[illegible]/170						
10.75	11.7				NL	<.2	2	<.2	150/[illegible]						
10.80	11.8				NL	<.2	1	<.2	172/[illegible]						

TESTLINE: 1	JULIAN DATE:	YEAR: 1981 -1982	TEMPLATE IDENTIFICATION: 1: 1,379

TRACKLINE NUMBER: 1a					Length SINGLE GOUGES					Length MULTIPLE GOUGES					CS: 310 °T
SEGMENT	WATER DEPTH (M)	TOTAL GOUGES	TOTAL NEW GOUGES	%	NEW SINGLE GOUGES	GOUGE DEPTH (M)	GOUGE WIDTH (M)	RIDGE HEIGHT (M)	Ø (°T)	NEW MULTI. GOUGES	NUMBER OF INCIS.	DEEPEST INCISION (M)	DISRUPT WIDTH (M)	Ø (°T)	Range = 100 m COMMENTS
LM/11	12.1	128	6	4.7											100 m range [illegible] resolution and accounts for
11.25	12.1				NL	.2	3	<.2	118/68						high total gouge count.
11.35	12.1				NL	<.2	3	<.2	[illegible]						
11.40	12.2									NL	2	.2	17	[illegible]	
11.75	12.2				NL	<.2	1	<.2	132/82						
11.85	12.2				NL	.2	13	.4	128/18						
MN/12	12.4	129	3	2.3											
12.50	12.6									NL	2	.4	13	97/47	
12.85	12.3				NL	1.0	7	.4	102/52						
NO/13	12.6	116	3	2.6											
13.85	12.9				NL	<.2	6	<.2	90/40						
13.95	12.9				NL	.5	11	.5	90/40						
13.99	12.9				NL	.2	5	<.2	90/40						
O/end	12.9														

TESTLINE: 2 | JULIAN DATE: | YEAR: 1977-1979 | TEMPLATE IDENTIFICATION: 1:1.633

TRACKLINE NUMBER: 11

CS: 358

SEGMENT	WATER DEPTH (M)	TOTAL GOUGES	TOTAL NEW GOUGES	%	Length SINGLE GOUGES: NEW SINGLE GOUGES	GOUGE DEPTH (M)	GOUGE WIDTH (M)	RIDGE HEIGHT (M)	Ø (°T)	Length MULTIPLE GOUGES: NEW MULTI. GOUGES	NUMBER OF INCIS.	DEEPEST INCISION (M)	DISRUPT WIDTH (M)	Ø (°T)	COMMENTS
AB/0	7.3	39	12	[illegible]											[illegible] line. Most older gouges gone.
0.10	7.8				NL	<.2	2	<.2	140/138						very small gouges
0.15	7.9									NL	4	<.2	42	27/25	(gouges spaced far apart (~5m))
0.25	8.6									NL	7	<.2	27	45/43	
BC/1	10.2	8	4	50.0											
1.20	10.5									NL	3	<.2	16	44/42	Termination: 154°T 42 154°T
1.99	11.5				NL	<.2	2	<.2	17/15						continues into next segment
CD/2	11.5	5	1	20.0											[illegible] of sand waves were many gouges used to be -
2.01	11.5				NL	<.2	2	<.2	17/15						[illegible] 169°T [illegible] continued from previous seg.
DE/3	11.7	24	22	91.7											2.3 m shoal. New gouges on shoal crest. Sed waves sea-
3.50	10.9				24	<.2	1	<.2	113/111						ward of shoal / on inside of shoal Termination: 111°T
3.65	9.5									NL	13	<.2	75	114/112	[illegible] in shoal crest. Most gouges on crest
3.65	9.5				31	<.2	1	<.2	40/38						Termination: 38°T
3.70	10.1									38	2	<.2	6	149/147	Termination: 147°T
3.70	10.1				48	<.2	2	<.2	163/161						Termination: 161°T
3.70	10.1				45	NC	3	NC	65/163						Termination 163°T
3.70	10.1				NL	<.2	2	<.2	38/36						
3.70	10.1				23	<.2	2	<.2	[illegible]/175						Termination: 175°T
3.90	12.1				NL	<.2	2	<.2	11/17						seaward of shoal
EF/4	12.4	3	1	[illegible]											[illegible] direction analysis (?)
4.85	13.1				NL	<.2	7	<.2	85/83						[illegible]

TESTLINE: 2	JULIAN DATE:	YEAR: 1977-1978	TEMPLATE IDENTIFICATION: 1:1,633

TRACKLINE NUMBER: 17 — CS: 358 T

SEGMENT	WATER DEPTH (M)	TOTAL GOUGES	TOTAL NEW GOUGES	%	Length NEW SINGLE GOUGES	SINGLE GOUGES: GOUGE DEPTH (M)	GOUGE WIDTH (M)	RIDGE HEIGHT (M)	ø (°T)	Length NEW MULTI. GOUGES	MULTIPLE GOUGES: NUMBER OF INCIS.	DEEPEST INCISION (M)	DISRUPT WIDTH (M)	ø (°T)	COMMENTS
FG/5	13.5	62	30	48.4											[illegible] Normal to line [illegible]
5.05	13.5									NL	5	<.2	30	129/118	[illegible] count may be higher of total gouges.
5.30	13.6				40	NC	2	NC	57/55						
5.50	14.0									94	5	NC	22	09/07	
5.50	14.0									200	7	NC	30	29/26	Termination: 26 T 26 [illegible]
5.95	14.2									NL	2	<.2	16	146/144	
5.99	14.3				NL	.2	7	.4	28/26						con't into next segment
5.99	14.3									NL	9	NC	25	150/148	148 25
GH/6	14.3	32	17	53.1											
6.01	14.3				NL	.2	7	.4	28/26						Poor resolution of gouges normal to trackline.
6.01	14.3									NL	9	NC	25	150/148	
6.10	14.4				NL	<.2	2	<.2	55/53						
6.20	14.4									NL	2	<.2	16	65/63	
6.40	14.5				NL	<.2	5	.2	52/50						
6.40	14.5				NL	<.2	1	<.2	12/10						
6.65	14.6				NL	<.2	2	<.2	52/50						
6.80	14.8				NL	<.2	2	<.2	85/83						
HI/7	15.1	13	4	30.8											[illegible] fraction features.
7.35	14.7									NL	4	<.2	20	61/59	
IJ/8	14.5	51	23	45.1											[illegible]
8.50	11.4				NL	<.2	1	<.2	[illegible]/98						Between years
8.50	11.4				NL	<.2	1	<.2	125/123						
8.50	11.4				NL	<.2	1	<.2	125/[illegible]						
8.50	11.4				NL	<.2	2	<.2	[illegible]/[illegible]						
8.50	11.4				NL	<.2	1	<.2	112/[illegible]						

TESTLINE: 2	JULIAN DATE:	YEAR: 1977-1978	TEMPLATE IDENTIFICATION: 1:1.633

TRACKLINE NUMBER: 17 — CS: 358°T — 125 ft [illegible]

SEGMENT	WATER DEPTH (M)	TOTAL GOUGES	TOTAL NEW GOUGES	%	Length SINGLE GOUGES: NEW SINGLE GOUGES	GOUGE DEPTH (M)	GOUGE WIDTH (M)	RIDGE HEIGHT (M)	Ø (°T)	Length MULTIPLE GOUGES: NEW MULTI. GOUGES	NUMBER OF INCIS.	DEEPEST INCISION (M)	DISRUPT WIDTH (M)	Ø (°T)	COMMENTS
8.50	11.4				NL	<.2	[illegible]	<.2	115/113						
8.50	11.4				46	<.2	1	<.2	[illegible]/00						
8.50	11.4				NL	<.2	2	<.2	57/120						
8.50	11.4									NL	2	<.2	5	03/01	
8.50	11.4				NL	<.2	2	<.2	55/53						
8.50	11.4				NL	NC	5	NC	125/123						Termination: 303°T
8.50	11.4				NL	<.2	2	<.2	125/123						
8.50	11.4				NL	<.2	1	<.2	100/98						
8.50	11.4				NL	<.2	1	<.2	115/113						
8.50	11.4				NL.	<.2	2	<.2	140/138						
8.50	11.4				NL	<.2	1	<.2	158/156						
8.50	11.4				NL	<.2	1	<.2	01/179						
8.50	11.4				NL	<.2	2	<.2	115/113						
8.50	11.4				NL	<.2	1	<.2	176/174						
8.50	11.4				NL	<.2	1	<.2	50/48						
8.50	11.4				NL	<.2	1	<.2	151/149						
8.50	11.4				NL	<.2	2	<.2	158/156						
JK/9	14.4	18	0	0.0											18 gouges are very faint [illegible] DUE TO small ice)
KL/10	15.3	13	8	69.2											1.0 m Shoal [illegible] waves on shoal [illegible]
[illegible]	14.3				31	NC	3	NC	[illegible]/15						[illegible]
[illegible]	14.3				12	NC	2	NC	[illegible]/13						
[illegible]	14.3									NL		[illegible]	[illegible]	[illegible]/107	
[illegible]	14.7				22	NC	3	NC	[illegible]/149						
[illegible]	14.9									NL	[illegible]	[illegible]	[illegible]	[illegible]/02	
[illegible]	15.0				NL	[illegible]	2	[illegible]	[illegible]/6						

768

TESTLINE: 2		JULIAN DATE:			YEAR: 1977-1978					TEMPLATE IDENTIFICATION: 1:1.633					
TRACKLINE NUMBER: [illegible]					Length SINGLE GOUGES					Length MULTIPLE GOUGES					CS: 358°T
SEGMENT	WATER DEPTH (M)	TOTAL GOUGES	TOTAL NEW GOUGES	%	NEW SINGLE GOUGES	GOUGE DEPTH (M)	GOUGE WIDTH (M)	RIDGE HEIGHT (M)	Ø (°T)	NEW MULTI. GOUGES	NUMBER OF INCIS.	DEEPEST INCISION (M)	DISRUPT WIDTH (M)	Ø (°T)	Range [illegible] COMMENTS
LM/11	15.7	17	13	[illegible]											[illegible]
11.60	16.4				[illegible]	NC	2	NC	[illegible]/20						
11.70	16.2									[illegible]	[illegible]	NC	13	[illegible]	
11.80	16.6				NL	<.2	2	<.2	48/46						
11.85	16.7									NL	4	NC	27	90/88	
11.90	16.3				NL	<.2	2	<.2	112/110						
11.99	16.7				NL	.2	8	.3	[illegible]						
MN/12	16.7	15	11	73.3											
12.10	16.9				NL	.4	3	<.2	77/75						
12.15	16.9									NL	3	<.2	17	115/113	
12.15	16.9				NL	<.2	1	<.2	99/97						
12.15	16.9				NL	<.2	2	.2	62/60						
12.20	16.8				NL	.2	3	.3	80/56						
12.45	16.9				NL	<.2	2	<.2	90/88						
12.50	17.0									NL	3	<.2	25	90/88	
NO/13	17.5	27	17	60.7											
13.05	17.5				NL	.5	20	.3	[illegible]/88						
13.15	17.5				NL	<.2	2	<.2	127/125						
13.25	17.5									35	3	NC	16	27/25	Termination: 205°T
13.30	17.5				NL	.4	10	.8	93/91						
13.35	17.6				NL	.2	4	<.2	[illegible]						
13.35	17.6				NL	<.2	2	<.2	[illegible]/56						
13.35	[illegible]				NL	.4	8	.2	[illegible]/98						
13.40	17.7									NL	2	<.2	8	[illegible]	
13.45	18.0									NL	6	.5	[illegible]	[illegible]	

TESTLINE: 2	JULIAN DATE:	YEAR: 1977-1978	TEMPLATE IDENTIFICATION: 1:1,633

TRACKLINE NUMBER: 17					Length SINGLE GOUGES					Length MULTIPLE GOUGES					CS: 358°T
SEGMENT	WATER DEPTH (M)	TOTAL GOUGES	TOTAL NEW GOUGES	%	NEW SINGLE GOUGES	GOUGE DEPTH (M)	GOUGE WIDTH (M)	RIDGE HEIGHT (M)	Ø (°T)	NEW MULTI. GOUGES	NUMBER OF INCIS.	DEEPEST INCISION (M)	DISRUPT WIDTH (M)	Ø (°T)	[illegible] COMMENTS
OP-14	18.3	17	7	41.2											[illegible]
14.25	18.3				NL	<.2	2	<.2	69/67						
14.65	18.4				NL	<.2	2	<.2	73/71						
14.99	18.5									NL	5	.5	55	98/96	
P-end	18.5														

1

TESTLINE: 2	JULIAN DATE:	YEAR: 1978-1979	TEMPLATE IDENTIFICATION: 1:1.633

TRACKLINE NUMBER: 31					Length SINGLE GOUGES					Length MULTIPLE GOUGES					CS: 358
SEGMENT	WATER DEPTH (M)	TOTAL GOUGES	TOTAL NEW GOUGES	%	NEW SINGLE GOUGES	GOUGE DEPTH (M)	GOUGE WIDTH (M)	RIDGE HEIGHT (M)	Ø (°T)	NEW MULTI. GOUGES	NUMBER OF INCIS.	DEEPEST INCISION (M)	DISRUPT WIDTH (M)	Ø (°T)	Range: 125 m COMMENTS SS#10 Pdls #10a.
AE/0	6.5	9	0	0.0											[illegible] ties of sand.
BC/1	9.9	6	1	16.7											[illegible] reworking?
1.15	10.2				NL	<.2	3	<.2	45/46						Sand ribbons (darker return) with ripples: Trough Ø = 64°T
															[illegible] wavelength, ht = <.2 m reworking indicated
CD/2	11.3	25	25	100.0											
2.95	11.4									NL	11	<.2	50	22/20	
2.99	11.3									NL	14	<.2	47	20/18	
DE/3	11.3	44	44	100.0											
3.55	10.1				NL	<.2	3	<.2	57/55						3.5 [illegible] of end of segment. 'Post' gouging
3.55	10.1				NL	<.2	2	.3	65/63						[illegible] sed. [illegible] on seaward side of shoal
3.60	9.2									25	6	<.2	15	19/17	
3.60	9.2				c2	<.2	2	<.2	116/114						
3.65	9.1				NL	<.2	2	<.2	108/106						
3.65	9.1				NL	<.2	1	<.2	125/123						
3.65	9.1				NL	<.2	1	<.2	135/133						
3.70	9.5									NL	27	.2	103	147/145	Pressure ridge scour
3.75	10.2				NL	.2	3	.2	98/96						
3.75	10.2									NL	[illegible]	<.2	7	50/48	Gouges on seaward side of shoal
3.80	11.6				NL	<.2	2	<.2	52/50						
3.85	11.8				NL	<.2	3	<.2	92/90						
EF/4	12.1	12	12	100.											
4.10	12.3				NL	<.2	2	<.2	13/11						
4.25	12.5				NL	<.2	2	<.2	17/15						
4.25	12.5				NL	<.2	3	<.2	61/59						
4.40	9.8				NL	<.2	2	<.2	79/77						Termination 287°T
															[illegible]

TESTLINE: 2					JULIAN DATE:				YEAR: 1978 - 1979			TEMPLATE IDENTIFICATION: 1 : 1.633			
TRACKLINE NUMBER: 31					Length SINGLE GOUGES					Length MULTIPLE GOUGES					CS: 358°T
SEGMENT	WATER DEPTH (M)	TOTAL GOUGES	TOTAL NEW GOUGES	%	NEW SINGLE GOUGES	GOUGE DEPTH (M)	GOUGE WIDTH (M)	RIDGE HEIGHT (M)	Ø (°T)	NEW MULTI. GOUGES	NUMBER OF INCIS.	DEEPEST INCISION (M)	DISRUPT WIDTH (M)	Ø (°T)	COMMENTS
4.40	11.8				NL	<.2	2	<.2	94/92						
4.40	11.8				NL	<.2	2	<.2	130/128						Termination: 128°T
4.50	11.9									NL	4	<.2	10	133/131	
4.50	11.9									NL	2	<.2	4	128/126	
FG/5	13.2	20	1	5.0											reworking of seafloor.
5.60	14.0				NL	<.2	2	<.2	74/72						
GH/6	14.1	6	0	0.0											ICE DETOUR AT END OF LINE
HI/7	15.0	1	0	0.0											Sed. waves indicate reworking of seafloor. θ=175°T λ=2m
IJ/8	14.4	23	20	87.0											3.7 m shoal mid segment. MOST GOUGING on shoal
8.50	13.1				NL	<.2	2	<.2	88/86						crest. Reworking of old gouges indicated.
8.55	12.0				18	<.2	2	<.2	124/122						Termination: 122°T
8.55	12.0				NL	<.2	3	<.2	164/162						
8.60	11.3									NL	6	<.2	12	03/01	
8.60	11.3				NL	<.2	2	<.2	118/116						
8.60	11.2				NL	<.2	1	<.2	120/118						
8.65	11.6									NL	2	<.2	11	126/124	
8.75	13.1									NL	7	<.2	17	170/168	
JK/9	14.6	1	0	0.0											reworking.
KL/10	15.1	14	9	64.3											1.8 m shoal in a segment.
10.55	13.9									15	3	<.2	7	166/164	Termination: 166°T
10.60	14.2									30	3	NC	7	[illegible]/16	Termination 166°T
10.95	15.3				NL	.2	3	<.2	/11						

TESTLINE: 2	JULIAN DATE:				YEAR: 1978-1979					TEMPLATE IDENTIFICATION: 1:1.633					
TRACKLINE NUMBER: 21					Length SINGLE GOUGES					Length MULTIPLE GOUGES					CS: 358 °T
SEGMENT	WATER DEPTH (M)	TOTAL GOUGES	TOTAL NEW GOUGES	%	NEW SINGLE GOUGES	GOUGE DEPTH (M)	GOUGE WIDTH (M)	RIDGE HEIGHT (M)	Ø (°T)	NEW MULTI. GOUGES	NUMBER OF INCIS.	DEEPEST INCISION (M)	DISRUPT WIDTH (M)	Ø (°T)	COMMENTS
LM/11	15.5	2	0	0.0											
MM/12	16.3	4	1	25.0											
12.50	16.6				NC	NC	3	NC	115/113						Termination: 113°T
11/end	NMP														loss of fathogram

TESTLINE: 2	JULIAN DATE: 215	YEAR: 1979-1980	TEMPLATE IDENTIFICATION: 1:1.379

TRACKLINE NUMBER: 16

SEGMENT	WATER DEPTH (M)	TOTAL GOUGES	TOTAL NEW GOUGES	%	SINGLE GOUGES: Length NEW SINGLE GOUGES	GOUGE DEPTH (M)	GOUGE WIDTH (M)	RIDGE HEIGHT (M)	Ø (°T)	MULTIPLE GOUGES: Length NEW MULTI. GOUGES	NUMBER OF INCIS.	DEEPEST INCISION (M)	DISRUPT WIDTH (M)	Ø (°T)	CS: 358 °T Range: 125 m COMMENTS SS # 5 Rolls # 116
AB/0	6.9	5	0	0.0											
BC/1	7.9	0	0	0.0											
CD/2	11.3	1	0	0.0											Sand waves - bottom mounted crest orien: 160°T λ = 2m
DE/3	11.5	26	21	80.8											2m step at [illegible] [illegible] gouging on shoal crest
3.15	11.6									NL	4	<.2	27	[illegible]/85	
3.45	10.8									32	3	<.2	8	[illegible]/176	
3.45	10.8				20	<.2	1	<.2	177/172						
3.60	9.2									NL	9	.2	36	110/108	Pressure ridge scouring
3.70	10.1				NL	<.2	2	<.2	97/95						
3.70	10.1				37	<.2	1	<.2	128/126						
3.70	10.1				NL	<.2	2	.2	80/78						
3.75	10.9				44	<.2	3	<.2	05/03						
EF/4	12.2	9	0	0.0											
FG/5	13.3	1	1	100.0											
5.45	13.7				NL	<.2	2	<.2	40/38						Termination: 218°T
GH/6	14.1	7	2	28.6											Tick Marks - λ = 2m
6.60	14.5				NL	<.2	7	<.2	71/6[illegible]						Tick Marks - λ = 2m
6.75	14.7				NL	<.2	5	<.2	71/77						
HI/7	15.0	9	1	11.1											Change template 1:1.623
7.10	14.4				NL	<.2	2	<.2	14[illegible]/138						[illegible] 68° λ = 2m

2

TESTLINE: 2	JULIAN DATE: 215	YEAR: 1979-1980	TEMPLATE IDENTIFICATION: 1:1.633

TRACKLINE NUMBER: 16 | CS: 308 °T

SEGMENT	WATER DEPTH (M)	TOTAL GOUGES	TOTAL NEW GOUGES	%	Length SINGLE GOUGES: NEW SINGLE GOUGES	GOUGE DEPTH (M)	GOUGE WIDTH (M)	RIDGE HEIGHT (M)	ø (°T)	Length MULTIPLE GOUGES: NEW MULTI. GOUGES	NUMBER OF INCIS.	DEEPEST INCISION (M)	DISRUPT WIDTH (M)	ø (°T)	COMMENTS
IJ/8	14.2	17	14	82.4											3.7 m shoal at mid segment gouging on shoal.
8.45	13.0				NL	<.2	2	<.2	110/108						Termination: 288°T
8.50	12.5				NL	<.2	2	<.2	91/89						
8.50	12.0									NL	4	.2	14	115/113	Termination: 293°T
8.55	11.5									NL	4	<.2	15	120/118	Termination: 298°T
8.60	11.3				NL	<.2	4	<.2	93/91						
8.65	12.2				NL	<.2	3	<.2	109/107						
8.65	12.2				NL	<.2	2	<.2	72/70						
8.75	14.2				NL	<.2	2	<.2	55/53						
JK/9	14.2	0	0	0.0											
KL/10	15.0	3	2	66.7											2m shoal at mid segment, 1 low gouges seaward side.
10.60	14.4				NL	<.2	1	<.2	124/122						
10.65	14.7				NL	<.2	2	<.2	138/136						Termination: 136°T
LM/11	15.1	3	1	33.3											
11.05	15.1				NL	<.2	1	<.2	122/120						
MN/12	16.2	6	4	66.7											
12.40	16.5				NL	<.2	4	<.2	127/125						
12.70	16.4				NL	<.2	2	<.2	58/56						
12.80	16.7				NL	.3	3	.3	73/71						
12.95	17.2				NL	<.2	3	<.2	66/64						
															[illegible]
11/end	16.9														

TESTLINE: 2 | JULIAN DATE: 216 | YEAR: 1980-1981 | TEMPLATE IDENTIFICATION: 1: 1.633

TRACKLINE NUMBER: 26

CS: 358°T

SEGMENT	WATER DEPTH (M)	TOTAL GOUGES	TOTAL NEW GOUGES	%	Length NEW SINGLE GOUGES	GOUGE DEPTH (M)	GOUGE WIDTH (M)	RIDGE HEIGHT (M)	ø (°T)	Length NEW MULTI. GOUGES	NUMBER OF INCIS.	DEEPEST INCISION (M)	DISRUPT WIDTH (M)	ø (°T)	Range = 125 m COMMENTS SS#14 Bat. #18
AC/0	7.0	8	2	25.0											Fathogram malfunction until segment 7 (HI)
0.10	7.3				NL	<.2	5	<.2	83/81						Better resolution on 1981 sonar than 1980. Accounts for gouge [illegible]
0.60	—				NL	<.2	4	<.2	[illegible]/89						Termination: 266°T
CC/1	—	8	5	62.5											
1.05	—				NL	<.2	2	<.2	71/75						Termination: 255°T
1.15	—				NL	<.2	2	<.2	66/64						
1.35	—				NL	<.2	2	<.2	47/44						
1.35	—				NL	<.2	2	<.2	[illegible]/43						
1.70	—				NL	<.2	2	<.2	53/51						
CD/2	–	4	2	50.0											
2.10	–				NL	<.2	2	<.2	69/67						
2.99	–				NL	<.2	2	<.2	71/75						
DE/3	–	29	25	86.2											2.3 meter shoal at midsegment. Most gouging on shoal crest.
3.05	–				NL	<.2	2	<.2	97/95						
3.15	–									NL	2	—	23	[illegible]/88	
3.50	–									NL	5	<.2	15	128/126	
3.60	–				NL	<.2	3	<.2	47/45						
3.50	–				NL	<.2	3	<.2	127/125						
3.50	–									NL	3	NC	20	127/125	Termination: 125°T
3.55	–									NL	2	NC	15	[illegible]/117	Termination: 117°T
3.60	–									NL	4	NC	17	[illegible]/123	Termination: 123°T
3.60	–									NL	2	<.2	9	[illegible]/10	
3.60	–									NL	2	<.2	6	15/113	
3.65	–				NL	<.2	3	<.2	[illegible]						
3.70	–				NL	<.2	3	<.2	[illegible]/61						

2

TESTLINE: 2	JULIAN DATE: 216	YEAR: 1980-1981	TEMPLATE IDENTIFICATION: 1:1.633

TRACKLINE NUMBER: 26 — CS: 359°T

SEGMENT	WATER DEPTH (M)	TOTAL GOUGES	TOTAL NEW GOUGES	%	SINGLE GOUGES Length NEW SINGLE GOUGES	GOUGE DEPTH (M)	GOUGE WIDTH (M)	RIDGE HEIGHT (M)	Ø (°T)	MULTIPLE GOUGES Length NEW MULTI. GOUGES	NUMBER OF INCIS.	DEEPEST INCISION (M)	DISRUPT WIDTH (M)	Ø (°T)	COMMENTS
EF/4	—	9	7	77.8											
4.05	—				NL	<.2	1	<.2	15/13						
4.15	—				NL	<.2	2	<.2	32/30						
4.25	—				NL	—	4	—	106/104						
4.35	—				NL	NC	4	NC	170/168						Termination: 168°T
4.60	—				NL	<.2	2	<.2	83/81						
4.60	—				NL	<.2	2	<.2	107/105						
4.85	—				NL	<.2	2	<.2	[illegible]/40						
FG/5	—	8	6	75.0											
5.05	—				NL	<.2	3	<.2	120/118						Termination: 118°T
5.15	—				NL	<.2	2	<.2	124/122						
5.15	—				NL	<.2	2	<.2	117/115						
5.20	—				NL	<.2	2	<.2	115/113						
5.95	—				NL	<.2	1	<.2	55/53						
5.99	—				NL	<.2	1	<.2	125/123						Continues into next segment.
GH/6	—	6	2	33.3											
6.01	—				NL	<.2	1	<.2	[illegible]/123						
6.65	—				NL	<.2	2	<.2	107/105						
HI/7	14.6	0	0	0.0											
IJ/8	14.2	14	14	100.0											[illegible]
8.40	12.3				NL	<.2	3	.2	125/123						
8.45	11.5				NL	<.2	4	<.2	86/86						
8.45	11.5				NL	.2	3	.2	[illegible]/130						
8.45	11.5				NL	<.2	3	.2	125/123						

777

TESTLINE: 2	JULIAN DATE: 216	YEAR: 1980-1981	TEMPLATE IDENTIFICATION: 1: 1.633

TRACKLINE NUMBER: 26 — CS: 358°T

SEGMENT	WATER DEPTH (M)	TOTAL GOUGES	TOTAL NEW GOUGES	%	SINGLE GOUGES (Length): NEW SINGLE GOUGES	GOUGE DEPTH (M)	GOUGE WIDTH (M)	RIDGE HEIGHT (M)	Ø (°T)	MULTIPLE GOUGES (Length): NEW MULTI. GOUGES	NUMBER OF INCIS.	DEEPEST INCISION (M)	DISRUPT WIDTH (M)	Ø (°T)	COMMENTS
8.50	11.1				NL	.2	3	.2	[illegible]/36						
8.50	11.1				NL	<.2	1	<.2	52/50						
8.55	11.5				NL	<.2	3	<.2	56/54						
8.70	13.0									NL	2	.2	9	124/122	
8.75	13.3				NL	<.2	2	<.2	58/56						
8.75	13.3				NL	<.2	1	<.2	50/48						
8.80	13.4				NL	<.2	1	<.2	123/121						
8.80	13.4									NL	2	<.2	19	128/126	
JK/9	14.0	7	7	100.0											
9.05	14.0				NL	.2	3	.2	90/88						
9.10	14.0				NL	<.2	3	<.2	82/80						
9.10	14.0				NL	.4	5	.5	112/110						Termination: 110 °T
9.15	14.5				NL	<.2	3	<.2	48/46						
9.25	14.6				15	<.2	2	<.2	128/126						
9.40	14.8				NL	.2	2	<.2	95/93						
9.45	14.7				NL	<.2	4	<.2	110/108						Termination: 108°T
KL/10	15.0	7	7	100.0											[illegible] m Shoal at mid segment.
10.50	14.1				NL	.2	5	.3	53/51						
10.50	14.1				NL	<.2	6	.2	118/116						
10.50	14.1				NL	<.2	6	<.2	117/115						
10.75	15.0									NL	2	<.2	23	[illegible]/109	
10.85	15.3				NL	<.2	2	<.2	114/112						
10.90	15.3				NL	<.2	2	<.2	[illegible]/116						

4

TESTLINE: 2 | JULIAN DATE: 216 | YEAR: 1980-1981 | TEMPLATE IDENTIFICATION: 1:1.633

TRACKLINE NUMBER: 26 | CS: [illegible]

SEGMENT	WATER DEPTH (M)	TOTAL GOUGES	TOTAL NEW GOUGES	%	Length SINGLE GOUGES: NEW SINGLE GOUGES	GOUGE DEPTH (M)	GOUGE WIDTH (M)	RIDGE HEIGHT (M)	Ø (°T)	Length MULTIPLE GOUGES: NEW MULTI. GOUGES	NUMBER OF INCIS.	DEEPEST INCISION (M)	DISRUPT WIDTH (M)	Ø (°T)	COMMENTS
LM/11	15.3	15	14	[illegible]											
11.15	15.6				NL	<.2	3	<.2	95/93						
11.30	15.5				NL	N/C	1	N/C	168/126						Termination: 039°T [illegible]
11.35	15.5				NL	.3	10	.3	119/117						
11.55	16.0				NL	.2	13	<.2	112/110						
11.60	16.0				NL	.5	10	.4	100/98						
11.65	16.0				NL	.2	2	<.2	[illegible]						
11.70	16.4				NL	<.2	1	<.2	118/116						
11.80	16.0				NL	.1	5	.5	101/99						
11.85	16.0				NL	<.2	3	<.2	102/100						
11.90	15.5				NL	<.2	2	<.2	103/101						
11.90	15.5				NL	.8	3	<.2	113/111						
11.95	15.8				NL	1.4	8	.9	69/67						
11.95	15.9				NL	.3	4	.3	106/104						
11.95	15.9				NL	.2	2	.4	109/107						
MN/12	16.0	23	19	82.6											
12.01	16.0				NL	.2	2	<.2	122/120						
12.20	16.4				NL	<.2	2	<.2	111/109						
12.25	16.8				NL	.2	5	<.2	66/64						
12.25	16.8				NL	.2	3	.2	133/131						
12.30	16.7				NL	<.2	2	<.2	135/133						
12.35	16.6				NL	.2	3	.2	[illegible]						
12.35	16.6				NL	<.2	3	<.2	123/121						
12.35	16.6				NL	.2	2	<.2	74/72						
12.40	16.6				NL	.2	2	.2	36/34						
12.45	16.6				NL	<.2	2	<.2	[illegible]						
12.50	16.4				NL	<.2	2	<.2	[illegible]						[illegible]

TESTLINE: 2 | JULIAN DATE: 216 | YEAR: 1980-1981 | TEMPLATE IDENTIFICATION: 1:1,633

TRACKLINE NUMBER: 2 | CS: 356°T

SEGMENT	WATER DEPTH (M)	TOTAL GOUGES	TOTAL NEW GOUGES	%	Length SINGLE GOUGES: NEW SINGLE GOUGES	GOUGE DEPTH (M)	GOUGE WIDTH (M)	RIDGE HEIGHT (M)	Ø (°T)	Length MULTIPLE GOUGES: NEW MULTI. GOUGES	NUMBER OF INCIS.	DEEPEST INCISION (M)	DISRUPT WIDTH (M)	Ø (°T)	COMMENTS
12.80	17.2				NL	<.2	3	<.2	114/112						
12.85	17.0									NL	3	<.2	25	107/105	
12.90	17.0				NL	<.2	2	<.2	137/135						
12.90	17.0				NL	.2	5	<.2	70/68						
12.99	17.2									NL	2	.3	25	89/78	
NO/13	17.2	16	8	50.0											
13.01	17.2				NL	<.2	4	<.2	103/101						
13.25	17.4				NL	.2	4	.2	92/90						
13.30	17.5				NL	.3	5	.3	116/114						
13.50	17.5				NL	<.2	2	<.2	121/119						
13.65	17.8				NL	.2	3	<.2	129/127						
13.80	18.0				NL	<.2	3	<.2	98/96						
13.90	17.8				NL	<.2	4	<.2	97/95						
13.95	17.7				NL	.2	2	<.2	120/118						
0/end	17.4														

1

TESTLINE: 3	JULIAN DATE: 250	YEAR: 1981-1982	TEMPLATE IDENTIFICATION: 1:1.067

TRACKLINE NUMBER: 12					Length	SINGLE GOUGES				Length	MULTIPLET GOUGES				COURSE: 000 °T
SEGMENT	WATER DEPTH (M)	TOTAL GOUGES	TOTAL NEW GOUGES	%	NEW SINGLE GOUGES	GOUGE DEPTH (M)	GOUGE WIDTH (M)	RIDGE HEIGHT (M)	Ø (°T)	NEW MULTI. GOUGES	NUMBER OF INCIS.	DEEPEST INCISION (M)	DISRUPT WIDTH (M)	Ø (°T)	COMMENTS SS# 6 BATS# 8
AB/0	11.5	6	6	100.											Fathometer 1m too shallow. Add 1m to
0.10	11.3				35	<.2	2	<.2	167/167						water depths.
0.40	11.9									NL	3	<.2	13	168/168	Sonar only fair quality All gouges
0.40	11.9				13	<.2	2	<.2	170/170						are small discontinuous scratches on seafloor.
0.45	12.0				16	<.2	1	<.2	156/156						
0.95	12.4				34	<.2	3	<.2	112/112						
BC/1	12.5	7	7	100.											
1.05	12.6				15	NC	3	NC	167/167						
1.05	12.6				NL	<.2	1	<.2	159/159						
1.30	12.9				NL	<.2	2	<.2	133/133						
1.45	13.3									NL	3	<.2	13	165/165	
1.90	13.3				NL	<.2	1	<.2	133/133						
CD/2	12.3	6	6	100.											Shoal (3m high) at end of segment. Gouges on crest
2.75	10.2									NL	2	<.2	7	142/142	
2.85	10.7				NL	<.2	1	<.2	167/167						
2.85	10.7				NL	<.2	2	<.2	152/152						Termination: 152°T
2.90	11.4				NL	<.2	2	<.2	151/151						
2.90	11.4				NL	<.2	1	<.2	150/150						
DE/3	12.0	15	11	73.3											Change template — 1:1.633
3.01	12.0				NL	NC	3	NC	97/97						Termination: 97°T
3.05	12.4				12	<.2	1	<.2	116/116						[illegible] at end of [illegible]
3.25	13.3				NL	<.2	2	<.2	122/122						
3.30	13.5				NL	<.2	1	<.2	117/117						
3.30	13.5				NL	<.2	1	<.2	118/118						
[illegible]	13.7				NL	<.2	2	<.2	91/91						

2

TESTLINE: 3 | JULIAN DATE: 250 | YEAR: 1991-1982 | TEMPLATE IDENTIFICATION: 1:1.067

TRACKLINE NUMBER: 12 | COURSE: 222°T

SEGMENT	WATER DEPTH (M)	TOTAL GOUGES	TOTAL NEW GOUGES	%	SINGLE GOUGES: Length NEW SINGLE GOUGES	GOUGE DEPTH (M)	GOUGE WIDTH (M)	RIDGE HEIGHT (M)	Ø (°T)	MULTIPLET GOUGES: Length NEW MULTI. GOUGES	NUMBER OF INCIS.	DEEPEST INCISION (M)	DISRUPT WIDTH (M)	Ø (°T)	COMMENTS
3.45	14.1				NL	<.2	2	<.2	94/94						
3.55	14.4				NL	<.2	2	<.2	131/131						
3.60	14.6									NL	2	<.2	8	142/142	
3.70	14.8				NL	<.2	2	<.2	132/132						
EF/4	15.0	9	9	100.											
4.05	15.2				NL	<.2	2	<.2	112/112						change from ... 1:1.067
4.15	15.3				NL	<.2	2	<.2	115/115						
4.15	15.3				NL	<.2	1	<.2	130/130						
4.40	15.4				NL	<.2	1	<.2	139/139						
4.60	15.9				NL	<.2	6	<.2	142/142						
4.70	16.5				NL	NC	3	NC	61/61						Termination: 222°T
4.75	16.7				NL	<.2	2	<.2	159/159						Termination 341°T
4.75	16.7				NL	<.2	1	<.2	150/150						
4.80	16.8				13	<.2	2	<.2	90/90						Termination 330°T
FG/5	17.8	7	2	28.6											
5.20	18.8				NL	<.2	5	<.2	141/141						Regain adding 1.5 m to water depth measurement.
5.25	18.9				NL	.2	5	<.2	113/113						16: 119
GH/6	20.5	70	5	7.1											
6.30	20.5				NL	<.2	2	<.2	101/101						
6.40	20.7									NL	4	.2	10	136/136	
HI/7	21.6	67	3	4.5											
7.20	22.0				NL	<.2	2	<.2	149/149						
7.65	22.6				NL	<.2	2	<.2	118/118						
7.80	22.7				NL	<.2	3	<.2	123/123						

TESTLINE: 3 | JULIAN DATE: 200 | YEAR: 1981-1982 | TEMPLATE IDENTIFICATION: 1:1,067

TRACKLINE NUMBER: 12

COURSE: 222°T

SEGMENT	WATER DEPTH (M)	TOTAL GOUGES	TOTAL NEW GOUGES	%	Length NEW SINGLE GOUGES	SINGLE GOUGES GOUGE DEPTH (M)	GOUGE WIDTH (M)	RIDGE HEIGHT (M)	Ø (°T)	Length NEW MULTI. GOUGES	MULTIPLET GOUGES NUMBER OF INCIS.	DEEPEST INCISION (M)	DISRUPT WIDTH (M)	Ø (°T)	COMMENTS
IJ/8	22.4	81	0	0.0											Perfect record match.
JK/9	22.7	72	4	5.6											
9.90	22.4									NL	4	<.2	50	126/126	large unaltered areas between incisions.
KL/10	22.5	41	0	0.0											[illegible] record match.
LM/11	22.2	124	22	17.7											Sonar missing at end of segment.
11.25	21.7									NL	14	.2	87	113/113	[illegible] ridge type [illegible].
11.30	21.4									NL	5	.2	18	117/117	
11.40	21.4				NL	.2	4	.6	177/177						
11.45	21.5									NL	8	<.2	25	142/142	
11.45	21.5									NL	2	.2	29	114/114	
11.55	21.6				NL	<.2	2	<.2	130/130						
11.55	21.6				NL	<.2	2	<.2	92/92						
MN/12	21.7	86	8	9.3											18m Fish just before [illegible] N. (4.2m drop).
12.60	21.2									NL	2	.3	22	126/126	[illegible] difficult.
12.75	21.1									NL	4	.2	26	111/111	
12.80	20.9									NL	2	.2	23	101/101	
NO/13	21.0	268	134	50.0											Change in [illegible] [illegible]. Seafloor
13.01	21.0				NL	NC	7	NC	16/16						saturated with gouges. Number of new gouges
13.10	23.3									NL	17	.4	57	114/114	is a conservative count.
13.15	23.5				NL	<.2	1	<.2	140/140						
13.15	23.5				NL	<.2	2	<.2	142/142						
13.20	23.0									NL	19	.2	47	143/143	
13.30	23.4									NL	6	.3	22	111/111	

TESTLINE: 3	JULIAN DATE: 250	YEAR: 1981-1982	TEMPLATE IDENTIFICATION: 1:1,067

TRACKLINE NUMBER: 12					Length	SINGLE GOUGES				Length	MULTIPLET GOUGES				COURSE: 003°T
SEGMENT	WATER DEPTH (M)	TOTAL GOUGES	TOTAL NEW GOUGES	%	NEW SINGLE GOUGES	GOUGE DEPTH (M)	GOUGE WIDTH (M)	RIDGE HEIGHT (M)	Ø (°T)	NEW MULTI. GOUGES	NUMBER OF INCIS.	DEEPEST INCISION (M)	DISRUPT WIDTH (M)	Ø (°T)	COMMENTS
13.30	23.8				NL	.3	3	.4	[illegible]						
13.30	23.8				NL	.3	5	.1	[illegible]						
13.35	23.8				NL	.2	5	.2	[illegible]						
13.35	23.8									NL	10	.2	35	123/123	
13.45	23.8									NL	9	.4	57	117/117	
13.55	23.9									NL	18	.8	108	122/1[illegible]	
13.60	24.0									NL	7	<.2	12	123/123	
13.70	24.2									NL	8	.2	50	123/123	
13.75	24.2									NL	2	NC	11	[illegible]/161	
13.75	23.2									NL	2	.5	14	146/146	
13.75	23.9									NL	1	.4	19	98/98	
13.80	24.0									NL	2	NC	12	[illegible]	
13.90	24.2									NL	27	.8	132	123/123	
OP/14	24.1														[illegible] 1/2 OF SEGMENT. CAN NOT MATCH BETWEEN RECORDS. PROBABLY LARGE NUMBER OF NEW GOUGES (AS IN Seg. 13)

TESTLINE: 4	JULIAN DATE:	YEAR: 1977-1978	TEMPLATE IDENTIFICATION: 1: 1.935

TRACKLINE NUMBER: 10, 11

SEGMENT	WATER DEPTH (M)	TOTAL GOUGES	TOTAL NEW GOUGES	%	Length SINGLE GOUGES: NEW SINGLE GOUGES	GOUGE DEPTH (M)	GOUGE WIDTH (M)	RIDGE HEIGHT (M)	Ø (°T)	Length MULTIPLE GOUGES: NEW MULTI. GOUGES	NUMBER OF INCIS.	DEEPEST INCISION (M)	DISRUPT WIDTH (M)	Ø (°T)	CS: 027°T COMMENTS
AB/0		—	—	—											No Sonar this Segment
															Sonar # 4 Rolls # 7
BC/1	3.3	59	4	6.8											[illegible] 977 records. Strudel
1.01	3.3				NL	<.2	2	<.2	117/141						[illegible]
1.70	4.9				NL	<.2	2	<.2	[illegible]/6[illegible]						
1.85	5.0				NL	.3	8	<.2	44/11						
1.90	5.0				NL	NC	1	NC	15[illegible]/17[illegible]						
CD/2	5.3	36	6	15.4											
2.25	5.7				NL	.2	6	<.2	62/87						
2.30	5.8				NL	<.2	1	<.2	29/56						
2.65	6.3				NL	<.2	1	<.2	31/56						
2.70	6.5				NL	<.2	2	<.2	11/44						
2.85	6.7				48	NC	1	NC	32/57						
2.85	6.7				32	NC	2	NC	20/47						
DE/3	6.9	14	7	50.0											
3.15	6.8				17	NC	2	NC	133/160						
3.20	7.0				NL	.2	2	.2	155/165						
3.25	7.2				22	NC	4	NC	17/114						
3.65	7.7				NL	<.2	2	.2	79/125						
3.95	7.9									25	3	NC	10	-2/49	
EF/4	8.0	27	4	14.8											[illegible] (showing [illegible])
4.25	8.0				68	NC	1	NC	65/72						[illegible] moves out of sand between
4.30	8.3				NL	<.2	1	<.2	39/66						[illegible]
4.50	8.5				NL	<.2	5	<.2	111/129						
4.95	8.9				NL	<.2	3	<.2	91/10						

785

786

2

TESTLINE: 4	JULIAN DATE:	YEAR: 1977-1978	TEMPLATE IDENTIFICATION: 1:1.935

TRACKLINE NUMBER: 10, 11					Length SINGLE GOUGES					Length MULTIPLE GOUGES					
SEGMENT	WATER DEPTH (M)	TOTAL GOUGES	TOTAL NEW GOUGES	%	NEW SINGLE GOUGES	GOUGE DEPTH (M)	GOUGE WIDTH (M)	RIDGE HEIGHT (M)	Ø (°T)	NEW MULTI. GOUGES	NUMBER OF INCIS.	DEEPEST INCISION (M)	DISRUPT WIDTH (M)	Ø (°T)	COMMENTS
															[illegible] more consolidation sediments that may contain older gouges.
FG/5	8.8	15	4	26.7											[illegible] gouges [illegible] ice-rafted - rough bottom [illegible] suggested.
5.30	9.2				NL	.2	4	<.2	60/57						
5.30	9.2				NL	<.2	2	<.2	[illegible]						
5.45	9.5				NL	NC	2	NC	[illegible]/14						
5.60	9.6				NL	.4	7	.4	116/143						
GH/6	9.8	29	6	20.7											bottom has been smoothed all new gouges are very small
6.10	9.7				25	NC	2	NC	28/65						all old gouges are [illegible] shape = [illegible] 38°T
6.40	10.1									65	2	<.2	7	17/46	
6.40	10.1				72	NC	2	NC	07/24						
6.50	10.3				50	NC	2	NC	3[illegible]/62						
6.95	10.2				43	<.2	1	<.2	16[illegible]/16						
HI/7	10.5	24	5	20.8											[illegible]
7.25	10.6									58	2	NC	14	15/42	
7.55	11.0				NL	.2	5	.2	118/145						
7.65	11.0				NL	<.2	1	<.2	10/37						
7.99	11.0				NL	NC	2	NC	51/70						continues into next segment.
IJ/8	11.0	47	4	25											[illegible]
8.05	11.1				NL	<.2	2	<.2	51/78						
8.65	11.9									NL	3	<.2	15	1[illegible]/14	Terminating direction - 149°T
JK/9	12.0	63	6	9.5											[illegible]
9.25	11.9									NL	2	.2	15	[illegible]/1[illegible]	
9.10	12.0				53	NC	3	NC	[illegible]/29						[illegible] - [illegible]°T

TESTLINE: 4 | JULIAN DATE: | YEAR: 1977-1978 | TEMPLATE IDENTIFICATION: 1:1,935

TRACKLINE NUMBER: 10,11

					Length SINGLE GOUGES					Length MULTIPLE GOUGES					
SEGMENT	WATER DEPTH (M)	TOTAL GOUGES	TOTAL NEW GOUGES	%	NEW SINGLE GOUGES	GOUGE DEPTH (M)	GOUGE WIDTH (M)	RIDGE HEIGHT (M)	Ø (°T)	NEW MULTI. GOUGES	NUMBER OF INCIS.	DEEPEST INCISION (M)	DISRUPT WIDTH (M)	Ø (°T)	COMMENTS
9.80	12.5									50	3	NC	17	35/62	
KL/10	12.6	117	11	9.4											[illegible]
10.10	12.6				NL	<.2	2	<.2	123/151						
10.20	12.9				NL	.2	4	.2	91/118						
10.30	12.9									NL	4	<.2	23	103/130	
10.35	13.0				NL	.2	2	<.2	20/47						
10.60	13.0				NL	<.2	1	<.2	65/92						
10.65	13.2									NL	2	.4	8	121/149	
10.75	12.9				NL	.2	3	<.2	131/158						
LM/11	13.4	120	24	20.0											
11.05	13.3									NL	9	.3	41	131/158	
11.10	13.5				NL	.2	2	<.2	111/138						
11.20	13.5									NL	2	.4	18	98/125	
11.55	13.6									NL	2	.3	12	95/122	
11.80	14.0									NL	5	<.2	25	51/78	
11.85	13.9									NL	5	.3	35	60/[illegible]	
ML/12	14.1	102	5	4.9											
12.05	14.0				NL	.2	3	<.2	66/93						
12.15	14.0				NL	<.2	2	<.2	113/140						
12.30	14.5				NL	<.2	2	<.2	72/99						
12.99	14.7				NL	NC	3	NC	18/45						[illegible] - 225°T
12.99	14.7				28	NC	9	NC	126/153						
MN/13	14.7	127	19	15.0											
13.65	15.1				NL	NC	2	NC	69/96						Terminates direction - 276°T

TESTLINE: 4					JULIAN DATE:			YEAR: 1977-1978		TEMPLATE IDENTIFICATION: 1:1.935					4
TRACKLINE NUMBER: 13,14					Length SINGLE GOUGES					Length MULTIPLE GOUGES					CS: 02[illegible]°T
SEGMENT	WATER DEPTH (M)	TOTAL GOUGES	TOTAL NEW GOUGES	%	NEW SINGLE GOUGES	GOUGE DEPTH (M)	GOUGE WIDTH (M)	RIDGE HEIGHT (M)	Ø (°T)	NEW MULTI. GOUGES	NUMBER OF INCIS.	DEEPEST INCISION (M)	DISRUPT WIDTH (M)	Ø (°T)	COMMENTS
13.70	15.0				NL	.3	6	.7	77/131						
13.80	15.0				NL	.5	3	.4	70/111						
13.85	15.1									NL	4	.3	19	153/00	
13.95	15.2									NL	7	NC	39	152/179	
13.95	15.2									NL	5	NC	18	15/42	Terminates direction - 222°T
OP/14	15.2	245	98	40.0											Start line 11 Template I.D.: 1:1695
14.01	15.3									NL	5	NC	23	32/59	very heavy multiplet
14.05	15.5									NL	12	.5	45	152/179	scouring for entire
14.15	15.7									NL	4	.3	28	102/127	segment
14.20	15.7									NL	10	.5	29	145/175	
14.30	14.5									NL	6	1.2	16	146/173	*Change to Narrow
14.30	14.5									NL	5	.5	23	62/95	Beam Ducer may account for
14.40	14.5									NL	7	.8	18	123/150	bathymetry discrepancy
14.40	14.4									NL	8	.3	36	68/95	for rest of record.
14.45	14.5									NL	11	.3	42	115/142	
14.60	14.7				NL	.3	3	<.2	107/134						
14.70	14.7									NL	10	.6	36	119/146	
14.75	14.8									NL	7	.5	18	127/154	
14.85	14.7				NL	.3	4	.2	07/34						slope:
14.90	14.7									NL	2	.5	13	127/141	
14.90	14.7									NL	2	.2	10	81/108	
14.90	14.7									NL	5	.3	30	127/151	
14.95	14.7									NL	2	.2	12	113/140	[illegible]
OP/15	15.0	157	45	28.[illegible]											
15.01	15.0									NL	2	.2	12	117/144	
15.05	14.2									NL	4	.5	27	120/147	

TESTLINE: 4	JULIAN DATE:	YEAR: 1977-1978	TEMPLATE IDENTIFICATION: 1:1,935

TRACKLINE NUMBER: 10,11					LENGTH SINGLE GOUGES					MULTIPLE GOUGES					CS: 0-7°T
SEGMENT	WATER DEPTH (M)	TOTAL GOUGES	TOTAL NEW GOUGES	%	NEW SINGLE GOUGES	GOUGE DEPTH (M)	GOUGE WIDTH (M)	RIDGE HEIGHT (M)	ø (°T)	NEW MULTI. GOUGES	NUMBER OF INCIS.	DEEPEST INCISION (M)	DISRUPT WIDTH (M)	ø (°T)	COMMENTS
15.10	14.4				NL	.2	4	.3	77/101						
15.25	14.5									NL	16	.5	118	115/142	
15.35	14.6									NL	5	.3	16	110/137	
15.45	14.7									NL	12	.3	115	104/131	
15.50	14.8				NL	<.2	2	<.2	108/135						
15.55	15.0				NL	.2	5	<.2	110/137						
15.60	15.0				NL	.5	4	.4	112/137						
15.70	15.1				NL	.4	3	.3	74/101						
15.99	15.3				NL	.4	8	.5	104/131						continues into next segment.
QR/16	15.8	110	11	10.0											begin add .5m to fathogram - machine malfunction
16.01	15.8				NL	.4	8	.5	104/131						
16.15	15.9									NL	2	.3	17	80/107	
16.85	16.5				NL	.4	7	.3	97/124						
16.90	16.5									NL	3	.4	16	103/130	
16.99	16.6									NL	4	.3	70	106/133	continues into next segment.
RS/17	16.6	125	21	16.8											
17.01	16.6									NL	4	.3	70	106/133	
17.15	16.6				NL	.4	7	.5	102/129						
17.25	16.8				NL	.5	8	.4	95/122						
17.35	17.0									NL	3	.5	25	90/117	
17.40	17.1									NL	5	.5	32	[illegible]/127	
17.50	17.2				NL	.3	2	<.2	117/144						
17.55	17.3									NL	3	.2	15	117/144	
17.85	17.5									NL	[illegible]	.2	27	[illegible]	

TESTLINE: 4	JULIAN DATE:	YEAR: 1977-1978	TEMPLATE IDENTIFICATION: 1:1.935

TRACKLINE NUMBER: 10,11					long'l SINGLE GOUGES					MULTIPLE GOUGES					CS: 027°T
SEGMENT	WATER DEPTH (M)	TOTAL GOUGES	TOTAL NEW GOUGES	%	NEW SINGLE GOUGES	GOUGE DEPTH (M)	GOUGE WIDTH (M)	RIDGE HEIGHT (M)	ø (°T)	NEW MULTI. GOUGES	NUMBER OF INCIS.	DEEPEST INCISION (M)	DISRUPT WIDTH (M)	ø (°T)	COMMENTS
ST/18	17.5	127	13	10.2											
18.05	17.7				NL	.2	14	<.2	90/117						
18.20	17.6				45	NC	2	NC	75/102						
18.25	17.8				NL	.5	3	.2	110/137						
18.30	17.8				NL	.3	3	.2	110/137						
18.30	17.8				NL	.2	2	<.2	112/139						
18.75	18.0				NL	.3	12	.2	104/131						
18.85	18.0									NL	7	.3	23	142/169	
TU/19	18.2	97	0	0.0											many gouges appear reworked by hydrolics
UV/20	18.7	120	6	5.0											hyrolic reworking indicated.
20.30	18.7									NL	3	.4	12	111/138	
20.40	18.8									NL	2	.4	17	99/126	
20.60	18.8				NL	.3	3	.4	114/141						
VW/21	19.0	117	7	6.0											hydrolic reworking indicated
21.30	19.1									NL	2	NC	12	133/160	Termination: 340°T Discontinuous
21.30	19.1									NL	3	.3	16	136/163	Termination: 343°T
21.30	19.1				NL	NC	3	NC	136/163						Discontinuous
21.35	19.1				NL	NC	2	NC	136/163						
WX/22	19.3	93	2	2.1											SLIGHTLY WEST OF LINE. hydrolic reworking
22.80	19.6									NL	2	1.2	1[illegible]	[illegible]	
XY/23	19.6	91	0	0.0											hyrdolic reworking (on line)

790

TESTLINE: 4 | **JULIAN DATE:** | **YEAR:** 1977-1978 | **TEMPLATE IDENTIFICATION:** 1:1.935

TRACKLINE NUMBER: 12,11

SEGMENT	WATER DEPTH (M)	TOTAL GOUGES	TOTAL NEW GOUGES	%	Length: SINGLE GOUGES NEW SINGLE GOUGES	GOUGE DEPTH (M)	GOUGE WIDTH (M)	RIDGE HEIGHT (M)	ø (°T)	Length: MULTIPLE GOUGES NEW MULTI. GOUGES	NUMBER OF INCIS.	DEEPEST INCISION (M)	DISRUPT WIDTH (M)	ø (°T)	CS: 027 °T COMMENTS
YZ/24	19.9	112	6	5.4											
24.75	19.9									NL	3	NC	11	33/60	Termination. 240°T
24.90	19.6				NL	NC	4	NC	62/87						Termination: 269°T
24.90	19.6									55	2	NC	13	130/157	Termination: 157°T
ZAA/25	19.7	148	5	3.4											Large pressure ridge gouge in segment
25.55	19.8									NL	2	<.2	12	92/119	
25.60	19.8									NL	3	.3	27	97/124	
AABB/26	19.7	188	5	2.7											West of line. Bottom coming up. Many wide
26.50	19.2									NL	5	.5	28	94/121	pressure ridge gouges
BBCC/27	18.5														West of line. Unable to correlate older gouges
															on record. Appears as though many new gouges
															have been formed on offshore shoal.

TESTLINE: 4					JULIAN DATE: 219				YEAR: 1978-1980				TEMPLATE IDENTIFICATION: 1:1.633		
TRACKLINE NUMBER: 20					Length SINGLE GOUGES					Length MULTIPLE GOUGES					CS: 0.2 [illegible] T
SEGMENT	WATER DEPTH (M)	TOTAL GOUGES	TOTAL NEW GOUGES	%	NEW SINGLE GOUGES	GOUGE DEPTH (M)	GOUGE WIDTH (M)	RIDGE HEIGHT (M)	Ø (°T)	NEW MULTI. GOUGES	NUMBER OF INCIS.	DEEPEST INCISION (M)	DISRUPT WIDTH (M)	Ø (°T)	COMMENTS SS#7 Rolls#14,15
AC/0	—	—													NO SWAK - NO EA[illegible]
BC/1	3.1	25	5	20.0											Bottom contains many reexposed gouges and
1.15	3.3				NL	<.2	1	<.2	148/175						causes difficulty in observing new ones.
1.50	4.0				NL	<.2	1	<.2	44/71						
1.60	4.2									NL	2	<.2	7	176/23	
1.80	4.8				NL	<.2	1	<.2	50/77						
CD/2	5.1	24	3	12.5											
2.05	5.2				NL	.2	5	.2	52/79						Termination Direction 259°T
2.40	5.9				NL	<.2	2	<.2	65/92						
2.50	6.0				NL	<.2	3	<.2	50/77						
															* *
DE/3	6.6	23	0	0.0											sand waves on seafloor. Their shifting reexposes
															old gouges in troughs. Many gouges that are
EF/4	7.6	18	4	22.2											on 1978 record are gone (covered by sand) while
4.60	8.3				NL	<.2	1	<.2	136/163						many reexposed older gouges on 1980 record
4.90	8.3									38	3	<.2	21	150/177	were not observed on the 1978 record.
															These old gouges have orientations of 90-80°T.
FG/5	8.8	26	4	15.4											sand waves have period of 100-150 m with 20-40 m
5.20	8.7									NL	2	<.2	4	160/97	height. * *
5.30	9.0				NL	.4	5	.4	23/60						
5.35	9.0				NL	<.2	3	<.2	122/149						
GH/6	9.2	48	5	104											
6.80	10.4				NL	<.2	1	<.2	21/51						
6.90	10.3									NL	3	<.2	.2	45/72	
6.95	10.2				50	NC	2	NC	16/43						

1

TESTLINE: 4 | **JULIAN DATE:** 21[illegible] | **YEAR:** 1978-1990 | **TEMPLATE IDENTIFICATION:** 1:1.633

TRACKLINE NUMBER: [illegible]

					Length SINGLE GOUGES					Length MULTIPLE GOUGES					CS: [illegible]
SEGMENT	WATER DEPTH (M)	TOTAL GOUGES	TOTAL NEW GOUGES	%	NEW SINGLE GOUGES	GOUGE DEPTH (M)	GOUGE WIDTH (M)	RIDGE HEIGHT (M)	Ø (°T)	NEW MULTI. GOUGES	NUMBER OF INCIS.	DEEPEST INCISION (M)	DISRUPT WIDTH (M)	Ø (°T)	COMMENTS
HI/7	10.5	[illegible]	[illegible]	[illegible]											
7.05	10.5				[illegible]	NC	[illegible]	NC	—						* SEMI-CIRCULAR
7.40	10.5				NL	NC	3	NC	123/150						MOST OF THE NEW GOUGES ARE IN THE SAND WAVE
7.40	10.5				NL	<.2	1	<.2	109/136						AREAS (CRESTS AND SIDES).
7.80	10.8				NL	<.2	2	<.2	20/197						
7.85	10.9				NL	<.2	2	<.2	67/94						
7.90	11.0									NL	3	<.2	7	178/25	
7.95	11.0				NL	<.2	1	<.2	145/172						
IJ/8	11.1	—	—												OFF LINE.
JK/9	12.0	—	—												OFF LINE.
KL/10	12.6	57	52	33.1											
10.05	12.5									NL	5	.3	23	18/45	
10.05	12.5									NL	4	<.2	30	[illegible]	
10.20	12.6									NL	6	.2	38	52/79	
10.30	12.9									NL	2	NC	6	[illegible]	
10.35	12.9									NL	2	<.2	11	29/55	
10.50	13.0									NL	2	.2	9	[illegible]	
10.50	13.0									NL	2	.5	20	110/137	
10.70	13.1				NL	.2	5	<.2	[illegible]						
10.70	13.1				NL	<.2	6	<.2	35/62						
10.75	13.1									NL	21	.2	[illegible]	163/11	
10.80	13.0				NL	.3	4	.4	104/131						
10.[illegible]	13.1				NL	[illegible]	6	<.2	[illegible]/121						
10.95	13.2				NL	.2	[illegible]	<.2	[illegible]						

TESTLINE: 4	JULIAN DATE: 219	YEAR: 1978-1980	TEMPLATE IDENTIFICATION: 1:1.253
TRACKLINE NUMBER: 20	Length SINGLE GOUGES	Length MULTIPLE GOUGES	CS: 227°T

SEGMENT	WATER DEPTH (M)	TOTAL GOUGES	TOTAL NEW GOUGES	%	NEW SINGLE GOUGES	GOUGE DEPTH (M)	GOUGE WIDTH (M)	RIDGE HEIGHT (M)	Ø (°T)	NEW MULTI. GOUGES	NUMBER OF INCIS.	DEEPEST INCISION (M)	DISRUPT WIDTH (M)	Ø (°T)	COMMENTS
LM/11	13.2	111	20	18.0											
11.25	13.4				NL	<.2	1	<.2	14/41						
11.40	13.5				NL	.4	2	.5	71/98						
11.40	13.5									NL	2	NC	7	168/11	[illegible] 191°T
11.60	13.7									NL	15	.3	62	32/59	
11.85	13.9				NL	.6	3	.7	98/125						
MN/12	14.0	64	10	15.6											
12.15	14.0									NL	2	.2	15	42/69	
12.35	14.2				NL	.3	2	.2	122/149						
12.35	14.2				NL	.5	5	.5	38/65						
12.50	14.3				NL	.5	13	.7	82/109						
12.80	14.5				NL	.4	11	.8	95/122						
12.90	14.6									NL	2	.4	17	142/169	
12.90	14.6				NL	.4	5	.4	42/69						
12.95	14.6				NL	.3	11	.4	48/75						
MO/13	14.7	149	21	14.1											NL LINE AT BEGINNING OF SEGMENT.
13.25	14.9				NL	.2	2	.3	38/65						
13.65	15.1									NL	7	<.2	35	138/165	
13.70	15.1									NL	6	<.2	25	134/161	
13.75	[illegible]				NL	<.2	2	<.2	94/121						
13.75	15.1				NL	.3	2	<.2	104/131						
13.80	15.1				NL	<.2	2	<.2	71/98						
13.80	15.1				NL	<.2	2	<.2	[illegible]						
13.85	15.2				NL	<.2	2	<.2	[illegible]/91						
13.95	15.2									NL	2	.4	16	74/101	

4

TESTLINE: 4 | JULIAN DATE: 219 | YEAR: 1978-1980 | TEMPLATE IDENTIFICATION: 1:1.633

TRACKLINE NUMBER: 20

SEGMENT	WATER DEPTH (M)	TOTAL GOUGES	TOTAL NEW GOUGES	%	Length SINGLE GOUGES NEW SINGLE GOUGES	GOUGE DEPTH (M)	GOUGE WIDTH (M)	RIDGE HEIGHT (M)	Ø (°T)	Length MULTIPLE GOUGES NEW MULTI. GOUGES	NUMBER OF INCIS.	DEEPEST INCISION (M)	DISRUPT WIDTH (M)	Ø (°T)	CS: [illegible] COMMENTS
0P/14	15.2	[illegible]	31	25.4											[illegible]
14.01	15.1									NL	1	.8	35	[illegible]/57	
14.10	15.3				NL	.4	2	.2	113/140						
14.15	15.2				NL	.3	3	.3	[illegible]/106						
14.15	15.2				NL	.6	3	.3	84/111						
14 25	15.2				NL	.7	25	.9	70/111						
14 30	15.3				NL	.2	2	.4	101/128						
14 30	15.3				NL	.2	2	.3	102/129						
14.30	15.3				NL	.3	3	.3	102/129						
14 35	15.5									NL	1	.4	37	90/117	
14.40	15.5									NL	2	.5	36	153/00	
14.50	15.3				NL	.5	5	.2	42/69						
14 55	15.4									NL	2	.2	20	87/114	
14.60	15.3				NL	.3	3	.2	91/118						
14.60	15.3				NL	<.2	2	<.2	111/138						
14.60	15.3				NL	.5	3	.2	100/127						
14.70	15.5				NL	.5	3	.3	94/121						
14.70	15.4				NL	.3	2	<.2	86/113						
14.75	15.5				NL	.3	1	.2	75/102						
14 80	15.5				NL	.2	5	.2	74/101						
P/15	15.6	—	—												[illegible] FOR ICE
AR/16	16.6	—	—												[illegible] - TURN FOR ICE
R/end	—														[illegible]

TESTLINE: 4	JULIAN DATE: 239	YEAR: 19??-1982	TEMPLATE IDENTIFICATION: 1:1.935

TRACKLINE NUMBER: 4 — CS: 027°T

SEGMENT	WATER DEPTH (M)	TOTAL GOUGES	TOTAL NEW GOUGES	%	Length SINGLE GOUGES: NEW SINGLE GOUGES	GOUGE DEPTH (M)	GOUGE WIDTH (M)	RIDGE HEIGHT (M)	Ø (°T)	Length MULTIPLE GOUGES: NEW MULTI. GOUGES	NUMBER OF INCIS.	DEEPEST INCISION (M)	DISRUPT WIDTH (M)	Ø (°T)	COMMENTS SS#2 Bat#2
AE/0	—	—	—	-											[illegible] SEGMENT LENGTH
															[illegible] TO HIGHER SHIP SPEED.
BC/1	—	—	—	-											No SONAR FOR FIRST TWO SEGMENTS.
CD/2	5.0	39	0	0.0											Range on Sonar resolution only 75m on each side.
															MANY OF 19?? GOUGES SEEN.
DE/3	6.8	19	0	0.0											Fathogram reads 1m too SHALLOW - add 1m
															[illegible]
EF/4	7.8	24	3	12.5											
4.40	7.8				NL	<.2	2	<.2	[illegible]						
4.45	7.9				NL	<.2	1	<.2	22/49						
4.50	8.0				NL	<.2	2	<.2	125/152						
FG/5	8.5	29	1	3.4											Sand waves. [illegible] SCOUR MARKS AT PT. F
5.25	8.6				NL	<.2	3	<.2	[illegible]						
GH/6	9.5	33	1	3.0											
6.25	9.6				NL	<.2	4	.2	[illegible]						
HI/7	10.3	16	6	37.5											Poor Sonar limits total gouge count
7.01	10.3				NL	NC	4	NC	[illegible]						[illegible]
7.45	10.4				NL	<.2	2	<.2	64/91						
7.60	10.[illegible]				NL	.2	3	.2	[illegible]						
7.75	[illegible]				NL	<.2	2	<.2	[illegible]						
7.95	[illegible]				NL	.2	[illegible]	.2	[illegible]						
7.[illegible]	[illegible]				NL	.2	3	<.2	115/142						
IJ/8	[illegible]	—	—												[illegible]

796

TESTLINE: 4	JULIAN DATE: 2??	YEAR: 1980-1982	TEMPLATE IDENTIFICATION: [illegible]

TRACKLINE NUMBER:

CS: [illegible]

SEGMENT	WATER DEPTH (M)	TOTAL GOUGES	TOTAL NEW GOUGES	%	SINGLE GOUGES: Length NEW SINGLE GOUGES	GOUGE DEPTH (M)	GOUGE WIDTH (M)	RIDGE HEIGHT (M)	Ø (°T)	MULTIPLE GOUGES: Length NEW MULTI. GOUGES	NUMBER OF INCIS.	DEEPEST INCISION (M)	DISRUPT WIDTH (M)	Ø (°T)	COMMENTS
J?/9	11.6	—	—	–											[illegible]
KL/10	12.3	93	8	8.6											
10.30	12.?				NL	.3	3	.2	32/117						
10.35	12.?				NL	.2	3	<.2	37/57						
10.50	12.?				NL	.6	3	.9	100/117						
10.50	12.?				NL	.2	2	.2	66/93						
10.70	12.5				NL	.9	3	.6	95/122						
10.70	12.5									NL	2	.6	13	57/84	
10.80	12.7				NL	.7	10	.9	66/93						
LM/11	12.8	75	13	17.?											
11.15	13.0									NL	4	.2	14	28/55	
11.15	13.0				NL	.4	3	.2	103/130						
11.40	13.5									NL	4	.6	30	32/59	
11.50	13.5				NL	.5	3	.8	32/59						
11.60	13.6									NL	2	.5	18	75/102	
11.70	13.7				NL	NC	5	NC	16/[illegible]						
MN/12	14.0	58	8	13.8											
12.20	14.0									NL	4	.5	16	08/35	[illegible]
12.50	14.2									NL	2	.5	30	110/137	
12.55	—									NL	2	NC	15	12/39	[illegible]
NO/13	—	194	17	16.?											[illegible]
13.01	—									NL	4	.5	[illegible]	[illegible]	[illegible]
13.01	—									NL	2	—	16	[illegible]/74	[illegible]
13.11	—				NL	—	9	—	[illegible]						[illegible]

3

TESTLINE: 4					JULIAN DATE: 237				YEAR: 1981-1982			TEMPLATE IDENTIFICATION: 1:1,935			
TRACKLINE NUMBER: 4					Length	SINGLE GOUGES				Length	MULTIPLET GOUGES				COURSE:
SEGMENT	WATER DEPTH (M)	TOTAL GOUGES	TOTAL NEW GOUGES	%	NEW SINGLE GOUGES	GOUGE DEPTH (M)	GOUGE WIDTH (M)	RIDGE HEIGHT (M)	Ø (°T)	NEW MULTI. GOUGES	NUMBER OF INCIS.	DEEPEST INCISION (M)	DISRUPT WIDTH (M)	Ø (°T)	COMMENTS
13.15	—				NL	—	17	—	83/110						No FATHOGRAM
13.30	—				NL	—	2	—	37/64						No FATHOGRAM
13.50	14.7				NL	<.2	2	<.2	45/72						
13.75	14.9									NL	2	.6	22	100/127	
13.75	14.9				NL	.2	6	.4	55/82						
13.90	14.8				NL	.6	8	.9	78/105						
13.99	14.7									NL	3	.9	25	61/88	continues into next segment
OP/14	14.7	102	19	18.6											
14.01	14.7									NL	3	.9	25	61/88	
14.15	14.9				NL	.5	8	.3	14/41						
14.20	15.0									NL	9	.2	55	80/107	
14.40	15.1									NL	3	.5	36	80/107	
14.45	15.1				NL	.6	6	.4	48/75						
14.50	15.2				NL	.3	3	.4	100/127						
14.55	15.2				NL	.6	5	.3	55/82						
P/end	15.6														end of

798

TESTLINE: 5	JULIAN DATE:	YEAR: 1979-1980	TEMPLATE IDENTIFICATION: 1:1.633

TRACKLINE NUMBER: 25 — COURSE: 006°T

SEGMENT	WATER DEPTH (M)	TOTAL GOUGES	TOTAL NEW GOUGES	%	SINGLE GOUGES: Length NEW SINGLE GOUGES	GOUGE DEPTH (M)	GOUGE WIDTH (M)	RIDGE HEIGHT (M)	Ø (°T)	MULTIPLET GOUGES: Length NEW MULTI. GOUGES	NUMBER OF INCIS.	DEEPEST INCISION (M)	DISRUPT WIDTH (M)	Ø (°T)	COMMENTS SS# 9 Roll# 17
AC/0	3.8	3	1	33.[illegible]											COMPARISON OF BATHYGRAMS SHOW THAT EXTENSIVE SEDIMENT
0.35	5.0				65	<.2	1	<.2	30/36						MOVEMENT TOOK PLACE BETWEEN RECORD YEARS. MANY BOULDERS
															ON SEAFLOOR
BC/1	9.2	0	0	0.0											SEDIMENT RIPPLES A=174°T λ=2m
															many boulders on seafloor.
CD/2	11.1	12	12	100											Boulders end shoreside of shoal. Gouges associated with shoal.
2.80	12.5				NL	<.2	2	<.2	132/138						Shoal near pt. D is now 1.5m high (was 1.2m in 1979)
2.80	12.5									NL	4	<.2	13	130/136	change template 1:1.067
2.80	12.5				18	<.2	2	<.2	123/129						Shoal has become more rounded.
2.80	12.5									NL	2	<.2	5	07/13	
2.85	13.9				NL	<.2	2	<.2	168/174						
2.85	13.9				18	<.2	1	<.2	145/151						
2.85	13.9				26	<.2	1	<.2	123/129						
2.90	14.4				NL	<.2	1	<.2	109/115						
DE/3	14.5	12	12	100											SEDIMENT RIPPLES θ=004°T λ=1m
3.05	14.6									NL	12	NC	25	16/22	Change template to 1:1.633
EF/4	16.0	—	—	.											OFF LINE FOR MOST OF SEGMENT.
F/end	18.9														

TESTLINE: 6	JULIAN DATE: 222	YEAR: 1979-1980	TEMPLATE IDENTIFICATION: 1:1.379

TRACKLINE NUMBER: 24					Length	SINGLE GOUGES				Length	MULTIPLET GOUGES				COURSE: 023°T
SEGMENT	WATER DEPTH (M)	TOTAL GOUGES	TOTAL NEW GOUGES	%	NEW SINGLE GOUGES	GOUGE DEPTH (M)	GOUGE WIDTH (M)	RIDGE HEIGHT (M)	ø (°T)	NEW MULTI. GOUGES	NUMBER OF INCIS.	DEEPEST INCISION (M)	DISRUPT WIDTH (M)	ø (°T)	COMMENTS 55# 9 End #17
AC/0	5.3	4	—												Cotton [illegible] [illegible] boulders – [illegible] [illegible]
															[illegible] [illegible] RECORD NO 1979 RECORD UNTIL
CC/1	8.0	26	—												[illegible] E.
CD/2	9.5	23	—												
DE/3	10.1	21	—												
EF/4	11.1	29	3	10.3											Boulders on seafloor.
4.05					NL	<.2	1	<.2	56/84						
4.20					NL	<.2	5	<.2	13/63						
4.50					NL	<.2	3	<.2	1?/15						
FG/5	12.0	34	—												OVER 1/2 OF 1979 SONAR MISSING.
GH/6	13.6	13	5	38.5											
6.20	13.8									NL	2	NC	6	49/52	
6.30	13.9				NL	<.2	2	<.2	43/11						
6.30	13.9				NL	NC	3	NC	173/21						
6.70	14.5				NL	<.2	1	<.2	120/196						
HI/7	14.5	14	4	28.6											
7.15	15.0									NL	2	<.2	3	115/22	
7.65	15.1				NL	<.2	2	<.2	41/26						
7.70	15.3				NL	NC	2	NC	-1/19						47 1?
I/end	15.9														

800

TESTLINE: 6	JULIAN DATE: 210	YEAR: 1990-1991	TEMPLATE IDENTIFICATION: 1:1.279

SEGMENT	WATER DEPTH (M)	TOTAL GOUGES	TOTAL NEW GOUGES	%	NEW SINGLE GOUGES	GOUGE DEPTH (M)	GOUGE WIDTH (M)	RIDGE HEIGHT (M)	Ø (°T)	NEW MULTI. GOUGES	NUMBER OF INCIS.	DEEPEST INCISION (M)	DISRUPT WIDTH (M)	Ø (°T)	COMMENTS
TRACKLINE NUMBER: 13					Length SINGLE GOUGES					Length MULTIPLE GOUGES					CS: 029°T SS#10 Bot#13
AB/0	5.7	0	0	0.0											[illegible] covered by [illegible].
															[illegible] .5m correction to water depths.
BC/1	8.2	25	0	0.0											change template - 1:1.633
CD/2	9.6	25	2	8.0											sonar quality poor. change template - 1:2.894
2.70	10.1				NL	<.2	1	<.2	43/71						
2.85	10.3				NL	<.2	1	<.2	25/63						
DE/3	10.5	38	5	13.2											poor quality sonar. change template - 1:1.633
3.40	10.6				NL	<.2	1	<.2	58/						
3.90	11.1									NL	4	<.2	15	155/03	
EF/4	11.2	36	1	2.8											
4.50	11.8				NL	NC	2	NC	24/22						
FG/5	12.3	26	2	7.7											
5.35	12.9				NL	<.2	2	<.2	47/15						
5.65	13.3				NL	<.2	1	<.2	13/41						
GH/6	13.5	16	0	0.0											sonar quality [illegible]
HI/7	14.5	14	0	0.0											
I/end	15.8														

801

TESTLINE: 6	JULIAN DATE: 244	YEAR: 1991-1992	TEMPLATE IDENTIFICATION: 1:1.879

TRACKLINE NUMBER: 6 — CS: 0-8°T

SEGMENT	WATER DEPTH (M)	TOTAL GOUGES	TOTAL NEW GOUGES	%	SINGLE GOUGES (Length): NEW SINGLE GOUGES	GOUGE DEPTH (M)	GOUGE WIDTH (M)	RIDGE HEIGHT (M)	Ø (°T)	MULTIPLE GOUGES (Length): NEW MULTI. GOUGES	NUMBER OF INCIS.	DEEPEST INCISION (M)	DISRUPT WIDTH (M)	Ø (°T)	COMMENTS SS#3 Eats#3
AB/0	5.3	4	1	25.0											[illegible] covers [illegible]. Resolution better than 1991
0.80	7.5				NL	<.2	2	<.2	21/55						record. [illegible] covers may be higher
BC/1	7.8	46	5	10.9											[illegible] resolution accounts for greater total gouge count
1.55	8.2				NL	.7	2	.3	37/65						Change template - 1:1.860
1.90	8.6				NL	<.2	2	<.2	28/6						
1.90	8.6									NL	3	<.2	10	08/30	36
															[illegible] program beginning to give too shallow of a
CD/2	9.3	54	1	1.9											measurement. Begin adding .5m to water depth.
2.45	9.6				NL	.5	3	.4	18/46						Change template - 1:2.894
DE/3	10.0	36	0	0.0											
EF/4	11.0	51	1	2.0											change template - 1:1.860
4.25	11.0				NL	NC	5	NC	23/51						Termination direction: 51°T
FG/5	11.8	55	18	32.7											Boulders still seen on sonar. Change template -
5.10	11.6									30	8	<.2	40	06/24	1:1.861
5.75	12.6				17	<.2	5	<.2	13/41						
5.85	12.7									37	7	<.2	32	04/32	
5.90	12.9				NL	<.2	2	<.2	30/58						
5.90	12.9				NL	<.2	2	<.2	32/60						
GH/6	13.5	20	1	5.0											[illegible]
6.95	14.5				NL	NC	1	NC	166/14						[illegible] to water depth.
HI/7	14.7	10	1	10.0											
7.21	14.7				NL	<.2	4	<.2	166/14						[illegible] 1:2.864

TESTLINE: 6 | JULIAN DATE: 244 | YEAR: 1981-1982 | TEMPLATE IDENTIFICATION: 1:1.935

TRACKLINE NUMBER: 6 | CS: 323°T

SEGMENT	WATER DEPTH (M)	TOTAL GOUGES	TOTAL NEW GOUGES	%	Length SINGLE GOUGES: NEW SINGLE GOUGES	GOUGE DEPTH (M)	GOUGE WIDTH (M)	RIDGE HEIGHT (M)	Ø (°T)	Length MULTIPLE GOUGES: NEW MULTI. GOUGES	NUMBER OF INCIS.	DEEPEST INCISION (M)	DISRUPT WIDTH (M)	Ø (°T)	COMMENTS
IJ/8	15.5	11	1	9.1											[illegible] change [illegible]
8.50	15.8				NL	<.2	2	<.2	147/195						Termination direction - 355°T
JK/9	16.2	126	15	11.9											off course for last part of segment. Cross 18m
9.70	17.9									NL	15	NC	57	158/06	bench at [illegible] mark. template change - 1:1,379
KL/10	19.3	132	15	11.4											
10.15	20.2									NL	4	NC	10	18/46	
10.15	20.2				NL	NC	5	NC	36/64						
10.25	20.0									NL	8	NC	33	107/15	
10.40	20.2				NL	NC	3	NC	11/47						
10.90	21.6				NL	.2	2	<.2	52/80						
LM/11	21.7	125	0	0.0											
MN/12	23.2	133	6	4.5											
12.10	23.3									NL	4	.2	17	55/83	
12.35	23.8									NL	2	<.2	8	137/165	
NO/13	25.2	85	0	0.0											Excellent record match
OP/14	26.0	84	0	0.0											
PQ/15	26.5	98	1	1.0											
15.35	27.2				34	NC	5	NC	20/28						
Q/end	27.4														end of 1981 survey

TESTLINE: 7 | **JULIAN DATE:** | **YEAR:** 1981-1982 | **TEMPLATE IDENTIFICATION:** 1:1633

TRACKLINE NUMBER: 3

SEGMENT	WATER DEPTH (M)	TOTAL GOUGES	TOTAL NEW GOUGES	%	Length SINGLE GOUGES: NEW SINGLE GOUGES	GOUGE DEPTH (M)	GOUGE WIDTH (M)	RIDGE HEIGHT (M)	Ø (°T)	Length MULTIPLE GOUGES: NEW MULTI. GOUGES	NUMBER OF INCIS.	DEEPEST INCISION (M)	DISRUPT WIDTH (M)	Ø (°T)	CS: 333 T — COMMENTS
AB/0	5.5	14	4	27											SS#4 Est.# 5
0.50	6.3				NL	<.2	2	<.2	120/120						appears to be a 1m discrepancy in bathymetry
0.55	6.4				NL	<.2	1	<.2	112/112						depth between the two records - machine malfunction?
															Resolution on this record is better; but is variable
BC/1	6.7	40	2	5.0											throughout.
1.01	6.7				NL	<.2	5	<.2	127/127						
1.80	7.0				50	NC	2	NC	147/147						
CD/2	7.1	42	2	4.8											
2.55	7.3				NL	<.2	1	<.2	145/138						Gouges do not cross under ship but are very small
2.70	7.3				NL	<.2	2	<.2	138/138						
DE/3	7.4	79	7	8.9											
3.01	7.4				55	<.2	1	<.2	158/153						
3.01	7.4				NL	<.2	1	<.2	91/91						
3.05	7.5				NL	<.2	2	<.2	130/130						
3.10	7.5				NL	<.2	3	<.2	91/91						
3.40	7.7				NL	<.2	1	<.2	49/49						
3.95	8.2									NL	2	<.2	10	116/116	
EF/4	8.2	44	2	4.5											TEMPLATE CHANGE: 1:1.379
4.40	8.5				NL	<.2	2	<.2	60/60						
4.45	8.5				NL	NC	2	NC	52/52						
FG/5	9.0	68	15	22.1											
5.25	9.1									NL	3	<.2	7	[illegible]	
5.30	9.1									NL	2	<.2	13	113/113	
5.40	9.2				NL	<.2	2	<.2	[illegible]						

805

TESTLINE: 7	JULIAN DATE:	YEAR: 1981-1982	TEMPLATE IDENTIFICATION: 1:1.379

TRACKLINE NUMBER: 8					length SINGLE GOUGES					length MULTIPLE GOUGES					CS: 000°T
SEGMENT	WATER DEPTH (M)	TOTAL GOUGES	TOTAL NEW GOUGES	%	NEW SINGLE GOUGES	GOUGE DEPTH (M)	GOUGE WIDTH (M)	RIDGE HEIGHT (M)	ø (°T)	NEW MULTI. GOUGES	NUMBER OF INCIS.	DEEPEST INCISION (M)	DISRUPT WIDTH (M)	ø (°T)	COMMENTS
5.40	9.2				NL	<.2	1	<.2	[illegible]/15						
5.40	9.2				NL	<.2	2	<.2	[illegible]						
5.45	9.2									NL	2	<.2	11	120/120	
5.50	9.3				NL	NC	3	NC	22/22						Curvilinear shape 22 170
5.55	9.3				NL	<.2	1	<.2	45/45						
5.60	9.3				NL	.2	3	.3	70/70						Tick marks in trough
5.80	9.4				NL	<.2	2	<.2	62/62						
5.99	9.5				NL	NC	1	NC	156/156						Curvilinear shape (con't into next segment) 156
GH/6	9.5	56	8	14.3											
6.01	9.5				NL	NC	1	NC	13/13						(con't from 5.95)
6.20	9.6				NL	<.2	2	<.2	167/167						
6.35	9.8				NL	<.2	1	<.2	50/50						
6.50	9.9				NL	<.2	1	<.2	15/15						
6.55	9.9				NL	<.2	1	<.2	23/23						
6.70	10.0				NL	<.2	1	<.2	14/14						Termination: 194°T
6.75	10.0				NL	<.2	2	<.2	127/127						
6.95	10.2									NL	2	.2	19	72/72	
HI/7	10.2	79	8	10.1											
7.05	10.2									NL	2	.2	17	76/76	
7.15	10.3									NL	2	.3	13	13/13	
7.20	10.4				NL	<.2	1	<.2	50/50						
7.30	10.4				NL	<.2	2	<.2	48/48						Found in g[illegible] 48/130
7.35	10.4				NL	<.2	3	<.2	113/113						
7.35	10.4				NL	<.2	2	<.2	18/18						

3

TESTLINE: 7					JULIAN DATE:				YEAR: 1981-1982				TEMPLATE IDENTIFICATION: 1:1.379			
TRACKLINE NUMBER: 8					Length SINGLE GOUGES					Length MULTIPLE GOUGES						CS: 022°T
SEGMENT	WATER DEPTH (M)	TOTAL GOUGES	TOTAL NEW GOUGES	%	NEW SINGLE GOUGES	GOUGE DEPTH (M)	GOUGE WIDTH (M)	RIDGE HEIGHT (M)	Ø (°T)	NEW MULTI. GOUGES	NUMBER OF INCIS.	DEEPEST INCISION (M)	DISRUPT WIDTH (M)	Ø (°T)	COMMENTS
IJ/8	10.8	42	4	12.7											
8.50	11.3				130	<.2	1	<.2	169/169						
8.80	11.5									52	2	NC	10	00/00	
8.95	11.7				NL	<.2	2	<.2	95/95						
JK/9	11.7	47	9	19.1											
9.25	12.0				NL	<.2	2	<.2	58/58						
9.40	12.1				NL	<.2	2	<.2	60/60						
9.55	12.3				NL	<.2	1	<.2	26/26						
9.70	12.3									NL	3	<.2	23	118/118	
9.99	12.5				NL	<.2	2	<.2	143/143						continue into next segment
9.99	12.5				NL	<.2	3	<.2	146/146						
9.99	12.5				NL	NC	2	NC	09/09						
KL/10	12.5	56	14	25.0											
10.01	12.5				NL	<.2	2	<.2	143/143						from previous segment
10.01	12.5				NL	<.2	3	<.2	146/146						
10.01	12.5				NL	NC	2	NC	09/09						
10.45	12.7				NL	<.2	2	<.2	66/66						
10.50	12.7				NL	<.2	2	<.2	35/35						
10.65	12.8									NL	3	<.2	6	24/24	Terminates · 24°T
10.90	12.9				NL	NC	3	NC	22/22						Sine in shape 22 167
10.90	12.8				NL	NC	2	NC	—						Circular
10.95	12.9				NL	<.2	1	<.2	167/167						
10.99	13.0				NL	<.2	1	<.2	161/161						
10.99	13.0				NL	NC	1	NC	163/163						
10.99	13.0				NL	NC	2	NC	165/165						[illegible]

806

TESTLINE: 7 | JULIAN DATE: | YEAR: 1981-1982 | TEMPLATE IDENTIFICATION: 1:1.379

TRACKLINE NUMBER: 3 | CS: 222°T

SEGMENT	WATER DEPTH (M)	TOTAL GOUGES	TOTAL NEW GOUGES	%	Length SINGLE GOUGES: NEW SINGLE GOUGES	GOUGE DEPTH (M)	GOUGE WIDTH (M)	RIDGE HEIGHT (M)	Ø (°T)	Length MULTIPLE GOUGES: NEW MULTI. GOUGES	NUMBER OF INCIS.	DEEPEST INCISION (M)	DISRUPT WIDTH (M)	Ø (°T)	COMMENTS
LM/11	13.0	82	23	28.0											ICE DETAIL IN MID SEGMENT; POSSIBLE LOW VALUE FOR NEW
11.01	13.0				NL	NC	2	NC	165/165						GOUGES. NOT CONSISTENT FROM LAST SEGMENT
11.05	13.0				NL	<.2	1	<.2	06/06						
11.05	13.0				62	<.2	2	<.2	20/20						
11.10	13.0				NL	<.2	2	<.2	06/06						
11.10	13.0				NL	<.2	1	<.2	123/123						
11.15	13.1				NL	<.2	2	<.2	27/27						
11.15	13.1				NL	<.2	2	<.2	171/171						
11.15	13.1									NL	2	<.2	5	164/164	
11.15	13.1				NL	NC	3	NC	172/172						
11.15	13.1				65	NC	3	NC	158/158						
11.15	13.1				68	NC	3	NC	158/158						
11.20	13.2									NL	2	<.2	11	07/07	
11.25	13.3				NL	<.2	2	<.2	148/148						
11.55	13.8				NL	<.2	1	<.2	178/178						
11.55	13.8				NL	<.2	1	<.2	178/178						
11.75	14.0				NL	<.2	2	<.2	140/140						
11.99	14.3				NL	NC	2	NC	164/164						Termination: 344°T
11.99	14.3				NL	NC	3	NC	162/162						cont. into next seg. Termination: 342°T
11.99	14.3				NL	NC	3	NC	162/162						cont. into next seg. Termination: 342°T
11.99	14.3									NL	2	<.2	8	135/135	cont. into next seg.
LM/12	14.3	156	15	9.6											
12.01	14.3				NL	NC	3	NC	162/162						
12.01	14.3				NL	NC	3	NC	162/162						
12.01	14.3									NL	2	<.2	8	[illegible]	
12.30	14.3									NL	[illegible]	.3	16	[illegible]	
12.50	14.5				NL	.2	3	<.2	11/11						

5

TESTLINE: 7 | JULIAN DATE: | YEAR: 1981-1982 | TEMPLATE IDENTIFICATION: 1:1.379

TRACKLINE NUMBER: | CS: 000°T

SEGMENT	WATER DEPTH (M)	TOTAL GOUGES	TOTAL NEW GOUGES	%	SINGLE GOUGES: Length NEW SINGLE GOUGES	GOUGE DEPTH (M)	GOUGE WIDTH (M)	RIDGE HEIGHT (M)	Ø (°T)	MULTIPLE GOUGES: Length NEW MULTI. GOUGES	NUMBER OF INCIS.	DEEPEST INCISION (M)	DISRUPT WIDTH (M)	Ø (°T)	COMMENTS
12.70	14.6				NL	NC	3	NC	15/15						Termination: 15°T
12.70	14.6				NL	.2	1	<.2	87/87						
12.85	14.8				NL	<.2	2	<.2	131/131						
12.90	14.7									NL	3	.2	22	135/135	
12.99	15.0				NL	<.2	2	<.2	138/138						Continues into next segment
NL/13	15.0	141	9	6.4											Ice detour at end of seg. New Gouge count may be low
13.01	15.0				NL	<.2	2	<.2	138/138						
13.05	15.0				NL	<.2	2	<.2	139/139						
13.05	15.0				NL	<.2	2	<.2	145/145						
13.15	14.8				NL	.2	3	.4	109/109						
13.25	15.2				NL	<.2	3	.2	130/130						
13.30	15.3				50	NC	4	NC	105/105						Termination: 105°T
13.35	15.3				NL	<.2	2	<.2	153/153						
13.35	15.3				NL	<.2	2	<.2	146/146						
13.55	15.5				NL	.2	2	<.2	125/125						
DP/14	15.9	120	18	15.0											
14.05	15.8									NL	2	.2	8	120/120	
14.10	15.9				NL	.2	1	.2	105/105						
14.10	15.9				NL	.5	2	.2	125/125						
14.20	16.0				NL	.4	5	<.2	95/95						
14.20	16.0				NL	NC	2	NC	130/130						
14.25	16.1				NL	.3	1	<.2	111/111						
14.25	16.1									NL	2	.2	7	115/115	
14.25	16.1				NL	.2	2	.3	125/125						
14.25	16.1				NL	.2	2	.2	105/105						
14.30	16.2									NL	2	.2	22	130/130	

6

TESTLINE: 7 | JULIAN DATE: | YEAR: 1991-1992 | TEMPLATE IDENTIFICATION: 1.1.379

TRACKLINE NUMBER:

CS: 200°T

SEGMENT	WATER DEPTH (M)	TOTAL GOUGES	TOTAL NEW GOUGES	%	Length SINGLE GOUGES: NEW SINGLE GOUGES	GOUGE DEPTH (M)	GOUGE WIDTH (M)	RIDGE HEIGHT (M)	ø (°T)	Length MULTIPLE GOUGES: NEW MULTI. GOUGES	NUMBER OF INCIS.	DEEPEST INCISION (M)	DISRUPT WIDTH (M)	ø (°T)	COMMENTS
14.45	16.2				NL	.5	3	.4	[illegible]/118						
14.55	16.3				NL	.5	3	<.2	126/126						
14.60	16.3				NL	.7	5	.4	173/173						
14.75	16.6									NL	2	.2	25	73/73	
PQ/15	16.8	103	.12	11.7											
15.05	16.9				NL	.3	4	.2	94/94						
15.15	16.9				NL	<.2	3	<.2	96/96						
15.15	16.9				NL	<.2	3	<.2	88/88						
15.20	17.0				NL	.2	5	.3	92/92						
15.20	17.0				NL	<.2	3	<.2	121/121						
15.30	17.1									NL	2	.4	30	95/95	
15.35	17.2				NL	<.2	2	<.2	63/62						
15.40	17.3				NL	<.2	3	<.2	94/94						
15.45	17.3				NL	NC	2	NC	175/175						odd shape
15.50	17.3				15	NC	2	NC	162/162						
15.50	17.3				12	NC	2	NC	158/158						
QR/16	17.7	85	1	1.2											
16.45	18.5				NL	<.2	2	<.2	46/46						
R/end	18.6														end of 1991 DATA

608

TESTLINE: 8			JULIAN DATE:			YEAR: 1981-1982				TEMPLATE IDENTIFICATION: 1:1.633					
TRACKLINE NUMBER: 7					Length SINGLE GOUGES					Length MULTIPLE GOUGES					CS: 99°T
SEGMENT	WATER DEPTH (M)	TOTAL GOUGES	TOTAL NEW GOUGES	%	NEW SINGLE GOUGES	GOUGE DEPTH (M)	GOUGE WIDTH (M)	RIDGE HEIGHT (M)	Ø (°T)	NEW MULTI. GOUGES	NUMBER OF INCIS.	DEEPEST INCISION (M)	DISRUPT WIDTH (M)	Ø (°T)	COMMENTS SS# 3 Bats# 4
AB/0	7.1	0	0	0.0											Sediment rifting and possible boulders
															θ = 155°T λ = 2.5 m
BC/1	10.6	0	0	0.0											Possible boulders -
															Machine malfunction: add
CD/2	11.9	16	12	75.0											.5 m to all depth measurements -
2.15	12.3														Sonar record less clear than 1981 record
2.15	12.3									NL	2	<.2	17	160/166	Bathymetry (depth) seems far off for 1982 record
2.15	12.3				NL	<.2	1	<.2	133/139						
2.15	12.3				NL	<.2	2	<.2	143/154						
2.15	12.3				NL	<.2	1	<.2	57/63						
2.15	12.3				NL	<.2	1	<.2	148/154						
2.35	12.8									NL	5	<.2	28	04/10	
2.65	14.0				NL	<.2	2	<.2	127/133						
DE/3	14.1	60	1	1.7											
3.45	14.5				NL	<.2	3	<.2	13?/1??						Break in slope mid-seg.
EF/4	16.8	69	12	17.4											
4.30	17.8									NL	3	<.2	15	65/71	
4.40	17.9									NL	3	<.2	11	46/52	
4.70	18.8									NL	6	<.2	32	157/163	
FG/5	17.8	63	2	3.2											Start adding fudge factor for depth of 1.5 m
5.05	19.8									NL	2	<.2	12	[illegible]	
GH/6	20.5	127	2	1.6											1.5 m bench at end of segment. Change
6.40	20.5				NL	<.2	3	<.2	45/51						in gouge character seaward of bench.
6.85	21.5				NL	<.2	2	<.2	[illegible]						continues into next segment

810

TESTLINE: 8	JULIAN DATE:	YEAR: 1981-1982	TEMPLATE IDENTIFICATION: 1:1.633

TRACKLINE NUMBER:				1	Length SINGLE GOUGES					Length MULTIPLE GOUGES					CS: 006 °T
SEGMENT	WATER DEPTH (M)	TOTAL GOUGES	TOTAL NEW GOUGES	%	NEW SINGLE GOUGES	GOUGE DEPTH (M)	GOUGE WIDTH (M)	RIDGE HEIGHT (M)	Ø (°T)	NEW MULTI. GOUGES	NUMBER OF INCIS.	DEEPEST INCISION (M)	DISRUPT WIDTH (M)	Ø (°T)	COMMENTS
HI/7	22.5	167	4	2.											It is perfect match and bathymetry is still
7.01	22.5				NL	<.2	2	<.2	20/26						.5 m shallow on 1982 record. Start adding 2 m
7.50	23.2				NL	.3	2	<.2	33/39						to measurements
7.65	23.4				NL	<.2	2	<.2	45/51						
7.75	23.2				NL	.3	2	<.2	115/121						
IJ/8	24.3	130	1	0.8											Change in scale make depth 2.5 m shallow - add 2.5
8.99	25.8				NL	NC	3	NC	05/11						continues into next segment.
JK/9	25.8	129	5	3.9											
9.01	25.8				NL	NC	3	NC	5/11						
9.40	26.2									NL	4	.8	25	126/132	
KL/10	27.0	116	—												Ice detours and high density gouging make new gouge counting impossible
L/end	27.7														

TESTLINE: 9	JULIAN DATE: 237	YEAR: 1979-1982	TEMPLATE IDENTIFICATION: 1:1.379

TRACKLINE NUMBER: 1 | COURSE: 0[illegible]0 °T

SEGMENT	WATER DEPTH (M)	TOTAL GOUGES	TOTAL NEW GOUGES	%	SINGLE GOUGES: Length NEW SINGLE GOUGES	GOUGE DEPTH (M)	GOUGE WIDTH (M)	RIDGE HEIGHT (M)	Ø (°T)	MULTIPLET GOUGES: Length NEW MULTI. GOUGES	NUMBER OF INCIS.	DEEPEST INCISION (M)	DISRUPT WIDTH (M)	Ø (°T)	COMMENTS SS#1 EPTS#1
BC/0	6.0	7	7	100											[illegible] conditions make bathymetry
0.10	6.1				NL	<.2	5	<.2	[illegible]						record very poor. Sand ripples in segment.
0.25	6.7				NL	<.2	1	<.2	145/165						Bdc [illegible] shallow by approx .5 m (add to depth)
0.25	6.7				NL	<.2	2	<.2	145/165						
0.30	6.9				25	<.2	2	<.2	[illegible]/73						
0.35	6.3				17	<.2	2	<.2	10/30						
0.35	6.3				8	<.2	1	<.2	20/40						
0.50	7.1				30	<.2	2	<.2	[illegible]/[illegible]						
BC/1	7.7	10	10	100											change template to 1:1.067
1.40	7.9				NL	.3	4	.2	111/131						
1.50	8.0				10	<.2	2	<.2	65/85						
1.60	8.0				NL	<.2	1	<.2	110/[illegible]						
1.65	8.2				NL	<.2	2	<.2	90/115						
1.75	8.4				NL	.2	2	<.2	[illegible]						
1.90	8.5									NL	3	.2	32	88/108	
1.99	8.5									NL	2	NC	7	178/18	Continues into next segment
BC/2	8.5	16	16	100											change template to 1:1.379
2.01	8.5									NL	2	NC	7	178/18	
2.05	8.5				NL	.3	4	.1	[illegible]/110						
2.05	8.5				NL	.2	3	<.2	[illegible]						
2.15	[illegible]				NL	NC	4	NC	[illegible]						
2.20	[illegible]				NL	<.2	2	<.2	[illegible]/62						
2.20	[illegible]				NL	<.2	2	<.2	[illegible]/113						
2.20	[illegible]				NL	<.2	2	<.2	[illegible]/62						
2.60	9.0				NL	NC	3	NC	[illegible]/21						
2.60	9.0				NL	—	5	—	[illegible]						[illegible] makes gouge depth impossible to measure

812

TESTLINE: 9 | JULIAN DATE: 237 | YEAR: 1979-1982 | TEMPLATE IDENTIFICATION: 1:1.271

TRACKLINE NUMBER: 1 | COURSE: [illegible]°T

SEGMENT	WATER DEPTH (M)	TOTAL GOUGES	TOTAL NEW GOUGES	%	Length: NEW SINGLE GOUGES	SINGLE GOUGES: GOUGE DEPTH (M)	GOUGE WIDTH (M)	RIDGE HEIGHT (M)	Ø (°T)	Length: NEW MULTI. GOUGES	MULTIPLET GOUGES: NUMBER OF INCIS.	DEEPEST INCISION (M)	DISRUPT WIDTH (M)	Ø (°T)	COMMENTS
2.65	9.0				NL	NC	5	NC	22/22						Termination: 202°T
2.80	9.2				NL	<.2	2	<.2	33/15						
2.80	9.2				NL	<.2	2	<.2	13/43						
2.85	9.2				NL	NC	8	NC	12/32						Termination 212°T
2.99	9.3				NL	.3	6	.2	15/35						Continues into next segment
2.99	9.3				NL	—	3	—	11/31						Continues into next segment
															*
DE/3	9.3	1	1	100											[illegible] FEATURES ARE HIGHLY AFFECTED BY LARGE
3.01	9.3				NL	.3	10	.2	15/35						SWELL CONDITIONS. THE [illegible] RESOLUTION IS ALSO VERY POOR.
															[illegible] SEGMENT FE/3 ON ONLY LARGE GOUGES WILL
EE/4	10.0	10	7	70.0											BE MEASURED (5 m WIDE OR GREATER). NUMBERS WILL
4.20	10.2				NL	.3	5	.2	100/120						[illegible] ONLY REFLECT THESE ICE GOUGE FEATURES
4.25	10.2				NL	NC	4	NC	90/10						
4.35	10.3				NL	.5	7	.5	16/66						
4.65	10.5				NL	—	5	—	15/115						[illegible]
4.75	10.7				NL	.6	6	.6	62/82						
4.99	10.8									NL	2	<.2	11	15/35	continues into next segment.
FG/5	10.9	9	5	[illegible]											
5.01	10.9									NL	2	<.2	11	15/35	
5.40	11.0				NL	<.2	12	<.2	109/129						
5.75	11.4				NL	.5	5	.3	99/119						
5.99	11.7				NL	1.1	15	.9	11/31						continues into next segment.
GH/6	11.8	2.0	2.3	76.7											OF THE SEVEN [illegible] belong to a multiplet
6.01	11.8				NL	1.1	15	.9	17/37						Start adding 1m to [illegible]
6.10	12.0									NL	2	<.2	10	62/82	

TESTLINE: 9 | JULIAN DATE: 237 | YEAR: 1979-1982 | TEMPLATE IDENTIFICATION: 1:1.379

TRACKLINE NUMBER: 1 | COURSE: [illegible]

SEGMENT	WATER DEPTH (M)	TOTAL GOUGES	TOTAL NEW GOUGES	%	SINGLE GOUGES: Length NEW SINGLE GOUGES	GOUGE DEPTH (M)	GOUGE WIDTH (M)	RIDGE HEIGHT (M)	Ø (°T)	MULTIPLET GOUGES: Length NEW MULTI. GOUGES	NUMBER OF INCIS.	DEEPEST INCISION (M)	DISRUPT WIDTH (M)	Ø (°T)	COMMENTS
6.40	11.9									NL	2	—	13	20/40	[illegible] to resolve gouge depths
6.40	11.9				NL	—	5	—	60/80						
6.50	12.1									NL	6	.9	47	50/70	Terminates: 250°T
6.55	12.0									NL	6	.6	30	56/76	Terminates: ends at large (3m) shoal or moraine at mid segment.
6.70	12.1									NL	5	—	34	49/69	
															— — —
HI/7	12.4	19	18	94.7											
7.15	12.5				NL	.4	5	.2	128/148						
7.20	12.5				NL	—	5	—	62/82						
7.40	12.6				NL	NC	5	NC	33/53						
7.45	12.6				NL	—	8	—	111/131						
7.50	12.6									NL	6	NC	37	39/59	
7.55	12.8				NL	—	7	—	126/146						
7.70	12.8				NL	NC	25	NC	18/38						Terminates: 218°T
7.80	13.0									NL	4	.7	28	27/47	Terminates: 224°T
7.99	13.0									NL	2	—	13	24/44	Continues into next segment.
IJ/3	13.0	13	12	92.3											
8.01	13.0									NL	2	—	13	24/44	
8.25	—									NL	3	—	25	53/73	Terminates: 253°T
8.45	13.2				NL	—	12	—	64/84						
8.50	13.1									NL	2	.7	24	64/84	
8.55	13.2				NL	.5	6	<.2	73/93						
8.80	13.5				NL	.3	8	.2	43/63						
8.90	13.3									NL	2	.9	24	[illegible]	

814

TESTLINE: 9 | JULIAN DATE: 239 | YEAR: 1973-1982 | TEMPLATE IDENTIFICATION: 1:1.379

TRACKLINE NUMBER: 1 | COURSE: 020°T

SEGMENT	WATER DEPTH (M)	TOTAL GOUGES	TOTAL NEW GOUGES	%	SINGLE GOUGES: Length NEW SINGLE GOUGES	GOUGE DEPTH (M)	GOUGE WIDTH (M)	RIDGE HEIGHT (M)	Ø (°T)	MULTIPLET GOUGES: Length NEW MULTI. GOUGES	NUMBER OF INCIS.	DEEPEST INCISION (M)	DISRUPT WIDTH (M)	Ø (°T)	COMMENTS
13.90	16.8				NL	—	5	—	65/85						
13.90	16.8				NL	—	9	—	29/49						continues into next segment.
13.99	17.0				NL	—	7	—	127/147						continues into next segment.
OP/14	17.0	26	16	61.5											
14.01	17.0				NL	—	9	—	29/49						
14.01	17.0				NL	—	7	—	127/147						continued from previous segment
14.01	17.0									NL	2	—	12	[illegible]/20	
14.15	17.1				NL	—	10	—	81/101						
14.20	17.1				NL	—	7	—	82/102						
14.20	17.1									NL	2	—	8	128/148	
14.25	17.2				NL	—	5	—	07/27						
14.30	17.2				NL	—	10	—	71/91						
14.60	17.4									NL	5	—	53	51/71	
14.85	17.5				NL	—	7	—	162/82						
PQ/15	18.2	12	7	58.3											fall ogrom now ~ 2.0m too shallow at scale chg.
15.20	18.2				NL	—	5	—	58/78						
15.50	18.4				NL	—	11	—	105/125						
15.55	18.3				NL	—	13	—	125/145						
15.75	18.[illegible]				NL	—	8	—	173/13						
15.85	18.5				NL	—	15	—	[illegible]/17						
15.90	18.6				NL	—	8	—	84/104						
15.95	18.7				NL	—	1	—	88/108						
															[illegible]
Q/end	18.7														

815

816

TESTLINE: 9	JULIAN DATE: 237	YEAR: 1979-1982	TEMPLATE IDENTIFICATION: 1:1,379

TRACKLINE NUMBER: 1 — COURSE: 020°T

SEGMENT	WATER DEPTH (M)	TOTAL GOUGES	TOTAL NEW GOUGES	%	SINGLE GOUGES — Length: NEW SINGLE GOUGES	GOUGE DEPTH (M)	GOUGE WIDTH (M)	RIDGE HEIGHT (M)	Ø (°T)	MULTIPLET GOUGES — Length: NEW MULTI. GOUGES	NUMBER OF INCIS.	DEEPEST INCISION (M)	DISRUPT WIDTH (M)	Ø (°T)	COMMENTS
JK/9	13.5	9	2	22.2											
9.35	14.0				NL	—	5	—	13/[illegible]						
9.80	13.5				NL	—	13	—	171/11						
KL/10	14.0	16	11	68.8											
10.40	14.4									NL	3	<.2	23	46/66	
10.50	14.3				NL	.2	6	.2	140/160						
10.65	14.4									NL	2	<.2	17	62/82	
10.80	14.4									NL	5	<.2	35	04/24	←24°→
LM/11	14.6	13	4	30.8											
11.15	14.7				NL	—	8	—	90/110						Poor fathogram
11.70	15.1				NL	NC	12	NC	86/106						
11.85	15.4									NL	2	NC	18	22/42	Termination · 222°T
MN/12	15.4	17	7	41.2											fathogram unusable for gouge depth measures
12.15	15.4				NL	—	12	—	30/50						
12.15	15.4				NL	—	11	—	41/61						
12.70	15.7				NL	—	6	—	00/20						= sinuous but still // to track
12.85	16.0				NL	—	13	—	54/74						
12.95	16.2									NL	3	—	19	40/60	
NO/13	16.2	20	12	60.0											Still to sin[illegible] on [illegible] compared to 1976.
13.05	16.1				NL	—	5	—	13/[illegible]						fathogram unusable for gouge depth measures
13.15	16.0				NL	—	8	—	93/113						
13.20	16.1				NL	—	8	—	60/80						
13.60	16.6									NL	4	—	42	57/[illegible]	
13.65	16.7									NL	[illegible]	—	12	00/20	sinuous but parallels trackline. Continues into next segment

TESTLINE: 1 | JULIAN DATE: 238 | YEAR: 1977-1978 | TEMPLATE IDENTIFICATION: 1:1.860

TRACKLINE NUMBER: 14.19

SEGMENT	WATER DEPTH (M)	TOTAL GOUGES	TOTAL NEW GOUGES	%	Length SINGLE GOUGES: NEW SINGLE GOUGES	GOUGE DEPTH (M)	GOUGE WIDTH (M)	RIDGE HEIGHT (M)	Ø (°T)	Length MULTIPLE GOUGES: NEW MULTI. GOUGES	NUMBER OF INCIS.	DEEPEST INCISION (M)	DISRUPT WIDTH (M)	Ø (°T)	COMMENTS CS = 205°T
AB/0	4.2	0	0	0											
															CS # 5 Pts # 8,10
BC/1	7.5	8	2	25.0											Beginning of trackline
1.50	7.8									73	2	NOT CROSSED	18	110/55	totally reworked bedrock
															3m shoal at pt. B.
															Termination at 1.5 direction – 235°T
CD/2	7.7	8	6	75.0											
2.20	8.0									NL	2	<.2	5	145/90	
2.80	8.5									NL	4	<.2	15	140/85	
DE/3	8.8	2	0	0											Sed. ripples (few)
EF/4	9.6	8	0	0											Sed. ripples (few)
FG/5	10.0	8	6	75.0											Sed. ripples (heavy concentration)
5.40	10.0				175	<.2	1	<.2	160/105						Orien. = 1??°T λ = 2m
5.65	10.0				63	<.2	2	<.2	160/105						
5.85	9.9				41	<.2	1	<.2	35/160						termination direction – 160°T
5.85	9.9				35	<.2	1	<.2	35/160						termination direction – 160°T
5.85	10.1				32	<.2	1	<.2	35/160						termination direction – 160°T
[illegible]	10.0				127	<.2	1	<.2	170/115						
															reworking bottom [illegible] (?) sed. waves (few)
GH/6	10.0	3	0	0											
															Sed. waves – [illegible] orien = 115°T λ ~100m
HI/7	10.5	5	0	0											
IJ/8	10.4	11	1	5.0											[illegible] termination [illegible] hooked and unclear
9.60	11.5				NL	.2	3	<.2	[illegible]/150						[illegible] – 150°T

TESTLINE: 1		JULIAN DATE: 238			YEAR: 1977-1978					TEMPLATE IDENTIFICATION: 1.1.860					
TRACKLINE NUMBER: 14,19					Length SINGLE GOUGES					Length MULTIPLE GOUGES					
SEGMENT	WATER DEPTH (M)	TOTAL GOUGES	TOTAL NEW GOUGES	%	NEW SINGLE GOUGES	GOUGE DEPTH (M)	GOUGE WIDTH (M)	RIDGE HEIGHT (M)	Ø (°T)	NEW MULTI. GOUGES	NUMBER OF INCIS.	DEEPEST INCISION (M)	DISRUPT WIDTH (M)	Ø (°T)	COMMENTS CS = 305°T
JK/9	11.5	75	18	24.0											[illegible] gouges
9.25	11.6									NL	3	NC	17	155/160	have [illegible]
9.25	11.6									NL	2	NC	11	155/160	[illegible]
9.35	11.7				NL	.2	3	<.2	130/75						
9.40	11.7									NL	2	.2	14	130/75	
9.65	11.9				280	<.2	2	<.2	00/125						
9.85	11.9									135	4	<.2	13	20/145	
9.99	12.0									831	4	NC	9	75/130	continues to next segment.
KL/10	12.0	76	5	6.6											
10.25	12.1									same as above	4	NC	9	05/130	
10.55	12.3				25	<.2	2	<.2	60/55						
LM/11	12.5	91	4	4.3											
11.30	12.6				50	<.2	7	<.2	120/65						START Trackline 19
11.60	12.7				108	NC	3	NC	170/115						terminates [illegible] masked [illegible] 115°T
11.80	12.8				138	<.2	11	<.2	110/135						
11.80	12.8				NL	<.2	2	<.2	150/105						terminates direction - 315°T
MN/12	12.8	94	15	16.0											
12.30	13.0				NL	<.2	2	<.2	170/115						
12.45	13.0									NL	4	<.2	23	55/00	
12.45	13.0				117	<.2	5	<.2	55/00						
12.45	13.0									NL	7	NC	65	55/00	
12.65	13.0				163	NC	2	NC	175/120						
12.75	13.0				43	NC	2	NC	05/120						

TESTLINE: 1		JULIAN DATE: 241			YEAR: 1977-1978					TEMPLATE IDENTIFICATION: 1:1.860					
TRACKLINE NUMBER: 14,19					Length SINGLE GOUGES					Length MULTIPLE GOUGES					
SEGMENT	WATER DEPTH (M)	TOTAL GOUGES	TOTAL NEW GOUGES	%	NEW SINGLE GOUGES	GOUGE DEPTH (M)	GOUGE WIDTH (M)	RIDGE HEIGHT (M)	Ø (°T)	NEW MULTI. GOUGES	NUMBER OF INCIS.	DEEPEST INCISION (M)	DISRUPT WIDTH (M)	Ø (°T)	COMMENTS
NO/13	13.2	141	21	14.9											
13.01	13.2									NL	4	<.2	14	00/125	
13.60	13.4									NL	5	NC	40	110/115	terminates direction - 125°T
13.60	13.4									NL	2	.3	13	140/85	
13.70	13.4				NL	<.2	3	.4	160/105						
13.90	13.5									NL	9	.2	21	160/105	continues to next segment.
OP/14	13.5	137	18	13.1											
14.10	13.8				35	<.2	2	<.2	130/75						
14.15	13.8									NL	9	.2	21	160/105	
14.25	13.5									NL	3	<.2	8	155/100	
14.50	13.9									NL	4	<.2	12	155/100	
14.80	13.8				NL	NC	2	NC	05/130						
PQ/15	14.0	61	8	13.1											[illegible] from reworking. North of line.
15.80	14.3									NL	8	.3	60	54/[illegible]	
QR/16	14.3	71	4	5.6											[illegible] floor North of line.
16.05	14.3									NL	2	.2	20	151/76	
16.65	14.5									NL	2	.5	17	144/60	
RS/17	14.9	69	0	0.0											[illegible]
ST/18	15.0	64	0	0.0											[illegible]
TU/19	15.2	102	0	0.0											[illegible]

TESTLINE: 1	JULIAN DATE: 241				YEAR: 1977-1978					TEMPLATE IDENTIFICATION: 1:1,860					
TRACKLINE NUMBER: 14, 19					Length SINGLE GOUGES					Length MULTIPLE GOUGES					CS: 305°T
SEGMENT	WATER DEPTH (M)	TOTAL GOUGES	TOTAL NEW GOUGES	%	NEW SINGLE GOUGES	GOUGE DEPTH (M)	GOUGE WIDTH (M)	RIDGE HEIGHT (M)	Ø (°T)	NEW MULTI. GOUGES	NUMBER OF INCIS.	DEEPEST INCISION (M)	DISRUPT WIDTH (M)	Ø (°T)	COMMENTS
UV/20	15.5	118	0	0.0											[illegible]
VW/21	15.7	108	10	9.3											
21.30	15.6									NL	5	.4	21	147/94	
21.50	15.6									NL	5	.5	28	164/103	
WX/22	15.8	81	4	4.9											
22.40	15.9				NL	<.2	2	<.2	96/131						
22.99	16.0									NL	3	.3	21	152/97	Continues into next segment.
XY/23	16.0	79	5	6.3											
23.01	16.0									NL	3	.3	21	152/97	
23.55	16.0				NL	<.2	2	<.2	112/107						
23.55	16.0				NL	.3	18	.3	124/69						Termination: 249°T
YZ/24	16.5	58	0	0.0											
Z/end	16.7														